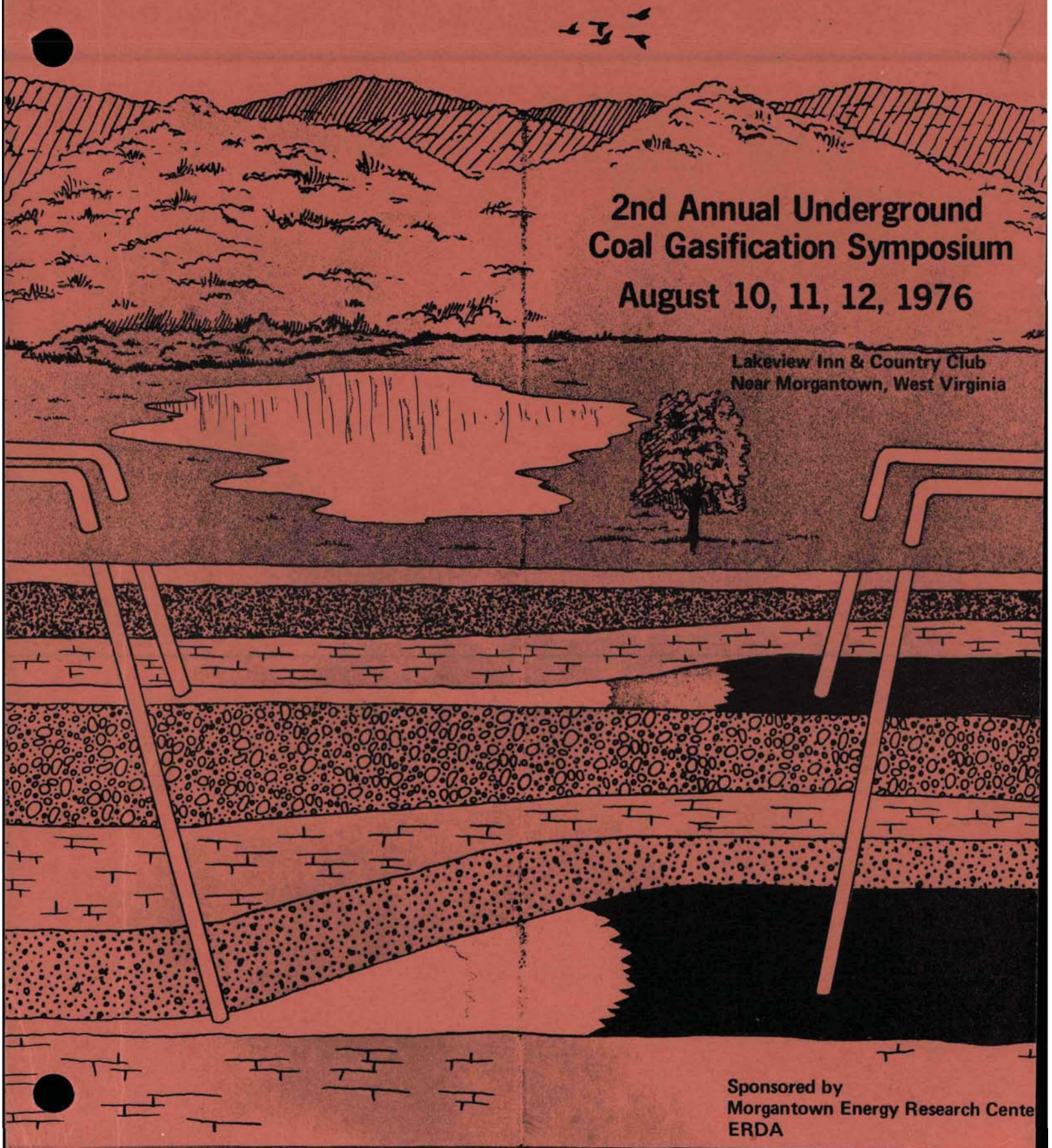


2nd Annual Underground Coal Gasification Symposium

August 10, 11, 12, 1976

Lakeview Inn & Country Club
Near Morgantown, West Virginia

Sponsored by
Morgantown Energy Research Cente
ERDA

DISCLAIMER

This report was prepared as an account of work sponsored by an agency of the United States Government. Neither the United States Government nor any agency Thereof, nor any of their employees, makes any warranty, express or implied, or assumes any legal liability or responsibility for the accuracy, completeness, or usefulness of any information, apparatus, product, or process disclosed, or represents that its use would not infringe privately owned rights. Reference herein to any specific commercial product, process, or service by trade name, trademark, manufacturer, or otherwise does not necessarily constitute or imply its endorsement, recommendation, or favoring by the United States Government or any agency thereof. The views and opinions of authors expressed herein do not necessarily state or reflect those of the United States Government or any agency thereof.

DISCLAIMER

Portions of this document may be illegible in electronic image products. Images are produced from the best available original document.

PROCEEDINGS

SECOND ANNUAL UNDERGROUND COAL GASIFICATION SYMPOSIUM

AUGUST 10-12, 1976

LAKEVIEW INN AND COUNTRY CLUB

MORGANTOWN, WEST VIRGINIA

NOTICE
This report was prepared as an account of work sponsored by the United States Government. Neither the United States nor the United States Energy Research and Development Administration, nor any of their employees, nor any of their contractors, subcontractors, or their employees, makes any warranty, express or implied, or assumes any legal liability or responsibility for the accuracy, completeness or usefulness of any information, apparatus, product or process disclosed, or represents that its use would not infringe privately owned rights.

SPONSORED BY

MORGANTOWN ENERGY RESEARCH CENTER, ERDA

PROCEEDINGS EDITOR : L. Z. SHUCK

ASSOCIATE EDITOR : J. D. SPENCER

COORDINATOR: HILMA D. BARLOW



DISTRIBUTION OF THIS DOCUMENT IS UNLIMITED

MORGANTOWN ENERGY RESEARCH CENTER, ERDA

MORGANTOWN, WEST VIRGINIA 26505

TABLE OF CONTENTS

ITEM	PAGE NO.
Message from the Chairman	vii
Welcome Address by A. A. Pitrolo	viii
Opening Remarks by L. Z. Shuck	ix
Keynote Address by H. D. Guthrie	xi
Luncheon Address, Jay Hilary Kelley	xii
Plenary Paper PP-1, the 1976 ERDA In Situ Coal Gasification Program P. R. Wieber and A. P. Sikri	1
SESSION I - MAJOR PROJECT STATUS REPORTS	
MPR-1 "Feasibility Studies of In Situ Coal Gasification in the Warrior Coal Field" G. W. Douglas.	18
MPR-2 "Results and Status of the Second Hanna In Situ Coal Gasification Experiment" L. A. Schrider, C. F. Brandenburg, D. D. Fischer, and D. A. Northrop.	36
MPR-3 "Lawrence Livermore Laboratory In Situ Coal Gasification Program" D. R. Stephens, F. O. Beane, and R. R. Hill.	53
MPR-4 "Status of the MERC In Situ Gasification of Eastern U.S. Coals Project" L. Z. Shuck, J. Pasini III, J. W. Martin, and L. A. Bissett.	65
MPR-6 "Texas Utilities Program Status Report" B. R. CLements and J. F. Grant.	86
MPR-7 "Research on In Situ Gasification of Texas Lignite at the University of Texas" T. F. Edgar, W. R. Kaiser, and T. W. Thompson.	90
MPR-8 "In Situ Combustion of Coal for Energy" R. F. Chaiken.	96
SESSION II - ENVIRONMENTAL STUDIES	
ENV-1 "Groundwater Contamination from In Situ Coal Gasification: Laboratory and Simulation Studies" J. F. Henry, W. Bertsch, and M. D. McKinley.	105

TABLE OF CONTENTS (CON'T)

ITEM		PAGE NO.
ENV-2	"Preliminary Laboratory and Modeling Studies on the Environmental Impact of In Situ Coal Gasification" J. H. Campbell.	119
ENV-3	"Hydrogeologic Assessment of an Underground Coal Gasification Project Site, Grant District, Wetzel County, West Virginia" C. W. Byrer.	140
SESSION III - PROCESS ECONOMICS		
EC-1	"Factors Influencing the Economics of Large-Scale In Situ Coal Gasification Operations" M. K. Buder, A. I. McCone, R. A. Fascher, and O. N. Terichow.	145
EC-2	"An Economic Evaluation of Underground Coal Gasification" A. M. Garon.	155
EC-3	"The Economics of Underground Coal Gasification" A. J. Moll.	169
EC-4	"Economics of Marketing Synthesis Gas Produced by Underground Coal Gasification" D. L. Bidlack and R. L. Arscott.	179
EC-5	"Economic Comparison of Producing SNG by Lawrence Livermore Laboratory's In Situ Coal Gasification Process with Lurgi Aboveground Coal Gasification" R. Z. Mason and D. E. Hall.	188
SESSION IV - MONITORING AND INSTRUMENTATION		
MI-1	"Remote Monitoring of an In Situ Coal Gasification Process" L. W. Beckham and L. C. Bartel.	214
MI-2	"Real Time Process Monitoring in Underground Coal Gasification" D. E. Eastwood, D. F. Moore, S. B. King, W. V. Lanum, J. K. Eastlack, and J. W. Jennings.	226
MI-3	"Electromagnetic Wave Propagation Within a Subsurface Coal Seam for In Situ Gasification Application" J. J. HOlmes and C. A. Balanis.	238
MI-4	"Monitoring of Emissions from an In Situ Coal Gasification Experiment" D. D. Fischer.	242

TABLE OF CONTENTS (CON'T)

ITEM		PAGE NO.
SESSION V - THEORETICAL PROCESS MODELING		
TPM-1	"Modeling and Computer Simulation of Reaction Kinetics Associated with the Underground Gasification of Coal" S. M. Farouq Ali and M. L. Pasha.	249
TPM-2	"Chemical Reactor Modleing of In Situ Coal Gasification" T. F. Edgar and T. H. Tsang.	256
TPM-3	"Thermoviscoelastic Considerations Associated with Underground Coal Gasification" S. H. Advani, L. Z. Shuck, and Y. T. Lin.	266
TPM-4	"A Theoretical Analysis of Soviet In Situ Coal Gasification Field Tests" D. L. Whitman.	272
SESSION VI - STRUCTURAL AND ROCK MECHANICS		
SRM-1	"Calculations of Fracture and Permeability Enhancement from Underground Explosions in Coal" T. R. Butkovich.	285
SRM-2	"Design Criteria for Hydraulic Fracture of Coal Beds" S. H. Advani, H. Y. Chang, L. Z. Shuck, and H. V. Ganga Rao.	295
SRM-3	"Hydraulic Fracturing Thin Coal Seams in Preparation for In Situ Gasification" T. Warren and A. Hayatdavoudi.	300
SRM-4	"Rock Mechanics Aspects of In Situ Gasification with Special Reference to Texas Lignite" T. W. Thompson.	306
SRM-5	"Mechanical Properties of Coal for Simulation of Underground Gasification Processes" H. D. Shoemaker, L. Z. Shuck, R. R. Haynes, and S. H. Advani.	316
SESSION VII - FIELD AND SYSTEMS STUDIES		
FS-1	"Some Insights from Temperature Measurements on Recent Underground Coal Gasification Experiments" S. G. Beard and R. P. Reed.	328
FS-2	"Practical Considerations in Designing an UCG Field Test" G. Campbell, T. Sterner, and A. Humphrey.	339

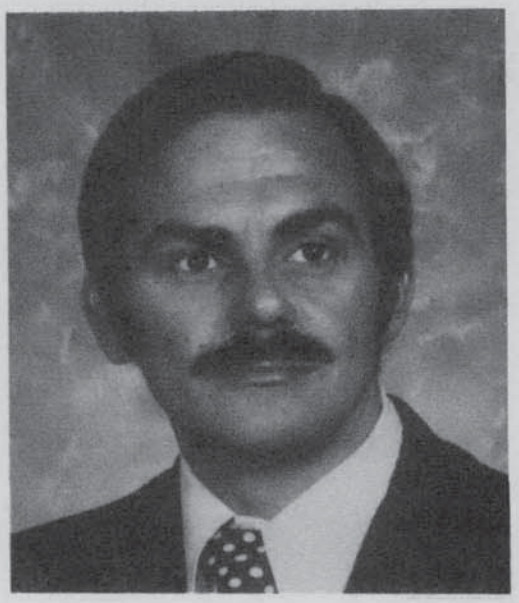
TABLE OF CONTENTS (CON'T)

ITEM		PAGE NO.
FS-3	"Post Burn Analysis Techniques APplicable to Underground Coal Gasification" R. M. Boyd.	344
FS-4	"Status of the Linked Vertical Well Process in Underground Coal Gasification" C. F. Brandenburg, D. D. Fischer, G. G.Campbell, R. M. Boyd, R. D. Gunn, and D. A. Northrop.	354
FS-5	"Utilization of Low Btu Gas from In Situ Coal Gasification for On-Site Power Generation" R. E. D. Stewart.	372
SESSION VIII - UCG TECHNOLOGY AND PROGRAMS IN OTHER COUNTRIES		
FTP-2	"In Situ Gasification in Australia; Prospects, Potential and Research Activities" I. McC. Stewart.	382
FTP-3	"Prospects and Problems for UCG in Britain" F. Williams.	388
SESSION IX - LABORATORY EXPERIMENTATION		
LE-1	"Two Dimensional Studies of Coal Pyrolysis: Preliminary Results" R. C. Forrester III.	402
LE-2	"Reaction Kinetics of COal Char Gasification Under Conditions Expected in Underground Coal Gasification" J. E. Young, R. Lo, and J. Fischer.	411
LE-3	"Lawrence Livermore Laboratory In Situ Coal Gasification Program" Underground Reaction Modeling and Laboratory Combustion Tube Experiments" R. Rozsa and C. Thorsness.	422
LE-4	"Laboratory Evaluation of the Subatmospheric Pressure Underground Gasification Concept for Thin Seams" O. J. Hahn and J. E. Jones, Jr.	430
LE-5	"Studies of Model Coal Tunnel Fires" R. F. Chaiken and J. M. Singer.	434
LE-6	"In Situ Hydrocarbon Recovery Simulation Laboratory Research at Morgantown Energy Research Center" L. Z. Shuck, G. E. Fasching, J. W. Martin, and L. A. Bissett	452

TABLE OF CONTENTS (CON'T)

ITEM		PAGE NO.
SESSION X - POTPOURRI BRIEFS		
PB-1	"An Ammonia Injection Scheme for Fracturing and Permeability Enhancement of Coal Beds" R. Datta.	467
PB-3	"Laser Coal Drilling Studies" S. V. Gunn.	471
PB-4	"Review of Current UCG Model Capabilities" W. K. Sawyer.	477
PB-5	"A Generalized Theory for Diffusive Fluid Flow Through Solid, Permeable Media" J. F. Seeberger.	489
PB-6	"Surface Directional Permeability Analyzer" J. C. Huston, L. Z. Shuck, and B. E. Slonneger.	507
PB-7	"Algorithm for Cost Effectiveness of Directional Versus Vertical Well Drilling" B. E. Slonneger.	519
PB-8	"Real Mass and Energy Transport Coefficients Determined from UCG Process Simulation Experiments" M. T. Pellegrin.	526
PB-9	"Fundamental Aspects of In Situ Electro-carbonization and Electrogasification of Coal" Erich Sarapuu	541
APPENDICES		
A-1	Symposium Staff and Session Chairmen	553
A-2	List of Attendees	554
A-3	Registration Statistics	562
A-4	Photographs of Symposium Events	563
A-5	Submitted Biographical Sketches	573
A-5	Duplication of the Program Outline	574

MESSAGE FROM THE CHAIRMAN



This Symposium is intended to stimulate an open exchange of information on the newly emerging technology in the United States of In Situ Coal Gasification. The technical feasibility of this process has been well established in the Soviet Union during their 40-plus years of development and industrial utilization. We must now evaluate and utilize their technology while embarking upon new innovative programs to implement the existing and newly developed UCG technology into our own industrial, economic, resource and environmental systems. This process may offer a means for extracting energy from coal and for providing relief to our energy demands.

During the evolvement of a new technology it is desirable to not only discuss established conventional methodology, but also seek new ideas and achieve quick reviews. A session with this specific objective is added at the end of the Symposium. Topics of unproven, advanced techniques or methods with preliminary results ready for critiquing are included.

A total of fifty-two papers will be presented during the Symposium. I am confident that with your open and candid discussion this Second Annual Underground Coal Gasification Symposium, like the first, will be a great success.

L. Zane Shuck

L. Zane Shuck
Symposium Chairman

SECOND ANNUAL
UNDERGROUND COAL GASIFICATION SYMPOSIUM
WELCOME

by

A. A. Pitrolo, Director, Morgantown Energy Research Center

On behalf of the Energy Research and Development Administration and the Morgantown Energy Research Center, I would like to welcome you to the Second Annual Underground Coal Gasification Symposium and to Morgantown, West Virginia.

Several things come to mind relating to the background of Underground Coal Gasification. While both the British and Russians claim to have invented the idea, the Soviets are more verbal about crediting the concept to D. I. Mendeleev, who created the periodic table. In 1888 in his work, "The Future Power Resting on the Banks of the Donets," he wrote "that a time will soon come when special plants will be built for converting coal into combustible gases. Moreover gas gives the highest temperatures, higher than coal itself, which is why even now coal is completely converted into combustible gas in simple installations called generators-a time will probably even come when coal will no longer be taken out of the ground but be converted there into combustible gases that will then be carried by pipelines over long distances."

Experiments in UGC began as early as 1913 in Britain, which were later followed by the work of many countries, including the United States. The enthusiasm for UGC has evolved through several cycles, the high point being the Russian work in the 1930's and 1940's, followed by world-wide activity in the 50's and the current effort of the 70's. Each of these periods of time were highlighted by a flurry of activity and enthusiasm which fell short of reaching true commercialization. So here we are again on the verge of UGC technology breakthroughs, and possibly this thrust will result in a commercially viable process.

I believe the momentum can be depicted at this time by the large participation and the extremely high quality and wide assortment of papers at this symposium. Here we have a room full of people exceeding 100. A few years ago we could have all gathered in the back of a Volkswagen or the phone booth at the reception desk. Today we are talking about seven active projects which will be conducted in 1977 in the United States and Canada. Other countries such as Austria, Belgium, Australia, Poland, England, Germany, and others are indicating considerable interest and initiating their own major UGC programs. UGC itself must be viewed as an interesting approach to satisfy major energy demands. It has far-reaching potential of utilizing the coal in place, precluding costly extraction and, furthermore, utilizing resources that could be sealed forever in the earth. In addition, it offers a very attractive energy source at much reduced cost than other comparable conversion processes.

UGC is truly a systems technology and cuts across virtually every technical discipline from the point of the resource determination, the exploitation, the conversion, and end use. This is again clearly shown by the wide array of papers to be presented in the next three days. We will all go home much more informed and ready to pursue the next course-which is the maturing of the technology toward commercialization.

With this short introduction, I would like to turn the meeting over to Dr. Zane Shuck the Symposium organizer.

SECOND ANNUAL
UNDERGROUND COAL GASIFICATION SYMPOSIUM
OPENING REMARKS

by

L. Z. Shuck, Symposium Chairman

Good Morning, I would also like to welcome you to the Second Annual Underground Coal Gasification Symposium. It has been very encouraging to us to see such a large number of people with a good distribution between government, industry and universities, interested in UCG technology and this Symposium. A list of the registrants will be distributed tomorrow.

We have a very compact program with over fifty-two planned presentations and other activities during these three days. In the interest of conserving time I would now like to make some general announcements.

First, I would like to introduce those persons responsible for making arrangements and who will be providing assistance during the next three days. Will the following please stand and be identified:

Jack Spencer ----- Vice Chairman and Treasurer
Hilma Barlow ----- My secretary and symposium coordinator
Chuck Whieldon --- Accomodations and arrangements
Judy Bennett ----- Special travel and hostess
Bill Samples ----- Photographer and A-V arrangements
Bob Davis -------- Photographer and A-V arrangements .

You may arrange with Bill Samples to pick up a slide tray and view your slides in advance in Room 603 below which has been reserved for this purpose.

I would now like to introduce the Session Chairmen who will be responsible for keeping us on schedule. Will the Session Chairmen please stand and be identified:

Paul Wieber ---------- Session 1
Leo Schrider ---------- Session 2
Doug Stephens --------- Session 3
Chuck Brandenburg ------ Session 4
Ed Byars -------------- Session 5
Walt Sawyer ----------- Session 6
Tom Edgar ------------- Session 7
Al Sikri -------------- Session 8
Dave Northrup --------- Session 9 .

All speakers should arrange to meet your Session Chairman and discuss any special arrangements, if any, for your presentation. Introductions of the speakers will be very brief in the interest of time, but detailed biographical sketches of all speakers will be included in the proceedings. Please save your questions until after each presentation to guarantee the speaker the allotted time and then step to the microphone and identify yourself first.

There are a few other announcements at this time:

All authors should leave a biographical sketch with Mrs. Barlow before leaving the Symposium.

There will be a group photograph taken of all participants at 6:15 p.m., Tuesday, on the lawn across from the Pro Shop.

The Proceedings will be designated by MERC/SP-76-3 and will be available later from the National Technical Information Service (NTIS). All paid registrants will be mailed copies.

An additional 75 seats have been added to the Allegheny flights departing to Pittsburgh, Friday between 8:00 a.m. and Noon, so you should have no difficulty getting to Pittsburgh Friday morning.

If you will not be attending the luncheon, please notify Ms. Barlow.

The sessions will not be interrupted for messages, but all messages will be posted on a board in the hall prior to each intermission.

I would like to again call your attention to the Potpourri Session X in which new concepts and ideas are to be presented. If you have a topic please notify me or Dave Northrup up to one hour before the session begins and it will be included. I am sure that this session along with the others will provide a very interesting and thought-provoking meeting. The success of a symposium depends upon participation by everyone so I encourage each of you to openly and candidly discuss the issues of UCG.

At this time I would like to introduce to you our Keynote Speaker. He is the new Director, Division of Oil, Gas and Shale Technology in Fossil Energy, ERDA, in whose Division ERDAs' UCG programs are sponsored. He has spent 33-plus years with Shell Corporation in research, marketing, manufacturing and management. He is a chemical engineer from the University of Iowa and he served as President of AICHE in 1969.

He has been a University Lecturer, a member of numerous advisory boards and professional societies, but this is his first time with the Feds. I decided that he must be either just a little crazy or a real tiger to accept the challenge of such a demanding position at this point in his career. Well, after talking with him last night and learning that he has five (5) daughters, I decided that he is a well seasoned TIGER.

It is indeed a pleasure to introduce to you Mr. Hugh Guthrie. Hugh it is a real honor to have you as our Keynote Speaker.

SECOND ANNUAL UNDERGROUND COAL GASIFICATION SYMPOSIUM
KEYNOTE ADDRESS

by

Hugh D. Guthrie, Director, Division of Oil, Gas, and Shale Technology, ERDA

This is a good audience. You represent all of the three major areas for application of technical discipline and understanding--industry, education, and government. If we are to make energy a continuing supporter rather than a deterrent to progress, all three must contribute. This meeting--The Second Annual Symposium on Underground Coal Gasification--represents a potential for encouraging that interaction, and the recent research results merit your time and participation.

As I thought about this particular subject, to me it illustrates very clearly the definition of engineering from the original issue of the Encyclopedia Brittanica. This issue defines engineering as the "art and science of weaving technology into the fabric of society." Think about that a little bit. I don't know of any definition that has more meaning to the subject of this meeting. That's the job you have to do, not just to establish that underground coal gasification is feasible and economic. You have the job of, in some way, weaving that technology into the fabric of scoiety. The need is there, the time is now, and I think, as Augie indicated to you, the potential is trememdous.

That's the message that I would like to leave with you this morning and like you to think about as you move through this symposium. View this as an opportunity to bridge across those differences of understanding that will always exist between industry, Government, and education, and to recognize that success in any project depends upon the human individuals involved. Each of you should ask himself, "Why am I important to this program? What contribution will I make? What will be my personal milestone that I hope to have achieved when the Third Annual Symposium rolls around?" If each of you does this, your being here will be one of the important times in your lives. Collectively, your being here will be one of the important times for this country in which we live.

I'm delighted to be here and am looking forward to sharing in both the formal and informal discussions.

FEDERAL-STATE ENERGY CONSIDERATIONS

by

Jay Hilary Kelley, West Virginia University

One of the favorable fallouts from the 1973-74 energy crisis is the new awareness created among the public and also among scholars, researchers, and teachers about energy and minerals. If it had not been for the energy crisis, we probably would not at this time have an Energy Research and Development Administration. We probably would not have as many University people focusing into energy areas. All of this is good for the minerals professions because it bolsters their ranks and draws a wide public cognizance to the need for conservation and study.

The energy crisis marked the climactic end to a fundamental philosophy for America--and the world. Although some people still hold the conviction that cheap energy will continue, the most knowledgeable persons regard this a naive pipe dream. The forced acceptance of the end of the era of free energy is indeed a bitter pill for many to swallow. Moreover, the prospect of scarce energy has wide implications for our most treasured way of living--perhaps forecasts an end to many fruits of modern technology for the masses.

With the ominous prospect of scarce energies for all time, it is certainly within our abilities to alleviate future crises and seek new sources of energy and techniques to obtain energy from sources that appear at present to be inaccessible. There are vast quantities of these so-called marginal sources such as in very thin seams of coal and deposits of coal left underground after mining. We are, therefore, pleased that the federal Energy Research and Development Administration has undertaken the aggressive study of how in situ coal might be converted to gas.

But states which are producers of energy such as West Virginia also have a concern. The purpose of my discussion today is to try to place in perspective the relative roles of the producing states and the federal government. I will begin with a series of statements or shall we say assumptions which guide our thinking on this subject. With appropriate comments then I will attempt to draw some conclusions.

The first statements pertain to mineral resources. The question is not <u>will</u> coal or other minerals be mined. The question is <u>when</u> will they be mined? As recently as four years ago a fellow dean in a non-technical discipline asked me in all seriousness: would it be possible that the remaining coal would not need to be mined with the prospect of free nuclear and hydrogen energy. This thought should be a mute question for this audience.

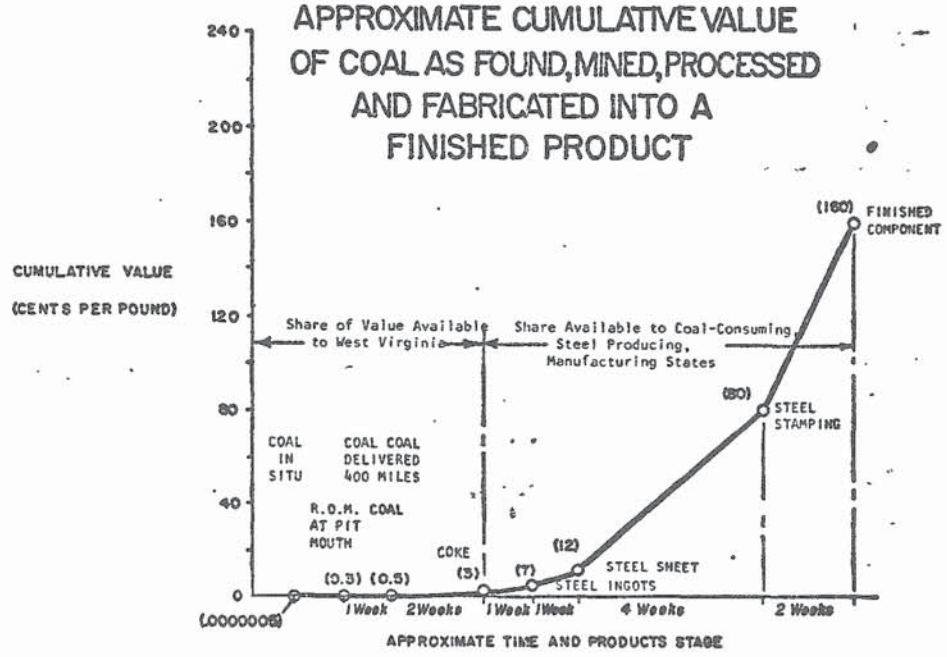
<u>Mineral resources are capital assets and the wealth produced by mining them should be considered capital assets</u>. Any economic rents such as severance taxes or profits are included as potential wealth replacement to a region.

<u>These capital assets should not be expended for sustaining operations</u>. If a producing region is not to be exploited and left impoverished or if production is to be nurtured and enhanced for

longer periods of time, supporting facilities and cultural improvements should be provided and are proper replacements for the exploited mineral.

Value added in the extraction of minerals is miniscule alongside of the value added in products using the minerals. Figure 1 shows this concept graphically. The curve represents approximate values of one pound of coal from the time it is discovered in the earth to the time it is sold in the market place as a component of, say, an automobile. The in situ value of a pound of coal is very inexpensive but as a block of coal is developed for mining and as it is mined and coked it picks up value possibly up to 3¢ a pound, but the real value added in absolute terms occurs after the coke is converted to steel, shapes, stampings, and finally finished products. We see that the value of a pound of coal in an automobile is approximately 160¢. You will note that a producing region such as West Virginia has access to the lowest value-adding portion of this curve on the left side of the chart, while coal consuming and manufacturing states enjoy much greater value adding on the right side of Figure 1. This leads then to the following three statements. The economic rents available to a coal producing region are miniscule compared to regions having other sectors of commerce.

FIGURE 1



If the value added in a particular sector of commerce is small, then the economic rents based on the value is also likely to be small.

And a producing region benefits less from its own resources than do consuming regions. Indeed, the value to a manufacturer having a guaranteed source of raw materials, i.e., minerals, is greater than the actual cost paid for those minerals. It is, therefore, understandable that the residents of a producing region are resistant to outside demands for the mineral if the prices received for it does not adequately cover the region's social and environmental costs plus a share in the total value added.

The next group of statements pertain to the federal mineral concerns.

The federal government has access to economic rents from the heavily value-adding sectors which use minerals.

The total manufacturing industry of the United States draws on the raw products such as coal from producing states like West Virginia. Wherever these manufacturing sectors of commerce exist in the United States, they are subject to federal taxation and the economic rents obtainable from these sectors of commerce are large since the value added in these other sectors is large.

The federal government has a responsibility in assuring that there are adequate future sources of minerals. In former years, nations secured mineral resources by colonizing producing areas of the world. With colonialism now obsolete, nations must pay more attention to internal sources as well as to obtaining sources through international politics.

The viability of a reliable minerals source is a function of the health of the producing region. Therefore, the federal government should have a special concern for the conditions of internal producing regions.

Now the following statements pertain to research and development activities.

Research competence follows money. It has been said as a way of rationalizing the particular support for various research projects favoring a few geographic areas that the scientific and technical competence exists in this location or that location. My thesis says that if the working conditions and the money are made available, good research people will move anywhere.

A typical success rate for R&D projects is about 10%. This means that nine projects in ten are not successful. Thus, the only payoff for the nine unsuccessful projects is in trained manpower, provided that persons trained can be retained organizationally to work in related projects.

R&D projects sponsored by governments become public information and not proprietary to a region. Thus, research that is sponsored by a state should be considered available to other states.

Small research budgets cannot compete with massive research budgets. By this we mean that a state like West Virginia cannot possibly support research efforts in the mainstream of federally supported projects and expect to make an impact.

Problem solving is best performed where the problems are. This statement, of course, gives recognition to the fact that the best transfer of technology is by people, and that people who work in the locations of problems tend to become problem solvers there, instead of elsewhere where they would not be exposed to those problems.

University research is most useful if it relates directly to education. Again this reflects that the problem is first one of manpower and second one of finding specific results to a problem.

The next set of statements pertain to the priorities that states should follow in allocating economic rents that they can collect.

1) The first priority is for producing states to invest in capital facilities in the particular producing county and these facilities should be first in direct support of mineral production and then in support of public conveniences. This is simply good horse sense--just as the wise farmer puts his first money into his barn and his second money into his home. 2) At the state level states should invest in capital facilities in support of the production of coal and minerals, and 3) States should invest in non-tangible assets such as manpower development and certain highly specific research usable in the mineral industries of the state.

For all the foregoing statements we would like then to draw some conclusions:

Coal producing states should monitor and secure for their mineral industries an adequate return which will pay all costs plus wealth replacement for the mineral extracted and capital generation. In this effort the producing states should pay particular attention to the political sub unit of the state where the production originates.

The federal government should support the coal producing states to maintain their economic and social health.

The federal government should assume the major responsibility for research over the broad spectrum from mineral production to mineral utilization and conservation.

This is what ERDA is doing for coal and other sources of energy and it delights us greatly to cooperate in this effort that ERDA is addressing as in this symposium today. We are appreciative of the new look being established at MERC and we look forward to many fruitful interactions.

The 1976 ERDA In Situ Coal Gasification Program

by

P. R. Wieber, ~~Acting Branch Chief~~
A. P. Sikri, ~~Chemical Engineer~~
In Situ Coal Gasification Branch
ERDA HQ, Washington, D. C.

ABSTRACT

This paper presents the status and plans of the ERDA in situ coal conversion program. Management, planning and overall technical direction are emphasized.

The history of underground coal gasification up to the formation of ERDA is briefly outlined. The pre-1970 programs in the Soviet Union, Great Britain and the United States are reviewed. In the 1970's, interest in underground gasification revived. Field projects at the Morgantown and Laramie Energy Research Centers were started by the Bureau of Mines and at the Lawrence Livermore Laboratory by the Atomic Energy Commission. These were combined under ERDA as the core of the present program.

The relationship of the in situ coal conversion program within the ERDA structure and goals is explained. The Underground Coal Gasification Branch is in the Division of Oil, Gas, and Shale Technology (OGST), one of five Fossil Energy Divisions. The in situ coal program is administered by the Branch, and the program objective is to develop commercially feasible processes for reacting coal in place to produce energy and fuels. Much of the present program is carried out by the ERDA field centers. The Branch intends to coordinate and execute the program by building a management team comprised of Headquarters, Operations Offices, and Energy Research Centers and National Laboratory personnel. The respective roles of the team members are outlined.

The various elements which affect the program strategy are presented and discussed. These elements include resources, product options and markets, expected economics, environmental impacts, technical options, and development paths to commercialization. All these elements are controlled by the constraints that in situ coal processing is a field-located operation. Commercial feasibility may not only require process scale-up, but also proof that the processes are applicable to a number of sites with similar coal resources.

The 1976 program status is reviewed. The major field projects are Linked Vertical Wells (LERC), Packed Bed (LLL), and Longwall Generator (MERC). Sandia Laboratories is providing instrumentation support to LERC. The program includes supporting research, and there are also university projects funded by Fossil Energy Research and some environmental studies funded cooperatively, by Environment and Safety. The Fiscal Year 1977 planned program is outlined. Steeply Dipping Beds will be added as a fourth major field project. Anticipated program activities and proposed funding for FY 1978 and beyond are presented.

1. INTRODUCTION

In situ coal conversion can be defined as the production of fuels and energy from coal in place. This form of processing is being developed as an option to meet the energy needs of the nation by the Energy Research and Development Administration (ERDA). This paper briefly reviews the history of

underground conversion, then concentrates on the management, proposed strategy, and plans by which the ERDA program intends to carry in situ coal processes to commercial feasibility.

The ERDA In Situ Coal Conversion (ISCC) program has the following near-term objectives: To develop and demonstrate a commercial technology for converting coal in place into low and medium Btu gas. To support the transfer of this technology into the commercial industrial sector through cooperative programs with industry. To explore advanced concepts for producing a wider products range from a variety of coal resources [1].

The ISCC program must deal with a unique set of problems compared to other coal programs in ERDA. Since the resource must be used in place with minimal modification, the process must deal with the geology of the coal and of its surroundings. Thus, the process design will be a function of coal rank, thickness, depth, dip, mineral content and wetness, and also of the structure, strength and hydrology of the over- and underburden. The major process problem is developing and proving reliable control of the underground reaction zone, so that product quality and production rate can be maintained while using as much of the coal in the seam as possible.

The past work in ISCC has shown that the production of low Btu gas with air as the gasifying reactant is technically feasible ([2] and [3], for example), and it remains to demonstrate the economics and reliability of these processes for commercialization. But there is also evidence that steam/oxygen in situ gasification giving a medium Btu gas is also feasible [4]. There are many other in situ processes which can be explored such as liquefaction, chemical comminution, recovery of energy from coal in abandoned mines, and cyclic processes. A variety of techniques need to be developed and tested to improve process efficiency. The proposed program intends to fill these needs.

ISCC carries a higher risk than processes which are entirely surface-based and can thus be carefully controlled. These risks make industry cautious about investing their R&D dollars. But the promise is also great, including lower capital investment, lower product selling price, and less adverse environmental impact compared to mining plus surface processing. In addition, commercial in situ processes could easily triple the U. S. coal reserves. These characteristics make the ISCC program especially suitable for a cooperative program of development with industry.

2. HISTORY

Origin

The idea of in situ coal gasification is not new. It was first suggested by Siemens [5] in 1868 for the gasification of waste oil and of slack. In 1888, Mendeleev [6], a Russian chemist, suggested the true underground gasification of coal. In 1909, a patent on this subject was granted to an American, Anson G. Betts [7]. He proposed a method of gasifying coal in the bed by igniting the base of one or more shafts or boreholes, supplying it with air and steam, and withdrawing the gas formed through the boreholes. In 1912, Ramsey began the first experimental work in retorting coal underground at Durham, Great Britain, but was unable to complete it due to outbreak of World War I.

Soviet Work

In 1913, Lenin talked about underground coal gasification to improve the working conditions of Soviet mine workers. In 1933, he recommended that the Soviet Union initiate experimental work to get the miners out of the mines. The work was interrupted in 1941 by World War II, but resumed in 1945, and went into industrial use in the 1950's. From 1933 to 1939, three distinct methods of underground coal gasification were developed. Considerable success was claimed and at least one method was tried on an industrial scale. Nusinov [8] has published an account of the work during this period. Status of much of the Soviet work through 1958, has been summarized in a Belgian article by Crombrugghe [9]. Among the methods studied in the Russian work were the: Chambers method; Borehole-Producer method; Stream method; Percolation or filtration method. The details of these methods are described by Elder [10].

In 1955, annual gas production at the Moscow region plant [11] had reached 16 billion cubic feet ($4.5 \times 10^9 m^3$). This gas could operate a 15 megawatt electric generating station on the basis that 10,000 Btu ($10.6 \times 10^6 J$) is required to generate one kilowatt-hour of electrical energy. During the same year, operations at Yuzhno-Abinsk were started in a 20 foot (6 meter) thick, steeply dipping (about 75°) bituminous coal bed. The Soviets experienced relatively problem-free start up and operation. The facility produced about 40 million standard cubic feet per day ($1.1 \times 10^6 m^3$/day) of 120 Btu per cubic foot ($4.5 \times 10^6 J/m^3$) gas.

References at end of paper

The Soviet work has included: gasification of high moisture lignite, high volatile bituminous, and semi-anthracite coal; enhancement of natural permeability; mined underground galleries; directional drilling through predetermined curved paths; and oxygen enriched air. Although detailed Soviet data since 1965 have been limited, this work is still underway in three sites, two in nearly level coal beds and one in a steeply dipping bed.

British and European Work

During the late 1940's work was performed in Belgium, Italy, Poland, Czechoslovakia, Morocco and Great Britain [12]. The British experiments involved nearly level coal beds in fairly thin seams (about 3 feet thick). The major British project at Newman Spinney used an array of horizontal boreholes and a mined gallery (borehole producer method). It produced very low quality gas (about 60 Btu/scf or 2 X $10^6 J/m^3$), but had large recovery of coal (87%).

United States Work

In 1946, the work in the United States was undertaken largely by the Bureau of Mines at a site near Gorgas, Alabama [13]. The high volatile bituminous coal bed at Gorgas was nearly level and under three feet thick. High gas loss was a major problem at Gorgas. This work focused on areas showing short range attractiveness that could be accomodated by limited budgets, and it ended in 1959.

In 1968, Gulf Research and Development Company conducted an in situ coal experiment [14]. The product gas was relatively high in heating value (270 Btu/scf or 10 X $10^6 J/m^3$). The coal bed was excavated to allow a first hand examination of the reacted coal bed. The test was actually a pyrolysis experiment and Gulf was also interested in the resultant coke.

In 1971, the results of a state-of-the-art appraisal for the Bureau of Mines by Arther D. Little, Inc. stimulated a decision to reinstitute experimental work in the United States [15]. Field experiments at the Bureau of Mines Center at Laramie, Wyoming were authorized in 1972 and started in early 1973. This work used linkages between vertical boreholes in a 30 foot thick Western subbituminous coal seam at a site near Hanna. The Bureau of Mines Center here at Morgantown, now called the Morgantown Energy Research Center (MERC), proposed their concept in 1972 for using directional drilling in thin Eastern coal seams.

The idea for the rubblized deep bed or packed bed concept from the Atomic Energy Commission's Lawrence Livermore Laboratory (LLL) was proposed in 1972, and a site evaluation and laboratory effort was started officially in 1974. This method involves explosive fracturing of the coal underground followed by steam/oxygen gasification in a vertical direction.

On October 11, 1974, the President signed the Energy Reorganization Act of 1974 to law. One effect of this act was the incorporation of the Department of Interior's Office of Coal Research, non-regulatory activities of the Atomic Energy Commission, and certain energy projects of the National Science Foundation, the Bureau of Mines, and the Environmental Protection Agency. ERDA has been given a broad charter to develop new and improved energy sources and utilization technologies consistent with sound environmental and safety practices. The Laramie, Morgantown, and Livermore major projects were transferred to this new agency under the fossil energy program.

In the private sector, the Texas Utility Service, Inc. (TUSI) has started an underground coal gasification project to produce low Btu gas from lignite beds in East Texas at a depth of over 200 feet (60 meters). Soviet technology will be used based on a licensing agreement between TUSI and V/O Licensintorg of Moscow. The pilot operation is expected to start around late 1977. The low Btu gas will be utilized in TUSI boilers to generate steam and power. The detailed geologic and hydrologic mapping was to begin June 1975, and hearings by the Texas Water Quality Control Board took place recently.

3. PROGRAM MANAGEMENT

The in situ gasification program is administered and managed by ERDA Headquarters, assisted by the Operations offices and Field Laboratories. Specific projects are managed and executed by the ERDA "in-house" Energy Research Centers and the National Laboratories and through industrial contracts.

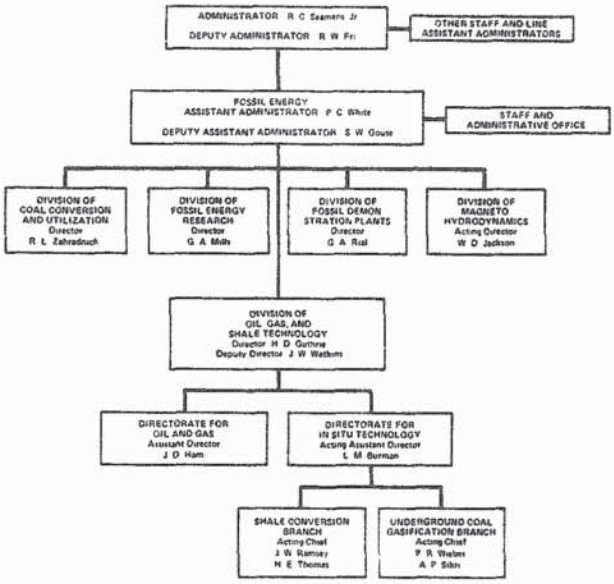


Figure 3-1 Headquarters Organization Relevant to Underground Coal Gasification

ERDA Headquarters Organization

The relevant organization in ERDA Headquarters is shown in Figure 3-1. The ERDA management structure is hierarchial by function. All ERDA programs are under the Administrator, Dr. Robert C. Seamans, Jr. The Assistant Administrator for Fossil Energy, Dr. Philip C. White and his Deputy, Dr. S. William Gouse, Jr. are responsible for the fossil fuels programs.

Coal programs are found in all five line Divisions in Fossil Energy. Fossil Energy Research funds basic and applied research that supports the major missions. Coal Conversion and Utilization carries out coal process development through the pilot plant stage, and Fossil Demonstration Plants funds demonstration-scale projects. The Division of Magnetohydrodynamics handles that speciality, again through the pilot stage. The Division of Oil, Gas, and Shale Technology is responsible for advanced techniques for oil and gas recovery, oil shale, and in situ coal conversion. Field demonstrations for oil and gas recovery do not involve large surface plants and hence are funded through the Division.

The Underground Coal Gasification Branch is contained within the Division of Oil, Gas, and Shale Technology because, 1) the processes are field oriented like petroleum recovery, rather than chemical-process plant design, 2) the methods and problems of fire-flooding of oil deposits and tar sands and in situ production from oil-shale retorting are similar to those of in situ coal processing, and 3) as with petroleum and other in situ technology, process development toward the commercialization of in situ coal conversion requires both production scale-up and verification of process performance at a number of similar sites. The Underground Coal Gasification Branch funds all of the in situ coal conversion work excepting university projects funded by Fossil Energy Research. Coal Conversion and Utilization is developing turbine and hot gas cleanup systems for low Btu gas from surface-based gasification processes. Most of their results should be directly applicable to in situ gasification. Thus the in situ coal conversion program is free to concentrate its resources on problems uniquely associated with underground processing.

Program Execution

The in situ coal conversion program is executed by the in-house Energy Research Centers and National Laboratories and through contracts with industry. Management and administration of the program is assisted by the ERDA Operations Offices at Albuquerque, Oak Ridge, Chicago and especially San Francisco.

The primary in-house laboratories are the Laramie and Morgantown Energy Research Centers and the Lawrence Livermore and Sandia (Albuquerque) National Laboratories. These facilities are involved in major field tests of process concepts. Sandia is also the primary in-house developer of instrumentation and process control methods. Supporting research is being done at the Oak Ridge and Argonne National Laboratories.

Industrial participation in the program has been minimal. This is due in part to the historical approach of the Bureau of Mines and the Atomic Energy Commission toward developing underground coal gasification. The ERDA program was formed using projects from those Agencies. Increased industrial involvement will be sought in future years.

Management Team Development

In situ technology has a broad base of activity. It incorporates a variety of processes being field tested in major coal resources at several geographic sites. The technical program activities range from engineering science, through drilling and geology, to equipment design and measurements technology. Environmental impacts, socioeconomic impacts, and supply-transportation-market relationships are complex. It is thus necessary to utilize all available resources within the ERDA system to carry out the program effectively.

A management team concept is being developed by the Underground Coal Gasification Branch to meet the program needs. The first stage of this process was the formulation of in-house working group which meets every six months to discuss the part progress and future plans in specific technical areas. Technical areas are: Geology, Site Preparation and Field Testing; Modeling and Laboratory Experimentation; Instrumentation and Process Control; and Environment and Safety.

The Working Groups serve several functions. They provide the field performers with an opportunity for an up-to-date exchange of experience in the specialties. They provide Headquarters with a program cross-cut of the status of the technical area, and hence assist program management. Finally, they provide a forum for a regular exchange of ideas, priorities, and concerns between the field and Headquarters.

As a second step in developing a management team, and pending Division approval, the Branch intends to institute a Management Working Group. This group will be comprised of a project leader from each of the primary in-house Laboratories and Operations Offices. The Management Working Group will meet on an ad hoc basis to discuss management issues such as advanced program plans, increasing industrial participation in the program, improving project team interactions, and so forth.

As a third part of management team development, and pending management approval, an active role for Operations Offices would be defined. Industrial interactions are the main business of the Operations Offices, and their increased participation will be most useful as more industry is brought into the program.

The duties of the three components of the Management Team are thus roughly seen as follows.
Headquarters: Carry out advance planning and budgeting, select and review projects, set project overall objectives and technical direction, and interact with Congress and ERDA top management. The ultimate authority for all projects resides in Headquarters.
Operations Offices: Carry our contracting actions, provide Technical Project Officers for some projects, provide technical and management coordination between industrial and in-house projects, interface with ERDA Regional Offices, and assist Headquarters in program formulation and planning.
In-house Laboratories: Provide the detailed technical planning, management and execution of in-house projects, propose new projects, assist in the technical management of industrial contracts as Technical Project Officers, and assist the Operations Offices and Headquarters in program formulation and planning.

This development of the Program Management Team is an ongoing process. Its ultimate goal is the best allocation of personnel resources within ERDA to implement the in situ coal conversion program.

4. PROGRAM STRATEGY

Resources

Coal resources can be classified into four catagories for in situ gasification. They are:

1. Beds with low dip (less than 45°)
   a. Beds less than 15 feet thick (4.6 meters);
   b. Beds between 15-50 feet thick (4.6-15 meters);
   c. Beds greater than 50 feet thick (15 meters);

2. Beds of all thicknesses and greater than 45° dip.

Total coal sources in the conterminous U. S. at depths of 6000 feet (1830 meters) or less are estimated to be 4,270 billion tons (Bt) [12] as updated from the U. S. Geological Survey of January 1, 1974. 2,350 Bt (55%) are in beds less than 15 feet thick; 1,230 Bt (29%) in beds 15-50 feet thick; and 550 Bt (13%) in beds greater than 50 feet thick, all with less than 45° dip. In addition, 110 Bt (3%) are in beds of all thicknesses dipping 45° or greater. The deposits in Alaska are estimated to be 270 Bt.

Only a portion of the coal resource would be suitable for in situ gasification. About 10% of all four categories would be strippable or too shallow to be of interest. About 50% of the thin and steeply dipping beds are either faulted or inaccessible. About 25% of the 15-50 foot and over 50 foot thick beds might be inaccessible for similar reasons. An estimated 50% of the remaining coal in all categories would be too deep. With these reductions, the coal available for in situ gasification in different categories is as shown in Table 4-1.

4-1 Categories of Coal Reserves and Amount Available for In Situ Gasification

Category	Total U. S. Resource 1974 USGS Estimate (billion tons)	Estimated Resource for In Situ Gasification* (billion tons)		
		Total	Eastern**	Western***
1. Low Dip (<45°)				
a) Thin beds, 5-50 feet (1.5-4.6 m)	2,350	530	220	310
b) Medium beds, 15-50 feet (4.6-15 m)	1,230	410	3	407
c) Thick beds, 50 feet (15 m)	550	190	0	190
2. Beds of all thicknesses >45° dip	110	25	2	23
Total estimated coal for In Situ Gasification		1,155	225	930

* Based on Reference 12
** Eastern coal comprised of Interior, Gulf, and Eastern provinces
*** Western coal comprised of Rocky Mountains, Northern Great Plains, and Pacific Coast provinces

It is evident that, based on conservative estimates we have an enormous resource of about 1,155 Bt of coal which is suitable for underground gasification, equivalent to 5,000 Quads of gas. Most of this coal is concentrated in the Western states of Wyoming, North Dakota, Montana, Colorado, New Mexico, Utah, Washington, and Arizona as shown in Table 4-1. This comes to 930 Bt, leaving 225 Bt for the Eastern states (Interior, Gulf, and Eastern provinces).

Table 4-2 shows a comparison of eastern and western coals. The energy needs in the eastern states are much larger than those in the western states, but the eastern coal has thin seams, low reactivity and permeability, high sulfur content, swelling characteristics, and surface land conflicts. Conversely, the Western coal is a very desirable coal for in situ gasification but has smaller local markets. Both resources are treated by the in situ coal program, with more emphasis on the western coals due to their relative ease of gasification.

Table 4-2 Comparison of Eastern and Western Coals

Characteristics	Eastern Coal	Western Coal
Thickness	Low	Low to Very High
Rank	Bituminous	Bituminous, Subbituminous, Lignite
Heating Value	High	High to Low
Relative Permeability	Low	High
Sulfur Content	High	Low
Reactivity	Low	Low to High
Water Availability	Generally High	Generally Low
Local Markets	High	Low
Swelling	High to Medium	Low to Zero
Availability of Transportation Systems	Generally Good	Depends on Product but Generally Poor
Socioeconomic Impacts	Minor	Major
Surface Land Conflicts	High	Low

Products

The products that can be derived from in situ gasification are:

1. Low Btu gas [up to 200 Btu per standard cubic feet (Btu/scf) or 7.5 X 10^6J/m^3];
2. Medium Btu gas [200-500 Btu/scf or (7.5-19) X 10^6J/m^3];
3. Methanol;
4. Chemical feedstocks.

The low Btu gas can be utilized on-site for electrical power generation or process heat. The medium Btu gas can be purified and upgraded to a substitute for natural gas which can be supplied to the national pipeline network. Methanol can be utilized as a fuel for automotives and as a boiler fuel.

Markets

Table 4-3 Product and Utilization

Product	Use	Transportation To Market
Low Btu Gas (<200 Btu/scf)	Electrical power Process heat Chemicals/fertilizer	Wired Local piping only Road and rail
Medium Btu Gas (200-500 Btu/scf)	Chemical Feedstock Process to synthetic natural gas	Road and rail Pipeline

Table 4-3 shows the utilization of the products and how they can be transported to the market areas. The markets for in situ gasification will depend a great deal on the national and local supply and demand levels of energy. ERDA estimates [16], that if no new initiatives are taken, the total U. S. energy consumption will increase at the average rate of 3.5% until 1985 and 3% thereafter. Total annual consumption is estimated to be 80 Quads (10^{15} Btu or 1.06 X 10^{18}J). This will increase to about 160 Quads by the year 2000. This increase in consumption will have to be partly supplied by synthetics from coal and shale.

Stanford Research Institute (SRI) [17] and Oak Ridge Institute for Energy Analysis at Oak Ridge [18] predicted the demand for synthetic gases from coal. SRI's approach was to predict the demand for synthetic gases from coal. SRI's approach was to predict the demand based on supply and demand

curves, for a product and its substitutes. The Oak Ridge projections extrapolate the product growth rate, the growth rate of competing products, and the growth of their principal uses. Figure 4-1 shows low and high projections for all types of synthetic coal gas by the two estimates. The large spread (3:1) between the high and the low estimates indicates the uncertainty in the projections. Figure 4-2 presents a breakdown by SRI of the projected demand for high and low Btu gas.

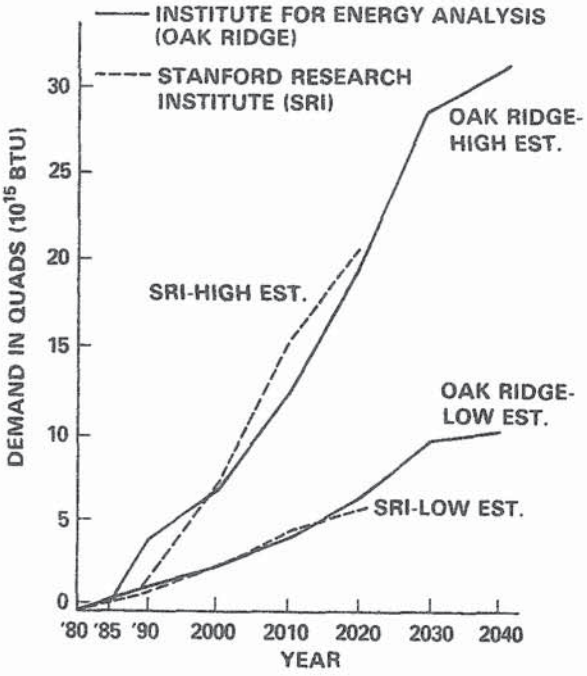


Figure 4-1 Projected Demand for Synthetic Gases from Coal [12]

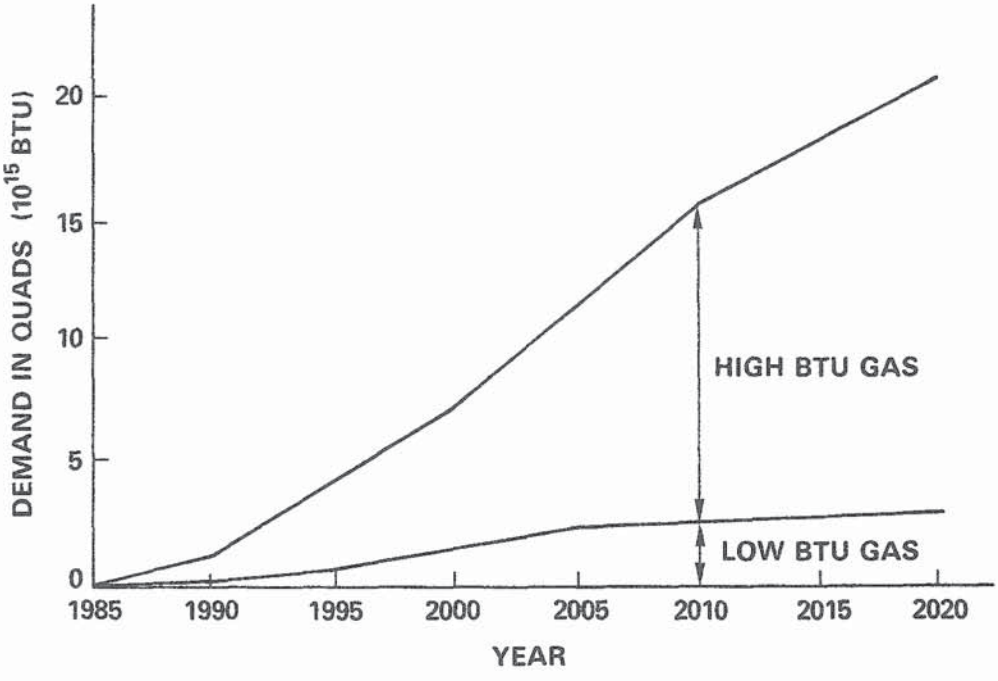


Figure 4-2 Stanford Research Institute High Projection For High and Low Btu Synthetic Gas From Coal [12]

Since the transport of low Btu gas (up to 200 Btu/scf or 7.5 X $10^6 J/m^3$) is uneconomical, the product must be used within a short distance of the site where it is being generated. Some of the uses for low Btu gas are electrical power generation and industrial heating to generate steam for a wide variety of industrial applications. In addition to these uses, there are other markets which have not been fully analyzed at this time. These are: residential-commercial heating (in 1952, a building containing eight apartments in the city of Tula, Russia was equipped to use such gas [19]), as a carrier gas for MHD [12], and as a fuel when mixed with powdered coal or atomized fuel oil. The market for electrical power generation will depend in part whether the combined-cycle operation fueled by in situ low Btu gas is competitive with direct coal firing. In areas near an in situ coal gasification process the market will depend upon the electricity demand within that local area. The national market has been studied by SRI and Oak Ridge and is very high regardless of which projection is considered.

Medium Btu gas [200-500 Btu/scf or (7.5-19) X $10^6 J/m^3$], can be generated by injecting oxygen and steam during gasification. This gas can replace low Btu gas with higher efficiency, or it can be purified and upgraded to a product containing over 90 mole percent methane. Since the supply of natural gas is diminishing and the cost of importing liquified natural gas is constantly increasing, the market for synthetic gas will be increasing. The high Btu gas can be transported by the extensive gas pipeline network in the continental United States. The current customers for residential, commercial, and industrial sectors should be able to use the product with no equipment modifications.

Methanol can be produced by the conversion of methane, carbon monoxide, hydrogen, and carbon dioxide from underground coal gasification. Methanol can be used as a fuel when mixed with gasoline (up to 15%) and as a boiler fuel for power generation and industrial heating. SRI's demand projections for power-turbine fuels show a buildup starting from 1985 to a steady level of 2.5 Quads by the year 2000. Higher market projections can be expected if methanol costs are lower.

Hydrogen produced during underground coal gasification can be marketed as a feedstock for the production of ammonia, urea and other chemicals. It can also be used as a feed for several oil-refining processes.

Economics

Table 4-4 Electric Power Price Estimates Using Low Btu Gas or Coal and 70% Base Loading

Process	Capital Cost $/Kilowatt	Price Mills per Kilowatt-Hour	Assumed Power Plant Efficiency %
Western In Situ, 900 MW	210	8.4	49
Western Conventional Power	300	8.9-11.1	37
Western Surface Low Btu/ Combined Cycle	350	17.2-20.9	34
Eastern In Situ, 265 MW	448	18.2	29
Eastern Conventional Power	360	12.7-14.3	35
Eastern Surface Low Btu/ Combined Cycle	375	20.5-23.0	34

Prices based on regulated utility with 65% debt at 9% interest, 15% return on equity and 48% tax rate. Conventional power plant assumed to have 28 years depreciable life, while low Btu combined cycle turbine plants have 10-year depreciable life. All costs (except Battelle) adjusted to first quarter 1975 (reference 12).

Table 4-4 shows the base load (70%) electric power price estimates using low Btu gas or coal [12]. These data are based on assuming a 65/35 debt-to-equity ratio, 28 year depreciation life, and the power plant efficiencies listed in the table. The efficiencies are questionable, and they make comparisons difficult. The power generated from in situ western coal is approximately the same as the power generated from the direct fired western coal. However, both of these processes produce power cheaper than by surface gasification of coal. If strip mining is restricted due to environmental reasons, the cost of mined coal would rise and make underground processing more favorable.

The economics of power generation from eastern coal are quite different from those of western coals. In this case the power generated by an underground process is more expensive than coal-fired power. This is due to high capital costs for the eastern in situ gasification plant. These costs are very dependent upon the ruggedness of local sites, and a general comparison may not be valid.

Two independent industrial cost analyses on high Btu gas from the Packed Bed in situ process have been reported. They are by Gulf Research and Development Company [20], and Amoco Production Company, Pacific Gas and Electric Company, and William Brothers Process Services [21]. Table 4-5 shows the comparison of these two studies in terms of total plant investment, working capital, and output price for underground and surface processes to produce 100 billion scf of high Btu gas (945 Btu/scf) per year. The study shows the following: the costs involved for the total plant investment and working capital are lower for the in situ process as compared with the El Paso Natural Gas (EPNG) costs; the gas selling price is highly dependent upon the efficiency of the in situ process design.

Table 4-5 Price Estimates for Coal Based High Btu Gas*

Evaluator	Total Plant Investment $MM	Working Capital $MM	Price $MM Btu**
1. Gulf R&D			
a) In Situ	435-470	8-10	$1.60-1.73
b) EPNG Lurgi	840	12	3.02
2. Amoco et al			
a) In Situ	570-640	23-62	1.85-4.49
b) EPNG Lurgi	855	33	2.85-4.35

* Mid-1975 dollars; 100 billion scf/yr. (945 Btu/scf) output

** The spread in gas costs is due to using optimistic and conservative designs with coal use efficiencies from 50 to 100%.

Environmental Impact

In situ coal gasification should be less severe in environmental impact than conventional coal mining. The mineral solids, otherwise appearing as wastes, remain underground. Also, the cost of surfact reclamation will be lower for underground gasification than for surface mining. Environmental problems can be caused directly by the gasification process such as water and air pollution, and subsidence.

The major environmental impact on the land can be possible erosion, temporary reduction in agricultural capability, and disruption of underground and surface formations. Immediate roof collapse or early subsidence could result in gas leakage to the surface through geologic faults. This can hopefully be avoided by siting in geologically sound areas at greater depths. The environmental impact on water could include the disruption of surface and underground water supplies and contamination of aquifers with chemicals and minerals released by the gasification zone. There is some laboratory evidence that the surrounding coal will partially cleanse the water from the reaction zone, and careful siting will help minimize impacts. This potential problem will be studied as part of the program. The product gas must be handled carefully to avoid leakage to the atmosphere. It is expected to contain praticulate matter, trace elements, tars, and harmful gaseous constituents 12 . If the untreated product gas is combusted, it might contain particulate matter, nitrogen and sulfur oxides, and unburned hydrocarbons. These problems should be similar to those for surface gasification processed and should be controllable by known technology. The socioeconomic effects in terms of number of operating personnel and their safety are poorly defined, but they should be less for underground coal gasification campared with surface processing of coal due to the expected smaller surface plants and need for fewer operators. There will be some safety problems associated with drilling, gas leakage, tar handling and surface plant operation but these can be handled with proper attention. One of the ways to insure minimal environmental impact will be to have a thorough analysis made of water, air, land, and living systems before, during and after each phase of test programs. A wide variety of instruments both downhole and at the surface, will be used to monitor a gamut of parameters to insure a thorough assessment of environmental impacts for the development of adequate controls. Table 4-6 shows a comparison of the environmental and safety problems as compared with mining and surface gasification. It shows that in situ gasification poses less severe problems with possible means for control. Low impacts must be assured to incorporate this type of processing into the nation's energy supply.

Technical Considerations

Two facets of in situ coal processing dominate the technical program. First, the process must be operated in a location where conditions which are imperfectly known. These uncertainties make process control a primary requirement for success. Second, the characteristics of the coal in situ and its surroundings vary with geographic location and must be accomodated by the process design. This can lead to different processes for different coal resources.

Table 4-6 Environment and Safety Compared to Mining Plus Surface Gasification

Parameter	Plus	Minus	Control
Water	Less need in process and lower quality	Surface and aquifer disruption and contamination	Site Selection; chemical neutralization
Air		Chemical and particulate emissions	Site to avoid faults; go deeper
Land Disruption	Less than strip mining; Cheap repairs and restoration	Unpredictable subsidence	Design process to control drop; go deeper
Socioeconomic	Potentially less people imported into region; Reduce mine safety problems	Increase drilling safety problems	Safety Procedures

Successful process control will give a gas of predictable heating value (quality) at differing operating conditions. The quality should be as high as possible. Gas leakage and seam water influx must be controlled. As much as possible the coal in the seam should be gasified in the reaction zone. Good process control requires a better understanding of the underground reaction-zone behavior. But it is impossible to completely simulate in situ conditions in the laboratory, and for this reason, will-instrumented field testing is the highest priority activity. Next is process modeling, the method by which the process design can be carried from site to site. Last, but certainly not unimportant, is laboratory experimentation supporting the modeling of the process.

A good process design positions the reaction zone as precisely as possible and also provides means for directional propagation of the reaction through the coal seam. There are two methods for controlling zone propagation. These are channel formation and field permeability control. Channel formation, using boreholes, gives the highest directional reliability but also the poorest positioning of the reaction zone if the gasification is moving along the axis of the borehole. Field permeability control by explosive fracturing gives poorer directional control, but as long as the packed bed is maintained without channeling, the gasification zone is relatively thin and well positioned.

As mentioned earlier, the process design must deal with a variety of in situ conditions. Some of the coal characteristics which affect the design are the coal rank, thickness, depth, angle of dip, water, and mineral content. The structure of the rocks above and below the coal affects gas losses, water infusion, and subsidence. The geographic location of the resources, transportation networks and markets specify the type of product from the process, such as low verses medium Btu gas. All of these factors demand attention in the process design and lead to alternate process concepts. Fortunately, some techniques are applicable to a number of coal resources so each process is not necessarily unique. The major process concepts and some of the advanced concepts for different resources are discussed in the Program Status and Plans section.

Instrumentation and environmental effects are very important program areas. The underground test will be of little value without adequate data to describe the process behavior. Unfortunately the current status of non-invasive instruments gives inadequate resolution or requires an interpretive model to transform the signal to the desired measurement. Downhole instrumentation can give the necessary resolution, but it is expensive to implant, it is usually lost in the test, and there is never enough of it. Improved invasive and surface-based non-invasive measurement techniques will benefit the program by eventually cutting test costs while improving data recovery. The ultimate benefit is better process control at lower costs for commercial processes. The potential environmental benefits to underground processing should be verified. The state environmental requirements for field testing, ERDA's internal review of environmental assessments, and process studies on emission-control technology assure that environmental R & D is intimately built into the process development. An environmental crosscut of all project research will be made to highlight this activity.

R & D Program Formulation

In Situ coal processing R & D has a number of unique features which can be exploited to accelerate process commercialization. The strategy presumes that the necessary gas cleanup, utilization in turbines and boilers, use as a chemical feedstock, or upgrading to synthetic natural gas, either

exists or is being developed elsewhere in the government and industry. Then delivery of a gas with suitable production characteristics over a sufficiently long time to verify process economics will demonstrate that the process is commercially feasible.

The unique ISCC program characteristics are:

1. Field tests of one module (the smallest pattern of wells which will be repeated) usually are relatively large scale but short term. For example, the Hanna No. 2 test gasified about 100 tons of coal per day and produced up to 12 million scf/day (340,000 m^3/day). This is equivalent to about 8 megawatts of electricity, but this phase of the test lasted only a few months.
2. The final field test below a pilot scale would generally gasify more than one module to study module interactions. This would produce even greater amounts of gas. Hanna No. 3 could produce 40-50 million scf/day (1-1.5 X $10^6 m^3$/day).
3. Scaleup to the equivalent of a pilot stage requires more modules to extend the time of maximum production. The extended tests will verify the needed process economic data. This multimodule large-scale test should also show the technical feasibility of components which are unique to in situ conditions.
4. Further scaleup to a "demonstration" adds even more modules and provides no new information to the underground process design. Likewise, it has been assumed that all additional surface processing and utilization of the gas is "off the shelf" and need not be tested further.
5. A process must be applicable to many sites with similar coal resources to be commercial. The applicability of an in situ process could be verified by conducting a relatively simple test at several sites as is done in advanced petroleum-recovery techniques.

The consequences of this analysis are clear. ISCC process development should need to be carried only through the multi-module large-scale test in conjunction with small-site applicability tests to verify commercial feasibility. This strategy will be tested during the next few years. If it is correct, the first commercial ISCC process could be ready before 1985.

5. PROGRAM STATUS AND PLANS

Present and Potential Projects

There are four major process concepts being developed within the ERDA program. These are the Linked Vertical Well, Packed Bed, Longwall Generator, and Steeply Dipping Bed concepts. The basic concepts are introduced in this section, and their current design will be the subject of many papers in this Symposium. Although a limited type of coal resource is inherent to each process, the real limits of each process have not yet been verified.

The Linked Vertical Well (LVW) process is shown in Figure 5-1. It is being developed by the Laramie Energy Research Center in subbituminous coal at a site near Hanna, Wyoming. Vertical wells are drilled into the coal seam and linked by reverse combustion to form permeable, hot char paths which are gasified by forward combustion. The figure illustrates an areal sweep test which was tried in the recent Hanna test. The LVW process applies to medium western seams, approximately 15-50 feet (4.6-15 meters) thick. Air gasification gives a low Btu gas for electrical power generation.

The Packed Bed (PB) process is seen in Figure 5-2. The process is being developed by the Lawrence Livermore Laboratory in subbituminous coal at a site near Gillette, Wyoming. Chemical explosives produce rubblized underground reactor which is gasified in a vertical fashion by steam and oxygen. The product will be a medium Btu gas suitable as a chemical feedstock or for upgrading by further surface processing to a synthetic natural gas. The process applies to very thick deep western seams greater than 50 feet (15 meters) thick.

The Longwall Generator (LG) process is shown in Figure 5-3. This concept is being developed in bituminous coal at a site near Pricetown, West Virginia by the Morgantown Energy Research Center. Boreholes are used because the eastern coals have very low permeability. Deviated wells are drilled to within the coal bed in long parallel rows. The coal between the rows is gasified with air to make a low Btu gas.

A concept for Steeply Dipping Beds (SDB) is illustrated in Figure 5-4. This project is in the planning stage and will be run by industry under a competitively procured contract. Boreholes are drilled through the coal and surrounding burden to the desired seam depth. These are linked across the coal strike, and the combustion zone moves up the seam. The Soviets have an SDB pilot plant. A list of advanced concepts and potential resource-oriented projects is given in Table 5-1. These items will be considered for inclusion in future program plans.

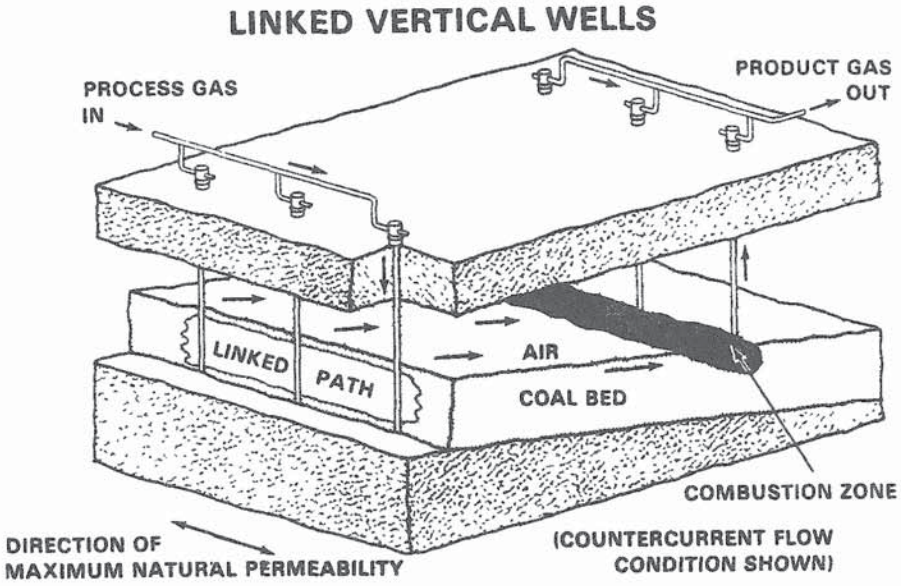


Figure 5-1 The Linked Vertical Well Concept

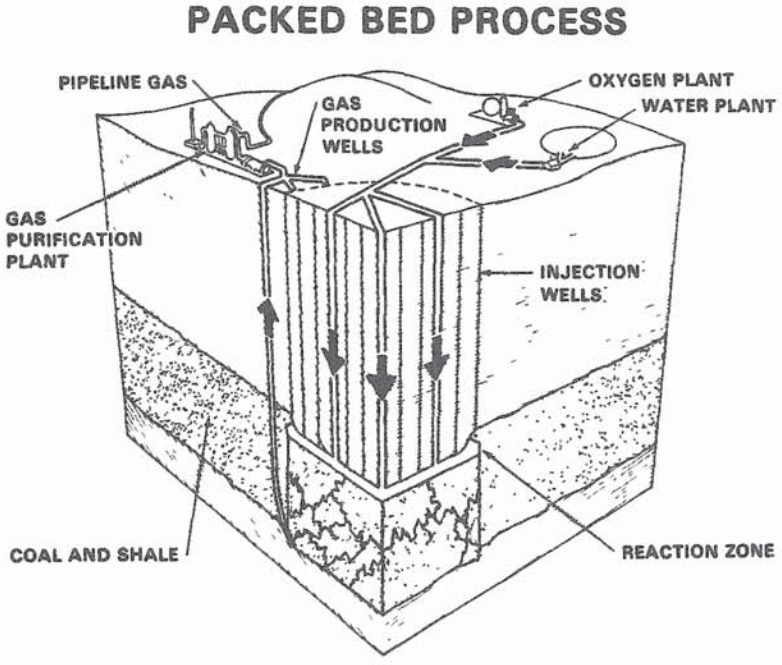


Figure 5-2 The Packed Bed Concept

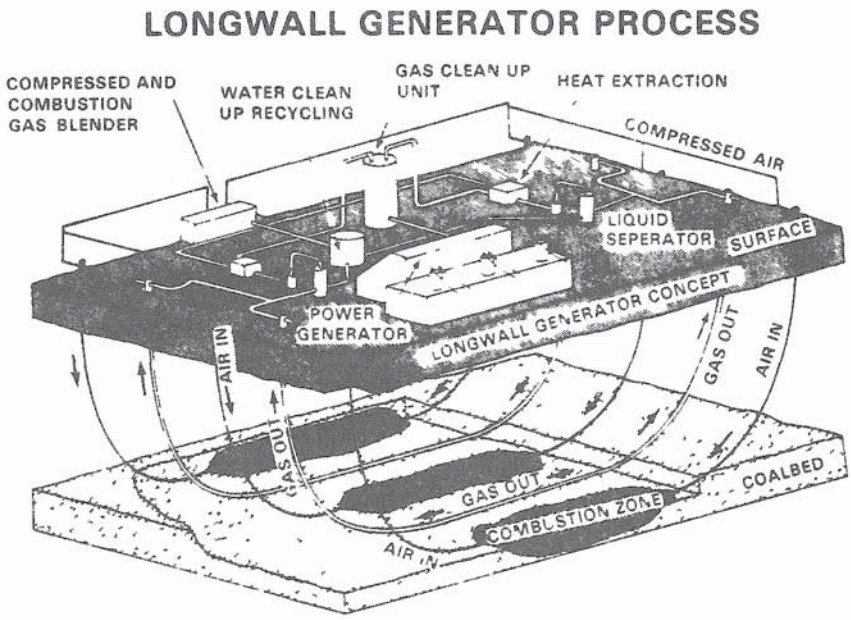


Figure 5-3 The Longwall Generator Concept

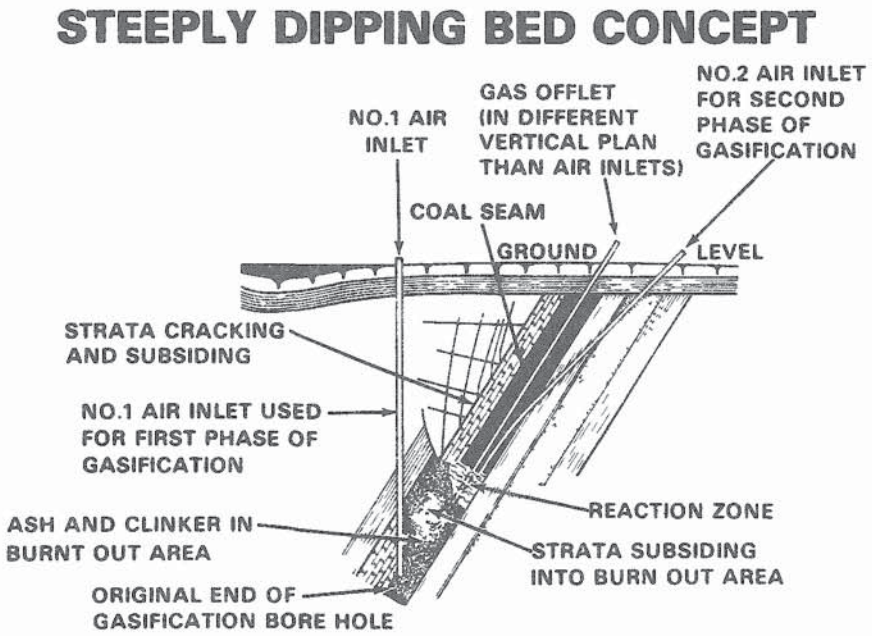


Figure 5-4 A Steeply Dipping Bed Concept

Table 5-1 Advanced Concepts and New Resource Objectives

Gasification in Semiarid Regions
Underground Mechanical Gasifiers
Liquefaction
Chemical Comminution
Gasification of Abandoned Coal Mines
Processes Using Partial Mining
Cyclic Processes
Combined Coal-Oil Shale and Coal-Oil Processes

Lignite Gasification
Multiple Seams with Non-Coal Breaks
Seams with High Mineral Matter (Dirty Seams)
Very Wet Seams
Very Thin Seams
Anthracite Gasification

Fiscal Year 1976 Highlights

Major advances in the program in fiscal year 1976 are highlighted here and will be discussed in detail in other papers at this Symposium

The LVW process development concluded a remarkable test at Hanna, producing gas with a heating value in the 170 to 180 Btu/scf (6.3-6.7 X $10^6 J/m^3$) range. Production went as high as 12 million scf per day (3.4 X $10^6 m^3$/day). Sandia Laboratories is using the Hanna site for instrumentation development and to support the Laramie Energy Research Center in data gathering and analysis. This was one of the best instrumented tests in the world. In addition, a measurement of gaseous particulates and trace emissions was made at intervals during the burn. This process is in the most advanced stages of development and will move toward a final major field test before scaleup.

A preliminary test of the PB process was started last fall with a two-spot explosive fracture. The resulting permeability enhancement appeared to be below expectations, but current field tests are providing more precise measurements of permeability distributions. Gasification with air will take place this fall. Two independent process analyses of the PB concept by the Resource Sciences Corporation with other industrial partners and by Gulf Research and Development were completed in late FY 1975 and FY 1976.

The LG concept relies on a capability of placing the deviated well in the coal seam. A 2,000-foot long (610 meters) long well was drilled into a six-foot (1.8 meter) thick seam at a depth of 850 feet (260 meters). The hole was turned almost horizontally and runs for about 500 feet (150 meters) inside the seam. The deviated well is being analyzed for further experimental options that would lead to a first gasification test.

The supporting research program is making progress in modeling, pyrolysis and char gasification under in situ conditions, and in the area of coal and rock mechanics. A variety of instrumentation techniques at the Hanna site was tested during the recent burn and their effectiveness is being evaluated. Plans for the SDB project have commenced.

Thus the first full program year under ERDA has been very productive. In particular, the Hanna 2 test should provide a big boost to in situ coal processing in the United States.

Fiscal Year 1977 and Beyond

A projected milestone chart for the program is shown in Figure 5-5, and the proposed budget backing this schedule is shown in Table 5-2. The budget numbers are projected and not approved beyond FY 1977.

Table 5-2 Proposed Budget for In Situ Coal Conversion
(in Million Dollars)

Fiscal Year	75	76	TQ	77 1/	78 1/	79 1/	80 1/	81 1/	82 1/
Authorization	6.5	6.2	1.7	8.2	30.0	49.0	56.0	64.0	68.0

1/ This is not an approved ERDA budget.

The LVW process development will run its last major field test in FY 1978 and FY 1979. A large scale multimodule feasibility test will be cost shared with industry. Testing should start in FY 1981 and should be completed in FY 1983. At the same time, small tests will be run at a number of different sites to verify process applicability. By the strategy outlined earlier, the process should be ready for commercialization at that time. The PB project will run a preliminary air gasification in FY 1977 (#1 on the figure). The first steam-oxygen test should occur in FY 1978 (#2). Two tests at a deep site (#3 and #4) in FY 1980 and 1981 would lead to a large scale multimodule project starting in FY 1981. The LG process will begin a series of three successively larger field tests through FY 1978 to 1980. A scaleup should occur in FY 1981.

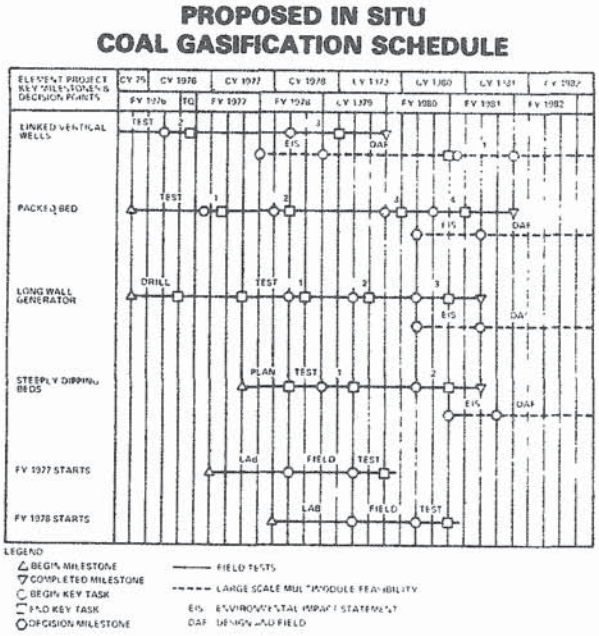


Figure 5-5 Proposed In Situ Coal Gasification Schedule

The FY 1976 program is heavily weighted toward in-house projects. We are planning increased opportunities for industrial participation starting in FY 1977 with an industry-run project on Steeply Dipping Beds. Proposals will be sought for an initial phase, followed by two tests in later fiscal years. Scaleup is anticipated in the early 1980's. Other possibilities are finding industrial partners to participate in the present in-house laboratories' projects.

Milestone lines are shown for FY 1977 and FY 1978 new starts. These starts will concentrate on laboratory and conceptual work, although the FY 1978 budget could permit some preliminary field work. The FY 1977 new starts are tentative. They could include starts on dry seams, lignite gasification and implanted mechanical-gasifier concepts. The FY 1978 new starts could include concepts for in situ liquefaction, recovery of coal energy from abandoned mines, and applications to very thin seams. In conclusion, the future plans will build upon past accomplishments to deliver commercial processes to use the vast coal resources in our Nation.

CONCLUDING REMARKS

The proposed budget is admittedly optimistic and was developed assuming that each new concept would carry through all scaleup phases. The totals, although large, are consistent with development costs of surface-based coal-conversion processes. If the strategy we propose is valid, several processes could be commercialized by 1985. We believe that the FY 1976 program accomplishments will attract the support of government and industry that is needed to move this program forward toward that goal.

REFERENCES

1. A National Plan for Energy Research, Development & Demonstration: Creating Energy Choices for the Future, Program Implementation , Vol. 2, ERDA 76-1, (1976)

2. Schrider, L. H. and Jennings, J. W.: An Underground Coal Gasification Experiment, Hanna, Wyoming, Soc. Pet. Eng., Paper No. SPE 4993, (1974)
3. Gregg, D. W., Hill, R. W., and Olness, D. U.: An Overview of the Soviet Effort in Underground Gasification of Coal, ERDA Lawrence Livermore Laboratory, UCRL-52004, (Jan., 1976)
4. Stephens, D. R.: Personal Communication, (July, 1976)
5. Siemen, W.: Transactions of Chemical Society, 21, 279 (1868)
6. Mendeleev, D. I.: Severney Vestnik (St. Petersburg), (1888) No. 8, Sect. 2, 27-73; No. 9, Sect. 2, 1-35; No 10, Sect. 2, 1-21; No. 11, Sect.2, 1-16; No. 12, Sect. 2, 1-26.
7. Betts, A. G.: Britain, Patent 21674 (1909)
8. Nusinov, G. O.: Underground Gasification of Coal, Moscow-Leningrad Gosstoptekhnisdat, Second Edition, (1941) 140
9. Crombrugghe, O.: Ann. Mines Belg., (1959) 478-534
10. Elder, J. L.: The Underground Gasification of Coal, Chemistry of Coal Utilization, Supplementry Vol., Lowry, H. H. (editor), (1963) 1023-1040
11. Kulish, F. D.: Podzemnaya Gazifikatsiya Uglei, (1957), No. 2, 27-31
12. Rupert, R. C., Choate, R. and others: Energy Extraction from Coal In Situ - A Five Year Plan, TRW Systems & Energy, Vol. 2 (1975)
13. Dowd, J. J., Elder, J. L., Capp, J. P. and Cohen, P.: Experiment in Underground Gasification of Coal, Gorgas, Alabama, R. I. 4164, (Aug., 1947)
14. Fair, J. C., Larson, O. A., Hasiba, H. H.: An Evaluation of In Situ Coal Gasification, Gulf Research and Development Company, Pittsburgh, Pennsylvania, (Nov., 1975)
15. Outlook for Research and Development in the Underground Gasification of Coal, Preliminary Report to Office of Research and Development Energy Policy and National Science Foundation, (Nov., 1975)
16. Creating Energy Choices for the Future, A National Plan for Energy Research and Development Administration, ERDA-48, Vol. 1, (1975)
17. Stanford Research Institute, Western Energy Resource Study, Economics, Data Review Package, (May, 1975)
18. The Institute for New Energy Analysis, The IEA Simulation Model, (Jan., 1975)
19. Gvozdev, A. P., Sokolov, V. V., and Shapito, M. I.: Utilization of Gas from Underground Gasification of Coal, Nanchn, T. R. Vses, Nanchn-Issled, Institute Podzemn, Gazifik, Uglei, No. 1, (1961) 102-106
20. Arscott, et al.: The LLL In Situ Coal Gasification Research Program in Perspective, A Joint GR&DC/LLL Report, (June, 1975)
21. Goddin, C. S., Hall, D. C., and Mason, R. Z.: Evaluation of the Lawrence Livermore Laboratory, In Situ Coal Gasification Concept, A Joint Report by Amoco Production Company., Pacific Gas and Electric Company, and William Brothers Process Services, Inc., (April, 1976)

FEASIBILITY OF IN-SITU COAL GASIFICATION IN THE WARRIOR COALFIELD: A PROGRESS REPORT[1]

by

George W. Douglas[2] and Wendell M. Beavers[3]

ABSTRACT

A two-year research effort is being conducted to determine the feasibility of in-situ gasification in the Warrior Coalfield of Alabama. This work is sponsored by the National Science Foundation. The Geological Survey of Alabama has located a preliminary test site on University of Alabama-owned coal lands and has begun geological studies of the area. A laboratory combustor has been constructed to investigate in-situ burning in cracks. Early tests show that forward burning in a swelling coal results in crack stoppage while reverse burning proceeds satisfactorily.

INTRODUCTION

This research project is being conducted as an investigation into the feasibility of underground coal gasification in the Warrior Coalfield and is sponsored by the National Science Foundation. The project as originally conceived is to be in two phases. Phase I, now in progress, is primarily a laboratory investigation into the techniques of in-situ gasification of coals typical to this coalfield. Some field work is being carried out by the Geological Survey of Alabama to support the laboratory investigations. Phase II is planned to follow Phase I and will be primarily field combustion tests using the results of Phase I.

The Warrior Coalfield of Alabama is the largest and most productive of the coalfields of the state and carries the largest reserves. In addition to the seams that are now being stripped or deep mined, there are numerous thin seams less than 36 inches (91 cm.) in thickness which cannot economically be recovered by conventional technology. Indirect mining techniques such as in-situ gasification could hold the key to economic use of this coal.

The coals of the Warrior Coalfield are of Pennsylvanian age and of high volatile bituminous and medium volatile bituminous rank. Table 1 shows analyses and certain properties of some Warrior field coals. The coals listed in this table were selected to include coals typical of the range of properties found in the field.

---

[1]Approved for publication by the State Geologist

[2]Associate Professor of Mechanical Engineering, University of Alabama

[3]Geological Survey of Alabama, P.O. Drawer O, University, Alabama 35486

Coalbed	Proximate Analysis				Ultimate Analysis						Petrography		GI	FSI
	M	VM	FC	A	C	H	O	N	S	Ash	Vitrain	Fusain		
Black Creek	2.6	36.4	57.1	3.9					1.5					3½
Black Creek	4.1	36.7	55.0	4.2	76.3	5.6	10.8	1.7	1.5	4.2		6.0	44	
Black Creek	4.0											6.3		1
Black Creek	3.1	36.0	58.3	2.6	79.2	5.7	9.7	1.7	1.1	2.6				
Black Creek	0.9	35.5	59.6	4.0					0.9	4.0		6.0		5½
Blue Creek	no data, area of interest													
Carter	2.8	33.7	58.1	5.4					1.2	5.4				4½
Corona	3.3	37.8	49.1	9.8	71.1	5.4	9.8	1.6	2.3	9.8			50	
Jagger	3.3	32.8	54.5	71.9	71.9	5.1	11.0	1.7	0.9	9.4			53	
Mary Lee	1.2	27.9	55.0	15.9	71.4	4.6	5.8	1.5	0.8	15.9	61.0	7.0		
Mary Lee		27.6	62.5	9.9							68.0	6.0	8	
Milldale	3.0	31.2	61.1	4.7	80.0	5.4	6.8	1.5	1.6	4.7			69	8
Milldale	1.8	32.5	56.8	8.9					1.2	8.9		7.0		7½
Pratt	1.5	35.5	52.9	10.1	74.1	5.2	6.8	1.5	2.3	10.1				
Pratt				7.9						7.9				7½
Pratt	1.3	31.4	65.0	2.3	83.6	5.4	6.5	1.7	0.6	2.3	51.0	5.0		
Pratt		30.5	66.5	3.0							77.2	6.8		7
Utley	1.1	25.9	64.6	8.4					2.1	8.4		3.3		9+
Utley	1.1	21.3	70.6	7.0					0.8	7.0		26.0		4½
Utley	1.2	25.6	69.6	3.6					1.1	3.6	63.0	6.4		9+

Table 1. Analyses of some Warrior Field coals

FIELD WORK

Introduction

Geologic investigations were undertaken in the vicinity of Adger, Alabama, to aid in the selection of a suitable test site and to provide data on any factors that may affect the experimental gasification process. A site was chosen in extreme southern Jefferson County approximately 2 miles (3.2 km) north of Adger in the Southwest 1/4 of Section 6, Township 19 South, Range 5 West (Fig. 1). This site lies near the southeastern limit of the Warrior Coalfield in the Valley and Ridge physiographic province of the southern Appalachian system.

The nature of the project dictated that a coal seam of sufficient thickness for the combustion process with approximately 250 feet (76 m) of overburden be accessible without road building. Existing subsurface information indicated that the potential site in Section 6 was underlain by the Gwin coal seam at a depth of just over 200 feet (61 m). Subsequent drilling at the site showed the Gwin seam to be present with 34 inches (86 cm) of coal and an overburden thickness of 260 feet (79m).

Upon selection of the site, a detailed geologic study was begun to determine the lithologic and structural nature of the coal-bearing formation and the thickness and extent of the Gwin seam.

Regional Geology

The subsurface of the Warrior Coalfield includes several groups of coal seams all of which occur in the Pottsville Formation, a widely occurring sequence of sandstones, siltstones, conglomerates, and shales deposited during Pennsylvanian time. The Gwin coal seam is situated in the Middle Pottsville (Fig. 2) and crops out in several locations within the area between Adger and Oak Grove, Alabama, (Fig. 3). The Gwin seam in this area dips slightly to the southeast toward the axis of the Blue Creek anticline.

Except for scattered deposits of recent stream alluvium, the Pottsville Formation is the only formation cropping out in the study area. The Pottsville sediments consist of sequences of very fine to medium grained, subangular to angular, poorly sorted, micaceous sandstones, muddy siltstones, conglomerates, and mudshales and clayshales.

Several coal groups occur in the Pottsville Formation with beds of various thicknesses (Fig. 2). The Gwin seam (34 inches (86 cm) of coal at the gasification site) varies in thickness over the study area. A coal isopach map was compiled from outcrop and subsurface data (Fig. 4).

Structural features in the study area are directly related to the Birmingham Anticline system, a distinctive northeast trending tectonic feature marking the end of the Appalachian Mountains in Alabama. The majority of postulated faults in the vicinity of the gasification site strike toward the northeast (Fig. 3). Jointing in the study area has also been shown to be greatly influenced by the anticline system and can be observed in practically all outcrops of competent rocks in the Pottsville Formation. Streams in the study area tend to follow dominant joint planes along parts of their paths. A Rose diagram, compiled from approximately 200 measurements, show the distribution of joint orientations in the area of the gasification site (Fig. 5). The majority of joints measured in the study area show a dip of 80 to 89° or are vertical.

Geology of the Experimental Site

The gasification site lies on a narrow ridge at a surface elevation of approximately 620 feet (189 m) (MSL). The study area occurs in the drainage area of Valley Creek which flows into the Black Warrior River. The immediate area of the test site is drained by Lick Branch and Johnson Branch into Valley Creek.

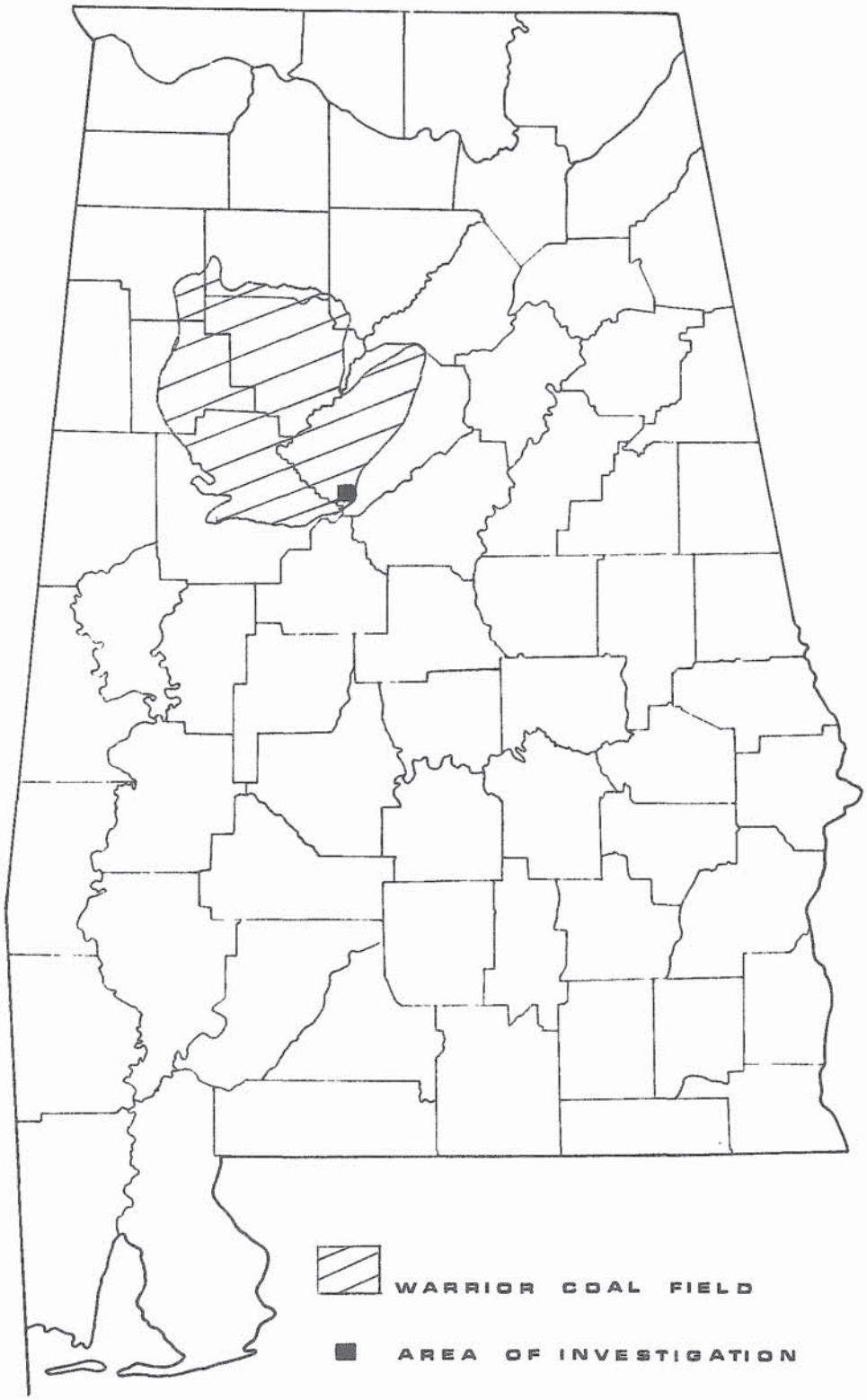


Figure 1.--Location of the experimental in-situ gasification study area with respect to the Warrior coal field in Alabama.

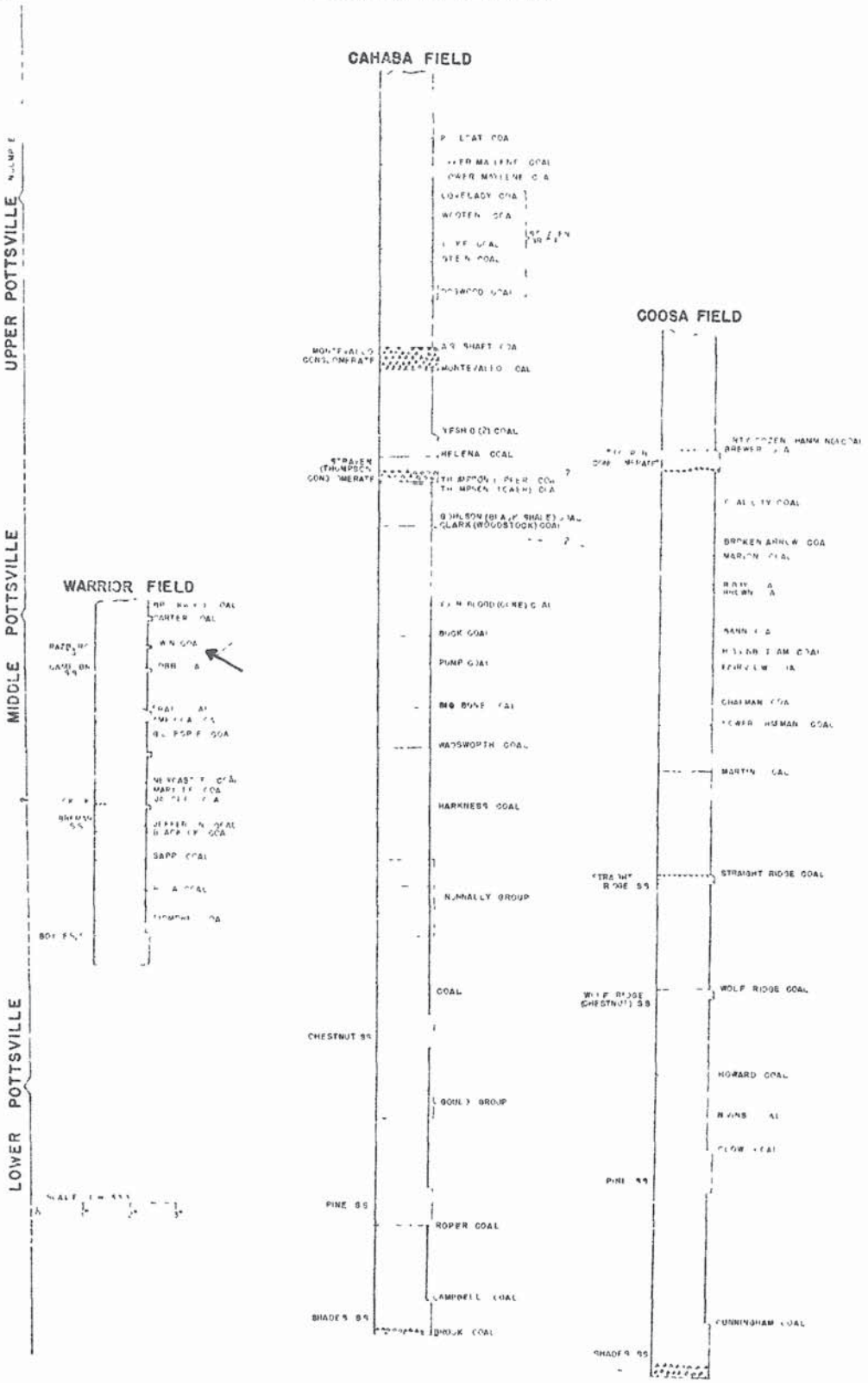


Figure 2.--Stratigraphic positions and correlations of coal groups in Alabama (after Shotts, 1960).

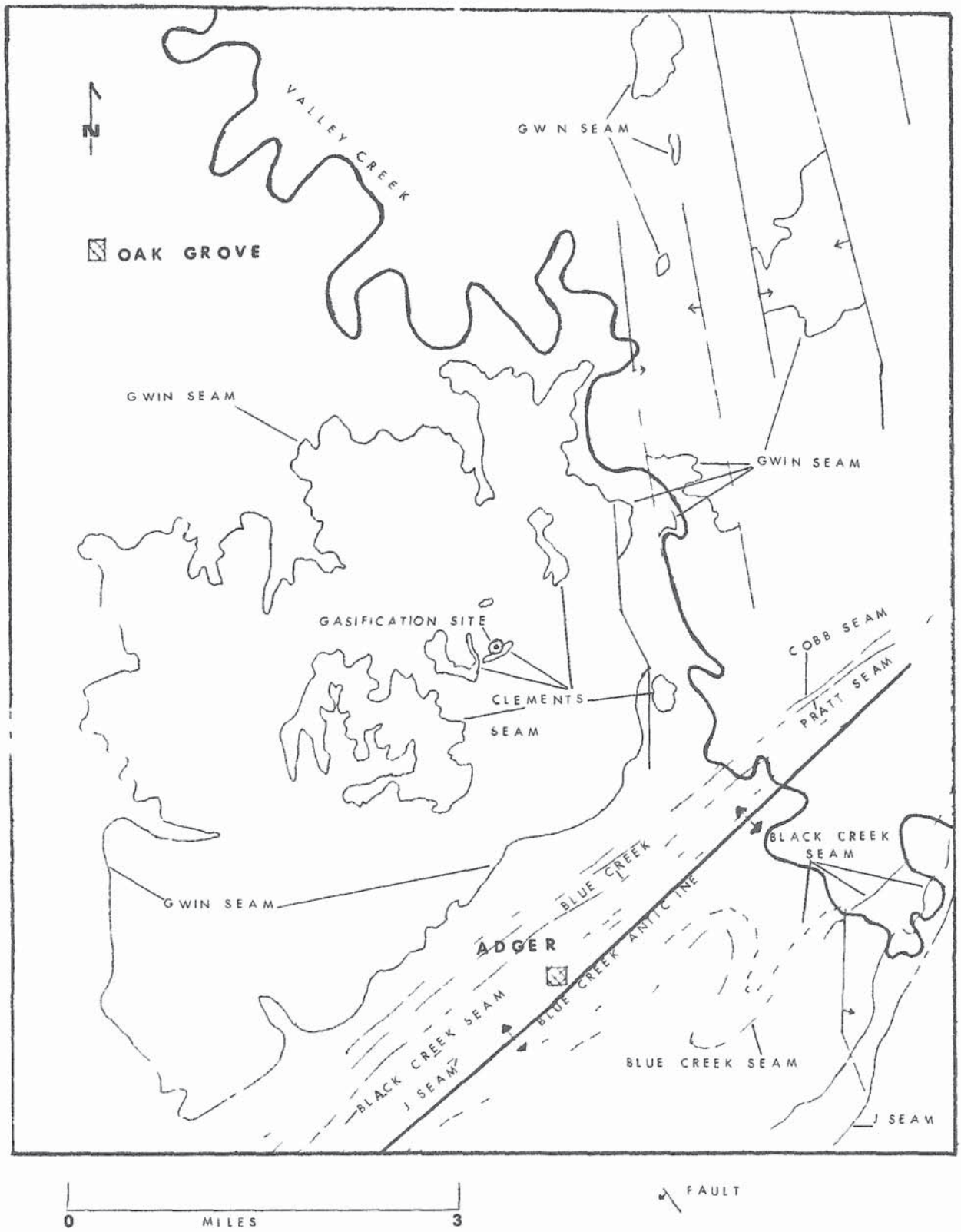


Figure 3.--Outcrop map of coal seams in area of in-situ gasification site.

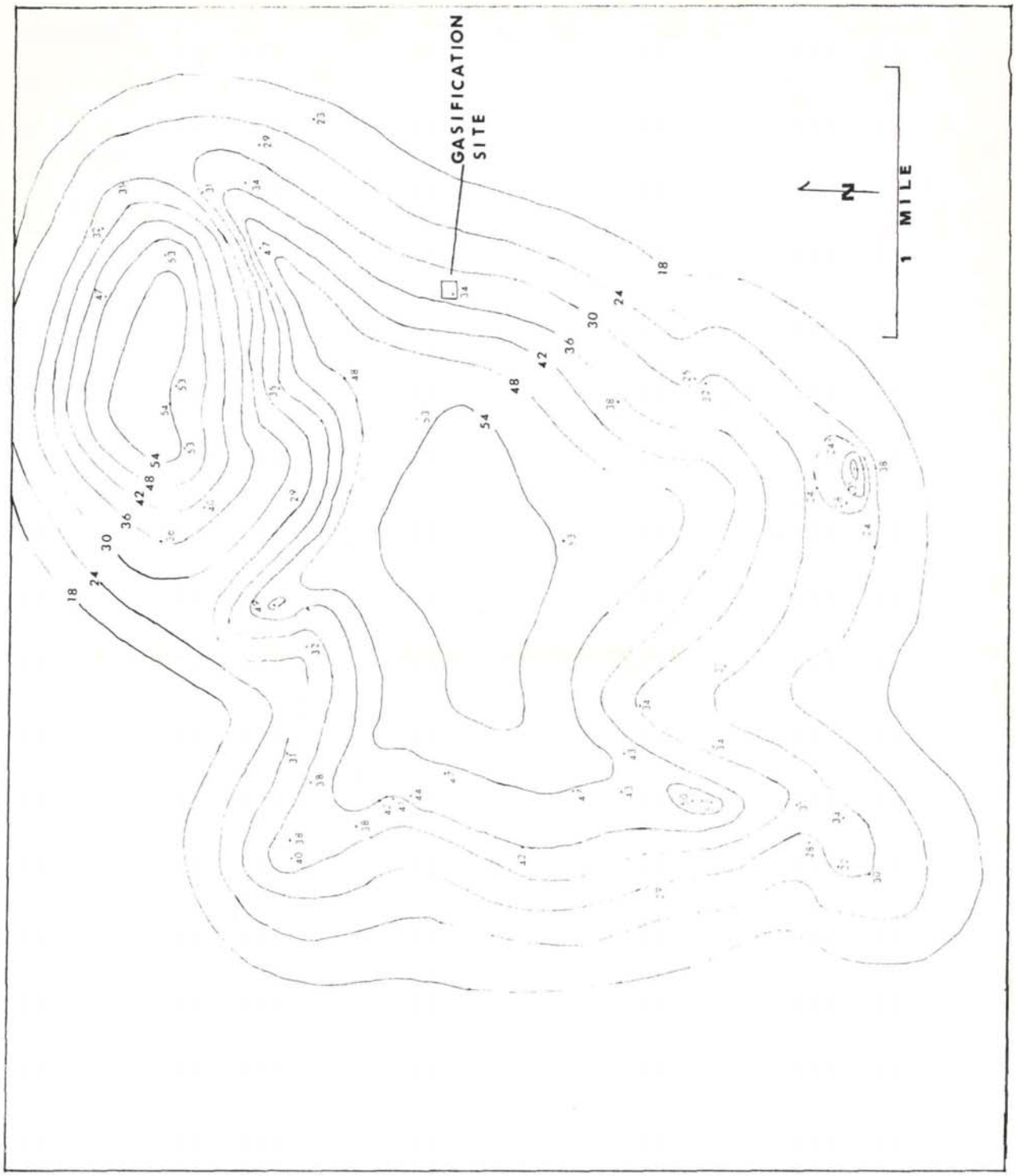


Figure 4.--Coal isopach map of the Gwin seam in study area.

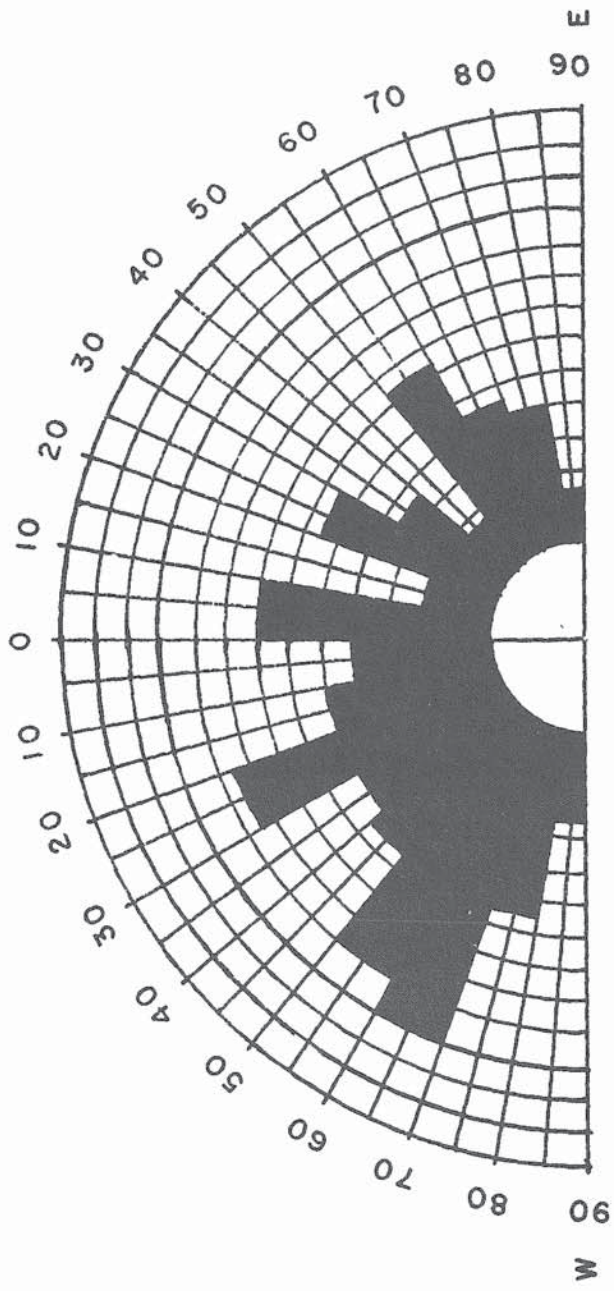


Figure 5.--Rose diagram showing dominant joint orientation in study area.

Immediately underlying the surface of the site is approximately 18 feet (5.5m) of surface mine spoil and weathered Pottsville sediments consisting of sand, clay, and gravel. At a depth of 20 feet (6 m), the Clements coal seam lies at an elevation of 600 feet (183 m). Figure 6, a lithologic log for In-Situ Gasification Core Hole 1-A, shows sediment types down to a depth of 284 feet (87 m). The Gwin seam occurs in Core Hole 1-A at a depth of 257 feet (78 m) or an elevation of approximately 365 feet (111 m). The Gwen seam at this position is several feet thick with layers and partings of clay shale.

Faulting in the vicinity of the site is probably limited to two faults 1 to 1.5 miles (1.6 to 2.4 km) east of the two core holes (Fig. 7). There may be another fault with a displacement of 80 to 100 feet (24 to 31 m) in the southeast corner of section 6 about 1/2 mile (0.8 km) from the site. If present, this fault could effect the experimental processes.

Jointing occurs in the Pottsville Formation over the entire Warrior Coalfield. Joint orientations were taken in two outcrops, one 100 yards (91 m) northwest of the site and the other 1 mile (1.6 km) northeast of the site (Table 2). These measurements demonstrate the variability of joint orientations near the gasification site.

Table 2.--Joint orientation at two outcrops near the gasification site

Location: NE¼SW¼ Sec. 32, T. 18 A., R. 5 W.				
N85E	N68E	N4E	N26W	N20W
N80E	N60E	N11W	N21W	N26W
Location: NE¼SW¼ Sec. 6, T. 19 S., R. 5 W.				
N25W	N31W	N20E	N3E	
N24W	N64W	N80E		

Conclusions

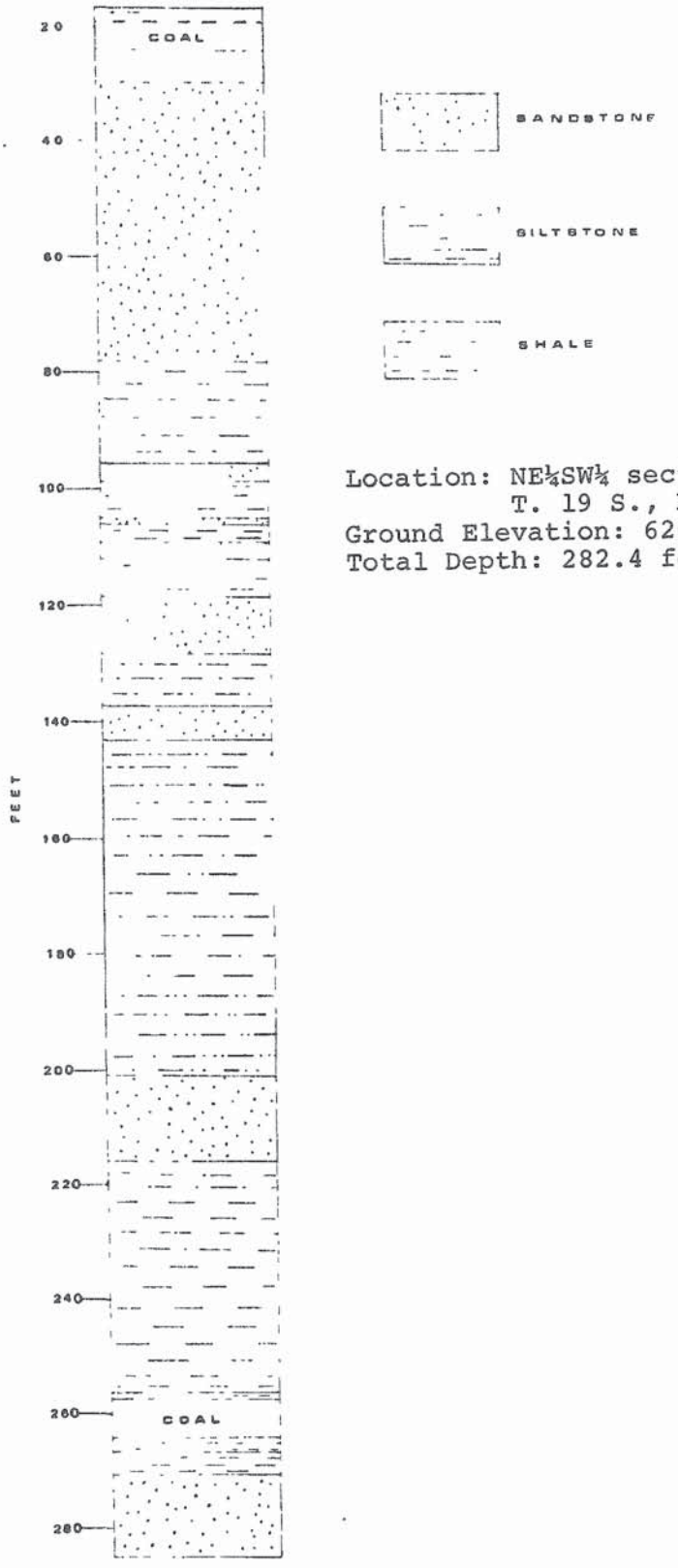
The site selected for in-situ gasification is located near the southeastern limit of the Warrior Coalfield. The Gwin seam, at a depth of 260 feet (79 m), will be the coal bed tested. The Gwin seam is overlain by a sequence of sandstones, siltstones, and shales typical of the Pottsville Formation. Subsurface data indicates the presence of two faults near the site with the possibility of a third fault in Section 6. The area has common jointing showing a relatively high variability in orientation.

LABORATORY STUDIES

In-situ gasification of thin seams of bituminous coal presents problems somewhat different from those associated with thick seams of lower ranked coals. Although field permeability tests have not yet been conducted on the test site, it is known that the bituminous seams of the Warrior Coalfield generally have extremely low permeability. Thus, some means of linking, probably hydraulic fracturing, will be necessary. Such fracturing methods produce large numbers of small cracks through which the air and combustion products can pass. Hence, the combustion zone can be expected to progress through relatively narrower cracks rather than across a broad front or through large diameter bore holes. The laboratory combustor which is described in the next section was designed to allow studies of crack burning.

Laboratory Combustor

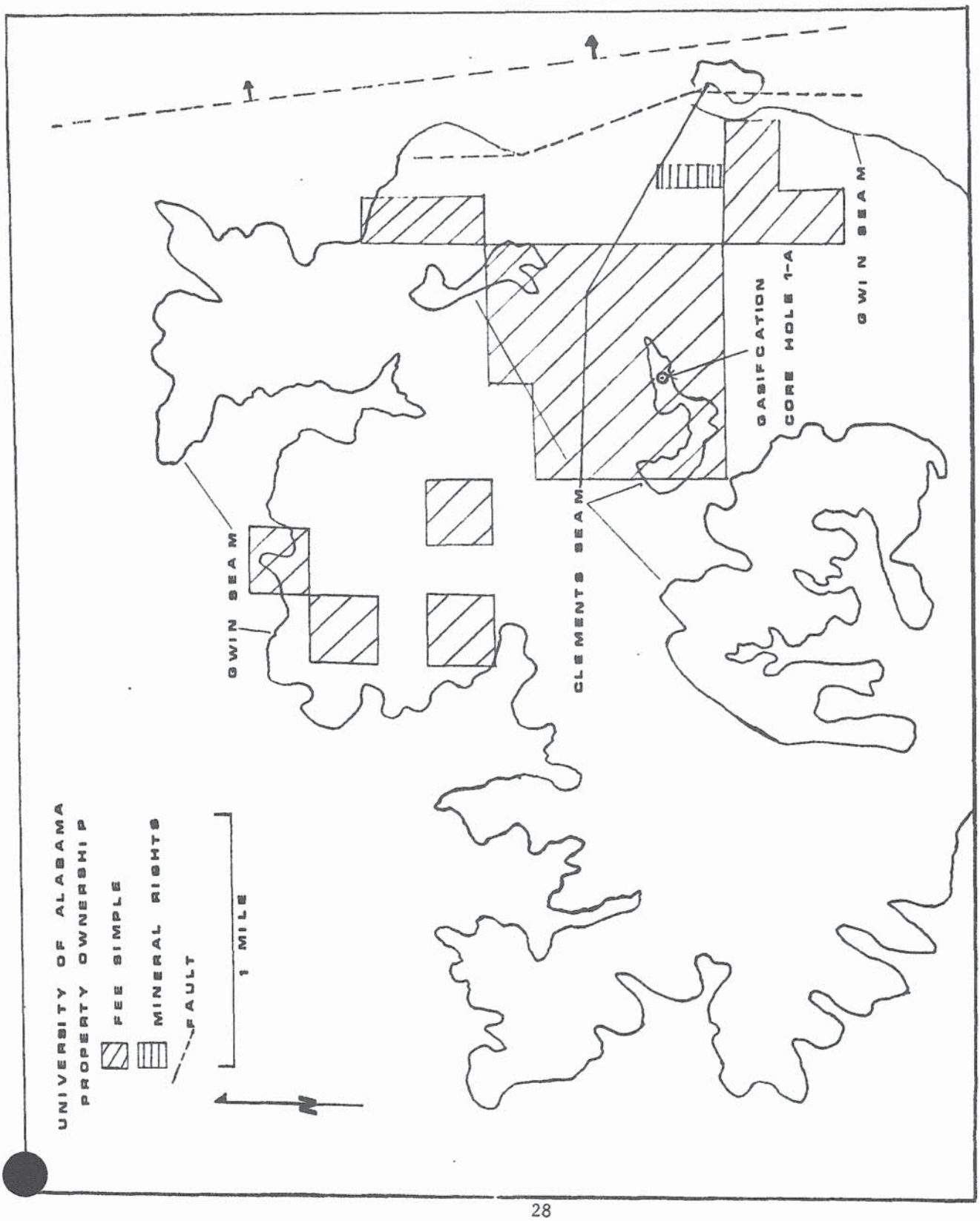
Two primary design considerations for the laboratory combustor are the ability to carefully arrange the coal samples within the combustor so that cracks of various sizes can be simulated and the need to study the sample in the combustor after a partial burn without destroying it. Further, instrumentation such as



Location: NE¼SW¼ section 6, T. 19 S., R. 5 W.
Ground Elevation: 620 feet
Total Depth: 282.4 feet

Figure 6.--Lithology present in In-Situ Gasification Core Hole 1-A at experimental gasification site.

Figure 7.--Map of coal outcrops, faulting, and property ownership in immediate vicinity of study area.



pressure probes, sampling tubes, and thermocouples must be capable of flexible placement in and around the sample. These requirements dictate that the combustor be accessible along one complete side as shown in Figure 8.

The combustor currently in use is constructed from 0.25 inch (0.64 cm.) steel plate and lined with fire brick. The result is a 7 by 7 inch (18 X 18 cm.) cross-sectional area for the coal sample and the combustor can accommodate a sample up to 24 inches (61 cm.) in length. Instrumentation ports are spaced along each side so that pressures, temperatures, and gas samples can be taken at any desired location in the coal. Since heat loss at the walls will be a problem, especially on a combustor of this size, electrical strip heaters will be placed along the side.

The coal is set into place by means of Steelkon refractory cement and the top of the combustor is sealed with an asbestos gasket. Small cracks in the refractory resulting from shrinkage while drying are sealed with Sodium Silicate. It has been found that this produces a satisfactory seal at low gasification pressures of about four inches of water. However, great care must be taken when installing the instrumentation to guard against leaks through the fire brick liner. The present method of sealing the coal sample will allow tests only at pressures slightly above atmospheric. Since a major part of the investigation is the relation between product gas composition and combustion parameters, any leakage around the burning zone cannot be tolerated.

A schematic of the total system is shown in Figure 9. The air supply system and product gas collection system is arranged so that either forward or reverse combustion can be tested as well as periodic cycling between the two. The product gas can be vented directly to the atmosphere or passed through a water scrubber and an after burner before venting. The sampling port for the gas chromatograph is placed after the water scrubber and samples are automatically drawn every fifteen minutes. Samples for the chromatograph can also be taken from within the combustor if desired.

Results to Date

Results of the laboratory combustion tests to date have been mainly of a qualitative nature. Several of the early tests were aborted due to system leaks and there was a lengthy delivery time on much of the instrumentation. The gas chromatograph in particular is essential to quantitative results and this instrument is now operational.

The first several tests were forward combustion runs whose main purpose was to check out the system and to help establish the proper flow parameters. A typical coal sample for these runs was prepared from lumps approximately 4 inches X 4 inches (10 cm. X 10 cm.) in cross-section and 6 inches (15 cm.) long. The butt ends were sawed smooth and a crack 1/16 in. (0.13 cm.) wide was prepared down the length of the sample. Figure 10 shows this arrangement. Table 1 lists properties of some Warrior field coals. Since these are swelling coals, one object of the forward combustion tests was to determine the extent of crack stoppage. In all of the forward tests crack stoppage due to swelling and tar condensation resulted in excessively high pressure drops causing leaks and thus aborting the run.

More recent tests have been conducted in the reverse combustion mode, and, of course, do not exhibit the crack stoppage due to swelling as before. A typical result of a reverse run is shown in Figure 11. There is a thin carbonized zone ranging from 0.5 to 2.5 inches (1.3 cm. to 6.4 cm.) in thickness followed by ash on the downstream side. The carbonized zone is quite porous and apparently allows diffusion of air along its length causing the combustion zone to spread away from the crack. This means that the reaction is somewhat diffusion limited so that an attempt to increase the reaction rate by increasing air flow results in much of the excess air being blown through the combustion zone without reacting.

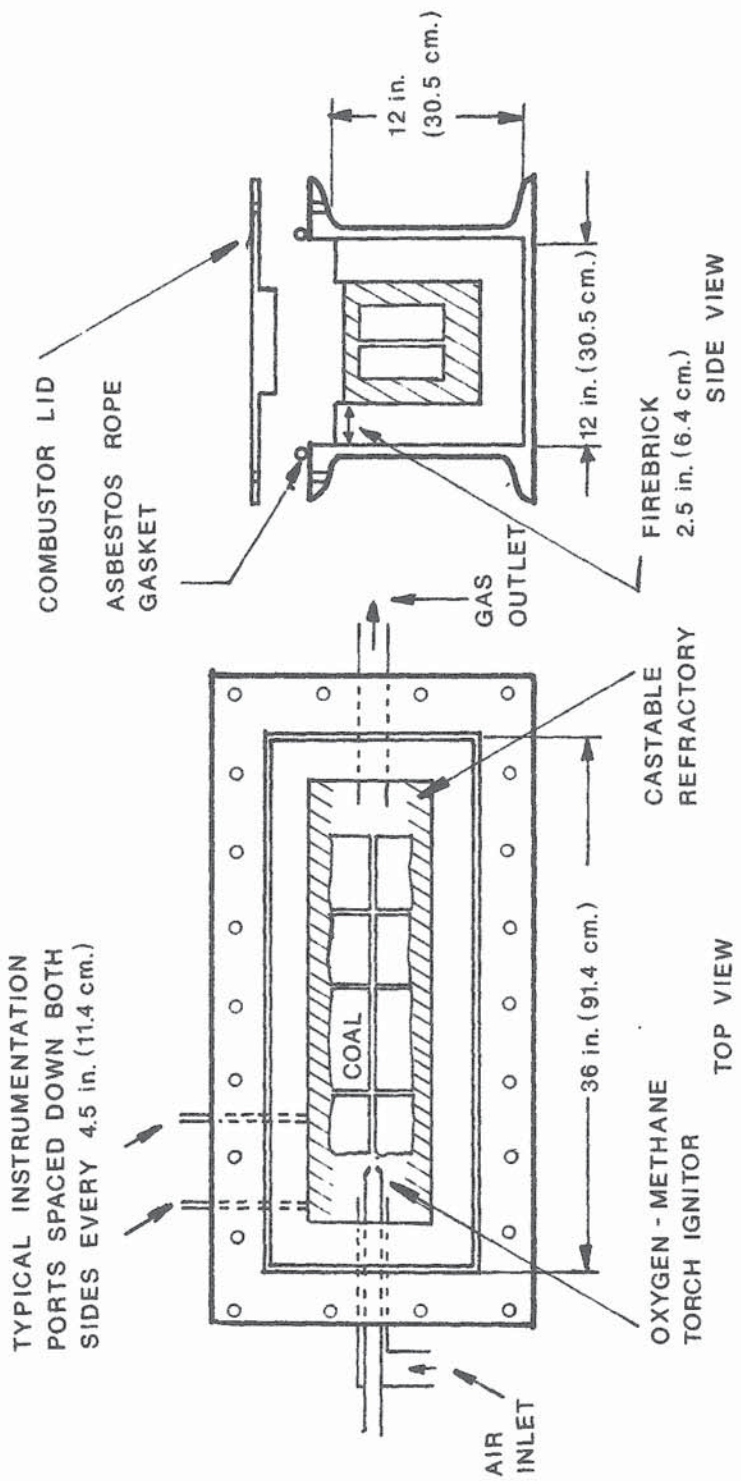


Figure 8.--Schematic of Laboratory Combustor

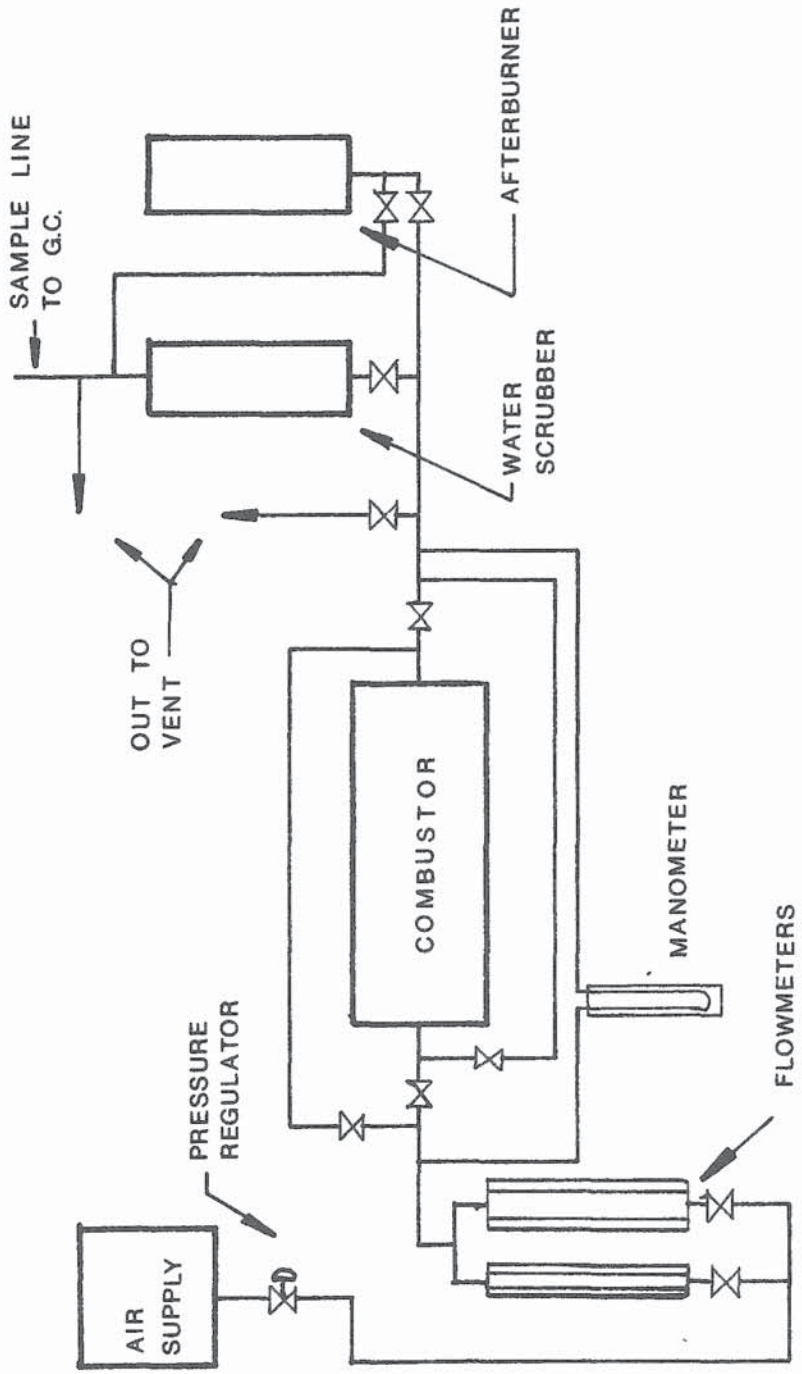


Figure 9.--Schematic of Combustor System

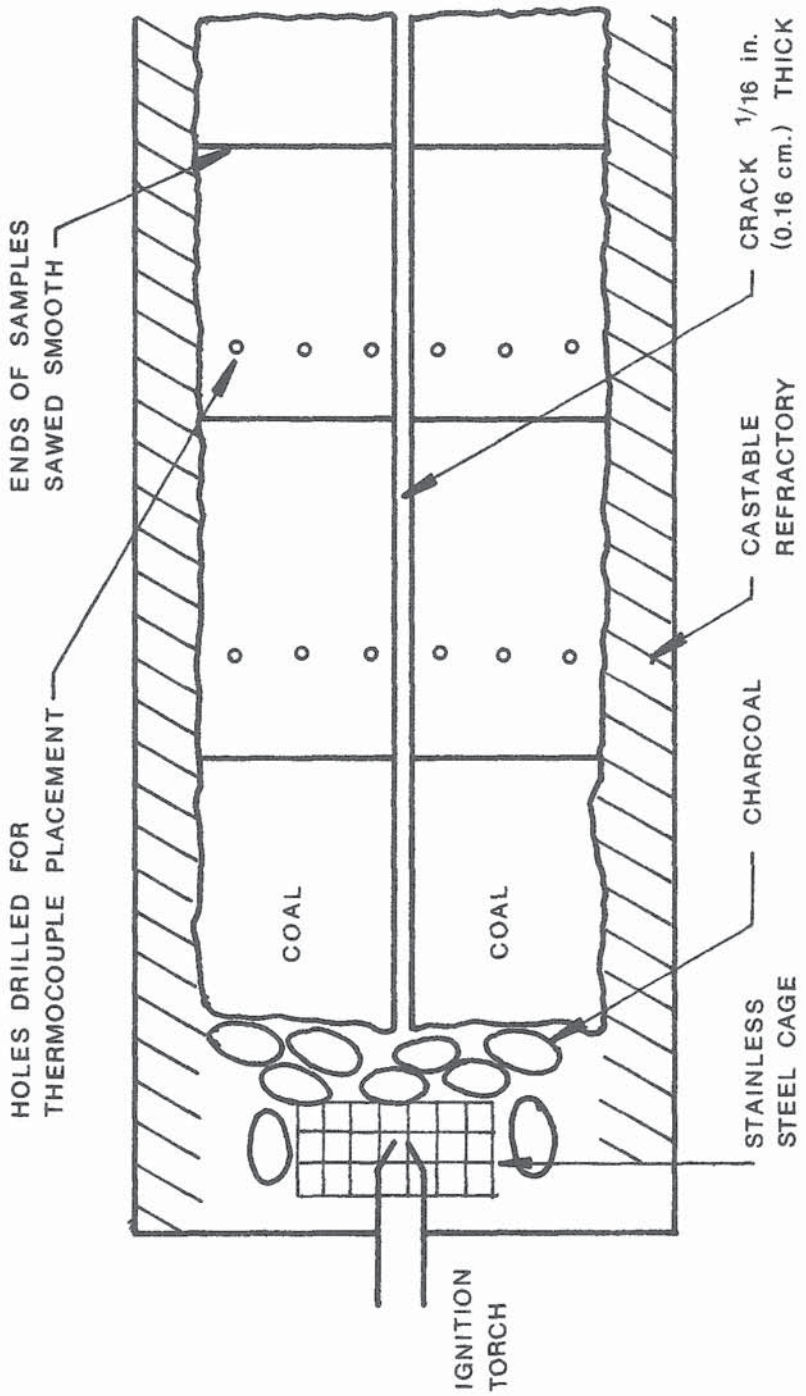


Figure 10.--Typical coal sample placement in combustor

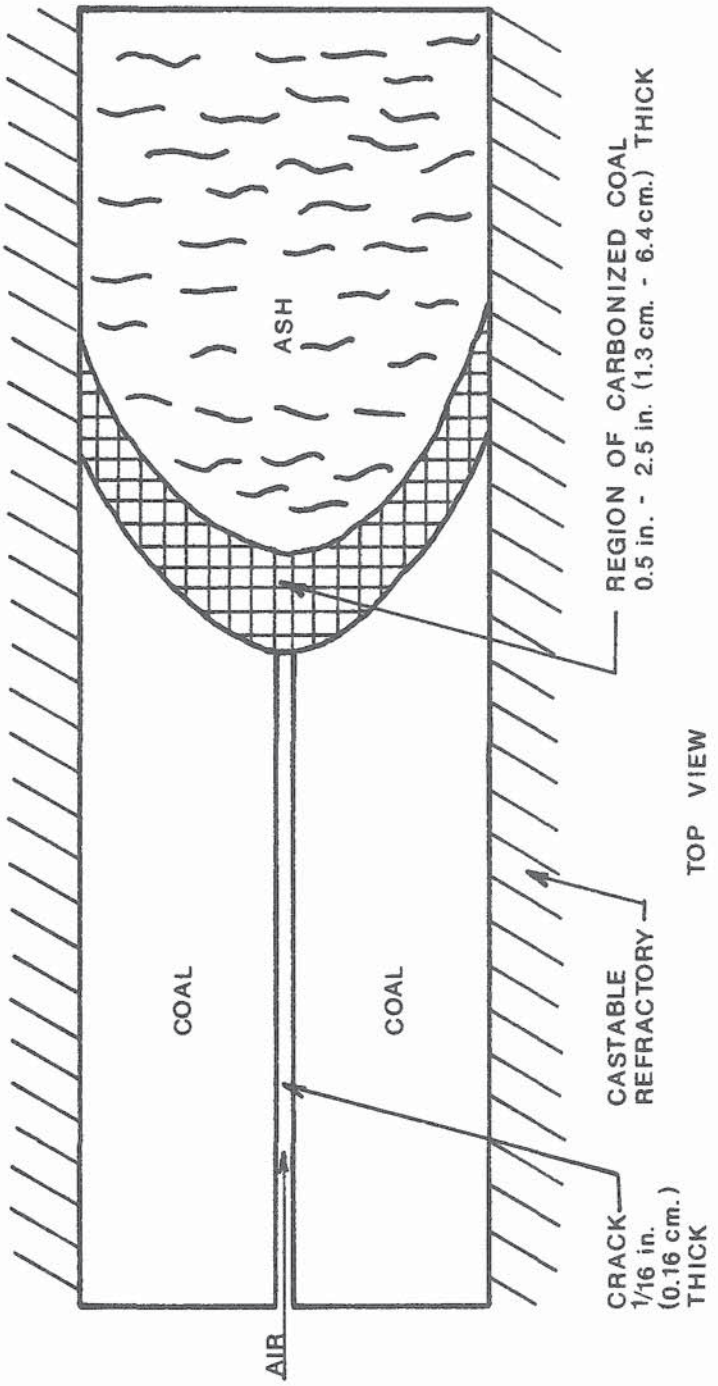


Figure 11.--Reverse Burn - Shape of Combustion Zone

The problem of crack burning in a swelling coal seems to be one of how to produce a sufficient volume of acceptable gas without closing the air passages. Tests are underway to determine the optimun air supply for reverse burning as well as an attempt to correlate crack size with pressure drop as combustion proceeds in forward mode.

Conclusions

Tests so far have shown that in-situ gasification of swelling bituminous coals which have been hydraulically fractured will be sensitive to crack stoppage in forward combustion. This is not the case for reverse combustion. Further tests are indicated which will determine an optimum air flow for a desired product gas in reverse combustion as well as a possible correlation of crack size with degree of stoppage in forward combustion.

George W. Douglas is an Associate Professor of Mechanical Engineering at The University of Alabama. He received a PhD in Mechanical Engineering from Tulane University in 1967.

RESULTS AND STATUS OF THE SECOND HANNA IN SITU COAL GASIFICATION EXPERIMENT

C. F. BRANDENBURG,[1] D. D. FISCHER,[1]
D. A. NORTHROP,[2] AND L. A. SCHRIDER[3]

ABSTRACT

The second Hanna experiment has demonstrated the feasibility of successfully gasifying coal in situ under controlled conditions. This experiment was designed as a three-phase study. Phase I was conducted from April through August 1975. This test showed that: (1) reverse combustion linking could be controlled; (2) the preferred flow direction was up-dip and along the minor fracture trend; (3) completion of wells near the bottom of the seam prevented gas overriding; (4) during a 38-day gasification test between two wells gas production averaged 2.7 MM scfd (8.1×10^4 scmd) of 152 Btu/scf (5.36 megajoules/scm) gas with consumption of 48 tons (44 tonnes) of coal per day. It was also determined that the system could be turned down by a factor of 10 with only a 20 percent drop in gas heating value with less than a 6-hour response time to bring the system back to full operation.

Phase II was completed in May 1976 and consisted of linking two wells (7 and 8) by reverse combustion, linking two wells (5 and 6) by reverse combustion, and gasifying the coal between Wells 5 and 6. Because of the extensive instrumentation it has been shown that the linkage path is a narrow channel that can be placed at the bottom of the coal seam. Further, the combustion front in gasifying between two wells was about 50 feet (16 m) across and completely utilized the entire 30 feet (9.1 m) coal section. During a 27-day gasification test production of 8.6 MM scfd (0.26 MM scmd) of 175 Btu/scf (6.17 megajoules/scm) gas with consumption of over 100 tons (91 tonnes) of coal per day (equivalent to 240 Bbls of oil per day) was achieved. Phase III, the line drive portion of Hanna II, was completed on July 30, 1976. The attempt to create a broad linkage pathway between the 5-6 and 7-8 lines by injecting simultaneously at Wells 7 and 8 was unsuccessful. A narrow link formed close to the line between Wells 6 and 8. Phase III was modified to another two-well burn from Well 8 to Well 7.

An extensive instrumentation effort has been fielded as an integral part of this program. Both diagnostic and remote monitoring techniques have been fielded utilizing a combination of instrumentation wells within the experimental region and near-surface arrays. The primary diagnostic information is obtained from extensive thermocouple arrays from which the location, extent, and movement of the combustion front is clearly evident. Gas sampling canisters, pressure transducers, tilt meters, and displacement gauges provide additional diagnostic information. Emphasis has been placed on the development of surface or remote instrumentation techniques based upon acoustic, seismic and electrical phenomena which would provide an overall picture or map of the changing process and which would be used in designing an overall process control system.

---

[1] ERDA, Laramie Energy Research Center, Laramie, Wyoming.
[2] Sandia Laboratories, Albuquerque, New Mexico.
[3] ERDA, Morgantown Energy Research Center, Morgantown, West Virginia.

The Hanna II experiment has provided further insight into the successful operation of an in situ coal gasification project. Completion of this test has determined that sustained production of high quality low-Btu gas can be achieved. The effects of air injection rate, backpressure, and water influx rate have been better defined. Completion of larger planned tests should yield the final refinements necessary for pilot plant and commercial operation.

INTRODUCTION

Previous authors have reported the results of several field tests of underground coal gasification [1].[4] Prominent among these are the Russian work [1,2] (which has included commercial utilization of UCG), the British tests [3], and early U.S. experiments [4-7]. In 1973 the Bureau of Mines initiated the first of a series of field experiments near Hanna, Wyoming. This first test is designated Hanna I and has been previously detailed [8-11].

Based upon the encouraging results of Hanna I, a second experiment, designated Hanna II, was initiated in 1975. This experiment was divided into three parts, called Phases I, II, and III. Phase I has already been reported [8-12] and will only be referred to as a basis of comparison. The results of Phases II and III are the subject of this report.

ORGANIZATION OF HANNA II EXPERIMENT

The location of Hanna II is about 800 feet (244 m) west of the site of Hanna I. The coal is the same 30 feet (9.1 m) Hanna #1 seam as previously used at a depth of approximately 275 feet (84 m). Geological details have previously been presented [8,9,11].

Phase I of Hanna II was initiated to further study the reverse combustion linkage process to determine the effects of formation anisotrophy on the linkage and subsequent gasification and the utility of downhole instrumentation for process characterization. This test was conducted from April through August 1975 [12] and showed: (1) Reverse combustion was a reliable and controllable technique for seam preparation; (2) Completion of the wells near the bottom of the seam resulted in placement of the link in the bottom half of the seam; (3) The preferred flow direction was up-dip and along the indicated minor fracture trend; (4) During the 38-day gasification period between two wells, 2.7 MM scfd (8.1×10^4 scmd) of 152 Btu/scf (5.36 megajoules/scm) gas were produced with 48 tons (44 tonnes) of coal being gasified; and (5) The air injection rate could be cut by a factor of 10 with only a 20 percent drop in gas heating value with less than a 6-hour response time to return the system to full operating conditions. Further details are given in Reference 12.

Based upon the results of Phase I, Phases II and III were designed as a four-well experiment, as shown in Figure 1. Wells 5, 6, 7, and 8 were drilled 60 feet (18.3 m) apart to the Hanna #1 seam, the pattern being located about 150 feet (46 m) northwest of the Phase I pattern. Wells designated by alphabetic characters were instrument wells, described below.

The experimental plan for Phase II was to link Wells 7 and 8 by reverse combustion with ignition at Well 7, to link Wells 5 and 6 by reverse combustion with ignition at Well 5, and then gasify in the forward combustion mode between Wells 5 and 6 with injection at Well 6. In Phase III simultaneous injection into Wells 7 and 8 would be initiated to effect a broad reverse combustion linkage between the 5-6 pathway by utilizing the 7-8 linkage as a line source for air injection. Once this broad linkage was established, the plan was to gasify the area encompassed by the four wells by injection into Wells 7 and 8 with production from Wells 5 and 6.

[4]References given at end of paper.

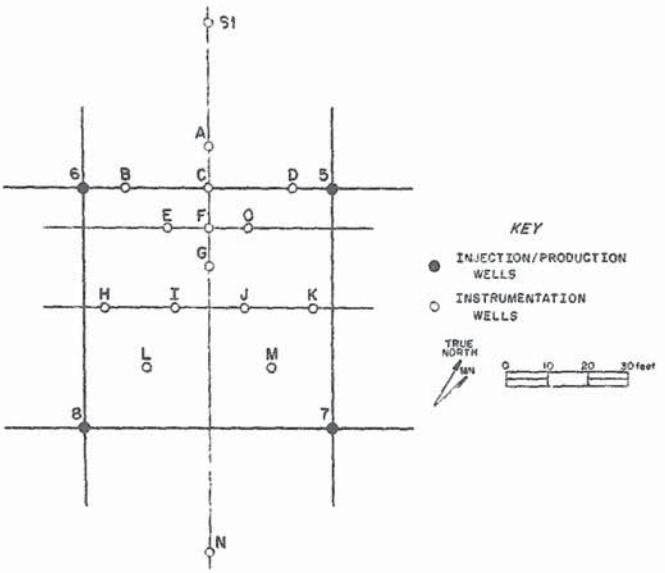


Figure 1 - Well Pattern of Injection-Production and Instrumentation Wells for Hanna II, Phases II and III.

INSTRUMENTATION

An extensive instrumentation effort was fielded as an integral part of this experiment. As illustrated in Figure 2, both diagnostic and remote monitoring techniques were emplaced utilizing a combination of instrumentation wells within the experiment region (Wells A through O and S1, Figure 1) and near-surface arrays. The diagnostic techniques were designed to give an in situ definition of the gasification process. Emphasis was also placed on the development of surface or remote instrumentation techniques based upon acoustic, seismic, and electrical phenomena which would provide an overall picture or map of the changing process and which would be utilized to design a process control system in conjunction with the data gathered on operating conditions by LERC.

The data were collected and recorded in an instrument trailer provided by Sandia Laboratories of Albuquerque, in which all instrumentation data described in this section were recorded, and LERC's HP-2100 computer, which was used to provide real time analysis of a majority of the temperature data from Wells A-O. The critical process parameters were recorded hourly by LERC's computer system and were permanently stored and available on instant recall. The LERC portion of the system is described elsewhere [13].

The instrumentation techniques fielded by Sandia on the Hanna II experiment and their present status are summarized in Table 1. Details and results from Phase I have been given elsewhere for the overall effort [12,14,15], thermal instrumentation [12, 16,17] and the remote monitoring techniques [18-20]. The major instrumentation effort was associated with Phases II and III and a summary of the instrumentation locations for these phases is given in Table 2. With the addition of redundant channels and diagnostic circuits, over 600 channels of information were recorded throughout the entire experiment period. This voluminous field data is being reduced and analyzed; preliminary results are given below for currently available information (through July 1976).

In-seam gas samples were obtained from Wells C and D via long-line gas sampling techniques. Pressure transducers were installed at the surface on the sampling lines and static in-seam gas pressures were measured at times gas samples were not being withdrawn.

Two electrical techniques are being developed for remote monitoring applications and are depicted in Figure 3; both utilize the same surface and downhole potential probe arrays. The feasibility of the Modified Schlumberger Technique (MST) was demonstrated on Phase I [18]; preliminary data on Phases II and III indicate that the direct excitation potential technique (DEPT) is more sensitive to changes in the coal seam and less sensitive to surface conditions than the MST. The linking between Wells 7 and 8 is indicated by the low resistivity region (decrease of 20 percent) in the DEPT data shown in Figure 4. However, close correlation of model calculations and field data are necessary to accurately interpret the results. DEPT model calculations utilizing a Green's function integral approach are underway.

The feasibility of a passive acoustic technique to locate the source of discrete acoustic signals was demonstrated on Phase I [18,19]. However, the utility of the technique is hampered presently by attenuation, the inexact definition of signal arrivals, and the lack of an automated signal monitoring and analysis system. Discrete passive signals whose sources are located in the overburden have again been observed in Phase II. Signals were first noted after gasification had proceeded for several days and when high temperatures were noted at the top of the coal seam. The frequency of these acoustic events, presumably due to cracking of strata in the overburden, increased continuously for the remainder of the phase.

Downhole-to-downhole and downhole-to-surface induced seismic techniques are based upon detection of changes in seismic signals whose source-to-geophone paths are

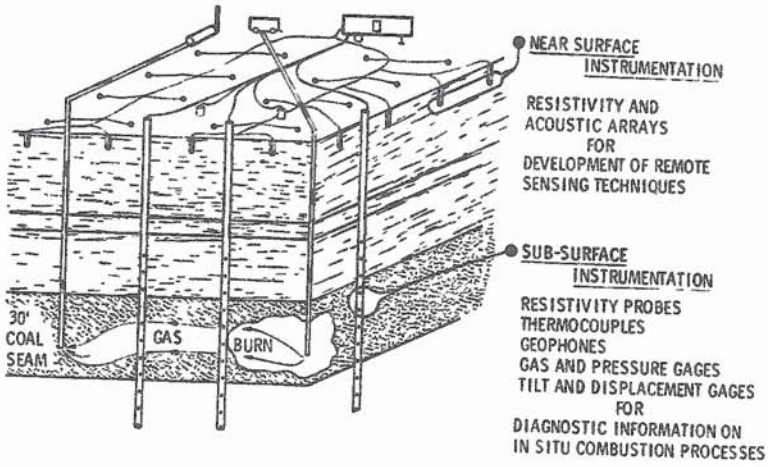
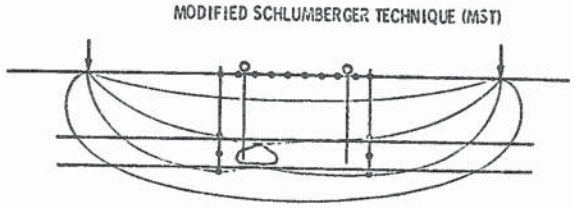


Figure 2 - Schematic of Remote and Sub-Surface Instrumentation Techniques Utilized in Hanna II.



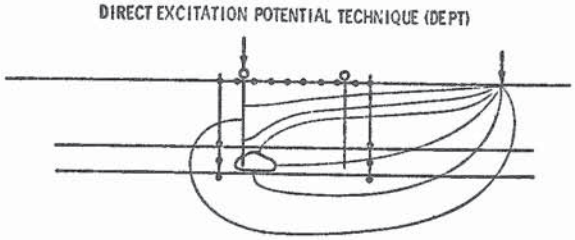


Figure 3 - Two Electrical Techniques Being Developed for Remote Monitoring Applications.

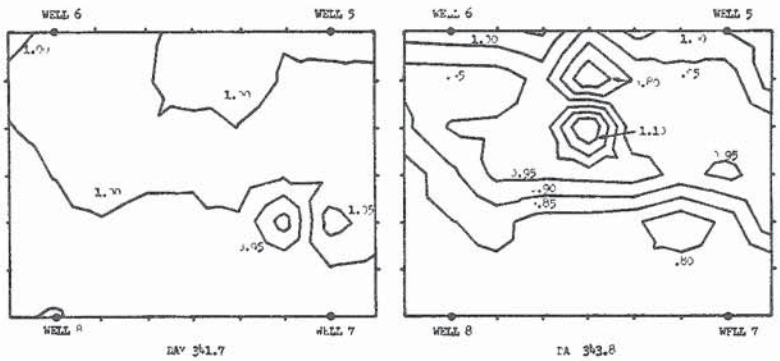


Figure 4 - Results of DEPT Electrical Technique Before and After Combustion Linkage of Wells 7 and 8.

Table 1

Instrumentation Techniques to be Fielded and Evaluated on

The Second Hanna In Situ Coal Gasification Experiment

	Technique	Phase 1	Phase 2	Phase 3
REMOTE	ELECTRICAL (surface and downhole)			
	Modified Schlumberger (MST)	X	X	X
	Direct Excitation (DEPT)		X	X
	Telluric Current		X	X
	PASSIVE ACOUSTIC	X	X	X
	INDUCED SEISMIC			
	Downhole-Downhole		X	X
	Downhole-Surface		X	X
DIAGNOSTIC	THERMAL			
	Low Temperature	X	X	X
	High Temperature		X	
	IN-SEAM GAS SAMPLING			
	Composition	X	X	X
	Pressure	X	X	X
	DISPLACEMENT		X	X
	TILT		X	X

Table 2

SUMMARY OF INSTRUMENTATION FIELDED FOR PHASES 2 AND 3 OF THE HANNA II UNDERGROUND COAL GASIFICATION EXPERIMENT

Instrumentation Well	A	B	C	D	E	F	G	H	I	J	K	L	M	N	O	Total
Low Temperature Levels[1]	10	9	10	10	8	9	9	10	10	10	10	10	10	7	9	141
High Temperature Levels[2]		3	3		3	3										12
Resistivity Probes[3]	3	3	3	3	3[4]	3[4]	3	3	3	3	3	3	3	3	3	48
Geophones	10	10	10	10	10	10	10[5]	10	10	10	10	10	10	10	10	150
Gas Sampling Canisters		1	1	1	1	1	1		1	1					1	9
Downhole Pressure Transducers			1			1	1									3
Surface Pressure Transducers		1	1	1	1	1	1		1	1					1	9
Tilt Meters		2	2			2		2	2	2	2					14
Displacement Levels			4		4		4									12
																398
Plus Surface: Geophone Array (20 ft depth)																15
Resistivity Probe Array																81
													Total			494

NOTES:
(1) Up to six-fold redundancy at most levels plus resistance and noise measurements greatly increase the total number of thermal channels available.
(2) Different materials fielded for evaluation.
(3) Three probes also fielded in shot-well, S1.
(4) High temperature sensors and cables fielded in these wells.
(5) Different geophone spacing to measure vertical attenuation.

intersected by the process. A five-layer seismic velocity model has been derived for the coal seam and the surrrounding formations based upon pretest data from Phase II.

RESULTS OF PHASES II & III

Linkage of Wells 7 and 8 was completed during December 1975. The combustion zone was extinguished by injecting water. Wells 5 and 6 were linked during April 1975. The details of these two linkages have been presented elsewhere [21].

During gasification from Well 6 to Well 5, three planned injection rates of 1700, 2500, and 3500 scfm (51, 75, and 105 scm/min), respectively, were utilized for periods of 3+, 5+, and 17+ days, respectively.

The gas composition, injection and production rates, injection and production pressures, product gas temperature at the wellhead, and product gas gross heating value are shown in Figures 5-9.

Figure 5 shows the gas composition was constant and uniform until near the end of the 5-6 gasification phase. No dramatic change in gas composition or heating value occurred during the planned abrupt increases in injection rate. The ratio of production rate to injection rate was consistently greater than 1.7 to 1. At 3500 scfm (105 scm/min) injection, the production rate was about 6000 cfm (180 scm/min) or 8.6 MM scfd (0.26 MM scmd) of 175 to 185 Btu/scf (6.17 to 6.52 megajoules/scm) product gas. All instrumentation in Wells A, B, C, D, E, F, G, and O was consumed upon completion of the 5-6 gasification. Wells H, I, and J were showing temperature increases at the 0 and 10 feet (3.05 m) levels from the bottom of the seam when the 5-6 gasification phase was completed on May 30. In addition, leakage of product gas to Well S1 occurred on May 30. Temperature measurements in S1 on May 31 showed a peak temperature of 88° F (31° C) at ∿12 feet (3.7 m) above the bottom of the seam. Therefore, at the midpoint of the 5-6 line the reaction front could have been as wide as 60 feet (18.3 m) assuming it had approached within a few feet of S1 and within a few feet of the H-I-J line as indicated from thermal data.

The movement of the gasification front is seen from the observation wells (Figures 10-11) as it swept across the well pattern: first near the bottom of the coal seam and then upwards at each location. The data indicate essentially complete utilization of the coal seam in the area of the instrumentation wells. Observed lateral and vertical rates of reaction zone advance were 0.5-1.5 ft/day (0.15-0.46 m/day) and 0.8-2.2 ft/day (0.24-0.67 m/day), respectively.

The total utilization for the linkage and gasification of 5-6 was 2520 tons (2290 tonnes). This is 1000 tons (907 tonnes) more than estimated from linear extrapolation of the data gathered from the gasification between Wells 1 and 3 (Phase I) during June and July 1975. The improved gas quality and resource utilization appear to be the result of the significantly higher injection rates used and of the backpressure on the system which maintained the proper air/water ratio necessary for efficient in situ gasification [21].

Upon conclusion of Phase II, Phase III was begun immediately. The original plan was to inject into Wells 7 and 8 to draw the combustion zone from the 5-6 gasification to the previously completed 7-8 link in a reverse combustion mode and then to gasify back toward the 5-6 line along the broad path thus formed. To this end injection into Wells 7 and 8 was begun. Linkage occurred in four days. A total of only 2.6 MM scf (7.78×10^4 scm) of air was injected and no temperature increases were seen at any instrument wells other than H and I. The linkage, therefore, was a narrow channel rather than a broad front. A series of tests to determine the location of the linkage path were initiated. By injecting and producing various combinations of wells it was determined that the linkage was on the Well 8 end of the 7-8 linkage path and that there was combustion along this path.

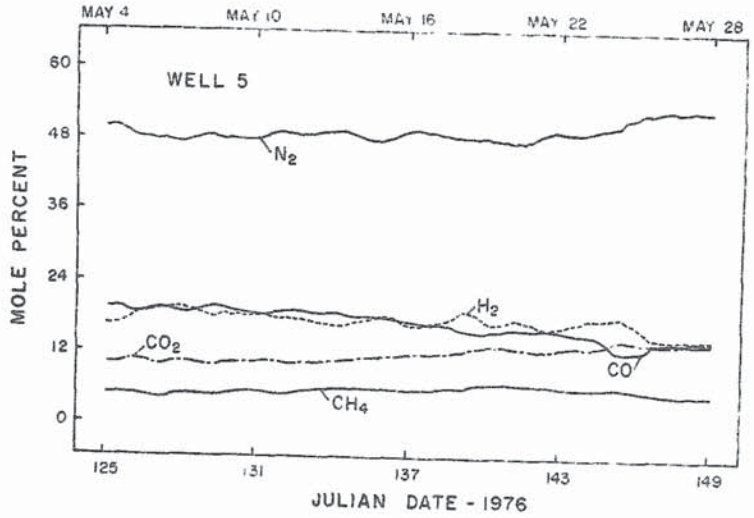


Figure 5 - Product Gas Composition During Gasification between Wells 5 and 6.

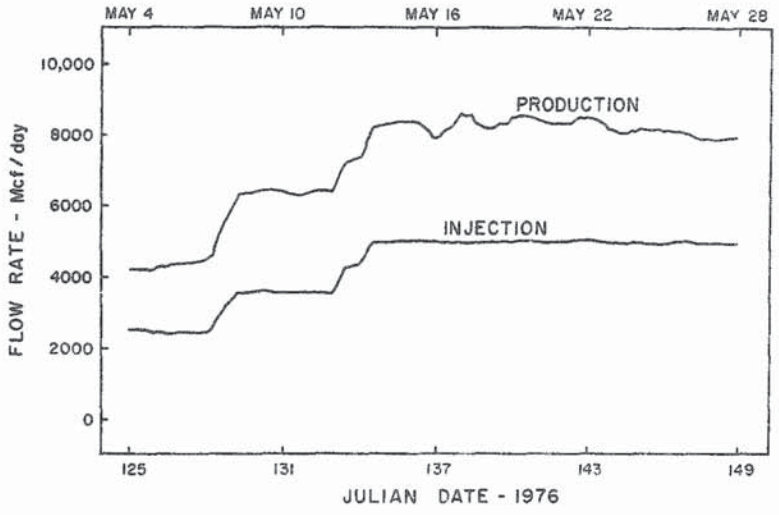


Figure 6 - Air Injection and Gas Production Rates During Gasification Between Wells 5 and 6.

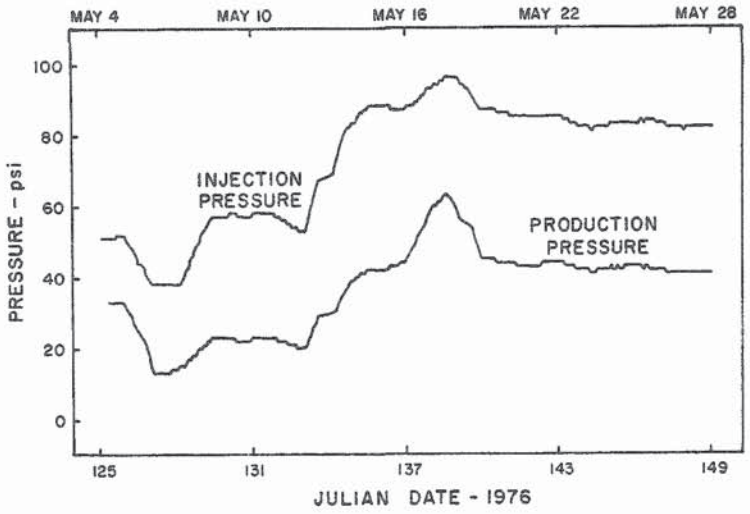


Figure 7 - Air Injection and Gas Production Pressures During Gasification between Wells 5 and 6

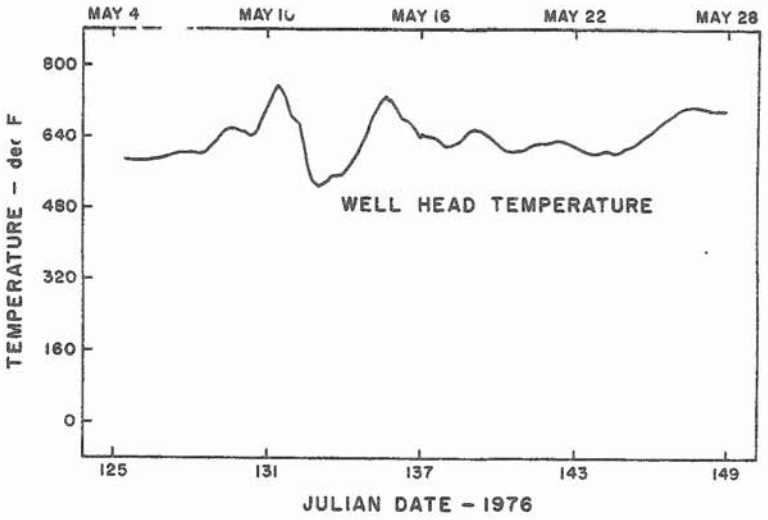


Figure 8 - Wellhead Product Gas Temperature During Gasification Between Wells 5 and 6.

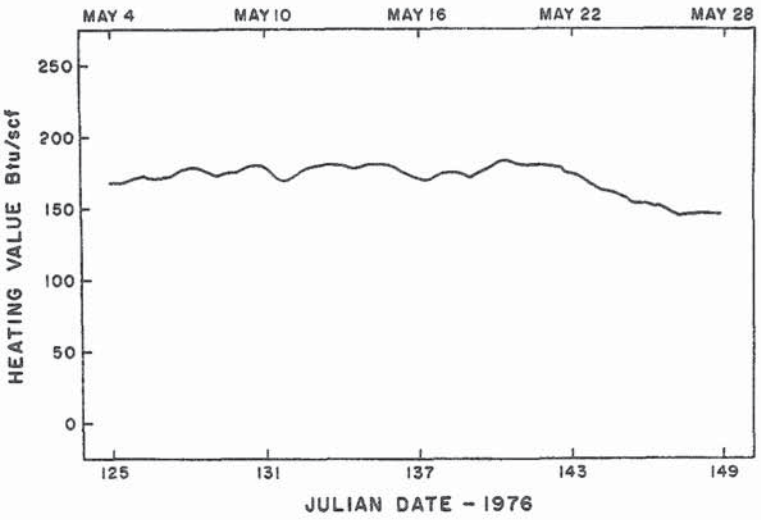


Figure 9 - Gross Heating Value of Dry Product Gas During Gasification Between Wells 5 and 6.

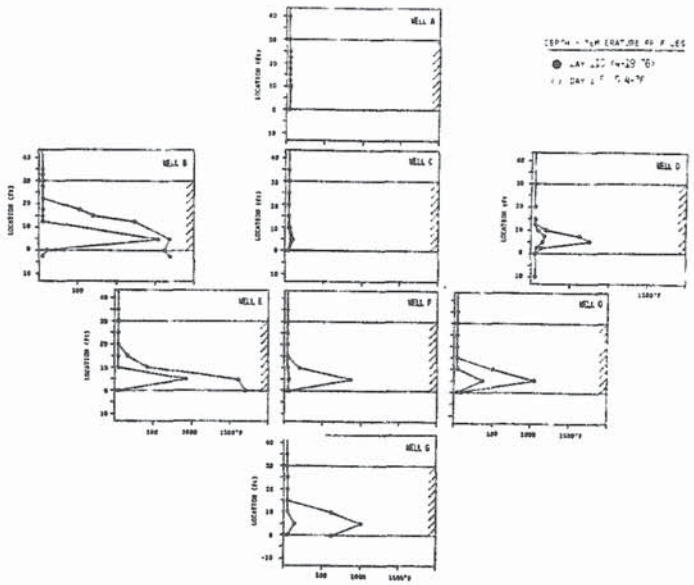


Figure 10 - Thermal Profile from Instrumentation Wells on Two Selected Days During Linkage and Gasification Between Wells 5 and 6.

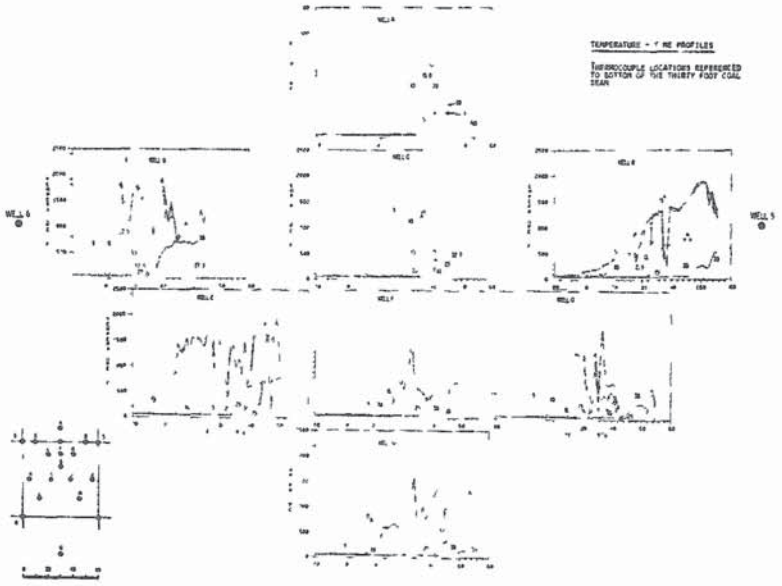


Figure 11 - Thermal Histories Seen From Instrumentation Wells During Linkage and Gasification Between Wells 5 and 6

In view of the high resource recovery during Phase II and the apparent failure to initiate the line drive, it was decided to investigate the results of two 2-well burns side by side. Accordingly air injection into Well 8 was begun with production from Well 7. During this interim period, 680 tons (614 tonnes) of coal were utilized.

Operating conditions were deliberately varied during this operation to study the effects of various operating parameters as well as the controllability of the process. Thus, while a direct comparison of two parallel gasifications was not made possible, further insight into the UCG process itself was made possible. Because of the voluminous amount of data acquired, full interpretation of the results has not yet been made. However, some effects are visibly discernible and some preliminary conclusions can be drawn from the test.

The product gas composition, production and injection rates, injection and production pressures, production wellhead temperature, and gross heating value are shown in Figures 12-16. The trends exhibited by these results contrast with those in Phase II (Figures 5-9) and in some ways resemble the results of Phase I [12], especially in the heating value of the product gas.

The injection rates utilized were 2500, 3500, and 4500 scfm (75, 105, and 135 scm/min). The other parameter which was varied was the backpressure on the system. During the individual injection rate periods, this parameter was varied from 10 to 80 psig (6.89×10^4 to 5.52×10^5 Pa). Increasing the backpressure produced an immediate small increase in the methane, hydrogen, and carbon dioxide concentrations while the carbon monoxide concentration dropped. Releasing the backpressure yielded the opposite effects.

Approximately 3490 tons (3160 tonnes) of coal were utilized during the 7-8 gasification phase, a significantly higher value than during Phase II. Again a higher injection rate was achieved between Wells 7 and 8 then in Phase II and is apparently responsible for this higher utilization although some unknown portion of this tonnage must be attributed to bleed down of the 5-6 system.

The outstanding differences between Phase II and Phase III are the results of excess water [21] during Phase III which greatly lowered the heating value and thermal efficiency. A more favorable air/water ratio could not be obtained because of the inability to increase the air injection rate beyond 4500 scfm (135 scm/min) during Phase III.

The total utilization during Phases II and III was 6690 tons (6070 tonnes). This is in comparison with 4600 tons (4170 tonnes) contained within the 60 feet by 60 feet (18.4 by 18.4 meters) well pattern indicating outstanding sweep efficiency.

CONCLUSIONS

The results of Phases II and III, of Hanna II, show a marked improvement over previous achievements during Hanna I and Phase I, Hanna II. The reasons for these improvements are the higher injection rates utilized and backpressuring of the formation. The original line drive system proposed for Phase III was unsuccessful but the resource utilization achieved during both Phases II and III indicates that such a system is unnecessary for high sweep efficiencies. Operation of two-well systems side by side offers the simplest process possible while still allowing production of high quality low-Btu gas over sustained periods at high rates. Even in a system such as that existing in the Hanna #1 seam, excess water can be a hindering factor in the in situ gasification process. Both increased air injection rates and backpressuring of the system can be used to moderate its influence but dewatering may be required. The results of Hanna II indicate the viability of underground coal gasification as a controllable source of low-Btu gas and additional planned experiments at Hanna should further elucidate the applicability of UCG to commercial operations as an alternate energy source.

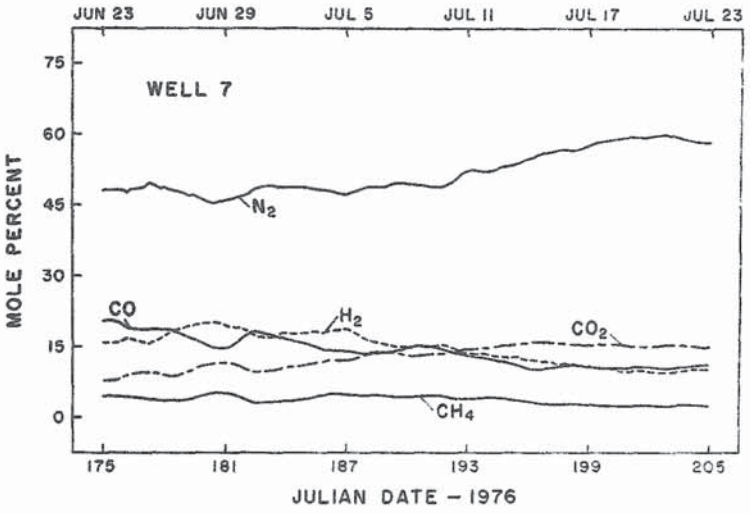


Figure 12 - Product Gas Composition During Gasification Between Wells 7 and 8.

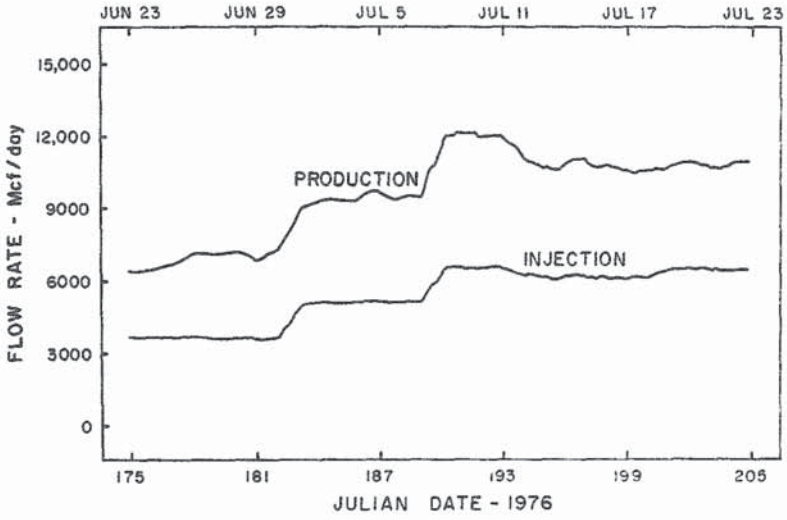


Figure 13 - Air Injection and Gas Production Rates During Gasification Between Wells 7 and 8.

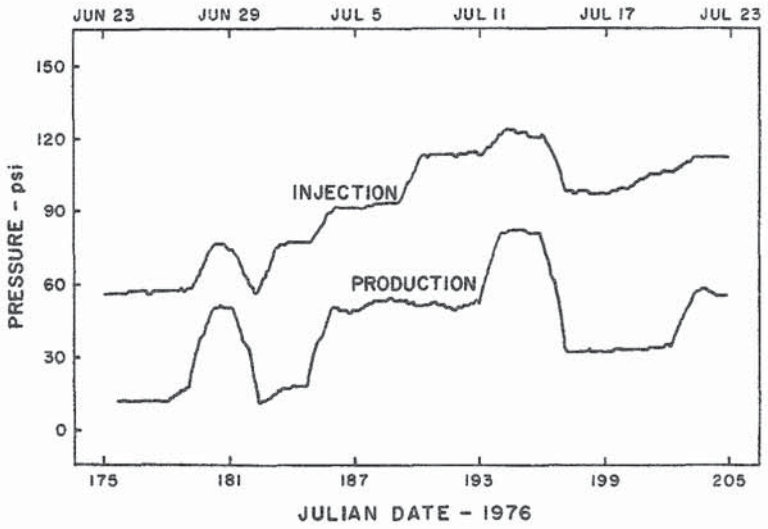


Figure 14 - Air Injection and Gas Production Pressures During Gasification Betweens Wells 7 and 8.

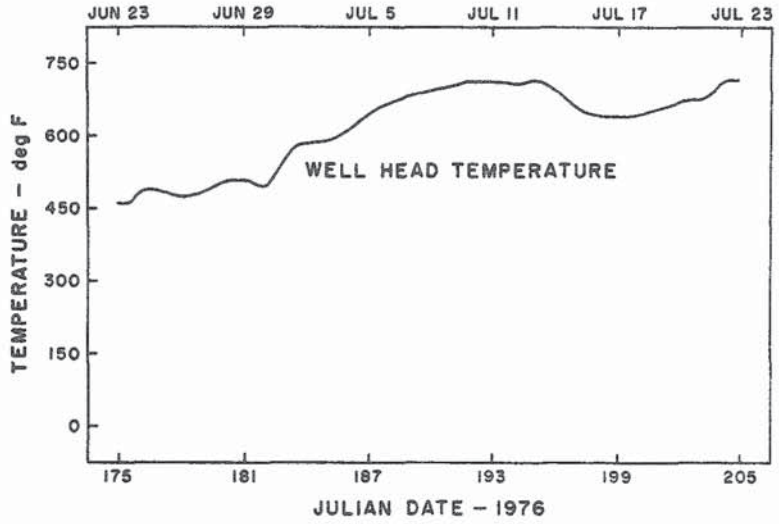


Figure 15 - Wellhead Product Gas Temperature During Gasification Between Wells 7 and 8.

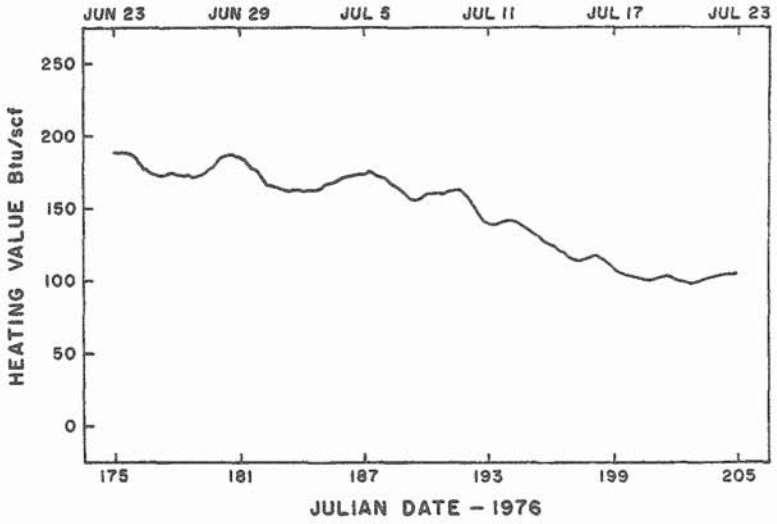


Figure 16 - Gross Heating Value of Dry Product Gas During Gasification Between Wells 7 and 8.

REFERENCES

1. A. D. Little, Inc., "A Current Appraisal of Underground Coal Gasification," Report No. C-73671 (Dec. 1971), 121 pp.

2. Skafa, P. V., Underground Gasification of Coal, Translated from Gosudarstvennoe Hauchno-Tekhnicheskoe Izdatel'stvo Literatury Po Gornomu Delu, Moscow (1960), 324 pp.

3. Sir Alexander Gibb and Partners, The Underground Gasification of Coal, Sir Isaac Pitman & Sons, Ltd., London (1964).

4. Dowd, J. J., J. L. Elder and J. P. Cohen, "Experiment in Underground Gasification of Coal, Gorgas, AL," BuMines RI 4164 (Aug. 1947), 62 pp.

5. Elder, J. L., M. H. Fies, H. G. Graham, R. C. Montgomery, L. D. Schmidt, and E. T. Wilkins, "The Second Underground Gasification Experiment at Gorgas, AL," BuMines RI 4808 (Oct. 1951), 72 pp.

6. Capp, J. P., J. L. Elder, C. D. Pears, R. W. Lowe, K. D. Plants and M. H. Fies, "Underground Gasification of Coal - Hydraulic Fracturing as a Method of Preparing a Coalbed," BuMines RI 5666 (1960), 50 pp.

7. Capp, J. P., and K. D. Plants, "Underground Gasification of Coal with Oxygen-Enriched Air," BuMines RI 6042 (1962), 14 pp.

8. Campbell, G. G., C. F. Brandenburg, and R. M. Boyd, "Prelimiary Evaluation of Underground Coal Gasification at Hanna, Wyoming," BuMines TPR 82 (Oct. 1974), 14 pp.

9. Schrider, L. A., J. W. Jennings, C. F. Brandenburg, and D. D. Fischer, "An Underground Coal Gasification Experiment, Hanna, Wyoming," SPE 4993, presented at the SPE Fall Meeting of AIME, Houston, TX (Oct. 6-9, 1974), 25 pp.

10. Brandenburg, C. F., D. D. Fischer, G. G. Campbell, R. M. Boyd, and J. K. Eastlack, "The Underground Gasification of a Subbituminous Coal," presented at the Div. of Fuel Chem., Am. Chem. Soc. National Spring Meeting, Philadelphia, PA (Apr. 1975), 11 pp.

11. Schrider, L. A., C. F. Brandenburg, D. D. Fischer, R. M. Boyd, and G. G. Campbell, "The Outlook for Underground Coal Gasification," presented at the 1975 Lignite Symposium, Grand Forks, ND (May 1975), 32 pp.

12. Brandenburg, C. F., R. P. Reed, R. M. Boyd, D. A. Northrop, and J. W. Jennings, "Interpretation of Chemical and Physical Measurements from an In Situ Coal Gasification Experiment," SPE 5654, presented at the SPE Fall Meeting of AIME, Dallas, TX (Sept. 28-Oct. 1, 1975), 28 pp.

13. Eastwood, D. E., J. K. Eastlack, J. W. Jennings, S. B. King, W. J. Lanum, and D. F. Moore, "Real Time Process Monitoring in Underground Coal Gasification," Paper MI-2, presented at 2nd Annual Underground Coal Gasification Symposium, Morgantown, WV (Aug. 10-12, 1976).

14. Stoller, H. M., L. A. Schrider, and D. A. Northrop, "The Status of Instrumentation and Process Control Techniques for In Situ Coal Gasification," presented at the 22nd ISA International Instrumentation Symposium, San Diego, CA (May 25-27, 1976).

15. Bartel, L. C., S. G. Beard, L. W. Beckham, R. P. Reed, and R. W. Seavey, "Instrumentation Results from an In Situ Coal Gasification Experiment," SPE 6151, to be presented at SPE Fall Meeting of AIME, New Orleans, LA (Oct. 4-6, 1976).

16. Beard, S. G., and R. P. Reed, "Some Insights from Temperature Measurements on Recent Underground Coal Gasification Experiments," Paper FS-1 presented at 2nd Annual Underground Coal Gasification Symposium, Morgantown, WV (Aug. 10-12, 1976).

17. Reed, R. P., "Branched Thermocouple Circuits in Underground Coal Gasification Experiments," Proc. 22nd ISA International Instrumentation Symposium, San Diego, CA (May 25-27, 1976).

18. Beckham, L. W., L. C. Bartel, and R. W. Seavey, "Remote Monitoring of an In Situ Coal Gasification Process," paper MI-1, presented at 2nd Annual Underground Coal Gasification Symposium, Morgantown, WV (Aug. 10-12, 1976).

19. Beckham, L. W., "Analysis of Passive Acoustic Signals Generated by an In Situ Coal Gasification Process," Sand. Lab. Rept. SAND-76-0124 (March 1976).

20. Bartel, L. C., "Model Calculations of Electric Fields Measured with a Fixed Stationary Array to Monitor In Situ Coal Gasification," Sand. Lab. Rept. SAND-76-0076 (Feb. 1976).

21. Fischer, D. D., C. F. Brandenburg, S. B. King, R. M. Boyd, and H. L. Hutchinson, "Status of the Linked Vertical Well Process in Underground Coal Gasification," paper FS-4, presented at 2nd Annual Underground Coal Gasification Symposium, Morgantown, WV (Aug. 10-12, 1976).

NOTE: Any reference to specific brand names does not imply endorsement by ERDA.

LLL In-Situ Coal Gasification Program*

BY

D. R. Stephens, F. O. Beane, and R. W. Hill

University of California, Lawrence Livermore Laboratory
Livermore, California 94550

INTRODUCTION

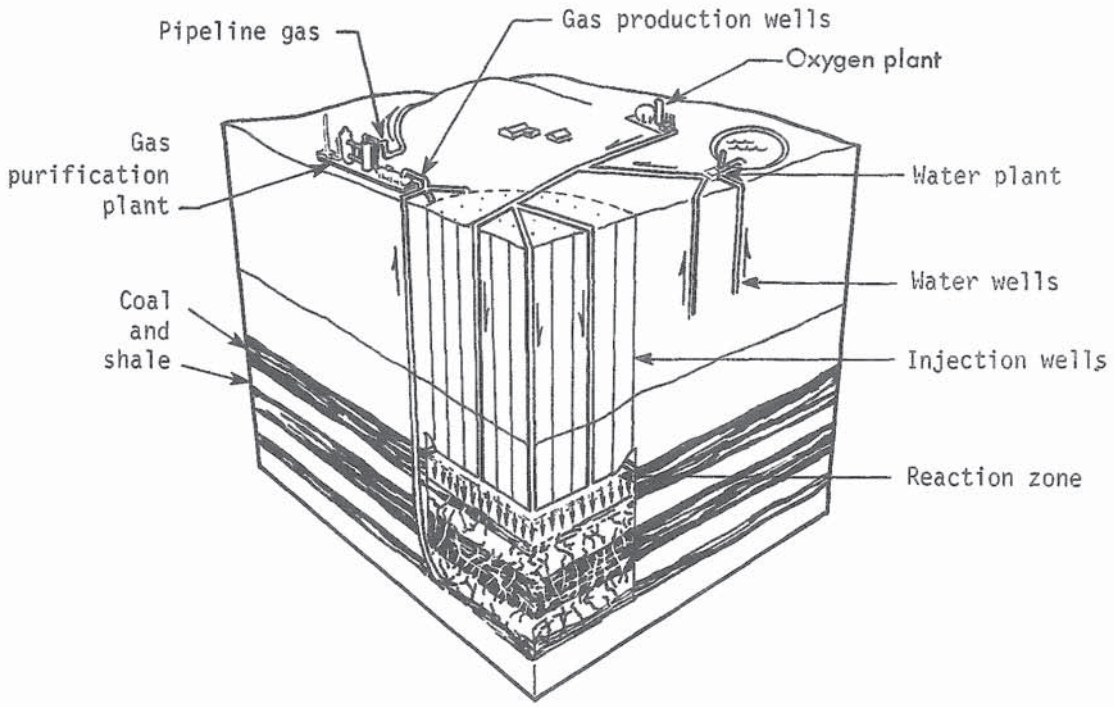
The conversion of coal into a clean, combustible gas can permit environmentally sound utilization of our principal fossil resource. If the conversion to gas can be accomplished with the coal underground (in-situ coal gasification) then additional environmental and economic advantages can be realized. In-situ coal gasification offers four potential advantages over conventional mining and subsequent surface processing:

- The product may be cheaper because of lower capital investment.
- Environmental damage is likely to be lower.
- Hazards to miners are avoided.
- It may be possible to exploit coal resources found at depths too great to be economically attractive for conventional strip- or deep-mining operations. Such resources include the thick, deep seams found in some western states and Alaska.

A unique approach to in-situ coal gasification was originated at LLL in 1972. In this approach, an array of chemical explosives is detonated to enhance the permeability of a reaction zone within a thick bed of coal (15 m or more). Our objective is to develop a commercial process for gasifying deep (150-1000 m), thick western coals to produce pipeline quality gas. A permeable, fractured coal bed within a relatively impermeable medium should permit intimate mixing of the coal and reactants (oxygen and steam) and allow heat transfer and reactant access to the coal. The low permeability of the surroundings should minimize leakage of reactants and products from the fractured zone. In essence the LLL concept is an underground packed-bed reactor. In 1974 ERDA initiated a major program aimed at exploiting the new concept. Laboratory experiments, computational studies, and an extensive field effort are in progress.

Access to the in-situ reactor will be through collection wells drilled to the bottom of the fractured coal and through reentered explosive holes, which will serve as injection wells. We plan to inject oxygen rather than air. After a suitable combustion zone has been established, the injected oxygen will be replaced by the appropriate mixture of oxygen and steam. Under suitable conditions the gas that is produced underground should consist primarily of methane (the principal constituent of natural gas) carbon monoxide, carbon dioxide, and hydrogen. These underground products will be cleaned and upgraded in a surface plant to provide pipeline-quality gas.

*Work performed under the auspices of the U.S. Energy Research & Development Administration under contract No. W-7405-Eng-48.



Packed bed concept

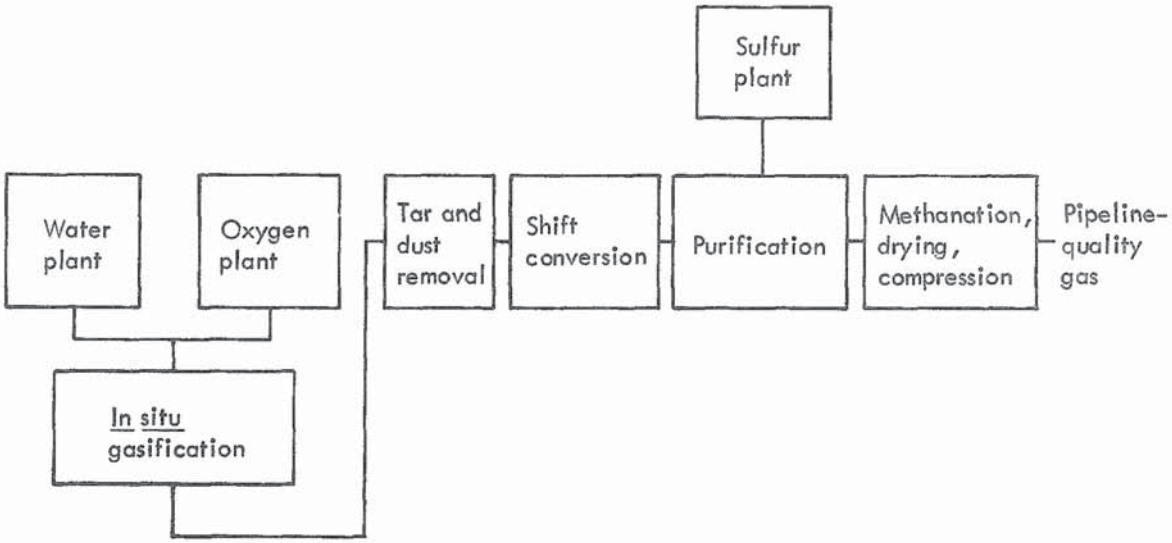


Fig. 1. Artists' conception and process diagram of one plan for a packed bed, in-situ gasification plant.

The surface facility for pipeline gas production will include oxygen-, water-, and gas-treatment plants. Water will be obtained from a suitable aquifer, stored in a pond, and pumped underground as needed. An in-situ gasifier may not require as much high quality water as a surface gasifier. Water requirements in general are expected to be less. Figure 1 is a schematic of one plan for an in-situ gasification plant.

SUMMARY OF RESULTS

We conducted a successful deep exploratory drilling program, which delineated potential coal sites in southeast Montana and northeast and southwest Wyoming. A deep site in the Powder River Basin of Wyoming and a shallow site at Hoe Creek, Wyoming were chosen for further characterization. Characterization of the shallow site provided the background for field gasification experiments.

We conducted a number of coal fracture experiments including a coal-outcrop field experiment in Kemmerer, Southwest Wyoming. Measured permeabilities and fracturing were in good agreement with preshot predictions from one- and two-dimensional stress-strain codes and serve as process design information for future field fracture experiments.

We gasified coal in 1-ft and 5-ft long packed-bed reactors with steam and oxygen and obtained gas qualities almost equal to those obtained in the Lurgi process. We also measured the progress of thermal waves and compared the data with our modeling calculations. We found that Wyoming subbituminous coals shrink upon heating and their permeabilities increase several orders of magnitude. Thus, it appears that swelling and softening of these coals will not cause problems in in-situ process operations, and, in fact, high temperatures will produce a desirable increase in permeability.

Modeling studies were initiated to consider convective instabilities, coal plasticity, and the effect of the spatial distribution of collection and production pipes on resource recovery. A one-dimensional reaction code, which included eight reacting species was developed and applied to results from the 5-ft reactor. Environmental models were developed for migration of water-soluble contaminants and for air quality. Adverse environmental consequences appear to be small. These laboratory experimental and modeling efforts, combined with the modeling and experimental fracturing work conducted at Kemmerer, provided the design bases for our planned Hoe Creek gasification experiment.

Two feasibility studies involving ERDA, LLL, and industry were conducted during the fiscal year. The objectives of the studies were to evaluate the commercial potential of the LLL packed-bed concept, to examine coal resources available for the concept, and to make recommendations for the R&D programs necessary to demonstrate the process. The feasibility studies with both Gulf Research and Development Company and Resource Sciences Corporation (RSC) resulted in favorable reviews. DuPont, American Oil Company, Rocky Mountain Energy Company and Pacific Gas and Electric Company are cooperating with RSC in the later study.

These independent studies identified three potential major advantages for the packed bed process. The first is that over 100 billion tons of deep, thick western coal are amenable for the process which would be otherwise not available for energy extraction. Most of this resource is in the Powder River Basin of Wyoming and Montana. The second is that pipeline quality gas can be produced for 60-70% of the cost of Lurgi gasification with reasonable sweep efficiencies (~70%) and moderate explosive requirements. The third potential advantage is that SNG should be produced via the packed bed process with less environmental consequences than by conventional surface gasification.

The following sections describe the LLL field program. The presentations by Rozsa and Thorsness, Butkovich, Campbell, and Gregg, Hill, and Olness describe our laboratory program in more detail.

SITE SELECTION

An exploratory drilling program, which was carried out from December 1974 to March 1975, led to the selection of the Hoe Creek site for LLL's initial shallow gasification experiment — see Fig. 2. Five sites in the Powder River Basin of Wyoming and Montana and one site in the Hams Fork coal region near Kemmerer, Wyoming were investigated. Shallow site selection criteria were:

1. Thick coal (15-50 ft thick)
2. Shallow depth (less than 300 ft)
3. Relatively flat coal bed
4. Low permeability overburden
5. No significant aquifer in the coal or overburden
6. Suitable terrain for surface plant operations
7. Close to utilities and all weather roads
8. Remote enough to avoid interferences with other operations

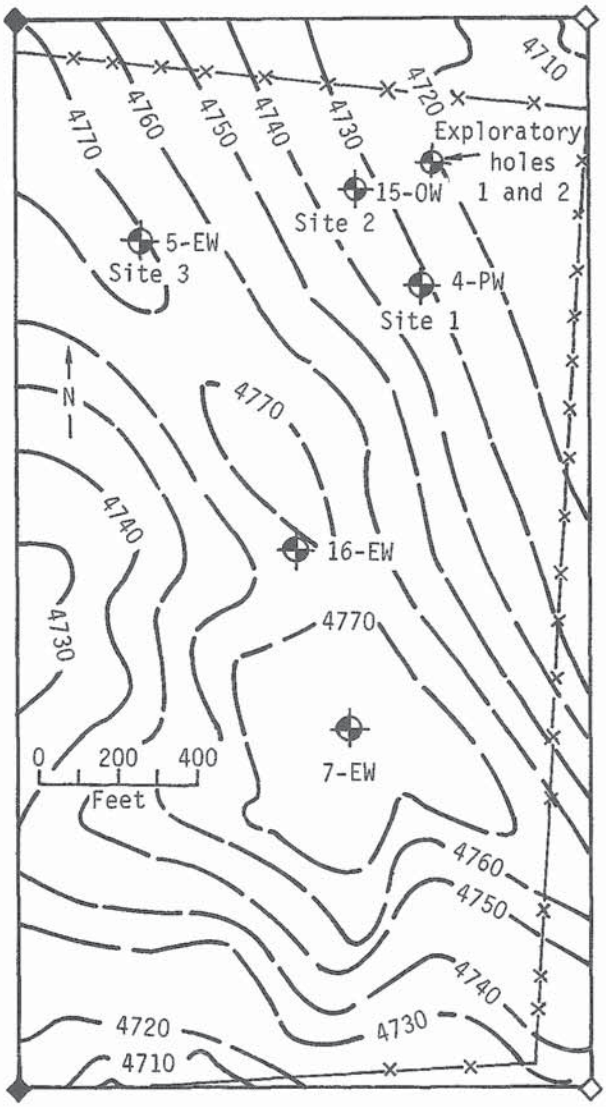


Fig. 2. Site characterization wells at the Hoe Creek site, Campbell County, Wyoming (W1/2 SW1/4 Sec. 7, T47N R72W). The contour interval is 10 ft.

SITE CHARACTERIZATION

The objectives of the characterization program were to determine: (1) near surface lithology (-250 ft), (2) the hydraulic characteristics (both horizontal and

vertical) of the coal bed and associated strata, (3) native fracture orientation in the coal bed, (4) hydraulic head as a function of depth and (5) native ground water quality. Results are shown in Fig. 3.

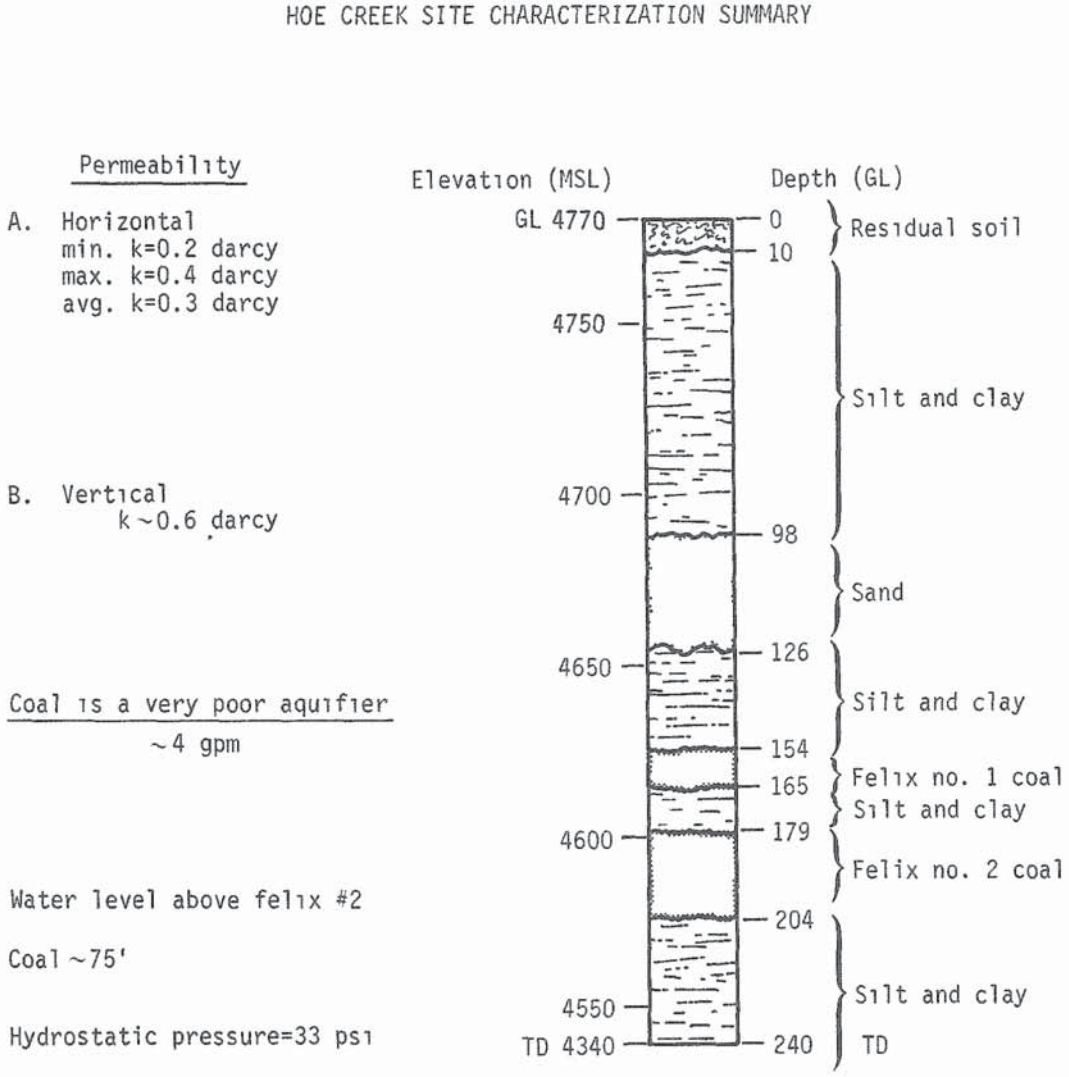


Fig. 3. Typical Hoe Creek site characterization information. The well log shown is from well 5EW at site 3.

In addition to the characterization work accomplished at sites I, II, and III, two other exploratory wells were drilled in an attempt to more closely define the deeper Wyodak-Anderson coal seam.

HOE CREEK EXPERIMENT NO. 1

Experiment No. 1 was a "simple 2-spot fracturing experiment" that was carried out at site I on November 5, 1975. It consisted of two -750 lb. explosive charges fired simultaneously at the bottom of the Felix #2 coal seam. The objectives of this experiment were to study the following, prior to committing the 5-spot test Experiment No. 2.

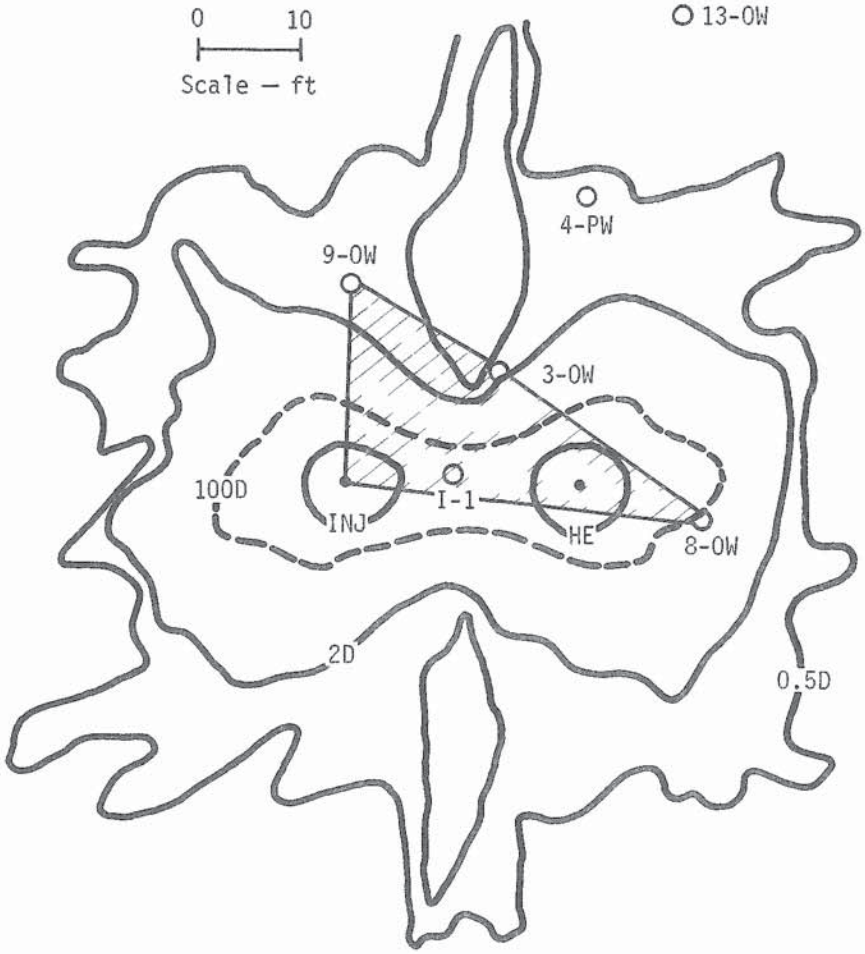
- Well and instrument survivability, post fracture drilling and well completion problems.
- Effects of two simultaneous explosions of the coal seam and overburden, with particular emphasis on post fracture coal permeability and air flow characteristics.
- Problems associated with gasification of the fractured coal.

Post fracturing it was determined that; instrumentation (thermocouples) could be located within 12 ft of an explosive charge without damage, steel cased wells suffered little damage except for cement bonds near the coal seam, all P. V. C. cased holes within 20 ft of an explosive charge suffered severe damage at the coal/overburden interface.

An instrument hole located between the two explosive charges was completed post fracture without problems. Its nearest approach to a charge was 11 ft.

An accelerometer array at the surface indicated a maximum displacement of .55 ft, and indicate spall to a radius of 425 ft. The maximum residual surface uplift was .2 ft. The total volume calculated from the residual uplift is approximately 2500 cubic ft.

A standard core barrel was run through the overburden and into the Felix #2 coal seam. About 1 ft of fractured coal was recovered. The core through the overburden did not indicate any vertical fracturing.



Plan view of Hoe Creek Experiment No. 1. The contours denote the predicted permeabilities. The shaded area denotes permeabilities of 1.5 to 4.0 D, as measured in hydrological tests.

Fig. 4. See text.

Post fracture characterization (using hydrology) is compared to predictions in Fig. 4. The data show stimulated coal permeabilities: from 0.3 d preshot to about 2 to 4 d postshot. The experimental data are consistent with the preshot predictions normal to the line connecting the two explosive holes but are lower by about an order of magnitude between the two charges.

The third goal, gasification of the fractured coal, was postponed because the communication between the injection and production wells was insufficient for successful gasification.

EXPERIMENT NO. 2

The 5-spot test designated Experiment No. 2 was in preparatory drilling work at the time of explosively fracturing Experiment No. 1. The drilling operation on this experiment was suspended December 2, 1975, due to the anomalous and unexpected permeability data obtained from Experiment No. 1.

HOE CREEK EXPERIMENT NO. 1: PHASE-2 PLANNING

Since there is essentially no flow from the injection well to the original production well we plan to gasify between the existing injection well and a new production well placed within the fracture zone at about the 2 darcy (D) boundary (see Fig. 5). We are planning a forward burn gasification from the injection well to the new production well after the coal in the fractured zone is dewatered. If forward gasification fails due to liquid plugging or insufficient gas flow, we plan to backward burn a high permeability path to the production well and then forward gasify.

We will ignite the coal in the injection well cavity near the top of the seam. If the high-permeability region is predominantly toward the bottom of the coal, and if the coal can be adequately dewatered, then the hot gas flow should proceed downward through the heavily crushed coal and outward to the production well. The drying and shrinking of the fractured coal by the hot gases should form a bed of broken coal with a large surface area.

DRILLING AND WELL COMPLETIONS

We are constructing the well plan shown in Fig. 5.

All of the new wells are within the calculated 2-darcy region where, presumably, considerable fracturing has taken place. The dewatering wells are arranged to surround the fractured zone.

The instrument holes are located so as to give burn profile information at several intervals along the expected flow path. Well 1-5 is to be completed as both an instrument and pump well, if possible. This is to allow for the large uncertainties in our present dewatering calculations.

Five core holes are being drilled to provide direct information as to the degree of fracturing caused by the explosions.

SUBSURFACE INSTRUMENT EMPLACEMENT

There are six new instrument wells. Two wells 1-1 and 1-2, were completed for Phase 1 and each already contains three thermocouples and a bubbler tube. The HE hole also has a pin-type water-depth gauge and a bubbler tube.

The new wells each contain seven thermocouples, a water-depth gauge through the coal, and a bubbler or pressure tube at the bottom of the coal. The dewatering and production wells have four thermocouples fastened to the outside of the casing.

We plan to try high-frequency electromagnetic attenuation (HFEM) measurements through the burn front during gasification. Results from this unproven experimental technique will be compared with thermocouple readings. We will use the existing plastic-cased wells, 8-OW, 9-OW, and 11-OW, for this experiment.

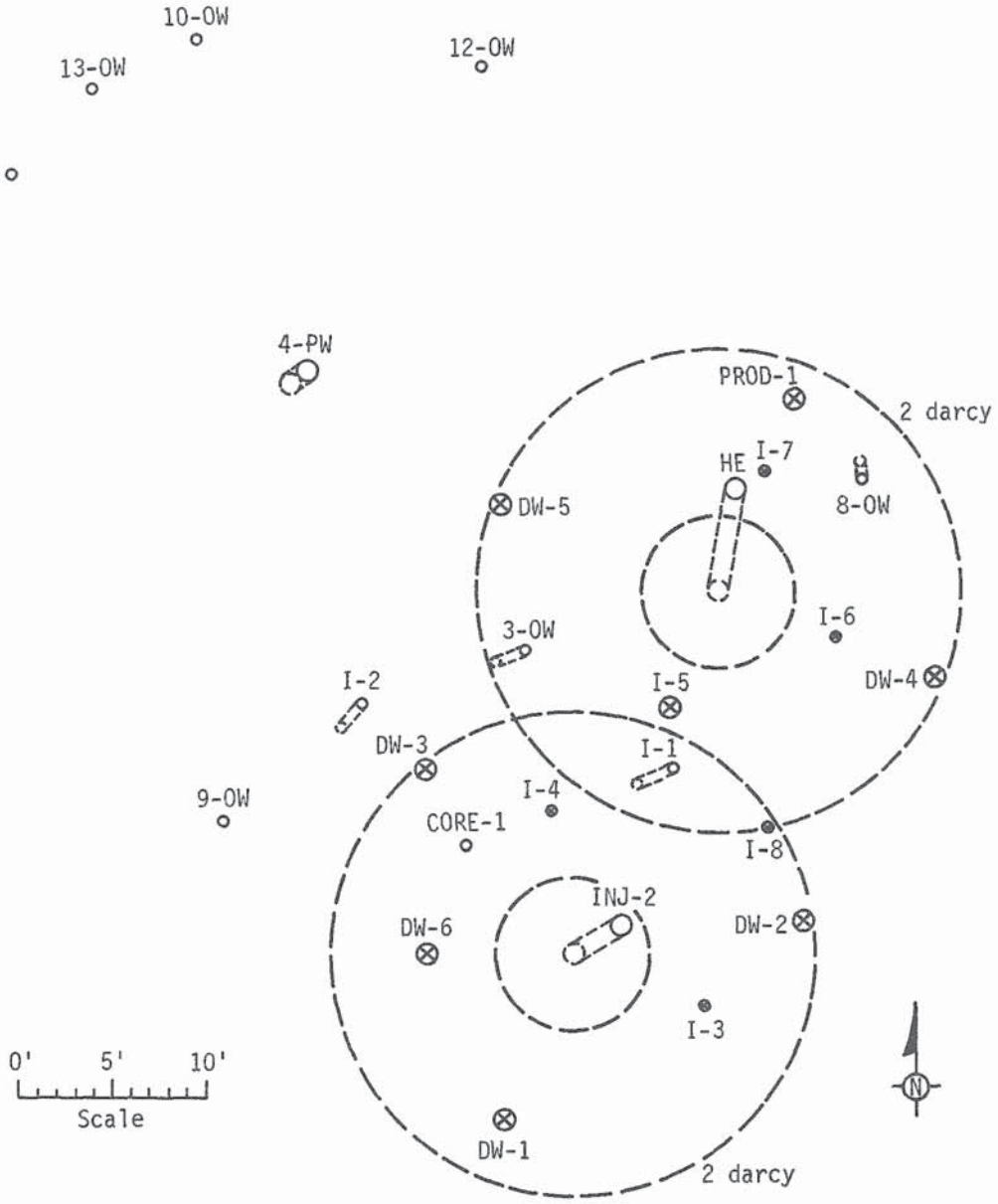


Fig. 5. Hoe Creek Experiment 1 phase 2 site plan. Existing holes shown as open circles with hole drift indicated by dashed lines. Wells to be drilled are indicated by crosses. Large circles indicate calculated postshot cavities and 2 Darcy permeability limits.

WATER PERMEABILITY TESTS

Three major areas in which permeability information is important are explosive fracturing effects, dewatering, and gasification. Because the explosively fractured region is heterogeneous, permeability characterization is difficult. Raw hydrology

data are reasonably straightforward to obtain and their reduction to permeabilities is also straightforward by means of homogeneous mathematical models; however, models that allow computations of two or three-dimensional permeability distributions are not yet perfected.

We will determine the overall and local permeabilities along the gasification path and to the dewatering wells with homogeneous models. We will then test to obtain data for evaluation of permeability change with distance from the injection well (an explosive charge location) for at least three radial distances in the sector away from the second charge. In these measurements we will conduct some tests by water injection as well as by pumped withdrawal. The injection results may be more comparable to those obtained at Kemmerer.

These tests will improve our ability to predict fracturing and permeability. We hope to get answers to some of the following questions:

1. Are there explosive interaction effects?
2. Is there a compacted region associated with the explosive charge?
3. Is there a high-permeability region, possibly 100 D, close to the explosive wells?
4. Is there a relationship between permeability and a calculable fracture parameter?

DEWATERING

Dewatering will proceed as a continuation of permeability testing. The goal is to lower the water level in the Felix No. 2 coal to near the base of the coal and maintain it there along a path between the injection and production wells for gas flow testing and gasification.

Prediction of the time required for initial dewatering is uncertain. Within 1 week we should know the effectiveness of the dewatering system and what we can gain by continued pumping for a reasonable time.

AIR FLOW TESTS

After dewatering and prior to ignition of the coal we will make a series of air flow tests at several injection pressures. These will give us improved guidance for startup and allow us to better estimate gasification times and preburn gas losses. These tests are to be made between the injection and production wells. During one of the air flow tests a gas tracer will be added to give an estimate of the gas-filled volume in the coal.

GASIFICATION

Our primary gasification goals are:

- Measure flow resistance during forward burn — How does the flow rate vary? Do liquid products plug the flow paths?
- Investigate gas override — Is the major permeability path along the bottom of the coal or did the HE lift the roof and provide a flow path along the top of the coal?
- Dewatering — How well can we dewater the fractured coal, and is that adequate for gasification?
- Study the effect of the rate of water inflow on gas quality — What happens if we shut off the pumps for a while?
- Burn front geometry vs time — Do we get a volume burn with a broad, flat burn front or does the burn form a long, narrow channel?
- Gas composition vs time — How erratic is the burn? At what point does oxygen breakthrough occur?
- Gas losses — A nitrogen balance will show the severity of gas losses as a function of time.
- Environmental issues — We need air quality measurements both on- and offsite during gasification. We need to monitor water pollution during the burn and for a long time after the burn.

DRYING-PYROLYSIS TIME

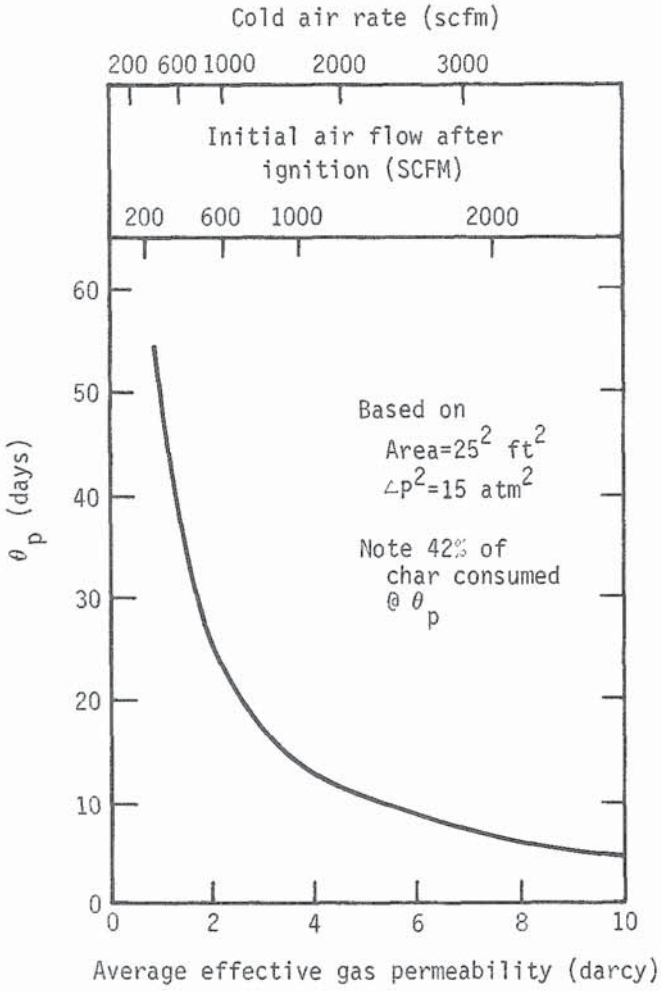


Fig. 6. Calculated time to dry and pyrolyse a coal block 25 ft wide, 25 ft high, and 32 ft long as a function of gas permeability, cold air flow rate and air flow rate right after ignition.

- Subsidence — Subsidence should not be a serious environmental problem for such a small experiment, but it may have an important impact on pipe survival during and after gasification.
- Resource recovery — Since there is no well-established boundary to this experiment, resource recovery as an area phenomenon is more or less a matter of definition. However, we can look for unburned coal within the burned-out region.
- As a contingency if forward gasification is unsuccessful: determine the effect of explosive fracture on backward burning — Both temperature profile and pressure-flow characteristics should be helpful in making this study.

After the gas tracer tests have been completed and a steady air flow has been reestablished through the fractured coal, an electric ignitor will be used to light the coal. If there is sufficient gas flow and liquid plugging does not become a serious problem, the gasification will be carried out entirely in the forward-burn mode.

Some of the system characteristics that will change during gasification and that can be measured are:

1. Product composition,
2. Gas losses,
3. Pressure drop across the formation,
4. Temperature response of the system,
5. Water influx rate,
6. Resource recovery.

However, we can only vary three parameters: flow rate, back pressure, and dewatering or water intrusion rate. Since we cannot decouple parameters completely, we will make only a few large changes in each one in an attempt to understand the effects of such change.

Some very crude estimates can be made for the time required for gasification and the flow rates to be expected by assuming a particular set of initial conditions. Figure 6 shows the time required to dry and pyrolyze all of the coal between the injection and production wells assuming a 25 × 25 ft cross section. The cold air rate is measured before ignition, while the initial air flow refers to the flow a few hours after ignition when the burn has been established. The time required to burn the remaining char is about 15 days assuming an air flow rate of 1000 scfm.

ENVIRONMENTAL TESTS

Very little experimental data are available concerning the environmental impact of in-situ processing. In order to adequately assess the impact of future large-scale projects we must learn all that we can from our small-scale experiment. We are planning a realistic program of water quality measurement from a series of wells to be drilled along the natural underground flow paths. Air quality will be monitored during the gasification phase of the experiment both as a safety precaution and for environmental data.

POSTBURN DIAGNOSTICS

After the burn has been completed and the area has cooled, a series of cores and/or logs taken at various locations will be necessary to define the lateral extent of the cavity and the character of the residue in the cavity.

SELECTED BIBLIOGRAPHIES

1. Higgins, G.H.: A New Concept for In Situ Coal Gasification, Lawrence Livermore Laboratory, Rept. UCRL-51217, Rev. 1 (1972).
2. Maimoni, A. and Stephens, D.R.: In-Situ Coal Gasification An Update of the National Research Program, Lawrence Livermore Laboratory, Preprint, UCRL-77102 (1975).
3. Mead, W., Ed.: LLL In Situ Coal Gasification Program, Quarterly Progress Report, July through December 1974, Lawrence Livermore Laboratory, Rept. UCRL-50026-74 (1975).
4. Stephens, D.R., Ed.: LLL In Situ Coal Gasification Program, Quarterly Progress Report, January through March 1975, Lawrence Livermore Laboratory, Rept. UCRL-50026-75-1 (1975).
5. Stephens, D.R., Ed.: LLL In Situ Coal Gasification Program, Quarterly Progress Report, April through June 1975, Lawrence Livermore Laboratory, Rept. UCRL-50026-75-2 (1975).
6. Stephens, D.R., Ed.: LLL In Situ Coal Gasification Program, Quarterly Progress Report, July through September 1975, Lawrence Livermore Laboratory, Rept. UCRL-50026-75-3 (1975).
7. Stephens, D.R., Ed.: LLL In Situ Coal Gasification Program, Quarterly Progress Report, October through December 1975, Lawrence Livermore Laboratory, Rept. UCRL-50026-75-4 (1976).
8. Stephens, D.R., Ed.: LLL In Situ Coal Gasification Program, Quarterly Progress Report, January through March 1976, Lawrence Livermore Laboratory, Rept. UCRL-50026-76-1 (1976).

9. Stephens, D.R., Ed.: LLL In Situ Coal Gasification Program, Annual Report Fiscal Year 1975, July 1974 through June 1975, Lawrence Livermore Laboratory, Rept. UCRL-50032-75 (1975).
10. Stone, Randolph and Snoeberger, David F.: Evaluation of the Native Hydraulic Characteristics of the Felix Coal (Eocene, Wasatch Formation) and Associated Strata, Hoe Creek Site, Campbell County, Wyoming, Lawrence Livermore Laboratory, Rept. UCRL-51992 (1976).

STATUS OF THE MERC IN SITU GASIFICATION OF EASTERN U.S. COALS PROJECT

by

L. Z. Shuck, J. Pasini III, J. W. Martin
and L. A. Bissett, MERC, ERDA

INTRODUCTION

The MERC underground coal gasification (UCG) project, initiated in 1971, and first funded in 1973, was designed to investigate the recovery of Eastern bituminous coalbeds in order to provide an energy source close to the high demand centers of the Eastern United States. It was clear in 1971 that UCG processes had never been theoretically analyzed or characterized, and that many different and contradictory concepts of the process mechanisms existed. There was an obvious need to develop the basic UCG technology to quantitatively and scientifically describe mechanisms which control the process in different rank coals and coalbed conditions. Many concepts remain controversial today, and mechanisms taking place, for example, in Lignite and subbituminous coals are often confused with those of bituminous coals. Before process optimization on such variables as BTU value, gas composition, energy out/energy in, cost per BTU or constancy of energy can realistically be considered, more basic knowledge of the processes in each type coal must be gained.

It was also evident that a more efficient scheme than radial flow-gasification was desirable, and perhaps necessary, for logistic and environmental reasons. Line drive techniques used for secondary recovery of oil in the petroleum industry and the longwall mining of coal suggested that a similar scheme should enhance UCG efficiency. Success in the Eastern U. S. also means simultaneous gasification of multiple, thin, undulating coalbeds. Other constraints prevalent in the Eastern U.S. such as dense populations and rugged terrain in the same areas of major coal deposits, which were already being extracted, required a new approach to UCG.

The successful development of a process with so many unknown mechanisms obviously required some means of gathering more detailed information than could be obtained from remote field experimentation. Thus, laboratory simulation experiments were planned to reveal the mechanical, physical and chemical mechanisms of the processes in different rank coals and under a wide variety of conditions. Thus, status of the technology and this rationale led to the design of a balanced program at MERC of theoretical, laboratory and field studies, including in-house research and contracts with industry and universities. The general organization scheme for pursuing these activities is illustrated in Figure 1. Resource characterization, linking methods, site development and environmental assessment will be described later under field results. Preliminary economic evaluations have been made [1,2] and will not be discussed further here. R&D technology transfer was planned through the direct involvement of industrial and university participation in the project. Industrial participation solicited early in the project development resulted in a cooperative agreement between the parties, Consolidation Coal Company, Continental Oil Company and MERC of the USBM at the time. This agreement provided that mineral and surface rights to the Pittsburgh coalbed be supplied by the industrial parties and that the field project be mutually developed. Other contracts and grants were let with universities and industry as illustrated in Table 1. Each of these contracts plays a key role in the MERC project for developing fundamental UCG technology.

References at end of paper

FIGURE 1

MERC UCG Project Management & Research Activities

Three primary mechanisms were identified as controlling factors to be better understood and characterized in a scientific manner. These mechanisms are reaction kinetics, structural effects on the process, and mass and energy transport phenomena. Contracts with universities shown in Table I were let to supplement the MERC in-house modeling and computational efforts.

UCG reaction kinetics grants and contracts have been in effect at Penn State University since 1973. The objectives of these studies are to develop predictive, simulation models of analytical and numerical type for both the stream and through-borehole and the filtration or permeation type UCG process conditions. The through-borehole simulation models are used to estimate process control parameter effects and ranges such as the axial to transverse burn velocity ratios for ignition of long boreholes in either forward or reverse burn modes. Numerous other valuable design data such as gas compositions and temperature distributions as functions of borehole dimensions can be generated. Results of this study have been presented [3, 4, 5] and will be updated later in this symposium.

Structural effects of the UCG process are only considered in the literature with respect to subsidence of the overburden and its environmental impact. On the contrary, the tectonic and thermal stress effects upon the in situ gasification process have been identified in the MERC studies as one of the principal controlling factors. The tectonic stresses in combination with thermally induced stresses are believed to be of major consequence in the rate oxidizing fluids penetrate, and the products are disposed from, the moving boundaries of the reaction zone. Somewhat as in longwall mining, the planned collapse configuration of the overburden structure on the viscoelastic, partially devolatized and gasified coal bed can greatly enhance total resource recovery efficiency, and perhaps gas quality. Permeability modifications also, as a result of the induced stresses, can be investigated. These studies have been underway for two years using numerical computer codes developed at West Virginia University [6, 7, 8], and recent results will also be discussed later here in the program.

The other fundamental UCG mechanisms include energy and mass transport processes. The flow of fluids under gravity, free and forced convection and diffusion through, to and from the coalbed are ctitical to an understanding of reservoir response times, gas losses, water penetration and general process control and optimization. The flow of fluids and thermal energy must be investigated under widely varying conditions and temperature ranges to place the process upon a scientific basis. A contract to investigate these mechanisms has been in effect for over a year at West Virginia University.

In situ process monitoring is critical in the R&D phases of UCG. Few measurement techniques though lend themselves to the disclosure of unique process characteristics. The MERC project reflects more emphasis on real time monitoring and control systems. One promising technique for monitoring in-the-plane changes, as introduced by an advancing reaction zone or changing fluid volumes, is being investigated at West Virginia University. This technique utilizes radial scanning electromagnetic wave transmission and reflection principles to detect such effects as water and tar movements and the gasification zone interface. The basic effect upon which the technique is founded is that coal electrical wave propagation constants, such as electrical conductivity, change by several orders of magnitude. Typically, the electrical resistivity may decrease from 10^5 ohm-meter to less than 1 ohm-meter during the phase transitions. This work will be described later by Dr. Balanis in more detail.

The major contractual work and budget expenditures have been for field development. Contracts have included the drilling of three vertical wells and one deviated well, cleaning out and plugging back to the coalbed one vertical well, and general site construction and maintenance.

Other contracts have been let to assess advanced techniques of drilling holes in coal. The ability to use conventionally drilled vertical wells down to the coalbed and then drill straight holes parallel to and through the coalbed, perhaps connecting other vertical wells has advantages over all existing gasification schemes and can also provide another means of establishing a longwall generator. A. U. S. patent has been issued on a method of laser drilling to privide such an alternative means of linking [8]. Some preliminary coal drilling experiments with a commercially available one-kilowatt CW CO_2 laser beam demonstrated that if the gas generated could be disposed into the coal, drilling rates up to 2-3 inches per second of approximately 1/8 inch diameter holes could be achieved at an actual laser operating cost of $3.00 per hour. Based upon the preliminary drilling experiments, each rank and type coal has drastically different drilling characteristics which suggests custom procedures for each coalbed. The Pittsburgh bituminous, Hanna subbituminous, Texas lignite, anthracite and other coals along with oil shale were tested in the laser drilling effects experiments.

References at end of paper

TABLE I

MERC UCG PROJECT CONTRACTS

ORGANIZATION	CONTACT OR PRINCIPAL INVESTIGATOR	TPO	TELE. NO.	ADDRESS	CONTRACT NO.	INITIATION DATE	TERMINATION DATE	CONTRACT TITLE
WVU	Dr. S.H. Advani	LZS	(304) 293-3111	525 Engineering Sciences West Virginia University Morgantown, WV 26506	E-(40-1)-5088 $165,085 (155,517)	05-01-76	04-30-79	Structural Mechanics Simulation Associated with UCG
WVU	Dr. Gordon Hopkins	LZS	(304) 293-3111	Engineering Sciences West Virginia University Morgantown, WV 26506	GO 155034 $15,000	12-74	05-31-76	Simulation of Fluid Flow Associated with UCG
WVU	Dr. H.W. Butler Dr. S.H. Schwartz	LZS	(304) 293-5360	327 Engineering Sciences West Virginia University Morgantown, WV 26506	E-(40-1)-5080 $79,771	06-01-76	04-30-77	A Study of Thermal and Fluid-Mechanical Aspects of UCG
WVU	Dr. C.A. Balanis	LZS	(304) 293-5180	929 Engineering Sciences West Virginia University Morgantown, WV 26506	E-(40-1)-5081 $33,263 (29,996)	05-01-76	04-30-77	Feasibility Study of Electromagnic Instrumentation for In Situ Gasif. Appl.
WVU	Dr. R.R. Haynes Dr. W.R. Powell	LZS	(304) 293-3770	Engineering Sciences West Virginia University Morgantown, WV 26506	GO 155031 $23,507	12-31-75	04-30-76	Dynamic Reflective Photoelasticity Study of Rock Fracture Mechanisms
Physics International	Nancy Sheppard Contract Admin.	LZS	(415) 357-4610	2700 Merced St. San Leandro, CA 94577	E-(46-1)-8002 $3,000	05-05-75	Continuing	Pisces Codes
ERDA Berkley Computer Center, Univ. Calif.	Eric R. Beals S. Moore	LZS	415-843-2740 FTS 88-415-843-5351	Lawrence Berkley Laboratory Univ. of California Berkley, CA 94720	W-7405-ENG-48 $4,000 ($1,700)	01-19-76	09-30-76	Computer Rental
ROCKETDYNE DIV.	Dr. Stanley Gunn	LZS	88-508-884-3466	6633 Canoga Ave. Canoga Park, CA 91304	E-(46-1)-8037 $10,000	03-01-76	05-01-76	Laser Coal Borehole Dril. Tech.& Feasibility Asses.
ROCKETDYNE DIV.	Dr. Stanley Gunn	LZS	88-508-884-3466	6633 Canoga Ave. Canoga Park, CA 91304	E-(46-1)-8049 $7,933 (7,345)	07-01-76	09-02-76	Laser Drilling in Coal Samples
Chisler Brothers	Bob Chisler	GER	(304) 879-6522	P.O. Box 101 Pentress, WV 26544	E-(46-1)-8026 $39,400	10-23-75	06-30-76	Clean Out Snodgrass Abandoned Well
Chisler Brothers	Bob Chisler	GER	(304) 879-6522	P.O. Box 101 Pentress, WV 26544	E-(46-1)-8032 $73,200 (orgin.)	12-09-75	12-08-76	Service Project
Penn State Univ.	Dr. Farouq Ali	LZS	88-455-0101	26 Mineral Industries Bldg. Penn State University University Park, PA 16802	E-(40-1)-8018 $50,000	07-01-75	06-30-76 N-C EXT 08-15-79	Modeling & Computer Simul. of Reac Kinetics Assoc. w UCG
Paramount Exploration, Inc.	Harold Rosenberg Jim Fritz	JPIII	212-838-3413 412-627-6144	Box 551 Waynesburg, PA 15370	$939,600	07-01-75	06-76	Drill Deviated Hole

From the encouraging results of these effects experiments, a technology assessment contract was let to the Rocketdyne Corporation. From the conclusions of the technology assessment study, it was decided to further pursue the technique with some well defined laboratory drilling feasibility tests. One of the major objectives of this latter contract is to determine the actual pressure difference required as a function of beam intensity and drilling rate to displace the high temperature liquid and gaseous products into the existing and newly created fractures in the coal. In the process of drilling holes over 20 feet in length, it is anticipated that intermittent drilling and fluid injection-hole scavenging will result in the optimal drilling rate per unit of power required and per unit cost.

THE LONGWALL GENERATOR (LWG) CONCEPT

The objective of the MERC UCG project is to develop a feasible scheme of gasifying in situ the Eastern bituminous coals under the various prevailing constraints. The scheme must be realistic in terms of commercial large scale development to have any impact upon the Eastern U. S. energy problem. A realistic scheme cannot be based upon closely spaced vertical wells and must be specially suited for bituminous coal characteristics.

The field project is designed to utilize new directional drilling technology in the Eastern, thin, bituminous coalbeds in order to develop a new general UCG scheme known as the Longwall Generator (LWG) Concept [9], illustrated in Figure 2. The LWG concept is often misunderstood due to the flexibility and large number of variations possible, some of which have been publicized and investigated experimentally and theoretically at MERC. The LWG is the only known scheme which satisfies the topological and environmental constraints in the Eastern U.S., makes maximum use of the tectonic stress field, and has a maximum theoretical sweep efficiency of 100%. The LWG can be developed for forward or reverse gasification, for filtration or stream methods, with or without lateral gas removal, and all possible combinations of these basic modes. Certain schemes have not been publicized due to patentability investigations. Various geometry or modifications to the basic LWG considered to accommodate different field initial and operating conditions are as follows:

(a) Directional, parallel holes drilled down to and through coalbed and back to the surface for medium depth coalbeds.

(b) Directional, parallel holes drilled only down to and through the coalbed.

(c) Directional, parallel holes drilled down to and through coalbed and intersected at end with a vertical hole.

(d) As in (b) and (c) with vertical monitoring and control wells.

(e) As in (b) with hydraulic fracturing between wells.

(f) As in (d) with hydraulic fracturing in vertical wells.

(g) Laser drilled horizontal holes (from vertical conventionally drilled holes) and liquid explosive enlargened to provide similar LWG schemes, as shown in Figure 3.

In these schemes, the fluids are forced through the coalbed in a forward or reverse mode called "diffusive", "permeation", or "filtration" gasification as differentiated from the "stream" or "through-borehole" method.

Using combinations of directional and laser drilling along with "through-borehole" or "stream" gasification, numerous other geometries are possible as illustrated in Figure 4. The combined directional and laser drilling linking methods create a LWG same as the Linked Vertical Well (LVW) method but with positive directional control. Combinations of "stream" and "filtration" gasification in forward and reverse modes for the geometries shown in Figure 2 may be most effective in the swelling, coking coals. The effects of tectonic stresses and directional permeabilities can be fully utilized with these schemes.

The LWG scheme currently being developed is shown in Figures 2 and 5. There are several options for preburn bed characterization and gasification with the two parallel, directionally drilled holes and each with a vertical hole intersecting at the blind end. This versatility is important in developing the best scheme for particular coalbed conditions such as slope, water influx rate

Reference at end of paper

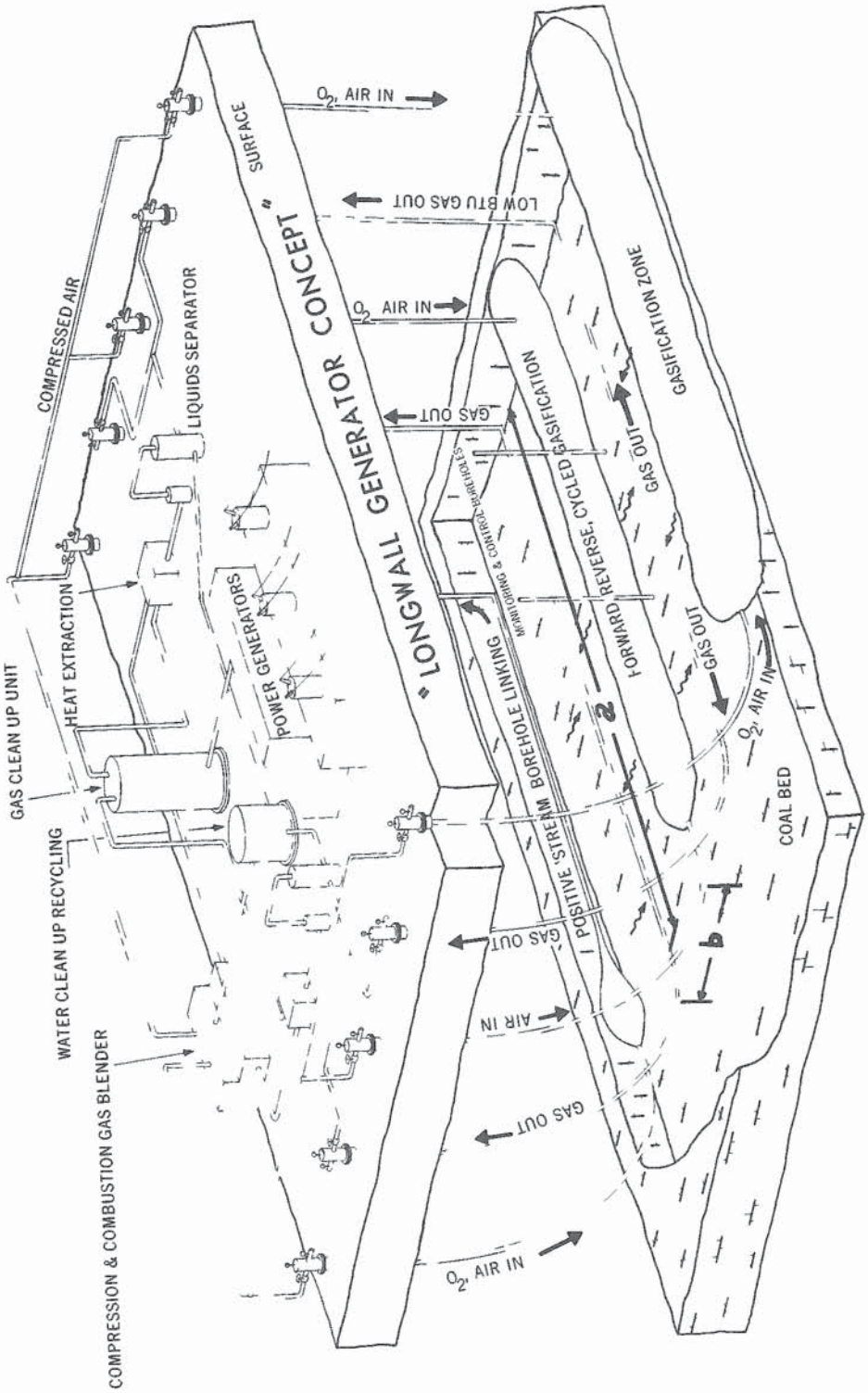


Figure 2. - One Variation of the Longwall Generator Concept

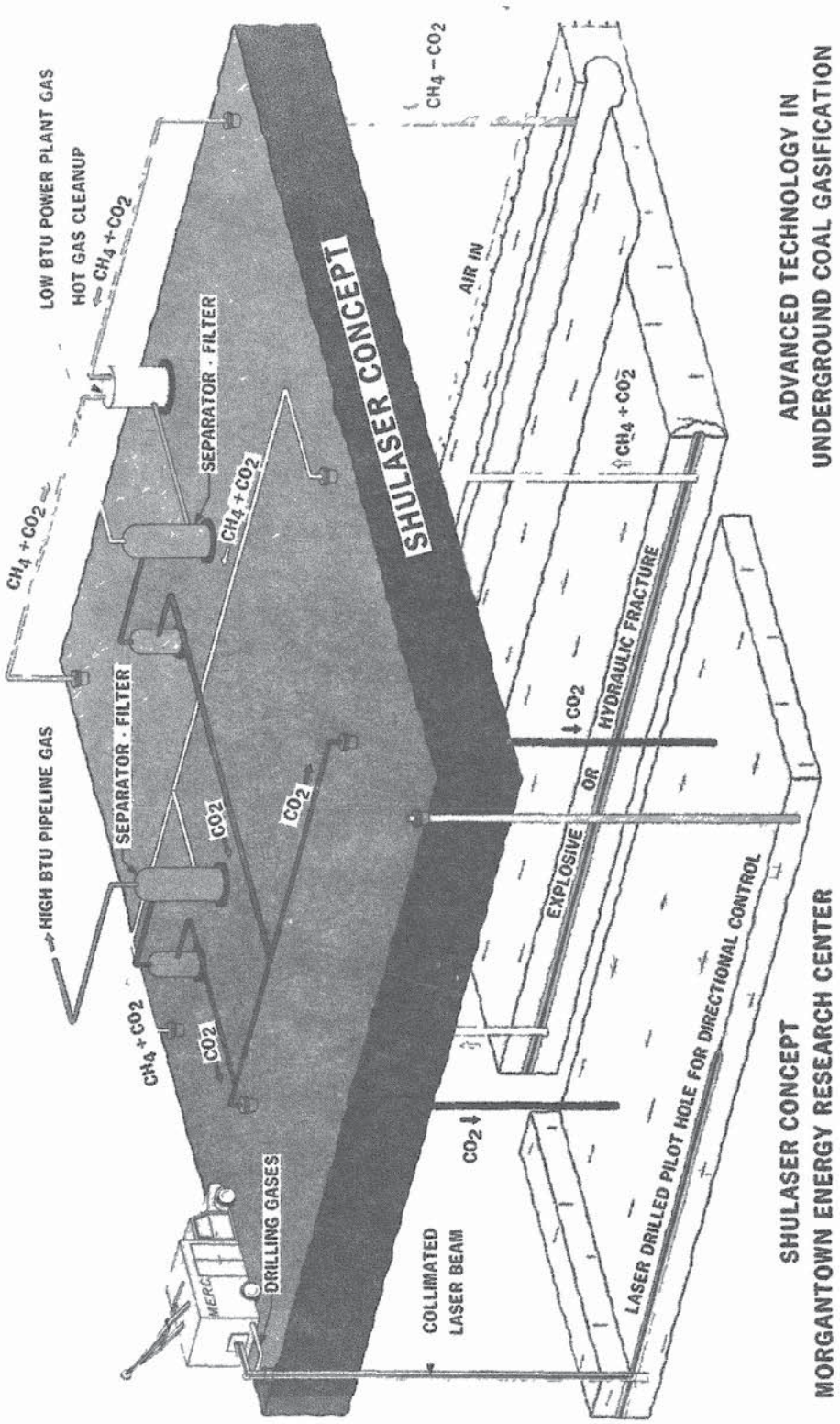


Figure 3.- Laser Drilled, Horizontal Pilot Holes for Creating a Longwall Generator

and directional mechanical and flow properties. Different options would be exercised also depending upon such coal properties as swelling or shrinking upon heating, volatility, reactivity, and coking characteristics.

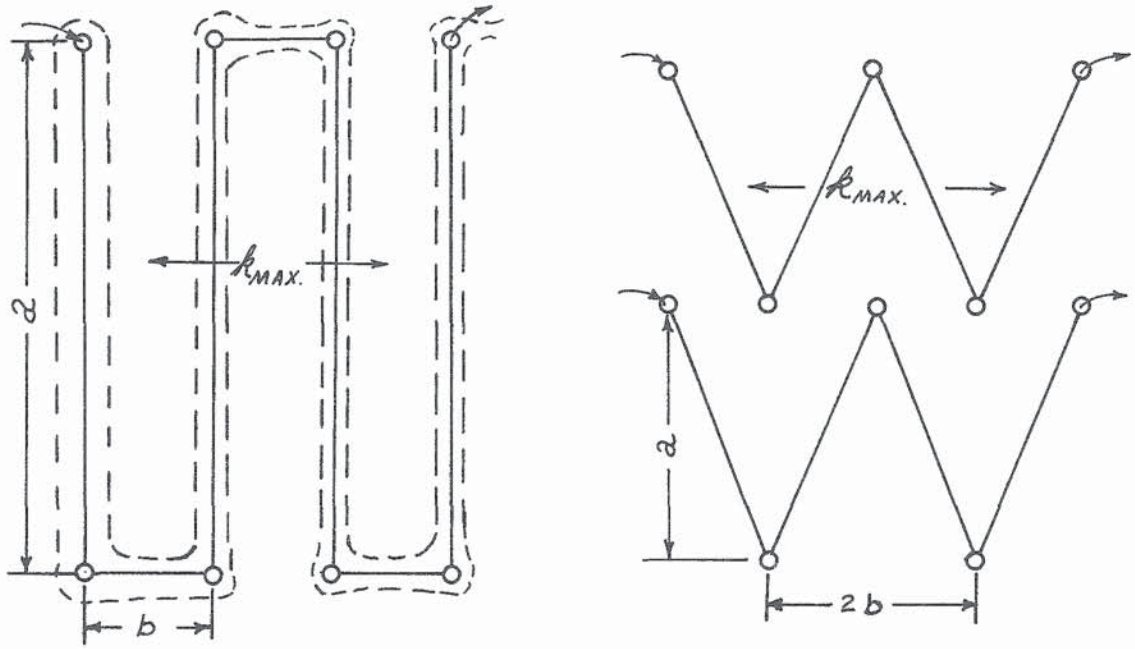


Figure 4

Rectangular and Triangular Patterns for Combinations of Stream and Filtration Gasification Schemes

Selection of the best combination can be made on the basis of one or more variables which may be chosen for process optimization. Uniformity of an advancing burn profile under the filtration method is a stability problem. As a result there are combinations of coal properties that result in linearly unstable profiles called channeling or fingering. Shrinking, reactive, noncoking coals fall into this category as will be discussed later. One profile stabilizing effect of the LWG is independent of all the coal properties except the directional mechanical properties. This stabilizing effect is due to the process induced stresses resulting from the LWG geometry. The phenomenon of "rock bursts" and other coal fracturing due to material removal during mining and the increased stress intensity near free surfaces is well known. The magnitude of the induced tectonic stresses of interest is a monotonically increasing function of the radius of the cavity or the arch effect of the roof. The linear LWG geometry being theoretically of infinite radius provides the maximum stresses for maintaining a uniform linear burn profile of all the possible UCG geometrical schemes. The significance increases approximately linearly with depth at the rate of one psi/ft. The ultimate strengths of coal along the cleat planes are exceeded typically below 500 feet for most Eastern coals. Thus, depending upon the overburden structure the coal is fractured at the thermal interface and the coke formed is squeezed to flow with less than 30 psi stress in the direction of the advancing burn zone. Ideally the roof subsides uniformly as a wave moving with an advancing slope which is determined by the coalbed thickness and the overburden and coal temperature-dependent, mechanical properties. Obviously, the stresses effective in advancing a fractured interface decrease from a maximum with a straight line to a minimum of zero as the radius of a perturbation, channel or effectively the arch length approaches zero.

Step D in Figure 5, the production of CH_4, is performed only for a period of a few months for the purpose of directional flow bed characterization and to drive some compressors to defray part of the compression costs. Earlier plans to reinject CO_2 separated from combustion products have been discontinued pending further laboratory studies. In the single lab test conducted to date with preburn

CO_2 injection, it was not possible to ignite the coal sample during 16 hours of heating even after creating a vacuum to remove the CO_2. Under otherwise similar conditions, the samples were ignited in less than two hours. This experiment will be discussed later under laboratory studies.

Prior to coal ignition much reservoir data must be obtained. Of fundamental importance to process understanding, modeling and control is the rate of water influx as a function of reservoir and wellbore pressures. These data, along with effective permeabilities, can be obtained through "draw-down" pumping tests wherein rates, pressures and water levels are measured. This would appear to be a necessary step in any experimental or production test when the coalbeds are not steeply dipping.

Use of directionally drilled holes can reduce surface degradation and environmental impact equal to or less than conventional oil and gas well drilling patterns, whereas vertical well UCG schemes require drilling on less than 100 foot square network spacing. Such spacing would not only totally destroy the surface environment, but would also not be feasible in much of the Eastern U. S. terrain overlaying major coal deposits.

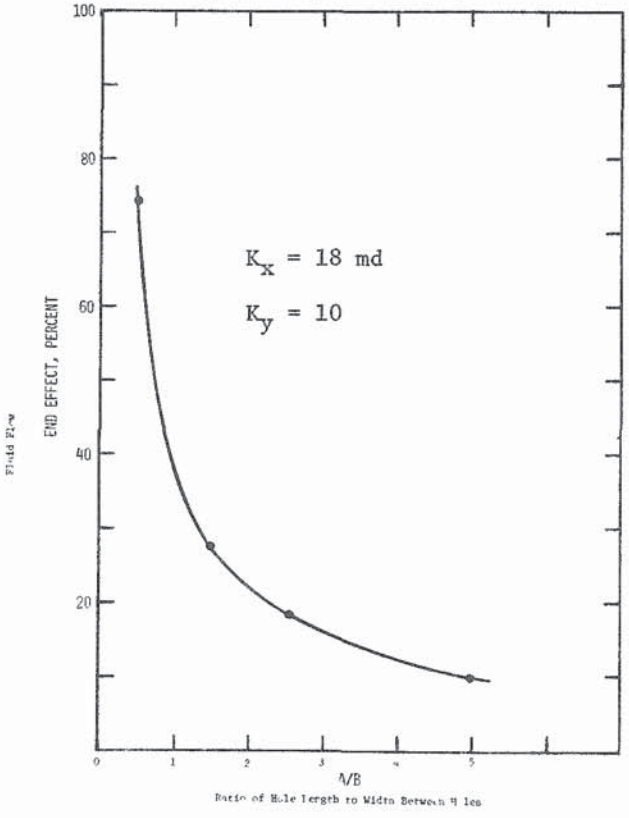
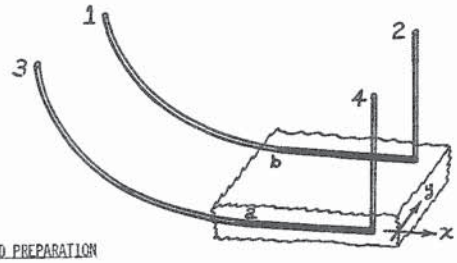


Figure 6

Illustration of the Whole Length to Whole Spacing Ratio upon Fluid Losses Outside the Recovery Zone



I. BED PREPARATION

A. PUMP WATER OUT OF 4
B. PRODUCE CH_4 OUT OF 4
" " " " 3 AND 4 (LOW P.P.)
C. PUMP WATER OUT OF 2
D. PRODUCE CH_4 OUT OF 2
" " " " 1 AND 2
" " " " 1 AND 1, AND 3 AND 4
E. INJECT AIR IN 1 OR 2 UNTIL O_2 ↓ AND CH_4 ↑ IN 3 AND 4
F. " " " " " " H_2O CONTENT ↓ " " " "
G. MISCELLANEOUS PRESSURE INTERFERENCE AND OTHER TESTS BETWEEN STEP A AND G

II. WELLBORE IGNITION

A. DECREASE AIR RATE IN 1 AND 2 TO PRESET VALUE
B. VENT 3 WHILE HEATING 4
C. INJECT IN 3 AND REVERSE BURN FROM 4 TO (a)

III. BLOCK REVERSE BURN

A. WHEN IGNITION REACHES (a) CHANGE MODE
B. INJECT IN 1 AND 2 AND PRODUCE GASES OUT 3 AND 4

Figure 5

The MERC Longwall Generator Development Scheme (1/2 unit shown)

Similar directional drilling techniques formed the basis for large industrial UCG projects planned after 30 years of process development in the Soviet Union in the early 60's and prior to their discovery of large natural gas reservoirs.

Rows of parallel deviated holes drilled in excess of 1,000 feet apart should greatly improve the sweep or total resource recovery efficiency. Different network spacing ratios of length to width, a/b as shown in Figure 2, were considered to evaluate fluid flow patterns. Results of calculations using the MERC field project design data are shown in Tables II and III. Figure 6 illustrates that when the length-to-width ratio is greater than 5, the flow to other areas in the coalbed under such conditions is less than 10 percent. This 10 percent loss corresponds to 100 foot spacing between the two 500 foot long holes of the planned field project with an assumed directional permeability ratio of 18 to 10 md or 1.8.

Large(L/D > 1,000)borehole ignition presents a separate problem to be analyzed. It is desirable to have the entire length ignited uniformly prior to forward or reverse gasification between parallel boreholes. Three methods of borehole ignition have been considered.

Table II. Comparison of Stabilized Gas Flowrates Between Horizontal Boreholes in Coalbed Obtained from Linear Steady-State Equation and One-Dimensional Gas Reservoir Simulator

T(°F)	k(md)	P_{in}(psia)	P_{out}(psia)	Stabilized Flowrate(SCF/day) from Steady-State equation	Stabilized Flowrate(SCF/day) from Gas simulator	Percent Difference
100	10	600	100	1,070,663	1,065,179	-0.510
300	10	600	100	788,910	784,896	-0.510
100	10	600	300	826,963	825,831	-0.140
300	10	600	300	609,405	608,474	-0.150
100	10	500	100	734,214	731,459	-0.370
300	10	500	100	540,960	538,961	-0.370
100	10	500	300	489,426	489,475	0.010
300	10	500	300	360,630	360,655	0.007

Table III - Two-Dimensional Gas Flow Between Horizontal Boreholes

in Coalbed After 46 days

Pore initial = 200 psia μ = 0.02 cp
Pore in = 500 psia Z = 0.98 h = 6 ft.
Pore out = 100 psia T = 100°F Kx/Kv = 1.8

No.	Job	Hole Length "a" (Ft)	Kx (md)	Ky (md)	Q in (SCF/day)	Q out (SCF/day)	One-Dim.* Steady State Flow, Qss (SCF/day)	End Effect (Actual) Q out-Qss	a/b	End Effect (percent) Q out-Qss x 100 / Qss
1		500	90	50	8,278,488Δ	7,320,938Δ	6,592,500	728,438Δ	5	11.0Δ
2		500	18	10	1,664,584	1,449,928	1,318,500	131,428	5	10.0
3		500	3.6	2	343,064	286,070	263,700	22,370	5	8.5
4		150	90	50	3,227,332Δ	2,578,340Δ	1,977,750	600,590Δ	1.5	30.3Δ
5		150	18	10	653,036	504,870	395,550	109,320	1.5	27.6
6		150	3.6	2	134,948	97,274	79,110	18,164	1.5	23.0
7	43	50	18	10	347,390	229,964	131,850	98,114	0.5	74.4
8		250	18	10	944,072	774,544	629,250	115,294	2.5	18.3

* Based on 732,500 (avg. from Table II) for Kx = 10 md and Hole length(a) = 500 ft.

Δ Boundary effects present

(a) The use of solid or liquid propellant with built-in oxidizer injected into coal borehole and ignited at one or both ends at regular intervals.

(b) The use of a concentric tube expendable gas burner or a retrievable, slowly traversing gas igniter.

(c) A through borehole forward or reverse burn to propagate a flame front along the entire length of the hole prior to changing from through-borehole stream to the filtration burn mode.

This latter method is in many respects the most desirable if the ratio of axial to radial burn velocity can be controlled between 10 and 100. Although several variables influence the control of this ratio, perhaps the single most important one is whether the coal is a coking and swelling type or a noncoking, shrinking type.

A proposal from United Technology Corporation was submitted to ERDA in November, 1974, to study the ignition problem and generate experimental and empirical design models of cases (a) and (b). This proposal has not been funded to date, so these two methods have not been technically evaluated. Method (c) has been only partially evaluated due to limited resources. Calculations from the numerical models generated under ERDA Contract E-(40-1)-8018 by Dr. Farouq Ali, PSU, predict that a nominal 3.12 foot diameter hole would result by the time the burn front travels from one end to the other of an initially 4-3/4 inch diameter hole, 500 feet long. Small scale laboratory tests on Pittsburgh bituminous coal samples at the same average air velocity of 7.5 feet per second yield an axial burn front velocity of 0.5 ft/hr which would require 1,000 hours or 41.7 days for through-borehole ignition of the entire 500 foot hole and less than 1/3 this value for the radial burn velocity.

Thus, for the Pittsburgh coal, method (c) is the only method partially evaluated. Similar experiments conducted on Texas Lignite indicate entirely different results. Radial burn velocities remain on the same order as axial velocities. The apparent explanation is that the highly reactive coals shrink, crack and completely gasify, leaving a void behind, whereas the Pittsburgh bituminous coal swells, expels liquids and forms a porous matrix of coke which is not readily gasified. This coke layer provides a mass and energy transport barrier which greatly retards the radial burn velocity, since counter-diffuse flow of the oxidizer and products of reactions must transpire through this matrix. With lower air velocities, as the hole diameter upstream increases, the erosive effect becomes negligible and the coke layer becomes increasingly more of a barrier until upstream radial burn velocity approaches zero and flame extinction is possible while burning continues downstream. These distinctions in behavior of different coals under in situ gasification conditions are still frequently confused or disregarded. Such observations and hypotheses were made from MERC laboratory experiments two years ago and presented at the First Annual UCG Sumposium at Laramie, July, 1975. Unfortunately, the asymptotic radial burn velocity values and upstream flame extinction as functions of hole diameter cannot be realistically evaluated in the laboratory due to small scale effects.

In general, this problem is one of non-stationary fields, reacting multi-specie boundary layers, multiple phase transitions in a fissured, nonisotropic medium. The coal is not in any sense a classical porous medium with an invariant structure. Phase transformations destroy the initial structural-flow properties and generate a new set of space, stress and time dependent properties behind the advancing front. These basic regimes are idealized as discrete zones illustrated in time frames 1 through 4 in Figure 7 and in detail in Figure 8.

The virgin coal ($R > R_4$) is not an isotropic porous medium, but composed of orthogonal cleat systems and fissures which may be preferentially opened or closed by directional thermal and tectonic stresses. If the cleats were randomly oriented and of random size, in the limit as the cleat spacing becomes small, the assumption of porous medium becomes plausible. However, the face cleats may be continuous up to a few feet resulting in structured flow similar to parallel flow between impermeable laminations with occasional discontinuities. Flow in these fissures is best described by capillary flow models. The coke zone ($R_2 \geq R \geq R_1$) can more realistically be represented as a porous, permeable medium.

The radial burn velocity is controlled by flow through this coke zone which is governed by several driving forces. For the purpose of simply discussing the most significant forces in a quantitative manner, some gross assumptions are necessary. In the simplest case of steady state, single

phase, non-reacting, two-component mass transfer, two mass potentials are readily identified:

1) Forced convection due to the pressure gradient ∇P, or as usually stated in one dimension,

$$\text{Darcy's Law, } \dot{m} = -\frac{k}{\mu}\frac{\Delta P}{\Delta R} \simeq \frac{k}{\mu}\frac{P_3 - P_2}{R_3 - R_2} \qquad (1)$$

$$\text{which is also} \simeq \frac{k}{\mu}\frac{P_2 - P_1}{R_2 - R_1} \qquad (1a)$$

and

2) Diffusive transfer due to species concentration gradients ∇C_i. Assuming only two species O_2 and CO_2 in equimolar counterdiffusion, the mass flux is given by Ficks Law

$$N_{O_2} = -D\,\nabla C_{O_2} \qquad (2)$$

where D is the diffusion coefficient. Although kinetic theory gives a basic expression for D,

$$D = \frac{bT^{3/2}}{P(V_{O_2}^{1/3} + V_{CO_2}^{1/3})^2}\sqrt{\frac{1}{M_{O_2}} + \frac{1}{M_{CO_2}}} \qquad (2a)$$

other empirical expressions provide better agreement with experiments. There are obviously many mechanisms whose relative effects are not disclosed by this simple model. They need to be evaluated, if possible, under controlled experimental conditions, and compared with progressively more models.

The steady state thermal energy transport is, by conduction,

1) Fourier's Law $q_k = -k\,\nabla T$ (3)

2) convection, $q_c = -h\,\Delta T$ (4)

and

3) radiation, $q_R = \sigma F_{i,j}(T_i^4 - T_j^4)$ in the porous coke (5)

zone ($R < R_2$) depending upon confining stress and the resulting porosity.

Other driving forces and phenomena must be investigated in this process, such as:

(a) Thermal diffusion known as the Soret effect.

(b) Other coupled phenomena such as heat flux due to a concentration gradient or the Dufour effect.

(c) Distributed source and sink terms due to phase changes and chemical reactions.

(d) Effects of 3-phase multi-component mass transfer upon the mass transfer coefficients.

(e) Energy and mass transfer within each phase as well as between phases.

Methodical comparison of well defined and controlled laboratory experiments with different models incorporating the effects separately can hopefully reveal the controlling or most significant driving forces and effects. This is one of the principal objectives of the MERC In Situ Hydrocarb Recovery Simulation Laboratory. There are, however, formidable problems in conducting well define and instrumented experiments that reveal the information needed. Thus, initially attempts were made to measure overall effective heat and mass transfer coefficients. Some of this work will be

described later by Pellegrin.

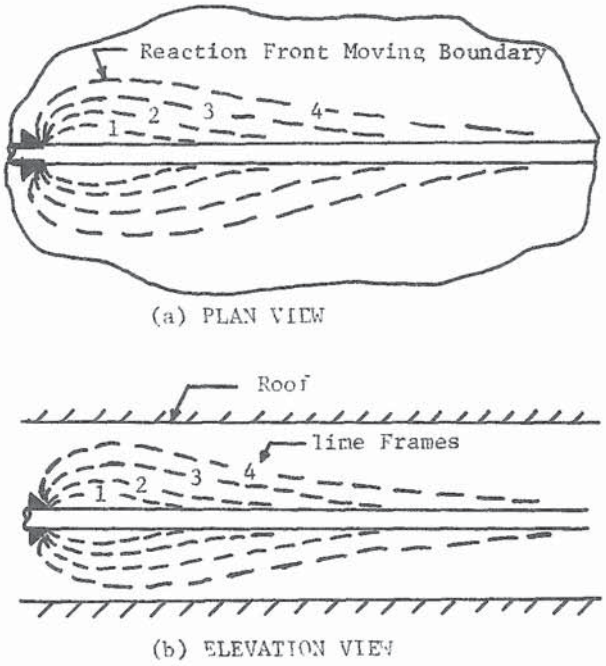


Figure 7

Through-borehole Ignition Burn Profiles

Realistic models of the stream gasification scheme do not exist and this is one of the reasons for contracts E-(40-1)-8018 and E-(40-1)-5080. Since accurate, quantitative analyses do not exist, estimates on final hole radius at this time would be very hypothetical.

Figure 8 illustrates the conditions existing for a coking coal, which are not restricted to borehole ignition, but representative of the general stream method of gasification. Gases flow along the borehole of initial radius R_o according to the pressure difference $(P_2 - P_1)$ and to or from the coalbed depending upon the value of $(P_4 - P_1)$. Through control of the difference $(P_4 - P_1)$ the ratio of receding coke surface directional velocities V_{RS1}/V_{ZS1} can be controlled, perhaps to the degree that $V_{RS1} \to 0$ and extinction results.

The option for such control is enhanced by the porous coke barrier of thickness $(R_2 - R_1)$. Since the oxydizing agent must pass through this zone, the primary reactions occurring in the zone of thickness $(R_3 - R_2)$ are highly dependent upon the pressure difference $(P_4 - P_1)$. In certain subbituminous coals and lignite, this layer does not exist. When the layer of coke does exist, the in situ conditions for further gasification of the coke are critical.

The potentials ∇T and ∇C are interdependent on ∇P and other coal and coalbed properties. These mutually dependent potentials are strong functions of coal reactivity, swelling, shrinking, coking and other thermal-mechanical-chemical properties. In practice, P_1 and P_2 could be adjusted as necessary to limit $\dot{m}_{H_2O}, CH_4$ based initially upon reservoir evaluation tests of $\dot{m}_{H_2O}$ versus $(P_5 - P_2)$, although economically P_2 should $\to P_{atm}$.

P_5 can be controlled by the adjacent directionally-drilled, parallel boreholes. The surface temperatures necessary for the normal velocity of the coke interface V_{NC} to be greater than zero are in excess of 1600° F. Laboratory tests have demonstrated that coke temperature T_C And V_{NC} are strong functions of V_{air} with a narrow range between extinction as illustrated qualitatively in Figure 9 for the Pittsburgh coal with coke gasification conditions not easily achieved. This leads to an apparent contradiction with "observed results in the field" that as the air injection rate is increased the gas quality and quantity continue to increase. This observation however must be qualified as to coal type, operating conditions, injection and production geometry and what happens to the flow paths within the coalbed.

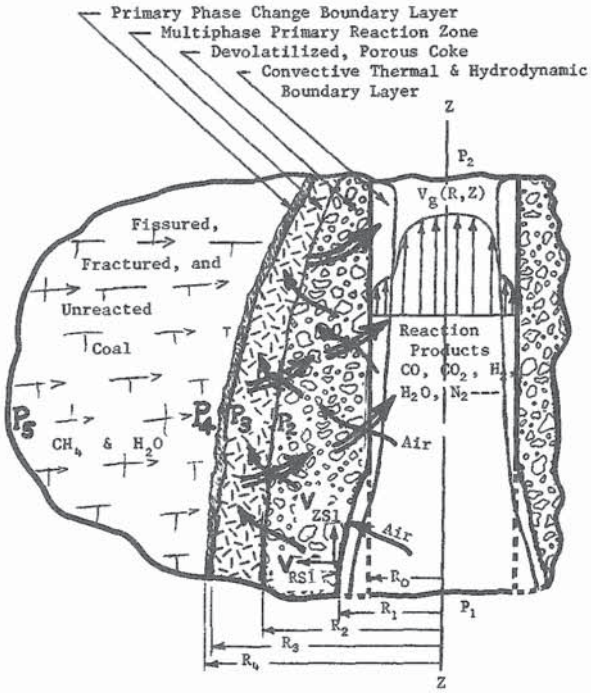


Figure 8

Illustration of Forced Convection and Molecular Counter-Diffusion of Air Components and Multicomponent Reaction Products Through Coking Coal During Borehole Ignition for In Situ Gasification

From laboratory experiments the estimated dimensions are $(R_4 - R_3) \leq 0.1$ inch, $0.1 \leq (R_3 - R_2) \leq 0.50$ inch and $(R_3 - R_2) > 2$ inches. However, the laboratory samples were not subjected to externally applied stresses which can greatly change the coke layer thickness and permeability. The layer defined by $R_3 - R_2$ does not exist in some lignite and subbituminous coals under stream gasification. The thermal and convective boundary layers may be turbulent or laminar. Fundamental potential theory explains the general mechanisms of mass and energy transport to and from the primary reaction zone. However, rigorous solutions for the multiphase, simultaneously expanding and receding surfaces and multicomponent counterdiffusion with temperature dependent reactions do not exist. Solutions obtained for transpiration cooling of ablating heat shields with chemical reactions, and the burning of solid rocket propellants are probably the closest related problems that have been solved, and these solutions are not close enough to be realistically applied. Modification and application of these empirical programs and techniques are the subject of the United Technology proposal. Discussion of some of these techniques and the large L/D borehole ignition problem will be discussed by Robert Hermsen of UTC in Paper No. PB-3.

These coal-specific properties are all fundamental to the burn front profile problem. The burn front profile is a stability problem dependent upon both the coal and coalbed properties and such imposed conditions as geometry and pressure differences. It appears that the filtration LWG burn profile is unstable in a volatile, reactive, shrinking, noncoking coal which would quickly result in "burn-through" and the stream gasification method. It is believed that forward gasification in such coals results in greater profile instability than the reverse burn mode. However, flame front curvature stability must be investigated by considering all the significant stablizing and nonstablizing forces. This is not simple, due to all the unknown conditions in any coalbed. However, some attempt must be made at identifying the most influential forces and factors and measuring their relative importance. Some factors to be considered are:

(a) directional permeability ratio
(b) directional fissure and fracture systems
(c) directional water flow channels
(d) faults, clay or shale stringers
(e) directional coal mineral compositions and thermo-chemical characteristics
(f) tectonic stress field magnitudes and directions
(g) pressure sources or sinks within the coalbed
(h) coal behavior when subjected to elevated temperatures in terms of i) dilatations, ii) phase changes, iii) chemical reactivity, iv) mechanical strength, v) thermoviscoelastic flow
(i) coalbed dip and strike directions with respect to burn direction
(j) instantaneous pressure differences and burn velocities
(k) forward, reverse or cyclic combustion
(l) steady state burn velocity

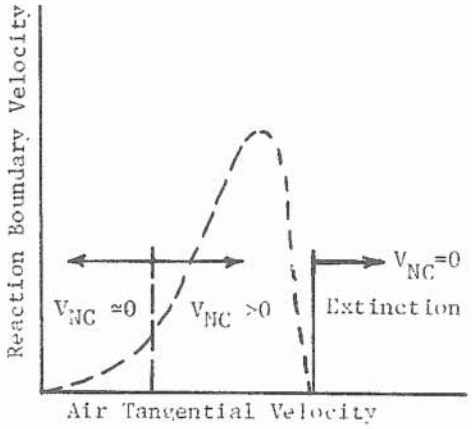


Figure 9

Qualitative Air Tangential Velocity Effect Upon Radial Burn Velocity.

As in the analysis of any such problem, it is necessary to solve it with a specific combination of conditions corresponding to a specific coal and coalbed region. A realistic analysis obviously is beyond the present state-of-art and knowledge of UCG processes and mechanisms. Before curvature stability of the reaction zone can be rigorously investigated, the fundamental processes of reaction kinetics, fluid flow, mass and energy transport, and structural behavior under steady state conditions must be modeled to a reasonable degree of accuracy. This is the essence of MERC contracts E-(40-1)-8018, E-(40-1)-5080, and E-(40-1)-5088, respectively.

Burn profile curvature stability is obviously a time dependent, non stationary field problem and perhaps an order of magnitude more complicated than the steady state problem. It is necessary to know the basic heat and mass transfer coefficients before the dimensionless parameters which describe transient transport processes can be evaluated. The temperature and specie concentration fields and their phase relations under prescribed conditions must be modeled previous to answering the burn profile curvature stability problem. Particular dimensionless numbers necessary for describing for example the temperature field are the Fourier, Biot, Margulis, Kossovich, Posnov, Predvodilelev numbers for both mass and heat transfer.

The swelling and coking coals produce a sealing and fluid redistribution effect which serves as a burn profile stabilizing factor. It is this effect along with the planned longwall tectonic stress effect which will hopefully render stable LWG burn profiles. The stabilizing effect due to swelling only has been demonstrated in laboratory experiments. However, the most immediately productive and results oriented approach is simply to conduct a field test on a sufficiently large scale in a near-surface coalbed which can be cheaply and redundantly monitored and post-burn excavated so that the resultant of all the acting forces can be measured and evaluated. The tectonic stress effects would not be adequately tested unless the depth were greater than 100 feet.

FIELD PROJECT

The MERC UCG site is located in Wetzel County, West Virginia, near the community of Pricetown. At this location, the Pittsburgh coal is nominally six feet thick and 885 feet below the surface. The directionally drilled holes are oriented N17°E to intersect orthogonally the face cleats or major coalbed permeability direction. Hole deviation of approximately 4-1/5 degrees per 100 feet is necessary to intersect the coalbed at the edge of the planned gasification site approximately 1100 feet horizontally from where the holes are started. The status of the field project is as follows:

(a) Site preparation is complete with improved roads to the drilling areas and over the burn zone, and two trailers with electric, telephone, water and sewage facilities have been installed.

(b) Drilled, obtained and analyzed oriented cores from two vertical wells, V-1 and V-2, for bed characterization.

(c) Completed water quality monitoring experiments in 30 domestic water wells within a three mile radius of the site.

(d) Electrical resistivity surveys were conducted over the planned burn zone to detect faults.

(e) Cleaned out and plugged back to the coalbed an old gas well, V-4, within 400 feet of the burn zone, which will be used as a monitoring hole.

(f) Drilled and cased one deviated hole to the coalbed and extended the open hole 500 feet through the coalbed.

Figure 10 illustrates the total field drilling plan with the completed directionally drilled hole, D-1. A vertical well, V-3, is planned to intersect the blind end of D-1. Details of the actual hole configuration are given in Figures 11 and 12.

In drilling the first directional hole, many delays and problems were encountered. The use of unproven and newly developed drilling motors with insufficient spare parts contributed significantly to the delays. Table IV summarizes the delays and their associated causes. Many of the equipment reliability problems have since been solved through redesigns and extensive testing. A second hole is planned in order to adequately test the Longwall Generator Concept.

SUMMARY

There are numerous coalbeds in the Eastern U.S. near the large energy demand centers which cannot be recovered by conventional methods. Most of these coals are the coking type which represents a different problem from subbituminous coal and lignite. It is these differences of coking, swelling and fluid phase transition that are considered to cause problems in conventional UCG schemes that are now being investigated in the MERC research program, to render feasible such new, innovative schemes as the Longwall Generator Concept. Variations of this concept, in conjunction with directional drilling, will hopefully add a new dimension to our means of recovering energy from the Eastern U. S. coalbeds.

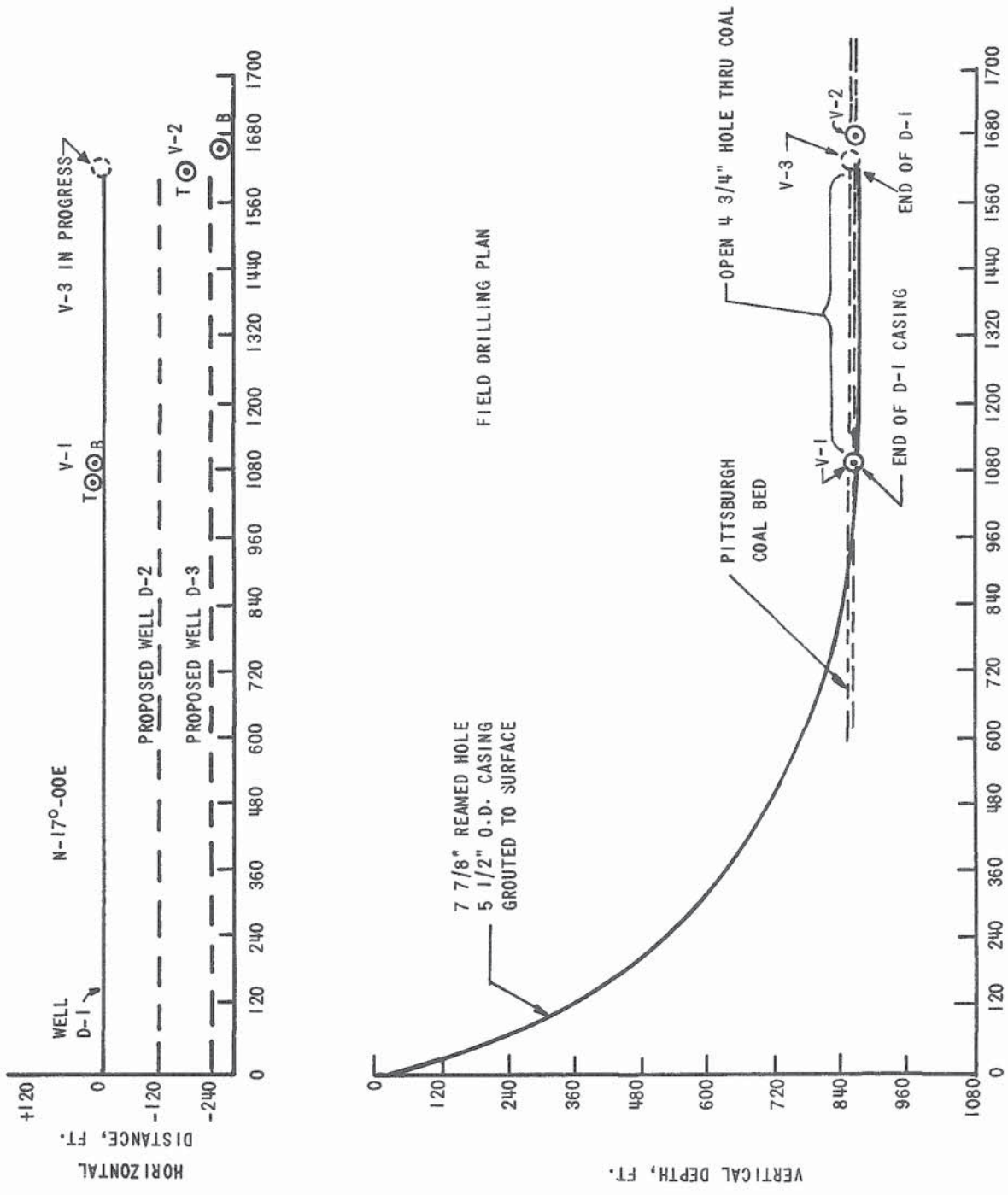

FIELD DRILLING PLAN
WELL D-1
N-17°-00E
V-1
V-3 IN PROGRESS
PROPOSED WELL D-2
PROPOSED WELL D-3
V-2
HORIZONTAL DISTANCE, FT.
+120
0
-120
-240
0 120 240 360 480 600 720 840 960 1080 1200 1320 1440 1560 1680 1700
7 7/8" REAMED HOLE
5 1/2" O.D. CASING
GROUTED TO SURFACE
PITTSBURGH
COAL BED
OPEN 4 3/4" HOLE THRU COAL
END OF D-1 CASING
END OF D-1
VERTICAL DEPTH, FT.
0 120 240 360 480 600 720 840 960 1080
HORIZONTAL DISTANCE

FIGURE 10

TABLE IV

D-1 DIRECTIONAL DRILLING TIME ANALYSIS

DATE	WORK HOURS		DELAY HOURS							OFF TIME
	Drilling 3-in.	Other Rig Uses	Wait on Dyna Drill	Wait on Cement to Set up	Wait on Tools and Parts	Work on Rig	Work on Mud Pump	Fish For Tools and Rods	Misc.	
Aug.75	85.8	84.7		69.5						
Sep.75	222.8	70.5	122.0	38.0			2.7			
Oct.75	362.0	146.5	210.6			7.4	17.5			
Nov.75	341.8	191.8	179.8						6.7	
Dec.75	239.0	178.3	182.8	65.5		24.0	30.3			24.0
Jan.76	321.2	162.0	11.3		1.5	0.8	2.6		4.8	
	Ream to 7-3/8"									
Feb.76	93.5	86.8		43.8	17.0		11.4		23.5	
Mar.76	446.0	129.0			24.6	57.3	1.6	79.1	6.4	
Apr.76	31.8	21.8		56.0	55.8	23.1	0.6		28.7	280.0
	Cement in 5-1/2" O.D.		Casing							
Apr.76		135.8								
Start	to Drill Through Coal									
Apr.76	28.9	57.6								
May.76	116.5	115.1	7.5			1.2			0.8	
Jun.76	154.1	187.9	9.0		77.7	35.7	1.5		14.9	40.0
	Ream Through Coal									
Jun.76	112.9	86.3								
Jul.76		23.6							16.4	
TOTAL	2556	1678	723	273	177	149	68	79	102	344

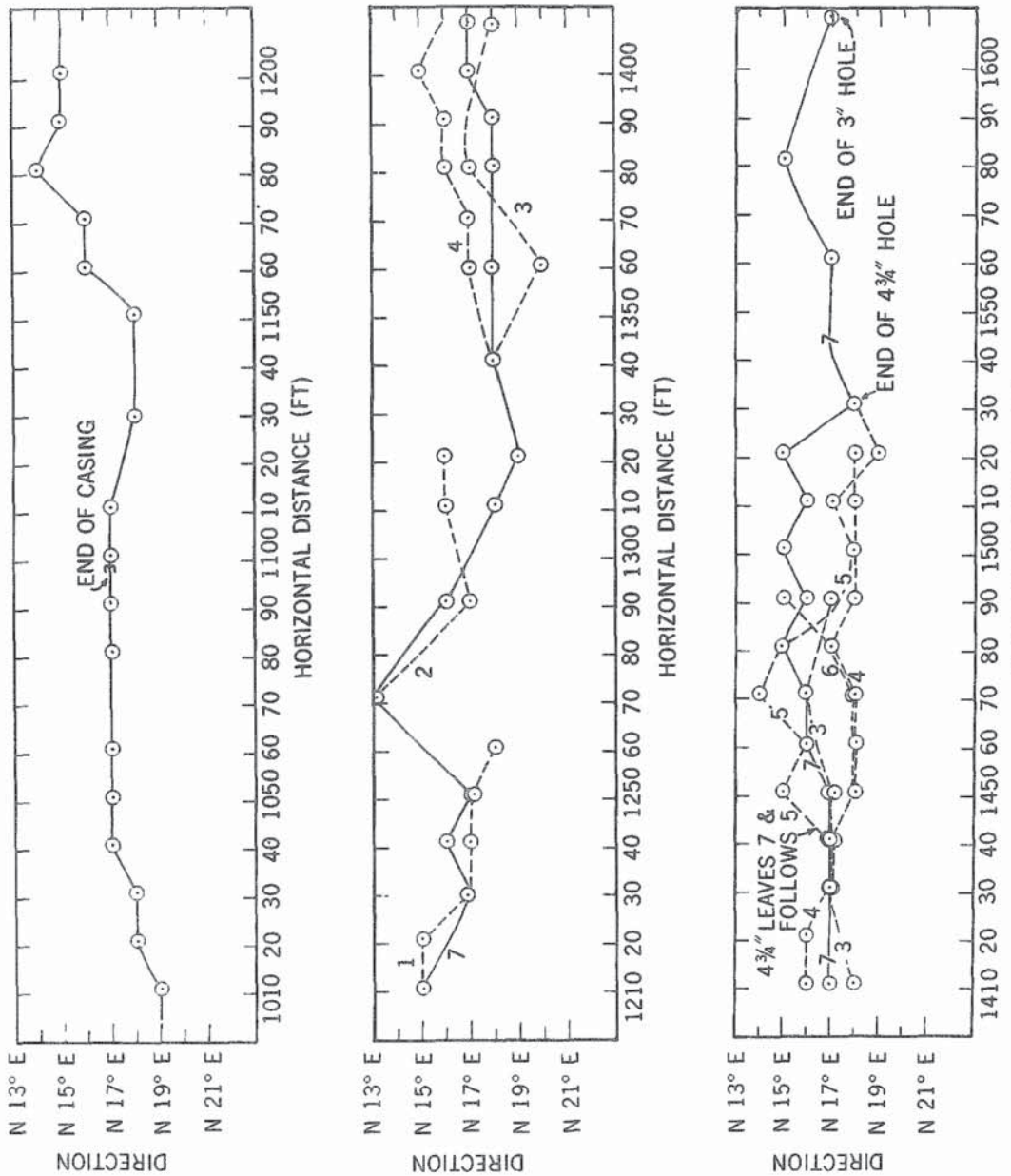


Figure 11. - Survey of the Directionally-Drilled Hole Through Coalbed - Plan View

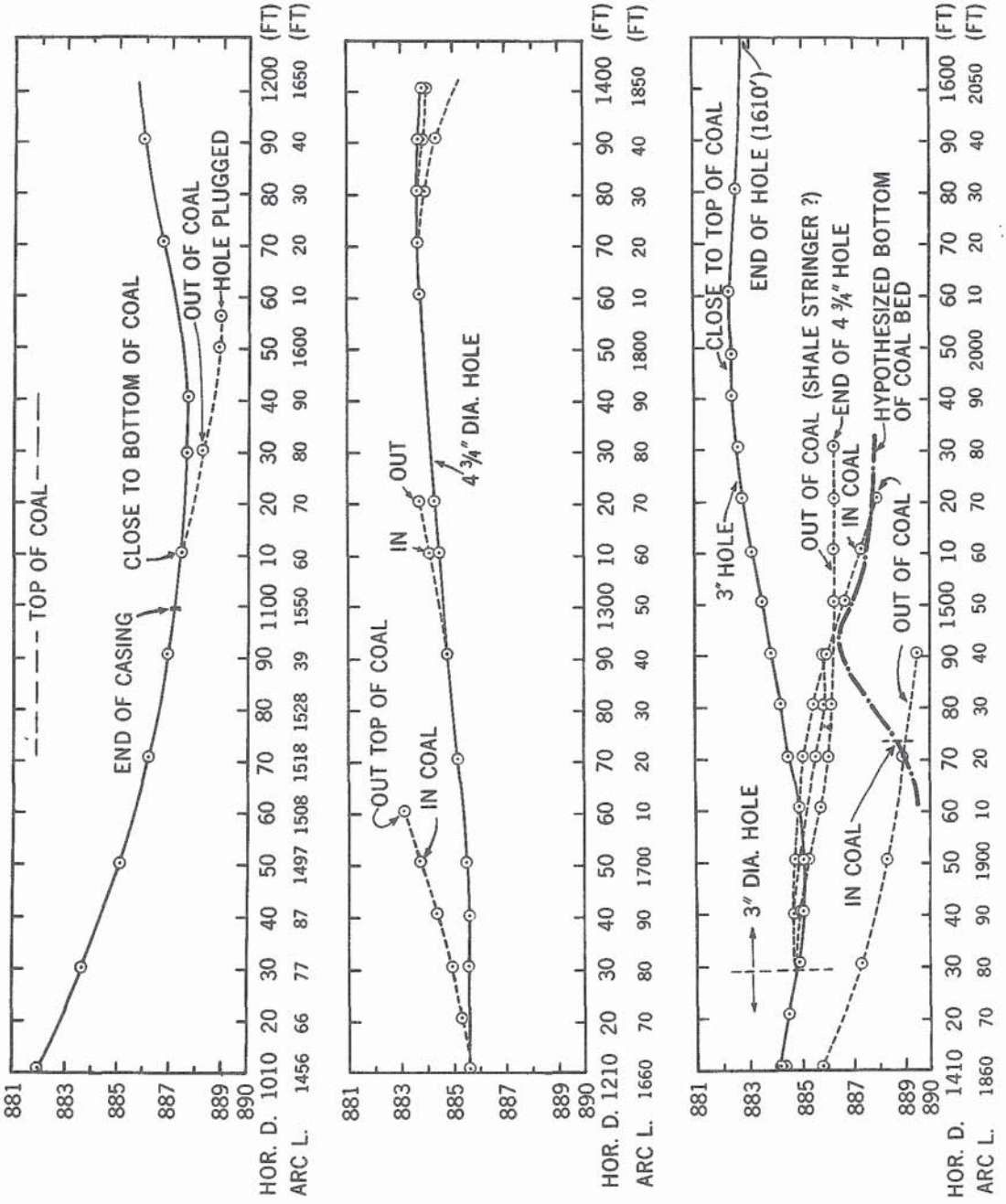


Figure 12. - Survey of the Directionally-Drilled Hole Through COalbed--Elevation View

REFERENCES

[1] Rice, Richard L., and William K. Overbey, Jr. "Preliminary Cost Evaluation, Underground Gasification of Eastern Coal Utilizing the Longwall Generator Concept," May, 1974, 8 pp.

[2] Rice, Richard L., K-H. Frohne, T. J. George, A. S. Moore, and M. Zulkoski. "Project Cost Estimates--Underground Gasification of Coal---," April, 1974, 30 pp.

[3] Farouq Ali, S.M., "Modeling and Computer Simulation of Reaction Kinetics Associated with the Underground Gasification of Coal," USBM Grant No. G0133094 Final Report, November 14, 1975, 169 pp.

[4] Farouq Ali, S.M. and M. L. Pasha, "An Advanced Mathematical Model of Underground Coal Gasification Using Steam-Air Mixtures," SPE Paper 6186, Presented at 51st Annual Fall Meeting SPE, New Orleans, La., October 3-6, 1976.

[5] Farouq Ali, S. M. and M. L. Pasha, "Numerical Modeling of Underground Coal Gasification by the Stream Method and Borehole Linking, Final Report, U.S.ERDA Contract E(46-1)-8018.

[6] Advani, S. H. and Y. T. Lin, "Structural Mechanics Simulations Associated with Underground Coal Gasification," USBM Grant No. G0155033 Final Report, MERC/CR-7611, National Technical Information Service, Springfield, Va., May, 1976, 85 pp.

[7] Advani, S. H., L. Z. Shuck, Y. T. Lin, H. Y. Chang, "Thermomechanics Simulations Associated with Underground Coal Gasification," Presented at 17th U.S. Symposium on Rock Mechanics, Snowbird Resort, Utah, August 25-27, 1976, Conference Proceedings, 7 pp.

[8] Shuck, L. Z., "Method for Laser Drilling Subterranean Earth Formations," U.S. Patent No. 3,977,478, August 31, 1976.

[9] Komar, C. A. , J. Pasini III, W. K. Overbey, Jr., "Longwall Generator Concept," Patent Applied For.

TEXAS UTILITIES PROGRAM STATUS REPORT

by

B. R. CLEMENTS, Texas Utilities Service, Inc.

I was to share this presentation with Joe Grant who is our Operating Engineer, but I'm sorry to report that Joe's back in Texas, pretty busy. We planned on Thursday to start putting air into the ground to try to dry the coal out that we're going to gasify and hopefully, next Monday or Tuesday, we'll light our first fires. We're going to do a very short burn...what we call a technical test site just to prove that we CAN start a fire and we're going to make a couple of links. I'll talk more about that later.

When I first was talking to Paul and Zane Shuck about making some sort of a presentation, I told him that we really hadn't done much and there was not a lot that we could really tell you about. So they asked me to share some of the experiences that we had in the Soviet Union with you. And when you visit different places, different things impress different people. Especially, when the place is as paradoxical as the Soviet Union is. One of the things that impressed me over there was their sanitary facilities. I want you to notice the safety precautions with the non-skid there on the shoe track. After a month over there, the month of August, you can believe that I had a high respect for the term "Communist movement."

In November of 1974, Jack Peterson talked to our management about coal or lignite gasification. Jack had talked to several companies around the country trying to get together a coalition to buy the Soviet technology.

Our management decided that we would try to get into this field for two reasons: (a) We had lignite that was too deep to strip, that is we had leases on some and we owned some, and of course, as all utility companies right now, (2) we need fuel. We're in a good fuel position. We have lignite leases throughout east Texas but we believe that you just can't turn down any source of fuel that you can get these days. So, in November of 1974, Jack and our president, Mr. Perry Brittain, went to the Soviet Union to discuss gasification with them (actually for our president to see what was going on and to see if they were really using this technology). We started negotiating with the Soviets and in March of 1975, a group of us went over to Moscow and Mr. Brittain signed an agreement with the Russians for complete usage of this technology and exclusive rights in the United States. As soon as the agreement was signed, they started giving us the information. They had agreed to give us their mistakes and all of their data, whether it was good or bad. And so far, we've found them to be very cooperative. We have had no problems at all with the information. One thing was sort of funny to me this morning when Zane Shuck said what he did about the Soviets starting out in a pretty rough fashion. They did...but we consider them to be very sophisticated right now in coal gasification. But, the first day, after we signed the agreement, the Russians were all sort of vying with each other to be the first to start cutting us in on the "hot word."

Dr. Pronin, who is considered by the Russians to be the father of their modern coal gasification program, listened to the exchange for two or three days. Their hydrologists, geologists and

engineers were talking to us. The last day before we were going to leave...Dr. Pronin indicated for me to come over to him and as I walked over the corner with him and an interpreter, he said, (through the interpreter)..."Don't they overdo it? You should just go out and drill some holes, start your fire and back away." So, the way they started (Zane was pretty much right). They started in pretty rough fashion.

We got our first bit of printed documentation in June of 1975. Ron Brimhall, who is the hydrologist on the project from Research Sciences Corporation, our interpreter, and I went over and we received the first part of the documentation. Jack brought the rest of the documentation back in November of 1975. So, we now have all the printed documentation that we're going to receive.

In August of last year, as a matter of fact, just about the time the First Annual Symposium for Coal and Lignite Gasification was taking place in Wyoming, we went over to the Soviet Union to spend a month. We took 5 engineers, an hydrologist, a geologist, a drilling engineer, and our own interpreter and translator. We spent three weeks down in the Uzbekistan. We flew into Tashkent from Moscow. We had spent about 24 hours in Moscow, and flew down to Tashkent and spent about three weeks out there about 90 kilometers southeast of Tashkent. They actually have a project going out there and have had for years. In the mornings mainly, we would break up into groups according to disciplines - our hydrologists with theirs, our geologists with theirs, our drilling engineer with theirs, and the 5 engineers with their engineers. In the afternoons, generally, we'd go out into the field.

As this slide depicts, one of our groups standing around a well, and I think in this particular case, they were just changing it from an injection well to a gassing well. The gentleman in the back there is Dr. Pronin, the one I mentioned earlier. He is about 75 years old and quite a gentleman. And I don't care what you're doing...whether it's swimming, drinking vodka, or gasifying coal...he'll hang in there with you!

There you see a field...the pipes coming in from the different areas there, kind of strung out...the gathering pipes into the major pipe, with the plant in the background. The plant is pretty rustic, and has been there awhile. Again this slide shows more piping. They use the heat from the gathering pipes to heat their injection air. This is the major pipeline that goes from the field to the plant where the gas is utilized. They have a plant that must be over 5 or 6 kilometers from where they're gasifying. It is approximately a 600 megawatt plant, and on any given day...about 60 megawatts would be using gas from the gasification plant.

Another slide of the pipeline. Closer to the plant. Taken at a different time of the year than when we were over there...This one taken in November. And a slide of the field with the plant and the generation plant utilizing the gas. The funny thing about it is that the gas is made and sold to the Ministry of Electricity in Moscow. We asked permission to go over and see the plant where this gas was being used, to see what size of burner they were using, and so forth.

They said, "Well, only if you insist!" And I said, "Well, I insist!"
It took them four days to get us permission. They had to go back to Moscow to the Ministry of Gas and the Ministry of Gas talked to the Ministry of Electricity. No new technology was involved. The plant was built in the early 50's.

By the way any comments I make about things like that...I'm in no way belittling the Soviets. I just don't like their form of government! So...the individual persons I have a good word for... and we had good working relationships with them. I don't mean to demean individuals. As a matter of fact, I can tell you a quick sea story.

As you know, they do drink a little vodka over there...and as we were getting ready to leave after a month's trip, one of the Soviets who had been with us the whole time, poured a couple of glasses of vodka. There must have been 4 to 6 ounces in a glass...and I don't drink much myself. But I watched those Russians pretty carefully and this guy had tears in his eyes...literally had tears in his eyes...and he said, "Mr. Clements, after working a month together, we're like brothers...". He said our countries should only exchange information...never a missle exchange, never a bomb exchange...but always information and brotherly love. Ad he said, the Soviet word for "down the hatch" and we downed the vodka. As I said, he had tears in his eyes before, and I had tears in my eyes afterward! It laid me back a little bit.

This is a closer slide of the plant where this gas is being burned and I don't show this in Texas because I don't want people to think that's the kind of gas or what it's gonna look like, but of course, they're stripping coal there also and the rest of the 540 to 570 megawatts of generation

is produced by burning bituminous coal. We asked them if they had any sort of ecology program and they looked sheepish and said "yes, we do." But the further you get from Moscow, the less it is enforced. We said, "Well what happens to a guy, if the government owns a plant...you can't fine the government; you can't do this and you can't do that." Well, they said, "We have a pretty good system. We have a plant manager, of course, the first time he gets a warning...the second time, he gets fined, and the third time, he goes to jail." And so, I'm sure that the plant manager is just as interested in ecology as we are! It's a different system.

This is looking at the edge of the gasifier back across the northern section of the valley that we were in. I brought these slides mainly for the coal people that are here. That's the beginnings of an open-pit mine and again, we asked permission to go over to see the open-pit mine and it took them again four days for us to get permission.

It turned out to be very interesting. It's about 600 feet deep to the bottom and there are several layers of coal. We went over to the plant and we got the usual speech about how they had overcome us in mining coal and how they were going to overcome us in almost everything that you could think of, and I noticed that we got the same speech at the five or six different plants. Each plant manager had the same speech. Seriously, it's as if they were written by one guy and then passed out.

There is a closer slide of the mine. You can see a little town in the background. Up that hill, there are two little towns. One, where the trees are on the left and one back to our right as you face it. They intend to go right up the side of that mountain stripping or open-pit mining...and destroy the little towns in the process. And they are already building houses in town for the people and have told the people that they would have to move and of course, since the government owns the coal and they own the houses, well, the people don't have much choice but to move. You can see the size of those full-size railroad cars there in the lower right hand corner of the slide. They have no plans at all to do any sort of reclamation. They are taking this overburden and moving it out on trains for contruction work elsewhere. That's not all one seam, it's multi-seams.

As I told you, we spent three weeks in Angren down by Tashkent. Next, we went out to their plant in Siberia at Uzno Abinsk and spent a week. The dewatering they're doing with those big pumps you see in this slide - there's a lot of water in this area...and there's the gathering system. The wells are along the mid picture going back to your left...going down away from the picture. You see the pipe in the background, by the white houses - that's their gathering system. Now, they're using this gas in Uzno-Abinsk for commercial purposes. They've got 14 small industries in the town of Kiselvsk and they use this gas for these industries. There's not any power plant using it. We were taken to a bakery to show us what kind of burners they were using. We actually saw how they were doing it. The Btu content of the gas is higher in Angren than in Uzno-Abinsk because of the difference in the type of coal. The cold prevents strip mining there in the wintertime, so they triple their output of gas from gasification. We had frost there in August, so I don't know what they call WINTER! In the dead of winter, it's just too cold to strip mine, so they do triple or quadruple their output of gas. This slide shows the location of Lake Fairfield...that's about 90-95 miles south-southeast of Dallas and that's where our first site will be. We have strip mines and lignite burning plants at several locations in East Texas. We have four 750 megawatt units going in at Martin Lake. We have two 575 and one 750 at Monticello. At Fairfield we have two 575's. I'd like to point out to you that we're not about to substitute gasification for stripping. That's just not our plan. We figure we're getting 90+ percent of the coal to the burners by stripping and if we get an in situ commercial plant, we'll probably end up with 30-50 percent somewhere, we're not sure exactly. So, we're not going to replace strip mining with in situ coal gasification. However, if any of you come to Texas, and would like a trip down to see the reclamation project that we're doing, we don't think strip mining is doing any long term damage. We're doing one hell of a good job reclaiming the land and we don't apologize to anybody for strip mining.

I just want to show you...this is our in situ site, fairly close to the two units at what we call Big Brown Steam Electric and we're really "poor boying it". After hearing Mr. Northrup this morning talk about all this instrumentation and gear the guys at Lawrence Livermore Labs have, I'm ashamed to get up here, because we're really just using the bare essentials on instrumentation. We have, of course, got thermocouples in the ground to determine the temperatures. Let me drop back a little bit and talk about water problems.

In December of 1975, we requested permits from the Texas Air Control Board and the Texas Water Quality Board. We requested permits without hearings. That's one of the ways you can get a permit

in Texas. By requesting one without a hearing. Well, the Air Control Board looked over the situation, looked over the data we had from the Soviet Union, and the data we had gotten together. They granted us, in February of 1976, a permit without a hearing. I think the Air Control Board is going to be one of our biggest boosters. The Water Quality Board told us right away, back in December, that there was no way that we'd get away without a hearing. So we submitted data in February of this year, requesting a hearing for a permit. We had a hearing in June of this year and on July 30, we were issued a water quality permit. We're in business. We have all the permits we need from the State to go ahead.

One of the purposes of this technical test site is to determine just what we do to the water. This slide shows our flare. I apologize for the simplicity as we just don't have much money. We're paying for ours out of revenues and stockholder's pockets. I don't mean anything to be snide, but we have no partners in this at all except for Research Science Corporation of Tulsa, Oklahoma.

Back in March of 1976, we determined the maximum magnitude and direction of the permeability of the layers of the coal we were going to work with. It was a very simple task. We just drilled a group of holes on a semi-circle and put a hole in the middle. We pumped air into the middle hole until we started getting air out of the other holes. Of course, the most air came out in the direction of maximum permeability of the lignite. It was a very simple test.

I know you can't read this slide. It just indicates to you that we're going to gasify this layer here, Unit 13, and indicates to you that we're down about 230 feet for our first test.

The day we were leaving the Soviet Union the first time, one of the old men who'd been in the program as long as Dr. Pronin came up to me and said, "Clements, I can tell you how to be successful." I said, "Gee, I sure appreciate whatever you can tell me, man. I'd like to have it." He said, "Buy yourself a coal seam about 30 meters thick with 20 to 30 meters of clay on either side, and you've got it made!" Well, our coal seam is two meters. So, maybe I'm in trouble. But, he was really serious. Just go out and find yourself a big thick seam and one that's got clay on both sides and you're in business. I'd sure like to find one. Can you help me, Leo?

This is our technical test site. The only three wells we're going to use as far as any burning or gassing are these three in red. The others are all monitoring wells. Water monitoring wells. We have them instrumented with thermocouples. We're going to start the fire here and link down to TTS-1a in this direction and we're going to link, of course, back to TTS-9. Once we've made this link, we're going to gasify in this area while we're making the other link. We don't expect the test to last over 6-8 weeks. We have a permit from the water quality board for 3 months. SOMEONE ASKS A QUESTION, WHICH IS NOT HEARD. This sounds weird...but with this license, I'm not allowed to talk about this. Kinda corny, but that's the way it is.

This is strictly a research project with the Texas Utilities. The Soviets don't like for us to say that, but it is. We're using money out of our R&D funds, and we are no way right now committed to anything but just this test site that I've indicated here. Of course, the thing that will tell us "yes" or "no" is the economics.

I'm on the carpet to tell our management in December whether or not I recommend a pilot plant. The TTS is a demonstration plant. The economics is what's going to determine for us whether or not we continue. Back in 40's when the man who is now our manager of coal and lignite started buying leases in Texas, he literally had to slip in and out of the building, he was razzed so much. People would say,"here comes the coal miner." Now the coal miners are the backbone of our company.

If gas were still 15 cents per million Btu's in Texas, I don't think any of us would be here at an underground gasification symposium. Right now, we're paying in Texas on new gas up to $2.00 per million Btu's. So all of you who live outside Texas and have the increase approaching, remember that we're still paying a lot more than that.

Those of us in our group feel that we have something that can compete with natural gas at $2.00 per million Btu's. The Texas Railroad Commission controls gas prices and usage within the state of Texas. The commission has ordered a 10% cutback in boiler usage of natural gas by 1980 and a 25% cutback by 1985.

RESEARCH ON IN SITU GASIFICATION OF TEXAS LIGNITE AT AT THE UNIVERSITY OF TEXAS

by

T. F. Edgar
W. R. Kaiser
T. W. Thompson
The University of Texas
Austin, Texas 78712

ABSTRACT

The important technical and economic factors for using UCG for recovery of Texas Lignite are discussed. The UCG research currently being conducted at The University of Texas at Austin currently involves the Departments of Petroleum Engineering, Chemical Engineering, Mechanical Engineering, Civil Engineering, and Geology. A description of activities in each disciplinary area will be given. Of particular interest are projects on rock mechanics and permeability studies, environmental impact of UCG, methods of utilizing low Btu gas, and various chemical reaction studies, ranging from small scale isothermal kinetics research to combustion tube experimental systems. Recent results of this research project will be highlighted; more complete details are available in semi-annual reports issued by The University of Texas.

TEXAS DEEP BASIN LIGNITE

Underground coal gasification is currently of great interest as an extraction method for Texas lignite, mainly for those deposits which lie below strip mining depth. Field and laboratory work is presently underway at Texas Utilities Generating Company (Dallas), University of Texas at Austin, and Texas A&M. Texas lignite resources, located mainly in East Texas, are very large and moderately low in sulfur (1.0 - 1.5% dry basis). Recent mapping of lignite lands by Kaiser (1974) of the Bureau of Economic Geology, have indicated roughly 10 billion tons at stripping depth. More impressive, the deep-basin lignites (those lying between depths of 200 to 5,000 feet beneath the surface) have been estimated to be in excess of 100 billion short tons, which is the Btu equivalent of ten times Texas's proven reserves of oil and gas. Obviously all of this lignite cannot be recovered, but the order of magnitude is still significant.

The principal deposits of Texas lignite occur north of the Colorado River. Near-surface deposits, those found at 0 to 200 feet below the surface, occur within the outcrop of the main lignite-bearing geologic units. Deep-basin deposits, those found at greater than 300 feet below the surface, occur downdip and coastward from the near-surface lignite (Figure 1), with a dip of approximately one degree. The major deep-basin deposits occur in a broad arc which widens gradually from Gonzales County northeast to Cherokee County, where it splits and wraps around the north and south flanks of the Sabine uplift (Panola and adjacent counties).

Primary commercial lignite deposits are found in lower Eocene rocks (Wilcox Group); deposits of secondary importance, in terms of resources and grade, are found in upper Eocene rocks (Yegua Formation and Jackson Group). Lignite of prime impor-

ferences at end of paper.

tance occurs as a component facies of ancient fluvial and deltaic rocks. Fluvial lignites occur in the Wilcox and Yegua north of the Colorado River. Deltaic lignites occur in the Wilcox, Yegua, and Jackson between the Trinity and Colorado Rivers and Trinity River and southwest flank of the Sabine uplift in the deep basin.

TECHNICAL FEASIBILITY OF UCG IN TEXAS

It appears that Texas lignite may be especially suited for this process for the following technical reasons:

(1) The overburden (usually clay or mud) tends not to form extensive fissures and cracks and is relatively impermeable to gas flow. The lignite also has an extremely high natural field permeability ($\sim$1 darcy) and thus should require pneumatic fracturing only; the overburden would resist and cushion the propagation of artificial fractures to the land surface. A tight seal around the gasification region would allow relatively high pressure operation and higher flow rates, minimizing leakage and improving yields.

(2) The reasonably thick lignite seams (5 to 20 feet thick) would yield good utilization of the heat evolved during in situ gasification. Russian data (Gregg et al., 1976) indicate that seam thicknesses over five feet are quite feasible for UCG, while thinner seams (e.g., two feet thick) are not feasible, due to relatively high heat losses.

(3) The mud roof and floor for Texas lignite would tend to settle down gradually during gasification. This phenomenon would also help prevent excessive production of CO_2 (formed by oxygen bypassing) due to void space and thus would improve the yield of product gas. A higher sweep efficiency might also be expected.

(4) Texas lignite is very reactive, and thus may allow wider reaction fronts (higher sweep efficiencies).

ECONOMIC FEASIBILITY OF UCG IN TEXAS

While the Texas lignite appears to be technically amenable to underground gasification, the economics of in situ production also appear to be favorable, when compared to coal deposits elsewhere in the U.S. A high thermal efficiency would certainly increase the net value of the low Btu gas. Other factors can be cited:

(1) The high permeability would yield significant cost savings in two areas. Fracturing is obviated, and the well density can be much lower, thus lowering the drilling costs tremendously.

(2) The thickness of the seams and the existence of multiple seams would yield a high energy content per well drilled, thus saving drilling costs and making the necessary operating field much smaller in size.

(3) Above ground coal processing equipment and gasifiers, which contribute one-fourth of the total costs of the produced gas in the Lurgi process, would be eliminated.

(4) Deposits of Texas lignite are located within 100 miles of the major demand centers of Texas, including Houston, Dallas, Austin, and San Antonio (Figure 1).

The depths at which in situ gasification can be applied are dependent upon drilling costs and technology. Current drilling and completion costs probably limit its application to less than 2,000 feet. For a 1000 MW plant, a six-foot lignite seam, and a sixty per cent recovery of coal as low Btu gas, an areal extent of 1.50 square miles per year would need to be gasified.

There appear to be several modes of utilization for low Btu gas produced from Texas lignite:

(1) direct combustion to produce electricity: projected improvements in gas turbine generators (combined cycle) could yield efficiencies approaching 50% (compared with 37% in conventional power plants) with low Btu gas from UCG.

(2) direct heating in industrial processes: low Btu gas could replace natural gas for direct firing of industrial processes. With the heavy concentration of energy-intensive industry in Texas, such a fuel would be very useful.

(3) chemical feedstock: much of the petrochemical industry now requires liquid petroleum or natural gas as a starting point for the manufacture of chemicals. The low Btu gas could serve as a basic building block for the production of organics. Gasification with pure oxygen is a necessity in this application.

A recent study (Ozturegen, 1975) at the University of Texas at Austin has evaluated the economics for in situ gasification of Texas lignite. Figure 2 shows

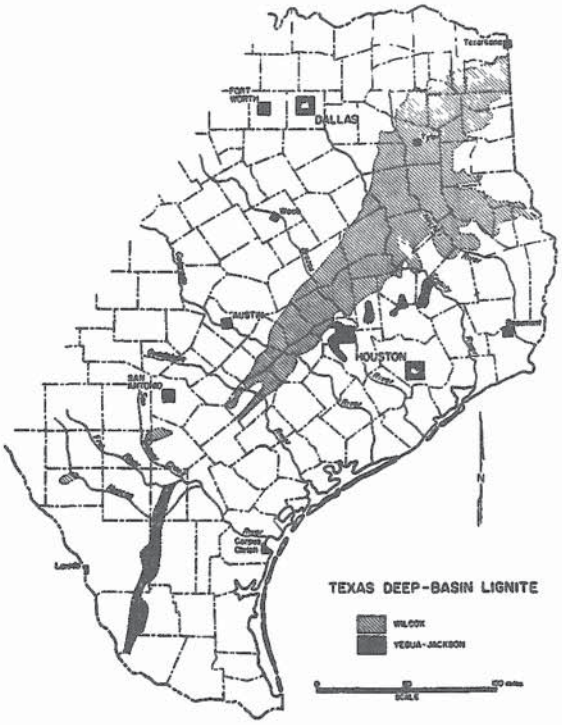


Figure 1. Distribution of Texas deep-basin lignite

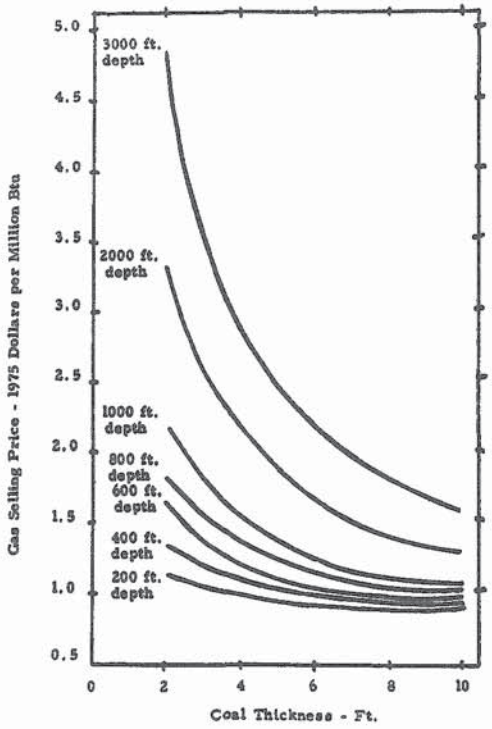


Figure .2: Gas Selling Prices with Height of Overburden as a Parameter

the projected cost in cents per million Btu of a clean low Btu gas (hydrogen sulfide removed as a function of seam thickness and depth beneath the surface of the earth. The utility financing method was used. As can be seen from the figure, the cost of the gas produced appears to level off at approximately a six-foot seam thickness. It is apparent from the figure that for underground coal gasification a low Btu gas can be produced competitively for overburden to seam thickness ratios approaching 150 to one and possibly even higher. The equivalent strip mining ratio will probably approach fifteen to one in the future. Thus, a tenfold enhancement in economic recovery potential is offered by in situ gasification. Some of the assumptions used in developing these curves included a drilling cost proportional to the depth and a borehole spacing of 75 feet by 75 feet, which was the spacing normally used in the Russian operations. At this time the optimum (economic) well spacing for underground coal gasification is not known. It is obviously desirable to maximize the borehole spacing, since the amount of energy recovered per hole drilled is the most significant economic factor in underground coal gasification.

Other assumptions made in the economic analysis include a gasification efficiency of 80 per cent and a contact efficiency of 75 per cent, thus giving an overall resource recovery of 60 per cent. This means that 60 per cent of the latent energy available in the coal underground is recovered in the form of a low Btu gas. These data are comparable to those obtained in the Russian commercial operations. The heating value of the gas produced during underground coal gasification is related to the thermal efficiency of the process and varies with the moisture content and heating value of the coal gasified as well as the amount of water influx.

UCG RESEARCH AT UT-AUSTIN

An interdisciplinary project on UCG, involving the Departments of Chemical Engineering, Petroleum Engineering, Civil Engineering, and Mechanical Engineering, the Bureau of Economic Geology, and the Center for Earth Sciences and Engineering, has been underway at the University of Texas at Austin since 1972. Principal funding for the project has come from the National Science Foundation (Research Applied to National Needs); additional funding has been received from the State of Texas and the following private companies: Texas Utilities Company, Continental Oil Company, Mobil Oil Corporation, Shell Development Company, E. I. DuPont de Nemours, Dow Chemical Company, and ARCO.

The purpose of the proposed research is to develop the necessary theory and understanding of the in situ gasification process so that it can eventually be commercialized for the large deposits of deep basin Texas lignite. The proposed laboratory and pilot scale work is necessary because field testing is uneconomic for every potential site; an engineering and geological design basis, which does not presently exist, must be developed before economic application of the technology can be realized.

The research is oriented towards developing mathematical models, suitable for design scale-up, which can be used for optimizing operation and design of in situ gasification. In a similar vein, the geological, chemical, and physical conditions which are conducive to application of underground gasification are being determined. The final result of the research will be a method of evaluating the potential of in situ gasification for a given site. At maximum, the research data would be used to design a field test, which hopefully would ultimately lead to commercialization of the process.

The long-term objectives of the project are as follows:

(1) To demonstrate that in situ gasification can be operated and controlled satisfactorily on a pilot scale.
(2) To determine which geological, physical, and chemical conditions are conducive to application of underground gasification.
(3) To develop a fundamental understanding of the dominant physical and chemical processes occurring and to use this information to design a field test to determine the validity of the theory.
(4) To obtain detailed engineering and geological data on several candidate in situ gasification sites, based on core drilling at those sites.

In order to arrive at a fundamental understanding of the in situ gasification process and to construct valid mathematical models, laboratory scale experiments in the petroleum and chemical engineering area are being undertaken. The basic process sequence proposed for in situ gasification of Texas lignite in the Russian

percolation process:

(1) in situ drying with air or hot product gas, causing cracks in the lignite and increasing the permeability.
(2) backward burning to create a zone of very high permeability between injection and production holes.
(3) after completion of step (2), forward burning to maximize sweep efficiency.

The goals of the research are as follows:

(1) measurement of lignite reaction properties--
laboratory scale experiments are underway to investigate the kinetics and transport effects of lignite pyrolysis, lignite char oxidation, the char-steam reaction, and the water gas shift reaction (in the presence of char). Transport/reaction models will be proposed and the data correlated. Effect of ash slagging on the reactions will also be studied.

(2) analysis of lignite permeability/pore structure--
experiments with backward burning in a natural fracture system is being performed in retorts and combustion tubes. The effects of temperature on lignite pore structure will also be investigated.

(3) development of combustion tube experiments with pulverized lignite--
forward and backward burning will be attempted and data collected for later modeling. Kinetic models developed in (1) above can be verified in this study.

(4) evaluation of low Btu gas utilization--
conceptual design for cleanup and gas turbine use of low Btu gas and integration with in situ reactor is being studied. An engineering and economic evaluation of petrochemicals production is also being performed.

(5) analysis of potential groundwater pollutants during UCG--
investigation of amount of toxic chemicals and solids dissolution in groundwater and effect of temperature during gasification is in progress. Transport of pollutants and monitoring and restoration techniques are being evaluated.

(6) rock mechanics and permeability tests of lignite and overburden--
Young's modulus, Poisson's ration, compressive and tensile strength, and coefficient of expansion are being determined for various samples. The effect of stress on permeability has been measured.

(7) evaluation of subsidence effects--
a finite element program in conjunction with mechanical properties is being used to determine subsidence patterns. Effects of temperature will be studied.

(8) performance of field permeability tests--
field tests using water and air packers and tracers will be run to obtain field directional permeabilities. Correlation with geology and lab work will be attempted. Coring will also be performed.

(9) completion of lignite resource assessment--
this will involve some field work to tie surface and subsurface geology together. A limited coring and logging program is planned to fill in the gaps on existing resource maps. Criteria for in situ site selection from a geological point of view will be developed. A possible correlation between lineament direction and directional properties will be investigated.

(10) assessment of hydrological and other environmental factors--
hydrological parameters and their effect on groundwater movement in the Wilcox and Yegua sands will be studied. An environmental impact statement will be initiated.

The detailed progress of the above research have been presented in several Semi-Annual Reports (Edgar, 1975, Edgar et al., 1976a, 1976b). These reports can be obtained from the principal author.

REFERENCES

1. Edgar, T. F., "In Situ Conversion of Texas Lignite to Synthetic Fuels," Semi-Annual Report to NSF-RANN, Austin, Texas, April, 1975, 43 p.

2. Edgar, T. F., Kaiser, W. R., and Thompson, T. W., "In Situ Conversion of Texas Lignite to Synthetic Fuels," Semi-Annual Report to NSF-RANN, Austin, Texas, November, 1975, 110 p.

3. Edgar, T. F., Kaiser, W. R., and Thompson, T. W., "In Situ Conversion of Texas Lignite to Synthetic Fuels," Semi-Annual Report to NSF-RANN, Austin, Texas, June, 1976, 137 p.

4. Gregg, D. W., Hill, R. W., and Olness, D. N., "An Overview of the Soviet Effort In Underground Gasification of Coal," UCRL-52004, Lawrence Livermore Laboratory, January, 1976.

5. Kaiser, W. R., "Texas Lignite: Near-Surface and Deep-Basin Resources," The University of Texas at Austin, Bureau Econ. Geol., Rept. Inv. 79, 1974, 70 p.

6. Ozturegen, F., "An Economic Study of In Situ Gasification of Texas Lignites," M.S. Thesis, University of Texas at Austin, September, 1975, 113 p.

IN SITU COMBUSTION OF COAL FOR ENERGY
A PROGRESS REPORT

by

R. F. CHAIKEN AND J. M. SINGER, U. S. BUREAU OF MINES
PITTSBURGH MINING AND SAFETY RESEARCH CENTER

ABSTRACT

Work progress on the Bureau of Mines In Situ Closed Trench Facility at Bruceton is reviewed. With this trench facility, large quantities (∿30 tons) of rubblized coal and other carbonaceous material (e.g., roof strata materials plus coal) can be burned in a simulated in situ geometry. Utilizing a straight burn channel (∿1 ft^2 opening and a 2.5 ft web thickness), it is expected that ∿1 Megawatt thermal power should be generated for several days at optimum trench burning conditions. Results of further theoretical analyses that have been carried out on the conductive heat losses from an IC combustor are reported.

INTRODUCTION

The Bureau of Mines' In Situ Combustion (IC) concept [1] differs from Underground Gasification (UG) of coal [2] in the aspect, whereas UG strives to maximize the combustible gas content of the exhaust from an underground combustor, IC strives to maximize the sensible heat content of the exhaust. In essence then, a UG combustor will operate under overall fuel-rich coal fire conditions, while an IC combustor will operate under overall stoichiometric to oxygen-rich fire conditions. In either case, the long term control of the underground combustion process is one of the major technical problems to be resolved before an in situ gasification process can achieve commercial utility as a source of energy. Herein, we believe, lies a distinct technical advantage of the IC concept; viz., that coal can be burned completely in place for long periods of time to produce high temperature (∿2000°F) gaseous combustion products. The heat from these products, if recovered, could then power an on-site steam turbine electrical power plant.

As far as we know, no organization has ever attempted a field test specifically designed to demonstrate the long term feasibility of the IC concept; however, the results of previous UG field experiments, such as the Bureau's Gorgas, Ala. experiment [3] and Great Britain's Newman Spinney experiment [4], suggest evidence in support of the IC concept [1]. Also, it is well known that coal fires in out crop seams and abandoned coal mines can thrive unattended for many years (better than 75 years in some instances). [5]

In FY 76, the Bureau of Mines initiated a modest project under its Advanced Mining Systems Program to develop a relatively small scale simulated underground coal burning experiment suitable for obtaining information pertinent to a future field demonstration of the IC concept. While extrapolation of small scale fire data to a full scale underground combustor is tenuous, it is believed that useful data on ventilation fire control and air pollution control can be obtained. Also, it should be possible to test instrumentation designs and high temperature gas handling techniques.

References at end of paper

This report describes the status of our simulated underground combustor as well as the results of some further theoretical analyses that have been carried out on the conductive heat loss from an IC combustor.

CLOSED TRENCH BURN FACILITY

Taking a cue from the British work [4], it was thought that the burning of coal in a closed trench could adequately simulate certain aspects of an IC process, in particular the effect of channeled air ventilation flow velocity on the combustion efficiency and composition of the exhaust products. Also, the development and operation of a closed trench burn facility would allow a good opportunity to test potential high temperature materials of construction, instrumentation designs, and ventilation and air pollution control techniques. It is recognized that such trench burns will not yield any data on potential problems related to ground subsidence or gas leakage to strata. Only a field burn experiment in an actual coal seam can provide this type of information.

With this viewpoint, we designed the trench facility shown in Figure 1 which is currently under construction at Bruceton. The facility is composed of a cement and insulating brick lined rectangular trench with inside dimensions 40' long, 6'8" wide and 9'6" high. Up to 30 tons of rubblized coal and other carbonaceous material (e.g., coal and roof strata) can be burned in the trench. In operation it is planned to have one or more air channels formed from metal grates passing through the coal rubble. The top of the trench will be sealed with a sand covered metal door. For a single straight through 12" rectangular air channel, the coal zone will have a minimum web thickness of 2-1/2 ft enabling the burn to proceed for an estimated 24 to 36 hours before the coal devolatization (pyrolysis) wave reaches the trench wall. Under steady state operating conditions, approximately one Megawatt of thermal power should be developed. The ventilation system for the trench will consist of a 15,000 cfm fan capable of developing an 18" H_2O pressure drop. Operating in exhaust mode (see Figure 2), the fan will pull combustion air into the trench, exhaust products through the trench/incinerator system, and "bleed" air into the ventilation duct just prior to the fan housing. The bleed air mixing with combustion products serves to cool the exhaust prior to its passing through the fan housing and emission to the atmosphere. The final gas emission temperature will be considerably less than 250°C, the maximum fan operating temperature.

The incinerator unit is designed to reduce smoke emissions during the trench burn, particularly during fire start-up. A separate gas burner/air injector system at the entrance to the incinerator can be operated as either an after burner to reduce the smoke concentrations, or as a fuel injector to reduce the O_2 levels in the exhaust.

It is planned to develop servo-control techniques for operating the combustor. Through these controls we will attempt to maintain a constant exhaust gas composition and constant thermal output during a burn. Also during a burn, a number of probes will be employed to follow gas and coal temperatures, gas compositions, pressure drops and flow velocities. These data will be collected and organized (ADP system), and subsequently analyzed to yield information on optimum operating conditions for the combustor. In the course of operations, it is planned to evaluate a number of high temperature materials of construction (e.g., pipes, valves, probes, etc.) for potential use in a field demonstration experiment.

As indicated previously, the trench burn facility has not yet been built, although complete construction designs have been specified for all parts of the system, all major equipment components have been ordered, and a construction contract is underway. We anticipate that operation of the trench will begin before the end of 1976.

HEAT BALANCE IN IN SITU COMBUSTION

In a previous report [1], a very simple steady-state model of the conductive heat loss from a burning coal seam was postulated which suggested that an in situ combustor would have negligible conductive heat loss to the surrounding strata. This problem has been looked at more realistically, but still with a relatively simple steady-state model, which now suggests that minimum conductive heat losses of 10 to 15% can be expected.

Briefly, the model consists of a rectangular channel which moves normal to its long axis of length ℓ, at a constant coal burning velocity B through a coal seam of thickness h (see Figure 3). It is postulated that the roof fall is such that a constant channel width w is maintained. Considering the combustor to be a well mixed stirred reactor with constant roof and floor temperature equal to the temperature of the combustion products, the conductive heat loss is essentially the one-

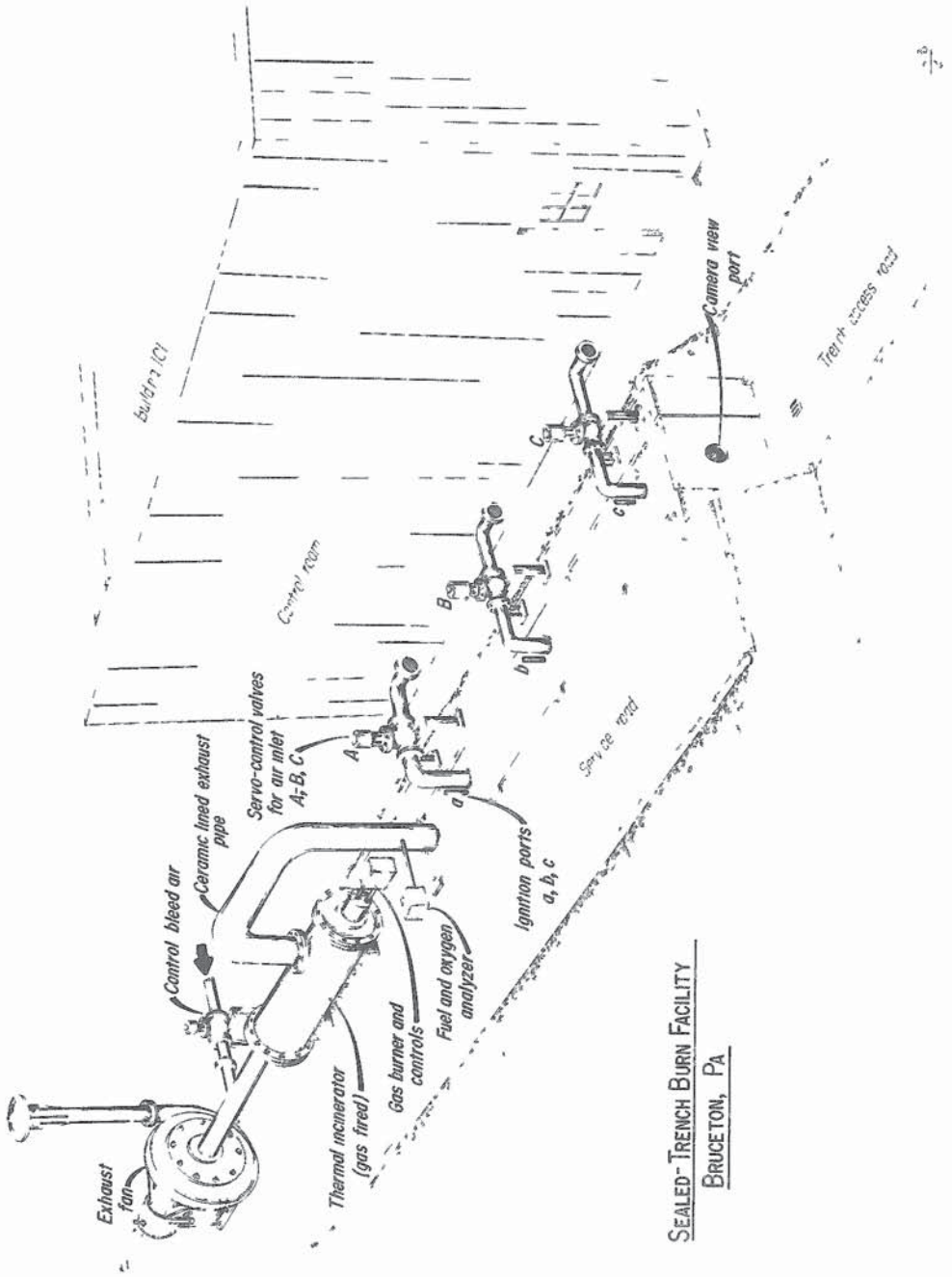


FIGURE 1. Sealed-Trench Burn Facility, Bruceton, Pa.

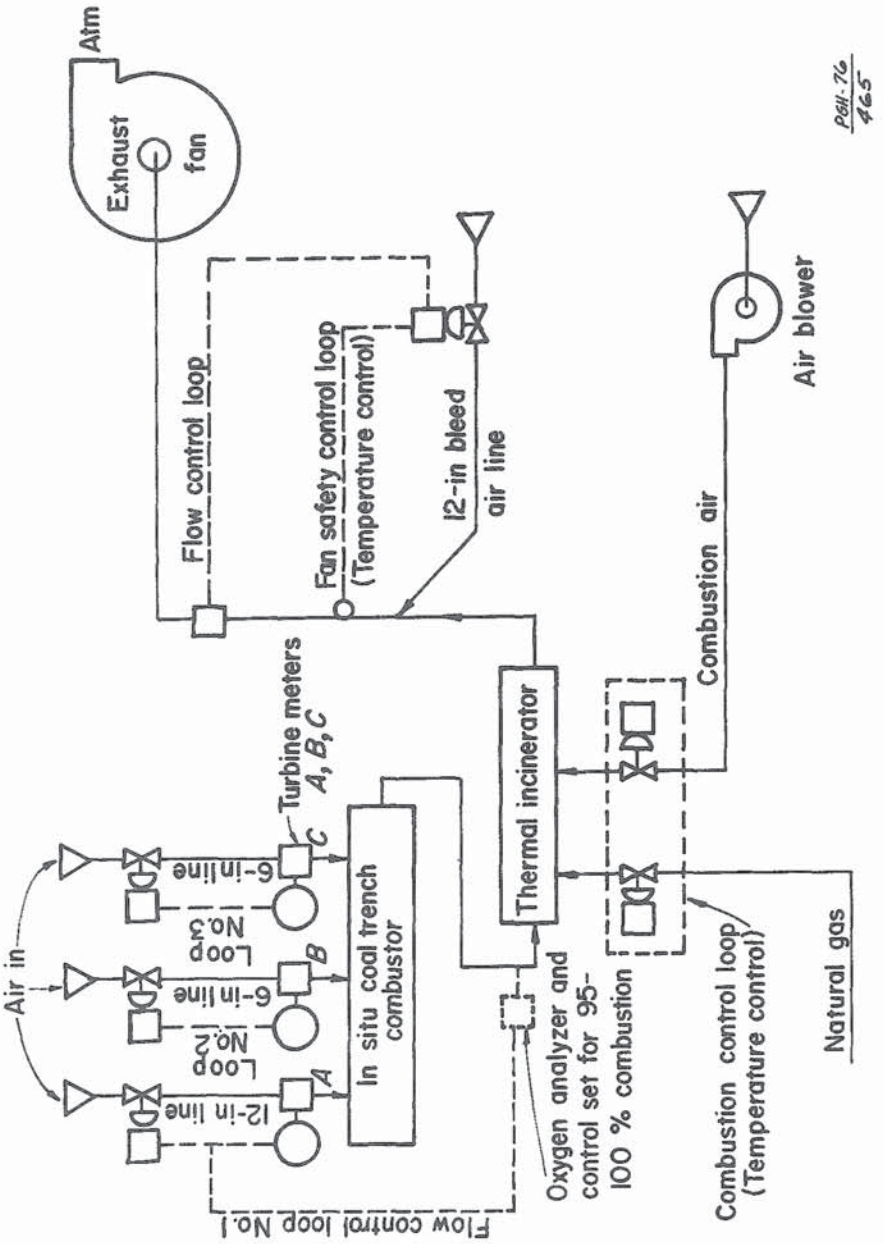


FIGURE 2. Control Diagram for Bureau of Mines In Situ Coal Trench Combustor.

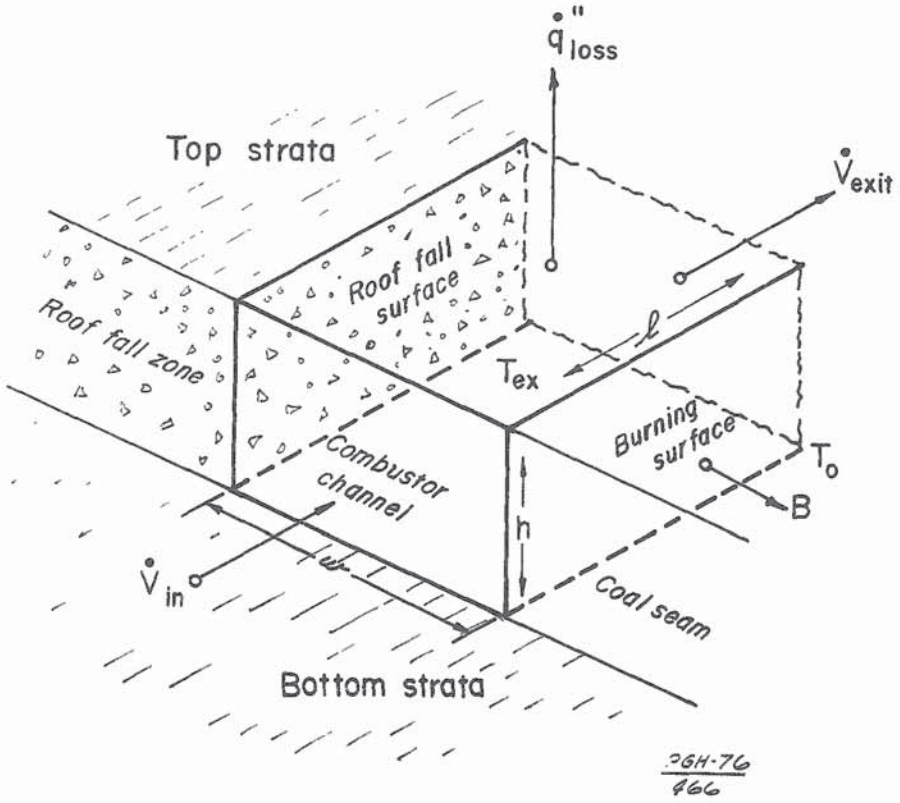


FIGURE 3. Model Coal Seam Combustion Channel.

dimensional heat flow from the roof and floor (area = $2w\ell$) to the surrounding rock strata. Gas leakage to the strata is assumed to be neglible.

The heat conduction problem is essentially identical to that treated by Warner and Szekely [6] so that we can write directly for the total steady rate of heat loss per unit length of channel (equation 9 of [6]).

$$\dot{Q}'_{\ell} = 4\lambda\Delta T \sqrt{\frac{wB}{\pi\kappa}}, \quad \text{cal/cm-sec} \qquad (1)$$

where λ and κ are the thermal conductivity and thermal diffusivity of the strata, respectively and $\Delta T = (T_{ex} - T_o)$ is the temperature difference between the hot combustion products and the ambient condition.

The steady-state energy balance for the combustor is then

$$\rho_s B\Delta H h\ell = C_p \rho_g \dot{V}_{exit} \Delta T + 4\lambda\Delta T\ell\sqrt{\frac{wB}{\pi\kappa}} \qquad (2)$$

where ρ_s and ΔH are the density and heat of combustion, respectively, of the coal; C_p, ρ_g and $\dot{V}_{exit}$ are the heat capacity, density and volumetric exhaust flow rate, respectively, of the hot combustion gases.

The LHS of equation 2 is the total rate of heat input due to the coal combustion process, and the first term of the RHS is the total rate of heat flow due to the exhaust of hot gas from the channel.

Solving for the reciprocal temperature, we obtain

$$(\Delta T)^{-1} = \frac{C_p \rho_g \dot{V}_{exit}}{\rho_s B\Delta H\ell h} + \frac{4\lambda}{\rho_s B\Delta H h}\sqrt{\frac{wB}{\pi\kappa}}. \qquad (3)$$

It can be noted that the quantity $\rho_s B\ell h$ is simply the coal mass burn rate, while the quantity $\rho_g \dot{V}_{exit}$ is the total mass exhaust rate (i.e., the sum of the coal burning rate and ventilation air intake rate). The ratio ϕ of these two quantities is related simply to the mass stoichiometry of the coal combustion process. Equation 3 can then be rewritten as

$$(\Delta T)^{-1} = \frac{C_p \phi}{\Delta H} + \frac{4\lambda}{\rho_s \Delta H h}\sqrt{\frac{w}{\pi\kappa B}} \qquad (4)$$

where $\phi = \dfrac{\text{mass of gas products}}{\text{mass of coal burned}}$ (5)

The quantities ϕ, ΔH and C_p can be readily evaluated from chemical equilibrium calculations allowing ΔT to be calculated for any assumed values of the strata thermal transport coefficients and coal burning velocity.

It can also be noted from equation (4) that the fractional heat loss, E_L, and thermal efficiency, E_H of the combustor can be defined by the quantities

$$E_L = C_p \phi\Delta T/\Delta H \qquad (6)$$

and

$$E_H = \frac{4\lambda\Delta T}{\rho_s \Delta H h}\sqrt{\frac{w}{\pi\kappa B}} \qquad (7)$$

Sample calculations of ΔT and E_L were carried out for a 150 cm ($\sim$5 ft) thick bed of Pittsburgh seam coal surrounded by a sandstone type strata. Table 1 lists the assumed physical properties of

the strata and coal and coal burning velocity.

Table 1. Input Physical Property Data for Numerical Calculations

$\lambda = 4 \times 10^{-4}$ cal/cm-sec-°C	$\rho_s = 1.3$ gm/cm^3
$w = 600$ cm	$\kappa = 10^{-4}$ cm^2/sec
$h = 150$ cm	$T_o = 27°C$
$B = 2 \times 10^{-4}$ cm/sec	

Table 2 lists the variation of C_p and ΔH with ϕ as determined by chemical equilibrium calculations. Figure 4 depicts the calculated results for variation of ΔT and E_L with ϕ.

Several points are worth noting from these data. First is the fact that E_L decreases with increasing ϕ and reaches a value of 11 to 12% for $\phi > 12$. Since stoichiometric burning occurs at $\phi \sim 11$, this means that E_L is lowest in the oxygen-rich regime of combustion. The exhaust temperature in the range of $\phi = 12$ to 17 (i.e. T = 1100° to 1200°C) should be quite respectable for purposes of steam production. A second point to note is that for fuel rich burning conditions ($\phi < 11$) the heat losses increase fairly rapidly, approaching 30% at $\phi = 5$. This suggests that if this type of channel combustor is operated as an underground gasifier, fractional large heat losses will be sustained.

Table 2. Calculated Equilibrium Properties of Coal Combustion Products*

Ash Free Pittsburgh Seam Coal: $CH_{0.782}N_{0.018}O_{0.068}S_{0.0058}$

ϕ = mass gas products / mass coal	ΔH_{comb} cal/gm	Adiabatic T °C	$\overline{C}_p$ cal/gm-°C
5	1390	981	0.337
7	3130	1450	0.342
9	4820	1810	0.433
11	6630	2020	0.442
13	7610	1980	0.493
15	7860	1810	0.375
17	7910	1640	0.336

*NASA/LEWIS Equilibrium Code

It can also be noted from equation 7 that the geometric scaling factor for E_L is the ratio $\sqrt{w}/h$. It is reasonable to expect that if an effective constant width burning channel does form during an actual IC process, the effective width of the channel will be directly related to the coal seam thickness, i.e., thicker coal seams will support wider burn channels. Using the input data of Table 1, it is calculated that a value of $\sqrt{w}/h \sim 0.2$, will lead to $E_L \sim 15\%$ and $\Delta T \sim 1100$. For a 150 cm (5 ft) thick seam, this implies that the value of w should not exceed 900 cm (30 ft), which is not an unreasonable result. For a seam thickness of 60 cm (2 ft), the corresponding value of w is 144 cm ($\sim$4.8 ft), which again is not unreasonable.

From the above results, it might be concluded that in the absence of gas leakage from an IC channel to the ground strata, as much as 80 to 90% of the heat of combustion of the coal will appear as sensible heat in the exhaust gas. However, too little information is available on the nature of the roof-fall process and its accompanying effects on channel width and gas leakage to assume at this time that such high thermal efficiencies will be achieved in a practical in situ combustion scheme.

REFERENCES

1. Chaiken, R. F., "In Situ Combustion of Coal for Energy", BuMines Technical Progress Report No. 84 (Nov. 1974), 12 pp.

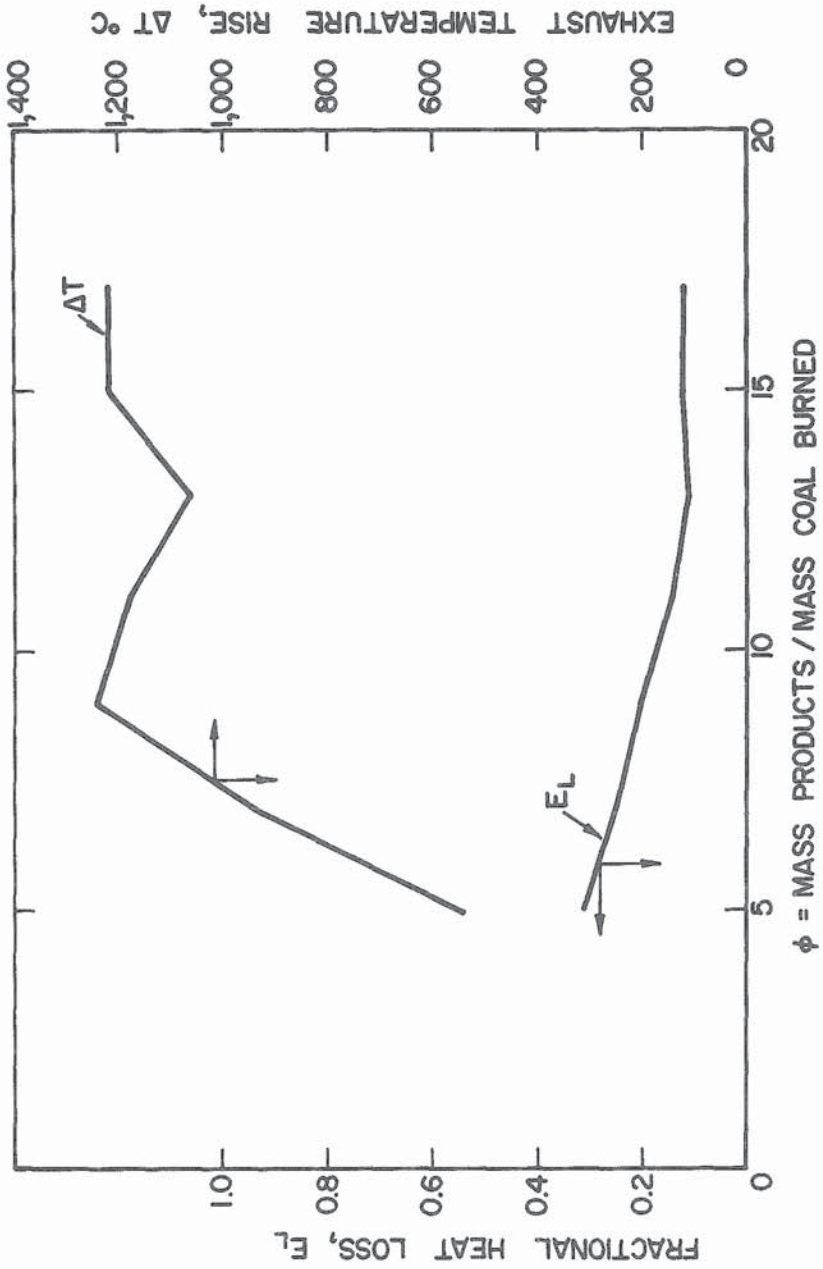


FIGURE 4. Variation of Fractional Heat Loss, E_L and Exhaust Temperature, ΔT on Stoichiometry Ratio ϕ = (mass products)/(mass coal).

2. Wang, C. S., Capp, J. P., Wane, M. T., and Boshkov, S. H., In Situ Gasification and Liquefaction Mining Systems. Ch. in SME Mining Engineering Handbook, Port City Press, Baltimore, Md., U. 2, 1973, pp. 21-78 to 21-96, 21-112 to 21-116.
3. Elder, J. L., Fies, M. H., Graham, H. G., Montgomery, R. C., Schmidt, L. D., and Wilkins, E. T., "The Second Underground Gasification Experiment at Gorgas, Ala., BuMines RI 4808, 1951, 72 pp.
4. Gibb, Sir Alexander, and Partners, "The Underground Gasification of Coal", Report to the National Coal Board, Pitman & Sons, London (1964), 205 pp.
5. Magnuson, M. O., "Control of Fires in Abandoned Mines in the Eastern Region of the United States", BuMines IC 8620 (1974), 53 pp.
6. Warner, F. E. and Szekely, J., "Underground Gasification of Coal: Part II, A. I. Ch.E.-I. Chem. E. Symposium Series No. 2. London: Instn. Chem. Engrs. (1965), pp. 49-55.

GROUNDWATER CONTAMINATION FROM IN-SITU COAL GASIFICATION: LABORATORY STUDIES

by

J. F. Henry
M. D. McKinley

ABSTRACT

A feasibility study for in-situ coal gasification in the Warrior coal field of Alabama is being conducted. As part of this study, estimates of the effect of a coal gasification operation on the groundwater are being made. The levels of contaminants to be expected by leaching of chemicals from burned-out coal seams by groundwater flowing through the area were predicted by experimental simulation in the laboratory. In most cases the levels of contaminants never exceeded the recommended limits for public water supplies. In those cases where the level of contaminants in the water was initially high, the concentration rapidly decreased so that no long-term problems are predicted.

INTRODUCTION

The University of Alabama is conducting a feasibility study of in-situ coal gasification in the Warrior coal field of Alabama in cooperation with the Geological Survey of Alabama and Alabama industries. The major portion of the funding for the study is from the National Science Foundation.

One aspect of the feasibility study deals with the possible effects of a gasification operation on the groundwater. The groundwater in Alabama is plentiful and is of good quality, so that contamination of the groundwater would be a serious problem. Most potential coal seams for in-situ gasification in Alabama lie below the water table, so direct contact between the groundwater and the gasified seam would take place. There are two potential sources of groundwater contamination that are of concern. Gas which leaks from the seam being gasified will contain water-soluble contaminants that will be absorbed by the groundwater. This absorption will occur only as long as the gasification is going on, and will cease whenever gas production is stopped. This type of contamination is not being considered here. Another possible source of groundwater contamination that is of more long-term concern is by leaching of soluble contaminants from a previously gasified zone by groundwater which is migrating through the region. This latter case is the one being considered here.

After the coal has been gasified from a portion of a coal seam, the residue and surrounding strata will cool by conduction and by seepage of water into the region. Because the coal seam is below the water table, migration of groundwater through the burned-out region because of hydraulic gradients will cause leaching of chemicals from the residue into the groundwater. A burned-out region would contain regions where there is only ash, regions where there is carbonized coal, while other regions would have partially carbonized coal in varying states of

carbonization. There would also be regions which did not get very hot which would contain condensed tars. Thus, water migrating through a burned-out zone would contact everything from ash to unaffected coal. Therefore, one would expect both organic and inorganic compounds to be extracted.

Although the environmental considerations of UCG are important, little work has been done on the subject to date. An indication of the types of contaminants to be expected can be obtained, however, by examining the results of studies made in connection with above-ground coal gasification processes. Table 1 shows the approximate composition of a coal tar sample, and Table 2 shows the types of contaminants found in process water in an above-ground gasification test. While these results indicate the types of compounds to be expected, they are not adequate for an environmental assessment of UCG.

Table 1

Some of the Contaminants in Coal Tar (1)

	Percent
Naphthalene	10.9
α-Monomethylnapthalene	1.0
β-Monomethlnaphthalene	1.5
Acenaphthene	1.4
Fluorene	1.6
Phenanthrene	4.0
Anthracene	1.1
Carbazol and kindred nonbasic nitrogen-containing bodies	2.3
Phenol	0.7
Phenol homologs (largely cresols and xylenols)	1.5
Tar bases (mostly pyridine, picolines, lutidines, quinolines, and acridine)	2.3
Total	28.3

Table 2

Contaminants in Product Water from Coal Gasification (2)

α, β Napthol	Isopropyl phenol
Benzofuranol	Phenol
Indanol	Xylenols
Trimethylphenol	Cresols
Methylethylphenol	Methyl pyridine
Ethylphenol	Ethylpyridine
Indole	Catechol

References at end of paper

The work described here is a combined laboratory and modeling effort to assess the long-term effects of UCG on groundwater by the leaching mechanism described above. The laboratory work consists of gasifying coal and then conducting leaching experiments on the residue to determine the type and concentration of contaminants in the water as a function of time by standard water quality analysis. The dispersion of contaminants from the gasified region is to be predicted by mathematical modeling. This work is still in progress, so the analysis is not complete. A more complete report will be issued when this phase of the study is complete.

Geology of Proposed Gasification Site

The Warrior coal field of Alabama is the largest and most productive of the coal fields in the state and carries the largest reserves. It lies in the west-central part of the state, consisting of a 12-county area. It lies almost entirely in the basic of the Black Warrior River, which has an area of about 5800 square miles (15000 km^2). Structurally, the Warrior coal field is a broad, gentle syncline pitching toward the southwest. This coal field contains many coal seams overlaying each other at different depths. Many of the seams are thin (less than 36 inches), and the coal is generally a swelling, coking-type bituminous coal.

In order to be able to assess the feasibility of underground coal gasification in the Warrior coal field, a prospective site has been located on University of Alabama lands in Jefferson County. The property is located in Section 6, T. 19 S., R.5 W. (Yolande 15' quardangle). The coal seam which was chosen is the Gwin seam, which lies under 260 feet (79.2 m) of overburden and is 34 inches (0.86 m) thick. This coal lies in the Lower Pottsville formation.

In order to be able to simulate leaching experiments in the laboratory, it is necessary to estimate the velocity of groundwater migration in the region. Unfortunately, only limited data are available for making this estimate. Gilluly, et al (3) state that the water table "is a somewhat flattened replica of the surface topography." Over a small region, the hills and valleys obscure the general slope of the land, but looking at a larger region, one can estimate this slope. In our case, a study of USGS topographic maps of the region show that our proposed site lies in a region where the slope is from Rock Mountain down toward Branch Creek, which is a year-round creek. Figure 1 shows a cross-section of the land in an almost north-south direction from Branch Creek to Rock Mountain passing through our proposed site. The dry-season water table is plotted starting at Branch Creek and is extended at a slope the same as that of the general terrain. The wet weather water table varies and at some times it extends to the surface at several points where there are seasonal streams. Note that the coal seam involved as the test case here lies below the dry-season water table.

In the lower Pottsville formation, fractures of various sizes, both joints and faults, are so numerous that the permeability of all the formation strata is increased considerably over what it would be if there were no fractures. Drahovzal, et al (4) state that the fractures occur in such a way that on a regional basis the hydrodynamic properties of the strata are approximately isotropic. Thus, on a regional basis we can apply Darcy's law to calculate the velocity of water in the region of interest. The permeability of the lower Pottsville region is about 150 darcys (5), and the pressure gradient is approximately 50 feet of water per mile, (9.5 m/km) from the estimate above. These data combine to give superficial water velocity of 1600 ft/yr (0.0015 cm/sec). This estimated velocity was the basis for the water flow rates used in the extraction experiments described below.

EXPERIMENTAL

Coal

Adequate samples of the Gwin coal seam were not available at the time this study was begun, so samples of a similar coal from this region were used. The analysis of the coal used in this study is given in Table 3.

FIGURE 1. CROSS-SECTION OF SITE VICINITY

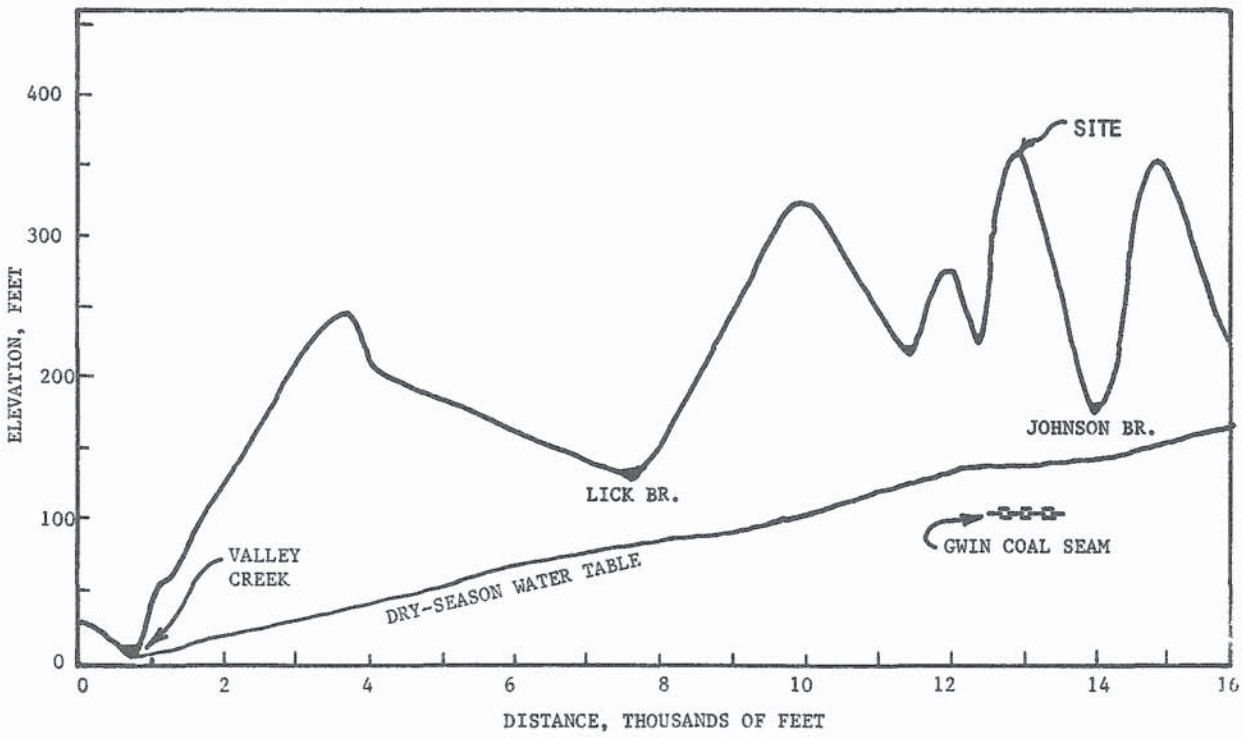


Table 3
Properties of Coal Used

Dry Basis

	Before Carbonization	After Carbonization
	Proximate	
Volatile Matter	32.91	5.41
Fixed Carbon	64.63	62.28
Ash	2.46	32.31
Sulfur	1.88	0.86
Heating value, BTU/lb	14,649	9,613
	Ultimate	
Carbon	80.54	61.81
Hydrogen	5.59	1.89
Nitrogen	1.76	1.01
Sulfur	1.92	0.81
Ash	2.60	32.31
Oxygen (by difference)	7.59	2.12

Pyrolysis

Laboratory gasification experiments began at the same time as the work described in this report, so that adequate supplies of coal residue produced under conditions simulating underground gasification were not available. Therefore, it was necessary to produce coal residue in a simple apparatus that would give a product containing coal in various stages of gasification from ash to only slightly affected coal. The apparatus used for this is shown in Figure 2. In this apparatus, large chunks of coal were charged, and heat was provided by a gas burner. Air flow was by natural connection. It was necessary to use large chunks of coal, because large passages for air were needed in order to prevent plugging of the apparatus by the swelling coal. Four runs were required to produce enough residue for the leaching experiments. It took about one hour of heating to raise the temperature throughout to about 650 °F. After 650 °F was reached, it took only a few minutes for the temperature to exceed 1200 °F and flame to shoot out the top of the vessel. At this time the air flow was restricted to cause partial combustion, and after a few minutes the air flow was stopped altogether. The vessel was allowed to cool by natural convection before removing the residue. Table 3 shows the results of the pyrolysis. This indicates that some of the coal was completely burned and some was pyrolyzed, as indicated by the large increase in ash. Because there is some volatile matter remaining, some of the coal was not completely pyrolyzed. Thus, a mixture of coal in various stages of gasification was prepared. The coal residue was broken and separated into three sizes for the leaching experiments as shown in Table 4.

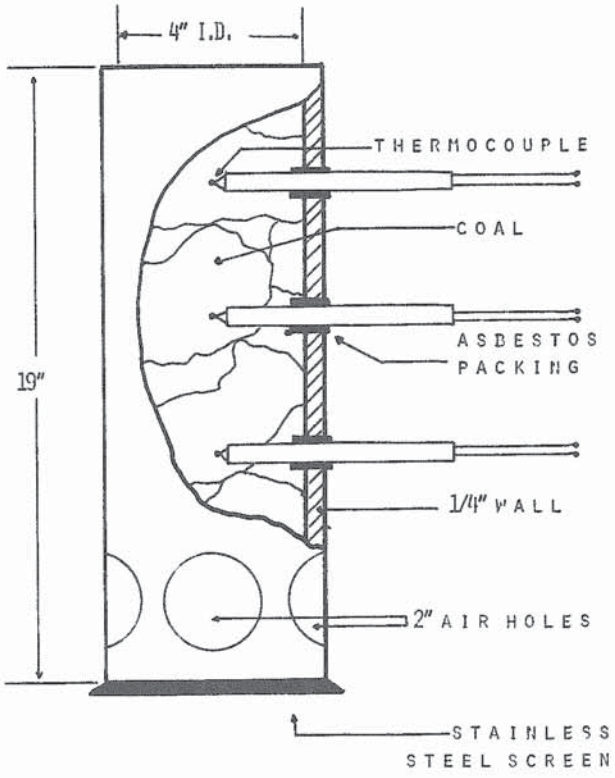


FIGURE 2. CHAR PRODUCER

Table 4

Residue Particle Sizes

Particle size	Mesh size	Average diameter
Large	-1.050 inches to +0.742 inches	0.896 in. (2.28 cm.)
Medium	-3 + 6	0.197 in. (0.500 cm.)
Small	-10 + 35	0.0407 in. (0.103 cm.)

Leaching Experiments

The apparatus for the leaching experiments is shown in Figure 3. Before the extraction experiments were begun, the equipment and all sample collection vessels and storage bottles were cleaned with detergent, rinsed well with tap water, and rinsed with methanol to remove as many external contaminants as possible. Only glass bottles with ground glass stoppers were used for storage. The equipment was assembled and flushed with tap water for two days. After this, the water flow rate was reduced to that calculated to match the estimated groundwater velocity (1.89 cm^3/min), and for almost 5 days blank samples were collected to be used to

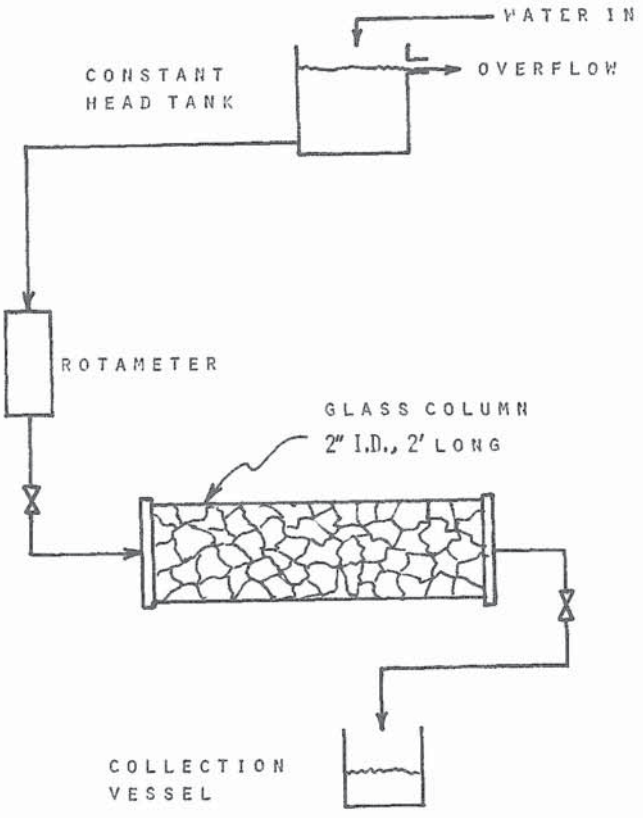


FIGURE 3. LEACHING APPARATUS

determine the background level of contaminants present in the system. Table 5 gives additional pertinent data on the packed tube experiments.

Table 5

Packed Tube Properties

	Particle mass needed to fill tube (grams)	Volume of water in tube packed with particles (ml)	Water residence time in tube (hours)	Duration of run (days)
Minimum size	648	605	5.35	27.196
Middle size	520	680	6.00	28.250
Maximum size	446	765	6.75	31.479

The coal residue was then packed into the glass pipe and the water was fed into the pipe at a rate that gave the same superficial water velocity as calculated for the test site. This rate is 1.9 cm^3/min. Table 5 gives the data regarding the packing of the pipe. These residue densities correspond to a situation where over 50 percent of the coal in the seam is completely gasified.

The water collected was analyzed for soluble contaminants by the recommended standard methods of analysis of water (6).

DISCUSSION OF RESULTS

The leaching experiments have now been completed for all of the particle sizes, but the chemical analysis of the effluent water is not complete. Analyses for metals in the water are not complete and are not reported here. Analyses for other organic and inorganic components are complete for the large and the small particle sizes, but are still in progress for the middle-sized particles. The available experimental results as a function of time are presented for each particle size in Figures 4 - 9.

Figure 4 shows the BOD content of the effluent water. There is no universally applied standard for the limits of BOD in water, but Table 6 shows that for the Tuscaloosa, Alabama sewage treatment plant a level of 36 mg/l is allowed and 26 mg/l is typical. The levels of less than 4 mg/l found for all samples here are considerably less than these sewage-treatment plant effluents.

Figure 5 shows the COD content of the water. Again, there are no universally applied standards, but an average of 98 mg/l found in the last monthly average for the Tuscaloosa sewage-treatment plant effluent can be used for comparison (Table 6). In the similog plot on Figure 5 the straight lines indicate exponential decay of the COD concentration in the water. Although the initial values of COD are relatively high, the water was crystal clear.

The organic acid content in the effluent is shown in Figure 6. Again, exponential decay of the concentration is indicated. Since the nature of the contamination problem from organic acids depends upon the nature of the acids, no general criteria for water quality based on the gross amount of acids have been set.

The maximum recommended ammonia (reported as nitrogen) in public water supplies has been set at 0.5 mg/l (Table 6). Figure 6 shows that the level of ammonia is initially considerably higher than this, but after about 700 hours the level in the effluent approaches this recommended value.

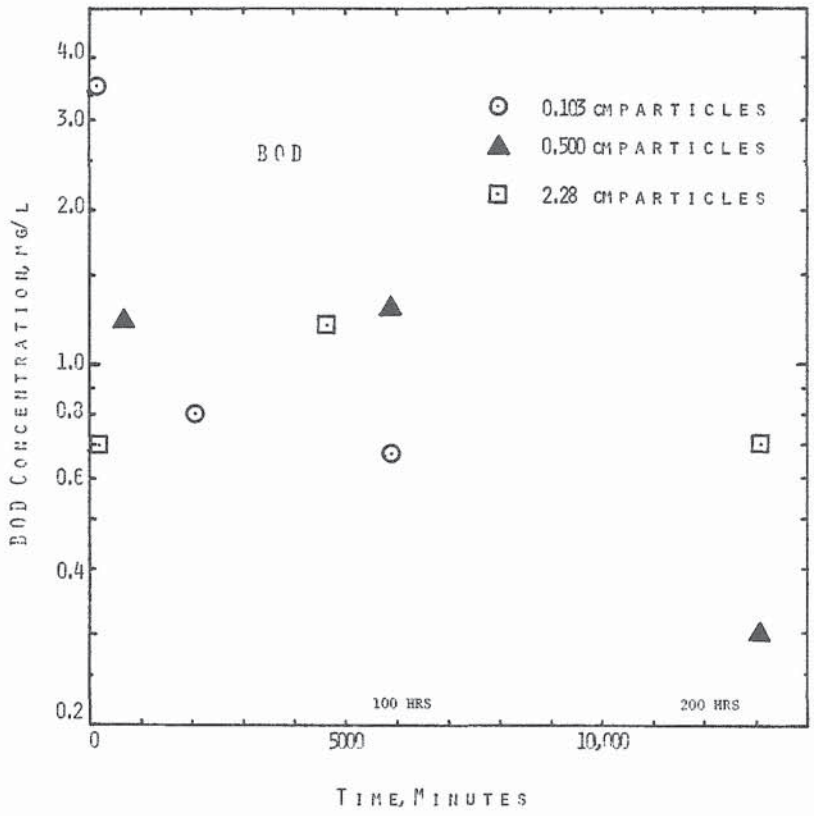


FIGURE 4. BOD CONTENT OF WATER

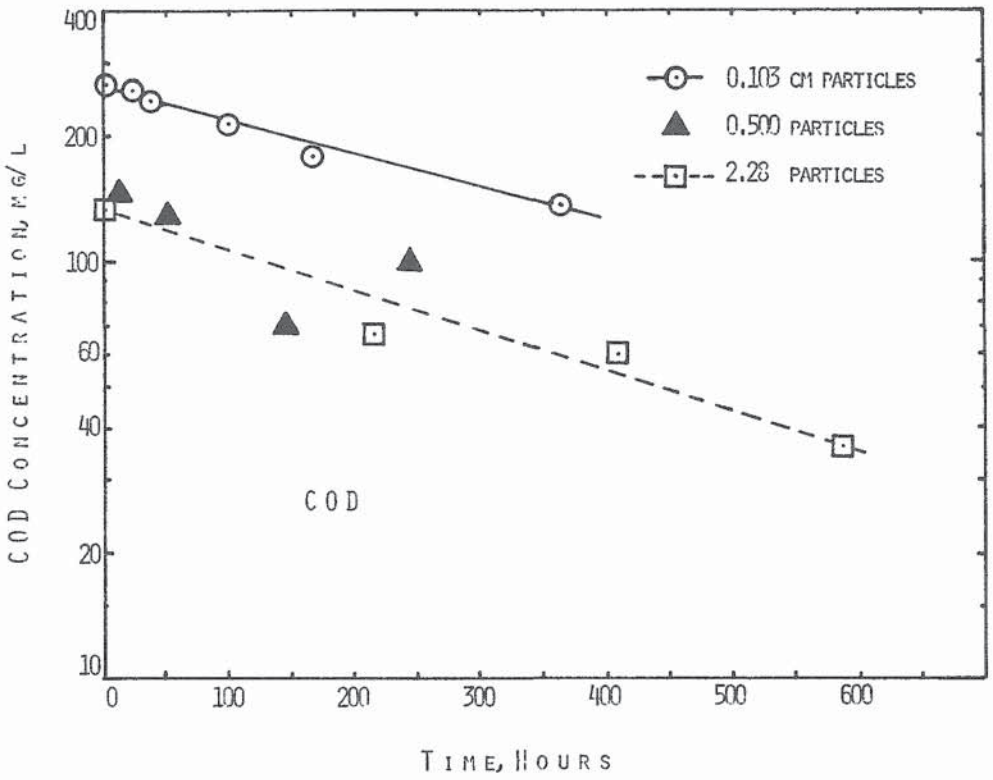


FIGURE 5. COD CONTENT OF WATER

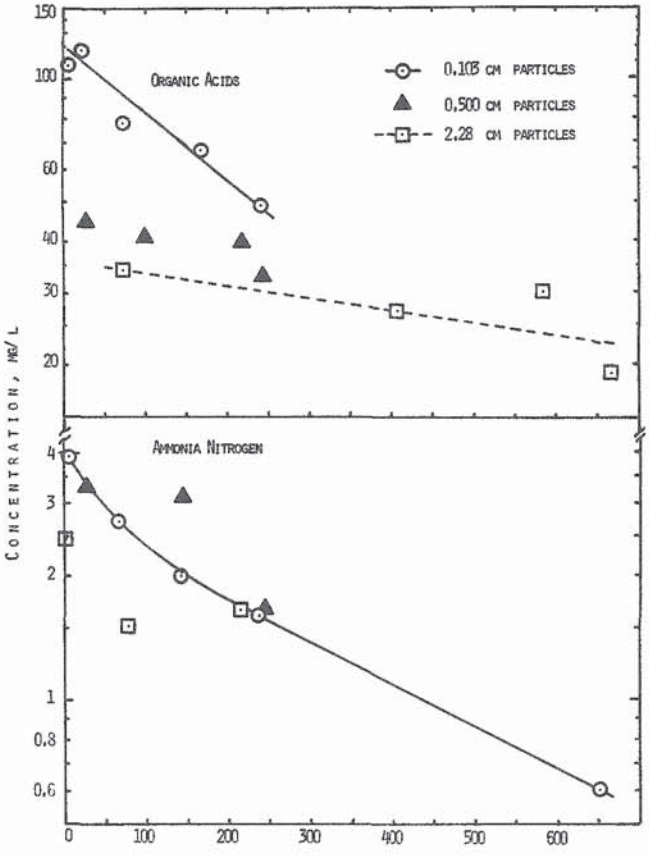


FIGURE 6. WATER ANALYSIS RESULTS

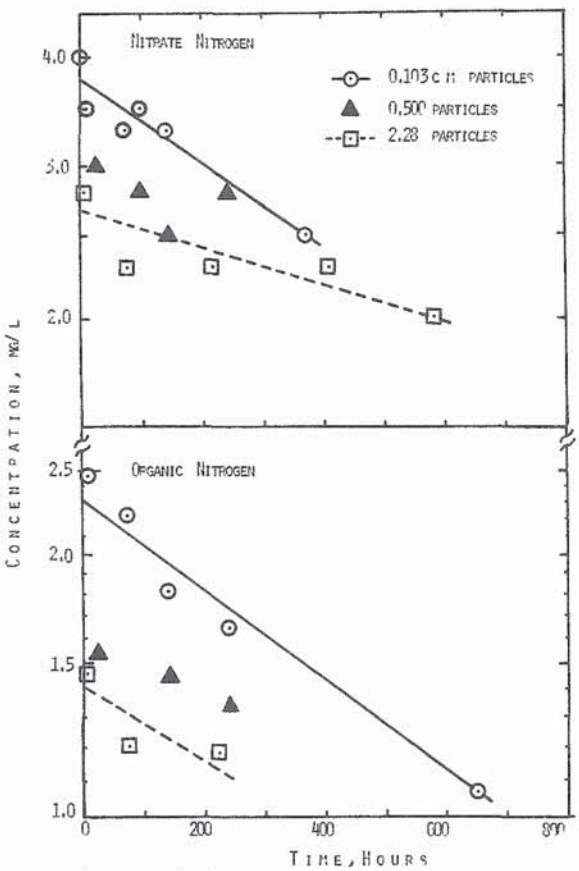


FIGURE 7. WATER NITROGEN CONTENT

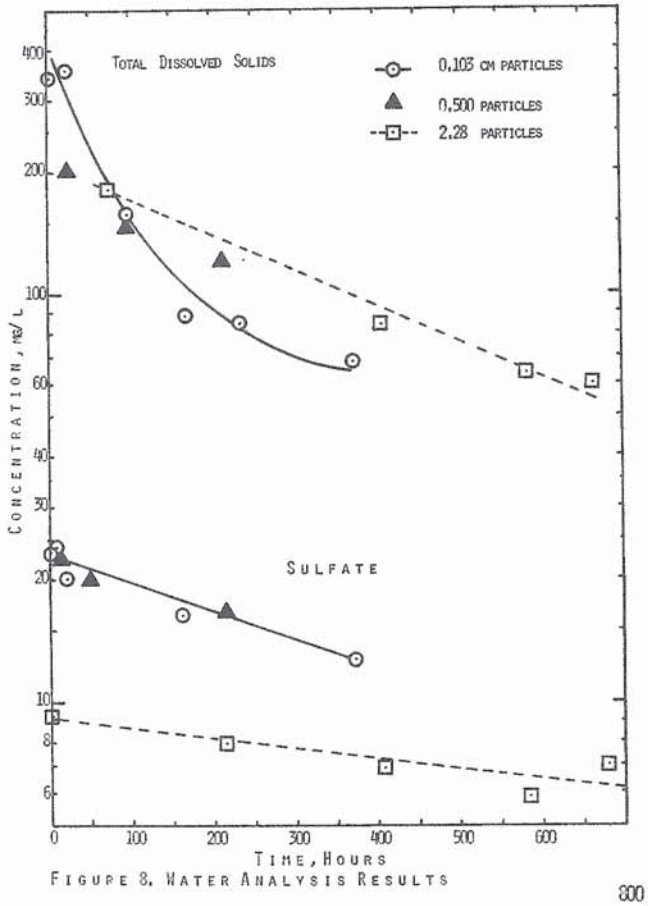


FIGURE 8. WATER ANALYSIS RESULTS

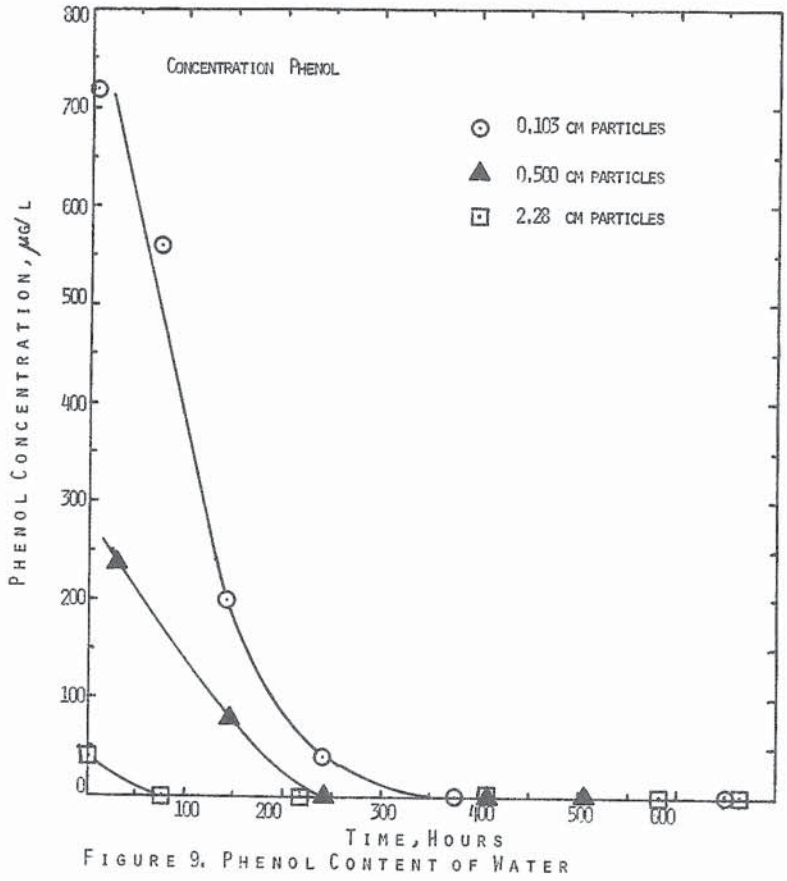


FIGURE 9. PHENOL CONTENT OF WATER

Table 6

Reference Compositions for Contaminants in Water

Inorganic components not including metals	
Ammonia (as N)	0.5 mg/l[d]
BOD	26.4 mg/l[a]
	36 mg/l[b]
COD	98 mg/l[c]
Nitrate (as N)	10 mg/l[g]
Nitrite (as N)	10 mg/l[d]
Sulfate	250 mg/l[d]
Total dissolved solids	500 mg/l[f]
Organic components	
Nitrogen, organic	no standard[e]
Organic acids	no standard[e]
Phenols	1 µg/l[d]

[a]Effluent average for June 25 - July 24, 1976, of samples taken 7 days per week, Tuscaloosa (Alabama) Wastewater Treatment Plant, 1976a. (7)

[b]Effluent monthly average set by EPA as suitable for Tuscaloosa Wastewater Treatment Plant, Tuscaloosa (Alabama) Wastewater Treatment Plant, 1976 b.

[c]Effluent average for June 25 - July 24, 1976, of samples taken 5 days per week, Tuscaloosa (Alabama) Wastewater Treatment Plant, 1976 b. (8)

[d]Recommended maximum level for public water supply (Water Quality Criteria 1972, March 1973, Section II).

[e]Concentration levels indicative of a contaminant problem vary, making it difficult to set a standard or a recommended limit. (9)

[f]Desirable maximum level for public water supply; may be exceeded if concentration of other individual substances remain below recommended limits (Water Quality Criteria 1972, March 1973, Section II).

[g]Maximum level set by law for public water supply (Federal Register, December 24, 1975).

Table 6 shows that the maximum legal level of nitrate (reported as nitrogen) in public water supply is 10 mg/1. Figure 7 shows that all values meaured here were below this value and decreasing rapidly. No nitrite was found in the samples. Organic nitrogen is also shown on Figure 7, but, again, as for organic acids the contamination problem and the relevant standards depend upon the chemical nature of the contaminant and the intended use of the water. No long-term effects are indicated for organic nitrogen because of the rapid decrease in concentration observed in Figure 7.

The total dissolved solids in the samples is shown in Figure 8. These values are all below the desirable level for public water supply as shown in Table 6. Figure 8 also shows the sulfate composition to be well below the recommended level for public water supplies.

Figure 9 shows that initially the phenol concentration greatly exceeds the maximum recommended value of 0.5 µg/1 for public water supply. After 400 hours of leaching, however, the amount of phenols remaining in the water was undetectable.

In summary, these results show that for most of the contaminants observed the levels at no time exceeded the recommended maxima. For those few cases where the levels were initially high, the values decreased rapidly so that no long-term contamination problem is anticipated.

FUTURE WORK

The analyses for the medium-sized particles for the contaminants reported will be completed, as will the analyses for Cr, Cu, Na, Ni, Mn, and Zn in all of the samples.

The interpretation of the data is not complete. The effect of the dimensions of the system, compared to the particle size, on the effluent composition must be considered. The fact that the initial concentration levels for a particular contaminant were not the same for all particle sizes indicates that a rate-limiting process for the solubility or leaching in some cases is important. This will be investigated further.

Mathematical models for the dispersion of contaminants in the water flowing through a gasified zone have been derived. These will be used to show the concentration distribution around a burned-out site as a function of time and distance from the site.

References

1. Rhodes, E. O., "The Chemical Nature of Coal Tar," Chapter in "The Chemistry of Coal Utilization," Vol. 2, H. H. Lowry, editor, John Wiley and Sons, New York, 1945, p. 1287.

2. Schmidt, C. E., Sharkey, A. G., and Friedel, R. A., "Mass Spectrographic Analysis of Product Water from Coal Gasification," U. S. Bureau of Mines TPR 86 (1974).

3. Gilluly, J., Waters, A. C., and Woodford, A. O., "Principles of Geology," W. H. Freeman and Co., San Francisco (1959).

4. Drahovzal, J. A., Ward, W. E. II, and Evans, F. E. Jr., "Fracture Analysis in a Selected Area of the Warrior Coal Field, Alabama," Geological Survey of Alabama, Division of Energy Resources Research, Office of Coal Research, University, Alabama (1976).

5. Powell, W. J., District Chief, Water Resources Division, U. S. Geological Survey, Private Communication (1975).

6. "Standard Methods for the Examination of Water and Wastewater," American Public Health Assoc., Inc., New York, (1965,1976).

7. Tuscaloosa (Alabama) Wastewater Treatment Plant. Monthly report to the EPA for June 25 - July 24, 1976. Unpublished.

8. Tuscaloosa (Alabama) Wastewater Treatment Plant. Unpublished data for June 25 - July 24, 1976.

9. Whittle, G. P., Professor of Civil Engineering, The University of Alabama. Private communication. August 6, 1976.

Biographical Sketch

Dr. Marvin D. McKinley received his B.Ch.E., M.S.E., and PhD degree (1963) from the University of Florida in Chemical Engineering. After two years with E. I. duPont de Nemours and Company in Orange, Texas, he joined the faculty of The University of Alabama. He is currently associate professor of chemical engineering at The University of Alabama.

Jonathan F. Henry received his B.S. in Chemistry from The University of Alabama in 1974. He has been a graduate council fellow and graduate council research fellow while pursuing his M.S. degree in Chemical Engineering at The University of Alabama. Upon graduation Mr. Henry will be employed by the Continental Oil Company at Aberdeen, Mississippi.

Preliminary Laboratory and Modeling Studies on the Environmental Impact of "In-Situ" Coal Gasification

BY

J. H. Campbell and H. Washington

Lawrence Livermore Laboratory, University of California
Livermore, California 94550

ABSTRACT

A preliminary laboratory and modeling study on the environmental impact of "in-situ" coal gasification field testing is reported. Experiments were conducted on the aspects of ground water pollution; water leaching, transport, and dispersion of pollutants. The major inorganic contaminants leached from the coal ash were determined to be Al^{+3}, Ca^{+2}, and OH^{-}, while the principal organic pollutants were found to be phenols. A simple calculational model is used to predict the movement of the polluted ground-water. This model inputs information from laboratory experiments for the rate at which the above pollutants are removed from the gasification zone and the degree with which they are sorbed by the surrounding coal. It was discovered that ungasified coal has a strong beneficial effect on retarding the dispersion of the pollutants.

The problem of air pollution resulting from the flaring of the production gas was also examined. The extent of the air pollution plume that develops from this flaring is predicted using a simple computer model. These predictions have been carried out for a set of atmospheric and flare operating conditions that may be encountered during field tests. It was determined that the LLL field experiments will adequately meet air quality standards, even under adverse conditions.

I. INTRODUCTION

Currently, LLL is developing a method for "in-situ" gasification of subbituminous western coal [1]. This concept requires the explosive fracturing of a coal seam at depths of 300 to 600 m, igniting the top of the permeable fractured area, and then injecting steam and oxygen to convert the coal into fuel gases.

Of particular importance to the recovery of any fossil fuel is the effect the process will have on the environment. For "in-situ" gasification, there are three major areas of environmental concern, ground water pollution, air pollution, and ground subsidence. These areas are well recognized [2] and a number of papers have appeared in the Soviet literature related to subsidence and ground water problems faced during gasifier operation [3-6]. However, the Soviets have only been concerned with these effects on the process itself and not with the impact of the "in-situ" process on the environment.

References at end of paper

We consider the ground water and air pollution problems associated with "in-situ" coal gasification field testing, particularly the environmental aspects of the Hoe Creek I field test [2-7]. Our air pollution results are pertinent only to field testing and may not be applicable to large commercial "in-situ" operations. However, the ground water contamination and pollutant transport results are generally applicable to large operations.

GROUND WATER CONTAMINATION FROM IN-SITU GASIFICATION

Physical Description of the Problem

A simplified picture of the ground water pollution associated with "in-situ" gasification is given in Fig. 1. A void is left after gasification of the coal seam. Ash remains where the coal has been completely removed and surrounding the ash bed is a ring of char where heat has pyrolyzed the coal but the char has not been gasified. Outside the char ring is a zone contaminated by gases and tars that have migrated out of the gasifier during gasification.

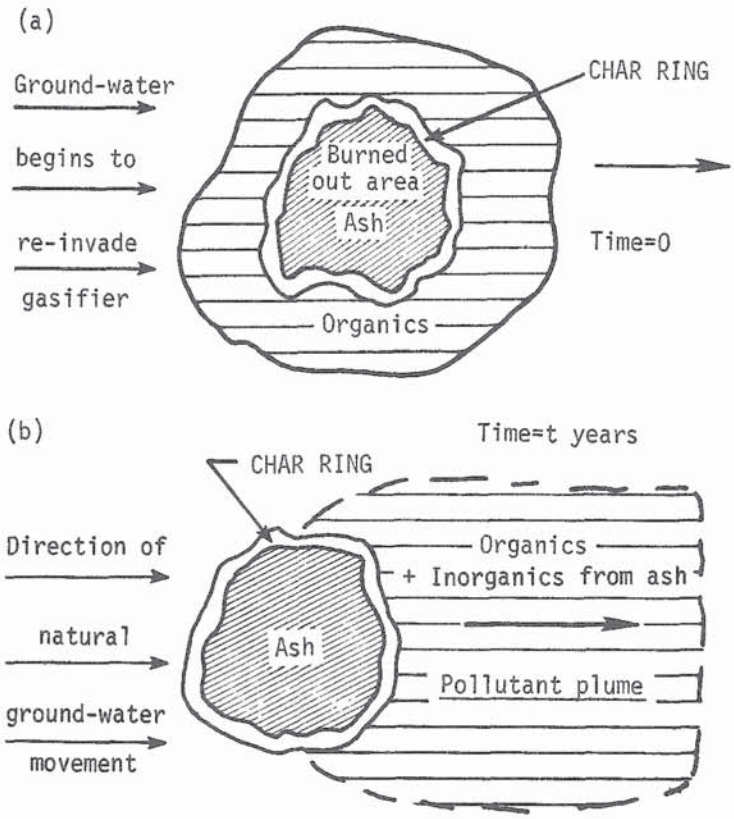


Fig. 1. Plan view of the post-gasification void (a) and the plume that develops as a result of the re-entry of ground water (b).

After gasification, water slowly enters the gasifier and, after a period of time, the natural flow through the coal aquifer is reestablished (Fig. 1b). The pollutants originally contained in or near the gasification zone are leached out and carried downstream by the flowing ground water. The hydrodynamic transport and dispersion of these pollutants in a porous rock media determines the distribution and concentration of the contaminants after they enter the ground water.

To predict the pollutant distribution as a function of time we need a model that accurately describes the process and reliable input parameters that describe the conditions under which the process takes place.

In the following sections, a computer model that calculates ground water pollutant transport and dispersion, the results of experiments used to determine model input parameters, and the results from the calculated prediction for the ground water pollutant distribution based on the above model and input data are presented.

Computer Transport Model

The model used to describe the movement of pollutants in ground waters is based on recent work by Holly et al [8]. They have developed a mathematical model for hydrodynamic transport of radionuclides in porous media based on the Transport Equation that accounts for dispersion and sorption of the pollutants as well as for different boundary conditions for the release of contaminants into the environment. An approximate two-dimensional solution is also given that incorporates the lateral dispersion of the pollutants.

The equation describing the one-dimensional transport of a solute by ground water flow is

$$B \frac{\partial C}{\partial t} - D \frac{\partial^2 C}{\partial x^2} + V \frac{\partial C}{\partial x} = 0 \ , \tag{1}$$

where x is the distance in direction of ground water flow in metres, C is the concentration of the solute in concentration units, D is the coefficient of dispersion in square metres per year, and v is the flow velocity of the ground water in metres per year. The retardation factor, B, accounts for the sorption of the solute on the porous media and is defined as

$$B = 1 + \left(\frac{1 - \phi}{\phi}\right) K_d, \tag{2}$$

where ϕ is the porosity and K_d is the distribution coefficient (the ratio of the concentration of the solute in the solid to its concentration in the liquid phase).

To solve Eq. (1), the initial condition is taken as

$$C(x,0) = 0 \text{ for } x > 0 \ . \tag{3}$$

The experimental results in the next section show the release of contaminates into the ground water to decrease approximately linearly with time, leading to the following boundary conditions:

$$C(0,t) = (C_o - kt) \quad \text{where} \quad 0 \leq t < t' \ , \tag{4}$$

$$C(0,t) = 0 \quad \text{where} \quad t > t' \ , \tag{5}$$

and where k is the rate of change of concentration with time (conc. units/y) and t' is the time at which C at x = 0 becomes zero (C_o/k). The solution to Eq. (1) under the above conditions is

$$C(x,t) = \frac{1}{2}\left\{\left(C_o - kt + \frac{Bkx}{v}\right) \operatorname{erfc} \frac{(x - vt/B)}{(2\sqrt{Dt/B})}\right\} + \left(C_o + kt - \frac{Bkx}{v}\right) \exp(vx/D) \operatorname{erfc} \frac{(x + vt/B)}{(2\sqrt{Dt/B})} \tag{6a}$$

for $t \leq t'$, and

$$C(x,t) = \frac{1}{2}\left\{\left(C_o - kt + \frac{Bkx}{v}\right) \operatorname{erfc} \frac{(x - vt/B)}{(2\sqrt{Dt/B})} + \left(C_o + kt - \frac{kBx}{v}\right) \exp(vx/D) \operatorname{erfc} \frac{(x + vt/B)}{(2\sqrt{Dt/B})}\right\} - \frac{1}{2}\left\{(C_o - k(t - t') + kBx/v) \operatorname{erfc} \frac{(x - v(t - t')/B)}{(2\sqrt{D(t - t')/B})} + (C_o + k(t - t') - kBx/v) \exp(vx/D) \operatorname{erfc} \frac{(x + v(t - t')/B)}{2\sqrt{D(t - t')/B}}\right\} \tag{6b}$$

for $t > t'$.

Note that Eq. (6b) is simply Eq. (6a) minus a similar term with $t = (t - t')$.

To properly model the dispersion of the pollution plume in both the x and y direction (i.e., in the direction of flow and lateral to the flow) we must solve the transport equation in two dimensions. Unfortunately, analytical solutions for the

two-dimensional case are difficult to obtain. Holly et al. [8], have found an approximate solution to the two-dimensional case by assuming that the dispersion in the y direction (lateral) is independent of the processes in the x direction (flow). Under this assumption, the concentration at any position and time is simply the product of Eq. (6) and the solution for lateral dispersion. The solution for lateral dispersion is

$$C(y,t) = \frac{1}{2} C_o \left\{ \operatorname{erf}\left(\frac{(R - y)}{2\sqrt{D_1 t/B}}\right) + \operatorname{erf}\left(\frac{(R + y)}{2\sqrt{D_1 t/B}}\right) \right\} , \qquad (7)$$

for $t > 0$ and where R is the radius of the source in metres and D_1 is the lateral dispersion coefficient in square metres per year. The boundary conditions are given as

$$C(y,0) = C_o \quad \text{where} \quad y \leq R ,$$
$$C(y,0) = 0 \quad \text{where} \quad y > R . \qquad (8)$$

The approximate two-dimensional solution is then the product of Eqs. (6) and (7):

$$C(x,y,t) = \frac{C(x,t) \cdot C(y,t)}{C_o} . \qquad (9)$$

In this work we have used Eqs. (6), (7), and (9) to predict the post-gasification transport and dispersion of pollutants originating from an "in-situ" coal gasifier.

To accurately describe the pollutant movement from the above equations, we also need the following input parameters: (1) identity and concentration of the pollutant species (C_o), (2) size of the pollutant source (R), (3) the rate of change of pollutant source concentration with time (k), (4) ground water flow velocity and direction (V), and (5) sorptive properties of the porous media (i.e., coal). Values for these input parameters are determined from the results of the laboratory and field studies.

Laboratory and Field Results

Aquifer Properties. The input parameters used to describe the porous media into which the pollutant is released are site specific. Because this report considers only the LLL Hoe Creek, Wyoming gasification test, we report geophysical and hydrological data relevant only to that area.

The Hoe Creek gasification site is located approximately 20 miles south of Gillette, Wyoming. The experiment will be conducted in the Felix No. 2 subbituminous coal seam that lies at a depth of approximately 40 m and is approximately 7.6 m thick. The coal seam is nearly horizontal ans has a tilt of less than 1°.

Immediately above and below the Felix No. 2 seam lie silt-clay aquitards (Fig. 2). The water table is about 20 m below the surface and therefore, the only aquifiers present are the sand below 20 m and the Felix No. 1 and No. 2 coal seams. Details of the hydraulic characteristics of the Hoe Creek site have recently been reported by Stone and Snoeberger [9].

The ground water flow in Felix No. 2 is in the easterly direction at a maximum velocity of 43.0 m/y, based on regional hydraulic gradient data from the U.S. Geological Survey. Recent hydrology experiments by LLL at Hoe Creek revealed much smaller local flow velocities, on the order of only several metres per year. However, no quantitative numbers are available. Therefore, for the model calculations, 43.0 m/y has been used for the ground water flow velocity to establish a maximum distance that the plume might travel.

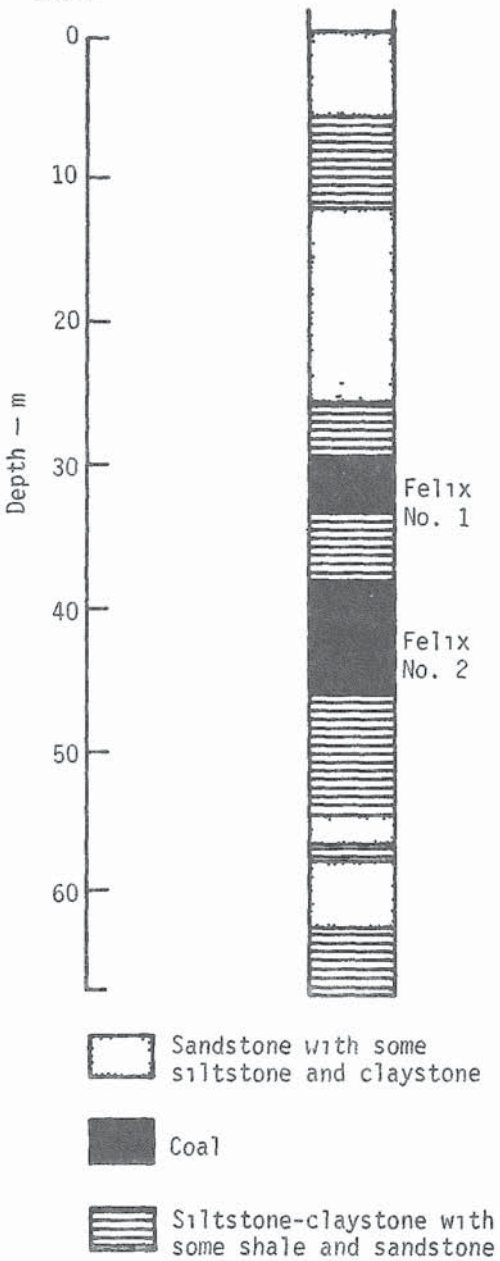


Fig. 2. Subsurface geology at the Hoe Creek coal gasification site.

The total porosity (ϕ) of the coal is about 0.33, whereas the interconnected flow porosity is estimated to be only 0.05. Porosity effects are discussed in more detail in the model calculation section.

Source Properties: Inorganic Contaminants. The pollutants carried by the ground water can be divided into two general categories, inorganic and organic contaminants. The principal potential source of water soluble inorganic pollutants is the ash material.* The approximate composition of the ash material, for a typical subbituminous coal expressed in its constituent oxides, is given in Table I. The coal is composed of approximately 9% ash by weight (on a dry basis). (Core samples of coal from Hoe Creek were not available at the time this work was done. Hence a similar coal from the Roland Seam of the Wyodak Mine was used.)

It is estimated that between 2.2 to 3.70 $\times 10^5$ kg [10] of dry coal will be consumed during the Hoe Creek I experiment. This implies that a maximum of 3.3×10^4 kg of ash will remain in the gasification void. Based on the layout of the experiment (Fig. 3), this corresponds to a gasified zone approximately 7.6 m high, 10.7 m long, and 5.2 m wide. At a flow rate of 43.0 m/y and a flow porosity of 0.05 for the surrounding coal, the volumetric flow through the ash bed is 175 m^3/y.

As the ground water flows through the gasification void, the soluble components of the ash are leached out. The degree to which the ash material is leached was determined from a series of ash samples subjected to distilled water washings in an attempt to simulate the flow of ground water through the ash and the resulting concentration of contaminants that would be released. The water, after passing through the ash, was analyzed for three major soluble components in the ash, Al^{+3}, Ca^{+2}, and OH^- ions.†

The ash sample was taken from a laboratory gasification reactor that had been operated at approximately 1273K. Samples of ash material (10 to 11 g) were slowly leached with 25-ml aliquots of distilled water at a flow rate of approximately 17 ml/h. The water samples collected at the downspout were analyzed by atomic absorption spectrophotometry to determine the concentrations of Ca^{+2} and Al^{+3}: pH was also measured with a pH meter. The decrease in concentration of Ca^{+2}, Al^{+3}, and OH^- with volume of H_2O washed through a 10.7-g ash sample is shown in Figs. 4 and 5. The quantity of water necessary to wash the ash "clean" of these three species can be estimated from the laboratory

*A number of other important water soluble species may be generated during gasification, in particular thiocyanates and cyanates [11]. These have not been included in this preliminary study, but they will be considered in future work.

†It was beyond the scope of this study to consider all possible soluble ash species. For this reason only the major species were chosen. It is emphasized, however, that treatment of the leaching and transport of most other soluble species can be done in a manner similar to that described in this manuscript.

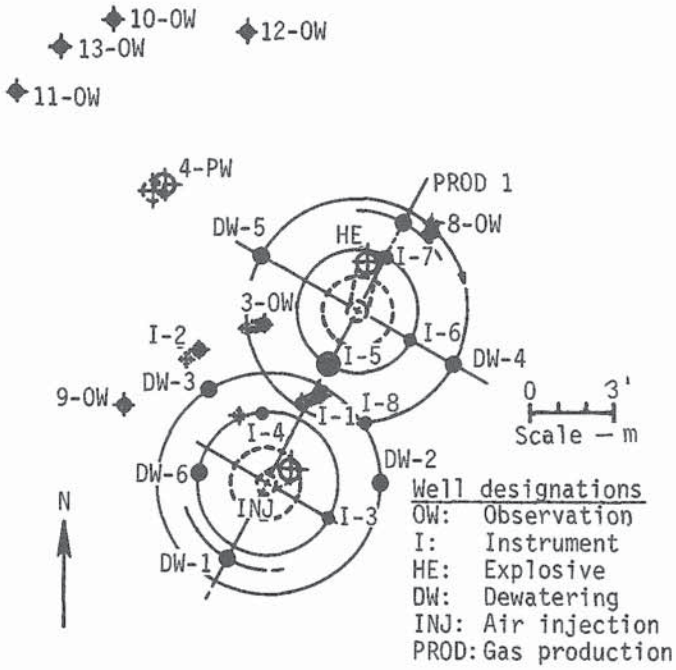


Fig. 3. Diagram of the well-hole locations at the Hoe Creek coal gasification site.

Table I. Mineral analysis of ash (as constituent oxides) from Wyodak Mine, Roland Seam subbituminous coal.

Mineral	Wt. %
Phos. pentoxide, P_2O_5	0.39
Silica, SiO_2	35.38
Ferric oxide, Fe_2O_3	2.03
Alumina, Al_2O_3	19.80
Titania, TiO_2	1.23
Lime, CaO	18.37
Magnesia, MgO	4.56
Sulfur trioxide, SO_3	16.98
Potassium oxide, K_2O	0.51
Sodium oxide, Na_2O	0.65
Undetermined	0.10
	100.00

leaching results. (For the OH^- ion, "clean" is assumed to be pH < 10.0). The total volume of water necessary to leach clean the Hoe Creek ash bed (3.3×10^4 kg) at a flow of 175 m^3/y and the necessary time can then be calculated (see Table II).

Up to this point, the effect of the temperature at which the ash was formed has been neglected. Experiments conducted on the ash from a Wyoming subbituminous coal (Roland Seam, Wyodak Mine) indicated that the ash fuses at 1513K. Therefore, ash subjected to temperatures greater than 1513K become glass-like on cooling (obsidian) and can withstand ground water leaching. Ash samples subjected to temperatures between 1273 and 1573K for 1 h show a decrease in the amount of leachable material with increasing heat treatment temperature. This is illustrated in Fig. 6 by the plot of the pH of water leachant from ash treated at 1273, 1373, and 1573K. Thus, it can be concluded that high temperature operating conditions may be more environmentally favorable because they appear to substantially reduce the amount of ground water contamination from the ash.

Table II. Volume of water V_T, necessary to leach "clean" 1 g of ash and 3.3×10^4 kg of ash from the gasifier, V_T' as well as time, t, required to leach the ash bed clean with a flow rate of 175 m^3/y.

Ion	V_T(1)	V_T'(1)	t(y)
Ca^{+2}	0.140	4.6×10^6	26.0
Al^{+3}	0.037	1.2×10^6	7.0
OH^-	0.140*	$4.6 \times 10^{6*}$	26.0

*Volume necessary to drop the concentration of hydroxyl ion by an order of magnitude.

Source Properties: Organic Contaminants. The organic contaminants originate from the tar left in or near the gasification void. The ground water moving through the post-gasification zone leaches out the water soluble components of the tar and transports then downstream. Concentrations of organic species encountered in the groundwater have been studied by several investigators. An analysis of waste water from coking plants by Jüntgen and Klein [11] determined phenol

and pyridine base concentrations to be on the order of 1000 to 3000 mg/l and 100 to 500 mg/l, respectively. Water samples collected from the LLL "in-situ" simulation reactor have soluble organic tar concentrations (phenols) between 1000 to 2000 mg/l [12] while water samples from laboratory pyrolysis experiments have concentrations of ∿1000 mg/l of organic compounds [13].

It is difficult to accurately estimate the size and time dependence of the source of organic species. Unlike the ash components, the organic contaminants can be swept out into the surrounding coal during the gasification process. It is likely, however, that the size of the area contaminated by these materials will be limited by the dewatering operations that are planned for the Hoe Creek operation. During dewatering, the formation water is removed from the coal seam and a depression in the height of the water level near the gasification zone is produced. The water surrounding this depression effectively forms a "seal" that prevents movement of gasification products further out into the coal seam. Therefore, the size of the depression of the water level can be used as an estimate of the maximum area possibly contaminated by tar species.

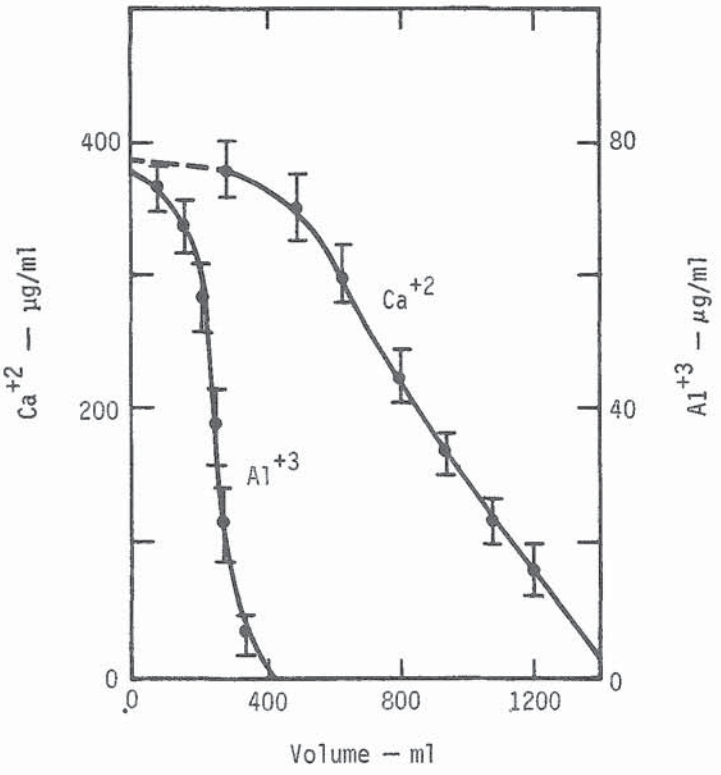


Fig. 4. Concentrations of Al^{+3} and Ca^{+2} metal ions leached from coal ash (10.7-g sample) in the water vs the volume of water washed through the ash. The ash was formed at 1273K.

Rozsa and Thorsness [14] have recently calculated the size of the dewatering depression for the Hoe Creek gasification experiment. They report a drawdown of greater than 1 m in the coal inside a 27-m radius from the center of the gasifier (Fig. 3). This radius is used as an estimate for the size of the area (i.e., the organic source) contaminated by the components. This estimate is probably pessimistic. In a more realistic view, the gaseous tars will probably condense within a few meters of the gasifier. Those tars that remain suspended as droplets in noncondensible gas will then be filtered out by the coal. Therefore, the area actually contaminated by organic materials should be much less than the area enclosed by the 27-m radius.

The time dependence of the source is also difficult to estimate because the actual quantity of tar deposited in the coal is unknown. For this reason, it assumed that all the soluble tars are released as a "slug", 54 m in diameter. Furthermore, the concentration of the tar in the slug is assumed to be 2000 mg/l, the maximum concentration observed in water samples taken from the LLL "in-situ" simulator.

All of the above assumptions tend to overestimate the water contamination resulting from the release of organic tar materials during gasification.* However, because we are presenting a conservative case, these values have been used as input for the transport calculations.

*Assuming a porosity of 5% and a concentration of organics in solution of 2000 mg/l, it can be shown that the "slug" contains 3.5×10^3 kg of dissolved tar. This is 15% of the maximum amount of tar that could be produced from the coal.

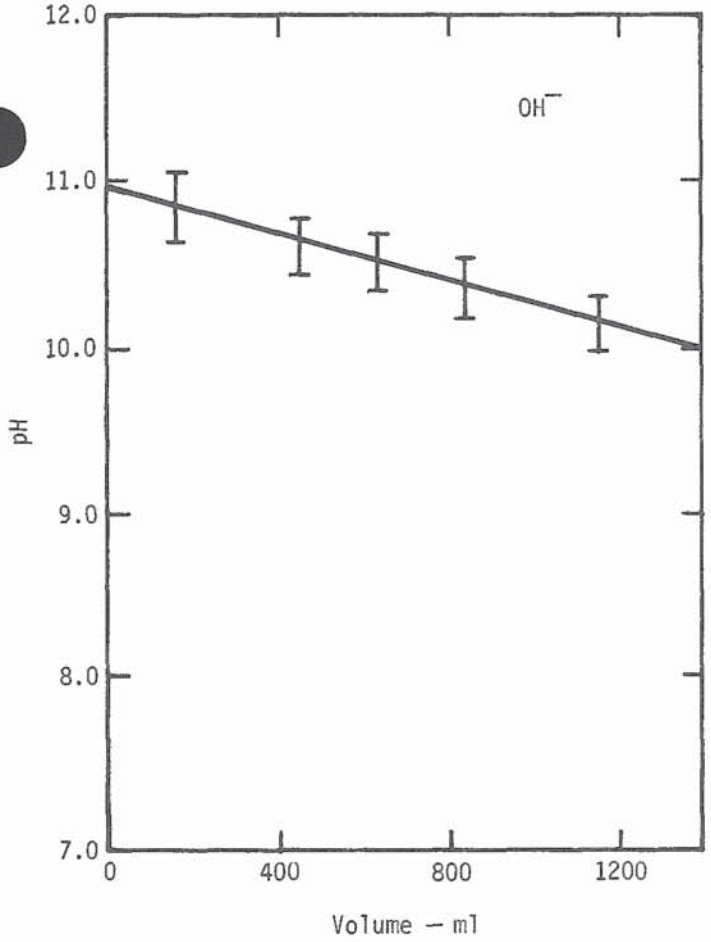


Fig. 5. Determination of the concentration of OH^- ion leached from coal ash (10.7-g sample), based on a plot of pH vs volume of water washed through the ash. The ash was formed at 1273K.

Sorption Effects. The rate of transport of the pollutants through the aquifier surrounding the gasifier strongly depends on the sorption properties of the porous media. Sorption of the pollutants retards the motion of the plume. This retardation effect is expressed by the quantity B (given in Eq. (2)) that depends on the porosity (ϕ) of the media and the distribution coefficient, K_d.

A series of laboratory experiments have been carried out to determine K_d for the water soluble tar components (principally phenols) as well as for the major inorganic species, Ca^{+2}, Al^{+3}, and OH^-, in contact with unheated subbituminous Roland Seam coal.

The sorption isotherms for the organic components in the wastewater are plotted in Fig. 7. These results were obtained by equilibrating known concentrations of wastewater solutions with various weights of subbituminous coal. The equilibration time was about 48 to 72 h and the particle size of the coal was between 1.7 to 3.35 mm. The amount of organic material in the water was analyzed by a gas chromatography method. The gas chromatograms of the original aqueous tar solutions showed four major peaks.* After allowing the solution to equilibrate with the coal, the chromatograms showed the same proportional reduction in amplitude of each peak. Hence, there was no apparent preferential adsorption of these tar components on the coal. The amount of material sorbed on the coal was then obtained by comparing the measured concentrations of organics in control samples with the concentration in solutions that had equilibrated with the coal.

A comparison of the sorptive properties of this subbituminous coal with data reported for several activated carbons [11] reveals that the coal has a sorptive capacity of approximately 10 times less than that of activated carbons. The general shape of the sorptive isotherm vs concentration, however, is nearly the same for both materials.

The distribution coefficient, K_d, for the organic components in the water depends strongly on the original concentration of the organics. At high concentrations, $K_d \simeq 2.0$, whereas at low concentrations, $K_d \simeq 50.0$. Because the maximum organic concentration is approximately 2000 mg/1, a value of $K_d = 2.0$ was used in the transport calculations.

The experimentally measured sorption isotherm for Ca^{+2} is shown in Fig. 8. It was obtained using the same coal and procedure as was used in the organic sorption experiment, except that the analyses were done by atomic absorption

*This is not meant to imply that there are only four water soluble tar components. Undoubtedly there are many others, most of which are at low concentrations, below the limits of detection of this method.

spectrophotometry. The sorption of Ca^{+2} by subbituminous coal is considerably less than that observed for organic materials; K_d is approximately 1.0 and, over the range plotted, is independent of concentration.*

The distribution coefficient for Al^{+3} was essentially infinite for sample concentrations ranging from 265 to 924 mg/l.* In all cases, the concentration of Al^{+3} left in solution (equilibrated with the coal) was below the spectrophotometer detection limit (<1.0 mg/l).

The sorption of the hydroxide ion on the coal matrix was not determined because the OH^- reacts readily with the phenolic end groups in the coal:

$$\text{Coal-OH} + M^+OH^- \rightleftharpoons \text{Coal-O}^-M^+ + H_2O \ .$$

Unfortunately, attempts to titrate the coal with NaOH were unsuccessful because of the poor endpoint. Blom [15] has reported that approximately 6% by weight of subbituminous coal exists in the form of phenolic oxygen, corresponding to 3.75 mmol phenolic groups/g coal. From this, it is possible to estimate the amount of coal necessary to neutralize the OH^- released by the ash. From the leaching experiments (see Fig. 5) we can calculate that about 5×10^{-2} mmol of OH^- are released per gram of ash. It is unlikely all the phenolic groups can react with the OH^- and thus, using a conservative estimate that 0.0375 mmol of the phenolic groups per gram of coal react (i.e., 1%), we can calculate that OH^- from 1 g of ash will be neutralized by approximately 1.5 g of coal.

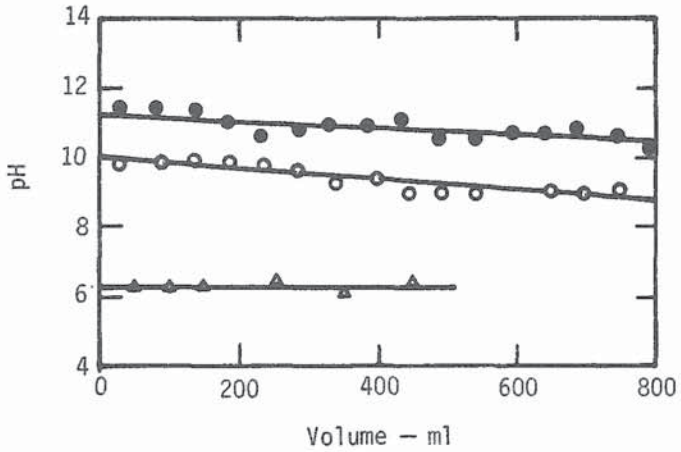


Fig. 6. Effects of ash heat-treatment temperature on the pH of the water leachant. Here, • represents 1273K ash, o represents 1373K ash, and Δ represents 1573K ash (fused).

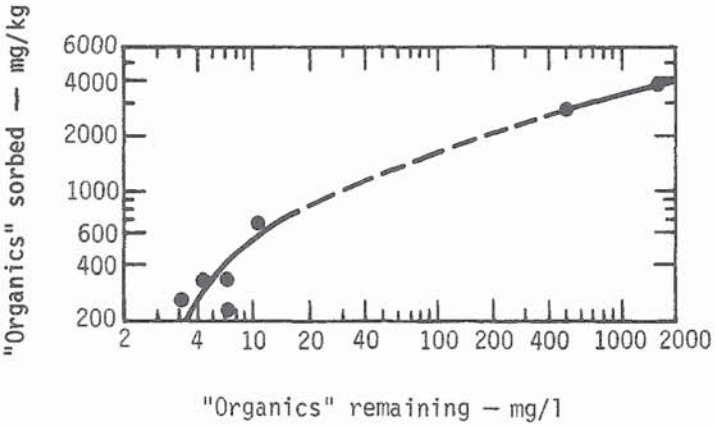


Fig. 7. Sorption isotherm for soluble organic components from coal tar.

Model Calculations

From the laboratory and field data presented in the preceding sections, it is possible to derive a set of input parameters for model calculations of the pollutant plume transport and dispersion (see Table III). The values used for the dispersion coefficients (D and D_1 in Eqs. (6) and (7), respectively) were obtained from Scheidegger [16].

Two parts of Table III require some clarification. First, in relation to "source properties" it has been assumed that the ash sources are depleted linearly

*The Ca^{+2} solution was prepared from $CaCl_2$. The Al^{+3} solution was prepared from $AlK(SO_4)_2$. All materials were of reagent grade purity.

with time (i.e., there is a constant water flow rate through the ash). Hence, the rate of change of pollutant source concentration is merely C_o/T_o. From the data in Figs. 4 and 5, it can be seen that this is a good approximation. The greatest uncertainty occurs at short times when only a small volume of water has leached through the ash. In this region, the concentrations of Ca^{+2} and Al^{+3} in solution are nearly constant. For the organic contaminants, it is assumed they are released as a slug. Because the flow rate is 43.0 m/y and the diameter of the "organic" source is approximately 54 m, the slug is released over a period of between 1 to 2 y. (A value of 2 y is used in the calculations.)

Table III. Summary of input parameters used for model calculations. Data obtained from field and laboratory experiments.

I. Aquifer Properties

Flow velocity (V)	43.0 m/y
Total porosity (ϕ_T)	0.33
Interconnected (flow) porosity (ϕ_F)	0.05
Flow direction	easterly
Dispersion coefficients $\left(\frac{m^2}{y}\right)$,	$D = 1.5$, $D_1 = 0.15$

II. Source Properties

Material	Radius, R (m)	Initial concentration, C_o (conc. units)	Time to deplete source* (y) T_o	Rate of change of pollutant source conc. (C_o/T_o) (mg/l y)
ASH Ca^{+2}	5.2	400 mg/l	26.0	15.4
ASH Al^{+3}	5.2	80 mg/l	7.0	11.4
ASH OH^-	5.2	1.0×10^{-3} mol/l**	26.0	3.8×10^{-4} mol/l y
Organics	26.8	2000 mg/l	2.0	0.0 (slug release)

*At flow rate of 43.0 m/y.
**pH = 11.0.

III. Coal Sorptive Properties

Material	Distribution coeff., K_d	Retardation factor B††
Ca^{+2}	1.0	14.4
Al^{+3}	$\sim \infty$	$\sim \infty$
OH^-	(reacts with coal)	—
"Organics"	2.0†	27.8

†At 2000 mg/l
††From Eq. (9) and $(1 - \phi_T)/\phi_F = 13.4$.

The second point in Table III that requires clarification is the method by which the retardation factor, B, is calculated. In coal, not all the pores are interconnected (i.e., not all the porosity is open to flow). For example, in a typical subbituminous coal the interconnected porosity is approximately 0.05, whereas the total porosity (void) is 0.33. Therefore, to describe the retardation effects in coal, we must rewrite Eq. (2) in the form

$$B = 1 + \frac{1 - \phi_T}{\phi_F} k_d , \qquad (10)$$

where ϕ_T is the total porosity and ϕ_F is the porosity available to flow. The quantity $(1 - \phi_T/\phi_F)$ is the ratio of coal to water flowing through the coal in a given unit volume. Hence, for a total porosity of 0.33 and a flow porosity of 0.05, there is 0.67/0.05 or 13.4 times as much coal as flowing water.

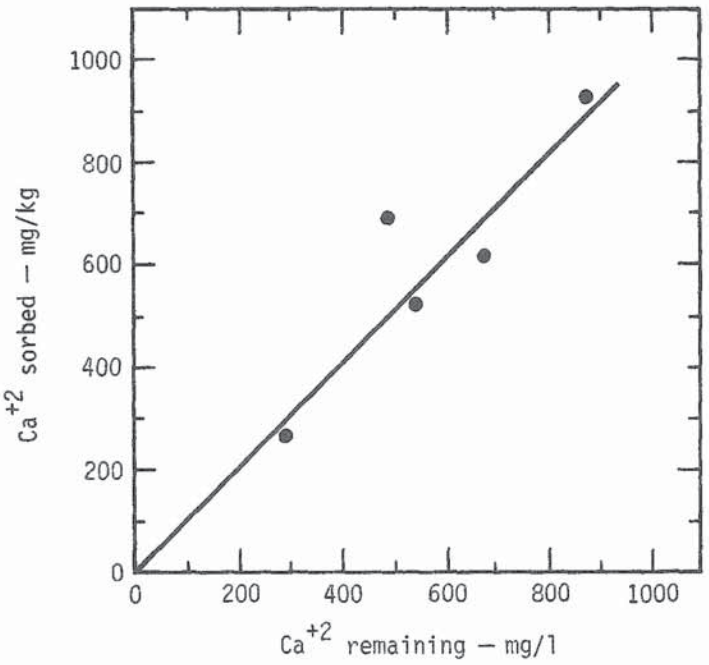


Fig. 8. Sorption isotherm for Ca^{+2} ions on subbituminous coal.

To calculate the plume transport and dispersion, a computer code was written incorporating Eqs. (6), (7), and (9). The results of the calculations are shown in Figs. 9 and 10. Input parameters from Table III were used in these calculations.

Organic Pollutant Plume. Aerial views of the plume of organic materials at times of 10, 100, and 1000 y following gasification are presented in Fig. 9. The plume is symmetric about the x axis and thus, only one half of the plume is shown. The solid lines depict contour lines connecting points of equal concentration. The contour intervals are 0.05 times the initial source concentration; (e.g., the source concentration for the phenols is 2000 mg/l and thus, the contour interval is 100 mg/l). Because of the strong sorption effects of the coal, the plume only moves 1500 m in 1000 y and is reduced to a concentration of 200 mg/l. Furthermore, the plume is only about 60 m in diameter. It is important to realize this is a pessimistic case. From the data in Fig. 7 it can be seen that the sorption of the coal increases as concentration decreases. For an organic concentration of 200 mg/l (as at 1000 y), remaining in solution, K_d = 10.0 or 5 times higher than the value of 2.0 chosen for the model calculation.* Hence in a more realistic case, the organics become almost completely adsorbed (i.e., infinitely retarded) after 1000 y. Thus, from these calculations, we conclude that even with pessimistic values for input parameters, the coal has a strong cleansing effect on the organic pollutant plume.

Inorganic Plume. Aerial views of the calculated plume containing Ca^{+2} ions at times 10, 100, and 1000 y following gasification are shown in Fig. 10. Because of the symmetry of the plume, only one half is shown. The contour intervals represent concentration changes of 20 mg/l. The plume calculations here are much more realistic because K_d does not vary significantly with concentration. The plume concen-

*The simple model used here does not account for the concentration variation of K_d.

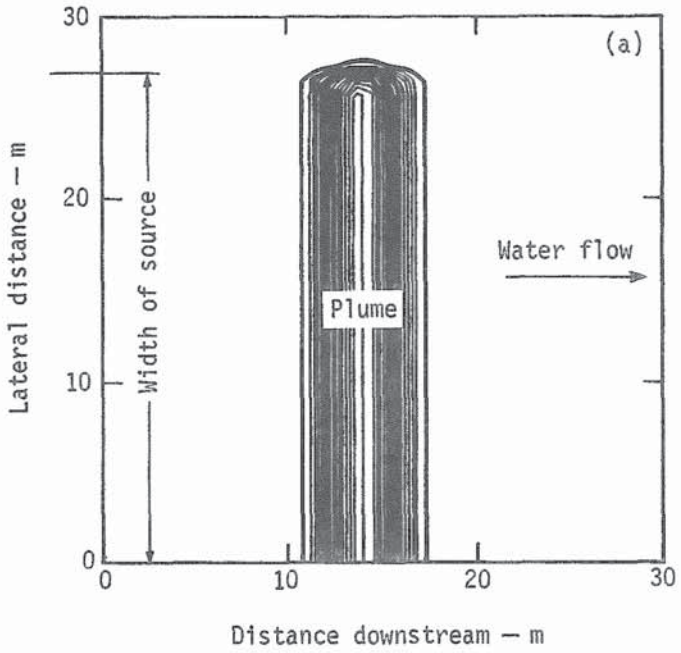


Fig. 9a. Calculated pollutant plume of organic wastes in ground water, 10 years following gasification. Water flow velocity is 43.0 m/y. Contour lines connect points of equal concentration: contour intervals represent concentration changes of 100 mg/l. Only half the plume is shown because it is symmetrical about the x axis.

concentration decreases in the direction of the gasifier as a result of the change in the source concentration with time. The plume is roughly 5 to 15 m in width and 80 m in length. After 1000 y, the plume has extended about 3000 m downstream and the maximum concentration is 45% that of the source. The results of the plume calculations demonstrate the ability to predict plume transport and dispersion, given a set of appropriate input parameters. Current predictive capability is limited by the lack of further laboratory and field input data and by the inability of the computer code to account for reactions between the coal and the OH^- groupings or between different species in solution.

The particular field data that lead to the greatest uncertainties in the calculations are the ground water flow velocity (V) and the porosity open to flow (ϕ_F). The upper limit on the flow velocity is about 43.0 m/y. The true flow velocity is probably much lower and thus the distance the plume travels is significantly reduced. Similarly, the value for flow porosity used in the calculations ($\phi_F = 0.05$) is also an upper limit. If instead, $\phi_F = 0.01$, the retardation factor, B, is increased approximately fivefold, and consequently the size and distance the plume moves is reduced 80%.

The significance of our calculations is that they represent essentially the "worst" case. As a result, limits can be set on the size and distribution of the pollutant plume. Furthermore, and perhaps more importantly, this analysis illustrates the strong cleansing effect the coal has on the contaminated water. Currently LLL is initiating a more extensive field and laboratory study to further quantify the input data and refine the code.

AIR QUALITY CONSIDERATIONS FOR HOE CREEK I

The principal gas products from "in-situ" gasification are H_2, CO, CO_2, CH_4, and H_2O, as well as lesser amounts of C_2H_4, C_2H_6, C_3H_8, and H_2S. During a gasification field test, these products are flared and yield principally, H_2O, CO_2, and SO_2. To avoid any possible adverse air quality conditions at the gasification site, it is necessary that the exhaust stack be of sufficient height to provide adequate dispersion and dilution of these combustion products.

Plume dispersion calculations have been carried out for the Hoe Creek I experiments using a code developed by Peterson, Crawford and Lawson [17]. Basically, the code uses the Gaussian plume diffusion model [18] for calculating pollutant concentration as a function of distance downwind from a continuously emitting point source. The basic plume diffusion equation used by the code is

$$X = \frac{Q}{2\pi\left(\sigma_y\sigma_z + \frac{CA}{\pi}\right)u} \exp\left(-\frac{y^2}{2\sigma_y^2}\right)\left\{\exp\left[-\frac{(z-h)^2}{2\sigma_z^2}\right] + \exp\left[-\frac{(z+h)^2}{2\sigma_z^2}\right]\right\}, \quad (11)$$

where: X is the concentration in units per cubic metre; Q is the source strength in units per second; σ_y is the horizontal standard deviation in cross wind direction in metres; σ_z is the vertical standard deviation in metres; u is the wind speed in metres per second; h is the height of plume centerline above ground in metres; CA is the cavity dilution term to account for wakes produced by structures where C is taken as 1 and A is the cross sectional area of the structure in square metres; y is the cross wind distance in metres; and z is the vertical distance in metres.

The theory used by Peterson et al., is taken largely from Ref. [18]. The code combines many of the different equations in this publication and automates the calculation. Furthermore, the code solves for three specific concentrations; along the axis of the plume (y = o and z = h), at the ground level under the plume center line (y = o and z = o), and sector averaged (over 22.5° sector) at ground level. For a more complete description of the code the reader is referred to the original work by Peterson et al. [17].

Input Parameters and Assumptions. The input required to use the code include wind speed data, local meteorological conditions, surface topography, as well as wet and dry deposition velocities. The source characteristics are also part of the required input, in particular, the source height, composition, heat flux, and flow rate.

Wind speeds, mean mixing heights [19] and atmospheric stability data [20] for the Powder River Basin area are presented in Table IV and Fig. 11. In all the calculations, we have used a neutral air stability category. From Fig. 11 it is apparent that this stable condition is most probable. Unstable conditions lead to slightly higher ground level pollutant concentrations but these instabilities occur only about 10% of the time. The Hoe Creek I experiment will be conducted in the late fall and thus, the average wind velocities and mixing heights for that season have been assumed (Table IV). Furthermore, morning conditions are used because, on the average, this is the worst period of the day. The wind is predominantly from the west.

The effects of precipitation have been neglected because most precipitation will probably occur as snow and the solubility of gases in snow is quite low [17]. Rain, on the other hand, tends to greatly increase the ground deposition velocity and to decrease the pollutant concentration in the plume.

A schematic diagram of the flare to be used during the Hoe Creek experiment is shown in Fig. 12. It is approximately 5 m high and 1.5 m in diameter. The

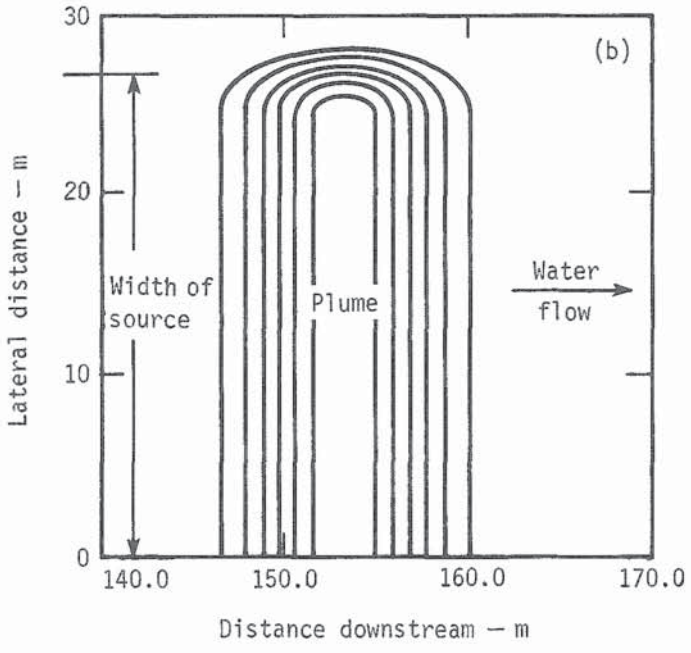


Fig. 9b. Calculated pollutant plume of organic wastes in ground water 100 years following gasification. (Same conditions apply as in Fig. 9a.)

expected composition of the gasification products to be fed to the flare is given in Table V; the heating value is about 4.8 MJ/std m^3 (130 Btu/scf). Maximum product gas flow into the flare is expected to be about 57 std m^3/min (2000 scfm). It will be mixed and combusted with air, blown in at a rate of 114 std m^3/min (4000 scfm) so that a 2/1 air/product mixture is achieved. Based on design analysis [21], the flare operating temperature will be about 1400K and the effluent heat flux about 275 MJ/min.

The effective height of the flare is a sum of the actual flare height (5.0 m), the plume rise due to the velocity (momentum) of the effluent gases, and the bouyancy rise. The bouyancy rise is a function of the temperature of the emitted gases and the atmospheric conditions and is calculated automatically by the computer code, using the input effluent heat flux. The plume rise resulting from momentum, however, is not calculated by the code and thus, must be included in the height inputed to the code.

The maximum momentum rise of the plume, H_{mv}, is easily calculated from the relation [22]

$$H_{mv} = \left(\frac{4.77}{1 + 0.43(u/V_s)}\right)\left[\frac{(QV_s)^{1/2}}{u}\right], \qquad (12)$$

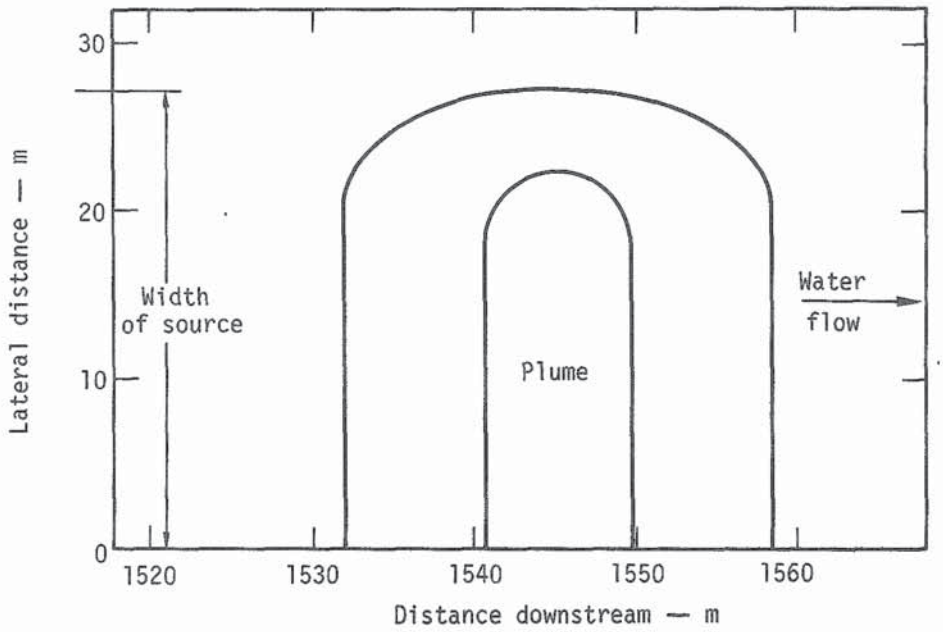


Fig. 9c. Calculated pollutant plume of organic wastes in ground water 1000 years following gasification. (Same conditions apply as in Fig. 9a.)

Table IV. Powder River Basin estimated mean mixing heights and wind speeds.

Time	Annual avg.		Winter		Spring		Summer		Autumn	
	am	pm	am	pm	am	pm	am	pm	am	pm
Mixing heights (m)	300	2000	300	1100	400	2600	300	3000	250	1900
Wind speed (m/s)	4.9	7.2	4.9	5.8	5.4	8.1	4.0	6.7	4.0	6.7

where u is the wind velocity and V_s is the stack exit velocity, both in metres per second. Q is the gas flow rate from the stack in cubic metres per second, measured at the absolute temperature at which the density of the stack gases would be equal to that of the ambient atmosphere (here, that temperature is approximately 298K). Based on the dimension of the flare (Fig. 12) and a total gas flow rate of 170 m^3/min, H_{mv} is calculated to be about 5.0 m. Hence the effective stack height is 10.0 m.

The flare will be physically situated on nearly level ground. A recent land survey of the area classes the topography of the site as gently rolling hills. Within the site boundaries, the changes in elevation are no greater than 23 m. The gasification site is on the northeast side of a gently sloping hill, the ridge of which is about 10 m above and 200 m west of the site. The only buildings on the site will be a few trailers and low work sheds. Thus, the influence of wakes near

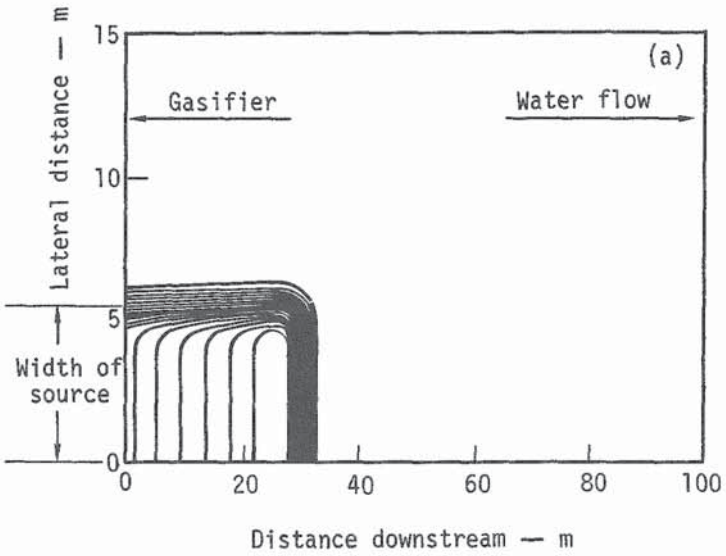


Fig. 10a. Calculated pollutant plume of Ca^{+2} ions leached from ash into ground water 10 years following gasification. Water flow velocity is 43.0 m/y. Contour lines connect points of equal concentration: contour intervals represent concentration changes of 20 mg/1. Only half the plume is shown because it is symmetrical about the x axis.

Table V. Approximate gas composition expected during the Hoe Creek I gasification experiment (using air).

Gas	Volume, %
H_2	16-17
CO	21-23
CO_2	5-7
CH_4	1.5-2.5
H_2S*	<0.1
N_2	56.5-50.4

*This is a maximum value and assumes all the sulfur in the coal to be released in the form of H_2S.

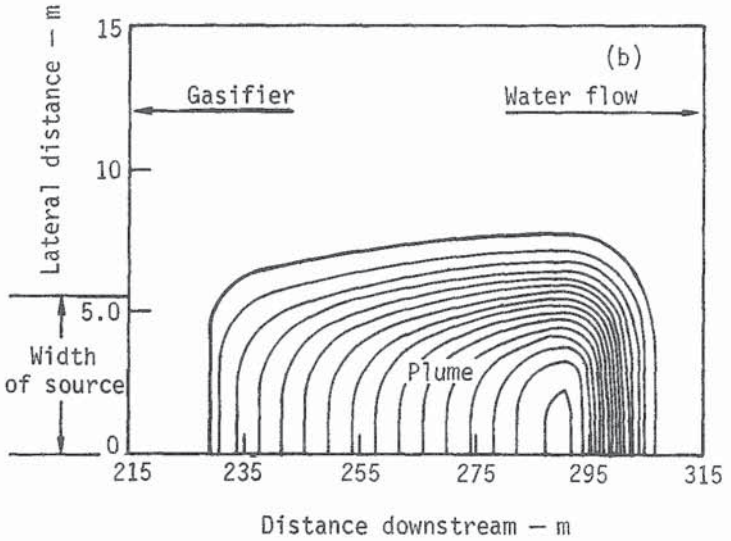


Fig. 10b. Calculated pollutant plume of Ca^{+2} ions leached from ash into ground water 100 years following gasification. (Same conditions apply as in Fig. 10a.)

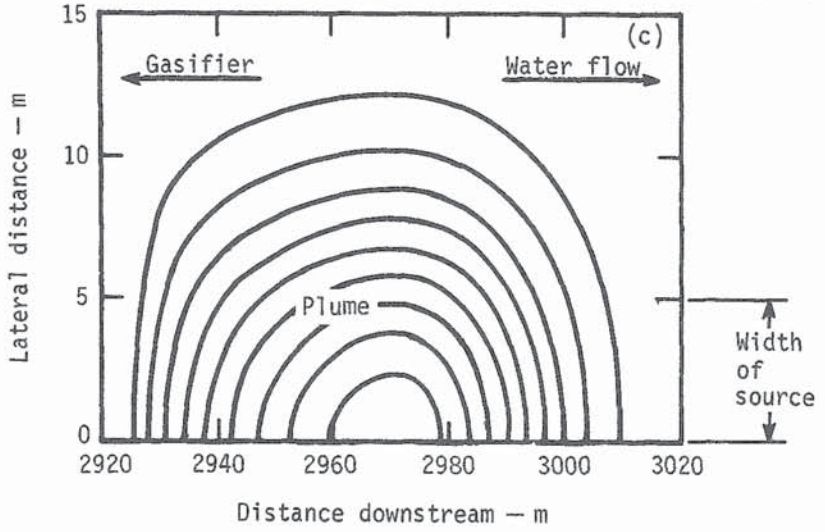


Fig. 10c. Calculated pollutant plume of Ca^{+2} ions leached from ash into ground water 1000 years following gasification. Note the "tail" of gradually decreasing Ca^{+2} concentration resulting from the leaching effect. (Same conditions apply as in Fig. 10a.)

large buildings can be neglected. (See Table VI for a summary of the input data for these model calculations.)

Calculated Results. The results of the plume calculations are shown in Figs. 13 and 14. The data are plotted in terms of units per cubic metre vs distance downstream from a source emitting at the rate of 1 unit/s. The results shown in Fig. 13 are for the ignited flare, whereas Fig. 14 corresponds to a malfunctioning flare which is extinguished. Notice the much lower ground level concentrations occurring with the ignited flare and resulting from the bouyancy produced by the heat from the burning gases.

To obtain the true effluent concentration at a

Table VI. Summary of input data used for air quality calculations.

Source	Flare Operating Condition	
	Ignited	Extinguished*
Effective source height (m)	10.0	10.0
Temperature (K)	1400	398
Gas flow rate (std m^3/min)		
Fuel	57	57
Air	114	114
Heat flux (MJ/min)	275	8.5**

Atmospheric conditions and site characteristics	
Wind speed (m/s)	4.0
Stability category	neutral (D)
Mixing height (m)	250
Topography	level

*The extinguished condition would result from a flare malfunction. Because it would lead to abnormally high ground level concentrations, it is included in the calculation.

**Based on gas heat capacity of 8.0 cal/g-mol °C and an exit temperature of 60°C for the air-fuel mixture.

particular point downstream, we merely multiply the concentration shown in either figure by the appropriate source strength given in Table VII. For example, the CO concentration 200 m downstream from the extinguished flare is $(0.21)(4 \times 10^{-5}) = 8.4 \times 10^{-6}$ m^3 SO_2/m^3 air, or 8.4 ppm. The advantage of a normalized source is that only one calculation is required to determine the downstream concentration of all effluents.

The calculated center line ground level concentrations of effluents at 100, 200, 500, and 1000 m downstream from the source are summarized in Table VIII. In all cases, the ground level concentrations are at acceptable levels. In particular, sulfur emissions (as H_2S or SO_2) do not exceed 0.04 ppm, even under the malfunctioning flare conditions.

Table VII. Source strengths for various effluent gases calculated from the gas composition of Table V and a flow rate of 57 std m^3/min.

Flare Operation	Gas	Source Strength (m^3/s)
Ignited	CO_2	0.27
	SO_2	0.00095
Extinguished	CO_2	0.057
	CO	0.21
	H_2	0.16
	CH_4	0.019
	H_2S	0.00095

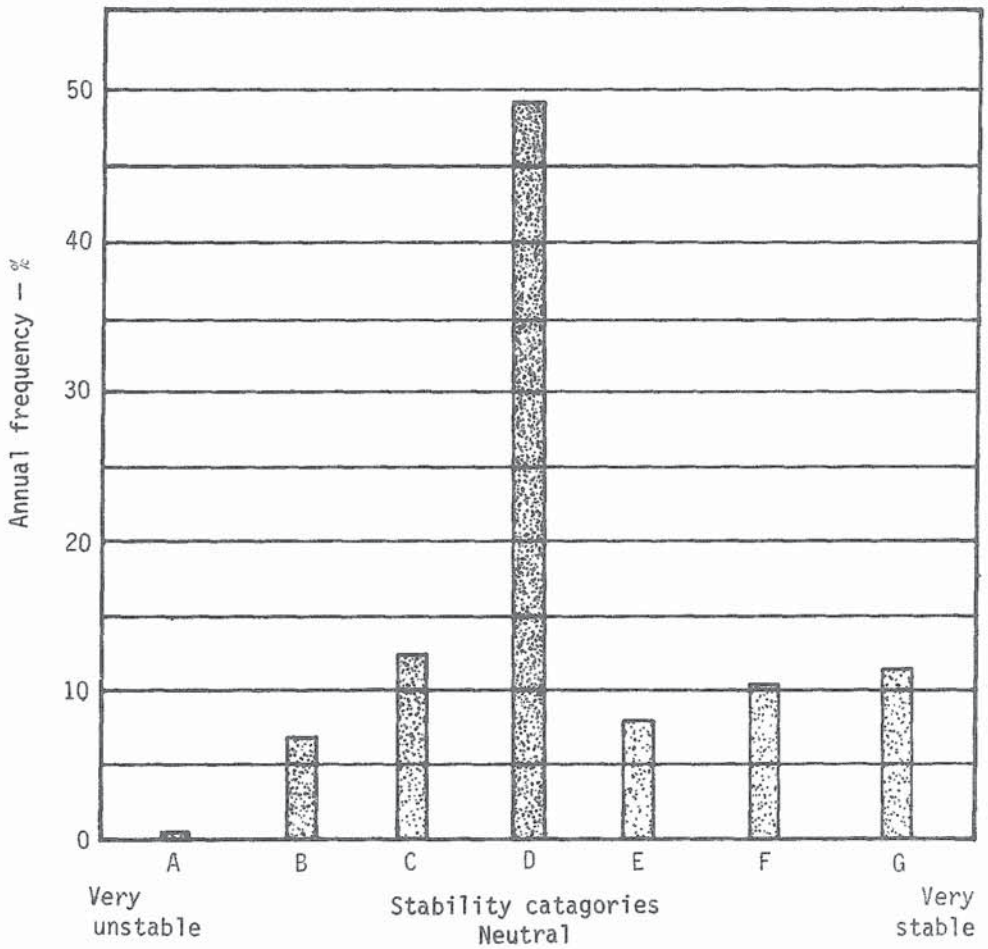


Fig. 11. Frequency of occurrence of various Pasquill stability categroies in the Powder River Basin.

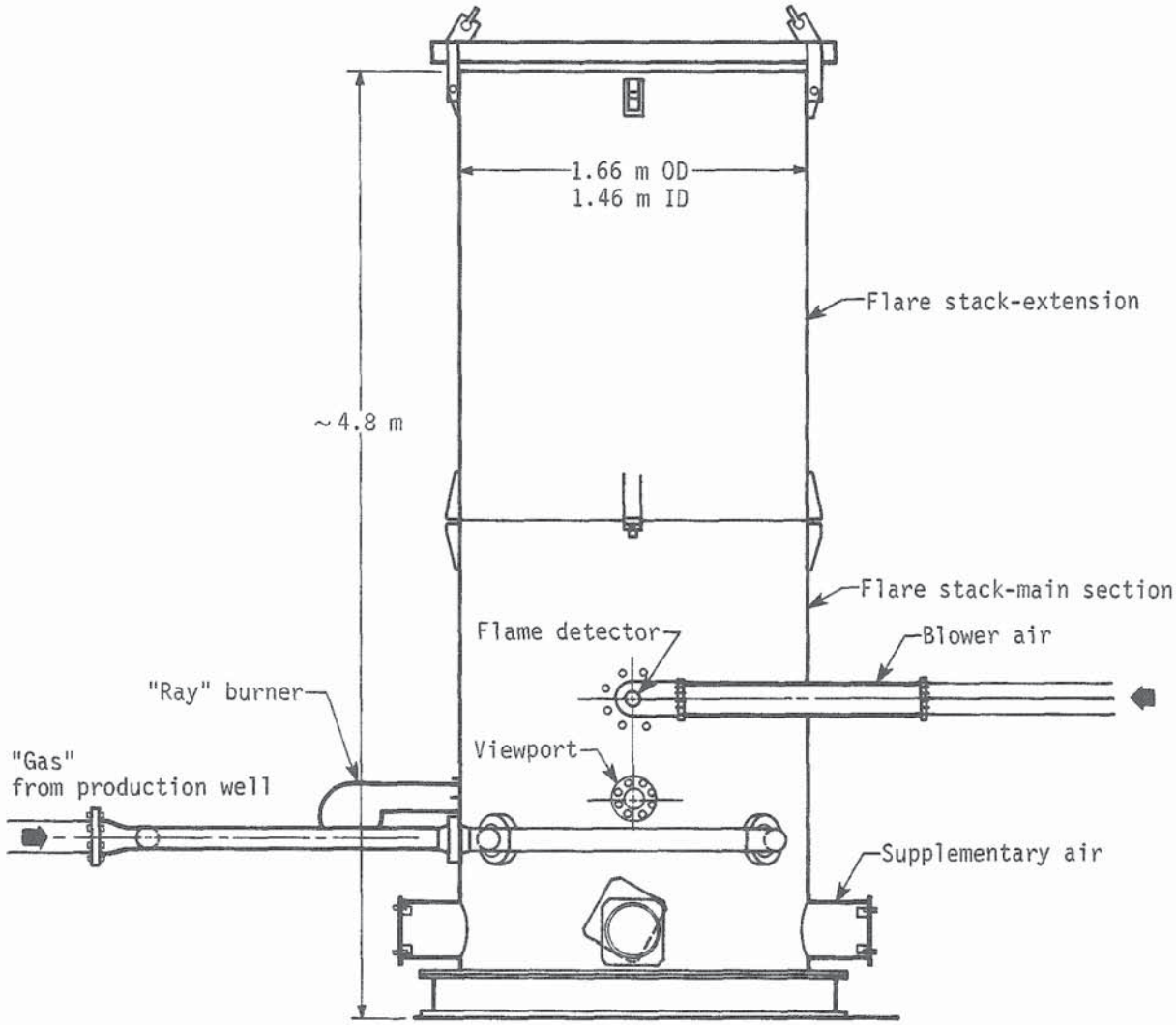


Fig. 12. Diagram of the product gas flare.

Therefore, based on the above calculations, we conclude that the Hoe Creek I gasification experiment will not produce adverse air quality conditions, even under the worst operating conditions.

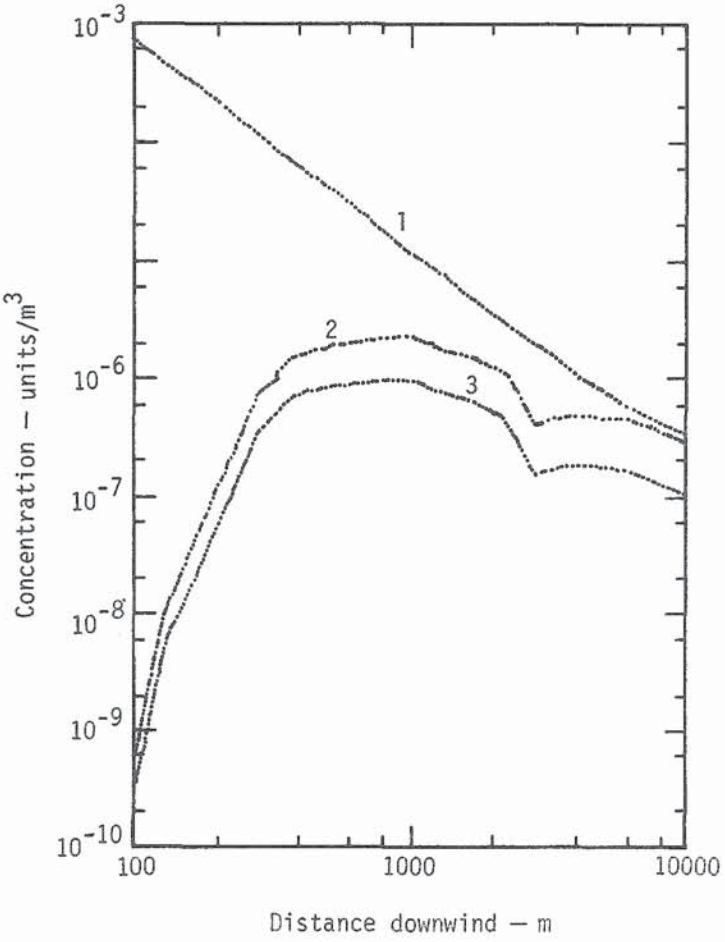


Fig. 13. Calculated normalized concentration vs distance downwind from a continuous source. Results are for average autumn morning weather conditions, assuming that the flare is ignited. Curve (1) presents the plume center line concentration, curve (2) presents the ground level concentration on the center line, and curve (3) the sector averaged curve, presents the ground level concentration, averaged over a 22.5° sector originating at the flare.

Table VIII. Centerline ground level concentrations downwind from a 57-std m^3/min continuous source. Results are calculated using Figs. 13 and 14 as well as the results from Table VII. The effective stack height is 10.0 m.

Flare operation	Gas component	Ground level concentration, downwind (ppm) 100 m	200 m	500 m	1000 m
Ignited	CO_2	<.01	.03	0.5	0.7
	SO_2	<.01	<.01	<.01	<.01
Extinguished	CO_2	0.5	2.3	2.3	0.8
	CO	1.7	8.4	8.4	3.2
	H_2	1.3	6.4	6.4	2.4
	CH_4	0.2	0.8	0.8	0.3
	H_2S	<0.1	0.04	0.04	0.01

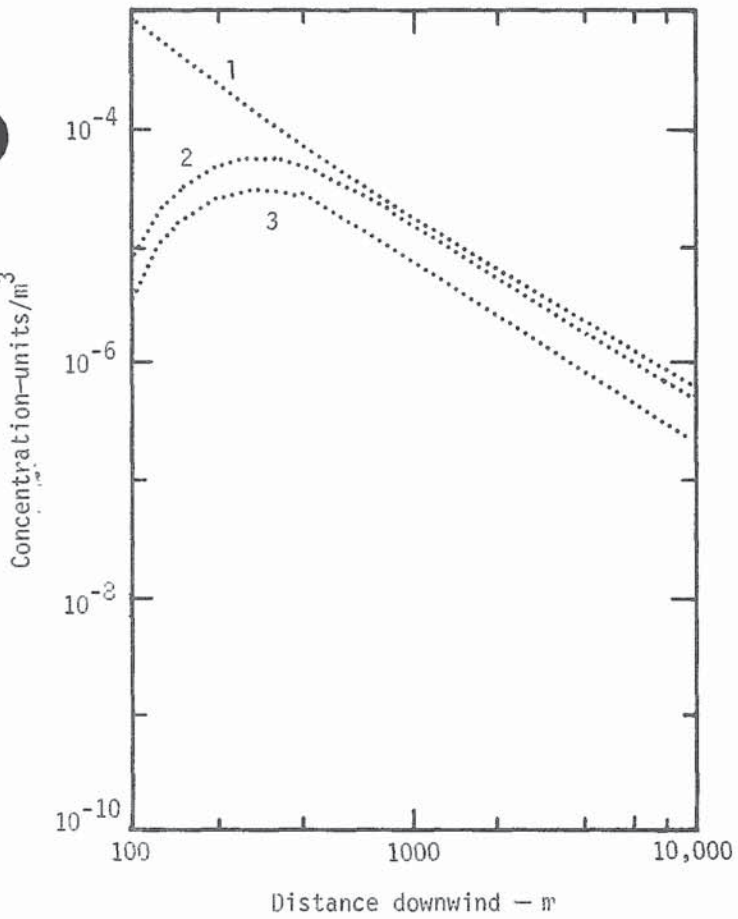


Fig. 14. Calculated normalized concentration vs distance downwind from a continuous source. Results are for average autumn morning weather conditions, assuming that the flare has malfunctioned and has been extinguished. Curve (1) presents the plume center line concentration, curve (2) presents the ground level concentration on the center line, and curve (3), the sector averaged curve, presents the ground level concentration, averaged over a 22.5° sector originating at the flare.

ACKNOWLEDGMENTS

The authors gratefully acknowledge the technical support of Patricia Rosseler in conducting the coal sorption experiments. The support from the LLL General Chemistry Division, particularly the fine work of Jack Clarkson, Kay Leach and Robert Lim is appreciated. The helpful discussions with Patrick Kinney, Warren Mead, and Ken Peterson are acknowledged.

This work was performed under the auspices of the U.S. Energy Research & Development Administration, under contract No. W-7405-Eng-48.

REFERENCES

1. Stephens, D.R., Pasternak, A., and Maimoni, A.: "The LLL In-Situ Coal Gasification Program," Lawrence Livermore Laboratory, (1974) Rept. UCRL-75990.
2. Mead, W.: "Draft Environmental Assessment of Application by ERDA For A Special Land Use Permit For Use of Public Lands in Wyoming For In-Situ Coal Gasification Experiments," Lawrence Livermore Laboratory, (1976) Rept. UCID-17011.
3. Fedorov, N.A.: "Some Problems of Control of The Process of Underground Gasification of Coals," Podzemnaya Gazifikatsiya Uglei, (1957) No. 1, 16-21.
4. Kononov, V.I.: "Effect of Artificial Heat Sources on the Formation of the Composition of Underground Waters and on the Underground Water Regime," UCRL-Trans. 10812, Gidrogeoterm. Usloviya Verkhn. Chastei Zemnoi Kory, AN SSSR, Geol. Inst. (1964) 35-51.
5. Bogoroditskii, K.F.: "Effect of the Coal Gasification Process on the Ground — Water Regime," UCRL-Trans. 10858, Trudy Lab. gidrogeol. problem im. F.P. Savarenskogo, AN SSSR, (1960) 23, 114-121.
6. Bogoroditskii, K.F.: "The Role of Water in the Transfer of Chemical Elements in Areas of Underground Gasification of Coal," Geokhimiya, (1961) 75-83; Geochemistry (1961) 1, 88-98.
7. Stephens, D.R., Ed.: "LLL In Situ Coal Gasification Program Quarterly Progress Report, January through March 1976," Lawrence Livermore Laboratory, (1976) Rept. UCRL-50026-76-1.
8. Holly, D.E., Guinasso, N.L., Jr., and Essington, E.H.: "Hydrodynamic Transport of Radionuclides: One-Dimensional Case with Two-Dimensional Approximation." Teledyne Isotopes, Nevada Operations, Rept. NVO-1229-179.
9. Stone, R. and Snoeberger, D.F.: "Evaluation of the Native Hydraulic Characteristics of the Felix Coal (EOCENE, WASATCH FORMATION) and Associated Strata, Hoe Creek Site, Campbell County, Wyoming," Lawrence Livermore Laboratory, (1976) Rept. UCRL-51992.
10. Thorsness, C.B.: Lawrence Livermore Laboratory, private communication (1975).
11. Jüntgen, H. and Klein, J.: "Purification of Waste Water from Coking and Coal Gasification Plants Using Activated Carbon," in Proc. of American Chemical Society, Div. of Fuel Chemistry (1974) 19, 67.
12. Rozsa, R.: Lawrence Livermore Laboratory, private communication (1976).
13. Campbell, J.H.: "Pyrolysis of Subbituminous Coal as it Relates to In-Situ Gasification: Part II Characterization of Liquid and Solid Products," Lawrence Livermore Laboratory, (1976) Rept. UCRL-52035-2.
14. Stephens, D., Ed.: "LLL In-Situ Coal Gasification Program Quarterly Progress Report: April through June 1976," Lawrence Livermore Laboratory, (1976) Rept. UCRL-50026-76-2.
15. Blom, L.: Ph.D. thesis, University of Delft, Holland (1960). Data reported in: Chemistry of Coal Utilization, H.H. Lowry, Ed., (John Wiley and Sons, New York, 1963) 267.
16. Scheidegger, A.E.: Physics of Flow Through Porous Media (McMillan, New York, 1974)
17. Peterson, K., Crawford, T.W., and Lawson, L.A.: "CPS: Continuous Point Source Computer Code for Plume Dispersion and Deposition Calculations," Lawrence Livermore Laboratory, (1976) Rept. UCRL-52049.
18. Slade, D.H., Ed." Meteorology and Atomic Energy, (U.S. Atomic Energy Commission/Div. of Technical Information, Springfield, VA (1968) 445.
19. Mixing Heights, Wind Speeds and Potential for Urban Air Pollution throughout the Continuous U.S., Environmental Protection Agency, January 1972.
20. USDC, NOAA, Environmental Data Service, Monthly and Annual Wind Distribution by Pasquill Stability Classes, Moorcraft, Wyoming, 1973.
21. Wong, R.: "In-Situ Coal Gasification Flare, Thermal and Flow Analysis," Lawrence Livermore Laboratory, (1976) Rept. UCRL-52085.
22. Buonicore, A.J. and Theodore, L.: Industrial Control Equipment for Gaseous Pollutants, Vol. II, (CRC Press, Cleveland, 1975).

HYDROGEOLOGIC ASSESSMENT OF AN UNDERGROUND COAL GASIFICATION PROJECT SITE GRANT DISTRICT, WETZEL CO., W. VA.

by

T. L. SOLE, GEOLOGIST, SKELLY AND LOY ENGINEERS
C. W. BYRER, GEOLOGIST, MORGANTOWN ENERGY RESEARCH CENTER

ABSTRACT

This hydrogeologic investigation provides baseline data on water quality and aquifer properties for the area surrounding the underground coal gasification site near Pricetown, West Virginia. Stratigraphic and domestic water well studies show that most wells are in shale aquifers of the Middle Dunkard Group; these wells yield about 1 to 8 gallons per minute of relatively good-quality water, except for excessive dissolved iron, manganese, arsenic, and lead in some wells. Moderate to low permeabilities of 0.032 to 0.18 millidarcys and transmissivities of 268 to 1003 gallons per day per foot were measured for shallow aquifers. Aquifer permeability and well productivity are significantly higher for wells within 35 feet of mapped fracture traces.

INTRODUCTION

The purpose of this study was to collect hydrogeologic baseline data for the Underground Gasification of Coal (UGC) Project in West Virginia. In order to assess the environmental conditions of such a project, knowledge of the ground water conditions both at the near-surface and at depth are necessary. This study was conducted prior to the initiation of any construction or excavation at the UGC site so that possible environmental changes resulting from the project could be later determined. The study is represented in part by a M.A. thesis in geology, by Sole [5].*

To date incomplete data are available for the hydrogeologic conditions at depth, therefore this report entails an assessment of the near-surface conditions only. Data are presented on water well and aquifer productivities, ground water quality, shallow aquifer porosity, and stratigraphy.

---

*References at end of paper

METHODS OF INVESTIGATION

Geologic knowledge of the area was derived from fieldwork, well logs, and previous investigations. Aquifer units were identified stratigraphically by correlating water well elevations and depths to stratigraphic cross-sections prepared from geologic logs. A water-well survey was conducted to collect information about well depth, accessibility of wells for quality sampling and pumping tests, and other well data. Pumping tests were then conducted on the available wells in order to determine well productivity, aquifer transmissivity, and aquifer permeability. Finally, lineaments were mapped from aerial photography and statistical tests were performed to determine relationships between lineament proximity to wells, and well and aquifer properties.

LOCATION AND STRATIGRAPHY

Location:

The study area is centered around the community of Pricetown, Wetzel County, West Virginia. Pricetown is located in the eastern portion of Wetzel County, near the Wetzel-Marion County border. The study area is for the most part contained by four small drainage basins (Figure 1).

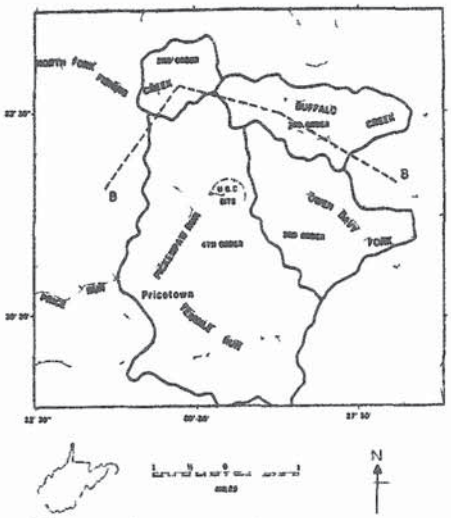


Figure 1 - Location Map of UCG Site.

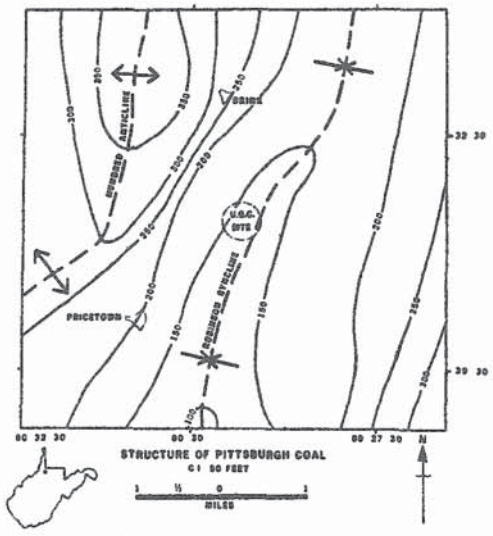


Figure 2 - Structure of Pittsburgh Coal, C.I.=50 ft.

Structurally, the area lies on the eastern flank of the Hundred Anticline and across the Robinson Syncline [3]. Figure 2 shows the structural contour map of the Pittsburgh Coal in the study area [2].

The exposed strata in the Pricetown area belong to the Dunkard Group [3]. A stratigraphic cross-section is presented in Figure 3. The stratigraphic representation and lithologic logs are useful as indicators of the sedimentary environment of the area, which in turn allows the determination of aquifer types, and other information needed in the evaluation of geologic conditions.

The Dunkard sedimentary environment in this area was initially a deltaic, interdistributary bay which later changed to an alluvial plain setting with a small lake and flood plain environment. The alternating sandstones, siltstones, shales, coal beds, and occasional limestones show that the Dunkard was deposited in a cyclothemic pattern [4]. Those stratigraphic units which are significant aquifers in this area are the Ninevah Sandstone, Pricetown Number One Shale, Pricetown Number Two Shale, and the Fish Creek Sandstone.

The Ninevah Sandstone has high porosity and poor cementation, and its coarse porous nature makes it a fairly good hillside aquifer [3].

The important unit below the Nineveh is the Pricetown Number One Shale [5]. This unit is a combination of grey, green-grey, red, and sandy shales.

Below the Pricetown Number One Shale is the Fish Creek Sandstone. This unit is important because it contains many of the water wells in the Pricetown area. It ranges from 30 to 50 feet in thickness. It is greenish-grey in color, medium grained and to some extent micaceous. It ranges in composition from a fine, silty sandstone to a sandy shale depending upon the exact location [3]. In bulk it would probably not make a very

good aquifer, but due to the highly fractured nature of the Pricetown area, it serves as a highly productive unit.

Immediately below the Fish Creek Sandstone and Coal is the Pricetown Number Two Shale [5]. It is of the same approximate composition and texture as the Pricetown Number One Shale. These two shale units were given specific names in the study area because a significant number of the water wells in the Pricetown area are in these units. The stratigraphic units between the Pricetown Number Two Shale and the Pittsburgh Coal are very poor aquifers. The area immediately above the Pittsburgh Coal consists of several significant lithologies.

One prominent lithology is the Redstone or Sewickley Limestone. Similar in composition to the Benwood Limestone, the Redstone ranges in thickness up to 100 feet. Below the Redstone Limestone is the Redstone Coal. The interval between the Redstone and Pittsburgh Coals is a layer of limey shale and shaley limestone sometimes included in the Redstone unit. The bottom of the Monongahela is marked by the Pittsburgh Coal. It ranges in thickness up to 10 feet and is the coal seam in which the UGC Project will be conducted [3].

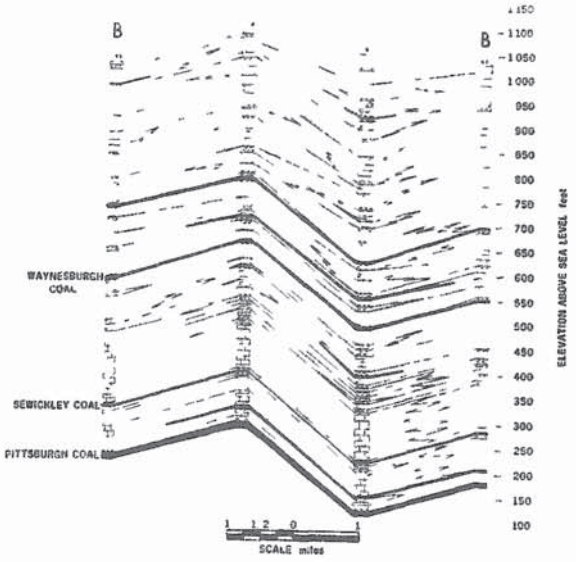


Figure 3 - Stratigraphic Cross Section B-B'.

Most of the units immediately above the Pittsburgh are poor aquifers with very low permeabilities; consequently, little to no water production should be expected from these units.

In the study area, aquifer definitions are difficult to apply, not because of structure but because of the deltaic nature of the sedimentay environment of the area [4]. Many of the sandstone units are discontinuous over very short distances making a good definition of these units difficult. The aquifers of the study area are probably either channel sands or unconfined shales [1].

DOMESTIC WELL SURVEY

In order to assess the near surface hydrogeologic conditions in the study area, a domestic water-well survey was conducted. This survey involved interviewing well owners, and was patterned after the U.S. Geological Survey's method for such well surveys. Information gathered from this survey included the well location, well owner, use made of both the well and water withdrawn from it, depth of well, depth of casing, type of casing, well diameter, drilling date, drilling contractor, the type of covering on the well (well finish), drilling method, pump type, power type used to operate the pump, and static water level depth. Some of the surveyed wells were sampled for water quality and others for both water quality and productivity.

DETERMINATION OF AQUIFER TYPE AND GROUND WATER QUALITY

By using core logs obtained from the Mountaineer Coal Company and correlating the logs in the study area, stratigraphic cross-sections were prepared and used to determine the principal aquifers of each well as in Figure 3. The elevations of the water wells and their depths were correlated to the cross-sections in order to make the aquifer determinations.

About 75 per cent of the wells in the study area occur in a shale aquifer. Since the Fish Creek Sandstone is an extremely discontinuous unit in this area and since it alternates between an argillaceous sandstone and arenaceous shale, it is difficult to attach stratigraphic names to the aquifers without a more in-depth analysis. All the wells do, however, occur in the Green Formation [5].

Twenty-seven of the wells surveyed were selected for quality analysis on the basis of accessibility and permission from the owner for sampling. Each of the wells was sampled once and analyzed for a variety of water-quality parameters mentioned earlier in this report. Most of the water

quality parameters were well within recommended standards for drinking water quality set by the West Virginia State Board of Health [7]. Even though some of the wells exceed the standards, they are probably not contaminated to a dangerous level [5].

In surveying these wells it was noted that some of the wells with high trace metal concentrations are often located near storage sheds where pesticides and garden chemicals are kept. Some wells are also down slope from gardens and garbage dumps. Still others are near garages and roads. Any one or a combination of these would account for the high arsenic and lead concentrations. The dissolved iron and manganese could be occurring naturally, since the wells are in shale aquifers or are uncased through a shale unit. Clay minerals are the probable source of these two elements, with pyrite being a supplemental iron source. Also, there seems to be no significant difference in the water quality between aquifers.

WELL AND AQUIFER PRODUCTIVITY

To evaluate the productivity of the wells and aquifers in the study area, four well productivity parameters were tested on eight wells [6]. These parameters include specific capacity, specific capacity index, transmissivity and permeability. Also porosities were calculated for some of the near surface aquifers in the area.

The results of the pumping tests show that there is no real distinguishing difference between the sandstone aquifers and the shale aquifers. Some of the wells in shale units had high productivities and some in the sandstone units had low productivities and vice versa. It was initially expected that the shale wells would be more productive than the sandstone wells. The concentration of fracture zones in the vicinity of the pumped wells apparently accounts for the relatively high permeability and productivity of the shale wells [6].

FRACTURE TRACES AND GROUND WATER

One important feature of structural significance to hydrogeologists is the fracture trace. Well yields are commonly 10 times greater for fracture trace wells than for wells drilled on random locations. Such high well yields result partially from the relatively high porosity and permeability associated with the closely spaced joints and solution cavities in the fracture zone beneath a fracture trace.

Fracture traces should also make good water well locations in shale and sandstone terrains. To test this hypothesis, fracture traces were first mapped in the study area from both high altitude color infrared (CIR) photographs and multispectral scanning, 9.0-11.4 millimicron (MSS) imagery. These types of photography are superior for detection of fracture traces [5].

The prime significance of fracture traces in the UGC area, is that they represent zones of relatively rapid ground water flow in fractures. Such zones are probably, therefore, the most likely avenues for the introduction and migration of ground water pollutants. The likelihood of future ground water pollution in the near-surface aquifers (used by present domestic wells) as a result of the UGC project is remote. However, if such pollution should occur, it is perhaps most likely to originate from organic and inorganic chemical species migrating from the burn zone up fracture zones, and then laterally along fracture zones in shallow aquifers to water wells. It is uncertain at present as to whether fracture zones penetrate from the surface to the burn horizon (roughly 1,000 feet below the surface).

REFERENCES

1. Donaldson, A. C.: Some Appalachian Coals and Carbonates: Models of Ancient Shallow Water Deposition, W. Va. Geological Survey, 1969, 384 p.
2. Haught, O. L.: Oil and Gas Fields Map, Marxhall, Tyler and Wetzel Counties, W. Va. Geological Survey, 1955.
3. Hennen, R. V.: County Report, Marshall, Tyler, and Wetzel Counties, W. Va. Geological Survey, 1909, 654 p.
4. Malone, R. D.: Stratigraphy of the Dunkard Group in West Virginia, Pennsylvania, and Ohio. Unpublished M.S. Thesis, West Virginia University, 1969.
5. Sole, T. L.: The Hydrogeology and Groundwater Geochemistry of Pricetown, Wetzel County, W. Va. Unpublished M.A. Thesis, West Virginia University, 1975, 79 p.
6. Sole, T. L., Byrer, C. W., Rauch, H. W., and Overbey, W. K.: Hydrogeologic Assessment of an Underground Coal Gasification Project Site, Grant District, Wetzel Co., West Virginia. MERC/TPR 1976, 50 p.
7. West Virginia State Board of Health. Public Water Supply Regulations, 1969.

FACTORS INFLUENCING THE ECONOMICS OF LARGE-SCALE IN SITU COAL GASIFICATION OPERATIONS

by

M.K. Buder R.A. Fisher
A.I. McCone O.N. Terichow
M.J. Wong
Bechtel Corporation, San Francisco, California

ABSTRACT

In a study of large-scale underground coal gasification (UCG) plants, the preparation and operation of the UCG field were found to be major contributors to product costs. The costs of UCG fields were based on expenditures mainly for drilling, linking, gas collection, and oxidant injection. In situ gasification costs, when compared to those of aboveground gasification, were generally found to be lower, in some cases by as much as 25 percent.

These results arose from a recent study undertaken by Bechtel Corporation, sponsored by the National Science Foundation. Bechtel applied state-of-the-art UCG technology to conceptualize large-scale power and SNG plants, derive preliminary economics based on both eastern and western U.S. coal, and compare them to previously established costs for surface gasification. In a brief study, Bechtel derived order-of-magnitude capital and operating costs for four different power plants (~900 MWe) and four plants producing substitute natural gas (~275 MM SCFD, 7.8 MM Nm^3/D). Data for the study were summoned from previous experience and from UCG process sponsors. The only instance, it was found, where UCG was more expensive than aboveground gasification was for power generation in the eastern U.S. Since the cost estimates were conservative and there is ample room for technological advance in UCG, lower costs for in situ gasification than those found by Bechtel are possible.

Past studies have shown how parameters such as seam depth, seam thickness, and well spacing influence UCG economics. The results of this study point out that drilling and piping costs, which are related to the above parameters, have an important effect on overall costs for large-scale UCG operations. Where these and other UCG field costs begin to raise the cost of raw gas produced in situ above the cost of raw gas from conventional gasifiers, it becomes clear that drilling and piping costs are governing parameters for UCG economics. In the study, for example, costs for power production using UCG in the East were high because the coal seam to be gasified was very thin and lay 1000 ft (305 m) deep.

Metric conversion factors and references are included at the end of this paper.

INTRODUCTION

Underground coal gasification (UCG) has been proposed as an alternative to aboveground gasification for the production of electrical power or substitute natural gas (SNG). A concise economic comparison of both methods of producing power and SNG was undertaken in late 1975 by Bechtel Corporation [1]. The study, which was funded by

the National Science Foundation, was a preliminary assessment of UCG on a large, commercial scale based on both eastern and western U.S. coal.

Because of the abbreviated nature of the study, certain assumptions were made, and cost estimates remained on the order-of-magnitude level. Modular costs for surface facilities were derived in previous studies and coupled as required with the UCG field costs (drilling, linking, piping, etc.). The generation of these field costs resulted in product costs for in situ gasification plants which were closer to surface plant product costs than expected. Since the cost estimates were conservative and there is ample room for technological advance in UCG, lower product costs than those derived for UCG in this study are possible. An analysis of the results points out some areas of UCG where there is a need for technological development.

PLANTS STUDIED

The study involved four power generation facilities and four large SNG plants. Table 1 shows their production capacities corresponding to plant type and location. A total of eight plants covers the production of power and SNG by surface and underground gasification of both western and eastern coals. The plants are composed of aboveground modules, and in the case of in situ gasification, they are also composed of UCG fields. These are the sites for drilling, linking, and piping operations. The components of these plants are listed in Table 2.

Table 1

PRODUCTION CAPACITIES OF THE PLANTS STUDIED

Plant Location	Type of Plant	Production Capacity	
		Power	SNG
West	Surface	934 MWe	275 MMSCFD
	UCG	824 MWe	260 MMSCFD
East	Surface	934 MWe	275 MMSCFD
	UCG	824 MWe	260 MMSCFD

Table 2

COMPONENTS OF THE PLANTS STUDIED

Desired Product	Plant Components	
	Surface	UCG
Power	Coal Handling Coal Gasification Ash Disposal Gas Purification Sulfur Recovery Combined-Cycle Power Plant Utilities and Compression	UCG Field Gas Purification Sulfur Recovery Combined-Cycle Power Plant Utilities and Compression
SNG	Coal Handling Coal Gasification Ash Disposal Gas Purification Shift Conversion and Methanation Sulfur Recovery Oxygen Plant Utilities and Compression	UGC Field Gas Purification Shift Conversion and Methanation Sulfur Recovery Oxygen Plant Utilities and Compression

Definition of the aboveground facilities was based on past experience. Appropriate plant modules were taken from past work as required and integrated into the plant configuration. The capacities of all plant elements were matched, and the utility requirements were balanced. All plants were envisioned as self-sustaining, that is, process energy requirements would be entirely satisfied without reliance on external sources.

The reference modules used from previous projects often consisted of more than one of the plant components shown in Table 2 lumped together. Therefore, in some cases, the costs of separate plant components as listed in Table 2 were never segregated. For example, in the SNG plants, the capital and operating costs for gas purification, sulfur recovery, shift conversion, methanation, and compression were never separated. These costs were available in the form of a single cost figure and were used as such in the study. Also, in the surface plants it was convenient to include dust removal in the Winkler gasification module, whereas for UCG, tar and dust removal were a part of the gas purification costs.

No detailed engineering or cost analyses were required for the surface facilities, for which designs and cost estimates were already available. However, some conceptual design and assemblage of cost information were necessary to describe the UCG field components shown in Table 2. Expenditures related to the UCG field account for all functions exclusive of surface gas

processing, such as well drilling, linking, gas collection, and air or oxygen injection.

UCG PROCESSES AND FIELDS

One of two in situ gasification techniques was applied, depending on plant location. In the West, the Linked Vertical Well (LVW) process being developed by ERDA's Laramie Energy Research Center (LERC) was employed. This process was chosen because of the successful, sustained test runs achieved at Hanna, Wyoming, since the experimental field program began there in 1972. The eastern UCG plants were based on the Longwall Generator (LWG) concept being developed by the Morgantown Energy Research Center (MERC). The LWG concept has not yet been tested at the Pricetown, W.Va. test site, but drilling operations have been underway. MERC's LWG concept is well suited for the thin, deep bituminous coal seams common in the East.

Variations of both of these UCG methods have been successfully applied in the U.S.S.R., where commercial-scale in situ gasification first evolved. Both the LVW and LWG techniques are being developed to attain commercial-scale in situ gasification of relatively thin, flat coal seams in this country. LERC's LVW process uses reverse combustion to establish a linked path between boreholes. The sequence of steps leading to gasification is shown in Figure 1 [2,3]. The LWG concept is illustrated in Figure 2. Parallel boreholes are directionally drilled from the surface to enter the seam and run along it horizontally for a distance of 500 feet. Combustion proceeds in an areal sweep pattern from one well toward the adjacent parallel well [4]. It should be noted that the information used herein reflects the status of these UCG techniques at the time this economic study was undertaken. Since then, rapid, continuing development has had an evolutionary effect on UCG.

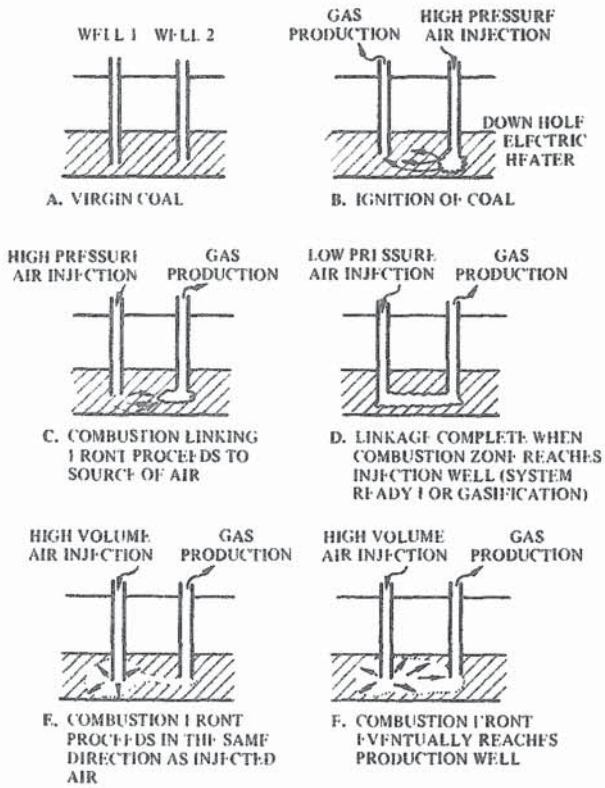


Figure 1

STEPS LEADING TO GASIFICATION IN LVW PROCESS

To supply the large quantities of gas needed to produce the amounts of power and SNG noted earlier, immense UCG fields were conceptualized. Their size, configuration, and mode of operation were defined with the help of information supplied or verified by the process developers. Following the definition of as many major process parameters as possible and their practical limitations, assumptions had to be made in areas where data were dubious or unavailable.

The rationale used to adequately delineate the UCG fields for subsequent cost estimation is outlined in stepwise fashion below. Table 3 lists the quantities used (either fixed or assumed as noted) for the major parameters defining the UCG fields. Using these figures, the field layouts and operational logistics were developed as follows:

- Power Plants

(a) Calculate volume of coal to be gasified annually. This is derived

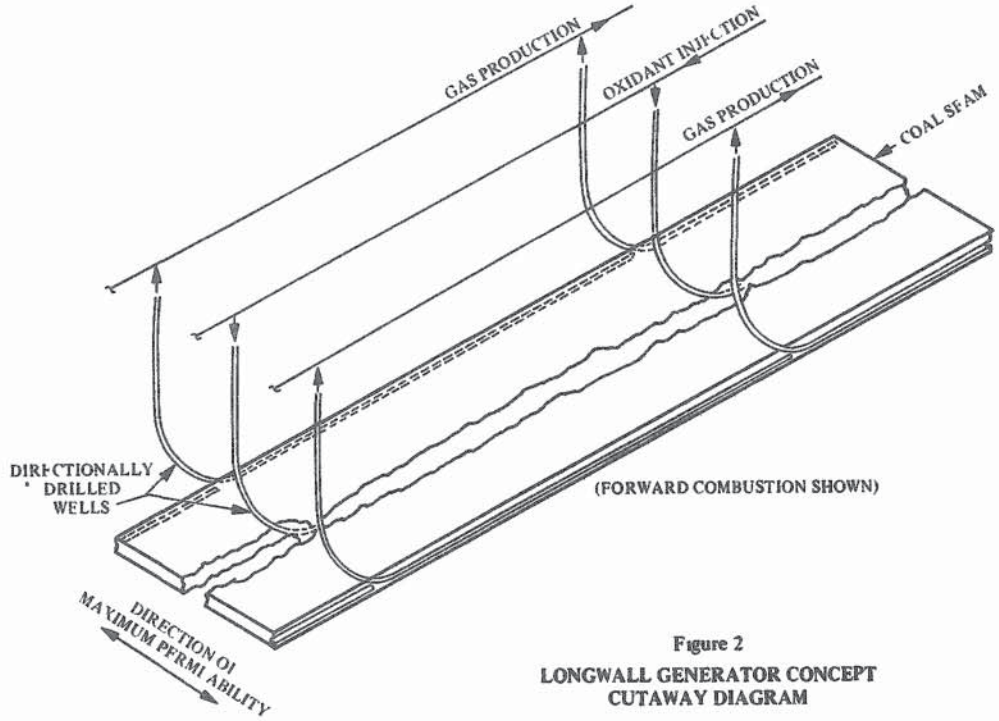


Figure 2
LONGWALL GENERATOR CONCEPT
CUTAWAY DIAGRAM

Table 3
DATA USED IN DEFINITION OF UCG FIELDS

Parameter	West (Site: Hanna, Wyoming)		East (Site Pricetown, West Virginia)	
	Power	SNG	Power	SNG
HHV of raw gas (Btu/SCF, dry)	126 [a]	300 [b]	126 [a]	300 [b]
Raw gas production rate (billion Btu/hr)	8 19	14 6	8 19	14 6
Coal required to produce 10^9 Btu raw gas (lb/billion Btu)	142,000 [c]	142,000 [b]	129,000 [d]	129 000 [b]
Coal specific gravity	1 25 [b]	1 25 [b]	1 5 [b]	1 5 [b]
Average seam thickness (ft)	30 [a]	30 [a]	6 [e]	6 [e]
Average seam depth (ft)	350 [a]	350 [a]	1000 [e]	1000 [e]
Borehole spacing (ft x ft)	100 x 100 [f]	100 x 100 [f]	100 x 500 [g]	100 x 500 [g]
Efficiency of energy recovery from coal to raw gas	50% [b]	50% [b]	50% [b]	50% [b]
Gas production capacity per well (million SCFD)	7 [f]	7 [f]	9 [g]	9 [g]

[a] Average value taken from Hanna No 1 experiment by LLRC [b] Assumed value [c] Based on carbon balance from Hanna No 1 experiment Values for power and SNG production are assumed identical [d] Same as c, but adjusted to reflect use of bituminous coal whose HHV is assumed to be about 10% greater than that of the subbituminous coal gasified at Hanna [e] Values consistent with Pricetown, W Va site [f] Values suggested by LLRC [g] Values suggested by MERC

from the raw gas production rate, the gas yield per unit weight of coal, and the specific gravity of the coal. Operation was assumed to be continuous, year-round (365 days, 24 hours per day).

(b) Calculate the land area required annually. Combined use of the coal seam thickness and the assumed 50 percent coal recovery efficiency gives the area of the seam which must be gasified each year. This corresponds to the land area required if the seam is assumed to be horizontal.

(c) Calculate the number of production wells required annually and on a continual basis to meet gas production needs. Since each borehole is associated with a fixed area of the coal bed, given a predetermined well spacing, the number of boreholes required annually can be found from the annual land allotment. The single-well production rate, the gas heating value, and raw gas production rate are used to derive the number of wells required in continual operation.

(d) Calculate air injection requirements. The ratio 1.5 volumes of gas to one volume of air, a result of the Hanna #1 experiment, was used.

(e) The number of air injection wells in operation was fixed at half the number of gas producing wells. The reason for this will become apparent below, where the field layouts are presented.

- SNG Plants

The UCG field design calculations for the SNG plants proceeded in similar fashion as those for the power plants. As shown in Table 3, it was assumed that the coal requirements for producing low- and medium-Btu gas are equal for UCG. To remain conservative, it was also assumed that the oxygen requirements for UCG, which would probably fall between Lurgi and Winkler requirements in actuality, were at the high end of the scale, that is, consistent with Winkler oxygen requirements. This is because UCG heat losses exceed surface reactor heat losses, and experience in the U.S.S.R. has shown oxygen losses to be high.

Table 4
UCG FIELD CALCULATION RESULTS

Design Parameter	West		East	
	Power	SNG	Power	SNG
Volume of coal gasified annually (ft^3)	1.31×10^8	2.33×10^8	9.89×10^7	1.76×10^8
Number of production wells required annually	870	1,550	660	1,170
Number of production wells required over 30-year plant life	26,100	46,500	19,800	35,100
Number of production wells for rated output	222	166	174	130

Table 4 lists the more significant results obtained from the calculations described above. These results were used to establish the actual field layout and mode of operation for each UCG plant. Field layout and operation were similar for the LVW and LWG methods, with the following exceptions:

- Different well spacing
- Linking required in LVW case only

The fields were designed so that three rows of wells would be in simultaneous operation. Air or oxygen is injected in the center row, and gas is produced from the flanking rows. Thus, the length of the rows is determined by the product of half the number of wells needed for the rated capacity and the well spacing. This dictates the field width, and the number of wells needed for 30-year plant life dictates the field length.

Figure 3 illustrates the mode of operation envisioned. It shows a section of a UCG field with the wells in a square pattern as in the LVW layout. After drilling and linking (if LVW) the wells of rows 1, 2 and 3, high-volume air injection and gas production are initiated as shown. Prior to the depletion of these rows, the wells for rows 4 and 5 are drilled, linked (if LVW), and connected to the air injection (row 4) and gas collection (row 5) pipe networks. Row 3 is reused for gas production

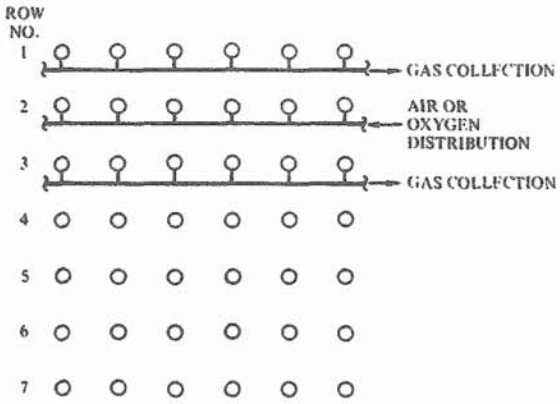


Figure 3
UCG FIELD OPERATION

with gasification occurring in the opposite direction. Upon depletion of the coal between rows 1 and 3, the newly prepared rows are put into operation, and the piping and casings are removed from rows 1 and 2 for reuse on rows 6 and 7. In this manner, gas production progresses down the field with drilling, casing, linking, and piping operations taking place simultaneously to prepare new rows for gasification.

The overall UCG field sizes, exclusive of the surface plant facilities, are given below. Thirty-year field life is assumed:

UCG Field Size	West		East	
	Power	SNG	Power	SNG
mi x mi	2.1x4.5	1.6x10.6	8.3x4.4	6.2x10.3
km x km	3.4x7.2	2.6x17.1	13.4x7.1	10.0x16.6

It was projected to locate the surface facilities in the center of the plot, thereby rendering the overall plot dimensions somewhat greater than those given above. A conceptual layout for the plot is shown in Figure 4.

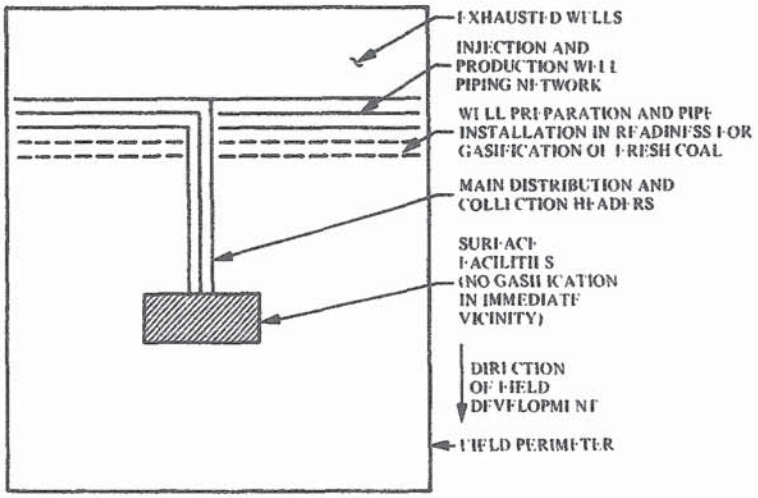


Figure 4
UCG FIELD PLOT PLAN
(NOT TO SCALE)

COST EVALUATIONS

Capital and operating costs for the eight plants considered were estimated on an order-of-magnitude basis. The rationale for cost estimating relied heavily on costs derived in previous Bechtel experience and on information supplied by UCG process developers.

The development of capital costs was based on conceptual plant designs incorporating scaled versions of similar plants or equipment dealt with in previous projects or studies. This was not entirely possible for the UCG fields, since they represent a novel approach and are somewhat speculative in design. Capital costs for the UCG fields are comprised of the following components:

- One full row of drilled and cased air- or oxygen-injection wells. This is a one-time cost, since subsequent oxidant injection is accomplished using idle gas production wells. All drilling is done on a long-term contractual basis.
- Compressors and other equipment needed for linking in the western LVW fields.
- The main piping runs from the surface facilities to the extreme rows of wells; also sufficient piping to run parallel along six rows of wells. All pipe comes in portable sections, each installed with a block valve.
- Structures, shops, and miscellaneous facilities.
- Site preparation and roads, taken as 1 percent of total capital cost for UCG field.
- Other costs, such as field instrumentation, also taken as 1 percent of UCG capital costs.
- Engineering and home office costs.

These capital costs were augmented by a distributable charge* of 20 percent and by a construction duration factor of 1.35. The latter corresponds to 6.5 percent compounded escalation and 10 percent compound interest during a construction period of 3.5 years. Both capital and operating costs include a 20 percent contingency allowance. Identical materials and labor costs were assumed in the West and the East.

Operating costs are divided into two segments: the costs of operating the surface facilities and the UCG fields. The major components of surface facility operating costs are listed below:

- Cost of coal, taken at $0.47/MM Btu ($1.87/MM kg-cal) in the West and twice that in the East.
- Operating labor, derived by factoring from previous plant designs.
- Maintenance and supplies, assumed to total twice the operating labor costs.
- Chemicals, estimated from reference plants.

The cost components for UCG field operation are outlined as follows:

- Drilling subcontract, including casing. For the LVW fields in the West the drilling of each 10- to 14-inch (25.4 to 35.6 cm) well was taken as $6,000 plus $25 per foot ($82/m) including casing [5]. MERC estimated that each directionally drilled borehole for the LWG field would cost $100,000. Drilling was planned to proceed continually during plant operation to provide the required number of production wells annually.
- Piping relocation, involving the dismantling of 100-ft (30.5 m) sections of pipe ranging from 20 to 40 in. (50.8 to 101.6 cm) in diameter, moving them, and reassembling them where needed.
- Linking operations (LVW fields only)

*Indirect costs, such as temporary buildings, miscellaneous construction services (clean-up, material handling, guards, etc.), construction equipment, supplies, and utilities during construction, supervision, etc.

• Coal royalty, assumed at 12.5 percent of value of annual raw gas production. Raw gas cost was estimated to be $0.64/MM Btu ($2.54/MM kg-cal) [5].

Based on the cost components outlined above, capital and operating costs were derived for each case studied. Table 5 presents a compilation of capital costs for the surface facilities, and Table 6 lists UCG field costs. It should be noted that 60 to 70 percent of the capital costs for the UCG fields represent expenditures for piping. It is also of interest that drilling costs represent 35 to 41 percent of the operating costs for UCG fields in the West and 72 to 75 percent in the East. It was found that the five-fold difference in coal seam thickness between the East and the West was predominantly responsible for the gap in drilling costs for the two locations.

Table 7 summarizes all capital and operating costs, and gives the product costs for all eight cases. The average capacity utilization designated for the power plants was 65 percent and for the SNG plants 91 percent. For comparison, based on the same coal costs used in the study, conventional power plants with flue gas desulfurization capability generate power for 28.3 and 32.6 mills/kWh in the West and East, respectively.

The results presented in Table 7 indicate that the cost of SNG from western coal will benefit most from the application of UCG. However, no such advantage for UCG is apparent for power production in the East. The site sensitivity of these UCG costs must be kept in mind when making comparisons.

It is noteworthy that since the completion of this study, further advances have been made by LERC on the LVW process. The Hanna No. 2 experiments, which are now complete, have produced results which would effectively improve the economics stated herein. The developers have increased the heating value of the gas produced to 175 Btu/SCF (1557 kcal/Nm^3), have augmented the gas production-to-air ratio from 1.5 to 1.8 and have succeeded in producing 8 to 12 MM SCFD (227,000 to 283,000 Nm^3/day) per well. LERC is also confident that 60 percent coal recovery can be attained, and that increasing the well spacing to 150 ft (45.7 m) will be feasible.

Table 5

CAPITAL COSTS OF THE SURFACE FACILITIES
(Millions of Dollars)

Mode of Gasification	Power	
	Surface	UCG
Plant Component		
Coal handling	23	
Coal gasification	231 [a]	
Gas purification and sulfur recovery	58	70 [a]
Raw gas compression	63	70
Combined-cycle power plant	250	250
Miscellaneous utilities and waste disposal	85 [d]	60 [b]
Total	710	450

Mode of Gasification	SNG	
	Surface	UCG
Plant Component		
Coal handling	45	-
Coal gasification	373 [a]	-
Syngas purification and methanation [c]	400	420 [a]
Oxygen plant	190	190
Miscellaneous utilities and waste disposal	152 [d]	150 [b]
Total	1,160	760

[a] This figure also includes dust removal facilities. [b] Treatment of condensibles from UCG is included. [c] Includes compression, gas sweetening, sulfur recovery, CO shift, and methanation. [d] A large percentage of this is for ash disposal.

Table 6

UCG FIELD COSTS
(Millions of Dollars)

Product	Power		SNG	
Plant Location	West	East	West	East
Capital Costs	105	110	115	150
Annual Operating Costs				
Drilling subcontract	15.4	78.2	27.4	139.2
Coal royalty	6.8	6.8	12.1	12.1
Piping (labor)	1.2	3.5	2.2	7.4
Linking (labor)	2.2		4.0	
Material	0.1	0.1	0.2	0.2
Capital-related (@ 18%)	18.7	20.0	21.3	27.3
Total	44.4	108.6	67.2	186.2

Table 7

COST SUMMARY
(Millions of Dollars)

Product	Power				SNG			
Location	West		East		West		East	
Mode of Gasification	Surface	UCG	Surface	UCG	Surface	UCG	Surface	UCG
Capital Costs	710	555	710	560	1160	875	1160	910
Annual Operating Costs								
UCG fields	-	44.4		108.6		67.2		186.2
Surface facilities								
Coal	29.0		58.1		79.[illegible]		159.4	
Operating and maintenance	52.4	40.1	52.4	40.1	102.0	77.7	102.0	77.7
Capital-related (@ 18%)	127.8	81.4	127.8	81.4	208.1	135.9	208.1	135.9
Total	209.2	165.9	238.3	230.1	389.8	280.8	469.5	399.8
Annual Product (kWh)	5318	4692	5318	4692			-	-
(10^{12} Btu)	-	-	-	-	84.4	79.7	84.4	79.7
Product Costs (mills/kWh)	39.3	35.4	44.8	49.1				
($/10^6$ Btu)					4.62	3.52	5.56	5.02

CONCLUSIONS

The results of this study show up to 25 percent savings when employing UCG rather than surface gasification for the production of power and SNG. The economic outlook for the large-scale commercialization of UCG is promising, especially since the opportunity for technological advances in UCG is extensive. The pattern uncovered by the analysis of the results gives some suggestion as to how future developmental effort may be directed to further improve process economics.

In the West (LVW process), combined operating costs for well drilling and piping constitute about 17 percent of the total plant operating cost for both power and SNG production. For the East (LWG concept), this percentage rises to 42 percent, partly because of coal seam geometry and partly on account of more costly drilling methods. The major UCG field costs, drilling and piping, can be reduced to make UCG even more attractive. To accomplish such cost reduction, the total number of wells required could be decreased by proper site selection, and by process and equipment development. The following factors are significant in reducing costs:

- Coal seam thickness should be maximized to the extent practical for the UCG technique employed. Seam thickness is the most significant cost related effect, since it influences both drilling and piping requirements.

- Coal seam depth should be minimized, although one of the unique features of UCG is the ability to extract very deep coal reserves.

- Coal heating value per unit volume is another site related consideration and should be maximized.

- The maximum possible well spacing should be employed. Developmental work continues in this area.

- Techniques which optimize the degree of coal recovery must be developed and employed.

- Improved and less costly drilling techniques must be developed.

The heating value of the gas produced and the production rate per well do not affect the total number of wells required for a certain Btu output, but they do alter the shape or mode of operation of the UCG field. Apart from efforts to decrease the costs of drilling and piping, other parameters such as gas/oxidant ratio can be improved to lower costs. This was recently accomplished for the LVW process at Hanna.

The design, development, and operation of large UCG fields requires further attention, not only from an economic standpoint, but also from an engineering point of view. Combined effort from the disciplines of petroleum engineering, mining technology, geology, chemical engineering, chemistry, and others will be necessary. Potential problems such as pipe failure due to ground subsidence must be evaluated. As further progress in UCG process development brings in situ gasification closer to commercial realization, it would be appropriate to expend some effort in the study of UCG fields.

ACKNOWLEDGEMENT

The technical support and assistance offered by the ERDA personnel at LERC and MERC is greatly appreciated.

METRIC CONVERSION FACTORS

1 ft = 0.3048 m
1 SCF = 0.0283 Nm^3
1 lb = 0.4536 kg
1 Btu = 0.252 kg-cal
1 Btu/SCF = 8.899 kg-cal/Nm^3

REFERENCES

1. "Preliminary Economics and Comment, In-Situ Gasification of Coal for Power and SNG," prepared for Office of Energy R&D Policy, National Science Foundation, Washington, D.C. by Bechtel Corporation, San Francisco, Ca.; November 1975.

2. Shrider, Leo A. and Jennings, James W., "An Underground Coal Gasification Experiment, Hanna, Wyoming," AIME Paper No. SPE 4993 presented at the 49th Annual Fall Meeting of the SPE, Houston, Texas; October 6-9, 1974.

3. Brandenburg, Charles F., Reed, Ray P., Boyd, R. Michael, Northrop, David A. and Jennings, James W., "Interpretation of Chemical and Physical Measurements from an In-Situ Coal Gasification Experiment," AIME Paper No. SPE 5654 presented at the 50th Annual Fall Meeting of the SPE, Dallas, Texas; September 28-October 1, 1975.

4. Shuck, L. Zane and Pasini III, Joseph, "A Report on Progress in Underground Coal Gasification," presented at the International Energy Engineering Congress, Chicago, Illinois; November 4-5, 1975.

5. Jennings, James W., "Some Economic Considerations of Underground Coal Gasification," AIME Paper No. SPE 5429 presented at the SPE-AIME Northern Plains Section Regional Meeting, Omaha, Nebraska; May 15-16.

An Economic Evaluation of Underground Coal Gasification

BY

A. M. Garon, Gulf Research & Development Company
Pittsburgh, PA 15230

ABSTRACT

A computer-programmed economic evaluation was developed to include all of the components of a hypothetical commercial underground coal gasification installation. The capital requirements and operational expenses for production operations, gas purification plants, oxygen manufacture and air compression were obtained from Gulf experience and a variety of other sources. Data from Lurgi pressure gasification tests were used in the base case calculations for production gas quantities and compositions and for the oxygen requirements. Sales prices were determined for three different product gas options, water or steam injection and two different base cases. One base case represents gasification in Illinois using pneumatic linking and the other represents operations in Wyoming using linking by backward burning.

The gas prices were determined as functions of the coal process parameters, the seam parameters, the operational parameters and the process efficiencies. Nominal values for these parameters were assumed for the base case calculations, and each of the parameters was varied relative to the base case values to determine its effect on the product prices.

INTRODUCTION

Gulf Research & Development Company (GR&DC) began investigating in-situ processing of coal for energy recovery during the early 1960's. Laboratory experimental work in the production of liquid and gaseous products from coal was performed along with a feasibility study and a preliminary economic analysis. A field test was conducted at the Pittsburg and Midway Coal Company Colonial Mine in Kentucky in 1968 [1]. Interest in underground coal gasification at GR&DC has increased in recent years after several years of only minor activity. In-house evaluation of ongoing work included a recent joint study with Lawrence Livermore Laboratory on their deep, thick coal-seam gasification concept [2].

An extensive study and economic evaluation of underground coal gasification has been conducted over the past several years. Comprehensive economic evaluations based on available data were desired to provide a basis for decisions on the value of pursuing the development to a commercial level. The objectives of the economic analysis and marketing study were the following: (a) Determine the cost of various product options using reasonable estimates where factual information does not exist. (b) Determine the sensitivity of product cost to variations in system parameters over reasonable ranges. Analyze the information from this parameter study to identify important parameters and important ranges of these parameters. (c) Maintain the link between these results and reality. Assumptions which are required to perform such a study at this early stage should always be kept in mind when evaluating the results and formulating conclusions. (d) Compare cost estimates from this study with competing fuels in the energy market. (e) Apply the results of the study to point out questions which

References at end of paper

need to be answered in future R&D work and to characterize the role underground gasification might play in filling the energy needs of the country.

Preliminary results of the economic analysis were presented at the American Nuclear Society Meeting in November, 1975, and published [3]. These results included the costs of producing several product options from a commercial application of forward combustion of coal in Illinois from vertical boreholes using pneumatic pressure linking. The effects of several of the variables on the results were shown. A marketing analysis of coal-derived gas based on end-use options in the Illinois basin was also included. Additional economic results for hypothetical commercial underground coal gasification plants are presented in this paper. The economic model now includes options not previously considered. The possibility of not injecting water, or injecting steam rather than water, has been included. Operation with Western conditions has been included along with the possibility of linking by backward burning with air or oxygen injection rather than linking by pneumatic pressure. The program has been expanded to enable the results to be based on current cost data using the Nelson Refinery Construction Cost Indexes. A second paper, presented by D. L. Bidlack [4] at this Symposium, discusses the economics of marketing synthesis gas produced by underground coal gasification for the manufacture of ammonia and methanol. These results are based on the gas production costs presented here.

DISCUSSION OF ECONOMIC MODEL

A computer-programmed economic model was developed and used to calculate results for hypothetical commercial underground coal gasification plants. The major assumptions used in the economic model are discussed below along with descriptions of the gasification concepts, the process data, the commercial production system and physical plant, and the cost data.

Gasification Production Concepts

Underground coal gasification can be performed through a series of vertical wells similar to a fireflooding enhanced recovery project. Generally, however, some type of linking technique must be used to provide communication between the wells. In the GR&DC Colonial Mine test [1] linking was accomplished using pneumatic pressure in an Eastern bituminous coal. The Laramie Energy Research Center (LERC) has successfully used linking by backward burning in a Western subbituminous coal in its tests near Hanna, Wyoming [5-7].

The GR&DC underground coal conversion test was conducted in a relatively thin (3 m) seam of moderately swelling bituminous coal by using high injection pressures (about 29.4 kPa/m of overburden or 1.3 psi/ft) to maintain a flow path between injection and production wells. The familiarity with the pneumatic linking technique, as applied to thin seams, led to the choice of this system for a part of the analysis. The coals of the Illinois basin were chosen for this study, both on the basis of similarity to the coal encountered in the Kentucky test and on the basis of major industrial energy demands nearby.

The Hanna tests are being conducted in a thicker seam (9 m) of subbituminous coal. The coal is preprocessed by backward burning between wells to establish communication. One advantage of this technique is that it enables much lower injection pressures to be used, reducing the possibility of gas losses. The current interest in this field test and availability of data led to the choice of this type of system for the other part of the analysis.

The two gasification schemes postulated in this paper have been extrapolated from the GR&DC test and the Hanna tests. The Gulf test was limited to dry combustion with air injection, using the heat of combustion for in-place retorting. However, it is assumed that gasification could be achieved from the same test configuration if water or steam were injected. The Hanna test was also performed with air injection and no water injection, although water from the coal seam entered the reaction zone. In both cases it is assumed that results with oxygen injection could be predicted from those with air. Although backward-burn linking has been performed with air injection, injection of oxygen with the same oxygen requirement per unit of linking length has been assumed for linking when oxygen is used for gasification.

These two schemes are presented as two possible alternatives of many, each with advantages and disadvantages. Potential marketing advantages exist for the Eastern situation because of the proximity of suitable deposits to industrial and population centers. However, bituminous coals require

special consideration in the choice of linking technique because their high volatile matter content leads to potential liquid plugging problems and their tendency to swell on heating can reduce flow permeability. Although Western coals are more distant from potential markets, the subbituminous coals have advantageous properties for fluid flow and reactivity, and the energy resource is more concentrated due to thicker seams. No further attempt is made to compare the two methods with the many other possible gasification techniques.

There is some technological information available about each of the two schemes which can be used in the economic evaluation. However, there are many unknown quantities. Thus, in situations where the current technology has not provided sufficient input for the economic analysis, assumptions had to be made based on the best available information. In addition, questions regarding subsidence, liquid plugging and other mechanical aspects of the process are not considered.

Gasification Process Data

Performance of the underground gasifier is a major unknown. Information on the injection parameters, such as the oxygen required per unit mass of coal and the water to oxygen ratio is needed, along with the amount and composition of the gas produced. These parameters affect the amount of coal resource required, oxidant capacity, and design and cost of the purification and/or methanation facilities.

Some of these data are availablefrom the Hanna project. However, the Hanna tests were performed in small patterns and part of the results were inferred from mass balance calculations. Thus, the Hanna data were not used in the base case calculations but were used in a separate economic analysis for comparison with the base case results.

It was decided that data from the Lurgi gasifier tests in Westfield, Scotland, [8,9] should be used as input for the base case calculations. The Westfield data are from systematic, well-documented tests that included both Illinois Nos. 5 and 6 coals, the seams of greatest importance in the Illinois basin, and a Western subbituminous coal named Rosebud. Reports from the underground gasification experiments at Hanna have indicated that, for their test conditions, underground gasification results have been "similar" to those reported for a Lurgi gasifier [6]. Despite many differences in operating conditions it was felt that the Lurgi data were, at least, indicative of the reactivity of the coals of interest and would provide valid comparisons between the results with different coals. The Lurgi data used in the base case calculations are shown in Table 1.

TABLE 1

LURGI COAL GASIFICATION DATA USED IN BASE CASE STUDIES*

Coal		Illinois #6 (SROM)	Rosebud (CG)
Proximate Analysis -	weight pct		
Moisture		13.68	24.70
Ash		9.12	9.73
Volatile Matter		33.96	29.20
Fixed Carbon		43.24	36.37
Coal Heating Value	MJ/kg (Btu/lb)	25.1 (10820)	20.0 (8611)
Oxygen Requirement			
per unit mass of coal	kmol/t(mscf/ton)	14.8 (11.2)	7.1 (5.4)
per unit of gas produced	kmol/kmol	0.183	0.119
Steam Requirement			
per unit mass of coal	kg/kg	2.63	1.25
per unit mass of oxygen	kg/kg	5.26	5.13
decomposition	pct	23.5	45.4
Gas Production			
per unit mass of coal	kmol/t(mscf/ton)	80.9 (61.4)	60.8 (46.2)
Liquid Production			
per unit mass of coal			
Tar	kg/t (lb/ton)	18.5 (37)	19 (38)
Oil	kg/t (lb/ton)	4.5 (9)	21 (42)
Benzol	kg/t (lb/ton)	8.0 (16)	6.5 (13)
Product Gas Properties			
composition	mole pct		
H_2		39.8	41.2
CO		16.3	15.1
CH_4		8.7	11.2
C_2H_6		0.5	0.5
Illuminants		0.1	0.0
CO_2		32.1	30.4
H_2S		1.1	0.5
Inerts		1.4	1.1
heating value	MJ/kmol (BTU/scf)	248 (281)	269 (305)

*Data from the Lurgi Pressure Gasification Plant at Westfield, Scotland.[8-9]

One possible major difference between the conditions under which Lurgi data were obtained and the postulated operating conditions for the underground gasification scheme is the state and quantity of the injected water. The Lurgi gasifier requires steam injection, whereas it is uncertain for the in-situ case whether steam is required, whether liquid water injection is possible, or if the system can be operated with no water injection. Although the Hanna test utilized nearly ideal conditions of natural ground-water flow to provide the required water, it is not felt that this fully justifies commercial operation with no water injection or even the use of liquid water. It is not known, at this point, whether the Hanna results could be obtained if the same water volumes came into the system from the wellbores. To account for this uncertainty in the required injection phase, results are obtained for both water and steam injection. The same process data are used for both conditions; it is simply a question of which injection phase is required to obtain the postulated results.

A surface gasifier of the type used in Westfield tests is constrained to operate at a temperature below the ash fusion point of the coal. Temperature control is maintained by injecting excess steam. Since slag removal is not a problem in the in-situ process, higher gasification temperatures requiring less steam

or water could be tolerated. Although water costs are only a small part of the overall cost of gas production, the cost of steam generation can be quite large. Thus, the water or steam injection requirements for the base cases were set equal to the amount of water actually consumed by the reaction in the Lurgi gasifier rather than the quantity injected. The effect on the gas price of varying this quantity was then investigated.

Commercial Gas Production System

The conceptual commercial gas production system employs a line drive configuration consisting of a number of five-spot patterns, as shown in Figure 1. Choice of this configuration is based on the initial test experience and conventional oilfield practice. Fluid produced from this array of wells is conducted to a transportable field production station. Here the gas is cooled, coal liquids and liquid water are separted, and the produced gas is compressed for transmission to the gas treatment plant. The production station is located near the active pattern to reduce gathering line pressure drop. The gas treatment facility, however, is located at a fixed site outside the active area for protection against surface subsidence. Also located at the gas plant site are the oxygen plant or air compressors and water supply system. Delivery lines run to the active site where distribution lines connect to each injection well. Figure 2 shows a schematic diagram of this piping system.

With pneumatic linking, no advance preparation of the coal seam is required since linking is accomplished by the pressure of the injection fluids. As the coal within each line drive pattern is consumed, an adjacent pattern, which has been previously piped, is gradually brought on stream to provide a continuous flow of product gas. Manifold piping for two patterns must therefore be provided. Each succeeding line drive is connected to the main lines prior to ignition, using the piping from the burned-out pattern. With linking by backward burning, gas must be injected before the gasification operation, requiring addition piping so that the area can be prepared in advance.

The burned out area is sometimes used for disposal of excess water, necessitating more pipe. In most cases the production water is reinjected for gasification. However, when the amount of water produced is greater than the desired injection quantity, the excess is injected into disposal wells. Also, in Illinois where water is plentiful, fresh water is used for steam generation, and all the produced water is disposed.

At periodic intervals, the field production station is moved as the advancing active zone approaches. Sufficient excess equipment capacity reduces the effect of this move on continuous gas production capability.

Physical Plant

The commercial gasification system is comprised of three distinct operational areas: the production facilities, the production field station and the main plant. In addition, numerous pipelines are required to interconnect the different facilities.

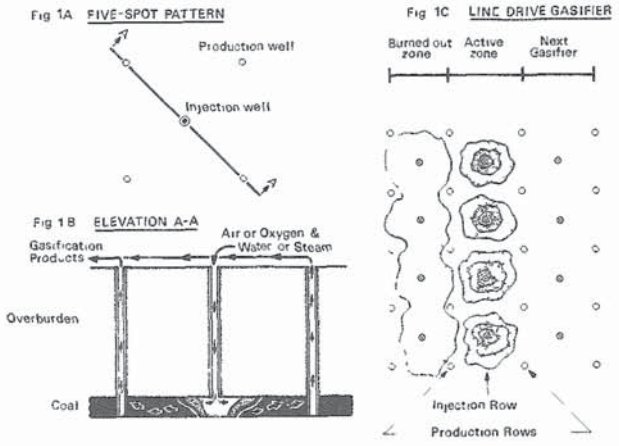


FIGURE 1 - GAS PRODUCTION CONFIGURATION

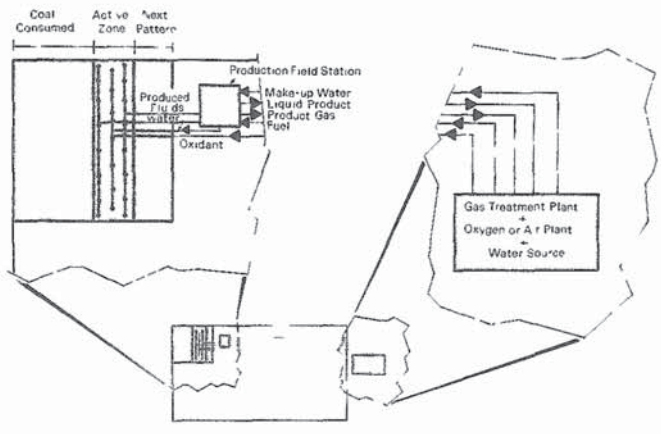


FIGURE 2 PLAN VIEW OF SURFACE FACILITIES

The field production facilities include the injection, production and disposal wells, the steam generators and the equipment and wells utilized for linking operations. Injection and production wells are assumed to be cased and cemented through the coal. The production well casing I.D. is a function of gas flow rate and a specified pressure drop criterion. The steam generators are located near the injection wells to reduce heat losses. In Wyoming thermosludge steam generators [10] are used to enable utilization of production water. The steam generators are moved along with the production area, and sufficient extra capacity is included to enable interruption-free relocation.

The field station includes gas coolers, field separators for gas and liquid separation and gas clean-up, and compressors required for transmission of the produced gas to the central treatment facilities. Separators, oil dehydrators, gas coolers, liquid storage facilities and compressors are sized according to assumed or calculated conditions using accepted formulae. Compressor interstage temperature is limited to 150°C. Flexibility for continuous operation is provided by requiring 25% production equipment standby capacity.

The central gas treatment plant design varies according to end product requirements. A gas produced with oxygen may be upgraded by acid gas (H_2S + CO_2) removal to provide medium-heat-value gas for fuel or synthesis feedstock. This gas is defined here as synthesis (SYN) gas. It may also be converted into synthetic pipeline gas (SPG) by shift conversion, purification, and then methanation to a pipeline quality of 834 MJ/kmol (945 Btu/SCF). A gas produced from air injection has a low heat value but would be suitable for nearby consumption as a fuel once sulfur compounds are removed. This type of product gas will be called low heating value (LHV) gas. The hot potassium carbonate process, as described by McCrea and Field [11], is used for both SYN gas and LHV gas purification plants. Process parameters are adjusted to remove nearly all CO_2 in the case of the SYN gas, but only about 25% of the CO_2 with more selective H_2S absorption in the LHV gas case. If CO_2 can be tolerated in the end product, savings are realized both in plant capital and energy requirements. A Claus sulfur plant is used to convert H_2S in the concentrated acid gas stream to elemental sulfur for byproduct sales.

The oxygen plant or the air compressor facility is located near the main gas treatment plant. The oxygen plant requirement is calculated with a maximum single train size of 0.66 Mt/a (2000 tons/day). Air compression is by gas turbine powered compressors of approximately 7500 kW (10,000 HP) capacity. Capital cost, as well as operating cost, varies with the required injection pressure. This, in turn, is a function of the linking technique, the assumed pressure gradient required to maintain gas flow underground, depth of cover and pressure drop in the surface piping.

The piping requirements can be divided into four systems: an oxygen or air system, a product system, a water system, and a fuel gas system. Pipe diameters and wall thickness are calculated according to flow rate, fluid pressure and pressure drop requirements. All piping is assumed to be carbon steel, except for the oxygen lines which must be stainless steel.

In order to supply the energy requirement of the gasification plant, a portion of the produced gas is split off for use as plant fuel. Selective H_2S and partial CO_2 removal is used to desulfurize the fuel gas. This fuel is used in gas turbines and boilers to provide gas compression at the field production station, regeneration steam for the gas purification process, shift conversion steam, power for the sulfur plant, oxidant at the required injection pressure for gasification and linking, steam for injection, and final compression of the product gas to the required delivery pressure. The fuel purification plant is integrated into the product purification facility for the SYN gas or LHV gas product options. For the SPG option the fuel purification plant is located within the field station. Only a small amount of energy is purchased as commercial electrical power.

Cost Analysis

The capital requirements and operational expenses for the production operations, gas purification plants, oxygen manufacture and air compression were obtained from Gulf experience and a variety of other sources. Every effort was made to design surface-system components and estimate equipment capital costs accurately so that the principal uncertainty in the results would lie in the gasification assumptions.

Drilling and completion costs have fluctuated wildly in the last several years under demand pressures and equipment shortages. However, recent data on a large number of infill holes, as well as published costs [12], were used to estimate drilling costs of $62/m ($19/ft), drilled, cased and cemented, plus $4400 fixed cost per injection well and $3300 for each production well. Casing is considered non-recoverable but tubing and packers used in the injection well are reused.

Surface piping material costs of $0.50/kg for carbon steel and $3.20/kg for stainless steel came from a variety of sources [13, 14]. Labor costs for installing piping were derived from a correlation [15] of extensive data from the literature, including a pipeline industry survey report [16]. Half of this value is charged for disassembling installed piping systems.

Compressor and steam generator capital cost data were taken from recent manufacturers' literature and quotations. The costs of tankage, separators and gas coolers came from Gulf data and assorted references [13, 17]. The costs of clearing, grading and building access roads, electrical substations and water supply systems came from Gulf data and Guthrie's manual [13].

Cost data for the oxygen plant and the SPG plant were provided by the GR&DC Planning and Economics Division [18]. The SPG plant costs were based on submissions to the FPC for surface plant construction. Cost and operating data for the hot carbonate gas clean-up process came from McCrea and Field [11]. Higher capital requirements for the gas processing plants of 7% are used for Wyoming. A ten percent higher cost for labor intensive construction operations in Wyoming was used to account for the more severe weather conditions.

Annual capital charges are 13% of total capital for utility financing based on 75/25 debt equity ratio, 15% return on equity, 8.5% interest rate, 48% federal income tax and 4% depreciation (25-year term). For equity financing, the annual charge is 24% of total capital based on 20% return on capital before taxes and 4% depreciation. All of the results are indexed to June, 1976.

The calculations which are used for evaluating the economics of a hypothetical commercial underground coal gasification plant are tedious, but not very complex. There are a great number of calculations required for each individual case study, and the results from many cases are needed to evaluate the effect of each parameter. Since a great number of parameter studies were desired, a computer program was written to perform the calculations. Thus, equipment sizing, line sizing and cost estimation are automatically performed and the total costs are properly accumulated. The program allows a wide selection of options to be executed as desired. The program also includes the capability for direct plotting of the results using the CRT plotter.

RESULTS

The costs of producing SPG, SYN gas and LHV gas from hypothetical commercial underground coal gasification plants with both water or steam injection were calculated for each of two locations. The parameters which were specified for the base cases are discussed. The results are presented along with a comparison with projected SPG costs from surface gasification plants. An analysis of the effects of variations of each of the parameters is presented.

Base Case Parameters

The base case parameters which were chosen represent a blend between realistic conditions and the ideal case. Realistic values were used where suitable data were available such as for seam depth or thickness. Optimistic values were used where no suitable data existed, such as for gas losses or sweep efficiency. The base cases are not intended to represent the optimal conditions nor the most realistic. They simply represent a base upon which to study the effect of parameter variations.

The values of the parameters which define the base cases are listed in Table 2. Process data from Lurgi gasification was used to represent the in-situ process, Illinois No. 6 coal from the Illinois basin for the Eastern base cases and Rosebud coal from the Powder River basin for the Western cases. Justification for the remainder of the parameter values is discussed below.

The depth and thickness of the coal seam at the Illinois location were chosen after reviewing several publications of the Illinois State Geological Survey on coal resources in the counties which

TABLE 2

BASE CASE PARAMETER VALUES

Location		Illinois	Wyoming
Coal Process Data*			
Name		Ill. #6 (SRDM)	Rosebud (CG)
Gas Produced	kmol/t (mscf/ton)	90.9 (61.4)	60.8 (46.2)
Oxygen Required	kmol/t (mscf/ton)	11.8 (11.2)	7.1 (5.4)
Water Consumed	kg/kmol (lb/lb)	39.6 (1.236)	74.5 (2.329)
Oxygen Ratio			
Gas Composition		Lurgi Results*	Lurgi Results*
Coal Seam			
Thickness	m (ft)	3.05 (10)	9.14 (30)
Depth	m (ft)	183 (600)	183 (600)
Linking Procedure			
Method		Preburn	Backward Burn
Injection Pressure	kPa/m (psi/ft)	29.4 (1.3)	22.6 (1.0)
Oxygen Required	kmol/m (mscf/ft)	0 (0)	39.2 (13)
Operational Procedure			
Injection Pressure	MPa (psi)	5.34 (790)	1.38 (200)
Production Pressure	MPa (psi)	3.34 (50)	0.34 (50)
Production Rate/well	mol/s (mmscf/day)	69 (5)	69 (5)
Well Spacing**	m (acres)	0.5 (2)	0.8 (2)
Aspect Ratio		1.0	1.0
Process Effectiveness			
Sweep Efficiency	PCT	100	100
Oxygen Utilization	PCT	100	100
Gas Recovery	PCT	100	100
Gas Delivery Pressure			
SPG	MPa (psi)	6.90 (1000)	6.90 (1000)
SYN Gas	MPa (psi)	3.10 (450)	3.10 (450)
LHV Gas	MPa (psi)	1.21 (175)	1.21 (175)
Plant Capacity			
Energy Output	GJ/s (MMBtu/day)	1.76 (144)	1.76 (144)
Volume Output of SPG Equivalent	kmol/s (MMSCF/day)	2.11 (152.2)	2.11 (152.2)
Time Base		June, 1976	June, 1976

* Results from Lurgi pressure gasification tests at Westfield, Scotland (see Table 1).
** Ratio of distance between production rows to distance between production wells in a row.

contain the deeper part of the Illinois basin [19-21]. Depths as great as 370 m (1200 ft) have been recorded for the No. 5 coal; half that depth was chosen for the base case. The coal resources of Wyoming are more plentiful and distributed over a wide range of seam thicknesses and depths [22]. A depth of 180 m (600 ft) was also chosen for this location to simplify the comparison of base case results. In general, Eastern coals are contained in rather thin seams, while thicker deposits are more likely in the West. However, since the Illinois Numbers 5 and 6 coals are not greatly separated, seam thickness is taken to represent net coal rather than a single physical dimension. For example, the Illinois coals are each 1.5 m (5 ft) in some areas of the Illinois basin and the two constitute the base case net coal thickness of 3 m (10 ft). Implicit in this interpretation is the assumption that multiple overlying seams can be gasified either simultaneously or sequentially. A larger seam thickness of 9 m (30 ft) was chosen for the Wyoming location. Seam thickness as a parameter in this investigation reflects only on the magnitude of the coal resource per unit land area. Variation in heat loss and product composition with seam thickness is not considered.

Linking by pneumatic pressure was used in the East and linking by backward burning in the West. A pressure of 29.4 kPa/m (1.3 psi/ft) of overburden was used in the Eastern cases to obtain and maintain sufficient injectivity, as encountered in the Gulf field test [1]. For linking by backward burning, pressures up to the fracture pressure were specified, and 39.2 kmol/m (10 mscf/ft) of oxygen were injected. However, this linking technique enabled the use of lower injection pressures for gasification; an injection pressure of 1.38 MPa (200 psi) was used. A production wellhead pressure of 0.34 MPa (50 psi) was maintained for both locations. Well spacing and flow rate of product gas from a single wellhead were set at reasonable levels. The plant capacity was based on one half the size of the proposed surface gasification plants. The product gas delivery pressures were derived from approximate linear scaling of pressure to gas heating values using the SPG values as the reference point. This choice is arbitrary and its effect was examined along with the effects of all the other parameters.

Optimum values for the process effectiveness parameters were chosen for the base case calculations. No gas was lost and no coal bypassed by the reaction front. Actual values of these numbers would vary with local geology, hydrology, operating pressures, etc. These base case values were chosen to represent the ideal case and the parameter study shows the effect of relaxing this assumption.

Base Case Results

The results of the economic analysis for the base cases are presented in Table 3 for each injection phase and product option under consideration. The total capital requirements for the SPG option are \$497 X 10^6 for the Eastern case and \$352 X 10^6 for the Western case, if water injection is sufficient. If steam injection were required about 12% additional capital would be necessary. The SYN gas and LHV gas plants require less capital as shown. The capital requirements are approximately 30 to 50% lower for the Western cases than the Eastern.

The manufacturing expense, the sales price with both utility and equity financing, and the by-product credits are also given in the Table. The sales prices are without the by-product credit which was obtained assuming complete recovery of the by-products listed in Table 1 plus the sulfur removed

TABLE 3 BASE CASE ECONOMIC RESULTS

	Illinois Base Cases						Wyoming Base Cases					
Product Option	SPG		SYN GAS		LHV GAS		SPG		SYN GAS		LHV GAS	
Water or Steam Injection	water	steam	water	steam	water	steam	water	steam	water	steam	water	steam
Capital Requirement - 10^6												
Production System	128	164	104	133	168	126	93	120	76	99	97	122
Oxygen or Air Plant	198	231	168	198	174	148	86	94	69	82	38	43
Gas Plant including product compression	171	171	91	93	45	47	173	173	91	93	29	31
Total	497	566	363	424	338	421	352	387	229	269	163	196
Total Manufacturing Expense - \$/GJ	0.87	1.00	0.68	0.79	0.68	0.85	0.57	0.69	0.41	0.48	0.34	0.40
Sales Gas Price without byproduct credit												
Utility Financing \$/GJ	2.17	2.48	1.63	1.90	1.56	1.95	1.19	1.66	1.01	1.19	0.76	0.92
Equity Financing \$/GJ	3.27	3.73	2.43	2.94	2.30	2.88	2.27	2.50	1.51	1.77	1.10	1.35
Byproduct Credit \$/GJ	0.18	0.20	0.15	0.18	0.15	0.19	0.22	0.25	0.14	0.22	0.17	0.20

Note: \$/GJ = 0.95 x \$/MMBTU.

from the gas. The sales prices for the SPG, SYN gas and LHV gas options with water injection in dollars per GJ are 2.17, 1.63 and 1.56, respectively, for the Illinois case and 1.49, 1.01 and 0.76 for the Wyoming case with utility-type financing. (A price of $1.00/MMBTU is equivalent to $0.95/GJ.) If it were necessary to inject the water as steam, the product prices would be 10 to 25% greater, depending on the product option; prices with equity financing are about 50% higher. Information about the sales and production gas volumes and energy utilization within the plant is shown in Table 4. The fraction of the production gas going to sales is significantly greater for the Western case.

TABLE 4 GAS PRODUCTION AND UTILIZATION FOR BASE CASES

		Illinois Base Cases						Wyoming Base Cases					
Product Option		SPG		SYN Gas		LHV Gas		SPG		SYN Gas		LHV Gas	
Water or Steam Injection		water	steam	water	steam	water	steam	water	steam	water	steam	water	steam
Sales Gas													
Volume Rate	kmol/s	2.10		4.73		11.33		2.10		4.51		8.85	
	(MMscfd)	(152)		(342)		(819)		(152)		(326)		(640)	
Heating Value	MJ/kmol	834		371		155		834		389		199	
	(BTU/scf)	(945)		(420)		(176)		(945)		(441)		(225)	
Produced Gas													
Volume Rate	kmol/s	15.23	17.48	13.30	15.24	22.13	26.32	11.42	13.03	9.97	11.35	12.82	14.69
	(MMscfd)	(1101)	(1264)	(962)	(1102)	(1600)	(1903)	(826)	(942)	(721)	(821)	(927)	(1062)
Heating Value	MJ/kmol	248		248		147		269		269		187	
	(BTU/scf)	(281)		(281)		(166)		(305)		(305)		(212)	
Production Gas Utilization (pct of total production)													
Sales Gas		46.6	40.6	53.3	46.5	54.1	45.5	57.1	50.1	65.4	57.5	73.2	63.9
Field Compressor Fuel		8.3	8.7	8.1	8.3	15.8	16.8	7.1	7.4	7.0	7.1	10.7	11.1
Field Steam Boiler Fuel		0	7.8	0	7.8	0	7.8	0	9.1	0	9.1	0	9.1
Fuel Gas Purification Plant Fuel*		0.4	0.8	1.0	1.4	3.7	4.4	0.3	0.8	0.9	1.3	1.7	2.3
Oxygen or Air Plant Fuel		24.8	24.8	24.8	24.8	20.5	20.6	12.9	12.9	12.9	12.9	8.1	8.1
Product Gas Plant and Compressor Fuel		19.9	17.3	12.8	11.2	5.9	5.0	22.5	19.8	13.7	12.1	6.3	5.5

*Does not include fuel for purification of fuel for the SPG or oxygen plants for the SPG option.

The fact that the economics are much more favorable for the Western cases than for those in the East is an important result of this study. Thus, it is interesting to examine the differences in the economics. The five base case parameters which differ from East to West are the location, the seam thickness, the gasification injection pressure, the linking technique and the coal process data. The effects on the economics of SPG production of changing these parameters is as follows. Beginning with the Eastern base case, changing only the location (to Wyoming) increases the cost by 3%. Increasing the thickness decreases the cost by 7%. Changing the linking procedure, without reducing the injection pressure, increases the cost by 2%, but the lower injection pressure saves 9%. Changing of the coal from the Eastern bituminous to the Western subbituminous has the largest effect, decreasing the cost by 20%.

The absolute values of the costs presented above have no meaning unless in the context of competition in the energy marketplace. A second paper [4] utilizes the production costs generated here to demonstrate the potential for in-situ generated gas from coal in the market. In addition, although it is not the purpose of this paper to discuss the marketing aspects of coal gasification, a comparison between the economics of projected surface SPG plants [18] to the base case results is presented in Table 5. The SPG prices for the in-situ plant were 31 and 37% lower than those from the surface plant for the Illinois and Wyoming locations, respectively. The significance of these differences should not be overinflated by forgetting how the base case parameters were chosen.

TABLE 5 COMPARISON OF ECONOMICS OF PROJECTED SURFACE SPG PLANTS TO BASE CASE RESULTS

Location	Illinois			Wyoming	
In-situ or Surface Gasification	In-Situ*	In-Situ**	Surface	In-Situ*	Surface
Plant Capacity - kmol/s	2.11	3.04	3.04	2.11	3.17
- MMscf/day	152.2	214.1	214.1	152.2	152.2
Capital Requirement - 10^6	847	971	1,179***	450	719***
Sales Gas Price - $/GJ (Utility Financing)	2.17	2.17	3.19	1.49	2.37

* Base case results with water injection and no by-product credit
** Same as results except for larger plant capacity.
*** Does not include capital for mine.

In the base case calculations, results were obtained for two coals, one each for the Eastern and Western locations. Additional results were obtained for all five of the coals and the various grading analyses for which data were reported from the tests of American coals at Westfield [8-9]. The results were similar for all of the bituminous coals. However, the average costs of SPG, SYN gas and LHV gas are approximately 25, 35 and 50% greater, respectively, for the three bituminous coals than for the subbituminous coal for both base case locations.

Additional calculations were performed using the process data from the Hanna I and the Hanna II tests along with the other base case assumptions in both locations. The resulting gas prices, presented in Table 6, are much higher than the base case results. It should be remembered, of course, that the Hanna process data include the field operation process inefficiencies that were set at optimum values in the base case assumptions. On the other hand, the Hanna data were obtained from a small test in an isolated pattern; more favorable results would hopefully be obtained in a commercial-sized operation. Considerable improvement was even seen between the two tests. However, despite these considerations, the cost differences are quite large, and at this point it can only be suggested that the real costs might be somewhere in between.

Parameter Study Results

The major parameters were varied over reasonable ranges to determine the gas cost sensitivity. For the purpose of this study, parameters which are related through the physics of the underground gasifier were decoupled. For example, injection gas flow rate and injection pressure were varied independently, while they are in reality interdependent. The volume of air injected must be five times the volume of oxygen injected for similar gasification rates, yet the base cases for both air and oxygen are examined holding the injection pressure constant. This decoupling must be kept in mind when examining the results of the parameter study. Results for the Eastern and Western locations were generated using their respective base case parameters.

A summary of the effects of the parameters on the price of SPG produced with steam injection is presented on Figure 3 which shows the percentage change in energy price for 10% increases and decreases in each of the parameters for both locations. It can quickly be seen that the parameters which most strongly affect the costs are the gas produced and oxygen required per ton of coal, the methane content of the produced gas, and the fractions of oxygen utilization and gas recovery. The effects are much stronger for the Eastern base case conditions than for the Western conditions.

Although Figure 3 provides a useful, illustrous summary of the parameter effects, it has a serious shortcoming. It shows the results for 10% parameter variations while, in reality, the possible or probably ranges of each of the parameters differ widely from each other. The figure would be more useful if it showed the effects of parameter variations of a given fraction of their expected range. However, with the current state of the art, it would be difficult to estimate the probable range for each of the parameters, and in some cases the results would be quite arbitrary. An alternate representation of the results of the parameter study is given in Table 7 which shows the effects of larger variations of the parameters in addition to the results for the 10% variations.

TABLE 6 ENERGY COSTS FOR IN-SITU GASIFICATION BASED ON PROCESS DATA FROM HANNA AND BASE CASE ASSUMPTIONS

Location and Linking Method	Eastern Location - Pneumatic Linking						Western Location - Backward Burn Linking					
Product Option	SPG		SYN Gas		LHV Gas		SPG		SYN Gas		LHV Gas	
Water or Steam Injection	water	steam	water	steam	water	steam	water	steam	water	steam	water	steam
HANNA I Test Results												
Capital Requirement - 10^6	854	1405	712	1193	1846	*	724	1138	589	958	793	*
Sales Gas Price - $/GJ												
Utility Financing	3.85	6.51	3.27	5.65	8.50	*	3.07	4.89	2.56	4.18	3.47	*
Equity Financing	5.74	9.61	4.85	8.29	12.58	*	4.67	7.41	3.86	6.30	5.23	*
HANNA II Test Results												
Capital Requirement - 10^6	731	1044	526	761	712	2453**	638	892	432	625	455	864
Sales Gas Price - $/GJ												
Utility Financing	3.41	5.01	2.48	3.71	3.49	13.22**	2.76	3.92	1.91	2.80	2.11	3.95
Equity Financing	5.03	7.32	3.64	5.39	5.06	18.64**	4.17	5.89	2.86	4.18	3.11	5.86

* Insufficient energy produced for internal consumption.

** Only 12% of produced energy is contained in product.

$/GJ = 0.95 x $/MMBTU.

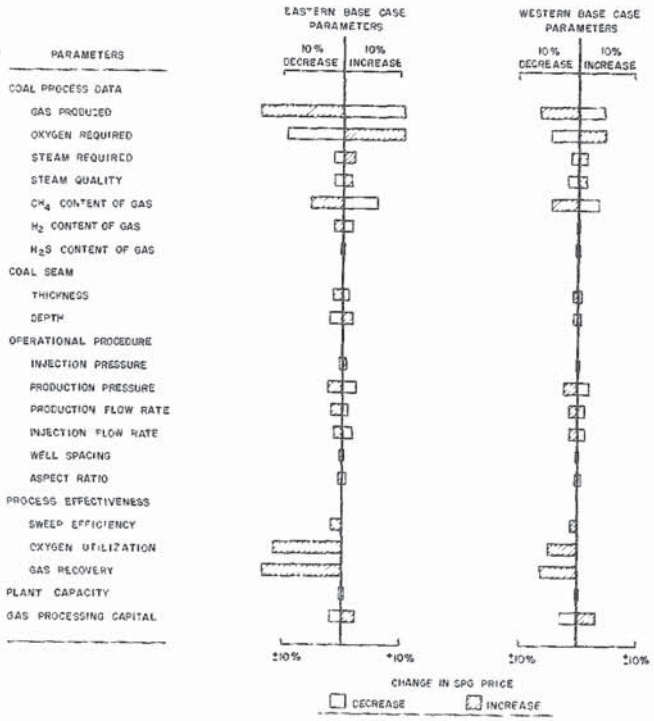


FIGURE 3 EFFECT OF PARAMETERS ON SPG PRICE

Because of space limitations, the computer-generated figures for only a few of the individual parameters are included and only for the Western location. These figures show the energy costs for the three Product options with the two injection phases plotted against the parameter being evaluated. The energy costs used in the figures are without by-product credit and for utility financing. Each of the curves is comprised of 20 to 30 individual points from separate calculations, connected with straight lines. The effects of the separate parameters on the energy costs are discussed below.

Coal Process Data. In the base case calculations, it has been assumed that the process data from Lurgi gasification are representative of the underground process. In reality it is possible that this is not the case. Perhaps, due to the inability to control the underground process as carefully as a Lurgi gasifier, the use of less optimistic process data would be more realistic. On the other hand, it is possible that superior gas composition can be achieved in the underground reactor where gas residence times are likely to be longer and equilibrium conditions (higher methane concentrations) are more likely to be approached. The importance of the process data on the product costs was demonstrated using data from several coals. In addition, the various process data are investigated individually. The amount of gas produced and the oxygen required per unit mass of coal are the most important process parameters. The effects of these two parameters on the energy costs are shown on Figures 4 and 5. Results from Lurgi gasification experiments have shown that the oxygen requirements are lower for the more reactive

TABLE 7 SUMMARY OF EFFECT OF PARAMETERS ON COST OF PRODUCING SPG WITH STEAM INJECTION

Parameter	Eastern Location: Figure Number	Eastern Location: Effect on SPG Cost of Parameter Variation of -50%	-10%	+10%	+50%	+100%	Western Location: Figure Number	Western Location: Effect on SPG Cost of Parameter Variation of -50%	-10%	+10%	+50%	+100%
Coal Process Parameters												
Gas Produced	11		+14.0	-10.7			12		+6.2	-4.7		
Oxygen Required	14		-9.5	+10.7			15		-4.3	+4.9		
Steam Required	18	-8.0	-1.4	+1.8	+9.4	+22.8	19	-5.4	-1.2	+1.6	+7.8	+15.9
Steam Quality	20		-1.3	+1.3			21		-1.4	+1.4		
CH_4 Content of Gas	22	+38.0	+5.5	-5.9			23	+31.5	+4.5	-3.5		
H_2 Content of Gas	24		+1.3	-1.3			25		+0.1	-0.1		
H_2S Content of Gas	26	-1.2	-0.2	+0.2	+1.2	+2.5	27	-0.5	-0.1	+0.1	+0.5	+1.0
Coal Seam												
Thickness	28	+12.9	+1.6	-1.0	-4.2	-6.3	29	+7.4	+0.7	-0.7	-2.6	-3.6
Depth *	32	-9.4	-2.1	+1.6	+8.2	+14.0	33	-4.3	-0.6	+0.6	+3.3	+7.4
Linking Procedure												
Injection Pressure			-	-				0.0	0.0	0.0	0.0	
Oxygen Required			-	-			34	-0.5	-0.1	+0.1	+0.5	+1.0
Operational Procedure												
Injection Pressure	35		-0.7	+0.7			36	-1.5	-0.2	+0.2	+1.1	+2.3
Production Pressure	37	+18.1	+2.4	-2.2	-9.2	-16.0	38	+14.4	+2.2	-1.9	-7.0	-13.0
Production Flow Rate Per Well	39		+1.9	-1.0	-4.0	-5.4	40	+14.4	+1.4	-1.1	-3.8	-5.1
Injection Flow Rate Per Well	42		+1.5	-1.4			43		+1.4	-0.8		
Well Spacing	44	+6.3	+0.6	-0.2	-0.8	-0.6	45	+2.7	+0.2	-0.1	0.0	+0.7
Aspect Ratio	46	+6.3	+0.7	-0.5	-2.4	-3.9	47	+4.4	+0.5	-0.4	-1.8	-2.6
Process Effectiveness												
Sweep Efficiency	48	+15.0	+1.9	-			49	+10.4	+1.2	-		
Oxygen Utilization	50		+11.8	-			51	+81.5	+5.1	-		
Gas Recovery	52		+13.6	-			53	+99.3	+6.5	-		
Plant Capacity	56	-2.1	-0.7	+0.7	+3.3	+11.8	57	+2.1	+0.3	-0.3	+1.14	+5.1
Gas Processing Capital	62		-2.1	+2.1			63		-3.0	+3.0		

* With injection pressure proportional to depth.

coals [23]. Since the lower rank coals and their chars are generally more reactive, the costs of in-situ gasification would generally be less for the lower rank coals.

The amount of water or steam that is injected for the in-situ base cases was taken as the amount of water actually consumed in the Lurgi process. Since the required quantity of water injection is unknown as is the required injection phase, results were obtained for the energy cost as a function of the water to oxygen injection ratio varying from zero to twice the base case values for both injection phases (Figure 6). If water can be injected, its quantity has little effect on the energy costs. However, the costs increase very quickly as steam injection quantities are increased. (In the base case calculations, the steam is generated at 80% quality, and both the liquid and vapor are injected, together making up the required injection quantity. The effect on the energy cost of varying the steam quality is thus essentially the same as varying the amount of steam.)

The effects of varying the methane content, the hydrogen content and the hydrogen sulfide content of the produced gas from the base case values are shown on Table 7. The concentrations of each of these gases was varied individually, keeping the relative concentration of the remainder of the gases and all the other parameters constant. The energy cost decreases for increasing methane or hydrogen concentrations and increases for higher hydrogen sulfide contents. The effect of equal percentage changes of methane is much greater than for hydrogen. A ten-fold increase in the hydrogen sulfide content increases the cost of SPG by about 20% in the East but by less than 10% in the West.

Seam Characteristics. The effect of the thickness of the coal seam on the energy costs is shown on Figure 7. Although the cost decreases with increasing thickness, increases beyond, say, 10 m have

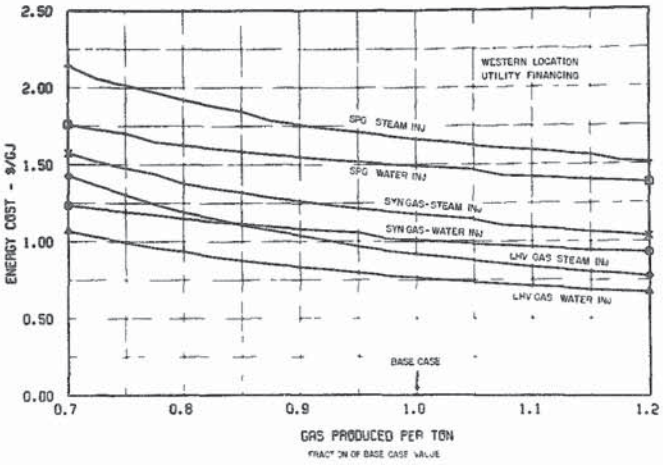


FIGURE 4 ENERGY COST VS GAS PRODUCED PER UNIT MASS OF COAL

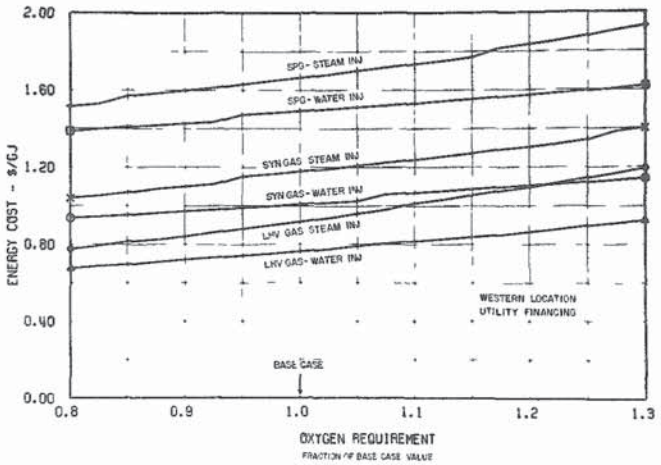


FIGURE 5 ENERGY COST VS OXYGEN REQUIRED PER UNIT MASS OF COAL

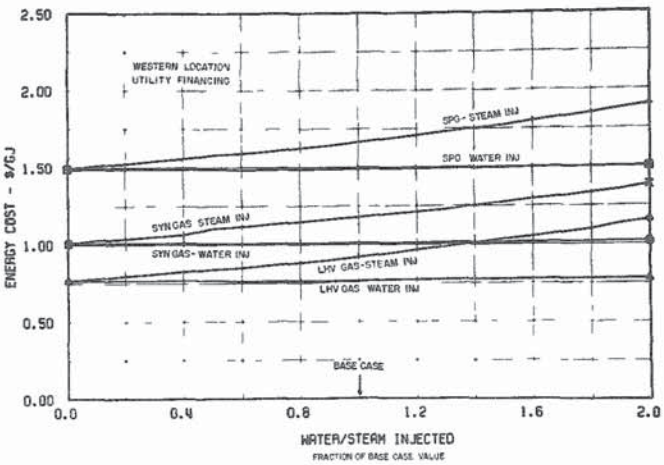


FIGURE 6 ENERGY COST VS AMOUNT OF WATER OR STEAM INJECTED

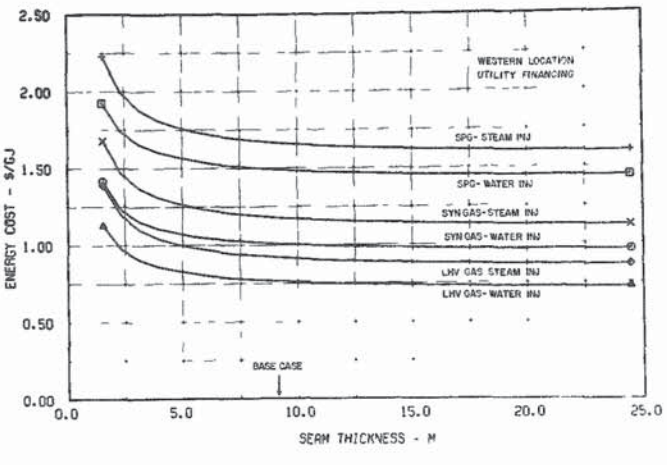


FIGURE 7 ENERGY COST VS SEAM THICKNESS

a diminishing influence. The effect of the seam depth is linear and not too great for the Western conditions. However, a greater influence is seen in the East where the injection pressure is a stronger function of depth.

Linking Procedure. For backward burn linking, the effects of the linking pressure and the oxygen requirement were investigated. The pressure was found to have an insignificant effect on the energy costs where the base case oxygen rate was injected or even with five times that amount. The effect of the amount of oxygen required was found to be quite small; a five-fold increase raises the energy costs by only about five percent. However, the influence would be greater for thinner coal seams.

Operational Parameters. The injection and production pressures, the flow rates and the well spacings are in reality tied together by some physical relationships which could be different for the two linking procedures. However, for the purpose of this study, these parameters are decoupled; i.e., each is varied while holding the remaining ones constant.

Lower product costs result from reduced injection pressures, as would be expected. However, where gas losses are not linked to the pressures, the effect of the injection pressure is not large. The effect of the production wellhead pressure (Figure 8) is more dramatic. At low production pressures, cost increases reflect both the increase in production compressor horsepower and in fuel-gas consumption. Although operations at very low injection pressures might seem desirable to reduce injection costs, it is much better to increase the reservoir pressure (barring large increases in gas losses) and avoid compressing larger volumes of production gas from low absolute pressures.

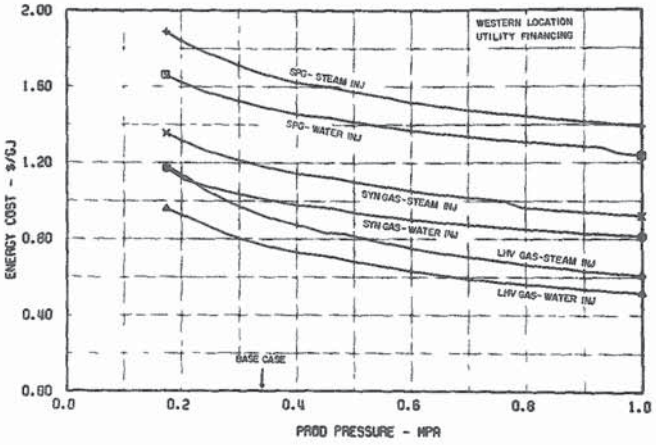


FIGURE 8 ENERGY COST VS PRODUCTION WELLHEAD PRESSURE

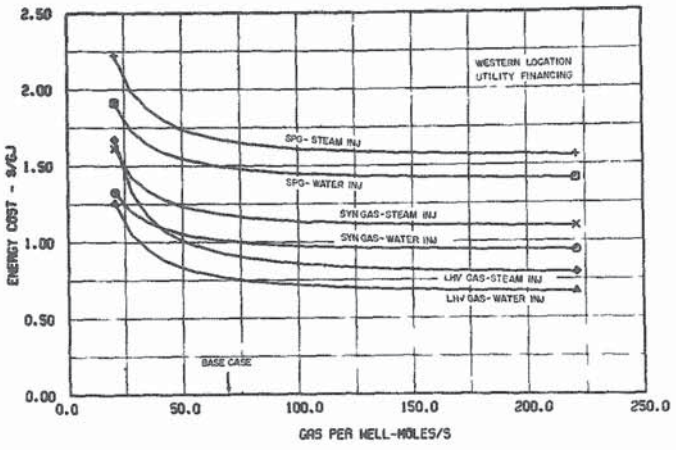


FIGURE 9 ENERGY COST VS PRODUCTION FLOW RATE PER WELL

The effects of varying the production flow rate (Figure 9) or the injection flow rate were investigated. The energy cost decreases rapidly with increasing production gas flow at low values and continues to decrease at diminishing rates at higher gas flow values. The effect of air injection rates on the results for the LHV gas option is quite severe because of the larger gas quantities that must be injected to achieve an equivalent amount of gasification.

Although the well spacing is likely to affect many of the other factors, its influence on the energy cost was investigated using constant values of the other parameters since the physical mechanisms are not known. The results show that no further costs savings will result from well spacings greater than about 1 ha (2.5 acres). In fact, some cost increases can occur, particularly for the air injection cases due to the additional piping and compression which is required as the facility is enlarged.

Process Effectiveness. Three parameters which gauge the effectiveness of the underground part of the process, the sweep efficiency, the oxygen utilization and the gasification product gas loss, were investigated. Reducing the sweep efficiency from the ideal situation of the base case to 90% increases the energy cost by only about 2%. The effects of injected gas losses and product gas losses are much more severe as shown on Table 7. A 10% loss of either gas results in cost increases of about 13% in the East and 6% in the West.

Plant Parameters. The energy costs as a function of the final pressure at which the gases are delivered are shown on Figure 10. A pressure of 6.9 MPa (1000 psi) is the only pressure

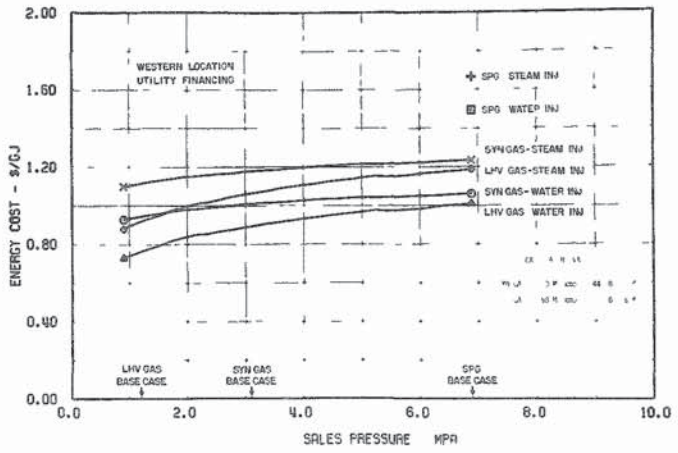


FIGURE 10 ENERGY COST VS SALES GAS DELIVERY PRESSURE

considered for SPG. The cost advantage enjoyed by the LHV gas over the SYN gas for the base case results is partially due to its lower sales pressure. The cost advantage diminishes if equal and increasing gas delivery pressures are specified. The effect is more severe for the Eastern LHV gas since its heating value is 20% lower than that of the Western LHV gas. Due to the higher heating values of the oxygen-produced SYN gas, the cost increase with pressure is much more gradual. The positions of the curves with respect to the SPG points suggests that some of the other gases could be transmitted over moderate distances at some cost benefit over SPG for the Western conditions.

Over a reasonable range of plant sizes, restricted only by limits on the cost estimating technique used for the SPG plants, the energy prices for oxygen generated gases are relatively unaffected by the underground gasification plant capacity. An increase in gas cost is noted for large air-blown plants, particularly in the Eastern cases. As the plant capacity becomes larger, the injection and gathering pipeline networks cover a larger land area, especially for the thinner Eastern seams. The cost for the air-blown plant is more sensitive since its pipeline network handles about five times as much gas for injection and twice as much gas for production because of nitrogen dilution.

A great effort has been made to accurately determine the capital requirements and operating expenses for each of the system components. However, the capital requirements of the gas processing plants were, perhaps, the most difficult to accurately predict. For this reason, the effect of variations in this capital cost was evaluated. The results indicated that a 10% change in the gas processing capital results in a change of the energy cost by 3% or less for all of the cases.

CONCLUSIONS

The costs of manufacturing SPG, SYN gas and LHV gas from a hypothetical, commercial underground coal gasification plant have been estimated based on certain assumptions for an Eastern and a Western location. The assumptions which were made and the base parameters which were specified must not be ignored when evaluating the results. Specifically, it should be remembered that some effects, such as subsidence and heat loss, and the physical relationships between these effects and the parameters and between the parameters themselves have not been considered. The following conclusions can be stated within the confines of these limitations:

(1) The capital requirements are less and the prices are lower for gas production based on subbituminous coals rather than bituminous coals. In addition, the effects of the parameters on the results are less important.

(2) SPG can be manufactured cheaper by underground coal gasification than by mining followed by gasification on the surface.

(3) SYN gas could be used locally for fuel or, perhaps, even at moderate distances from the plant with some cost benefits over SPG. Air-produced LHV gas has little if any cost advantages over oxygen-produced SYN gas. Although LHV gas cannot be economically converted to SPG, it can be used as a local source of fuel.

(4) The produced gas must be at some minimum pressure to be usable. It is economically advantageous to obtain a portion of this pressure at the production wellhead rather than in subsequent surface compression.

(5) The higher pressures required for pneumatic linking increase gasification costs due to higher capital costs and plant fuel consumption and penalties incurred by possible increased gas losses.

(6) Parameter studies show that there are two main types of parameters which most significantly affect the energy costs. These are the coal process parameters and the gas loss parameters. Thus, additional research should be directed toward these parameters.

(7) The price predictions based on the limited process data from the Hanna tests are greater than those based on Lurgi process data. The resulting cost predictions for gasification with air injection are particularly high.

ACKNOWLEDGEMENTS

The contributions of J. C. Fair and D. L. Bidlack in developing portions of the economic model are gratefully acknowledged. In addition, the helpful discussions with R. L. Arscott, the assistance of P. J. Kokales and the permission by GR&DC for publication are sincerely appreciated.

REFERENCES

1. P. Raimondi, P. L. Terwilliger and L. A. Wilson, Jr., "A Field Test of Underground Combustion of Coal", J. Pet. Tech., Jan., 1975.
2. Joint GR&DC/LLL Report, "The LLL In-Situ Coal Gasification Research Program in Perspective", TID-26825, June 10, 1975.
3. J. C. Fair, O. A. Larson and H. H. Hasiba, "An Evaluation of In-Situ Coal Gasification," Energy, Vol. 1, pp. 77-94, 1976.
4. D. L. Bidlack and R. L. Arscott, "Economics of Marketing Synthesis Gas Produced by Underground Coal Gasification", Presented at the Second Annual Underground Coal Gasification Symposium, Morgantown, August, 1976.
5. L. A. Schrider and J. W. Jennings, "An Underground Coal Gasification Experiment, Hanna, Wyoming", SPE Paper No. 4993, presented at the Annual Fall Meeting, Houston, October, 1974.
6. D. D. Fischer and L. A. Schrider, "Comparison of Results from Underground Coal Gasification and from a Stirred-Bed Producer", presented at the National AIChE Meeting, Houston, March, 1975.
7. C. F. Brandenburg, R. P. Reed, R. M. Boyd, D. A. Northrop and J. W. Jennings, "Interpretation of Chemical and Physical Measurements from an In Situ Coal Gasification Experiment" SPE Paper No. 5654, presented at Annual Fall Meeting, Dallas, Sept., 1975.
8. D. C. Elgin and H. R. Perks, "Results of Trials of American Coals in Lurgi Pressure-Gasification Plant at Westfield, Scotland", Proceedings of the Sixth Synthetic Pipeline Gas Symposium, Chicago, October, 1974.
9. "Trials of American Coals in a Lurgi Gasifier at Westfield, Scotland," R&D Report No. 105, Final Report to ERDA and AGA, NTIS FE-105, November, 1974.
10. R. J. Hull, "The Thermosludge Water Treating and Steam Generation Process", JPT, December, 1967.
11. D. H. McCrea and J. H. Field, "The Purification of Coal Derived Gases: Applicability and Economics of the Benfield Processes", Paper No. 296, American Institute of Chem. Engrs., 78th National Meeting, August, 1974.
12. "1973 Joint Association Survey of the U.S. Oil and Gas Producing Industry, Section I: Drilling Costs", API Statistical Publications, Washington, D.C., February, 1975.
13. K. M. Guthrie, Process Plant Estimating Evaluation and Control, Craftsman Book Company of America, Solana Beach, CA, 1974.
14. S. P. Marshall and J. L. Brandt, "1974 Installed Cost of Corrosion Resistant Piping", Chem. Engr., October 28, 1974.
15. J. C. Fair, GR&DC, Production Department, Private Communication, December, 1975.
16. "Pipeline Economics", Oil & Gas J., August 12, 1974.
17. J. M. Campbell, Gas Conditioning and Processing, Campbell Petroleum Series, Norman, OK, 1974.
18. D. L. Bidlack, GR&DC, Planning and Economics Division, Private Communications, March 31, 1975, July 7, 1975, April 20, 1976 and June 25, 1976.
19. G. H. Cady et al, "Subsurface Geology and Coal Resources of the Pennsylvania System in Certain Countiesof the Illinois Basin", Report of Investigations, No. 148, Illinois State Geological Survey, 1951.
20. G. H. Cady, "Coal Resources of Franklin County, Illinois", Circular No. 151, Illinois State Geological Survey, 1949.
21. J. A. Harrison, "Subsurface Geology and Coal Resources of the Pennsylvania System in White County, Illinois", Report of Investigations No. 53, Illinois State Geological Survey, 1951.
22. H. L. Berryhill, Jr., D. M. Brown, A. Brown and D. A. Taylor, "Coal Resources of Wyoming", Circular 81, U.S. Geological Survey, June, 1967.
23. P. F. H. Rudolph, "The Lurgi Process - The Route to S.N.G. From Coal" presented at the Fourth Synthetic Pipeline Gas Symposium, Chicago, October, 1972.

THE ECONOMICS OF UNDERGROUND COAL GASIFICATION

by

A. J. Moll, Stanford Research Institute, Menlo Park, California

ABSTRACT

Two economic criteria must be met for underground coal gasification to be competitive. First, the product gas must be produced and transported to users at an attractive price compared with competitive fuels. Second, the value assigned to the coal gasified must be equal or greater than any alternate use for that coal. The alternate value of the coal in place depends on the mining cost, percentage coal recovery, coal transportation costs, and value to potential users.

In this paper speculative economics are presented for some of the methods being pursued today in the United States. Financial and technical factors that are important to the required price for the gas are identified. The relative effects of investment, coal royalties, and other operating costs are compared. The effect of plant capacity on gas cost is found to be less than expected. The importance of requirements for air compression, well drilling, gas purification, and resource recovery efficiency are shown.

The likely role of underground gasification in the energy picture is discussed. An analogy is drawn with geothermal steam.

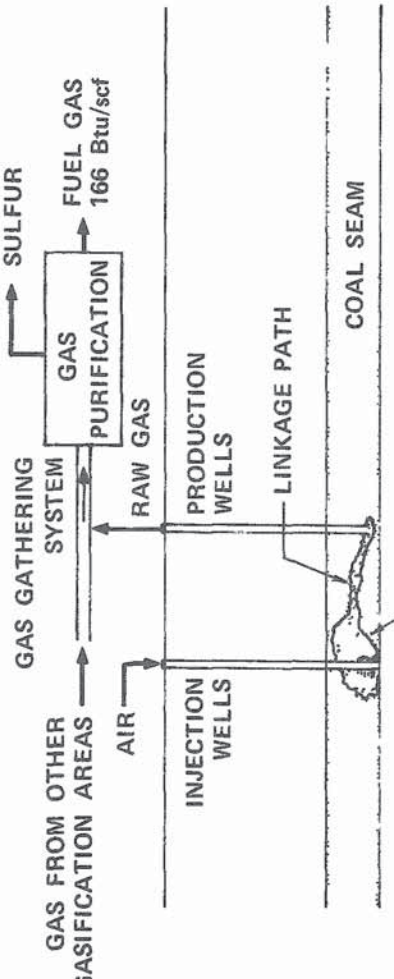
DISCUSSION

The commercialization of underground coal gasification (UCG) will depend on the answer to the question, "How much does it cost?" This paper represents a preliminary attempt to place a cost on UCG, as illustrated by the production of low-Btu gas from Wyoming coal. The costs presented in this paper are based on an application similar to that being tested by the Laramie Energy Research Center but is not meant to apply exclusively to this method.

A highly simplified diagram of a UCG facility is shown in Figure 1. Not shown are the intricacies of the gas gathering system and the fact that the raw gas may have to be quenched to avoid damaging the gas gathering pipeline. In the gas purification operation both particulates and sulfur must be removed. A cyclone or wet scrubbing technique is visualized for particulate removal. Sulfur removal is assumed to be accomplished by means of the Stretford process, an effective means of removing hydrogen sulfide from low sulfur gases.

Figure 1

LOW Btu GAS BY UNDERGROUND COAL GASIFICATION



The Wyoming subbituminous coal being gasified is assumed to lie in a seam 30 feet thick at a depth of 600 feet. This coal is assumed to have a heating value in place of 8500 Btu per pound and a sulfur content of 0.7 weight percent. Injection and production wells are assumed to be spaced 100 feet apart. The gas production rate per production well is taken to be 11 million standard cubic feet per day. The heating content of the gas is 166 Btu per standard cubic foot. These figures are typical of recent values achieved at the Hanna test site. The facility evaluated is one with a capacity equivalent to 500 megawatts of electricity generation at a heat rate of 10,000 Btu per kilowatt; therefore, 5 million Btu of product fuel gas are produced per hour. An operating factor of 90 percent is assumed.

The scale of such an operation is impressive. Over a plant life of 20 years, a total of over 20 thousand producing wells will be required. On the average, over three new wells will be required each day of operation. Over 400 miles of gas gathering pipelines will be required. In spite of this, the entire 20 year operation consumes less than 3,000 acres of coal land. The maximum distance of any well from a central point where gas purification operations can take place would be 3 miles. Naturally, the total acreage of coal land required increases inversely with the coal seam thickness.

A recovery rate of 50 percent is assumed based on production of raw gas and heating value of the coal in place. The requirements for fuel in gas purification and to raise steam for compressor turbine drives accounts for 20 percent of the raw gas; therefore, the overall recovery efficiency is 40 percent. This overall recovery efficiency at the present time must be regarded as hypothetical. Much data must be accumulated before this number can be firmed up.

Low-Btu gas is expensive to transport; therefore, this evaluation assumes the presence of an on-site power plant. The costs of this power plant are not included. The product from the UCG facility being evaluated here is clean low-Btu gas delivered over the fence to a power plant.

This economic evaluation is based on regulated utility debt/equity financing. A four year construction period is assumed with a 20 year plant life. The capital is raised by 65 percent debt and by 35 percent equity of the operating company. The interest on the debt is assumed to be 10 percent, and the return on equity is assumed to be 15 percent, in line with regulatory practice. An allowance of 52 percent income tax is included. This may be considered to be 48 percent federal income tax and 4 percent state income tax. Depreciation is calculated by the straight line method. Fixed costs, including 2 percent for general and allocated expenses and 2.5 percent for property taxes and insurance, are assumed. Dollar costs are in constant 1976 dollars.

Investments for a 500 megawatt facility are listed in Table I. These investments are based on the previously described facility. It should be noted that most of the required equipment is standard design--pipelines, compressors, gas purification systems. The problem in making the investment estimate is how much of the standard equipment will be required. If the UCG method used does not work as efficiently as assumed here, naturally the amount of these facilities will increase. However, the investments shown here are regarded as reasonable based on the progress of the Hanna tests. The total capital investment of $126 million compares very favorably with estimates for other advanced low-Btu gasification systems.

Table II shows a listing of operating costs and components of required gas selling price. Two items in particular are noteworthy on this table. These are the drilling expense and the gathering system modifications. For this evaluation these items have been expensed rather than capitalized. These two items would add over $300 million to the investment if they were capitalized. Much of this investment would be deferred for over 10 years.

The main item not needed in these operating costs is that for mined coal. A charge of 5 cents per million Btu is included based on a liberal coal royalty of 70 cents per ton--in this case, assumed to be per ton gasified. The total required price for the gas produced is estimated to be $1.22 per

Table I

LOW-BTU GAS BY UNDERGROUND GASIFICATION
ESTIMATED CAPITAL INVESTMENT

(Gas Production Rate: 5 Billion Btu/Hr, 166 Btu/Scf)

	Millions of Dollars
PLANT SECTION INVESTMENT	
AIR INJECTION COMPRESSION	$ 24
GAS PURIFICATION	26
GAS GATHERING PIPELINE SYSTEM	10
UTILITIES	15
GENERAL FACILITIES	25
TOTAL PLANT FACILITIES	$100
LAND	1
INTEREST DURING CONSTRUCTION	16
START-UP COSTS	6
WORKING CAPITAL	5
TOTAL CAPITAL INVESTMENT	$128
DEPRECIABLE INVESTMENT	$122
DEBT CAPITAL	83
EQUITY CAPITAL	45

Table II

ESTIMATED OPERATING COST AND REQUIRED SELLING PRICE

(Gas Production Rate: 5 Billion Btu/Hr, 150 Btu/Scf)

	Dollars per Million Btu in Product Gas
COAL ROYALTY AT $0.70/T GASIFIED	$0.05
MAINTENANCE MATERIALS	0.05
OTHER MATERIALS	0.02
DRILLING EXPENSE	0.34
GATHERING SYSTEM MODIFICATION	0.08
LABOR RELATED COSTS	0.13
FIXED COSTS	0.11
PLANT DEPRECIATION, 20-YEAR	0.15
TOTAL OPERATING COSTS	0.93
RETURN ON RATE BASE AND INCOME TAX	0.29
REQUIRED PRICE, UTILITY CALCULATION	1.22
REQUIRED PRICE, 15% DCF CALCULATION	1.37

million Btu based on utility type financing. A required price of $1.37 is estimated by a discounted-cash-flow calculation based on 15 percent return on equity, also assumed to be 35 percent of the total investment.

Tables III and IV show capital investments and operating costs for a 50 megawatt equivalent facility. The total required price per million Btu is a little more than 50 percent higher than for the 500 megawatt facility. This increase is regarded as relatively modest compared to similar situations involving other methods of synthetic fuel production. One concludes that economies of scale are somewhat less important for UCG than, for example, synthetic natural gas (SNG) production in surface facilities. Figure 2 shows the effect of capacity on required gas price.

Also shown on Figure 2 is the effect of a 50 percent overrun in investment. The effect of investment on required gas price is linear. Even the 50 percent overrun curve yields attractive gas prices. However, at the present stage of development one cannot be assured that investments of several times that estimated here might not be required. Conversely, new developments may actually yield a lower investment as we proceed along the learning curve.

The effect of resource recovery is shown in Figure 3. It is seen that reducing the overall resource recovery to 20 percent from 40 percent increases the required price to $1.79 from $1.22. The variation of resource recovery shown on Figure 3 only considers changes in percentage of the coal gasified. Changes in the gasification process are not considered, for example, which increase the amount of air injected per unit of gas produced.

Numerous other sensitivity analyses are possible which are not shown here. The most important variables include debt/equity ratio, interest rate, project lifetime, construction schedule, load factor, resource recovery, well spacing, coal seam thickness.

This economic analysis, though incomplete, shows the economic promise of UCG. The utilization of the product fuel gas is a potentially limiting factor on commercialization of UCG. It appears likely that for the foreseeable future fuel gas made by UCG will be used to fuel power plants and perhaps to supply local industrial fuel needs. More widespread usage would depend on the development of UCG methods for producing SNG.

If low-Btu fuel gas is the product of UCG, it would be expected that a slow, orderly development would be followed beginning with small facilities. An appropriate analogy is that of geothermal steam. Geothermal steam also depends on a great deal of well drilling costs and the logistics of utilizing the product.

Much data must yet be accumulated before a definitive engineering estimate of UCG is possible. However, it is shown that the economics of underground coal gasification are potentially attractive. It is clearly time to begin to put dollar signs on underground coal gasification and to evaluate development programs accordingly.

Table III

ESTIMATED CAPITAL INVESTMENT

(Gas Production Rate: 500 Million Btu/Hr, 166 Btu/Scf)

	Millions of Dollars
PLANT SECTION INVESTMENT	
AIR INJECTION COMPRESSION	3
GAS PURIFICATION	4
GAS GATHERING PIPELINE SYSTEM	1
UTILITIES	2
GENERAL FACILITIES	10
TOTAL FACILITIES	20
LAND	neg
INTEREST DURING CONSTRUCTION	1
START-UP COSTS	2
WORKING CAPITAL	2
TOTAL CAPITAL INVESTMENT	25
DEPRECIABLE INVESTMENT	23
DEBT CAPITAL	16
EQUITY CAPITAL	9

Table IV

ESTIMATED OPERATING COST AND REQUIRED SELLING PRICE

(Gas Production Rate: 500 Million Btu/Hr, 166 Btu/Scf)

	Dollars per Million Btu in Product Gas
COAL ROYALTY AT $0.70/T GASIFIED	$0.05
MAINTENANCE MATERIALS	0.10
OTHER MATERIALS	0.02
DRILLING EXPENSE	0.34
GATHERING SYSTEM MODIFICATION	0.05
LABOR RELATED COSTS	0.25
FIXED COSTS	0.22
PLANT DEPRECIATION, 20-YEAR	0.30
TOTAL OPERATING COSTS	1.33
RETURN ON RATE BASE AND INCOME TAX	0.56
REQUIRED PRICE, UTILITY CALCULATION	1.89
REQUIRED PRICE, DCF CALCULATION	1.98

Figure 2

REQUIRED PRICE FOR FUEL GAS BY UNDERGROUND GASIFICATION OF WYOMING SUBBITUMINOUS COAL

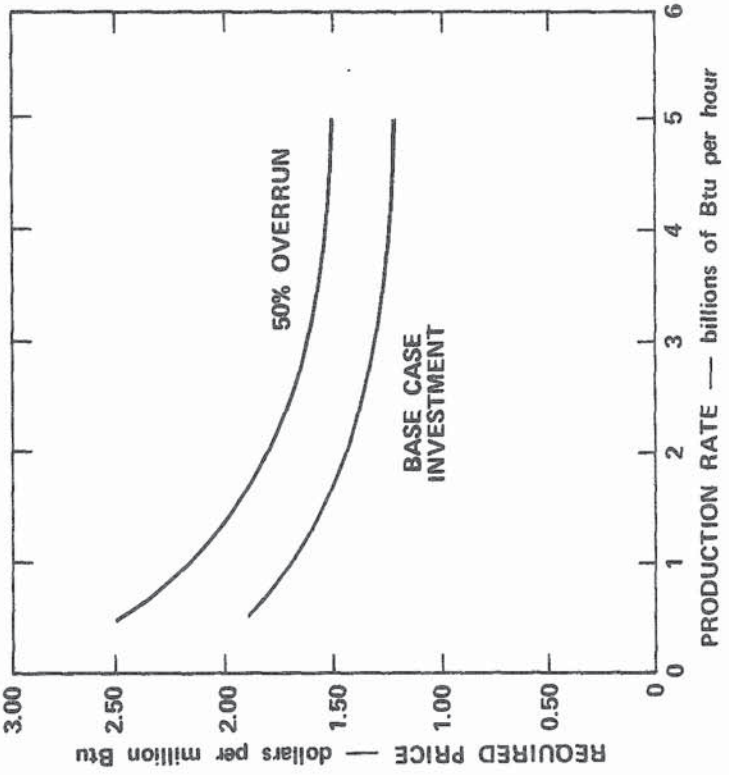
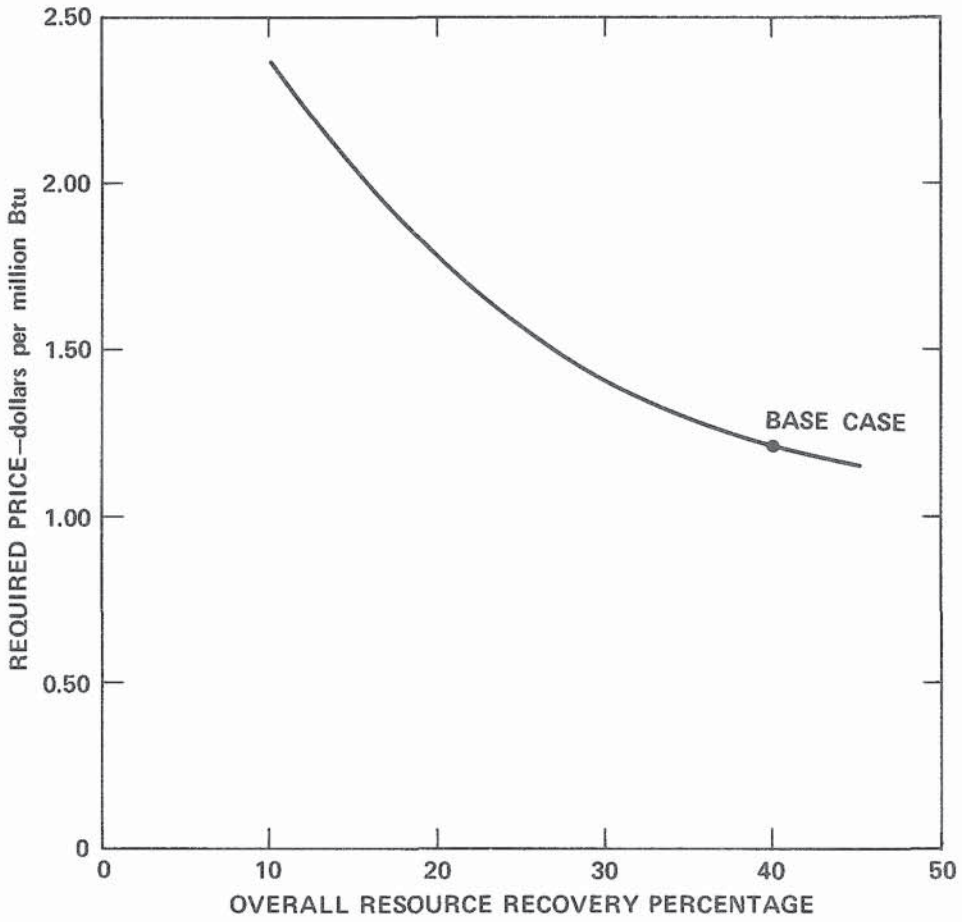


Figure 3
EFFECT OF RESOURCE RECOVERY



Economics of Manufacturing Synthesis Gas Produced by Underground Coal Gasification

BY

D. L. Bidlack and R. L. Arscott

Gulf Research & Development Company
Pittsburgh, Pennsylvania USA

ABSTRACT

The major options for utilizing the products from underground coal gasification are very dependent on whether air or oxygen is used as the gasifying agent. If air is used, the low heating value gas produced is suitable only for local generation of electricity or use as a fuel in the vicinity of the gasifier. If oxygen is used, the medium heating value gas can be utilized for the manufacture of methane, as a chemical feedstock for such products as methanol or ammonia or as a fuel. This paper concentrates on the economics of marketing synthesis gas for the manufacture of methane, methanol and ammonia. The current and projected markets are examined together with the production and transportation costs. Currently the petrochemical industry utilizes 7.2% of the total U.S. natural gas production and the demand is expected to grow especially if methanol finds wide acceptance as a fuel. When this increased demand is coupled with the decreased supply of natural gas, the potential for synthesis gas derived from coal gasification becomes substantial.

The manufacture of methanol and ammonia is currently concentrated in the Gulf Coast area because of the accessibility of natural gas. Because of this situation, one of the options which has been studied is to manufacture a gas for synthesizing methanol at an underground coal gasification facility located in the Wyoming-Montana area and either pipeline the gas to existing synthesis plants on the Gulf Coast or feed the gas to newly built plants near the gasification facility. Both the gasification facility and the pipeline would be large enough to supply several synthesis plants. If the methanol synthesis gas is pipelined to the Gulf Coast, the price of methanol is $178/t ($161/ST) which is $49/t ($44/ST) higher than methanol made from natural gas priced at $1.25/kmol ($1.50/10^3 SCF). The situation changes, however, when the synthesis gas is used in Wyoming or Montana; the price of methanol would be reduced to $97/t ($83/ST). Manufacturing ammonia from underground coal gasification derived synthesis gas shows similar economics. These economics assume utility-type financing for the synthesis gas production facilities. This makes the methanol made from synthesis gas produced by underground coal gasification competitive with that made from natural gas at its current price, but would require the construction of a whole new synthesis industry near the coal deposits. Building the synthesis plants requires less capital, however, than building the pipeline.

The capital requirement for underground production of methanol synthesis gas is only 65% of that required if the synthesis gas is made via Lurgi gasifiers in an aboveground facility. Methanol made from the underground produced gas costs $63/t ($57/ST) less than methanol synthesized from gas made in the aboveground plant. Similarly, the capital requirement for manufacturing substitute natural gas (SNG) via underground coal gasification is 76% of the capital requirement for an

aboveground facility. The price of the SNG is \$1.66/GJ (\$1.76/10^6 Btu) if the gas is produced by underground coal gasification which is 71¢/GJ (75¢/10^6 Btu) less than that produced in an aboveground plant.

INTRODUCTION

The growing shortage of natural gas and the abundance of coal in the U.S. will lead inevitably to the utilization of coal to produce substitutes for natural gas as a fuel and a chemical feedstock. Gasification of mined coal has been demonstrated, but serious constraints are evident because of the capital intensive natural of the processes, the environmental, labor and health problems involved with mining coal and the cost and logistics of transporting and handling solid fuel. Underground coal gasification is being developed at a slow pace, but holds tremendous potential to reduce the above mentioned problems associated with mining and processing coal.

The major options for utilizing the products from underground coal gasification are very dependent on whether air or oxygen is used as the gasifying agent. If air is used, the low heating value gas produced is suitable only for local generation of electricity or use as a fuel in the vicinity of the gasifier. If oxygen is used, the options are much greater. For example, the produced gas can be utilized as a synthesis gas for the manufacture of methane, methanol, ammonia and other chemicals, as a synthesis gas for the catalytic production of high grade liquid fuels, or utilized directly as a medium heating value gaseous fuel.

This paper concentrates on the economics of manufacturing synthesis gas by underground gasification of coal and the utilization of the produced gas to make methane, methanol and ammonia. It is assumed that synthesis gas would be produced by underground coal gasification at coal deposits in, say, Wyoming or Montana; upgraded to the composition required for synthesis in an aboveground facility; and then either pipelined to existing chemical synthesis plants in Texas and Louisiana or used at newly constructed synthesis plants located near the production facility in Wyoming or Montana. The synthesis gas production facility would be large enough to supply several synthesis plants.

BACKGROUND TO THE AMMONIA AND METHANOL INDUSTRY

Historically, chemicals derived from synthesis gas, such as ammonia, methanol, Oxo compounds, etc., have relied on steam reforming natural gas to generate the synthesis gas. However, shortages of natural gas have presented problems for manufacturers of these chemicals in recent years. For example, curtailments in natural gas caused a reduction in ammonia production of 117 000 t (128 000 ST) in 1972, 285 000 t (315 000 ST) in 1973, and 350 000 t (380 000 ST; more than 2% of capacity in 1974) [1]. Methanol production has also been reduced because of natural gas curtailments. Currently, no interstate natural gas is available for new plant facilities. Manufacturers are therefore looking for alternative feedstocks.

The petrochemical industry in the United States consumed about 580×10^{15} J (550×10^{12} Btu) of natural gas as feedstock and 1090×10^{15} J (1030×10^{12} Btu) as fuel in 1974 [2]. This amounts to 7.2% of the total U.S. natural gas production. Much of the natural gas feedstock is steam reformed to make synthesis gas for synthesizing ammonia. In 1973, 364×10^{15} J (345×10^{12} Btu) [1] of natural gas were used for ammonia feedstock or about 1.5% of the total U.S. production of natural gas. Another 262×10^{15} J (248×10^{12} Btu) of natural gas were used as fuel for ammonia plants. Overall, the ammonia industry consumed about 2.6% of the natural gas in 1973

Methanol also consumes a large amount of synthesis gas derived from natural gas - about 97×10^{15} J (92×10^{12} Btu) or 0.4% of the total natural gas production for 1973. Methanol production also consumed 36×10^{15} J (34×10^{12} Btu) of fuel in 1973 and presumably this was also mostly natural gas. Thus, feedstock alone for ammonia and methanol production accounts for almost 2% of the total natural gas production for 1973.

References at end of paper

Overall, the manufacture of ammonia and methanol consumed about 3% of the natural gas production in 1973. Although this is relatively small, natural gas supplies are declining rapidly so that, unless alternatives are found for natural gas reforming to make the synthesis gas, the proportion of the natural gas used to make ammonia and methanol would have to increase just to satisfy present demands.

Tables I and II show the location of the United States ammonia and methanol capacity in 1974. Ninety-six percent of the methanol capacity is located near the source of natural gas in Texas and Louisiana. Only 38% of the ammonia capacity is located in Texas and Louisiana while the rest is distributed near the main agricultural areas of the country where ammonia derivatives are used as fertilizer.

TABLE I

DISTRIBUTION OF METHANOL MANUFACTURING CAPACITY FOR THE UNITED STATES IN 1974

STATE	CAPACITY, 10^6 t/a	PER CENT
TEXAS	2 4	63 8
LOUISIANA	1 2	32 3
FLORIDA	0 2	3 9
TOTAL	3 8	100 0

TABLE II

DISTRIBUTION OF AMMONIA MANUFACTURING CAPACITY FOR THE UNITED STATES IN 1974

REGION	CAPACITY 10^6 t/a	PER CENT
TEXAS/LOUISIANA	5 8	38 4
SOUTHEAST (FL, GA, NC, TN, AL MS, AR)	2 7	17 9
CORN BELT (IA, MO, IN, OH)	2 0	13 2
PLAINS STATES (NE, KS, OK)	2 0	12 9
WEST (CA, AZ, ID, WY, WA, OR, UT)	1 6	10 4
EAST (VA, PA, WV, NY)	1 1	7 2
TOTAL	15 2	100 0

FIGURE 1

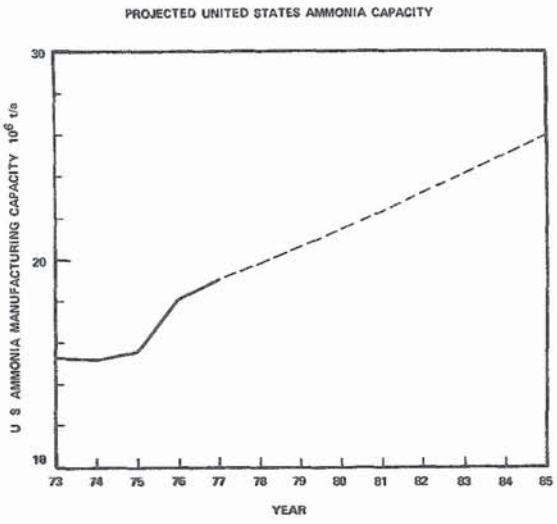


Figure 1 projects the capacity for ammonia production in the U.S. to 1985. The capacity increases for 1975, 1976 and 1977 are based on announced construction [3]; for subsequent years they are based on an expected average capacity increase of 4% per year [4].

Methanol capacity cannot be so easily projected since there is much speculation that methanol usage will not be confined to chemicals in the future. One optimistic group speculates that worldwide methanol production will be increased in 1980 by ten-fold over 1970 production and will have such diverse uses as substitute natural gas (SNG) feedstock, gas turbine fuel, gasoline substitute or additives, boiler fuel, and source of protein [5]. Most of these speculations are based on manufacturing methanol in large capacity plants from low cost natural gas in the Middle East and, therefore, do not apply directly to a study based on coal gasification. One interesting related concept would be the use of methanol as a slurry medium for transporting coal [5]. This proposal would transport 9×10^6 t/a of coal from Wyoming to Oregon, a distance of 1280 km (800 mi). With a 50% slurry, this would require manufacturing 9×10^6 t/a of methanol which is over twice the 1974 capacity (see Table I).

PRICE OF NATURAL GAS AND SUBSTITUTE NATURAL GAS

For the first six months of 1975, new contracts for intrastate natural gas reportedly averaged \$1.42/kmol (\$1.70/10^3 SCF) on the Texas Gulf Coast and \$1.10/kmol (\$1.31/10^3 SCF) in southern Louisiana [6]. This is an overall average of about \$1.25/kmol (\$1.50/10^3 SCF). The current price is somewhat higher and intrastate sales have been reported in the region of \$1.68/kmol (\$2.00/10^3 SCF). The FPC have recently announced a decision to raise the ceiling of new interstate natural gas to \$1.2/kmol (\$1.42/10^3 SCF).

The price of coal-derived substitute natural gas is calculated on Table III for both underground coal gasification and for aboveground gasification in Lurgi gasifiers. Both cases assume a Western subbituminous coal and the volume of gas produced is about half that proposed in the El Paso and WESCO projects [7, 8]. The manufacture of SNG via Lurgi coal gasification is well known and will not be repeated here. The major assumptions for the calculation of the underground gasification costs are a gas product yield and composition similar to the Lurgi process, no loss of injected or produced gas from the underground reactor and no significant problems due to subsidence or poor control of the underground process. Obviously these assumptions have yet to be demonstrated on a commercial basis. Departures from the above specifications and details of the process are discussed by Garon [9].

As shown in Table III, the capital requirement for the underground coal gasification case including the field production equipment is \$394 x 10^6 which is 76% of the capital required for the aboveground case. Assuming utility-type financing with 13% capital charges, the 25-year average price of the SNG in the underground case is \$1.66/GJ (\$1.75/10^6 Btu) or \$1.38/kmol (\$1.65/10^3 SCF). For aboveground gasification, the price of SNG is \$2.37/GJ (\$2.50/10^6 Btu) or \$1.97/kmol (\$2.36/10^3 SCF). Capital charges at 13% assumes a 75/25 debt/equity ratio, 15% return on equity, 8.5% interest rate, 48% federal income taxes, and 4% depreciation. A 10% contingency is included in the capital cost.

It is interesting to note that in the WESCO application for the FPC rehearing dated May, 1975, a price of \$2.1/kmol (\$2.50/10^3 SCF) was proposed.

TABLE III

ECONOMICS OF MANUFACTURING SNG
152 TJ/d (144 X 10^9 Btu/d)
WYOMING–MONTANA LOCATION

METHOD OF GAS PRODUCTION	UNDERGROUND	ABOVEGROUND
UPGRADING PLANT	ABOVEGROUND	ABOVEGROUND
CAPITAL REQUIREMENT, 10^6		
FIELD PRODUCTION EQUIPMENT	79	–
UPGRADING PLANT	243	417
INTEREST DURING CONSTRUCTION, START–UP, ETC	66	94
WORKING CAPITAL	6	8
TOTAL CAPITAL REQUIREMENT	394	519
SNG PRICE, ¢/GJ		
FIELD OPERATION EXPENSE	23 2	–
UPGRADING PLANT OPERATING EXPENSE	54 8	89 5
COST OF COAL AT \$3 858/t (\$3 50/ST)	–	42 2
BY–PRODUCT CREDITS	– 14 7	30 2
PRICE OF SNG, UTILITY–TYPE FINANCING WITH 13% CAPITAL CHARGES	166 0	236 8

TABLE IV
GAS COMPOSITIONS

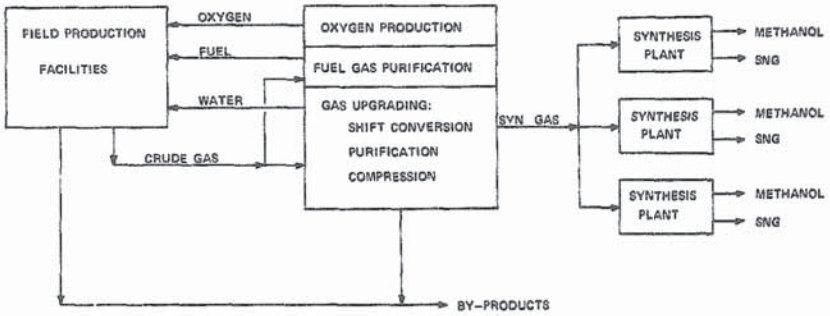
COMPOSITION, DRY, VOL %	CRUDE GAS	METHANOL SYNTHESIS GAS	AMMONIA SYNTHESIS GAS	BY–PRODUCT SNG (TYPICAL)
H_2	38 5	69 1	73 5	2 6
N_2	0 3	0 4	24 5	1 8
CO	19 4	17 6	– –	0 1
CO_2	29 4	6 3	– –	0 3
H_2S	0 3	– –	– –	– –
CH_4	11 1	14 9	2 0	95 1
C_nH_m	1 0	0 7	– –	– –
TOTAL	100 0	100 0	100 0	100 0

THE MANUFACTURE OF METHANOL AND AMMONIA

In each of the cases presented in this report, the coal gasification facilities are about half the size of one of the large substitute natural gas manufacturing plants such as envisioned by El Paso and WESCO [7, 8]. The crude gas produced by coal gasification is upgraded in an aboveground plant to the composition required for synthesis. The gasification and upgrading facilities would be located in Wyoming or Montana; however, as shown in Tables I and II, much of the usage for the synthesis gas is on the Gulf Coast. The synthesis gas industry would, therefore, have the option of building new synthesis plants near coal deposits in the Wyoming/Montana area or building a pipeline to the existing plants in Texas and Louisiana. In the cases involving the pipeline, it was assumed that one large diameter pipeline would be used to transport the production of more than one synthesis gas facilities. The capacity of the ammonia and methanol synthesis plants is assumed to be 907 t/d (1000 ST/SD) of product.

FIGURE 2

MANUFACTURE OF METHANOL SYNTHESIS GAS



The case involving methanol from synthesis gas made by underground coal gasification is shown in Figure 2. Production of crude gas by underground coal gasification is described elsewhere and will not be repeated here [9]. Briefly, field production consists of injecting oxygen and water into the gasification zone to produce a crude gas rich in hydrogen and carbon monoxide as well as CH_4, CO_2 and H_2S (see Table IV). After cooling, which condenses liquid hydrocarbons and water, the gas is piped to the upgrading plant. At the upgrading plant, the gas is compressed to about 2900 kPa (400 psig); shifted according to the shift reaction,

$$CO + H_2O \longrightarrow H_2 + CO_2, \quad (1)$$

to adjust the H_2/CO ratio to about 3.4; purified to remove H_2S and CO_2; and, finally, compressed to pipeline pressure.

At the methanol synthesis plant, the synthesis gas is compressed to about 10,000 kPa (1500 psig) and reacted over a catalyst according to the following reaction:

$$CO + 2H_2 \longrightarrow CH_3OH. \quad (2)$$

The reactor effluent is cooled to condense the methanol and unreacted gases are recycled to the reactor (synthesis loop). The synthesis gas contains the CH_4 from gasification as well as other non-reacting components; these are removed from the synthesis loop by means of a purge stream. The purge stream, rich in CH_4 and unreacted CO and H_2, is methanized to convert the CO and H_2 to more CH_4 according to the reaction,

$$CO + 3H_2 \longrightarrow CH_4 + H_2O, \quad (3)$$

and sold as substitute natural gas (SNG).

Each synthesis gas production facility is sized for producing 416×10^6 mol/d (348×10^6 SCF/SD) of synthesis gas; the pipeline is sized for 850×10^6 mol/d; and each synthesis plant is sized to produce 907 t/d (1000 ST/SD) of methanol which requires 170×10^6 mol/d. Thus, each pipeline would supply about five synthesis plants and two production facilities of the size assumed for this study would be required to supply the pipeline to capacity. In addition to the 907 t/d of methanol, each synthesis plant manufactures 33.7×10^6 mol/d (28×10^6 SCF/D) of SNG.

Ammonia synthesis takes place in a synthesis loop similar to methanol synthesis according to the reaction,

$$3H_2 + N_2 \longrightarrow 2NH_3. \quad (4)$$

However, the composition of the synthesis gas is considerably different than the methanol synthesis gas as shown on Table IV and thus requires additional steps in the gas upgrading plant. First of all, the gas is shifted according to the shift reaction (1), to utilize essentially all of the CO to produce H_2; secondly, because ammonia is fairly difficult to separate from the methane in the synthesis loop, methane is cryogenically separated from the synthesis gas at the upgrading plant and sold as by-product SNG; thirdly, nitrogen from the air separation (oxygen) plant is added to the synthesis gas; and, finally, traces of CO and CO_2 poison the synthesis catalyst so that these components are removed by methanation.

Auxiliary heat requirements for the field and upgrading facilities are supplied by utilizing about 26% of the crude gas production after purification to remove H_2S. Water for gasification is provided by utilizing the water condensed from the crude gas plus the blowdown from the cooling water system, boilers, etc. The gasification water containing phenols, NH_3, etc. is used without treatment.

In order to compare the cost of manufacturing methanol and ammonia via underground coal gasification with the cost via surface gasification, a Lurgi surface coal gasification process was considered as a producer of synthesis gas. Run-of-mine subbituminous coal is received at coal preparation facilities where it is crushed and sized to minus 50 mm to 9.5 mm (2 in x 3/8 in), minus 9.5 mm to 1.5 mm (1/16 in), and less than 1.5 mm (fines). The larger sizes of coal are fed to the Lurgi gasifiers for gasification with steam and oxygen. The crude gas is cooled to condense water and liquid hydrocarbons in a tar separator unit and then upgraded to the required synthesis gas composition in the same way as the underground coal gasification cases. Auxiliary heat requirements are supplied by burning some of the fines; the remaining fines are sold as a by-product. The water condensed from the crude gas is treated in a Phenosolvan plant to recover phenols and ammonia, combined with other wastewater streams, treated to remove the last traces of any contaminants, and recycled to the plant utilities.

ECONOMICS

The economics for manufacturing methanol synthesis gas are shown on Table V. As shown, the capital requirement is $\$332 \times 10^6$ for the underground case which includes the investments for field equipment and the upgrading (aboveground) facilities, interest during construction, start-up expenses, etc., and working capital. Similarly the capital requirement for the aboveground plant is $\$511 \times 10^6$. The price of the synthesis gas is calculated on a utility-type basis as described previously for the SNG cases and on an equity basis, assuming 20% return on capital before taxes and 4% depreciation. With underground gasification, the price of the synthesis gas is 49¢/kmol (58¢/10^3 SCF) with utility-type financing and 73¢/kmol (87¢/10^3 SCF) with equity financing. With aboveground gasification, the synthesis gas is priced at 81¢/kmol (97¢/10^3 SCF) with utility-type financing and \$1.22/kmol (\$1.46/10^3 SCF) with equity financing.

Table VI shows the price of the synthesis gas for the four cases when the cost of pipelining to the Gulf Coast is added. The distance from Wyoming and Montana to the Gulf Coast is approximately 2250 km (1400 miles). To transport the capacity of two synthesis gas production facilities requires a 90 cm (36 in) pipeline with an investment of about $\$400 \times 10^6$. The transportation expense is 41.8¢/kmol (50¢/10^3 SCF).

TABLE V

ECONOMICS OF MANUFACTURING METHANOL SYNTHESIS GAS

416 X 10^6 mol/d (348 X 10^6 SCF/SD)
WYOMING–MONTANA LOCATION

METHOD OF GAS PRODUCTION	UNDERGROUND	ABOVEGROUND
UPGRADING PLANT	ABOVEGROUND	ABOVEGROUND
CAPITAL REQUIREMENTS, $10^6		
FIELD PRODUCTION EQUIPMENT	66	–
UPGRADING PLANT	205	411
INTEREST DURING CONSTRUCTION, START-UP, ETC	56	93
WORKING CAPITAL	5	7
TOTAL CAPITAL REQUIREMENT	332	511
SYNTHESIS GAS PRICE, ¢/k mol		
FIELD OPERATION EXPENSE	7 4	–
UPGRADING PLANT OPERATING EXPENSE	15 7	29 9
COST OF COAL AT \$3 858/ t (\$3 50/ST)	–	14 0
BY-PRODUCT CREDITS	– 6 0	– 11 3
PRICE OF SYNTHESIS GAS, UTILITY-TYPE FINANCING WITH 13% CAPITAL CHARGES	48 7	81 2
PRICE OF SYNTHESIS GAS EQUITY FINANCING WITH 20% RETURN ON CAPITAL AND 4% DEPRECIATION	73 0	122 1

The total capital requirement for a 907 t/d (1000 ST/SD) synthesis plant is \$50 x 10^6 which includes the investments for process, utilities, and off-sites, interest during construction, start-up expenses, etc. and working capital. Figure 3 shows the price of methanol (calculated on an equity basis) plotted against the price of the SNG by-product for the case with the synthesis gas pipelined to the Gulf Coast and the synthesis gas production financed with utility-type financing. Also plotted on Figure 3 is the price of methanol manufactured via steam reforming natural gas. Figure 3 shows that neither case where the methanol is made from coal-derived synthesis gas is competitive with methanol made via steam reforming natural gas. With natural gas priced at the nominal price of \$1.25/kmol (\$1.50/10^3 SCF) , methanol would be priced at \$129 /t while in the underground gasification case, with SNG priced at \$1.25/kmol, the methanol is priced at \$178/t, a difference of \$49/t (\$44/ST). Natural gas would have to be priced at \$1.82/kmol (\$2.17/10^3 SCF) before the underground case becomes competitive. With the synthesis gas production calculated on an equity financing basis, as shown on Figure 4, the methanol made from coal-derived synthesis gas becomes even less competitive.

The situation changes when the synthesis plants are located near the synthesis gas production facilities. As shown on Figure 5, assuming utility-type financing and SNG at \$1.25/kmol, methanol made from underground coal gasification-derived synthesis gas is priced at \$97/t (\$88/ST) which is \$32/t less than the price of methanol made by steam reforming natural gas.

As mentioned earlier, SNG made by underground coal gasification would be priced at \$1.38/kmol (\$1.65/10^3 SCF). Methanol made from steam reforming SNG at \$1.38/kmol is priced at \$135/t which is \$42/ t (\$38/ST) more than the price of methanol synthesized from gas made via underground coal

TABLE VI

PIPELINING COST TO TRANSPORT METHANOL SYNTHESIS GAS FROM WYOMING-MONTANA PRODUCTION SITE TO GULF COAST

LENGTH OF PIPELINE	2250 km (1400 mi)
PIPELINE DIAMETER	90 cm (36 inch)
CAPACITY	600 X 10^6 mol/d (670 X 10^6 SCF d)
PIPELINE COST	41 8 ¢ k mol (50 ¢ 10^3 SCF)
PIPELINE INVESTMENT	\$400 X 10^6

METHOD OF GAS PRODUCTION	FINANCING METHOD FOR SYNTHESIS GAS PRODUCTION	SYNTHESIS GAS PRICE AT PRODUCTION SITE ¢ k mol	SYNTHESIS GAS PRICE DELIVERED TO GULF COAST ¢ k mol
UNDERGROUND	EQUITY	73 0	114 8
UNDERGROUND	UTILITY	48 7	90 5
ABOVEGROUND	EQUITY	122 1	163 9
ABOVEGROUND	UTILITY	81 2	123 0

TABLE VII

ECONOMICS OF MANUFACTURING AMMONIA SYNTHESIS GAS METHANE REMOVED FROM GAS CRYOGENICALLY AND SOLD AS SNG

377 X 10^6 mol / d of $H_2 + N_2$

65 X 10^6 mol /d of SNG

METHOD OF GAS PRODUCTION	UNDERGROUND	UNDERGROUND
UPGRADING PLANT	ABOVEGROUND	ABOVEGROUND
CAPITAL REQUIREMENTS \$$10^6$		
FIELD PRODUCTION EQUIPMENT	68	–
UPGRADING PLANT	217	419
INTEREST DURING CONSTRUCTION START-UP ETC	59	94
WORKING CAPITAL	5	7
TOTAL CAPITAL REQUIREMENT	347	520
SYNTHESIS GAS PRICE ¢/k mol of H_2+N_2		
FIELD OPERATION EXPENSE	8 1	–
UPGRADING PLANT OPERATING EXPENSE	19 1	34 4
COST OF COAL AT \$3 858 / t (\$3 50/ST)	–	14 7
BY-PRODUCT CREDITS (EXCL SNG)	-6 6	-11 4
CREDIT FOR SNG	- 21 7	21 7
PRICE OF SYNTHESIS GAS UTILITY-TYPE FINANCING WITH 13% CAPITAL CHARGES	35 2	70 6
PRICE OF SYNTHESIS GAS EQUITY FINANCING WITH 20% RETURN ON CAPITAL AND 4% DEPRECIATION	63 3	116 6

FIGURE 3

PRICE OF METHANOL SYNTHESIZED FROM SYNTHESIS GAS PRODUCED BY COAL GASIFICATION VERSUS STEAM REFORMING NATURAL GAS

	LOCATION	FINANCING
S G PRODUCTION	WYOMING MONTANA	UTILITY
METHANOL SYNTHESIS	GULF COAST	EQUITY

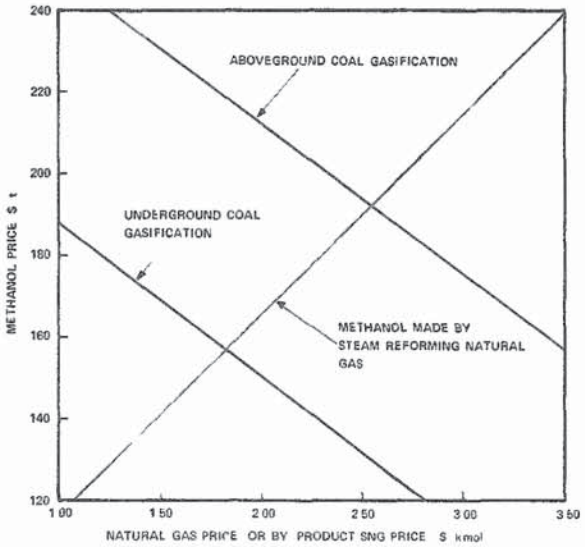


FIGURE 4

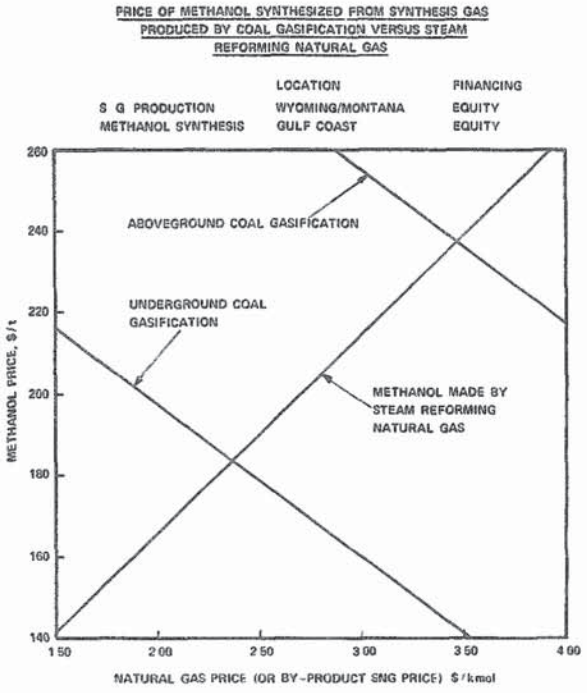


FIGURE 5

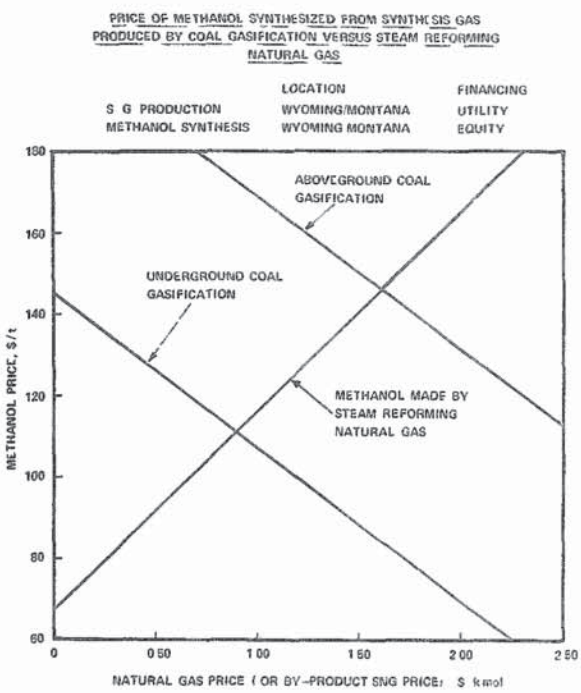


FIGURE 6

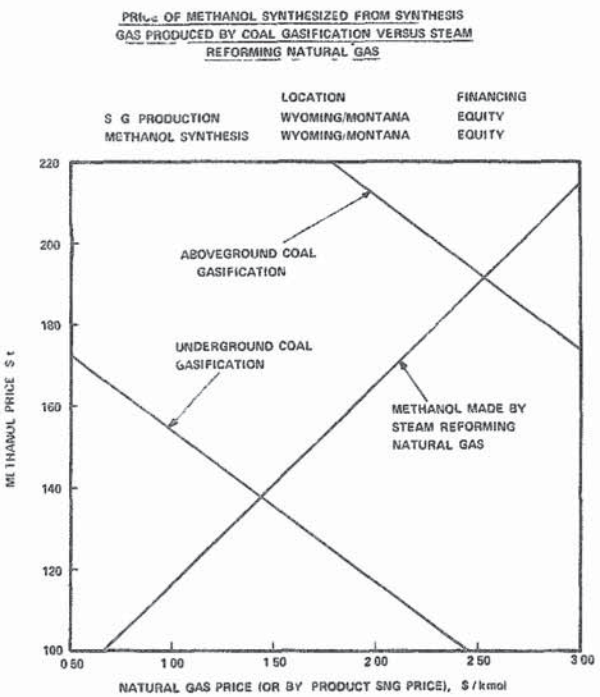
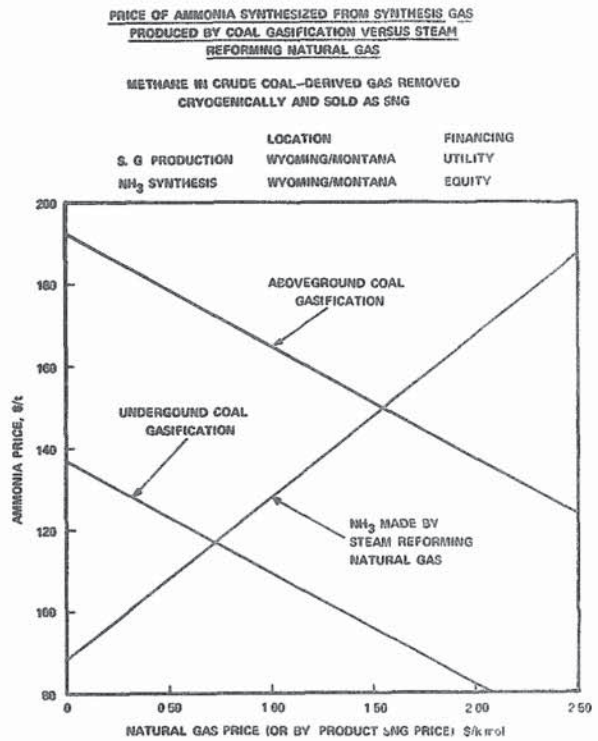


FIGURE 7



gasification. This shows the advantage of making synthesis gas which can be used directly in synthesis plants over making SNG which can be steam reformed to make the methanol.

Figure 5 (as well as Figure 3) shows that the price of methanol synthesized from gas made by underground coal gasification is $63/t ($57/ST) less than the price of methanol made by above-ground coal gasification.

Figure 6 shows that, with equity financing, methanol synthesized from gas made via underground coal gasification is competitive with that made from steam reforming natural gas at $1.44/kmol ($1.72/10^3 SCF) which is within the range of current intrastate natural gas prices.

Table VII shows the economics of producing the ammonia synthesis gas by the underground method and aboveground in Lurgi gasifiers. As in the methanol synthesis gas case, both the capital requirement and the price of synthesis gas is significantly lower for the underground coal gasification case than for the aboveground case. Figure 7 shows that the economics for manufacturing ammonia are also similar. Ammonia synthesized from gas produced by underground coal gasification is competitive with that made from natural gas at 72¢/kmol (86¢/10^3 SCF). Only the case with the synthesis plant located near the gas production facilities and with the gas production facilities financed with utility-type economics is shown, but the other cases showed results similar to the corresponding methanol cases.

CONCLUSIONS

1. Under the assumptions made in this study, the production of synthesis gas for the manufacture of methane, methanol and ammonia is cheaper by underground gasification than surface gasification

2. The manufacture of methanol and ammonia using synthesis gas derived from underground coal gasification is competitive with steam reforming of natural gas at current gas prices assuming the synthesis plants are located near the coal field.

3. It is substantially more economical to build new ammonia and methanol synthesis plants near the coal fields of Wyoming and Montana than pipe the synthesis gas to current plants near the Gulf Coast. The investment for five synthesis plants would be $250 x 10^6 which is 63% of the cost of the pipeline.

ACKNOWLEDGEMENTS

The authors wish to express their gratitude to Gulf Research & Development Company for permission to publish this paper.

REFERENCES

1. "Industrial Energy Study of the Industrial Chemicals Group", performed by International Research and Technology Corporation for the U.S. Department of Commerce, Industrial Energy Analysis Group and the Federal Energy Office, Contract No. 14-01-0001-1654, August, 1974, PB 236 322/AS.
2. Chemical and Engineering News, pp 12-16, August 25, 1976.
3. "World-Wide HPI Construction Boxscore", Hydrocarbon Processing, October, 1975.
4. Greek, G. F.: "Ammonia Squeeze Loosens, Outlook Stays Good", Chemical and Engineering News, pp 10-13, April 18, 1975.
5. Burke, D.P.: "Methanol", Chemical Week, pp 33-42, September 24, 1975.
6. Chemical and Engineering News, p 7, January 5, 1976.
7. Application of El Paso Natural Gas Company to the Federal Power Commission, November 7, 1972, Revised October 8, 1973.
8. Application of Western Gasification Company, (WESCO), to the Federal Power Commission, February 2, 1973, Revised November 16, 1973.
9. Garon, A. M.: "An Economic Evaluation of Underground Coal Gasification", UCG Symposium, Morgantown, West Virginia, August, 1976.

ECONOMIC COMPARISON OF PRODUCING SNG BY LAWRENCE LIVERMORE LABORATORY'S IN SITU COAL GASIFICATION PROCESS WITH LURGI ABOVEGROUND COAL GASIFICATION

by

R. Z. Mason, Williams Brothers Process Services, Inc.
D. E. Hall, Pacific Gas and Electric Company

ABSTRACT

The in situ coal gasification concept of the Lawrence Livermore Laboratory has been technically and economically appraised on paper by an industrial team consisting of the Resource Sciences Corporation, Amoco Production Company, E. I. du Pont de Nemours & Co., Inc., Pacific Gas and Electric Company, and Rocky Mountain Energy Company. The conceptual plan and the industry evaluation are summarized. The stoichiometry, field design, crude gas processing, utilities requirements and estimated investment and operating costs are discussed briefly. Problem areas to developing the technology are stressed. Economic appraisal of conservative and optimistic cases indicates that pipeline quality natural gas produced by this technology will be competitively priced with synthetic natural gas produced by other technology which is under consideration today if the assumptions made in the appraisal prove to be valid.

INTRODUCTION

The Lawrence Livermore Laboratory (LLL) concept for in situ gasification of thickly bedded deep coals is presented in Figure 1. An array of blastholes is drilled into a coal bed located at 500 to 3000 foot depth. Chemical slurry explosive is emplaced within the coal bed and detonated to create permeability. Some of the blastholes are reentered and completed to permit injection of oxygen and steam into the top of the fractured coal bed. Gasification products are removed using wells completed into the bottom of the rubblized bed. The crude gas is processed in surface facilities to yield gas of pipeline quality.

BASIS OF ECONOMIC EVALUATION

This paper represents an assessment of the economic potential of the LLL in situ coal gasification concept in its present preliminary stage of development. Using both optimistic and conservative estimates of several important process and economic parameters, a cost range for the pipeline quality gas product has been estimated and is compared with similar computations for a Lurgi gasification complex using stripmined coal.

Stoichiometry

Capacity - To expedite estimating the costs of surface processing facilities, the calculations are based on a project capacity that corresponds to that for the proposed Burnham coal-gasification complex of the El Paso Natural Gas Company (EPNG). The EPNG project is based on the gasification of surface-mined coal from the Navajo tribal lands in San Juan County, New Mexico and is described in detail in the EPNG application to the Federal Power Commission for a Certificate of Public Convenience and Necessity [1]. Figure 1 is a simplified flow diagram presenting the basis for the scoping economics.

References at end of paper

BASIS FOR SCOPING ECONOMICS

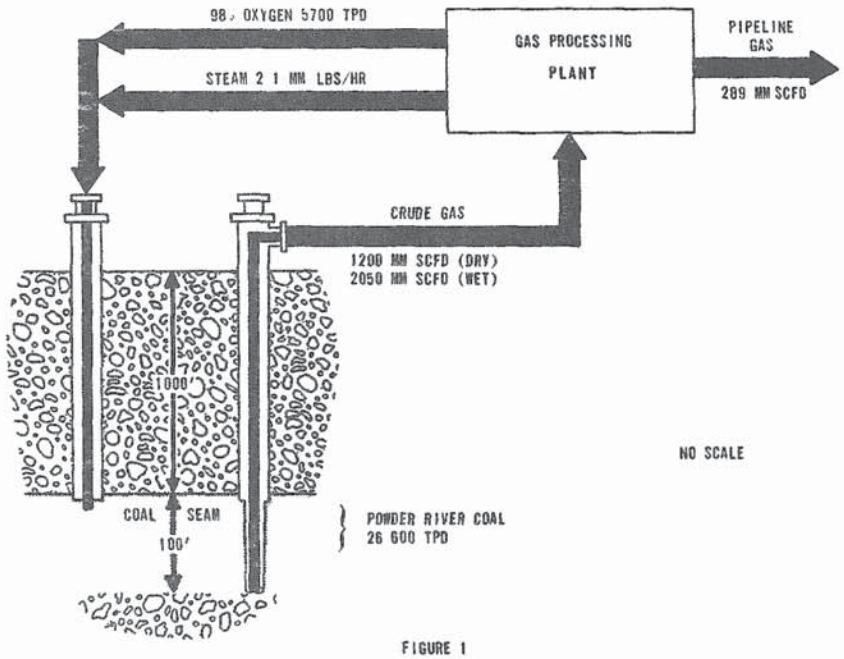


FIGURE 1

The design capacity of the EPNG project is 289 MMSCF per stream day of pipeline-quality gas, with a higher heating value of 954 Btu/SCF. Based on a 90.4% onstream efficiency, the average pipeline gas production is 261 MMSCF per calendar day.

Coal Source - Subbituminous coal from the Powder River Basin, Wyoming is assumed to be the basic raw material for the in situ process in this evaluation. This coal is similar in composition to the EPNG Burnham coal. (See Table I which presents the design criteria for the LLL in situ project as well as two Lurgi gasification complexes: the EPNG complex, which uses New Mexico subbituminous coal, and the American Natural Gas Service Company (ANG) complex, which uses North Dakota lignite.) The average depth to the top of the Powder River Basin coal seam is assumed to be 1000 feet, and the average seam thickness to be 100 feet. The density of the coal is 87.4 lb/ft [3].

Crude-Gas Composition - An important assumption is that the composition of the crude gas produced by the in situ gasification of Powder River coal is the same as that produced from the aboveground Lurgi generators specified in the EPNG project (see Table II) [2]. Reaction conditions for the Lurgi reactor and the in situ process at 1000 ft. are comparable in that both processes accomplish gasification at a pressure of about 450 psi by the injection of oxygen diluted with steam. Figure 2 shows a sequence of reaction zones for the Lurgi reactor. In the initial high-temperature combustion zone inlet oxygen reacts with char to yield carbon dioxide. This zone is followed by the gasification zone, in which endothermic reactions of carbon dioxide and steam with char yield carbon monoxide and hydrogen. Methane is produced by the exothermic hydrogenation of carbon monoxide and char [3]. The gasification zone is followed by the coal-pyrolysis and drying zones. The same sequence of reaction zones would occur in the in situ process. In the Lurgi reactor, however, the coal bed moves downward with the reaction zones in a fixed position, whereas for the in situ processing of the coal the converse is true.

TABLE I

Criteria Used in the Design of Two Lurgi Coal Gasification Complexes and the LLL In Situ Gasification Project

Category	ANG[a]	EPNG[b]	Predicted for in situ[c]
		Plant	
Capacity (MMSCF/day)	275	289	289
Operating factor (%)	91	90	90
Higher heating value of SNG (Btu/SCF)	979	954	954
Oxygen requirement (tons per day)	5,419	5,720	5,720
Oxygen purity (%)	99.5	98	98
Plant water requirement (GPM)	7,912	5,600	5,600
Proportion of crude gas sent to shift converter (%)	40	55	
Sulfur recovery system	Claus and Stretford	Stretford	Stretford
Fuel for steam generation	Coal	Low-Btu gas	Crude Gas
		Coal	
Coal requirement (tons per day)	36,800	29,800	26,590
Coal analysis, as received (wt.%):			
Coal (MAF)	56.6	64.5	72.2
Moisture	36.0	16.3	21.4
Ash	7.4	19.2	6.4
Total	100.0	100.0	100.0
Ultimate coal analysis (MAF) (wt.%):			
Carbon	71.5	76.3	72.4
Hydrogen	4.8	5.6	5.2
Nitrogen	1.4	1.3	1.2
Sulfur	1.3	1.1	1.1
Oxygen	21.0	15.7	20.1
Total	100.0	100.0	100.0
Higher heating value of coal (Btu/lb)	6,822	8,872	
		By-products	
Tar (gal/day)	83,672	240,950	293,200
Tar oil (gal/day)	137,556	119,420	145,100
Naphtha (gal/day)	46,241	68,730	68,700
Crude phenol (gal/day)	28,112	29,220	35,600
Ammonia (tons per day)	220	219,290[d]	234
Sulfur (tons per day)		148	160

[a] American Natural Gas Service Company. Type of coal: North Dakota Lignite.
[b] El Paso Natural Gas Company. Type of coal: New Mexico subbituminous.
[c] Powder River Basin (Wyoming) coal.
[d] Gallons per day.

TABLE II

Lurgi Gas Compositions [a]

Component	Concentration (mole %) Crude gas[b]	Pipeline gas
CO_2	28.0	1.8
CO	20.2	--
CH_4	11.1	92.9
H_2	39.0	4.2
C_2H_6	1.0	--
N_2	0.3	1.1
H_2S	0.4	--
	100.0	100.0
Molecular weight	21.1	16.2
Gross heating value (Btu/SCF)	324	954

[a]From the EPNG Lurgi design of October 1973.

[b]Excluding water, tar, phenol, and ammonia.

REACTION ZONES IN LURGI GASIFIER

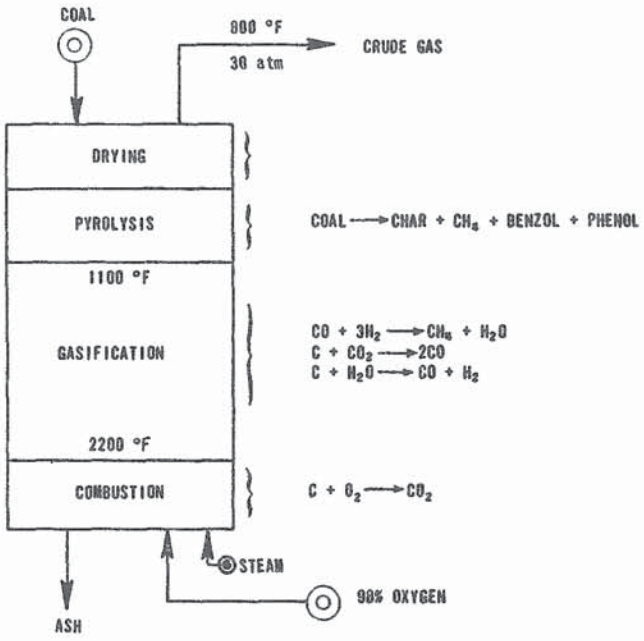


FIGURE 2

The crude gas from the EPNG Lurgi reactors has a heating value equal to 79% of the Burnham coal consumed. If the secondary gasification reactions do not proceed as efficiently in the in situ process as in the Lurgi reactor, due to poor contacting or heat leak, the carbon dioxide content of the crude gas will be higher and the heating value lower. For surface facilities with fixed oxygen-plant and gas-purification capacity, a lower gasification efficiency would result in lower pipeline-gas output. The Lurgi crude-gas composition given in Table II is that produced under controlled reaction conditions, feeding carefully sized coal (8 to 44 mm) to the gasifier. Less efficient contacting, with lower gasification efficiency, seems likely in the in situ operation, and the assumption of an average crude-gas composition identical with that from the Lurgi reactor is considered optimistic. This is a matter that can be resolved only by field in situ tests.

Material Balance

Based on the assumed crude-gas composition, the coal and oxygen requirements for the in situ combustion of Powder River coal have been estimated [4, 5, 11]. Production rates for the project are summarized in Table III. (Note that the coal and oxygen requirements include the in situ generation of fuel gas for the project.)

The steam-injection rate is based on maintaining the same mole ratio of steam to oxygen as for the EPNG project, which corresponds to about 11 mole % oxygen in the steam-oxygen mix. This represents considerably more steam than is required for the gasification stoichiometry and is determined primarily by the need to limit the combustion temperature.

TABLE III

Module Details and Stream-Day Rates

	Conservative case, 25-hole module	Optimistic case, 9-hole module
Powder factor (lb explosive per ton of coal)	2.5	1.0
Modules required at 100% sweep efficiency (first 2 years)	62	36
Modules required at 100% sweep efficiency (After second year)	56	33
Blasthold underream diameter (in.)	17	24
Blasthole spacing (ft)	38	83
Blastholes per module at 1100-ft depth	25	9
Injection wells per module	12	4
Production wells per module	5	1
Explosive charge per blasthole (lb)	14,750	29,400
Coal fractured per blasthole (tons)	6,300	30,100

Operating parameters	Total Project	Per module	Per hole	Per module	Per hole
Coal burn rates					
Gasification (tons per day)	21,900				
Fuel (tons per day)	4,690				
Total	26,590	428.9	17.2	738.6	82.1
Injection rates					
Oxygen (98%) (tons per day)	5,720	92.3	7.69	158.9	39.7
Oxygen (98%) (MMSCFD)	135	2.17	0.18	3.75	0.94
Steam (550 psig) (M lb/hr)	2,090	33.7	2.81	58.1	14.51
Steam (550 psig) (MMSCFD)	1,050	16.9	1.41	29.2	7.29
Production rates					
Crude gas--dry (MMSCFD)	1,190	19.25	3.85	33.16	33.16
Water in gas (MMSCFD)	856	13.81	2.76	23.78	23.78
Total	2,050	33.06	6.61	56.94	56.94
Pipeline gas (MMSCFD)	289	4.66	0.93	8.03	8.03
Pipeline gas (MMSCF/yr)	95.4	1.54	0.31	2.65	2.65

FIELD DESIGN

Explosive Fracturing

Permeability is generated in the coal bed by blasting with slurry explosives. There is considerable uncertainty about the efficiency of blasting in coal beds that do not have a free surface in proximity to the charge. Du Pont experience on blasting coal with dynamite on one free face indicates a "lower" powder factor of about 2.0 lb per ton of coal shattered. For the projected in situ operation at 1000-ft depth with large-diameter blastholes and no free surface, an "upper" powder factor of 5.0 is considered "realistic." By using a high-efficiency slurry explosive like Du Pont EL-836, the lower and upper limits on the powder factor are reduced to 1.0 and 2.5 lb per ton of coal shattered, respectively. With the powder factor fixed, the effective fracture radius can be calculated for a blasthole of given diameter.

Module Design

The industrial evaluation team considers that, to provide the gas treatment plant with a continuous feed of reasonably uniform composition and temperature, it is essential to conduct the gasification in multiple modules, or clusters of wells. [6] An important factor in module design is the need to control subsidence. This restriction may impose an upper limit on module diameter and a lower limit on barrier thickness. After combusion in adjacent modules is completed, positive control of subsidence might be accomplished by blasting in the surrounding barrier and/or overburden, to fill the cavity with rubble. [6] Another consideration is the width of coal barrier required to effectively isolate adjacent modules. Here again, field studies are needed to establish optimal module design.

In this evaluation, subsidence-control considerations are assumed to impose a maximum width of about 200 ft. Two module designs--conservative and optimistic--are evaluated; the details are given in Figures 3 and 4. The conservative design uses 25 blastholes, underreamed to 17 in. within the coal seam, located on a square pattern. Using the Du Pont upper powder factor for EL-836, (2.5 lb of high explosive per ton of coal fractured) the well spacing is found to be 38 ft and the quantity of coal fractured amounts to 158,000 tons per module, with a horizontal fractured section that is 190 ft square. The optimistic design (1 lb of high explosive per ton of coal fractured for EL-836) uses nine blastholes, underreamed to 24 in. within the coal seam. Well spacing is 83 ft, and the quantity of coal fractured is 271,000 tons per module, with a fractured section 249 ft square. Additional module details, including flow rates for the injection and production wells, are given in Table III. The flow rates are based on a module burn life of one year.

CONSERVATIVE MODULE DESIGN - 25 HOLE

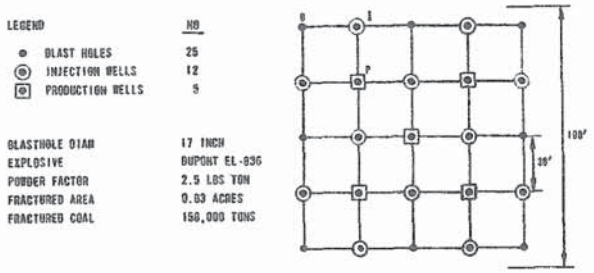


FIGURE 3

OPTIMISTIC MODULE DESIGN - 9 HOLE

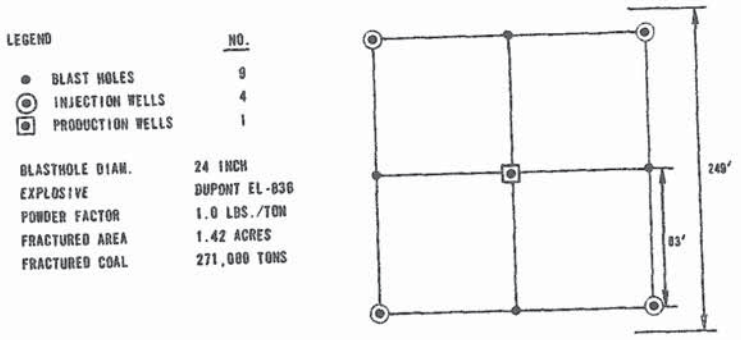


FIGURE 4

Well Design

The blastholes are drilled with a truck-mounted rig, using a Dyna-Drill downhole motor to obtain close directional control. [7] For the conservative module design, an 8.75-in. hole is drilled to 1100 ft, and the bottom 100 ft in the coal is underreamed to 17 in. For the optimistic design, a 12.25-in. hole is underreamed to 24 in. The permissible hole drift is limited to 4.4 ft for the 17-in. hole and 6.2 ft for the 24-in. hole. Except for 20 ft of surface conductor pipe, the blastholes are not cased. Liquid-slurry explosive is introduced to fill the underreamed hole in the coal bed, and the hole is stemmed with water, sand, or drill cuttings before detonation.

Injection and production wells are completed in some of the blastholes after detonation, as shown in Figures 3 and 4. This presumes that damage to the blastholes is minor, so that cleanout can be accomplished and casing run and cemented. The injection wells are cased to the top of the coal bed, with a 30-ft Incoloy section set immediately above the bed. The production wells are completed with a 130-ft recoverable Incoloy liner extending to the bottom of the coal seam. It may not be practical to complete the production wells in the blastholes. These wells would extend into the most highly fractured region of the coal bed. By-passing of oxygen-rich gas downward along the production liner could be excessive. It might be necessary to drill production wells in a less fragmented part of the bed or in the barriers between modules. One possibility is to use, instead of blasting, hydraulic fracturing initiated in the lower part of the bed, in the production-well locations.

Ash and coal tar entrained in the combustion gases represent a potential plugging problem for the production wells. Provision is made to circulate hot gas liquor through tubing installed in each production well. The liquids and suspended solids are separated from the crude gas in surface separators, an operation analogous to that accomplished in the wash coolers of the Lurgi process.

The well-completion specifications used in this study incorporate know-how gained from Amoco's in situ work in the Athabasca tar sands and, of course, are only tentative, pending field tests of the LLL concept.

Field Surface Facilities

Details on the piping, spearators, and well instrumentation for the conservative-case modules are shown in Figures 5 and 6. Gas-liquid separators are provided for each production well.

INJECTION WELL PIPING SYSTEM
CONSERVATIVE 25 HOLE DESIGN

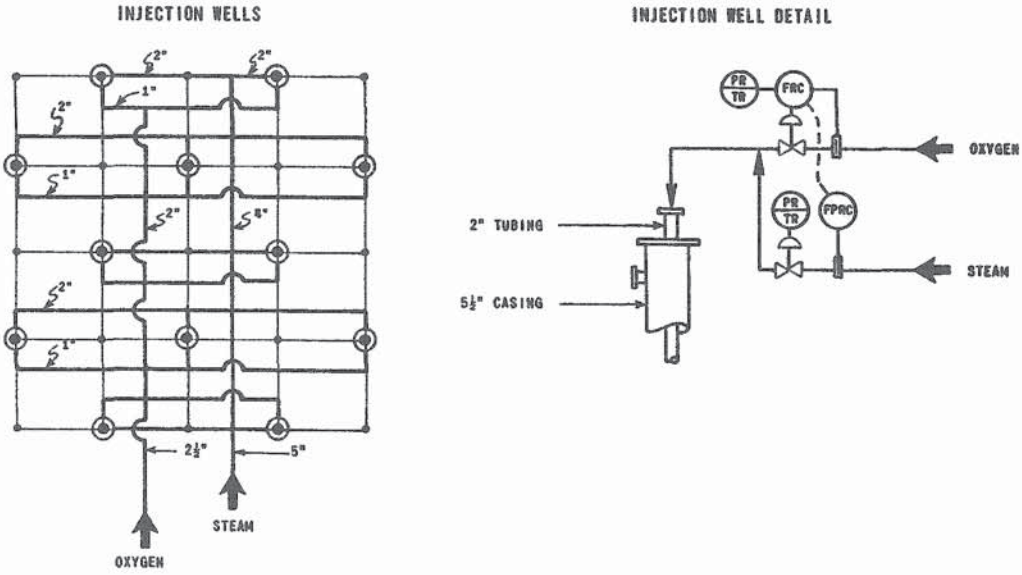


FIGURE 5

PRODUCTION WELL PIPING SYSTEM
CONSERVATIVE 25 HOLE DESIGN

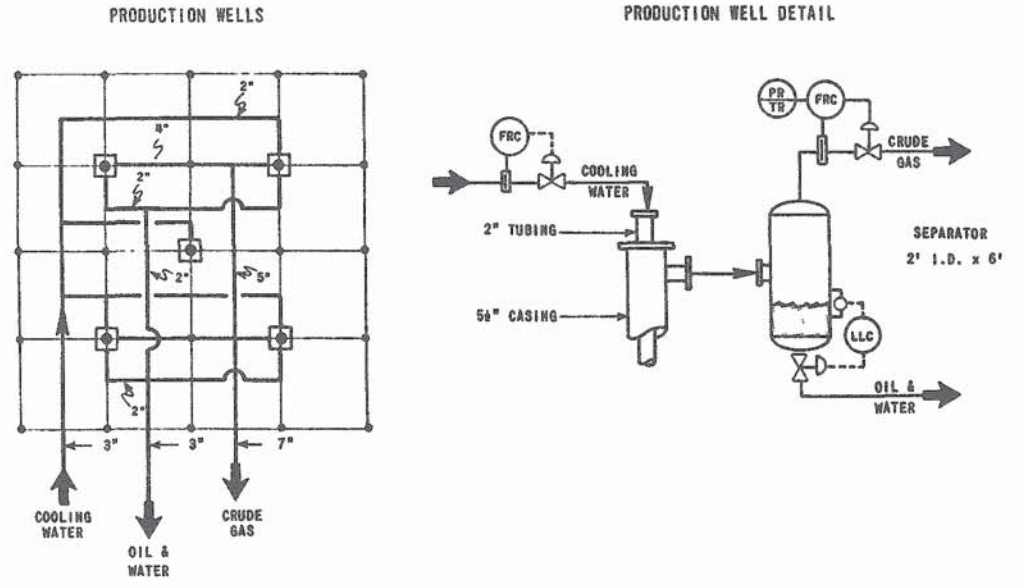


FIGURE 6

Instruments to record temperature and pressure, and control steam, oxygen, produced gas and gas liquor flows are provided as necessary for each well. The individual modules are tied into header systems to transfer steam, oxygen, crude gas, oil, and water between the plant and field (see Figure 7).

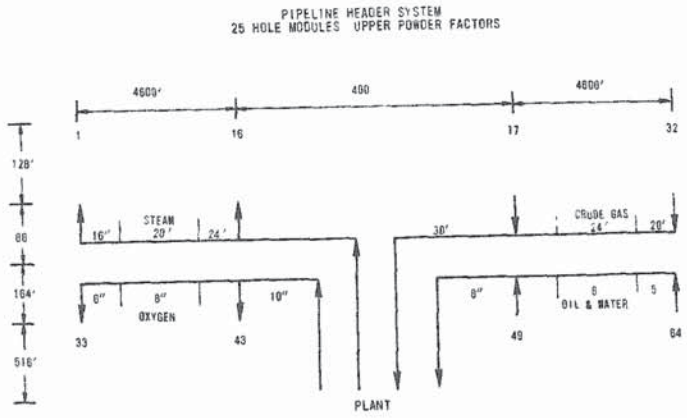


FIGURE 7

PLANT DESIGN

Gas Processing

The design of the gas-processing plant is identical with that described in the EPNG application, except that the Lurgi aboveground coal gasifiers and associated coal- and ash-handling equipment are deleted. Hot crude gas collected from the field separators is pipelined to the plant, where it is cooled to about 350°F in waste-heat boilers generating 100-psig steam. A portion of the cooled gas is diverted to the shift unit, where carbon monoxide is catalytically reacted with steam at about 700°F by the water-gas shift reaction:

$$CO + H_2O \longrightarrow CO_2 + H_2$$

The proportion of gas sent to the shift unit (about 55%) is regulated to maintain an H_2/CO ratio of 3.75 in the combined gas feed to the subsequent methanation unit. The crude- and shifted-gas streams are further cooled in separate waste-heat boilers and air coolers, to condense out oil and water. In the EPNG plant, tar oil, crude phenol, and ammonia are recovered as salable by-products. The yield and economic recovery levels of by-products for the in situ project are not known. For example, it might be more economical to dispose of the gas liquor, containing dissolved phenols and ammonia, by reinjection into the modules. In the present evaluation, however, the complete investment for by-product recovery is included.

The cooled gas is sent to a Lurgi Rectisol unit, where it is purified by contact with cold methanol in several stages. The first stage, operating at 32°F, removes light naphtha and water. The second stage, at -50°F, removes carbon dioxide, hydrogen sulfide, and carbonylsulfide, which are processed in a Stretford unit to recover elemental sulfur. The purified gas is sent to the methanation unit, where carbon monoxide and hydrogen are reacted over nickel catalyst to yield methane.

$$CO + 3H_2 \longrightarrow CH_4 + H_2O$$

Utilities

The oxygen plant has a design capacity of 5720 TPD of 98% oxygen. Compressors are installed

to deliver oxygen to the field transfer lines at 500 psig.

In the EPNG installation, plant water requirements are met by transporting river water through a 40-mile pipeline. To supply the Powder River in situ plant, deep wells drilled into the Madison aquifer may be necessary. The cost of each 13,000-ft well equipped with a 1500-gpm downhole pump is estimated to be $980,000. It is assumed that the costs of water wells and raw-water-treating facilities would be comparable to the cost of the EPNG river-water system.

In the EPNG proposal, a battery of 10 air-blown Lurgi gasifiers is included to supply fuel gas for the plant energy requirements. The fuel gas is sweetened, but not upgraded by shifting or methanation. For the in situ process, the necessary fuel gas is assumed to be obtained by additional in situ gasification with 98% oxygen. The total oxygen tonnage, including fuel-gas generation, for this in situ facility is comparable to that specified for the EPNG project. This is in consequence of the lower computed oxygen requirement per ton of Powder River coal, due to the higher oxygen content of the coal itself.[4] In actual practice, plant fuel might be obtained more economically from other sources, such as coal, or by using air rather than oxygen for combustion in separate gasification modules.

The steam requirement for the in situ injection wells might advantageously be supplied by batteries of gas-fired skid-mounted field boilers. These units can feed water with dissolved-solids content of up to 8000 ppm, producing high-pressure steam of 80% quality or better. Their feasibility has been demonstrated by commercial "steam-flooding" operations in heavy-oil fields.

Detailed utility and energy balances have not been prepared for the in situ process: the assumption was made that investment and operating costs for utilites and other OSBL facilities are comparable to those in the EPNG estimate.

INVESTMENT AND OPERATING COSTS

The investment and operating costs estimated for late 1974-early 1975 included no provision for inflation during the construction and startup period nor the 25-year project life. The capacity of each gasification plant design is assumed to be 289 MMSCF per stream day. Product and operating cost estimates assume that the facility operates 330 days each year (90.4% operating factor). The unit price of gas is therefore based on a gas production rate of 95.37 billion SCF/yr. The cost of gas for each case is computed for two rates of return (10 and 12%) after taxes. The rate of return is calculated by the discounted-cash-flow (DCF) method over the life of the project. Interest on borrowed capital is at 10% per annum.

Field Costs

Details of the cost estimates for preparing 17- and 24-in. under-reamed blastholes, including explosive charges, are given in Table IV. The costs are based on contracting out the drilling and blasting operations. This is common practice in the oil industry, since drilling contracts can usually be negotiated at a lower overall cost than is incurred by purchasing rigs and operating within a corporate drilling department. The costs in Table IV reflect economies resulting from essentially continuous rig operation drilling a large number of closely spaced holes. [7]

Details of the injection- and production-well completion costs, based on reentering and completing the blastholes after detonation, are given in Table V. The initial wells are drilled in the year prior to production and during the first year of operation. The costs cover all new wellheads, casing, tubing, and liners. It is assumed that wells completed in subsequent years will use salvaged wellheads, tubing, and liners, at a 10% replacement cost on wellheads and tubing, and a 20% replacement cost on liners. Rig time on subsequent completions is reduced from five shifts to four shifts to reflect the learning curve.

The installation costs for initial and subsequent modules, based on the blasthole and completion costs described above, are summarized in Table VI. The estimated costs cover lines, separators, instruments, roads, and lease preparation and include cost allowances for well plugging and subsidence control. The subsidence-control costs are based on drilling four 17-in. blastholes and blasting the barrier walls surrounding the module. It is not known whether this procedure would be effective or the cost allowance sufficient.

TABLE IV

Blasthole Costs for LLL In Situ Process[7]

Parameter	Conservative case, 25-hole module	Optimistic 9-hole module
Hole diameter		
Diameter of 1000-ft hole (in.)	8-3/4	12-1/4
Diameter of underreamed bottom 100 ft (in.)	17	24
Cost of drilling		
Set 20-ft conductor and cement	$ 1,400	$ 2,000
Rig rental and labor (14 shifts at $600)	8,400	8,400
Downhole motor	2,000	2,000
Bits	1,200	1,500
Underreamer	2,000	2,400
Mud and chemicals	1,000	1,500
Survey	600	600
Subtotal	$ 16,000	$ 18,400
Cost of explosives		
Load E1-836 at $0.32/lb	$ 4,700	$ 9,400
Primer cord and caps	100	100
Stem hole with water	100	100
Subtotal	$ 4,900	$ 9,600
Total	$ 21,600	$ 28,000

TABLE V

Well Completion Costs for the LLL In Situ Process[a]

Item	Twenty-five hole modules						Nine-hole modules					
	Injection			Production			Injection			Production		
Intangible costs:					Initial wells							
Rig time (five shifts)			$ 3,000			$ 3,000			$ 3,000			$ 3,000
Bit			400			400			400			400
Mud and chemicals			500			500			500			500
Cement			3,500			3,500			3,500			3,500
Perforating			2,000			2,000			2,000			2,000
Subtotal			$ 9,400			$ 9,400			$ 9,400			$ 9,400
Tangible costs:	Depth (ft)	Diam. (in.)		Depth (ft)	Diam. (in.)		Depth (ft)	Diam. (in.)		Depth (ft)	Diam. (in.)	
Casing	970	5.5	$ 4,400	970	5.5	$ 4,400	970	5.5	$ 4,400	970	7	$ 5,400
Incoloy sections	30	4.5	1,200	130	4.5	3,800	30	4.5	1,200	130	5.5	5,000
Tubing	1000	2	2,200	1000	2	2,400	1000	3	2,900	1100	2.5	2,400
Wellhead			4,000			4,000			4,000			5,000
Packers and miscellaneous			2,000			4,000			2,000			4,000
Subtotal			$ 13,800			$ 18,600			$ 14,500			$ 21,800
Total costs per well			$ 23,200			$ 28,000			$ 23,900			$ 31,200
Intangible costs:					Subsequent wells							
Rig time (four shifts)			$ 2,400			$ 2,400			$ 2,400			$ 2,400
Bit			400			400			400			400
Mud and chemicals			400			400			400			400
Cement			3,500			3,500			3,500			3,500
Perforating			1,600			1,600			1,600			1,600
Pull tubing and Incoloy			1,200			1,800			1,200			1,800
Subtotal			$ 9,500			$ 10,100			$ 9,500			$ 10,100
Tangible costs:												
Casing			$ 4,400			$ 4,400			$ 4,400			$ 5,400
Incoloy- recovered with 20% loss			300			800			300			1,000
Tubing--recovered with 10% loss			300			300			300			300
Wellhead--recovered with 10% loss			400			400			400			500
Packers and miscellaneous			2,000			4,000			2,000			4,000
			$ 7,400			$ 9,900			$ 7,400			$ 11,200
Total costs per well			$ 16,900			$ 20,000			$ 16,900			$ 21,300

[a] Estimated costs to complete each such well.

TABLE VI

Module Installation Costs for the LLL In Situ Process[a]

(Thousands of Dollars)

	Initial modules				Subsequent modules			
	25-hole modules		9-hole modules		25-hole modules		9-hole modules	
	Number of wells	Annual cost	Number of wells	Annual cost	Number of wells	Annual cost	Number of wells	Annual cost
Wells:								
Blastholes	25	$ 418	9	$ 166	25	$ 418	9	$ 166
Injection wells	12	278	4	96	12	203	4	68
Production wells	5	140	1	31	5	100	1	21
Subtotal		836		293		721		255
Other equipment:								
Lines within module		10		11		4		4
Pro-rata header lines		30		42		14		17
Power lines		1		1		1		1
Separators		28		18		9		6
Instruments		102		30		36		11
Roads and lease preparation		3		5		3		5
Miscellaneous		3		3		3		3
Subtotal		177		110		70		47
explosive charge		123		86		123		86
Ignition		12		4		12		4
Well plugging		63		27		63		27
Subsidence control:								
Blastholes (four at 17 in.)		67		67		67		67
Explosives		20		20		20		20
Stemming and plugging		10		10		10		10
Subtotal		97		97		97		97
Total cost per module		$ 1,308		$ 617		$1,086		$ 516
Tangible fraction		0.24		0.25		0		0

[a]Estimated cost to prepare each such module.

For the in situ operation, the number of modules burned per year, and thus the field investment, is a direct function of the sweep efficiency (i.e., the fraction of coal in the module that is burned before oxygen breakthrough). Table VII shows the direct field investment for three sweep efficiencies and two module designs for the LLL in situ process. [8]

Annual operation and maintenance costs per module are given in Table VIII. The operating labor requirements are based on five man-minutes per well per shift, which is considered to be a high workload. [8] The various operating-cost bases are included in Table VIII.

TABLE VII

Direct Field Investment LLL In Situ Process[a]

(Millions of Dollars)

	Conservative case 25 hole module			Optimistic case 9 hole module		
	100% Sweep efficiency	70% Sweep efficiency	50% Sweep efficiency	100% Sweep efficiency	70% Sweep efficiency	50% Sweep efficiency
Capitalized well costs	17 4	24 9	34 [illegible]	3 2	4 [illegible]	[illegible] 3
Pipelines etc	21 9	31 5	43 9	[illegible] 9	11 4	15 9
Field direct investment	39 3	56 4	78 [illegible]	11 1	0	-2 1
Number of modules required per year	62	89	124	36	52	2

[a]Direct field investment required to prepare the total number of modules necessary to produce the required volume of crude gas for the first two years

TABLE VIII

Annual Operating Costs per Module, LLL In Situ Process

(Thousands of Dollars)

Type of expenditure	25-hole module	9-hole module
Investment		
Wells	836	293
Other equipment	177	110
Total	1013	403
Number of operating wells	17	5
Operating labor (man hours per shift)	1 4	0 4
Operating costs		
1 Operating labor at $15 000 per man-year	11	3
2 Maintenance labor at 3% of investment	30	12
3 Supervision at 15% of items 1 and 2	6	2
4 Labor benefits at 20% of items 1-3	9	3
Maintenance materials at 2% of investment	20	8
5 Field overhead at 20% of items 1-3	9	3
6 Insurance and miscellaneous at 2% of investment	20	8
General administrative expenses at 2% of investment	20	8
Total	125	47

Table IX summarizes the annual field operating expenses for the two module designs at three levels of sweep efficiency.

The capital costs estimated in the El Paso Natural Gas Company's 1973 application to the Federal Power Commission for a strip mine to produce approximately 9.3 miolion tons per year of Burnham coal are as follows:

Type of expenditure	Millions of dollars
Leasehole acquisition	23.1
Initial mining equipment	47.2
Miscellaneous	1.4
Total to mid-1973	71.7
Escalation to early 1975	109.6

The estimated early 1975 cost closely approximates the cost estimated by the American Natural Gas Service Company for a mine that would produce approximately 10 millon tons of North Dakota lignite ($106.2 million).[9] In addition to the above, an expenditure of $2 million per year of capital expenses will be incurred over the life of the project. To simplify cost accounting, this item is included in the operating expenses.

Typical operating costs for large strip mines in the United States are given in Table X. The cost estimates are similar to those predicted by the American Natural Gas Service Company, except that the royalty and labor-related costs reflect the more recent United Mine Workers (UMW) contract. The royalty for coal burned in the in situ process is set at $0.48 per ton, the difference being the amount of the UMW royalty.

Gas-Processing Plant Costs

The most recent detailed cost estimate published for the EPNG project was made in 1973. A breakdown of the Lurgi coal-gasification process costs, as reported in the 1973 El Paso FPC application, is given in Table XI, which also shows the estimated 1973 cost for a processing plant to purify the crude gas produced by the in situ process. These costs were obtained by deleting the costs for the Lurgi coal gasifiers and the associated coal- and ash-handling equipment.

Since the EPNG estimate was prepared in mid-1973, inflation has dramatically increased the cost of construction and operation of gas-processing facilities. In early 1975, the American Natural Gas Service Company filed an application with the FPC for a Lurgi coal gasification complex that will be located in Mercer County, North Dakota and is quite similar in design and capacity to the EPNG complex (see Table I.) The installed-plant cost for this facility exceeds 650 million dollars. The cost estimates in the ANG application are believed to be a sound basis for adjusting the EPNG cost estimate to late 1974 and early 1975. The resulting estimate of the invesment cost for the gas-processing plant as of late 1974-early 1975 are as follows:

	Millions of dollars	
	Lurgi	In Situ
EPNG estimate mid-1973	353.7	259.5
Escalate to late 1974-early 1975	540.7	431.0
Coal handling facilities	40.8	-
Location bonus and construction housing	56.4	56.4
Miscellaneous	29.5	21.6
	667.4	509.0

TABLE IX

Annual Operating Expenses--Field Program

(Millions of Dollars)

Item	25-hole module			9-hole module		
	100% Sweep efficiency	70% Sweep efficiency	50% Sweep efficiency	100% Sweep efficiency	70% Sweep efficiency	50% Sweep efficiency
Number of modules per year	56	80	112	33	47	66
Maintenance materials, and supplies	1.2	1.7	2.4	0.3	0.4	0.5
Wages and salaries, etc.	3.9	5.5	7.7	0.9	1.3	1.8
Administrative expenses	1.6	2.3	3.2	0.4	0.6	0.8
Royalty	4.2	4.2	4.2	4.2	4.2	4.2
Module installation	60.8	86.9	121.6	17.0	24.3	34.1
Total	71.7	100.6	139.1	22.8	30.8	41.4

TABLE X

Operating Expenses of a Strip Mine Producing 9.3 Million Tons per Year

(Thousands of Dollars)

Item	Cost per ton	Total annual cost
Labor-related costs	$1.70	$15,800
Supplies	0.78	7,300
Royalty	0.72	6,700
Capital expenditures	0.22	2,000
Administrative and general	0.10	900
Total	$3.52	$32,700

TABLE XI

Direct Investment--Surface Plant[a]

	EPNG[b]	Adjusted to in situ gasification
Process		
Gas production	$ 64.4	$ --
Crude-gas shift	7.7	7.7
Gas cooling	8.1	8.1
Gas purification	31.0	31.0
Refrigeration	9.6	9.6
Methanation	18.6	18.6
Gas compression and dehydration	5.7	5.7
Phenol extraction	7.0	7.0
Gas liquor separation and stripping	11.6	11.6
Lock gas storage and compression	1.9	--
Sulfur recovery	8.2	8.2
Subtotal	$ 173.8	$107.5
Utilities		
Fuel-gas production	21.6	--
Fuel-gas cooling	1.5	1.5
Fuel-gas treating	3.8	3.8
Air compression	20.5	20.5
Steam and power generation	30.2	30.2
Oxygen production	22.4	22.4
Oxygen compression	6.5	6.5
Raw-water treating	6.7	6.7
Cooling water system	5.8	5.8
Miscellaneous	5.7	5.7
Subtotal	$ 124.7	$103.1
OSBL facilities		
Ash dewatering and transfer	6.3	--
Raw-water pumping, pipeline and storage	14.3	14.3
Buildings, land and site improvements	11.2	11.2
Electrical distribution	6.8	6.8
Pipe headers and lines	10.6	10.6
Storage and loading	2.6	2.6
Settling ponds	3.4	3.4
Subtotal	$ 55.2	$ 48.9
TOTAL INVESTMENT	$ 353.7	$259.5

[a]In millions of dollars.

[b]From the El Paso Natural Gas Company's 1973 FPC application.

Estimated annual operating expenses for the Lurgi plant and the in situ surface plant are shown in Table XII. The bases for estimating the operating expense are as follows:

1. Maintenance materials and supplies for both the Lurgi process and in situ operation are estimated to cost 1.8% of the appropriate total direct plant investment, excluding the provision for taxes, location bonus, and construction housing.

2. The EPNG estimate of catalyst and chemicals cost is escalated to reflect the Chemical Week chemical price index of 185 for early 1975 versus 113 for mid-1973--ratio of 1.64

3. Water purchased for both plants amounted to nearly 4 billion gal/yr and is estimated to cost $0.05 per 1000 gallons.

4. Power purchased is estimated to cost 11 mils/kW-hr. A Lurgi plant requires nearly 450 million kW-hr. per year, while the in situ operation is estimated to need 415 million kW-hr each year.

5. Wages and salaries, etc., are estimated to be $20,000 per year for maintenance and operating personnel and $25,000 for supervisory and staff personnel. These estimates include a contingency for fringe benefits and other payroll burdens. The total payroll exceeds 600 for the Lurgi plant and is estimated to be 450 for the in situ plant.

6. General and administrative expenses for both the Lurgi process and the in situ operation are estimated to be 1% of the total direct plant investment.

TABLE XII

Annual Operating Expenses for the Surface Plant

Item	Lurgi	In situ
Investment, excluding taxes, relocation bonus, construction housing (millions of dollars)	611	452.6
Operating labor (estimated per shift)	57	39
Estimated total personnel	600	450
Annual operating costs (millions of dollars)		
Maintenance materials and supplies at 1.8% of investment	11.0	8.1
Chemicals and catalysts	5.8	5.8
Water purchased	0.2	0.2
Power purchased	5.0	4.6
Wages and salaries	12.7	9.5
General administrative expenses	6.1	4.5
Total	40.8	32.7

Total Project Capital and Operating Costs

Table XIII summarizes the direct plant and field investment for each design considered and enumerates the associated indirect investment. The following bases were used to estimate the indirect investments:

1. Interest during construction estimated at 15% of the total direct investment.

2. Contingency estimated at 10% of the total direct investment.

3. Startup expenses and working capital, each estimated at one-fourth of the total project operating expenses.

The consolidated annual plant and field operating expenses are given in Table XIV for each of the sweep efficiencies for the in situ coal-gasification process. For comparison, consolidated costs for the Lurgi process are also given.

BY-PRODUCTS

The yields of by-products predicted for the EPNG Lurgi plant and the LLL in situ process are given in Table XV.

The annual revenue from the sale of these by-products was originally estimated by EPNG to be $15.8 million per year. The by-product revenue given in Table XV reflects the increase in the Chemical Week chemical price index during the period between the filing of the EPNG application to FPC and early 1975.

FINANCIAL ANALYSIS

The preceding estimates of investments, annual operating expenses, and product yields were used as the basis for estimating the sale price of gas for the Lurgi operation and each of the in situ designs. It was determined that the sale price would be sufficient to yield a satisfactory rate of return on investment.

Table XVI shows a pro forma income statement and unit price of gas sufficient to yield a 10% discounted cash flow (DCF) rate of return (after tax) on invested capital. At the current cost of money, a 10% DCF would require a highly leveraged financial structure (approximately 25% equity-75% debt) for a project to be financially attractive. At 75% debt such a project would return about 16% on equity investment. This is the type of financial structure proposed for many of the coal-gasification plants currently before the Federal Power Commission. Table XVII presents a pro forma income statement and unit price sufficient to yield a 12% DCF return. This rate of return reflects the historical financial structures of utilities (about 50% equity-50% debt) and the current cost of money. At 50% debt such a project would also return 16% on equity investment.

RESULTS AND RECOMMENDATIONS

An analysis of Tables XVI and XVII reveals the economic significance of various process assumptions. Comparison of the unit gas price for the 25- and 9- blasthole well designs demonstrates the importance of the ability to fracture the coal efficiently. If the nine-hole design proves technically feasible, the price of SNG from the in situ operation would be in the range of $1.40 to $1.65 per thousand cubic feet at a 12% DCF return. In this price range the in situ operation has definite economic merit. Currently intrastate gas sales are being made at about $2.00 per thousand cubic feet.

In reviewing Tables XVI and XVII, it should be kept in mind that the 25- and 9-blast hole in situ gas-generator configurations are for scoping purposes only. The 25-well gas-generator configuration is considered to represent a conservative design in that the quantities of explosives and the blasthole diameters and spacing should provide adequate fracturing of the coal body to create the necessary coal permeability. On the other hand, the optimistic nine-hole configuration provides a minimum quantity of explosives that can be expected to fracture the coal properly.

TABLE XIII

Capital Investment Summary

(Millions of Dollars)

Item	Lurgi plant	LLL in situ process					
		25-hole module			9-hole module		
		100% Sweep efficiency	70% Sweep efficiency	50% Sweep efficiency	100% Sweep efficiency	70% Sweep efficiency	50% Sweep efficiency
Plant investment	667.4	509.0	509.0	509.0	509 0	509.0	509 0
Field investments:							
Strip mine	109.6						
Capitalized well		17.4	24.9	34.7	3.2	4.6	6.3
Pipelines, etc.		21.9	31.5	43.9	7.9	11.4	15.8
Direct investment	777.0	548.3	565.4	587.6	520.1	525.0	531.1
Indirect investments:							
Interest during construction	116.6	82.2	84.8	88.1	78.0	78.8	79.7
Contingency	77.7	54.8	56.5	58.8	52.0	52.5	53.1
Working capital	18.4	26.1	33.3	47.0	13.9	15.9	18.5
Startup expense	18.4	26.1	33.3	47.0	13.9	15.9	18.5
Subtotal	231.1	189.2	207.9	232.9	157.8	163.1	169.8
Total Investment	1008.1	737.5	773.3	820.5	67[illegible] 9	688 1	708.9

TABLE XIV

Annual Operating Costs--Total Project

(Millions of Dollars)

Item	Lurgi process	LLL in situ process					
		25-hole module			9-hole module		
		100% Sweep efficiency	70% Sweep efficiency	50% Sweep efficiency	100% Sweep efficiency	70% Sweep efficiency	50% Sweep efficiency
Maintenance materials and supplies	20.3	9.3	9.8	10.5	8.4	8 5	8.6
Chemicals	5.8	5.8	5.8	5.8	5.8	5.8	5.8
Water purchased	0.2	0.2	0.2	0.2	0.2	0.2	0.2
Power purchased	5.0	4.6	4.6	4.6	4.6	4.6	4.6
Wages and salaries, etc.	28.5	13.4	15.0	17.2	10.4	10.8	11.3
Administrative expenses	7.0	6.1	6.8	7.7	4.9	5.1	5.3
Royalty	6.7	4.2	4.2	4.2	4.2	4.2	4.2
Module installation		60.8	86.9	121.6	17.0	24.3	34.1
Total	73.5	104.4	133.3	171.8	55.5	63.5	74.1

TABLE XV

Yields of By-Products for the EPNG Lurgi and LLL In Situ Processes

By-product	Yield (lb/hr) EPNG Lurgi process[a]	LLL in situ process[b]
Tar	$ 7,300	$ 8,900
Tar oil	28,000	34,000
Naphtha	20,000	20,000
Crude phenol	9,100	11,100
Ammonia	17,600	21,400
Sulfur	15,600	16,800
Annual revenue	$ 26,800,000	$29,800,000

[a]Burnham coal.

[b]Powder River Basin coal.

TABLE XVI

Financial Analysis of Coal Gasification Concepts--10% DCF Rate of Return

(Millions of Dollars)

Item	Lurgi plant and strip mine	LLL in situ coal gasification					
		25-hole module			9-hole module		
		100% Sweep efficiency	70% Sweep efficiency	50% Sweep efficiency	100% Sweep efficiency	70% Sweep efficiency	50% Sweep efficiency
Revenue:							
By-product sales	26.8	29.8	29.8	29.8	29.8	29.8	29.8
Gas sales	173.3	166.9	200.0	244.2	110.8	120.0	132.1
Total revenue	200.1	196.7	229.8	274.0	140.6	149.8	161.9
Expenses:							
Maintenance material	20.3	9.3	9.8	10.5	8.4	8.5	8.6
Chemicals and catalysts	5.8	5.8	5.8	5.8	5.8	5.8	5.8
Water purchased	.2	.2	.2	.2	.2	.2	.2
Power purchased	5.0	4.6	4.6	4.6	4.6	4.6	4.6
Wages, salaries, etc.	28.5	13.4	15.0	17.2	10.4	10.8	11.3
Administrative expenses	7.0	6.1	6.8	7.7	4.9	5.1	5.3
Well expenses		60.8	86.9	121.6	17.0	24.3	34.1
Subtotal	66.8	100.2	129.1	167.6	51.3	59.3	69.9
Taxes on income	--	--	--	--	--	--	--
Property tax and insurance	15.5	11.0	11.3	11.8	10.4	10.5	10.6
Royalty on coal	6.7	4.2	4.2	4.2	4.2	4.2	4.2
Depreciation	40.3	29.5	30.9	32.8	27.1	27.5	28.0
Subtotal	62.5	44.7	46.4	48.8	41.7	42.2	42.8
Total	129.3	144.9	175.5	216.4	93.0	101.5	112.7
Return	70.8	51.8	54.3	57.6	47.6	48.3	49.2
Cash flow	111.1	81.3	85.2	90.4	74.7	75.8	77.2
Unit gas price ($/MCF)	1.81	1.74	2.08	2.55	1.15	1.25	1.38

TABLE XVII

Financial Analysis of Coal Gasification Concepts--12% DCF Rate of Return

(Millions of Dollars)

Item	Lurgi plant and strip mine	LLL in situ process					
		25 module			9-hole module		
		100% Sweep efficiency	70% Sweep efficiency	50% Sweep efficiency	100% Sweep efficiency	70% Sweep efficiency	50% Sweep efficiency
Revenue							
By-product sales	26.8	29.8	29.8	29.8	29.8	29.8	29.8
Gas sales	209.0	193.0	227.5	273.3	134.8	144.4	157.1
Total revenue	235.8	222.8	257.3	303.1	164.6	174.2	186.9
Expenses:							
Maintenance materials	20.3	9.3	9.8	10.5	8.4	8.5	8.6
Chemicals and catalysts	5.8	5.8	5.8	5.8	5.8	5.8	5.8
Water purchased	.2	.2	.2	.2	.2	.2	.2
Power purchased	5.0	4.6	4.6	4.6	4.6	4.6	4.6
Wages, salaries, etc.	28.5	13.4	15.0	17.2	10.4	10.8	11.3
Administrative expenses	7.0	6.1	6.8	7.7	4.9	5.1	5.3
Well expenses		60.8	86.9	121.6	17.0	24.3	34.1
Subtotal	66.8	100.2	129.1	167.6	51.3	59.3	69.9
Taxes on income	18.3	13.4	14.1	14.9	12.3	12.5	12.8
Property tax and insurance	15.5	11.0	11.3	11.8	10.4	10.5	10.6
Royalty on coal	6.7	4.2	4.2	4.2	4.2	4.2	4.2
Depreciation	40.3	29.5	30.9	32.8	27.1	27.5	28.0
Subtotal	80.8	58.1	60.5	63.7	54.0	54.7	55.6
Total	147.6	158.3	189.6	231.3	101.3	114.0	125.5
Return	88.2	64.5	67.7	71.8	59.3	60.2	61.4
Cash flow	128.5	94.0	98.6	104.6	86.4	87.7	89.4
Unit gas price ($/MCF)	2.18	2.01	2.37	2.85	1.40	1.50	1.65

Therefore it is expected that the actual explosives requirement will be somewhere between the conservative and optimistic estimates. That being so, the expected price of pipeline-quality gas made by the LLL concept under evaluation would fall somewhere between the values presented in Tables XVI and XVII and Figure 8. (The actual quantity of explosives required, hole diameter and spacing, and other parameters must be developed through field testing.) The projected sales price of gas produced by aboveground gasification via the EPNG Lurgi plant has also been calculated for 10 and 12 DCF, and the results are presented in Tables XVI and XVII and Figure 8.

It should also be remembered in reviewing these data that this economic evaluation is for but a single isolated case. The case evaluated considered a 100-ft-thick coal seam with 1000 ft of overburden. Within reasonable limits, as the coal seam gets thicker or as the overburden depth diminishes, the economic incentive for constructing facilities based on this technology would improve. Conversely however, thinner seams or deeper coal would require higher gas prices to yield the same rate of return.

The effect of the assumptions of sweep efficiencies on the economics can be seen (Tables XVI and XVII and Figure 8) by comparing the unit prices for a given module design. For example, at 12% DCF and the 25-blasthole module design, a sweep efficiency of only 50% will result in a price of $2.85 per thousand cubic feet, or an increase of 42% over the price of gas at a sweep efficiency of 100%. The efficiency of energy recovery by this technology must also be determined by field testing.

If none of the by-products is recoverable or if only partial recovery and sale of by-products is possible, a higher gas price would be required to provide the same rate of return.

If the gasification reaction and crude-gas composition are less favorable than has been predicted, the entire process design and economic comparison presented in this report are invalid. It is possible that the processing of coal in situ could be more favorable than in the Lurgi gasifier due to longer residence times and the catalytic effect of shales and extraneous materials present. This too can best be determined by field testing.

In the absence of actual field test data, it is impossible to make a factual assessment of the economic feasibility of the LLL in situ concept. On the basis of best judgments, however, it is considered that gas produced by this technology can be priced competitively. It is therefore recommended that field tests be carried out as soon as possible to obtain firmer estimates of key process parameters. Thereafter an economic feasibility determination can be made on the basis of sounder technology than exists today.

This paper essentially presents the economics section of a much broader study done under a contract whith the Resource Sciences Corporation (RSC) holds with ERDA. [11] Participating in that study were RSC's industrial partners Amoco Production Company, E. I. duPont de Nemours & Co., Inc., Pacific Gas and Electric Company, and Rocky Mountin Energy Company. A similar paper was presented at the Centennial meeting of American Chemical Society (ACS), April 7, 1976. [10] That paper assumed the same basic technical considerations as presented herein, but the ACS Symposium Committee on Comparative Economics for Synfuels Processing had requested the economics be presented on quite different economic considerations.

REFERENCES

1. Second Supplement to the Application of El Paso Natural Gas Co. for a Certificate of Public Convenience and Necessity, FPC Docket No. CP 73-131, October 8, 1973.

2. R. L. McGalliard, Amoco Production Company, private communication, December 17, 1974.

3. P. H. F. Rudolph, "The Lurgi Process--The Route to SNG from Coal," paper presented at the Fourth Synthetic Pipeline Gas Symposium, Chicago, October 30, 1972.

4. R. Z. Mason, Williams Brothers Process Services, private communication, January 6, 1975.

5. R. Z. Mason, Williams Brothers Process Services, private communication, January 15, 1975.

6. K. L. Hujsak, Amoco Production Company, private communication, January 20, 1975.

7. B. V. Randall, Amoco Production Company, private communication, February 12, 1975.

8. C. S. Goddin, Amoco Production Company, private communication, April 18, 1975.

9. Application of Michigan Wisconsin Pipeline Company and American Natural Gas Service Company for a Certificate of Public Convenience and Necessity, FPC Docket No. CP 75-278.

10. "Evaluation of the Lawrence Livermore Laboratory In Situ Coal Gasification Concept," C. S. Goddin, D. E. Hall, and R. Z. Mason, American Chemical Society, April 7, 1976.

11. "An In-Depth Evaluation of LLL's R&D Program for the In Situ Gasification of Deep Coal Seams," February 24, 1976, Prepared for ERDA Under Contract Nos. W-7405-Eng-48 (LLL) and AT (04-3)-1009 (RSC), TID-27008.

12. D. E. Hall, Pacific Gas and Electric Company, private communications, January 1976.

REMOTE MONITORING OF AN IN SITU COAL GASIFICATION PROCESS

by

L. W. BECKHAM, L. C. BARTEL, and R. W. SEAVEY
Sandia Laboratories
Albuquerque, New Mexico 87115

ABSTRACT

Electrical resistivity, passive acoustic, and thermal measurements were made during Phase 1 of the Hanna II in situ coal gasification experiment. The resistivity and acoustic techniques are under investigation for remote monitoring; the thermal measurements provide diagnostic information and the correlation to the process. We present here: (1) the model for the electrical measurements which is derived from the nodal potentials in a resistance network chosen to represent the overburden, coal seam and underburden as well as representative calculations where the presence of various wells is taken into account; (2) comparison of field resistivity data and model calculations from which we determine the path of the reaction zone; (3) models to determine the foci of discrete acoustic events based on compressional wave arrival times; and (4) source locations for acoustic events during gasification, which are in the overburden and are associated with subsidence and cracking over the gasified area. Correlations between the thermal data and the individual techniques result in a consistent picture of the overall gasification process.

INTRODUCTION

Phase 1 of the Second Hanna in situ coal gasification experiment was conducted by the Laramie Energy Research Center (LERC) from February, 1975 until September, 1975 at Hanna, Wyoming. Sandia Laboratories fielded instrumentation for this experiment with the intent of obtaining diagnostic information useful for process understanding and evaluating remote monitoring techniques which would provide information as to the spatial extent of the gasification process. Among the measurement techniques employed were in situ thermometry for direct sensing with electrical resistivity and passive acoustics methods designed to provide remote estimates as to the spatial effects of the process.

These two remote techniques were considered for the following reasons:

(a) The electrical resistivity of coal during in situ coal gasification changes by several orders of magnitude as the reaction zone proceeds between the recovery and injection wells. The wet, virgin coal has a resistivity of 200-250 ohm-m, the dry unaltered coal at ambient temperature has a resistivity in excess of 10^5-10^6 ohm-m and upon devolatization and reaction the resistivity decreases continuously, while hot ($>650°C$), carbonized coal has a resistivity of about 1-10 ohm-m [1].

(b) Various investigators since the early 1940's have measured the acoustic emission properties of material under stress with the intention of using such data as a diagnostic tool for determining impending failure. The Bureau of Mines has conducted an extended study of applying various passive techniques in an effort to understand and determine the stability of underground and surface excavations in rock and soil [2]. Hence, the detection of sufficient acoustic emission might allow for the mapping of the burn region as a function of time.

References at end of paper

In this paper, models for the resistivity and passive acoustic techniques will be presented along with a description of Phase 1 of the Hanna II in situ coal gasification experiment and the instrumentation used to monitor process-related activity. In addition, results for both remote techniques will be presented; results from the resistivity technique will illustrate its usefulness for estimating the spatial extent of the reaction zone while the sources of passive acoustic emissions will be shown to be located in the overburden, associated with the gasification process and representative of subsidence and/or cracking over the reaction region. Thermal measurements will provide the correlation of the remote techniques to the gasification geometry.

MODELING OF THE REMOTE TECHNIQUES

(a) Resistivity Technique [1]

This electrical method utilizes the voltage produced by the current driven between two current electrodes in order to determine an apparent resistivity of the earth. Using the fact that

$$\bar{J} = \sigma \bar{E} \tag{1}$$

and the equality (no sources or sinks of current)

$$\bar{\nabla} \cdot \bar{J} = 0 \quad , \tag{2}$$

where $\bar{J}$, $\bar{E}$, and σ are the current density, the electric field, and the conductivity, respectively, we may model the overburden, coal seam and underburden as a group of finite elements. The resulting model provides a linear matrix equation for the unknown potentials at each nodal point. Specifically, the matrix representation is

$$S \phi = I \quad , \tag{3}$$

where S is the square conductance matrix, ϕ the column matrix for the potentials and I is the column matrix for the current injected into the nodal points from an external source. The conductance matrix is derived from the connection of nodal points in the x, y, and z directions.

For the model calculations here, there is a current source and a current sink at the surface of the earth; no current flows through the surface of the earth except at these points. The horizontal boundaries are assumed to be far enough away so that no current flows through them. In addition, an insulating basement is assumed. Finally, no current flows through the plane connecting the current source and sink; this symmetry is utilized in the calculations. The effects of the conducting casings of the injection and recovery (production) wells are simulated as follows. The casings provide a low resistance path from the coal seam to the surface of the earth. For conduction in the z-direction (vertical direction in Fig. 1) the resistance of the material in a volume and that of the well casing are treated as resistances in parallel. The effects of the casings are ignored for conduction in the horizontal direction.

A schematic for the layout of the model calculations is shown in Fig. 1. In the calculations, the current electrodes A and B are taken to be at the surface of the earth. The potentials obtained from the model calculations are used to calculate the electric field everywhere. A fixed, stationary, surface array of voltage electrodes measures the electric field at the surface. The electric field E_x is defined as $|E_x| = |\Delta\phi|/|\Delta x|$ where $\Delta\phi$ is the potential difference between two points a distance Δx apart.

In plotting $|E_x|/I$ versus x in Fig. 2, the value for $|E_x|$ is plotted mid-way between the positions of the potentials used to determine $\Delta\phi$; I is the current. The calculated points are connected by straight lines. Here VB denotes E_x for the wet, virgin coal, UC denotes E_x for the island of the dry, unaltered coal created by air injection, and the numbers denote E_x for various lengths of the low resistance, carbonized (linkage) path as it grows within the island of dry unaltered coal from the recovery well (R) to the numbered surfaces 1, 2, 3 and 4 to the injection well (I). The letter L denotes the linking of the injection and recovery wells via the low resistance, carbonized coal; this linking will be referred to as electrical linking. The insets in the figure shows the location of the wells and the low resistance path. The electric field component E_x is calculated in the centerline between I and R and 3 m off centerline as shown.

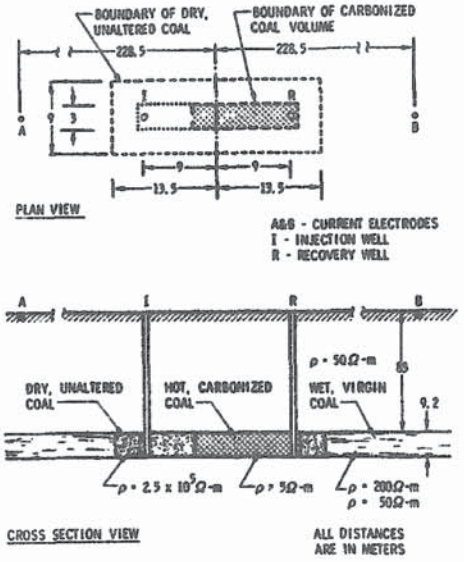


Fig. 1. Schematic Layout of the Model Calculations.

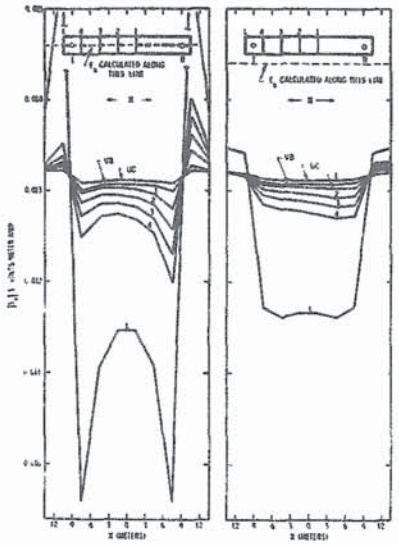


Fig. 2. Model Calculations of $|E_x|$ I vs x. The inset shows the location of the hot carbonized coal path, the location of the injection well I and the recovery well R, and the traverses of E_x on centerline and 3 m off centerline.

The apparent resistivity is proportional to $\Delta\phi/I$ so that the behavior of the apparent resistivity in the field measurements would be similar to that of $|E_x|/I$ as shown in Fig. 2.

Inspection of Fig. 2 shows that when electrical linking has occurred, there is a saddle in the electric field (or apparent resistivity). The lows in $|E_x|$ are near the wells and the crest of the saddle centered between the wells and over the low resistance path. As will be shown, these saddle features were observed in the field data when the injection and recovery wells were electrically linked.

(b) Passive Acoustic Technique

There are several methods of determining the spatial origin of a seismic-acoustic wave propagating within the earth. Eaton [3] describes a method and gives a computer program for determining hypocenters of earthquakes in an earth consisting of uniform flat layers over a half space. In general, however, these techniques involve obtaining the least-squares estimate of the signal source coordinates by minimizing the difference squared between the observed compressional and/or shear wave arrival times and a closed form expression for the theoretical times as determined from a selected structural model. Two least-squares approaches are presented here to illustrate the techniques used for the acoustic signals observed in a geophone array during Phase 1 of the Hanna II in situ coal gasification test. In both cases, an infinite homogeneous media is assumed and compressional arrival times used as input into the appropriate code. The use of a model homogeneous in velocity is justified by the short distances traveled by the acoustic waves.

(1) Non-linear Least Squares

In the non-linear case, the velocity and the spatial origin of the signal source are unknown. The objective function of the least-squares optimization problem is

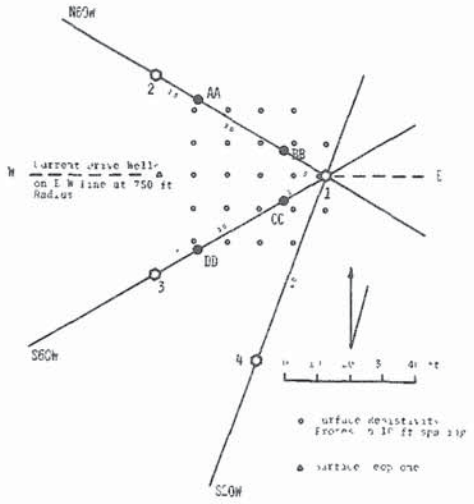


Fig. 3. Phase 1 Well and Instrumentation Layout - May, 1975.

$$f(X,Y,Z,V) = \sum_{i=1}^{N-1} \sum_{j=i+1}^{N} (V(t_i - t_j) - (D_i - D_j))^2, \qquad (4)$$

where the t_i are observed arrival times, the D_i unknown distances and N the number of geophones used. Code FLEXIPLEX [4] allows for arbitrary constraints to be placed on the unknowns so that a solution limited in space may be found.

(2) Linear Least Squares

This alternate technique, described in considerable detail elsewhere [5], assumes a known velocity. The approach is to use the geophone nearest the event as a time reference, eliminate the non-linear terms resulting from distance expressions and then minimize the objective function

$$f(X,Y,Z) = \sum_{j=1}^{N'} (A_j X + B_j Y + C_j Z - E_j)^2 , \qquad (5)$$

where the constants A_j, B_j, C_j, and E_j are derived from the elimination of the non-linear terms and

$$N' = (N-1)(N-2)/2 , \qquad (6)$$

where N is the number of geophones available. The standard deviation of the solution is defined as

$$SD = (f(X^*,Y^*,Z^*)/N')^{1/2} , \qquad (7)$$

where X*, Y*, and Z* are the most likely source coordinates obtained by minimizing Eq. 5.

EXPERIMENTAL DESCRIPTION AND INSTRUMENTATION

(a) Gasification Procedure and Experiment

Phase 1 of the Hanna II in situ coal gasification test was designed to determine in situ permeability, to examine pneumatic and combustion linkage of wells and to conduct a brief gasification test in an implementation of the linked vertical well concept [6-8].

Brandenburg et. al. [9] have adequately described the first phase of the Hanna II gasification process from inferences made on the thermal data. Hence, herein we will limit the discussion to the general considerations of the Hanna II, Phase 1 linkage and gasification. Fig. 3 provides a plan view of the experiment with associated surface instrumentation.

The test consisted of two major periods of linkage and gasification; the periods have been denoted as Phase 1a and Phase 1b. In both phases of linkage, reverse combustion was used to establish sufficient permeability for gasification. Phase 1a was a linkage and sustained gasification between Wells 1 and 3 of Fig. 3. Phase 1b was similar except that linkage and gasification occurred between the line connecting Wells 1 and 3 and Well 2. During Phase 1a, air injection was at Well 3 and recovery at Well 1. However, for Phase 1b, Well 3 was shut in with injection and recovery at Wells 2 and 1, respectively. Table I supplies a summary of major Phase 1 activity.

(b) Instrumentation

Both electrical and passive acoustic data were collected daily throughout the course of the experiment. Each technique will be discussed.

Table I. Summary of Phase 1 Activities

DAY (1975)	ACTIVITY	DATE (1975)
97	Air injection initiated at Well 1	April 7
108	Air Injection changed to Well 3	April 18
139	Air Injection phase terminated	May 19
141	Heater started in Well 1; Phase 1a initiated	May 21
145	Heater removed; air injection switched to Well 3 and production at Well 1	May 25
155	Reverse combustion linkage completed, Phase 1a	June 4
192	Phase 1a Terminated; initiated Phase 1b Air injection switched to Well 2 and production remained at Well 1	July 11
203	Reverse combustion linkage completed, Phase 1b	July 22
240	Phase 1b Terminated; air injection halted	August 28

(1) Electrical Measurements:

The resistivity experiment was designed to measure the change in apparent resistivity of the earth due to the in situ coal gasification process. The surface potentials generated by the injected current were measured to provide changes in this apparent resistivity as a function of time.

The current source electrodes consisted of 30-foot (9.1 m), 7-inch (17.8 cm) cased wells located 750 (227 m) feet east and west of the geometrical center of Wells AA, BB, CC, and DD in Fig. 3. The current source generated a three-cycle, bi-polar square wave current of four-second period and approximately 18 amperes peak-to-peak. Rechargeable batteries were used for the current supply.

Eighteen surface potential difference measurements were made from a grid of twenty-three potential electrodes as shown in Fig. 3. This arrangement is similar to the Schlumberger technique[10]. Potentials between each east-west pair were measured. The probes were emplaced below frost-line a depth of five (1.5 m) to six (1.8 m) feet and contained a copper sulphate solution which passed slowly through a ceramic frit to insure a conductive, non-polarizing contact with the earth. Strong background DC potentials on the order of 70 mv were noted for this area and capacitors were installed on each probe circuit to eliminate them.

Analog records of the potentials between each pair of potential electrodes, as well as the current, were recorded on magnetic tape every four hours.

(2) Passive Acoustic Measurements:

Vertical axis geophones with a sensitivity of 0.6 volts/in/sec (0.24 volts/cm/sec) were used to monitor passive acoustic activity. These geophones exhibit a reasonably flat spectrum from 10-1000 Hz, and a representative set of nine geophones tested proved to lie within five percent of manufacturer's specification [11]. The geophones were grouted in Wells AA-DD at locations of -5(-1.5), 6(1.8), 21(6.4) and 57(17.3) feet (meters) referenced to the coal seam floor. Outputs of these sensors were amplified and preserved daily over arbitrary five minute intervals on a standard fourteen track magnetic tape instrumentation recorder.

Both analog passive acoustic and surface resistivity data were recorded using voltage controlled oscillators with sensitivities and bandwidths chosen to be consistent with sensor response. Analog data were returned to the Sandia Data Processing Center, filtered, digitized and placed on tapes which were in a format compatible with the CDC 6600 in order to allow further analysis.

RESULTS FROM PHASE 1

(a) Phase 1a

Selected temperature measurements during Phase 1a are presented in Figures 4 and 5. These figures indicate the rapid temperature rise near midseam from Day 156 to Day 158. These rapid rises followed the linkage on Day 155 (as indicated by the significant decrease in injection pressure at Well 3). Brandenburg et. al. [9] have shown that these data suggest that the hot, thermal linkage was localized near midseam.

Large decreases in the resistivity during Phase 1a were measured by probes in the vicinity of the 1-3 line on Day 157. These changes are indicated in Figure 6 which provides resistivity contours normalized to pre-experiment values for before and after the linkage. These decreases were due to the electrical linking of Wells 3 and 1, the injection and recovery (production) wells. They were not noted near Wells 2, AA and BB and occurred two days after the subsurface porous link was established as defined by the pressure drop and corresponded to the time of the temperature increases at midseam in Wells CC and Well DD. Note the resistivity saddle which appears along the 1-3 line after electrical linking and as predicted by the model calculations. This saddle indicates the linkage path is along the 1-3 line as expected and the path is confirmed by the thermal measurements.

The reason for the delay of the electrical indication following linkage was that the temperature of the initial carbonized coal link was probably not sufficiently high to give a low resistivity path. With the beginning of gasification, such high temperatures (> 1200°F (>650°C)) were obtained. During gasification the volume of the cavity expanded so that the combustion front moved away from the injection well, Well 3. Indication of the increase in volume of the cavity near the injection well is given in Fig. 5 by the temperature rises at levels 25 and 30 in Well DD. With this growing cavity, good electrical "contact" was lost between Well 3 and the combustion region; this lead to an increase in the resistivity approximately two days after the electrical linking as shown in Fig. 2 when the low resistivity path does not connect the well casings.

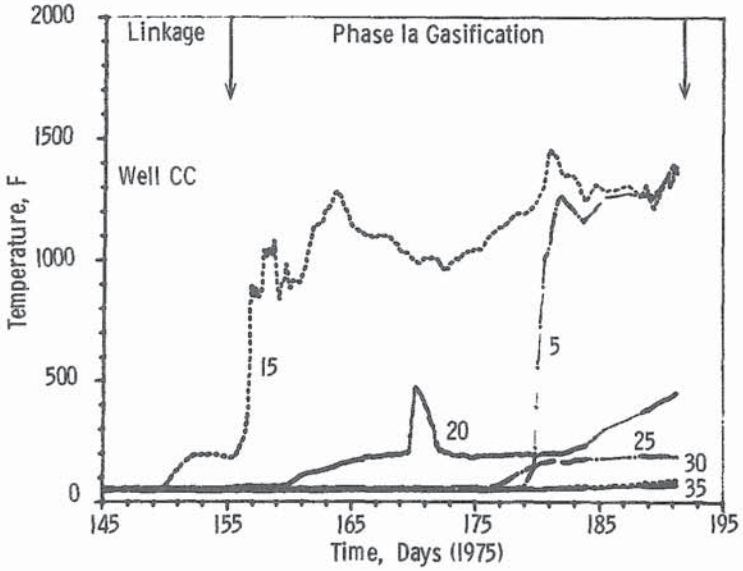


Fig. 4. Selected temperatures in Well CC during Phase 1a. Thermocouple locations (feet) are referenced to the bottom of the 30 foot (9.1 m) coal seam.

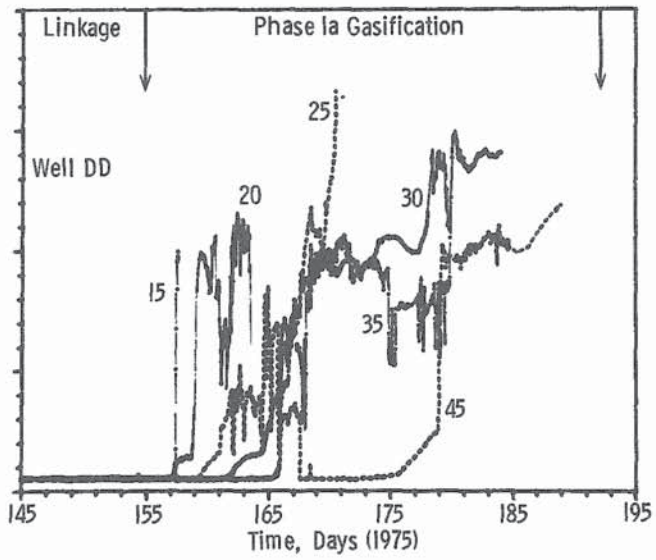


Fig. 5. Selected temperatures in Well DD during Phase 1a. Thermocouple locations (feet) are referenced to the bottom of the 30 foot (9.1 m) coal seam.

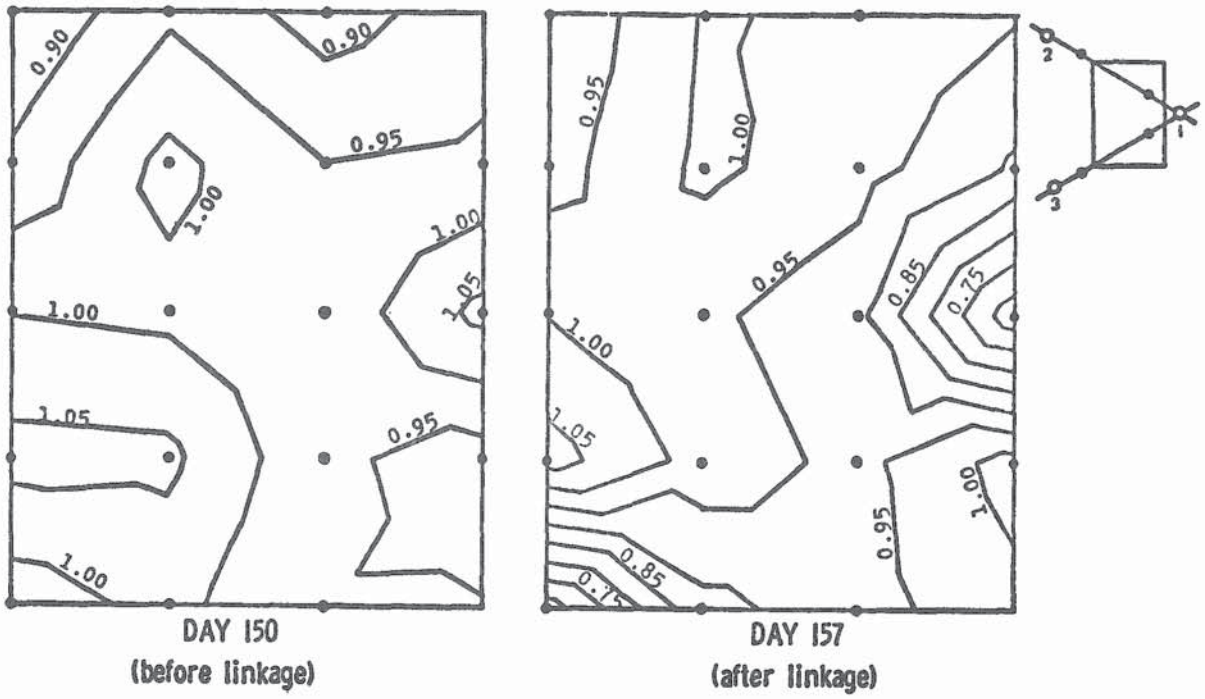


Fig. 6. Normalized resistivity plots from a surface probe array. The resistivity was normalized to its pre-experiment value. The array location relative to wells is shown at the top of the figure.

Soon after linkage in Phase 1a was completed, temperatures rose to approximately 1000°F (537°C) at two levels in Well DD and at midseam in Well CC. By Day 168 temperature increases to approximately 1000°F (537°C) from midseam to the seam top indicated widespread combustion in the vicinity of Well DD. The temperature rise at the 5-foot (1.5 m) level in Well CC and the absence of high temperatures in the upper part of the seam suggests that at this location combustion had moved into the lower half of the seam but not into the upper part of the seam by Day 192 when all the thermocouples in Well CC failed. In Well DD the initial erratic temperature variations in the major reaction zone have been interpreted to indicate local collapse of coal and roof materials [12]. The measurement of approximately the same temperature at several levels in Well DD suggests that the collapse and mixing of material in the reaction zone resulted in uniform temperatures across the seam. Due to equipment failure, no resistivity data were collected during the latter part of the gasification period.

Three basic acoustic signal types were observed during the first phase of the Hanna II test [5]. The first type detected was a continuous burning noise induced in a geophone because of the proximity of the instrument to the process. Such signals provided no process information because of their low level and ill-defined character. The second type, of a discrete nature, generally lasted for a few seconds and died out. Because of an insufficient number detected and/or a waveform too complex to accurately determine compressional or shear wave arrival times this type was also useless in the correlation of process related activity. The third and most useful type observed consisted of relatively high frequency pulse-like signals with clearly evident compressional arrival times. An example of the appearance of a signal resulting from such an event and observed in a geophone above the coal seam is presented in Fig. 7.

Data of this type were monitored daily over five minute intervals throughout the course of the experiment. Since the source location techniques require a minimum of five geophones for a unique result, the detection of a signal in at least five geophones was the criterion used to define that an acoustic event had occurred. The frequency of occurrence of these events is presented in Fig. 8. The indication here is that the dominant activity occurs during gasification and after the creation of void-like regions in the seam. Especially on Days 167-170, the thermal data suggested local collapse of coal and roof material near Well DD as indicated by comparison of Figs. 5 and 8.

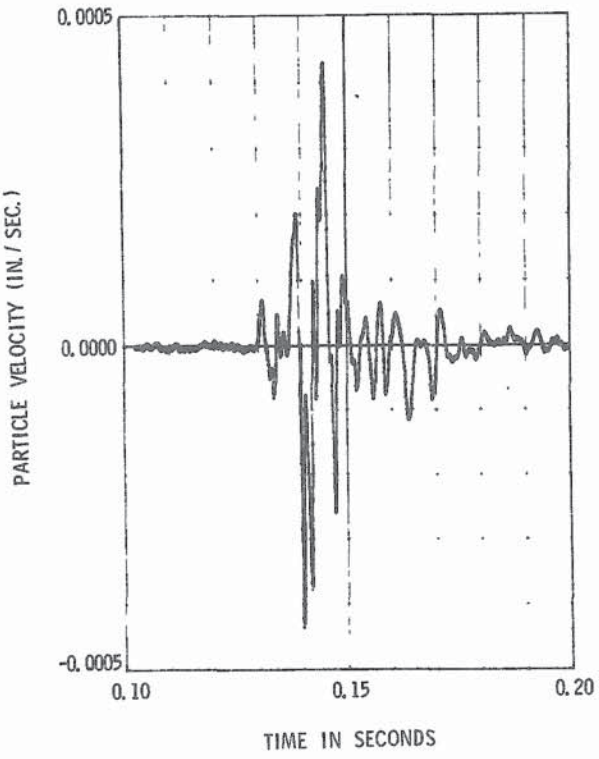


Fig. 7. Representative acoustic signal observed in geophone array.

By visually inspecting the records for signal arrival times and using the linear source location technique described above, several source locations were obtained and are displayed in Fig. 9. These data are from Day 168 and Day 171 and indicate a predominance of activity in the overburden. The fact that overburden activity is the major source of data throughout the course of the experiment is substantiated by signal levels, i.e., signals in geophones above the coal seam invariably will have greater amplitude than those in or below the seam. The interpretation of the source locations obtained for these two days is that the majority of activity appears to be occurring above the line connecting Wells 3 and 1 and relatively close to Well DD. The source of these signals is most likely subsidence and cracking in the overburden over the gasified area.

(b) Phase 1b:

Figures 10 and 11 provide thermal profiles for Wells AA and BB during Phase 1b. Note that linkage was detected on Day 203 from observations of the pressures and flows. Using Figures 10 and 11 one may conclude that the linkage was not on a line connecting Wells 1 and 2 (see Fig. 3) and that excessive thermal fluctuations are not evident near the injection well (i.e. in Well AA).

Conclusions of an off-line linkage for Phase 1b are substantiated further by the resistivity technique. Normalized resistivity contour plots for Phase 1b are shown in Fig. 12. From this figure, it is evident that the resistivity decreased near Well 2 when electrical linkage was established. The contours shown on Day 206 indicate the loss of electrical contact with Well 2 and the development

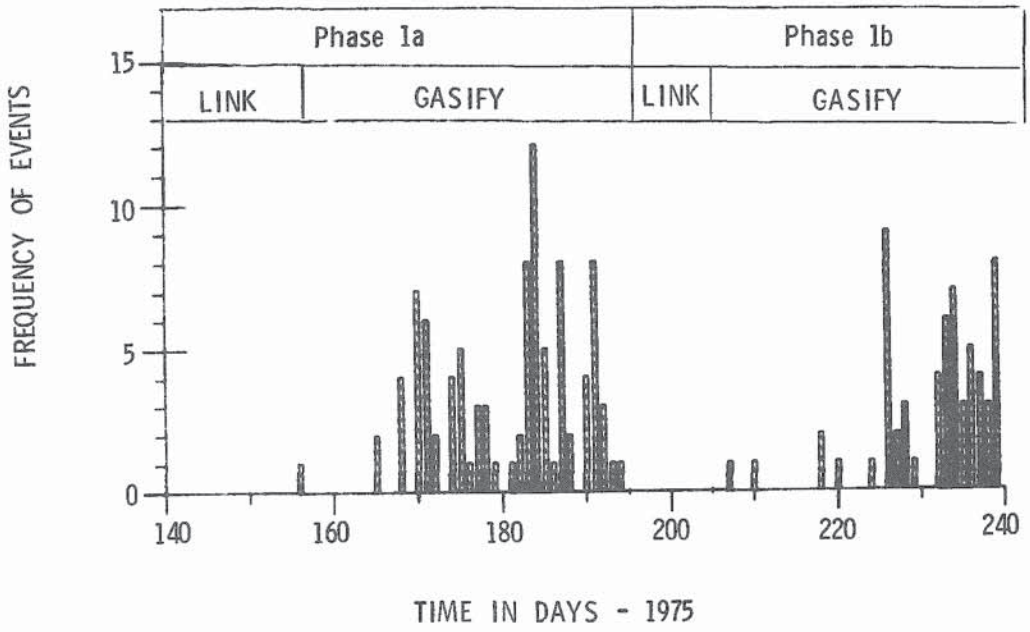


Fig. 9. Distribution of acoustical data with time during Phase 1.

of a resistivity saddle in the upper left hand corner of the array. The contours shown on Day 218 show a general increase in the resistivity along with the resistivity saddle between Well 2 and the 1-3 line. The probable reasons for this increase were: (1) a large area was affected leading to a larger island of dry, unaltered, high resistivity coal, and (2) even though the void was surrounded by hot, conducting coal, the larger void lead to an increased electrical resistance of the coal seam and thus increased resistivity. The resistivity saddle is probably centered over the cavity surrounded by hot, carbonized coal resulting from gasification in Phase 1b. Because of the limited extent of the resistivity array, the boundaries of the cavity can not be determined but only estimated. The lack of a significant temperature rise recorded in Well BB supports the assumed location of the path.

Inspection of Fig. 8 will indicate that similar passive acoustic activity was observed during Phase 1b as compared to Phase 1a. Unfortunately, the loss of most of the geophones due to process-related effects precluded additional source locations. However, signal levels were again greatest in the overburden suggesting that subsidence was the major cause of passive acoustic activity.

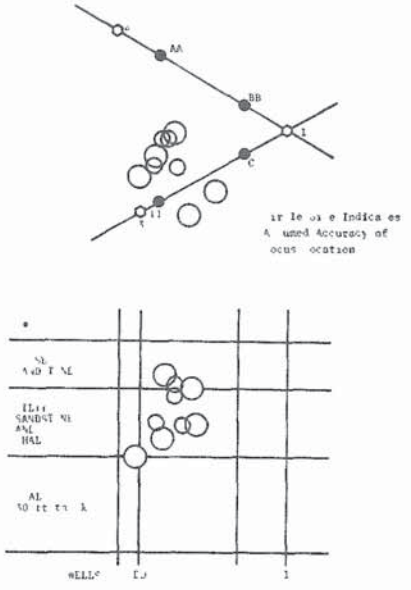


Fig. 9. Discrete signal source locations Day 168 and Day 171.

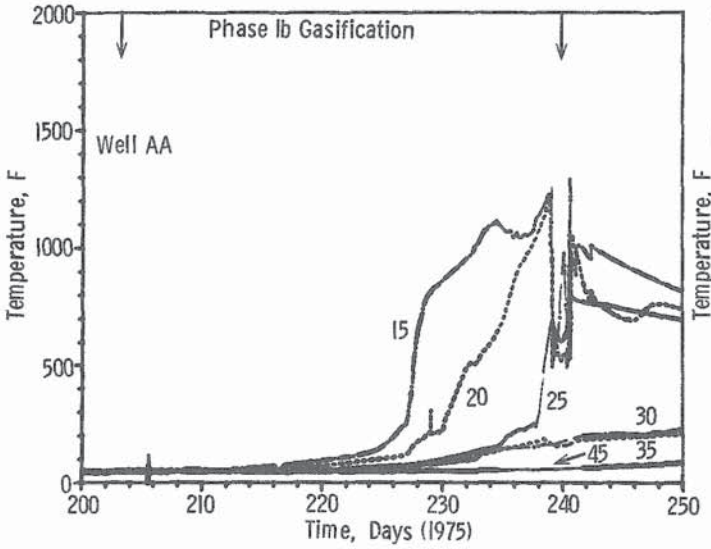


Fig. 10. Selected temperatures in Well AA during Phase 1b and quench. Thermocouple locations (feet) are referenced to the bottom of the 30 foot (9.1 m) coal seam.

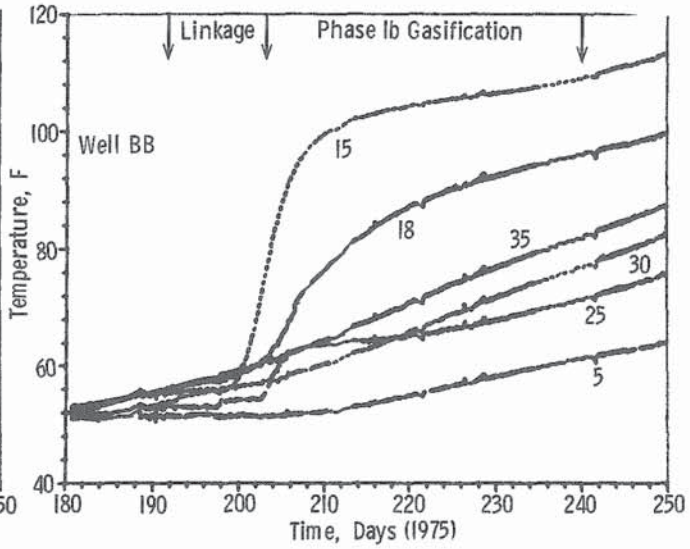


Fig. 11. Selected temperatures in Well BB during Phase 1b thermocouple locations (feet) are referenced to the bottom of the 30 foot (9.1 m) coal seam.

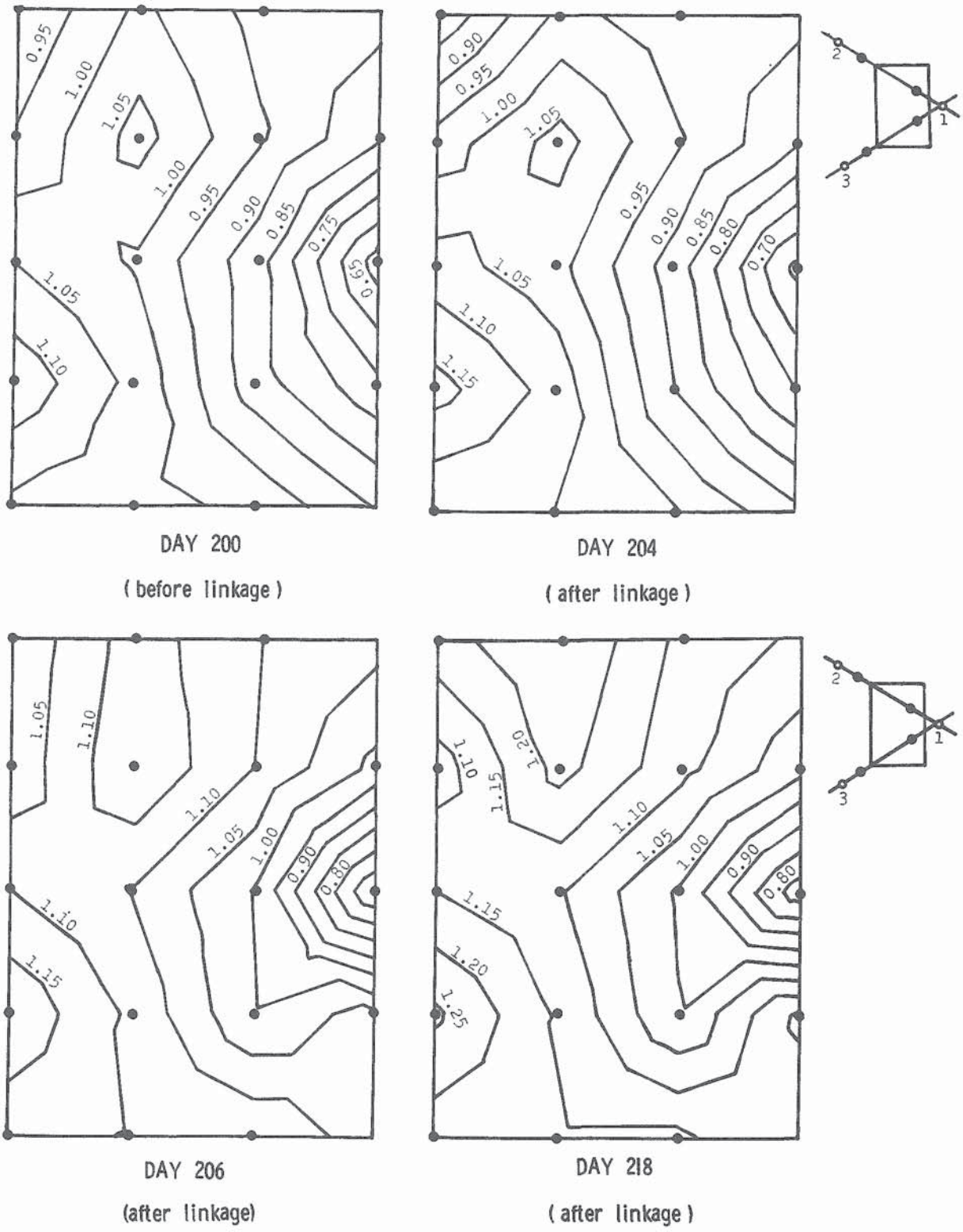


Fig. 12. Normalized resistivity plots from a surface probe array. The resistivity was normalized to its pre-experiment value. The array location relative to wells is shown.

CONCLUSIONS

Model calculations of the modified Schlumberger resistivity technique [10] have predicted the behavior of the surface electrical potentials observed over an in situ coal gasification process at Hanna, Wyoming. Models for determining the foci of discrete acoustic emission signals have located the sources of useful signals observed during this test in the overburden above the burning coal seam; these data occur during gasification and not during the thermal reverse combustion linkage period. Correlation with thermal measurements confirms that both models provide a reasonable spatial representation of the process, i.e.: (1) the resistivity method allows for the remote detection of linkage and of variations of the motion of the process in two dimensions, and (2) the detection and location of acoustic emission data indicates that gasification of the coal seam produces subsidence and cracking in the overburden and that these data are representative of the creation of void like regions within the seam.

The resistivity and passive acoustic techniques show promise in that they are feasible for remotely monitoring the extent of the process. More extensive modeling is required for the following reasons: (1) the resistivity model requires refinement so that the edges of the reaction zone are more clearly defined, and (2) the development of an automated detection and source location scheme is necessary so that large volumes of acoustic data may be processed during gasification. In addition, because of severe signal attenuation, efficient means of detecting low level events will be required for this technique to be incorporated into an in situ coal gasification process monitoring scheme. Model studies to reach both of these goals are currently underway.

ACKNOWLEDGMENTS

The authors are grateful to D. A. Northrop, S. D. Stearns, R. P. Reed, S. G. Beard and J. A. Beyeler for many helpful comments and suggestions. S. A. Winters and R. N. Sanderville were responsible for the data collection system. R. J. Beyatte, W. B. Miller and H. A. Schuler processed the majority of data through Sandia's Data Processing Center. Many other Sandians were either directly or indirectly responsible for the successful completion of this work. The Laramie Energy Research Center personnel are due considerable credit for executing a successful gasification experiment as well as providing an atmosphere amenable to the study of this problem.

This work was supported by the Division of Oil, Gas, and Shale Technology, United States Energy Research and Development Administration. Dr. Paul C. Wieber of that organization is manager of the in situ coal gasification program.

REFERENCES

1. Bartel, L. C.: "Model Calculations of Electric Fields Measured with a Fixed, Stationary Array to Monitor In Situ Coal Gasification," Sandia Laboratories Report, SAND76-0076 (Feb. 1976).

2. Blake, W., Leighton, F., and Duval, W. I.: "Microseismic Techniques for Monitoring the Behavior of Rock Structures," Bureau of Mines Bulletin 665 (1974).

3. Eaton, J. P.: "HYPOLAYR, A Computer Program for Determining Hypocenters of Local Earthquakes in an Earth Consisting of Uniform Flat Layers Over a Half Space," U.S. Geological Survey, Open File Report.

4. Himmelblau, D. M.: Applied Nonlinear Programming, McGraw-Hill, New York (1972) Chapter 8.

5. Beckham, L. W.: "Analysis of Passive Acoustic Signals Generated by an In Situ Gasification Process," Sandia Laboratories Report, SAND76-0124 (March, 1976).

6. Campbell, G. C., Brandenburg, C. F., and Boyd, R. M.: "Preliminary Evaluation of Underground Coal Gasification at Hanna, Wyoming," BuMines TPR 82, (Oct. 1974), 14pp.

7. Schrider, L. A. Jennings, J. W., Brandenburg, C. F., and Fischer, D. D.: "An Underground Coal Gasification Experiment, Hanna, Wyoming," paper SPE 4993 presented at SPE 49th Annual Fall Meeting, Houston, Oct. 6-9, 1974.

8. Brandenburg, C. F., Fischer, D. D., Campbell, G. C. Boyd, R. M., and Eastlack, J. K.: "The Underground Gasification of a Subbituminous Coal," Am. Chem. Soc. National Spring Meeting, Philadelphia, April 1975.

9. Brandenburg, C. F., Reed, R. P., Boyd, R. M. Northrop, D. A., and Jennings, J. W.: "Interpretation of Chemical and Physical Measurements from an In Situ Coal Gasification Experiment," Paper SPE 5654 presented at SPE 50th Annual Fall Meeting, Dallas, Sept, 28-Oct. 1, 1975.

10. Bartel, L. C.: Sandia Laboratories, Personal Communication.

11. Beyeler, J. A.: Sandia Laboratories, Personal Communication.

12. Beard, S. G. and Reed, R. P.: "Some Insights from Temperature Measurements on Recent Underground Coal Gasification Experiments," to be presented at the 2nd Annual Underground Coal Gasification Symposium, Morgantown, West Virginia, August 10-12, 1976; proceedings will be published.

REAL TIME PROCESS MONITORING IN UNDERGROUND COAL GASIFICATION

D. E. EASTWOOD,[1] J. K. EASTLACK,[2] J. W. JENNINGS,[3]
S. B. KING,[1] W. J. LANUM,[1] AND D. F. MOORE[1]

ABSTRACT

The LERC Hanna II experiment uses a multiprogramming system for real-time data acquisition, analysis, and display. Within the framework of the real-time executive program for the computer, time-scheduled user programs are executed and data accumulated. The time scale of the experiment permits averaging of data over one-hour intervals, but the sampled data before averaging may be displayed or plotted for observation and control. The data include pressure, temperature, and flow information and on-line gas analyses. From this information, material balance and other calculations essential to an insight into underground processes may be calculated on demand. Computer control of the position of selected valves has also been utilized.

Hourly averaged data are written into a disc file, which each midnight receives a name unique to the day just ended. The hourly history files are available for access by time-sharing programs, of lower priority than the data acquisition programs. A user file directory permits accumulation of information about the daily files, and makes the files easily transportable to another computer system. The real-time data acquisition and processing has permitted a degree of understanding and operator control which has contributed greatly to the success of the project.

INTRODUCTION

This paper describes the contributions of the computer data acquisition system to the LERC Underground Coal Gasification project. These contributions include immediate display of data; calculation of flow rates and material balances; trend analysis and plotting of temperature, pressure, flow, gas composition, and heating value data; storage of gas analysis data; and complete access to data files without interference with the real-time data acquisition. It is the opinion of all project personnel that these real-time acquisition and analysis capabilities have made significant contributions to the success of the experiments.

All of the authors listed have contributed to the initiation or evaluation of the data acquisition system. Specific acknowledgment should be given to Dr. Jim Jennings and to then graduate student, Jim Eastlack, for the initial recognition of the potential value of a computerized experiment and for the bulk of the program development. Much of the material for this paper has come from Eastlack's thesis [1].[4]

---

[1]ERDA, Laramie Energy Research Center, Laramie, Wyoming.
[2]Atlantic Richfield Company, Midland, Texas.
[3]Texas A&M University, College Station, Texas.
[4]Reference given at end of paper.

We will describe the physical computer installation, the logical program structure, the communication of information among programs, the nature of the data received from the experiment and the kinds of output information available to project personnel. We will also indicate what has been done toward computer control of the underground experiment, and the capabilities of the system for handling the more extensive data expected from Hanna III.

PHYSICAL INSTALLATION

The computer used is the Hewlett Packard Model 2100, shown in Figure 1 in the computer room used at the present time. There were severe dust and electrical power problems in the original installation, as may be imagined from the exposed nature of the Hanna site. The improved facility pictured has a separate heating and air conditioning unit, humidifier, electrostatic precipitator, and lightning arrestors on all feasible input data and power lines. The computer room is separated from the outside by at least two doors at each entry (Figure 2), but there is still some problem with dust. For Hanna III and subsequent experiments we plan a more completely sealed computer installation in a movable building.

COMPUTER SYSTEM CONFIGURATION

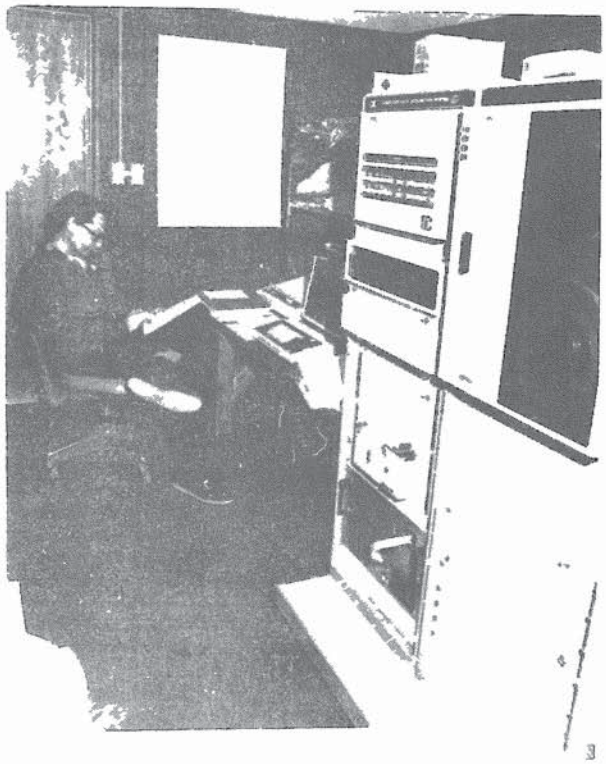
The central and peripheral equipment making up the Hanna II data system is shown in Figure 3. The shaded boxes represent data input or control components. The 100 channel data logger, originally planned not only as an input channel but also as a back-up device which could continue to record data even if the computer went down, has proven to be less reliable than the computer and has now been removed from the system with the chromel-alumel thermocouples and pressure sensors being connected directly to the low-level and high-level analog-to-digital (A/D) channels. The system capacity at present is 112 low-level and 48 high-level channels. Most of the thermocouple lines were provided by Sandia and are also recorded by them on data-logger/magnetic tape equipment for later analysis at Albuquerque. Our experience has been that the immediate availability of this data through the computer, together with the ability to compute flow rates and other derived values, has given the project engineers a far greater understanding of the developing underground experiment than could be obtained by manual readings and hand calculations.

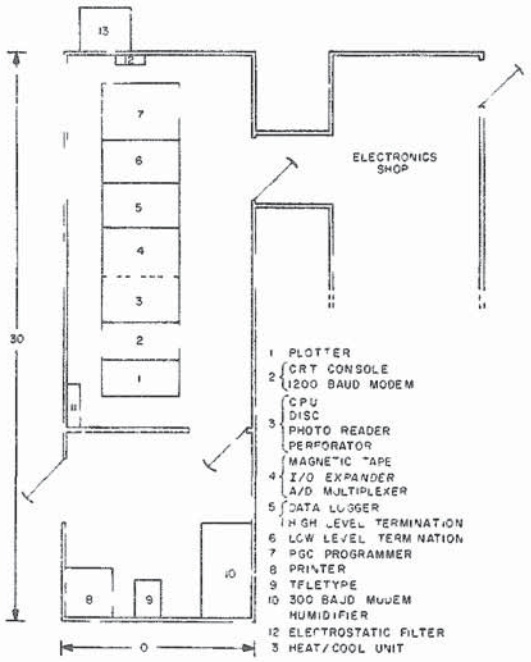
MEMORY UTILIZATION

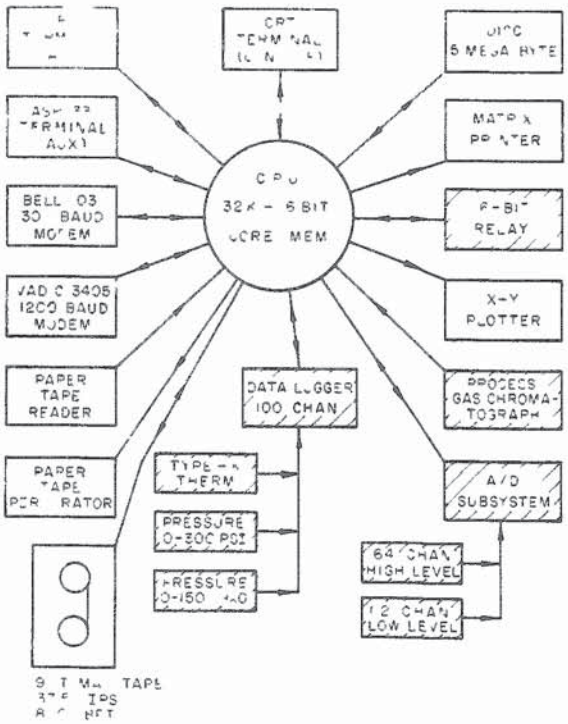
The programs for the Hanna II project operate through the Hewlett-Packard Real-Time Executive system, RTE II, which has proven to be reliable and to have most of the capabilities needed. This paper will not go into detail on the system organization, but some perspective may be gained by looking at the project's utilization of the 32-k memory (Figure 4). This is a simplified picture of the proportion of memory devoted to the operating system (shaded) and to the major types of user programs (dotted background). The RTE II System has enough capabilities that almost all the application programs could be written in FORTRAN IV. The FORTRAN COMMON Region (shown as white) is the central communication area for real-time data acquisition and display. Notice that the shaded system area takes up about one-half of the 32-k memory, which may seem like a lot, but it performs many functions for the users. The space not used by the system is divided into several regions, the most important being the foreground area used for the real-time programs (about 7744 locations including COMMON) and that for the background programs (about 11200 locations). Programs from the disc unit are brought in and written out from these regions according to the needs of the real-time system and the requests of the project engineers for data display. The point to notice here is that the system usage of memory would not need to be greatly increased if the memory size were doubled, assuming that the system retained its present functions, so that almost all the additional memory could be used for application programs. Thus an increase of memory size to 64k would increase the space available to user programs from 19k to about 48k or about 250 percent. That would allow more frequently-used programs to be permanently resident in memory, increasing the efficiency of operation and making it feasible to handle larger quantities of data. Thus the already proven system design for Hanna III may easily be extended to handle future needs.

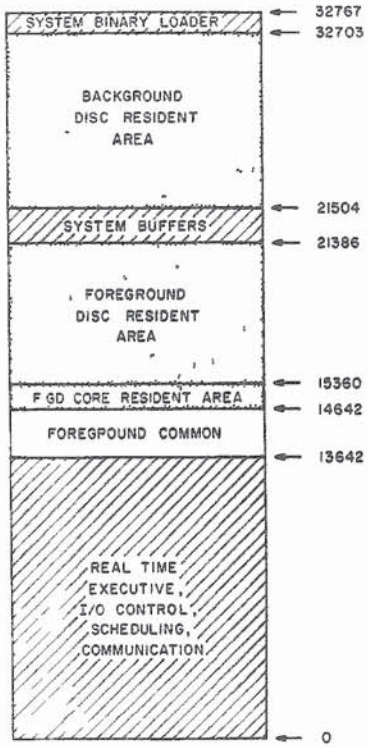
PROGRAM STRUCTURE

The requirements of the real-time data acquisition programs, shown in Figure 5, determine the structure of all other programs. A single program is time-scheduled to run every five minutes. The control program initiates the execution of two data acquisition programs, which access low-level and high-level analog-to-digital channels and deposit the raw data in the FORTRAN COMMON region. A sequence of other programs follow, as indicated in the figure, to convert the data to meaningful units and to take care of routine functions. Each hour the 5-minute data is averaged,




13
12
7
6
5
4
3
2
1
30
ELECTRONICS SHOP
8
9
10
0
1 PLOTTER
2 CRT CONSOLE
1200 BAUD MODEM
3 CPU
DISC
PHOTO READER
PERFORATOR
4 MAGNETIC TAPE
I/O EXPANDER
A/D MULTIPLEXER
5 DATA LOGGER
HIGH LEVEL TERMINATION
6 LOW LEVEL TERMINATION
7 PGC PROGRAMMER
8 PRINTER
9 TELETYPE
10 300 BAUD MODEM
HUMIDIFIER
12 ELECTROSTATIC FILTER
13 HEAT/COOL UNIT


CRT TERMINAL
DISC 5 MEGA BYTE
BELL 03 300 BAUD MODEM
CPU 32K - 8 BIT CORE MEM
8-BIT RELAY
VAD C 3405 1200 BAUD MODEM
X-Y PLOTTER
PAPER TAPE READER
DATA LOGGER 100 CHAN
PROCESS GAS CHROMATOGRAPH
PAPER TAPE PERFORATOR
A/D SUBSYSTEM
PRESSURE 0-300 PSI
64 CHAN HIGH LEVEL
12 CHAN LOW LEVEL


SYSTEM BINARY LOADER
32767
32703
BACKGROUND DISC RESIDENT AREA
SYSTEM BUFFERS
21504
21386
FOREGROUND DISC RESIDENT AREA
FGD CORE RESIDENT AREA
15360
14642
FOREGROUND COMMON
13642
REAL TIME EXECUTIVE, I/O CONTROL, SCHEDULING, COMMUNICATION
0

stored on disc, and printed. Every eight hours, a shift summary of averaged data is printed and a complete copy of the data disc is written to tape for backup. At midnight, the name of the disc file containing the last 24 hours of data is changed to identify the file by Julian date, and a new daily file is created. One removable disc holds about 60 days of data.

In addition to thermocouple and transducer analog signals sampled on a scheduled basis, there is an analog signal read from the process chromatograph on an interrupt basis. A bleed stream from the production gas line is passed through a gas clean-up system which is in turn sampled every 15 minutes by the process chromatograph. During the chromatographic analysis, analog signals (proportional to component concentration) from the chromatograph are read by the computer and at the end of an analysis a gas composition is calculated. This analysis is stored on a disc file until the end of the hour. At that time all analyses for the hour are printed out on the line printer and stored in another disc file with the previous hours' gas analyses for that day. At midnight the disc file with the day's content of gas analyses is given a Julian day name allowing this to be accessed the same as all other operating data. To supplement the process chromatograph an additional chromatograph is used for sampling gas manually instead of automatically. This chromatograph is used for three different purposes. First, to sample those instrument wells which contain gas canisters within the coal seam to determine gas composition at locations other than production wells. Secondly, to sample production gas during the linkage phase when production flows and pressures are very low making automatic sampling difficult. Lastly, as a back-up for the automatic process chromatograph. These samples are collected in a sample bottle and injected by hand into the chromatograph. Analyses are entered into the computer by hand where they are stored in a disc file with the operating data and can be accessed by various programs.

The automatic operation of the time-sequenced programs is supplemented by a variety of programs for data analysis and display. Usually the hourly-averaged data is more than sufficient for the experiment, which has a duration measured in months. However, when conditions are changed or when underground events seem to be occurring rapidly, an automatic printout of the 5-minute data can be initiated. The latest 5-minute data is always available for examination on one of the terminals, or a copy may be sent to the printer by operator action at any time. Current temperature data from instrumentation wells can be plotted by level as a bar graph. The temperature distribution in several wells as a function of level may be displayed in tabular form. The current pressures and flow rates may also be displayed or printed.

All of the foregoing are programs for examining the latest data. Other programs which can access the previous data on the disc file, by hour and by day, are even more important for understanding the progress of the experiment. These include programs for obtaining hourly data either in a tabular format or with X-Y plotting routines. Data from each 60-day period must be handled separately at present, but this may be done during the course of the experiment by changing discs which takes about three minutes.

PROGRAM MODULARITY

The functional separation shown in Figure 5 is reflected in the program modules. The modules are small, easy to understand and to change. Many modules are independent of the detailed nature of the experiment, i.e., during data acquisition all channels are read; the absence of data is indicated by an external switch setting. Those modules which must apply specific information about the experiment, such as what conversion factors to use on what channels, use values stored in the COMMON data base whenever these factors are subject to change. Other programs use data description techniques to reduce dependence of their logical structure upon the specific experimental setup.

EXAMPLES OF COMPUTER OUTPUT

Before describing the various outputs available to the users of the Hanna computer, we should emphasize, as illustrated in Figure 3, the different interactive terminals incorporated into the present system. On site there are two CRT's, a teletype, and a TI Silent 735 terminal that may interact with the system. In addition there is a 120 character/Sec TERMINET terminal in Laramie that has the same accessibility as the on-site terminals. All of the user requested outputs, except X-Y plotting outputs, can be obtained on any of these terminals.

The scheduled hourly output of averaged 5 minute data appears in Figure 6. It includes all recorded channels of temperature, pressure and calculated flows for the hour. A similar type

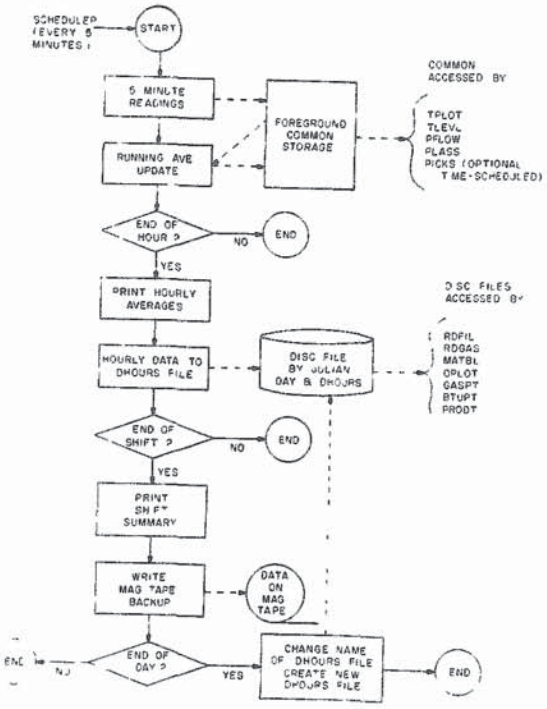


Fig. 5 - Data Acquisition Program Sequence

HOURLY REDUCTION OF OPERATING DATA
BEGINNING AT TIME 286 12 5 4

LOW LEVEL APX —— TEMPERATURES IN DEG. F

	1	2	3	4	5	6	7	8
0	-999.00	588.84	-999.97	161.84	-999.98	679.44	68.93	41.89
8	78.40	1381.48	1478.34	1586.48	1949.88	1943.72	1214.10	1216.13
16	1224.48	1233.68	1231.76	251.51	522.80	276.80	113.56	110.88
24	63.56	59.08	41.76	89.31	89.43	1446.48	14 [illegible]	1399.96
32	1397.56	1363.92	1398.48	1464.16	267.80	231.16	1346.24	435.74
40	-999.00	86.16	35.84	562.71	448.48	471.76	316.48	113.78
48	-999.00	-999.00	-999.00	-999.00	-999.00	-999.00	-999.00	-999.00
56	-999.00	-999.00	-999.00	-999.00	-999.00	-999.00	-999.00	-999.00
64	-98.10	743.01	156.00	1212.24	1024.20	15.20	16.16	16.10
72	46.00	46.00	48.76	98.48	57.56	-999.00	-999.00	-999.00
80	-999.00	-999.00	-999.00	-999.00	-999.00	-999.00	-999.00	-999.00
88	-999.00	-999.00	-999.00	-999.00	-999.00	-999.00	-999.00	-999.00
96	-999.00	-999.00	-999.00	-999.00	-.30	23.16	2.40	1.15
104	63.20	-.56	1.70	.10	2.18	-999.00	-999.00	-999.00
112	-999.00	-999.00	-999.00	-999.00	-999.00	-999.00	-999.00	-999.00
120	-999.00	-999.00	-999.00	-999.00	-999.00	-999.00	-999.00	-999.00
128	-999.00	-999.00	-999.00	-999.00	-999.00	-999.00	-999.00	-999.00
136	-999.00	-999.00	-999.00	-999.00	-999.00	-999.00	-999.00	-999.00
144	-999.00	-999.00	-999.00	-999.00	-999.00	-999.00	-999.00	-999.00
152	-999.00	-999.00	-999.00	-999.00	-999.00	-999.00	-999.00	-999.00
160	-999.00	-999.00	-999.00	-999.00	-999.00	-999.00	-999.00	-999.00
168	-999.00	-999.00	-999.00	-999.00	-999.00	-999.00	-999.00	-999.00
176	-999.00	-999.00	-999.00	-999.00	-999.00	-999.00	-999.00	-999.00
184	-999.00	-999.00	-999.00	-999.00	-999.00	-999.00	-999.00	-999.00
192	-999.00	-999.00	-999.00	-999.00	-999.00	-999.00	-999.00	-999.00
200	-999.00	-999.00	-999.00	-999.00	-999.00	-999.00	-999.00	-999.00
208	-999.00	-999.00	-999.00					

HIGH LEVEL APX —— STATIC & DELT P, ETC

0	-9999.00	-9999.00	49.28	1.00.33	-9999.00	-9999.00	110.44	137.34
8	-9999.00	-9999.00	50.06	138.24	11.19	11.57	13.51	-9999.00
16	.10	.05	-9999.00	-9999.33	-9999.00	-9999.00	-9999.00	-9999.00
24	-9999.00	-9999.00	-9999.00	-9999.00	-9999.00	-9999.00	-9999.00	-9999.00
32	-9999.00	-9999.00	-9999.00	-9999.00	-9999.00	-9999.00	-9999.00	-9999.00
40	-9999.00	-9999.00	-9999.00	-9999.00	-9999.00	-9999.00	-9999.00	-9999.00

FLOW RATES IN CUBIC FEET PER MINUTE (CFM)
-9999.00 3137.39 -9999.00 5214.61 -9999.00 1678.36

AVG WIND SPEED IN MPH= 11.2 AVG OUTSIDE TEMP IN DEG F= 73.4
WIND MILL FACTOR= 73.9

Fig. 6 - Hourly Average Printout

printout for the shift summary appears every eight hours and is an average of the last eight hourly reports. The purpose of the shift summary is to provide a convenient form of summarized data for on-site personnel rather than to serve as a timely reporting procedure. If the optional program to output all 5 minute operating data is running, the same format as the hourly is presented every 5 minutes. This is for those periods of relatively rapid transitions. These typically are printed on the matrix line printer. Figure 7 is an example of the gas analysis format from the process chromatograph which is printed every hour.

Channels which have no data are indicated by the value - 999.9. The no-data condition is signalled by setting a switch on a separate control panel, which allows any computer channel to be marked inactive. Such a situation exists when a sensor is under manual test or when a thermocouple is known to have burned out.

As shown in Figure 5, there are several user programs that can access the current or last 5 minute data that resides in the COMMON area. Figures 8, 9, 10 and 11 illustrate four of the possible formats that can be called at any terminal. The first method (Figure 8) displays all channels in the hourly average format and the second (Figure 9) outputs just the static pressures, delta pressures, temperatures and calculated flows for the active flow channels at any time. The third method (Figure 10) gives a bar graph of the temperature profile from the thermocouples in any instrument well in the pattern. A more versatile method (Figure 11) displays the temperature profile of up to seven wells in a tabular format.

The aforementioned programs access the most recent data collected. Additional programs access past data on disc files as shown in Figure 5. The RDFIL (short for READ FILE) program allows access to previously collected data in one of three ways which can be specified by the operator. The first method allows listing all operating data for any hour in a format identical to an hourly print out. The second method is to list up to 6 channels of either temperature, pressure or flow in a tabular form for the entire day as illustrated in Figure 12. As demonstrated, the six flow channels are listed for the entire day in the units MCF/DAY. Figure 13 illustrates the third option available to a RDFIL user which is the gas analysis for a selected hour.

Figure 14 shows the output from a program RDGAS (short for READ GAS) which lists the concentration of a selected component in the gas analysis over a selected time period. In this particular case the component code is 5 which corresponds to carbon monoxide and its concentration from midnight on day 110 till 11 pm on the same day. Figure 15 is a sample output of MATBL (short for MATERIAL BALANCE) which calculates a material balance from gas composition and average injection and production rates stored on a disc file.

As mentioned previously, the Hanna computer facility also includes an X-Y plotter which is used extensively for analyzing trends in the data collected. The capabilities at present include plotting any channel of temperature, pressure, flow, gas component(s) or the heating value of the produced gas. These may be plotted from 1 to 60 days at the discretion of the operator with the flexibility of manually setting the Y-axis scale or allowing autorange of the Y-axis. Figure 16 portrays one of the uses of the X-Y plotter and its associated programs. In this case, a plot of heating value of the gas over a time period of 10 Julian days is shown. Figure 17 shows a plot of injection rate, which corresponds to channel #4, for 30 days. Figure 18 demonstrates the capability of plotting gas composition with time. The figure doesn't demonstrate one added feature of the plot which is different colors for each component and separate component labels at the top.

COMPUTER CONTROL

In future experiments the computer will be used to control as well as monitor the process. The present experiment uses an electropneumatic valve to control air injection. The desired flow rate is obtained by manual adjustment of a rheostat. The computer has been used to control this valve in an on-off mode in conjunction with some tests that were made to estimate the volume of the cavity. Computer control has a two-fold advantage when compared with manual control. The controlled variables can be maintained more precisely and the experiment can be conducted with greater flexibility.

An overview of the proposed computer control system is shown in Figure 19. The computer, D/A converters, and several analog control loops are shown. The computer specifies the flow rate set point to each control loop through a D/A converter. Each control loop maintains its flow rate at the specified set point. One advantage of this approach is greater reliability through manual

GAS ANALYSIS HOURL REPORT

DATE APR 18 1976 DAY 108

TIME OF PRINTOUT = 3 HOURS 54 MIN 50 SEC

COMPONENT	STREAM	TIME	
	4	4	999
	2 5	2 20	2 35	0 0
SO2	00	00	00	-999 99
H2O	00	00	00	-999 99
H2	21 87	22 26	22 50	-999 99
O2	55	23	06	-999 99
N2	46 61	46 42	44 33	-999 99
C1	3 84	3 89	4 84	-999 99
C0	11 75	11 55	10 72	-999 99
C2	42	41	43	-999 99
CO2	14 13	14 21	13 89	-999 99
C3	20	00	3 27	-999 99
*C3	14	50	31	-999 99
IC4	00	00	00	999 99
NC4	00	00	00	999 99
H2S	00	00	00	999 99
TOTAL	99 81	99 46	99 57	999 99
POUNDS CARBON	3499 00	3559 00	4468 00	-999 99
POUNDS OXYGEN	3874 00	3868 00	2851 00	999 99
POUNDS HYDROGEN	591 00	606 00	847 00	-999 99
POUNDS SU FUR	00	00	00	999 99
*ONS GASIFIED	2 21	2 16	1 19	999 99
TONS CARBONIZED	46	74	5 65	-999 99
H2O IN BARRELS CONSUMED	6 53	6 28	1 74	999 99
HEATING VALUE BTU SCF	162 56	168 69	245 46	999 99

Fig 7 - Last 5 Minute Report of Analysis

OPERATING DATA AT TIME = 216 11 20 0

LOW LEVEL APX —— TEMPERATURES IN DEG. F

	1	2	3	4	5	6	7	8
0	-999.98	364.38	-999.98	-999.98	-999.98	-999.98	69.88	69.88
8	69.08	1155.78	1198.88	1145.48	1157.48	1156.58	1249.48	1258.88
16	1238.08	1185.78	1185.78	-97.88	1341.48	178.18	-999.98	-999.98
24	77.78	74.28	47.88	77.73	98.38	-999.98	-999.98	1258.08
32	1249.48	442.68	442.68	1184.78	1178.88	798.18	944.68	795.78
40	-999.98	69.88	78.68	836.98	648.38	876.78	68.98	843.58
48	-999.98	-999.98	-999.98	-999.98	-999.98	-999.98	-999.98	-999.98
56	-999.98	-999.98	-999.98	-999.98	-999.98	-999.98	-999.98	-999.98
64	-53.88	532.98	215.28	1194.38	142.82	63.68	58.18	68.18
72	61.88	67.18	79.48	184.18	188.58	-999.98	-999.98	-999.98
80	-999.98	-999.98	-999.98	-999.98	-999.98	-999.98	-999.98	-999.98
88	-999.98	-999.98	-999.98	-999.98	-999.98	-999.98	-999.98	-999.98
96	-999.98	-999.98	-999.98	-999.98	-1.48	29.98	1.98	1.98
104	55.88	-.28	1.98	-.48	4.98	-999.98	-999.98	-999.98
112	-999.98	-999.98	-999.98	-999.98	-999.98	-999.98	-999.98	-999.98
120	-999.98	-999.98	-999.98	-999.98	-999.98	-999.98	-999.98	-999.98
128	-999.98	-999.98	-999.98	-999.98	-999.98	-999.98	-999.98	-999.98
136	-999.98	-999.98	-999.98	-999.98	-999.98	-999.98	-999.98	-999.98
144	-999.98	-999.98	-999.98	-999.98	-999.98	-999.98	-999.98	-999.98
152	-999.98	-999.98	-999.98	-999.98	-999.98	-999.98	-999.98	-999.98
160	-999.98	-999.98	-999.98	-999.98	-999.98	-999.98	-999.98	-999.98
168	-999.98	-999.98	-999.98	-999.98	-999.98	-999.98	-999.98	-999.98
176	-999.98	-999.98	-999.98	-999.98	-999.98	-999.98	-999.98	-999.98
184	-999.98	-999.98	-999.98	-999.98	-999.98	-999.98	-999.98	-999.98
192	-999.98	-999.98	-999.98	-999.98	-999.98	-999.98	-999.98	-999.98
200	-999.98	-999.98	-999.98	-999.98	-999.98	-999.98	-999.98	-999.98
208	-999.98	-999.98	-999.98					

HIGH LEVEL APX —— STATIC & DELT P. ETC

0	-9999.00	-9999.00	6.38	40.53	-9999.00	-9999.00	-9999.00	-9999.00
8	-9999.00	-9999.00	-74.25	-44.55	-12.28	11.55	-18.01	-9999.00
16	9.37	14.62	-9999.00	-9999.00	-9999.00	-9999.00	-9999.00	-9999.00
24	-9999.00	-9999.00	-9999.00	-9999.00	-9999.00	-9999.00	-9999.00	-9999.00
32	-9999.00	-9999.00	-9999.00	-9999.00	-9999.00	-9999.00	-9999.00	-9999.00
40	-9999.00	-9999.00	-9999.00	-9999.00	-9999.00	-9999.00		

FLOW RATES IN CUBIC FEET PER MINUTE (CFM)

-6943.75 344.24 -6943.75 -6943.75 -6943.75 -6943.75 -6943.75

AVG WIND SPEED IN MPH= .0 AVG OUTSIDE TEMP IN DEG F= 69.8
AVG CHILL FACTOR= 69.8

Fig 8 - Last 5 Minute Reading of All Channels

#	TEMP	STATIC	DELTA	FLOW
2	601.4	45.37	69.75	1740.65
4	158.7	106.87	131.85	4191.78
6	707.3	45.75	123.98	4957.01
17		59.63		
18		65.25		

OUTSIDE TEMP = 87.3 DEG. F
WIND SPEED = 15.9 M.P.H.
WIND DIREC. = 312.7 DEG. FROM NORTH
WIND CHILL = 85.5 DEG. EQUIV
BAR. PRESS. = 11.6 PSIA
TIME NOW = 209 16 50 53

Fig 9 - Last 5 Minute Reading of Flows

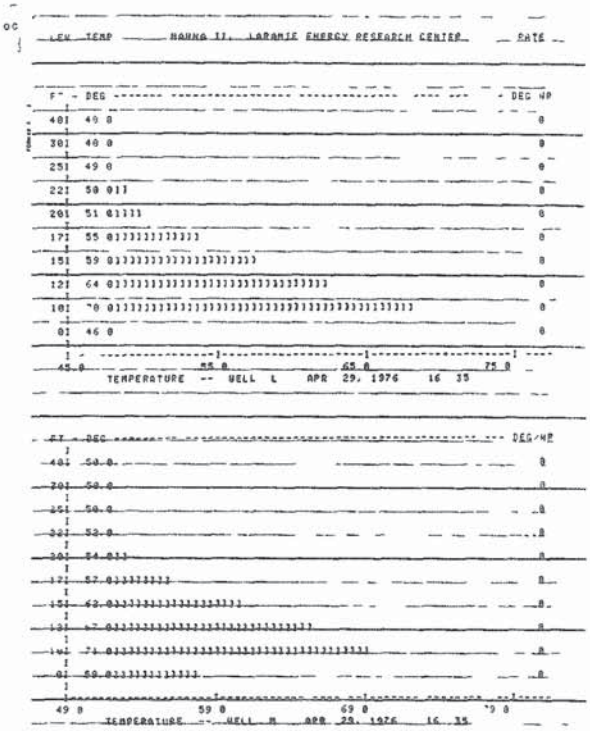


Fig 10 - Bar Graphs of Temperature Profiles

TEMPERATURE PROFILES, HANNA II, LARAMIE ENERGY RESEARCH CENTER

30	748.0	46.0	47.0	47.0	48.0	48.0	55.0
22	731.0	.0	.0	0	0	0	0
20	.0	217.0	51.0	51 0	50 0	51 0	50 0
15	.0	826.0	467 0	594 0	386 0	182 0	0
13	1188.0	.0	.0	0	0	0	0
12	0	.0	.0	.0	0	0	893 0
10	0	0	0	.0	.0	878.0	0
5	1128.0	792.0	1727.0	796 0	1241 0	0	1262 0
0	1189.0	1352.0	1559.0	811.0	1570 0	1784 0	1333 0
LEV	WELL B	WELL E	WELL C	WELL F	WELL G	WELL D	WELL B

TEMPERATURE PROFILES, WELLS BEEFGOD MAY 13, 1976 11 5

40	0	0	.0	0	0	48 0	50 0
30	47.0	48.0	48.0	48 0	48 0	48 0	50 0
25	0	.0	.0	0	0	49 0	51 0
22	48.0	.0	49.0	50 0	49 0	50 0	52 0
20	0	49 0	.0	0	0	52 0	54 0
17	0	.0	.0	0	0	55 0	57 0
15	51.0	50.0	51.0	52 0	48 0	59 0	62 0
12	0	.0	.0	.0	0	64 0	67 0
10	114.0	52.0	54.0	59 0	51 0	70 0	71 0
0	58 0	52.0	53.0	54 0	51 0	46 0	59 0
LEV	WELL A	WELL H	WELL I	WELL J	WELL K	WELL L	WELL M

TEMPERATURE PROFILES, WELLS AHIJKLM MAY 13, 1976 11 5

Fig. 11 - Tabular Display of Temperature Profiles

FLOW RATE DATA FOR DAY 207

HOUR	FLOW 1	FLOW 2	FLOW 3	FLOW 4	FLOW 5	FLOW 6
MCF 0	-9999.0	3161.1	-9999.0	6401.6	-9999.0	7806.7
MCF 1	-9999.0	3108.6	-9999.0	6431.0	-9999.0	7690.5
MCF 2	-9999.0	3136.9	-9999.0	6636.9	-9999.0	7758.7
MCF 3	-9999.0	3141.7	-9999.0	6603.4	-9999.0	7755.0
MCF 4	-9999.0	3089.8	-9999.0	6650.1	-9999.0	7654.2
MCF 5	-9999.0	2948.6	-9999.0	6590.4	-9999.0	7496.1
MCF 6	-9999.0	2980.6	-9999.0	6624.3	-9999.0	7646.8
MCF 7	-9999.0	3019.5	-9999.0	6553.2	-9999.0	7733.1
MCF 8	-9999.0	3163.4	-9999.0	6069.1	-9999.0	7993.7
MCF 9	-9999.0	3111.5	-9999.0	6528.9	-9999.0	7846.9
MCF 10	-9999.0	2979.7	-9999.0	6540.5	-9999.0	7578.3
MCF 11	-9999.0	2978.3	-9999.0	6474.2	-9999.0	7611.6
MCF 12	-9999.0	2991.6	-9999.0	6471.2	-9999.0	7596.2
MCF 13	-9999.0	2994.8	-9999.0	6460.8	-9999.0	7626.5
MCF 14	-9999.0	2985.2	-9999.0	6453.2	-9999.0	7593.7
MCF 15	-9999.0	2973.7	-9999.0	6082.9	-9999.0	7545.1
MCF 16	-9999.0	2900.3	-9999.0	6020.5	-9999.0	7374.1
MCF 17	-9999.0	2808.2	-9999.0	5625.3	-9999.0	7133.9
MCF 18	-9999.0	2858.9	-9999.0	6285.8	-9999.0	7256.1
MCF 19	-9999.0	2859.8	-9999.0	6319.0	-9999.0	7333.3
MCF 20	-9999.0	2840.4	-9999.0	6301.4	-9999.0	7361.3
MCF 21	-9999.0	2812.4	-9999.0	6191.9	-9999.0	7277.7
MCF 22	-9999.0	2842.1	-9999.0	6423.3	-9999.0	7325.6
MCF 23	-9999.0	2851.3	-9999.0	6384.9	-9999.0	7345.6

PROGRAM TO OUTPUT HOURLY SUMMARY DATA ON LU = 7
INPUT 0 FOR TODAY'S DATA, ELSE NUMBER OF DAY WANTED

Fig. 12 - RDFIL Display of Flow Rates For a Day

```
ANALYSIS DATA DURING HOUR      206   12    5    0

FLOW NUMBER      =    7
HYDROGEN         =   9.770
OXYGEN           =    .210
NITROGEN         =  59.600
METHANE          =   2.560
CARBON MONOXIDE  =  10.260
ETHANE           =    .190
CARBON DIOXIDE   =  16.610
NORMAL PROPANE   =    .100
PROPENE          =    .000
ISØ-BUTANE       =    .000
NORMAL BUTANE    =    .000
HYDROGEN SULFIDE=     .000
ARGON            =    .710

PROGRAM TO OUTPUT HOURLY SUMMARY DATA ON LU =  7
INPUT Ø FOR TODAY'S DATA, ELSE NUMBER OF DAY WANTED
```

Fig. 13 - RDFIL Display of Gas Analysis For a Selected Hour

```
ANALYSIS VALUES

---- GAS ------- CODE ------
  HYDROGEN          1
  OXYGEN            2
  NITROGEN          3
  METHANE           4
  CARBON MONOXIDE   5
  ETHANE            6
  CARBON DIOXIDE    7
  NORMAL PROPANE    8
  PROPENE           9
  ISØ-BUTANE       10
  NORMAL BUTANE    11
  HYDROGEN SULFIDE 12
  ARGON            13
  CO/METHANE RATIO 14
  CO + H2          15

VALUES FOR CODE    5

  DAY   HOUR      DATA

  110     Ø      8.18
  110     1      8.17
  110     2      7.90
  110     3      8.24
  110     4      7.85
  110     5      8.22
  110     7      8.21
  110     8      8.09
  110     9      8.01
  110    11      7.62
  110    14      6.73
  110    15      6.53
  110    16      6.55
  110    17      6.40
  110    18      6.23
  110    19      6.12
  110    20      5.93
  110    21      5.79
  110    22      5.64
  110    23      5.53
```

Fig. 14 - RDGAS Display of Concentration of Selected Gas Component

```
          DATE      MAY  14,1976          DAY  134
          TIME  =     1

**************************************************

------ COMPONENT VALUES IN PER-CENT ------

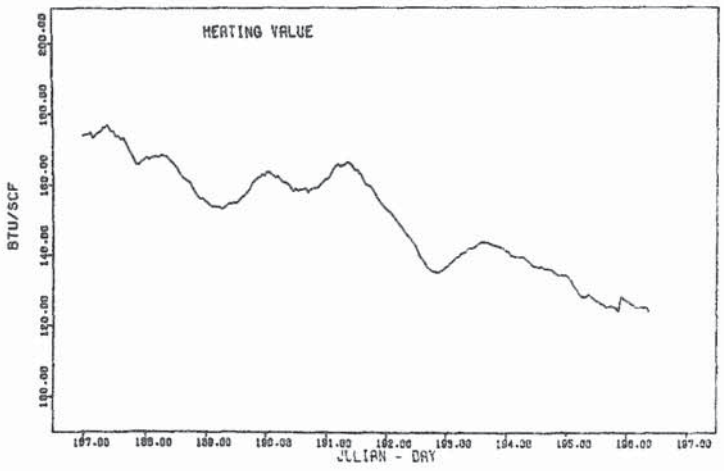
   WELL NUMBER              =    5
   HYDROGEN (H2)            =   16 12
   OXYGEN                   =    54
   NITROGEN (N2)            =   48 57
   METHANE (CH4)            =    5 58
   CARBON MONOXIDE (CO)     =   17 94
   ETHANE (C2               =    58
   CARBON DIOXIDE (CO2)     =    9 96
   NORMAL PROPANE           =    05
   PROPENE                  =    09
   ISO-BUTANE (I-C4)        =    00
   NORMAL BUTANE (N-C4)     =    00
   HYDROGEN SULFILE (H2S)   =    00
   ARGON                    =    50

   ------  TOTAL  -------    =  100 01

   AIR INJECTION RATE       =  4987929   SCF/D
   GAS PRODUCTION RATE      =  0042024   SCF/D

**************************************************
**                                              **
**                                              **
**     CARBON --- (POUNDS)          =  89273    **
**                                              **
**     OXYGEN --- (POUNDS)          =  43763    **
**                                              **
**     HYDROGEN --- (POUNDS)        =  12553    **
**                                              **
**     COAL AFFECTED --- (TONS)     =  89 631   **
**                                              **
**     TONS (MAF) COAL GASIFIED     =  43 631   **
**                                              **
**     TONS (MAF) COAL CARBONIZED   =  52 830   **
**                                              **
**     BARRELS OF WATER CONSUMED    =  39 317   **
**                                              **
**                                              **
**************************************************
```

Fig 15 - MATBI Display of a Material Balance Calculation



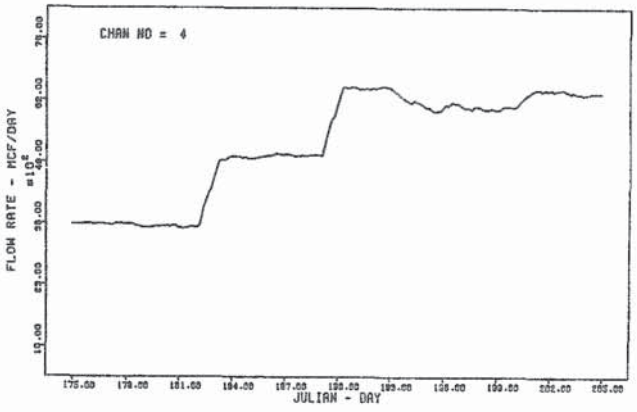


Fig. 17 - X-Y Plot of Injection Rate (Flow Channel #4)

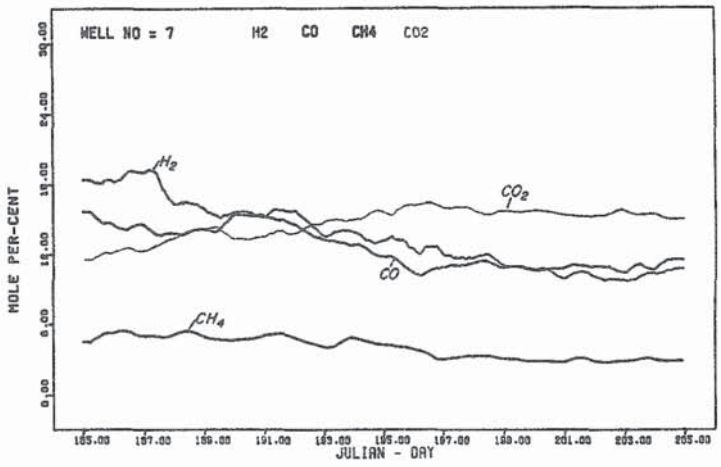


Fig. 18 - X-Y Plot of Gas Composition

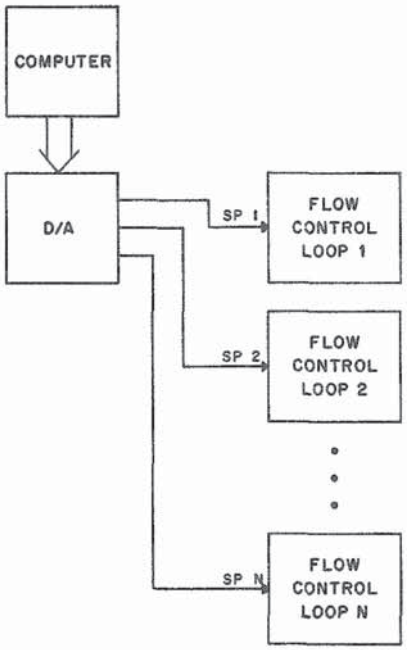


Fig. 19 - Valve Control Overview

backup. In the event of a computer failure the set point to each control loop can be manually specified, thus maintaining automatic control of each flow. Two general methods of control are possible. The first method is to specify that each flow be some desired function of time (constant, ramp, etc.). For the second method, the computer is used to optimize the process (maximize gas quality for example) by controlling the air injection at various wells. Since the method of control is software dependent, it can be changed as needed.

A typical control loop is shown in Figure 20. The flow rate Q can be related to static pressure P, differential pressure ΔP, and absolute temperature T as shown where C is a constant of proportionality. The control loop calculates the flow, compares it with the specified set point, and adjusts the valve as required to make Q=SP. The pressure, temperature, and valve control transducers operate with 4 - 20 mA or 1 - 5 volt signals.

SUMMARY

All data in the form of temperatures, pressures and calculated flows are collected automatically every 5 minutes throughout the life of an experiment. Gas composition is recorded on an interrupt basis as analyses are performed by an on-line chromatograph. Hourly averages are printed as a hardcopy and stored on a disc file for later access. Every eight hours all information on a data disc is copied onto magnetic tape in case of a system malfunction that could ruin a disc.

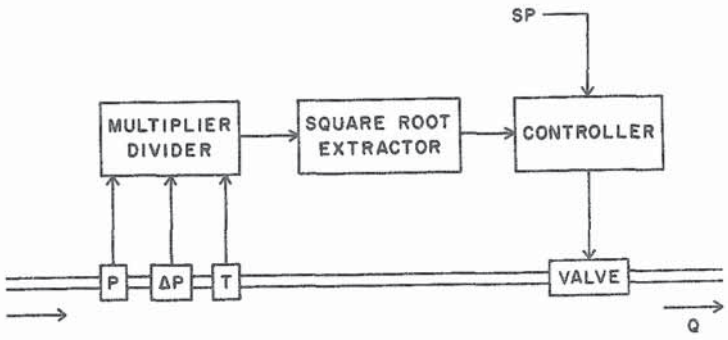
At any time during operations, a user may access the most recent 5 minute data in several forms. In addition, a user may access past data in a disc file through use of several programs either in a tabular format or through plotting programs and an X-Y plotter.

The incorporation of automatic controls operated by the computer should increase the performance of future experiments. With expansion in memory capacity of the computer system, the proven system will develop into an even more reliable and indispensible tool for the future experiments at Hanna which will be larger and more complex.

REFERENCE

1. Eastlack, J. K.: "Development of Data Acquisition System for an In-Situ Coal Gasification Experiment," M.S. Thesis, Department of Mineral Engineering, University of Wyoming, May 1976.

NOTE: Any reference to specific brand names does not imply endorsement by ERDA.



ELECTROMAGNETIC WAVE PROPAGATION WITHIN A SUBSURFACE COAL SEAM FOR IN-SITU GASIFICATION APPLICATION

by

JOHN J. HOLMES AND CONSTANTINE A. BALANIS
DEPARTMENT OF ELECTRICAL ENGINEERING
WEST VIRGINIA UNIVERSITY
MORGANTOWN, WEST VIRGINIA 26506

ABSTRACT

To aid in the design of an electromagnetic system for the detection, monitoring, and mapping of the burn front of an underground coal gasification (UCG) process, an analytical model has been developed that will predict the magnitude of the electromagnetic field reflected from the gasified portion of the coal seam.

The coal and gasified section have been modeled electrically as lossy media, surrounded above and below by relatively high conducting overburden and underburden. Vertical and horizontal electric and magnetic dipole antennas have been investigated, utilizing a geometrical optics formulation which also takes into account the physical roughness of the coal-overburden (underburden) and coal-gasified section boundaries. Although the model is two-dimensional in nature, the results prove to be applicable.

THEORY

The development of an efficient underground coal gasification (UCG) process may become an important step in achieving energy self-sufficiency. To realize the benefits of UCG, monitoring systems are being developed that use electromagnetic transceivers to detect, monitor, and map the burn front of the UCG process. To aid in the design of these systems, an electromagnetic model of the subsurface gasified coal seam has been developed.

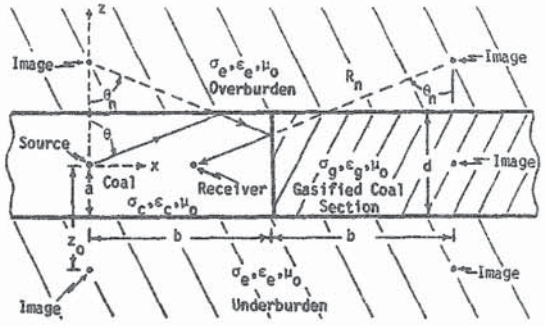


Fig. 1. Geometry of monitoring system.

A subsurface coal seam and gasified coal section, each of height d, are surrounded above and below by an overburden and underburden, as shown in Fig. 1. It is assumed that each one of the media is of finite electrical conductivity ($\sigma \neq 0$). To detect the leading edge of the gasified section, it is recommended that the transmitter and receiver be located in the same section, as shown in Fig. 1.

Electromagnetic waves emitted by the source are represented by rays, some of

which reflect from the overburden, underburden, and/or the coal-gasified section interface. The reflected rays are taken into account by introducing fictitious sources(images) placed beyond the boundaries, some of which are shown in Fig. 1. For any observation point, in the presence of a gasified section, there are in general three components of field that will contribute. These are

a. The direct ray from the source to the observation

b. Rays that are reflected from the overburden and underburden

c. Rays that are produced as in a and b and undergo reflection from the gasified section.

Utilizing a two-dimensional geometrical optics technique of [1], the field of an infinitesimal horizontally-oriented magnetic dipole (located at x = z = 0) is given by

$$H_y = -\gamma^2 MK/4\pi, \tag{1a}$$

where

$$K = K^+ + K^-, \tag{1b}$$

$$K^+ = \sum_{n=-\infty}^{\infty} F^{2|n|} F' \exp(-\gamma r_n^+)/r_n^+ [1 + 1/\gamma r_n^+ + 1/\gamma^2 r_n^{+2}], \tag{1c}$$

$$K^- = \sum_{n=-\infty}^{\infty} F^{|n|+|n-1|} F' \exp(-\gamma r_n^-)/r_n^- [1 + 1/\gamma r_n^- + 1/\gamma^2 r_n^{-2}], \tag{1d}$$

$$r_n^+ = [(x - 2b)^2 + (2nd - z)^2]^{1/2}, \tag{1e}$$

$$r_n^- = [(x - 2b)^2 + (2nd - 2a - z)^2]^{1/2}, \tag{1f}$$

M = magnetic dipole moment (amp - m^2),

γ = complex propagation constant of the coal,

F = reflection coefficient[coal-overburden (underburden) interface],

F' = reflection coefficient (coal-gasified section interface).

The expression above describes the field of the rays that are reflected from the gasified section. Setting b=0 and F'=1 in Eqs. (1c) - (1f) yields the rays that travel to the receiver without being reflected by the gasified section. The equation can be reduced even further, to isolate the direct wave, by using only the n=0 term in Eq. (1b) with b=0 and F'= 1.

The reflection coefficients F and F' in Eqs. (1c) and (1d) take into account boundary roughness [1]. Although plane wave reflection coefficients are used for F and F', even though the boundaries are in the near field of the antenna, the error produced can be small for conducting media [2]. This allows Eq. (1) to be used for electrically small gasified coal seams. Similar models have been formulated for infinitesimal vertical electric and magnetic and horizontal electric dipoles, but are not included here.

COMPUTATIONS

If in Eq.(1) b=0 and F'=1, the model of Figure 1 reduces to a homogeneous coal seam

References at end of paper

discussed by Emslie and Lagace [3]. To fit their theoretical data and the measured data of Cory, which were included in [3], conductivities of 1.1×10^{-4} mhos/m and 2.5 mhos/m were used for the coal and overburden-underburden, respectively. These conductivities are in the range of those reported elsewhere [3],[4]. Comparison of

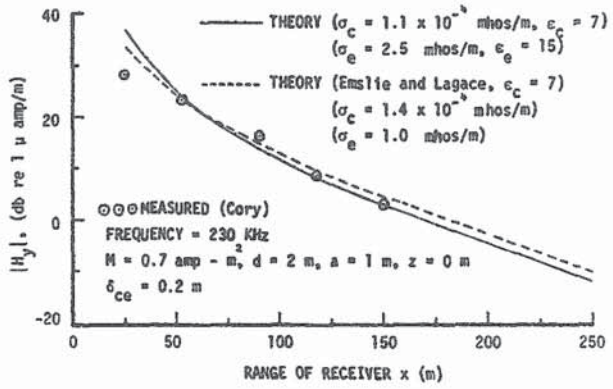


Fig. 2. Horizontal magnetic dipole inside a homogeneous coal seam.

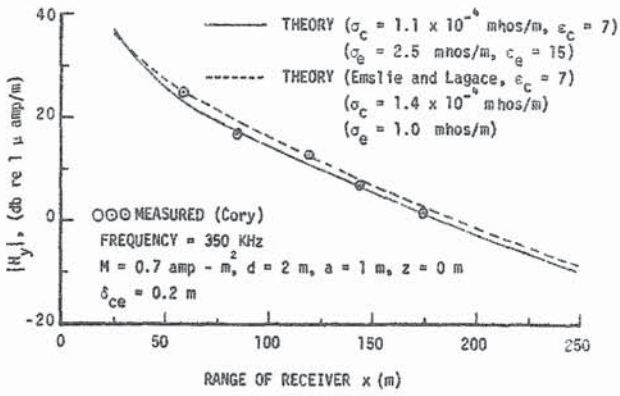


Fig. 3. Horizontal magnetic dipole inside a homogeneous coal seam.

Eq.(1) with the data of [3] in Figs. 2 and 3 show good agreement in shape and magnitude.

Using the parameters given in Figs. 2 and 3 and a standard deviation of 0.2 m for the coal-gasified section and coal-overburden (underburden) boundary roughness, the field strength of a reflected wave from the coal-gasified section interface can be determined for various distances as shown in Fig. 4. It is assumed that the receiver and transmitter are located at the same position. Indications are that a strong reflected field can be expected for the cases investigated.

In Fig. 4 the field reflected from the front edge of the gasified section of the coal seam was shown. In addition to that field, there are other components which travel to the receiving station without being reflected from the gasified section. These components can be obtained by setting b=0 and F'=1 in Eqs. (1a)-(1f). Adding the other components to the field reflected from the coal-gasified coal interface gives the total field at the receiving station of Fig. 1. The total y component of the H-field produced by the infinitesimal horizontal magnetic dipole (H_y^t) is given by

$$H_y^t = H_y + H_y\Big|_{\substack{b=0 \\ F'=1}} , \qquad (2)$$

where H_y and $H_y\Big|_{\substack{b=0 \\ F'=1}}$ can be computed from Eqs.(1a)-(1f).

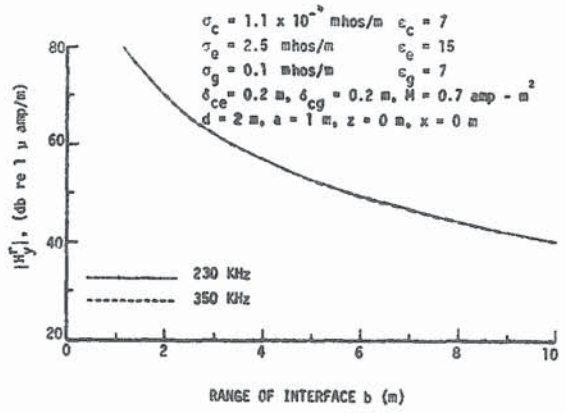


Fig. 4. Reflected field strength of horizontal magnetic dipole inside a gasified coal seam.

References at end of paper

When the receiver is located some distance away from the transmitter, the direct and the reflected waves interfere to form a standing wave pattern, as shown in Figs. 5 and 6. These curves were computed for a constant source current which explains the rise in field strength with frequency.

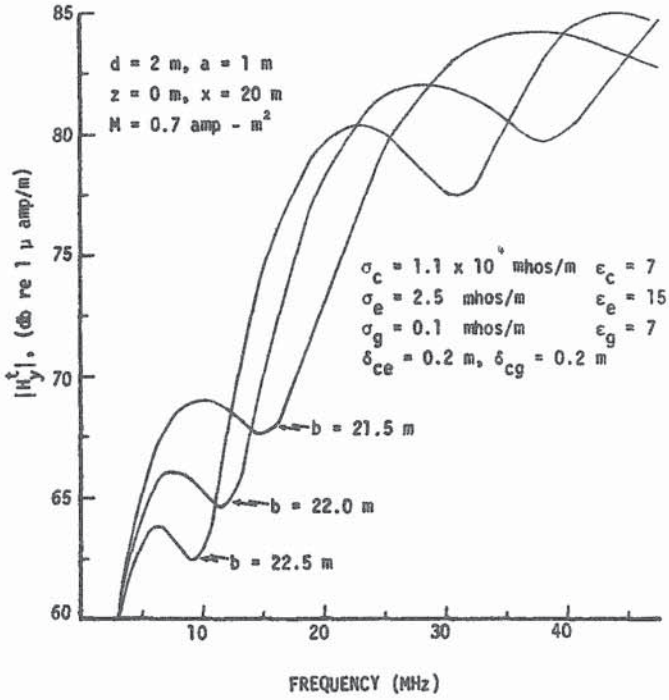


Fig. 5. Frequency response of a horizontal magnetic dipole inside a gasified coal seam (receiver near interface).

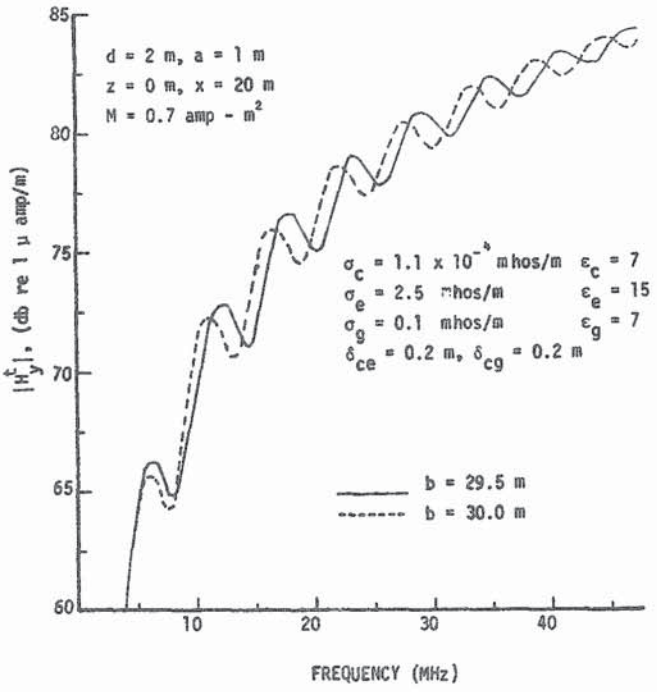


Fig. 6. Frequency response of a horizontal magnetic dipole inside a gasified coal seam (receiver away from interface).

The frequency responses of Figs. 5 and 6 suggest that a swept frequency monitoring system can be used to detect and monitor the leading edge of the gasified section. This system would require the detection of the peaks and/or nulls formed by the received signal as the transmitter's frequency is varied through some preset band. The distance of the interface can then be determined from response curves similar to those shown.

ACKNOWLEDGEMENTS

This work was sponsored by the Energy Research and Development Administration under Contract No. E(40-1)-5081 with Dr. L.Z. Shuck as technical project officer.

REFERENCES

[1]. Mahmoud, S.F., and Wait, J.R., "Geometrical Optical Approach for Electromagnetic Wave Propagation in Rectangular Mine Tunnels," Radio Science, Vol. 9, No. 12, pp. 1147-1158, December, 1974.

[2]. Lytle, R.J., et. al., "Monitoring Fluid Flow by Using High-frequency Electromagnetic Probing," Lawrence Livermore Laboratory, UC-11, January, 1976.

[3]. Emslie, A.G., and Lagace, R.L., "Propagation of Low and Medium Frequency Radio Waves in a Coal Seam," Radio Science, Vol. 11, No. 4, pp. 253-261, April, 1976.

[4]. Balanis, C.A., Rice, W.S., and Smith, N.S., "Microwave Measurements of Coal," Radio Science, Vol. 11, No. 4, pp. 413-418, April, 1976.

MONITORING OF EMISSIONS FROM AN IN SITU COAL GASIFICATION EXPERIMENT

DENNIS D. FISCHER
ERDA, LARAMIE ENERGY RESEARCH CENTER,
LARAMIE, WYOMING

ABSTRACT

Product gases produced from an in situ coal gasification experiment conducted by the Laramie Energy Research Center (LERC) at Hanna, Wyoming, have been monitored for particulate matter content and the concentrations of fourteen trace components. Six monitoring periods for each component were conducted at the wellhead during distinctly different operating conditions in order to determine concentration changes during different times in the lifetime of a two-well system.

The monitoring was conducted by Radian Corp. of Austin, Texas, under contract to LERC. Particulate matter in the product gas stream was monitored for particle size distribution as well as for bulk density and bulk elemental composition. The fourteen trace components which were monitored were carbonyl sulfide (COS), carbon disulfide (CS_2), ammonia (NH_3), hydrogen cyanide (HCN), mercury (Hg), lead (Pb), cadmium (Cd), arsenic (As), selenium (Se), sodium (Na), potassium (K), lithium (Li), vanadium (V), and calcium (Ca).

The results of the monitoring will be presented. The implications of the monitoring with regard to utilization of low-Btu gas produced by UCG will also be discussed.

INTRODUCTION

Experiments to determine the technical, environmental, and economic feasibility of underground coal gasification (UCG) have been conducted by ERDA's Laramie Energy Research Center at a site near Hanna, Wyoming, since March 1973 [1-7].[1] These tests have yielded significant technical success. Production of up to 11.5 MM scfd[2] of 175 Btu/scf low-Btu gas has been achieved during the latest experiment.

Combustion of this low-Btu gas at the UCG site to generate electricity is considered the most promising application for the process. Prior to designing a surface utilization system for the product gas, determination of the concentrations of various trace components in the dirty product gas stream is necessary. These data can then be used in designing the necessary gas scrubbing and cleaning facilities in order to meet the desired specifications for combustion in a boiler or in a gas turbine. The monitoring, therefore, has two purposes. It establishes baseline data for design of surface utilization facilities as well as determining any special environmental impacts on air quality associated with the UCG process and utilization of the low-Btu product gas.

Radian Corporation of Austin, Texas, was contracted to perform the monitoring. The monitoring consisted of six monitoring periods at a production well. The components to be determined were

---

[1]References at end of paper.
[2]Conversion from English to metric units given in Appendix A.

the following: total particulate loading; bulk density and elemental composition of the particulate matter; particulate concentration as a function of size distribution; and concentrations of ammonia (NH_3), carbonyl sulfide (COS), carbon disulfide (CS_2), hydrogen cyanide (HCN), mercury (Hg), cadmium (Cd), arsenic (As), lead (Pb), selenium (Se), sodium (Na), lithium (Li), potassium (K), calcium (Ca), and vanadium (V). The results for each of six monitoring periods will be presented and discussed.

MONITORING LOCATION

The well pattern used during the recently completed UCG experiment is shown in Figure 1. Wells 5, 6, 7, and 8 were air injection - production wells. All other wells shown were instrumentation wells for use in monitoring the UCG process. These wells were instrumented by Sandia Laboratories from Albuquerque, New Mexico.

Wells 5 and 6 were linked with ignition taking place in Well 5. Gasification from Well 6 to Well 5 was conducted from May 5 through May 31, 1976, at three programmed air injection rates of 1700 scfm, 2500 scfm, and 3500 scfm. Two monitoring periods were conducted at Well 5 during each of these different air injection rates.

MONITORING

Six monitoring periods were conducted during the gasification period. The dates and the operating parameters for the gasification process for each monitoring period are shown in Table I.

Particulate concentrations as a function of size distribution were determined using an Andersen Cascade Impactor. Samples of bulk particulates were collected in a cyclone followed by a backup filter for bulk density and bulk elemental composition determinations.

Separate sampling runs during each monitoring period were made to collect the following gaseous species:

(1) COS and CS_2

(2) Trace metals and NH_3

(3) HCN

RESULTS

All available results for each of the six monitoring periods are shown in Tables II-VII. As can be seen, the particulate loading during the first two monitoring periods was extremely low (<.0025 gr/scf) with the majority of the particulate matter being <2 μ. Table V shows that, for the sample collected on May 4, the particulate matter appears to be coal particles or possibly char produced by low-temperature (<500° C) carbonization.

The total loading increased significantly during the next two monitoring periods (Table III) to .034 and .36 gr/scf, respectively. The .36 gr/scf loading was the highest observed. The increase was expected because the reaction zone proceeds toward the production well thereby reducing the path length to the wellhead. The natural filtering efficiency of the coal seam is therefore reduced due to this shorter path length. Again, greater than 50 percent of the particulate matter was less than 2 μ. The C-H-O analysis of the particulates collected on May 10 (Table V) are significantly different from the sample on May 4 but again appear to be coal particles.

The samples from May 13 and May 15 shown in Table IV show sizable reductions in particulate loading compared to the sample collected on May 10. No explanation for this decline is presently available. On May 13 >50 percent of the particulates were <2 μ. The May 15 sample (Table IV) was the only sample to show a significantly different size distribution. Here >85 percent of the particules were >2 μ indicating that the natural filtering efficiency of the coal seam had changed dramatically allowing larger size particles to be produced to the surface. The C-H-O analyses (Table V) of the May 15 sample show only a change in oxygen content when compared with the May 10 sample .

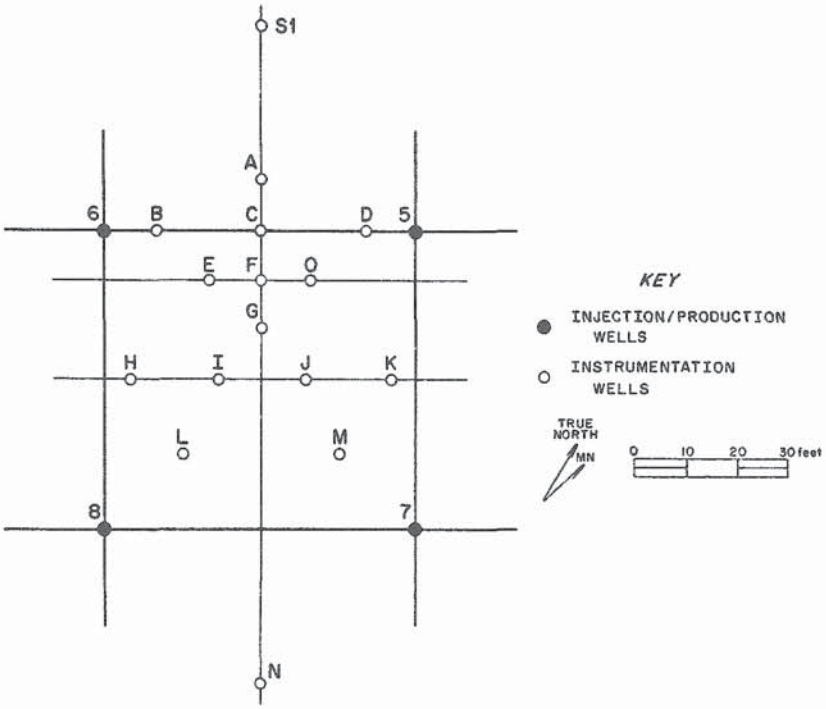


Figure 1 - Well Pattern Used During Phases II & III, Hanna II

TABLE I: UCG Operating Parameters During Each Monitoring Period

Date		Temperature (° F)	Velocity (feet/second)	Injection Rate (scfm)	Production Rate (scfm dry)	Static Pressure at Well 5 (psia)	Moisture Content (percent)
5/2/76	Range Average	556-603 582	372-399 387	1700 ±50 --	2696-2777 2735	32-33 32.5	-- 10.6
5/4/76	Range Average	600-617 610	370-404 396	1700 ±50 --	2736-3070 2981	36.5-43 37.3	-- 13.4
5/8/76	Range Average	650-686 669	711-730 715	2500 ±50 --	4563-4685 4589	-- 33	-- 13.1
5/10/76	Range Average	768-786 782	722-773 761	2500 ±50 --	4102-4392 4323	32-33 32.5	-- 15.3
5/13/76	Range Average	585-608 597	630-644 644	3500 ±50 --	5316-5683 5449	47-50 47	-- 18.4
5/15/76	Range Average	662-681 666	614-636 626	3500 ±50 --	6099-6225 6127	52-57 55	-- 13.9

TABLE II: Particle Size Distribution on May 2 and May 4, 1976

May 2

Size Range (μ)	Particulate Concentration (gr/MM scf)	Fraction (percent)
>15.0	80	3.3
15.0-9.3	250	10.4
9.3-6.2	--	--
6.2-4.4	100	4.2
4.4-2.7	100	4.2
2.7-1.39	140	5.8
1.39-0.87	130	5.4
0.87-0.62	--	--
<0.62	1600	66.7
Total	2400	100.0

May 4

Size Range (μ)	Particulate Concentration (gr/MM scf)	Fraction (percent)
>13.3	--	--
13.3-8.3	74	3.7
8.3-5.5	28	1.4
5.5-3.8	162	8.1
3.8-2.4	262	13.1
2.4-1.25	254	12.7
1.25-0.78	220	11.0
0.78-0.52	301	15.0
<0.52	701	35.0
Total	2003	100.0

TABLE III: Particle Size Distribution on May 8 and May 10, 1976

May 8

Size Range (μ)	Particulate Concentration (gr/MM scf)	Fraction (percent)
>10.6	828	2.4
10.6-6.7	777	2.3
6.7-4.5	704	2.0
4.5-3.2	761	2.2
3.2-2.0	1,436	4.2
2.0-1.0	5,474	15.9
1.0-0.62	5,006	14.6
0.62-0.41	5,531	16.1
<0.41	13,832	40.3
Total	34,349	100.0

May 10

Size Range (μ)	Particulate Concentration (gr/MM scf)	Fraction (percent)
>8.8	8,300	2.3
8.8-5.5	11,300	3.1
5.5-3.7	16,100	4.5
3.7-2.6	17,500	4.9
2.6-1.6	22,000	6.1
1.6-0.82	41,500	11.5
0.82-0.50	62,300	17.3
0.50-0.33	71,700	19.8
<0.33	109,800	30.5
Total	360,300	100.0

TABLE IV: Particle Size Distribution on May 13 and May 15, 1976

May 13

Size Range (μ)	Particulate Concentration (gr/MM scf)	Fraction (percent)
>10.3	960	4.9
10.3-6.4	974	4.9
6.4-4.3	684	3.5
4.3-3.1	1,062	5.4
3.1-1.9	697	3.5
1.9-0.97	1,285	6.5
0.97-0.59	2,471	12.5
0.59-0.40	3,861	19.6
<0.40	7,730	39.2
Total	19,725	100.0

May 15

Size Range (μ)	Particulate Concentration (gr/MM scf)	Fraction (percent)
>10.7	47,300	37.2
10.7-6.7	26,900	21.1
6.7-4.5	23,900	18.8
4.5-3.2	12,100	9.5
3.2-1.9	3,860	3.0
1.9-1.0	4,250	3.3
1.0-0.61	1,880	1.5
0.61-0.40	1,770	1.4
<0.40	5,250	4.1
Total	127,210	100.0

TABLE V: Elemental Composition and Bulk Density of Selected[1/] Particulate Fractions

Component[2/]	Date of Collection: May 4	May 10	May 15
Na_2O	0.14	--	0.24
K_2O	0.14	--	0.32
Li_2O	--	--	--
CaO	4.19	--	1.23
MgO	0.27	--	1.29
Al_2O_3	0.89	--	7.10
Fe_2O_3	4.83	--	2.50
TiO_2	0.28	--	0.34
SiO_2	3.83	--	13.05
Total Oxides[3/]	13.66	--	25.81
C	78.72	60.33	58.06
H	6.47	1.01	3.26
O	7.87	2.62	11.08
Total	106.72	--	98.21
Bulk Density[4/] (g/cm^3)	0.77	0.51	1.33

1/ Cyclone collection only. Particulate fraction >2μ.

2/ All values as weight percent unless otherwise noted.

3/ Percent values corrected to pre-extracted weights. Total oxides should equal ash content.

4/ Samples packed in 16 lambda capillary tubes for density measurements.

TABLE VI: Concentration of NH_3, HCN, COS, and CS_2 for Each Monitoring Period

Date	NH_3 (percent)	HCN (ppm)	COS (ppm)	CS_2 (ppm)
May 2	0.13	1.0	3.0	4.7
May 4	0.14	10.0	2.8	2.2
May 8	0.21	9.4	1.7	9.0
May 10	0.28	0.17	0.57	9.8
May 13	0.18	6.9	1.5	7.4
May 15	0.14	0.43	1.1	8.9

TABLE VII: Trace Metal Concentrations for Each Monitoring Period

Component+	May 2	May 4	May 8	May 10	May 13	May 15
Na	0.92	3.97	12.9	0.49	4.35	<0.05
K	0.16	0.10	0.04	0.12	0.05	<0.02
Li	<0.06	<0.06	<0.06	<0.06	<0.06	<0.06
Ca	0.43	0.84	0.48	0.80	0.42	0.37
V	0.034	0.097	0.071	0.064	0.063	0.064
Hg	0.0068	0.0042	0.0130	0.0140	0.0076	0.0077
Pb	0.012	0.030	0.033	0.021	0.016	0.011
Cd	0.00054	0.00047	0.00022	0.000089	0.000083	0.00040
As	0.0066	0.0117	0.036	0.088	0.075	0.029
Se	0.0355	0.0137	0.0101	0.0186	0.0156	0.0169

+All concentrations ppm (v/v) on a moisture-free basis.

Further analyses of the three selected particulate samples are shown in Table VI. A final report giving data from all analyses should be available in September 1976.

The concentrations of NH_3, HCN, COS, and CS_2 for each monitoring period are shown in Table VI. NH_3 shows no dependence on time of collection remaining reasonably constant and lower than expected. The coal at the Hanna site contains 1.25 percent N. Using the rule of thumb developed for surface gasifiers that 80 percent of the N in the coal is converted to NH_3, the concentrations of NH_3 in the product gas for each of the six monitoring periods should have been 0.60 percent. Based on the results shown in Table VI, either this rule of thumb is invalid or, more likely, water and tars in the product gas scrub out some of the NH_3 thus acting as a natural scrubbing system.

The HCN, COS, and CS_2 concentrations shown in Table VI are low as expected. COS and CS_2 concentrations appear to be time dependent with COS trending downward and CS_2 trending upward. There is some question as to the validity of the HCN analyses. Coal tars collected during the sampling may have interfered in the analyses thus yielding high HCN values.

The available data for trace metal concentrations are shown in Table VII. As can be seen, only Na and Ca approached or exceeded 1 ppm. The primary concern associated with Na, Ca, V, Li, and K is their corrosive effects should the low-Btu gas be expanded through a turbine for power generation. The other five trace metals are of environmental concern.

CONCLUSIONS

The monitoring indicates that no unexpectedly high concentrations of any species determined were produced during the monitoring of the UCG test at Hanna. Although only a first effort at determining the concentrations of these various components, the techniques used were efficient and rapid. Certainly further monitoring of future UCG tests will be necessary for these components as well as others before a sufficiently broad data base can be established, but these data do indicate that no unforeseen problems should be encountered.

ACKNOWLEDGMENTS

I would like to thank the staff from Radian Corporation for their efficient and professional conduct of this monitoring work as well as the other staff members associated with LERC's UCG project for their assistance in ensuring that necessary equipment was available at the Hanna site for use during the monitoring.

REFERENCES

1. Campbell, G. G., Brandenburg, C. F., and Boyd, R. M.: "Preliminary Evaluation of Underground Coal Gasification at Hanna, Wyoming," BuMines TPR 82, October 1974, 14 pp.

2. Schrider, L. A., Jennings, J. W., Brandenburg, C. F., and Fischer, D. D.: "An Underground Coal Gasification Experiment, Hanna, Wyoming," SPE 4993, presented at the SPE Fall Meeting of AIME, Houston, Tex., Oct. 6-9, 1974, 25 pp.

3. Brandenburg, C. F., Fischer, D. D., Campbell, G. G., Boyd, R. M., and Eastlack, J. K.: "The Underground Gasification of a Subbituminous Coal," presented at the Div. of Fuel Chemistry, Am. Chem. Soc. National Spring Meeting, Philadelphia, Penn., April 1975, 11 pp.

4. Fischer, D. D., and Schrider, L. A.: "Comparison of Results from Underground Coal Gasification and From a Stirred Bed Producer," presented at the National AIChE Meeting, Houston, Tex., Mar. 16-20, 1975, 34 pp.

5. Fischer, D. D., Brandenburg, C. F., and Schrider, L. A.: "Energy Recovery From In Situ Coal Gasification," Energy Sources, Vol. 2, No. 3 (1975), pp. 281-292.

6. Schrider, L. A. Brandenburg, C. F., Fischer, D. D., Boyd, R. M., and Campbell, G. G.: "The Outlook for Underground Coal Gasification," presented at the 1975 Lignite Symposium, Grand Forks, N. D., May 1975, 32 pp.

7. Brandenburg, C. F., Reed, R. P., Boyd, R. M., Northrop, D. A., and Jennings, J. W.: "Interpretation of Chemical and Physical Measurements From an In Situ Coal Gasification Experiment," SPE 5654, presented at the SPE Fall Meeting of AIME, Dallas, Tex., Sept. 28-Oct. 1, 1975, 28 pp.

APPENDIX A - CONVERSIONS

1 ft = 0.3048 m

1 scf/min (60° F) = 0.029931 scm/min (0° C)

1 MM scf/day (60° F) = 29931 scm/day (0° C)

1 Btu/scf (60° F) = 35247.7 joules/scm (0° C)

$$\mu g/m^3 = ppm(v/v) \times \frac{Mol.\ Wt.}{.02404}$$

$$1 \frac{gr}{scf} = 2165\ mg/scm$$

NUMERICAL MODELING OF THE STREAM METHOD OF UNDERGROUND COAL GASIFICATION

by

S. M. Farouq-Ali, Pennsylvania State University, Univ. Park, Pa.
M. L. Pasha, Pennsylvania State University, Univ. Park, Pa.

ABSTRACT

In the past, a series of analytical models of underground coal gasification by the stream method were developed. In order to extract a closed form solution the models necessitated a number of restrictive assumptions, including steady state combustion.

The present model is a numerical extension of the previous models, and as a result, it is considerably more general. A channel of two-dimensional (r, x) axisymmetrical geometry, in a coal seam, is considered. The channel is ignited at one end, and thereafter, gas is injected. As a result, the channel walls recede, and the combustion zone advances with time. Reaction kinetics are assumed to be diffusion controlled, and temperature and gas composition-dependent. The numerical solution used employs an implicit finite difference scheme. The resulting algebraic equations were solved by the Alternating Direction Implicit Procedure (ADIP). The moving coal boundary, being the result of erosive burning, was handled by means of a time-dependent coordinate transformation, which made the transformed boundary stationary in time, even though the actual boundary moved. This considerably simplified the numerical grid used, though at the expense of complicating the equations.

This paper essentially gives the mathematical technique developed. The numerical results will be relegated to a later comprehensive report.

The model developed is designed to be of immediate application to underground coal gasification schemes employing the stream method. In particular, it is intended to simulate the borehole linking phase of the underground coal gasification field test being conducted by the Morgantown Energy Research Center in the Pittsburgh coal.

INTRODUCTION

In recent years, underground coal gasification has gained renewed importance as an important process for in situ recovery of low-grade coal. As a result, after a period of some 10 years of inactivity in this area, a number of field tests are currently underway in the U.S., Canada, and other countries. At the same time, a number of mathematical treatments of the gasification process as well as the associated chemical kinetics have been published.

Earlier, Magnani (1) and Magnani and Farouq Ali (2, 3) reported a series of mathematical models of underground coal gasification, for linear and two-dimensional geometries, having increasing degrees of complexity. These models were designed to simulate the stream method of underground coal gasification, wherein a horizontal borehole is initially ignited at one end, and air (with possibly steam and oxygen) is injected to promote the advance of the combudtion front both axially and radiall

Although several reaction regimes were considered, the models essentially simulated the producer gas stoichiometry. In a later work, Farouq Ali and Pasha (4) extended the linear model to include six reactions involving carbon-steam and carbon-hydrogen as well as oxidation reactions, in addition. This model was further extended (5, 6) to incorporate as many as 14 gasification reactions, and variable velocity and channel cross-sections. All of the aforesaid models were of steady state type, which was necessitated in view of the analytical approach employed. This permitted the extraction of closed form solutions, which, though complex, were useful for carrying out parameter sensitivity studies. Apart from this, the analytical models were also of considerable value for carrying out pseudo-steady state simulations of unsteady state gasification.

It should be noted that while this study has been devoted to the stream method of underground gasification, a number of other simulation studies have been reported, which consider other gasification processes. These include the works of Kotowski and Gunn (7), Gunn and Whitman (8), Winslow (9), Thorsness and Rosza (10), Edgar (11), as well as several papers on coal reactivity and reaction kinetics.

The present study represents the extension of the authors' previous steady state models to the unsteady state conditions. A two-dimensional geometry is considered, with gasification occurring inside an initially cylindrical, horizontal channel, which subsequently assumes various axisymmetrical cross-sectional profiles as a result of erosive burning of the channel walls. In view of these and other complicating features, the present model utilizes a numerical solution scheme. This paper essentially describes the solution procedure employed. Computational results will be reported in a more extensive report.

MODEL DETAILS

The principal assumption is that the coal consists of 100% carbon. However, the model allows for "source terms" in all components considered, i.e. influx of any of these, e.g. water, as a function of distance and time may be simulated.

The gasification channel is initially assumed to be of cylindrical geometry, one extremity of which is ignited. The injected gas consists of air and any other gases. The channel walls subsequently recede radially and the profile thus changes as a function of distance and time. Seven gasification reactions are assumed to occur. All reactions, except the hydrogen and carbon monoxide oxidation, occur at the solid surface to which the oxygen arrives by diffusion through the boundary layer. The net heat generated at the solid surface, as well as that generated in the gas phase as a result of oxidation reactions, is assumed to be conducted into the coal both radially and axially, and also convected by the gas. Both convective and radiative exchanges of heat between the coal and the gas are considered. The outlet boundary is taken to be adiabatic.

The gas diffusion coefficients are assumed to be the same for all species, although the temperature dependence is taken into account. The reactions are controlled by diffusion. The diffusion of the molecules of gas components is equal to their kinetic consumption at the surface of coal.

Effects such as ash deposition at the coal surface, fluid flow within the pores in the coal, swelling of coal, and roof collapse are not considered in this first numerical model. Some of these will be incorporated in the future simulations.

REACTION KINETICS

The present model considers the following seven reactions, occurring at the solid surface, or in the gas phase, as indicated. The heats of reaction are also given (12).

		ΔH, kcal
(1) $C + O_2 \xrightarrow{R_1} CO_2$	(solid surface)	- 94.0
(2) $C + CO_2 \xrightarrow{R_2} 2CO$	(solid surface)	+ 40.8
(3) $C + H_2O \xrightarrow{R_3} CO + H_2$	(solid surface)	+ 31.1

(4) $C + 2H_2 \xrightarrow{R_4} CH_4$ (solid surface) - 17.9

(5) $CO + \frac{1}{2} O_2 \xrightarrow{R_5} CO_2$ (gas phase) - 67.4

(6) $H_2 + \frac{1}{2} O_2 \xrightarrow{R_6} H_2O$ (gas phase) - 68.2

(7) $CO + H_2O \xrightarrow{R_7} CO_2 + H_2$ (solid surface) - 9.7

The expressions for the reaction rates R_i, as well as the constants involved, are given in Appendix A. It is noted that R_i are taken to be temperature- and composition-dependent, and in some cases incorporate the equilibrium "constants" as functions of temperature, based upon the data given by Von Fredersdorff and Elliott (13). Typically, $R_i = d[i]/dt$, where [i] is the concentration of species i.

MATHEMATICAL FORMULATION

Chemical Species Balance

Seven chemical species, other than carbon, are considered. These are: oxygen (1), carbon dioxide (2), carbon monoxide (3), water (4), hydrogen (5), methane (6), and nitrogen (7), and are represented in the following by the subscripts indicated in the parentheses. Define y_i as the concentration of the i^{th} species in the gas phase, in moles/ft^3. Then a molar balance for the i^{th} species, considering axial transport, and axial and radial diffusion, as well as generation (or consumption), gives

$$\frac{\partial y_i}{\partial t} + \frac{\partial}{\partial x}(v y_i) = \text{div } (D \text{ grad } y_i) + S_i, \tag{1}$$

$i = 1, 2, \ldots, 7$; where S_i are rates of generation. The equation utilizes cylindrical (r, x) coordinates. It is seen that $S_1 = -R_5 - R_6$, $S_2 = 2R_5$, $S_3 = -2R_5$, $S_4 = 2R_6$, $S_5 = -2R_6$, and $S_6 = S_7 = 0$, assuming no external sources.

The above equations are subject to the following boundary and initial conditions:

$$\text{At } x = 0,\ y_i = y_{io} \text{ (known)} \quad 0 \le r < r_1, t > 0$$

$$x = L,\ \frac{\partial y_i}{\partial x} = 0 \qquad 0 \le r < r_1, t > 0 \tag{2}$$

where L is the channel length, and the subscript "0" (zero), indicates known input values.

At $r = r_1$, the channel radius at any time and distance:

$$D \frac{\partial y_1}{\partial r} + \frac{r_1}{2} R_1 = 0 \tag{3}$$

$$D \frac{\partial y_2}{\partial r} + \frac{r_1}{2} (-R_1 + R_2 - R_7) = 0 \tag{4}$$

$$D \frac{\partial y_3}{\partial r} + \frac{r_1}{2} (-2R_2 - R_3 + R_7) = 0 \tag{5}$$

$$D \frac{\partial y_4}{\partial r} + \frac{r_1}{2} (R_3 + R_7) = 0 \tag{6}$$

$$D \frac{\partial y_5}{\partial r} + \frac{r_1}{2} (R_4 - R_3 - R_7) = 0 \tag{7}$$

$$D \frac{\partial y_6}{\partial r} - \frac{r_1}{2} \left(\frac{R_4}{2}\right) = 0 \tag{8}$$

$$\frac{\partial y_7}{\partial r} = 0 \tag{9}$$

Initial conditions are:

$$Y_i = Y_{i0} \quad 0 \leq r \leq r_1, \; 0 \leq x \leq L, \; t = 0 \tag{10}$$

Energy Balance for Solid

The solid temperature T_s is given by an energy balance on the coal as follows:

$$\nabla.(k_1 \nabla T_s) = \rho_1 C \frac{\partial T_s}{\partial t} \tag{11}$$

where k_1 is the thermal conductivity, ρ_1 is density, and C is specific heat of coal.

Equation (11) is subject to the following boundary and initial conditions:

$$T_s = T_{s\infty} \text{ at } r = r_o, \; 0 \leq x \leq L, \; t > 0$$

$$\frac{\partial T_s}{\partial x} = 0 \text{ at } x = L, \; r_1 < r < r_o, \; t > 0$$

$$T_s = T_o \text{ at } x - 0, \; r_1 < r < r_o, \; t > 0 \tag{12}$$

where $T_{s\infty}$ is the coal temperature at the outer radius r_o, assumed to be constant. The boundary condition at the solid-gas interface $r = r_1$ is given by

$$k_1 \frac{\partial T_s}{\partial t} = h (T_s - T_g) - \Sigma m_i' \Delta H_i + RHT, \tag{13}$$

where m_i' is the mass flux of the i^{th} species, H_i is the heat of reaction of the i^{th} reaction, RHT is radiative heat transfer, given by

$$RHT = A_1 \sigma (T_s^4 \varepsilon_g - T_g^4 \alpha_g), \tag{14}$$

and h is the convective heat transfer coefficient, expressed by Nusselt's equation; σ is the Stefan-Boltzman constant, ε_g and α_g are absorptivity and emissivity coefficients, and T_g is the gas temperature. Since the channel radius r is changing with time and distance, the area A_1 is given by

$$A_1 = 2\pi \int_o^L r (x, t) \, dx. \tag{15}$$

Notice that each term in the summation in Eq. (13) is of the form $M_i R_i \Delta H_i$, where M_i is the molecular weight of the i^{th} component, R_i is the reaction rate, and ΔH_i is the heat of reaction.

Energy Balance for Gas

The gas temperature T_g is given by the energy balance for gas, as follows

$$\nabla.(\Sigma_j \gamma H_j \nabla m_j) + \nabla.(k_2 \nabla T_g) + SH = \rho \frac{\partial H}{\partial t} + v\rho \frac{\partial H}{\partial x}, \tag{16}$$

where SH is heat generation in the gas phase, H is the enthalpy of the gas mixture, H_j is the enthalpy of the j^{th} component, m_j is the mass fraction of the j^{th} component, k_2 is the thermal conductivity of the gas mixture, $\gamma = \rho D$, where ρ is density of gas, and D is diffusion coefficient; H_j is taken as the sum of the energy of formation and the sensible heat, reffered to 25°C. Equation

(16) can be simplified to give

$$\sum_{j=1}^{7} [\rho m_j(T_g) C_{p_j}(T_g) \frac{DT_g}{Dt} - (C_{p_j}(T_g) \nabla T_g) . \gamma_j \nabla m_j] - \nabla . k_2 \nabla T_g + \sum_{j=1}^{7} H_j m_j' = M_1 (R_5 \Delta H_5 + R_6 \Delta H_6) \quad (17)$$

where m_j' is the rate of mass change. The above equation is subject to the following boundary and initial conditions:

$$T_g = T_{g\infty} \text{ at } x = 0,\ 0 \le r \le r_1,\ t > 0$$

$$\frac{\partial T_g}{\partial x} = 0 \text{ at } x = L,\ 0 \le r \le r_1,\ t > 0$$

$$k_2 \frac{\partial T_g}{\partial r} = h\,(T_s - T_g) + RHT,\ 0 \le x \le L,\ r = r_1,\ t > 0,$$

$$T_g = \text{finite at } r = 0,\ 0 \le x \le L$$

$$\text{and } T_g = T_{g\infty} \text{ at } t = 0,\ 0 \le x \le L,\ 0 \le r \le R. \quad (18)$$

Gas velocity v can be obtained from a total balance over the gas species, as follows:

$$v = \frac{\bar{D}}{Y} \frac{\partial Y}{\partial x} + \frac{1}{A_c Y} \int_o^x RT dx - \frac{1}{A_c Y} \int_o^x \frac{\partial}{\partial t}(A_c Y) dx + \frac{1}{A_c y} [A_c v Y - A_c \bar{D} \frac{\partial Y}{\partial x}]_{x=0}. \quad (19)$$

where $RT = (R_2 + R_3 - R_4/2 - R_5 - R_6)\, A_c$; and

where $Y = \Sigma \bar{Y}_i$, A_c is the instantaneous cross-sectional area, and a bar denotes an average over the channel cross-section. Writing a balance of carbon in the gas and taking into account the carbon burned, we have

$$A_c(-vy + \frac{\partial y}{\partial x} \bar{D}) + \int_x^L [\frac{\partial}{\partial t}(A_c y)]\, dx - \int_x^L [\frac{\partial}{\partial t}(\rho A_c/12)]\, dx = [-v A_c y]_{x=L} \quad (20)$$

where $y = \bar{y}_2 + \bar{y}_3 + \bar{y}_6$. This equation can be solved to obtain the cross-sectional area A_c, and hence the instantaneous channel radius r(x, t).

Treatment of the Moving Boundary

The equations developed above were reduced to dimensionless form, using $T = tD_1/L^2$ and $X = x/L$. Furthermore, two transformed coordinates U and V were defined as follows:

$$U = \frac{1 - e^{c_1 r/r_1}}{1 - e^{c_1}};\ (0 \le r \le r_1) \quad (21)$$

and

$$V = \frac{1 - e^{c_2} e^{-c_2 r/r_1}}{1 - e^{c_2} e^{-c_2 r_0/r_1}};\ (r_1 \le r \le r_0) \quad (22)$$

where, as before, r_1 is the channel radius and r_0 is the outer radius of the cylindrical coal seam element under consideration and c_1 and $c_2 > 0$. With these transformations, the boundary $r=r_1$ remains invariant, since U=1 and V=0. The actual and transformed grids are shown in Fig. 1. This technique was employed by Duda et el (14) for a moving boundary problem. Using Eqs. (21) and (22), Eq. (1) can be transformed into the following equation

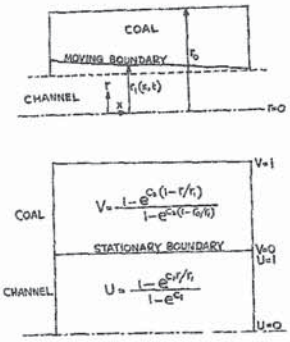


Figure 1 – Transformation of a moving burning boundary into a stationary boundary.

$$C_1 \frac{\partial y_i}{\partial U} + C_2 \frac{\partial y_i}{\partial X} + C_3 \frac{\partial^2 y_i}{\partial U^2} + C_4 \frac{\partial^2 y_i}{\partial X^2} + C_5 = \frac{\partial y_i}{\partial T} , \qquad (23)$$

where

$$C_1 = - \frac{\partial U}{\partial T} + DL^2 \frac{\partial^2 U}{\partial r^2} + L^2 \left(\frac{D'}{r} + \frac{\partial D'}{\partial r}\right) \frac{\partial U}{\partial r} + \left(\frac{\partial D'}{\partial X} - \frac{vL}{D0}\right) \frac{\partial U}{\partial X} + D \frac{\partial^2 U}{\partial X^2} ;$$

$$C_2 = \frac{\partial D'}{\partial X} - \frac{vL}{D0} ;$$

$$C_3 = D'\left[\left(\frac{\partial U}{\partial r}\right)^2 L^2 + \left(\frac{\partial U}{\partial X}\right)^2\right] ;$$

$$C_4 = D' ;$$

$$C_{5i} = 2D' \left(\frac{\partial U}{\partial X}\right) \frac{\partial^2 y_i}{\partial U \partial V} - \frac{Ly_i}{D0} \frac{\partial v}{\partial X} + \frac{L^2 S_i}{D0} ;$$

where $D' = D/D0$. In the same manner, the solid and gas energy balances, Eqs. (11) and (17) are transformed into the form of Eq. (23). The detailed expressions will not be given here, and will be included in a comprehensive report (15).

METHOD OF SOLUTION

The final partial differential equations, of the form of Eq.(23) were discretized, using a grid covering both the channel and the coal seam. The derivatives were approximated by finite differences using the standard techniques. The y_i, T_s and T_g terms were taken at the new time level, along with these same terms occurring in the reaction rate expressions. The coefficients, such as C_1, C_2, ... were evaluated at the previous time levels. Once the finite difference equations were obtained, they were solved individually by the Alternating Direction Implicit Procedure of Peaceman and Rachford. The equations were arranged in such a way that any y_i occurring in the reaction rate expressions were always at the new time level. The detailed finite difference equations are given in (15) in view of space limitations, and follow easily from the transformed partial differential equations. The same is true of the finite difference approximations of Eqs. (19) and (20).

The solution procedure was as follows. Starting with the initial and boundary conditions, each of the equations for y_i (i=1, 2, ...,7) and T_s and T_g were solved sequentially. At the first time step, the original channel radius and gas velocity were used in the calculation of the coefficients. At a subsequent time step, the finite difference approximations of Eqs. (19) and (20) were solved first, obtaining the gas velocity and channel cross-section, and hence $r_1(x, t)$, at each grid point. Next, the coefficients were calculated, and finally the gas species and the solid and gas temperature equations were solved. Except for the rather complex algebraic expressions, the programming was generally straightforward.

RESULTS

As of the writing of this paper, computer runs were still being conducted, and the data were being refined. The results obtained are typified by Fig. 2, which shows the actual grid and the transformed grid at several stages in the gasification process. Apart from the channel profile, gas composition and solid and gas temperatures are also obtained as functions of distance and time, and are used for calculating the gasification parameters.

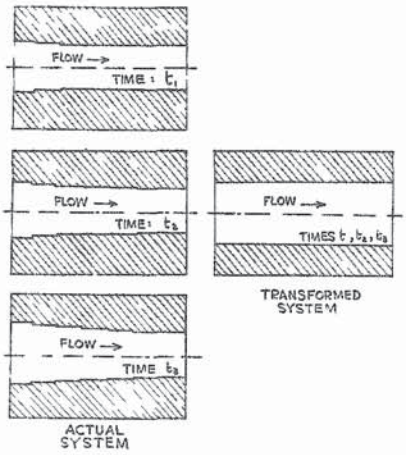


Figure 2 - Different stages in channel development in the actual and transformed coordinates.

ACKNOWLEDGMENTS

The authors are indebted to Dr. Zane Shuck and Mr. J. Pasini, III, for their suggestions in the development of this model in order that it may simulate MERC's field test.

REFERENCES

1. Magnani, C.F.: Mathematical Foundations for the Process of Underground Gasification of Coal, Ph.D. Thesis, Penn State U., August 1973.
2. Magnani, C.F., and Farouq Ali, S.M.: "Mathematical Modeling of the Stream Method of Underground Coal Gasification", SPE J. (Oct., 1975) 425-436.
3. Magnani, C.F., and Farouq Ali, S.M.: "A Two-Dimensional Mathematical Model of the Underground Coal Gasification Process", SPE 5653, presented at the 50th Annual Fall Meeting of Soc. of Pet. Engrs., Dallas, Texas, Sept. 28 - Oct. 1, 1975; 1-15.
4. Farouq Ali, S.M. and Pasha, M.L.: Computer Simulation and Economic Optimization of Underground Gasification of Coal, Final Report, Grant No. G0 133094, USDI, B. of Mines, Jan. 24, 1975, 1-95.
5. Farouq Ali, S.M., and Pasha, M.L.: Modeling and Computer Simulation of Reaction Kinetics Associated with the Underground Gasification of Coal, Final Report, Grant No. G0133094, USDI, B. of Mines, Nov. 14, 1975, 1-169.
6. Farouq Ali, S.M., and Pasha, M.L.: "An Advanced Mathematical Model of Underground Coal Gasification Using Steam-Air Mixtures", Paper SPE 6186, presented at the 51st Annual Fall Meeting of Soc. of Pet. Engrs., New Orleans, Oct. 3-6, 1976.
7. Kotowski, M.D., and Gunn, R.D.: "Theoretical Aspects of Reverse Combustion in the Underground Gasification of Coal", Report LERC/RI-76/4, U.S. ERDA, Laramie (March, 1976) 1-46.
8. Gunn, R.D., and Whitman, D.L.: "An In Situ Coal Gasification Model (Forward Mode) for Feasibility Studies and Design", Report LERC/RI-76/2, U.S. ERDA, Laramie (February, 1976) 1-39.
9. Winslow, A.: "Numerical Model of Coal Gasification in a Packed Bed", UCRL-77627, 16th Int. Symp. on Combustion, MIT, Cambridge, Mass. (Aug. 15-21, 1976) 1-24.
10. Thorsness, C.B. and Rosza, R.B.: Talk given at LLL, Livermore, Calif., May 18, 1976.
11. Edgar, T.F.: Talk given at LLL, Livermore, Calif., May 18, 1976.
12. Thring, M.W., and Essenhigh, R.H.: "Thermo-dynamics and Kinetics of Solid Combustion", Chap. 17 in Chemistry of Coal Utilization by Lowry, pp. 754-772, John Wiley & Sons, New York.
13. Von Fredersdorff, C.G., and Elliott, M.A.: "Coal Gasification", Chap. 20 in Ref. cited in (17), p. 895.
14. Duda, J.L., Malone, M.F., and Notter, R.H.: "Analysis of Two-Dimensional Diffusion Controlled Moving Boundary Problems", Int. J. Heat Mass Transfer, Vol. 18 (1975) 901-910.
15. Farouq Ali, S.M., and Pasha, M.L.: Numerical Modeling of Underground Coal Gasification by the Stream Method and Borehole Linking, Final Report for Contract E(46-1)-8018, U.S. ERDA (in preparation).

APPENDIX

Reaction Rates

The reaction rates employed were of the following forms:

$$R_1 = Ae^{-\Delta E/RT} p_{o_2} ;$$

$$R_2 = Ae^{(a/T-bT)} p_{co_2} ;$$

$$R_3 = Ae^{-\Delta E/RT} (p_{H_2 0} - \frac{1}{K_p} p_{co} p_{H_2}) ,$$

where $K_p = e^{-\Delta G/RT}$;

$$R_4 = Ae^{-\Delta E/RT} (p_{H_2}^2 - \frac{1}{K_p} p_{CH_4}) ;$$

$$R_5 = Ae^{-\Delta E/RT} p_{co} ;$$

$$R_6 = Ae^{-\Delta E/RT} p_{H_2} ;$$

$$R_7 = (\frac{k_1}{k_{-1}})^{\frac{1}{2}} p_{H_2}^{\frac{1}{2}} [k_2 k_3 p_{H_2} p_{co_2} - k_{-2} k_{-3} p_{co} p_{H_2 o}] / [k_{-2} p_{co} + k_3 p_{H_2}],$$

where k_1 and k_2 have the form $aT^{-b}e^{-\Delta E/RT}$; k_{-2}, k_3, and k_{-3} are of the form $ae^{-\Delta E/RT}$; and $k_{-1} = a/T$.

CHEMICAL REACTOR MODELING OF IN SITU COAL GASIFICATION

by

T. F. Edgar
T. H. Tsang
The University of Texas at Austin
Austin, Texas 78712

ABSTRACT

Conceptual models for underground coal gasification (UCG) are discussed. A combustion tube, which embodies a one-dimensional representation of UCG, is to be tested as a means of verifying one scale-up step from laboratory kinetics data. A simple approach for modeling sweep efficiency in a combustion tube is given and preliminary simulation results presented. Problems of developing more realistic one- and two-dimensional models are discussed.

INTRODUCTION

The Russians developed a commercial scale system for in situ gasification which is in operation at the present time. However. their results are in the form of field data (Gregg et al.. 1976). as are experimental tests by other investigators. Many things are still unknown about the process, mainly due to the absence of well-conceived laboratorv scale research on the many variables involved. It is clear that the kinetic-transport behavior of the gasification reactions determines the eventual product gas distribution and yield in terms of heating value. Recent work by Gunn and Whitman (1976) has demonstrated some aspects of this relationship using a one-dimensional packed bed reactor model. At this time no theory is available which will predict how the gasification reaction propagates in a coal seam and how the individual process variables affect the resulting product. By formulating and validating mathematical models for this process, economic design and operational control of gasification facilities can be achieved.

As an initial step, it is planned to couple laboratory scale and bench scale research so that a suitable one-dimensional transient model for a combustion tube with axial variation in composition and temperature and negligible radial variation can be developed. Presently small scale kinetics work is underway on the following subjects:

(1) pyrolysis of lignite
(2) oxidation and reduction of lignite char
(3) char-steam reactions
(4) gas phase oxidation of carbon monoxide to carbon dioxide.

References at end of paper.

The kinetic/transport models obtained in the above investigation will eventually serve as components of a combustion tube model. The combustion tube model can provide valuable information for the scale-up to two and three-dimensional reactors.

One of the unresolved analytical problems in the analysis of in situ coal gasification field data is the assessment of the in situ reactor geometry (sweep efficiency). This type of reactor is quite unconventional, since it has no fixed boundary. Also the internal geometry of the gas/solid interface is changing with respect to time; the evolution of such channels has a significant effect on product gas composition and the heat transfer characteristics of the in situ reactor.

CONCEPTUAL MODELS OF IN SITU GASIFICATION

The chemical processes that occur during in situ coal gasification are essentially the same ones that occur in conventional coal gasifiers. It is not proposed here to discuss basic coal chemistry, either gasification or devolatilization, since extensive information on this subject is contained, for example, in Lowry's Chemistry of Coal Utilization (1963). Therefore, only a general discussion will be given.

The basic coal gasification reactions are as follows:

(1) $C + O_2 = CO_2$ (oxidation)

(2) $C + CO_2 = 2CO$ (reduction)

(3) $C + H_2O = CO + H_2$ (carbon-steam)

(4) $CO + H_2O = CO_2 + H_2$ (water gas shift)

(5) $CO + 3H_2 = CH_4 + H_2O$ (methanation)

In most conventional gasifiers, it has been found that reaction (4) nearly reaches thermodynamic equilibrium, while the other reactions are kinetic in nature. The oxidation reaction is irreversible for all intents and purposes.

Since it is desirable to operate the in situ gasifier at low pressures in order to minimize the gas leakage problem, the amount of methane produced via the gasification reactions (such as $CO + 3H_2 = H_2O + CH_4$) will be rather small, certainly comprising less than one per cent of the total gas volume for air injection. Virtually all of the methane recovered from in situ gasification will be due to pyrolysis. The exact nature of the pyrolysis products will, of course, be dependent on the coal used. The interaction of pyrolysis, water influx, and gasification on the product gas composition will be different for forward burning and reverse burning.

As discussed by Thring and Essenhigh (1963), the mechanism of the oxidation kinetics consists of chemical kinetic, adsorption, and diffusion regimes. Of particular interest for in situ gasification is the expected particle size, which for UCG will be much larger than for pulverized fuel furnaces. The size of the particles will be controlled by the structural characteristics of the coal, since the rubble-ization of the coal seam proceeds by thermal fracturing. In general, it is assumed, therefore, that the controlling regime is diffusion through the boundary layer above about 1000°C and chemical reaction below this temperature. At extremely high temperatures, adsorption may become important. The kinetics for coal gasification are usually approximated in terms of reactions of carbon, hydrogen, and oxygen (rather than in terms of more complicated chemical constituents of coal).

Nusinov (1946) and Skafa (1960) have explained qualitatively the major mechanisms of gas formation in underground gasification. Certain zones have been identified when following the gas stream along its flow path in a coal seam under gasification. With air as the gasification agent, the first zone is the zone of oxidation, where practically all the oxygen content of the blast is depleted in contact with the coal by the reaction, $C + O_2 = CO_2$. As in gas producers, the oxidation zone should be rather short, often less than one foot, although this is affected by the presence of the channel. Much heat is evolved (a typical temperature is greater than 900°C), forming within the coal bed successive zones of high temperature coking, semi-coking, and drying. As long as free oxygen remains in the gas stream, the zone of oxidation persists. Depleted of free oxygen, the stream moves into a reduction zone (600° - 900°C), where carbon dioxide is reduced to carbon monoxide in contact with the hot coke; $C + CO_2 = 2CO$, and water vapor forms hydrogen and carbon monoxide, $C + H_2O = CO + H_2$, through the carbon-steam reaction, or carbon dioxide and hydrogen at lower temperatures, through the water gas shift reaction, $CO + H_2O = CO_2 + H_2$. While this zone is 6 feet or less in conventional gas pro-

ducers, it may extend to nearly 50 feet in UCG, yielding more efficient utilization of the heat produced. Due to these endothermic reactions, the temperature decreases and the gas enters a zone of dry distillation (200° - 600°C) where it mixes with the volatiles evolved from the coal. Finally, some moisture is added to the product gases before they leave the coal seam. A typical composition profile for UCG is shown in Figure 1 (Skafa, 1960).

The above description has placed all discussion within the context of a "simple" one-dimensional steady state model involving reaction kinetics and heat transfer; however, even the numerical simulation of such a system represents a formidable challenge. While the study of fixed bed reactor simulation is not a neglected subject, the consideration of a complex set of interacting reactions such as those mentioned earlier presents many unanswered questions.

SIMULATION RESULTS

In a rapidly decaying catalytic conversion process occurring in a fixed bed reactor, the "hot spot" travels from the inlet to the outlet of the reactor. Although the gasification of coke in a combustion tube is a gas-solid reaction, the evolution of the temperature profile exhibits behavior similar to the catalytic conversion process with catalyst decay. Since the catalyst activity, θ ($0 \leq \theta \leq 1$), characterizes the decaying process, it seems appropriate to define the weight fraction of coke gasified to characterize the gasification process. The weight fraction, W, like the catalyst activity, θ, is a function of time and position in the bed because it depends on the concentration and temperature profile in the bed. Profiles characteristic of the decay process have been presented by Butt (1972) and are shown in Figure 1. The catalytic activity variable can be replaced by weight fraction in the case of regeneration of coked catalysts or gas-solid reaction. A homogeneous model, where solid and gas phase temperatures are not distinguished, will be used.

Preliminary simulation runs were undertaken to demonstrate the usefulness of the weight fraction concept. If plug flow with no axial dispersion is assumed, the homogeneous transient model can be used with the pseudo steady-state assumption obtain an ordinary differential equation in a single variable, x* (dimensionless distance). In order to simplify the number of equations required, only the species of carbon and oxygen are assumed to react; surface reactions as well as gas phase oxidation of CO are allowed to occur. No momentum equation or change in porosity equation was utilized in these simulations. Constant gas velocity and physical properties were assumed.

The reactions used include two surface reactions:

(a) $C + O_2 \rightarrow CO_2$ $\qquad r_{O_2} = k_2 C_{O_2}$

(b) $C + CO_2 \rightleftneq 2CO$ $\qquad r_{CO_2} = k_f C_{CO_2} - \frac{k_f}{k_{eq}} C_{CO}^2$

and one gas phase reaction:

(c) $2CO + O_2 \rightarrow 2CO_2$ $\qquad r_{O_2} = k_1 (\frac{P_T}{14.7})^3 y_{CO}^2 y_{O_2}$

The combined kinetics for oxidation of carbon is

$$r_2 = \frac{1}{1/k_2 + 1/k_m} C_{O_2} = k_O^{(1)} C_{O_2}$$

where k_m, the mass transfer coefficient, is obtained from a j_D plot.

For the reversible reaction: $C + CO_2 \rightleftneq 2CO$, the reverse reaction is important only at low temperatures at which the mass transfer resistance ($1/k_m$) is negligible. Because of this, the interface compositions need not be retained, yielding a simplified kinetic expression:

$$r_{CO_2} = \frac{1}{1/k_f + 1/k_m} \left[C_{CO_2} - \frac{1}{k_{eq}} C_{CO}^2 \right] = k_O^{(2)} \left[C_{CO_2} - \frac{1}{k_{eq}} C_{CO}^2 \right]$$

Reaction rate parameters have been estimated from the literature (Lowry, 1963; Frank-Kamenetskii, 1955; Walker et al., 1959).

The mathematical reactor model in dimensionless form is

Mass Transfer:

$$\frac{\partial C^*_{O_2}}{\partial x^*} = -\frac{L}{u_o} k_1 \left(\frac{P_T}{14.7}\right)^3 \frac{C^{2*}_{CO}\, C^*_{O_2}}{C_{N_2}(1+C^*_{O_2}+C^*_{CO}+C^*_{CO_2})^3}\,\varepsilon - \frac{L}{u_o} k_o^{(1)} S_g C^*_{O_2} W \qquad (1)$$

$$\frac{\partial C^*_{CO}}{\partial x^*} = -2\frac{L}{u_o} k_1 \left(\frac{P_T}{14.7}\right)^3 \frac{C^{2*}_{CO}\, C^*_{O_2}}{C_{N_2}(1+C^*_{O_2}+C^*_{CO}+C^*_{CO_2})^3}\,\varepsilon + 2\frac{L}{u_o} k_o^{(2)} S_g \left[C^*_{CO_2} - \frac{C_{N_2} C^{2*}_{CO}}{k_{eq}}\right] W \qquad (2)$$

$$\frac{\partial C^*_{CO_2}}{\partial x^*} = 2\frac{L}{u_o} k_1 \left(\frac{P_T}{14.7}\right)^3 \frac{C^{2*}_{CO}\, C^*_{O_2}}{C_{N_2}(1+C^*_{O_2}+C^*_{CO}+C^*_{CO_2})^3}\,\varepsilon - \frac{L}{u_o} k_o^{(2)} S_g \left[C^*_{CO_2} - \frac{C_{N_2} C^{2*}_{CO}}{k_{eq}}\right] W + \frac{L}{u_o} k_o^{(1)} S_g C^*_{O_2} W \qquad (3)$$

Heat Transfer:

$$\frac{\partial T}{\partial x^*} = \frac{L}{u_o \rho_G C_p} k_1 \left(\frac{P_T}{14.7}\right)^3 \frac{C^{2*}_{CO}\, C^*_{O_2}}{(1+C^*_{O_2}+C^*_{CO}+C^*_{CO_2})^3}\,\varepsilon\,(-\Delta H_1) + \frac{L}{u_o \rho_G C_p} k_o^{(1)} S_g C_{N_2} C^*_{O_2} W(-\Delta H_2) \qquad (4)$$

$$+ \frac{L\, C_{N_2}}{u_o \rho_G C_p} k_o^{(2)} S_g \left[C^*_{C_{CO_2}} - \frac{C_{N_2} C^{2*}_{CO}}{k_{eq}}\right] W(-\Delta H_3) - \frac{4\, L\, U}{d_t u_o \rho_G C_p}(T - T_w)$$

Solid Consumption Rate:

$$\frac{dW}{dt} = -\frac{S_g M_C C_{N_2} W}{\rho_s}\left[2k_o^{(1)} C^*_{O_2} + k_o^{(2)}\left(C^*_{C_{CO_2}} - \frac{C_{N_2} C^{2*}_{CO}}{k_{eq}}\right)\right] \qquad (5)$$

Initial Condition: $t = 0,\ 0 \le x^* \le 1.0,\ W = 1.0$

Boundary Condition: $x^* = 0,\ t \ge 0$

$$C^*_{O_2} = C^*_{O_2}(0)$$

$$C^*_{CO} = 0.0$$

$$C^*_{CO_2} = 0.0$$

where $C^*_i = \frac{C_i}{C_{N_2}}$

$T = T_o$

Parameters chosen:

L: reactor length: 3.04 m (1.0 ft.)

u_o: Gas velocity: .076 m/s (15 ft/min)

ρ_G: Gas density: .469 kg/m^3 (.0293 lb/ft^3)

C_p: Specific heat of gas mixture: .025 cal/g ^oK (.25 Btu/lb ^oR)

M_c: Molecular weight of coke: 12

k_m: Mass transfer coefficient: .0064 to .0152 m/s (1.26 to 3.0 ft/min)

ε: porosity: 0.25

d_t: tube diameter: .05 m (.167 ft)

U: Overall heat transfer coefficient: 1.02 W/m^2 ^oK (0.18 Btu/ft^2min^oR)

C_{O_2}: 9.0 g-mole/m^3 ($x^* = 0$) (.00056 lb mole/ft^3)

C_{N_2}: 33.8 g-mole/m^3 ($x^* = 0$) (.002116 lb mole/ft^3)

P_T: reactor pressure: .007 MPa (1 atm)

S_g: Surface area per unit volume of bed: 164.5 m^{-1} (50 ft^{-1})

W: Weight fraction of ungasified coke $0.0 \leq W \leq 1.0$

$\bar{\rho}_s$: Bulk solid density: 240 kg/m^3 (15 lb/ft^3)

T_w: Reactor wall temperature: 1370^oK (2460^oR)

T_o: Inlet temperature: 1100^oK (2000^oR)

Solution Procedure:

(1) Let $W(x) = 1$. Initially, integrate the heat and mass transfer equations using Runge-Kutta 5th order integration.
(2) Store the calculated values of concentration and temperature at the grid points.
(3) Calculate $W(x)$ at $t + \Delta t$ by using the profiles and the solid consumption rate. Interpolation by grid points (i.e., Δx) is necessary for $W(x)$ where $W(x) \leq W(x + \Delta x)$.
(4) With the new $W(x)|_{t + \Delta t}$, go to (1) again until $t = t_f$.

Figure 2 gives the concentration profiles for CO, CO_2, and O_2; note that the outlet mole fraction of CO is 0.30, corresponding to a gas heating value of over 105 Btu/SCF. With pyrolysis effects, this value would be increased. Also a longer residence time would yield an increase in carbon monoxide production. Figure 3 illustrates the change in the temperature profile over time. Figure 4 shows how the combustion reaction proceeds in terms of weight fraction remaining.

Numerical experiments to test the effects of varying model parameters (grid size, porosity, heat transfer coefficients, mass transfer coefficient) gave the expected results. Hence, the simple numerical model behaved as expected. The "hot spot" travels toward the outlet of the reaction. The weight fraction decreases in a satisfactory way. As time elapses, the "hot spot" temperature decreases and the combustion zone (or reaction zone) spreads out, the lowering of "hot spot" temperature due to the fact that as time increases, the weight fraction of ungasified coke decreases, thus decreasing the amount of heat generated. Current efforts in numerical simulation have been oriented towards the development of a non-homo-

Current simulation efforts are oriented towards the development of a non-homophases) rather than the "homogeneous" model studied previously. This type of model will be necessary in order to predict two and three-dimensional behavior for in situ coal gasification as well as front movement velocities. These properties are not predictable through a one-dimensional model. Also there is some evidence

that the one-dimensional model without axial dispersion is inaccurate. The development of efficient numerical techniques for the non-homogeneous model is an important goal of this research. Once the assumptions of one-dimension and no dispersion are eliminated from the model, however, the numerical difficulties increase astronomically. The problem is no longer classified as initial value, but now is a two-point boundary value problem.

More often that not, a sophisticated model needs a sophisticated mathematical tool for solution. A numerical method, which is a mixture of orthogonal collocation and finite element methods and uses a direct solution for the profiles rather than a matrix inverse, is currently under study.

Why are finite elements useful when usually one is served rather adequately by finite difference methods? For solving the convection-diffusion type problem, use of the common finite difference method is not appealing because of two reasons:

(a) Many grid points have to be used. This leads to a large number of unknowns. The inversion of a large matrix may be a problem owing to round-off errors.

(b) The finite difference method usually utilizes a uniform grid size, though a nonuniform grid size is feasible. For some problems with steep gradients, the finite difference method of uniform grid size is not very suitable.

However, finite difference methods do allow easy formulation of problems. The mathematical manipulation of finite elements is somewhat complicated, which is a disadvantage. The finite element approach is a general method, and finite difference methods are a "subclass" of the finite element method. The finite element method also treats nonuniform grid spacing quite efficiently.

Orthogonal collocation is a method which entails approximate solution of a differential equation using, for example, a polynomial approximation. This approximation must however satisfy the differential equation exactly at a number of points, called collocation points, in the interval of solution (or domain of the independent variable). Thus, use of orthogonal collocation requires simultaneous solution of unknowns; an excellent book on the technique and its application to chemical reaction problems has been published by Finlayson (1972).

Use of orthogonal collocation method to solve diffusion-convection problems is best explained by the following case study: Finlayson (1972) used six interior collocation points to solve two coupled heat and mass equations with an axial dispersion tubular reaction model and got the same result as Lee (1968) who used finite difference method with 481 grid points. Furthermore, Finlayson (1974) pointed out that, for a solution of a certain O.D.E., the error was proportional to $(1/N)^{1.72N}$ where N was the number of collocation points. As N increases from 5 to 6, the error decreases by a factor of 100. By contrast, in a finite difference calculation of $0(\Delta x^2)$, where $N = 1/\Delta x$, a change of N from 5 to 6 leads to 1.4 factor improvement in the error, or if the method is of $0(\Delta x^4)$, there is a 2:1 factor improvement. Besides its accuracy, orthogonal collocation does not require the calculation of integrals which is a common and time consuming part of finite element method using a variational method. This is especially advantageous for non-linear differential equations (e.g., reaction rate equations). These advantages have led Finlayson (1974) to recommend orthogonal collocation on finite element for this type of problem.

The application of collocation to the reactor equations falls under the classification of DSCT (discrete space-continuous time), since the net result is converting a set of pde's to a larger set of ode's, where time is the independent variable. However, the right hand side of the ode's will contain many unknowns if an implicit method of integrating with respect to time is chosen (explicit methods avoid this difficulty at the expense of large errors and much computer time). In this work Crank -Nicholson and fully implicit schemes are being investigated.

The simultaneous solution of the nonlinear ode's is also not easy. Two methods of linearizing the nonlinear terms are being studied: quasilinearization (Newton's method) and forward projection. This latter method is easier to implement for nonlinear equations, but is not as accurate as quasilinearization. Once the set of equations is linearized, a large set of linear algebraic equations results. While a matrix converse solution is in theory possible, it is pragmatically out of reach because of the large matrices involved. Therefore, an iterative method which takes advantage of the sparseness of the matrices involved appears to be the most attractive approach at this time. The iterative method would require less computer storage and may be faster, since as many as 1000 unknowns may have to

be solved in the solution procedure.

ANALYSIS OF FORWARD VS. REVERSE COMBUSTION

Most successful underground coal gasification systems employ a reverse combustion step to create a zone of high permeability between injection of production boreholes. Reverse combustion is implemented when the propagation of the combustion front is opposite to the direction of the oxidant flow. Hence, this process operates through the process of heat conduction rather than convection, since the injected gases are not used to heat up the unburned coal. On the other hand, forward combustion, where the combustion focus and oxidant move co-currently, is a convection-driven process; here the hot product gases heat up the unburned coal prior to combustion. This is the same method used in conventional fixed bed coal gasifiers, such as in the Lurgi gasifier.

Coal gasification systems should have a preferred direction of combustion, which depends upon a combination of the operating parameters for gasification. In underground coal gasification, it has been found that for high pressure drops and low flow rates (low permeability), reverse combustion is preferred. After the path of high permeability is created, the preferred direction of combustion is the forward mode, corresponding to high flow rates and high permeability. The examination of moving reaction zones has been performed previously for regeneration of coked catalyst beds as well as for other systems. Vortmayer and Jahnel (1972) studied the moving reaction zone for the oxidation of ethane on palladium oxide catalyst, and they found that the zone movement depended upon the gas velocity, reactant concentration, and other system parameters. Similar analyses have been performed for oil and tar sands recovery: Berry and Parrish (1960) and Warrent al. (1960), although numerically.

Pitin et al. (1963) have reviewed field data for forward combustion, and have noted the following general trends:

(1) The velocity of the fire front is proportional to oxygen concentration in blast stream and inversely proportional to the coal moisture content.
(2) The combustion temperature increases with oxygen concentration in the blast stream and reaches a maximum for 30-35% oxygen, after which it declines.
(3) The combustion temperature is inversely proportional to the moisture content.
(4) For each coal rank, there is a minimum oxygen concentration in order for the combustion front to advance; below this value there is no movement.
(5) For each coal type there is an upper bound on allowable moisture content, above which the combustion front does not move for air injection.

The effect of various operating variables on the process of reverse burning has been investigated in several locations; the results were as follows (Lavrov et al., 1968):

(1) An increase in ash content of the coal from 30 to 45% resulted in a reduction in the cross-cutting rate by a factor of 2.5.
(2) As the porosity of the coal increased, the cross-cutting rate increased.
(3) The migration rate of the combustion focus increased with increasing inlet oxygen concentration.

It is planned to validate some of these trends both experimentally in a combustion tube and numerically with a computer simulator. The principal coal type to be investigated will be Texas lignite, which is a prime candidate for in situ gasification, mainly due to its location. Some variation in physical properties, e.g., ash and moisture content, will be obtainable through selecting different sampling sites.

In order to simulate in situ gasification on a bench scale, it would be desirable to obtain long cores of lignite, which then can be sealed into a combustion tube. However, it is virtually impossible to obtain sufficient lengths of unbroken cores for lignite or other sub-bituminous coal. On the other hand, it has been discovered in working with smaller samples that the thermal front during gasification fractures the lignite prior to actual combustion. Similar results have been reported by Lawrence Livermore Laboratory. This characteristic seems to be shared by low rank shrinking (as opposed to swelling) coals. Therefore, some simplification in the experimental procedure is attainable, i.e., pulverized coal can be used in lieu of a coal core. Sealing of a pulverized coal system in a combustion tube is not critical, since uniform flow through the system can be obtained. With a core, leakage around the perimeter is a common problem.

EXPERIMENTAL CONFIGURATION

In order to test modeling hypotheses for the fixed bed gasification system, it is necessary to construct a suitable experimental apparatus. The features of the experimental system, which is nearly completed, are as follows:

(1) The reaction will take place in a insulated vertical stainless steel tube, with a diameter of five centimeters and a length of one meter. The tube will be lined with refractory, because of the high temperatures occurring.

(2) Small particles of lignite of a narrow size range will be packed in the tube. The porosity of the carbon bed will be specified in order to sustain sufficient flow rates. Flow rate/pressure drop data will be checked with packed bed correlations.

(3) The flow rate of oxygen and nitrogen will be monitored from their respective cylinders by appropriate metering systems. Air injection will be used initially.

(4) At six points along the tube the temperature will be measured. Thermocouples capable of measuring temperatures up to 1100°C will be used for temperature measurements. Gas samples will be collected through sampling valves into evacuated sampling bottles.

(5) The reaction will be initiated at one end of the tube by an electrical heating element. Reverse combustion experiments will be performed initially because of their low operating temperatures (less than 700°C). This should maximize the life of the combustion tube. Such reverse combustion experiments will be followed by higher temperature forward combustion experiments.

REFERENCES

1. Berry, V.J., and Parrish, D.R., Trans, AIME, 219, 109 (1960).

2. Butt, J.B., "Catalyst Deactivation," Adv. in Chem., 109, 259 (1972).

3. Carey, G.F., and Finalyson B.A. Chem. Engr. Sci., 30, 587 (1975).

4. Dinsmoor, B., and Edgar, T.F., "Modeling of Gasification Channels," NSF-RANN Semi-Annual Report, The University of Texas at Austin, Austin, Texas, November 1975.

5. Finlayson, B.A., The Method of Weighted Residuals and Variational Principles, Academic Press, New York, 1972.

6. Finlayson, B.A., "Weighted Residual Methods and Their Relation to Finite Element Methods in Flow Problems," in Finite Element in Fluids, Wiley, New Yori, 1974.

7. Frank-Kamenetskii, D.A., Diffusion and Heat Exchange in Chemical Kinetics, Princeton University Press, Princeton, New Jersey, 1955.

8. Gregg, D.W., Hill, R.W., and Olness, D.O., "An Overview of the Soviet Effort in Underground Gasification of Coal," UCRL-52004 (1976).

9. Gunn, R.D., and Whitman, D.L., "An In Situ Gasification Model (Forward Mode) for Feasibility Studies and Design," LERC/RI-76/2, Laramie, Wyoming, February, 1976.

10. Lavrov, N.V., Nusinov, G.O., and Semenenko, D.K., Khimiya Tverdogo Topliva, No. 1, 113 (1968).

11. Lee, E.S., Quasilinearization and Invariant Imbedding, Academic Press, New York 1968.

12. Lowry, H.H., Chemistry of Coal Utilization, Wiley, New York, 1963.

13. Nusinov, G.O., Canad. Chem. and Proc. Ind., 30, 29 (1946).

14. Pitin, R.N., and Cheredkova, K.I., "Underground Processing of Fuels," TT-63-11063, p. 56 (1963).

15. Skafa, P.V., "Underground Gasification of Coal," Moscow, 1960.

16. Thring, M.W., and Essenhigh, R.H., "Thermodynamics and Kinetics of Solid Combustion," in Chemistry of Coal Utilization (H.H. Lowry, ed.), Wiley, New York, 1963.

17. Vortmayer, D., and Jahnel, W., Chem. Engr. Sci., 27, 1485 (1972).

18. Walker, P.L., Rusinko, F., and Austin, L.G., Adv. in Catalysis, 11, Academic Press, New York, 1959.

19. Warren, J.E., Reed, R.L., and Price, H.S., Trans, AIME, 219, 109 (1960).

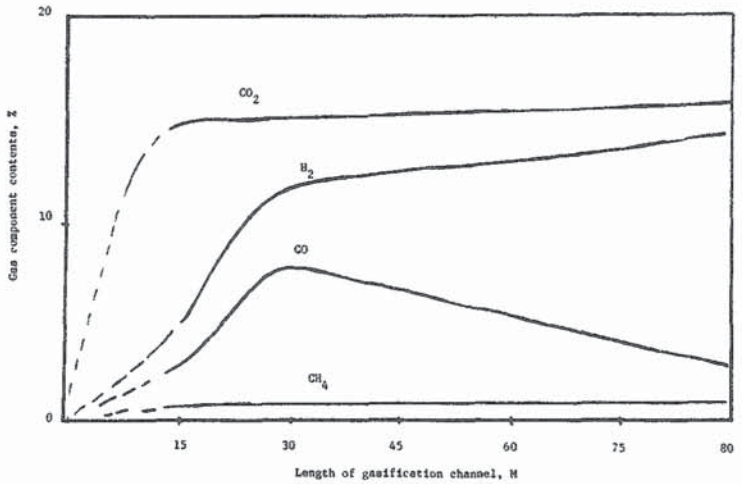


Figure 1. Change in the Composition of the Resultant Gas in the Gas Phase Along the Length of the Gasification Channel.

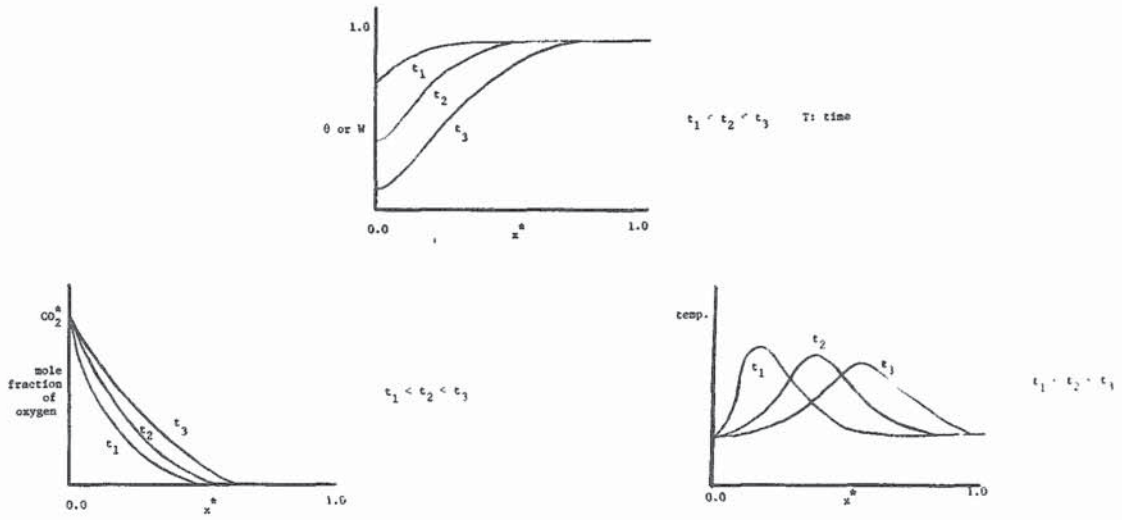


Figure 2. Typical Profiles for Packed Bed Catalyst Decay

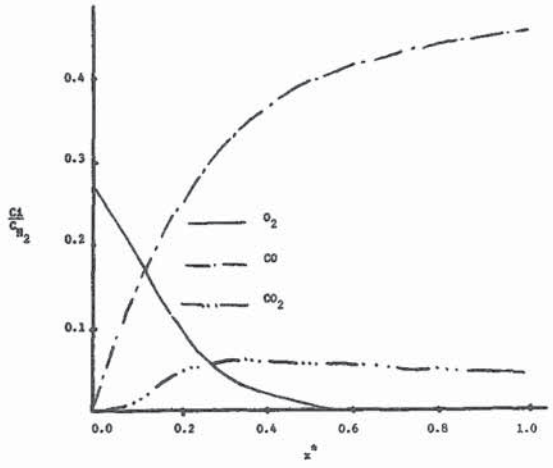


Figure 3. Simulated Composition Profiles, Combustion Tube

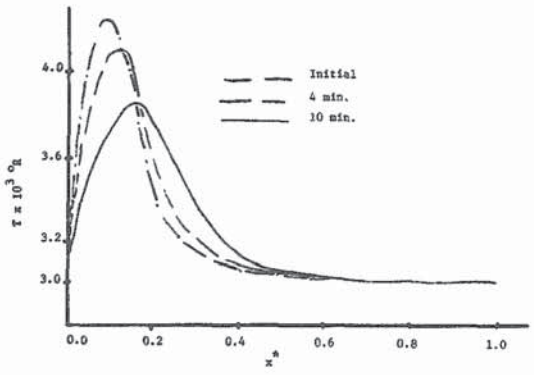


Figure 4. Simulated Temperature Profiles, Combustion Tube

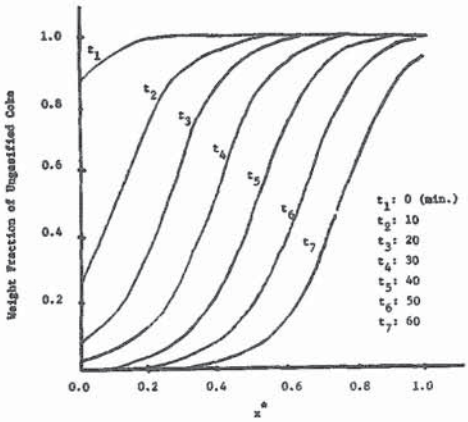


Figure 5. Simulated Sweep Efficiency, Combustion Tube

Thermo-Viscoelastic Considerations Associated With Underground Coal Gasification

by

Sunder H. Advani, West Virginia University
L. Zane Shuck, MERC, ERDA
Y. T. Lin, West Virginia University

ABSTRACT

Simplified thermoviscoelastic response solutions for circular cavity and line drive models, incorporating Pittsburgh coal properties at elevated temperatures, are presented. Preliminary results from a two dimensional finite element structural model representation of the coke, softened layer, coal media are given. The response of coal fissures to pressure and temperature loading is also discussed.

INTRODUCTION

The mechanical properties of coal at elevated temperatures govern, to a large extent, the basic mass and energy transport phenomena associated with the Longwall Generator Concept of Underground Coal Gasification. Delineation of the thermoviscoelastic response is therefore fundamental to the understanding of the basic mechanisms controlling UCG flame propagation and stability.

This abstract details the stress responses of simplified models represented by a circular cavity in the coal bed and a uniformly translating line drive. Finite element model results for a layered model are also presented. These models incorporate experimentally determined properties of Pittsburgh coal at elevated temperatures [1].

RESULTS

The stress equations governing the thermo-elastic response of a circular cavity in an infinite medium can be deduced from Muskhelishvli [2]. The radial and hoop stress expressions are

$$\sigma_{rr} = \frac{E\alpha}{2(1-\nu)} \frac{(T_o - T_\infty)}{(\log R_\infty - \log R_o)} \left\{\log r + \frac{1}{r^2} \frac{R_o^2 R_\infty^2}{R_\infty^2 - R_o^2} \log \frac{R_\infty}{R_o} - \frac{R_\infty^2 \log R_\infty - R_o^2 \log R_o}{R_\infty^2 - R_o^2}\right\} \quad (1)$$

$$\sigma_{\theta\theta} = \frac{E\alpha}{2(1-\nu)} \frac{(T_o - T_\infty)}{(\log R_\infty - \log R_o)} \left\{\log r - \frac{1}{r^2} \frac{R_a^2 R_\infty^2}{R_\infty^2 - R_o^2} \log \frac{R_\infty}{R_o} - \frac{R_\infty^2 \log R_\infty - R_o^2 \log R_o}{R_\infty^2 - R_o^2} + 1\right\} \quad (2)$$

Figure 1 illustrates the thermo-viscoelastic stress responses using equations (1) and (2) and the properties of Pittsburgh coal at elevated temperatures for $\theta_o = 600°F$ (fluidic state) at different time intervals. Corresponding solutions using a finite difference technique are also revealed for comparison in this figure.

References appear at end of paper.

Thermo-viscoelastic solutions for the problem posed by a line drive translating uniformly (velocity V) in the coal seam are obtained from the quasi-static temperature and stress relations.

$$T = \frac{(T_o - T_\infty)}{1 - e^{-(V/a)x'_\infty}} \; e^{-(V/a)x'} + \frac{T_\infty - T_o \; e^{-(V/a)x'_\infty}}{1 - e^{-(V/a)x'_\infty}} \tag{3}$$

and

$$\sigma_{yy} = \frac{-3\alpha(T_o - T_\infty)}{(J_s + 2J_c)} \tag{4}$$

Figure 2 shows the σ_{yy} profile computed from (4) along the moving x axis.

Figure 3 details the selected two dimensional rock, clay, and coal bed finite element model. The coke and softened layers around the volatilized cavity are also identified. The computed "instantaneous" temperature distribution [3] along the x axis is given in Figure 4. The following properties are assumed for the model in the stress evaluations:

PROPERTY	UNITS	COAL	ROCK	CLAY	COKE	SOFTENED LAYER 525°F	SOFTENED LAYER 300°F
E	psi	0.55×10^6	3.0×10^6	1×10^5	1.3×10^5	2×10^2	1.8×10^5
ν	-	0.44	0.22	0.45	0.25	0.47	0.47
α	-/°F	2.78×10^{-6}	4.50×10^{-6}	2×10^{-6}	4.50×10^{-6}	5.4×10^{-6}	5.4×10^{-6}
K	BTU/°F in.sec.	7.50×10^{-6}	2.5×10^{-5}	1.33×10^{-5}	2.79×10^{-6}	5.15×10^{-6}	5.15×10^{-6}
ρ	$lbm/in.^3$	0.046	0.086	0.046	0.037	0.028	0.028

The thermal stresses along the x axis are shown in Figure 5a with the hoop stresses around the cavity due to the primitive stresses and thermal loading revealed in Figures 5b and 5c respectively. The corresponding magnitudes of the hoop stresses due to the primitive stresses and thermal loading in the softened layer are of the order of 10 psi. In this context, local extrusion through the fissures can occur at these relatively small stress levels. Computations of critical differential crack pressures for crack extension and equivalent critical temperatures can be found in Reference [4]. These fissure response studies can lend fundamental insight on the suitabilities of the forward and reverse modes of combustion via fluid flow and heat transfer models.

NOMENCLATURE

E	Elastic modulus
J_c, J_s	Creep compliances in compression and shear respectively
K	Thermal conductivity
r	Radial co-ordinate
R_o, R_∞	Cavity and outer radii respectively
T	Temperature
T_o, T_∞	Cavity and outer surface temperatures respectively
V	Burn velocity
x	Axial co-ordinate
α	Coefficient of thermal expansion
σ_{ij}	Stress components
ρ	Mass density

REFERENCES

1. Shoemaker, H., L. Z. Shuck, R. Haynes, and S. Advani, "The Mechanical Properties of the Pittsburgh Coal at Elevated Temperatures," In Press, ASME Transactions, Paper to be presented at the 1976 International Joint Pressure Vessels and Piping Conference, Mexico City, Mexico, 1976.
2. N. I. Muskhelishvili, "Some Basic Problems in Theory of Elasticity," Noordhoff, Groningen, Netherlands, 1953.
3. Advani, S., L. Z. Shuck, Y. T. Lin, and H. Y. Chang, "Thermomechanics Simulations Associated with Underground Coal Gasification," In Press, 17th U.S. Symposium on Rock Mechanics, August, 1976.
4. Advani, S., L. Z. Shuck, and Y. T. Lin, "Thermal and Structural Response Evaluations for Underground Coal Gasification, SPE paper 6152, 1976.

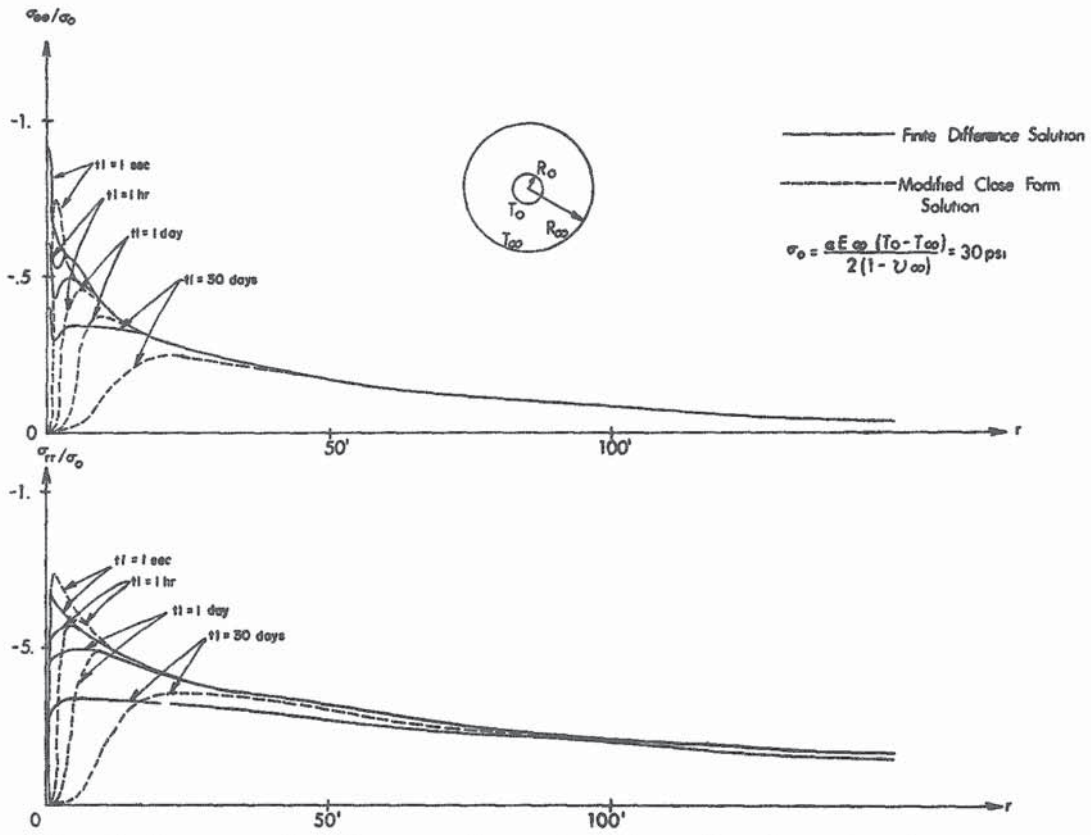


FIGURE 1. COMPARISON OF THERMO-VISCOELASTIC HOOP AND RADIAL STRESSES USING MODIFIED CLOSED FORM AND FINITE DIFFERENCE SOLUTIONS.

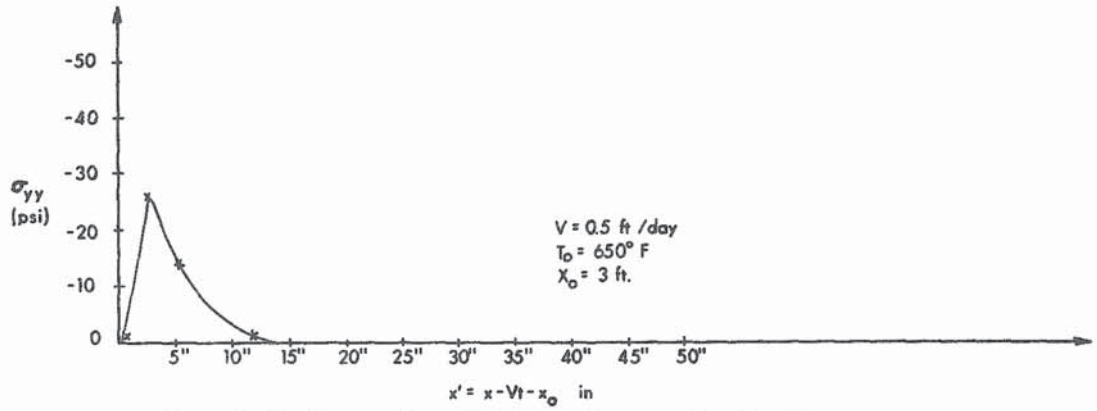


FIGURE 2. NON-VANISHING THERMO-VISCOELASTIC STRESS FOR LINE DRIVE MODEL.

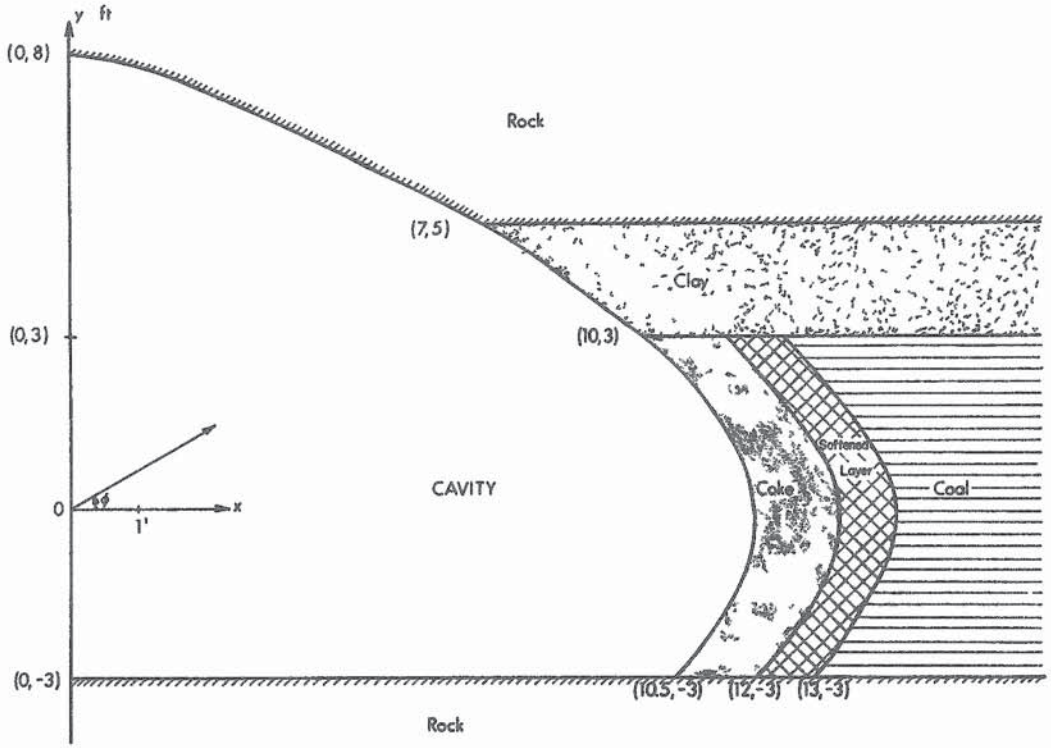


FIGURE 3. SELECTED TWO DIMENSIONAL ROCK, CLAY, AND COAL BED MODEL. COKE AND SOFTENED LAYERS ARE ILLUSTRATED.

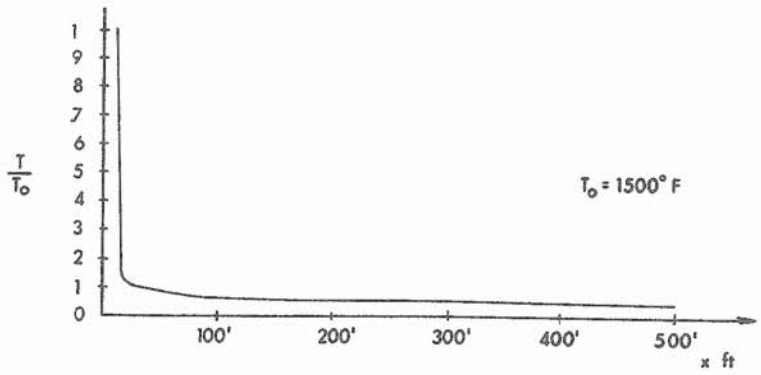


FIGURE 4. TEMPERATURE DISTRIBUTION FOR MODEL IN FIGURE ALONG X AXIS.

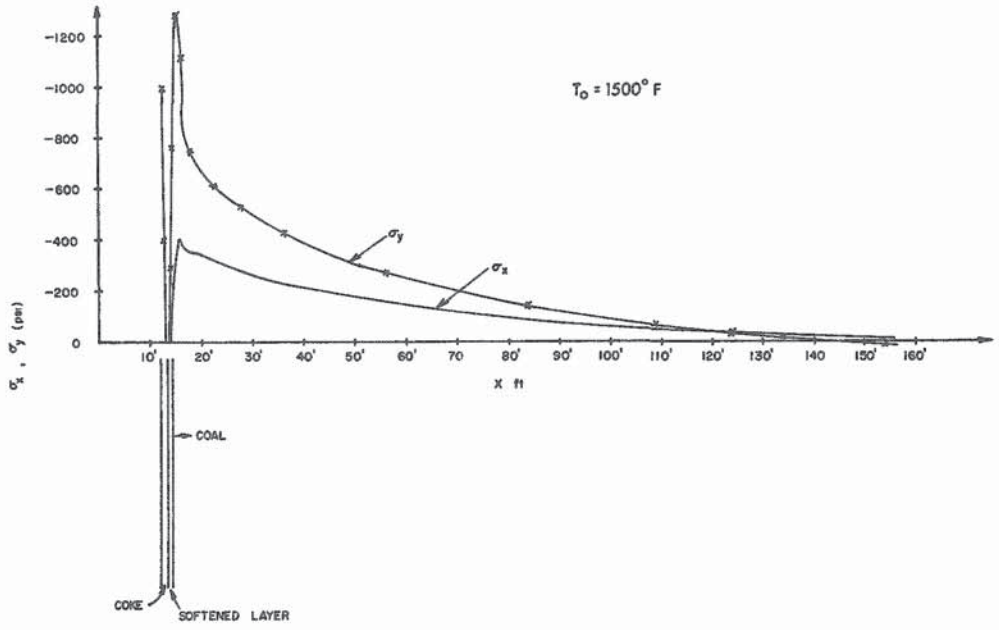


FIGURE 5A. STRESSES RESULTING FROM THERMAL LOADING.

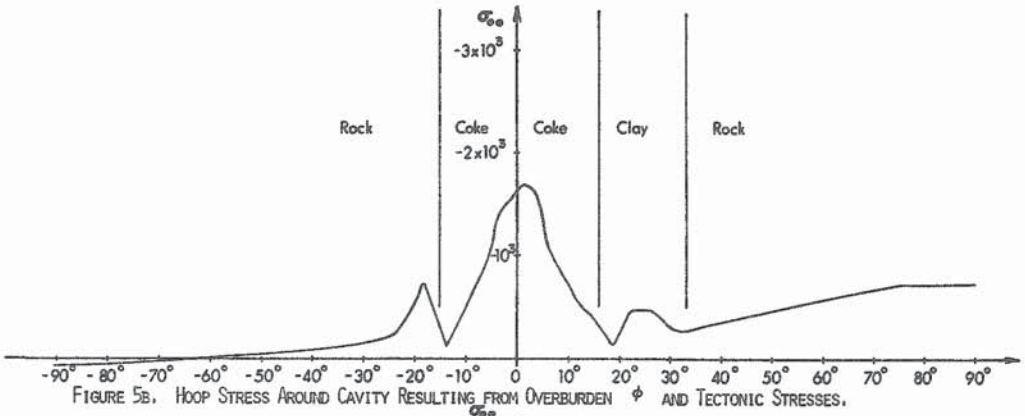


FIGURE 5B. HOOP STRESS AROUND CAVITY RESULTING FROM OVERBURDEN AND TECTONIC STRESSES.

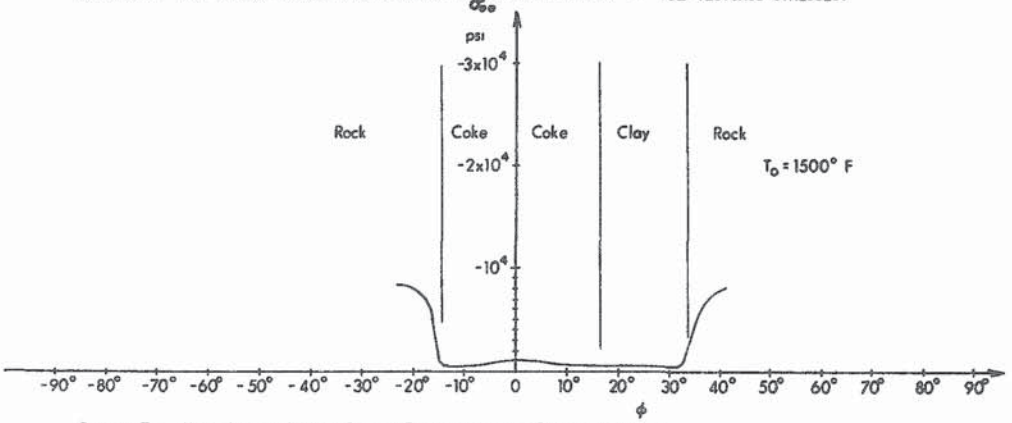


FIGURE 5C. HOOP STRESS AROUND CAVITY RESULTING FROM THERMAL LOADING.

A THEORETICAL ANALYSIS OF SOVIET IN SITU COAL GASIFICATION FIELD TESTS

R. D. GUNN,[1] D. W. GREGG,[2]
D. L. WHITMAN[1]

ABSTRACT

The Soviet literature contains a number of empirical correlations which interrelate important variables in the underground coal gasification (UCG) process. These correlations are based on the results of a massive field testing program conducted over a period of more than 40 years. Can the Soviet experience be used as a qualitative guide to this country's field testing of UCG which is still in its infancy? A theoretical analysis of Soviet field test data with the aid of a mathematical model helps determine the chemical and physical phenomena governing the behavior observed, and similar conditions and behavior can be expected in field tests in the United States. The mathematical model predicts such effects quantitatively.

INTRODUCTION

Underground coal gasification (UCG) has been field tested for more than 40 years. The process has been proven technically, but in the past it has not been economically attractive in competition with artificially cheap natural gas supplies. The availability of natural gas, however, is becoming increasingly restricted within recent years; and some large intrastate gas contracts have been negotiated at prices approaching $2.00/MM Btu ($1.90/billion joules).

At these prices gas produced in situ from coal may be competitive once the process is sufficiently understood to permit commercialization, and within the last three years there has been much renewed interest in UCG.

SOVIET TECHNOLOGY IN UCG

Probably any well conceived research program concerning in situ coal gasification must involve a serious study of the Soviet experience in field testing UCG. A review of the Soviet work in UCG very quickly shows that the amount of effort expended by the Soviets far exceeds the combined efforts of all other nations [1].[3]

The Soviet decision to pursue underground gasification of coal was made in 1928, and the first field experiments were performed in 1933 [2-3]. Their work has continued up to the present, with varying levels of effort that appeared to peak in the late 1960's. Skafa [4] indicates that there were as many as 3000 people working in the effort in 1963. It appears that this number might have more than doubled by the late 1960's, and then fallen off dramatically by the early 1970's.

---

[1]University of Wyoming and ERDA, Laramie Energy Research Center, Laramie, Wyoming
[2]Lawrence Livermore Laboratory, Livermore, California
[3]References at end of paper

The reduction in emphasis was probably due to their discovery of large resources of natural gas, and the construction of the necessary pipelines for its distribution. A crude economic estimate, taking into consideration the numerous commercial plants they constructed and operated as well as the number of people involved over the past 47 years, indicates that it might take as much as 10 billion 1976 dollars to reproduce their work.

Because only the Soviets have operated numerous commercial coal gasification power plants over long periods of time, it is important to understand what were their final process designs and why they settled on such designs. It is easy to conceive of numerous methods for UCG that address one particular problem or another, but in the operation of a successful commercial process it is obvious that all the problems that nature is going to generate have to be dealt with simultaneously in a satisfactory and harmonious manner. Only the Soviets have demonstrated that they have a system design that can be operated repeatedly in a predictable manner and can be transferred from one area to another where there are large differences in the geological nature of the coal seams [1].

The final design configurations that the Soviets settled on for gasification of horizontal and steeply dipping beds, which are essentially the same basic design at different angles to the surface, are deceptively simple. They both consist of establishing in preparation for gasification, parallel, highly-permeable channels in the coal. These channels are placed in the "bottom" of the seam so that as gasification is carried out and the channel burns and widens, overlying coal falls into the channel which both feeds the coal to the combustion zone and provides a large amount of coal surface area for efficient reaction with the gases.

The techniques of establishing the highly permeable channels were the subject of extensive work by the Soviets and constitute a major portion of the technology. Such channels, called "linking channels", were formed by four basic techniques, depending on the particular situation: (1) directional drilling, (2) countercurrent combustion, (3) electrolinking, and (4) hydrofracking. A more detailed description of these techniques is presented by Skafa [4].

The final design configurations for horizontal and steeply dipping beds are presented in Figures 1 and 2 respectively. In both cases, parallel channels are placed in the coal at the "bottom" of the seams and are connected at one end by a manifold, which is also underground. In the system for steeply dipping beds, the channels are always drilled along the coal seam from the surface, and the bottom manifold is formed by any of the linking techniques described above. In the system for horizontal beds, the channels not always formed by the same technique, but rather any one of the linking techniques mentioned above might be used with the choice being dependent on the nature of the coal and equipment available. A more detailed description of the logic of the systems and how they handle the large number of physical and chemical phenomena that operate in the systems is presented by Gregg et al. [1].

Figure 3 presents a map of the USSR showing underground coal gasification sites [1]. Of these sites, Lisichansk and Yuzhno-Abinsk are steeply dipping beds and the rest are horizontal beds. It is our understanding that three gasification stations, Podmoskovia, Yuzhno-Abinsk, and Angren are still operational, but not necessarily on a continuous basis.

The Soviet research effort concerning UCG has apparently been a primarily empirical approach in which a large variety of different concepts have been tested on a vast scale in the field. From this work the Soviets have developed a number of different empirical correlations interrelating various relevant parameters. These results represent a potentially valuable source of data, especially because many of the correlations represent literally millions of dollars of field testing. The basic defect in these data is that an interpretive or a theoretical discussion of them is almost never given. For this reason the applicability of the Soviet results to U.S. conditions is doubtful, the physical basis for the correlated behavior is often uncertain, and the interactive effect of many variables is unknown.

A MATHEMATICAL MODEL FOR UCG

Mathematical modeling is an important tool for interpreting complicated processes. A good mathematical model is generally a quantitative interpretation of the physical and chemical phenomena involved in the process being studied. Once a successful model has been developed, it can be used to determine which phenomena are most important, how the various phenomena interact, and what their effect is on the outcome of the process. Process design methods and equations are an example of useful mathematical models.

PLAN OF A SHAFTLESS GENERATOR MOSCOW REGION PLANT

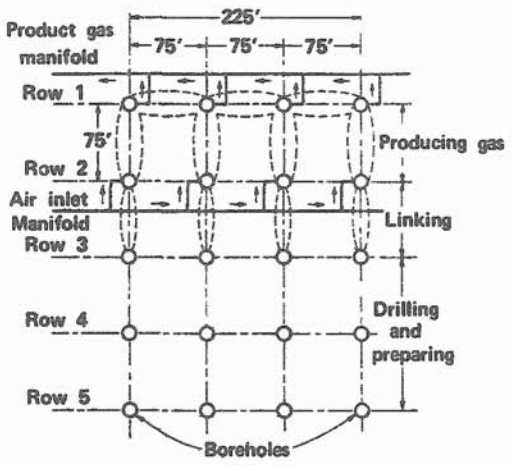


Figure 1.

TYPICAL SCHEME OF AN UNDERGROUND GAS GENERATOR FOR STEEPLY-DIPPING COAL BEDS: (a) PLAN VIEW (b) END ELEVATION.

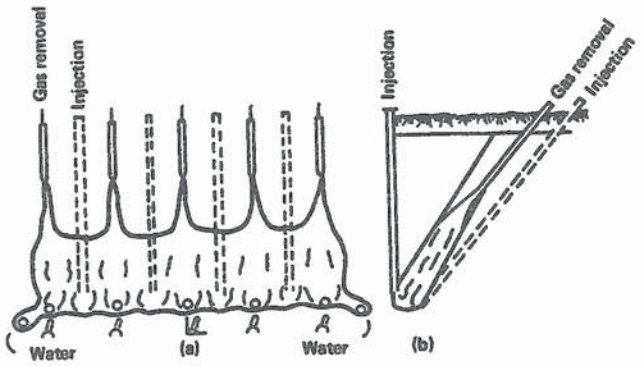


Figure 2.

UNDERGROUND COAL GASIFICATION SITES

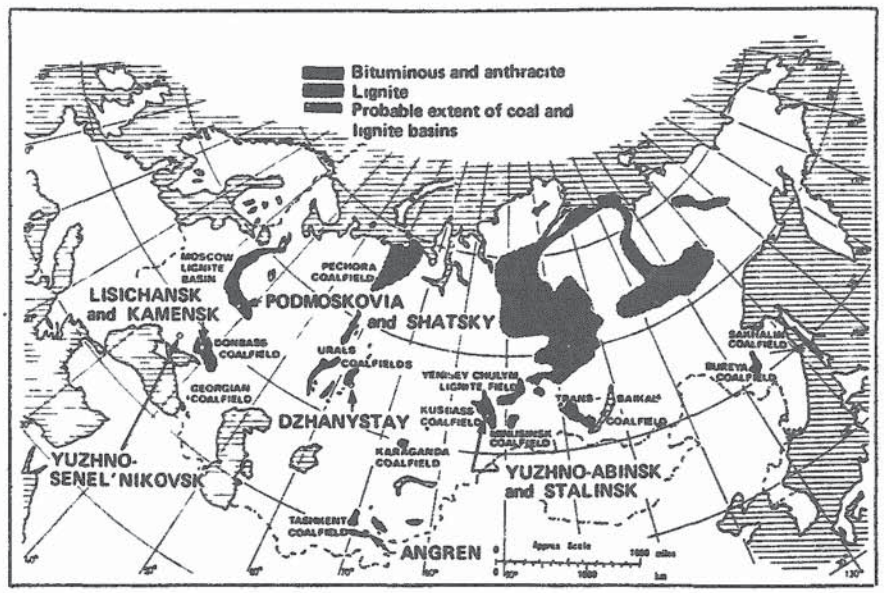


Figure 3.

Gunn and Whitman [5-7] have developed a successful model which is capable of predicting the performance of UCG tests with good accuracy. Since the model has been validated with actual experimental field data, it can be used now to interpret the results from Soviet field tests. The major purpose of this analysis is to determine the theoretical significance of the empirical correlations developed by the Soviets and to determine for comparative purposes the quantitative nature of similar correlations for UCG in subbituminous coal in the Hanna, Wyoming area.

The Hanna area has been selected because since 1973 a number of field tests have been carried out there by the Laramie Energy Research Center. These are probably the most thoroughly instrumented tests ever conducted, and correspondingly they have contributed much to current knowledge concerning the process. These are the only tests conducted within the United States since a single test by the Gulf Oil Company in 1969.

Figures presented later in this paper give comparisons of Soviet field data and corresponding data for UCG at Hanna, Wyoming. In most cases the data for Hanna are calculated and only a few points are actual experimental results. It has been explained earlier that the development of correlations from field data requires many field tests and an investment of millions of dollars. The Laramie Energy Research Center's field experimentation program at Hanna, Wyoming has not been extensive enough to permit development of completed correlations at this time; therefore, the mathematical model has been used to extrapolate to conditions not yet tested in the United States.

Much can be learned from the comparison between predicted data for Hanna and the Soviet data. In general, however, the similarities are expected to be only qualitative. The Soviet correlations are usually based on types of coal and conditions considerably different from those encountered in Hanna, Wyoming. Furthermore, the Soviet literature never provides sufficient data concerning coal properties and operating variables to permit the use of the mathematical model to predict the Soviet results directly.

LIMITATIONS

The effect of a number of variables upon the UCG process needs to be considered by the design engineer. An example of these types of information are:

1. Effect of air injection rate on gas heating values and compositions.
2. Effect of water intrusion rate on gas heating values and compositions.
3. Effect of oxygen enrichment on gas heating values and compositions.
4. Effect of coal ash content on gas heating value.
5. Effect of coal seam thickness on gas heating value.
6. Effect of well spacing and configuration on coal recovery.
7. Effect of air injection rate on rate of flame front propagation.
8. Effect of pressure on gas composition and heating value.

The first five items listed above are discussed in some detail in the remainder of this work. Items 6 and 7 are directly dependent upon the three dimensional flow patterns of gas and air through the coal. The mathematical model used in this work is a linear one; and, therefore, the model cannot predict data which depends directly on multidimensional flow. Item 8 and some related types of correlations for field experiments appear not to be available in the Soviet literature. In general the Soviets operated at pressures as low as possible in order to prevent gas losses from the coal seam. In addition the pressure dependence of laboratory kinetic and devolatilization data for Hanna coal has not been determined experimentally; and model predictions at higher operating pressures are probably inaccurate for this reason.

OPTIMUM AIR INJECTION RATE

The heating value of gas produced depends on the rate of air injection during forward combustion, and an optimum injection rate does exist. Figures 4 and 5 demonstrate the relationship between the heating value of produced gas and the air injection rate for four different

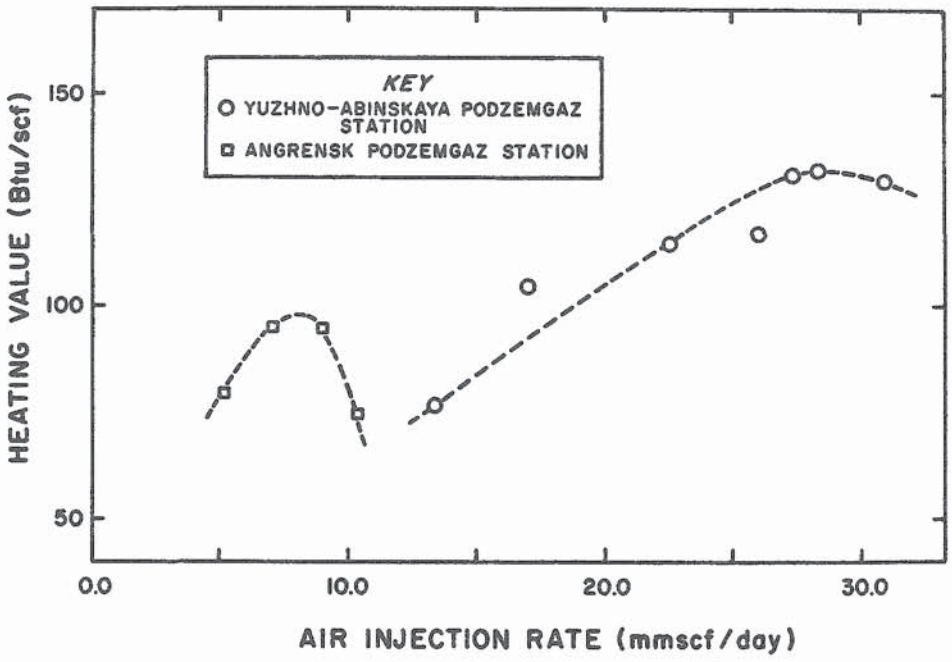


Figure 4.

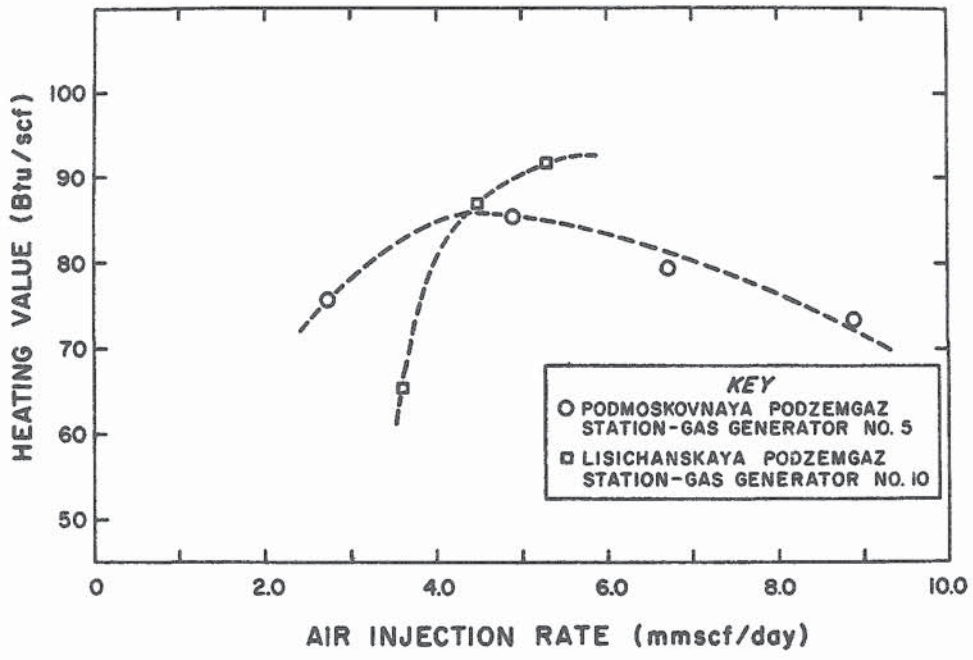


Figure 5.

locations in the Soviet Union. Figure 4 shows results obtained from field tests in lignite at Angren, Uzbekistan [8] and in highly volatile bituminous coal at Yuzhno-Abinsk, Siberia [9]. Figure 5 shows similar results for bituminous coal at Lisichansk in Southern Russia and for lignite in the Moscow Basin at Tula [4]. Figure 6 shows a comparable curve for Hanna No. 1 coal. The curve shown in Figure 6 is calculated, but the experimental point for the Hanna II Phase IA field test agrees closely with the calculated value.

The Hanna No. 1 seam in which the test was conducted is an aquifer. Thus water from the coal bed flowed into the combustion region throughout the test period. The rate of water intrusion generally increased during the field experiment. For the sake of consistency, however, the theoretical curve shown in Figure 6 is calculated on the basis of a fixed rate of water influx, that occurring on June 10, 1975. For this reason only a single field data point is included in Figure 6 corresponding to the air injection rate and heating value also for the June 10th period.

Figures 4, 5 and 6 all show a maximum in the heating value of gas produced as the air injection rate is increased. The mathematical model described earlier in this work provides a clear interpretation of the physical reasons for this maximum. These same reasons have also been cited by Skafa [4]. In reality it is the molar water/air ratio which is important rather than the air injection rate.

If water from the coal seam itself seeps into the combustion zone at a fairly constant rate, then at high air injection rates the water/air ratio is too low to provide the water needed for the gasification reaction,

$$C + H_2O \longrightarrow CO + H_2O \quad \text{(gasification reaction)}, \qquad (1)$$

and the heating value suffers. At low air flow rates the water/air ratio is too high. In this operating regime the gas heating value is controlled by the amount of heat available to drive the highly endothermic gasification reaction. The necessary energy is produced by the combustion of coal char; however, if too much liquid water seeps into the combustion zone, then a substantial part of the heat of combustion is lost in vaporizing the water. Thus, less energy is available for the endothermic reactions, and the gas heating value declines.

The maximum heating value for underground gasification does not coincide at the same water/air ratio as for the Lurgi process, because steam rather than liquid water is injected along with the air in the surface gasification process.

In a commercial operation a maximum heating value for the gas produced may not be a necessary objective. Even in this case, however, a too high water/air ratio is undesirable. With too much water a substantial part of the energy in the produced gas is tied up in the form of latent heat of vaporization. This latent heat is expensive and difficult to recover on a commercial basis.

Skafa [4] states that in the Soviet Union a major task of operating personnel is to maintain the air injection rate at its optimum value. As the burned out area gets larger during forward combustion, the rate of water inflow tends to increase; and, consequently, a higher air flow rate is also required for optimum conditions.

The intrusion of too much water in the gasification region has been a major problem in the Soviet Union. In some cases water drainage wells have to be drilled to reduce the rate of water influx. It seems probable, therefore, that too much water will also be a problem in the in situ gasification of coal in many areas of the United States.

WATER INFLUX RATE VS. GAS COMPOSITION

Data from Soviet and Hanna field tests indicate that gas compositions and heating values are functions of the air injection rate. As explained in the previous section this apparent correlation is actually a manifestation of the effect of the water/air ratio. Because this effect is directly related to the rate of water influx, a plot of heating value versus water influx (cubic meters per metric ton of coal consumed) should provide a more consistent method of comparing results for different field tests. Figure 7 shows such a plot for field test results at Hanna and at Yuzhno-Abinsk (seam IV Vrutrennyi) in Siberia [9]. The model shows good agreement with both sets of field test data. In addition the results of field experiments at the two different locations are quite similar.

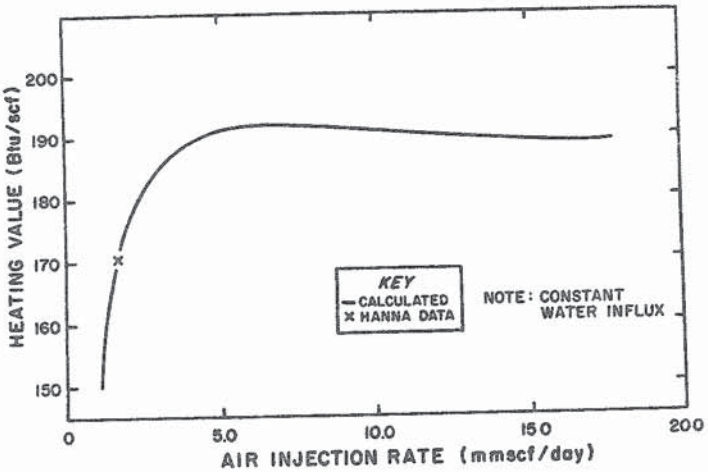


Figure 6.

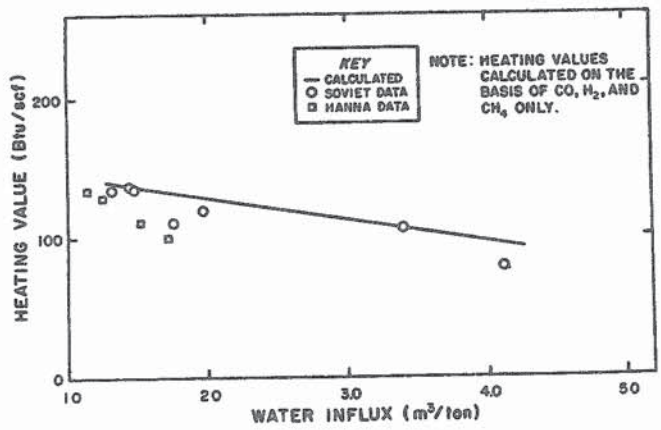


Figure 7.

Figure 8 depicts the relationship between the methane and carbon dioxide content of the gas produced and the water influx rate. Figures 9 and 10 are similar graphs for hydrogen and carbon monoxide respectively. In all three graphs the model calculations agree with the field data for the Yuzhno-Abinskaya tests [9] and with the Hanna field tests as well.

The field test sites in Wyoming and in Siberia are within 10° longitude of being on opposite sides of the earth. It is rather startling, therefore, that heating values and gas compositions are so similar. This similarity is even more striking when a comparison is made between the Siberian field tests and the model calculations. The calculations are based strictly on the laboratory data and properties of Hanna coal. The close agreement of model calculations with Siberian field data indicates that there is considerable similarity in the coal from the two locations.

The Hanna product is a high heating value subbituminous coal. The coal from Yuzhno-Abinsk has been described as a highly volatile bituminous coal [1]. The subbituminous classification apparently is not used in the Soviet Union.

It might appear surprising that the hydrogen and carbon monoxide content of the gas decrease as the water influx rate increases because these components both originate primarily from the water gas reaction (Equation 1). Figures 9 and 10 show that this decrease actually does occur, however. As explained in the previous section high water influx rates consume substantial amounts of energy in vaporizing the liquid, and this causes less energy to be available to support the highly endothermic water gas reaction.

Figure 8 shows the methane content of the gas is essentially unaffected by water influx rate. Methane is almost entirely a product of the devolatilization of the coal, and water has little effect on this process.

Some carbon dioxide is produced in the devolatilization process, but most of it originates from the combustion of coal char. At a constant air injection rate the absolute amount of carbon dioxide produced remains fairly constant even with an increasing water influx rate. However, additional water reduces the amounts of carbon monoxide and hydrogen generated, and less gas is produced. Consequently, the mole percent of carbon dioxide rises because the total amount of gas is less. Figure 8 illustrates this effect.

In addition to correlations of the type shown in Figure 7, the effect of water upon heating values and gas compositions is frequently represented in other ways in the Soviet literature [4,9]. For example, heating values are frequently plotted as a function of the water vapor content (gm/cubic meter) of the produced gas. When a too high water influx reduces the gas heating value for reasons already discussed in this section, the excess water turns up as a high steam content in the produced gas. No further discussion of this type of graph is included here because such correlations are simply a somewhat different manifestation of the same physico-chemical phenomena discussed earlier in this section.

OXYGEN ENRICHMENT

If a synthesis gas relatively free of nitrogen is desired, the injection of an oxygen-steam mixture is required. This process is used on commercial scale with Lurgi gasifiers. Much less frequently it is advantageous to use an oxygen enriched air mixture. For theoretical purposes, however, it is useful to compare model predictions with Soviet data for enriched air injection.

Figures 11 to 14 show the results of field tests conducted at Gorlovka in the Northern Donbass Coal Field in southern Russia [4]. The Soviet data agree semi-quantitatively with the calculated data based on Hanna. Quantitative agreement is not possible because the coal at Gorlovka is bituminous rather than subbituminous, the rate of water influx is unknown, and it is not certain if these tests were based on a permeation process. The trends of the data with respect to an increasing oxygen content are the same, however, because the same physical phenomena are involved for both sets of data.

For comparative purposes calculated data in Figures 11 to 14 are provided for two different water/enriched air ratios. This ratio which has a significant effect on produced gas compositions was not reported in the referenced source for the Soviet data.

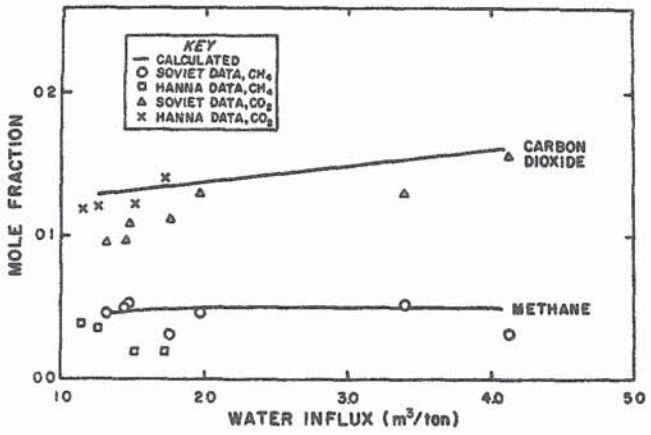


Figure 8.

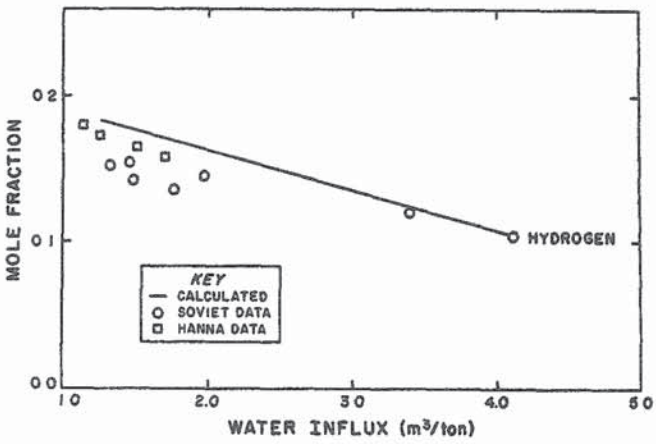


Figure 9.

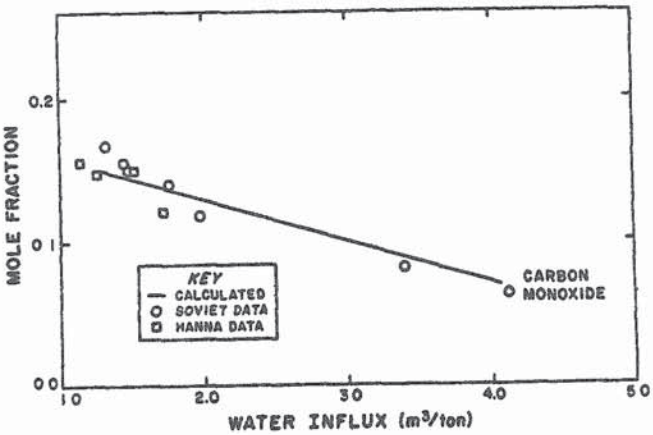


Figure 10.

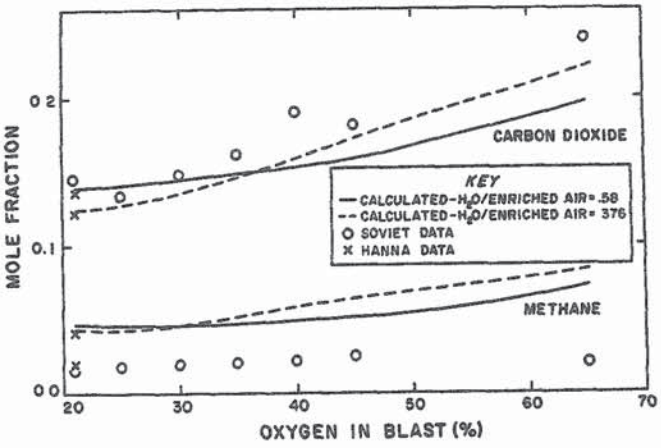


Figure 11.

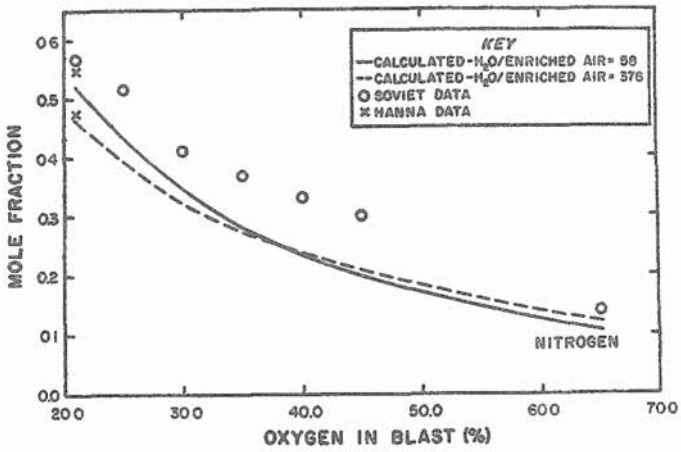


Figure 12.

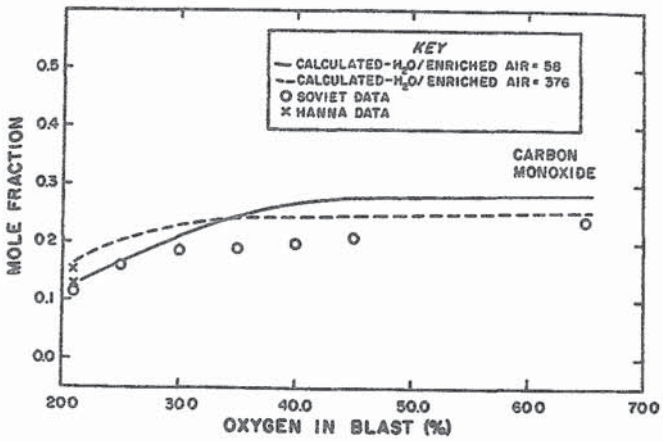


Figure 13.

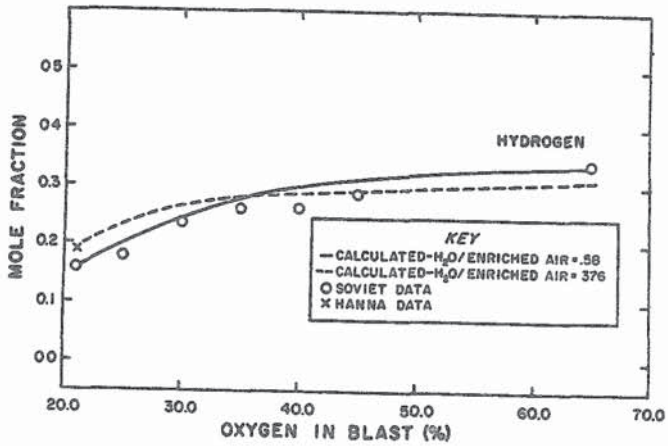


Figure 14.

It is intuitively apparent that with enriched air more oxygen is available for combustion, and thus more carbon dioxide should be present in the produced gas. Similarly enriched air contains a lower percentage nitrogen which also should be reflected in the composition of gas produced. As expected Figures 11 and 12 show that carbon dioxide increases and nitrogen decreases monotonically as more and more oxygen is used to enrich the air. The Hanna coal devolatilization products are much richer in methane than most other types of coal, and this fact is apparent in Figure 11.

The effect of oxygen enrichment on percentages of carbon monoxide and hydrogen is shown in Figures 13 and 14 respectively. The computed data are calculated on the basis of a constant rate of injection of enriched air and a constant rate of water influx, thus the water/air ratio remains constant for each of the calculated curves. The water/oxygen ratio, however, changes in direct proportion to the amount of oxygen in the injected air. Both calculated curves represent water influx rates which are greater than the optimum shown in Figure 6; and, therefore, higher water/oxygen ratios lead to higher percentages carbon monoxide and hydrogen and a higher heating value for the produced gas. Eventually the optimum water/oxygen ratio is exceeded, and the carbon monoxide and hydrogen content tends to level off.

The broken line curve in Figures 13 and 14 represents the lower water influx rate, that is, the influx rate closer to the optimum value. For this reason the broken line initially shows a higher quality gas than the solid line because a higher hydrogen and carbon monoxide content leads to a higher gas heating value. On the other hand for the lower water influx rate, the optimum water/oxygen ratio is exceeded more rapidly and levels off sooner; and the two calculated curves cross for this reason.

ASH CONTENT

In general no attempt is made in this work to interpret laboratory data reported in the Soviet literature. This section, however, is an exception. The effect of ash content of coal is technically an important consideration in designing an in situ coal gasification project. The Soviets report a correlation based on laboratory data of the heating value of gas produced versus coal ash content, but unfortunately a similar correlation of field test data has not been found. Figure 15 shows the correlation based on the Soviet laboratory data [4]. The calculated data based on Hanna No. 1 coal properties show the same trends as the laboratory data, but the heating value for the Hanna coal is much higher. The thirty foot thick seam at Hanna burns almost adiabatically because of the insulating properties of the cap rock and base rock. On the contrary the authors have found that heat losses from laboratory combustion tubes tend to be quite high. As explained in earlier sections any loss of heat causes a decrease in gas heating value, and heat losses probably explain the differences in the two curves in Figure 15.

A high ash content also leads to a decrease in gas heating value. With a higher ash content more thermal energy is adsorbed by it, and less energy is available for the endothermic gasification reaction which produces the fuel gases hydrogen and carbon monoxide.

For a thick seam, such as the Hanna No. 1 seam, Figure 15 shows that good heating values can be obtained even with ash concentrations as high as 60 percent. For thinner seams, especially those with a high water influx, the ash content can be much more critical because heat losses are large even without the presence of ash. For example the laboratory data, for which heat losses are believed to be large, show that gas heating value drops below 85 Btu/scf at ash concentrations greater than 60 percent. Heating values this low are generally to be avoided.

SEAM THICKNESS

Figure 16 shows the relationship between seam thickness and gas heating value. The figure also shows that the results are very sensitive to water intrusion rates. The curves based on Soviet data [10] are almost identical in shape to curves calculated for Hanna coal. The heating values are considerably higher for Hanna than for the Soviet field test. The Soviet data are based on experiments with hard (bituminous) coal from the Donbass and Kuzbass regions. These bituminous coals have less volatiles than those at Hanna; therefore, the methane content and the gas heating value should be lower for the Donbass and Kuzbass coals.

As with so many other correlations presented here thermal energy is the controlling factor in Figure 16. In a thick coal seam only a small fraction of the heat of combustion of coal char

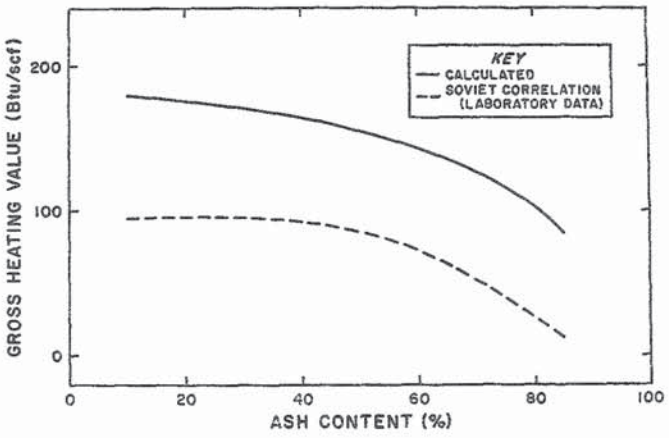


Figure 15.

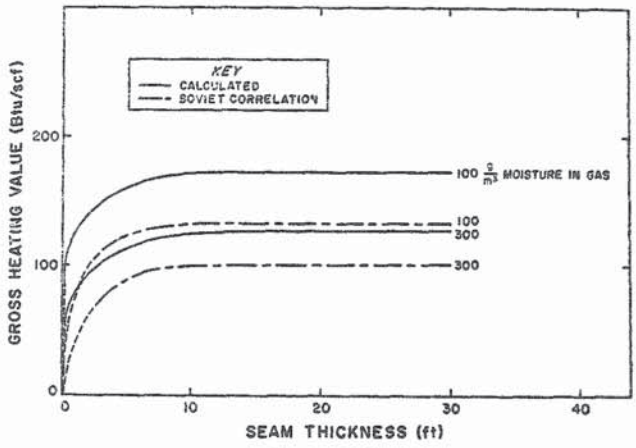


Figure 16.

is lost to cap rock and base rock. In thin seams the distance from the center of the coal to the edge is much less; hence, a much larger proportion of heat is conducted out of the coal into the surrounding rock. Due to this higher heat loss the gas heating value and the thermal efficiency of coal gasification in thin seams is less.

Actual heating values that can be obtained in a given thin seam will depend on many things such as the type of coal, ash content, air injection rate, rock properties, and water intrusion rate. For this reason the Soviet data are only a qualitative guide in areas outside of the Soviet Union.

CONCLUSIONS

The Soviet literature contains much field test data acquired at enormous cost. Because field tests are very expensive, it is important to make maximum use of these data. In all results considered here there is good qualitative, and sometimes nearly quantitative, agreement between model predictions and the empirical correlations derived from Soviet field tests. It is possible, therefore, to deduce the chemical and physical basis for the behavior observed in these field tests.

With the improved understanding derived from this study, the engineer can use the appropriate Soviet correlations as a qualitative guide to the design of underground coal gasification. The model provides a more concrete definition of the conditions and limitations implied by the correlations. At the same time it is possible with the aid of the model to develop quantitative correlations applicable to types of coal and to geological conditions different from those encountered in the Soviet Union.

A review of the results of Soviet field testing of UCG and of the physical and chemical reasons for their occurrence leads to two important conclusions. First a major controlling influence in UCG is the thermal energy balance. Factors which affect the thermal balance unfavorably are large heat losses from thin coal seams, loss of internal energy in the ash of high ash coal, and heat losses due to the vaporization of water. Second, excessive water influx into the combustion zone has been a major problem in the Soviet Union. It will probably present a major problem that must be remedied if UCG is to become a commercial process in this country.

ACKNOWLEDGMENT

The authors gratefully acknowledge financial support from the Northern Natural Gas Company and the Electric Power Research Institute.

REFERENCES

1. Gregg, D. W., Hill, R. W. and Olness, D. U.: "An Overview of the Soviet Effort in Underground Coal Gasification," Lawrence Livermore Laboratory, UCRL-52004, Jan. 29, 1976.

2. Kirichenko, I. P. and Ton, V. S.: "Underground Coal Gasification at the Lisichansk Mine," Gornyi Zhurnal III, 10-9 (1935).

3. Matveev, V. A.: "A Brief Report of Results and of the Most Pressing Problems in the Field of Underground Gasification of Coal," Podzem. Gaz. Uglei, No. 2, 4 (1957) [Eng. Transl. No. A. 1408/SEH (National Coal Board, Great Britain, 1957)].

4. Skafa, P. V.: "Underground Gasification of Coal," Lawrence Livermore Laboratory, UCRL-Trans-10880 (Sept., 1975).

5. Gunn, R. D.: "Mathematical Modeling of the Linked Vertical Well Process," talk presented at the First Annual Underground Coal Gasification Symposium, Laramie, Wyo., July 28-Aug. 1, 1975.

6. Gunn, R. D. and Whitman, D. L.: "An In Situ Coal Gasification Model (Forward Mode) for Feasibility Studies and Design," Laramie Energy Research Center, LERC RI 76/2, Feb., 1976.

7. Gunn, R. D., Fischer, D. D. and Whitman, D. L.: "The Physical Behavior of Forward Combustion in the Underground Gasification of Coal," SPE 6149 presented at SPE-AIME 51st Annual Fall Mtg., New Orleans, La., Oct. 3-6, 1976.

8. Lavrov, N. V., Kulakova, M. A. and Kazachkova, S. Ts.: "An Analysis of Several Technical Factors in the Underground Gasification of Brown Coal," Lawrence Livermore Laboratory, UCRL-Trans-10804 (Dec., 1974).

9. Kreinin, E. and Revva, M.: "Underground Gasification of Coal," Lawrence Livermore Laboratory, UCRL-Trans-10810 (Dec., 1974).

10. Antonova, R, I., Garkusha, E. G., Gershevich, E. G., Kreinin, E. V., Lavrov, N. V., Semenenko, D. K. and Fedorov, N. A.: "Some Regular Parameters of Underground Coal Gasification," Lawrence Livermore Laboratory, UCRL-Trans-10804 (Dec., 1974).

Calculation of Fracture and Permeability Enhancement From Underground Explosions in Coal*

BY

T. R. Butkovich, Lawrence Livermore Laboratory, University of California, Livermore, California

ABSTRACT

We use one- and two-dimensional computer programs to study explosive-induced fracturing and permeability enhancement. The total failure-induced deviatoric strain, a calculable parameter related to rock fracture, is used to correlate calculations with measurements. This parameter is made up of two parts, that associated with pure shear distortion and that associated with shear distortion from tensile failure. The total failure shear strain can be related to intensity of fracture, and the tensile portion can be related to the volume of tensile fractures. The latter value can be considered a measure of the crack volume generated following tensile failure. We correlate our calculations with measurements from field and laboratory experiments for both single and multiple explosions.

INTRODUCTION

The Lawrence Livermore Laboratory (LLL) scheme for in-situ coal gasification [1]† involves the use of chemical high explosives to fracture coal at depth, thereby increasing its permeability. The fractured, permeable, coal bed would then be ignited and supplied with a steam-oxygen mixture to form an underground retort. The gases produced would be recovered and processed on the surface to produce pipeline-quality gas. The design of such a retort requires a prediction of permeability enhancement within and around arrays of drill holes in which explosives are emplaced and detonated.

The SOC [2] and TENSOR [3] codes, designed to calculate stress fields resulting from the detonation of explosives in geologic media, are being used in an effort to predict permeability enhancement. The failure model used is based on measurements. It allows the rock to fail in a specified stress state, and the region of failure can thus be identified. However, the detailed condition of the fractured material is not presently available in the codes. Therefore, calculations and measurements of fracture and permeability enhancement must be closely coupled if we are to understand and model the behavior of geologic media subjected to a stress wave and displaced by the expanding working gases formed from the explosion products.

Predicting the extent of fracture around an underground detonation is important because to enhance permeability, one must first fracture the rock. One might expect that the more intensely the rock is fractured, the better the permeability enhancement. While this may be true in general, crushing the rock into many small particles

*This work was performed under the auspices of the U.S. Energy Research & Development Administration, under contract No. W-7405-Eng-48.

†References at end of paper.

could actually lower the permeability. Fracture is a necessary but not a sufficient condition for permeability enhancement. The fractures must remain open and connected; that is, fracture porosity must be created. Popular permeability theories such as the Blake-Kozeny-Carmen [4] theory relate permeability to fracture porosity.

The SOC and TENSOR codes do not calculate permeability per se. Instead, they compute a function ε_f, the total failure-induced deviatoric strain, which has been related to fracturing observed in connection with an explosion in granite [2], to explosive-fracture-intensity and permeability-enhancement measurements in a coal outcrop, and to fracturing caused by a small-scale explosion of a cylindrical charge in a coal block [5].

CALCULATION OF DAMAGE-INDICATING PARAMETER

SOC and TENSOR are Lagrangian codes designed to calculate the effects of underground explosions by solving the equations of motion based on the conservation of mass, momentum, and energy. SOC allows plane, cylindrical, and spherical geometries in one dimension. TENSOR is two-dimensional and can be set up to run in either axial cylindrical symmetry or plane strain. The codes require a description of the geologic materials, including elastic constants, pressure/volume relationships, and an experimentally determined failure criterion. The expansion adiabat and a rate of release of energy for the particular high explosive employed must also be provided. The codes calculate the propagation of the stress wave and the resulting changes in material density and velocities with distance. The calculations are normally run until the velocities in the region of interest approach zero.

Failure can occur in shear or tension. Shear failure is modeled through deviatoric stresses based on triaxial strength tests. Two failure surfaces are generated in K-$\bar{P}$ space, where K is the shear stress equal to $(\sigma_1-\sigma_2)/2$ (σ_1 is the axial stress and σ_2 is the confining stress) and $\bar{P}$ is related to the mean stress P by the equation $\bar{P} = P + K/3 = (\sigma_1+\sigma_2)/2$. One failure surface is measured on unfailed rock and the other on previously failed rock. The surfaces are actually lines above which a stable state of stress and strain cannot exist. In the brittle case, if the calculated state of stress crosses the failure surface measured on the unfailed rock, the stress relaxes back to a lower failed surface. At a brittle-ductile transition pressure, the two surfaces merge. Tensile failure occurs when either of the principal stresses are negative and the tensile strength is exceeded. This occurs whenever a stress state exists to the left of a 45° line in K-$\bar{P}$ space, as shown in Fig. 1.

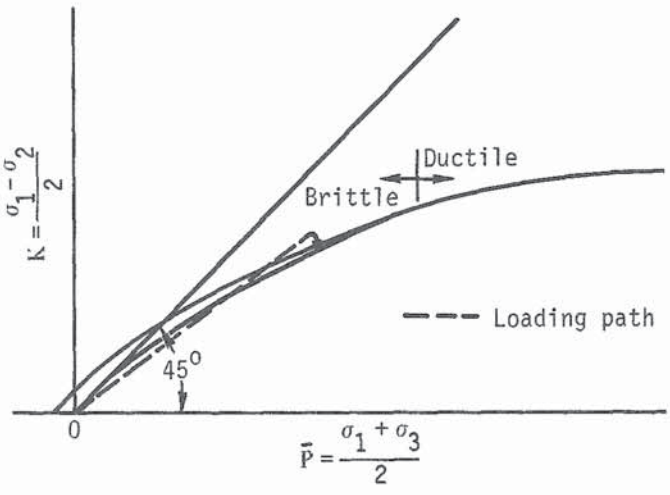


Fig. 1. Failure model used in SOC and TENSOR codes.

It is convenient to have some measure of the permanent damage to the material that has failed. In the elastic/plastic constitutive model used in SOC and TENSOR, the total strain is separated into elastic and plastic parts. As the material deforms, the strain and the elastic stress are calculated from relationships based on Hooke's law. If failure is occurring, the elastic increment of stress is based on the current value of strain. The part of the strain not associated with the elastic stress is the failure-associated distortional strain. That portion associated with pure shear distortion is denoted by ε_s, and shear distortion associated with tensile failure as ε_t, where the total failure shear strain is $\varepsilon_f = \varepsilon_s + \varepsilon_t$.

Schatz [2] has correlated ε_f with observed failure reported by Borg [6] for a 5-kt nuclear event (Hardhat) in granite. He showed that the observed "limit of intense fracture" is at a radius where the calculated $\varepsilon_f \approx 0.1 = 10\%$. The limit of microfracturing is at a radius where the calculated $\varepsilon_f \approx 0.01 = 1\%$, and the measured

collapse chimney height is at a radius about equal to the calculated limit of fracture, where $\varepsilon_f \rightarrow 0$. Schatz further reports that these correlations agree in a general way with laboratory observations of failure in granite, where the onset of observable fracture occurs with nonelastic shear strains of >1%, and where total sample destruction occurs with nonelastic shear strains of ~10%.

No explicit physical model couples the magnitude of ε_f with permeability enhancement.

EXPLOSIVE-ROCK-FRACTURING EXPERIENCE

Data on rock fracturing and permeability enhancement from explosive-generated stress waves and expanding working gas in the absence of a free surface is of primary interest. Unfortunately, there is at present only a limited amount of data from which these quantities can be related. Some information is available from measurements around underground nuclear explosions. Borg [7] has compiled and analyzed the available rock-fracture data from such explosions in various competent rocks. In the study, fracture was judged on the basis of in-situ permeability measurements, macrofracturing in cores and re-entry tunnels, and microfracturing in cores and collapse chimney heights. Horizontal fracturing was found to extend about 3.8 cavity radii (R_c) and pervasive fracturing about 2 R_c.

The Hardhat experiment, referred to earlier, provides the best data available on permeability enhancement from underground explosions in a hard rock [8]. Enhancement of two to three orders of magnitude was observed within a radius of 125 to 215 ft (38 to 66 m) from the shot point. Figure 2 shows the permeability data for Hardhat along with the calculated total failure strain related to scaled radius R/R_c. The fracture observations agree with Schatz' results (i.e., intense fracture correlates with $\varepsilon_f \gtrsim 0.1$, and the limit of detectable fracture correlates with $\varepsilon_f \approx 0.01$).

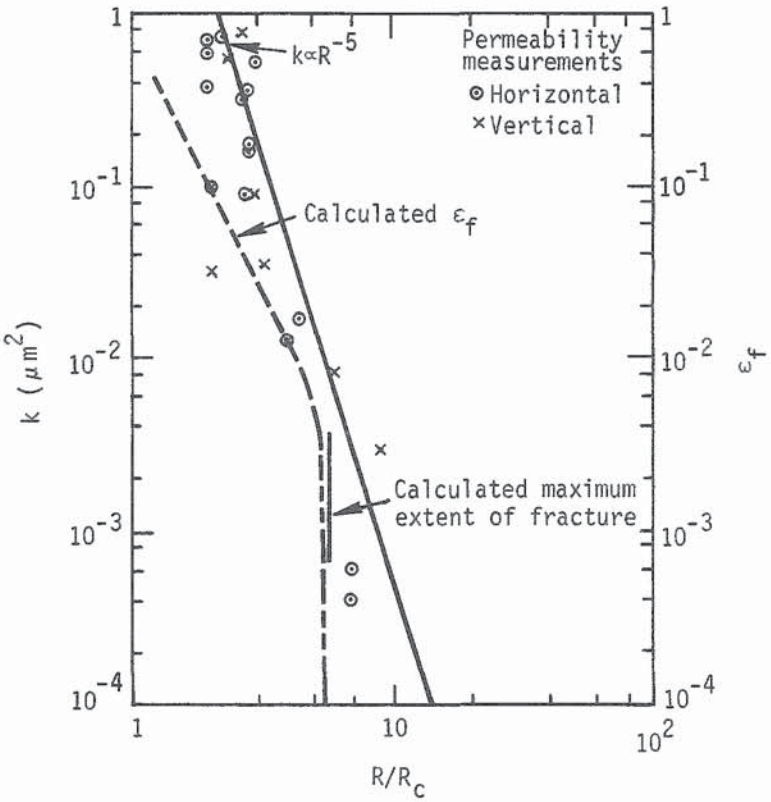


Fig. 2. Measured permeability and calculated ε_f vs distance (Hardhat event).

McKee and Hanson [9] have shown that in the elastic limit, explosively created permeability will fall off as R^{-5} in spherical geometry and as R^{-4} in cylindrical geometry. The Hardhat event, essentially a point-source spherical explosion, induced permeability that fell off as R^{-5}, in agreement with their analysis.

EXPLOSIVE-COAL-FRACTURING EXPERIENCE

A fracturing experiment was recently conducted in a coal outcrop near Kemmerer, Wyoming [5]. A 59.4-kg, 10-cm-diameter cylindrical charge with length/diameter = 55 was exploded with its center 15.2 m below the surface in the middle of the coal seam. Direct observations of the extent of fracturing were made in post-shot cores. Dye injection and other methods were used to distinguish pre- and post-shot fractures. Ease of drilling and the attenuation of acoustic waves as a function of frequency across the fracture region provided some indications. In general, these measurements indicate that the fractured region extends out to about 150 cm from the center of the shot hole. Although the exact cavity radius could not be measured, the calculated R_c was 18 cm. Based on this result, the fractured region extended to 8.3 R

Permeability measurements were taken using packers in the Kemmerer coal outcrop experiment. Pressure testing was performed using water injection until a quasi-steady pressure was attained. Although the data are quite scattered (Fig. 3), the linear-elastic solution for the fall-off of permeability with distance for cylindrical geometry ($k \propto r^{-4}$) fits quite well through the scatter of the data.

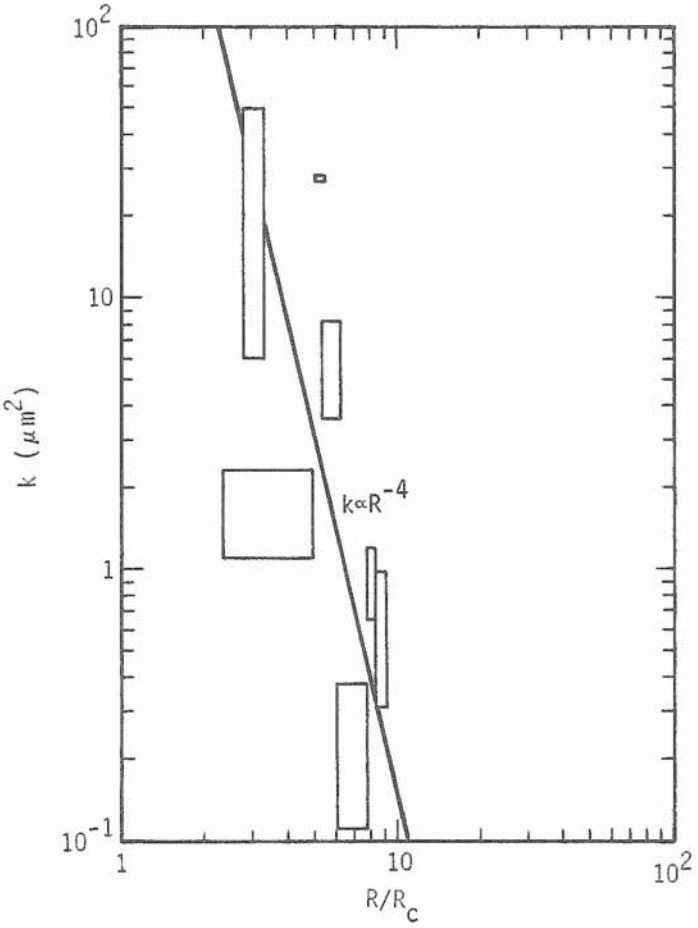


Fig. 3. Measured permeability for the Kemmerer-core-outcrop experiment showing $k \propto R^{-4}$.

Figure 4 shows the calculated total failure strain ε_f vs the scaled distance. The shot produced a significant permeability enhancement which also extended to a radius of about 1.5 m (8.3 R_c). Also shown are the measurements and observations which indicate significant enhanced fracturing out to this distance.

The lognormal least-squares fit of the permeability data for the Kemmerer coal outcrop experiment (Fig. 3) [10] produced the relationship,

$$k = 427\ (R/R_c)^{-3}.$$

This, along with the calculated ε_f vs R/R_c, produces a relationship between k and ε_f. Note that a fit with an exponent of -4 will also fit the data. Nevertheless, the best fit, plotted in Fig. 5, gives the relationship, $k \propto \varepsilon_f^{3/2}$, for values of $\varepsilon_f \gtrsim 0.01$, and $k \propto \varepsilon_f^{5/2}$ for values of $\varepsilon_f \lesssim 0.01$. The break in the curve occurs at about the radial limit of permeability enhancement.

A high-explosive fracturing experiment was also conducted in a coal block [5]. The block measured 1.2 m in diameter and 1.5 m high. Care was taken to preserve the original water content. Spall plates were attached to the outside of the block to simulate an infinite medium subjected to an explosive-induced stress wave. The explosive charge consisted of a 0.6-cm-diameter charge with its center at the center of the coal block and with length/diameter = 33.3. Figure 6 is a post-shot photograph of a cut through the cavity perpendicular to the axis of the charge. Epoxy resin was placed in the shot hole post shot and allowed to migrate into open fractures. The cavity radius is about 1.0 cm. Severe damage was observed out to about 2.0 cm (2 R_c). Maximum penetration of epoxy is about 7.0 cm (7 R_c). Also shown in Fig. 6 are the calculated radii of total failure strain (ε_f = 0.1 at about 2.8 R_c and ε_f = 0.01 at about 8.5 R_c).

The results of the permeability measurements were ambiguous. In spite of the great care exercised, removing the block from the coal seam and storing it seem to have prejudiced the results.

COMPARISON OF CALCULATED ε_f AND OBSERVED FRACTURE AND PERMEABILITY ENHANCEMENT FROM SINGLE EXPLOSIVE CHARGES

When an explosive is detonated underground, the gases produced expand and form a cavity. Computer calculations show that the expansion continues until the cavity

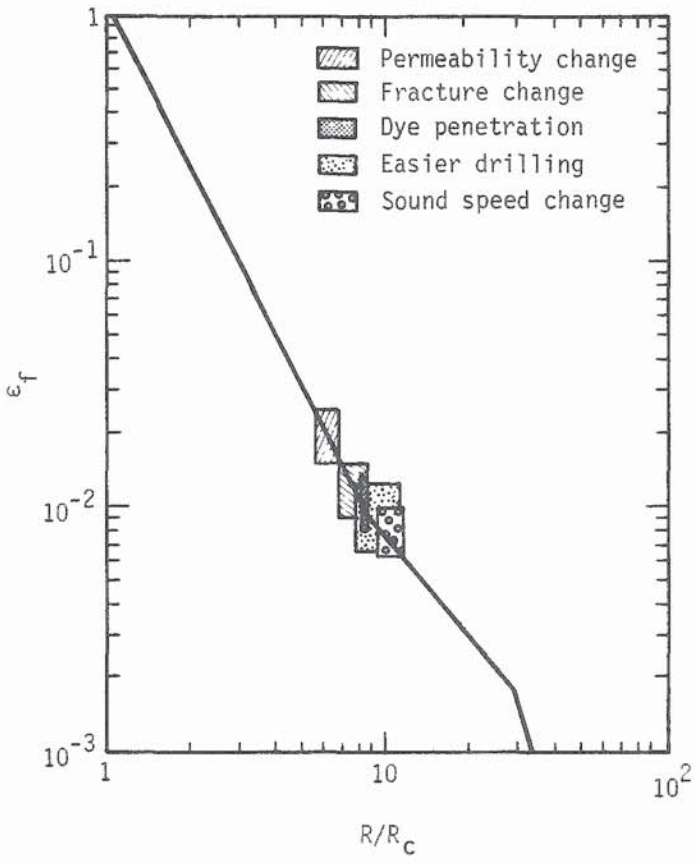


Fig. 4. Calculated failure strain vs distance showing fracture-indicating observation distances (Kemmerer coal outcrop experiment).

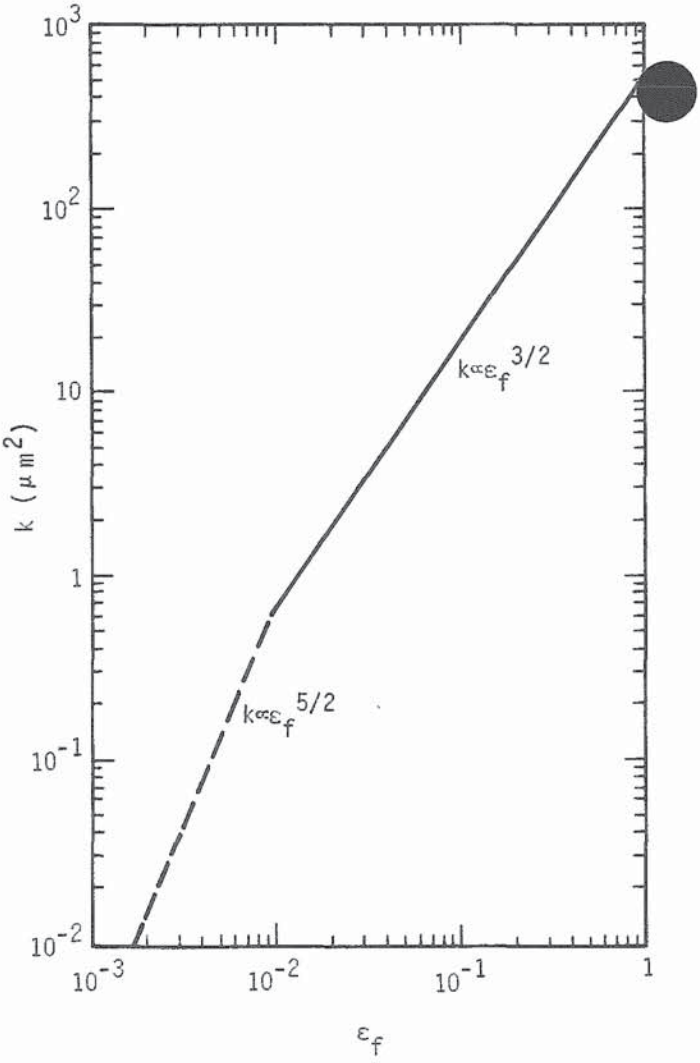


Fig. 5. Lognormal fit to permeability data vs ε_f (Kemmerer coal outcrop experiment).

pressure comes to equilibrium with the stresses in the surrounding rock. Strong rocks like granite support higher stresses than weak materials like coal. Similar materials will support higher stresses at great depths than near the surface because of the difference in overburden stress. Cavity expansion also depends upon the expansion adiabat for the particular explosive employed. Figure 7 shows that the expansion adiabats for Teledet* and EL-836 chemical explosives employed in our experiments are different. EL-836 will produce a significantly larger cavity in a given rock at a given depth than Teledet.

Butkovich [11] has shown that the calculated value of ε_f at a given radius from the center of the charge is directly related to the size of the explosion cavity R_c and that for spherical or cylindrical charges, the volume of rock within this radius is independent of the charge geometry. Since the volume of a sphere is related to R^3 and that of a cylinder to R^2, it should be expected that the multiple of R_c for a cylinder, F_c, should be related to the multiple of R_c for a sphere F_s, as $F_c = F_s^{3/2}$.

*Reference to a company or product name does not imply approval or recommendation of the product by the University of California or the U.S. Energy Research and Development Administration to the exclusion of others that may be suitable.

As mentioned earlier, Borg [7] reports data on rock fracturing from nuclear explosions. Her data show that the radius of "pervasive fracture" is on the order of 2.0 R_c. Since nuclear sources produce spherical cavities, the radius factor would translate to $2^{3/2} = 2.8$ for cylindrical geometry. For the Kemmerer coal outcrop experiment, SOC calculates that $\varepsilon_f = 0.1$ at a radius of 50 cm (Fig. 4), or 2.8 R_c. For the coal block experiment, $\varepsilon_f = 0.1$ at 2.8 R_c also. Schatz [2] calculated $\varepsilon_f = 0.1$ at 2.0 R_c for the Hardhat nuclear event in granite.

Borg reports observable horizontal fracturing in several competent rocks out to 3.8 R_c. In cylindrical geometry, this would translate to 7.4 R_c. Penetration of epoxy into fractures produced in the coal block experiment extended to 7.0 R_c. SOC calculates $\varepsilon_f = 0.014$ at 7.0 R_c and $\varepsilon = 0.01$ at about 8.5 R_c for both the Kemmerer field experiment and the coal block experiment. Kutter and Fairhurst [12] predict that for underground blasts of cylindrical charges, the radial fractures extend to 8 to 9 R_c.

It appears, then, that the code-calculated total failure strain ε_f can indeed be correlated quite well with fracture and fracture intensity, but correlation with permeability is another matter. For the Hardhat event, the measured postshot



Fig. 6. Photo of coal block showing the cavity, the maximum extent of epoxy penetration, and the radii at which various ε_f were calculated.

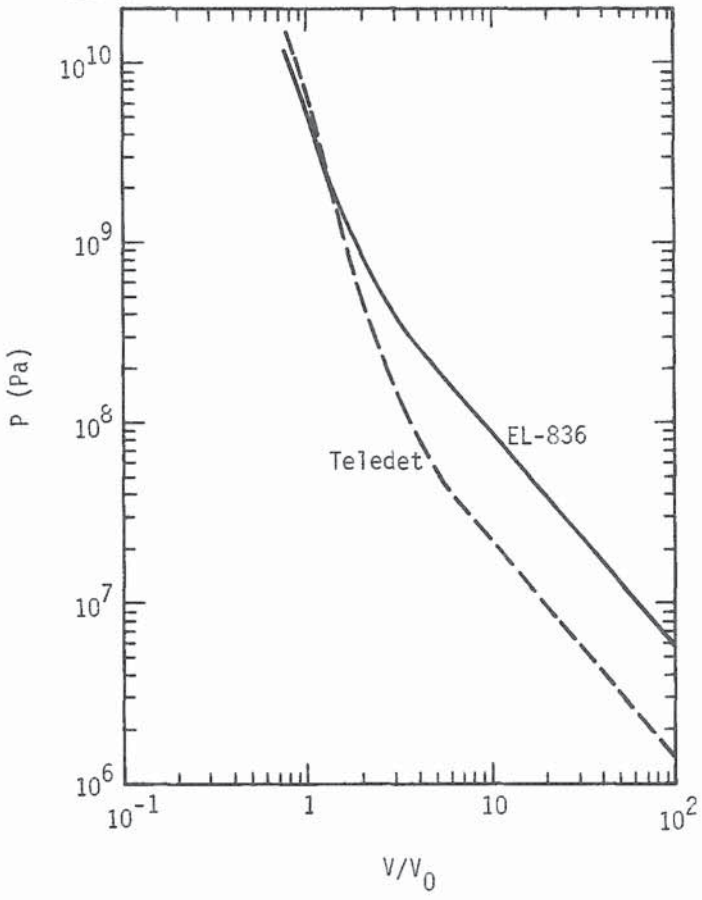


Fig. 7. JWL expansion adiabatics for two different explosives.

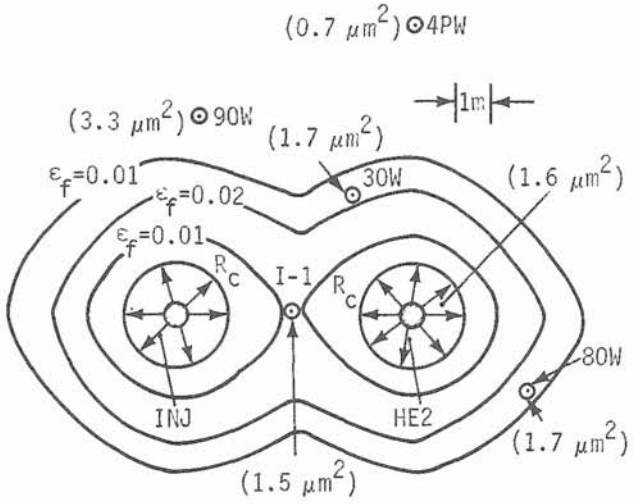


Fig. 8. Calculated contours of ε_f for the explosion of two 750-lb (340-kg) charges of EL-836 (Hoe Creek). The contours are shown on a cross section through the explosive charges. The values in parentheses are the measured average permeability between the injection hole and various other holes.

permeability ranged from about 1 μm^2 at about 2 R_c, where $\varepsilon_f \approx 0.1$, to about 0.018 μm^2 at 3.8 R_c, where $\varepsilon_f \approx 0.013$. For the Kemmerer coal outcrop experiment, the measured permeability (best fit to scattered data) at $(2.0)^{3/2} = 2.8\ R_c$, where $\varepsilon_f \approx 0.1$, exceeds 20 μm^2. At $(3.8)^{3/2}\ R_c \equiv 7.4\ R_c$, where $\varepsilon_f \approx 0.013$, the measured permeability was about 1.0 μm^2. These differences are undoubtedly due to differences in pre-shot fracture patterns and the associated background permeability as well as to the effect of the overburden stress. Hardhat was detonated 935 ft (285 m) below the surface where the lithostatic stress was about 75 bars (75×10^5 Pa), but the Kemmerer shot was detonated about 50 ft (15.2 m) below the surface, where the lithostatic stress was about 2 bars (2×10^5 Pa). However, if two similar HE fracturing experiments are carried out at about the same depths and in materials with similar properties, similar results might be expected.

A MULTIPLE-CHARGE EXPERIMENT IN COAL

An experiment to study simultaneous multiple explosions was carried out in a coal seam at Hoe Creek, Wyoming. The purpose of the experiment was to study the effect of charge interaction on fracturing and permeability enhancement. The plan is to gasify the fractured coal later. Two 750-lb (340-kg) charges of EL-836 were placed in 30-inch-diameter (76-cm) holes with length/diameter ≈ 1.0. This produces a nearly spherical expansion cavity.

A prediction of permeability for the Hoe Creek experiment was attempted using the relationship between k and ε_f obtained from the Kemmerer coal outcrop experiment. Permeability at the radial distance where $\varepsilon_f = 0.1$ should be in the tens of μm^2, about 2 μm^2 where $\varepsilon_f = 0.02$, and less than 1 μm^2 where $\varepsilon_f = 0.01$. The background permeability at the Hoe Creek site is reported to be about 0.5 μm^2 in the coal at shot depth. Figure 8 shows the contours for various values of ε_f (0.1, 0.02 and 0.01). The permeability measurements (shown in brackets at various locations about the shot holes) indicate that the average permeability is about 2 μm^2, except at hole 4PW, where it is near background. One would expect that permeability in hole I-1, on the

axis between the two detonations, would be highest due to the reinforcement of the shock wave shortly after the explosions and due to the subsequent opposing cavity growths in that direction. This is observed in the calculation in the distortion of the $\varepsilon_f = 0.1$ contour. However, the measured permeability is not enhanced as much as expected.

Post-shot coring in the Hoe Creek coal seam confirmed that the intensity of fracture on the same radius (about 2.4 m) around hole INJ is much greater between the two charges near I-1 than 180° opposite I-1 [13]. From this, one could infer that the necessary fracturing for high permeability obtained in the single, cylindrical Kemmerer experiment is present, however the fractures in the region between the explosives may not have remained sufficiently open and interconnected.

CALCULATED TENSILE FAILURE STRAIN

When tensile failure is occurring, a greater volume of material exists than would be inferred from the pressure/volume relationship for a material. This may be physically interpreted as the opening of a tensile void space. In the codes, the criterion for initiation of tensile failure is taken to be the same as for shear failure, although the relaxation scheme is different. This unified shear-tensile failure criterion corresponds to the notion that tensile failure must be preceded by the creation of cracks by large stress deviators. Once a crack has occurred for any reason, it is then free to open if there is a tension. Along with the opening of the crack, tensile relaxation occurs. All principle stresses which are tensile are allowed to relax. The magnitude of the tensile strain to relax these stresses should be a measure of the void volume of the tensile cracks.

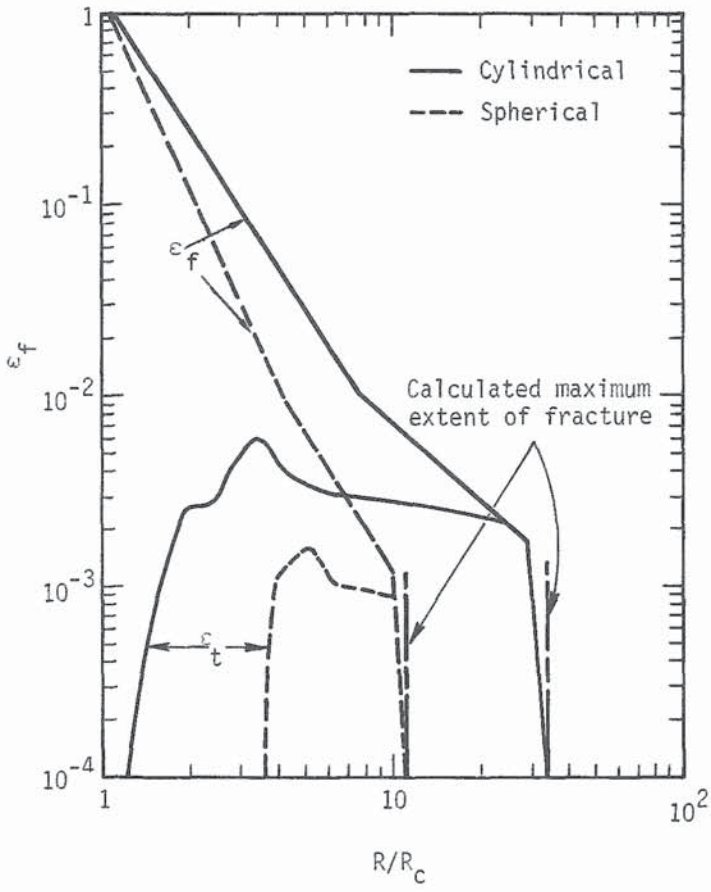


Fig. 9. SOC-calculated failure strains for Hoe Creek coal (spherical and cylindrical charges).

Two SOC calculations were run to study this effect, one in spherical and the other in cylindrical geometry. The calculations were made as nearly identical as possible in that the same material and explosive properties were used and similar zoning was employed. In Fig. 9, the tensile failure strain ε_t and the total failure strain ε_f are plotted vs distance. These results indicate that a much larger no-tensile-failure region occurs in spherical geometry (3.6 R_c) than in cylindrical geometry (1.2 R_c). A TENSOR calculation of the Hoe Creek multiple detonation, in which essentially spherical charges were employed, also showed a region of no tensile failure out to 3.6 R_c. Figure 10 shows a cross section of the explosive cavities indicating the region where no tensile failure occurs.

DISCUSSION OF RESULTS

That the code-calculable parameter, total failure strain ε_f, can be related to the intensity and extent of fracturing around an explosion cavity has been amply demonstrated. In both spherical-source nuclear explosions and cylindrical high-explosive sources, a value of $\varepsilon_f = 0.1$ would be calculated near the explosive cavity where the material is severely fractured, and a value of $\varepsilon_f = 0.01$ would be calculated near the outer boundary of observable fracture. Additional fracture occurs beyond this point, but in these regions $\varepsilon_f \lesssim 0.01$. The calculations as well as observations of fracture from a number of different experiments

show that ε_f and observed fracture intensity scales with the cavity radius R_c. Various conditions, such as the amount of the explosive, the overburden stress, the energy in the explosive, and the strength of the rock, affect R_c. In addition, it was shown that for a given case, the volume of rock within a radius of $\varepsilon_f = 0.01$, for example, is independent of the charge geometry.

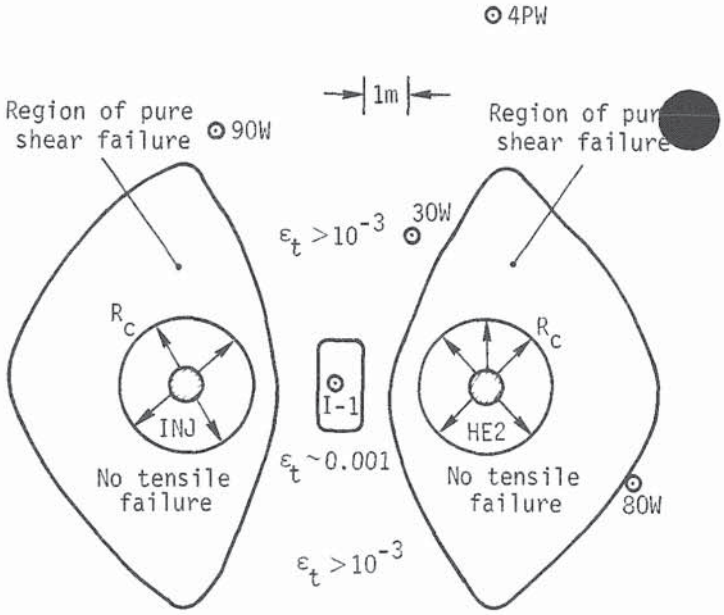


Fig. 10. Calculated regions of no tensile failure for the Hoe Creek explosion of two 750-lb (340-kg) charges of EL-836 shown on a cross section through the explosive charges.

Relating permeability to ε_f is another matter. Although fracture is necessary for permeability enhancement, it is not in and of itself sufficient. The fractures must remain open and connected so that fluids can flow through them. The Hoe Creek experiment demonstrated that although high values of ε_f are calculated between the two explosives and although post-shot coring showed that this region was very highly fractured, the permeability was essentially the same as on the same radius outside of the interaction region.

Fracturing is a complex process. Failure can occur in either shear or tension. The compressional shock wave that travels out from the explosive center initiates shear fracture, but it causes only a small displacement of the material. Most of the displacement is caused by the expanding cavity, which increases to many times the original HE volume. Fracture porosity necessary for permeability enhancement is created by the displacement of the free surface, by irreversible compression radially from the expanding cavity, or by tangential tension cracking. The region of pure shear failure is, in general, one where circumferential cracks predominate. Undoubtedly there is some connection between these cracks because in the Hoe Creek coal experiment permeability was measured through this region. Regions where radial-tension cracks occur, can be of high permeability. If tension failure occurs near the cavity boundary, then permeability can be expected to fall off as in the Kemmerer coal outcrop experiment.

It appears then that permeability enhancement can be related to some weighted combination of ε_s and ε_t, where ε_s is the failure strain from pure shear failure and $\varepsilon_f = \varepsilon_s + \varepsilon_t$. Work is proceeding to find this relationship.

REFERENCES

1. Stephens, D. R.: "In-Situ Coal Gasification," in Proc. Tri-State Fossil Fuels Energy Conf., Denver, Colorado (1974).
2. Schatz, J. F.: "SOC73, A One-Dimensional Wave Propagation Code for Rock Media," Rept. UCRL-51689, Lawrence Livermore Laboratory, Livermore, California (1974).
3. Burton, D. E., and Schatz, J. F.: "Rock Modeling in TENSOR74," Rept. UCID-16719, Lawrence Livermore Laboratory, Livermore, California (1974).
4. Carmen, P.: "Fluid Flow Through Granular Beds," Trans. Inst. Chem. Eng. London (1937) 15, 150.
5. Butkovich, T. R., and Hearst, J. R.: "Prediction and Determination of Explosive Induced Fracture," in Proc. of Explosive Engineers Conf. on Explosion and Blasting Techniques, Jan. 28-30, 1976, Louisville, KY, Rept. UCRL-77659, Lawrence Livermore Laboratory, Livermore, California (1976).
6. Borg, I. Y.: personal communication.
7. Borg, I. Y.: "Extent of Pervasive Fracturing Around Underground Nuclear Explosions," Int. J. Rock Mech. Min. Sci. (1973) 10, 11-18.
8. Boardman, C. R., and Skrove, J.: "Distribution in Fracture Permeability of a Granitic Rock Mass Following a Contained Nuclear Explosion," J. Pet. Tech. (1966) 18, 619-623.

9. McKee, C. R., and Hanson, M. E.: "Explosively Created Permeability from Single Charges," Soc. Pet. Eng. J. (1975) 15, 495-501.
10. McKee, C. R., Hanson, M. E., and Terhune, R. W.: "Permeability from Single and Multiple Detonation of Explosive Charges," Rept. UCRL-78207, Rev. 1, Lawrence Livermore Laboratory, Livermore, California (1976).
11. Butkovich, T. R.: "Correlation between Measurements and Calculations of High Explosive Induced Fracture in Coal Outcrop," Int. J. Rock Mech. Min. Sci. (1975) 13, 51-55.
12. Kutter, H. K., and Fairhurst, C.: "On the Fracture Process in Blasting," Int. J. Rock Mech. Min. Sci. (1971) 8, 181-202.
13. Ganow, H.: personal communication.

Design Criteria for Hydraulic Fracturing of Coal Beds

by

Sunder H. Advani, West Virginia University
L. Zane Shuck, MERC, ERDA
H. Y. Chang, West Virginia University
H.V.S. GangaRao, West Virginia University

ABSTRACT

Critical pressures for hydraulic fracture initiation and extension in coal beds are presented in terms of the primitive stress fields, geometry, fracture orientation, and material properties. Fluid flow considerations for incorporation in the structural models are also discussed.

INTRODUCTION

Hydraulic fracturing of coal seams can play a significant role in enhancing the permeability of coal beds and thereby permit efficient methane drainage and/or suitable well linking for underground coal gasification. The method of hydraulic fracturing [1], conventionally used for secondary stimulation of oil and tight gas reservoirs, has not been rigorously applied to coal seams. As a result, design criteria for predicting critical fluid pressures for fracture propagation and fracture orientations in terms of tectonic and overburden stresses, relative coal cleat orientations, coal bed geometric and material properties are lacking.

The objective of this abstract is to formulate criteria for hydraulic fracturing of coal beds from the vantage point of fracture mechanics. Governing equations and numerical results for vertical fracture initiation, extension, and inclination are given.

RESULTS

The two dimensional criteria for fracture initiation around a well bore with the dominant cleat system aligned with respect to the major tectonic stress is [2].

$$P_{critical} = \frac{\sigma_t - 3\sigma_2 + \sigma_1}{2 - \alpha(1-2\nu)/(1-\nu)} \tag{1}$$

With fluid flow penetration ignored, the governing equation is

$$P_{critical} = \sigma_{t_c} - 3\sigma_2 + \sigma_1 \tag{2}$$

The corresponding equation for fracture initiation along the dominant cleat system which is inclined at an angle θ_o with respect to the σ_1 stress is

$$P_{critical} = \sigma_{t_c} - (\sigma_1 + \sigma_2) + 2(\sigma_1 - \sigma_2)\cos 2\theta_o \tag{3}$$

For σ_1 = -8.28 MPa (-1200 psi), σ_2 = -4.83 MPa (-700 psi), θ_o = 6°, and σ_{t_c} = -0.69 MPa (100 psi), the critical pressure (above pore pressure) for fracture initiation is $P_{critical}$ = 7.05 MPa (1022 psi).

References appear at end of paper.

Fracture extension criteria, for the 2D model in Figure 1, can be formulated by employing the strain energy density(S) concept [3] and requiring that $dS/d\theta = 0$ and $d^2S/d\theta^2 \geq 0$. Figure 2 illustrates typical $P_{critical}$ versus crack inclination plots for various crack lengths using experimentally determined values of the critical strain energy density. Figure 3 reveals the critical pressure versus the three dimensional configuration relation as the crack progresses from an ellipse (with the vertical axis as the major axis) to the penny shaped crack and finally to a crack with semi-circular fronts [4]. The corresponding well bore pressure log is also illustrated. Three dimensional analysis of stress intensity factors, using finite element methods, is presented in Reference [3]. Fracture widths can be estimated from finite element model results or from closed form solutions for elliptic, penny shaped, and line cracks. For example, the elliptic crack fracture width is given by

$$W_f = \frac{2(1-\nu)b}{GE(k)} \quad [p - \sigma_2] \tag{4}$$

The computed fracture widths, for a 6 ft. thick coal seam, employing Pittsburgh coal properties range from 0.08 in. (elliptic crack) to 0.24 in. (line crack of length 20 ft.).

Coupling of the governing fracture mechanics equations and the fluid flow relations is currently in progress. The pressure profile in the fracture can be expressed by a modified form of Poiseuille's equations. The fluid flow from the crack into the coal can be assumed to be governed by the diffusion equation

$$K_x \frac{\partial^2 p}{\partial x^2} + K_y \frac{\partial^2 p}{\partial y^2} = \alpha\mu c \frac{\partial p}{\partial t} \tag{5}$$

Approximate solutions to equation (5) have been reported by Howard and Fast [5] with a one dimensional solution expressed by [6]

$$P(y,t) = (P_o - P_w) \text{ erf } [\frac{y}{2}\sqrt{\frac{\alpha\mu c}{Kt}}] + P_w \tag{6}$$

The pressure magnitudes will be incorporated in the multi layered coal bed finite element models for computing fracture dimensions and predicting fracture orientations.

NOMENCLATURE

b	Coal seam half thickness
c	Compressibility
erf [ ]	Ganssian error function
E(k)	Complete elliptic function of the second kind
G	Shear modulus
k_1	Stress intensity factor
K_x, K_y	Coal seam permeabilities
p	Pressure
P_o, P_w	Pore pressure and crack pressure respectively
σ_1, σ_2	Principal tectonic stresses
t	time
x,y	Cartesian co-ordinates
α	Permeability coefficient
μ	Dynamic viscosity
ν	Poisson's ratio

REFERENCES

1. Clark, J. B., "A Hydraulic Process for Increasing the Productivity of Wells," Trans. AIME, v. 186, pp. 1-8, 1949.
2. Haimison, B. and C. Fairhurst, "Initiation and Extension of Hydraulic Fractures in Rocks," Soc. Petrol. Engr. Jr., v. 7, No. 3, pp. 310-318, 1967.
3. Advani, S. H., L. Z. Shuck, H. Y. Chang, and H.V.S. GangaRao, "Analytical and Experimental Investigations on Induced Fracturing of Reservoir Rock," In Press, ASME, 1976, Paper No. PVP
4. Advani, S. H., L. Z. Shuck, H. Y. Chang, and H.V.S. GangaRao, "Material and Structural Simulations Associated with Hydraulic Fracturing," Proceedings, International Conference on Computer Simulation for Materials Applications, Nuclear Metallurgy, Vol. 20, Part 2, pp. 1011-1022, 1976.
5. Howard, G. C. and C. R. Fast, "Hydraulic Fracturing," SPE Monograph V. 2, 1970.
6. Shuck, L. A. and S. H. Advani, "Induced Stresses in Hydraulic Fracturing Operations," Proceedings 15th Conference on Rock Mechanics, ASCE, pp. 93-134, 1975.

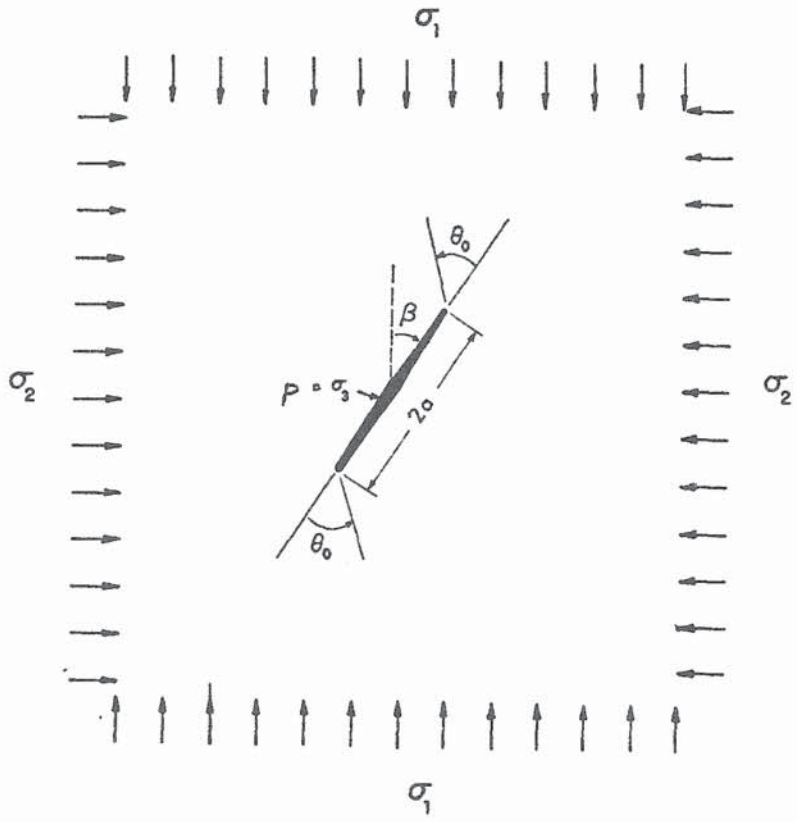


FIGURE 1. TWO DIMENSIONAL CRACK MODEL SUBJECTED TO TECTONIC STRESS FIELD.

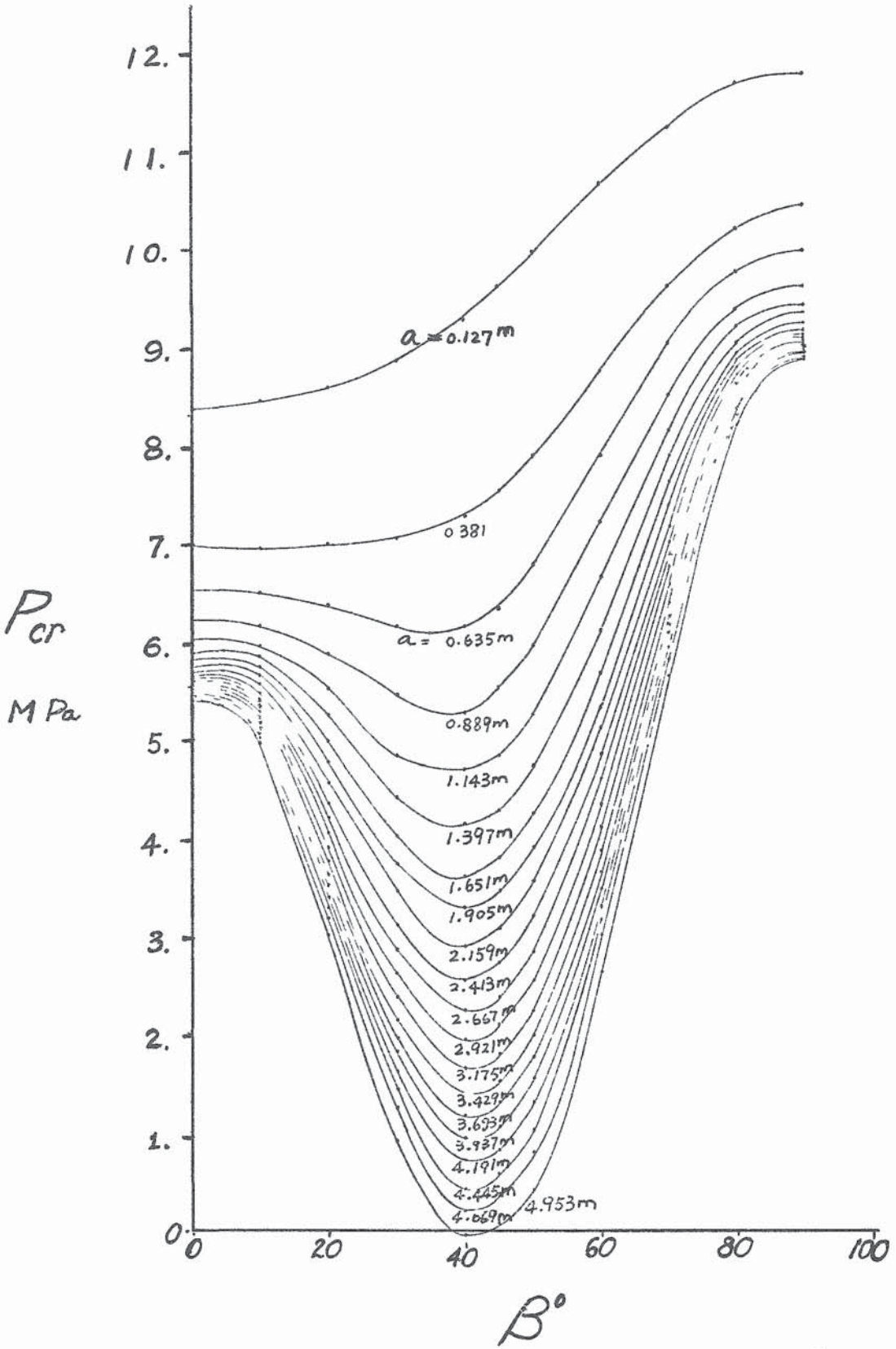


FIGURE 2. TYPICAL CRITICAL PRESSURE VS. CRACK INCLINATION CURVE FOR VARIOUS CRACK LENGTHS WITH σ_1 = -8.28 MPA(-1200 PSI), σ_2 = -4.83 MPA(-700 PSI), AND K_{1C} = 2.2 MPA $\sqrt{M}$ (2 KSI $\sqrt{IN.}$)

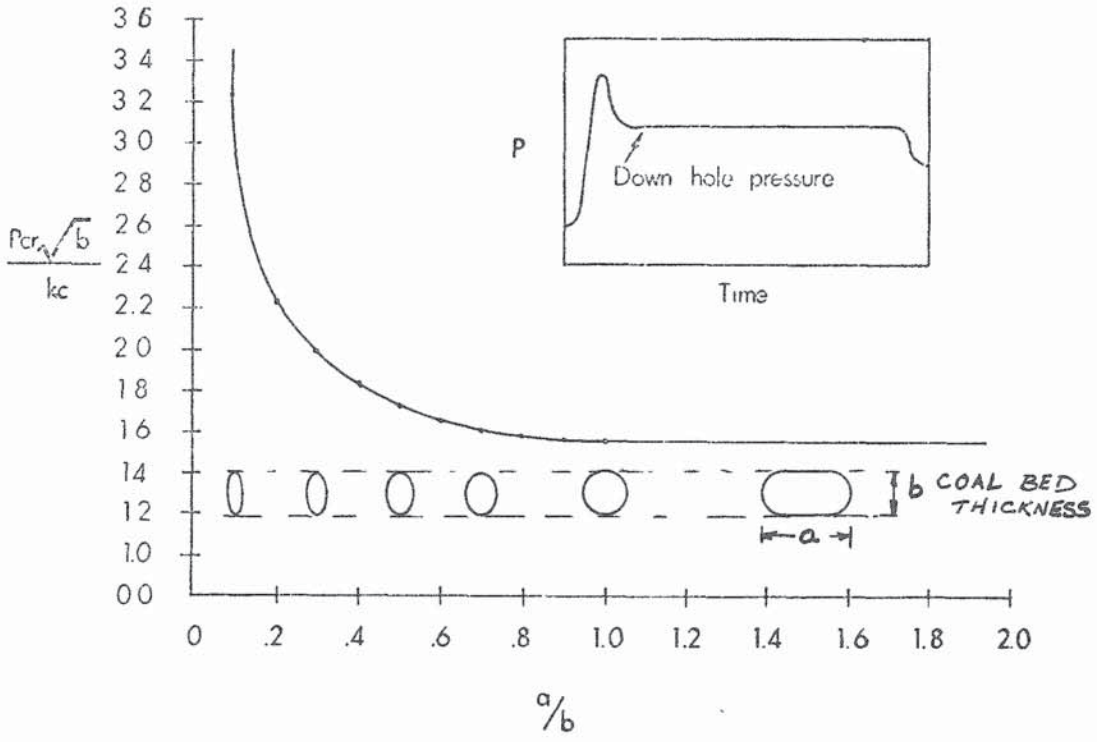


FIGURE 3. PLOT OF CRITICAL PRESSURE VERSUS THREE DIMENSIONAL CRACK CONFIGURATION. CORRESPONDING PRESSURE CURVE FROM HYDRAULIC FRACTURING DATA IS ALSO INDICATED.

HYDRAULIC FRACTURING THIN COAL SEAMS IN PREPARATION FOR IN SITU GASIFICATION

by

TOMMY M. WARREN, THE UNIVERSITY OF ALABAMA
ASADOLLAH HAYATDAVOUDI, THE UNIVERSITY OF ALABAMA

ABSTRACT

A THEORETICAL ANALYSIS HAS BEEN CONDUCTED TO DETERMINE THE EFFECT OF CLEATS ON THE HYDRAULIC FRACTURE DIRECTION OF COAL. EQUATIONS WERE DEVELOPED TO INDICATE CONDITIONS NECESSARY FOR THE HYDRAULICALLY INDUCED FRACTURE TO OCCUR ALONG THE CLEATS. THE MODEL WAS BASED UPON THE ASSUMPTION THAT COAL CAN BE MODELED AS AN ELASTIC MEDIUM WITH THREE UNEQUAL PRINCIPAL STRESSES INVOLVED. THE MODEL REPORTED HEREIN CAN BE UTILIZED IN THE DEVELOPMENT OF A WELL PATTERN FOR UNDERGROUND COAL GASIFICATION.

INTRODUCTION

A shortage of petroleum fuel products currently exists in the United States. One possible source of additional energy is the underground gasification of coal. Energy from the coal can be recovered in the form of a low quality gas by a partial combustion process. Figure 1 shows a well pattern that may be utilized in the underground gasification process. The wells are drilled through the coal seam and completed with casing cemented slightly below the top of the coal. The coal bed is prepared (linked) by some method that will increase the permeability between the wells. Air is passed between the wells and the coal gasified by an incomplete combustion process. As shown in Figure 1, each of these stages can be occurring simultaneously in various parts of the field. Reference 1 discusses the current state of technology of underground gasification.

Although coal gasification is an important alternative, it is expected to compliment conventional mining methods rather than replace them. Seams to be gasified will generally be those that are uneconomical to mine conventionally because of thinness, depth, or high ash content.

Bituminous, medium rank coal does not have adequate permeability to allow sufficient air to be injected to support the gasification process.[2] Therefore, some means of increasing the coal permeability must be utilized. The permeability can be increased by directional drilling, electrolinking, hydraulic fracturing, or controlled blasting. This paper discusses hydraulic fracturing because it seems the most promising for thin, shallow coal seams.

The permeability of the coal bed must be made great enough to allow sufficient air to be injected at pressures less than the over-burden pressure in order to minimize leakage. Hydraulic fracturing does not directly result in sufficient permeability to allow gasification to be initiated.[2,3] Once the fracture is created, air is injected at a low rate and a path with a small cross sectional area carbonized between the gasification wells by reverse combustion. After the linking process is completed, the air injection rate is increased and the coal gasified by forward combustion.

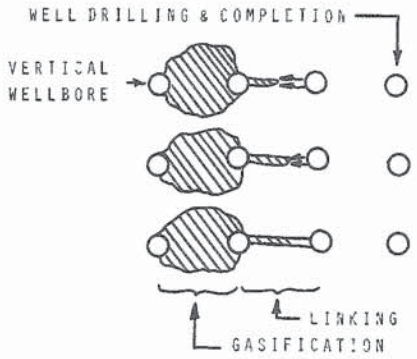


FIG. 1 DEVELOPMENT OF A GASIFICATION SYSTEM

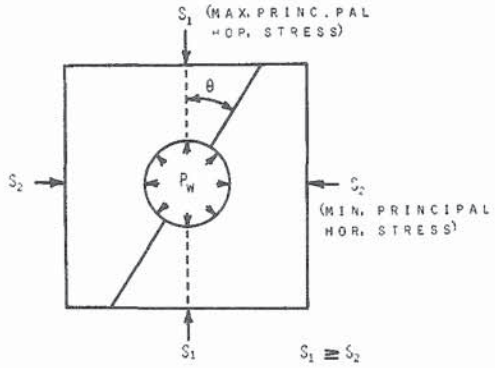


FIG. 2 STRESSES ACTING ON WELLBORE

Hydraulic fracturing of coal, even at relatively shallow depths, usually results in vertical fractures.[4] A knowledge of the fracture direction is required for the design of a well pattern for gasification. It is important to know that the fracture direction will be consistent for several fractures in a field. This requirement is necessary so that several parallel rows of wellbores can be drilled and fractured with the assurance that the fracture will follow the previously drilled row of wells.

PREDICTING FRACTURE DIRECTION

In order to develop a theory to be used in fracture prediction let us consider a homogeneous, isotropic, elastic, impermeable element of coal with a borehole in it. The coal will generally be under a stress system that can be resolved into three unequal principal stresses. Figure 2 shows a plan view of such a system, where S_1 and S_2 represent the two horizontal principal stresses. The largest horizontal principal stress is designated S_1. The term S_v represents the vertical principal stress, P_w represents the wellbore pressure, and P_o represents the pore pressure.

On any vertical plane located at an angle Θ (measured clockwise) from the direction of S_1, the normal stress on the Θ plane at the wellbore wall is a function of the principal stresses and the wellbore pressure. The stress term that results from the principal stresses can be obtained by the Kirsch's solution of the problem of a circular hole in an infinite plate.[5] The wellbore pressure term is the effective wellbore pressure which is the difference between wellbore pressure and the pore pressure.[6] In all the equations presented in this work tensile stresses are defined as negative and compressive stresses as positive. By the principle of superposition the magnitude of the tangential stress, S_Θ, at the wellbore wall is:

$$S_\Theta = S_1 + S_2 - 2(S_1 - S_2)\mathrm{Cos}(2\Theta) - P_w + P_o \ . \quad (1)$$

A fracture will occur when the magnitude of the tangential tensile stress at some point becomes greater than the tensile strength of the coal at that point. The wellbore pressure required to create a fracture at a point on the wellbore wall rotated Θ degrees from the direction of S_1 can be calculated by substituting the tensile strength, T_Θ, for S_Θ and solving for P_w.

$$P_{f\Theta} = S_1 + S_2 - 2(S_1 - S_2)\mathrm{Cos}(2\Theta) + T_\Theta + P_o \ . \quad (2)$$

Equation 2 gives the pressure required to form a vertical fracture in the Θ direction. The fracture will actually form at the value of Θ for which $P_{f\Theta}$, wellbore fracture pressure, is a minimum. $P_{f\Theta}$ will be a minimum for $\Theta = 0$ and $\Theta = \pi$. Thus in a homogeneous, isotropic, impermeable material the fracture direction will tend to occur in a direction parallel to the direction of the largest magnitude of compressive stress, consistent with earlier definitions.

Bituminous coal is not isotropic because of the presence of numerous vertical joints. All bituminous coals have vertical joints (cleats) that are extensive and usually well defined.[7] Normally two sets of cleats exist, usually oriented perpendicular to each other. The dominant set of cleats is usually perpendicular to the fold axis of the area. They are thought to be formed as extension fractures during the structural folding. The other set of cleats is usually discontinuous and not well defined.

Most cleats have been partially cemented back together and thus exhibit a non-zero tensile strength which is usually less than that of the coal matrix. Some coals have cleats that have not

been cemented back together and thus have a zero tensile strength across the cleat.

The cleats can be incorporated in the fracture model by assuming that a vertical plane of weakness exists at an angle Θ_c from the direction of the greatest horizontal principal stress. Θ_c would be expected to be small because the largest horizontal principal stress tends to be in the direction of the tectonic force that caused the folding and Θ_c is perpendicular to the folding. However, this may not be the case if erosion, uplifting, or later folding has altered the direction of the existing tectonic force.

Equation 2 can be applied to Θ_n and to Θ_c, where Θ_n is the normal direction that a fracture would be expected for an isotropic system (0°) and Θ_c is the cleat direction from the plane of the principal stress, S_1. The tensile strength perpendicular to the Θ_n direction is T_n and the tensile strength perpendicular to the Θ_c direction is T_c.

$$P_{f\Theta_n} = S_1 + S_2 - 2(S_1 - S_2)\text{Cos}(2\Theta_n) + T_n + P_o \ . \tag{3}$$

$$P_{f\Theta_c} = S_1 + S_2 - 2(S_1 - S_2)\text{Cos}(2\Theta_c) + T_c + P_o \ . \tag{4}$$

Subtracting equation 3 from equation 4 with $\Theta_n = 0$ gives

$$P_{f\Theta_c} - P_{f\Theta_n} = 2(S_1 - S_2) - 2(S_1 - S_2)\text{Cos}(2\Theta_c) + T_c - T_n \ . \tag{5}$$

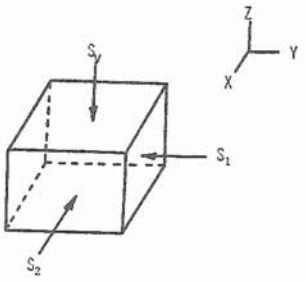


FIG. 3 COAL ELEMENT UNDER OVERBURDEN STRESS

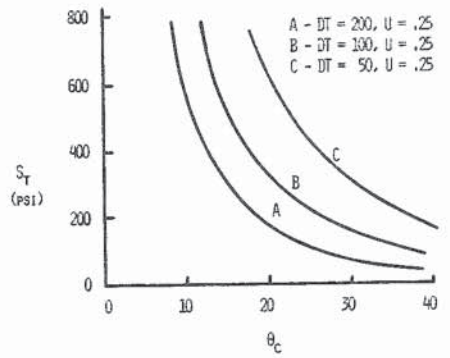


FIG. 4 CONDITIONS FOR FRACTURE TRANSITION FROM S_1 DIRECTION TO CLEAT DIRECTION

The condition necessary for the fracture direction to change from Θ_n to Θ_c is that $P_{f\Theta_c} - P_{f\Theta_n}$ pass through zero.

This transition can also be defined as

$$T_n - T_c = 2(S_1 - S_2)\ (1 - \text{Cos}\ 2\Theta_c) \ . \tag{6}$$

It should be noted that the pore pressure term is eliminated by this process and does not affect the transition equation. However, in reality, a pore pressure exists which might not obey Darcy's Law but rather obeys a diffusion overpressurization inherent in the affinity of gases to the coal surface even when coal is impermeable.

The difference in the horizontal principal stresses can be transformed into a function of the tectonic stress, S_t, the overburden stress, S_v, and Poisson's ratio, u. To do this we will make the following assumptions:

a. $S_2 \leq S_v$ to assure that a vertical fracture is formed.

b. The only tectonic force acting is in the S_1 direction.

c. Coal exhibits elastic properties.

If a cube of coal has a stress, S_v, placed on it in the z direction (Fig. 3) and the x and y directions are confined, an induced stress equal to $\frac{u}{1-u}S_v$ will be produced in the x and y directions. If a tectonic stress is added in the y direction, a similar stress will be induced in the x direction. By the principle of superposition the stress in the x and y directions are:

$$S_1 = S_t + \left(\frac{u}{1-u}\right)S_v \ . \tag{7}$$

$$S_2 = \frac{u}{1-u}\ (S_v + S_t) \ . \tag{8}$$

The difference in the horizontal stresses is then given by $\left(1 - \frac{u}{1-u}\right)S_t$.

Substitution of this into Equation 6 and letting $T_n - T_c = DT$ gives

$$DT = (1 - \frac{u}{1-u})2S_t(1 - \cos(2\Theta_c)) \quad . \tag{9}$$

The value of DT, difference between two tensile strengths, may range from 0 to 200 psi (1.38 MPa).[8] Poisson's ratio for coal may range from 0.25 to 0.50. Figure 4 shows Equation 9 plotted for various mechanical properties of coal. The significance of Figure 4 is that any point that falls to the left of the curve for the mechanical properties of a particular coal seam would indicate that the coal seam would fracture along the cleat direction.

A coal seam cannot be considered to be totally impermeable. There is essentially no permeability in the coal matrix, but a permeability does exist along the natural fracture system (cleats). This causes an additional tendency for coal to fracture along the cleats because of fluid penetration effects. As illustrated in Figure 5, fluid penetration into the cleat exerts a normal stress, S_k, on the faces of the cleat. The exact magnitude of this tendency has not been calculated, but it would seem to depend on

a. viscosity of the fracture fluid;

b. permeability along the cleat;

c. pressurization rate;

d. permeability perpendicular to cleat, and

e. physical and chemical properties of the coal.

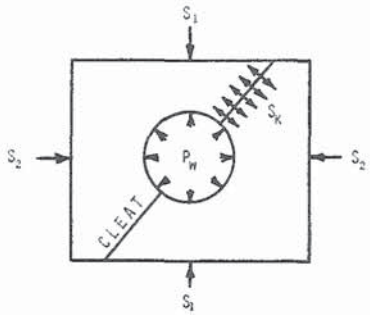


FIG. 5 EFFECT OF DIRECTIONAL PERMEABILITY

The effect of the stress caused by the permeability would be to reduce the fracture initiation pressure and to shift the curves in Figure 4 to the right. This would increase the tendency to fracture along the cleat direction and would reduce the pressure required to initiate the fracture. The probability of fracturing along the cleats can be increased by using a low viscosity fracturing fluid, possibly diesel oil, and a low injection rate to take advantage of the directional permeability.

DETERMINATION OF THE PRINCIPAL STRESSES

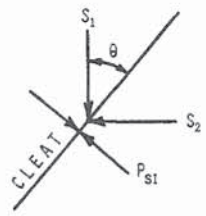
If the fracture is known to occur along the face cleats, the principal stresses and their directions may be calculated from data taken during the fracture job. Figure 6 shows the stress orientation around the cleat. The compressive stress tending to force the fracture closed will be just equal to the instantaneous shut-in pressure, P_{si}, after the fracture job.

$$P_{si} = S_1 \, \mathrm{Sin}\Theta + S_2 \, \mathrm{Cos}\Theta + P_o \quad . \tag{10}$$

$$P_{si} = (S_t + \frac{u}{1-u} S_v) \, \mathrm{Sin}\Theta + (S_v + S_t)(\frac{u}{1-u})\mathrm{Cos}\Theta + P_o \tag{11}$$

The above equation can be solved directly for S_t yielding

$$S_t = \frac{P_{si} - \frac{u}{1-u} S_v \, (\mathrm{Sin}\Theta + \mathrm{Cos}\Theta) - P_o}{\mathrm{Sin}\Theta + \frac{u}{1-u} \mathrm{Cos}\Theta} \quad . \tag{12}$$



$P_{SI} = S_1 \, \mathrm{Sin}\Theta + S_2 \, \mathrm{Cos}\Theta + P_o$

FIG. 6 DETERMINATION OF S_1 AND S_2

The values of all the variables in Equation 12 should be known except S_t and Θ. The following procedure can be utilized to determine the values of S_1, S_2 and Θ.

1. Assume a value for Θ.
2. Solve Equation 12 for S_t.
3. Solve Equations 7 and 8 for S_1 and S_2.
4. Calculate P_{fc} from Equation 2.
5. If the calculated P_{fc} equals the observed P_f, the above calculated values are correct. Otherwise iterate until P_{fc} equals P_f.

The compass orientation of S_1 and S_2 can be determined from the cleat direction and Θ. The cleat direction can be determined from a nearby outcrop of the coal seam or from oriented cores.

This information can be utilized in the planning of a linkage system for an underground coal gasification project. If a survey of the geology of the proposed area gives no indications of excessive tectonic stress and a well-defined cleat system exists in the coal, hydraulic fractures may be produced along the cleats. If quantitative data is available for the in situ stress system, Figure 4 can be utilized to obtain further indication of whether or not fractures will follow the cleats. This data can also be obtained during a test fracture job at the time of pilot testing of the gasification system. If Figure 4 indicates that the coal seam is to the left of its transition condition, hydraulically induced fractures should be consistently produced along the cleats.

FIELD DATA

Data from a field case is shown to illustrate how the above method can be applied. Figure 7 shows the injection rate and pressure curve for the Mary Lee seam which has been fractured.[4] (The hydraulic fracture job was done as an experiment to release methane gas from the seam prior to conventional mining.) It is assumed that the fracture occurred along the face cleat direction. The seam was approximately seven feet thick and 1,075 feet (327 m) deep. The surface fracture pressure and shut-in pressure is read from the injection pressure curve. These two pressures are converted to bottom hole pressures by the use of the fluid gradient in the well. The fracture initiation pressure is also corrected for friction losses in the tubing. Table 1 shows the observed and calculated values. It should be noted that the calculated P_{fc} was approximately equal to the observed fracture pressure and that the tectonic stress plots on Figure 4 to the left of the transition curve (DT = 100 psi). This would indicate that the fracture occurred along the face cleats.

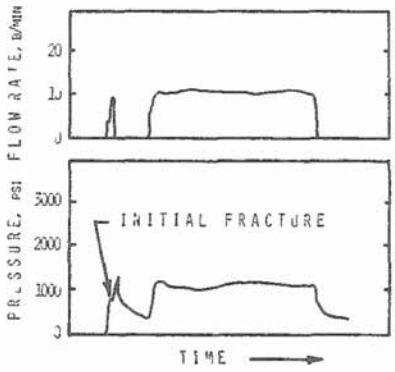


FIG. 7 INJECTION CHART FOR MARY LEE SEAM

TABLE 1

Depth	1,075 ft.	327 m
P_f	1,074 psi	7.40 MPa
P_o	399 psi	2.75 MPa
P_{si}	865 psi	5.96 MPa
S_1	392 psi	2.70 MPa
S_2	281 psi	1.94 MPa
S_t	167 psi	1.15 MPa
Θ	25°	0.436 rad
P_{fc}	1,079 psi	7.44 MPa

CONCLUSIONS

It has been shown that under certain conditions the fracture direction of a coal seam may be controlled by the joint system of the coal bed. When this occurs, the fracture direction should be consistent from well to well and can be predicted by the method discussed in this paper. A method has also been developed to calculate the principal horizontal stresses and their direction when the coal fractures along the cleat direction and the pore pressure is known. This information can be utilized to design a well pattern for underground coal gasification that will result in successful linkages between the wells.

ACKNOWLEDGEMENT

Thanks are due Dr. George Douglas, Dr. Marvin McKinley, and Professor Reynold Q. Shotts, the principal investigators of the NSF Funded Project AER75-04512/GSA75-35 for financial support given to this work.

REFERENCES

1. Arthur D. Little, Inc., "A Current Appraisal of Underground Coal Gasification," Report to the U.S. Bureau of Mines, No. C-73671, December 1971, 121 p.
2. Capp, J. P., et al, "Underground Gasification of Coal: Hydraulic Fracturing as a Method of Preparing a Coal Bed," U.S. Bureau of Mines RI-5666, 1960.
3. Capp, J. P., et al, "Underground Gasification of Coal: Second Experiment in Preparing a Coal Bed by Hydraulic Fracturing," U.S. Bureau of Mines RI-5808, 1961.
4. Elder, C. H. and Deul, Maurice, "Hydraulic Stimulation Increases Degasification Rate of Coalbeds," U.S. Bureau of Mines RI-8047, 1975.
5. Obert, L. and Duvall, W. I., "Rock Mechanics and the Design of Structures in Rock," John Wiley and Sons, Inc., New York, 1967, pp. 98-101.
6. Hubbert, M. K., and Rubey, W. W., "Role of Fluid Pressure in Mechanics of Overthrust Faulting," Bulletin of Geophysical Society of America, Vol. 70, 1959, p. 115.
7. McCulloch, C. M.; Deul, M.; and Jeran, P. W., "Cleat in Bituminous Coalbeds," U.S. Bureau of Mines RI-7910, 1974.
8. Evans, I. and Pomeroy, C. D., The Strength, Fracture, and Workability of Coal, Pergamon Press, Oxford, 1966, p. 81.
9. Kehle, Ralph O., "The Determination of Tectonic Stresses through the Analysis of Hydraulic Well Fracturing," Journal of Geophysical Research, Vol. 69, No. 2, Jan. 15, 1964, pp. 259-273.
10. Hubbert, M. K. and Willis, D. G., "Mechanics of Hydraulic Fracturing," AIME Transactions, Vol. 210, 1957, pp. 153-167.
11. Hamison, B. C., "Determination of In Situ Stresses around Underground Excavations by Means of Hydraulic Fracturing," Final Report to ARPA of the Department of Defense, Contract No. H0220080, 1974.

Rock Mechanics Aspects of In-Situ Gasification with Special Reference to Texas Lignite

BY

1. T. W. Thompson, THE UNIVERSITY OF TEXAS AT AUSTIN
2. K. E. Gray, THE UNIVERSITY OF TEXAS AT AUSTIN

ABSTRACT

If the 'in-situ' gasification of coal is to be achieved in a controlled manner, information is required on the behavior of the rock mass, and techniques must be available for the prediction of this behavior. Two aspects of the 'in-situ' rock characteristics are import, firstly the fluid flow during the initial linking phase and secondly the stability of the overburden, with particular reference to its influence on any overlying aquifers and on surface subsidence. In this paper these aspects are reviewed, with particular reference to the gasification of Texas lignite, preliminary data on rock properties is summarized, and the significance of these data to the underground gasification process discussed.

INTRODUCTION

The controlled operation of an underground coal gasification plant requires the ability to predict the 'in-situ' behavior of the relevant rock strata, which in turn presupposes a knowledge of the mechanical and physical rock properties. Without this ability unforseen economic and environmental problems may arise, with it optimal operating conditions may be achieved.

More specifically information and techniques are required to allow the prediction of gas flow during the early connection and linking phase, of heat loss through the surrounding strata, and of roof stability and subsidence during and after the productive life of the operation.

Before production can begin a connection must be established between the inlet and producing wells, and later in the process this connection must be maintained at a level sufficient to allow continuing production at the required rate. In planning this linking phase decisions must be made concerning the well separation and relative orientation, while permeability enhancement techniques, if any, must be chosen and designed. These decisions require a knowledge of the various components of the 'in-situ' permeability tensor of the coal, together with its fracturing characteristics. Information on the 'in-situ' stress field will also be needed. Swelling or shrinking characteristics of the coal could significantly effect link development in its later stages and must be known.

At a later stage the magnitude of heat losses to the surrounding strata may have a significant effect on the efficiency of the operation [1]. Heat losses could occur by conduction to the surrounding rocks or by gas leakage or excessive water influx due to roof fracturing. In either case the heat loss must be predictable, requiring a knowledge of the conduction characteristics of the surrounding rock and an estimate of the extent of roof fracturing.

Probably the most significant rock mechanics considerations are those concerned with roof stability. Roof fracturing may occur due to drying in softer more clayey

overburdens, or through mechanical failure due to lack of roof support. Under certain conditions total, or partial roof collapse may occur. The development of fracturing or roof collapse could allow excessive gas losses or water influx, and could lead to surface subsidence and loss of well-hole stability [1]. Fracturing will be minimized where plastic deformation of the overburden occurs at the high temperatures associated with the process, but surface subsidence effects may still be significant.

Part of the in-situ gasification research program at the University of Texas is directed towards the quantification of these factors and the development of methods for the prediction of their effects. The remainder of this paper is concerned primarily with this work, and hence is specifically concerned with the situation envisaged in gasifying the Texas Lignite deposits.

The Lignite deposits of Texas have been adequately described elsewhere [2]. Those with potential for gasification lie at depths between about 200 ft. (60 m) and 2000 ft. (600 m). They are compact rocks with poorly to well defined bedding and a normally high water content. Jointing is well developed. The immediate overburden varies between mud and a poorly consolidated fine grain sand with obvious closely spaced bedding. Carbonaceous material may be fairly abundant as partings along bedding planes.

Most of the work carried out to date in this project has used examples of these rocks obtained from the Alcoa strip mine at Rockdale, Texas.

THE FLOW OF GAS THROUGH LIGNITE

In establishing a connection between the inlet and producing wells, in the early stages of the gasification process, the air injection pressure must be sufficient to produce significant flow through the rock, and the wells must be sited to take advantage of the principal permeability direction.

The flow of fluid through saturated lignite will occur predominantly along the planes of fracture and weakness within the rock mass, that is along the near vertical joints and the near horizontal bedding. Flow through the intervening rock matrix will be minimal by comparison and may be neglected. In the lignite at the Alcoa strip mine, the only field occurrence examined in this context to date, two vertical joint sets are evident at an angle of slightly more than 90 degrees to each other, together with the near horizontal bedding. However, this lignite, and it seems reasonable to assume that other lignites from the same formation behave similarly, is characterized by the development of closely spaced fractures on drying and exposure to the atmosphere, these new fractures being roughly parallel to the originally visible joint planes.



Fig. 1 The Development of Dehydration Cracks in Texas Lignite

A laboratory investigation into the effect of drying and stress on the rock matrix permeability is currently underway. Tests are being conducted using a laboratory permeameter (Fig. 2). The core under test is held in a rubber sleeve inside a core holder. Confining pressure is provided by nitrogen, the same source being used for flow pressure. Cores are stored under water before use, then wipe dried, placed in their rubber jacket, weighed and their permeability measured. The core is then dried, still in its jacket, in a vacuum oven, reweighed and new permeability determined at various confining pressures. This process is repeated until it is judged that the core is fully dried or, as more usually happens, the core disintegrates.

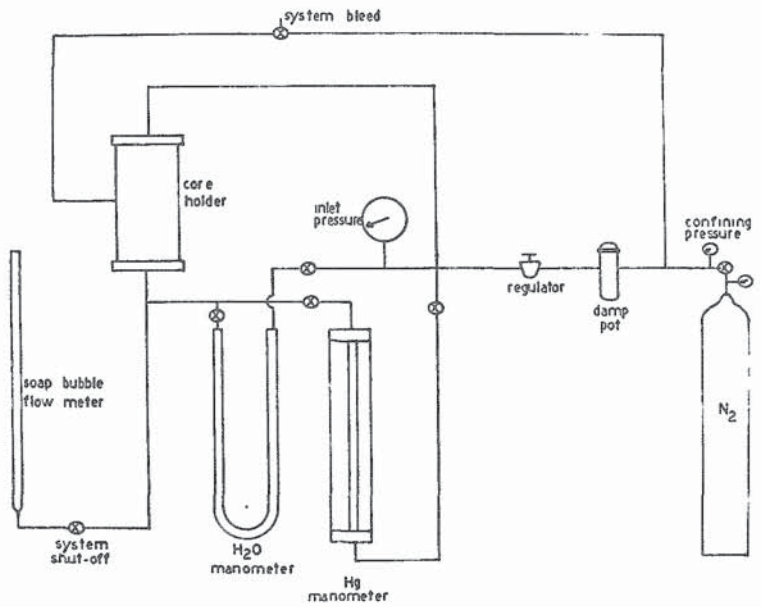


Fig. 2 Schematic Diagram of the Permeameter

Typical results from early tests are shown in Figures 3 and 4, the core from which these data were obtained having its axis perpendicular to the bedding. It will be seen that drying of the cores leads to appreciable permeability increase, this correlating with an increase of visible cracking. However, even where appreciable permeability is established, this is substantially reduced by the application of the fairly low confining pressures possible with the current equipment. Tests at higher confining pressures are planned in the near future.

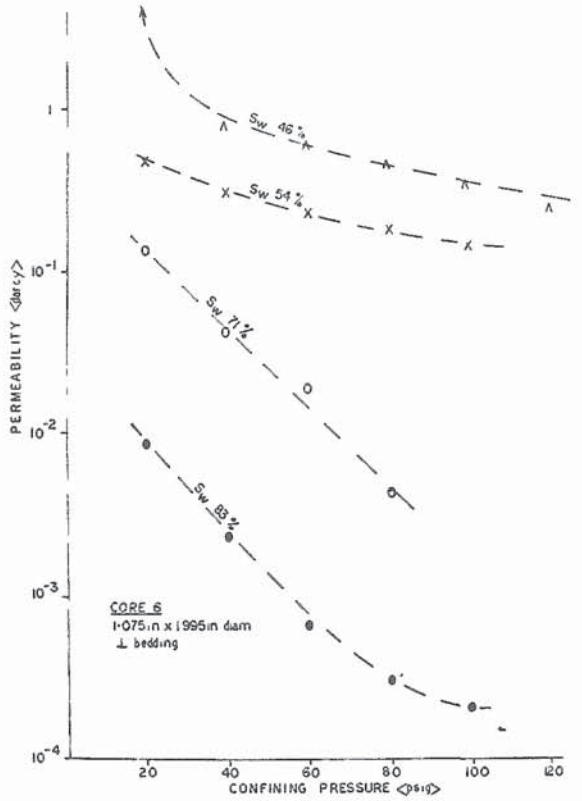


Fig. 3 Gas Permeability of Texas Lignite vs. Confining Pressure at Different Water Saturations (Sw)

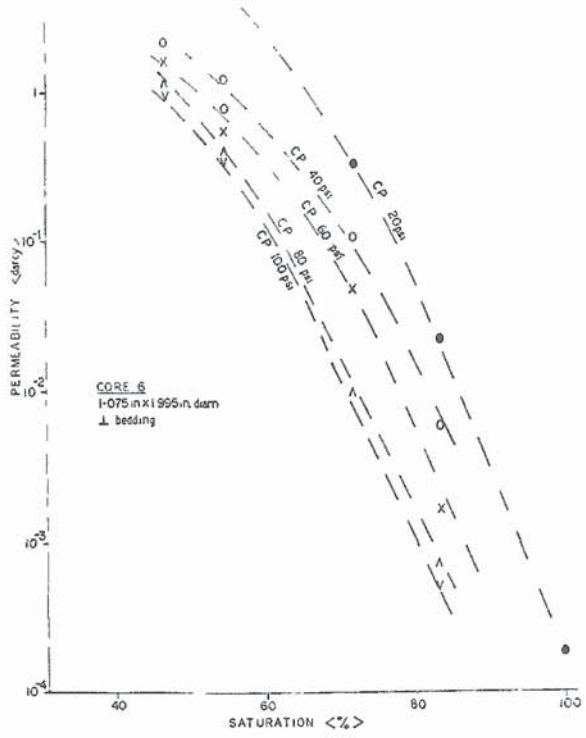


Fig. 4 Gas Permeability of Texas Lignite vs. Water Saturation at Different Confining Pressures (Cp)

While this effect may assist in the flow of gas in the later linking phase, the most significant factor in the early gas flow is likely to remain the fracture or joint permeability. This cannot be investigated satisfactorily in the laboratory, because of both the scale of phenomenon and the problems associated with specimen preparation.

Thus, the major problem in laboratory testing of any rock, and particularly one which, like the lignite, is weak and highly fractured, is the unavoidable natural selection which occurs during specimen preparation. Those parts of the rock mass which are either incipiently weak, or contain major fracture planes, are the parts which will have the most significant influence on permeability and those from which few, if any, specimens may be prepared. In this way a weighting of laboratory data in favor of the stronger, less permeable, parts of the rock mass is unavoidable. This effect will lead not only to an underestimate of permeability, which being a 'worst case' error in the present context may not be too serious, but could also lead to an erroneous identification of the direction of maximum permeability.

Because of these inherent uncertainties in the results of laboratory tests a back-up field test is also projected. This has the disadvantage that control of the external stress field and close monitoring of the degree of desiccation of the lignite are impossible. However, if a sufficient volume of rock is affected, the permeabilities measured in the field will be much more representative of the values required, that is, the values applying to an operational gasification unit, both in terms of relative and absolute values. A comparison of the field results to those from the laboratory will give a measure of the inaccuracy of the latter values, which will be of use in applying the laboratory results to different situations. It is also intended that the field test be used as a model for further tests which would be carried out on the site of a projected pilot operation.

ROOF STABILITY

Significant fracturing, deformation, or collapse, of the roof material may lead to excessive surface subsidence, and the possibility of loss of seal for the combustion products. An analysis of the behavior of the rock, therefore, is essential to the controlled operation of a gasification facility. Before this analysis can be conducted, however, certain data must be obtained and certain abilities developed. Rock testing must be carried out to determine the predominant deformation mechanisms and to evaluate the relevant mechanical parameters, computer techniques must be adapted to allow the simulation of the rock behavior, and operational data from pilot test sites must be collected for comparison with and possible modification of, the simulation predictions.

As the combustion chamber expands, roof support will be removed and the unsupported parts of the roof rock will be subjected to relatively high induced stresses, leading to deformation and the possibility of fracture and collapse. The most critical conditions will be associated with the tensile stress concentration in the unsupported roof, and the shear stress concentrations near the edge of the chamber, which could lead to shear fractures in the overburden and loss of stability of the boreholes (Fig. 5). As an added factor the drying effect of combustion could lead to dessication cracks in the immediate roof, while the high temperatures associated with the process could induce high thermal stresses in the roof rock as well as having an effect on the rock deformation behavior.

It must be appreciated that roof collapse may not necessarily be a disadvantage. A certain amount of closure of the combustion chamber can be of great assistance in maintaining the reaction at its most efficient level [3]. Moreover when the reaction is at a stage where the roof is composed of coal, roof collapse will be advantageous in giving a 'self-fueling' effect [1]. However, where the conditions are such that fracturing, excessive deformation or widespread collapse of the overburden occurs an unstable situation exists with the possibilities of gas leakage, water influx, and subsidence. This instability could be especially serious if connection is achieved between the gasification zone and any overlying producing aquifers.

THE MECHANICAL BEHAVIOR OF THE ROCKS

Rocks in general behave as rheological materials and may usually be described by

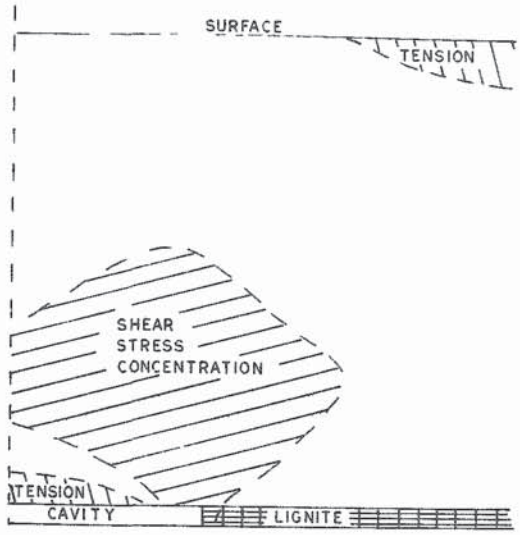


Fig. 5 Critical Zones of Tension and Shear Stress Concentration Above A Tabular Cavity

nonlinear elastic, visco-elastic and plastic elements in various combinations. They are, in addition, typically anisotropic and inhomogeneous. In general, the deformation of rocks may be described by a relationship of the form:

$\varepsilon = f(\sigma, t, T, S, H)$
ε = strain
σ = stress
t = time
T = temperature
S = moisture content
H = history of loading

Relationships of this form will be exceedingly complex and difficult to handle mathematically, so that simplification by neglect of relatively unimportant parameters is usually necessary, those most commonly neglected being moisture content and loading history. Most rocks may be reasonably well described by a non-linear viscoelastic relationship of the form [4]:

$$\varepsilon = A(T)\ \sigma^m t^n$$

with the possible addition, in the present context, of plastic elements at very high temperatures. Again, however, a relationship of this type tends to be difficult to handle mathematically for all but the most simple boundary value problems. As a result, most practical rock mechanics investigations rely upon further simplifications. Commonly used relationships are:

1. Linear viscoelastic
   $\varepsilon = f(t, T)\sigma$
2. Non-linear elastic
   $\varepsilon = f(\sigma, T)$
3. Linear elastic
   $\varepsilon = f(T)\sigma$
4. Elastic-perfectly plastic where it is assumed that the material is elastic up to some limiting stress and plastic at that stress.

Rock testing must be aimed at determining which of the available constitutive relationships is most suitable for each rock type, and at quantifying the relevant parameters. Since complex stress states will occur under critical conditions, and since rocks typically show different behavior in tension and compression the relevant parameters must be found for both states of stress. In addition the effects of anisotropy, temperature and moisture content must be investigated.

Preliminary uniaxial compressive and disc testing is currently under way with the intention of defining the orders of magnitude and the nature of the mechanical behavior of both the Texas lignite and the immediate roof rocks. Neither the testing, nor the full analysis of the data from completed tests are complete, and these will be reported later. However, some indication of the early results may be given.

Nominal 2 inches (51 mm) diameter cores of lignite and overburden have been tested under uniaxial compression using an MTS closed loop testing system which allows accurate control of loading. A further batch of 1 inch (25 mm) diameter cores have been tested using a Soiltest testing machine. Axial deformation is monitored by two strain gauged cantilevers attached to the upper specimen plate and activated by

push rods attached to the lower platen. Radial deformation is monitored by four strain gauged cantilevers equally spaced around a ring and activated by screws contacting the specimen [5]. The load and deformations are monitored at specified increments of deformation by a Data General Super Nova computer.

The lignite cores are tested over three load cycles, the first two to about 300 psi (2070 kN/m^2), the load being increased to failure on the third cycle, Figure 6 showing a fairly typical result. After an initial high strain crack closure region, the lignite shows a reasonably linear deformation response to load, and is approximately elastic up to at least moderate loads. A tendency to time dependent deformation at stress levels approaching the uniaxial compressive strength has been detected.

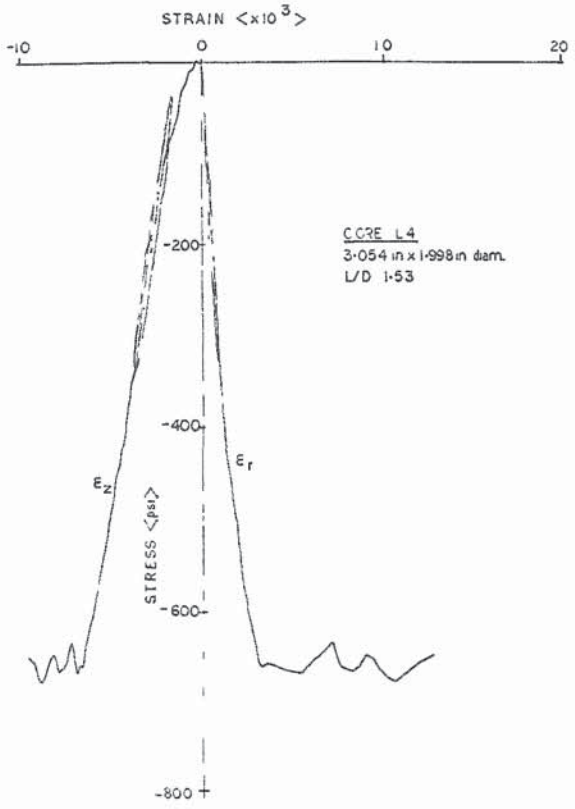


Fig. 6 Typical Stress-Strain Behavior of Texas Lignite Under Uniaxial Compression

The strength and deformation behavior of the lignite are variable, but there is a tendency for cores cut with their axis in the plane of the bedding to be weaker, to show a larger permanent deformation during initial loading, and have a lower modulus than those cut perpendicular to the bedding. Cores cut perpendicular to the bedding have uniaxial compressive strength ranging from 1010 psi (6960 kN/m^2) to 2010 psi (13860 kN/m^2) and Young's moduli in the third loading cycle between 1 x 10^5 psi (6.9 x 10^5 kN/m^2) and 1.3 x 10^5 psi (9.0 x 10^5 kN/m^2); cores cut parallel to the bedding have strengths ranging from 250 psi (1720 kN/m^2) to 860 psi (5930 kN/m^2) and Young's moduli between 2 x 10^4 psi (1.4 x 10^5 kN/m^2) and 1 x 10^5 psi (6.9 x 10^5 kN/m^2).

As already noted the overburden rock obtained from the Alcoa strip mine is an extremely weak and friable sand with obvious closely spaced bedding planes often incorporating carbonaceous partings. The inherent weakness of this rock has led to several problems both in preparation of samples and in testing.

The maximum length of core consistantly attainable has been 2.5 inches (63 mm), giving an L/D ratio of 1.25 and a consequent gross nonuniformity of the stress field in the specimens. It is hoped that a sufficient number of longer cores may be obtained in the future to quantify the effect of the L/D ratio, and hence to allow the bulk of the test program to be carried out on the shorter cores, or, failing this, that numerical simulation techniques will allow correction for the lack of uniform stress.

A wide variation in uniaxial behavior has been observed, due mainly to variations in lithology. The weaker varieties have strengths in the range 30 psi (210 kN/m^2) to 220 psi (1520 kN/m^2) and loading moduli of the order of 10^4 psi (6.9 x 10^4 kN/m^2). The harder rocks have strengths between 800 psi (5520 kN/m^2) and 1450 psi (10,000 kN/m^2) and moduli of the order of 2 x 10^5 psi (1.4 x 10^6 kN/m^2). No significant differences in behavior with core orientation have been detected to date.

Failure of these materials has typically been brittle, either on inclined shear planes, or axial planes of tensile splitting, the latter being observed most commonly in the cores tested with their axis parallel to the bedding.

A number of Brazilian disc tests have been conducted on the various overburden materials. Tensile strengths obtained by this method have ranged from 10 psi (70 kN/m^2) to 50 psi (340 kN/m^2) for the weaker material and from 95 psi (650 kN/m^2) to 125 psi (860 kN/m^2) for the stronger rock. No firm indications are available to date of any anisotropy of this parameter.

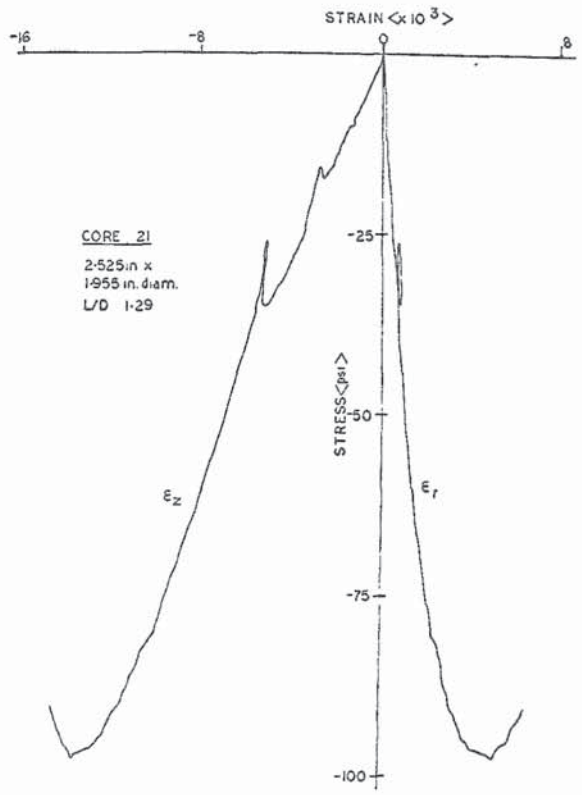


Fig. 7 Typical Stress-Strain Behavior of the Overburden Under Uniaxial Compression

All the cores tested up to the present have been saturated. It is to be expected that the cracking which occurs on drying will lead to an appreciable reduction in strength and modulus under uniaxial compression.

ROOF STABILITY AND SUBSIDENCE PREDICTION

In the calculation of stress and deformation fields in an anisotropic layered rock sequence where non-simple geometries are encountered, solutions for every particular set of boundary values must be obtained by numerical techniques, the most powerful and most commonly used of which is the finite element method. Codes based on this method are now widely available, many with geotechnical facilities, but in the majority of cases these assume linear or non-linear elasticity. It is envisaged that such a code will be used for the investigation of the lignite gasification overburden stability, with initial runs using an elastic model, later runs being carried out for a viscoelastic model after suitable code modification and extension, should this prove necessary.

A suite of finite element programs suitable for this application has been obtained by the University of Texas from the University of Nottingham, England and is currently undergoing implementation. This basic suite (Pafec 70+) [6] includes the facilities for applying gravity loading and thermal strain and can be used for two or three dimensional problems for anisotropic materials. It can also be used for obtaining plastic and non-linear creep solutions, and has been used to model subsidence above long wall mining operations in the U.K.

A preliminary estimate of the likely subsidence effects of roof collapse can be made using the empirical and analytical solutions obtained for subsidence over conventionally mined cavities.

As a general rule surface subsidence will depend upon the effective maximum convergence, S_m, in the extracted horizon and the depth, H. In practice three classes of subsidence can be distinguished, depending on the ratio of these two factors. Many other factors influence the subsidence effects, so these classes may only be regarded as broad generalizations. For higher ratios, $S_m/H>0.1$, discontinuous subsidence is often found with a distinct step in the vertical surface movement roughly above the edge of the mined out area. As the ratio decreases, $0.1>S_m/H>0.01$ subsidence outside the mined out area becomes more pronounced and cracks can be observed in the tensile zones. At low ratios, $S_m/H<0.01$, the surface subsidence is generally continuous and no cracks observed [7].

The most satisfactory analytical results for a stratified rock mass appear to be those based on a homogeneous transversely isotropic model. In a series of classic papers Berry and Berry and Sales [8] investigate this, and other models.

Figures 8 through 11 show the subsidence effects for various depths and chamber sizes calculated from Berry and Sales equations for the two-dimensional transversely isotropic case. The subsidence in this case is a function of the anisotropic material constants α_1 and α_2, where α_1 and α_2 are the two roots with positive real parts of:

$$\alpha^4 - 2k_2\alpha^2 + k_1^2 = 0.$$

and the parameters k_1, k_2 in this equation are given by:

$$k_1^2 = \frac{1 - \nu^2}{E_1 E_2 - \nu_2^2}$$

$$k_2 = \frac{E_1/2G - \nu_2(1 + \nu_1)}{E_1/E_2 - \nu_2^2}$$

Where E_1, E_2 are the horizontal and vertical Young's moduli respectively, ν_1, ν_2 are the ratios $-\varepsilon_x/\varepsilon_y$, $-\varepsilon_z/\varepsilon_y$, for uniaxial loading in the y (vertical) direction G is the shear modulus in the vertical direction. Figures 8 through 11 are based on values for α_1 of 4.45 and α_2 of 0.45.

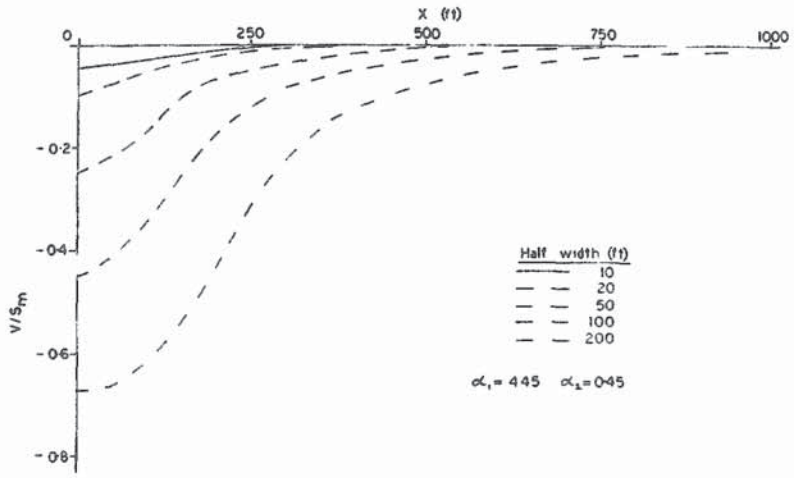


Fig. 8 Vertical Surface Subsidence (v) as a Function of Convergence (Sm) for Different Cavity Widths

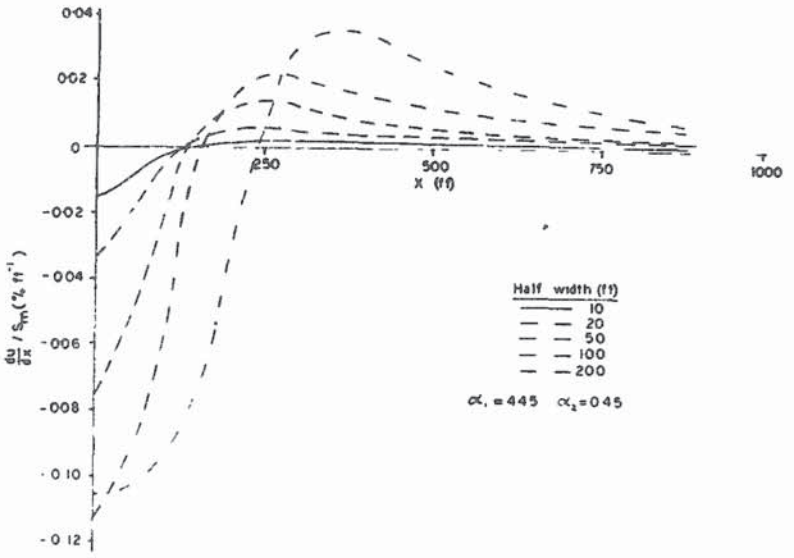


Fig. 9 Horizontal Surface Strain ($\frac{du}{dx}$) as a Function of Convergency (Sm) for Different Cavity Widths

As a general rule the most damaging effects of subsidence are the tilt and horizontal surface strain caused by differential settlement [7]. Figures 10 and 11 show the development of tilt on the sides of the subsidence basin, and of tensile surface strains towards the edge of the basin. Figures 12 and 13 illustrate the decrease in subsidence effects with increasing depth or decreasing cavity size.

The above theoretical results and discussion assume a continuous form of the subsidence profile, both on the surface and beneath it. A real possibility exists, however, for non-continuity of this profile, if the immediate roof is similar to that examined at the Alcoa site. It has already been stated that this material is weak and friable and it seems more likely that early total collapse of the roof would occur. In this case there is a real possibility of progressive caving which could extend some way to the surface particularly as the roof rock is fine grained and would be expected to show little bulking effect.

A rough estimate of the likely extent of caving may be obtained by considering the volume of caved rock as a function of the extracted volume and assuming the areal extent of the caved and extracted volumes to be the same. The caved volume may be written as [9]:

$$V_e = V_o\left(\frac{k}{k-1}\right)$$

where V_e is the extracted volume

k is a bulking factor which may range from 1.5 to 1.1 and will be near the lower value for powdered and highly compacted materials.

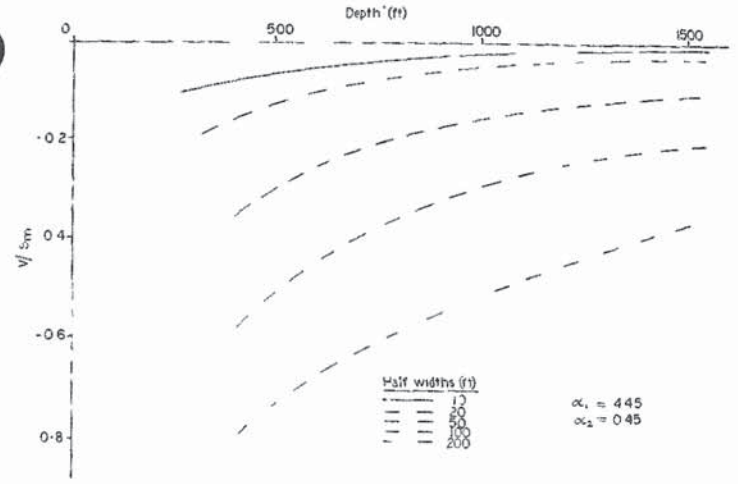


Fig. 10 Vertical Surface Subsidence (v) as a Function of Convergence (Sm) vs. Depth for Various Cavity Widths

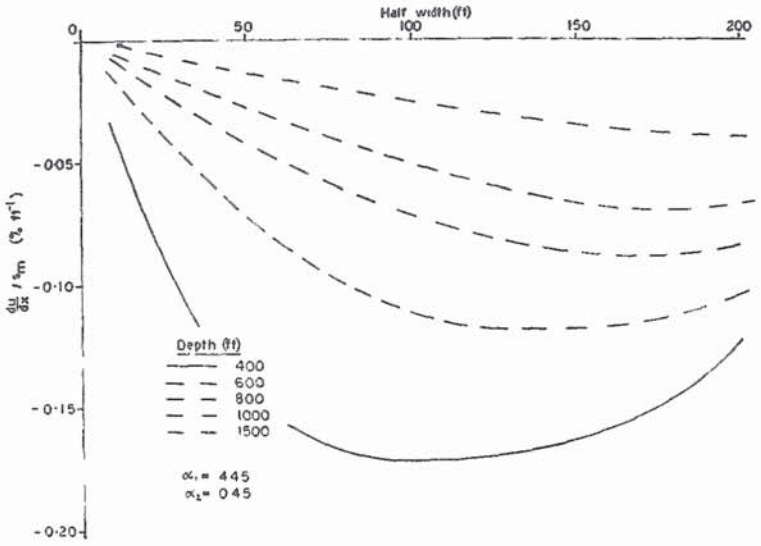


Fig. 11 Maximum Horizontal Surface Compression Strain ($\frac{du}{dx}$) as a Function of Convergency (Sm) vs. Cavity Width for Various Depths

Assuming the equivalence of areal extent this relationship may be written in terms of vertical extent of the caved zone (t_c) related to thickness extracted (t_e). In this case the ratio of $\frac{t_c}{t_e}$ varies from 11 for k=1.1 to 3 for k=1.5. Thus for a 10 ft. extracted thickness the caved zone could extend for as much as 110 ft. Though this would not extend to the surface it could lead to loss of seal for the gaseous products of combustion and could significantly effect the subsidence profile

CONCLUSIONS

In unaltered Texas Lignite fluid flow will be controlled by joint and bedding fractures and weakness planes, flow through the intervening rock matrix being minimal. However, on drying this rock is characterized by the development of closely spaced cracks roughly parallel to the original joint and bedding planes, and this effect could be significant to flow during linkage. Laboratory studies on the effect of drying and stress on crack development and thus on permeability indicate that this mechanism may be important in later link development, but that this importance will tend to decrease with depth.

In the Rockdale region of Central Texas the Lignite is overlain by a poorly cemented, weak sand, and it is probable that a similar overburden occurs in other localities. Early mechanical tests indicate that this rock has very low values of uniaxial compressive and tensile strengths, and a low deformation modulus. Early roof collapse seems inevitable, and it is important to be able to predict when this collapse will occur and in what manner and how far its effects will extend, since the Lignite is overlain in many places by producing aquifers, and roof collapse could have an appreciable effect on surface subsidence, especially in thick, shallow developments. Finite Element codes are being implemented to help this investigation.

ACKNOWLEDGMENTS

The authors are pleased to acknowledge the assistance of Mr. S. Sen who has carried

out the permeability tests and Mr. C. Stephenson on whom much of the work of specimen preparation and testing has fallen. Further thanks are due to Drs. T. F. Edgar and W. R. Kaiser, co-investigators in the University of Texas Lignite Gasification Project.

Financial support for this work has come from The National Science Foundation (RANN Division) and Texas Utilities Fuel Company. This support is gratefully acknowledged.

REFERENCES

1. Gregg, D. W., Hill, R. W., and Olness, D. N., "An Overview of the Soviet Effect in Underground Gasification of Coal," UCRL-52004, Lawrence Livermore Laboratory, January, 1976.
2. Kaiser, W. R., "Texas Lignite: Near-surface and Deep-basin Resources," The University of Texas at Austin, Bureau of Econ. Geol. Rept. Inv. 79, 1974.
3. Heide, K., Eilhaur, W., "Underground Gasification of Coal in the Soviet Union and Checkoslovakia," UCRL-Trans-10756, Lawrence Livermore Laboratory.
4. Jaeger, J. C. and Cook, N. A. W., "Fundamentals of Rock Mechanics," Methuen and Co. Ltd., London, 1969.
5. Menezes, J. "An Improved Technique for Rock Deformation Measurements and Application to Berea Sandstone," The University of Texas at Austin, M. S. Thesis, 1976.
6. Henshall, R. D. (ed.), "Pafec 70+," The University of Nottingham, 1974.
7. Salamon, M. D. A., "Rock Mechanics of Underground Excavation," Proc. 3rd Cong. Rock Mechs., V1B, 951-1099, 1974.
8. Berry, D. S. "An Elastic Treatment of Ground Movement due to Mining-Part I, Isotropic Ground," J. Mech. Phys. Solids, V8, 280-292, 1960: and Sales T. W., "Part II - Transversely Isotropic Ground," J. Mech. Phys. Solids, V9, 52-62, 1961. "Part III - Three Dimensional Problem, Transversely Isotropic Ground," J. Mech. Phys. Solids., V10, 73-83, 1962.
9. Obert, L. and Duvall, W. I., "Rock Mechanics and The Design of Structures in Rocks," Wiley, New York, 1967.

MECHANICAL PROPERTIES OF COAL FOR SIMULATION OF UNDERGROUND GASIFICATION PROCESSES

by

H. D. Shoemaker[1]
L. Z. Shuck[2]
R. R. Haynes[3]
S. A. Advani[4]

ABSTRACT

Mechanical properties of coal have been determined in an effort to advance in situ gasification processes. Experiments and apparatus were developed to evaluate the directional compressive and shear properties of coal at elevated temperatures. Both creep and stress-relaxation experiments were conducted to evaluate the viscoelastic properties in compression and shear, at temperatures between 75° and 650°F (24° and 343°C). The directional experiments involved loading and or deforming the specimen normal to the bedding planes, face cleats, and butt cleats; and on four different specimen sizes. Stress-strain relations and ultimate strengths were also determined at three different loading rates for these directions, specimen sizes, and temperatures. A time-temperature superposition shift function was used to represent the viscoelastic properties of coal. Four- and six-parameter viscoelastic fluid models and empirically derived polynomial representations are available for viscoelastically modeling coal as functions of temperatures.

Shallow and deep mine coal from the Pittsburgh coalbed were tested. Future tests will include other eastern bituminous, midwestern bituminous, western bituminous and subbituminous and lignites. The Pittsburgh coal was found to have the greatest ultimate strength and elastic moduli at 200°F (93°C) in both compression and shear, regardless of the orientation of loading or the loading rate. The ultimate strength in the normal to coalbed direction was approximately twice that in the face and butt cleat directions, independent of temperature. The ultimate strength is dependent upon the specimen size and loading rate. As the specimen size decreases, the strength increases; and as the loading rate increases, the strength increases. The ultimate strain is relatively constant for temperatures below the softening stage. At 575°-650°F (302°-343°C) the coal becomes fluidic, coalescent, and is well represented by a four-parameter fluid. Coal also obeys the time-temperature superposition principle.

INTRODUCTION

The mechanical properties of coal have been determined for numerous applications, most of them being related to surface processing. Although considerable mechanical property data has been generated on coal in the crushed and thermally modified states, the data required for the further development of certain in situ technology has been lacking.

---

[1]Mechanical Engineer, Morgantown Energy Research Center, ERDA
[2]Supervisory Mechanical Engineer, MERC, ERDA
[3]Mechanical Engineer, MERC, ERDA
[4]Professor, Mechanical Engineering and Mechanics Department, West Virginia University

One of the processes for extraction and conversion of coal being reevaluated in the U.S. is underground gasification. This is one of the few processes that could be implemented in a short time period to provide energy to the high demand centers of the U.S. This process has been used commercially for over 30 years in the Soviet Union [1, 2][5] and considered at different times by others [3]. However, the micro/macro mechanisms by which the processes advance through the coalbed have not been rigorously explained. Simulation or process modeling techniques have been of the lumped-parameter, black-box type.

Three basic mechanisms must be understood to improve in situ gasification technology. These mechanisms are mass and energy transport phenomena, reaction kinetics, and mechanical-structural effects. These basic mechanisms and their interactions are believed to control process advancement through the coalbed. Laboratory research at the Morgantown Energy Research Center [4] has demonstrated the importance of the mechanical-thermal-structural characteristics of coal in in situ process front dynamics. In fact, the thermally induced strains and tectonic stresses in conjunction with coalbed permeability are believed to be the predominate controlling factors in the rate of process advancement and stability.

The basic structural and constitutive properties of coal at elevated temperatures must be known in order to predict the effects of a gasification scheme with regard to roof collapse, coal fracturing, porosity, permeability, and surface subsidence with its direct effect on the environment as well as the gasification process.

Coal is somewhat of an elastic material, but shows definite similarities to viscoelastic materials as its properties vary with temperature. Hence, coal is a unique, difficult material to describe quantitatively. However, as our most abundant energy resource, the associated sciences of extraction, conversion, and utilization must be developed from a strong fundamental base through engineering applications.

This study represents an effort to provide somewhat more realistic and comprehensive data for computer models being developed [5, 6] with the capability of using such data to structurally model in situ processes. It was performed at the Morgantown Energy Research Center as part of the ERDA Underground Coal Gasification Program.

PREVIOUS INVESTIGATIONS

Most of the research performed to determine the strength of coal has been from uniaxial compression tests on cubical, rectangular, or irregular shaped specimens [7, 8, 9]. Coal has a greater ultimate compressive strength when loaded normal to the bedding planes (6,600-11,000 psi (4.55-7.58 x 10^7 N/m^2)), than when loaded normal to either the face or butt cleats [7, 8]. The ultimate strength increases when the stresses become representative of in situ tectonic stresses as shown from triaxial loading experiments [8, 10, 11, 12]. The ultimate compressive strength of coal whether loaded normal to the bedding planes or the cleat planes is test specimen size dependent [13, 14, 15], and increases exponentially with decreasing specimen size.

The relationship between stress and strain is nonlinear at the onset of loading, but approximately linear over a wide range prior to failure. The most significant nonlinear effect in the stress-strain curve at room temperature is the apparent closing of fissures in the specimen during initial loading [8, 16, 17]. Poisson's ratio as determined from compression tests, did not show a significant dependence on specimen orientation, and ranged from 0.37 to 0.44 [8]. If the principal material axes 1, 2, and 3 are defined as the normals to the face cleats, butt cleats, and bedding planes, respectively; then Poisson's ratios for Barnsley Hards coal were $\nu_{12} = 0.44$, $\nu_{23} = 0.37$, and $\nu_{31} = 0.41$ [8]. The average values reported for Poisson's ratios for the same material axes for Pittsburgh coal were $\nu_{12} = 0.34$, $\nu_{23} = 0.39$, and $\nu_{31} = 0.42$ [12]. Macrae and Mitchell [18] reported that the ultimate failure stress and deformation were notably time dependent. At room temperature, failure occurred after a high stress had been maintained on the specimen for an extended period of time. Sanada and Honda [19] have demonstrated that the time-temperature superposition principle can be applied to coal.

There is evidence that bituminous coal is a viscoelastic material which behaves like a viscous fluid at elevated temperatures. Brewer [20] states that when bituminous coal is heated under appro-

[5]Numbers in brackets refer to references at the end of this paper

priate conditions, it may exhibit plastic, viscous, or elastic flow, and often combinations of all three. In general, most of the eastern U.S. bituminous coals upon heating, coalesce to a more amorphous state, swell, effervesce, and become fluidic prior to the coking phase and final solidification.

EXPERIMENTAL PROCEDURE

In examining directional property effects upon burn front directional stability, subsidence, and various modes of failure, specific types of data are required. The basic properties required are directional and temperature-dependent stress-strain relations and failure stresses in compression and shear.

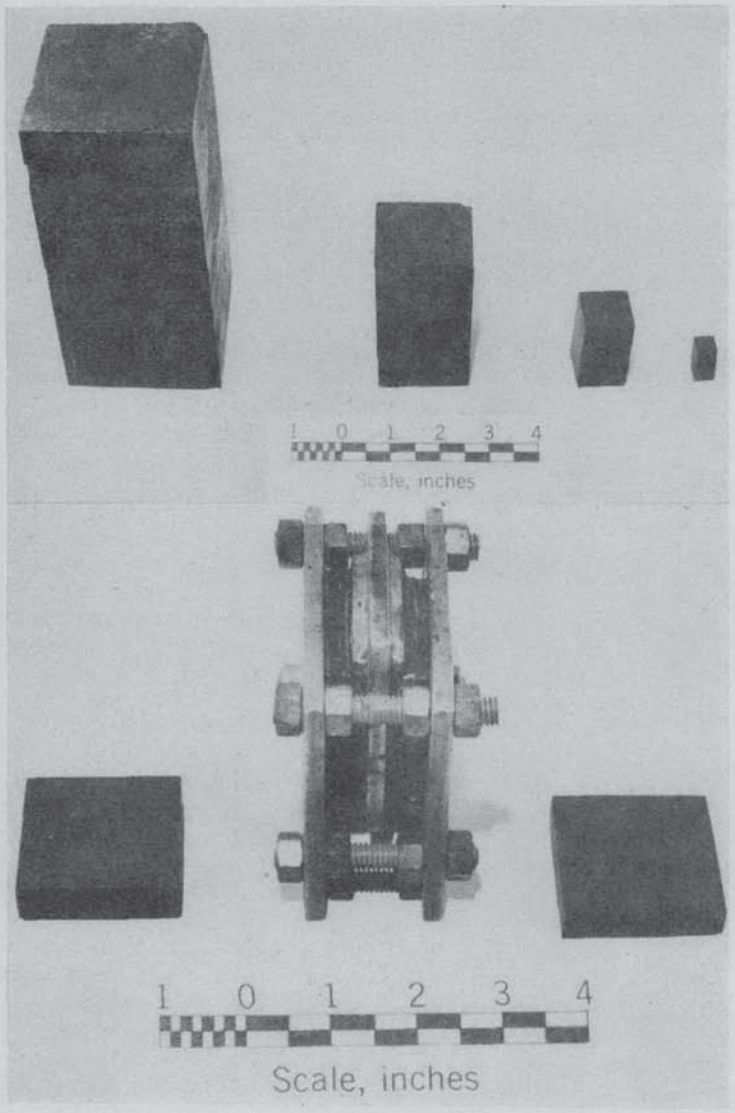


Figure 1. Pittsburgh Coal Specimens as used in Uniaxial Compression and Shear Experiments.

The Pittsburgh bituminous coal properties were evaluated in these tests. Samples were obtained from the working face of a mine near Mt. Morris, Pa., with a bed thickness of seven (7) to nine (9) feet (2.1-2.7 m) and approximately 480 feet (146 m) below the surface. A few samples of Pittsburgh coal were obtained from a strip mine near Bridgeport, W.Va., with a bed thickness of five (5) to six (6) feet (1.5-1.8 m) and 50-80 feet (15.2-24.4 m) below the surface. The test specimens were oriented with respect to the bedding planes, face cleats, and butt cleats; and cut into specimen sizes (Figure 1) from lumps obtained at random.

The research described here was organized as illustrated in Figure 2. The experimental apparatus used included provisions for determining the moduli of elasticity and rigidity (stress-strain curves to specimen failure) at various loading rates, and the viscoelastic[6] properties (Figure 3). All experiments were conducted in uniaxial compression and simple shear. The specimen loading chamber of the test apparatus was heated with inert gas and a heating coil surrounding the test area (Figure 3).

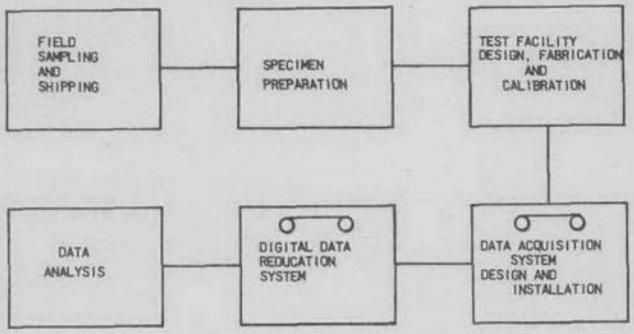


Figure 2. Major Tasks.

---

[6] Stress-relaxation as defined by the time dependent stress response of a material in a step constant strain is given as

$$Y(t) \triangleq \frac{1}{\varepsilon_o}\,\sigma(t)$$

Creep as defined by the time dependent strain response to a step stress is given as

$$J(t) \triangleq \frac{1}{\sigma_o}\,\varepsilon(t)$$

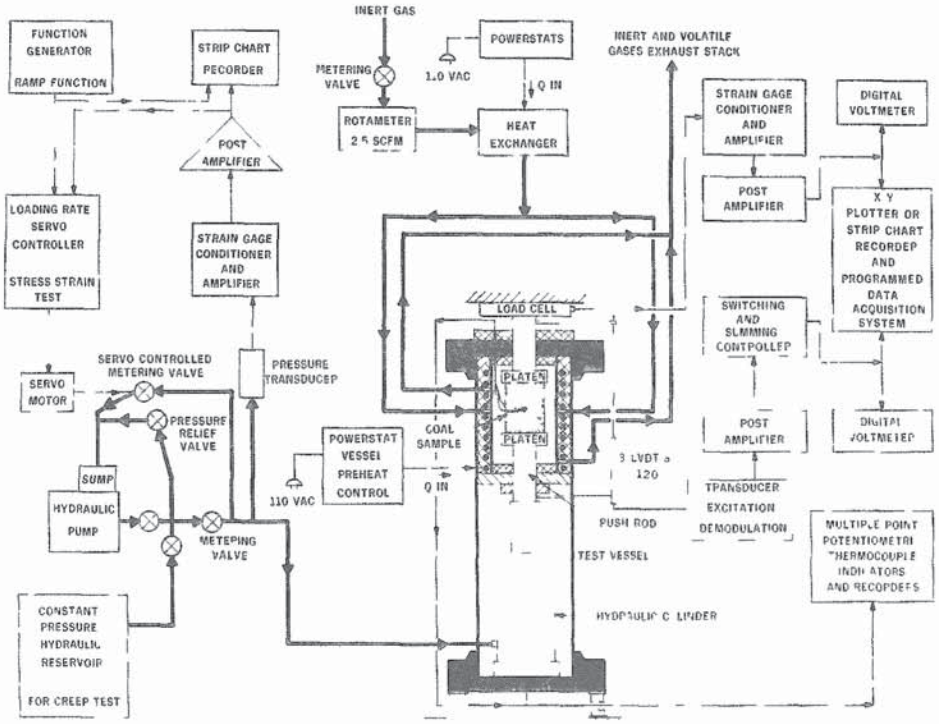


Figure 3. Elevated Temperature Stress-Strain, Stress-Relaxation, and Creep Test Apparatus.

The stress-strain experiments were conducted at various loading rates in both compression and shear to specimen failure (Figure 3). A constant loading rate was maintained by a servo-controlled metering value. The experimental apparatus for the stress-relaxation and creep experiments is shown in Figure 4, where gage blocks were used at Fulcrum A to calibrate for a prescribed deformation in the stress-relaxation experiments. Fulcrum A was removed for the creep experiments to apply a prescribed constant load.

The deformation of coal specimens in compression or shear was measured by a linear variable differential transformer (LVDT) with total system displacement resolution less than 0.001 inch (0.0254 mm). The system currently includes three LVDT's at 120° surrounding the test area. The loads applied during the compression and shear tests were measured by strain gage load cells (Figure 4) with total system resolution better than 2 lb (8.9 N) for the small specimens (1/2" and 1" square base and shear specimens) and 20 lb (89 N) for the larger specimens (2" and 4" square base). Total system calibration was performed at each temperature prior to each test. A stainless steel calibration specimen similar in size to the coal specimen was used to obtain the calibration curve. This calibration curve was subtracted from the coal data curve. The maximum uncertainty under the worst conditions was 4.8 percent and an average uncertainty of less than 2 percent was attained for both the load and displacement measurements.

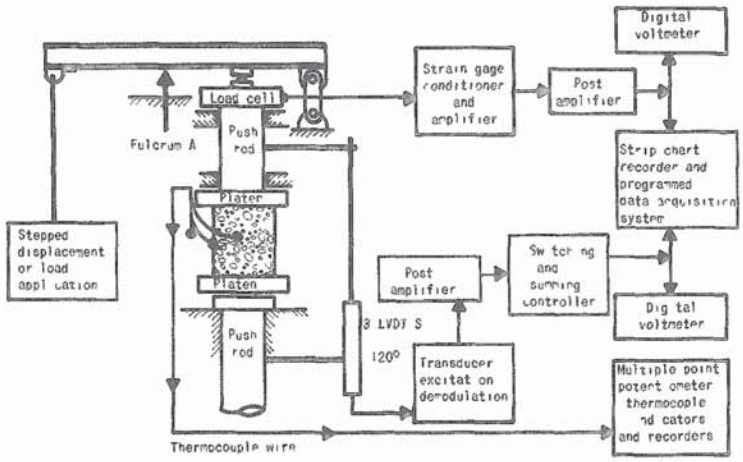


Figure 4. The Stress-Relaxation and Creep Apparatus and Instrumentation Schematics Shown with a Uniaxial Compression Specimen. Note that for the creep experiment, Fulcrum A is removed and the load adjusted to give a constant stress on the coal specimen.

When measurements were recorded at a particular elevated temperature, the test specimen chamber was maintained at the desired uniform temperature for the duration of the experiment (temperatures were measured by chromel-alumel thermocouples). The specimen was heated until it attained the test temperature and allowed to stabilize for approximately 10 minutes under no load. All experiments were conducted in the temperature range of 75°-650°F (24°-343°C).

The duration of application of the load or deformation varied between 2 and 7,200 sec. Other than the destructive test effects, sample degradation due to these time periods for temperatures up to 575°F (302°C) could not be detected. At 650°F (343°C), the duration of a test was only a few seconds so that sample degradation was minimal. No tests were performed above the phase transition temperatures around 650°F (343°C) because of sample degradation.

EXPERIMENTAL DESIGN

The independent variables or factors in the simplified factorial design for the compressive tests were coal specimen sizes, 1/2" x 1/2" x 1", 1" x 1" x 2", 2" x 2" x 4", and 4" x 4" x 8" (1.27 x 1.27 x 2.54 cm, 2.54 x 2.54 x 5.08 cm, 5.08 x 5.08 x 10.16 cm, and 10.16 x 10.16 x 20.32 cm); loading rate (for stress-strain relations) 100, 500, and 1,000 psi/min (0.069, 0.345, 0.690 x 10^7 N/m^2-min); orientation of loading in uniaxial compression was normal to the bedding planes, normal to the face cleats, and normal to the butt cleats; and temperature, 75°-650°F (24°-343°C). The variables for the shear tests were the same as for compression except six orientations of loading were used as illustrated in Figure 5 and only one specimen size of 1/2" x 2" x 2" (1.27 x 5.08 x 5.08 cm). The number of replications for the stress-strain relations was at least two for all tests and three for the 1" x 1" x 2" (2.54 x 2.54 x 5.08 cm) specimen loaded normal to the bedding planes at 500 psi/min (0.345 x 10^7 N/m^2-min).

The independent variables for the stress-relaxation experiments were the same as those used in the stress-strain relations except the percent of ultimate deformation as obtained from stress-strain relations (25, 50, and 75 percent ultimate deformation) replaced the variable loading rate. The number of replications was at least one for all tests and two for the 1" x 1" x 2" (2.54 x 2.54 x 5.08 cm) specimens deformed normal to the bedding planes at 50 percent ultimate deformation.

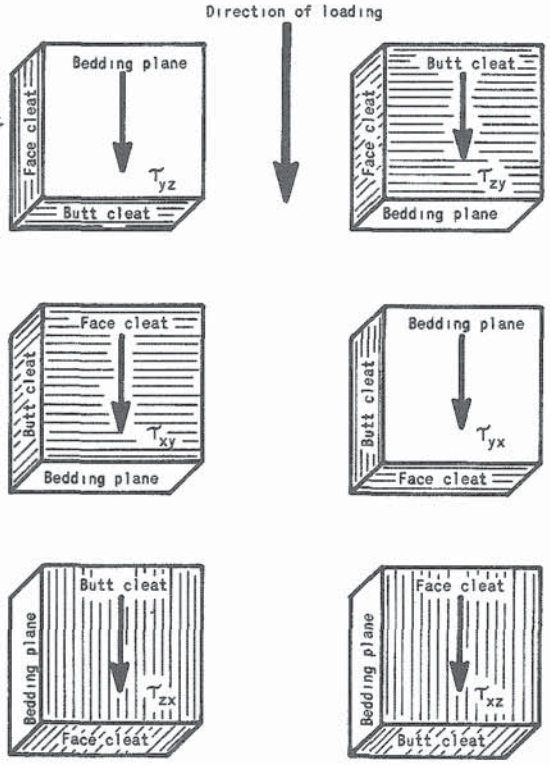


Figure 5. Shear Specimen Orientation Showing the Direction of Loading.

The independent variables for the creep experiments were the same as those used in the stress-strain relations except the percent of ultimate load (25, 50, 75 percent ultimate stress) replaced the variable loading rate. The number of replications was at least one for all tests and three for the 1" x 1" x 2" (2.54 x 2.54 x 5.08 cm) specimens loaded normal to the bedding planes at the constant stress levels 25, 50, and 75 percent ultimate stress.

There were approximately 500 separate experiments conducted in all. The variation in the data between replications was on the average no more than ± 15 percent of the measured values. The percent ultimate stress and percent ultimate strain indicate the range of viscoelastic linearity or nonlinearity.

RESULTS

Stress-Strain Relations -- Temperature has a dramatic effect upon the ultimate strength and ultimate strain of coal (Figure 6). Regardless of specimen size, the ultimate strength of coal is greatest at 200°F (93° C) (Figures 6 and 7). The ultimate strength is statistically[7] uniform for temperatures up to 350°F (177°C), where the ultimate strength diminishes to less than 100 psi at 650°F (0.069 x 10^7 N/m^2 at 343°C). The ultimate strain is statistically constant until the temperature of the specimen exceeds 500°F (260°C) where large finite strains occur. Notice, in Figure 8, the effect of specimen size on the stress-strain curves at 500°F (260°C) and also that the strip mine coal

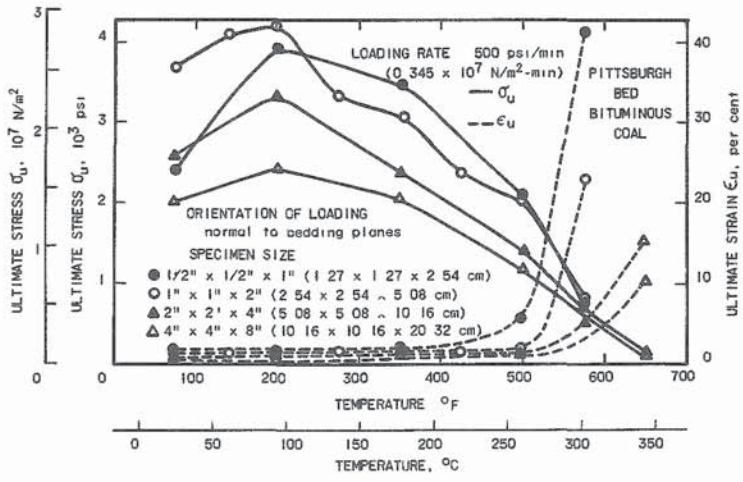


Figure 6. The Ultimate Stress and Strain-Temperature Curves Showing the Effect of Specimen Size of the Pittsburgh Coal when Loaded in Uniaxial Compression Normal to the Bedding Planes.

[7]The statistical test employed was the analysis of variance with an α error of 5 percent.

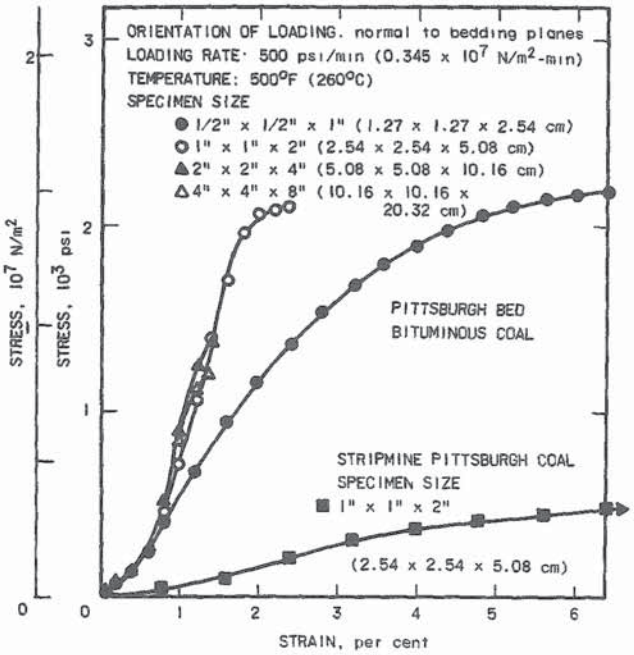


Figure 7. Stress-Strain Curves Loaded Normal to the Bedding Planes in Uniaxial Compression (Average Values) Showing the Effect of Specimen Size at 500°F (260°C).

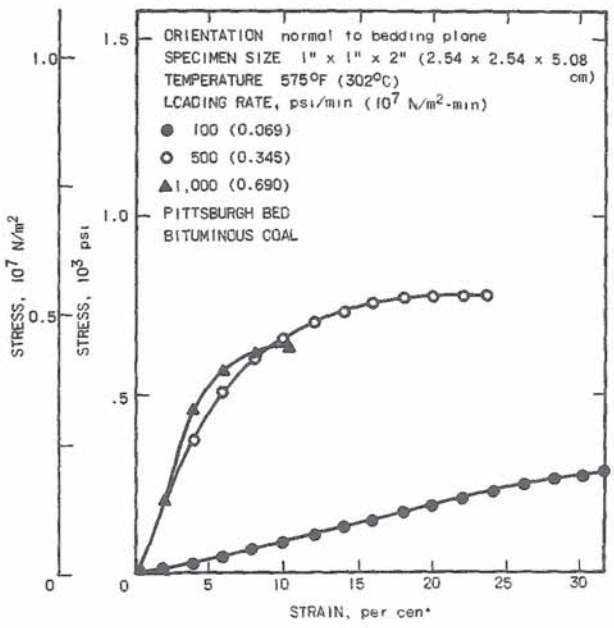


Figure 8. Stress-Strain Curves Loaded Normal to the Bedding Planes in Uniaxial Compression (Average Values) Showing the Effect of Loading Rate at 575°F (302°C).

softens at a lower temperature as compared to the deep mine coal.

The effect of loading rate upon the ultimate strength and ultimate strain is such that as the loading rate increases the ultimate strength increases while the ultimate strain decreases in both compression (Figure 9) and shear. Note the characteristic S-shape of the stress-strain curves with the initial part of the curve apparently representing closure of the fissures and the final part being the plastic flow of the coal prior to specimen failure.

The effect of orientation of loading upon the ultimate strength and ultimate strain as a function of temperature are demonstrated in Figure 10. The ultimate strength when loaded normal to the bedding planes is approximately twice that for loading normal to the face or butt cleats over the entire temperature range. The ultimate strain is relatively constant and independent of the orientation of loading for temperatures approaching 500°F (260°C). However, at temperatures above 500°F (260°C), the deformation for loading normal to the bedding planes is approximately four times that for loadings normal to the face and butt cleats.

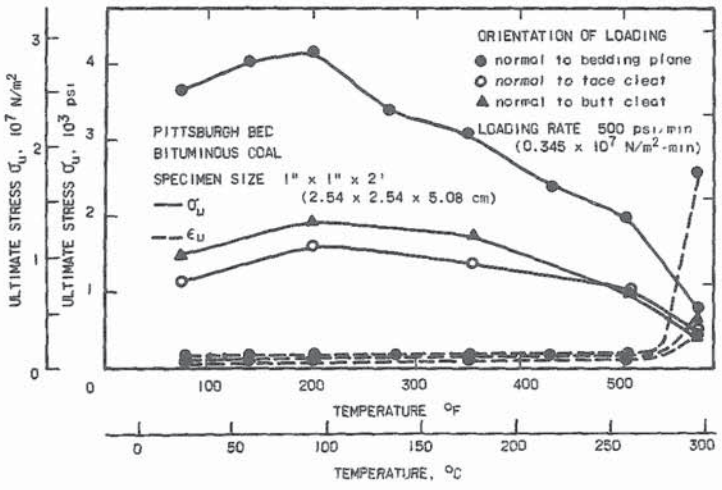


Figure 9. The Ultimate Stress and Strain-Temperature Curves Showing the Effect of Orientation of Loading on the Pittsburgh Coal When Loaded in Uniaxial Compression.

Figure 11 demonstrates that the ultimate shearing strength is the greatest at 200°F (93°C) regardless of the orientation of loading. In general, the shearing stresses do not vary more than 200 psi (0.138×10^7 N/m^2) from one another throughout the temperature range.

Stress-Relaxation Relations--The stress-relaxation experiments involved applying an instantaneous constant deformation on the coal specimen and allowing the stress to relax with time.

The effects of temperature in relaxation experiments are similar to those for the stress-strain. Figure 12 for shear, indicates that the relaxation moduli are similar for temperatures through 350°F (177°C) followed by decreasing relaxation moduli at the higher temperatures.

The Pittsburgh coal is viscoelastically nonlinear at the lower temperatures, 75°-500°F (24°-260°C), as the S-shape of the stress-strain curves indicate (Figure 8). However, at 575°-650°F (302°-343°C) the coal becomes essentially linear (Figure 13).

Creep Relations--The creep experiments involved applying an instantaneous constant load on the coal specimen and allowing the deformation of the specimen to change with time.

The effect of temperature in the creep experiments

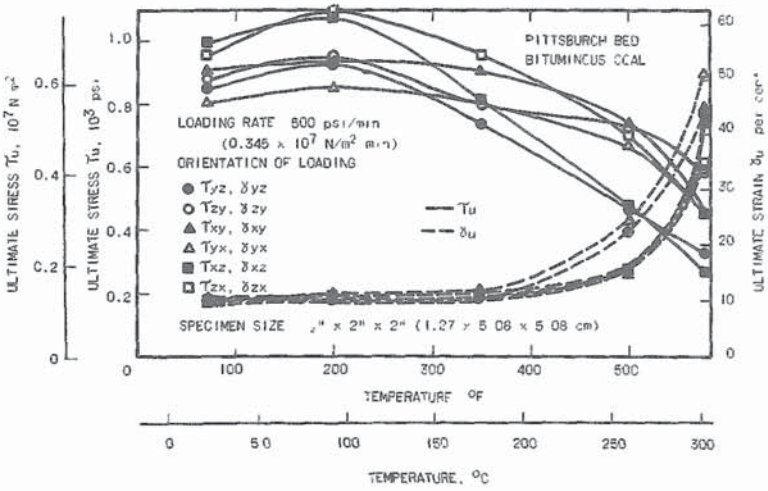


Figure 11. The Ultimate Stress and Strain-Temperature Curves Showing the Effect of Orientation of Loading in Shear on the Pittsburgh Coal.

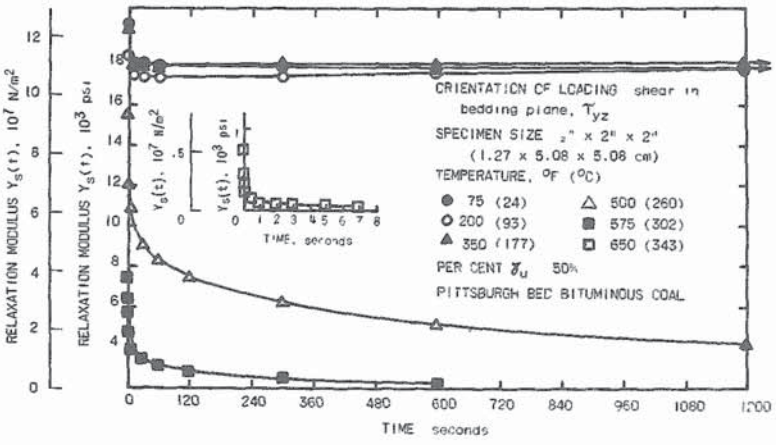


Figure 12. Relaxation Modulus-Time Curves Showing the Effect of Temperature (75°-650°F (24°-343°C)) on the Pittsburgh Coal When the Specimens are Loaded in Shear.

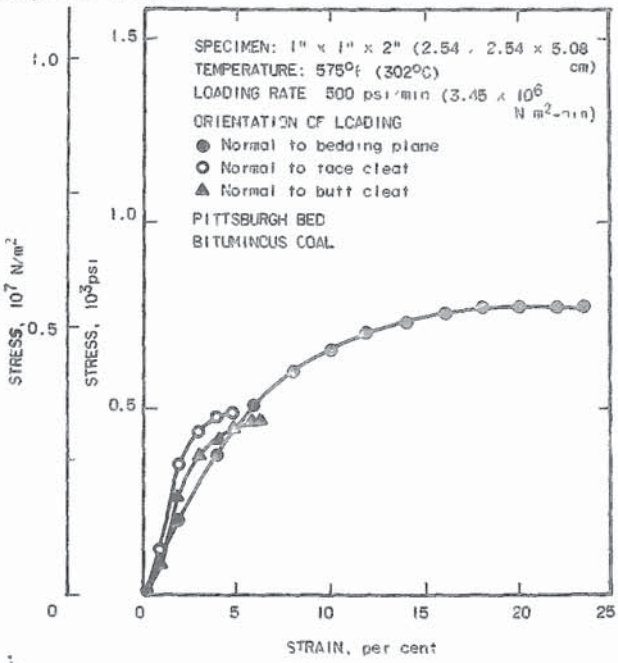


Figure 10. Stress-Strain Curves Showing the Effect of Orientation of Loading on the Pittsburgh Coal When Loaded in Uniaxial Compression (Average Values) at 575°F (302°C).

reflect the same results as for stress-strain and stress-relaxation experiments. The effect of specimen size upon the creep compliance in uniaxial compression is demonstrated in Figure 14, at 200°F (93°C). The smallest specimen size reflects the characteristic creep curve, while the larger specimens display a reverse creep at approximately one minute into the test. This swelling occurs in both compression and shear at temperatures of 200° and 350°F (93° and 177°C). At 500°F (260°C) and above, the coal softens and coalesces and cannot support a sustained load. Figure 15 represents a typical creep specimen at 650°F (343°C) after very large deformation occurs. Notice the tar bubbles along the edge as degradation occurs.

The effect of orientation of the constant applied load on the creep compliance is demonstrated in Figure 16 at 500°F (260°C). The curve represented by loading normal to the bedding planes in compression is very different from the others. It demonstrates failure in tertiary creep after approximately six minutes, while for the loadings normal to the face and butt cleats failure did not occur until much later (35 minutes). Similar directional properties between the face and butt cleat directions were observed in the stress-strain relations.

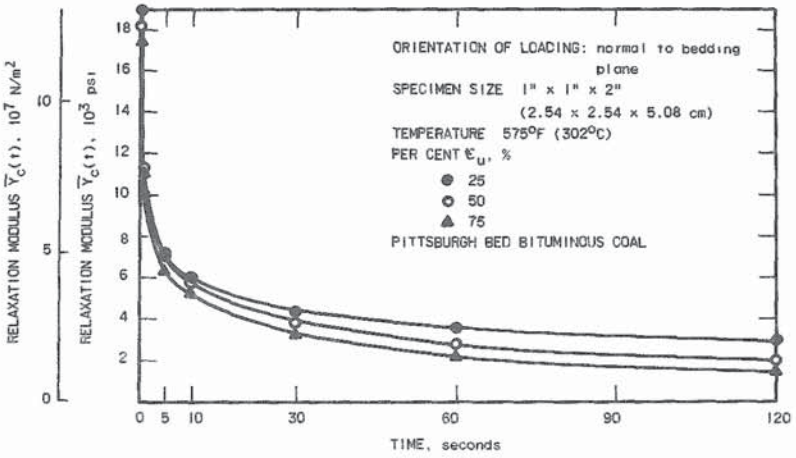


Figure 13. Relaxation Modulus-Time Curves Showing the Effect of Percent Ultimate Strain at 575°F (343°C) on the Pittsburgh Coal When Loaded in Uniaxial Compression.

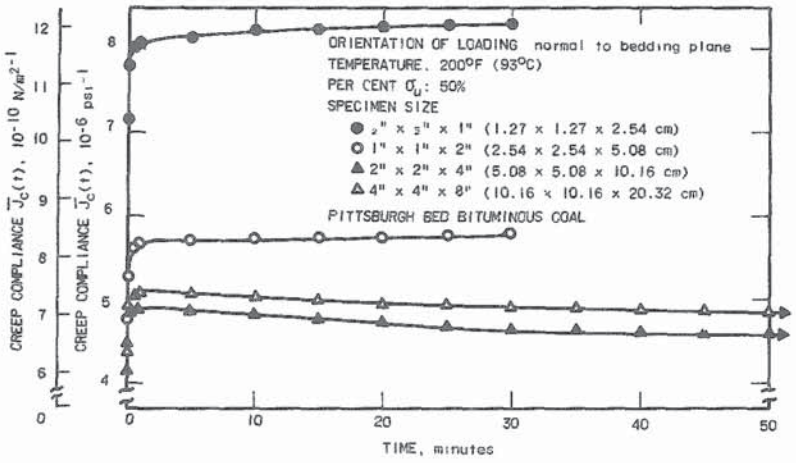


Figure 14. Creep Compliance-Time Curves Showing the Effect of Specimen Size at 200°F (93°C) on the Pittsburgh Coal When Loaded in Uniaxial Compression.

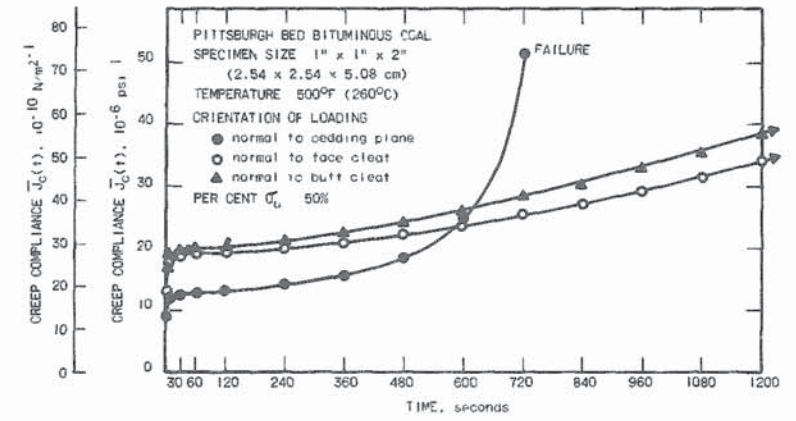


Figure 16. Creep Compliance-Time Curves Showing the Effect of the Orientation of Loading in Uniaxial Compression at 500°F (260°C) on the Pittsburgh Coal.



Figure 15. A Characteristic Creep Specimen Showing the Effect of Temperature (650°F (343°C)) on a Pittsburgh Coal Specimen (1" x 1" x 2" (2.54 x 2.54 x 5.08 cm)) When Loaded in Uniaxial Compression. The Specimen was Compressed to a Height of Approximately 1/2-inch (1.27 cm) at the Termination of the Test.

The effect of temperature on the creep compliance is represented in Figure 17 where the curves are similar for the temperatures 75°-350°F (24°-177°C) as observed for the stress-strain experiments. Figure 18 represents typical shear specimens following a creep experiment at 575°F (302°C) for shear in the bedding planes (τ_{yz}).

Time-Temperature Superposition of Coal--The time-temperature superposition principle implies that the variation of the creep function (or stress-relaxation function) with temperature is similar to the variation of the same functions with time. Figure 19 demonstrates that the Pittsburgh coal lends itself to the time-temperature superposition principle.

Viscoelastic Modeling of Coal--The behavior of viscoelastic materials can be represented by various models composed of springs and dashpots. Figure 20 demonstrates that the four-parameter fluid (Figure 21) can describe the Pittsburgh coal viscoelastic behavior at 575°F (302°C). However, this model does not reflect the primary creep of the Pittsburgh coal (Figures 22 and 23) as well at the lower temperatures, 75°-350°F (24°-177°C). These results were the same whether the constant stress was 25, 50, or 75 percent of the ultimate stress.

The primary creep of Figure 22 can be represented more fully by the addition of more spring-dashpot units as in Figure 24. Figure 25 demonstrates the viscoelastic modeling of the Pittsburgh coal by a six-parameter fluid. However, with increased parameters, the solution loses its uniqueness, and the values obtained for the individual parameters lose their significance.

DISCUSSION OF RESULTS

The tests conducted on the Pittsburgh coal are conventional ones used for determining the properties identified for elastic or viscoelastic isotropic, homogeneous materials. The stress-strain curves for coal represent a large variety of linear and nonlinear rheological properties including plasticity and creep, depending upon temperature. In reality, the Pittsburgh coal behaves as a plastic, elastic-plastic viscoelastic material under different conditions and none of the existing elastic-plastic or other known plastic theories are suitable for describing all the stress-strain-time characteristics. Similar phenomena was described by Brewer [20].

Theory does not support the phenomenon observed in coal that its strength increases with temperature before a final decrease to very small values (Figures 6, 9, and 11). However, Macrae and Mitchell [18] observed this characteristic in British coals. They postulated that the increased strength at approximately 212°-248°F (100°-120°C) was due to the weaker secondary forces of the van der Waals-type between structural units being affected and that heating affects the mode of fracture from tension at ordinary temperatures to shear at temperatures above 212°F (100°C). These results were generally validated in this investigation.

The shearing strengths from the shear tests were, in general, independent of the orientation of loading (varied less than 200 psi (0.138×10^7 N/m^2) over the temperature range, Figure 11). Hence, an assumption that $G_{yz}=G_{zy}$, and similarly for the other pairs, throughout the temperature range is representative of the shearing properties of the Pittsburgh coal (an average difference of 15 percent). However, the average difference of G_{yz}, G_{zy}, and G_{xz}, G_{zx} at 575°F (302°C) approached 45 percent.

The results for loadings normal to the face and butt cleats in uniaxial compression are also similar, but different from loadings normal to the bedding

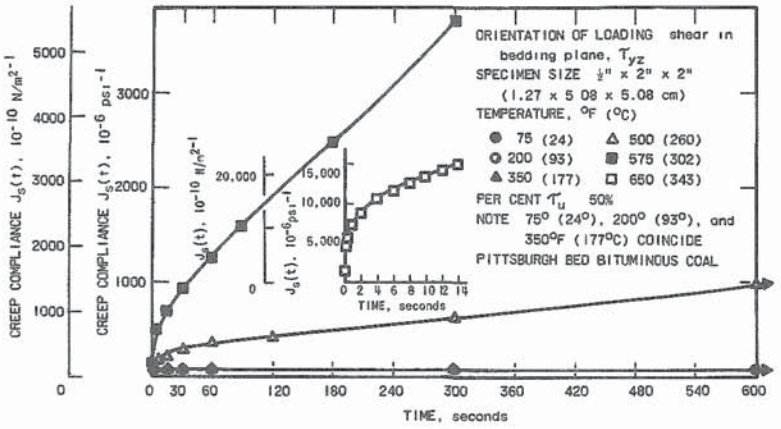


Figure 17. Creep Compliance-Time Curves Showing the Effect of Temperature (75°-650°F (24°-343°C)) on the Pittsburgh Coal When the Specimens are Loaded in Shear.

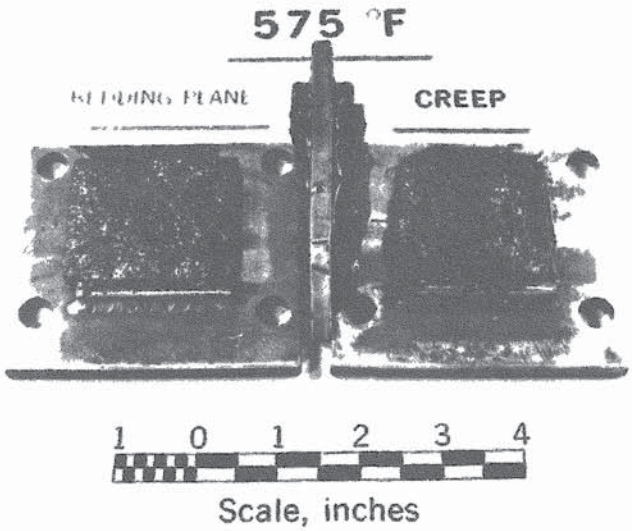


Figure 18. A Typical Creep Experiment Coal Specimen After Shear Deformation in the Bedding Planes (τ_{yz}) at 575°F (302°C).

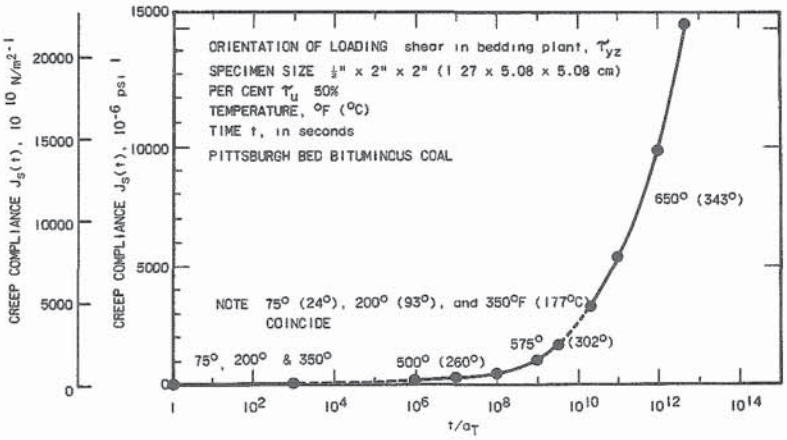


Figure 19. Time-Temperature Superposition Showing the Time Shift for the Pittsburgh Coal When Loaded in Shear.

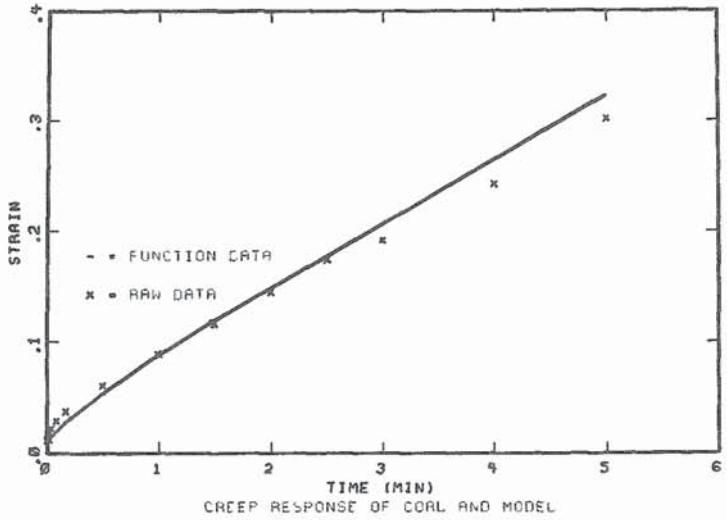


Figure 20. Viscoelastic Modeling of the Pittsburgh Coal at 575°F (302°C) Represented by the Four-Parameter Fluid. The Creep Curve is for the 1" x 1" x 2" (2.54 x 2.54 x 5.08 cm) Specimen, Loaded Normal to the Bedding Planes in Uniaxial Compression, the Percent σ_u was 50%, and the Initial Stress was 200 psi (0.137×10^7 N/m^2).

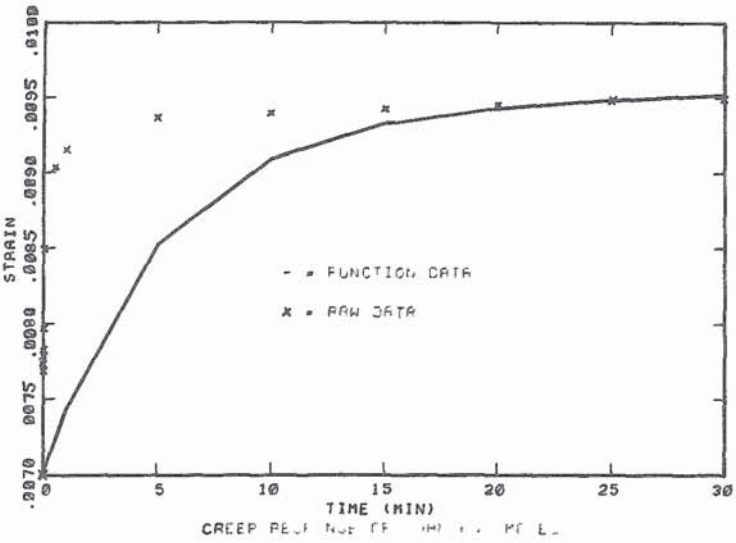


Figure 22. Viscoelastic Modeling of the Pittsburgh Coal at 75°F (24°C) Represented by the Four-Parameter Fluid. The Creep Curve is for the ½" x ½" x 1" (1.27 x 1.27 x 2.54 cm) Specimen, Loaded Normal to the Bedding Planes in Uniaxial Compression, the Percent σ_u was 50%, and the Initial Stress was 1,272 psi (0.877×10^7 N/m^2).

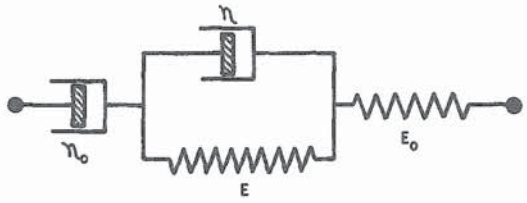


Figure 21. Burgers Model Illustrating the Behavior of Viscoelastic Materials [8,19,23,24].

planes (Figures 9, 10, and 16). This similarity indicates that at least along these two directions the Pittsburgh coal behaves as a transversely isotropic material as also observed [8, 17, 21, 22] for other coals. The Pittsburgh coal exhibits complex mechanical behavior and this apparent transversely isotropic behavior is somewhat surprising due to the obvious planes of symmetry of the face and butt cleats. Perhaps it would be more prudent to refer to some of these data as "structural responses" instead of the idealized material properties although this violation is routine in studying materials of complicated structure.

The reduced deformation in the face and butt cleat directions at elevated temperatures as compared to loadings normal to the bedding planes (Figures 9, 10, and 16) is apparently due to increased resistance to deformation in the face and butt cleat directions caused by the inter-layering of the organic and inorganic materials when the loading is parallel to the bedding planes. That is, the inorganic material has not softened at temperatures near 575°F (302°C); hence, restricting deformation (Figures 10 and 16).

The viscoelastic properties of the coal also represent a large variety of linear and nonlinear rheological properties. The Pittsburgh coal is viscoelastically nonlinear at the lower temperatures, 75°-500°F (24°-260°C), as evidenced by the S-shape of the stress-strain curves. However, at 575°-650°F (302°-343°C) the coal becomes nearly linear viscoelastically (Figure 13). This viscoelastic behavior would be expected as the coal begins to soften and coalesce at temperatures above 500°F (260°C) and since the stress-strain curves become more linear at low loading rates (see Figure 8). Another viscoelastic property demonstrates that the Pittsburgh coal can be represented by the time-temperature superposition principle (Figure 19). Similar observations have been reported on Japanese coals [12].

These data reflect qualitative and quantitative behavior of the Pittsburgh coal under many conditions, elastically and viscoelastically, essential to analyzing in situ coal processes such as gasification. This study has supplied realistic and comprehensive data for computer models [5, 6] to structurally model in situ processes, such as, overburden relaxation into the gasification zone and

the environmental impact of subsidence. These data also become useful in understanding the basic mechanisms involved in mass and energy transport and mechanical-structural effects in gasification processes. For example, decreased permeability shortly after initiation of a burn in modeling coal gasification processes in the laboratory with the Pittsburgh coal is readily understood to be due to the swelling and effervescent nature (bubbling of tars into the fissures) of the Pittsburgh coal at elevated temperatures. The tars, along with the swelling of the Pittsburgh coal, tend to restrict the outward movement (reduce permeability) of the burning front around a bore-hole as well as inhibit a forward burn along the bore-hole. However, the swelling, effervescent and coalescent nature of the Pittsburgh coal may also be an asset in the control of channeling or short-circuiting in the gasification process in that the fluidic coal will be forced into these channels by the pressure of the overburden and the swelling of the coal.

The data at normal temperatures should also be useful in studying methodology of coal extraction through conventional mining methods.

CONCLUSIONS

1. Temperature has a significant effect upon the mechanical and viscoelastic properties of the Pittsburgh coal in the range of 575°-650°F (302°-343°C).
2. The ultimate strengths (σ_u, τ_u) of the Pittsburgh coal are greatest at 200°F (93°C).
3. The ultimate strain in the stress-strain experiments for the Pittsburgh coal is relatively constant for temperatures through 500°F (260°C), becoming finite for 575°-650°F (302°-343°C).
4. The effect of orientation is such that the ultimate strength of the Pittsburgh coal, when loaded normal to the bedding planes, is approximately twice that for loading normal to the face and butt cleats, for the temperature range of 75°-650°F (24°-343°C).
5. The effect of orientation on the ultimate strain results in approximately four times the deformation, when loaded normal to the bedding planes as for loadings normal to the face and butt cleats at 575°-650°F (302°-343°C) and is perhaps due to the restrictive nature of inter-layering of organic and inorganic materials.

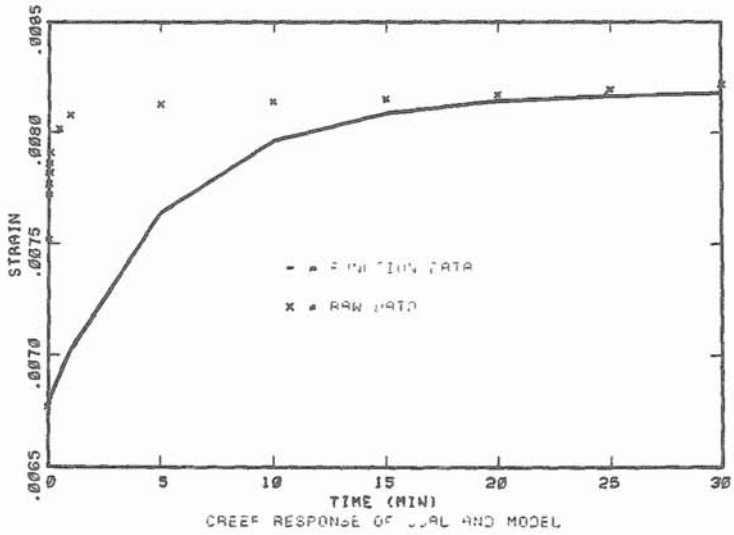


Figure 23. Viscoelastic Modeling of the Pittsburgh Coal at 200°F (93°C) Represented by the Four-Parameter Fluid. The Creep Curve is for the 1" x 1" x 2" (2.54 x 2.54 x 5.08 cm) Specimen, Loaded Normal to the Bedding Planes in Uniaxial Compression, the Percent σ_u was 50%, and the Initial Stress was 1,423 psi (0.981×10^7 N/m^2).

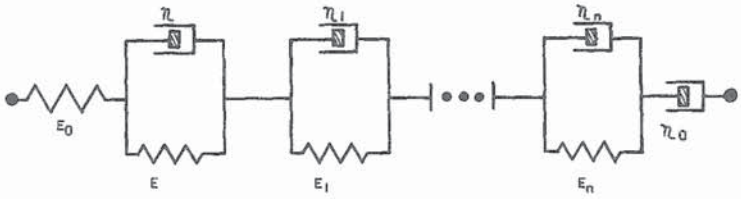


Figure 24. Generalized Kelvin Model Representation.

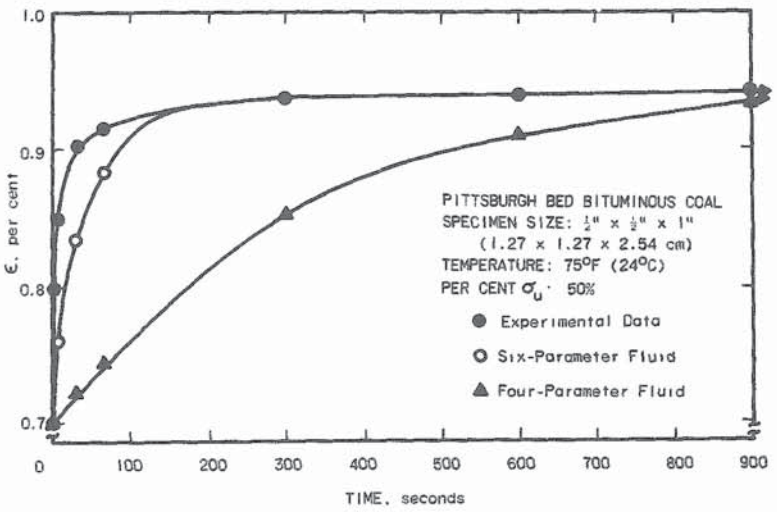


Figure 25. Viscoelastic Modeling of the Pittsburgh Coal When Loaded in Uniaxial Compression at 75°F (24°C) Represented by the Six-Parameter Fluid.

6. From the stress-strain, stress-relaxation, and creep experiments, the results for the face and butt cleats were similar regardless of temperature; hence, the Pittsburgh coal behaves somewhat as a complex transversely isotropic medium.
7. The Pittsburgh coal is nonlinear elastically due to the S-shape of the stress-strain curves, both in uniaxial compression and in shear.
8. The Pittsburgh coal responds as a nonlinear viscoelastic material at the lower temperatures, but becomes nearly linear at the softening stage of 575°F (302°C).
9. The Pittsburgh coal swells when subjected to a constant load or constant deformation in the temperature range of 100°-500°F (38°-260°C) after an initial contraction.
10. The Pittsburgh coal obeys the viscoelastic time-temperature superposition principle and can be modeled reasonably well with the four-parameter fluid from 75°-650°F (24°-343°C).

BIBLIOGRAPHY

1. Skafa, P. V. Underground Gasification of Coal. Translated from Gosudarstvennoe Hauchno-Teknicheskoe Izdatel'stov Literatury Po Gornomu Delu, Moscow (1960), UCLR Translation No. 10880, 324 pp.
2. Shuck, L. Z., and J. Pasini III. A Report on Progress in Underground Coal Gasification. Presented at the International Energy Engineering Congress, Chicago, Illinois, Nov. 5, 1975, 21 pp.
3. Little, A. D. A Current Appraisal of Underground Coal Gasification. Report to the U.S. Bureau of Mines, Report OCR-11-72 (Arthur D. Little, New York, December 1971), Report ADL-C-7367-1.
4. Shuck, L. Z., G. E. Fasching, J. W. Martin, and L. A. Bissett. In Situ Hydrocarbon Recovery Simulation Research at Morgantown Energy Research Center. ERDA (to be published).
5. Advani, S. H., and Y. T. Lin. Structural Mechanics Simulations Associated with Underground Coal Gasification. Final Report ERDA Grant No. G0155033, MERC/76-FCR-1, May 1976, 85 pp.
6. Sawyer, W. K., and L. Z. Shuck. Numerical Simulation of Mass and Energy Transfer in the Longwall Process of Underground Gasification of Coal. Presented at 4th Society of Petroleum Engineers of AIME Symposium on Numerical Simulation of Reservoir Performance, SPE Paper No. 5743, February 20, 1976, pp. 355-370.
7. Evans, I., and C. D. Pomeroy. The Compressive Strength of Rectangular Blocks of Coal. National Coal Board (England), Report 2077, October 1957, 15 pp.
8. Evans, I., and C. D. Pomeroy. The Strength, Fracture, and Workability of Coal. Pergamon Press, New York, 1966, 277 pp.
9. Rad, P. F. Mechanical Properties and Cutting Characteristics of Coal. Bureau of Mines Information Circular 8584, 1973, 46 pp.
10. Hobbs, D. W. Strength and Stress-Strain Characteristics of Coal in Triaxial Compression. J. Geol., v. 72, March 1964, pp. 214-231.
11. Pomeroy, C. D., and D. W. Hobbs. Fracture of Coal Specimens Subjected to Complex Stresses. Steel and Coal, v. 185, December 1962, pp. 1124-1133.
12. Ko, Hon-Yim, and K. H. Gerstle. Elastic Properties of Two Coals. International Journal of Rock Mechanics, Mineral Science, and Geomechanics, v. 13, 1976, pp. 81-90.
13. Bieniawski, Z. T. Effect of Specimen Size on Compressive Strength of Coal. International Journal of Rock Mechanics and Mineral Science, v. 5, July 1968, pp. 325-335.
14. Evans, I., C. D. Pomeroy, and R. Berenbaum. Compressive Strength of Coal. Coal, Eng., v. 38, 1961, pp. 75-87.
15. Gaddy, F. L. Study of Ultimate Strength of Coal as Related to Absolute Size of Cubinal Specimens Tested. Va. Polytechnical Inst., Eng. Expr. Sta., Ser. 112, August 1956, 27 pp.
16. Morgans, W. T. A. The Elastic Properties of Coal, III Static Compression Tests. National Coal Board (England) Report 2072, August 1957, 25 pp.
17. Morgans, W. T. A., and N. B. Terry. Measurement of Static and Dynamic Elastic Moduli of Coal. Fuel, v. 37, April 1958, pp. 201-219.
18. Macrae, J. C., and A. R. Mitchell. The Response of Bright Bituminous Coal to Undirectional Compression. Fuel, v. 36, October 1957, pp. 423-441.
19. Brewer, R. E. Plastic and Swelling Properties of Bituminous Coking Coals. Bureau of Mines Bulletin 445, 1942, 260 pp.
20. Sanda, Y., and H. Honda. Creep in Coal Over the Temperature Range 200 to 370°C. Fuel, v. 42, 1963, pp. 479-486.
21. Fitzgerald, D. Rheological Properties of Coal During Carbonization. Nature, v. 175, 1955, pp. 515-516.
22. Fitzgerald, D. Viscoelastic Properties of Coal During Carbonization. Fuel, v. 36, 1957, pp. 389-394.
23. Hearmon, P. F. S. The Elastic Constants of Anisotropic Materials. Rev. Modern Physics, v. 18, 1946, p. 409.
24. Schuyer, J., H. Dijkstra, and D. W. van Krevelen. Chemical Structure and Properties of Coal, VII—Elastic Constants. Fuel, (London), v. 33, 1954, pp. 409-419.

SOME OBSERVATIONS FROM TEMPERATURE MEASUREMENTS ON RECENT UNDERGROUND COAL GASIFICATION EXPERIMENTS

by

S. G. BEARD and R. P. REED
Sandia Laboratories
Albuquerque, New Mexico 87115

ABSTRACT

Recent underground coal gasification experiments at the Laramie Energy Research Center (LERC) field site at Hanna, Wyoming have been monitored with an array of subsurface thermocouples located in and near the coal seam. These temperature measurements are providing a quantitative basis for a specific understanding of thermal, chemical, and mechanical aspects of the underground gasification process. The subsurface measurements complement surface observations of process variables and allow direct deductions not available from surface measurements alone. This paper presents a description of the thermometry system, an example of data validation using diagnostic information provided by branched thermocouple circuits, and complete temperature histories from four instrument wells during the linkage, gasification, and cooldown stages of the Hanna II, Phase 1 experiment.

INTRODUCTION

The Hanna II Underground Coal Gasification Experiment has been in progress at the Laramie Energy Research Center (LERC) field site near Hanna, Wyoming since 1975 [1,2,3,4]. Low sulfur subbituminous coal from the Hanna Number 1 seam is being utilized in the test. The 30-foot thick seam lies 270 ft beneath the surface at the test site. The principal objectives of the experiment are to improve definition of significant parameters and to improve operational procedures and process control techniques toward optimized in situ gasification of coal. The experiment has been conducted in several phases. Phase 1, which involved four process wells, was a preliminary experiment to determine the directional variation of natural resistance to gas flow through the coal seam, to compare the effectiveness of pneumatic and thermal methods of improving flow communication (linking) between wells, and to conduct a short term gasification demonstration. Phase 2, isolated from the previous test, employed two process wells to confirm and refine the techniques of Phase 1 and to prepare the reaction bed for the following experimental phase. Phase 3 added two wells to form a square pattern bounding a region over which the coal was to be gasified.

In conjunction with this field experiment, Sandia Laboratories conducted an instrumentation and process control development program. Objectives were to develop and evaluate local and remote instrumentation techniques and to obtain diagnostic information on the gasification process. This paper addresses some details of the temperature measurements of Phase 1 of the Hanna II experiment.

Phase 1 of the Hanna II experiment extended from January through August, 1975. Sandia Laboratories fielded acoustic and electrical resistivity instrumentation arrays as part of the program to develop remote sensing techniques. An array of subsurface thermocouples was also fielded to obtain in situ data necessary not only for process definition and control but also for interpretation of the remote monitoring measurements provided by the resistivity and acoustic techniques.

References at end of paper

The history of temperature distribution through and above the coal seam over the duration of the experiment was the basic indicator to define actual subsurface events during retorting. Temperature measurements allowed the obvious direct measures: burn front location, speed of advance, and extent during both linking and gasification phases of the burn. However, detailed temperature profiles also allowed deduction of a number of other diverse features of the process including thermal, chemical, and mechanical behavior of material adjacent to the reacting region and thermal decay during the passive cooldown period. As the instrumentation experiments of Phase 1 were developmental and preliminary to more detailed studies to be conducted, the array of sensing points was not extensive. This information allowed a confirmation of the surface observations of subsurface events provided by coordinated resistivity, acoustic, and other techniques.

This paper presents a description of the thermometry system, an example of data validation using diagnostic information, and the complete temperature histories from four wells during the linkage, gasification, and cooldown phases of the experiment. The emphasis of the paper is on the specific time resolved information not available from surface measurements of process variables and on the less obvious benefits of in situ thermometry in underground coal gasification research.

TEMPERATURE INSTRUMENTATION

The Phase 1 process well and instrument well patterns are shown in Figure 1. Wells 1, 2, 3 and 4 were cased injection and production wells which were perforated over the lower third of the seam to localize the injected air flow linking path to the lower portion of the seam. The thermocouple assemblies and other subsurface instruments were installed in instrument wells AA, BB, CC, and DD. These 8-inch (20-cm) diameter instrument wells were drilled to the coal seam floor and were cased only at the surface. The steel surface casing of one well served as the common grounding point for all measurement systems. From the bottom of each well to slightly above the coal seam, the sensors were thermally coupled to the surrounding medium with a special coal-filled grout. The remainder of each well was filled with a conventional expansive pozzolan cement grout.

The locations of the thermal sensors in the overburden and coal seam are presented in Table I. All of the thermocouples installed in Phase 1 were of ANSI Type K (Chromel-Alumel) material. The elements were of 24 AWG wire insulated with MgO and sheathed with 1/8 inch (0.32 cm) o.d. Inconel-600. This material pair has a Relative Seebeck Coefficient of 21.4 μV/°F (38.5 μV/°C) at 32°F (0°C). It conforms to standard Type K characteristics within 4°F (2.2°C) from 32°F (0°C) to 535°F (277°C) and within 3/4 percent up to 2300°F (1260°C) for short-term heating under favorable conditions [5]. While the elements do not melt at temperatures up to 2550°F (1400°C), the combination is recommended for prolonged use in protected environments at temperatures up to only 1600°F (870°C) in this wire size.

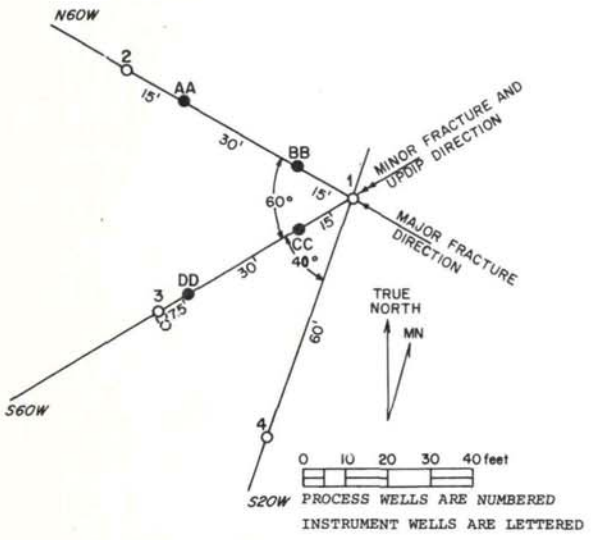


Fig. 1. Well Pattern for Phase 1 of the Hanna II Experiment.

For economy, a transition was made from metal sheathed thermoelements to a 12-pair direct-burial compensating extension cable in a sealed and potted junction canister. The splice was made about 50 ft (15 m) above the coal seam. Another splice was made at the surface, in a junction box, to an extension cable that led to the recording facility.

Conventional individual thermocouple circuits were installed in Wells AA and DD, and circuits of both conventional and branched form [6] were employed in Wells BB and CC. Branched thermocouple circuits are formed by interconnecting individual thermoelements. The theory of branched thermocouple circuits is developed elsewhere [6]. These unconventional circuits provide redundant measurement of temperature through alternate circuit paths and allow direct sensing of temperature differentials. They uniquely permit the direct diagnostic measurement of spurious nonthermoelectric emf and loop resistance. Branched thermocouple circuits can be used to improve data return and to allow the validation of temperature data. During Phase 1 usually not all of the available redundant and

Table I

Vertical Placement of Temperature Sensing Points Relative to Local Floor of Coal Seam (All Dimensions in Feet)

Nominal Level		Well AA	Well BB	Well CC	Well DD
80		79.8	80.1	79.0	80.3
45	Shale	44.9	45.0	44.9	44.9
35	Shale	34.9	35.0	34.9	35.0
30	Coal Seam	30.0	30.0	30.0	30.0
27.5	Coal Seam		27.5		
25	Coal Seam	24.9	25.0	25.0	25.1
22.5	Coal Seam		22.4		
20	Coal Seam	20.0	20.2	20.0	20.1
17.5	Coal Seam		18.0		
15	Coal Seam	15.0	15.0	15.0	15.0
12.5	Coal Seam				
10	Coal Seam				
7.5	Coal Seam				
5	Coal Seam		5.0	5.0	
2.5	Coal Seam				
0	Coal Seam				

diagnostic quantities were monitored continually. Many were manually sampled or recorded only during periods where noise was suspected.

Signals were recorded on microprocessor-based data acquisition systems (DAS) located in a mobile instrumentation trailer. Data were sampled at intervals up to four times per hour continually for the duration of the experiment. Temperatures were easily recorded in Fahrenheit units with 0.1°F (0.05°C) resolution with insignificant noise contamination so that small temperature increases could be observed. The high resolution is not costly and it allowed unique and important observations to be made during small temperature excursions. Although commercial tolerances on the thermocouples guarantee no greater than 4°F (2.2°C) accuracy, agreement between sensors during quiescent periods was within 0.5°F (0.28°C).

Data output was available in several forms. Front-panel digital displays, printed paper tape, and a telephone link to off-site experimenters provided prompt sampled data. These data were immediately available to all experimenters for open-loop process control. This prompt data also allowed daily evaluation of operations and experiment trends so that modifications of measurement procedures could be promptly effected. Reel-to-reel magnetic tape recordings provided the detailed data base for automatic data processing and in-depth analysis.

DATA VALIDATION USING DIAGNOSTICS FROM BRANCHED THERMOCOUPLES

Temperature data from in situ experiments commonly include intervals over which the signal is erratic and is suspected of being incorrect. Conversely, significant, but inobvious, errors often exist in apparently valid data. New diagnostic techniques especially developed for in situ studies were employed to validate some of the data from the Hanna II experiments. Details of the techniques and varied examples of its application have been reported elsewhere [6]. A simple example of an actual instance of subtle error and its detection by direct recording of noise emf and of redundant measures of temperature is given in Figure 2. This temperature record shows the passage of a gasification reaction front observed five feet from the seam floor in Well CC. Temperature at this location was sensed by a tip-branched thermocouple as shown in the figure.

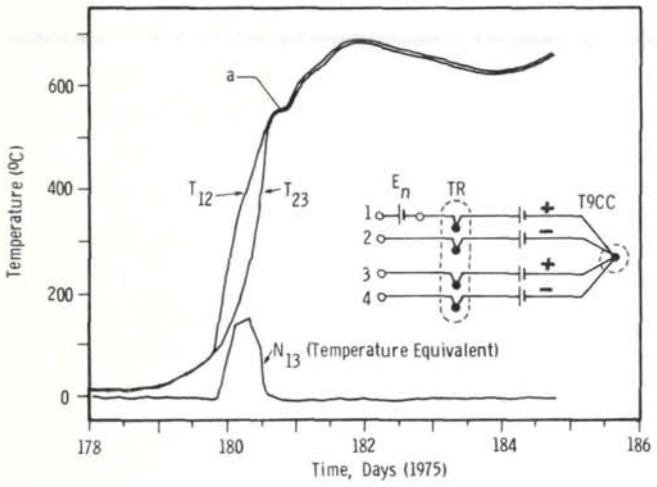


Fig. 2. Noise emf as a Diagnostic

Four redundant measures of temperature and two different measures of emf were available from this circuit [6]. Only two of the temperature measures, T_{12} and T_{32}, and one noise emf, N_{13}, were recorded over this particular time interval. The two temperature indications agreed within 0.2°F (0.1°C) until noon on Day 178. Then the temperature records diverged. The records merged again after one day and continued to agree within 5°F (3°C) at high temperature. The maximum discrepancy between the two records was 235°F (130°C). This difference was substantial -- over 40 percent of the average of the two indications.

D. C. noise emf measured over the same period was as great as 6232 μV. Converted to temperature equivalent, the peak noise was about 229°F (127°C), essentially the same as the discrepancy between temperature records. Throughout the 8-day period, the temperature-equivalent noise was within 0.2°F (0.1°C) of the difference between temperatures except around the time of peak noise.

In the example, even though the error was substantial it could not have been detected directly from either separate temperature record. Its location on the rise of the profile also made the error inobvious. In this instance, the large error did not seriously affect many uses of the data. However, considering the shape and magnitude of the noise pulse, it is obvious that, had the noise peak occurred eight hours earlier or thirty-six hours later, the qualitative effect or peak error would have been a serious handicap to accurate interpretation.

On the basis of the diagnostic measures, there is reason to reject data over the time interval of the noise; however, validation allows the conclusion that the peak amplitude and the profile feature, a, immediately following the noise episode are representative of the actual temperature experienced by the thermocouple in the reaction zone vicinity.

EXPERIMENTAL RESULTS

Phase 1 of the Hanna II experiment was conducted in the following sequence: (1) air injection tests to determine the directional variation of permeability of the coal seam, (2) Phase 1a: ignition, reverse combustion linkage, and forward gasification between Wells 1 and 3, (3) Phase 1b: reverse combustion linkage and forward gasification between Wells 1 and 2, and (4) cooldown of the reaction zone following termination of air injection. A summary of the Phase 1 activities is presented in Table II.

Directional Permeability and Pneumatic Linking Experiments

Directional permeability and pneumatic linking experiments were conducted from Day 97 to Day 139. Air was injected into Well 1 from Day 97 to Day 106; then injection was terminated in order to reduce pressure at Well CC where a small leak was noted. During this period the injection pressure was high, ~ 250 psig (1.724 MPa), and the total production flow rate from Wells 2, 3, and 4 was low, < 50 scfm (1.4 m^3/min). The direction of greatest flow was toward Well 3. From Day 107 to Day 139 air was injected into Well 3 in an attempt to pneumatically decrease flow resistance between Wells 1 and 3. A small increase of injectivity was noted but adequate flow linking between wells was not achieved. The injection pressure remained high, and the maximum output flow rates remained low at approximately 100 scfm. During this period the maximum flow rate was from Well 3 to Well 1 with lesser flow to Well 2 [4].

Table II

Summary of Hanna II, Phase 1 Activities

Day (1975)	Activity	Date (1975)
97	Air injection initiated at Well 1. Output at Wells 2, 3, and 4.	April 7
107	Air injection changed to Well 3. Output at Wells 1, 2, and 4.	April 17
139	Air injection linking experiment terminated.	May 19
141	Phase 1a initiated. Heater started in Well 1.	May 21
145	Heater removed. Air injection switched to Well 3 with production at Well 1.	May 25
155	Phase 1a reverse combustion linkage completed and forward gasification started.	June 4
192	Phase 1a terminated. Phase 1b initiated. Air injection changed to Well 2. Production remained at Well 1.	July 11
203	Phase 1b reverse combustion linkage completed and forward gasification started.	July 22
240	Phase 1b terminated. Air injection halted.	August 28

During the air injection phase preceding ignition, temperature elevations which were only a few degrees greater than the background values of 48-50°F (9-10°C) were observed. The history of these is presented in Figures 3 and 4. The small temperature elevations of up to 5°F (2.8°C) near midseam in all the wells were attributed to low temperature surface oxidation of coal by the injected air. The sensitive temperature measurement indicated the in situ air flow distribution. The temperature above the coal seam where there was no air flow did not change during this period. Even in Well CC where a small leak to the surface was experienced, the temperature 5 ft above the seam ceiling remained at 48°F (9°C).

When temperature changes in Wells AA, BB, and CC are compared, it is evident that the changes are more rapid, more prompt and of greater magnitude in Well CC (along the line of greater flow) than in Wells AA and BB.

During the pneumatic linking experiment the mean temperature of the outside ambient air was 40°F (4°C) and the diurnal variation at the surface was from 20°F (-7°C) to 61°F (16°C) [4]. Small diurnal variations ($< \pm 0.5$°F) ($\pm$ 0.3°C) in temperature indication were recorded on recording van temperatures as well as subsurface channels. No significant in situ temperature changes obviously related to the diurnal variation in injected air temperature have been observed. It is clear that the heating of the formation was from an exotherm rather than from mass transport of sensible heat from the injected air.

The preceding examples illustrate the practical usefulness of sensitive thermometry in providing a direct indication of flow distribution during the several stages of retort preparation.

Phase 1a

Phase 1a was initiated on Day 141 when heat was applied below coal midseam in Well 1. Although combustion was observed (by analysis of the product gas) within 12 hours, the electrical heating continuei to Day 145. During this period compressed air was injected into Well 1 and production gases were recovered from Well 3. Other wells were capped. On Day 145 the heater was removed, and the reverse combustion linking phase was begun when air injection was changed to Well 3 with production at Well 1. The period when the link was being established by burning was characterized by high pressures and low injection flow rates. This process continued until Day 155 when linking was achieved. When the link was established the injection pressure that could be maintained by the air compressors decreased to less than 50 psig (345 kPa), as the injection and production flow rates abruptly increased to ~ 900 scfm (25.5 m^3/min) and ~ 1700 scfm (48 m^3/min), respectively. During the relatively stable period of gasification which followed, production-to-injection flow ratios of ~ 1.75 and gas heating values greater than 150 Btu/scf (5.6 MJ/m^3) were observed. After Day 180 the values of these parameters began to decrease significantly and Phase 1a was terminated on Day 192 [4].

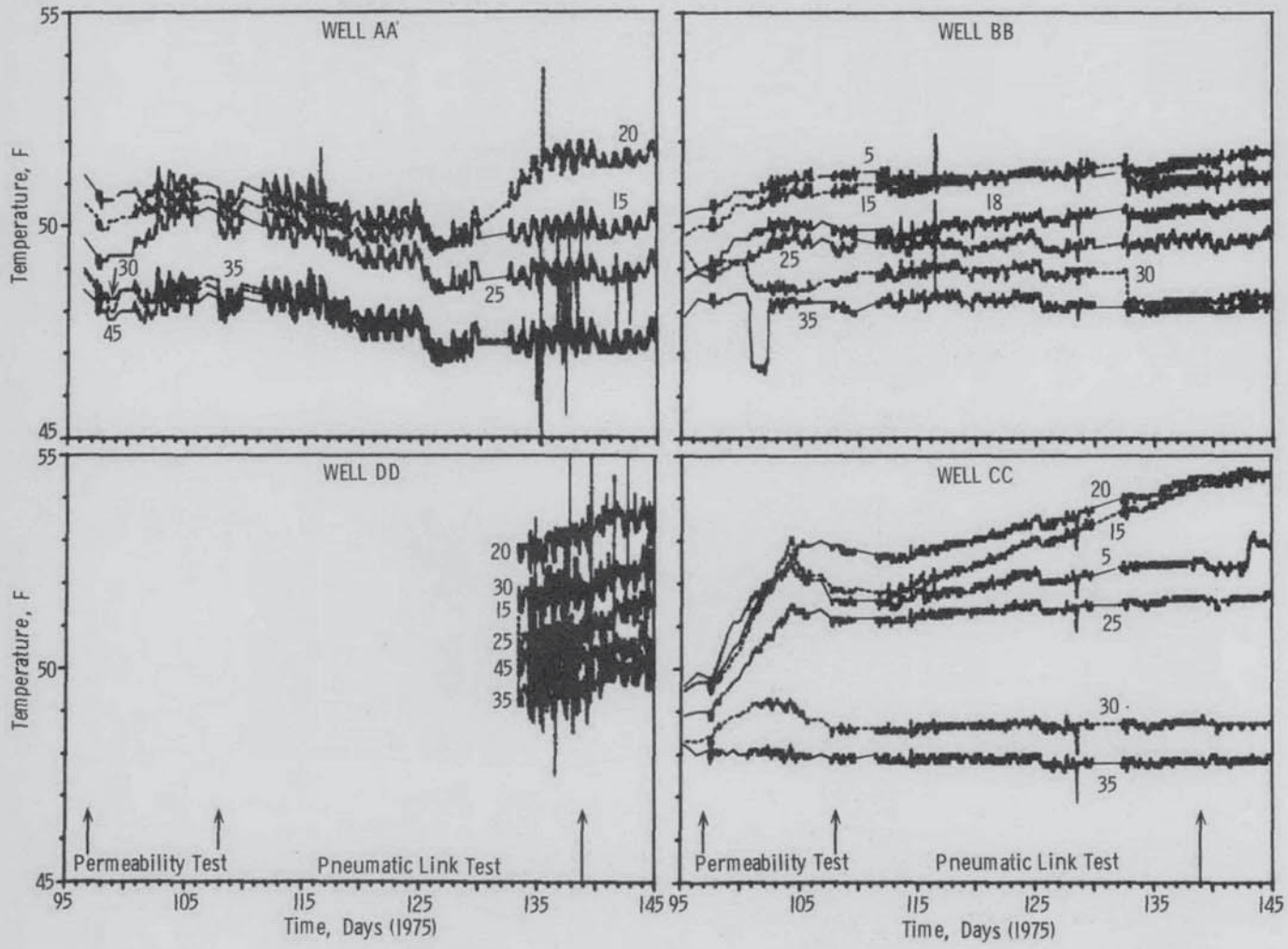


Fig. 3. Temperatures During Directional Permeability and Pneumatic Linkage Test (Thermocouple Levels (feet) Referenced to Bottom of Coal Seam)

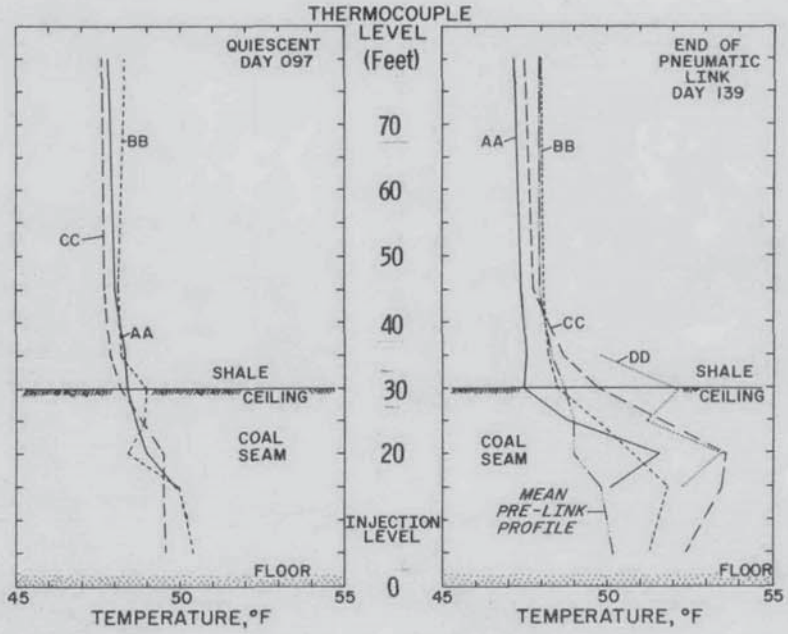


Fig. 4. Vertical Temperature Distribution Before and After Pneumatic Link Test

Temperatures measured in Wells CC and DD during Phase 1a link formation and gasification are presented in Figures 5 and 6. During the combustion linking period (Days 145-155), the only temperature change noted was an increase to approximately 200°F (93°C) at the midseam location in Well CC. No temperature increases were measured in Well DD, on the line between the same process wells, during this period. The immediate temperature elevation at only one isolated level in Well CC, the absence of any prompt increases in Well DD, and the subsequent rapid increases in Wells CC and DD shortly after the completion of linking indicated that the flow link was localized to a slender channel.

Soon after linking was completed, temperatures rose to approximately 1000°F (538°C) at two adjacent levels in Well DD and at midseam in Well CC. By Day 168 temperature increases to approximately 1000°F (538°C) from midseam to the seam top indicated widespread combustion in the vicinity of Well DD.

The initial erratic temperature variations in Well DD in the major reaction zone have been interpreted to indicate local collapse of coal and roof materials. The later indication of approximately the same temperature at several levels in Well DD suggests that the collapse and mixing of material in the reaction zone resulted in a temporary change to relatively uniform temperatures across the seam. (The uniform indication of the same temperature by more than one thermocouple in a well could also result from the failure of the thermocouples at a common level and the subsequent formation of new thermoelectric junctions at this location.) On Day 169 a large subsurface collapse was indicated simultaneously by the abrupt shaking of surface piping around Well 3 and the very rapid increase in temperature at several levels in Well DD. In Well CC the rapid temperature rise at the 20-ft level in Well CC on Day 169 and the subsequent decrease at this level suggests that temporary communication was established between this level and the reaction zone through fissures affected by the collapse.

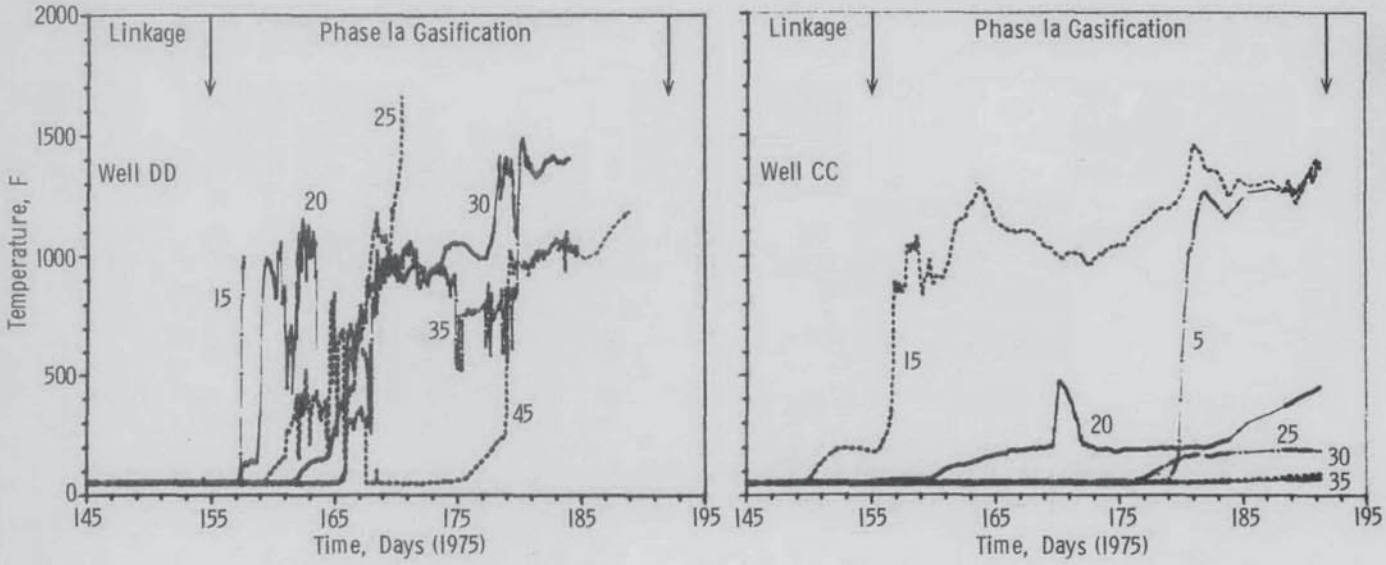


Fig. 5. Temperatures in Wells DD and CC During Phase la (Thermocouple Locations (feet) Referenced to Bottom of 30-foot Coal Seam)

The elevated temperatures 5 ft (1.5 m) above the coal floor in Well CC following Day 179 and the absence of high temperatures in the upper part of the seam indicate that at this location combustion had moved into the lower half of the seam but not into the upper half by Day 192 when all the sensors in Well CC failed.

Several distinct and physically characteristic temperature levels of the in situ process appear in the thermal data. These are approximately 49°F, 200°F, 1000 to 1500°F (10°C, 95°C and 500 to 800°C), and a few values are greater than 1500°F (800°C). Throughout the experiment, the sensors may have been near but separated laterally from the actual reaction zone so that all the observed temperatures, even though accurate, do not necessarily indicate the temperatures of the gas. The frequently observed abrupt increases in temperature to ~ 200°F (100°C) and the subsequent maintenance of this temperature level for several days indicate that the energy at that location is being utilized in water evaporation and volatilization instead of temperature increases of the solid coal.

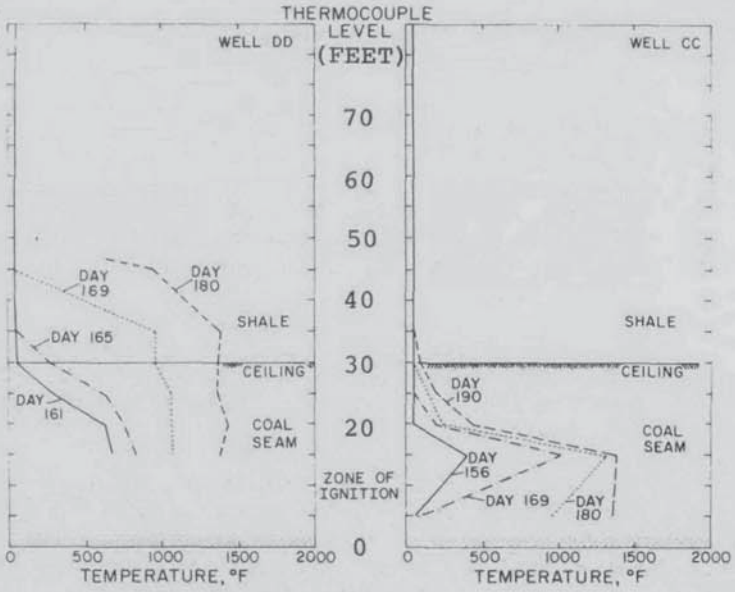


Fig. 6. Vertical Temperature Distributions During Gasification Test.

The temperature behavior observed in Well CC illustrates two modes of heat transfer seen throughout the experiment. The rates of temperature increase measured at the 20 and 25-ft (6.1 and 7.6-m) levels are similar to those computed with heat conduction theory [7]. The rapid rates of increase seen at the 5-ft (1.5-m) level in Well CC and at

many levels in Well DD are much greater than those associated with conduction alone and probably resulted from sudden exposure of the thermocouple to the hot gases by collapse or the movement of the reaction zone into a pre-existing system of fissures providing temporary direct communication between the thermocouple and reaction zone. The thermocouple responses in Well CC indicate that prior to Day 179 the vertical dimension of the reaction zone was 5 to 10 ft (1.5 to 3 m) and that it extended from approximately 15 ft (4.6 m) above the coal floor to a few feet above the 5-ft (1.5-m) level.

Phase 1b and Cooldown

Phase 1b was initiated on Day 192 when injection was shifted from Well 3 to Well 2. Wells 3 and 4 were capped. Reverse combustion linkage between Wells 1 and 2 was established on Day 203 with the characteristic increase in injection flow rates and the resulting decrease in injection pressure. Gasification conditions were maintained for 37 days, and Phase 1b was effectively terminated when air injection was halted on Day 240.

During Phase 1a (Day 141-192), the temperatures in Well AA remained at approximately 50°F (10°C) while in Well BB the temperatures increased from a range of 48-51°F to 50-57°F (9-10°C to 9-14°C). This latter rise is probably the result of thermal conduction from the combustion zone between Wells 1 and 3. The temperatures measured in Wells AA and BB during Phase 1b are presented in Figure 7. During the linkage and gasification stages of Phase 1b, the temperature profiles in Wells AA and BB showed that the linkage path was established near midseam in the second linking operation just as was observed in Phase 1a. The 110°F (43°C) maximum temperature in Well BB at the end of Phase 1b on Day 240 demonstrates that the linkage path from Well 2 to Well 1 did not lie along the direct line between these wells but passed from Well 2 to somewhere along the boundary of the zone affected in Phase 1a between Wells 1 and 3 and along this path to Well 1. The maximum temperature of 1100°F (593°C) in Well AA and the absence of rapid fluctuations attributed to subsidence suggest that the reaction zone was also located to the side of instrument Well AA.

Following the end of Phase 1b, the temperatures in Wells AA and BB were recorded occasionally and are presented in Figure 8. Temperatures were recorded automatically through Day 261 when regular recording was terminated to allow preparation of the system for Phases 2 and 3. During the initial cooling period a definite trend is evident within the seam. The temperature decrease for the 15-ft (4.6-m) level between Days 242 and 261 indicated that approximately 8 months would have been required for the temperature in the reaction zone to decrease exponentially from 1010 to 60°F (540°C to 15°C) by thermal diffusion. The temperatures in Well BB continued to increase slowly as a result of conduction and/or fluid convection from the hot reaction zone several feet from this well. The daily data fluctuations following Day 303 resulted from the measurement of thermocouple temperatures with less precise portable equipment during this period.

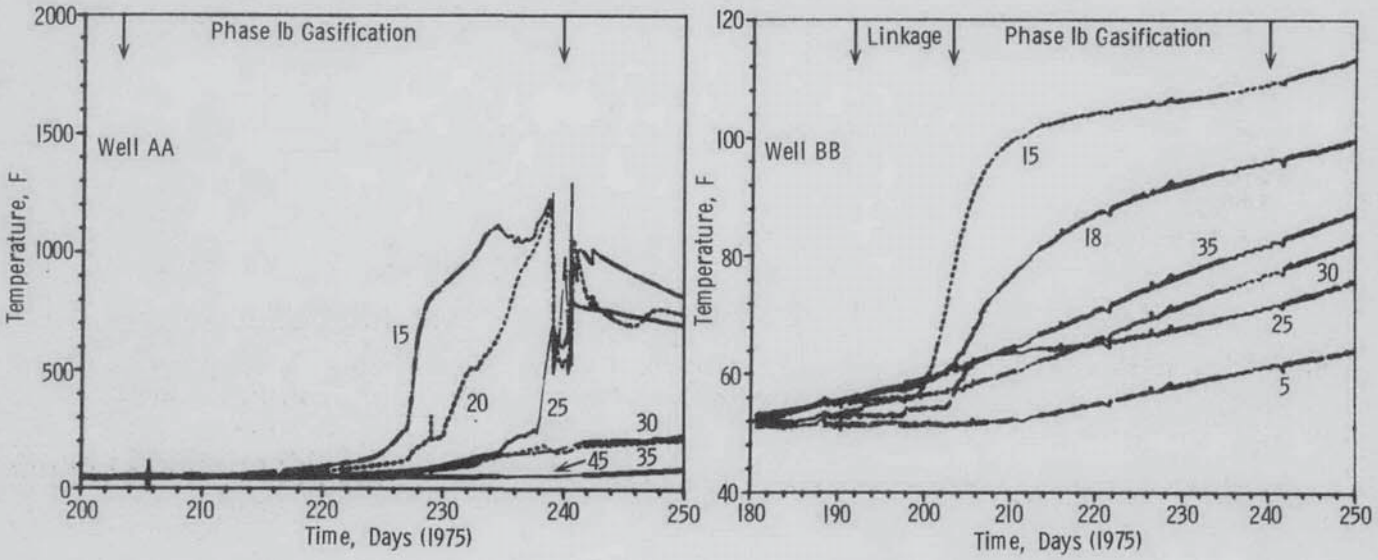


Fig. 7. Temperature Distributions in Wells AA and BB during Phase 1b (Thermocouple Locations (feet) Referenced to Bottom of 30-foot Coal Seam)

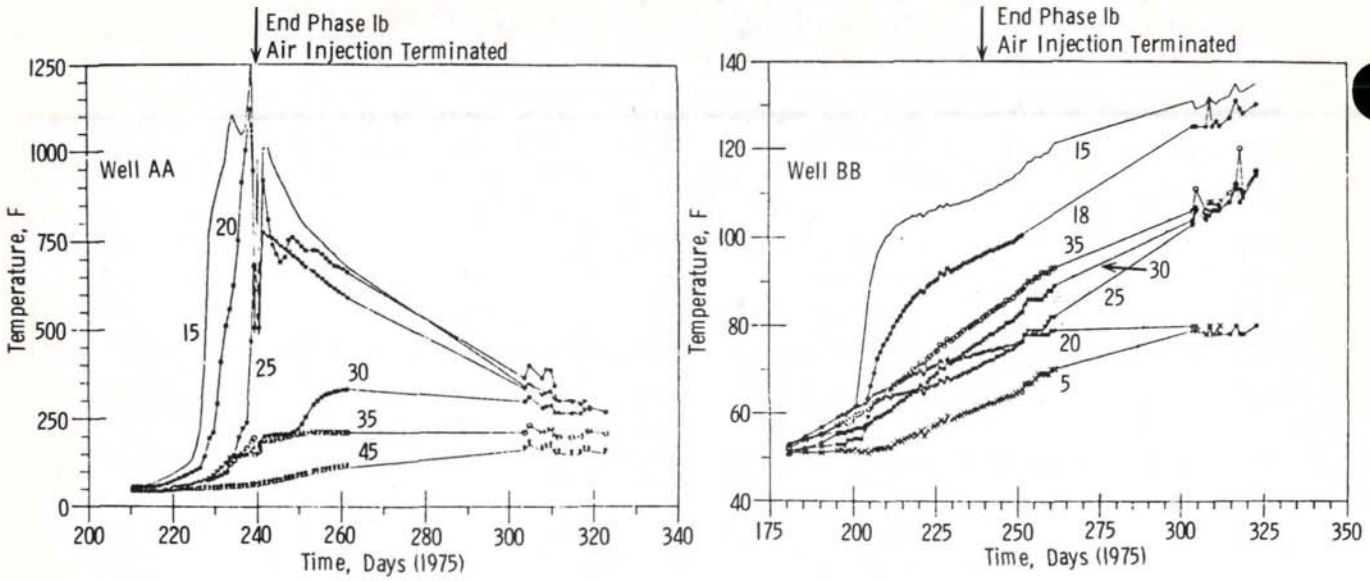


Fig. 8. Temperatures in Wells AA and BB During Phase 1b and Cooldown

Although the temperatures recorded for Well DD after Day 182 are indefinite, the indicated temperatures in this well have steadily decreased from 1400°F (760°C) at the end of Phase 1a (Day 192) to 225°F (107°C) on Day 322.

Phases 2 and 3 of the Hanna II Experiment

Preliminary thermal data for Phases 2 and 3 of the Hanna II experiment which were conducted during the spring and summer of 1976 will be presented in a joint LERC-Sandia Laboratories paper [2]. In these phases more extensive thermal sensor arrays were installed in 15 instrumentation wells. Although a more detailed description of the in situ process was obtained in Phases 2 and 3, preliminary examination indicates that the trends of temperatures and general thermal behavior in these phases were similar to those seen in Phase 1. Differences which exist reflect variations in particulars of operation of the two retort experiments.

CONCLUSIONS

The preliminary temperature measurements conducted during the Hanna II, Phase 1 experiments demonstrated the value of thermometry in depicting a variety of events in in situ gasification of coal. The thermocouple systems employed satisfactorily resolved detail of all stages of the gasification process from bed preparation through cooldown. Validation of data by special diagnostic techniques assured correctness of interpretation of much questionable data.

High temperature resolution thermometry proved useful in the early stages of reactor bed preparation allowing important direct observations of flow distribution. Some of the obvious details of the link forming process were observed, but spatial resolution was not sufficient on Phase 1 to fully resolve all important features of the linking process. Temperature structure revealing the mass transport of fluids in advance of the reaction zone and dimensions of the propagating reaction front have provided the basis for more detailed understanding of the subsurface process. Variations in subsurface temperatures and product chemical analysis in response to changes in the surface process variables (flow and pressure) were used in open-loop process control during the experiment and will allow a more specific insight into means of optimizing the gasification process. Maximum temperatures observed slightly exceeded the recommended maximum temperature (1600°F) for all common metal thermocouple materials and long term failures of many sensors was experienced. Although a few expensive refractory metal thermocouples are being employed to determine maximum temperatures in more recent experiments, most temperature features of operational significance appear to fall within the useful range of type K thermocouples.

The extensive thermometry arrays employed in the Hanna II experiment are essential to research and development studies exploring the specific processes in underground coal gasification. They have provided prompt and direct information allowing operational control of the process experiment. Thermometry of the extent used in these experiments is not expected to be used in routine commercial process control.

ACKNOWLEDGEMENT

The cooperation of L. A. Schrider, Dr. C. F. Brandenburg, and the many other members of the Laramie Energy Research Center staff in the Hanna experiment is appreciated. The Sandia personnel who fabricated and fielded the thermal sensors, operated and maintained the recording instruments, and reduced the data contributed greatly to this research.

This work was supported by the Division of Oil, Gas, and Shale Technology, United States Energy Research and Development Administration. Dr. Paul C. Wieber of that organization is manager of the in situ coal gasification program.

REFERENCES

1. Schrider, L. A. and Fischer, D. D., "In Situ Coal Gasification -- A Unique Means of Energy Recovery," Mech. Eng., 98, No. 3 (1976), 20-24.

2. Schrider, L. A., Brandenburg, C. F., Fischer, D. D., and Northrop, D. A., "Results and Status of the Second Hanna In Situ Coal Gasification Experiment," 2nd Annual Underground Coal Gasification Symposium, Morgantown, WV, August 10-12, 1976.

3. Stoller, H. M., Schrider, L. A., and Northrop, D. A., "The Status of Instrumentation and Process Control Techniques for In Situ Coal Gasification," 22nd International Instrumentation Symposium, San Diego, CA, May 25-27, 1976.

4. Brandenburg, C. F., Reed, R. P., Boyd, R. M., Northrop, D. A., and Jennings, J. W., "Interpretation of Chemical and Physical Measurements from an In Situ Coal Gasification Experiment," SPE 5654, 50th Annual Fall Meeting of the Society of Petroleum Engineers of AIME, Dallas, TX, September 28-October 1, 1975.

5. Powell, R. L., Hall, W. J., Hyink, C. H., Jr., Sparks, L. L., Burns, G. W., Scroger, M. G., and Plumb, H. H., "Thermocouple Reference Tables Based on the IPTS-68," NBS Monograph 125, U. S. Department of Commerce, March 1974.

6. Reed, R. P., "Branched Thermocouple Circuits in Underground Coal Gasification Experiments," Proceedings of the 22nd ISA International Instrumentation Symposium, San Diego, CA, May 25-27, 1976.

7. Northrop, D. A. (Editor), "Instrumentation and Process Control Development for In Situ Coal Gasification: Third Quarterly Report: June through August 1975," SAND75-0535, Sandia Laboratories, Albuquerque, NM, October 1975.

PRACTICAL CONSIDERATIONS IN DESIGNING AN UCG FIELD TEST

A. E. HUMPHREY,[1] T. E. STERNER,[1]
H. L. HUTCHINSON,[2] AND G. G. CAMPBELL[1]

ABSTRACT

Experience gained over the past four years in underground coal gasification by personnel at the Laramie Energy Research Center has shown the major areas of consideration for successful experiments are location and preparation of the test site, and operation of the test itself. Problems encountered during the selection, design and operation of the field test and some solutions to these problems will be discussed. In addition, the drilling, logging, dewatering and linkage techniques used at Hanna will be presented.

INTRODUCTION

Experience gained over the past four years in underground coal gasification (UCG) by personnel at the Laramie Energy Research Center has shown that the major considerations for successful experiments are location and preparation of the test site and operation of the test itself. From this experience a set of parameters have been defined for selecting, designing and operating a UCG test site.

The parameters to consider most carefully in site selection, when use of the linked vertical well technique is planned, are seam depth, seam thickness, overburden characteristics, seam water content, coal characteristics and dip.

Tests conducted by LERC have been in the Hanna I coal seam which is about 30 feet[3] thick and has about 7 degrees of dip at the test site [1].[4] These tests have been conducted at depths ranging from 400 to 275 feet below the surface [1,2,3]. From a technical aspect the depths in excess of 400 feet would appear to pose few additional problems but at present funding levels, concept testing at shallower depths is more economically attractive. Problems could arise if the test seam were in close proximity (less than 150 feet) to the surface. Communication with the surface might be established thereby causing leakage to the surface. Besides the obvious hazards of uncontrolled product gas release to the atmosphere, resource recovery would be reduced (less product gas per unit volume of air injected as well as less coal affected).

The overburden at the Hanna test site is a series of shales, siltstones and sandstones. With the presence of an aquifer 80 feet above the coal seam, and the coal seam itself being

---

[1]ERDA, Laramie Energy Research Center, Laramie, Wyoming.
[2]University of Wyoming and ERDA, Laramie Energy Research Center, Laramie, Wyoming.
[3]Conversion from English to metric units given in Appendix A.
[4]References given at end of paper.

saturated, effectively sealing the seam laterally, leakage of product gas has not been a problem in any of the tests thus far completed. The water in the coal seam not only helps seal the reaction vessel but also serves as an additional hydrogen source for the in-situ process [4]. Influx of water in excess of that required by the process will result in lower heating values of the produced gas. This influx of water has been controlled by increased back pressure and increased air injection rates [4].

The seam thickness and ash content affect the heating value of the produced gas and would be economic considerations more than concept testing considerations. In general, as the ash content of the coal increases or the seam thickness decreases, the heating value of the product gas decreases [5].

DISCUSSION OF CONSIDERATIONS

In the UCG experiments to date, linkage and gasification have been conducted between pairs of wells. Well spacings of 25 to 100 feet have been used and successful results have been obtained [1,2,3]. However, commercial applications will probably require longer spacings than 100 feet. Varied spacing of wells is planned in future tests to investigate this parameter. The optimum well spacing will be determined by economic as well as technical considerations and a particular spacing will probably not be applicable to all ranks and depths of coal. One thing which should be the same for all coals in which the linked vertical well process is to be applied is that the rows of wells (direction of gasification channel) should be along the direction of major permeability in order to minimize the reverse combustion linkage time requirements.

Information which should be available before drilling the entire pattern is the major and minor fracture and/or permeability orientation and dip of the coal seam. If it is not practical to drill and test 1 to 3 wells to obtain these data, the laboratory data derived from at least 1 oriented core may be used.

Drilling procedures used at Hanna have varied widely due to the large number of separate contractors engaged. A successful method has been settled upon and consists of using a 1500 rated drilling rig, heavy drill collar, flush joint 4 inch O.D. drill stem and 8 to 10 pound mud to stabilize the walls of the hole. Two methods of completion have met operational and process requirements.

The first method is to drill a 6 inch pilot hole to near the top of the coal seam, core from just above to just below the seam, then ream the entire hole to its final diameter. Next the open hole logs are run to get physical property and lithologic data. After logging is completed the casing is run into the hole with a float shoe on the bottom and centralizers on every third joint. The casing is set 15 feet below the bottom of the coal and a mud flush is used before cementing. After the cement has had 48 hours to set, a bond log, gamma ray log, and casing collar locator log are run to insure the casing string is intact and the cement bond is satisfactory. The casing is then perforated at the desired interval within the coal seam. This completes the method in which holes are cased through the seam.

The second method of completion is one in which an interval is left open to the coal below the casing. This method consists of drilling a 6 inch pilot hole to near the top of the coal, coring through the coal, then reaming to final diameter to the point at which the casing will be set (usually 2/3 of the way through the seam). The casing is then set on bottom and the remaining portion of the 6 inch pilot hole sanded back to the bottom of the casing. The hole is then cemented and a rubber plug is pumped down to within 15 feet of the bottom of the casing. After the cement has set, the cement and plug are drilled out and the sand is worked out of the lower portion of the hole, leaving an open interval within the coal.

The number of logs run depends on the information desired. Coal is characterized by high resistivities and high apparent porosities on Sonic, Neutron, and Density logs. As it is also desirable to identify and characterize the shale, sand, limestone, and clay areas, the Induction Electric, SP, and Laterolog are quite useful. The Caliper log is necessary to determine cement volumes needed. The drift log locates the bottom of the well relative to its surface location and is important in placement of instrument wells and is particularly useful in interpretation of data obtained from such wells. The logs mentioned are of necessity run in open hole. The logs preferred after casing and cementing are the Gamma for correlation of the open hole logs, the

Cement Bond to determine competency of the cement, and the Caliper and Collar Locator logs to determine that the casing has not parted or been damaged during reaming or well clean out.

Experience has shown that dewatering and drying the formation, particularly in the ignition well, is advantageous to ignition of the coal. The volume and the rate of movement of the water in the coal seam would dictate the extent of dewatering needed. Prior to air injection, bailing, air lift, or submersible pumping may be used. Generally bailing is inadequate and time consuming while submersible pumps will air lock once air injection is initiated. Submersible pumps also tend to plug and are not as dependable as the air lift method presently being used. The siphon jet (air lift) can be operated independent of the air being injected or gas being produced and, if desired, can be left in the well indefinitely. If excessive quantities of formation water are present, drilling, completing and equipping wells outside the pattern to remove such water may be necessary. These wells could be located such that they could be used later as injection and/or production wells as the system expands.

The procedure used at Hanna for formation dewatering is to inject air into the ignition well and produce from the well to which linkage is planned. Other wells not in use for gasification are closed in. This achieves a degree of localized dewatering between the wells to be linked. Once air injection is initiated for dewatering and drying, it is continued in the ignition well until ignition has been achieved and until air injection is switched to an adjacent well to initiate the reverse combustion linkage. Experience at Hanna has been that the coal should accept about 50 scfm of air at slightly less than lithostatic pressure and produce about half that amount within 48 hours of initiation of drying. Acceptance rates on this order are preferred before ignition but a successful link has been completed with initial acceptance rates of only 35 scfm.

The use of good engineering practice is always recommended for the layout of the surface facilities, materials selection and sizing. Many of the problems encountered at Hanna have resulted from trading preferred engineering practices for less desirable but more timely and economical practices.

Compression, flow monitoring and flaring facilities should preferably be located as close to the well pattern as is practical. By locating the monitoring facility close to the well pattern problems associated with signal transmission, sampling of product gas and overall supervision of the site can be reduced. By locating the compressors close to the well pattern both capital and operating costs will be reduced.

The site-specific problem of line freeze can be minimized by locating both the compressors and the flare close to the well pattern. The weather at the Hanna site is quite severe and all injection lines must be heat taped and insulated to prevent freezing of condensate in the air. Production lines should ideally be treated in a similar fashion (primarily during low flow conditions associated with linking), but the high temperatures experienced during the gasification phase are not amenable to use of currently available commercial insulating materials.

Locating the flare within a few hundred feet of the well pattern reduces the problems associated with condensing tars. Once the tars condense they are more difficult to dispose of than if they are burned in the vapor state in the homemade flares presently used. If the tars are allowed to condense, burning them would require some type of incinerator which would be considerably more expensive. If this expenditure is not acceptable and location of the flare near the wellhead is not feasible, an alternative is to dispose of them in a pit, which is not environmentally pleasing.

Three different flares have been designed and built at Hanna to burn the produced gas. The major problem in flare design is the broad range of water content, heating value and volumes that are encountered during the life of a UCG test. Produced gas volumes have ranged as high as 12 MM Scf/day with heating values as low as 85 Btu/scf. Two of the flares presently used are refractory lined and one is a standard oil field flare. All flares are fitted for propane injection during periods of high water concentrations.

Additional problems associated with the tars are their tendency to accumulate in valve seats, at the bottom of the production well during linkage, and in any low areas of the surface plumbing. The tar and water that condense in the casing must be evacuated from the production well as they will increase the backpressure on the production side of the linkage. The tar and water have been successfully airlifted at the site. Once production gas temperatures start to rise, the tars begin to cause other problems. The tar condensates that collect in the low areas of the surface

plumbing and in the seats of valves polymerize restricting flow and rendering valves inoperative. Globe valves and gate valves have been used with less than satisfactory results. We recommend that the valves used on the production lines have smooth flow lines with gates that sweep the seat face clean on each closing. The smooth flow lines of the valve would also help reduce some erosion problems that have been encountered. During short periods, high concentrations of fine particulates have been produced to the surface. These particulates are very abrasive and in the course of a few days will erode ell's, orifice plates and control valve gates to the point of replacement. These erosion problems were amplified by the use of improperly sized casing and surface piping. Stream velocities of 750 to 850 ft/sec were common during the final portion of both Phases II and III, Hanna II. Reduction of stream velocities to the range of 150 to 250 ft/sec and use of tee's to replace some ell's would almost completely eliminate surface piping erosion problems. A valve that will remain operative after being exposed to coal tar, abrasive particulate, 750 to 1000° F temperatures, and pressures in the 450 to 500 psig range has not been found. Use of valves with hard surfaced seats has helped and two valves are being tested that have flow characteristics that seem to reduce tar build up.

The metering devices used at Hanna are orifice flanges with graphite asbestoes gasket material. Meter runs are sized according to the production gas rate estimates. When the surface piping is sized properly, the meter run is usually 2 inches larger in diameter than the prodution piping diameter. The well spacing, seam thickness and anticipated water influx rates determine the injection rate which in turn determines the production rate to which the casing and production lines are sized.

The capacity of air compression is determined by the injection rate and injection pressure. Portable diesel powered air compressors have been used at Hanna due to an inadequate supply of electric power in the area. We have leased 3/2 the estimated air compressor requirements because of the frequent maintenance requirements as well as the need for backup capacity in case of major compressor malfunctions.

Linkage is one of the most critical phases in the testing sequence. The link must be kept low in the coal seam. This is accomplished by completing the wells at least 2/3 of the way through the coal seam or perforating the lower 1/3 of the casing, both of which were discussed earlier. After the dewatering and the drying phase has been completed (as described earlier), the lower 1/3 of the coal is ignited. This can be done in many ways. Two techniques tried at Hanna have been a propane heater [1,2] and an electric heater. Ignition does not seem to be as much of a problem as many would believe. During the 5-6 linkage of Hanna II, the coal autoignited during the drying phase when air preheated to approximately 250° F was being used to study its effects on permeability.

Once the coal is ignited air is injected for a period of a few hours in the ignition well to establish combustion. This injection cannot be continued since the forward burn will soon plug the formation [2]. After combustion has been established, injection is switched to the adjacent well and reverse combustion is used to complete the linkage. The procedure deemed most appropriate based on experience gained during Hanna II is constant pressure injection until an injection rate of 150 scfm is achieved. Then a constant rate of less than 150 scfm is maintained until linkage is completed. The pressure used during the constant pressure phase of linking is slightly less than lithostatic pressure. The reason for the constant volume injection in the second phase is two linkages performed during Hanna II gave evidence that the critical flux for reverse combustion was exceeded by maintaining a constant injection pressure rather than controlling the air injection rate.

A mini computer system is used on site for data acquisition and real-time data reduction [6]. The system monitors thermal data, flows and gas analysis. Because of the system, the number of personnel required for proper operation of the test site is reduced. An automatic on-line process gas chromatograph has been used for gas analysis and was interfaced with the computer system [6]. A manual gas chromatograph was used for back-up and for analysis of gas taken from instrument wells located in the well pattern and completed into the reaction zone but not connected to surface production lines. A bleed stream of gas was cleaned for the gas analyzers in a clean-up system in order to minimize contamination of packed columns in the gas chromatographs. The bleed stream was fed into a condenser first, which removed >95 percent of the tar and water. The condensate was collected in a sump and the gas was then passed through a rag filter. From there the stream entered an electrostatic precipitator to remove the very light oils and aerosols formed during the rapid cooling in the condenser. One additional step was taken to insure that no light oils passed into GC sampling system. The gas stream was passed through a loose column of resin. This system has worked quite well.

CONCLUSIONS

By careful planning problems associated with gasifying coal can be reduced. A careful design of surface facilities, always remembering that coal tar and water will be present in the production gas and that the gas will carry at times some small percentage of abrasive particulate, will reduce the problems associated with the operation of the site itself. Through experience gained during the tests at Hanna, the majority of the problems associated with operation of a UCG field test have been solved or their effects have been greatly reduced.

REFERENCES

1. Campbell, G. G., C. F. Brandenburg, and R. M. Boyd, "Preliminary Evaluation of Underground Coal Gasification at Hanna, Wyoming," BuMines TPR 82, October 1974, 14 pp.

2. Brandenburg, C. F., R. P. Reed, R. M. Boyd, D. A. Northrop, and J. W. Jennings, "Interpretation of Chemical and Physical Measurements from an In Situ Coal Gasification Experiment," SPE 5654, presented at the SPE Fall Meeting of AIME, Dallas, Tex., Sept. 28-Oct. 1, 1975, 28 pp.

3. Brandenburg, C. F., D. D. Fischer, D. A. Northrop, and L. A. Schrider, "Results and Status of the Second Hanna In Situ Coal Gasification Experiment," Paper MPR-2, presented at 2nd Annual Underground Coal Gasification Symposium, Morgantown, WV, Aug. 10-12, 1976.

4. Fischer, D. D., C. F. Brandenburg, S. B. King, R. M. Boyd, and H. L. Hutchinson, "Status of the Linked Vertical Well Process in Underground Coal Gasification," Paper FS-4, presented at 2nd Annual Underground Coal Gasification Symposium, Morgantown, WV, Aug. 10-12, 1976.

5. Gunn, R. D., D. W. Gregg, and D. L. Whitman, "A Theoretical Analysis of Soviet In Situ Coal Gasification Field Tests," Paper TPM-4, presented at 2nd Annual Underground Coal Gasification Symposium, Morgantown, WV, Aug. 10-12, 1976.

6. Eastwood, D. E., J. K. Eastlack, J. W. Jennings, S. B. King, W. J. Lanum, and D. F. Moore, "Real Time Process Monitoring in Underground Coal Gasification," Paper MI-2, presented at 2nd Annual Underground Coal Gasification Symposium, Morgantown, WV, Aug. 10-12, 1976.

APPENDIX A - CONVERSION FACTORS

1 ft = 0.3048 m

1 in = 2.54 cm

1 ft/sec = 0.3048 m/sec

1 gal = 3.785 l

1 scfm (60° F) = 0.029931 scm/min (0° C)

1 Btu/scf (60° F) = 3.52477×10^{-2} megajoules/scm (0° C)

° C = 5/9 (° F - 32)

1 psig = 6894.76 pascal

NOTE: Any reference to specific brand names does not imply endorsement by ERDA.

POST BURN ANALYSIS TECHNIQUES APPLICABLE TO UNDERGROUND COAL GASIFICATION

by

R. MICHAEL BOYD[1]

ABSTRACT

An important consideration in process development for in situ coal gasification is a means of measuring resource utilization and the location of the active combustion front by remote sensing. Efforts to develop measuring techniques applicable both during and after completion of a test burn have been underway at LERC for the past two years. Existing technology applied to post-burn evaluation has consisted of wire line drilling and coring, and conventional reflection seismic surveying. Research is underway to evaluate shear wave seismic surveying, high resolution shallow reflection seismic surveying, magnetic surveys to detect changes in iron minerals in the overburden as they are heated, and seam wave seismic surveys as means of real-time evaluation for process monitoring and control.

An area of concern in all types of in situ combustion processes is the need for remote sensing which accurately describes the size and shape of the consumed resource. Material balances in conjunction with certain forms of instrumentation are able to give reasonably accurate information on the amount of resource consumed at any given time, but do not indicate the shape of affected areas. It is apparent that a means for remote determination of resource utilization would be very useful at this time for comparing various in situ techniques. Possible future uses include prospecting for suitable gasification sites, determination of burn boundaries in relation to property lines and surface structures, and definition of in place resources for leasing agreements.

The evaluation of the Hanna I test site consisted of a seismic feasibility study, and drilling and coring to obtain samples for chemical analysis. The seismic investigation consisted of a shear wave refraction study done under contract by the Environmental Research Institute of Michigan(1). Shear waves were chosen for two reasons: 1) the high resolution shallow reflection work did not appear to be sufficiently advanced; 2) this wave type depends only on the rigidity of the medium for propogation Therefore it would not continue through the burned area if it was filled with air or water or some combination of the two (figure 1). ERIM was chosen to do the study because they are unique in having a generator which produces shear waves of sufficient strength and repeatability to reach the depths required. Although both P (compressional) and S (shear) waves are produced by their equipment. Only the horizontal component (SH) of the shear wave was used for this study. Other data collected in the field have been preserved for later expansion and continuation of the work reported here.

---

[1]ERDA, Laramie Energy Research Center, Laramie, Wyoming.

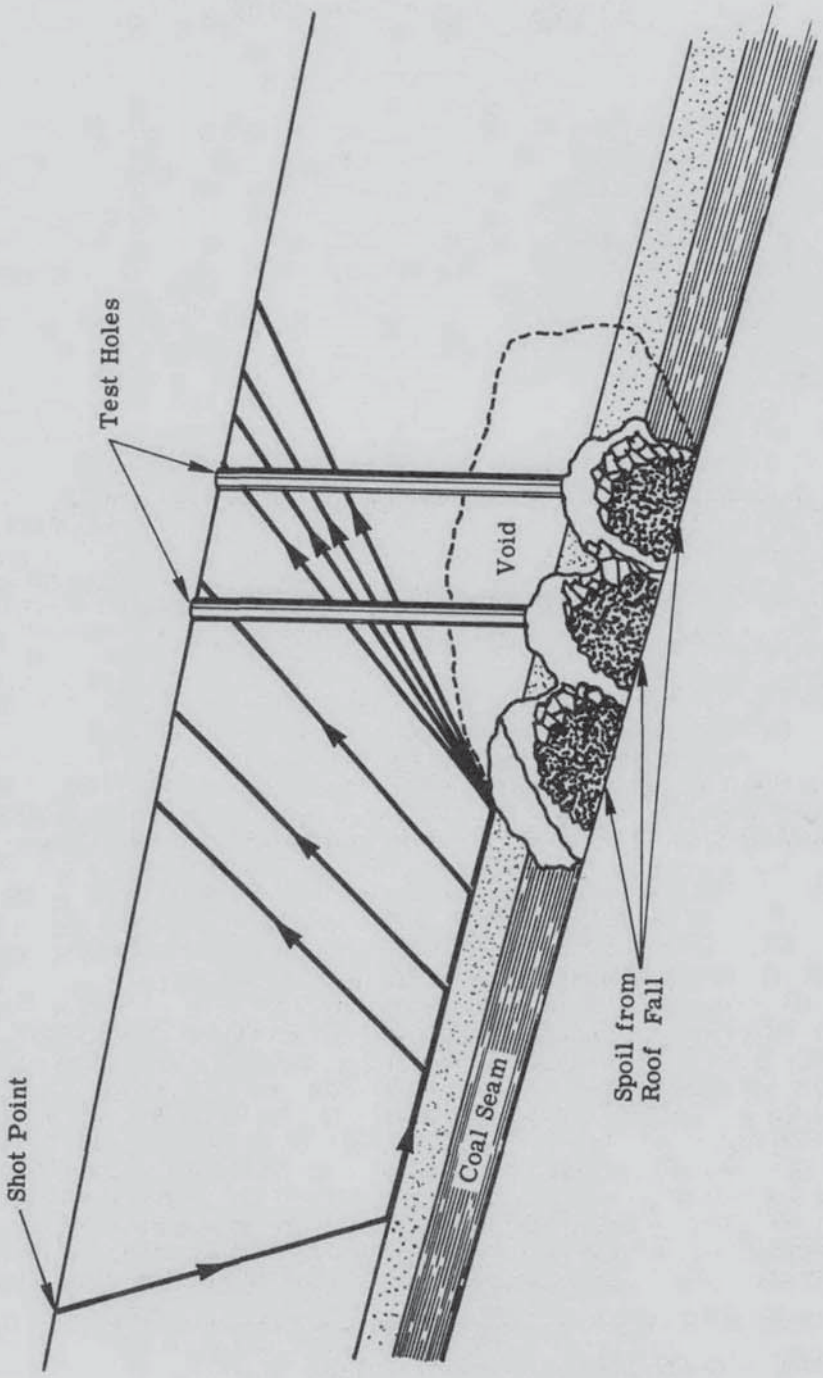


Figure 1 - Three dimensional sketch of Environmental Research Institute of Michigan's shear wave refraction technique.

Five double ended refraction lines were established using the orientation of various pairs of wells at the Hanna I site (figure 2)(2). It was intended that a series of lines passing through the burned area would give intercepts of the edges and thereby outline the area burned (figure 3). Four of the lines were 1035 feet (315m) in length, one was 1600 feet (488m). The 1600 ft. (488m) line was used to compare a fixed geophone array and a moving shot point with the moving array, fixed shot point used on other lines. The method used consisted of setting an array of 24 horizontal geophones oriented transverse to the line at 45 foot (13.7m) intervals and setting the source 782 feet (238m) from first one end and then from the other end of the line while moving the geophone array across the target area. In the case of the 1600 ft. (488m) line, the previously described method was used, then geophones were kept in a fixed array at 25 ft. (7.6m) spacing, and the source was moved across the target area. The shear wave generator was oriented perpendicular to the line first in one direction for several shots, then in the opposite direction for several shots. The reason for several shots was to "stack" the data to overcome high ambient noise conditions at the site caused by the operation of two drill rigs, an air compressor, and a large flare stack, in addition to 10-35 mph (16-56 km/hr) surface winds. On the seismogram (figure 4) the reversal of the generator is shown by the phase change of the shear waves. Note the P wave energy duplicates itself while the S waves come through at nearly the same amplitude but 180° out of phase. In this study a subjective criterion of a sharp decrease in SH wave amplitude was used to define the edge of the anomaly. This is undoubtedly not as precise a method as is possible, but some modeling of diffraction around the cavity is needed to determine the rate of decay of shear wave amplitude due to diffraction.

A layered model for travel times was used, and based on travel times the ray paths did not extend below the coal but penetrated to 380 ft. (116m) and propagated as head waves above the top of the coal. The intersections shown in (figure 3) are edges of the rubble zone of roof fall rather than edges of the burned area. The amount of diffraction, calculated from travel times, produces an offset of the cavity location about 330 ft. (101m) down each line, so the intersections shown on figure 3 are to be considered estimates until more work can be done on refraction modeling.

Because seismic and other geophysical technology is in the research stage, it cannot yet be relied upon to evaluate a test site. In addition to the shear wave study, eight evaluation holes were drilled and cores were taken from each. The locations of the holes were based on the probability of burning effects to the coal determined by duration of air injection and gas production during the Hanna I test. Because the greatest utilization should have occurred in the central portion of the pattern, the wells were drilled from the edge inward.

Holes 1 and 2 were to investigate the linkage path from well 15, a primary injection well, to the central combustion zone in the 5-7-8 area. The results indicate the linkage path had undergone forward combustion and the top 10-14 ft. (3-4.2m) of the seam had been consumed. Holes 3-4-5-8 were drilled to investigate the central burn areas, and the area gasified between well 9 and wells 5-7-8. This was the area of greatest utilization, where approximately 60% of the coal seam was consumed, but only the upper portion. This indicates overriding during the linkage to well 9. Overriding is a condition in which the injected air rises to the top of the coal seam and linkage and combustion are thereby limited to this area. It is caused by improperly locating the wells too high in the seam. For example, the wells used in the Hanna I test were completed 4 feet into the top of the coal seam. Holes 6 and 7 were to determine the extent of burning in the 5-8-12 direction and possibly locate the linkage to well 12. No signs of linkage or combustion were found in hole 6 in spite of a very good link between well 12 and wells 8-5-7. It is probable the linkage lies to the north of the 8-12 line, but no further drilling was done to locate it. Table I summarizes the results of coring in these holes.

TABLE I

Hole #	Depth to Solid Coal	Orig. Depth of Coal	Ft. of Coal Burned	% of Seam*
1	389	375	14	48
2	382	375	10	34
3	380	364	16	55
4	383	367	16	55
5	368	366	2	7
6	356	356	0	0
7	372.5	359	13.5	47
8	388.3	366	22.3	77
		Avg.:	14.5	50

*based on 29 ft. seam thickness

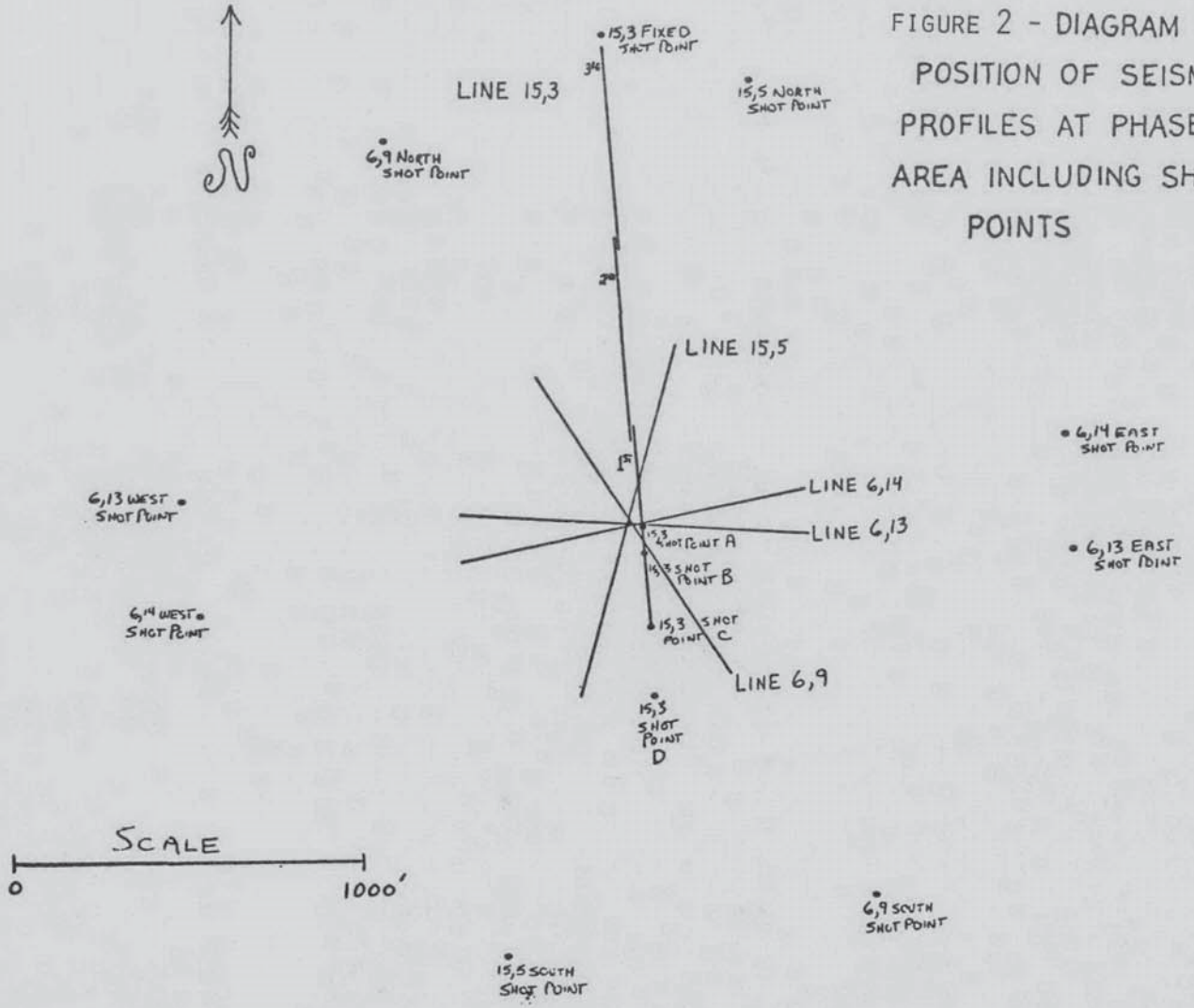


FIGURE 2 - DIAGRAM OF POSITION OF SEISMIC PROFILES AT PHASE I AREA INCLUDING SHOT POINTS

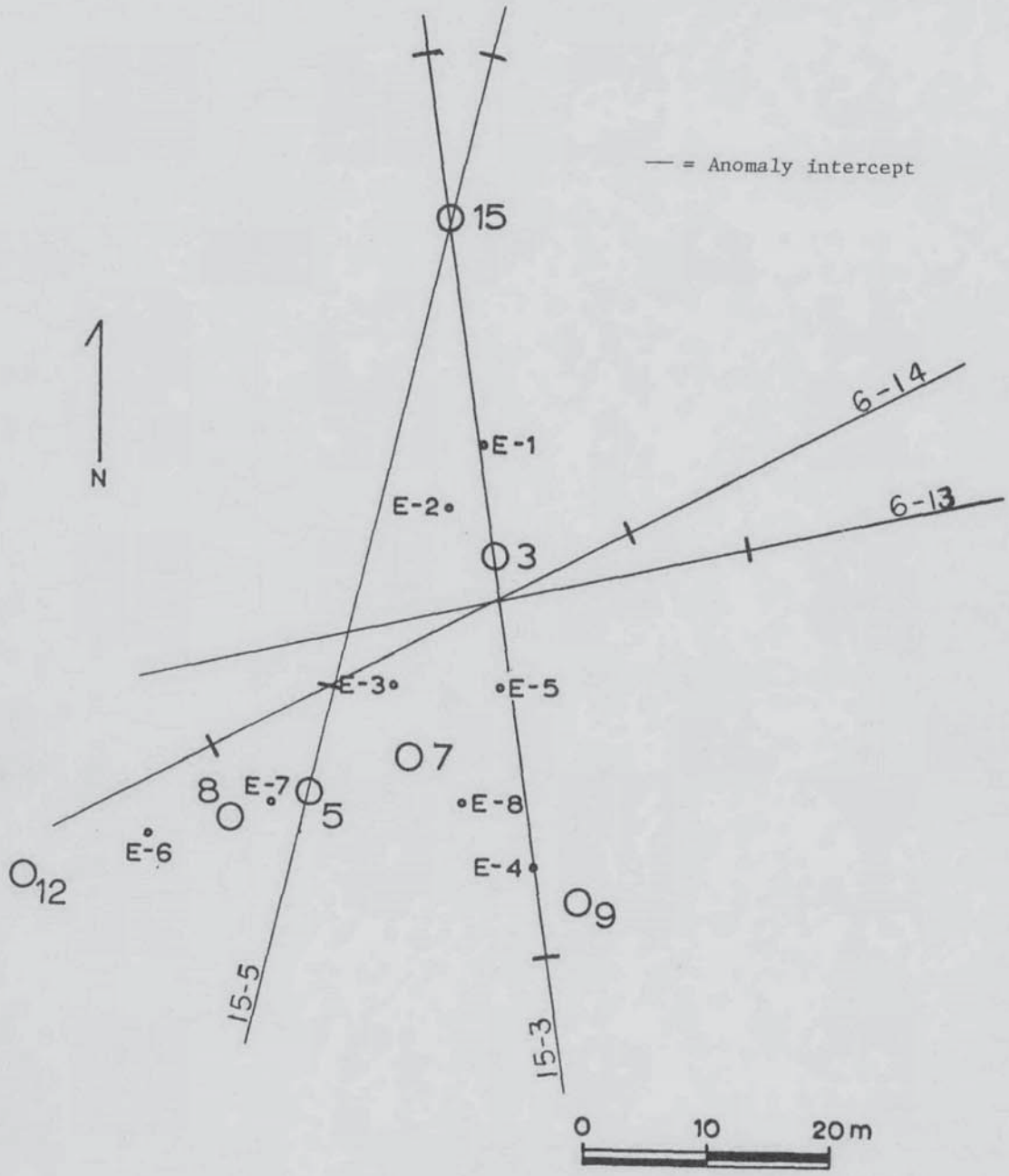


Figure 3 - Intercepts of seismic anomaly forming outline of roof fall.

Samples were taken in all the holes from the first solid coal encountered at the bottom of the of the interval burned. No carbonized layer could be found. Table II is a comparison of the analysis of fresh coal (samples taken prior to burning) and analysis of samples of core taken from the burned area. Note the composition of samples from the floor of the burned area is very similar in most cases to the range of normal variation of fresh coal. No visible effects of burning were apparent from study of the cores.

TABLE II

	Fresh Coal (Before burn)		Core Sample (After burn)	
	Range	Avg.	Range	Avg.
Moisture	3-12%	8%	4-11%	7%
Volatile Matter	16-49%	37%	17-40%	33%
Fixed Carbon	10-50%	43%	35-68%	49%
Ash	3-74%	34%	2-21%	11%
Sulfur	.3-4.2%	.8%	4-.6%	.5%
Carbon/ hydrogen ratio	11.7-14.3	13	11.8-22	13.2

However the range of variation is so great within the coal seam that comparison by this means is very unreliable. When the carbon/hydrogen ratio is calculated from a large number of samples taken from throughout the seam, we find a consistent basis for comparison. In spite of variations in ash content by a factor of 2 to 5 the C/H ratio is consistently between 12 and 14 to 1 (3, 4). In one sample from the burned area the C/H ratio was 22 to 1. This ratio is higher by almost a factor of 2 than that found in samples taken elsewhere from both affected and unaffected areas. It seems very likely that this sample was carbonized. One type of material balance calculation indicated large zones of carbonized coal should be present, but no such zones were found. It is possible that the zones were thin and therefore masked by the size of the sample, or perhaps they were very fragile and destroyed by the addition of water to cool the burned area.

Another observation from the drilling was the lack of a large open cavity. We had anticipated encountering such a cavity and intended to map it with a sonar logging tool. But what we encountered, 16 months after shutdown, was rubble and roof fall which filled the burned area nearly from floor to ceiling. A few voids, ranging from 6 inches to 1 foot in height were encountered, these were probably spaces between large blocks of roof material.

Figure 5 is a compilation of data gathered from drilling and seismic work and presents as complete an interpretation as possible from the evaluation work completed thus far. The main features to be noted are the lack of a well defined carbonized halo surrounding the gasification zone, and the utilization of just the upper portion of the seam, due to overriding, around the edges of the central burn area. Figure 6 shows a cross section from well 15 to well 9. Completion methods, as well as other operating practices, have since been changed and greatly improved utilization is anticipated when Hanna II is evaluated.

It can be concluded from the evaluation work thus far completed that: a) only the upper one half of the coal seam was utilized due to overriding by injected air; b) no large open cavity exists at the conclusion of gasification, instead the cavity created by burning coal is filled with caved roof material; c) no large halo of carbonized coal surrounds the gasified area; d) the use of shear waves to evaluate burned areas appears feasible and should be further developed and refined.

Other remote evaluation techniques, which appear to have a high probability of success, include high resolution shallow reflection seismic surveying, magnetometer surveying, and seam wave seismic surveying. The high resolution shallow reflection technique is presently in the research stage, but the technique is similar to conventional reflection surveying, except with very short sample intervals to utilize higher frequencies. In contrast to the shear wave study where energy in the 1-18 Hz range was used, the high resolution reflection work involves frequencies up to 300 Hz, thus the resolution is correspondingly greater. Due to the experimental nature of the work the costs are comparatively high, but it is hoped that a preliminary survey at Hanna Site II can be done within the next year.



Figure 4 - SHOT POINT C: SH ARRIVALS. Shear wave generator force directed to the right when first deflection is upward, facing left when first deflection is downward. From ERIM Rept. No. 116400-1-F.

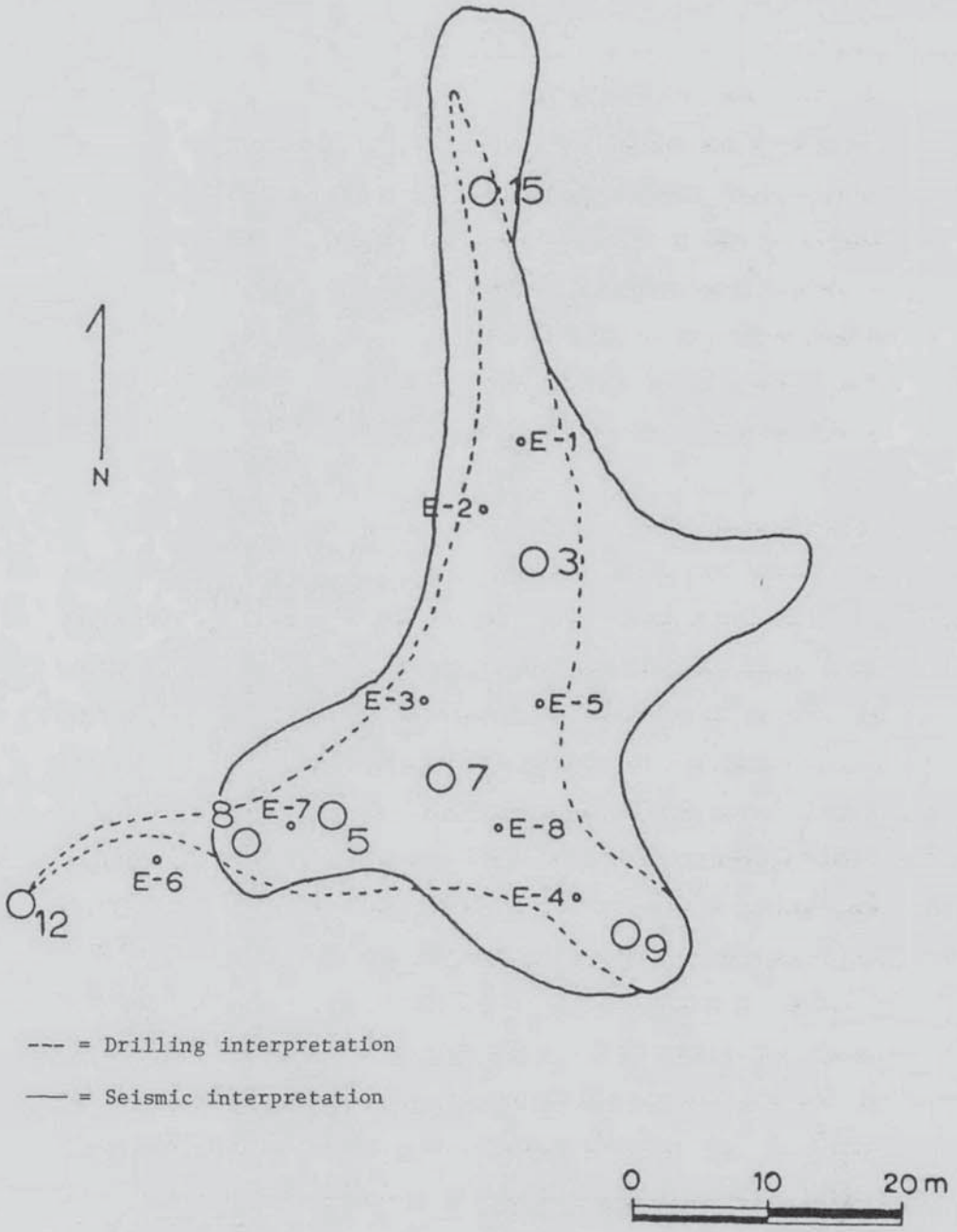


Figure 5 - Composite plot of seismic and drilling interpretation of burned area.

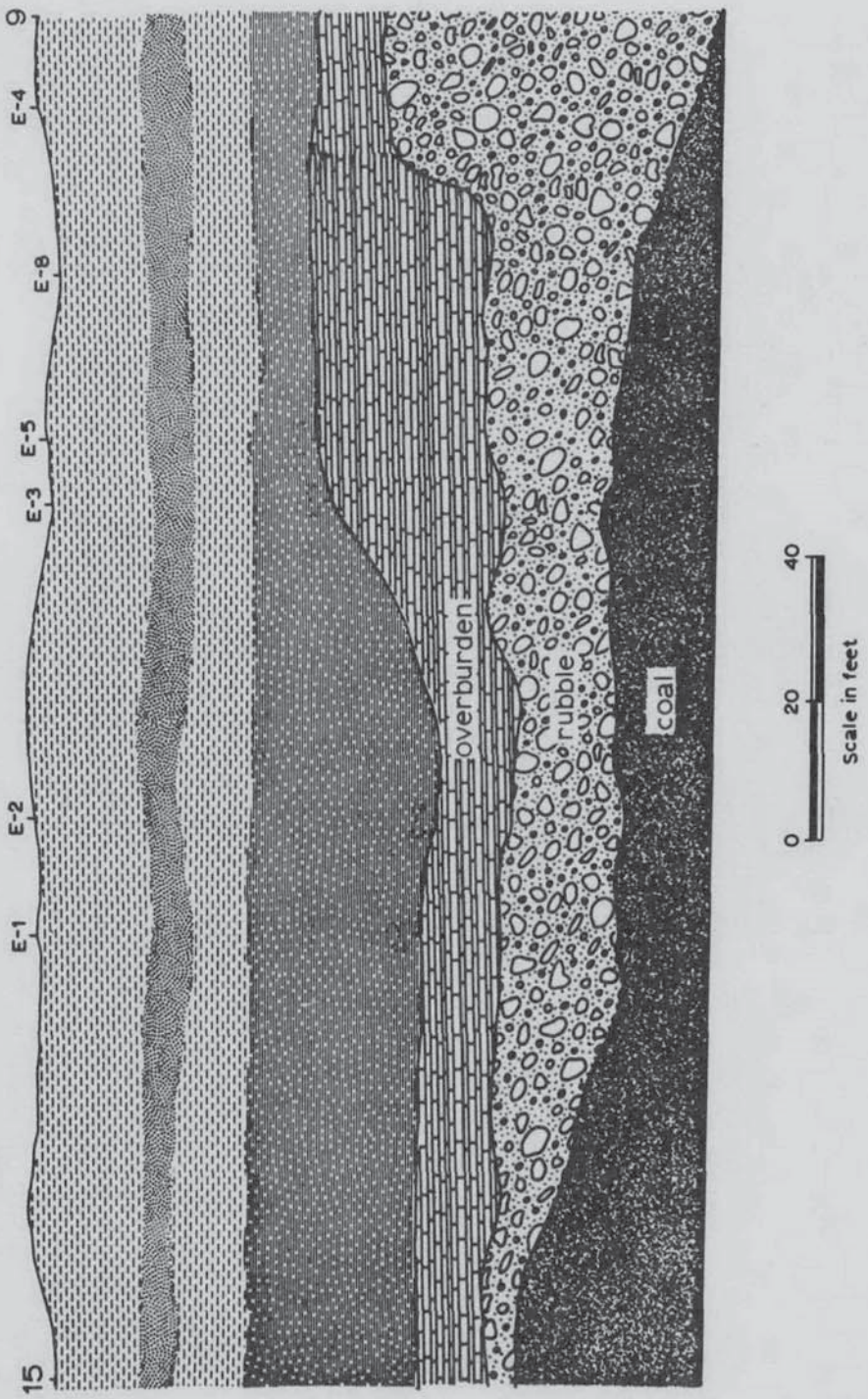


Figure 6 - Diagrammatic cross section through burn area looking east from Well 15 to Well 9.

Investigations by the Colorado School of Mines in using the coal seam as a wave guide also appear promising. In this work the source is placed within the coal seam, usually through a borehole, and the geophones are located some distance away in a vertical array also within the coal seam. The idea is to measure these waves at various distances from the source to determine the lateral continuity of the seam. This technique has been used in advance of longwall mining in Europe with great success.

Another area of interest being investigated by the U.S. Geological Survey is the change in magneti of iron minerals in overlying shales due to heating. Initial surveys run over areas of natural fires in coal seams shows a 6000 fold increase in magnetism. It may be possible to compare measurements made at the surface during a burn with those made prior to burning, and thus determine fire front locations.

These three methods appear to have a great chance for short-term development with a high probability of success, and it is hoped that their development will be pursued through the field test stage in the near future.

REFERENCES

1. Turpening, Roger M.: "Cavity Detection By Means of Seismic Shear and Compressional Wave Refraction Techniques," Final REport, Contract No. E(29-2)-3614 ERDA, Laramie Energy Research Center, June 1976, 102 pp.
2. Schrider, L. A., et.al.: "The Outlook from Underground Coal Gasification," presented at the 1975 Lignite Symposium, Grand Forks, North Dakota, May 1975, 31 pp.
3. Estep-Barnes, P. A., and Kovach, J.J.: "Chemical and Mineralogical Characterization of Core Samples from Underground Coal Gasification Sites in Wyoming and West Virginia," RI-76/2, Laramie Energy Research Center, ERDA, February, 1976, 39 pp.
4. Brandenburg, C. F., et.al.: "The Underground Gasification of a Subbituminous Coal," presented at the Div. of Fuel Chem., Am. Chem. Soc. National Spring Meeting, Philadephia, PA (April 1975), 11 pp.

STATUS OF THE LINKED VERTICAL WELL PROCESS IN UNDERGROUND COAL GASIFICATION

D. D. FISCHER,[1] C. F. BRANDENBURG,[1] S. B. KING,[1]
R. M. BOYD,[1] AND H. L. HUTCHINSON[2]

ABSTRACT

The Linked Vertical Well (LVW) process, which employs reverse combustion as a preparatory step to forward combustion gasification, will be described from both a practical and theoretical viewpoint. Fifty years of underground coal gasification experimentation has shown that, prior to efficient gasification, a "linkage" between injection and production boreholes must be prepared. The LERC experimentation has concentrated on the characterization and the development of reverse combustion linking such that it has become a predictable means of process control. The results of eight different reverse combustion links at Hanna indicate that subbituminous coal is ideally suited to reverse combustion linkage both from a controllability standpoint and the quantity of air needed to complete a linkage. Following reverse combustion linking, forward gasification ensues. Eight different well to well gasification periods have been completed since initiation of tests at Hanna. A detailed chemical and physical description of the recent results from Hanna II will be given. This latter experiment resulted in the gasification of 6690 tons (6070 tonnes) of coal and production of up to 12 MM scfd (0.36 MM scmd) of 175 Btu/scf (6.2 megajoules/scm) gas. The reasons for these improved process results will be discussed in detail.

INTRODUCTION

Testing of the linked vertical well (LVW) process for underground coal gasification (UCG) was initiated in March 1973 by the Laramie Energy Research Center (LERC) at a site near Hanna, Wyoming. Since that time the Hanna I and II experiments have been completed - Hanna II only recently. The results of Hanna I and of Phase I, Hanna II, have been previously reported [1-7].[3] This paper will present a detailed outline of the operating parameters used and data gathered during Phases II and III, Hanna II, with discussion and interpretation of the field data gathered from those two phases. The status of the LVW UCG process will be discussed as well as proposed future tests for further delineation of the commercial viability of the LVW process.

THE LINKED VERTICAL WELL (LVW) PROCESS

A schematic of the LVW process for a two-well system is shown in Figure 1. The steps involved are ignition, using a downhole electric heater with concurrent low-volume air injection to sustain combustion; switching air injection to the adjacent well in order to achieve a reverse combustion linkage; and high volume-low pressure air injection upon completion of the linkage phase to achieve efficient gasification conditions with the gasification zone proceeding from the air injection well to the production (ignition) well. This technique has been successfully utilized for eight

[1]ERDA, Laramie Energy Research Center, Laramie, Wyoming.
[2]University of Wyoming and ERDA, Laramie Energy Research Center, Laramie, Wyoming.
[3]References given at end of paper.

reverse combustion linkages followed by eight gasification periods utilizing two-well systems during Hanna I and Hanna II. The linkage distances achieved have varied from 25 feet (7.6 m) to 90 feet (27.4 m).

THE HANNA II EXPERIMENT

The site of Hanna II is approximately 800 feet (244 m) west and updip from the site of Hanna I. The 30 feet (9.2 m) thick Hanna #1 coal seam was again utilized. The depth to the top of the seam was approximately 275 feet (84 m) compared to 370 feet (113 m) for Hanna I.

Hanna II consisted of three phases. Phase I was conducted from July through August 1975. Detailed results of Phase I have been previously reported [7]. A summary of the results of that phase are shown in Table 1.

The well pattern for Phases II and III is shown in Figure 2. Wells 5 through 8 were for use as injection and/or production. All other wells shown were instrument wells with instrumentation designed and fielded by Sandia Laboratories of Albuquerque, New Mexico [8].

Phase II was planned to consist of the following steps:

(1) Link Wells 7 and 8 with ignition occurring at Well 7.

(2) Link Wells 5 and 6 with ignition occurring at Well 5.

(3) Gasification from Well 6 to Well 5.

Phase III - scheduled for immediate implementation upon completion of Phase II - was designated a line drive system and was to include the following steps:

(1) Simultaneous injection at Wells 7 and 8 to form a broad front reverse combustion link to the 7-8 linkage path.

(2) Gasification from the 7-8 line back toward the 5-6 line.

If successful, the line drive was projected to yield a higher areal sweep efficiency than experienced during other UCG tests.

RESULTS OF PHASE II

Reverse Combustion Linkage of Wells 7 and 8

Ignition at Well 7 was achieved on December 3, 1975, using a downhole electric heater. The flow rates and temperature data at the bottom of Well 8 are shown in Figure 3. The linkage proceeded as expected until December 6 when the injection rate more than doubled. No accompanying drop in injection pressure was observed. The injection rate continued to increase and on December 10, the production rate exceeded the injection rate. From previous linkages this event has always been an indication that completion of linkage was imminent. The temperature at the bottom of Well 8 also started to rise, a further and more credible indication of the imminence of linkage. The air injection rate continued to increase but the temperature at Well 8 started to decline. Total air injected at the time of peak temperature at Well 8 was 1.98 MM scf (5.93×10^4 scm) or 33 Mscf per lineal foot (3.24×10^3 scm/m) of well separation.

This corresponds with the air requirements previously reported for past linkages [7], but the accompanying drop in static injection pressure was not observed. The critical flux for reverse combustion had been exceeded causing the reverse combustion linkage to

TABLE 1: Summary of Phase I, Hanna II, Results

Average Operating Parameters

Gross Heating Value	152 Btu/scf
Daily Gas Production	2.7 MM scf
Daily Air Injection	1.9 MM scf
Daily Btu Production	420 MM Btu
Average Composition (vol. %)	
H_2	17.3
N_2	51.0
CO	14.7
CO_2	12.4
CH_4	3.3
Ar	0.6
H_2S	0.1
C_2-C_4	0.6

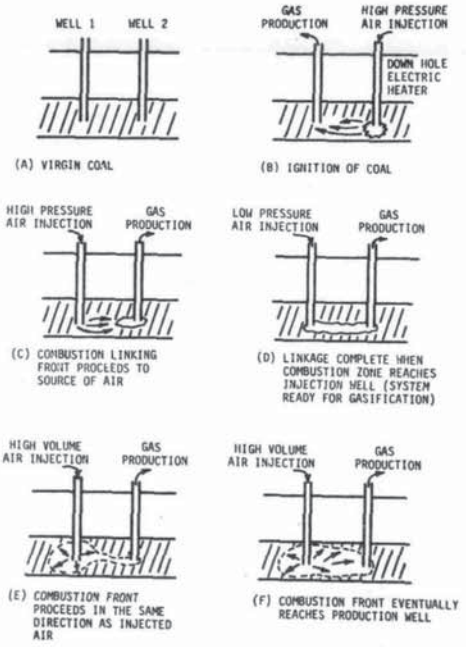


Figure 1 - Schematic of the LVW UCG Process.

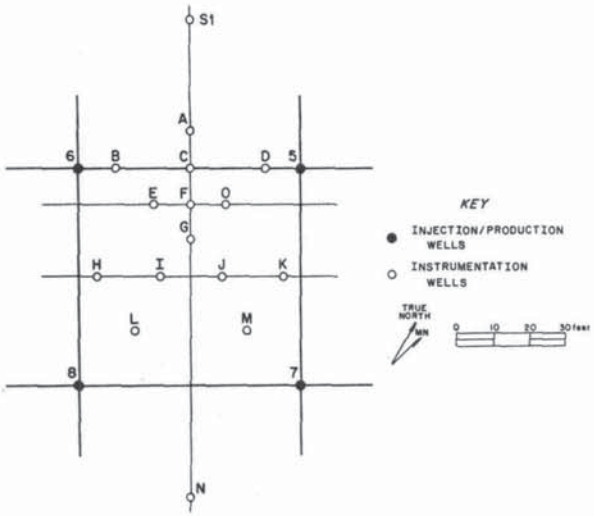


Figure 2 - Well Pattern used During Phases II & III, Hanna II.

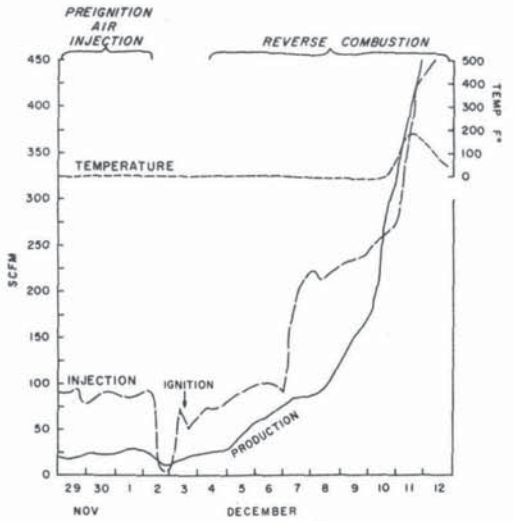


Figure 3 - Flow Rate and Temperature Data for the Linkage of Wells 7 and 8, Phase II, Hanna II.

revert to forward combustion. Linkage was achieved by pulsing air injection at Well 8 thereby leading to an injection rate of 950 scfm (28.4 scm/min) at 25 psig (1.72×10^5 Pa). Water was injected in January 1976 to ensure that the combustion zone was extinguished.

Material balance calculations indicated that about 91 tons (82.6 tonnes) of coal were consumed during the linkage. Seventy-five percent of this calculated volume was able to be filled with subsequent water injection, which was considered an excellent corroboation because the material balance calculation assumed no carbonized coal left along the linkage path. Since linkage is known to be a lower temperature process than gasification, carbonization should be the primary reaction mode. Only 18 tons (16.3 tonnes) of the calculated 91 tons (82.6 tonnes) were used during the reverse combustion linkage through December 11 and the remainder consumed during the forward combustion mode (which was primarily gasification) after that time. Thus the injected water volume matched the calculated volume very well indeed.

Reverse Combustion Linkage of Wells 5 and 6

Initial air injection tests prior to beginning the linkage of Wells 5 and 6 were begun on March 25, 1976. The initial air acceptance at Well 5 was 6 scfm (0.18 scm/min) at 250 psig (1.72×10^6 Pa) injection pressure, a rate deemed too low to sustain a reverse combustion link. This problem was rectified by additional perforations in the casing in Well 5, pressuring and depressuring Well 5 with pulsed air injection, and drying of the coal with a downhole heater. This resulted in the ability to inject >50 scfm (>1.5 scm/min) into Well 5. The coal was ignited on April 4 and the reverse combustion linkage initiated on April 6. On April 15 (see Figures 4 and 5) the injection pressure dropped from ≈250 psig (1.72×10^6 Pa) to ≈40 psig (2.76×10^5 Pa) at an injection rate of 350 scfm (10.5 scm/min) indicating that linkage had occurred. However, the thermocouples at the bottom of Well 6 did not indicate that a large combustion zone had reached Well 6. The air injection rate was maintained at a controlled rate of 100 to 150 cfm (3 to 4.5 scm/min) to maintain the combustion process in the reverse mode until April 22 with no further significant temperature increases at the bottom of Well 6. On April 23 the injection rate was increased to 500 cfm (15 scm/min) which required a pressure of 120 psig (8.27×10^5 Pa). These data indicated that, although a permeable pathway had been created by reverse combustion, it was not sufficiently open to allow efficient gasification at low pressures. This restriction was removed by switching the air injection back to Well 5 for 6 hours after which injection of 1500 cfm (44.9 scm/min) at 42 psig (2.9×10^5 Pa) was possible into Well 6. The 5-6 system was then ready for operation under conditions necessary for efficient underground coal gasification. Carbon balance calculations showed that about 330 tons (299 tonnes) of coal were utilized during this period. This is more than was used in the 7-8 linkage because of the greater difficulty incurred in achieving the link.

The temperature measured in Wells A through G and O during the linkage and gasification between Wells 5 and 6 are given in Figures 6 and 7. The thermal data defined the location of the reverse combustion linkage near the bottom of the coal seam and as a lateral arc between the injection and production wells, as the initial temperature rise at each instrumentation well occurred at either the 0 or 5 feet (1.52 m) level above the bottom of the coal seam. Figure 8 shows the approximate path of the linkage.

Gasification from Well 6 to Well 5

Operating conditions maintained during the 5-6 gasification phase consisted of three staged injection rates of 1700 scfm (50.9 scm/min), 2500 scfm (74.8 scm/min), and 3500 scfm (104.8 scm/min). The periods at these injection rates were 3+ days at 1700, 5+ days at 2500, and 17+ days at 3500 cfm beginning on May 4.

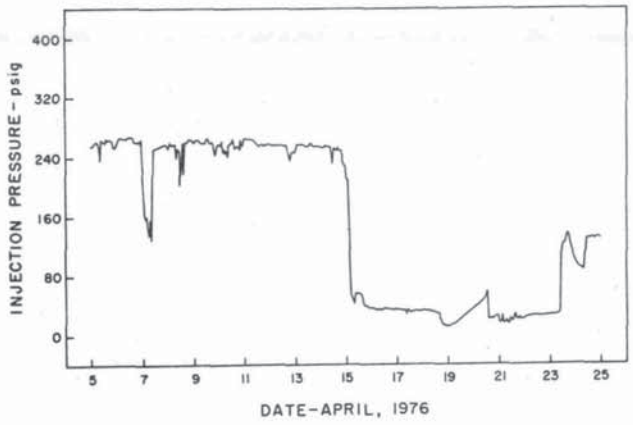


Figure 4 - Injection Pressure During the Linkage of Wells 5 and 6, Phase II, Hanna II.

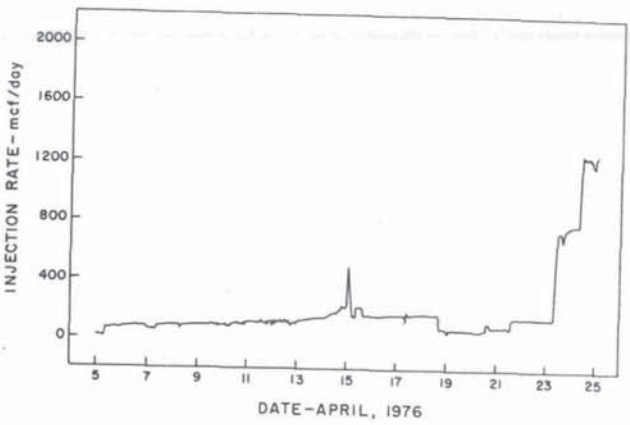


Figure 5 - Injection Rate During the Linkage of Wells 5 and 6, Phase II, Hanna II.

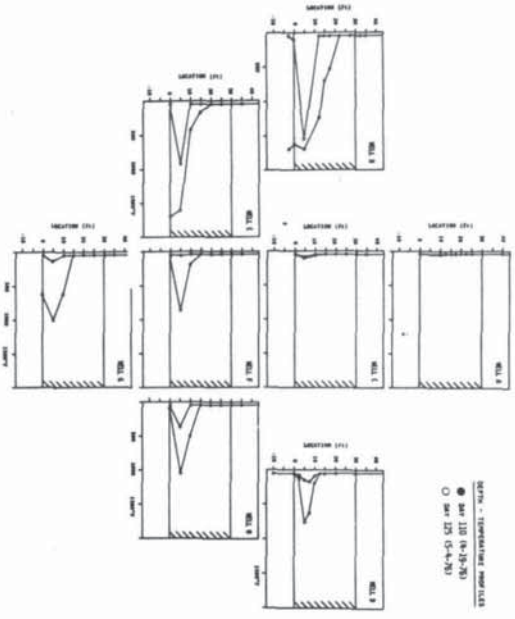


Figure 6 - Thermal Data Showing the Linkage Progress from Well 5 to Well 6, Phase II, Hanna II.

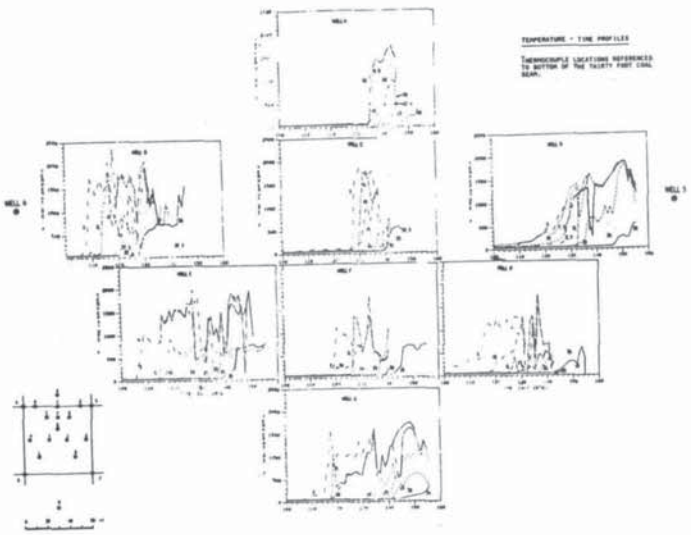


Figure 7 - Thermal Data Showing Gasification Front Movement from Well 6 to Well 5, Phase II, Hanna II.

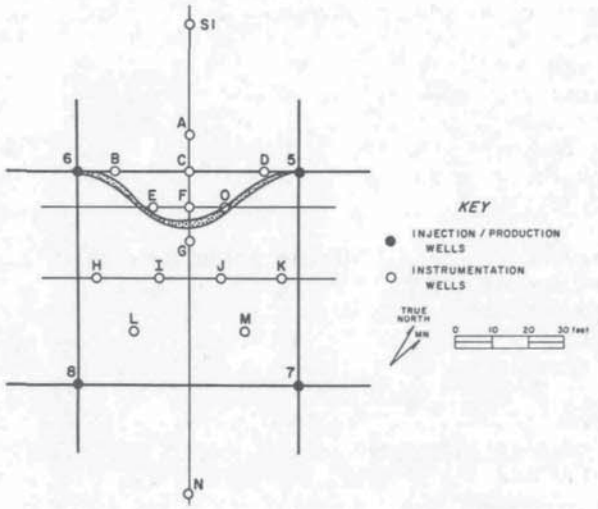


Figure 8 - Estimated Linkage Path between Wells 5 and 6, Phase II, Handa II.

The gas composition, injection and production rates, injection and production pressures, product gas temperature at the wellhead, and product gas gross heating value are shown in Figures 9-13.

As can be seen the gas composition was constant and uniform until near the end of the 5-6 gasification phase. No dramatic changes in gas composition or heating value occurred during the planned abrupt increases in injection rate. The ratio of production rate to injection rate was consistently greater than 1.7. At 3500 scfm (104.8 scm/min) injection, the production rate was about 6000 cfm (179.6 scm/min) or 8.6 MM scfd (2.6×10^5 scmd) of 175 to 185 Btu/scf (6.2 to 6.5 megajoules/scm) product gas. All instrumentation in Wells A, B, C, D, E, F, G, and O was consumed upon completion of the 5-6 gasification. Wells H, I, and J showed temperatures at or above the steam plateau at the 0 and 10 feet (3 m) levels from the bottom of the seam when the 5-6 gasification phase was completed on May 30. In addition, leakage of product gas to Well S1 occurred on May 30. Temperature measurements in S1 on May 31 showed a peak temperature of 88° F (31° C) at 12 feet (3.6 m) above the bottom of the seam. Therefore, at the midpoint of the 5-6 line the reaction front could have been as wide as 50 feet (15.2 m) assuming it had approached within a few feet of S1 and within a few feet of the H-I-J line as indicated from thermal data.

An additional 2190 tons (1990 tonnes) of coal were removed during the 27-day period from May 4-30 bringing the total utilization for the linkage and gasification of 5-6 to 2520 tons (2286 tonnes). This is 1000 tons (907 tonnes) more than estimated from linear extrapolation of the data gathered from the gasification between Wells 1 and 3 (Phase I) during June and July 1975.

Coal tar and water content of the product gas were measured on three separate occasions toward the end of the 5-6 gasification period. On a total wet gas basis, the weight percent water and tar were 12.6, 13.7, and 16.0 percent, and 1.7, 1.9, and 0.8 percent, respectively. The last readings of 16 percent water and 0.8 percent tar were gathered just before the end of the 5-6 gasification.

For the first time in the series of experiments at Hanna, a two-well system was taken near enough to completion to experience the production of large quantities of particulate matter through the surface piping. The particles, traveling at velocities of 760 feet per second (232 m/sec) eroded the Schedule 40 elbows in the 4 inch production piping to the point of leakage at several locations. This necessitated shut-down of injection into Well 6 and initiation of production through Well 6 with Well 5 shut in. After a few hours of bleed down, air injection was begun into Well 5 to ascertain that the burn between 5 and 6 was completed as would be evidenced by a decrease in gas quality and an increase in production gas temperature due to bypassing of oxygen. The product gas temperature at Well 6 increased from approximately 750° F (399° C) to greater than 950° F (510° C) within 12 hours as the gross heating value also declined. Injection was terminated and the 5-6 system was then allowed to bleed down.

PHASE III

Upon conclusion of Phase II, Phase III was begun immediately. The original plan was to inject into Wells 7 and 8 to draw the combustion zone from the 5-6 gasification zone back to the 7-8 link in a reverse combustion mode and then gasify along the broad path thus formed. To this end injection into Wells 7 and 8 was begun on May 31. Initial injection rates and pressures were 300 scfm (8.98 scm/min) at 260 psig (1.79×10^6 Pa) into 7 and 330 cfm (9.88 scm/min) at 260 psig (1.79×10^6 Pa) into 8. Production rates from 5 and 6, respectively, were 1800 and 900 scfm (53.9 and 26.9 scm/min). Well 6 was produced at a lower rate due to the high product gas temperature at Well 6. These rates continued until June 3 when linkage occurred. It was suspected that a narrow linkage channel was formed between the 7-8 linkage path and the flame front advancing from the 5-6 burn area. The channel was believed to have been located on the west side of the well pattern near Wells 6 and 8 because instrument wells H and I were the only two to show temperature increases during this linkage phase and because the product gas temperature

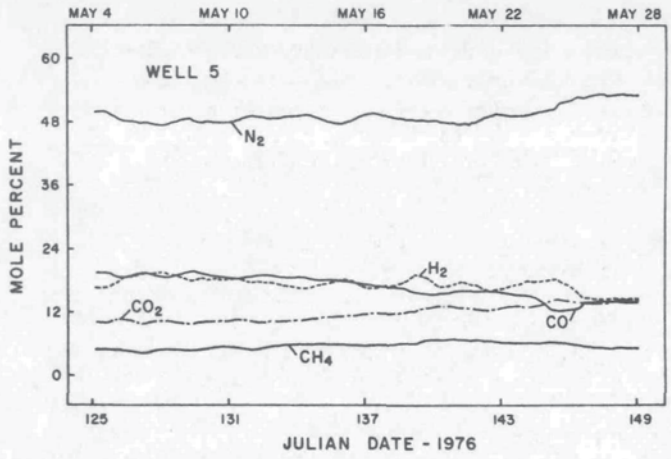


Figure 9 - Product Gas Composition, Phase II, Hanna II.

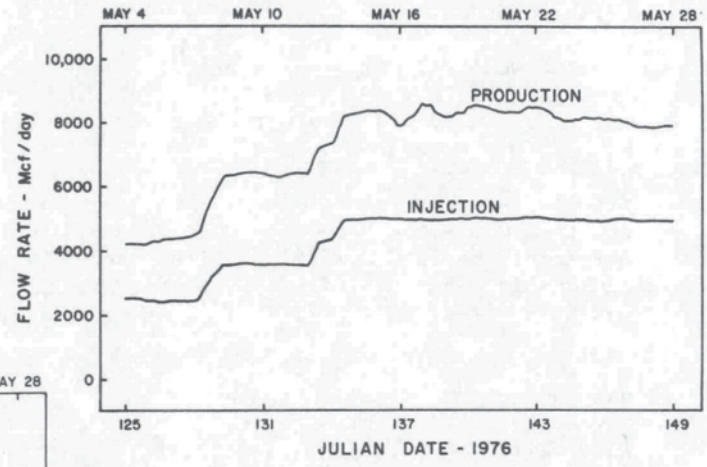


Figure 10 - Injection and Production Rates, Phase II, Hanna II.

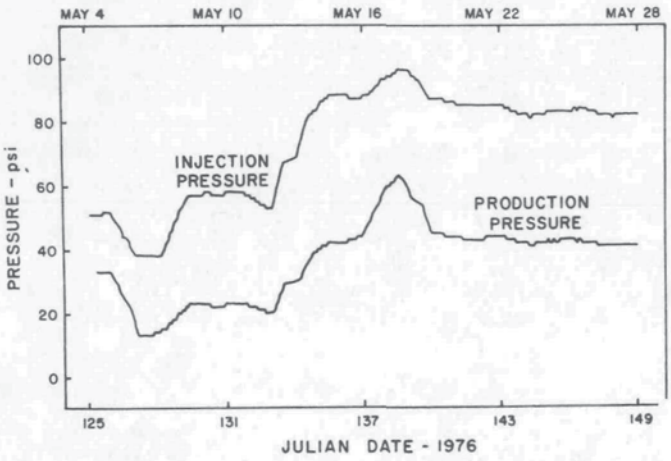


Figure 11 - Injection and Production Pressures, Phase II, Hanna II.

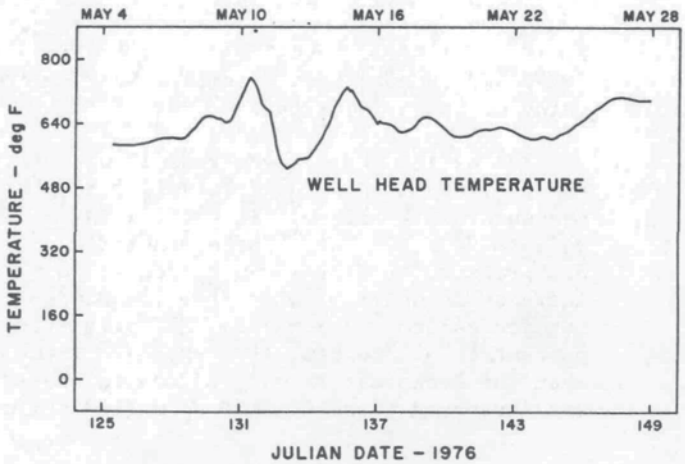


Figure 12 - Product Gas Temperature at Well 5, Phase II, Hanna II.

at Well 6 continued to increase during this time. Approximately 2.6 MM scf (7.78×10^4 m^3) of air were injected during the linkage, which is additional evidence that the linkage was a channel rather than a broad front. It was decided at this time to reduce the reservoir pressure from 230 psig (1.59×10^6 Pa) to 5 or 10 psig (3.45×10^4 to 6.9×10^4 Pa) to reduce the potential for leakage. The pressure drop through the reservoir at this time was 20 psig (1.38×10^5 Pa).

Air injection was ceased on June 5 and the system was allowed to bleed down. When the system reached 3 psig (2.07×10^4 Pa) and stabilized, a series of tests to determine where the linkage was located was begun. By injecting and producing various combinations of wells, it was determined that the linkage was on the Well 8 end of the 7-8 linkage path and that there was combustion along this path. It was decided to inject into Well 8 and produce Well 7 to increase the temperature along the linkage path bringing the coal surrounding Well 7 up to combustion temperature, and then to switch injection into Well 7 to drive a forward burn from existing combustion zones at both 7 and 8 towards Wells 5 and 6.

The wellhead temperature at Well 7 rose to 722° F (383° C) on June 16 and injection into both Wells 7 and 8 was begun. Initial injection was unbalanced, i.e., more air was injected into 7 than 8 to compensate for the closer proximity of the link and fire to Well 8. After a few hours of injection it became apparent that efficient gasification was not occurring. Gas compositions indicated primarily that carbonization was taking place. Temperatures in Wells H and I also started a downward trend. It appeared that ignition was not achieved at Well 7 in spite of what appeared to be favorable conditions. Air injection into Well 8 was first decreased and then ceased in an effort to improve gas quality, but the effort was unsuccessful. About 680 tons (617 tonnes) of coal were gasified during this period.

In view of the high resource recovery from the two well pattern (5-6 gasification) and the apparent failure to initiate the line drive, it was decided on June 21 to investigate the results of two 2-well burns side by side. Accordingly air injection into Well 8 was begun on June 22 with production from Well 7.

Gasification from Well 8 to Well 7

Operating conditions were deliberately varied during Phase III to study the effects of various operating parameters as well as the controllability of the process. Thus, while a direct comparison of two parallel gasifications was precluded, further insight into the UCG process itself was possible. Because of the voluminous amount of data acquired, full interpretation of the results has not yet been made. However, some effects are visibly discernible and some preliminary conclusions can be drawn from the test.

The production and injection rates, gas composition, injection and production pressures, production wellhead temperature, and gross heating value are shown in Figures 14-18. The trends exhibited by these results contrast with those in Phase II (Figures 9-13) and in some ways resemble the results of Phase I [7], especially in the heating value of the product gas.

The gasification began June 22 with injection into Well 8 at about 2500 scfm (74.8 scm/min) and production from Well 7 of about 4300 scfm (129 scm/min). The injection pressure was about 50 psig (3.45×10^5 Pa) while the production pressure was about 13 psig (8.96×10^4 Pa). These conditions were maintained until June 27, when the backpressure at Well 7 was raised to 50 psig (3.45×10^5 Pa). This was followed by an increase in heating value from 166 Btu/scf (5.85 megajoules/scm) to 185 Btu/scf (6.52 megajoules/scm) (Figure 18), due primarily to an increase in methane content from 4.0 percent to 5.5 percent (Figure 15). These conditions were maintained until June 29 when the backpressure was reduced to about 15 psig (1.03×10^5 Pa). The injection rate was increased to about 3450 scfm (103 scm/min). By July 1 the system had stabilized

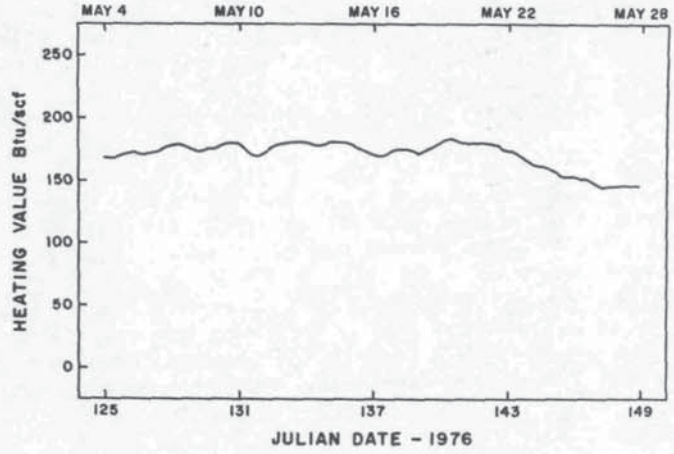


Figure 13 - Product Gas Cross Heating Value, Phase II, Hanna II.

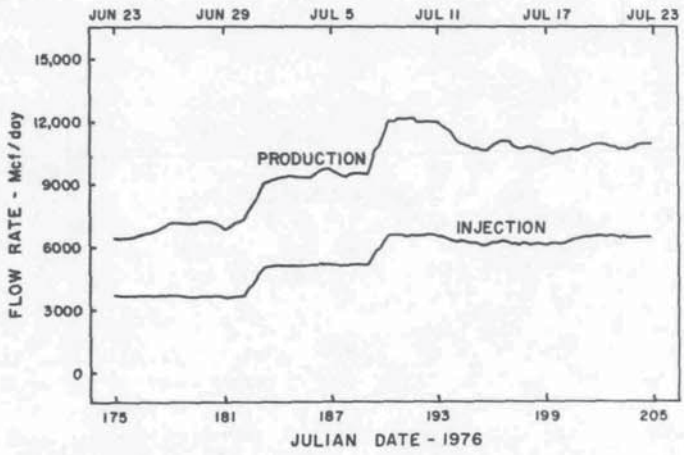


Figure 14 - Injection and Production Rates, Phase III, Hanna II.

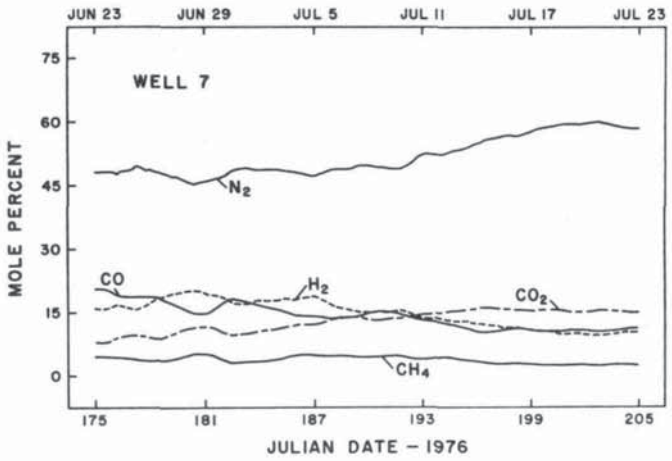


Figure 15 - Product Gas Composition, Phase III, Hanna II.

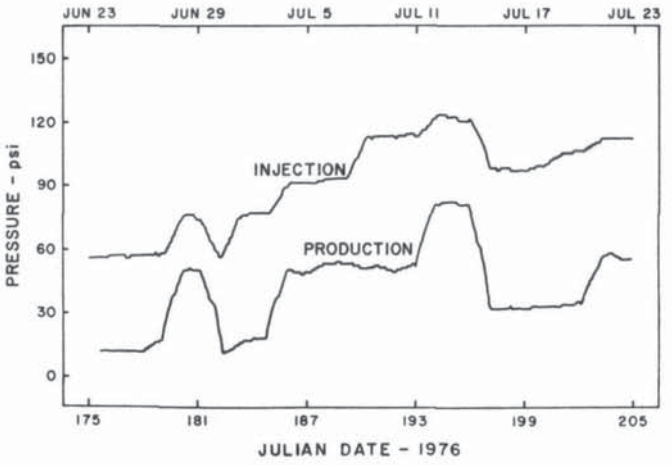


Figure 16 - Injection and Production Pressures, Phase III, Hanna II.

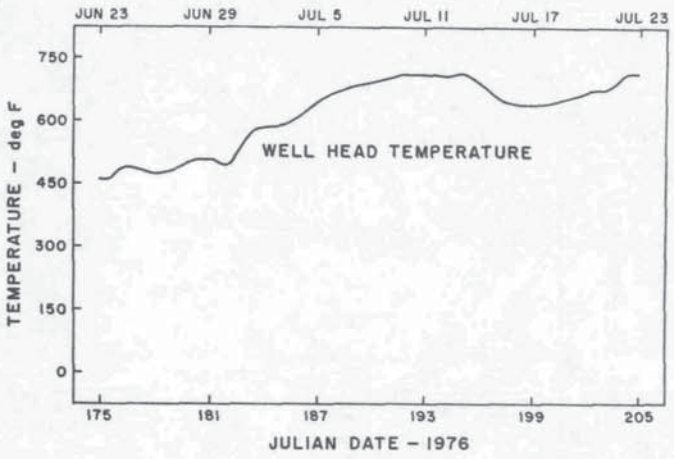


Figure 17 - Product Gas Temperature at Well 7, Phase III, Hanna II.

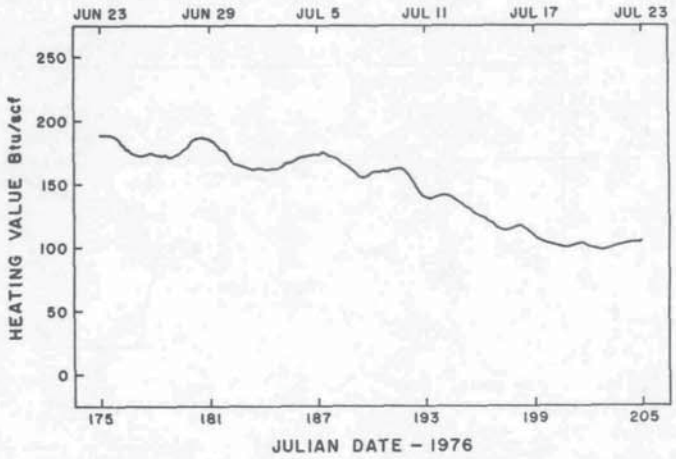


Figure 18 - Product Gas Cross Heating Value, Phase III, Hanna II.

and the product gas showed a heating value of about 165 Btu/scf (5.82 megajoules/scm), primarily due to the methane content having returned to about its former value of 4.0 percent. During the high pressure period, the carbon monoxide content dropped while the hydrogen and carbon dioxide content increased (Figure 15), which shows evidence of the water-gas shift reaction affecting the process.

On July 3 the system was again backpressured to about 50 psig (3.45×10^5 Pa) with the injection rate remaining constant. Again the heating value increased as the methane content, hydrogen and carbon dioxide contents increased, although none quite as high as during the previous increased pressure period. Although the rates and pressures remained essentially constant for the next few days, the product gas composition did not; the carbon monoxide content continued to decrease and the carbon dioxide content simultaneously increased, as Figure 15 shows.

Although the product gas composition showed no signs of stabilizing, it was decided to see what effect an increase in injection rate might have. Accordingly, on July 7 the rate was increased to about 4500 scfm (135 scm/min) with the backpressure of 50 psig (3.45×10^5 Pa) being maintained. The immediate effects were an increase in carbon monoxide content with an attendant decrease in carbon dioxide content and arresting of the decline in hydrogen content. The system remained stable for about two days, whereupon the carbon monoxide and hydrogen contents began to decrease with an attendant decrease in heating value and an increase in the carbon dioxide content.

The injection rate remained at about 4500 scfm (135 scm/min) for the rest of the test, but on July 11 the backpressure was increased from 50 to 80 psig (5.52×10^5 Pa) to see if the methane content could again be increased. A slight arresting of the heating value decline (Figure 18) was produced but it was short lived. Due to mechanical problems with the compressor system and the observed lack of improvement in gas quality, it was decided on July 14 to reduce the backpressure. Injection decreased slightly to about 4200 scfm (126 scm/min) when the backpressure was reduced to 30 psig (2.07×10^5 Pa), but these conditions were maintained for the rest of the experiment. It was felt desirable to increase the injection rate during this time to maintain gas quality but surface capabilities were unequal to the task. Gas quality continued to decline until about July 18, when the heating value stabilized at about 100 Btu/scf (3.52 megajoules/scm). From July 18 through July 30, when air injection was terminated, the heating value further declined to 80 to 90 Btu/scf (2.8 to 3.2 megajoules/scm). Upon termination all instrumentation in Wells H, I, J, K, L, and M had been destroyed.

The coal utilization during the 7-8 gasification period was 3490 tons (3167 tonnes). The total coal utilized during Phases II and III was 6690 tons (6070 tonnes). This is significant when one considers that the 60 by 60 feet (18.4 by 18.4 m) pattern contained only 4600 tons (4170 tonnes).

COMPARISON OF THE 5-6 AND 7-8 GASIFICATION PERIODS

Examination of the data from Phases II and III shows obvious dissimilarities. The difference in gross heating value performance (Figures 13 and 18) has already been mentioned. Further differences appear in the cold gas efficiencies (defined as the calculated dry gas production rate based on a nitrogen balance multiplied by the gross heating value divided by the total Btu content of the coal utilized as determined by material balance calculations, i.e., the heat of combustion of the product gas divided by the energy available in the coal gasified) and in the water-produced to coal-utilized ratio, where the water produced was calculated by subtracting the calculated dry gas production rate from the measured production rate and assuming the difference to be water vapor with the coal tars being neglected. This produced water reflects the original water present in the coal seam, the water of combustion (which is assumed negligible), water influx during gasification, and the water of carbonization.

As Figure 19 shows the gas quality and cold gas efficiency remained reasonably constant during Phase II until near the end of the 5-6 gasification period and the produced water-coal utilized ratio remained low until the same period.

In contrast, the data plotted in Figure 20 shows a higher initial water-produced to coal-utilized ratio during the 7-8 burn when compared with the 5-6 burn with a dramatic increase when the backpressure was reduced from 80 to 30 psig (5.52×10^5 to 2.07×10^5 Pa). The cold gas thermal efficiency and gross heating value were decreasing prior to this but dropped significantly after July 14, 1976.

The water influx rate, which should have increased as the surface area of the underground cavity increased, was apparently not the major cause of the gas quality decline near the end of Phase II (5-6 gasification). It appears that the injection rate was too low and should have been increased to maintain the air/water ratio.

Conversely, the water influx rate during the 7-8 burn did apparently cause the dramatic drop in thermal efficiency and heating value observed after July 14. Field measurements of weight percent water in the product gas stream show a significant increase after that time (Figures 21 and 22). Figure 21 compares the measured with the calculated weight percent water and Figure 22 the water content with backpressure.

The effect of increased water influx does appear to be partially controllable by increasing the injection rate or by increasing the backpressure, but further tests will be necessary to confirm this preliminary judgment.

Based on this comparison, a process control system based on measured water content in the product gas stream appears feasible. It would appear that completion of further planned tests to better determine a critical value for the ratio of produced water to coal utilized could yield control through a programmed injection rate to maintain this ratio below that critical value.

The sensitivity of resource utilization to air injection rate has also been indicated. During Phase II the maximum injection rate was 3500 scfm (105 scm/min) whereas during Phase III the maximum was 4500 scfm (135 scm/min). The material balance calculations show 2520 tons (2286 tonnes) utilized during Phase II and 3490 tons (3166 tonnes) during Phase III. Confirmation of this judgment awaits further seismic and coring evaluation to determine the differences between Phases II and III, but it appears that sweep efficiency is a function of flux rate.

FUTURE TESTING

Hanna III has been proposed as a 9-well pattern on 100 and 150 feet (30.5 and 45.7 m) spacings (Figure 23). Initial injection rates will be linearly scaled from Hanna II, e.g. for 100 feet (30.5 m) spacing the initial injection rate will be 1.67 times the maximum used in Hanna II. Excess air injection capacity will be on hand to allow injection of at least 50 percent more than the linear scaling calculation, should the data indicate the need. The injection rates will be computer controlled to gain experience valuable for pilot plant operations.

The conduct of an experiment of this size will also add information on one unknown variable--subsidence. The timing of subsidence could seriously affect the success of UCG. To date no subsidence to the surface has been observed at Hanna although coring of the Hanna I site has shown roof collapse up to 30 feet (9.1 m) above the coal seam. Russian experiments have shown that subsidence can be a major problem [9] because of gas leakage. Therefore, before UCG can be considered a viable process, the effects of subsidence on the process - both from a technical as well as an environmental viewpoint - must be determined.

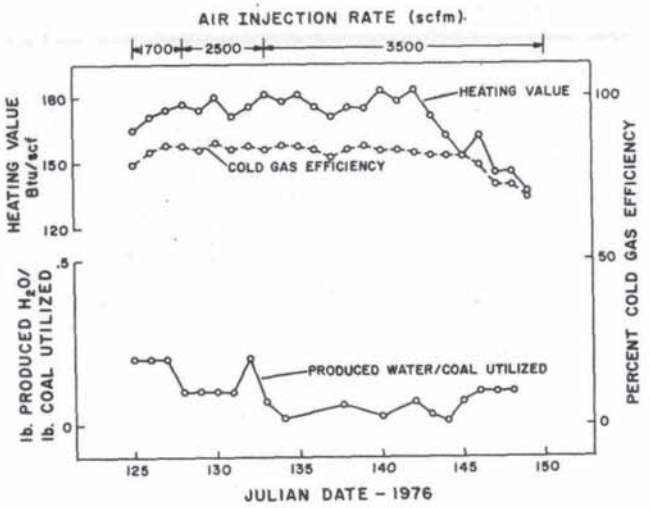


Figure 19 - Effects of Water Influx on Phase II, Hanna II, Results

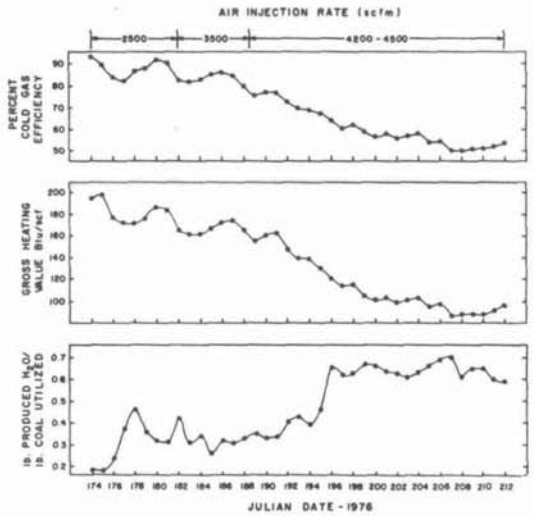


Figure 20 - Effects of Water Influx on Phase III, Hanna II, Results

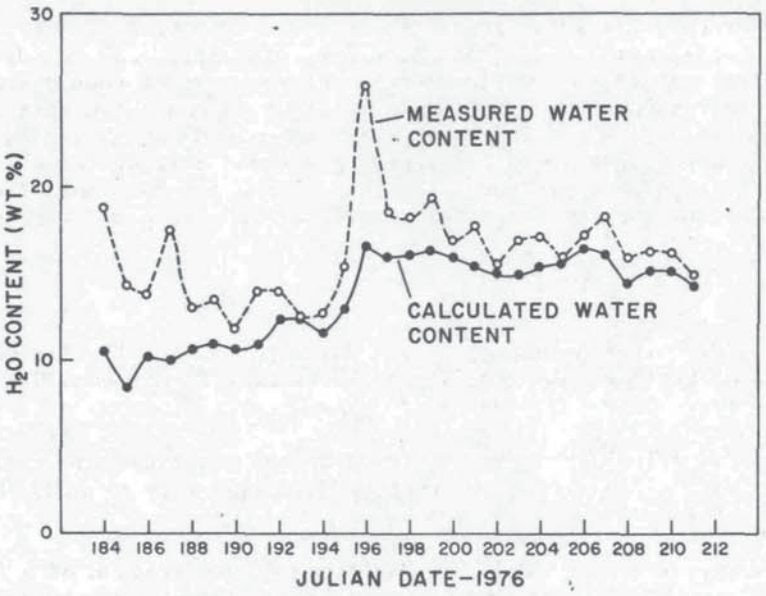


Figure 21 - Comparison of Measured and Calculated Water Content in Product Gas, Phase III, Hanna II.

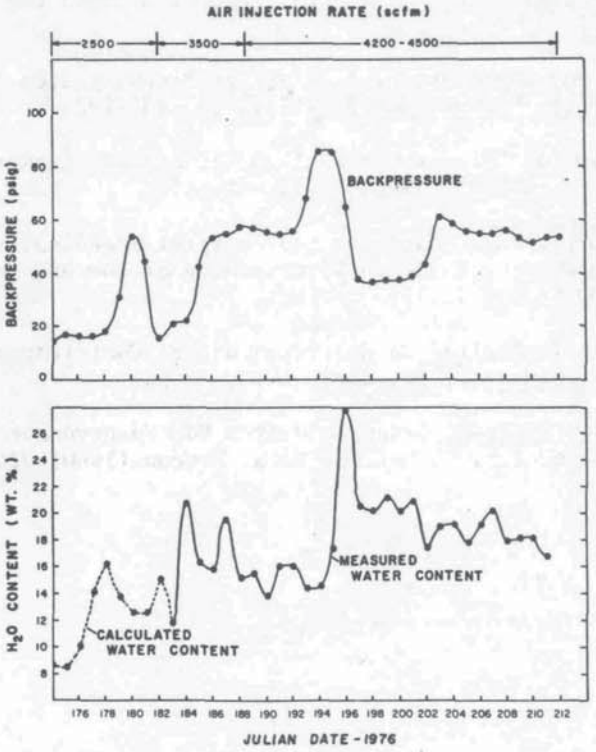


Figure 22 - Effect of Backpressure on Product Gas Water Content, Phase III, Hanna II.

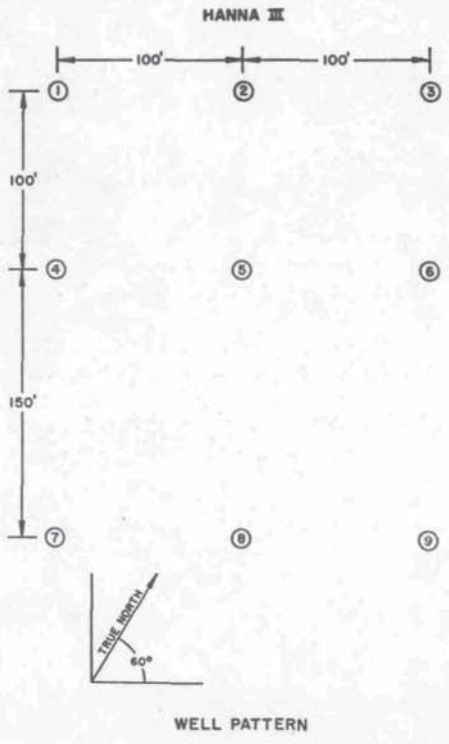


Figure 23 - Proposed Well Pattern for Hanna III.

STATUS OF THE LINKED VERTICAL WELL (LVW) PROCESS

The LVW process has shown remarkable success. The gas quality, thermal efficiency, and resource utilization efficiency have been extremely good. Additional testing to refine critical values for use in process control systems should ready the process for pilot plant operations. The completion of Hanna II has shown that operation of simultaneous two-well systems is the preferred method. High values of resource utilization can be achieved. Stable product gas gross heating value can be attained. Process control can be exercised. The LVW UCG process has shown itself to be a system worthy of consideration as a valuable source of low-Btu gas for meeting future U.S. power demand.

REFERENCES

1. Campbell, G. G., Brandenburg, C. F., and Boyd, R. M., "Preliminary Evaluation of Underground Coal Gasification at Hanna, Wyoming," BuMines TPR 82, October 1974, 14 pp.

2. Schrider, L. A., et al., "An Underground Coal Gasification Experiment, Hanna, Wyoming," SPE 4993, presented at the SPE Fall Meeting of AIME, Houston, Tex., Oct. 6-9, 1974, 25 pp.

3. Brandenburg, C. F., et al., "The Underground Gasification of a Subbituminous Coal," presented at the Div. of Fuel Chemistry, Am. Chem. Soc. National Spring Meeting, Philadelphia, Penn., April 1975, 11 pp.

4. Fischer, D. D. and Schrider, L. A., "Comparison of Results from Underground Coal Gasification and From a Stirred Bed Producer," presented at the National AIChE Meeting, Houston, Tex., Mar. 16-20, 1975, 34 pp.

5. Fischer, D. D., Brandenburg, C. F., and Schrider, L. A., "Energy Recovery from In Situ Coal Gasification," Energy Sources, Vol. 2, No. 3 (1975), pp. 281-292.

6. Schrider, L. A., et al., "The Outlook for Underground Coal Gasification," presented at the 1975 Lignite Symposium, Grand Forks, N. D., May 1975, 32 pp.

7. Brandenburg, C. F., et al., "Interpretation of Chemical and Physical Measurements From an In Situ Coal Gasification Experiment," SPE 5654, presented at the SPE Fall Meeting of AIME, Dallas, Tex., Sept. 28-Oct. 1, 1975, 28 pp.

8. Stoller, H. M., "In Situ Instrumentation Applied to Underground Coal Gasification," SAND-75-0459, Sandia Laboratories, Albuquerque, NM, Sept. 1975, 31 pp.

9. Skafa, P. V., Underground Gasification of Coal, Translated from Gosudarstvennoe Hauchno-Tekhnicheskoe Izdatel'stvo Literatury Po Gornomu Delu, Moscow (1960) 324 pp.

UTILIZATION OF LOW BTU GAS FROM IN-SITU COAL GASIFICATION FOR ON-SITE POWER GENERATION

by

R. E. D. STEWART
SANDIA LABORATORIES, ALBUQUERQUE, NEW MEXICO 87115

ABSTRACT

System studies are conducted which address the technological and economic aspects of utilization of low BTU gas from in-situ coal gasification for on-site power generation. Gas cleanliness requirements are established, and the applicability of commercially available gas cleaning processes/equipment is discussed. A parametric study of the thermodynamic efficiency of several power cycle configurations with various fuel inlet conditions and operating parameters is conducted. A typical low BTU fuel gas composition/heating value is assumed. The sensitivity of system performance to variations in fuel gas composition/heating value and production rate is also investigated, and some possible techniques for minimizing system sensitivity to such variations are discussed. A preliminary economic analysis using the discounted cash flow method is carried out to assess the relative economics of the various design alternatives for an integrated in-situ gasification/on-site power generation plant. Based on the results of the performance and economic evaluations, a conceptual integrated system design is established, and areas requiring further investigation are identified.

INTRODUCTION

Since the fall of 1972, ERDA has been conducting a series of experiments to investigate the technologic, economic, and environmental feasibility of underground gasification of a western subbituminous coal. The experiments are being conducted at a site near Hanna, Wyoming under the direction of the Laramie Energy Research Center (LERC). The experimental results to date have been generally successful, with sustained production rates of a few million SCF of gas per day with a heating value of 125-150 BTU/SCF [1, 2]. So far, all gas produced has been flared.

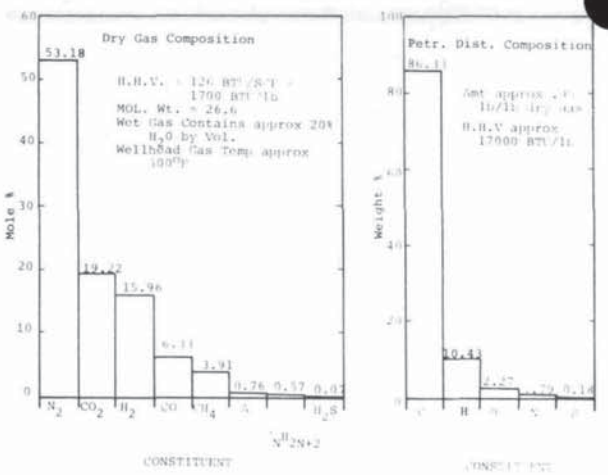
The system studies presented in this paper were initiated to assist LERC in the development of a conceptual pilot plant design which would utilize this low BTU gas for on-site power generation. The relative performance and economics of various potential design alternatives have been assessed, and areas where additional study and/or experiment may be required have been identified. The system studies are divided into four major areas, (1) fuel cleaning and purification considerations, (2) combustion thermodynamics and power cycle analysis, (3) cost estimates and economic analysis, and (4) conceptual integrated system design.

FUEL CLEANING AND PURIFICATION

GAS CHARACTERIZATION

A typical composition of the low BTU gas generated by the Hanna 1 experiment is given in Figure 1 [1]. Wellhead gas temperature and pressure for the Hanna 1 experiment were approximately 500°F and slightly above atmospheric pressure. The heating value of the dry gas averaged ~ 126 BTU/SCF. In addition to the dry components, the wellhead gas contained ~ 20% water vapor by volume (.169 lbs H_2O/1b of dry gas), .005 1b of petroleum distillate vapors per 1b of dry gas, and some entrained particulates. Recently completed particulate characterization tests indicate that while the average amount of particulates entrained in the gas flow is quite low, it is highly variable, with relatively large amounts occurring over brief time intervals [3].

Fig. 1 - Typical Low BTU Gas Characterization*



*Based on Hanna #1 Expr. March '73 - May '74

FUEL CLEANLINESS REQUIREMENTS

Fuel cleanliness requirements for power plants stem from two different sources; pollution regulations, and gas turbine limitations. Figure 2 summarizes maximum allowable levels of particulates, sulfur compounds, and trace metals. The following observations should be noted: (1) Local emission limits, where they exist, may be significantly tighter than the federal limits. This is illustrated using New Mexico as an example. (2) There are currently no particulate or SO_2 emission regulations, either state or federal, on gas fired power plants. This is due to the fact that, historically, gas fired plants have utilized clean natural gas. However, proliferation of coal gasification plants, both in-situ and above ground, can be expected to generate new and tighter regulations such as the one already proposed by the state of New Mexico. (3) Fuel sulfur limits will be dictated by SO_2 emission regulations. For the Hanna 1 gas, the sulfur, which is principally in the form of H_2S, is typically slightly under that permitted by federal emission regulations for coal fired power plants, but is significantly greater than that proposed for coal gasification plants in New Mexico. (4) In power plants utilizing the low BTU gas as a gas turbine fuel, maximum allowable particulate and trace metal contaminant levels will be dictated by gas turbine limitations. Note that the specific values given in Figure 2 apply to the gas turbine expansion gases rather than the fuel. The relation between allowable fuel contaminant concentration and allowable turbine expansion gas contaminant concentration, assuming clean air, is

Fig. 2-GAS CLEANLINESS REQUIREMENTS[1]

	PARTICULATES			SULFUR COMPOUNDS[2]			TRACE METALS
	FEDERAL	N. MEX.	TURBINE	FEDERAL	N. MEX.	TURBINE	TURBINE
COAL FIRED	0.1[3]	0.05	MAX SIZE = 10 0-10 ~ FEW PPM[4]	1.2[5]	0.34	NO LIMITATION	$N_a + K \leq .04$ PPM
OIL FIRED	NO REG.	0.005		0.8	0.34		$V \leq 0.04$ PPM[6]
GAS FIRED	NO REG.	NO REG.		NO REG.	NO REG.		$P_b \leq 0.10$ PPM
PROPOSED FOR GASIFICATION PLANTS	NO REG.	0.03		NO REG.	0.10		$C_a \leq 0.20$ PPM

(1) FOR NEW SOURCES AFTER 1973 (ALL UNSPECIFIED UNITS = LB/10^6 BTU)
(2) EMISSION LIMITS ARE FOR SO_2
(3) 0.1 LB/10^6 BTU ~ 0.0875 GR/SCF OF DRY GAS ASSUMING H.V. OF 126 BTU/SCF
(4) 10 PPM ~ 0.005 GR/SCF OF DRY GAS ASSUMING H.V. OF 126 BTU/SCF AND MOL. WT. OF 26.6
(5) 1.2 LB SO_2/10^6 BTU ~ .084 H_2S BY VOL. ASSUMING H.V. OF 126 BTU/SCF
(6) SIGNIFICANTLY HIGHER LEVELS OF V CAN BE TOLERATED BY USING Mg ADDITIVES

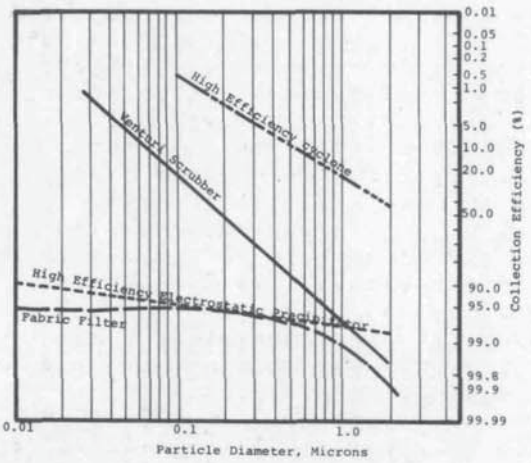
$$X_F = (1 + A/F)X_G ,$$

where X_F and X_G are the allowable contaminant concentrations in the fuel and turbine expansion gases respectively, in PPM by weight, and A/F is the air-fuel ratio on a mass basis.

FUEL CLEANING/PURIFICATION EQUIPMENT

There are four major types of particulate removal equipment. These are 1) cyclones, (2) scrubbers, (3) filters, and (4) precipitators. Figure 3 provides typical performance data comparisons for each of the four types of particulate removal apparatus [10, 11]. The following general statements apply. (1) Even the most efficient cyclones have relatively poor efficiency for particulates smaller than 5 to 10 microns, and thus are inadequate for cleaning gases for use in a gas turbine. Any of the remaining three types of particulate removal apparatus could be used. (2) Electrostatic precipitators work best when particulates are of a single type and a relatively uniform size, density, and concentration, which is not the case with in-situ gasification.[3]. Scrubber and baghouse performance are unaffected by such variations. (3) Scrubbers have the lowest installed cost, but the highest operating costs. (4) Baghouses have the highest efficiency, and also the highest maintenance cost, primarily because of the requirement for periodic bag replacement. (5) Electrostatic precipitators have the lowest total annualized cost. (6) High efficiency venturi scrubbers require water circulation rates of ~ 10 gal per actual ft^3 of gas scrubbed. A portion of this water flow must be either filtered or discarded and replaced with clean water as required to prevent the concentration of suspended solids from exceeding ~ 5% by weight. (7) Venturi scrubbers can provide simultaneous gas cleaning and cooling when this is desirable. (8) Venturi scrubbers are much smaller physically than either precipitators or baghouses. Because of their relatively small size they can be designed to handle gases at elevated pressures with little additional expense. This is not true of precipitators and baghouses.

Fig 3-Performance of Particulate Removal Apparatus



There are a very large number of gas purification processes for H_2S removal [12, 13]. Figure 4 lists and characterizes some of the more important ones. Based on this information and discussions with various process engineers, the Stretford process appears to be a prime candidate for the application of interest. Three major reasons are: (1) The process is highly selective to H_2S in the presence of the large quantity of CO_2 present in the low BTU gas, (2) it produces elemental sulfur directly as an end product rather than H_2S, which would require further processing via a Claus plant to convert it to elemental sulfur, and (3) the economics are favorable. A possible disadvantage of the Stretford process is the fact that the temperature of the gas being purified cannot exceed ~ 120°F.

Fig. 4–PROCESSES FOR H_2S REMOVAL

PROCESS	WET vs DRY	CHEMICAL vs PHYSICAL	H_2S SELECTIVITY	PRODUCT	TEMP. (°F)
• Solid Adsorbents	↑		↑		↑
• Iron Oxide	DRY	Chemical	Excellent	H_2S	Ambient
• Activated Carbon		Physical		S	
• Molecular Sieves	↓	Physical	↓	H_2S	↓
• Iron Oxide Suspensions	↑	↑	↑	↑	↑
• Ferrox	Wet	Chemical	Excellent	H_2S	Ambient
• Gluud					
• Manchester	↓	↓	↓	↓	↓
• Amine Solutions	↑	↑		↑	↑
• MEA, DEA		Chemical			
• TEA, MDEA	Wet		Poor	H_2S	Ambient
• ADIP			Fair		
• Sulfinol	↓	Chem. & Phys	↓	↓	↓
• Alkaline Salt Solutions	↑	↑	Poor	H_2S	70-400
• Tripotassium Phosphate			↓	↓	↓
• Benfeld					
• Catacarb	Wet	Chemical	Fair		Ambient
• Alkazid			Good	S	
• Stretford					↓
• Takahax	↓	↓	↓	↓	70-300
• Giammarco-Vetrocoke					
• Organic Solvents	↑	↑		↑	
• Rectisol			Good		
• Purisol	Wet	Physical	↓	H_2S	LO
• Selexol					Ambient
• Fluor Solvent	↓	↓	Fair	↓	↓

COMBUSTION THERMODYNAMICS AND POWER CYCLE ANALYSIS

PARAMETRIC EFFICIENCY ANALYSIS

Thermodynamic efficiency calculations were carried out based on the Hanna 1 fuel gas composition in conjunction with various power cycle configurations. Included were (1) a Brayton (gas turbine) cycle, with and without regeneration, reheat, and/or intercooling, (2) a Rankine (steam turbine) cycle, and (3) a combined cycle. The combined cycle utilized an unfired waste heat boiler to generate steam for the Rankine portion of the cycle. Gas turbine compression ratio and inlet temperature were treated as parameters with values ranging from 4 to 30 and 2000°F to 3000 F, respectively. Fuel supply temperature and pressure were also varied to determine the effect on overall system performance of gasifying at elevated pressures and/or conserving the sensible heat in the wellhead gas. Figure 5 summarizes the major results of the parametric efficiency study. In each case the power conversion cycle was charged with the energy required to compress the injection air needed for the gasification process. The following important points should be noted: (1) Results for regenerative Brayton cycles with more than one stage of intercooling and/or one or more stages of reheat did not differ appreciably from those obtained with one stage of intercooling. (2) Peak cycle efficiency increases signficantly with increasing turbine inlet temperature for all cycles. (Maximum turbine inlet temperature of commercially available gas turbines is ~ 2000°F, but is expected to approach 3000°F by 1985-1990 [14]. Peak steam temperature for commercially available steam turbines is currently 1000-1200°F and is not expected to increase significantly in the near future [15].) (3) The difference in cycle efficiency between low pressure cold (LPC) and high pressure hot (HPH) fuel gas inlet conditions is ~ 4-6 percentage points for all cycles except the conventional steam cycle whose efficiency is essentially unaffected by fuel inlet conditions. (4) The difference in cycle efficiency between low pressure cold (LPC) and high pressure cold (HPC) fuel gas inlet conditions, which is indicative of the incentive for gasification at elevated pressure, is significantly greater for regenerative cycles than for non-regenerative cycles. (In non-regenerative cycles, the work required to compress the low pressure fuel gas is used effectively to heat the fuel gas entering the combustion chamber, whereas in regenerative cycles the temperature of the fuel gas leaving the regenerator and entering the combustion chamber is only slightly affected by the temperature of the fuel gas entering the regenerator.) (5) For any given fuel inlet conditions and turbine inlet temperature, a regenerative gas turbine cycle yields a significantly higher efficiency than a simple gas turbine cycle. (6) For any given fuel inlet conditions and turbine inlet temperature, the efficiency of the combined cycle does not differ significantly from that for a regenerative gas turbine cycle with one stage of intercooling. (7) Peak efficiencies for regenerative and combined cycles occur at significantly lower compression ratios than those for simple gas turbine cycles.

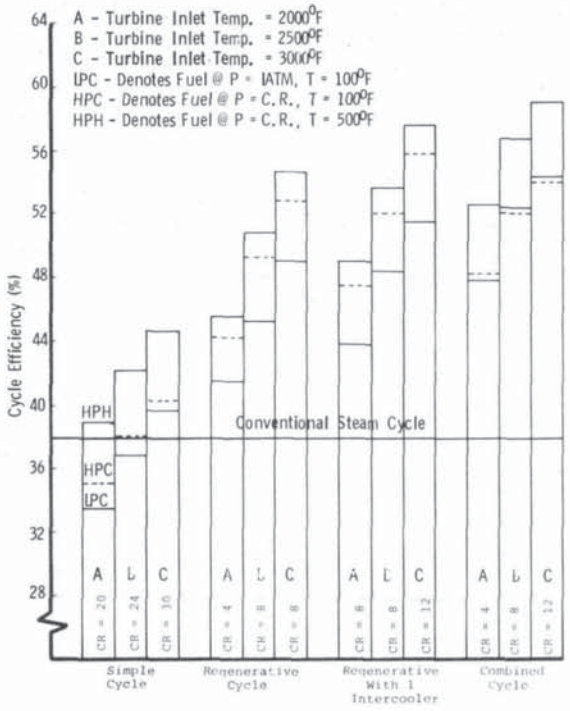


Fig. 5 - Approximate Peak Cycle Efficiencies for Various Cycle Configurations, Fuel Inlet Conditions, & Turbine Inlet Temperature Based on Hanna 1 low BTU Fuel Gas

SENSITIVITY ANALYSIS

While Figure 1 provides a typical fuel gas composition for the Hanna 1 experiment, mean fuel heating values averaged over successive two week intervals varied between - 48% and +31% from the average over the entire 5-1/2 month duration of the experiment [1]. Furthermore, the mean value of the ratio of gas produced to air

injected for successive two week intervals varied between -17% and + 9% from its average over the entire 5-1/2 month period. In view of this, calculations were carried out to determine the sensitivity of the performance of a simple cycle gas turbine to variations in fuel heating value and/or gas production-to-air injection ratio. The results indicate that a ±20% variation in fuel heating value will result in a ±250°F variation in combustion temperature, and a ±2 to 3 percentage point variation in cycle efficiency, provided no compensating adjustments in air or fuel flow rates are made. Similar results are obtained if the ratio of fuel gas produced to air injected is assumed to change by ±20% without any compensating adjustments. These numbers are large enough to be of concern. A 3% change in efficiency represents a significant change for a system being used for base load power generation. Also, a 250°F increase in turbine inlet temperature could significantly affect turbine blade life. Thus some technique to compensate for expected fluctuations in fuel composition/heating value and/or gas production-to-air injection ratio is required.

One potential technique for compensating for fuel gas fluctuations would be to utilize a feedback control system which would monitor certain system parameters, e.g., turbine inlet (or exhaust) temperature, fuel composition, etc., and use this information to regulate system flow rates. In fact, commercial gas turbine control systems utilize this technique, and are normally capable of handling fluctuations in inlet air and fuel conditions of ±10%, provided the changes do not occur too abruptly [16]. However, with in-situ gasification, there is a time lag between any change in air injection rate and the resulting change in fuel gas production rate. A simple mathematical analysis shows that this time lag renders control systems utilizing some of the simpler feedback control functions unstable. Additional analysis is needed to determine how this instability problem might best be handled.

Another potential technique for averaging out, at least to some extent, undesirable fluctuations in gas composition, heating value, and gas production rate would be to manifold the output from multiple gas generators before routing the fuel to the turbine. For example, assuming n independent in-situ gas generators each with output X_i, which is assumed to be normally distributed with mean μ_x and standard deviation σ_x, the average of these outputs, $y = 1/n \sum X_i$, will be normally distributed with mean $\mu_y = \mu_x$ and standard deviation $\sigma_y = \sigma_x/\sqrt{n}$. Thus, if X_i denotes heating value, and we set $\mu_x = 130$ BTU/SCF and $\sigma_x = \mu_x/6 = 21.67$ BTU/SCF*, then $n = 25$ is required to reduce the 3σ limits on y to ±10% of μ_y. Manifolding of this number of in-situ gas generators does not seem unreasonable for a large base load power plant, and would simplify phasing in replacement gas generators as necessary without significantly perturbing the level of power generation.

A third possibility, assuming gasification at elevated pressure is feasible, would be to regulate the output of an in-situ gasifier at the wellhead so that the gasifier cavity would behave as a large underground storage tank with varying internal pressure. One could also utilize old burned out gasifiers as storage reservoirs, and blend the output of active gasifiers with that from storage reservoirs. Additional study is needed to determine the best approach.

POWER CYCLE ECONOMICS

In the final analysis, it is the cost of the various available power cycle options which determines which one will be chosen. Cycle efficiency is only one factor which affects total power plant cost. The higher the cycle efficiency, the lower the fuel cost for a given plant output. Other factors affecting total power plant cost are plant capital costs and plant maintenance costs.

The usual approach for comparing power plant economics is to estimate fuel, capital, and maintenance costs for each different power plant, and then calculate and compare the electrical generation cost of each. An accurate estimate of plant capital costs requires detailed cost estimates based on well defined plant designs

* i.e., $3\sigma_x = \mu_x/2$, which assumes that the heating value of the gas produced by any individual gas generator will be between 65 and 195 BTU/SCF 99.7% of the time.

and locations, and this is beyond the scope of the present study. Therefore, a slightly different approach has been taken in order to provide some assessment of the relative economics of the various power cycle configurations. The approach taken was to estimate all parameters other than plant capital costs, and then calculate and compare the allowable capital investments for the various plants.

The calculations were made using standard discounted cash flow analysis [17]. Some typical results are shown in Figure 6. In interpreting the results of Figure 6, one must bear in mind that the ordinate is a measure of how much one can afford to invest in plant capital -- it does not represent either actual or estimated plant costs. Thus the crossover point of the two bottom curves does not necessarily imply, for fuel costs greater than 60¢/10^6 BTU, that a conventional gas fired steam cycle is economically superior to a simple cycle gas turbine plant. What it means is that for fuel costs greater than 60¢/10^6 BTU, one can afford to invest more money in a conventional gas fired steam plant than for a simple cycle gas turbine plant. For example, at a fuel cost of \$1/10^6 BTU, one can afford to invest ~ \$21/KW more in a conventional gas fired steam plant than in a simple cycle gas turbine plant. However, if the actual capital cost of a gas fired steam plant on a per KW basis is more than \$21 higher than a simple cycle gas turbine plant, then the latter is economically preferable to the former. Similarly, at a fuel cost of \$1/10^6 BTU, Figure 6 indicates that one can afford to invest ~ \$50/KW more for a regenerative gas turbine cycle than for a simple gas turbine cycle. Therefore, if a regenerator costs less than \$50/KW, a regenerative cycle is economically preferable to a simple cycle, and vice versa. Thus, results such as those given in Figure 6 can enable one to choose from among the various cycle configurations without obtaining detailed cost estimates of all system components.

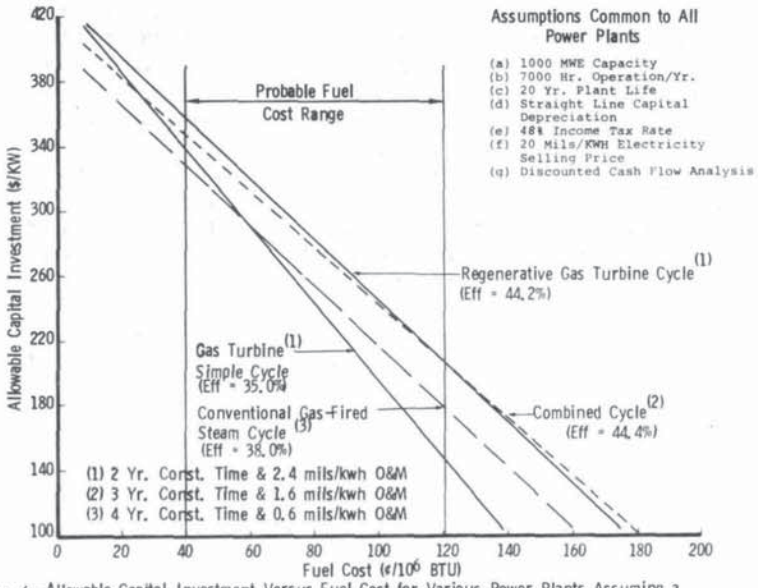


Fig. 6 - Allowable Capital Investment Versus Fuel Cost for Various Power Plants Assuming a Required Rate of Return of 15% on Capital Investment

CONCEPTUAL SYSTEM DESIGN

Based on the performance and economic considerations discussed above, the conceptual system design shown in Figure 7 has been synthesized. Referring to Figure 7, the low BTU gas generated by a number of individual in-situ gasifiers are manifolded to average out fluctuations in fuel gas composition, heating value, and production rate. A total of ~ 10^6 SCFM of dry gas needs to be generated for a 1000 MWE power plant. The wellhead gas is assumed to be produced at ~ 500°F and 10 atmospheres pressure*. The hot wellhead gas passes through a heat exchanger where it is cooled from ~ 500°F to ~ 280°F, which is still above its dew point, so that no water vapor condenses from the gas. The gas then enters the venturi scrubber, which removes any particulates, and also cools the gas to ~ 120°F, thereby resulting in condensation of most of the water and petroleum distillate vapors from the gas.

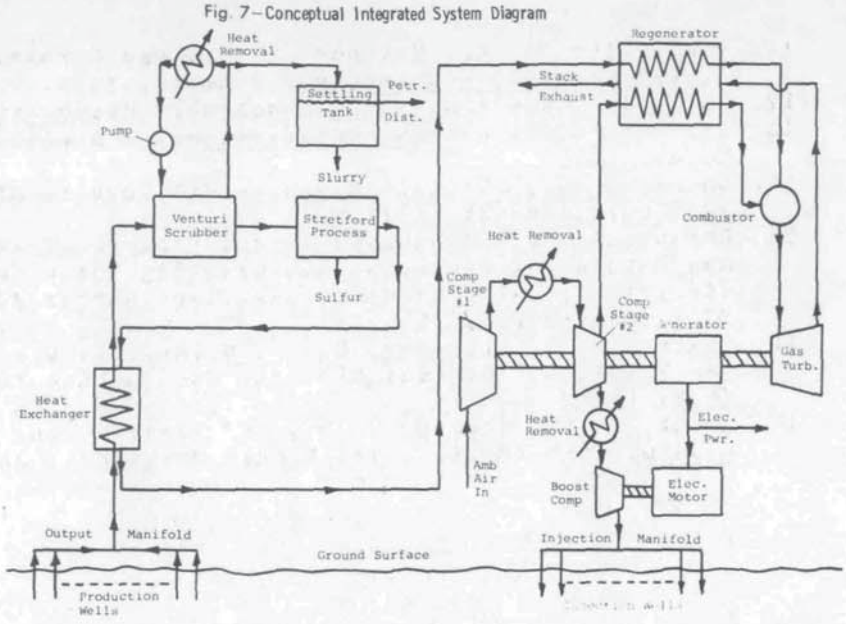
Heat is removed from the scrubber fluid flow loop by either an air cooler or a conventional cooling tower. (The same applies at other places in the system diagram where heat removal is indicated.) A fluid flow rate through the venturi scrubber of ~ 65,000 gal/min is required to cool and scrub the gas, assuming a 30°F fluid

* The feasibility of in-situ gasification at elevated pressure has not yet been demonstrated at the Hanna site.

temperature differential across the scrubber. The water (~ 1350 gpm) and petroleum distillates (~ 40 gpm) condensed from the gas stream by the scrubber is drawn off into a settling tank where the petroleum distillates are skimmed off, and the water/particulates slurry drained from the bottom of the settling tank and reinjected into the ground.

The clean saturated gas leaving the venturi scrubber at ~ 120°F is next processed for removal of the hydrogen sulfide and then routed back through the heat exchanger for sensible heat recovery. The gas leaves the heat exchanger at ~ 400°F and 10 atmospheres pressure, which constitute the fuel inlet conditions for the power cycle portion of the system.

Fig. 7—Conceptual Integrated System Diagram



The power cycle utilized is a regenerative gas turbine cycle with one stage of intercooling, a compression ratio of 10:1 and a turbine inlet temperature of 2000°F, consistent with currently available equipment. Approximately 13% of the air compressor output is routed through an aftercooler and booster compressor which boosts its pressure to 13 atmospheres* prior to injection for gasification. The calculated efficiency of the power cycle is ~ 48%.

* This assumes a 3 atmosphere pressure drop occurs across the in-situ gasifier which is consistent with results at lower gasification pressures.

REFERENCES

1. Fischer, D. D., Brandenburg, C. F., and Schrider, L. A., "Energy Recovery from In-Situ Coal Gasification," Laramie Energy Research Center, Laramie, Wyoming, 1974.
2. Schrider, L. A., Jennings, J. W., Brandenburg, C. F., and Fischer, D. D., "An Underground Coal Gasification Experiment,"Hanna, Wyoming, SPE 4993, Presented at The SPE Fall Meeting of AIME, Houston, Texas, Oct. 6-9, 1974.
3. Fischer, D. D., "Monitoring of Emissions from an In-Situ Coal Gasification Experiment," Laramie Energy Research Center, Laramie, Wyoming, 1976.
4. Fraas, A. P., "Survey of Turbine Bucket Erosion, Deposits, and Corrosion," ASME No. 75-GT-123, 1975.
5. Anon., "Fuel Specification - GT 73E, Revision E," Turbodyne Corporation, St. Cloud, Minnesota, Oct. 11, 1974.
6. Anon., "Plant Fuels & Lubricants - Fuels Specifications, Lubrication Specifications," Westinghouse Electric Corporation, Philadelphia, Pennsylvania.
7. Anon., "Gas Fuel Specification MS-57622," Westinghouse Electric Corp., Gas Turbine Systems Division, Lester, Pennsylvania, Jan. 6, 1975.
8. Vermes, G., "Standardization of Fuel Specifications," GTED Engineering, Westinghouse Electric Corp., Philadelphia, Pennsylvania, May 23, 1975.
9. Anon., "Specification for Gas Turbine Fuel Gases, GTS-60-1," General Electric Corporation, Schenectady, New York.
10. Anon., "Switch Back to Coal Puts Renewed Emphasis on Particulate Removal," Power, November, 1975.

11. Vandegrift, A. E., Shannon, L. J., and Gorman, P. G., "Controlling Fine Particles," Chemical Engineering, June 18, 1973.
12. Wall, J., "Gas Processing Handbook," Hydrocarbon Processing, April, 1975.
13. Riesenfeld, F. C., Gas Purification, 2nd Edition, Gulf Publishing Co., Houston, Texas, 1974.
14. Smock, R. W., "Utilities Battle Gas Turbine Maintenance Costs," Electric Light and Power, May 26, 1975.
15. Robson, F. L.,"Technological and Economic Feasibility of Advanced Power Cycles and Methods of Producing Nonpolluting Fuels for Utility Power Stations,"United Aircraft Research Laboratories, East Hartford, Connecticut, Distributed by NTIS, December, 1970.
16. Foster, A. D., Doering, H. E., Hickey, J. W., "Fuel Flexibility in Heavy-Duty Gas Turbines," General Electric Gas Turbine Products Div., Schenectady, New York, 1974.
17. Grant, E. L., Ireson, W. G., and Leavenworth, R. S., Principles of Engineering Economy, 6th Edition, The Ronald Press Co., New York.

NOTICE

Page Numbers 380 and 381 are not used in this report.

Missing Page
from
Original Document

Missing Page
from
Original Document

In-Situ Gasification In Australia; Prospects, Potential and Research Activities

by

I. McC Stewart, The University of Newcastle, N.S.W.

ABSTRACT

The industrial area of Australia has large cheaply mined coalfields close to industry and the coast. There are a number of deep, difficult or high sulphur seams which will only be workable by in-situ gasification. In South Australia and West Australia considerable proportions of the small coal reserves are only likely to be won by this method. Longer term cyclic or oxygen-steam gasification in-situ offers a high potential for low cost production of synthesis gas.

We are building up a research program based on the borehold system which avoids the channelling difficulties expectable in broken-bed systems. Computer analysis of the terminal reduction zone and of well stirred combustion zones indicates that a considerable minimum moisture content is desirable, that, particularly for moist coals, considerable reaction occurs within the coal bed and that either cyclic water-gas operation or cyclic oxygen-steam gasification offer potential for high efficiency with this system.

AUSTRALIAN COAL RESERVES

Australia is well endowed with coal. Large coal basins of bituminous coals extend along the Eastern coast.

In Queensland the major basin extends over two hundred miles north and south at from 60 to 100 miles from the coast. In N.S.W. the main basins extend from about a hundred and fifty miles of the central coastline inland north and west for about a hundred miles. There are large areas with a number of thick seams at less than a thousand feet deep suitable for low cost extraction by modern open-cast methods. In the South-east a very large basin of brown coal has major seams several hundred feet thick with comparatively low cover. Despite the high moisture content (65% wet basis) these coals are economically won by German up-cut dredger techniques and provide the basic energy source for the state of Victoria. The major ports and industrial developments in Australia are located reasonably close to the Victorian and N.S.W. coal fields while Queensland supplies a high proportion of our substantial coal export trade.

Natural gas resources supplying Queensland are negligible; for N.S.W., they will last about 25 years; for Victoria, they are somewhat more substantial.

The central southern state of South Australia is poor in energy resources. It shares the limited central Australian gas reserves with N.S.W. The limited reserves of coal are low grade lignites, some with difficult ash characteristics, and located in arid regions remote from any foreseeable load centres. There is a small but growing interest in the potential of in-situ gasification.

Western Australia is extremely rich in minerals, particularly iron ore nickel and bauxite; has a potentially large gas field off the remote north west coast but only limited coal reserves. The [illegible] coal reserves at depths workable by current practice are wet sub-bituminous low hydrogen coals in

a small basin at Collie, close to the main population centre. These provide most of the state's present energy requirements and are ample, if assessed by projection of present demands. However, half of these reserves are regarded as too deep for open-cast mining and, because of water and weak-roof conditions most seams are not suitable for conventional mining. For those which are being mined the practical recovery rate is very low. The State Energy Commission takes a long view on resource planning and assesses reserves on the basis of energy requirements for the primary processing of the large mineral reserves. On this basis it is interested also in the potential of very large seams of reasonable thickness of sub-bituminous coal at depths of several thousand feet (located during oil and artesian water exploration drilling). For these, as for the deeper Collie coals, it considers that the potential of in-situ gasification should be explored. While no major projects are in sight the Commission is actively encouraging the writer's program and is initiating discussions towards an initial experimental program.

PROSPECTS FOR IN-SITU GASIFICATION

There is a considerable potential for in-situ gasification in the coal rich Eastern states in two directions.

First there are seams adjacent to industrial areas which are not workable by conventional mining methods and appear suitable for "in-situ" techniques. A close association with the mining problems in a thick seam first roused the writer's interest in "in-situ" gasification. For several decades the "Great" seam, hard, high-volatile, bituminous coal, had provided the bulk of N.S.W. coal production. However, in many places several feet of high-sulphur coal had to be left unmined; spontaneous combustion was often disastrous, and at cover about 1200 ft. roof and floor conditions made mining impossible.

Secondly, and perhaps more significant in the long run, "in-situ" gasification with oxygen-water, or by a cyclic water gas reaction, Fig. 1, is potentially a much more attractive method of producing synthesis gas than any operations of coal mining followed by a gas producer installation. Any type of gas-producer, commercial or envisaged, involves high capital maintenance and operating costs and produces effluents (ash, foul water, etc.) which give environmental problems. It will be a long slow development to reach a commercially reliable technique, but there do not appear to be any impossible technical barriers.

The West Australian objective is equally long range, but part of what will eventually be a world wide task - the winning of energy from coal seams at great depths. Again the in-situ gasification technique appears the most likely for initial development. "In-situ" solvent extraction may come eventually but it would be logically associated with "in-situ" gasification.

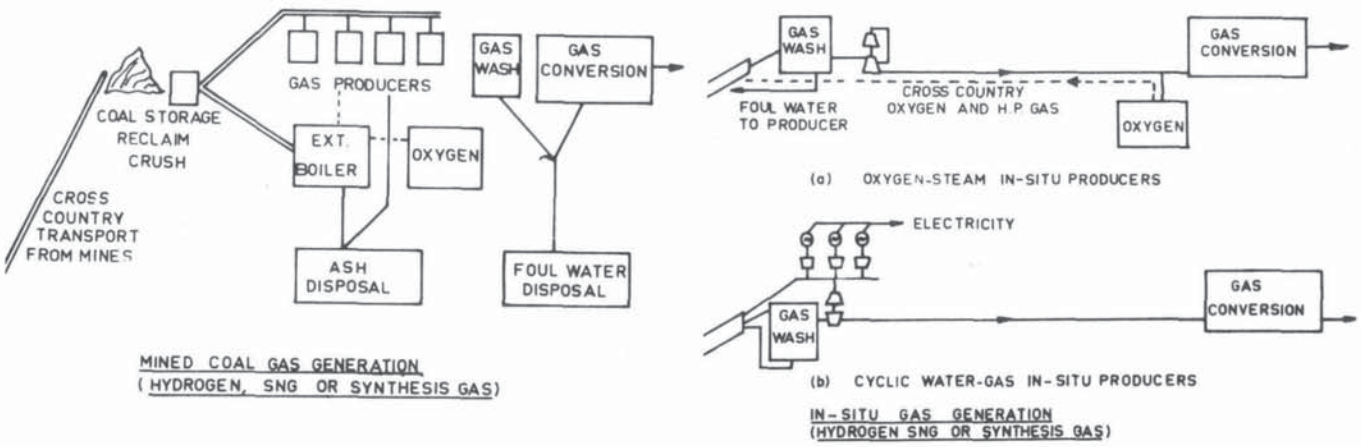
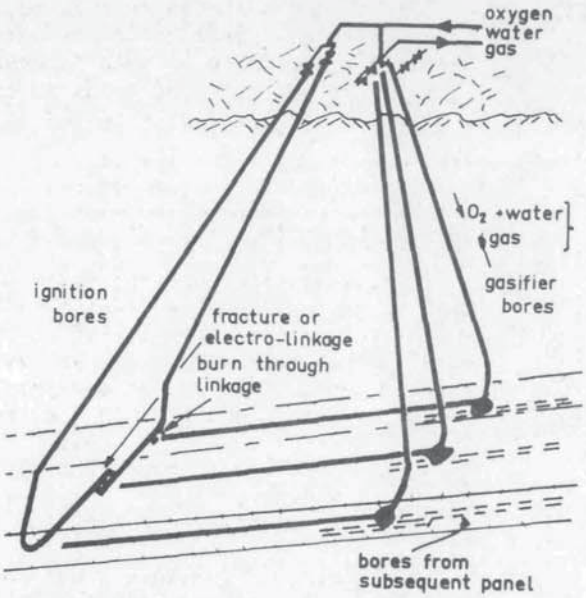


Fig. 1 - Synthesis Gas production from "in-situ" gasification
Left - Plant arrangement with oxygen gasification
Right - Water gas cycle with by-product electricity



POSSIBLE DEEP-SEAM HIGH PRESSURE GASIFICATION

Fig. 2 Possible high-pressure deep-seam gasification.

CURRENT RESEARCH DIRECTION

We are concentrating on borehole type systems (Fig. 2) for several reasons.

(1) The continuing Russian semi-commercial operations have developed effective techniques for linked borehole systems.

(2) A great deal of published data is available from British and U.S. trials of the 1945-1960 period and, to a lesser extent from Russian sources.

(3) The writer's early experience with combustion and producer gas operation on fixed beds of broken coal made him aware of the very real problem of self-propogating channelling from any unevenness in an unstirred bed. We do not have the resources to tackle this type of problem.

Analysis of the published material including available Russian work does suggest strongly that most of the effort was concentrated on mining and drilling techniques and that the combustion-reduction phenomena were observed by the classical mining method of "suck it and see" rather than by analysis at any depth. This is understandable in that the physical systems cannot be adequately modelled by algebraic techniques (despite a valiant attempt by Szekely) and that computers were not available during the period of intense activity prior to 1960.

The disappointing results of borehole systems are apparently due to the limited surface area available for the reduction reactions with resultant high gas exit temperatures and low cold gas efficiency. Provision of broken or fissured coal for the reduction reactions therefore looks very attractive. Having ruled that out of our terms of reference we looked in more detail at what happens in a borehole system and see that:

(1) Initial gas quality is high and gas exit temperature tolerable because of distillation of coal beyond the combustion and reduction surfaces. This "unsteady state" condition may last for several weeks but, whatever the surface available, the great proportion of the coal will be gasified with exit gas temperatures of 700°C or more. This not only represents at least 20% sensible heat loss with air gasification, but also gives borehole troubles. Apart from oxygen gasification the major possibility to alleviate this conditions is a regenerative cyclic process. Preliminary calculations indicate that for boreholes longer than, say, 200 metres, the internal surface of the borehole should be adequate, at reasonable ratings, for recovery of about 300° C at a 4 hour cycle or longer.

(2) In conventional borehole systems as in Fig. 3a the combustion zone is very inefficiently used. Where the gas passage is very wide compared with the height of the seam the combustion rate is limited to a low value by the rate of oxygen transport by turbulent diffusion. This results in the combustion zone extending over the large area up to the point where the gasification zone is sufficiently narrow. It is noted that the thin edge of the combustion zone is at the cold entry end of the zone. This edge will undoubtedly comprise coal broken by strata pressure and would be advantageous in the reduction zone. The desirable system would appear to be as in Fig. 3b; an intense combustion zone followed by a long reaction zone. There is a possibility that this also could be achieved by cyclic operation.

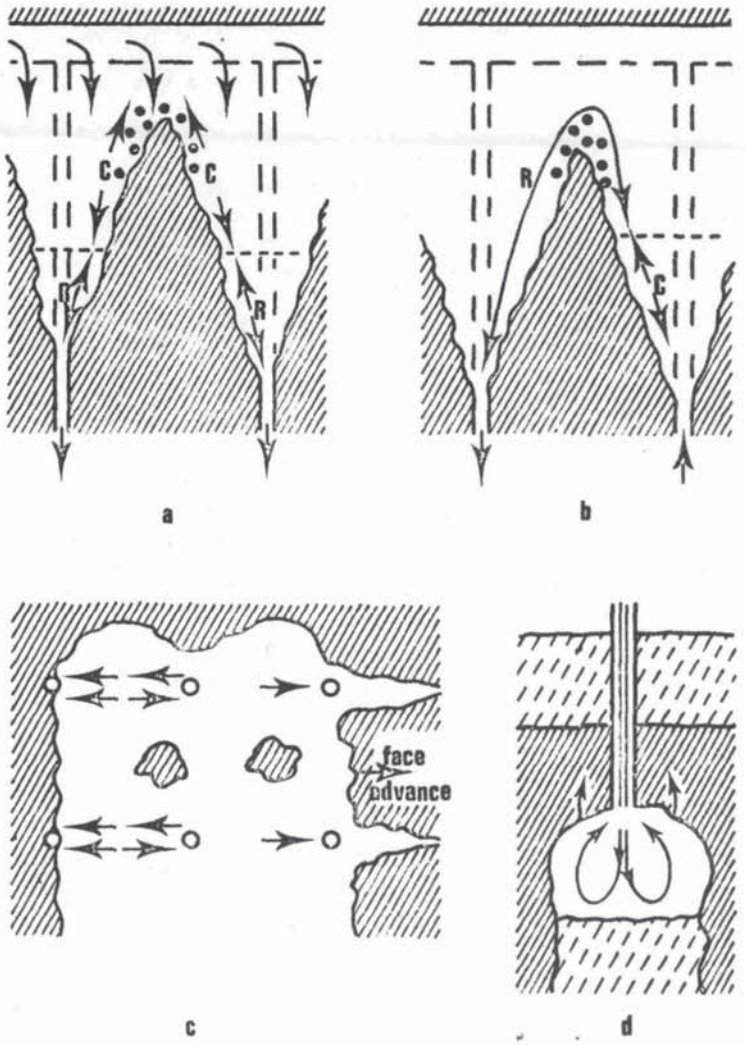


Figure 3 - (a) Simple Parallel Borehole system (British P5 trials) C - combustion zone; R - reaction zone
(b) Cyclic operation of system (a)
(c) A Russian vertical borehole system
(d) Vertical jet stirred zone deep seam (Arthur D. Little & Co. Report)

It should be noted at this point that upward borehold gasification of very thick seams is conceivable by such intense combustion systems (if roof break is controllable) and has been proposed [3]. (Fig. 3d)

References at end of paper

Our investigation program is directed then to analysis of the conditions for successful cyclic operation of an "in-seam" long borehole system. We have made a two dimensional computer analysis of the two major components of such a system:

(1) A reduction zone of tapering width.
(2) A jet-stirred combustion zone.

We have just completed, but not yet operated, a laboratory rig with 1" diameter boreholes in an artificial seam 6" thick and about 6' x 4' in plan area. This will be used to check the validity of our computer model before we move on to the three dimensional model which will be necessary to properly examine wide gasification passages.

The results of these computer models are being presented in detail to the XVI International Combustion Symposium in August. Before discussing the general results, the basic model of behavior of the coal face will be outlined.

THE COAL FACE MODEL

In front of a steadily advancing hot face there will be a temperature gradient. At the rate of advance of borehole systems this region of hot coal may extend for two or more feet. Within this region seam moisture will be evaporated and the coal volatiles distilled. These must escape to the face through natural cleat and ply cracks and have ample time to react with hot reactive coke at temperatures up to 1200°C. Even if only half of the water-vapour is decomposed these reactions for a high moisture high-volatile lignite can account for gasification over a large surface area of eighty percent of the fixed carbon in the coal. Thus for a high moisture coal the borehole system does provide for most of the reduction to occur on extensive cleavage surfaces, if this model is valid. We feel that behaviour cannot be otherwise unless the face successively flakes off due to high stress, (mechanical or at high combustion rates, thermal).

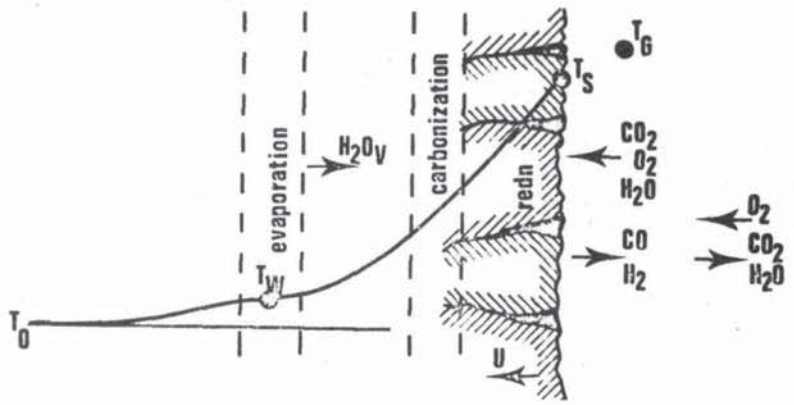


Figure 4 - Model of Coal Face Conditions

We believe that a laboratory test rig using cut blocks of coal about three feet square would test and quantify this behaviour. We hope to arrange such an experiment.

REDUCTION ZONE BEHAVIOUR

Using standard correlations for mass and heat transfer from a combustion gas stream we have computed for a number of coal types, seam heights and reduction zone widths the expected advance rate and gas compositions in the reduction zone. From the model discussed above it is clear that the reaction rate between the gas stream and the exposed face has only to be sufficient to gasify the balance of the fixed carbon after seam moisture has reacted with it. On this basis predicted results are comparable with what may be deduced from published information about field trials.

Sample results are shown in Fig. 5. There are several features of the results which are initially surprising but are the result of the fact that at temperatures above 1500K rates are controlled predominantly by mass transfer i.e. by the gas velocity in the main passage. As gasification proceeds and as the passage towards the borehole narrows, causing higher velocities, the effect of temperature becomes very significant. The assumption of zero-losses does represent a real case - the combination of say 15% heat loss to strata with a 15% energy recovery in preheat of the blast in a cyclic system. Curve (3) illustrates the great potential value of such a system. The computed effect of seam height shown between curves (1) and (2) is based on the assumption of equal losses in the combustion zone. This is reasonable if the total gas flow per borehole is the same for both the thin and thick seams. It suggests that the reported poor behaviour of thin seams cannot be accounted for solely by consideration of heat loss but that other factors, such as the blanketting effect of fallen roof, etc. must be taken into account.

The overall conclusions from computations to date are that tolerable performance at quite high ratings is achievable from a simple conventional borehole system, and that preheat by cyclic operation offers potential for high output high efficiency operation of bore-hole gasification systems. A three dimensional computer model is desirable for investigation of the wide sections of the zone.

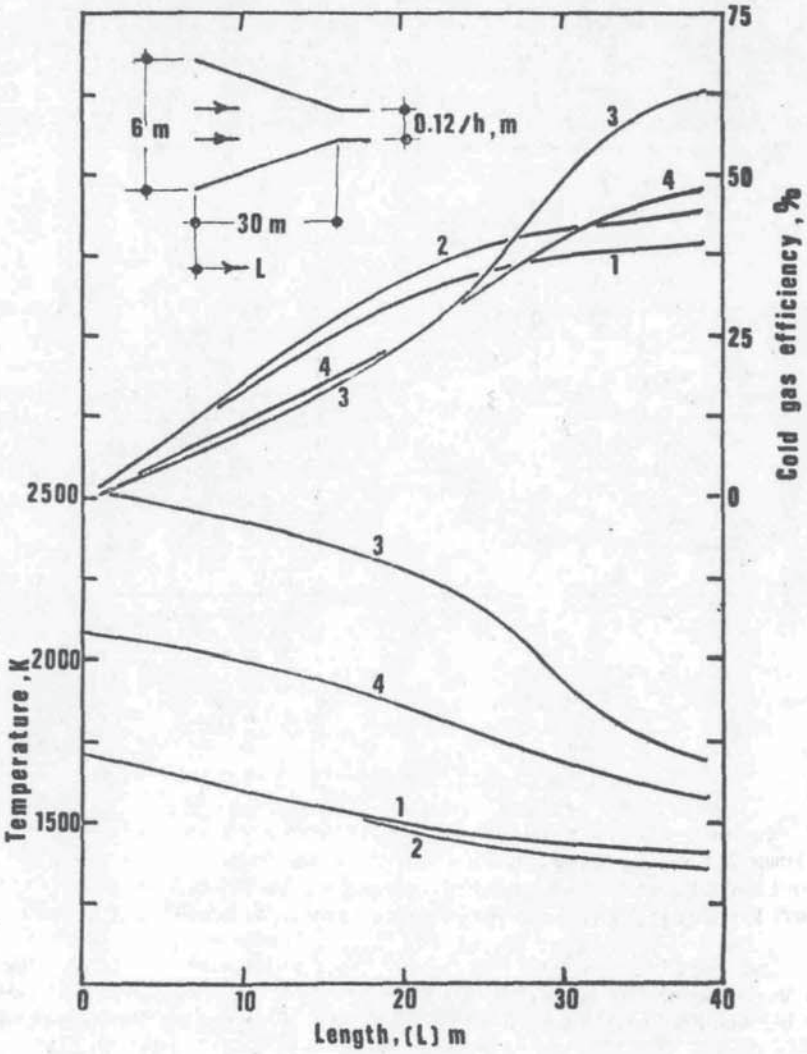


Figure 5 - PLUG FLOW REDUCTION; BROWN COAL

(1) Blast 20% moisture, 10% losses, seam 1.5 m
(2) Dry air; 0% losses, seam 1.5 m
(3) Dry air; 10% losses, seam 1.5 m
(4) Dry air; 10% losses, seam 1.5 m and K_R = 3 times K_R used previously.

STIRRED REACTOR TYPE OXIDATION ZONE

The jet issuing from a borehole into a wider space will produce a highly recirculating flow which may be analysed approximately as a well-stirred reactor and will tend to burn-out to a tulip-shaped zone somewhat wider than the 12° angle of normal jet spread. The size of this well-stirred

volume will depend very much on the system layout and strata conditions; - e.g. at some particular width, probably of the order of twenty feet, roof will fall and make a boundary to the opening. We have computed the conditions necessary to maintain ignition in such a system under quasi-steady state conditions (i.e. after coal faces and strata have reached fairly steady temperatures). The effect of moisture is very important. In a well-stirred system, once ignited, reaction goes right through to the production of some reducing gases and the effect of moisture on the reaction rate is very considerable. We predict that lignites and sub-bituminous coals will ignite at lower temperatures and produce more reductant gases than low moisture bituminous coals; in fact, that dry bituminous coals will not maintain ignition with bone dry air in this type of system.

Some typical figures are shown in Table I, below:

COAL	BLAST	COAL FACE m^2	TEMPERATURE IGNITION K	TEMPERATURE BURNING K	DRY COAL RATE Kg/sec	COMBUSTIBLE (CO & H_2) %
Bituminous 6.0% H_2O 40% vol d.a.f.basis	DA	100	1640	1900	0.155	Oxygen 7.2%
	DA	25	NO IGNITION		-	-
	080	25	1440	1735	0.365	10.12
	A20	10	1790	2055	0.214	4.70
	"	25	1625	2025	0.223	6.17
	"	100	1440	1990	0.230	7.16
Brown 35% H_2O 51% vol. d.a.f. low c.v.	DA	10	1700	1805	0.283	3.64
	"	25	1425	1730	0.321	6.93
	"	100	1200	1615	0.340	9.84

TABLE I: W.S.R. With Reacting Wall

BLAST
2 m^3/sec at 1 at
300K from borehole
of 0.35 m diameter

- DA - dry air
- A20 - 80% air 20% H_2O
- 080 - 20% oxygen 80% H_2O

We have had to make a great many assumptions, particularly with regard to the carbon reactivity in lump form. However, sensitivity tests on the model indicate that mass-transfer is far more important than reactivity. We expect to be able to check a number of these assumptions and the general validity of the model with our small laboratory model seam.

The conclusions are that with adequate control of blast moisture in relation to coal moisture and with oxygen gasification and/or preheat by cyclic operation a substantial degree of gasification can be secured in a jet stirred reactor of practicable dimensions.

Ignition in a plug flow situation is a more complex phenomenon with considerable dependence on the geometry of the system. With the uneven surfaces of a real system there must be recirculation zones. It is expected that the well stirred system will give qualitative indications of ignition behaviour in plug flow.

SUMMARY AND CONCLUSIONS

In-situ gasification has a real potential both for recovery of coal reserves not workable economically (or with adequate environmental control) by conventional methods, and for the production of synthesis gas more economically than by conventional means.

The borehole system has the advantages of avoiding the risks of channelling and of permitting sensible heat recovery by a cyclic operation. Computations of simple models indicate that, particularly for high moisture coals, a high proportion of carbon is gasified in the cleats and crevices of the bed. Under these conditions a cyclic air-steam or oxygen-water system should yield high quality gas at high efficiency and recovery.

PROSPECTS AND PROBLEMS FOR UCG IN BRITAIN

P. N. THOMPSON
J. R. MANN
F. WILLIAMS

OPERATIONAL RESEARCH EXECUTIVE
NATIONAL COAL BOARD

ABSTRACT

The Operational Research Executive of the National Coal Board has reassessed Underground Gasification in the contexts of the present and predicted future energy supply/demand scenarios in Britain.

For the immediate future, Britain's gas requirements will be met by natural gas drawn from the North Sea, but supplies are sufficient for only about 30 years. Alternative sources of gas will therefore be needed at about the turn of the century and UCG is judged to merit consideration as one possible source.

Two proven methods of UCG were used as the basis of cost models which are used to compare UCG gas with alternative fuels in terms of cost and resource utilisation efficiency.

The outstanding problems facing UCG in Britain are discussed and new methods of upgrading are suggested which could prove to be more economical than the methods considered in the past.

Britain intends to maintain an interest in UCG, even though there is no immediate urgency for its development, and is now considering possible ways of collaborating with these countries currently pursuing the development of UCG.

INTRODUCTION

The National Coal Board is responsible to the British Government for the efficient utilisation of the nation's coal reserves. Although the bulk of the production (currently about 115M tons) is produced by deep mining methods with an additional 10M tons produced by strip mining the Board has always been aware of the need to investigate alternative methods of working. It first took an interest in UCG in 1949 when it co-operated with the Ministry of Fuel and Power in an eleven year programme of Research and Development. The work, which was fully documented /1, 2/ was started in the face of the post war fuel crisis and abandoned in the fuel glut of 1959. It was a useful experience and a lot was learned about steering boreholes, and controlling the reaction, and even though the planned program was not completed, much valuable basic data was obtained. When in 1974 the country faced another fuel shortage, and interest in UCG was revived, the Board felt it was opportune to reassess the process and decided that its purposes would be best served by carrying out a thorough paper study rather than by committing itself immediately to more costly practical work. It was aware of the worldwide resurgence of interest in UCG and also of the tremendous technological advances that had come about in the drilling field since 1959. Accordingly it commissioned its Operational Research Executive to reappraise the whole process.

In evaluating the process a critical view had to be taken of:

1. The technical capability of the process to supply gas at a steady rate in the quantities and qualities required.

2. The cost of the final product and its sensitivity to various cost factors.

3. The comparison of UCG costs with these of other energy sources.

4. The availability of suitable coal reserves and the efficiency of utilisation of these reserves.

5. The potential uses of the product gas.

6. Environmental and safety effects.

7. The resource use of capital and labour.

8. The energy account in comparison with conventional mining.

In our studies we drew heavily on past U.K., U.S.S.R., and U.S.A. experience and we were helped in this respect by engaging Dr. Arthur E. Balfour as a consultant. We were also fortunate to have the opportunity of visiting the U.S.A. to see the new development work now going ahead and to meet many of the people currently occupied in the projects.

Our method was to build an economic model of the process and to use this model to predict gas production costs based on feasible methods of operation in the suitable sets of conditions we hoped to discover. The model was constructed entirely on the basis of proven technology, though, in the later phases of the work we did tentatively extrapolate along likely lines of development to give ourselves some indication of the way costs might be changing in the future, and also we hoped to suggest promising avenues of development.

In this paper we sketch out the British fuel scene, assess UCG as an optional energy source and then go on to discuss the problems that will have to be overcome to make UCG a commercial reality.

THE BRITISH ENERGY SCENE

The British Energy market is still recovering from the confusion caused by the after effects of the Yom Kippur war but gradually a pattern for the future is emerging. [3] It is now expected that up to the end of the century the British energy situation will be conditioned by the global trend in oil production. This is expected to reach a peak at about the year 2000 but before then the reductions in growth rates are expected to push prices up.

By the 1990's North Sea oil and gas supplies will probably be past their peak and declining quite quickly just at a time when imported oil will be becoming more expensive. Conservation measures are not likely to affect the picture to any great extent and the contribution which nuclear power will be able to make is still a matter of debate.

Thus the coal based contribution to the market in 2000 could be of the order of 200-350 mtce that is 1½ to 2½ times the present size of the industry.

There is no doubt that Britain's technically recoverable coal reserves are adequate to last for several 100 years even on a conservative estimate. There is no doubt that we have the technology and expertise to mine the coal, and most problems are likely to centre on our ability to mine it at high enough rates and at low enough cost. This of course is just the sort of challenge that brings out the best in any mining industry and there is general confidence within the NCB that this challenge can be met. However, as part of the demand will be for gas to replace natural gas, processes which convert coal into gas will be required and one which could eliminate the mechanical mining stage of the process should have a distinct advantage. If, in addition, UCG could be developed to economically extract the conjectured deeper-lying and presently unmineable reserves it could assume even greater long term significance.

COSTING THE UCG PROCESS

The economics of UCG follow rules similar to those encountered in strip-mining. Gas can be produced from thick shallow seams of clean coal at a lower cost than from thinner, deeper seams of higher ash content. A large proportion of the cost depends on the ratio of seam thickness to depth. It is therefore impossible to quote a single cost or even a narrow range of costs for UCG in general as any cost must be stated in the context of the thickness, depth, ash content, etc. of the coal seam in question.

Over the years a great many different methods of UCG have been suggested and tried. Clearly it would be impossible to model them all and so we selected two basic methods which seemed to have the potential for application on a commercial scale. They were the methods which looked most promising at end of the last development phase in 1959 and so contained the fruits of the experience of that time.

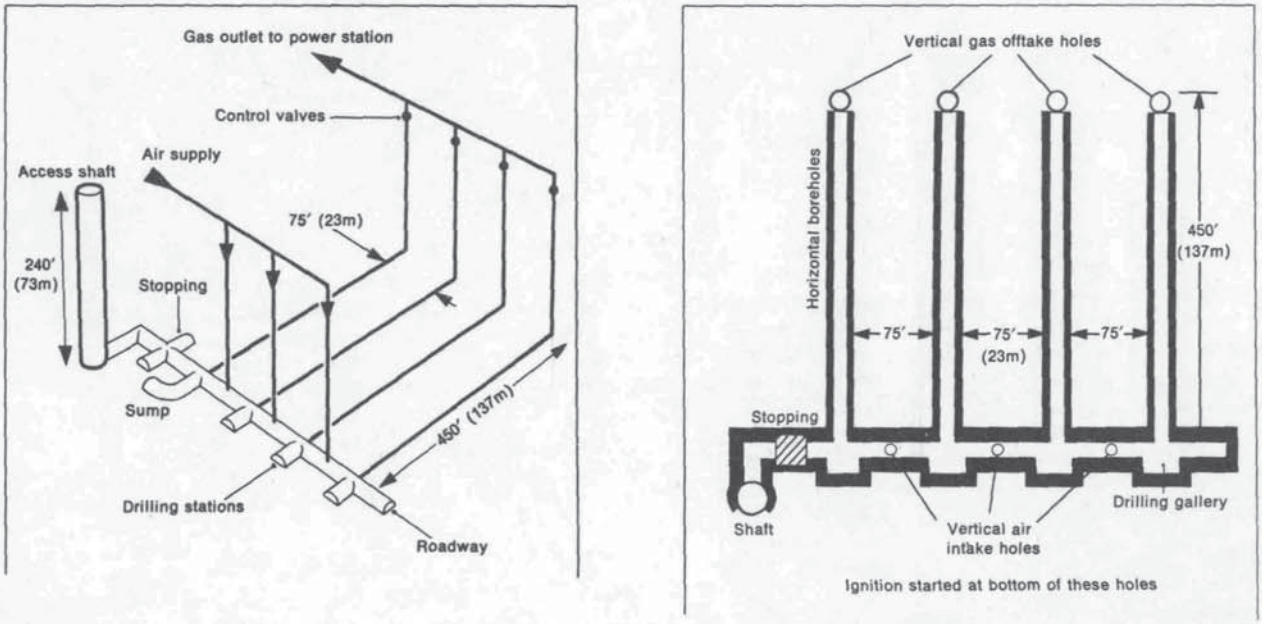
We chose the Preliminary Mining Method (Fig. 1) which was developed at Newman Spinney because it had been shown to work and because our initial calculations showed that it could have cost advantages over the alternative methods in suitable conditions. All the operations involved in the method are standard practice in mining and so costs are available. Modern equipment and techniques mean that the scale of operations can be enlarged without making any unreasonable assumptions and so cost estimates based on the method should be reliable.

We also chose the Vertical Drilling Method (Fig. 2) because this is the basic method on which almost all current developments are based. Since 1959 tremendous advances have been made in the fields of drilling and linking boreholes, and we believe the method has further potential which is still untapped.

When building our model we were careful to keep it as flexible as possible so that it could accommodate the widest possible range of conditions and process variations. We believe it can now accommodate almost all the proposed methods of UCG but we have not yet applied it to non-British coals because without access to detailed local knowledge on conditions and costs we have to rely on the dubious nature of costs converted into sterling on the basis of official exchange rates. In fact to make the model internationally useful it must be capable of working entirely in local currency with local costs and charges applicable to the local conditions. This aspect of the work is still under development and we look forward to an opportunity of running it in a real life situation.

Our main reservation about our work so far is whether results obtained on an experimental scale will really apply on a commercial scale. We believe the costs need to be no higher and we could suggest several reasons why they might be lower but until high production rates have been achieved in practice we must retain this caveat.

In order to produce comparative results it was necessary to base both methods on a set of central assumptions which are given in table 1.



Schematic

Plan View

Figure 1: P5 Layout at Newman Spinney

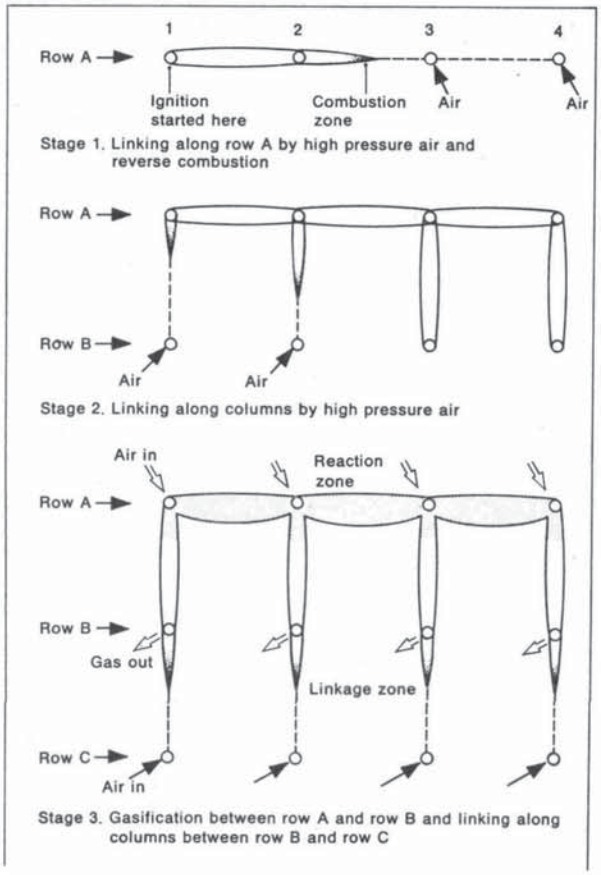


Figure 2: Vertical Drilling Method

	Vertical Drilling Method	Preliminary Mining Method
Vertical Boreholes	100 ft (30 m) apart (at corners of squares)	75 ft (23 m) apart (in rows 900 ft (275 m) apart)
Galleries	-	300 ft (90 m) long
Horizontal Holes	-	75 ft (23 m) apart 900 ft (275 m) long
Barrier Width	-	10 x seam thickness
Proportion of Coal Burnt	85%	85%
Proportion of Heat Gained	60%	60%
Overall Efficiency	51%	51%
Gas Calorific Value		
seams less than 6 ft (2 m) thick	80 Btu/ft^3 (3 MJ/m^3)	80 Btu/ft^3 (3 MJ/m^3)
seams 6 ft (2 m) thick or more	100 Btu/ft^3 (3.7 MJ/m^3)	100 Btu/ft^3 (3.7 MJ/m^3)
Leakage Rate	4%	4%
Operating Pressure	30 psig (2 bar)	30 psig (2 bar)
Reactant	Air	Air
Average Reactant Rate	100 ft^3/sec (2.83 m^3/sec)	100 ft^3/sec (2.83 m^3/sec)
Linkage Air Rate	66,000 ft^3/ft (6124 m^3/m)	-
Seam Thickness	> 3 ft (1 m)	> 3 ft (1 m)

[1] Pneumatic linkage assuming 66,000 ft^3 of air for each foot (6124 m^3 for each metre) of linkage in the coal. This is twice the rate being used in the Laramie experiment.

Table 1: Central Assumptions

We also assumed freedom from excessive faulting and non porous surrounding strata.

If the assumptions we have made do hold, then UCG gas with a calorific value of 80-100 Btu/ft^3 (3-3.7 MJ/m^3) can be produced for as little as 7p/therm (70p/MBtu), though the expected range of costs would fall in the 7-24p/therm (70-240p/MBtu) range. How these prices compare with the alternatives in the British market can be seen in Table II.

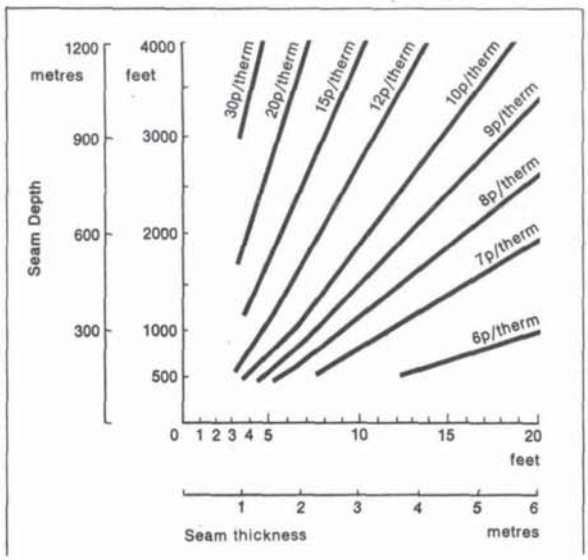
	UCG gas (80-100 Btu/ft^3)	Deep mined Coal	Strip mined Coal	Oil	SNG imported	NG from N. Sea
Fuel cost p/therm	7-24	4-12	3	9.5[1]	13-33	3-4
Recovery Efficiency	51%	60%	90%			

[1] Landed price at 1st January, 1976

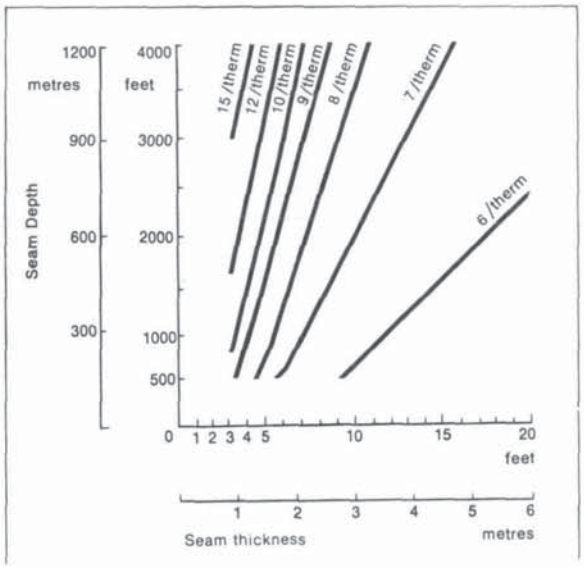
Table II: Comparative costs of UCG and alternatives

These figures are encouraging because they suggest that even when we are using 1950's methods and technologies UCG is still on terms with the competition.

The range of applicability of these figures can be seen from the cost contours in the following graphs.



Preliminary Mining Method



Vertical Drilling Method

These cost contours can be used to estimate the cost of producing gas from a range of combinations of seam thickness and depth. The curves are not linear as they take account of changing gas calorific value with seam thickness.

They also show that gas prices have a minimum at around 5-6p/therm which is due to the basic cost structure of the process which has capital and operational elements.

The costs for the preliminary mining method are lower and show less sensitivity to changes in seam depth and thickness. This is because the need for fewer boreholes more than compensates for the cost of the shaft and galleries. Also, for each unit of gas, the cost of linking by horizontal boreholes is less than the cost of pneumatic linkage.

The lower cost of the preliminary mining method does not mean we should abandon the vertical drilling development. The vertical drilling method has advantages in recovering seams not accessible to conventional mining for reasons of high temperature etc. and further developments which could increase the separation of the boreholes could bring the cost below that of the preliminary mining method, and more directly comparable with current deep mining costs.

Sensitivity analysis showed the effects of varying the central assumptions by 10% for better and for worse. The results shown in Table III show that the cost is affected by a disproportionately large amount, though we would hope that in practice there would be a compensating as well as compounding effect.

	Central Assumptions	10% change for the better	10% change for the worse
Vertical Drilling	12.4p/therm	10.5p/therm	15.3p/therm
Preliminary Mining	9.2p/therm	7.9p/therm	10.8p/therm

(4 ft thick seam, 1000 ft deep, coal calorific value: 12100 Btu/lb)

(1.2 m thick seam, 300 m deep, coal calorific value: 28144 Kj/Kg)

Table III: Example of the Sensitivity of UCG Gas Costs to Changes in the Central Assumptions

Both methods are noticeably sensitive to a change in the assumptions and not a particularly large one at that. This has its good and bad sides. A comparatively small drop in the efficiency or tightening of the operating rules could considerably alter the profitability of the plant. On the other hand improvements which are probably within our reach would cause a worthwhile reduction in costs.

A breakdown of costs of UCG compared with the costs of mining is given in Table IV.

	UCG gas	Deep mined coal
Labour	35%	52%
Power	12%	4%
Materials Repairs Depreciation Overheads	53%	44%

Table IV: Comparison of resource use of UCG and mining as a proportion of costs

UCG has a proportionately lower labour cost content than deep mined coal and so should gain in times of high wages costs, but it would lose out in times of high energy costs because of its higher power requirement. It would be difficult to measure the effect of the higher materials, repairs and other costs. We can see no obvious reason why UCG costs should not move more or less in line with inflation and deep mining costs.

In terms of manpower requirements UCG comes between deep and strip mining as Table V shows.

	Deep Mining	UCG	Strip Mining
Manshifts per M therms	1850	565	460

Table V: Comparison of Manpower Levels

In terms of capital input we estimate UCG to require about 20p/annual therm whereas deep mines require only 12p/annual therm.

The energy account for UCG is less favourable than that for either deep or opencast mining. Comparative figures are given in Table VI.

UCG	Deep Mining	Opencast
3:1 to 5:1	20:1	13:1

Table VI: Comparison of UCG Energy Output to Input ratio with these of mining

Here the figure for UCG more resembles a processing plant than an extractive process.

In making these comparisons we have been aware of the difficulty of comparing like with like and so we would regard the results as indicating little more than trends and orders of magnitude.

The costs we have been working with so far have been derived from hypothetical coal reserves and to see how they would work out in practice we applied them to four sample areas in Britain.

The NCB mining department were asked to nominate four areas which matched the specification we provided. Briefly what we asked for was: -

(i) There were to be at least 5M tons in the deposit so that an installation would have an adequate commercial life of up to 20 years.

(ii) It was not scheduled for deep, opencast or private mining as these were deemed to take priority over UCG, and it was not to be adjacent to any deep or private mine because of possible gas leakage.

(iii) It was not to be coal in pillars left to prevent unacceptable subsidence.

(iv) The seam thickness was to be at least 3 ft (1 m) but we included banded coals having a total thickness of over 3 ft (1 m).

(v) The depth of the seam was to be at least 100 ft (30 m) to minimise the risk of gas leaking to the surface.

(vi) The ash content was to be less than 60% including any dirt bands as ash contents above this might impede combustion.

(vii) The area had to be free from excessive faulting.

For coal reserves which fitted the description we wanted to know: -

1. The location
2. The depth range of the seam
3. The seam sections with thickness and ash contents of dirt and coal bands
4. Total tonnage available
5. Sulphur content
6. Calorific value
7. Rank
8. Volatile content
9. Nature of surrounding strata
10. Angle of dip
11. Details of faulting and folding

Four areas were nominated of which A is in a small coalfield in which all mining has now ceased, B is in a coalfield where mining is still going on but is isolated from working mines, C is an extension of an existing coalfield but isolated from it by a large fault and D is in a coalfield where mining has not yet started.

The coal in all four areas could conceivably be gasified with no great advances in technique. The resultant estimated costs, using the vertical drilling method are shown in Table VII.

Area	Seam thickness		Depth		Gas cost p/therm	Approx. size of power station supportable for 20 years (MW)
	(ft)	(m)	(ft)	(m)		
A	3-4.5	0.9-1.4	820	250	11.0	180
B	6-7	1.8-2.1	750-1200	230-370	8.7	200
C	15-21	4.6-6.4	3300	1000	8.4	1400
D	4-5.5	1.2-1.7	2000-2600	600-790	18.3	380

Table VII: UCG Cost for four example areas of coal

The costs produced suggest that UCG is not to be ignored and so when the need arises it should be one of the optional sources of gas that would have to be taken into consideration. In this event a comprehensive catalogue of British coals suitable for UCG would have to be drawn up and from this the most suitable areas selected for development.

THE OUTSTANDING PROBLEMS

UCG at present clearly stands in need of further development and to say that it is an option future energy source implies that the outstanding problems will be overcome. At present none of the problems appear to be particularly intractable though forward assessment of development problems is notoriously difficult. The emphasis of the various problems will also change with time but our present assessment is as follows:

Drilling Costs

The cost of drilling is at present the most influential variable and needs to be reduced either by reducing the number of holes required to gasify an area of coal or else by gasifying more than one seam from one set of holes.

The actual techniques of drilling have seen rapid development in recent years and further developments are in the offing. Rapid surveying techniques are currently widening the utility of deviated drilling and it would be reasonable to expect the accuracy of all forms of drilling to be improved if this were shown to be necessary.

Rotary and turbo drilling techniques have responded well to development pressures and for drilling straight holes the air percussive machines may yet have a contribution to make.

Linkage

High pressure air injection coupled with reverse burning now seems capable of consistently creating linkage paths in lignite and sub-bituminous coals but the low permeability of British coals may still present problems. Although several methods of inducing linkage through Bituminous coals have been suggested it cannot yet be guaranteed that it will always be possible to establish a path in the required direction. Holes can be drilled in the seam but applications of this method may be limited by considerations of depth and temperature. The possibility of laser linkage has been under consideration for some time and if the problems of smoke masking can be overcome then a breakthrough of considerable magnitude will have been achieved. If the laser could cut a fine channel between two distant holes, and this channel then enlarged by conventional means we might have the ability to create large economic gasifiers with extreme precision.

Ignition

Ignition does not seem to have caused any problems in the past, but since in any commercial scale application rapid and reliable ignition will be of crucial importance, this aspect of the process should not be overlooked.

Control of the Reaction

In any commercial scheme the watchwords will be reliability and consistency of output and in order to produce a consistent gas a high degree of control will be required. It is now virtually certain that modern equipment and techniques will give us the degree of control we need and this is likely to be proved in the current trials at Hanna.

At the same time, present indications are that the underground reaction should be aimed at producing a raw gas of about 80-100 Btu/ft^3 (3.3.7 MJ/m^3) and that any upgrading should be carried out in the more precisely controllable environment of a surface plant.

Leakage

In most of the tests carried out so far leakage has been accepted as a relatively minor disadvantage which has had little bearing on the test results. As the scale of operations and the working pressure increase, however, the problem of leakage will assume greater significance. Not only will it introduce an element of loss and inefficiency, but the increasing volumes of leakage gas will represent a potential hazard and also a bar to perfect process control.

The mechanisms of leakage and the relative importance of the various leakage paths will all require careful study.

The exploitation of coal abandoned in and around old mine workings is likely to depend very heavily on the possibility of reducing leakage to acceptable levels. Similarly the problem of gasifying a succession of seams lying one above the other will very largely be a problem of controlling leakage through the subsiding overburden. The breaking of borehole liners and seals may be particularly relevant in this connection though the problem of providing an efficient, high temperature grout seal will exist at the bottom of all gas off-take boreholes.

UCG in Faulted Areas

Trials have naturally been conducted in small areas virtually free from faults, but widespread application would mean that faulted areas would have to be dealt with. The presence of faults could interfere with orderly reaction progression just as they affect the advance of mine workings but in addition they could provide possible leakage paths. No experience has yet been gained in dealing with this question. Work would have to be done to show the extent of faulting that would stop the reaction, and the necessary design features of the underground gasifier to take account of this.

Roof Control

Presumably the roof of the seam caves in after the passing of the reaction front. The small amount of subsidence recorded in trials so far suggests that this may not be so, but is more probably due to the fact that only small areas have been gasified. The ash left behind could provide some support but just how much remains an unknown for the present. The behaviour of the roof would depend to some extent on the temperature of the reaction and on the effect of this temperature on the rock material itself.

Future work on UCG must be designed to provide data on how long the gasifier goaf could be expected to stay open sufficiently to allow the air to get through to the reaction. This data will have an important bearing on gasifier design.

Utilisation of the Gas

Generation of electricity has so far been the most popular use for UCG gas but we do not see this as the major commercial market. Britain's long term energy forecasts are currently based on the assumption that nuclear power will be generating much of the base load with fossil fuels helping to meet peak demands. Until we know more about the turn down potential of the UCG process we must regard it as a steady state process and this brings it into direct competition with nuclear power.

To generate electricity at maximum conversion efficiency it would be necessary to use gas and steam turbines in combination but the raw gas will not be fit to feed directly to a turbine. For this it would have to meet standards of cleanliness and consistency of calorific value which could only be achieved by surface treatment. We therefore, believe it will prove to be necessary to clean and upgrade the gas to some extent to allow it to be efficiently used and stored. Economic storage demands a concentrated energy form and concentrated energy forms appeal to wider markets.

All the indications are then that the future UCG plants will be producing a raw material which should be regarded as a basic energy source to be converted into electricity, gaseous or liquid fuels, or into synthetic chemical products.

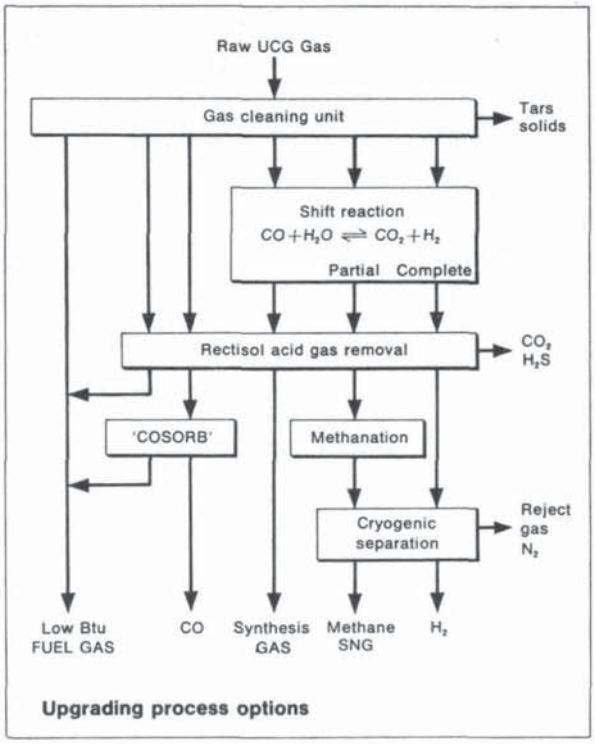
Gas Cleaning and Upgrading

The necessity to upgrade the raw UCG gas need not be a disadvantage as the vastly improved utility and marketability of the gas would far outweigh the likely financial costs involved in the sort of schemes we have been considering.

In the past, upgrading schemes have usually been based on the use of oxygen as the UCG reactant but in our assessment it is expensive, adding 6-15p/therm on to the cost of the raw gas, and the inherent hazards of handling bulk oxygen are a deterent. Oxygen would be required in quantities many times greater than the capacity of the largest separation plants currently in operation in Britain, and in addition, for some obscure reasons the experimental results on the use of oxygen are not encouraging. There are on the other hand several proven processes for utilising synthesis gas some of which are tolerant enough to accept raw UCG gas provided that catalyst poisons such as sulphur are removed beforehand.

We commissioned a review [4] of possible upgrading methods and this suggested that there are four processes which are worthy of further study.

The four selected upgrading process options are shown schematically in the block diagram and are: -



Upgrading process options

Upgrading to a Clean Fuel Gas

The raw gas is scrubbed and then freed of CO_2 and H_2S to yield a gas with the following compositions.

CO	11%
H_2	14.5%
CH_4	3%
N_2	70%

This gas should be suitable for fuelling a gas turbine and the added cost, based on the South African experience of the Rectisol process, should be about 0.5p/therm of raw gas.

Production of a methane SNG

The raw gas is subjected to the shift reaction to improve the H_2: CO ratio and then the Rectisol process removes the CO_2. The gases are next methanised to give a gas with the following compositions.

CH_4	11.5%
N_2	86.5%

Reasonably pure methane could then be extracted from the gas to give an SNG at an additional cost of about 4p/therm.

Production of Hydrogen

In this option the shift reaction is again used but this time pushed to completion to maximise hydrogen production.

$$CO + H_2O \longrightarrow CO_2 + H_2$$

The CO_2 is again removed by the Rectisol process and pure hydrogen separated cryogenically from the residual gas at a cost of about 2.2p/therm on top of the raw gas cost.

Production of pure CO

Carbon monoxide is a valuable basic building block in synthetic chemistry. It is difficult to separate cryogenically from N_2 but the recent development of the COSORB process gets around this difficulty. The process we envisage would generate a stream of 97.5% pure CO and also a stream of low Btu gas which is basically the residual H_2 and N_2 from the original gas. The operating costs of this process are estimated at around 7p/therm.

We must emphasise that in their present state these proposals are merely tentative and the costs particularly should be treated with caution. We do believe however, that the proposals are worthy of further study in greater detail.

Environment and Safety

The major British coalfields are generally associated with relatively high population densities and the coal seams themselves have been fairly extensively worked over the last hundred years. These two factors increase the chances that if and when UCG is introduced as a commercial process it will have some measurable impact on the population in terms of environmental pollution and safety. The very idea of UCG with fires raging away underground is highly emotive and so it is likely that we shall be dealing with real and imaginary nuisances and dangers.

On the nuisance level the main concern is likely to be the visual impact and the noise of the drilling rigs. Visual impact is difficult to assess but noise levels should be controllable below real nuisance levels. Dust, smell and traffic should all be less than with alternative ways of winning the coal.

In terms of real hazards the leakage of poisonous gas must be the main concern. Leakage into mines and into surface buildings are possibilities which must be avoided and so until more positive data is available we could not recommend UCG in any places where this was likely to happen.

Pollution of ground water is unlikely to be a major hazard but again until more data is available its effects should not be underestimated.

The industrial safety record of UCG shows every prospect of being good. Men would be working mainly in small teams and even with the preliminary mining method where some would have to be below ground they should not be exposed to any undue hazard. As in most industries the safety record will be determined mainly by the overall standards of site management and operation and the maintenance of a good working environment.

Use of Land

A possible disadvantage of UCG is that it needs at least temporary access to most of the surface overlying the coal. In Britain most land is intensively developed in some way and even in farming areas we are faced with the prospect of having to negotiate with large numbers of land owners. In this respect the preliminary mining method may be more acceptable reducing as it does the number of surface drilling sites required.

CONCLUSIONS

Our assessment of the prospects for UCG in Britain has to be in the context of the current energy situation and in the light of the investment that has already been made for the future.

Investment for the immediate future has been mainly centred on the oil and natural gas resources in the North Sea and on extensions of current conventional coal mining. Our assessment helps to confirm the wisdom of this course as UCG cannot rival these sources in terms of cost per therm produced. We therefore, have no grounds on which to recommend the immediate development of UCG in Britain. But the further outlook is different.

The reserves of oil and gas in the North Sea are known to be limited and when it becomes necessary to recover the energy by secondary and tertiary methods unit costs will rise. At this stage UCG may become competitive, and so we should keep the process under review.

Our present estimates of the cost of gas from UCG are largely based on old technologies and we have grounds for reasonable optimism that these costs can be reduced by development. The point at which UCG becomes competitive therefore depends on the rate at which oil and gas prices rise as well as on the rate and extent of the drop in UCG's own costs. It is consequently rather difficult at this time to suggest a timetable for developments.

In its present state the UCG process stands in need of further development. We see no insuperable problems and our only reservations about future costs are that all available costs are based on development scale work. Nowhere outside Russia has the process been operated on a commercial scale and until it has been, we must be cautious about the problems involved in scaling up the operations.

Some aspects of the UCG development programme now going on could bring spin off benefits to the conventional mining industry in the short term; deviated drilling for methane drainage for example, and these facets may repay more detailed study in the shorter term.

Our final conclusion then is that UCG is an option to be kept open in determining the pattern of Britain's future energy supply. It merits continued observation to monitor the changing economic relationship between this and other forms of energy supply and models developed in the course of this assessment will be valuable because of the rapid reappraisals which they will make possible.

The opinions expressed in this paper are entirely those of the authors and are not necessarily those of the National Coal Board.

REFERENCES

1. British Trials in Underground Gasification, 1949-55, HMSO.
2. The Underground Gasification of Coal, Sir Alexander Gibb and Partners, Pitmans, 1964.
3. Energy Prospects to Year 2000, The Future of Coal Supply and Demand in Europe, J. A. E. Beamish-Crooke, NCB Memorandum.
4. Technical Studies for Upgrading UCG gas, NCB PADB Report No. 75/30, 1975.

TWO-DIMENSIONAL STUDIES OF COAL PYROLYSIS: PRELIMINARY RESULTS

BY

R. C. Forrester III
Oak Ridge National Laboratory
Oak Ridge, Tennessee 37830

ABSTRACT

Two-dimensional pyrolysis behavior of large, instrumented blocks of subbituminous coal has been examined recently in studies conducted at the Oak Ridge National Laboratory (ORNL) in support of *in situ* coal gasification process development. Pyrolysis studies have traditionally dealt with small coal particles which were heated rapidly; but by contrast, *in situ* gasification involves slow heating of large coal blocks resulting from permeability enhancement operations or, perhaps, roof collapse. Experiments utilizing maximum reactor temperatures of 500° to 1000°C achieved over 4- to 50-hr time periods have produced data correlating tar and gas production rates and composition with maximum temperature and heating rate.

INTRODUCTION

In situ gasification of coal, presently under active study by the Energy Research and Development Administration, entails injection of oxygen or air with or without steam into a coal seam whose permeability has been increased previously by explosives, by high pressure liquid injection, or by some other means. The presence of injected oxygen permits ignition of the coal and subsequent maintenance of a combustion front which moves through the coal bed, producing a combustible product gas which is piped to the surface. Pyrolysis of the coal in front of the combustion front is an important part of the process, but pyrolysis studies have traditionally dealt only with small coal particles which were heated quite rapidly. By contrast, *in situ* gasification involves slow heating of large coal blocks resulting from permeability enhancement operations or, perhaps, roof collapse. Conversion of these large masses is necessary for improving overall utilization of the available resource.

The specific objective of the ORNL program supportive of underground coal gasification (UCG) development is the generation of data describing pyrolysis of large coal blocks under conditions which can be expected to occur underground. Such data can be used both in the development of computer codes that describe underground reactions and in the interpretation of field test results.

The need for laboratory data on two-dimensional pyrolysis reactions was recognized by researchers involved in early attempts to model UCG processes in a meaningful way. Few data were available for Western subbituminous coals which appeared to be likely candidates for UCG applications. Thermogravimetric analysis (TGA) studies were quickly carried out at the Laramie Energy Research Center (LERC) and at the Lawrence Livermore Laboratory (LLL) to meet interim data needs, and a supporting study of two-dimensional pyrolysis was established at the Oak Ridge National Laboratory.

APPARATUS

Simulation of the *in situ* pyrolysis process has consisted of experiments utilizing large,

instrumented blocks of subbituminous coal taken from the Roland-Smith seams near Gillette, Wyoming. Figure 1 is a schematic representation of the apparatus used in these experiments. The reactor is electrically heated and swept with a cylinder-supplied cover gas. Maintenance of a specified heating rate within the reactor is achieved through the use of a three-mode controller which can provide heat-up ramps of 0.1 to 10 C^{o}/minute. Reactor pressure is essentially atmospheric.

Fluids produced during pyrolysis are carried to a water-cooled mist eliminator-condenser which traps most of the tars, oils, and water, permitting noncondensable gases to be metered, sampled, and vented. Following each experiment, the apparatus is disassembled for recovery of trapped oils and for cleaning. Char remaining in the reactor is sampled for analysis and weighed.

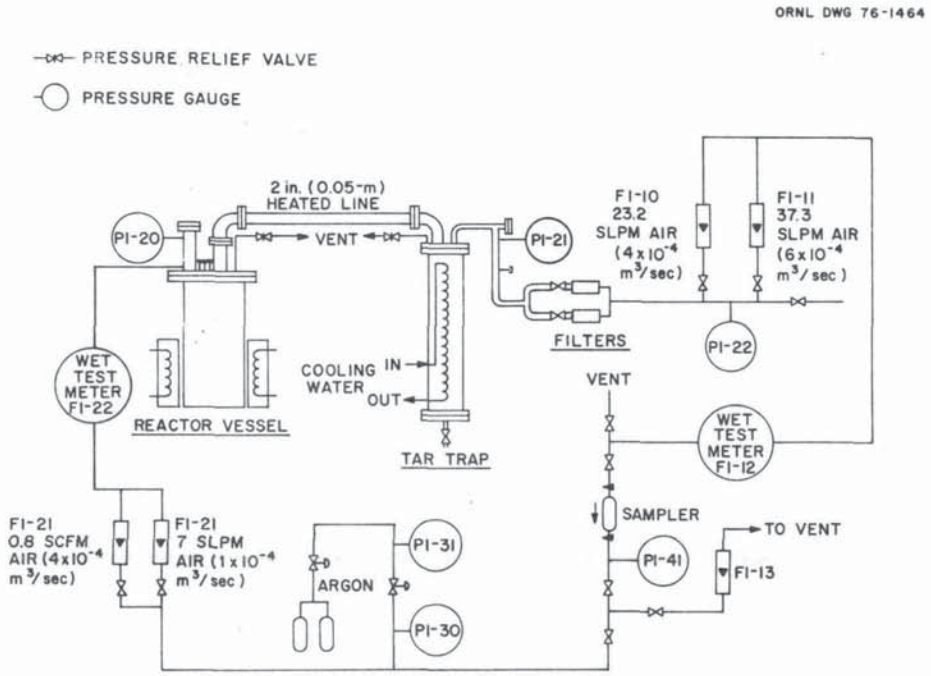


FIGURE 1. SCHEMATIC REPRESENTATION OF THE BLOCK PYROLYSIS EXPERIMENT.

SAMPLE PREPARATION

As mentioned previously, coal utilized in these pyrolysis studies comes from the Roland and Smith seams at the Wyodak Resources Development Corporation mine near Gillette, Wyoming. Table 1 compares results of our analyses of this coal with analyses performed by others on coals from the same seams. Our procedure for preserving the original condition of samples during storage includes (1) sealing the sample blocks in plastic bags at the mine mouth, (2) submersion in water upon receipt at the Laboratory, and (3) performing all necessary machining and drilling operations under a water spray. The efficiency of these procedures seems to be verified by the agreement shown in Table 1.

Preparation of pyrolysis test blocks requires that a 15-cm right circular cylinder be cut from larger, irregular blocks using a band saw. The blocks are drilled to accomodate 1.2-mm thermocouples before being placed in the reactor. Figure 2 shows a typical thermocouple placement pattern. All experiments have utilized as-received blocks without prior drying or excessive contact with air.

Table 1. Analyses of coal taken from the Roland-Smith seams as received from Wyodak Resources Development Corporation, Gillette, Wyoming

	Coal analyses made by					
				ORNL		
	Wyodak[a]	HRI[a]	Livermore[b]	Sample 2A	Sample 3A	Sample 3B
Moisture, wt %	21.7	26.2	20.4	27.0	27.9	27.9
Proximate Analysis Dry, wt %						
Ash	7.9	8.2	-	5.1	4.4	5.2
Volatile matter	45.0	43.6	-	45.2	45.9	49.3
Fixed carbon	47.1	48.2	-	49.7	49.7	45.5
Ultimate Analysis Dry, wt %						
Carbon	-	69.91	66.7	69.99	69.95	70.79
Hydrogen	-	4.29	5.14	4.47	4.48	5.24
Sulfur	-	1.00	1.09	0.38	0.55	0.53
Nitrogen	-	0.65	1.22	1.05	1.07	1.21
Oxygen (by difference)	-	15.95	18.35	19.05	19.49	17.06
Ash	-	8.20	7.5	5.06	4.46	5.17
Heating Value, Btu/lb	8900	-	-	-	8500	9100

[a]Data obtained from P. M. Lantz, ORNL/TM-4789 (May 1975).

[b]Data obtained from A. Pasternak et al., UCID-16265 (May 1973).

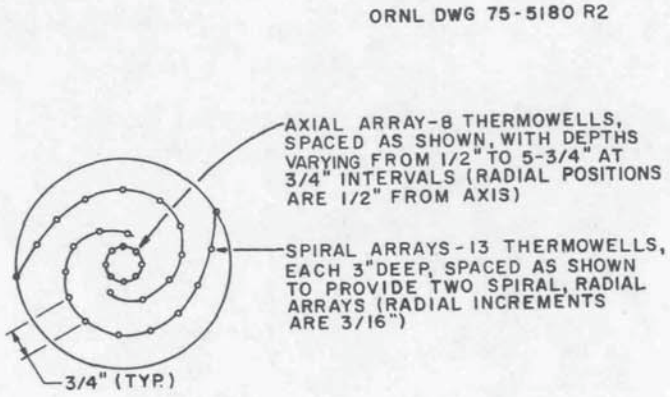


FIGURE 2. INSTRUMENTATION DETAILS FOR PYROLYSIS TEST BLOCK BP1-4.

EXPERIMENTAL PROCEDURE

After a test specimen has been placed in the reactor and a stable cover gas flow has been established, the reactor is heated at one of two heating rates chosen for these studies: 3.0 or 0.3 C^{o}/min. (Reactor temperature is referenced to a thermocouple at the surface of the coal block.) Block surface temperature is permitted to increase to a specified maximum temperature (500^{o} to 1000^{o}C) where it is held constant until interior thermocouples have reached T_{max} and gas evolution has ceased. Experiments to date have utilized argon or, in a few cases, nitrogen as the cover gas. The effects of reactive gases will be examined at a later date.

Typical thermal profiles produced by these experiments are shown in Figure 3. These profiles, which were measured using the thermocouple placement pattern shown in Figure 2, describe several interesting phenomena. First, no uneven burning effects were seen; all probes appear to describe a single thermal wave. This was observed to be the case even for specimens having large, deep cracks (> 5 mm) extending from the surface of the block nearly to the axis of symmetry. One observes further that axial probes at the top of the block measure temperatures which fall upon the radial profiles, whereas the bottom of the block does not appear to be heating. We conclude that pyrolysis of the block proceeds radially inward and axially downward, but not axially upward. Convective effects are probably responsible for this. Figure 4 reveals that heat transport within the wet coal

during the early stages of pyrolysis is primarily by conduction and is quite rapid until the boiling point of water has been reached throughout the block. Observe in Figure 3 that the temperature measured at the block's center is 100°C, as are those measured at locations lying between the center and the point at which the temperature gradient steepens. From that point, further heat transfer is restricted by the vaporization of water which results in the distinct "steam front" seen in Figure 3. Finally, the steep gradients seen in both figures show that heating rates experienced within the coal block bear little relationship to the nominal rate applied to the block surface. This is partly a result of slow movement of the "steam front" relative to the heating rate at the coal block surface, but several high-temperature experiments (T_{max} = 900-1000°C) showed the existence of predominent exothermic reactions at the center of the block which may also play a significant role in the observed behavior (1,2)

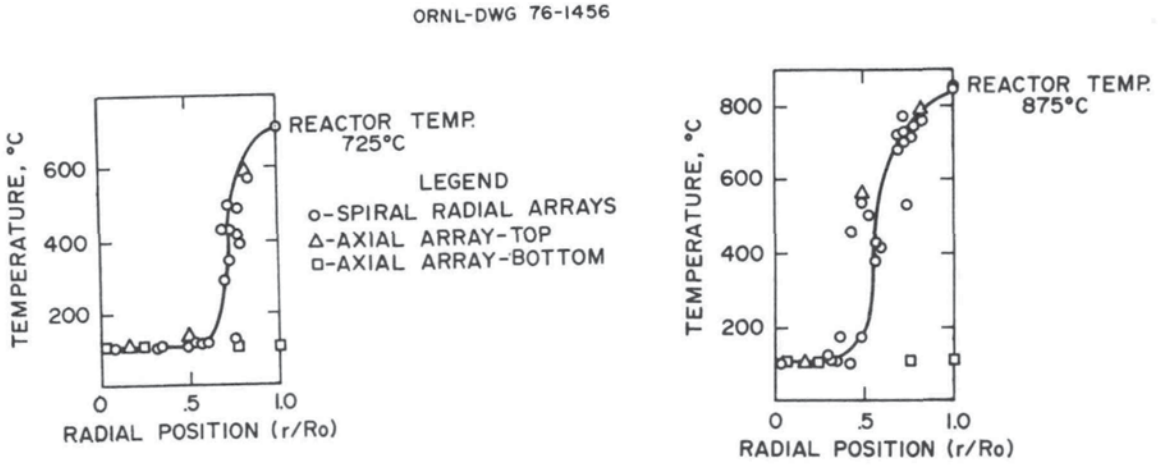


FIGURE 3. TEMPERATURE PROFILES OBSERVED DURING WHOLE-BLOCK PYROLYSIS EXPERIMENT BP1-4.

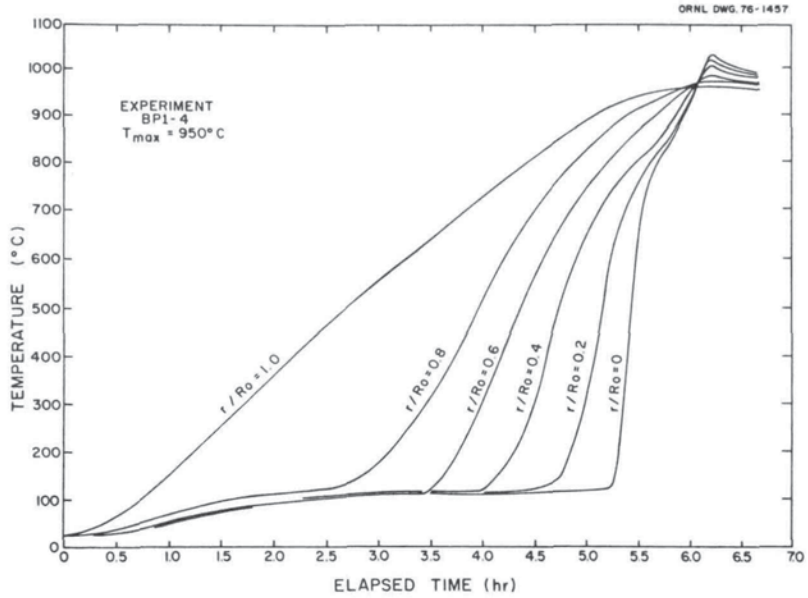


FIGURE 4. TEMPERATURE AT VARIOUS POSITIONS WITHIN SAMPLE BLOCKS AS A FUNCTION OF TIME.

Early experiments (3) utilized radial rather than spiral patterns for thermocouple placement, but close metal-to-coal-to-metal spacing resulted in higher effective thermal conductivities near the thermowells. Results shown in Fig. 3 indicate the close correlation shown by two different profiles in a single block. Later tests have also demonstrated good reproducibility between experiments (see Fig. 5).

In addition to monitoring temperatures within the coal and at various points about the apparatus, frequent measurements of reactor pressure, cover gas flow rate, liquid production rate, and gas production rate were made. Gas samples were taken at regular intervals. At the conclusion of each experiment, samples of the gross oil and water fractions produced and of the char remaining in the reactor were taken for detailed analysis.

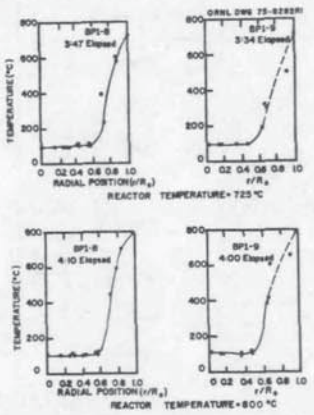


FIGURE 5. REPRODUCIBILITY OF BLOCK PYROLYSIS EXPERIMENTS.

RESULTS AND DISCUSSION

Experiments conducted to date provide some qualitatively predictable information about two-dimensional pyrolysis. Figure 6, for example, shows the variation in product split as a function of maximum pyrolysis temperature. As one would expect, the amount of gas produced increases with temperature at the expense of char (primarily) and liquid hydrocarbons. Heating rate, within the range examined, seems to have only a small effect upon this distribution. These results correlate well with those of Fieldner et al., whose experiments nevertheless dealt with the coking of Eastern bituminous coals in a 35-kg retort (4).

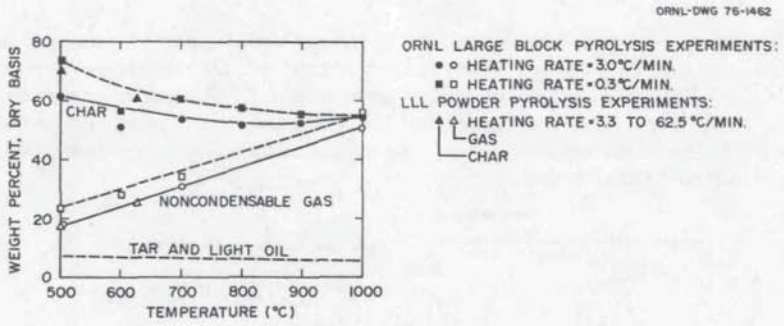


FIGURE 6. PRODUCT DISTRIBUTION AS A FUNCTION OF HEATING RATE AND MAXIMUM PYROLYSIS TEMPERATURE.

Chars. Analysis of chars produced by these experiments has been complicated by the repeated occurrence of pyrophoricity. When the reactor is disassembled and air is permitted to contact the char, self-heating is immediate and rapid, ignition sometimes taking place within a matter of minutes. Table 2 shows that the pyrophoric nature of the char is diminished as T_{max} is increased and that

ignition rarely occurs with those chars produced at temperatures above 700°C. Heating rate, within the range studied, appears to incluence this behavior slightly, but the type of coal is clearly an important factor. Samples obtained from LERC (Hanna No. 1 seam, for example, produce chars significantly less pyrophoric than those taken from the Roland and Smith seams. Reports of pyrolysis-enhanced reactivity could not be found in the literature; however, an experience of the British National Coal Board with a partially-coked bituminous coal was remarkably similar in that spontaneous self-heating and ignition were observed to occur (5)

Table 2. Pyrophoricity of chars produced by large block pyrolysis experiments using heating rates of 3.0 and 0.3°C /min.

Experiment number (BP2-)	Heating rate (°C/min)	Maximum pyrolysis temperature (°C)	Measured increase in temperature[a] (°C)
3	3.0	500	> 330
5[b]	3.0	500	22
8[c]	3.0	600	> 250
9[c]	3.0	700	224
12	3.0	800	> 258
15	3.0	900	192
4	0.3	500	264
6[b]	0.3	500	24
7	0.3	600	> 273
10	0.3	700	235
13	0.3	800	120
14	0.3	900	75

[a]Measured from 25°C after opening the reactor to the atmosphere. Entries indicating "greater than" a certain number of degrees refer to chars which were smothered with argon to prevent ignition.

[b]Sample was a 6-cm right circular cylinder of Hanna No. 1 coal (all others are Roland-Smith).

[c]Sample size was 6-cm dia. x 6-cm high (all other Roland-Smith samples were 15-cm dia. x 15 cm).

Some char samples have been recovered using techniques which avoid contact with air and have been subjected to ultimate analysis. Carbon and hydrogen content of these materials are shown in Figure 7 with a few data reporated by LLL for coal from the same mine. Heating values were found to lie between 12,200 and 13,100 Btu/lb with a general increase in heating value occurring as maximum pyrolysis temperature increased. Surface area and porosity determinations and the reactivity of a few selected samples with steam have also been reported (6,7).

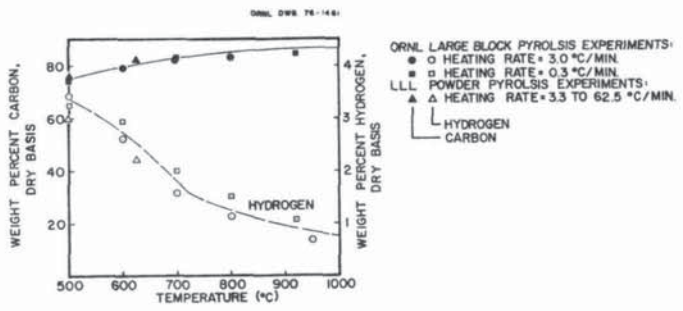


FIGURE 7. ANALYSIS OF CHARS PRODUCED BY TWO-DIMENSIONAL PYROLYSIS EXPERIMENTS.

Liquids. Liquids produced by the experiments have presented the most striking effect of heating rate variations. Tars produced at the lower heating rate are of lower average molecular weight and are decidedly less voluminous than those produced at 3.0°C/min. A sizable fraction of the tars produced at the higher heating rate is solid at room temperature, and these particular experiments produced essentially no light oils which could be separated from the aqueous liquor for meaningful analysis. Some tar constituents have been identified by gas/liquid chromatographic techniques reported in detail elsewhere (8).

Light oil production during the lower-heating-rate experiments, on the other hand, is significantly greater. The effect of maximum pyrolysis temperature upon the composition of these oils is shown by Figure 8. Note that the boiling range is narrowed and the oils become lighter as the maximum temperature increases. This result appears to be inconsistent with the observations made at the first field experiment at Laramie, but there are obvious reasons for this. Table 3 presents a comparison of the LERC and ORNL data, showing that the percentage of material boiling above 600°F is quite large for oils produced by our pyrolysis tests and by the LERC carbonization test, but much lower for the UCG test oils. The LERC assumption that only light oils will be carried to the surface is probably correct, but it is also likely that the reverse-burn configuration which produced LERC/1 caused a significant amount of cracking of the produced oils as our data (Figure 8) suggest. Table 4 details other characteristics of the light oils produced by these experiments.

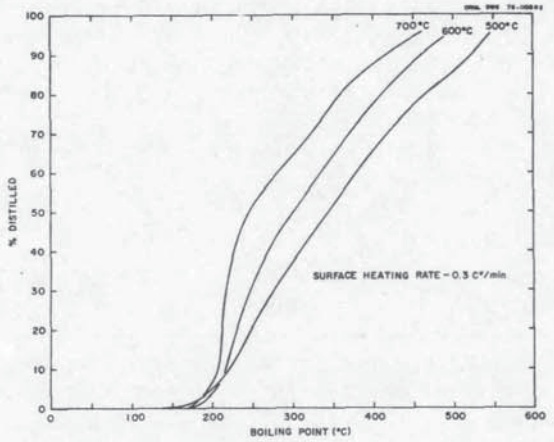


FIGURE 8. SIMULATED DISTILLATION CURVES FOR LIGHT OILS PRODUCED BY TWO-DIMENSIONAL PYROLYSIS EXPERIMENTS.

Table 3. Boiling range distributions by weight percent of light oils produced by large block pyrolysis compared with LERC determinations (9).

Sample description	100 – 400°F	400 – 500°F	500 – 600°F	600 – 700°F	700 – 800°F	800 – 900°F	900 – 1000°F	Residue
BP2-4	4.5	20.5	15.0	15.5	16.5	10.5	0	
BP2-7	4.5	31.5	17.5	15.0	11.0	15.0	0	
BP2-10	8.0	45.5	13.0	14.0	9.5	10.0	0	
LERC/1[a]	30.0	46.7	22.0	1.3	0	0	0	0
LERC/2[b]	6.2	16.9	25.6	28.2	16.0	5.3	1.8	0
LECR/3[c]	0	11.3	16.3	13.1	15.2	12.4	7.5	24.2

[a]Recovered from field experiment product stream during reverse-burn linkage operations.

[b]Recovered from field experiment product stream during cocurrent gasification.

[c]Laboratory carbonization at 500°C.

Table 4. Light oil production by large block pyrolysis experiments. (Heating rate for all experiments is 0.3°C/min.)

Experiment number (BP2-)	Maximum pyrolysis temperature (°C)	Heating value[a] (Btu/lb)	Density at 25°C (gm/cc)	Viscosity at 100°C (centistokes)
4	500	17,980	--	0.90
7	600	16,790	--	1.08
10	700	17,040	--	--
13	800	16,768	0.976	5.26

[a]Multiply Btu/lb by 2.326 to obtain kJ/kg.

Gases. Detailed analysis of gas production has been summarized in Figures 9 through 13. As shown in the first figure, there are three distinct regions of gas production: loss of adsorbed or loosely-bound volatiles, the so-called (10) primary pyrolysis stage and the secondary stage. Mazumdar states that 80% of the gas produced by pyrolysis is formed at or below 600°C during primary pyrolysis; however, these experiments would closely simulate the deviations from this rule observed in commercial coke-making practice wherein tars and steam interactions with the char/coke bed tend to increase the gas production at higher temperatures beyond what would be produced under "ideal" conditions. This is brought into focus by Figure 10, which shows the total gas production per kilogram of coal as a function of pyrolysis temperature and heating rate. Note that gas production at temperatures higher than 800°C is significatnly greater than that predicted by Mazumdar or observed by LLL during their powder pyrolysis experiments.

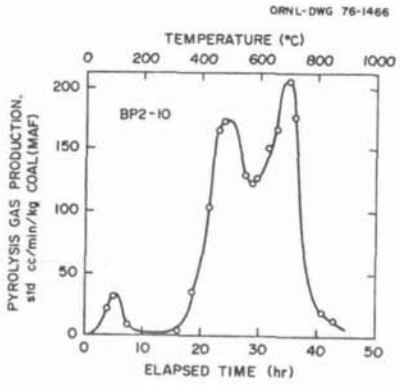


FIGURE 9. TOTAL GAS PRODUCTION RATES FOR TWO-DIMENSIONAL PYROLYSIS EXPERIMENTS AT 0.3 C°/MIN HEATING RATE.

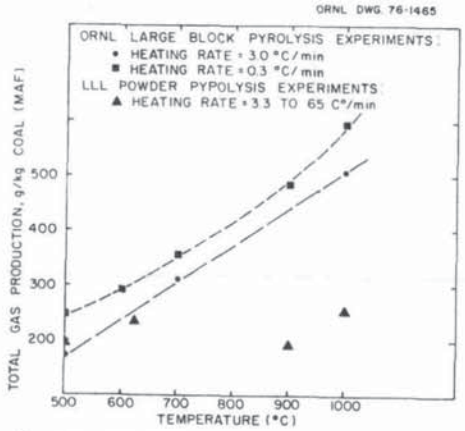


FIGURE 10. TOTAL GAS PRODUCTION AS FUNCTIONS OF MAXIMUM PYROLYSIS TEMPERATURE AND HEATING RATE.

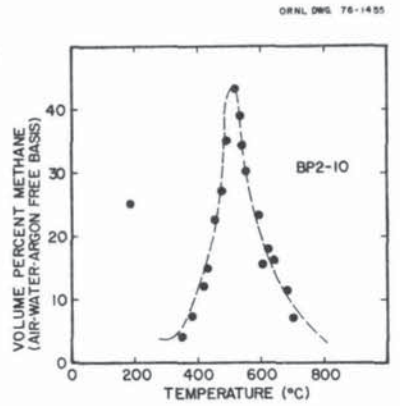


FIGURE 11. METHANE CONTENT OF PYROLYSIS GAS AS A FUNCTION OF BLOCK SURFACE TEMPERATURE. (HEATING RATE = 0.3 C°/MIN).

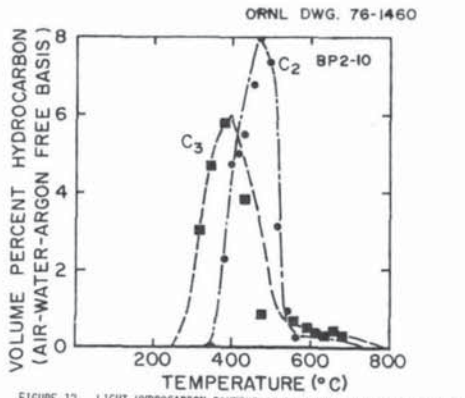


FIGURE 12. LIGHT HYDROCARBON CONTENT OF PYROLYSIS GAS AS A FUNCTION OF BLOCK SURFACE TEMPERATURE. (HEATING RATE = 0.3 C°/MIN).

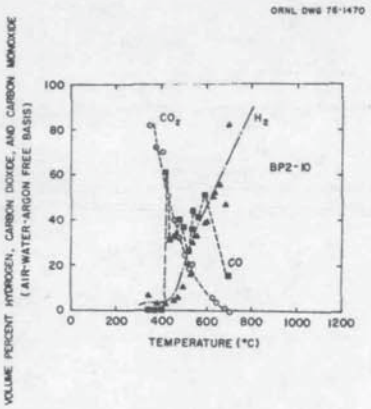


FIGURE 13. HYDROGEN, CO_2, AND CO CONTENT OF PYROLYSIS GAS AS A FUNCTION OF BLOCK SURFACE TEMPERATURE. (HEATING RATE = 0.3 C°/MIN).

The last figures summarize the change in composition of the pyrolysis gas with time for several experiments. Observe that methane evolution (Figure 11) is substantial during the primary pyrolysis stage but diminishes rapidly as the temperature increases beyond 600°C. This is true also of the light hydrocarbon gases (Figure 12). On the other hand, CO and H_2 production (Figure 13) begin at a relatively low rate and increase rapidly to account for nearly 90% of the total gas produced in the latter stages of pyrolysis. Carbon dioxide production, also shown in Figure 13, is observed to be negligible above 700°C.

CONCLUSIONS

Some of the preliminary data produced by these studies have been made available to the LLL modeling group and others, but variations in gas composition and production rates shown by more recent experiments to result from two-dimensional effects should be given serious consideration in future computer code development. It may even be appropriate, for example, to update one-dimensional codes presently in use as field test diagnostic tools to include two-dimensional pyrolysis product-split data. Most of these codes are presently written to include pyrolysis data obtained from TGA analyses of the coal to be gasified.

It would also be useful to expand the scope of these studies to include a look at the effects of pressure and reducing gas atmospheres upon Wyodak coals, followed by a few definitive experiments upon Eastern coals (both caking and non-caking) and some representative lignites. It is unlikely that extensive studies on other coal types would be required to obtain a reasonably accurate definition of two-dimensional pyrolysis behavior.

REFERENCES

1. R. C. Forrester III, "Experimental engineering support of an *in situ* gasification process," presented at the ORNL Chemical Technology Division's Annual Information Meeting, October 14-15, 1975.
2. J. N. Doggett, "Summary of large block oil shale retorting experiments," Lawrence Livermore Laboratory, UCID-16699, February 6, 1975.
3. J. P. Nichols (editor), "Coal technology program quarterly progress report No. 2 for the period ending March 31, 1975," ORNL-5049, August 1975.
4. A. C. Fieldner et al., "Methods and apparatus used in determining the gas, coke, and by-product making properties of American coals," U.S. Bureau of Mines Bulletin 344, March 1931.
5. John O. H. Newman, National Coal Board, Coal Research Establishment, personal communication, April 8, 1976.
6. J. Fischer et al., "Gasification of chars produced under simulated *in situ* processing conditions," Argonne National Laboratory, ANL-75-77, December 1975.
7. J. P. Nichols (editor), "Coal technology program progress report for July 1975," ORNL/TM-5037, October 1975.
8. J. P. Nichols (editor), "Coal technology program annual interim report for fiscal year ending June 30, 1975," ORNL-5069, October 1975.
9. S. B. King et al., "Characterization of nitrogen compounds in tar produced from underground coal gasification," presented at the Philadelphia meeting of the American Chemical Society, April 6-11, 1975.
10. B. K. Mazumdar and N. N. Chatterjee, "Mechanism of coal pyrolysis III: Relation to industrial practice," Fuel 52, p. 11, January 1973.
11. A. B. Macknick, "Pyrolysis of Wyoming subbituminous coal," Lawrence Livermore Laboratory, UCID-16710, March 10, 1975.
12. D. R. Stephens (editor), "LLL *in situ* coal gasification program quarterly progress report July through September 1975," UCRL-50026-75-3, October 31, 1975.
13. J. H. Campbell, "Pyrolysis of subbituminous coal as it relates to *in situ* gasification," Lawrence Livermore Laboratory, UCRL-52035, March 11, 1976.

Reaction Kinetics of Coal Char Gasification Under Conditions Expected in Underground Coal Gasification

BY

J. E. Young, Argonne National Laboratory, Argonne, IL
R. Lo, Argonne National Laboratory, Argonne, IL
J. Fischer, Argonne National Laboratory, Argonne, IL

ABSTRACT

This project, which is part of the Argonne National Laboratory energy program for ERDA, is directed toward support studies for the national endeavor on *in situ* coal gasification. The objective of this work is to determine the reaction-controlling variables and reaction kinetics for the gasification of chars resulting from pyrolysis of coal in underground gasification. The reactions to be studied include steam-char, CO_2-char, H_2-char, and the water gas shift reaction.

Studies are described concerning chars prepared from subbituminous coals obtained from the Wyodak-Anderson and Hanna seams in Wyoming. These studies include physical characteristics defined by surface area measurements and scanning electron microscopy. Results are reported for the reaction of steam with these chars.

Rate expressions are derived describing the reaction rate as a function of steam partial pressure, carbon consumption, and temperature. Pyrolysis of the coal under simulated underground gasification conditions results in a char with appreciably different characteristics from those of a char prepared externally to the reactor. The nature of these differing characteristics and their effects on the reactivity of the resulting char are discussed. The effects on these kinetics stuides caused by the catalysis of the water gas shift reaction by the mineral matter present in the coal are also discussed. In addition, the kinetics of the hydrogen-char reaction in the range of temperatures and partial pressures of hydrogen and steam expected in *in situ* gasification are described.

INTRODUCTION

The goals of the Argonne program of *in situ* coal gasification support studies are threefold: (1) To obtain kinetics data for use in mathematical models of the *in situ* gasification process, (2) To investigate effects of differing pyrolysis conditions on the reaction kinetics, and (3) To investigate the effects of using brackish water as the source of steam for underground gasification.

The mathematical models using our kinetics information are those prepared by the laboratories currently undertaking or planning actual field tests; Argonne is not carrying out a modeling effort for underground coal gasification. The reactions for which we plan to supply kinetic data are the reactions of steam with char, carbon dioxide with char, the water gas shift reaction, and the reaction of hydrogen with char. The source coals that to be studied include Wyodak and Hanna western subbituminous coals and Pittsburgh Seam eastern high-volatile bituminous coal.

The information presented in this paper includes preliminary kinetic data for the reaction of steam with chars prepared from Wyodak and Hanna coals. In addition, we discuss some differences in the physical nature of the Wyodak and Hanna chars, as well as the effects of these differences on the reactivity of these chars with steam.

EXPERIMENTAL

The kinetics studies are carried out in a packed bed differential reactor in which steam, carbon dioxide, and/or other reactants are blended with nitrogen to obtain the desired total pressure and partial pressure of reactants. Preparation of the char is carried out immediately prior to gasification in the reactor under conditions of pressure, heating rate, and sweeping gas composition similar to those encountered in underground gasification. The coals studied are characteristic of those expected to be utilized in *in situ* tests in the near future. The product gases are analyzed by means of an automated gas chromatograph, yielding concentration data for hydrogen, carbon monoxide, methane, and carbon dioxide.

A schematic diagram of the laboratory-scale char gasification system used in these studies is shown in Figure 1. The water for steam generation is supplied by a high-pressure positive-displacement metering pump. This pump provides a variable feed rate (which can be set at a minimum of 5 cm^3/hr). The water flows into a coiled-tube high-pressure steam generator which is encased in a split-type furnace. The steam is then blended with additional reactant or carrier gas (N_2, CO, CO_2, H_2) prior to entering the reactor. Both the steam and the reactant gas flows can be remotely switched to bypass the reactor, either for flow calibration purposes or during standby.

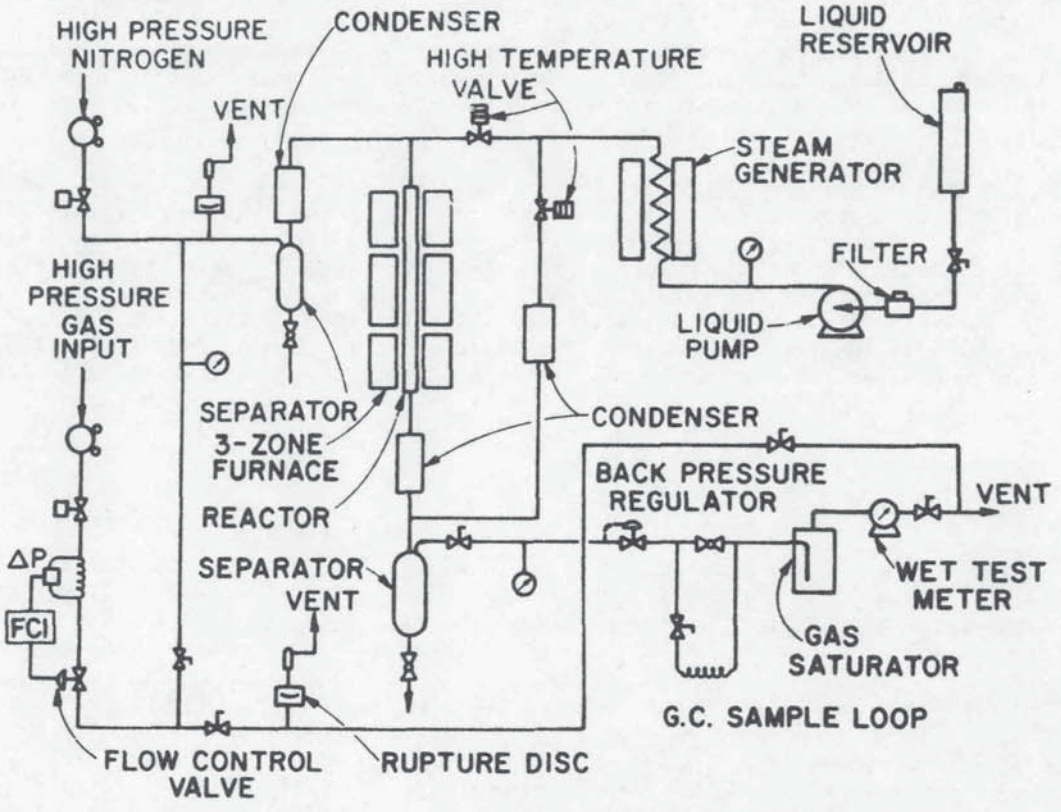


Figure 1. Schematic of Char Gasification System

The reactor vessel (1.6 cm ID x 91 cm long) is constructed of Type 316 stainless steel. The lower half of the reactor is filled with 120-mesh high-purity alumina. Above this is the 2 to 5-cm-deep char or coal bed, crushed to -4 +12 mesh. Above the char, the balance of the reactor is filled with 8-mesh alumina, which serves as a steam preheater section. The reactor is heated using a three-zone split-type tube furnace with 15.25, 30.5, and 15.25-cm-long heater sections. Reactor temperatures are monitored by means of a cluster of three thermocouples situated at the center axis of the reactor.

The kinetics experiments are carried out under differential conditions in order to accurately define the uniform partial pressure of reactants throughout the char bed and maintain nearly another must condition throughout the bed. In an experiment, the product stream after leaving the reactor is cooled in a high-pressure, water-cooled condenser, and the steam and hydrocarbon condensate is collected in a high-pressure separator vessel. The product gas is then let down to 172 kPa (25 psig) through a remotely controlled back-pressure regulator, and passed to the analytical section. At this point, the gas is fed to an on-line gas chromatograph and then to a wet-test meter for measurement of total product gas flow.

By means of the gas chromatograph, the product gas from the reactor is analyzed for H_2, CO, CH_4, and CO_2. The analysis is carried out utilizing a Hewlett Packard Model 5830A gas chromatograph equipped with both thermal conductivity detectors (TCD) and flame ionization detectors (FID). This unit is programmed for automatic operation of the gas sampling valves, switching of the detector signals, and integration of the areas of the peaks resulting from the various gas constituents.

Two chromatographic columns are used. A 91.4 cm (3 ft) long by 3.18 mm (1/8 in.) OD by 2.16 mm (0.085 in.) ID stainless steel column containing 80/100 mesh type 13X Molecular Sieve is used for separation of H_2, CH_4, and CO. Carbon dioxide is separated and measured, utilizing a 91.4 cm (3 ft) long by 3.18 mm (1/8 in.) OD by 2.16 mm (0.085 in.) ID stainless steel column containing 80/100 mesh Porapak Q-S.

Contamination of the Molecular Sieve column by CO_2 is prevented by inserting upstream from it an absorber consisting of a 30.5 mm (1 ft) by 4.76 mm (3/16 in.) OD by 3.17 mm (1/8 in.) ID stainless steel tube containing Ascarite. The Ascarite consists of sodium hydroxide on an inert support, and permanently absorbs any acid gases (CO_2 or H_2S).

The effluent from the Molecular Sieve column is monitored by means of a thermal conductivity detector and an FID placed in series. The TCD is used for detection of Hydrogen and CO; the FID is used for detection of methane. The CO_2 is detected by means of a TCD used in conjunction with the Porapak Q-S column.

Neon, the carrier gas, gives good sensitivity for all components in the product gas stream. 0.5-cm^3 samples are injected into each column for analysis. The column temperature is 35°C, detectors are operated at 100°C, carrier gas flow is 40 cm^3/min through each column. The total time necessary for a complete analysis and data output for the four components is approximately 6.5 min.

RESULTS AND DISCUSSION

A number of experiments have been carried out in order to characterize the chars formed from the Wyodak-Anderson and the Hanna coals and to define some of the differences between the two chars. It was anticipated that the conditions present during pyrolysis and occurring between the pyrolysis and gasification stages of the process would affect the reactivity of the resulting chars toward steam. Therefore, experiments were carried out to confirm this effect.

Samples of the Wyodak and Hanna coals were pyrolyzed in our reactor system and then removed from the reactor for characterization prior to gasification. The coals were crushed to -4 +12 mesh, and then pyrolyzed at 3°C/min to a maximum temperature of 700°C. The system pressure was 0.162 MPa with 2.5 liters (STP)/min nitrogen flowing through the reactor. Under these conditions, the average keep in linear velocity of gas through the coal bed was 3 cm/sec. After it was cooled in a nitrogen flow, the char was removed from the reactor. The ash content was measured and the percent carbon recovered was determined. For the Wyodak coal, 44 percent of the coal on an as-received basis was recovered as char, which had as ash content of 16 percent. For the Hanna coal, 60 percent of the coal (as received) was recovered as char. The ash content of the Hanna char was 6.1 percent.

Surface areas of these chars have been measured by nitrogen adsorption (BET method) and carbon dioxide adsorption. The results of these measurements are shown in Table 1. The surface areas of both the Wyodak and Hanna chars as determined by nitrogen adsorption are extremely low, while the areas determined by CO_2 adsorption are high. This indicates that most of the surface occurs in the micropore structure of the char.

Table 1. Surface Area (m^2/g)

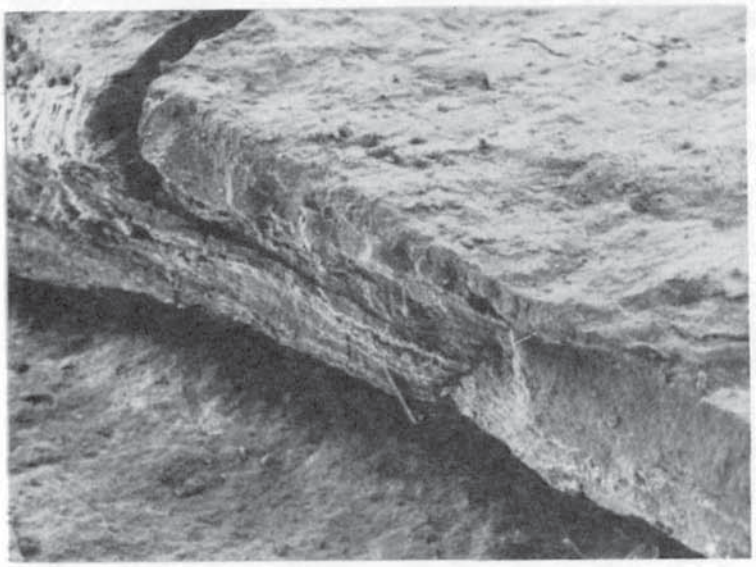
Pyrolysis Conditions		Wyodak BET	Wyodak CO_2	Hanna BET	Hanna CO_2
ANL					
3°C/min, 16 atm	700°C	1.2	455	0.2	549
ORNL					
3°C/min, 1 atm	650°C	4	320		
3°C/min, 1 atm	900°C	190	350		
LLL					
1 atm	675°C	211			
1 atm	800°C	124			

A char prepared at high pressure can be compared with a char prepared under similar heating conditions but at lower pressure. We have measured the surface area of a sample of Wyodak char obtained from Oak Ridge National Laboratory. This char was the product of a pyrolysis experiment in which a large block of coal was heated at a 3°C/min average heating rate, but under an atmosphere of argon at ambient pressure. This char, when heated to 650°C showed a very low surface area as determined by the surface area determined by CO_2 absorption was somewhat less than that obtained in the higher pressure pyrolysis experiment.

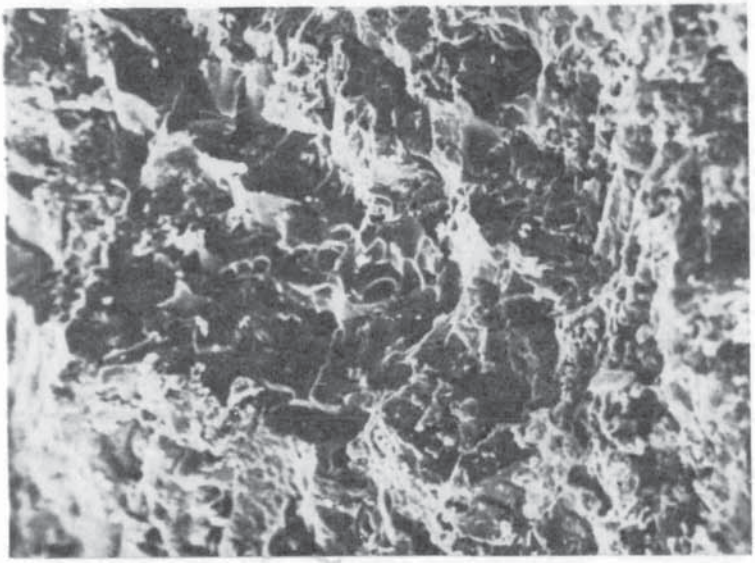
Surface areas measured for these chars appear to contrast sharply with those measured for a Wyodak char by Taylor and Bowen at Lawrence Livermore Laboratory (LLL).[1] This char was pyrolyzed in 0.1 MPa (1 atm) pressure of argon at an unknown heating rate. The BET determined surface areas of the chars pyrolyzed to both 675°C and 800°C at LLL are considerably higher than those obtained in our studies. Also, the char prepared at the higher temperature had a smaller area than did that prepared at lower temperature, which is an effect opposite to that observed in the case of the ORNL prepared char. The reason for these anomolies is not known.

Scanning electron micrographs have been taken of the Wyodak and Hanna chars prepared in our reactor. Figure 2a is a low-magnification view of the Wyodak char, showing the macrofissures formed during pyrolysis. This view shows two perpendicular surfaces of a char particle. These two surfaces differs greatly in structure, as seen in Figures 2b and 2c. Figure 2b shows a more detailed structure of the edge surface of the particle shown in Figure 2a. This surface contains a relatively small number of large fissures. However, there is also a great number of nearly round pores in this surface of the char, very closely spaced with diameters of 2-10 μm. In Figure 2c, we see the detailed structure of the flat surface of this same particle. Instead of rounded pores, there are many submicron sized cracks in addition to the large macrofissures.

The surface character of a particle of the Hanna char is shown in Figure 3a. The Hanna and the Wyodak chars differ considerably in physical appearance. The Hanna char has a glassy appearance after pyrolysis, with the particle edges and fissures generally at random angles. The Wyodak char has a matte, porous appearance, with many fissures occurring parallel or perpendicular to each other. Figure 3b shows a higher magnification view of one particle of the Hanna char. The microfissures observed in the Wyodak char did not appear in the Hanna char. With few exceptions, there was observed only the submicron sized pores that are apparent in Figure 2b. There appears to be a considerably smaller number of these pores in the Hanna char, although their sizes are roughly equal to the sizes of those observed in the Wyodak char. The bright specks in Figure 3b are mineral matter present in the char. X-ray analysis of the specks in this picture indicates the presence of iron, sulfur, aluminum, and silicon.



2a 36 μ



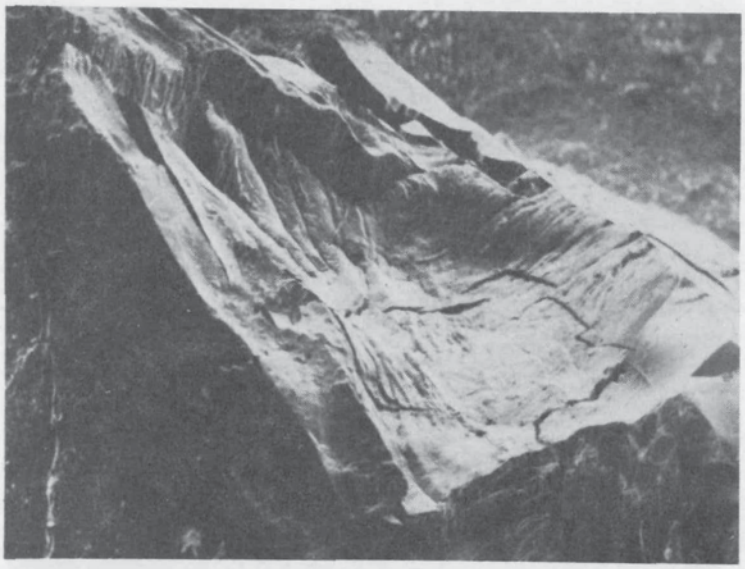
2b 5.6 μ



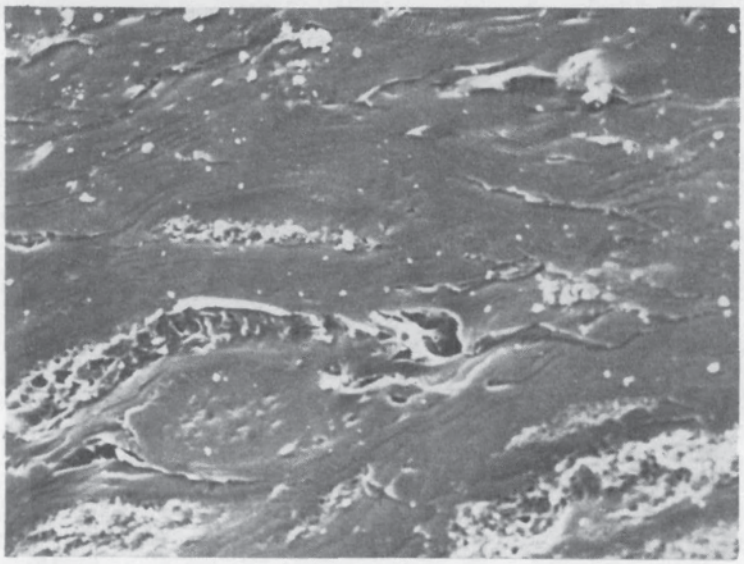
2c 1.1 μ

Fig. 2.

Scanning Electron Micrographs of Wyodak Char



3a ⟷ 105 μ



3b ⟷ 5.1 μ

Fig. 3.
Scanning Electron Micrographs of Hanna Char

From these micrographs and from the surface area determinations, it appears that the porosity of the Hanna char is considerably less than that of the Wyodak char, which would result in severe mass transfer limitations in the accessibility of reactants to the char surface. The kinetics data presented below support this observation.

It is evident in Table 1 that variation in the conditions during pyrolysis of the coal appears to have an effect on the physical nature of the char. For the reaction with steam, the reactivity of a char prepared in the gasification reactor immediately prior to gasification (internal pyrolysis) is compared in Fig. 4 with that of a char prepared externally and transferred in air to the gasification reactor. The externally prepared char is a portion of the product of the ORNL large-coal-block pyrolysis experiment described earlier in which the heating rate was 3°C/min, the final temperature was 800°C, and the pyrolysis atmosphere was 0.1 MPa (1 atm) argon. The char prepared in the ANL gasification reactor was pyrolyzed at a heating rate of 3°C/min to 700°C in 0.16 MPa (16 atm) absolute pressure of nitrogen, with a flow rate of 2.5 liters (STP)/min. Gasification of both samples was carried out at 700°C, with a partial pressure of 0.64 MPa (6.3 atm) steam, total system pressure of 0.16 MPa (16 atm).

In Fig. 4, the instantaneous reaction rate is expressed as grams carbon gasified/hr-g ash-free carbon remaining. On the abscissa, the fraction converted is plotted on an ash-free basis. The two chars initially have very similar reactivities, but as the carbon is consummed, the externally prepared char decreases in reactivity rapidly, eventually leveling off at a value equal to approximately 30% of the original reactivity. The reactivity of the char prepared in the ANL reactor immediately prior to gasification increased and then held a high value of reactivity until at least 50% of the char was consummed.

A relatively simple expression that has been used to describe the kinetics of the steam/char reaction is:

$$\frac{dc}{dt} = A(X_c)^n \ (P_{H_2O})^m \exp \ (\frac{-E_a}{kT}) \qquad (1)$$

where dc/dt = the instantaneous rate of gasification of the carbon

X_c = fraction of carbon remaining

P_{H_2O} = partial pressure of steam

E_a = activation energy (k cal g-mole)

T = reaction temperature (K)

k = gas constant (k cal g-mole)$^{-1}$ (deg K)$^{-1}$

A = experimentally determined proportionality constant

n = reaction order in carbon

m = reaction order in steam

The value of n is generally considered to equal 1 for the steam-carbon reaction. If this is true, then rearrangement and integration of equation (1) would yield:

$$\frac{dc}{X_c} = A \ (P_{H_2O})^m \exp \ \frac{-E_a}{kT} \ dt$$

$$\ln X_c = A \ (P_{H_2O})^m \exp \ \frac{-E_a}{kT} \ t + B$$

where t is time and B is the integration constant. If this reaction is indeed first order in carbon, then ln X_c or log X_c should be a linear function of time.

A plot of log X_c versus time is shown in Fig. 5 for both the internally and externally prepared chars. In the case of the internally pyrolyzed char, the reaction is very nearly first order with respect to carbon until more than sixty percent of the char is gasified. For the char prepared externally, the reaction appears to remain first order in carbon through the fifty percent conversion point, but the curve changes slope at approximately the thirty percent conversion point.

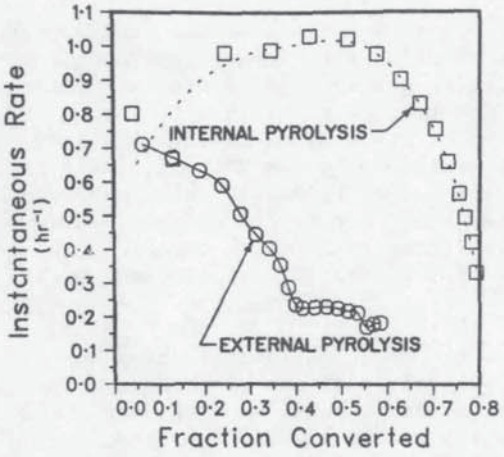


Fig. 4. Effect of Pyrolysis Conditions on Gasification Rates

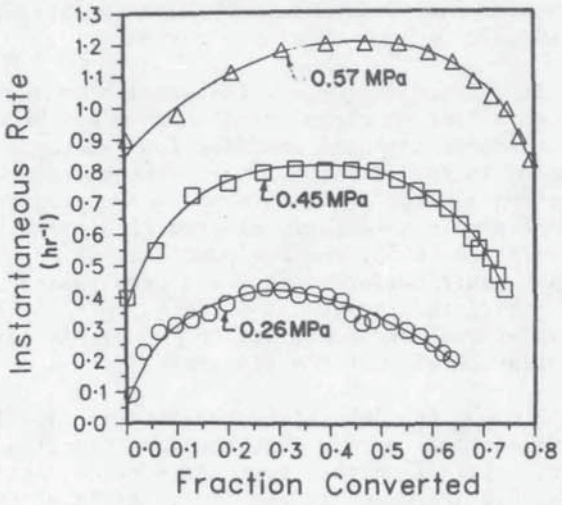


Fig. 6. Effect of Steam Partial Pressure on Gasification Rate (Wyodak char)

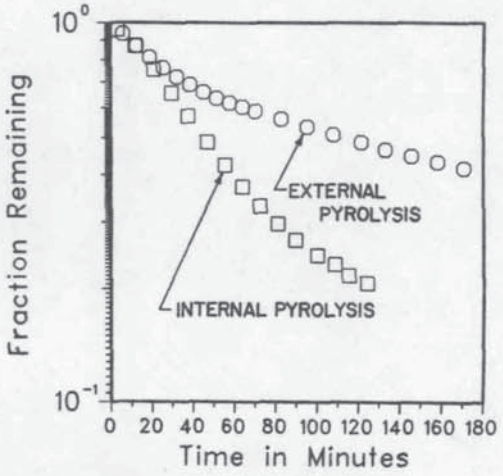


Fig. 5. Effect of Pyrolysis Conditions on Gasification Reaction Order

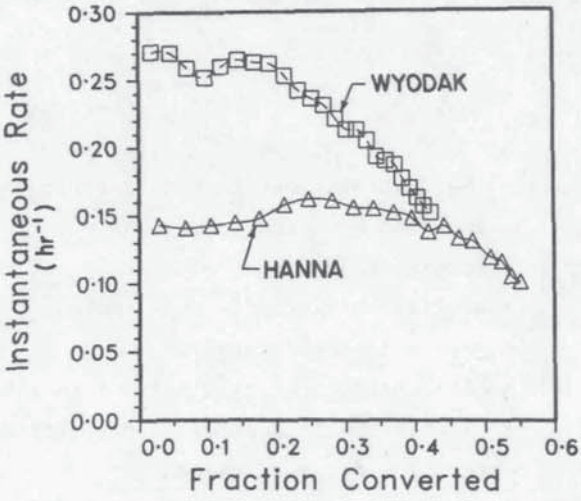


Fig. 7. Comparison of Reactivities of Hanna and Wyodak Chars

As a result of the above-described observations, all subsequent kinetic studies reported here have been carried out with pyrolysis performed in the gasification reactor immediately before gasification.

The effect of P_{H_2O} on the gasification rate is indicated in Fig. 6. Wyodak char was used, and the reaction temperature was 700°C. Up to this time, only three partial pressures of steam have been studied: 0.26, 0.46, and 0.57 MPa (2.6, 4.5, and 5.6 atm, respectively). As defined in Equation (1), the value of m appears to be 1.3 for conversion of the first twenty percent of the carbon and then decreases to 1.2 for conversion of the balance. However, it will be necessary to investigate a wider range of steam partial pressures to better define a value for the constant m in Equation (1).

The reactivities towards steam for the Wyodak and the Hanna chars under similar pyrolysis and gasification conditions are compared in Fig. 7. The reaction temperature for these experiments was 650°C, the steam partial pressure was 0.71 MPa (7.0 atm), and the total system pressure was 0.16 MPa (16 atm). The reaction rate for the Wyodak char is approximately twice that for the Hanna char. A reason (if only a partial reason) for this difference in reactivity can be found in the differences

in surface area and porosities. The Hanna char has a much smaller number of macropores, as can be observed in the photomicrographs. This would limit accessibility of the steam reactant to the interior of the carbon particle. In addition, the BET-determined surface area of the Hanna char was less, although the CO_2-determined surface area was approximately 20 percent greater. This would indicate that not all of the microporosity of the carbon indicated by CO_2 adsorption is available to steam as a reactant and specific reaction sites are required for the reaction.

The temperature dependence of the conversion rate for the Wyodak char is shown in Figure 8. Four temperatures have been investigated--600, 650, 700, and 750°C. Lower temperatures will be studied in the future. At each temperature, the multiple points plotted on the graph correspond to the conversion rates at the various stages of conversion--10%, 20%, 30%, etc. In most cases, the points are grouped closely enough that an average apparent activation energy can be determined throughout the range of conversion up to approximately 50% conversion. At 600°C, the reaction rate was so low, that only the rate at 10% conversion was obtained. The partial pressure of steam for all of these determinations was 0.71 MPa (7.0 atm). Between 600 and 700°C, the apparent activation energy is 318 kJ/mole (76 kcal/mole) while at higher temperatures, it decreases considerably. Between 700 and 750°C, the apparent activation energy is approximately 53 kJ/mole (15 kcal/mole). The radical decrease in E_a at higher temperatures points to rather severe diffusion limitations at these temperatures. The kinetics are no longer limited by the kinetics of the reaction, but the reaction rate is now fast enough that diffusion through the pore structure is the limiting factor.

In Reference (1), an apparent activation energy for the reaction of steam with Wyodak char was calculated to be 184 kJ/mole (44 kcal/mole) in the temperature range, 500 and 675°C. The partial pressure of steam in this study was 1 atm. Quite possibly, at this lower partial pressure of steam, diffusion limitations exert an effect, even at the lower temperatures.

In the case of the Hanna char, only three gasification temperatures have been studied at this time, 650, 700, and 750°C. Their effect on conversion rate is plotted in Fig. 9. It should be noted that at 750°C, the variation in conversion rate as a function of extent of conversion is much greater than at lower temperatures. The conversion rate at 50% conversion is more than a factor of two greater than the rate at 10% conversion. The apparent activation energy at 10% conversion is less that the E_a at 50% conversion in the 700-750°C temperature range. This change in apparent activation energy would be expected if micropore diffusion limitations were occurring. At the beginning of conversion, the pore structure has not yet been opened by partial consumption of the carbon, hence the diffusion limitations would be greater at the earlier stages of conversion. At the maximum conversion rate observed, the apparent activation energy is 113 kJ/mole (27 kcal/mole) between 700 and 750°C, but it appears to be approximately 222 kJ/mole (53 kcal/mole) between 650 and 700°C. Obviously a wider temperature range must be investigated to better define the range of activation energies encountered for this reaction. It also appears that for these chars, the apparent activation energy and the partial pressure of steam may be related. If this dependence is real, the reason for it is undoubtedly the limitations due to micropore diffusion.

The distribution of product gases for a typical steam-char gasification run is shown in Figure 10. No carbon monoxide was detected; only in the case of very low partial pressures of steam is carbon monoxide observed in the product stream. The ratio of H_2 to CO_2 is almost exactly 2:1, indicating that the water gas shift reaction ($CO + H_2O \rightarrow CO_2 + H_2$) was occurring to a great extent. In fact, the observed H_2 and CO_2 concentrations indicate that thermodynamic equilibrium for the water gas shift reaction is reached under our reactor conditions, most likely catalyzed by the ash content in the char. In the case of the Hanna chars, the hydrogen to carbon dioxide ratio is always somewhat less than 2:1, indicating the probability of a lesser extent of catalysis for the shift reaction with this char.

There is also a surprising amount of methane observed in the product gas stream. This methane persists for the duration of the experiment, indicating that it is not the result of continuing pyrolysis reactions occurring after introduction of the steam to the char. An experiment has been carried out in which the partial pressure of hydrogen was set equal to that expected in actual underground gasification. The results of this experiment are shown in Fig. 11. The Hanna coal was pyrolyzed in nitrogen at a heating rate of 3°C/min up to a final temperature of 700°C. At this point, no methane was detected in the gas stream. After the final temperature was reached, a blend of hydrogen and delium was introduced giving a hydrogen partial pressure of 138 kPa (20 psia) (at time = 0 in Figure 11). The average concentration of methane after introduction of the hydrogen was 0.015 mole %. After 60 min had elapsed, steam was introduced at a partial pressure of 0.33 MPa (3.3 atm). Upon introduction of the steam, the rate of production of methane doubled, and the production rate of methane was 20 percent of that of carbon oxides.

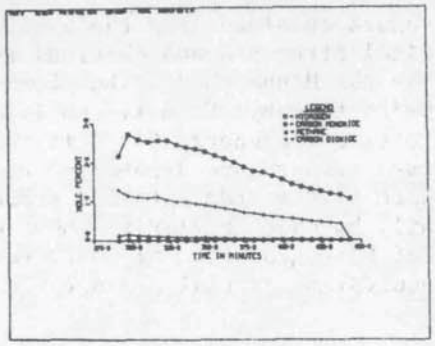


Fig. 10. Product Gas Composition Wyodak Char, Temp. 650°C, 7.36 atm Steam, 16.31 atm Total Pressure

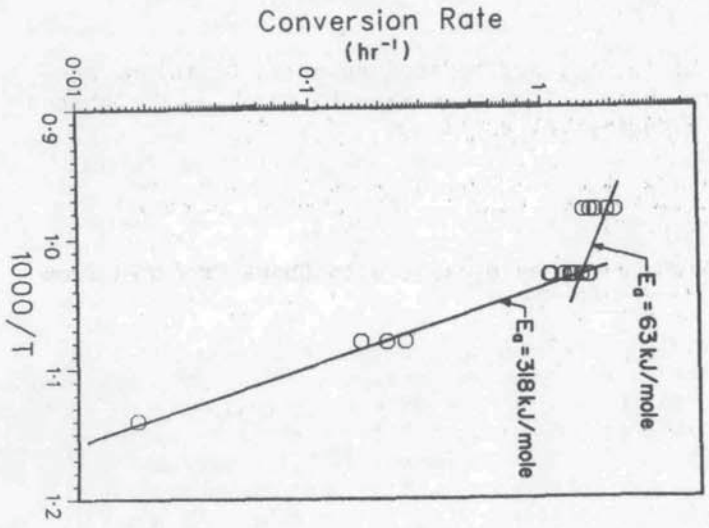


Fig. 8. Temperature Dependence of Gasification Rate, Wyodak Char

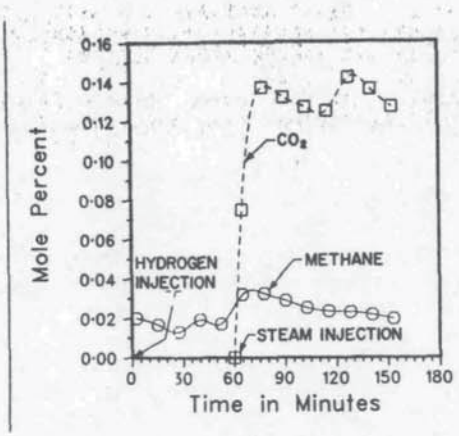


Fig. 11. Effect of Steam on Rate of Methane Formation, Hanna Char

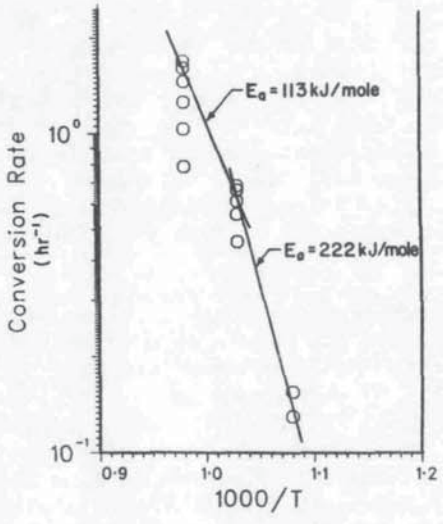


Fig. 9. Temperature Dependence of Gasification Rate, Hanna Char

In a similar experiment in which the steam partial pressure was 0.5 MPa (5 atm), the rate of methane production following steam injection was four to five times greater than that prior to the injection of steam. Insufficient experiments have been carried out to determine a kinetic model for this reaction, but it is apparent that there is a synergistic effect between hydrogen and steam for the production of methane. This phenomenon has been observed with both the Wyodak and the Hanna chars.

CONCLUSIONS

Preliminary information has been obtained regarding the kinetics of the reaction of steam with chars prepared from Wyodak and Hanna subbituminous coals. The chars have been prepared under conditions simulating those expected in underground gasification. It has been found that a close simulation of the actual pyrolysis conditions is necessary, since variations in the pyrolysis conditions have a significant effect on the reactivity of the chars toward steam.

The chars obtained from the Wyodak and the Hanna coals are quite different with respect to both physical structure and chemical reactivity. The Wyodak char is about twice as reactive toward steam as is the Hanna char. The steam-char reaction is first order in carbon, while the order in steam appears to range from 1.3 to 1.2, depending on the extent of conversion of the carbon. The apparent activation energy for this reaction ranges from 63 to 318 kJ/mole (15 to 76 kcal/mole); the observed temperature dependence of the activation energy indicates that the reaction is limited by diffusion of the reactants and products through the micropore structure of the char. Further studies will be made to clarify these diffusion limitations. The presence of steam promotes the reaction of hydrogen with the char, resulting in the formation of more methane than is formed with only an equivalent partial pressure of hydrogen.

ACKNOWLEDGMENTS

The authors wish to thank G. T. Chubb of the Biological and Medical Research Division, ANL, for taking the scanning electron micrographs of the chars. They also wish to thank J. E. Johnson and D. Bowyer for technical assistance during the experimental studies.

REFERENCES

R. W. Taylor, D. W. Bowen, Rate of Reaction of Steam and Carbon Dioxide with Chars Produced from Subbituminous Coals, UCRL-52002, January 16, 1976.

LAWRENCE LIVERMORE LABORATORY COAL GASIFICATION PROGRAM: UNDERGROUND REACTION MODELING AND LABORATORY COMBUSTION-TUBE EXPERIMENTS*

BY

R. ROZSA AND C. THORSNESS, LAWRENCE LIVERMORE LABORATORY,
UNIVERSITY OF CALIFORNIA, LIVERMORE, CALIFORNIA 94550

ABSTRACT

The in-situ coal-gasification concept currently under study at the Lawrence Livermore Laboratory calls for the fracturing of thick, deep, coal seams by means of chemical explosives. The high-permeability zone created by the blast would be ignited and reacted with a steam/oxygen mixture to produce medium-Btu gas. This gas could them be upgraded to pipeline quality in conventional surface facilities.

We discuss here recent calculational modeling and combustion-tube experiments carried out to evaluate the workability of the general coal-gasification concept. We seek specifically to predict and correlate reaction and thermal-front propagation rates and product-gas composition as a function of bed properties and process operating conditions.

Our preliminary model considers only one-dimensional transient Darcy flow in a permeable packed bed. The normal conservation equations are coupled by chemical reactions and heat and mass transfer. The combustion tube, 1.6 m long and 0.15 m in diameter, is designed for conditions up to 6.9 MPa (1000 psi) and 1300 K. It is equipped with electric heaters to reduce radial heat losses.

Results of a simulation of combustion-tube-reactor test runs are compared with observations. Good agreement is shown between calculated and experimentally observed reaction-front propagation rates as well as produced-gas compositions.

INTRODUCTION

In-situ coal gasification as a means of converting coal into a clean combustible gas has received renewed interest recently. It offers four potential advantages over conventional mining and subsequent surface processing:

- The product gas may be cheaper because of lower capital investment requirements.
- Environmental damage is likely to be lower.

*This work was performed under the auspices of the U. S. Energy Research & Development Administration, under contract No. W-7405-Eng-48.

- Hazards to miners are avoided.
- It may make possible the exploitation of coal resources too deeply buried for economic recovery by conventional strip or deep mining operations.

The Lawrence Livermore Laboratory (LLL) packed-bed concept was originated in 1972. Major program funding by the Energy Research and Development Administration (ERDA) began in 1974. The LLL concept is designed to provide medium-Btu gas from the thick, deeply buried, subbituminous coal deposits prevalent in the western United States. The product gas, after upgrading in a surface facility, would have sufficiently high energy density to make pipeline distribution economically attractive.

The packed-bed concept calls for creating a permeable zone of coal by detonating chemical explosives in an array of drilled boreholes. The resulting permeable zone is then ignited and a steam/oxygen reactant mixture supplied. The oxidation reactions produce a high-temperature zone, which propagates through the bed as a slow-moving thermal wave. This is shown schematically in Fig. 1. The thermal wave first dries the coal downstream of the reaction zone then pyrolyzes (devolatilizes) it forming a char. The char undergoes further reactions with the steam present. The major products of the overall process include H_2, CO, CH_4, and CO_2 as gases, and water and tar as liquids.

To further our understanding of the important parameters of the in-situ gasification process, mathematical modeling and laboratory experimentation have been carried out. Predicting resource recovery for a variety of different field geometries and operating conditions is the long-range goal of our modeling effort. This is a multidimensional, multiphase flow problem, but our preliminary model is a transient, one-dimensional description of the gasification process in a packed bed. It was developed to provide a framework in which to test the importance of accurately modeling the large number of physical and chemical processes involved in gasification. By comparing model results with carefully controlled experiments performed in a 1.6-m combustion-tube reactor, we can get an idea as to the relative importance of the various processes involved.

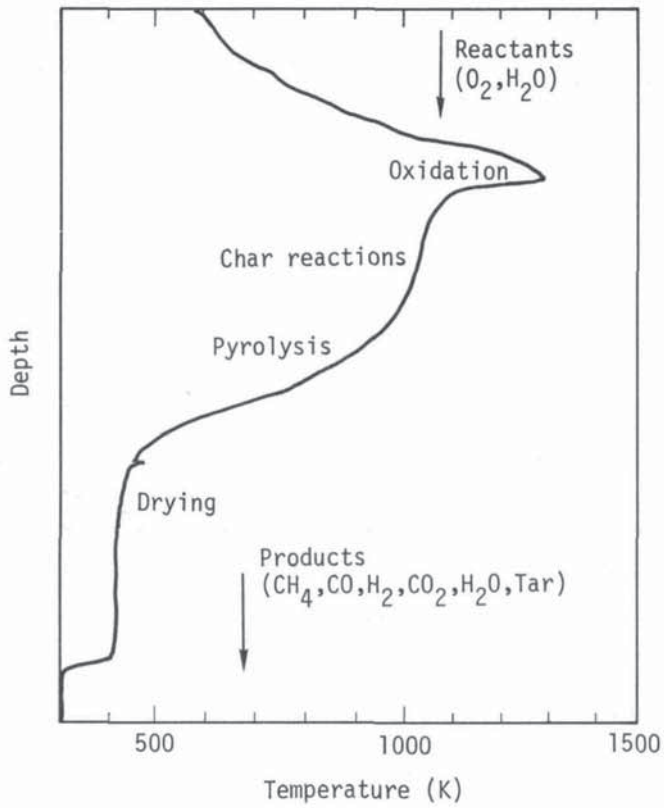


Fig. 1. Reaction schematic for in-situ coal gasification.

ONE-DIMENSIONAL MODEL

The model consists of mass balances for 13 species, energy balances on gas and solid phases, and a Darcy-flow momentum equation. The gas-phase species are N_2, O_2, H_2O, H_2, CH_4, CO, CO_2, and tar. The solid-phase species are coal, char, H_2O, and ash. The equations are coupled by source/sink terms involving heat and mass generation from 11 chemical reactions. Reactions include four heterogeneous gas-char reactions, the water-gas-shift reaction, coal pyrolysis, coal drying, steam condensation/vaporization, and three possible gas-phase oxidation reactions. Reaction rates are controlled by chemical kinetics at low temperatures, and are limited by mass transfer at higher temperatures.

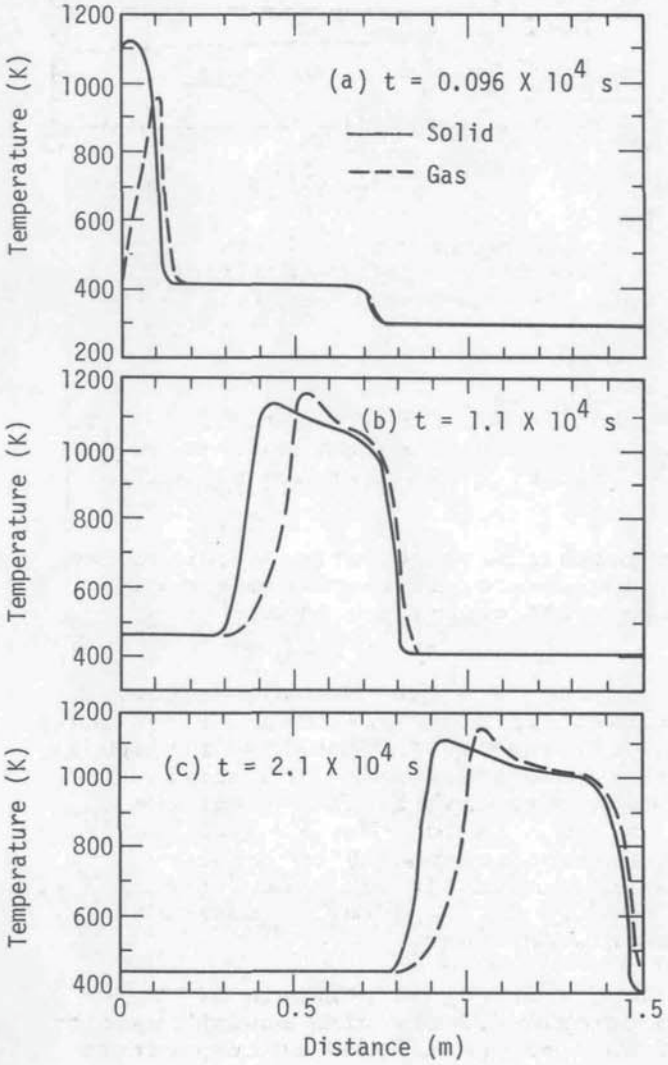
Several phenomena that may be very important for in-situ gasification are not considered in this model. These include effects of tar condensation and plugging,

gas losses to surroundings, water intrusion from surroundings, heat losses, and coal bed movement as a result of shrinking (or swelling) during drying and pyrolysis. The model could be extended to include in approximate fashion some of these effects, but this would require very careful consideration of how these essentially two- or three-dimensional phenomena might be represented in one dimension.

The system of differential equations is solved using finite-difference methods. The solution is performed on a grid system, which is allowed to evolve with time. Fine zoning is created where necessary to track high-gradient regions, and coarse zones are used where changes in the system in the space dimension are small. This allows long systems to be simulated with fewer grid locations than would be necessary with a constant grid system.

SAMPLE RUNS

A limited number of runs have been made with the current version of the numerical code. These consist of a simulation of the laboratory-scale experimental reactor and a first cut at a simulation of a field-scale system. Some results are shown in Figs. 2 and 3. Calculations of the temperature profiles clearly show the three fronts associated with the movement of the gasification processes through the bed. The leading steam-condensation front, which rapidly moves out of the bed, is followed by the drying/pyrolysis front. The third front is associated with the sharp negative temperature gradient that occurs where incoming reactants first contact



g. 2. Calculated temperature profiles for the 1.6-m-reactor simulation.

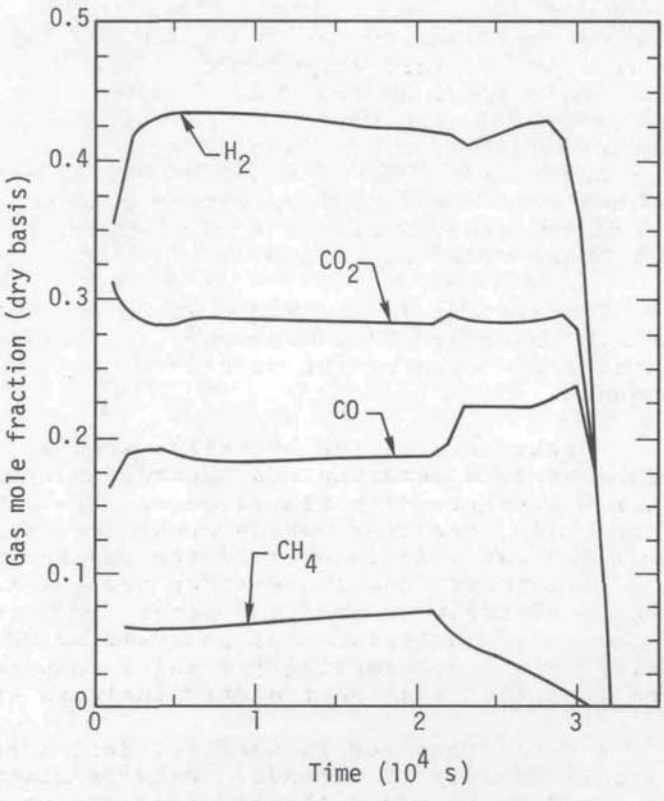


Fig. 3. Calculated effluent-gas composition for the 1.6-m-reactor simulation.

unconsumed char. The hot char zone grows as time progresses, indicating that the reaction and drying/pyrolysis fronts are moving at different speeds. As expected in a small particle system, the gas and solid temperatures are quite similar except in the vicinity of large gradients.

The effluent-gas composition is reasonably constant during the middle portion of the run, although slow trends are indicated due to the increase in the size of the hot char zone. The arrival of the pyrolysis zone at the exhaust end of the reactor causes an abrupt change in composition. After this time, CH_4 production steadily decreases due to less residence time of the gases in the shrinking hot char zone.

Calculation of a small field-scale (15-m) system shows similar thermal profiles. However, as shown in Fig. 4, the larger system with its extended char zone allows higher methane production.

DESCRIPTION OF THE 1.6-m REACTOR AND CONTROL SYSTEM

The coal gasification reactor is designed for operation at peak conditions of 6.9 MPa (1000 psia) and 1300 K to simulate the environment of deeply buried coal deposits. However, our current operating pressures are less than 0.69 MPa (100 psia) consistent with shallow field gasification tests.

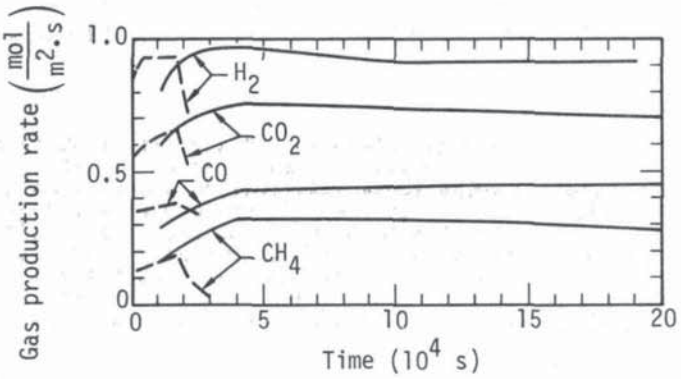


Fig. 4. Comparison of calculated effluent-gas composition (1.6-m reactor and 15-m field scale).

The reactor, shown in Fig. 5, consists of an inner thin-walled tube (310 stainless steel) 1.6 m long and 0.15 m in diameter. This tube, which houses the coal, is contained within a high-pressure outer tube 0.3 m in diameter. During operation, the annulus is pressure balanced with the inner tube using an inert gas. This design allows high-pressure operation with thin-walled tubing near the reaction zone to minimize heat-transfer effects (both radial and longitudinal). To further reduce radial temperature gradients, the annular region contains separately controlled electrically heated elements in 0.15-m lengths. This region is packed with loose fiber insulation.

Temperature is monitored with type K thermocouples sheathed with 310 stainless steel. There are 32 thermocouples placed in various locations in the packed coal and 16 are placed on the outside of the inner tube wall to monitor heater performance.

A schematic of the overall system is shown in Fig. 6. The reactant streams each contain a metering and monitoring system consisting of motor-driven valves and orifice-pressure-drop transducers. The products exiting the reactor flow through a water-cooled tar trap, which condenses the hydrocarbons and some of the water. The remaining water is removed in the condenser. The noncondensible gases continue on through a total-flow-integrating dry-gas meter and to a flare. Gas samples are withdrawn downstream of the flow meter for both gas-chromatograph (GC) and mass-spectrometer analysis. Gas analysis by GC is done continually (15-minute turnaround) during each run, sampling for major components H_2, CO, CO_2, and CH_4. Samples for more complete mass-spectrometer analysis are taken every hour.

A small computer is used for data acquisition, scanning 50 channels of temperature data every 15 seconds. Data is stored on cartridge disks with enough capacity for six 8-hour runs. Algebraic manipulation of data and generation of temperature plots are routine operations. The computer system also has sensing and feedback-control capability for many of the operating variables (e.g., reactant flows, pressure balancing, and back-heater control). We have not implemented these features

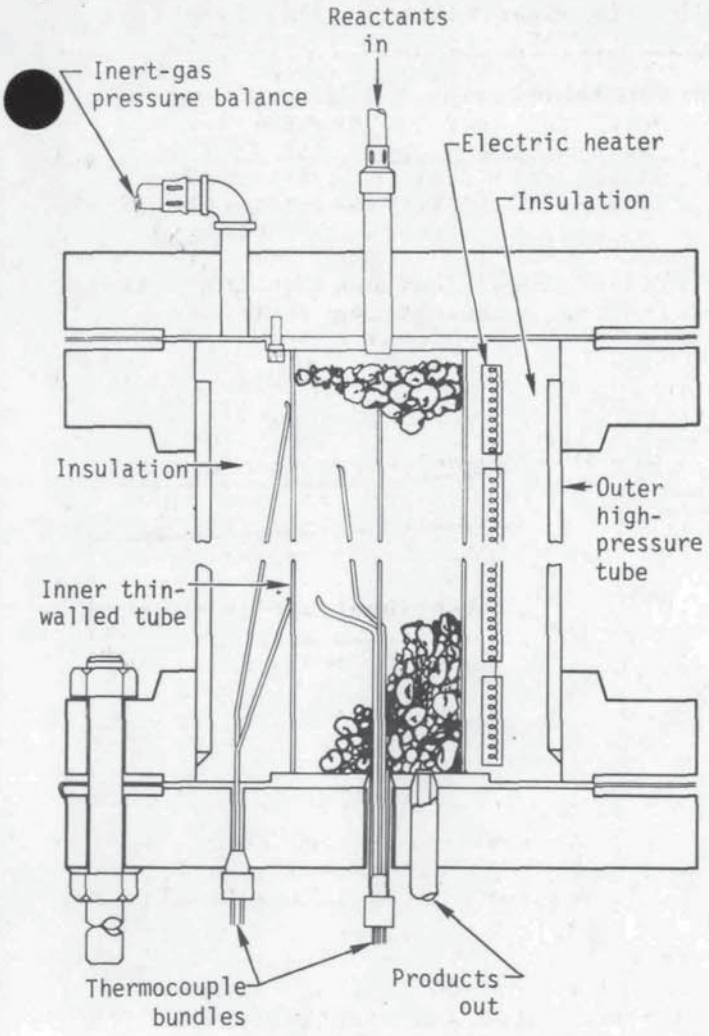


Fig. 5. Schematic of the 1.6-m coal gasification reactor.

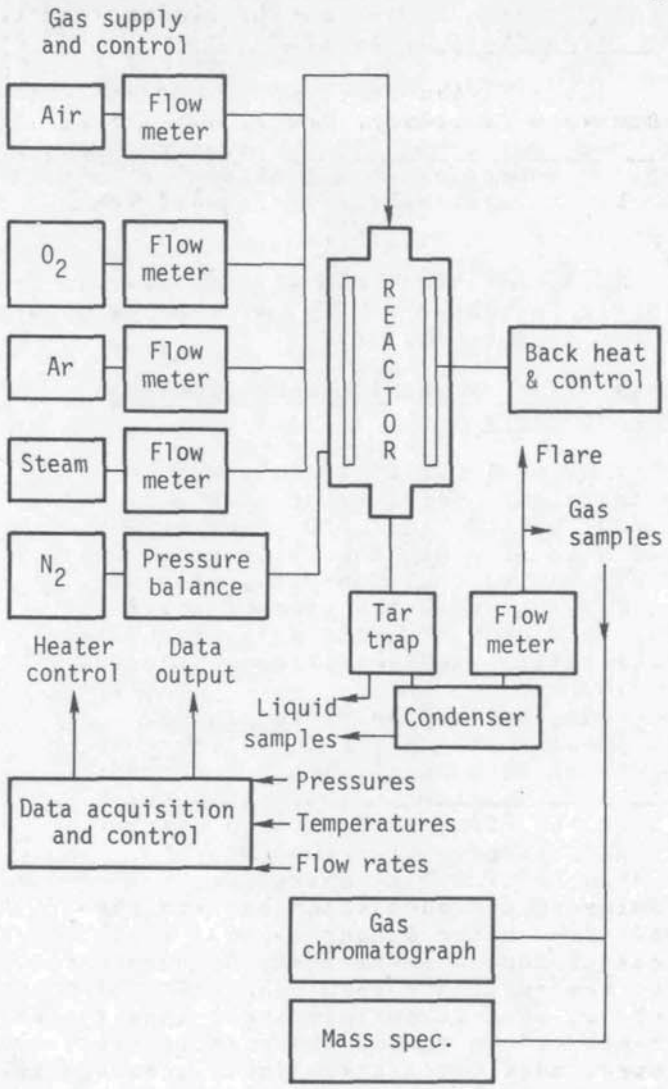


Fig. 6. Schematic of the 1.6-m coal gasification reactor system.

because operation in the manual mode has thus far been very stable. Later, when higher-pressure operation or long run times are used, some automatic control will be added for safety and convenience.

EXPERIMENTAL RUNS

The system was recently completed. To date, we have conducted seven experimental runs, each one lasting approximately 8 hours. A summary is given in Table 1. Runs 1, 2, 3, and 7 were used to shake down various parts of the operating system, the back-heaters, and the computer and to investigate various operating conditions. We varied the ratio of O_2 to steam in the feed streams and also tried two particle sizes of coal. The system was quite stable, and everything worked as planned.

Runs 4, 5, and 6 were conducted to investigate the effect of back-heating on the gasification process. With no back-heating, the outside-wall temperatures would only reach 700 K, while the center line in the coal was above 1000 K. With the back-heaters on, the outer wall could be raised to 1000 K, thereby reducing radial losses greatly.

Tables 2 and 3 show details of heat and material balances for runs 4, 5, and 6. Mass balances on the major streams showed a closure of better than 97%. Heat

Table 1. Summary of 1.6-m reactor experiments.

Run No.	Absolute pressure, MPa	H_2O/O_2, mole ratio	Particle size, mm	Remarks
1	0.52	3.7-4.8	3	First run, not back-heated, no computer operation
2	0.52	6.3	3	First back-heated run, first computer data acquisition
3	0.52	5.4-6.3	10	Not back-heated, larger particle size
4	0.52	5.9	10	New thermocouple-bundle design, base run for back-heating investigation (no back-heating)
5	0.52	5.9	10	Back-heated at low rate
6	0.52	5.9	10	Back-heated at high rate
7	0.24-0.52	4-7	10	Test of (O_2/H_2O reaction with char, variety of conditions tested

balances around the coal volume showed that the heat losses for run 4 were about 17 MJ over the 8-hour running time. This agrees with simple heat-conduction-loss calculations. Runs 5 and 6 showed no significant losses compared to the enthalpies of the major streams. The heat released during the oxidation reaction is about 40 MJ, or a factor of 2 to 3 greater than the heat losses for the run without back-heating. In runs 5 and 6 the electric heaters generated about 40 MJ of heat. However, most of this does not enter the coal or produced gas. It is instead lost to the outside. Energy balances on these reacting systems are difficult to close completely, but everything is within the expected range.

The predicted and experimentally observed thermal-front propagation rates are shown in Figs. 7 and 8. Both the reaction and drying/pyrolysis zone movements are affected by the degree of back-heating. It appears that run 5 had about the right amount, while run 6 had too much. Comparison of calculated and observed effluent-gas compositions (Table 4) also reveals very good agreement, although the difference between runs 4, 5 and 6 was not significant. The produced gas had a gross heat of combustion of about 11 MJ/m^3 (290 Btu/ft^3).

CONCLUSIONS

The one-dimensional model in preliminary form predicts reaction-zone propagation rates and produced-gas compositions rather well, as evidenced by our laboratory-scale reactor data. However, one cannot conclude from this that all formulations used are accurate. In fact, the good agreement probably indicates that the exact details and magnitudes of many of the processes are not important to overall system performance. Thus, even simpler models may do an adequate job of simulating the major features of the overall process.

The 1.6-m reactor is operationally stable and provides a good test bed for modeling evaluations. Back-heating is successful in reducing radial heat losses.

Modeling and laboratory work will continue. The sensitivity of calculated results to reaction-rate constants and transport coefficients will be investigated

Table 2. Mass balance for the 1.6-m reactor experiments (runs 4, 5, and 6).

Approximate amounts in major streams, kg

	Run 4	Run 5	Run 6
Reactant stream			
Wet coal	19.6	20.0	19.7
O_2	4.6	4.4	4.0
H_2O	15.3	14.6	13.4
Total	39.5	39.0	37.1
Product stream			
H_2O	17.6	15.9	14.6
Tar	0.9	0.7	0.9
Gas	18.7	19.8	19.5
Char/ash	2.3	2.0	1.7
Total	39.5	38.4	36.7

Approximate elemental balance, kg

	Run 4		Run 5		Run 6	
	in	out	in	out	in	out
C	8.47	8.33	8.64	8.41	8.49	8.21
H	3.14	3.11	3.10	3.00	2.94	2.89
O	26.9	27.4	26.3	26.3	24.7	25.0
Ar (tracer)	0.98	1.0	0.94	0.94	0.86	0.86

Table 3. Heat balances for 1.6-m reactor experiments (runs 4, 5, and 6).

Enthalpy, MJ (based on standard heats of formation at 298 K)

	Run 4	Run 5	Run 6
Feed streams (Temp., K)			
O_2/H_2O (440)	-200	-192	-176
Coal (300)	-144	-147	-144
Total	-344	-339	-320
Exit Streams (Temp., K)			
Char/ash/tar (980)	3	3	2
H_2O (400)	-232	-210	-193
Product gas (400)	-132	-135	-132
Total	-361	-342	-323
Loss from coal in reactor	17	3	3

by systematically varying the values over wide ranges. Different formulations will be tested to identify the most useful ones in terms of accuracy vs computer time. The 1.6-m reactor will continue to be used as a test bed with higher pressure experiments at a variety of different inlet compositions.

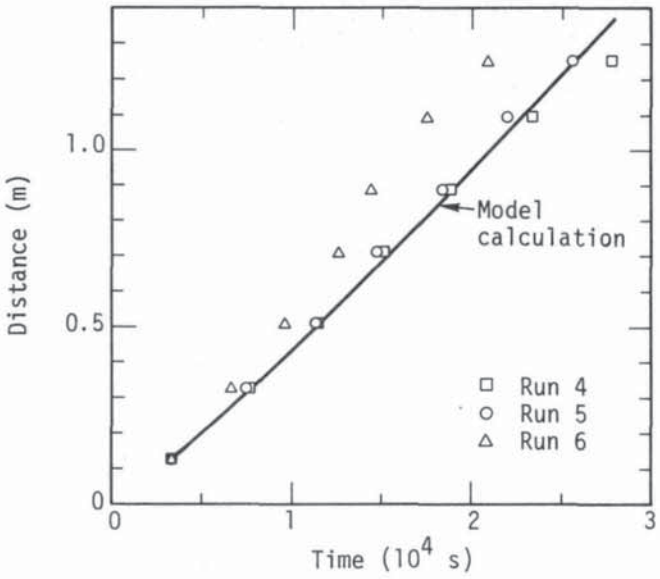


Fig. 7. Comparison of calculated and experimentally observed reaction-front propagation.

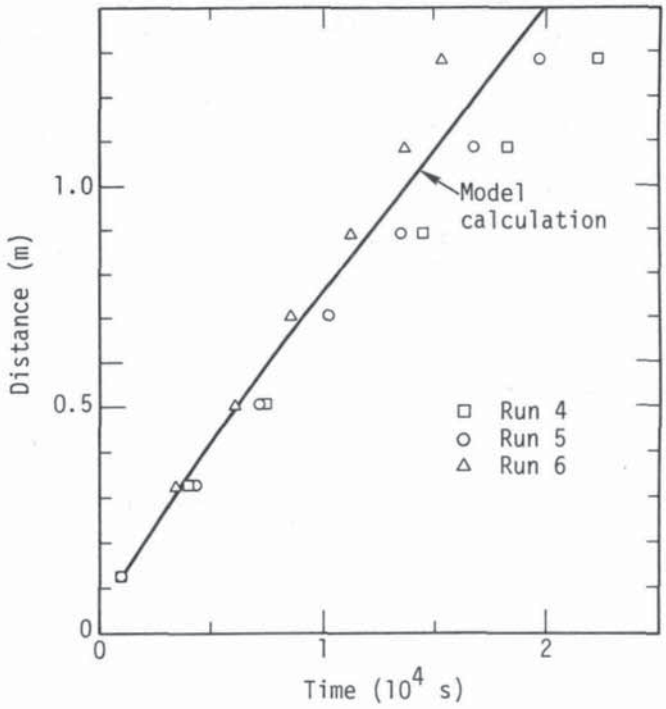


Fig. 8. Comparison of calculated and experimentally observed drying-front propagation.

Table 4. Comparison of calculated and experimentally observed effluent-gas composition.

	Product Gas (major constituents averaged over run), mole fraction			
	H_2	CO	CH_4	CO_2
Run 4	0.449	0.165	0.064	0.332
Run 5	0.446	0.190	0.069	0.295
Run 6	0.457	0.196	0.066	0.281
One-dimensional computer solution	0.441	0.206	0.058	0.295

Underground Gasification at the University of Kentucky

O. J. Hahn &
J. E. Jones, Jr.

Institute for Mining and Minerals Research
University of Kentucky
Lexington, KY 40506

I Introduction

Underground gasification experiments have been conducted in Belgium, France, Italy, Germany, Czechoslovakia, Poland, the U.S.S.R. and the United States. The only commercial operation has been reported in the Soviet Union. The factors that have made underground gasification remain attractive when compared to mining and surface processing are:

1. Greatly reduced capital requirements
2. Reduced manpower requirements
3. Recovery of otherwise unusable resources
4. Potentially, greatly reduced environmental impact

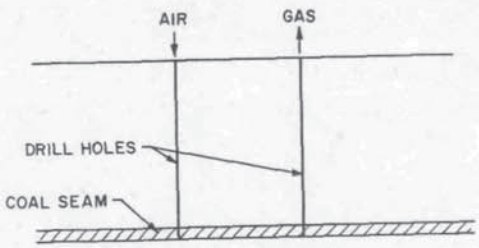


FIGURE 1
VERTICAL SHAFT METHODS

The processes which have been used in the past can be grouped into four general categories. These are:

1. Vertical shaft methods
2. Packed bed methods
3. Long wall techniques
4. Blind borehole techniques

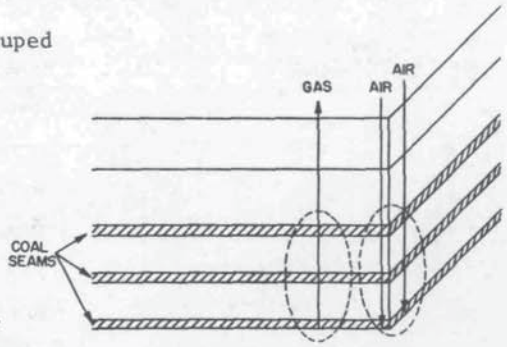


FIGURE 2
PACKED BED

These general schemes are shown in Figures 1 through 4. These techniques were developed for coal seams below the water table and of sufficient thickness to justify the relatively high percentage of drilling through the overburden versus drilling in the coal.

In the Appalachian region there are numerous coal seams which crop above the water table which are under 20 inches in thickness

or for which no underground mining system exists at present. The reserves which are in such thin or dipping seams in the United States are estimated to be between 150 million tons and 680 million tons. An underground gasification concept is proposed which relies on negative pressure in the gasification zone together with the use of an extension of the present technology of auger mining. In the initial tests the gasification ports are auger holes drilled horizontally from the surface; no special fracturing techniques are anticipated since the auger process increases the permeability of the pillars remaining between successive auger holes.

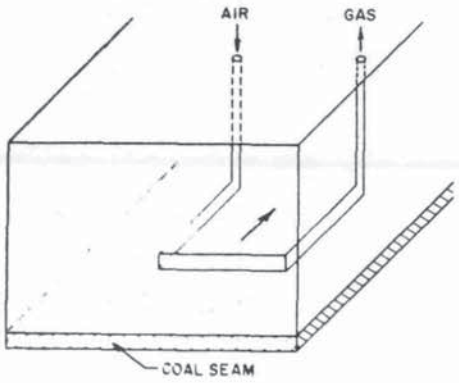


FIGURE 3
LONG WALL METHOD

II The Proposed Kentucky Underground Gasification Concept

The overall underground gasification concept can be seen in Figure 5. Auger holes are drilled from the bench or at bays inside a mine. These holes are drilled horizontally or dipping with the coal seam. In one auger hole air and steam are passed. This will go through the gasification zone and exit through the next auger hole as seen in Figures 6 & 7. Then the gasification zone is slightly subatmospheric; air will be entering through previous gasified zones and through the entry port. The steam/air ratio can be adjusted to compensate for air leakage from other areas. The next auger hole will not be drilled until the gasification in the previous zone has been nearly completed. Part of the gas of the gasification process can be used directly to power the augering process. The tars in the gas can be trapped in the coal from the next auger hole and are, thus, used to enrich the coal for future processes.

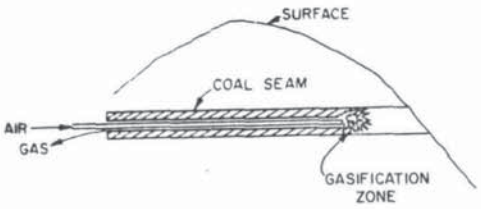


FIGURE 4
BLIND BORE HOLE TECHNIQUE

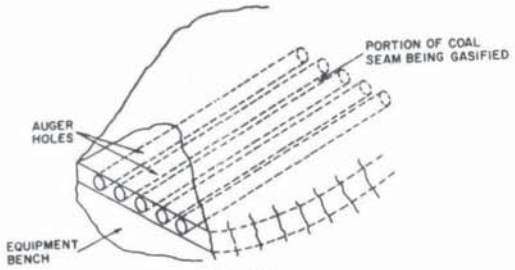


FIGURE 5
PLAN VIEW OF HORIZONTAL COAL SEAM BEING AUGER-MINED AND THE REMAINING COAL GASIFIED

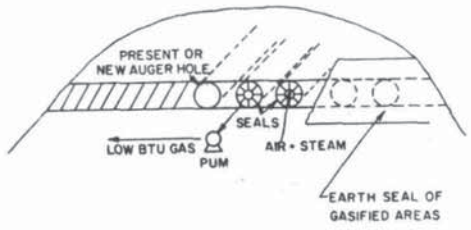


FIGURE 6
ENTRANCE VIEW OF COAL SEAM WITH AUGER-MINING AND GASIFICATION

III Gasification and Liquefaction

The evaluation of the concept starts with a review of the positive and negative aspects of the proposed process. The process uses much existing tehcnology, has minimal environmental effects, uses negative pressures, thus permitting a lower gasification temperature. The development areas include fire control and auger techniques to extend the present limit beyond the present of 600 feet to 2,000 feet. The evaluation of the concept began with a computer simulation to estimate the lowest temperature at which the gasification would proceed. Equilibrium thermodynamic calculations [1] gave the lowest temperature at 480°C. Laboratory measurements confirmed this number. The laboratory experiment was conducted in a quartz tube using fine coal in

the reverse burning process.

IV Permeability

Permeability tests have been conducted in the laboratory. These tests have been done on small undisturbed blocks of coal and between 2 inch holes drilled in large blocks of coal. The objective is to determine the difference in permeability of undisturbed coal as compared to bored coal and full scale augered holes in the field. Tests are also underway to determine the effect on permeability of moisture in the coal and burning of the coal. An example of the permeability data shown in Figure 8. The permeability experiments were run along two horizontal orientations of the coal thus giving the two curves. The natural permeability was found to be sufficient for the proposed process which will use low air flow rates. Field permeability tests were attempted in the summer of 1975. Adjacent 40" auger holes were capped externally and sealed internally at a depth of ten feet. The tests were terminated due to equipment failure and seal leakage. A new sealing system was designed and a site located for tests to be performed this summer. The tentative site has a 47 inch and a 11 inch coal seam separated by a 2 inch stringer. This coal, which covers about one acre, is located at the top of a knoll with 20 feet of over-burden. The nearest other coal seam, in case of loss of gasification control, if 150 feet below.

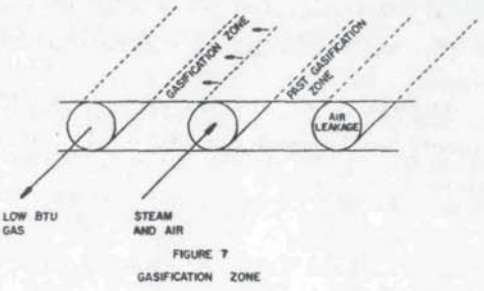


FIGURE 7
GASIFICATION ZONE

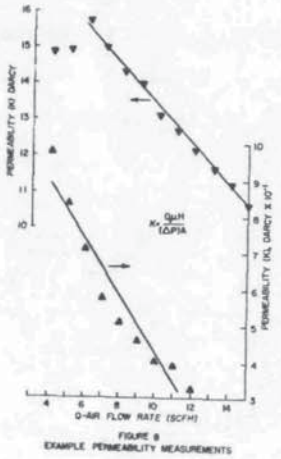


FIGURE 8
EXAMPLE PERMEABILITY MEASUREMENTS

V Gasification

Gasification tests have been run in the laboratory using the negative pressure concept with air to produce gases having heating values ranging from 80 to 200 Btu/SCF.

Tests have been run using crushed Eastern Kentucky coals in the quartz reactor system described previously. Gasification between auger holes has been simulated in the laboratory by gasifying between holes two inches in diameter into large blocks of coal. The combustion occurred without problems of channeling on tar plugging. Tests are being run to determine the optimum operating conditions including air flow rate, air to steam ratio, and temperature.

VI Summary

The negative pressure low temperature underground sification process appears to be technically feasible

based on modeling and laboratory results. The project is now moving into large scale field. The future progression of the project will be as follows:

(1) Field permeability tests between augered holes
(2) Preparation of impact reports for securing approval for field gasification tests
(3) Site preparation for gasification test
(4) Gasification of an edge section to test fire control
(5) Gasification of the mountaintop seam

As this work is progressing studies will be underway to improve auger techniques for use in conjunction with underground gasification and to develop product utilization and distribution schemes.

References

[1] Powell, T. C. and Hahn, O. J., "Thermodynamics of Underground Coal Gasification at Subatmospheric Pressure". Manuscript in preparation, IMMR, University of Kentucky, 1976.

EXPERIMENTAL COAL MINE FIRE RESEARCH*

by

R. F. CHAIKEN AND J. M. SINGER, U.S. BUREAU OF MINES
PITTSBURGH MINING AND SAFETY RESEARCH CENTER

ABSTRACT

Model ducts lined with coal are being employed to study the nature of coal mine fires, their rate of propagation, their influence on ventilation air flows and their response to sealing and other fire suppression measures. For scale modeling purposes it is planned to carry out these studies in various size ducts leading to a full size mine entry configuration in the Bruceton multiple entry experimental mine. At present, however, work is being carried out in a 9.1 meter long duct lined with 5 cm thicknesses of coal and insulating brick leaving a 23 by 23-cm-square opening for air ventilation.

A number of probes are employed to follow the course of the fire, which is ignited at the upstream end of the coalbed. Thermocouples monitor gas, coal, and brick temperatures; differential pressure probes monitor pressure drop across the fire zone and along the duct; calorimeters measure the amount and distribution of heat flux (radiation and convection) to the coal and brick surface; anemometers measure air velocity profiles. In addition, a number of gas sampling stations positioned along the duct allow for continuous monitoring of the nature of the combustion products (CO, CO_2, H_2, O_2 and CH_4).

Experimental data are presented related to various fire characteristics which are believed to be important in actual mine fires. For example, significant throttling of the ventilation air flow has been observed, along with stratified reverse flow of the gaseous combustion products upstream of the fire zone. These phenomena appear to relate in part to the rate of flame spread along the fire bed, the rate of advance of the devolatilization front into the coal, and the gasification rate of glowing coke.

I. INTRODUCTION

Fire represents one of the two most probable causes of major disasters (i.e., five or more fatalities) in underground coal mining in the United States. Fortunately, in recent years the incidence of injuries from coal mine fires has been small; however, the potential for a major mine disaster is ever present and the actual loss of coal production due to fire and the required sealing of entire mines or working sections is significant even today.

The U.S. Bureau of Mines at the Pittsburgh Mining and Safety Research Center has recently initiated a detailed experimental and theoretical study into the nature of coal mine fires, their rate of propagation, their influence on ventilation flows, and their response to sealing, for the distinct purpose of developing optimal methods for fire suppression and extinguishment. The modus operandi in this work is to investigate fire propagation in ventilated coal-lined ducts (i.e., simulated entries) of increasing size, leading eventually to a full-size mine entry configuration such as the

*Based partially on a paper presented at the IVth International Symposium on Combustion Processes, Częctochowa, Poland, Sept. 15-18, 1975.

Bruceton Multiple Entry Experimental Mine. A determination through these studies of the pertinent fire/ventilation/geometry scaling parameters should enable laboratory results to be extrapolated to actual mine conditions.

At present our fire studies have been confined to a 9.1 meter long insulated duct having a square opening of 23 by 23 cm for ventilation flow. Coal slabs 5 cm thick, are cemented to the walls of the duct to define a fire zone of varying length. It is the purpose of this paper to describe these fire duct experiments and some of the results that have been obtained on fire spread, fume and temperature production, and ventilation throttling. Associated studies on coal combustion and theoretical modeling of duct fires, which are also being carried out in our laboratories, will not be reported in detail here, but in other publications [1] [2] [3].

II. DESCRIPTION OF THE EXPERIMENT

A. Design

The experimental design is based on an attempt to simulate in small size a single mine entry in which a coal fire could be initiated and observed to propagate under the influence of a forced ventilation air flow. The desirability of having geometric symmetry for purpose of theoretical analysis and flat (as versus curved) walls for ease of construction prompted the choice of a square duct for our initial studies. A duct 9.1 meters in length with an internal cross section of 23 by 23-cm was chosen for convenience. The duct (figure 1) is essentially a steel trough made from 0.64-cm-thick metal sheets with 2-meter-long removable roof sections. It is completely lined on the inside with 5-cm-thick insulating fire brick except for a 1-meter-length on the upstream end which is lined to 10 cm thickness so that the insulation fits flush against the beginning of the coal zone. The coal zone is prepared by cementing 5-cm-thick coal slabs to the insulated floor and side walls (i.e., ribs). The roof is formed by supporting coal slabs on a steel wire mesh (5- by 10-cm openings) which stretches across the entry. Interlocking insulating brick is set on top of the roof coal followed by the steel roof plates to complete the enclosure of the coal zone. The coal slabs are oriented so that their bedding planes lie horizontal to the duct axis. For the most part the individual slabs are about 200 cm^2 in area and are butted against one another to minimize the crevice area. When necessary, smaller pieces of coal are used as crevice filler to yield a relatively continuous and somewhat smooth coal lining. To date, coal zones 1, 2, and 3 meters (nominal) in length have been burned.

Ventilation of the duct is achieved by a constant-speed fan (nominal air flow of 14 m^3/min) operating in exhaust mode (see figure 1). The fan, located outside the laboratory building, is connected to the downstream side of the duct through an uninsulated galvanized steel ventilation duct. Control of the air flow is obtained by (1) two slot dampers which bleed air directly to the fan intake, (2) a butterfly valve in the main ventilating duct, and (3) a variable-orifice plate at the exit of the fire duct. The bleed air at the fan intake also cools the combustion products before they pass into the fan housing. Cold intake air velocities up to 200 m/min can be readily achieved with this ventilation scheme, although the tests to date have mostly been carried out at 1 m/sec or less air flow.

Principal instrumentation for the fire duct is listed in Table 1, and includes thermocouples and an optical pyrometer for measuring gas, coal, and brick temperatures; calorimeters and radiometers to monitor total, convective, and radiative heat flux; pressure transducers to monitor the pressure drop across the fire zone; a venturi meter which monitors the total exhaust flow; and a hot film and/or vane anemometer to measure the intake velocity. Batch gas samples are taken from the duct at a number of positions for subsequent gas chromatography analysis of the major permanent gas combustion products.

Currently, the thermocouple data are recorded by a means of a 100-channel data logger equipped with temperature compensation inputs. Eventually we plan to have all transducer data, including gas analyses, recorded on-line in a digital format for computer processing.

The ignition source for the coal fires studied to date is a single ceramic gas-fired radiator (∿15 by 23 cm area, 4500 Kcal/hr) which is positioned at the upstream end of the coal zone. It is removed after the coal is ignited.

B. Operation

In carrying out the fire experiments, a cold air ventilation flow is first established. The ignitor is then inserted so as to ignite first the floor, then the side walls, and finally the roof.

References at end of paper.

TABLE 1. - List of Instrumentation.

Quantity	Type	Function	Location
35	Chromel-alumel thermocouples, bare, ungrounded 0.07 cm	Temperatures	Passageway in vertical and horizontal arrays
44	Chromel-alumel thermocouples sheathed, ungrounded, 0.051 cm	Temperatures	Imbedded in coal and fire-brick wall and at surface of coal
1-	Hot film anemometer[1]	Air flow into coal fire zone	At cross section 0.9 m from entrance
1-	Vane anemometer[2]	Air flow into coal fire zone and reversed flow	At cross section 0.9 from entrance
1-	Surface pyrometer[3] (Infrared radiation)	Surface temperature of 4-walls	3 m in front of entrance
6-	Pressure transducers[4] (variable reluctance type)	Pressure-drop across fire zone, and length of tunnel	Pressure-tap arrays in passageway
14-	Gas sampling probes	Burned gas product concentrations	In vertical and horizontal arrays 0.9, 1.5, 3.4, 5.2, 7.1 and 8.8 m from entrance.
3	Radiometers,[5] (BaF_2 windows, (Gardon-foil type)	Radiative flux, 1 to 30 micrometers	In fire zone, 1.6 and 2.3 m from entrance, and after fire zone, 3.0 m from entrance
3	Total calorimeters,[5] (Gardon-foil type)	Total thermal flux	In fire zone, 1.6 and 2.3 m from entrance, and after fire zone, 3.0 m from entrance
1	Weight cell[6]	Weight loss of a portion of coal	0.9 m long by 15.2 - cm wide coal floor
3	Lasers (0.63, 0.94 and 3.39 m wave length) and detectors	Smoke particle size downstream of fire	5.4 m from entrance
1	Smoke-particulate monitor[7]	Smoke concentration and average particle size downstream of fire	Probe taps at variable distances from entrance

[1]Disa Electronics, Franklin Lakes, N.J.
[2]Davis Instrument Manufacturing Co., Inc., Baltimore, Md.
[3]Ircon, Inc., Niles, Ill.
[4]Celesco Industries, Canoga Park, Calif.
[5]Thermogage, Inc., Frostburg, Md.
[6]BLH Corporation, Waltham, Mass.
[7]Environment-One, Schenectady, N.Y.
Reference to specific trade names is made to facilitate understanding and does not imply endorsement by the Bureau of Mines.

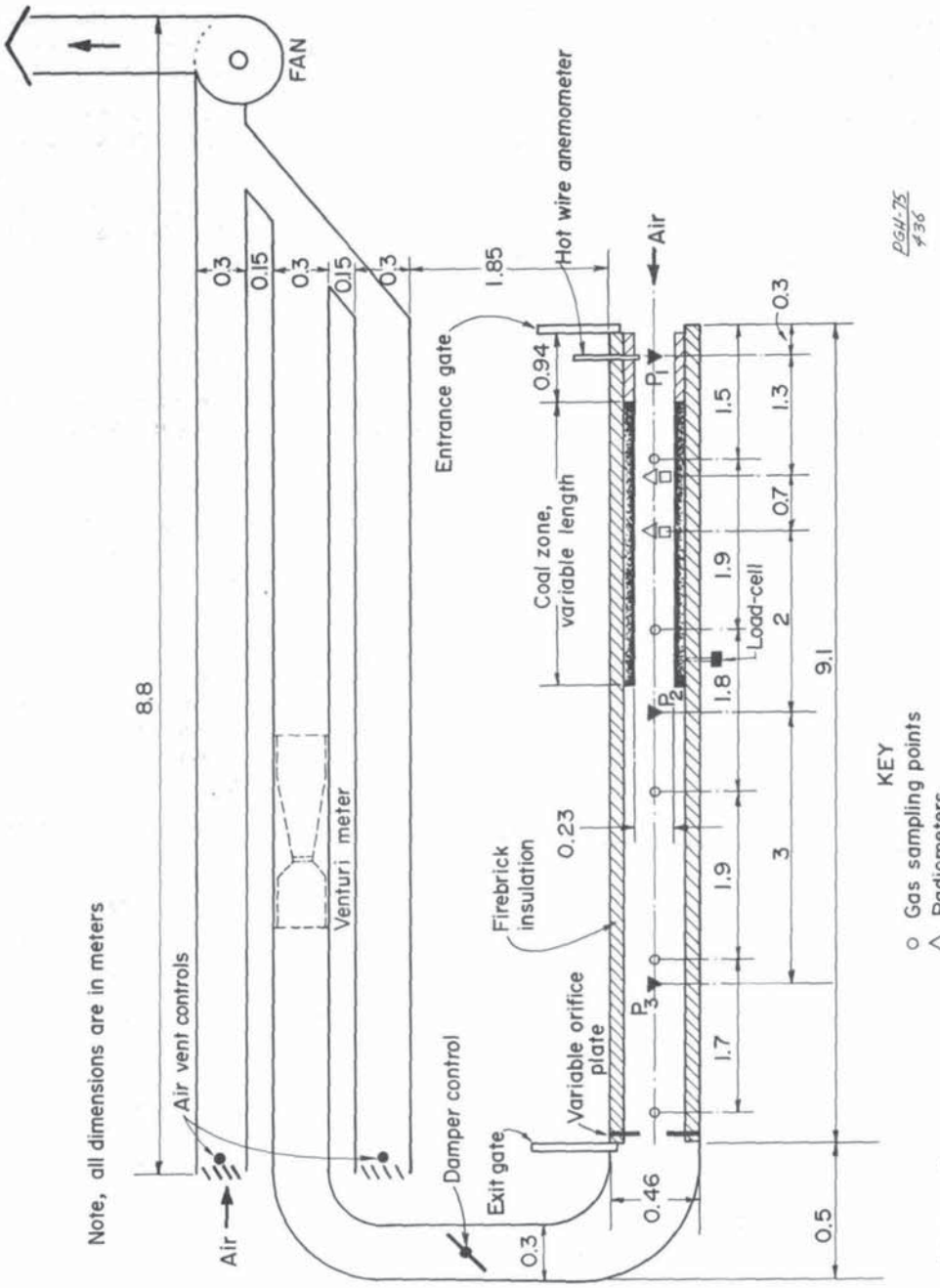


Figure 1. - Coal-fire tunnel schematic.

Until the roof is ignited, the fire spread downstream appears to be small. After roof ignition the ignitor is withdrawn from the duct. Generally the whole ignition process takes about 30 minutes.

All time measurements start at ignition. Typically, temperature data are recorded every 5 minutes, and other data every 15 to 30 minutes depending upon how long the fire has been burning. Some data, such as the response of thermocouples attached to the coal floor surface, are monitored continuously. Visual and photographic observations of the fire are made from the open upstream end of the duct during the entire course of the fire.

The fire, once started, is generally allowed to seek its own course in controlling the intake air flow; on occasion the ventilation flow was altered by means of the duct air controls.

III. EXPERIMENTAL RESULTS AND DISCUSSION

To date, five fire trials have been carried out involving four-wall coal zones of 1-, 2- and 3-meter (nominal) lengths and one fire for a 1-m long, 5-cm thick coal bed. Initial intake ventilation velocities of 0.5 and 1.0 m/sec have been employed. Figures 2-6 indicate data obtained from one of the four-wall experiments (experiment 4) involving a 3-m fire zone and a 1-m/sec initial air flow. The data are somewhat typical of the other experiments; however, in this particular fire a mild explosion (sans noise) occurred about 3 hours into the burn. The effect of this occurrence (as well as other events) is clearly depicted in the sudden changes in the time profiles of the data. This point as well as other details of the fire is discussed below along with general comments on the nature of the duct fires. Figure 7 indicate data for the floor bed fire.

A. Ignition and Propagation

In each case, ignition, for the four-wall fires, as evidenced by the fire being able to propagate downstream without added heat from the ignitor, occurred only after the floor, ribs and roof of the coal zone were set aflame. This sometimes took as much as one half hour of heating with the ignitor being manipulated to expose all four-walls to high temperature radiation. At 1 m/sec initial air flow, the fire in the 1- and 3-meter long coal zones spreads rather quickly, about 10 to 15 m/hr; however, at 0.5 m/sec ventilation flow (2-meter coal zone), the spread rate is considerably slower, about 1 to 2 m/hr. Direct measurement of the fire spread rate has been rather difficult in these experiments due to (1) the long ignition times which gradually preheats the entire coal zone to $\sim$200°C, and (2) the difficulty in distinguishing between flames moving in the gas stream above the coal surface and actual surface combustion. A coal floor bed fire, not surrounded by fire on adjacent walls and roof propagated much differently than the four-wall fire. Continuing fire propagation of the coal floor bed depended on the continuing presence of the ignitor at the upstream end of the coal zone. Data for experiment 1, a 1-m long coal bed fire, are shown in figure 7. Temperatures in the channel of the single bed fire did not exceed 480°C.

B. Temperature

In experiment 4 (3-m long, four wall channel the gas temperatures rose steadily after ignition to a maximum value of 1100°C (see figure 2). Sealing the fire caused a rapid drop in both gas and coal temperature ($\sim$1.50°C/min). It is interesting to note that in another case (experiment 2) the initial sealing was inadequate and led to slight air leakage. In this instance the temperature decrease was much slower ($\sim$0.15°C/min), and reopening the fire zone at a coal temperature of 500°C led to reignition of the fire. The velocity of the thermal wave into the coal as measured by the thermocouples was in approximate agreement with the coking rate (4 to 6 micrometers/sec) determined in laser-heating experiments (see Table 2). As seen in figure 2, the temperatures responded to transient fire transformations such as ventilation clogging and unclogging, explosion in the fire duct, and sealing of the fire duct.

C. Pressure Drop

During the course of the fire in experiment 4 (see figure 3), the pressure drop across the coal zone, like the temperature, rose steadily to a maximum and slowly decayed. The maximum pressure drop appears to depend upon both coal zone length and initial air flow, as can be seen from Table 3. The experimental values are in approximate agreement with pressure drops, P_L, calculated from the usual pipe flow expression

$$P_L = \frac{A_w}{A_x} \frac{\rho v 2}{2} \qquad (1)$$

where f is the friction factor; A_w, the wetted area; A_x, the cross sectional area; ρ, the gas density; and v, the average gas velocity. With v determined from the venturi flow measurement, $\dot{V}$ m^3/min (NTP),

TABLE 2. - CO_2 Laser Irradiation of Pittsburgh Seam Coal and Coke in Air Atmosphere.

Radiative flux, $\dot{q}''_R$, cal/cm^2-sec	COAL Weight Loss Rates, 10^{-4}xgm/cm^2-sec *	COAL Weight Loss Rates, 10^{-4}xgm/cm^2-sec **	COKE Weight Loss Rates, 10^{-4}xgm/cm^2-sec ***	COAL Rate of coke-layer advance, 10^{-4}xcm/sec
0.99	0.743	0.74	0.28	-
1.6	3.18	1.9	1.3	-
2.4	7.53	3.3	2.4	6.7
4.1	15.4	6.4	-	8.8

*Maximum rate in first minute
**Average rate in 30 minutes
***Coke sample completely devolatilized at 900°C before laser heating.

TABLE 3. - Maximum Pressure Drop Across the Fire Zone.

Exp't	Length of Fire Zone, meters	Initial Air Flow, m/sec	P_{LO}, mm H_2O	P_{LO}(fire/P_{LO}(cold) Exp't*	Calc.**
#2	2	0.5	0.05	76	-
#3	3	1.0	.06	50	-
#4	3	1.0	.06	40	53
#5	1	1.0	.05	8.4	13
#6	2	1.0	.06	32.0	33.4

*P_L/P_{LO} at ~2 hours after ignition.
**Calculated from equation 2. Venturi meter measurements not available prior to experiment 3.

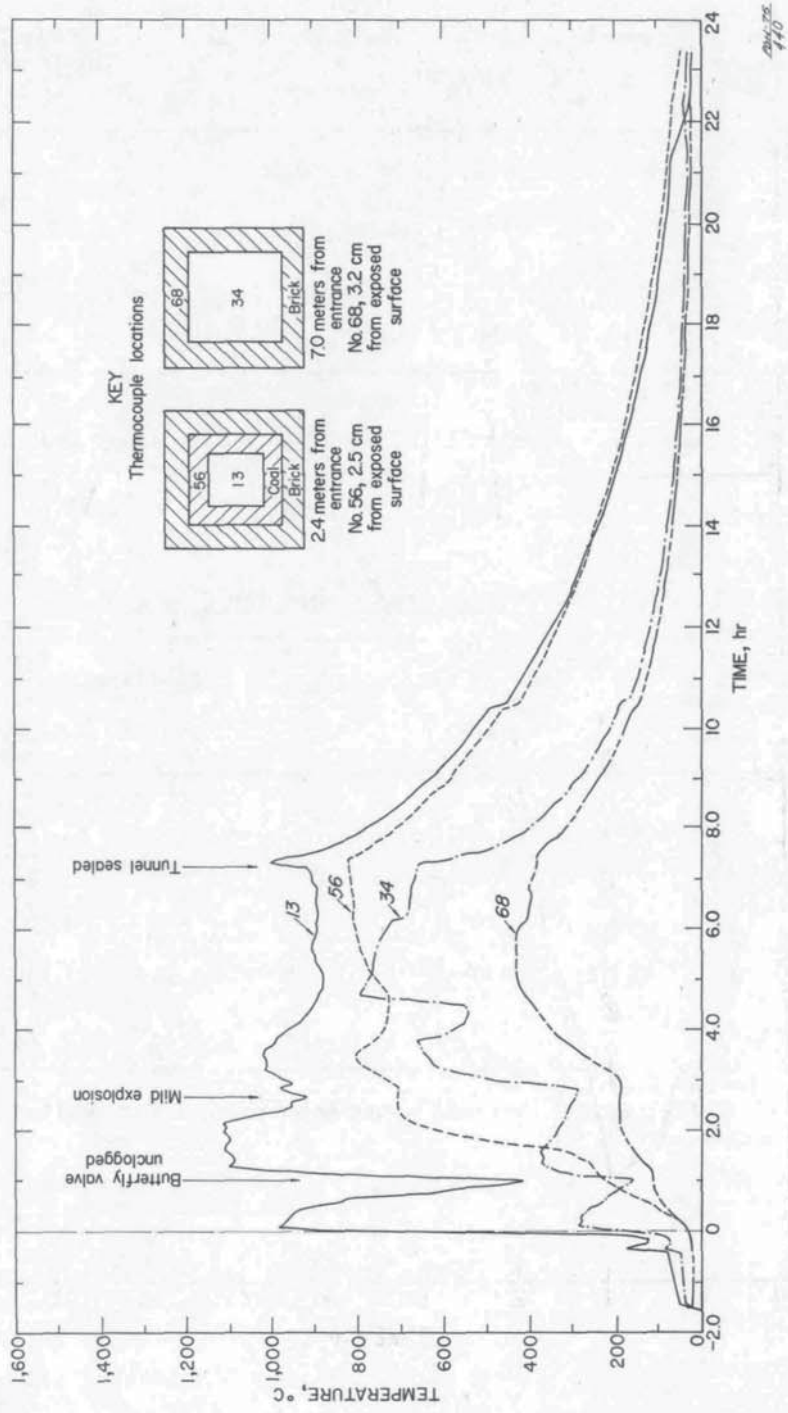


Figure 2. - Temperature-time profiles in passageway and walls. (Experiment #4, Pittsburgh seam coal, 3 m length x 5 cm thick walls, v_o = 1m/sec)

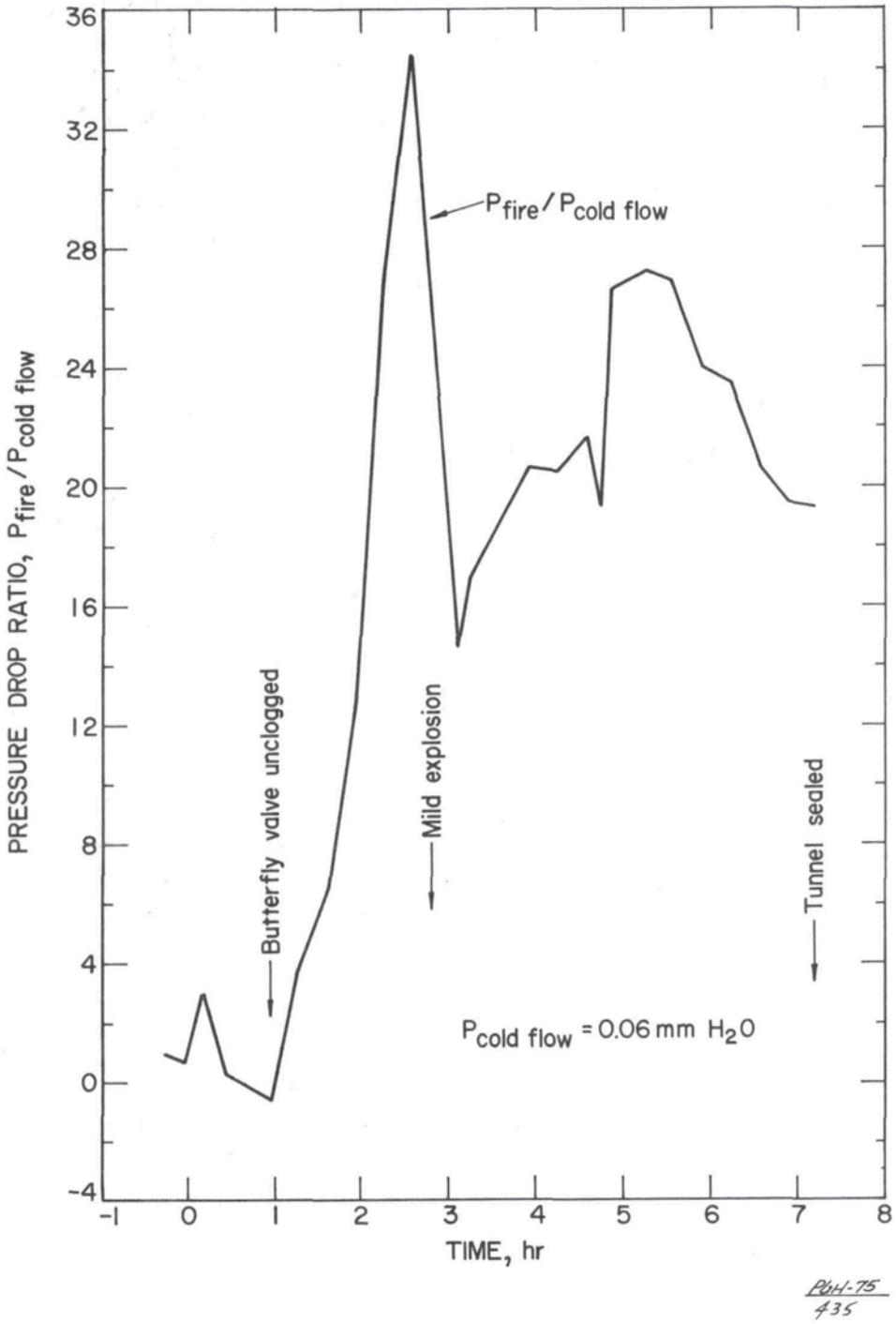


Figure 3. - Pressure-drop time profile across entire fire-zone length (Experiment #4, Pittsburgh seam coal, 3 m length x 5 cm thick walls, v_o = 1m/sec)

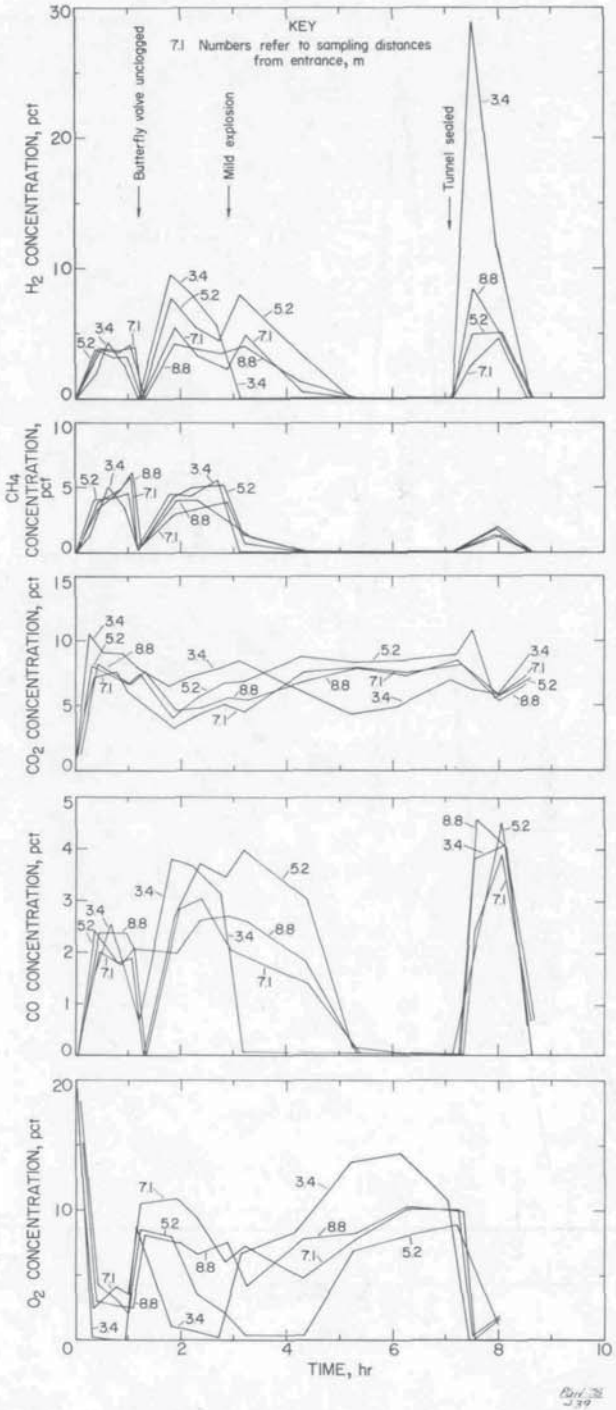


Figure 4. - Gas product composition - time profiles (Experiment #4, Pittsburgh seam coal, 3 m length x 5 cm thick walls, v_o = 1m/sec)

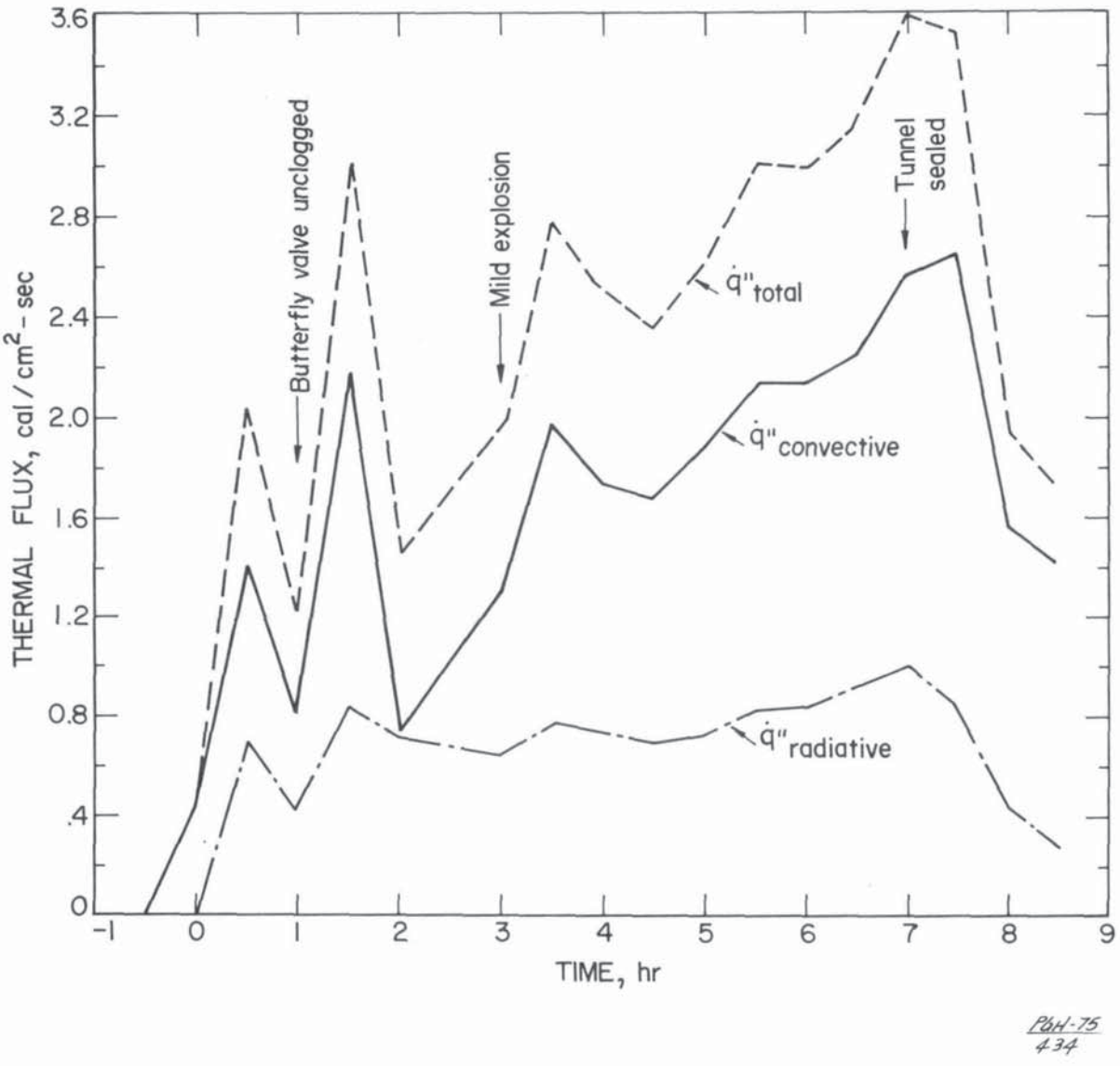
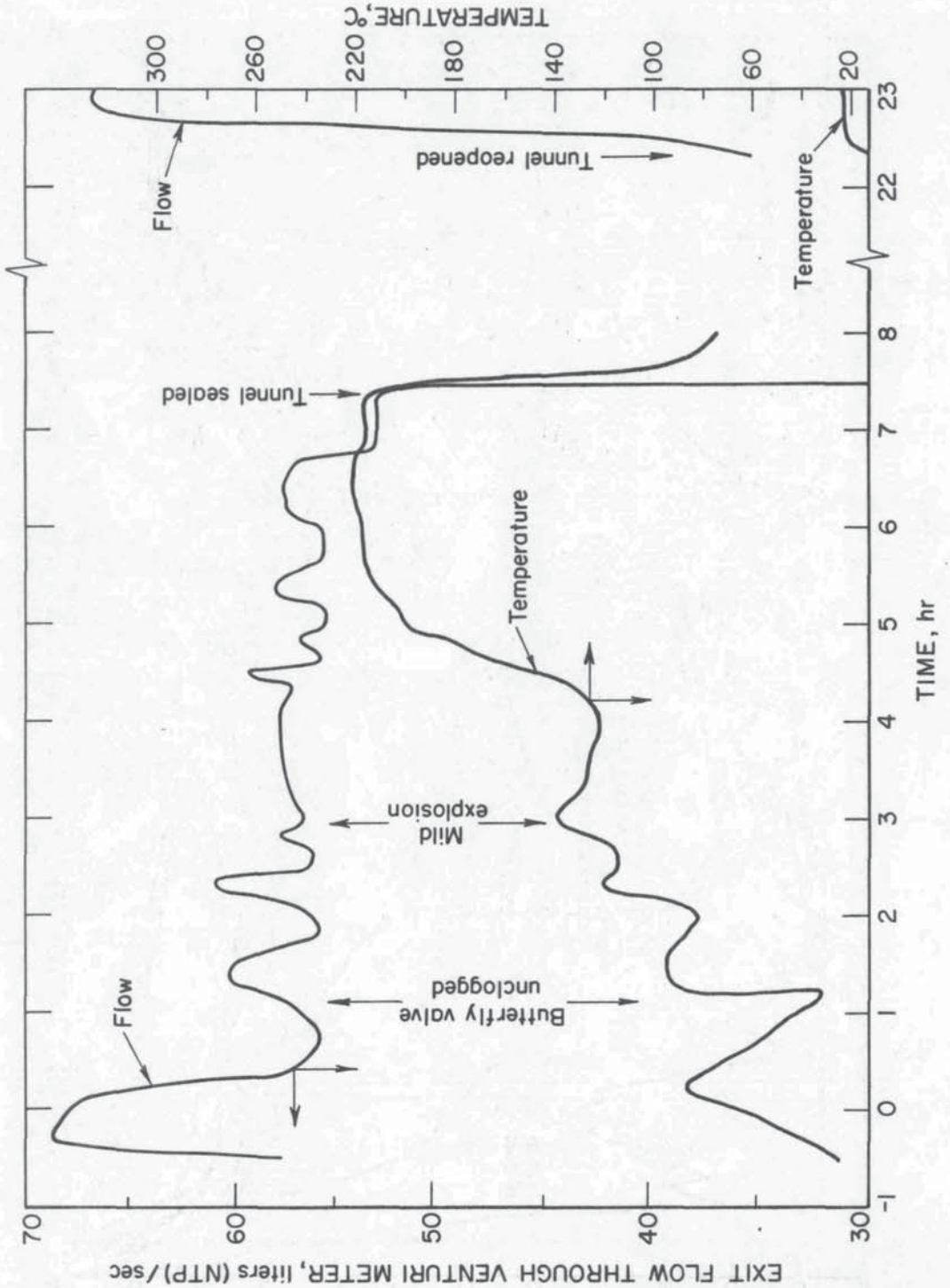


Figure 5. - Total, radiative, and convective thermal flux in coal fire-zone (Experiment #4, Pittsburgh seam coal, 3 m length x 5 cm thick walls, v_o = 1 m/sec).



PGH-75 437

Figure 6. - Total exit flow at venturi meter (Experiment #4, Pittsburgh seam coal, 3 m length x 5 cm thick walls, v_o = 1m/sec).

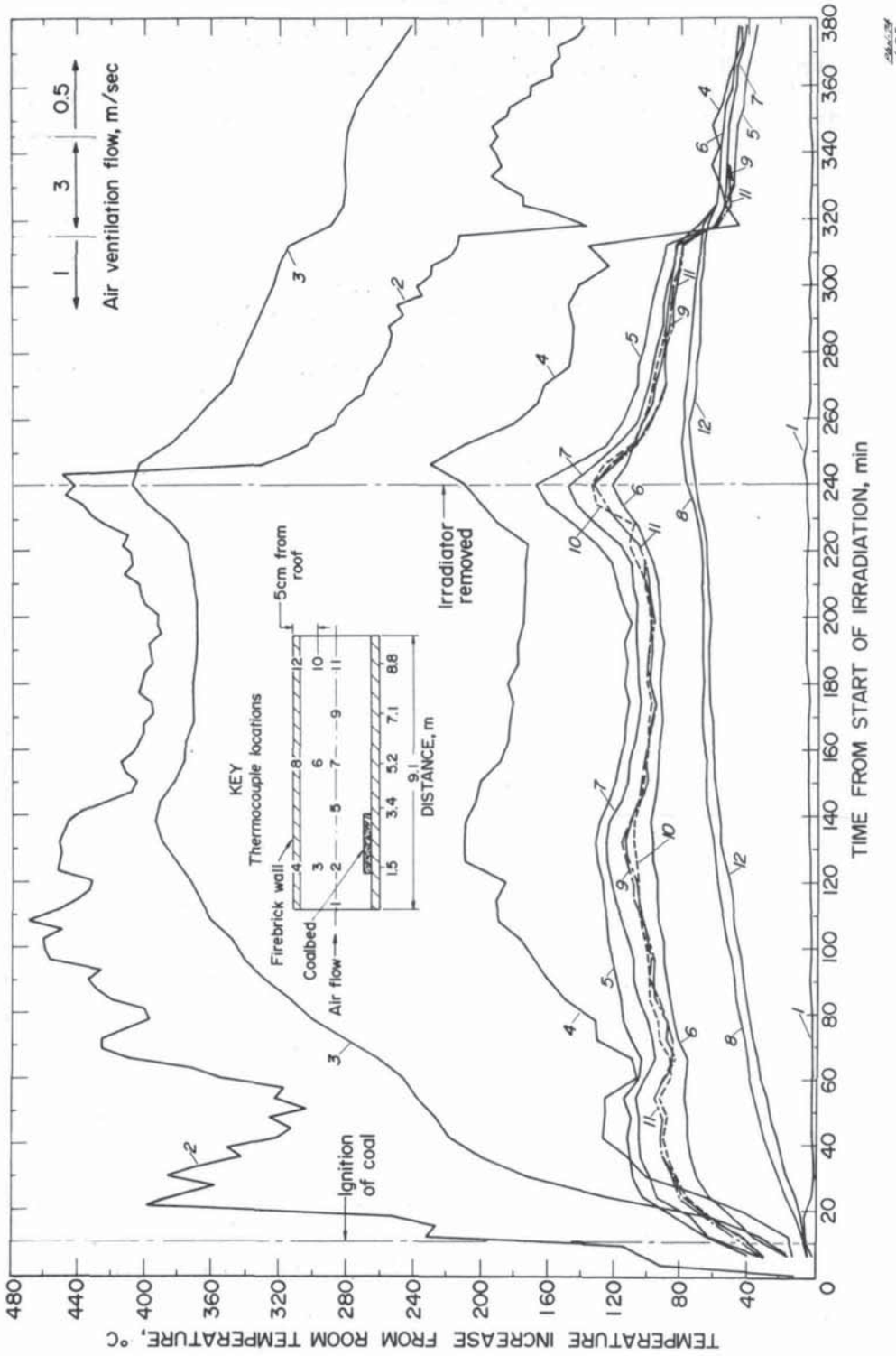


Figure 7. - Coal floor bed fire (Experiment #1, Pittsburgh seam coal, 1 m length x 5 cm thick, v_o = 1m/sec).

A_w expressed in terms of A_x for a square duct, and ρ determined from the ideal gas law assuming constant gas composition, the ratio of P_L(fire) and P_{LO}(cold) becomes

$$\frac{P_L(\text{fire})}{P_{LO}(\text{cold})} = \left(\frac{f}{f_o}\right)\left(\frac{A_{xo}}{A_x}\right)^{5/2}\left(\frac{T}{T_o}\right)\left(\frac{\dot{V}}{\dot{V}_o}\right)^2 \qquad (2)$$

Here, T is the absolute temperature and the subscript 0 refers to conditions before the fire. In utilizing equation 2, the factor in the square bracket is evaluated from cold air flow measurements taken before and after the fire.

It appears from these calculations that the two factors that most affect the pressure drop in the duct fires are (1) the change in A_x due to expansion of the coal during combustion and (2) the high temperatures developed in the fire zone. Surprisingly, $\dot{V}/\dot{V}_o$ remains relatively constant, probably due to the design of the ventilation system. The cross section effect is expected to decrease as we go to large ducts; however under actual mine fire conditions, roof falls may well be a major contributing factor to P_L(fire).

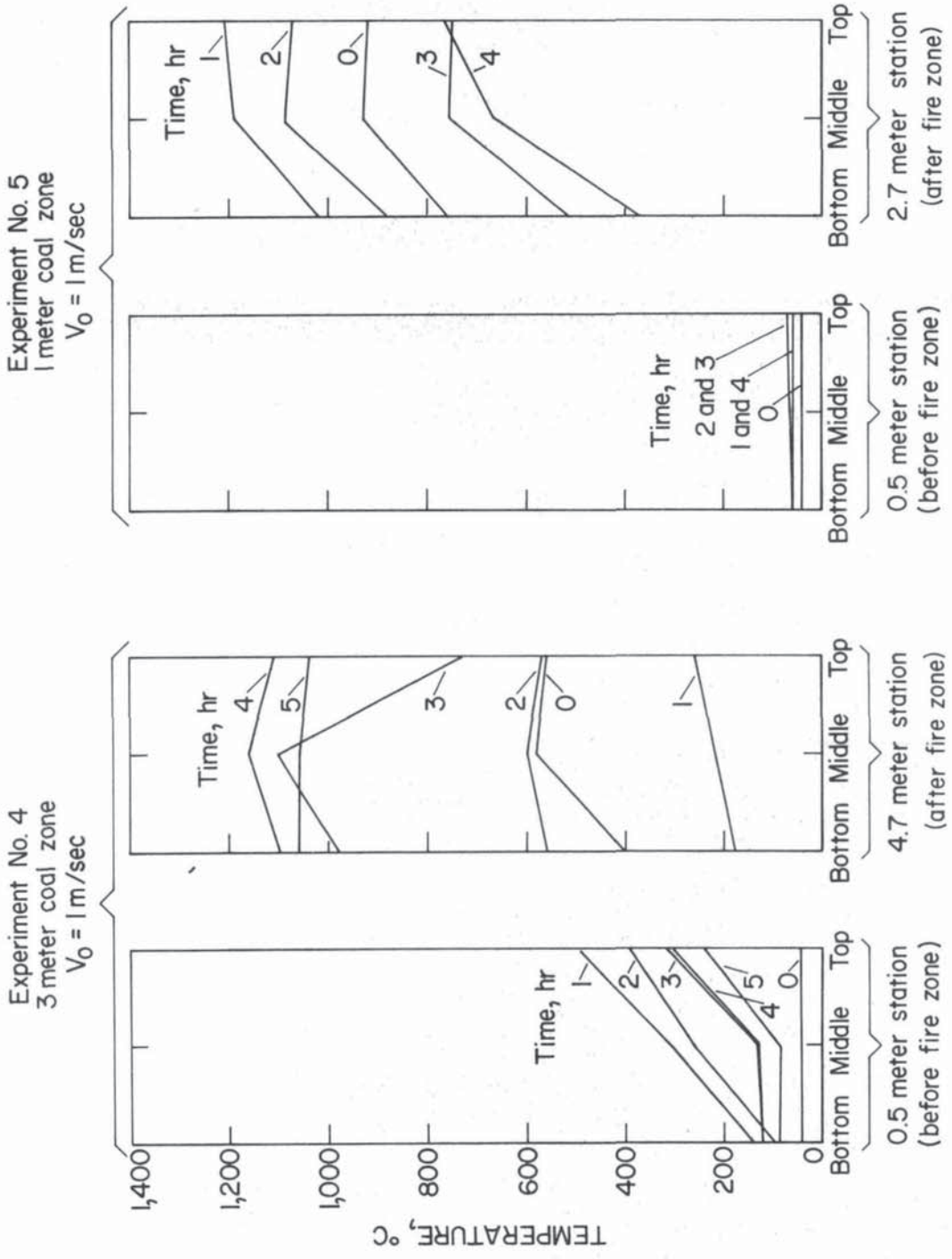
D. Reverse Stratified Flow

Except in the case of the 1-meter fire zone, considerable reverse flow is observed to develop in the upper level of the duct intake. At several periods of time, this flow as monitored by the vane anemometer actually exceeded the initial air velocity, leading to voluminous quantities of smoke pouring into the laboratory. Figures 8 and 9 show some of the temperature and velocity profiles at the intake 0.5 meter ahead of fire-zone lengths of 3 meters (experiment 4) and 1 meter (experiment 5). For comparison the temperature profiles at a station downstream of the fire are also depicted. It is readily seen that in experiment 4, the reverse flow can be highly stratified, filling as much as the top one-half of the entry with hot smoke laden gas. Analysis of the gas indicates that it contains some CO (<0.5 vol %), negligible H_2 and CH_4, and variable amounts of CO_2 and O_2. Thus, while the reverse flow does not seem to be an explosion hazard, it does present a toxic fume problem. The absence of combustible gas in the reverse flow stream is somewhat surprising since the downstream combustion products, at these same periods of time, generally contain substantial quantities of CO, CH_4, and H_2.

Several additional points can be noted from Figures 8 and 9. While the intake flow to the 3-meter fire zone becomes highly stratified, there appears to be little stratification of the downstream flow. On the other hand, with the 1-meter fire zone, the intake flow is not stratified but the downstream flow appears to be stratified. We have no good explanation for this, but feel confident that it relates to the difference in ventilation throttling by the two fires. Also, it is interesting that the maximum gas temperatures developed by the two fires are quite comparable despite the difference in ventilation throttling.

E. Gas Composition

In figures 4 and 10 we show for experiments 4 and 2, respectively, the concentration of the major permanent gases as determined by batch samples taken from stations along the length of the duct. The various curves are identified by the distance in meters between the duct intake and the sampling station. It is evident that there is considerable scatter in the individual data; however, the curves do appear to define trends with time. An explanation of these trends offers good insight into the course of the fire. Examination of the oxygen concentration data indicates that $[O_2]$ decreases the time from value of 20 vol pct at the ignition to some low value of 2-5 vol pct. It remains at this level for 2 to 4 hours at which time it gradually increases to an apparent steady value of $\sim$10 vol pct. The data for CO, H_2, and CH_4 show just the opposite trend, viz., their concentrations increase to some maximum and then decline to near zero at about the same point in time where the $[O_2]$ starts to increase. It is strongly suggested from these trends that the initial decrease in $[O_2]$ involves increased coal combustion as the fire spreads along the coal zone from the point of ignition. The combustion products, which are high in CO, H_2 and CH_4, indicate the primary fuel to be the volatile component of the coal ($\sim$35 wt pct for Pittsburgh seam coal), which reacts very rapidly in the gas phase to produce flame. When the entire coal zone is aflame, the $[O_2]$ level remains small and fairly constant as the coal steadily devolatilizes. Depletion of the volatile content of the coal leads eventually to coke combustion, which is a much slower surface-burning process (see table 2). This lowers the rate of coal gasification and the rate of oxygen consumption, leading to a decrease in ventilation throttling and an increase in $[O_2]$ in the exhaust. In a typical computation for a 3-meter long, 0.23- by 0.23-m coal corridor fire-zone (based on an average $\dot{m}''$ of 3×10^{-4} gm/cm^{2}sec) approximately 14g/sec of volatile matter will be emitted. Assuming an average molecular weight of 100 for the volatile matter [4], the additional volume (NTP) added to ventilation flow by rapid devolatilization would be 3500 cc/sec of which about 19.5 pct is combustible, based on Bureau of Mines



PH-75
432

Figure 8. - Temperature profiles across duct height, upstream and downstream of fire zone (Experiments #4 and #5).

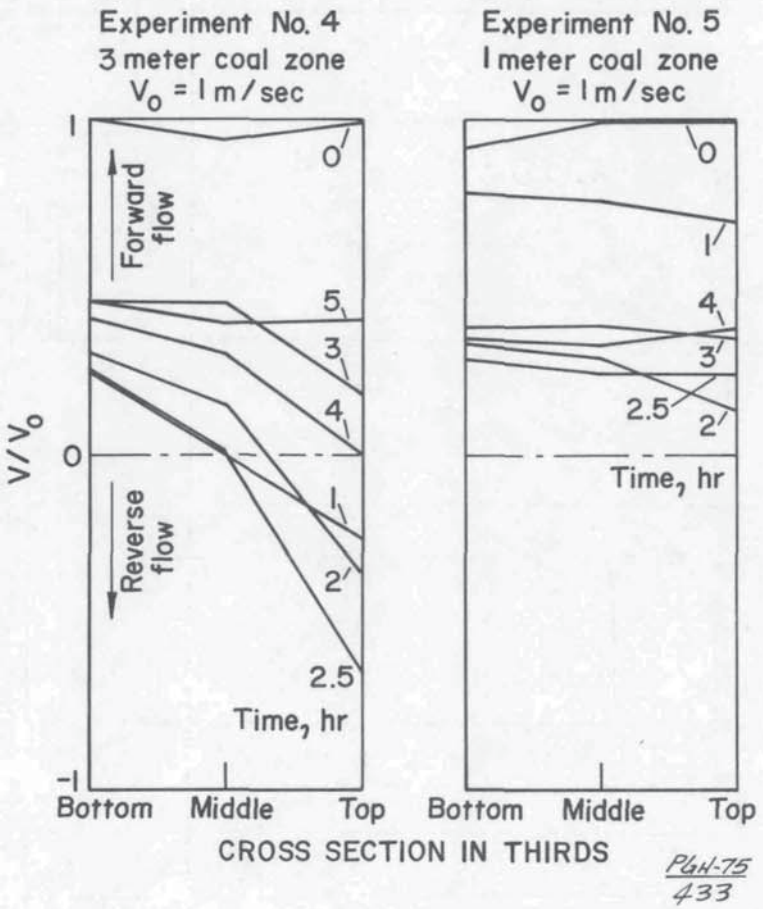


Figure 9. - Intake ventilation flow profiles through duct (Experiments #4 and #5).

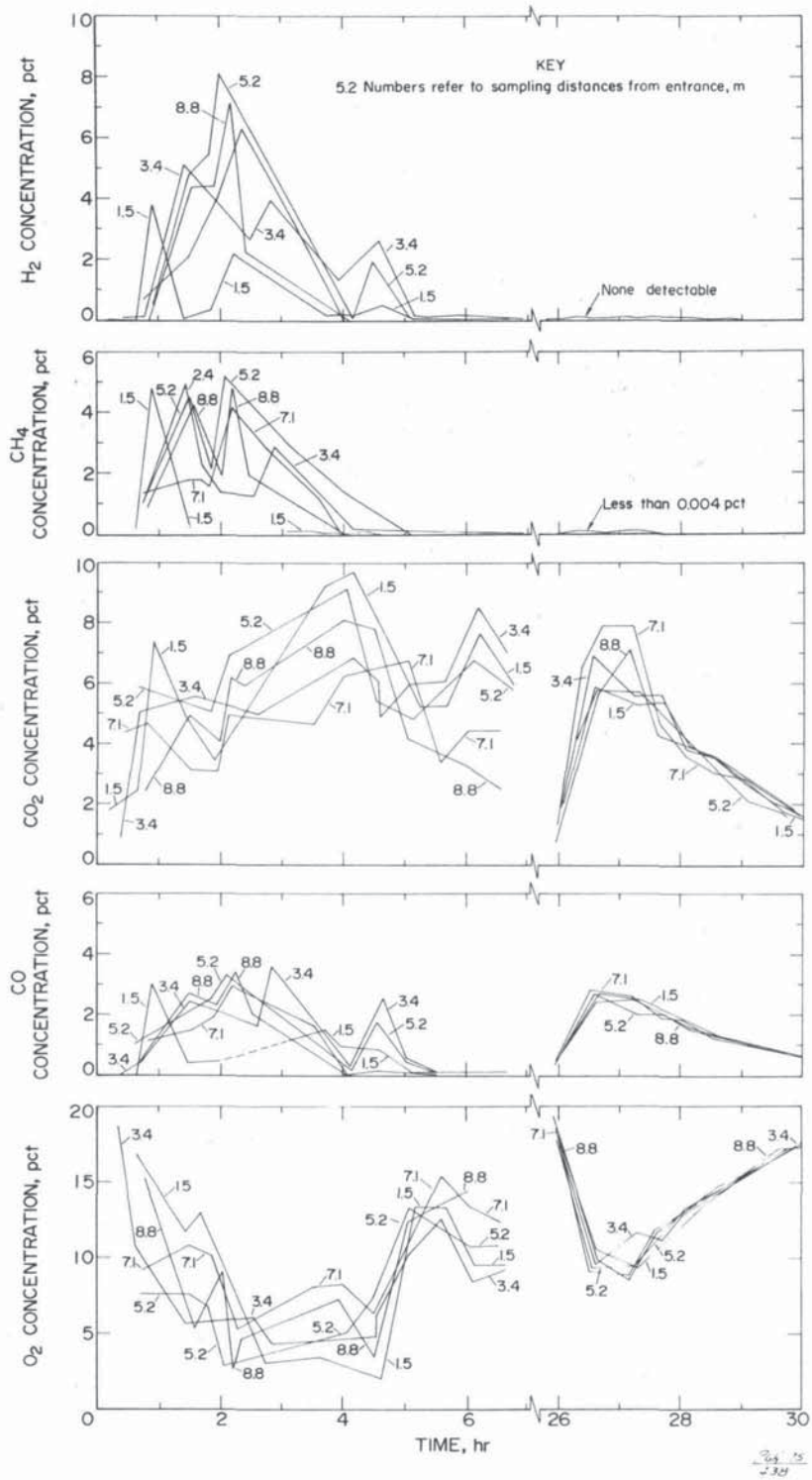


Figure 10. - Gas product composition-time profiles (Experiment #2, Pittsburgh seam coal, 2 m length x 5 cm thickwalls, v_o = 1m/sec).

Bulletin 571 [5]. Complete combustion of these products would consume about 1500 cc/sec O_2 in the devolatilization stage and about 3 times less in the glowing coke stage, accounting for the transformation from fuel-rich to oxygen-rich as the glowing coke stage was approached.

Two factors offer additional support for this explanation of the gas composition trends. First, the initial rate of decrease of $[O_2]$ could be expected to be related to the rate of fire spread. For experiment 2 the $[O_2]$ data indicate a spread rate of ∿12 m/hr. Both of these values are in agreement with visual observations. Second, the time period (2 to 4 hours) during which the $[O_2]$ remains at a constant low level should correspond to the time for devolatilization of the 5 cm thick coal lining. Laser heating experiments in our laboratory (table 2) indicate that the average linear rate of pyrolysis of coal to form coke at high total surface heat flux (2 cal/cm^2-sec) is ∿5x10^{-4} cm/sec. This would lead to a total time of 2.8 hours for devolatilizing a 5-cm-thick slab of coal.

It is evident from the gas sample data that considerable quantities of combustible gas are produced during the devolatilization stage of the coal fire and immediately after sealing the fire. In the former case, the $[O_2]$ is generally sufficiently low to prevent a flammable premixed gas mixture; however, during the course of oscillations in the fire intensity and ventilation flow, it is quite possible for the exhaust gases to become flammable. Also late in the fire, direct sealing almost surely leads to formation of a flammable gas, at least for a short transition time.

While no explosions have occurred in the fire duct after sealing, a mild explosion did occur in the open duct during experiment 4 (2.9 hours after ignition during the stage of rapid devolatilization). The explosion was not audible but it did cause considerable smoke and soot to be emitted from the duct intake. The event also altered all the measurements temporarily (see Figures 2-6).

F. Thermal Flux (Total, Convective, and Radiative)

The thermal flux quantities (total $\dot{q}''_T$, radiative $\dot{q}''_R$, and convective $\dot{q}''_C$) are shown in figure 5 for a pair of calorimeters and radiometers located in the coal-fire zone 1.68 meters from the entrance of the fire duct in experiment 4. Transformation of the coal burning zone from oxygen-rich (initial) to fuel-rich (during rapid devolatilization) to oxygen-rich (during glowing-coke degasification) and return to fuel-rich (during fire-duct sealing) is seen to be paralleled by the trend of thermal flux quantities, with the oxygen-rich flux values larger than the fuel-rich values. The radiative flux was consistently lower than the convective flux component during all stages of burning. Temperatures computed from the radiative flux based on the Stefan-Boltzmann formula, $\varepsilon = \sigma T_F^4$, where ε is the emissive power (cal/cm^2-sec) of a black-body, σ the Stefan-Boltzmann constant (1.36×10^{-12} cal/cm^2-sec-deg^4, and T_F the absolute temperature in °K, were in the range measured by the surface thermocouples and infrared surface pyrometer. As found for the fire temperatures, the maximum thermal flux quantities attained were about the same for all fires despite different air velocities and fire zone lengths.

FURTHER DISCUSSION

Application of the Froude modeling concept for fires in different sized ducts calls for the ventilation flow to be proportional to the square roof of the height of the fire duct. Analysis of the usefulness of the Froude principle as a scaling principle is somewhat questionable in the present fires owing to the transient behavior of the fire and its influence on the intake ventilation flow. However, the balance of inertial and buoyancy forces expressed in the Froude number, i.e., $Fr = \frac{(\Delta\rho/\rho)D}{v_o^2/g}$ (where $\Delta\rho$ and ρ are the average density difference between burned products and air, and the initial density of air respectively, D the duct height, v_o the ventilation speed, and g the gravitational constant) can be used to estimate a critical velocity to prevent flow reversal. Suppression of flow reversal in a dust with D = 23 cm might be expected to occur at Fr = 1. The computed value of v_o is about 1.5 m/sec. Thus, far, we find that a ventilation speed of 1 m/sec is not sufficient to prevent flow reversal in the 2- and 3-meter long coal fire zones, but is sufficient for the 1-meter-long zone. Apparently the ratio of length of fire zone to duct diameter, L/D, must be considered as a scaling parameter. Another difficulty in applying the Froude principle is that complete turbulent flow and rapid mixing of gases is assumed. This appears to be invalidated at the low ventilation air speeds in our small fire duct. The burned gas composition data at different heights in the coal fire zone indicate higher concentrations of unreacted fuel in the top portion of the duct, which suggests incomplete mixing. The appearance of stratified flow velocities has already been noted in figures 8 and 9.

SUMMARY

Experimental data have been presented for typical four-wall coal fires in a 9.1-meter-long, 23- by 23-cm open cross section fire duct. The data indicate the interdependence between fire-generated

parameters: Passageway and coal-wall temperature, differential pressure drops across the fire zone and fire duct, thermal flux to the coal and brick wall, stratified and reverse flow of the combustion products, and gas product-time profiles and explosibilities. The results can be interpreted in conjunction with separate measurements (laser irradiation) of the rates of coal devolatilization and coke combustion at fire-intensity surface heat fluxes. Planned future work with larger fire ducts should provide predictive equations and better understanding of fire-propagation processes in large scale coal mine corridors.

ACKNOWLEDGEMENT

The following personnel at the Pittsburgh Mining and Safety Research Center contributed to the execution of the work described in this paper. D. Chi, R. Markley, M. Harris and D. Martz who assisted in developing the computerized methods for data recording and retrieval; F. Ambrose and A. Bruszak, who handled much of the gas analyses; D. Lee who performed the laser-irradiation experiments; and A. Damick, C. Bennett, R. Diehl, W. Hoffman, and A. Page who executed the experimental tasks. Their efforts are gratefully appreciated.

REFERENCES

1. Edwards, J. C., Perlee, H. E., and Chaiken, R. F. Flame Spread in a Duct Fire. Presentation at ASME-AICHE Heat Transfer Conference, St. Louis, Mo., Aug. 9-11, 1976.

2. Lee, C. K., Singer, J. M., Chaiken, R. F. Coal Pyrolysis at Fire-Level Heat Flux. To be presented at Eastern Section Fall Technical Meeting of the Combustion Institute, Drexel University, Philadelphia, Pa., Nov. 18-19, 1976.

3. Hwang, C. C., Chaiken, R. F., Singer, J. M., and Chi, D. H. Reverse Stratified Flow in Duct Fires: A Two-Dimensional Approach. To be published in Sixteenth Symposium (International) on Combustion. Presentation at Cambridge, Massacheusetts, Aug. 15-21, 1976.

4. Field, M. A., Gill, D. W., Morgan, B. B., and Hawksley, P. S. W. Combustion of Pulverized Coal. The British Coal Utilization Research Association, Leatherhead, England, Cheng and Sons, Ltd., Banbury, England, 1967, p. 178.

5. Selvig, W. A., And Ode, W. H. Low Temperature Carbonization Assays of North American Coals, Bulletin 571, Bureau of Mines, 1957, 56 pp.

IN SITU HYDROCARBON RECOVERY SIMULATION LABORATORY RESEARCH AT MORGANTOWN ENERGY RESEARCH CENTER

by

L. Z. SHUCK
G. E. FASCHING
J. W. MARTIN
L. A. BISSETT

INTRODUCTION

Dwindling petroleum and natural gas reserves in the United States coupled with increasing demands for electrical power has precipitated a national effort to develop new sources of clean energy. Long term solutions to the energy problem appear to be feasible by developing or utilizing alternate forms of energy. Little or no relief is envisioned for the near to midterm (10 to 30 years) unless coal conversion processes are considered. Even then, it is problematic whether conventional and newly developed gasification processes can be commercialized soon enough to provide a significant impact on the energy industry. New mines and coal preparation plants must be constructed, workers trained to remove and process the coal, and systems developed and installed to clean up the dirty product gas before use, and the effluent before releasing it into the atmosphere. These necessary tasks are, to say the least, time consuming and the cost involved in each new construction and plant opening is phenomenal. In addition, using conventional mining techniques, only about one-half of the resource is recovered. These considerations have resulted in renewed interest in Underground Coal Gasification (UCG) and other in situ processes in oil shale, tar sands and petroleum reservoirs.

Over the past forty years, the UCG method of coal recovery has been studied in many countries throughout the world including Germany, Poland, Czechoslovakia, USSR, Belgium, Great Britain, France and the United States. For various reasons (but usually the ready availabilty of low cost petroleum and natural gas) the studies were discontinued. The commercial or industrial stage was achieved only in the Soviet Union. There it was developed to a high level and served as a major energy source for more than 30 years. Today, three UCG plants (podzemgaz stations) are supplying power to areas in the Soviet Union remotely located from oil and gas reserves.

Therefore, UCG has been thoroughly demonstrated to be technically feasible and economically viable in the USSR. The task remains to develop the UCG technology required for economical and optimum resource recovery of the United States coal reserves.

The development of in situ recovery processes whether in coal, oil shale, tar sands, petroleum and natural gas or geothermal type reservoirs can proceed along various paths. The most direct approach of immediately attempting a field-based recovery scheme is by far the most productive and enlightening into the real practical problems associated with the particular chosen reservoir and recovery scheme. However, even with substantial theoretical and practical engineering support, there are not only cost obstacles, but in some processes, limitations as to what can be observed from the field studies. By virtue of the remoteness, frequently only black-box input/output quantities are observable and measurable such that the real internal processes can only be hypothesized.

Rudimentary field tests may quickly achieve a process efficiency plateau, which even through trial and error, may not be greatly improved upon. Further development may then depend upon a

more basic scientific approach. This is the essence of the In Situ Hydrocarbon Recovery Simulation Laboratory developed at the Morgantown Energy Research Center. Improvement in the overall total energy resource recovery efficiency of only a few percent could mean the difference of whether UCG is utilized in the U.S. on a large commercial scale.

These laboratory studies can be conveniently catagorized according to four types:

(a) qualitative principle demonstration or illustration
(b) quantitative material property evaluation
(c) quantitative, simple, single-factor process simulation or "effects" studies and
(d) quantitative, total process simulation experiments.

Each of these catagorical experiments is important in developing the UCG process in the United States. Accurate concepts about "what happens" in a UCG process are vital to further process development. The UCG process is very multi-disciplinary in nature which has in part led to widely varying concepts. Many concepts of "the UCG process" are based upon limited experience with a specific type coal, and perhaps, concepts prevalent only in certain engineering or scientific disciplines. As has been demonstrated in the MERC simulation laboratory, the processes in different coals can be almost unrelated.

The differences lie in the significant or controlling multidisciplinary mechanisms involving both physical and chemical effects. In particular, the primary process mechanisms involve chemical reactions (kinetics and catalysis), heat and mass transport phenomena, bulk fluid flow, to, from, and through various geological and structural media (porous, permeable and fissured or fractured) and thermal-mechanical induced stress and strain variations (including tectonic effects) for a temperature and time dependent changing medium. These mechanisms are both externally and internally controlled depending upon the coal properties and the coalbed environment. Only the coalbed environment is subject to change by varying the process scheme and input/output parameters. Thus, the theme of in situ laboratory simulation is to vary and monitor the input/output parameters for various schemes and coal types and study the "internal" micro/macro effects as well as the overall black-box results. The MERC simulation facility was developed to expeditiously and comprehensively accomplish this theme.

Potential in situ conversion energy resources in the Eastern U.S. range from peat and lignite to bituminous and anthracite ranks, from thick to thin beds, and in depths from zero to several thousand feet below the surface. Therefore, wide versatility in simulation facilities is necessary to study recovery of each potential resource. These mechanisms play a different role for each type coal and as each time dependent phase is reached from the initial conditions of a liquid and gas fissure-filled, solid, coal matrix through various phase transitions to the eventual gaseous and liquid phase of all except the ash residue. None of these initial, intermediate or terminal conditions are measurable or observable under field conditions. Thus, laboratory experiments can play a major role in delineating the actual results of specific test conditions.

Experimentation

As discussed earlier, UCG experiments can be conveniently classified in categories to serve specific purposes. In the development of such a multidisciplinary technology, personnel with widely different backgrounds are necessarily involved. The fundamental disciplines may, for example, include geologists, mathematicians, petroleum reservoir and refinery engineers, chemists, physicists, mining, industrial, environmental, chemical, metallurgical, mechanical and electrical engineers, computer and instrumentation specialists. Therefore, education of personnel on as many aspects of the process as possible is critical to successfully developing the technology. For this purpose, simple demonstrations can very effectively convey some of the real physical and chemical characteristics of the process such that "correct physics" is understood and the equations are written to describe it as opposed to "applying existing models with appropriate assumptions."

The Oven Test

One such qualitative demonstration which shows important chemical reaction and structural or physical behavior critical to process modeling is shown in Figure 1 . Small equal size specimens of various types of coal are prepared and subjected to simultaneous, programmed changes in temperature in an air or nitrogen atmosphere in an oven with a special heat treated transparent glass* front. The role chemical reactions play in coal specimen degradation with temperature and time

* for example, Vycor glass

is easily demonstrated by conducting identical experiments with air and N_2 atmospheres. Such an experiment should be very informative to the mathematician pondering realistic structural and reaction models and assumptions, and at the same time, convincingly inform the chemist who wants to conduct char studies at high pressures or temperatures in an argon environment, of the relevance of such a test to the UCG process. This simple "Oven Test" reveals many other process characteristics to the astute observer, namely:

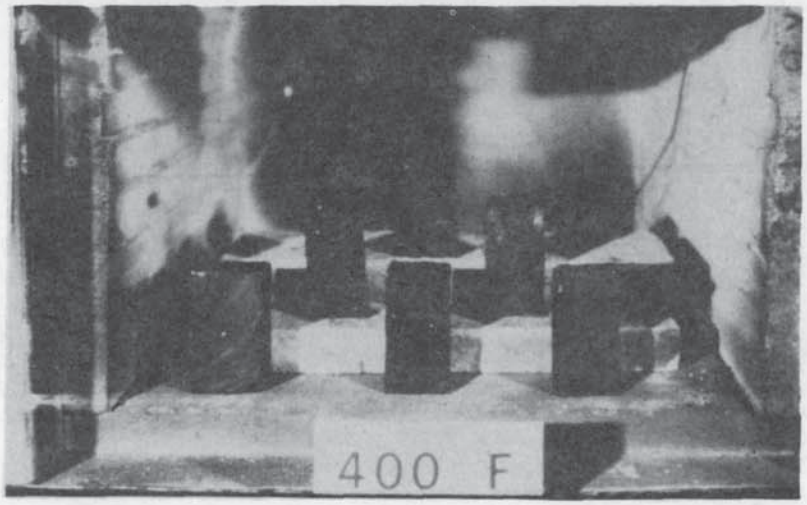


Figure 1. - Oven Test to Demonstrate Chemical and Structural Changes in Coal with Increasing Temperature

(1) As the coal swelling index was measured by heating powdered, compacted coal in a cup, the Oven Test gives quantitatively the swelling or shrinking ratio for solid rectangular blocks of coal under no external stress subjected to any prescribed temperature-time function provided by a temperature controllable oven.

(2) The critical temperature at which a particular coal will undergo self-sustained oxidation reactions in an air atmosphere is easily observed and indicative of the reactivity or activation energy.

(3) The temperature at which significant sample degradation occurs in terms of:

a. Viscous fluid state onset and loss of structural integrity
b. Preferred direction of thermal fracturing
c. Ratio of thermally-induced, orthogonal fracture widths

(4) The temperature at which any preferential directional flow of effluent gases from an oriented sample may occur and when or if free carbon is entrained in the effluent gases.

All of these characteristics are critical to a realistic understanding of the in situ process.

Conventional physical, chemical, electrical and thermal property determination-type tests are also a necessary part of UCG technology development. Although coal has been subjected to innumerable tests for more than 50 years, certain data necessary for UCG process engineering computations do not exist. One major reason for the lack of appropriate data is the emphasis on statistical sampling of a coalbed by first crushing the coal to a specific particle size. While being a valid technique for many coal evaluation purposes, such data on crushed and recompacted coal of a specific particle size may have little relevance to the in situ conversion of coal in its natural solid state.

Property Determination

Coal properties need to also be determined under a variety of conditions representative of the natural and progressively changing environment associated with UCG from the inception through the in situ gasification phase. In general, few, if any, of the chemical, physical, etc. properties have been so determined.

Coal beds are typically fractured and the fissures filled with a saturated water/gas solution. During initial injection of air/O_2 under some specific gasification scheme, these fluids are moved through the coal bed and possibly cycled through phase conversions. Then, after drying of the fissure cavities, these same surfaces may be subjected to convective and/or conductive thermal currents which initiate new mechanisms. The ensuing phase and property changes are very complicated and with negligible exception, have never been realistically modeled or characterized. It is these stages of the process which distinguish the behavior of different coals and suggest that

special recovery schemes be tailored to each type of coal. But first, the individual coal properties must be well defined under real in situ conditions.

Coal beds are known to have directional properties which can play a critical role in the in situ conversion/recovery process. The most common directional properties of a coal bed is the "pseudo permeability" due to the fissures which control fluid directional migration. This pseudo permeability is a function also of the bedding plane tectonic stress field which can be modified in various ways by the in situ gasification. The initial stress field modification occurs as a result of pressure gradients and thermal stress. Subsequently, the vertical tectonic stress becomes locally intensified due to the moving, free boundaries. These effective directionally-applied or relieved stresses can also play a dominant role in the mode of and direction of process advance or fluid ingress and egress.

To thoroughly analyze the coalbed structurally and evaluate the directional effects, the directional properties first have to be determined under temperature and time dependent in situ related conditions. Figure 2 illustrates an apparatus developed and used at MERC to determine the fundamental mechanical properties to facilitate structural modeling of the UCG process. Details of the apparatus construction and use along with results for the Pittsburgh coal have been reported [1]. Recent structural models developed with the capability of using these data have been discussed [2].

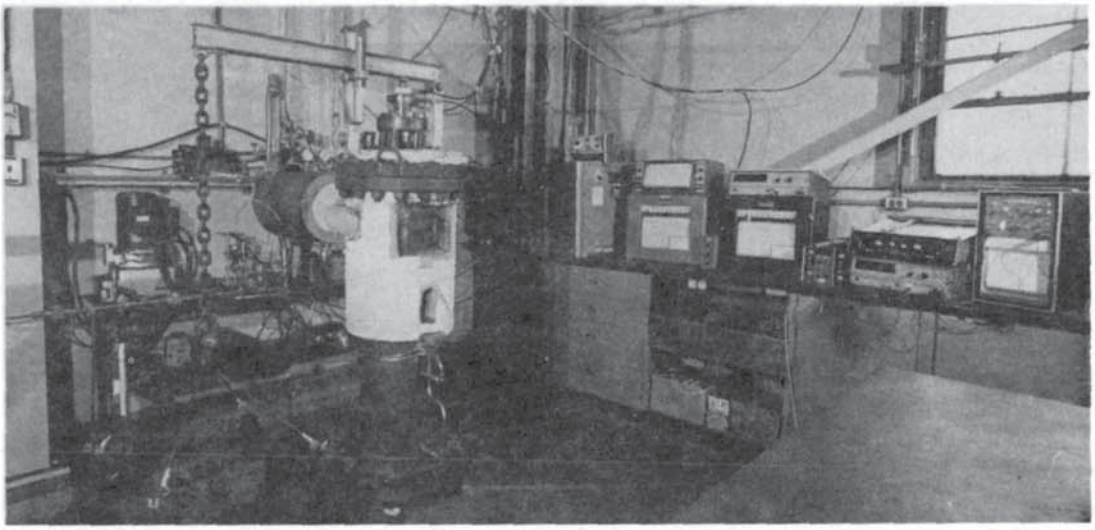


Figure 2. - Thermo-Mechanical Property Test Apparatus

Simulation Experiments

Historically, the UCG process has been developed largely on a field trial and error basis. Largely due to the remote nature of the process, little information has been generated on the "internal" mechanisms, and the associated theoretical analyses required for detailed engineering computations do not exist. The controlling mechanisms such as swelling or shrinking effects, tar distillates flow, water influx, thermal fracturing, and coke viscous flow under tectonic stress, roof subsidence, coal rank, reactivity, coking, heating value, ash and other mineral content effects, and thermal energy transport processes all are expected to play key roles and produce entirely different results for each coal type and set of coalbed conditions. Thus, a comprehensive laboratory simulation facility was planned to study the significance of these parameters singly and in various combinations.

Experiments can be of single, multiple, or total process purpose. Single factor tests which have been conducted include simple heat conduction with no convection affects and heat conduction with co-current and counter-current convection effects on water-saturated coal and dry coal at different temperature levels. Additional experiments have been performed to determine the effects of CO_2 injection on coal sample permeability and to define the permeability increase of the sample with air drying.

Single factor simulations of the UCG process are not always as simple as might be anticipated due to a large number of non-controllable variables not the least of which is the variability between coal specimens. The total number of factors which need to be investigated, if formulated in terms of a statistical factorial design test program, yield an impractical number of tests. Consider the factors listed in Table 1. To reduce the total number of experiments, multi-purpose tests are usually conducted approximating a unique combination of process simulation conditions.

Table 1. - In Situ Hydrocarbon Recovery Simulation Laboratory Test Variables

UCG SCHEME	COAL TYPE	GASIFICATION MODE	OXIDIZING AGENTS	COAL BED CONDITIONS	SIMULATION PURPOSE
Longwall Generator	Eastern Bituminous	Forward	Air	Horizontal	TOTAL PROCESS
Linked Vertical Well	Western Bituminous	Reverse	Oxygen Enriched Air	Dipping	Transfer Coefficients Conductive Heat Convective Heat Combined Heat & Mass
Packed Bed	Western Bituminous	Cyclic Forward-Reverse	Oxygen Enriched Air with Steam	Thick	Gas Composition Composition BTU
Steeply Dipping Bed	Lignite	Dynamic Flow Control		Thin	Burn Direction Effects Face Cleats Butt Cleats
Through Borehole		Dynamic Pressure Control		Deep	Total Recovery Efficiency Burn Stability
Blind Borehole				Shallow	Directional Permeability Effects
				Water Influx	CO_2 Permeability Enhancement Open Fractures Effects

In preparation for and during the tests, the procedures are designed to duplicate what could be done in the field.

A sample is obtained from a large block of coal such that sample orientation with respect to the coal seam bedding plane and the face and butt cleating system is known. This sample is sealed into the coal specimen either parallel or perpendicular to the bedding plane. The geometry of these simulated wells are carefully noted to determine whether the reaction front progresses in the direction of or perpendicular to the face cleating system. A pattern of small diameter holes is then drilled into the coal specimen and thermocouples are inserted to monitor temperatures throughout the reactor interior during the test. An oxidizing agent is supplied to the reactor inlet and the product gases are directed through a conventional gas clean-up train into a gas analysis system.

Both small (12-inch ID) and large (30-inch ID) reactor vessels are used in the tests. The smaller reactors, requiring more easily obtained small coal samples and less preparation time, are used to initially test out various concepts and procedures. For example, through borehole combustion is one method under consideration for igniting a horizontal hole in planned field tests. To test this concept, a single hole is drilled axially through the center of a sample cemented into a small reactor, the sample is ignited at one end, and the fire propagated along the hole in either the forward or reverse combustion mode. In several tests, a small section of coal was left in the center of the hole to simulate the possibility of blockages which may occur. Valuable information was obtained from these tests concerning the rate of reaction front preogression in forward and reverse burn modes, the magnitude of tar repolymerization and deposition problems, and the effects associated with the high swelling indices of eastern bituminous coals. The quality of the gas produced during these tests was low, as anticipated, due primarily to the lack of a strong reduction zone in the short reactors.

After initial testing in the small reactors, the larger reactor is used to integrate the various concepts and procedures to approximate a total process. For example, in a recently completed test, an attempt was made to ignite a center horizontal borehole by forward combustion, reverse link to two parallel horizontal boreholes located on 7-inch centers from the central

borehole, and finally, to forward gasify the hot bed of porous coke from the outer holes to the center. Many of the problems experienced in this test were predictable as a result of analysis of tests completed in the smaller reactors.

Laboratory Instrumentation

Extensive instrumentation has been incorporated in the UCG Simulation Laboratory to provide rapid and automatic monitoring and storage of process variables and to provide continuoud information necessary for manual or automatic process control. Measured parameters include temperatures, pressures, flows, and gas composition. Although most measurements result in analog signals which are directed to a computer-based automatic data acquisition and control system (ADACS), many critical signals are simultaneously directed to control panel meters for backup in the event of ADACS failure.

To sense the reaction temperatures, 1/16" or 1/8" diameter CH/AL thermocouples with 446 SS sheating are utilized. This type thermocouple is used throughout the system where corrosive atmospheres and high temperatures exist. In locations with lower temperatures and non-corrosive atmospheres CU/CN or FE/CN thermocouples suffice.

A resistance-type igniter using platinum wire wound solenoidally on a ceramic tube yields excellent performance as a heat source for sample ignition. The igniter maintains its integrity and is, therefore, reuseable in the same test, if necessary, and also in subsequent tests. The current and voltage is monitored by the ADACS, and, the power developed (controllable from 0 to 500 watts) and current are continuously updated on a 30-unit digital display array. The igniter length, ranging from 6-1/4" to 15", is determined by the gasification scheme being tested and the simulated well length. Thus, the total required ignition energy and flux intensity required under various conditions are known.

Pressures throughout the system are monitored by means of pressure transmitters which utilize a piezoresistive strain gauge pressure sensor. The 4 to 20 MA transmitter output signal is proportional to the process gauge pressure.

All flow measurements are made with integral orifice transmitters. The 4 to 20 MA transmitter output signals are converted to flow rates in the ADACS and corrected for temperature, pressure, and density effects.

Pneumatically-activated valves provide a means for automatically controlling flow rates and pressures. The output signals of transmitters associated with the valves are converted to proportional control signals in the ADACS which are sent to the proper valve controllers. The controllers develop correction signals regulating the opening and closing of the valves to maintain present flow rates and pressures. The conditions can be set manually or varied automatically by the ADACS.

Analysis of the product gas comspsition is accomplished by gas chromatography, mass spectrometry and chemoluminescense. Two independent, but synchronously operated, programmable gas chromatographs, using helium as the carrier gas, are the primary monitors of gas composition. The components determined by GC1 and the full-scale values are: hydrogen (50%), carbon dioxide (20%), ethane (2%), methane (50%), carbon monoxide (20%), argon (3%), oxygen (25%), and nitrogen (100%). The components determined by GC2 and the full-scale values are: hydrogen cyanide (.2%), butane (1%), hydrogen sulfide (3%), carbonyl sulfide (.1%), propane (1%), and sulfur dioxide (3%). Prior to each experiment, the chromatographs are completely recalibrated using certified cylinder calibration gases. Since the chromatographs are programmable, the control of analyzer valves, cycle timing, electrical zeroing, component range attenuator selection and signal output is automatic and continouus. Each chromatograph is equipped with a 10" recorder and, in addition, 0 to 10 volt output signals are developed corresponding to 0- to full-scale percent of each component. One complete analysis cycle for the 14 gas components (sample withdrawal to sample withdrawal) requires 850 seconds.

Although the process gas chromatograph is the workhorse of the industry, it is nearly useless to monitor the rapid changes occurring within the reactor during laboratory similitude experiments. Gas quality can vary up to several hundred BTU in less than five minutes and rapid gas composition updating is needed, therefore, to exercise control over the process.

To accomplish this, a mass spectrograph multiple gas analyzer is incorporated in the analysis system. Zero to 90 percent response for the spectrometer is typically less than 250 milliseconds and several thousand updates for each component is possible in the time required for one complete chromatograph cycle. In practice, however, the gas transport time between the reactor and the spectrometer is approximately two minutes. The gas components measured and the full-scale values are: nitrogen (100%), oxygen (20%), carbon dioxide (20%), hydrogen (20%), methane (50%), carbon monoxide (20%), hydrogen sulfide (5%), and sulfur dioxide (5%). These components will characterize in excess of 98% of the product gas on the average. Prior to each experiment, the spectrometer is calibrated using the chromatograph output as the standard and then checked using certified cylinder calibration gases. In addition to digital displays on the analyzer 0 to 10 volt output signals are developed corresponding to 0-to-full scale percent of each component.

One additional important aspect of the spectrometer is the capability to automatically sample up to four gas streams sequentially with dwell times programmable in fixed steps for each stream. The atmospheres normally measured in addition to the product gas is room air and cabinet air. The latter measurement is made to monitor the possible accumulation of explosive gases within the analyzer itself while the former measurement alerts personnel to the presence of toxic gases in the room air. Additional health monitors with alarms are provided for carbon monoxide and hydrogen cyanide. Also, this multiple stream sampling can be used to increase the rate that a single stream is measured.

The final gas analysis is to determine the oxides of nitrogen. Using chemoluminesence techniques, nitrous oxide and nitrogen dioxide in the gas stream is determined. No_x is then found by subtraction. In addition to panel meter indications,0 to 10 volt signals are developed corresponding to 0 to 1000 PPM full scale.

Figure 3 is a photograph of the UCG Simulation Laboratory gas analysis instrumentation as well as the automatic data acquisition and control system.

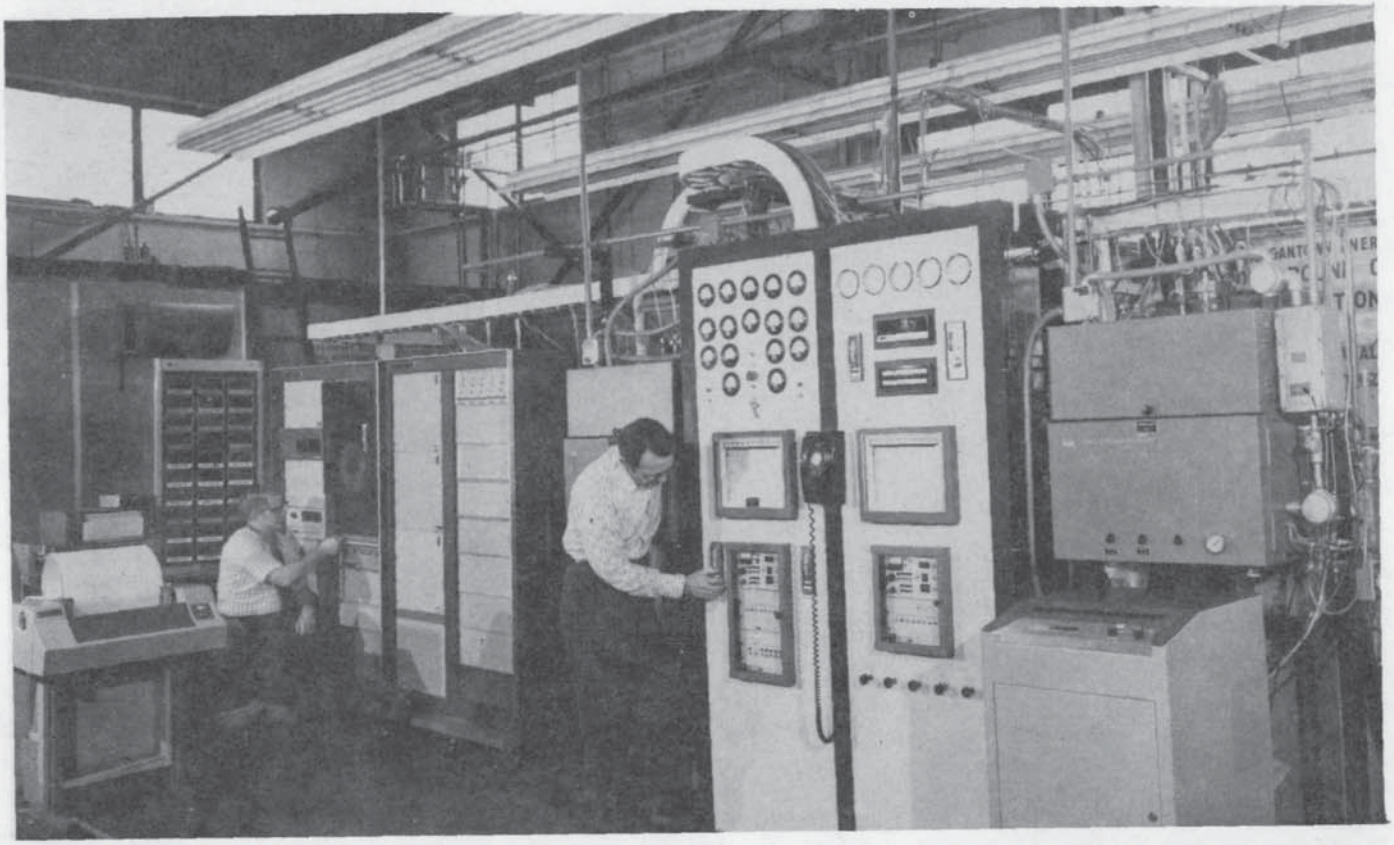


Figure 3. - In Situ Hydrocarbon Recovery Simulation Laboratory

Automatic Data Acquisition and Control System (ADACS)

The ADACS is a computer based, high speed, multiple channel data collection, processing, and control unit. The computer is interrupt driven with 32K of 16 bit core memory and, a 264 K drum provides a means for additional data and program storage and retrieval.

Although only 384 channels are currently available for analog data input (ranging from -10.24 to 10.24 volts), the system can be expanded to 2048 channels. The analog-to-digital converters have one bit for sign, a 4 bit range, and 11 bits for magnitude permitting a conversion resolution of 1 part in 2048. This is enhanced by automatic signal level ranging selectable over 12 ranges starting at 5 millivolts full scale. A portion of 144 bits of digital data input and output which is addressable in 16 bit words, is used to determine the status and the cycling of the gas chromatographs and to drive a 30 unit digital display array. Thirty-two channels of digital-to-analog converters, with 12 bit resolution, develop up to $\pm$ 10 volt analog signals to drive strip chart recorders and to provide control signals for regulating automatic instrumentation.

Two important features of the system include programmed automatic scan control and system calibration. The present scanning rate is up to 10,000 channels/second with a potential of 20,000 channels/second limited only by the magnetic tape recording rate and the need for converting digital voltage data to engineering units. Automatic calibration corrects for such things as drift in strain gage bridge excitation power supply voltages and for zero and gain variations in the converters.

Many peripherals have been added to the ADACS to facilitate operations during experiments and subsequent data analysis. These peripherals include: a teletypewriter consol for operator communication with the ADACS, 9-track and cassette magnetic tape recorders for data storage and software back-up, a 132 column lineprinter for hard copy of data at selected time intervals, and a 30-unit digital display array of selected process variables for rapid assessment of reaction progress by the operator. Any variable in the array can be programmed to flash to alert the operator when the variable exceeds predetermined limits.

Figure 4 is a block diagram illustrating the structure of the ADACS.

Software, written specifically for the data acquisition system and peripherals, provide the instructions necessary for scanning, converting, processing, storing, recording, displaying and printing of variables. Additional software updating is currently obtained using assembly language programming specific to the particular computer. This time-consuming, laborious task is performed by only one or two knowledgeable personnel which often impeded the use of the ADACS for experimentation.

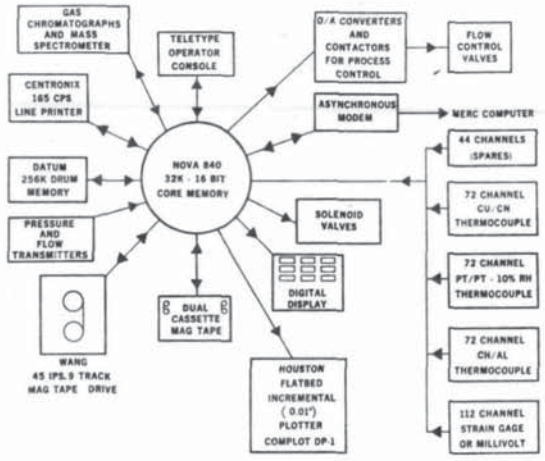


Figure 4.-UCG Data Acquisition and Control Systems

A 1.2 million byte disk and associated software for the ADACS enables programming in widely-known FORTRAN. Future software development will be accomplished in the fully compatible MERC central computer facility by MERC programmers. This acquisition will also facilitate bringing on line in the laboratory an x-y incremental plotter and a CRT graphics terminal. The incorporation of these two peripherals is very important to process control development since currently parameter variations are known only as a function of time during similitude tests rather than the possibly more important parameter-parameter relationships.

With this system, magnetic tapes of raw and some premassaged data are played back on the MERC central computer facility and, for example, one-inch thick reports of CalComp plots, tables, etc. of raw data as well as calculated data are automatically generated.

System and Process Flow Description

The system is designed to handle a variety of gasification schemes by providing versatility in input/output configurations, gaseous agents, (Figure 5) pressures and flow rates. Figure 5 is a flowsheet for the complete system showing not only the direction of gas flow, but also, the locations where system parameters are measured and the types of measurement made. Provision has been made for the injection of various gaseous agents into the system; carbon dioxide to determine the effects of CO_2 on coal permeability, nitrogen to preheat the system, air to provide oxygen during the combustion phase, and inert gas or nitrogen to quench the reaction. Modifications for steam/O_2 are nearing completion.

The reaction can be quenched manually at the conclusion of a test or automatically during a test. Solenoidal valves V10 and V11 and the pressure switch P10 form a fail-safe system. Power is required to close V10 in the inert gas line and open V11 in the air line. An interlock assures that the inert gas pressure at P10 exceeds 90 PSIG before power can be applied to the valves. Loss of system power, inert gas pressure or the rupturing of the rupture disk at the reactor exit causes immediate flooding of the system with inert gas.

Clean,dry air flowing into the system through the flow controlling automatic main gate valve V12 is heated prior to entering the reactor. Products of gasification exiting the reactor pass through a filter pot (not shown) and a heat exchanger for preliminary particulate and liquids removal prior to passing into the gas clean-up section. By incorporating two parallel gas clean-up sections, both large and small flows can be processed with minimum gas transport lag time to the analysis system. The maxi-section is equipped with a larger filter and precipitator as well as a high capacity heat exchanger. Selection of the proper section is controlled by air actuated by high temperature valves V17 and V18. Valves V16 and V19 permit preheating of the gas clean-up section not in use with nitrogen if the need for switching exists. Automatic valves 24A and 24B control the back pressure on the system with the excess gas being directed to the stack and flared. After passing through trace heated lines, the remaining stream is conditioned in dryers and filters prior to actual analysis.

Reactor Vessels

Similitude tests are conducted in three small (C-size) reactors and one large (D-size) reactor. Two of the C-size reactors are constructed from 12-inch schedule, 40 carbon steel pipe with 125# carbon steel slip on flanges, and the 23-1/4" long chamber is sealed with 125% carbon steel blind flanges. Each blind flange has a 1-9/16" diameter hole drilled in the center for air injection and product gas removal. Flange-type adapters are bolted into these holes during reactor preparation. Eighteen 1/4" I.D. and eighteen 1/2" I.D. pipe couplings are welded to holes drilled in the pipe to permit access to the reactor interior for the placement of thermocouples. The third C-size vessel is constructed with 316 stainless steel pipe and weld neck flanges. Vessel design was for 120 PSIG pressure at a shell temperature of 650°F.

Sample Collection and Preparation

Because of availability and ready access, local strip mines are most frequently used as the source of eastern bituminous coal samples. As soon as possible after the overburden is removed, large blocks of coal are sawed out of the coal seam. Every attempt is made to obtain blocks which may be easily trimmed to 20" x 20" x 15" and that there are no visible large fractures. As the coal is removed, the orientation with respect to the bedding plane, face, and butt cleats is recorded. For transportation to the laboratory, the coal is wetted down and wrapped in plastic to minimize water loss. Samples collected large distances from the laboratory (such as Texas lignite and Powder River Basin subbituminous) are shipped sealed in plastic with water saturated sawdust packed around the coal.

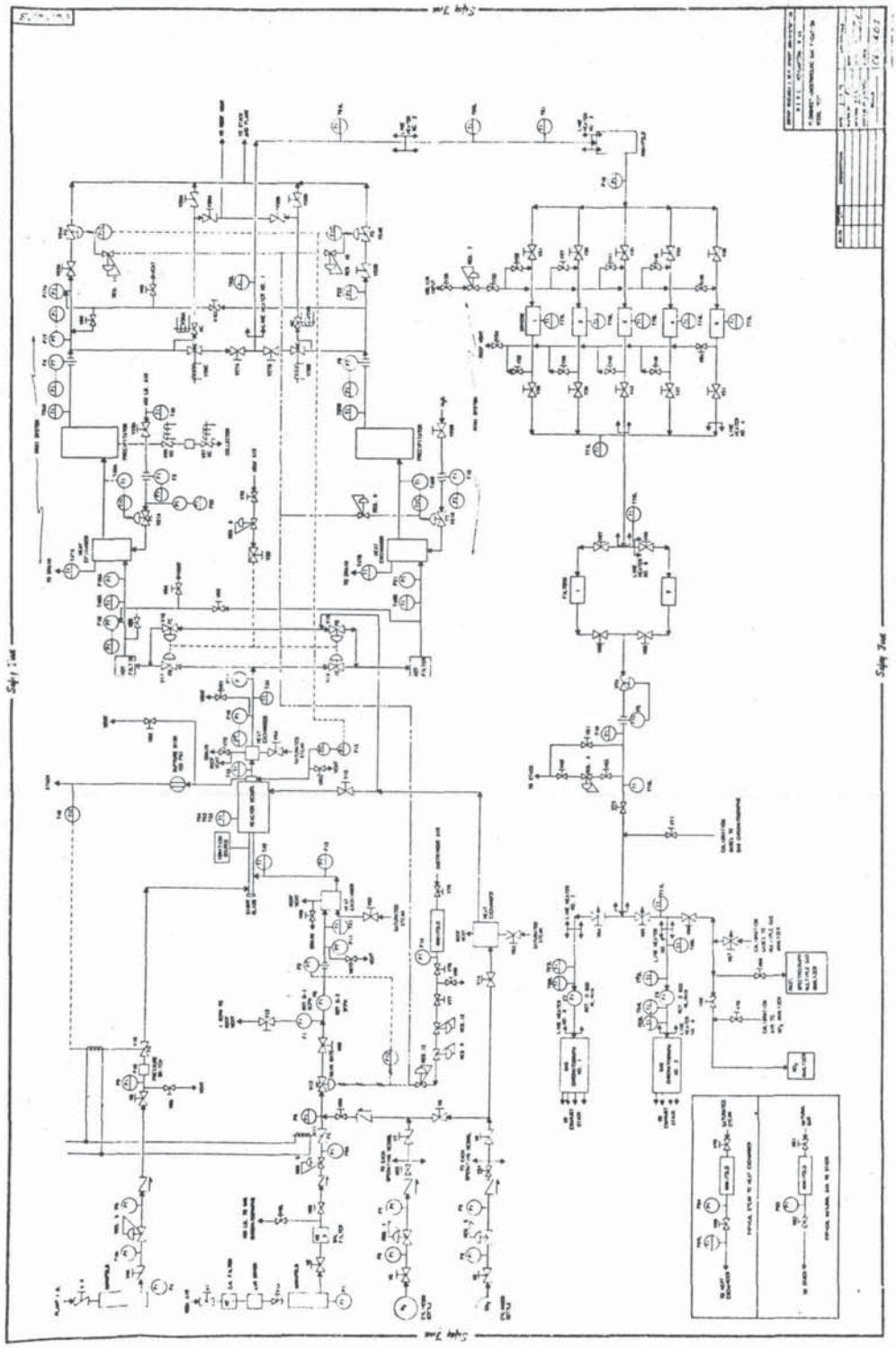


Figure 5. - System and Process Flow Sheet

Upon receipt at the laboratory, the samples are prepared for insertion in either of the two reactors depending on the simulation scheme to be tested. For the C-size reactor (12" I.D.), a 6" diameter by up to 15" long oriented core is obtained by wet coring methods. The core is immediately centered in a 10" diameter by 21" long 20-gage stove pipe and the remaining cavity is filled with castable refractory cement. After curing the 18 to 24 hours, the cement at the open ends of the stove pipe are coated with sauereisen cement to minimize further moisture loss and to minimize bypass of gases during the simulation test.

For the D-size reactor, (30" I.D.), the coal block is trimmed to 20" by 20" by 15". After centering the rectangular coal blcok in a 26" diameter by 21" long 20-gage metal cylinder, preparation proceeds as with the C-size reactor sample. Figure 6 shows the prepared samples prior to installation in the reactors.

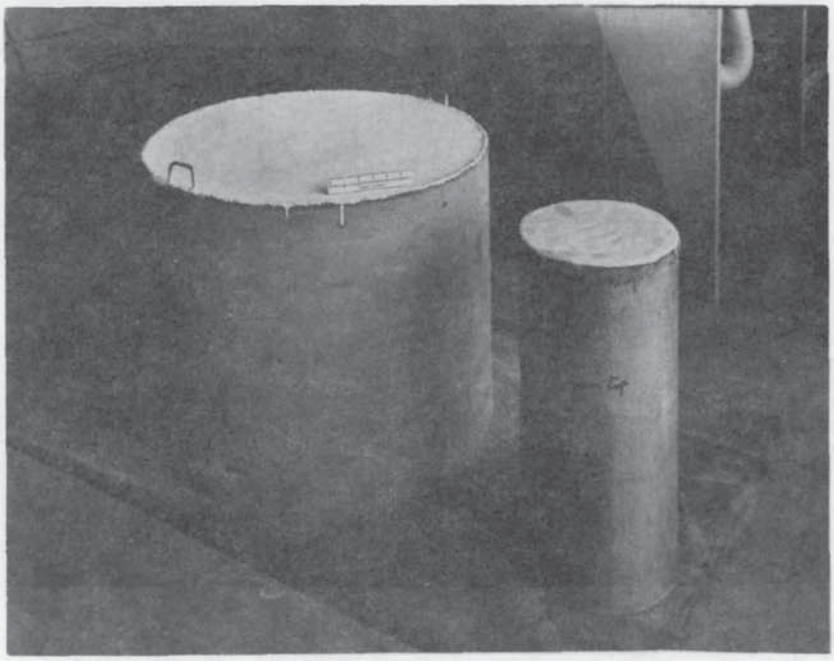


Figure 6. - Prepared Coal Samples Prior to Insertion in Reactors.

Reactor Preparation

Reactor preparation begins with the installation of one blind flange. The prepared sample is then centered in the reactor and rotated to the desired orientation with respect to the face and butt cleats, and, the remaining cavity is filled with castable refractory cement. After curing, the exposed cement is coated with a thin layer of sauereisen cement and, when dry, the surface is crisscrossed with beads of silicon rubber cement. The end flange (rotated such that the 1-9/16" holes in each flange are aligned) is then installed producing an airtight seal.

A one-inch diameter core drill is used through the flange holes into the coal sample to provide simulated wells for air injection and product gas removal. Ceramic tubes extending from the blind flanges and the coal surface are cemented into each hole. The wells are completed by installing the flange-type adapters over the ends of the ceramic tubes and bolting them to the blind flange. The selection of holes and the length of each well drilled into the coal sample is dependent upon the gasification scheme being simulated. The one-inch coal cores obtained during the drilling are chemically analyzed to characterize the sample.

Reactor preparation continues with the drilling of holes through the ports for placement of thermocouples within the reactor. The holes, 3/32" diameter of 5/32" diameter, are drilled radially into the coal sample to prescribed depths to accommodate 1/16" O.D. or 1/8" O.D. thermocouples. The thermocouples are sealed in with sauereisen cement to prevent hot gases accumulating in and leaking through the holes.

Reactor preparation is completed by piping the reactor into the system, connecting the thermocouples to the ADACS, and installing the igniter. Figure 7 shows the final preparation of the D-size vessel immediately before a longwall generator similitude experiment.

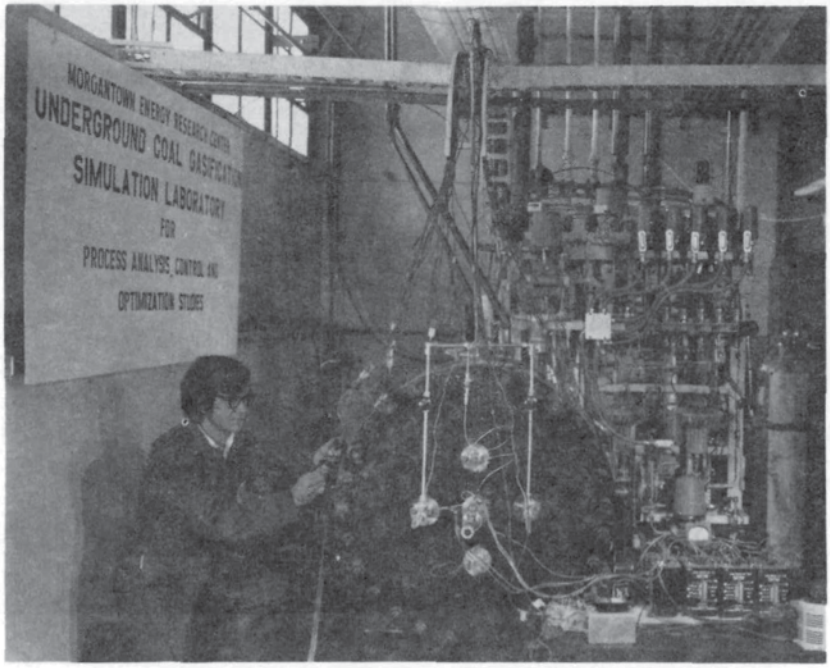


Figure 7. - Final Preparation of D-Size Reactor Vessel

Data Analysis and Presentation

A data base for the UCG Simulation Laboratory and field effort has been established in the MERC central computing facility. Data transfer from the ADACS is primarily by 9-track magnetic tape with subsequent data reduction and analysis performed by the facility. Standardized package routines are used to smooth and filter the data and to print tables of experimental results. Relationships of variables are previewed on CRT graphics terminals prior to selection or rejection for CalComp plotter publication quality output. For programs requiring the memory or speed of a larger computing system, the MERC facility provides a direct link, for both input and output, to the IBM 360/75 computer and associated peripherals at the West Virginia University Computer Center. A data report, generated for each similitude test conducted in the laboratory, characterizes the properties of the sample, describes the experimental conditions of the test, and presents the data in both tabular and graphical formats.

To illustrate the data presentation, portions of UCG Burn 6 will be discussed. This test was a modified blind borehole-type simulation performed in a C-size vessel on a 6-inch diameter by 15-inch long core of Mahoning Eastern Bituminous Coal. The core was inserted in the reactor with the bedding plane and face cleats parallel to the long axis of the vessel.

A one-inch diameter hole was drilled 5-1/2 inches into the coal from each end of the vessel leaving 4 inches of undrilled coal in the center. A reverse burn was conducted by igniting the hole on the production end and percolating air through the coal to the reaction zone. The process was controlled by automatic closed loop regulation of inlet air flow and reactor back pressure. The data acquisition rate was one scan of all system parameters each two seconds.

Figure 8 shows the system air input and product gas output flow rates and Figure 9 shows the system pressures during the test. It is of interest to note that after about nine hours, the air in pressure fell to almost that of the reactor out pressure probably as a result of a fracture developing from thermal stresses. The pressure rose slowly for 3-1/2 hours until finally, a drastic pressure increase occurred, indicating the complete resealing of the fracture and adjacent coal by repolymerization of tars and oils. When the reaction zone burned through this area, butn-through was complete and the test was terminated.

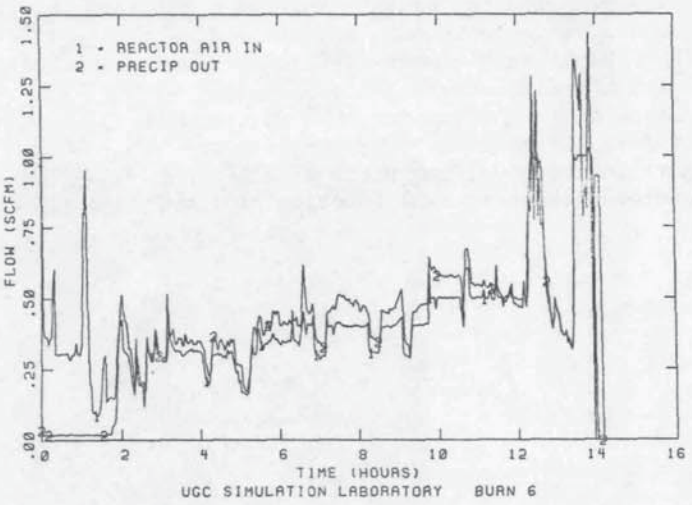


Figure 8. - System Flow Rates During a Similitude Test

Figure 10 illustrates the temperature distribution longitudinally along the reactor from level 2 (input end of the coal sample) to level 7 (output end of the coal sample) with about 2" separating each level. One thermocouple is inserted at each level with the tip 5/8" from the axial center of the vessel (8/8" into the coal). The movement of the reaction front during the reverse burn is delineated very readily in this figure. A characteristic loss of temperature in levels 6 and 7 is noted about 5-1/2 hours into the test when the igniter power was cut off. At 8-1/2 to 9 hours, the temperature of these levels increased rapidly since more air reached this area through the opened fracture.

The radial temperature distribution at level 7 during the test is shown in Figure 11. Thermocouples were placed 5/8", 1-1/4", and 2-1/4" from the axial center of the vessel. The outermost portions of the coal did not reach gasification temperatures during the test. It has been observed, in fact, that the complete reaction zone is on the order of 1 to 1-1/2" and the temperature differential in this 1-1/2" zone may reach 1000 to 1200°F.

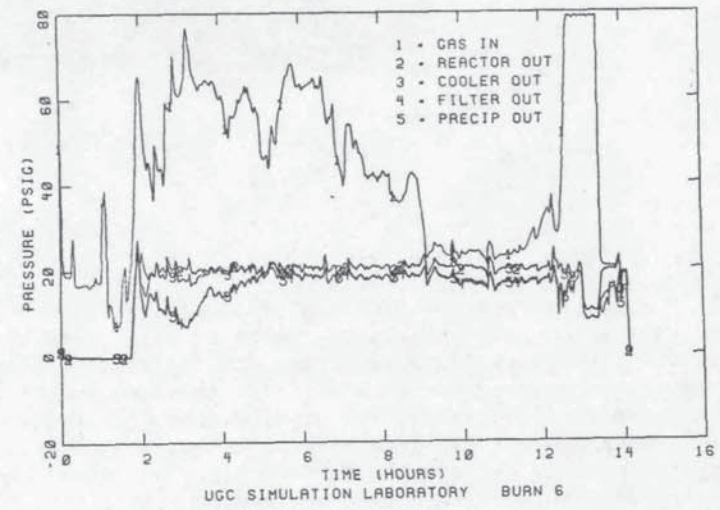


Figure 9. - System Pressures During a Similitude Test

Figure 12 shows the hydrogen and methane concentration in the product gas obtained during the experiment. The rapid changes in the gas composition are easily and accurately measured by the mass spectrometer multiple gas analyzer. In contrast, Figure 13, which

illustrates the heating value of the same product gas determined from gas chromatograph data, shows none of the intermediate gas heating values--a result of the slow response of the instrument.

The limited number of CalComp plots and the brief interpretation of each serves only to illustrate the vast amount of data accumulated. The complete report includes CalComp plots of all system parameters as a function of time, strip chart recordings, photographs of the sawed-open sample taken after quenching, chemical analyses of the sample before and after burning, and scanning electron microscope photographs of samples taken from and near the reaction zone. Cross correlation techniques are currently being investigated to delineate the effects of various system parameters on the remaining system parameters and these results will be included in the report in the future.

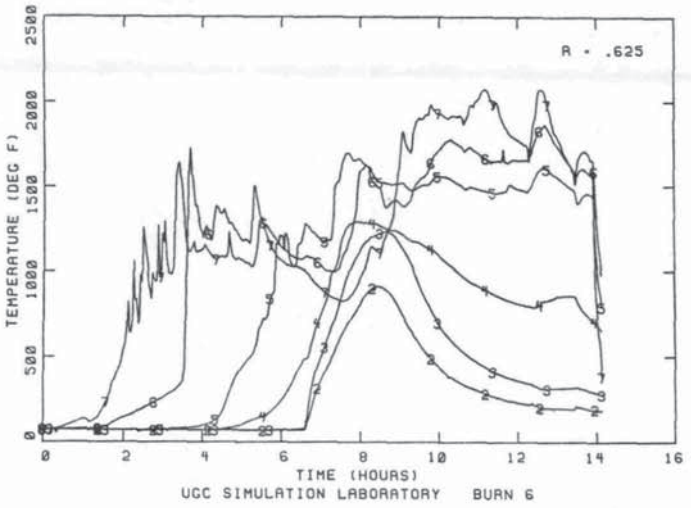


Figure 10. - Longitudinal Temperature Distribution During a Similitude Test

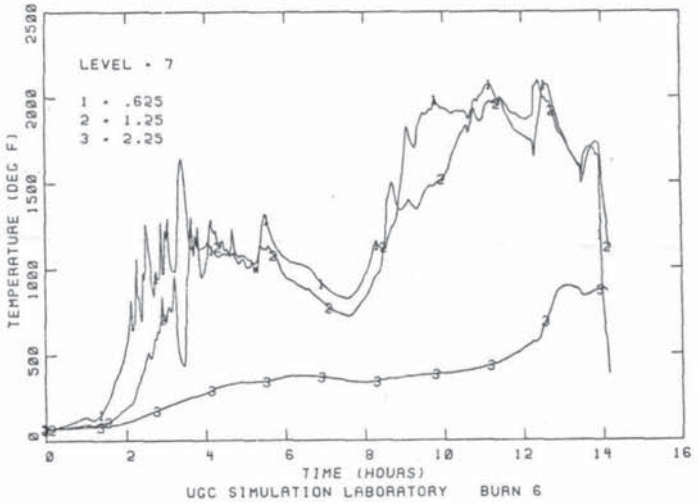


Figure 11. - Radial Temperature Distribution During A Similitude Test

REFERENCES

[1] Shoemaker, H. D., L. Z. Shuck, R. R. Haynes, and S. H. Advani. "The Mechanical Properties of the Pittsburgh Coal at Elevated Temperatures," an ASME publication, Paper No. 76-Pet-55, Presented at the Petroleum Mechanical Engineering and Pressure Vessels and Piping Conference, Mexico City, Mexico, September 19-24, 1976. Copies available from National Technical Information Service, Springfield, Va., 7 pp.

[2] Advani, S. H. and Y. T. Lin. "Structural Mechanics Simulations Associated with Underground Coal Gasification," MERC/CR-76/1, May 1976, 85 pp.

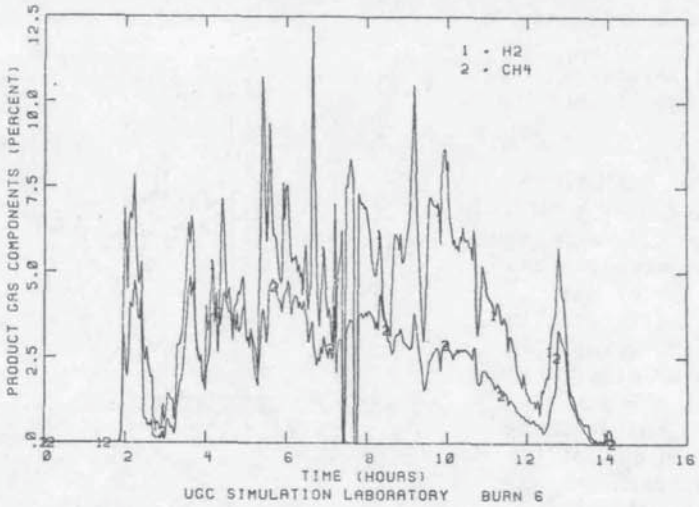


Figure 12. - Hydrogen and Methane Concentration in the Product Gas as Measured by the Mass Spectrometer Gas Analyzer

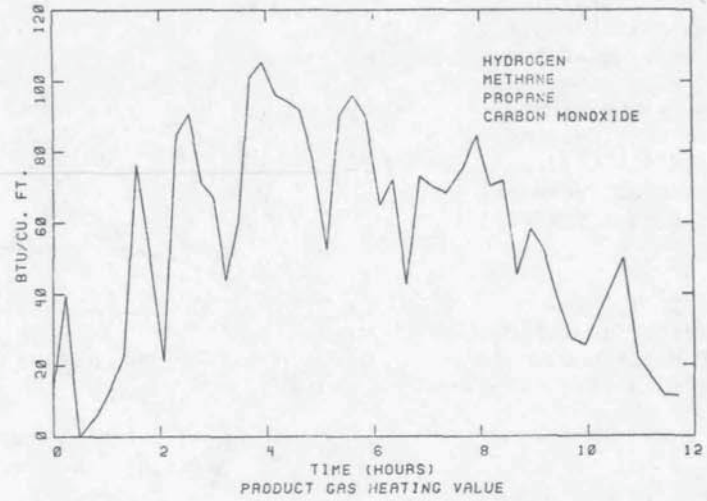


Figure 13. - Product Gas Heating Value Obtained From Gas Chromatograph Measurements

AN AMMONIA INJECTION SCHEME FOR FRACTURING AND PERMEABILITY ENHANCEMENT OF COAL BEDS

Rabinder S. Datta, Syracuse Research Corporation, Syracuse, N.Y.

ABSTRACT

A scheme is presented where the ammonia or other chemical is introduced into the coal bed. As a result of the unique effect of these chemicals on coal, fracturing and/or an increase in its permeability take place. This method can be very easily adopted to various underground gasification, degasification and mining systems.

INTRODUCTION

The Syracuse Research Corporation has been involved in the search for improved methods for cleaning coal. The technology developed has been patented (1) in a series of disclosures covering applications in the cleaning and mining of coal. The term 'chemical comminution' has been applied to this process.

Conventional methods of fracturing and/or increasing the permeability of coal, for either underground gasification, degasification or mining of coal, involves the use of underground galleries, boreholes, mechanical cutting or fragmentation using explosives, either separately or in conjunction with each other. The operations involved require an excessive energy expenditure and/or manpower. Chemical comminution, on the other hand, involves a selective fracture and/or increase in the permeability of the coal by the use of chemicals, for example ammonia, which are inexpensive, recoverable to a high degree, and operative under conditions which permit its utilization as an integral step in either an insitu gasification scheme, underground mining system or in the degasification of coal beds.

THE CHEMICAL COMMINUTION PROCESS

The chemical comminution process involves the penetration of certain low molecular weight compounds, characterized in part by molecular weights of 100 or less, throughout the naturally occurring system of faults, pores and other discontinuities in coal. This results in the weakening and disruption of the interlayer forces at the natural interfaces. Though no significant dissolution of the coal matrix has been found, this does not rule out the possibility that the chemicals selectively dissolve material, such as resins or waxes, and cause the

Reference at end of paper

increase in the permeability of the coal. The chemical seems to induce the breakage selectively along the bedding planes, the mineral matter constituents and the maceral boundaries (2). Figures 1 and 2 show an Illinois No. 6 coal sample before and after chemical treatment. Notice the extensive fracturing of the coal along the cleats and bedding planes.



Figure 1. Illinois No. 6 Coal Before Chemical Treatment

For any one coal, the rate and extent of the fragmentation can be regulated by varying the reaction conditions. This is indicated in Figure 3 where 3/4" x 1/4" Upper Freeport seam coal samples were subjected to a variety of exposure conditions.

GENERAL METHODOLOGY FOR PERMEABILITY ENHANCEMENT OF COAL BEDS

A general scheme, for increasing the permeability of a coal bed, involves:

1. Introduction of the comminuting agent. This requires that one or more access boreholes be drilled into the bed either vertically, horizontally or directionally. The chemical, for example ammonia, is pumped into the bed under pressure and maintained at that pressure for a predetermined length of time. Under certain circumstances a low level of hydraulic fracturing, using the comminuting agent as the fracturing medium, may be employed. The chemical would cause the coal to swell (3) and fracture without affecting the mineral matter in any way. The amount of swelling

Reference at end of paper

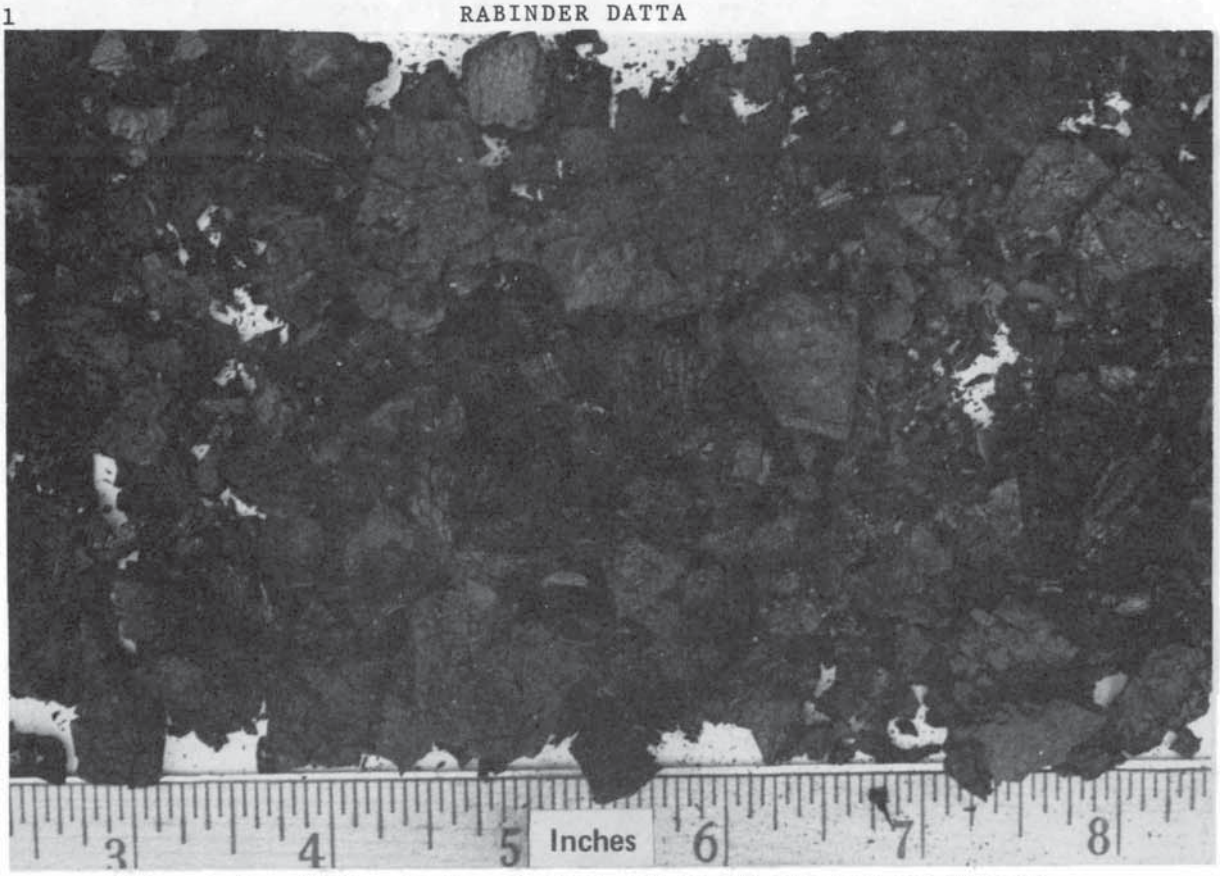


Figure 2. Illinois No. 6 Coal after 15 minutes in Liquid Anhydrous Ammonia at Atmospheric Pressure.

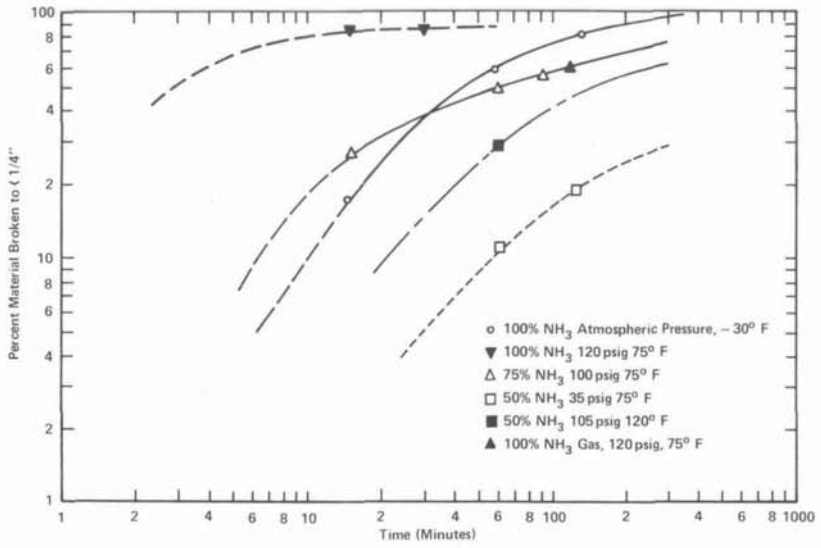


Figure 3. Chemical Comminution of 3/4" x 1/4" Upper Freeport Coal (Westmoreland County, Pa.) under Various Conditions

and consequently the pressure subjected on the surrounding strata would depend on the chemical used, and the reaction conditions (time, pressure, and temperature). Though not proven, it is conceivable that by the use of chemicals like methanol, small quantities of certain waxes and resins may be dissolved and thus help increase the permeability of the coal.

2. Extraction of the chemical. After a predetermined length of time the pressure in the bore hole is released causing the chemical, which has a low boiling point, to be boiled out of the bed. The gas is collected and reused or liquefied for reuse.

The net effect of the swelling and shrinking of the coal (but not the mineral matter) and the disruption of the bonding forces (in the coal) by the chemical, is the increased permeability and/or fracture of the coal bed.

CONCLUSIONS

This scheme claims to have advantages over the other methods (4) of increasing the permeability of coal bed. Since almost all of the ammonia is recoverable and only a few boreholes are required this method promises to be cheaper than other methods. Moreover, because the upper and lower strata are not disturbed the leakage of gases out of the bed and the influx of water into the bed can be more effectively controlled. Though the feasibility of the chemical comminution method as a coal preparation tool has been proved (5) a lot more work has to be done in the laboratory (and in the field) to prove the feasibility of the scheme presented.

REFERENCES

1. U.S. Patents 3,815,826 (6/11/74); 3,830,477 (11/26/74); 3,870,237 (8/11/75) and 3,918,761 (11/11/75).

2. Greer, R.T., "Microstructural Characterization of Iowa Coal," Iowa State University Project No. 0014, 1975.

3. Choi, D.S., and Parsons, R.C., "Method for Controlling Stress and Increasing the Strength of Support Members in Coal Mines." U.S. Patent No. 3,948,055, 1976.

4. Nadkarni, M.R., Bliss, C., Watson, W.I., "Underground Gasification of Coal," Clean Fuels from Coal, Symposium II, Institute of Gas Technology, IIT Center, Chicago, 1975, pp. 625-652.

5. Datta, R.S., Howard, P. and Hanchett, A., "Precumbustion Coal Cleaning Using Chemical Comminution." To be presented at NCA/BCR Coal Conference and Expo III, "Coal: Energy for Independence," Oct. 1976.

IGNITION OF COALBEDS FOR UNDERGROUND GASIFICATION

by

R. W. Hermsen

CHEMICAL SYSTEMS DIVISION
UNITED TECHNOLOGIES CORPORATION

1. INTRODUCTION

One of the most promising advanced concepts for underground coal gasification is the longwall generator scheme proposed independently by engineers in the USSR[1] and at MERC[2]. This method employs modern drilling techniques to produce a series of long (i.e., up to 3,000 ft.) horizontal holes through a coal seam perpendicular to the direction of major permeability. Alternate boreholes are ignited along their entire length and gasification is accomplished by reverse burning towards the non-ignited boreholes. As in longwall mining, greater total resource recovery efficiencies should be achieved, provided that ignition can be obtained uniformly over the entire length of the boreholes. If ignition is nonuniform or nonsustaining over a portion of the borehole length, recovery efficiency will be limited by premature burn-through and short circuiting of the borehole pattern.

The longwall generator presents a unique problem in ignition technology. Because of the extreme length-to-diameter ratio of the boreholes (10^3-10^4) it is not clear which, if any, of several proposed methods will result in uniform ignition of the coal. Better understanding of the criteria governing the sustained ignition of in-situ coal surfaces is needed. Design methods must be developed to guide selection of the best technique, configuration and igniter parameters, such as heat flux, duration and composition.

2. IGNITION REQUIREMENTS FOR DIFFERENT UCG CONCEPTS

Single point ignition schemes followed by reverse-burn linkage or by convective flame spreading are satisfactory for use with several UCG concepts (figure 1). These are the linked vertical well and line drive methods tested by LERC at Hanna, Wyoming[3], the LLL packed bed reactor concept[4] and the stream methods investigated in some USSR[5] AND UK[6] studies. In these instances the size and geometry of the region initially ignited is not critical nor is the time required to achieve stable ignition. Single point ignition has been accomplished with no apparent difficulty using down-hole torches and electric heaters, sometimes operated for several days.

More sophisticated techniques involving distributed ignition will probably be required for the longwall generator. This is a consequence of the strong dependence of resource recovery efficiency on the method of ignition and the rate of ignition spreading. Distributed ignition methods may also be useful for advanced versions of the line drive concept which use pneumatic, rather than combustion linking.

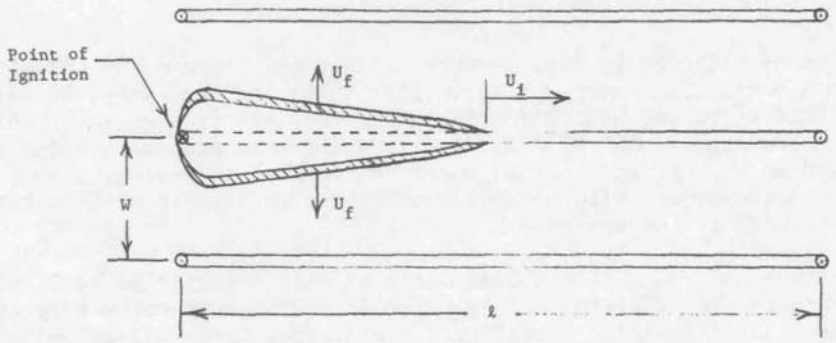
Whether discrete single or multiple point ignition schemes are practical for use with the longwall generator depends primarily on achieving high rates of convective flame spreading from the ignition site down the borehole. For a given hole spacing and length, the sweep efficiency depends on the ratio of the ignition propagation velocity, U_i, to the lateral velocity of the combustion wave, U_f (figure 2). High sweep efficiencies require high values of U_i ($U_i/U_f \sim 10^2$), which may or may not be achieved in practice. Sweep efficiency may be improved by decreasing the spacing between ignition points, at the cost of drilling additional vertical wells. Quantitative data on ignition propagation are needed to assess these tradeoffs.

IGNITION REQUIREMENTS FOR DIFFERENT UGC CONCEPTS

	Point Ignition	Linking	Convective Flame Spread	Distributed Ignition
Linked Vertical Wells	X	X		
Line Drive (LERC)	X	X - - - - - - - - - - - - - - - -		(X)
Packed Bed (LLL)	X		X	
Stream Methods	X		X	
Longwall	? - - - - - - - - - - - - - - - -		?	X

Figure 1

EFFECT OF IGNITION PROPAGATION VELOCITY ON RESOURCE RECOVERY EFFICIENCY



From geometric considerations sweep efficiency is

$$\eta \approx 1 - \frac{\tau_i}{2\tau_b}$$

$$\tau_i = \frac{\ell}{U_i}$$

$$\tau_b = \frac{W}{U_f}$$

For $\frac{\ell}{W} = 20$

$\frac{U_i}{U_f}$	η
10	0.50
50	0.80
100	0.90

Figure 2

3. IGNITION OF CHARRING MATERIALS

Although considerable work has been done on the ignition of coal particles, few studies have considered the ignition of in-situ coal surfaces. However, some idea of the expected behavior of coal can be obtained from extensive research on the ignition of slabs of other charring materials (e.g., cellulose)[7]. Regions of persistent (glowing) ignition, transient (flaming) ignition and non-ignition have been observed, depending on heat flux level and the total energy supplied to the solid (figure 3). At low, intermediate, and high flux levels, the ignition behavior is controlled by convective cooling, conduction of heat into the solid, and ablation of the exposed surface, respectively.

The minimum energy for persistent ignition is nearly a constant value for intermediate and high fluxes, indicating that a critical thermal wave thickness must be achieved to stabilize ignition. The lower limit for transient, or flaming ignition corresponds to reaching a constant solid surface temperature. This suggests that flaming ignition is controlled either by a lean limit criterion for the combustion of pyrolysis gases near the surface, or by the heterogeneous reaction of oxygen with char on the surface.

Assuming that the main features of the ignition behavior of cellulose slabs are applicable, some conclusions may be drawn concerning the principal factors governing ignition of in-situ coal surfaces. These are likely to be: pressure, and the igniter temperature, flow rate and composition, which together determine the heat flux and reactivity of the igniter gases; and the coal physical and thermodynamic properties, moisture, mineral content and permeability.

4. POSSIBLE IGNITION SCHEMES FOR LONGWALL GENERATOR

Several ignition schemes which may be considered for the longwall generator are listed in figure 4. Ignition at discrete points followed by convective flame spreading may be satisfactory if sufficiently high flame spreading rates can be attained, as discussed above. However, low flame spreading rates would lead to low sweep efficiencies or to unacceptably close well spacings.

A traversing igniter, such as a downhole torch which is slowly moved along the borehole, has the advantage of providing uniform heating. Although ignition is not simultaneous, this method should provide a more uniform burnback along the length of the hole. A serious potential disadvantage likely to be encountered is that considerable time may be required to ignite the entire borehole using a traversing ignition system.

Use of a distributed ignition source offers both uniform heating and rapid ignition, since the entire borehole surface is heated simultaneously. Two types of distributed ignition systems may be considered: a distributed gas flame, or picolo igniter, with multiple jets of flame impinging on the coal; and a pyrotechnic train placed in the hole prior to ignition.

A picolo igniter has great design flexibility and could easily be tailored to meet the ignition requirements of a given coal. It has the further advantage of variable duration; that is, it can be terminated or left on in response to outlet gas composition and coal temperature. The major disadvantage is the inherently high cost of a picolo igniter.

Ignition using a train of pyrotechnic material in the borehole offers all the advantages of a distributed ignition system at a low cost. It is also a flexible approach with respect to loading density and composition, which may be tailored within a spectrum ranging from a source of heat and oxygen to a gasless source of heat alone. Potential disadvantages of this approach are 1) the duration is fixed by the design and 2) the heat flux may be too high for maximum effectiveness.

5. APPROACH TO DETERMINE IGNITION BEHAVIOR OF IN-SITU COAL SURFACES

Further research is needed to determine the ignition behavior of in-situ coal surfaces and to provide a basis for selecting the best type of ignition system for the longwall generator. The program should include experimental studies to establish ignition criteria and analytical studies to provide scale-up techniques.

An experimental approach for determining the ignition behavior of coal surfaces is illustrated in figure 5. A slab of coal may be ignited in the apparatus by convective heating in a stream of hot gases issuing from a precombustor. The flow rates of fuel, oxygen and nitrogen into the precombustor may be independently regulated to provide control of total flow rate, temperature and composition of the ignition gases. The desired pressure level is maintained in the test section by means of a sonic choke at the exit. Instrumentation includes a transducer to monitor pressure in the test section, heat flux gages before and aft of the coal sample, and thermocouples to measure inlet gas temperature

IGNITION BEHAVIOR OF CELLULOSIC MATERIALS

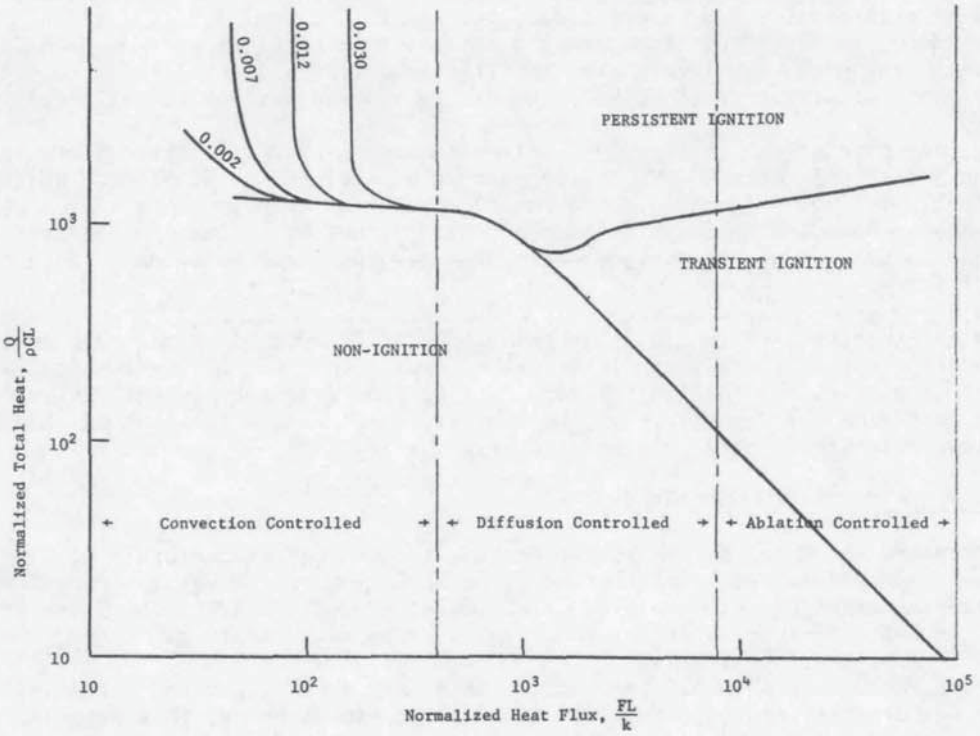


FIGURE 3

POSSIBLE IGNITION SCHEMES FOR LONGWALL GENERATOR

Ignition Scheme	Advantages	Disadvantages
1. Ignition at Discrete Points — Convective Flame Spreading	low cost	may lead to low sweep efficiency
2. Traversing Igniter	uniform heating	ignition not simultaneous, may be slow
3. Distributed Ignition Source		
(a) Gas Flame (Picolo)	uniform ignition	high cost
(b) Pyrotechnic — oxidizing or gasless	uniform ignition probably low cost	heat flux may be too high for maximum effectiveness

FIGURE 4

IGNITION BEHAVIOR EXPERIMENT

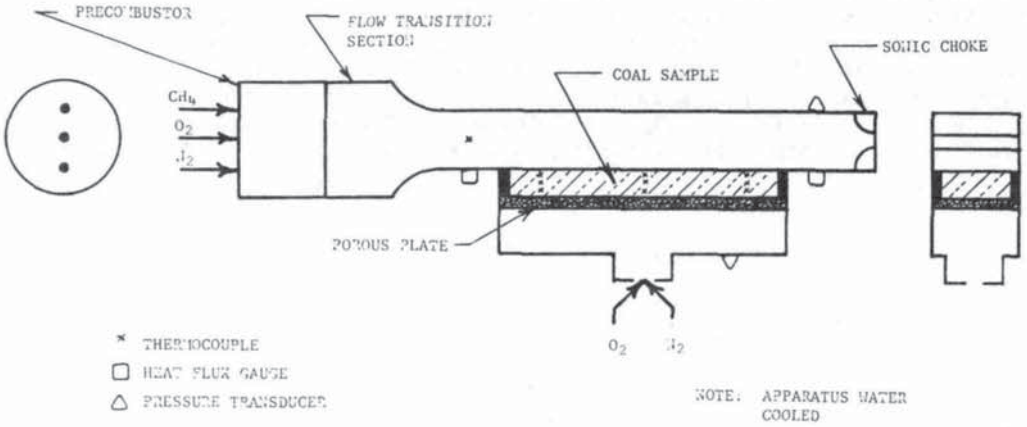


FIGURE 5

ANALYTICAL MODEL OF IGNITION PROCESS

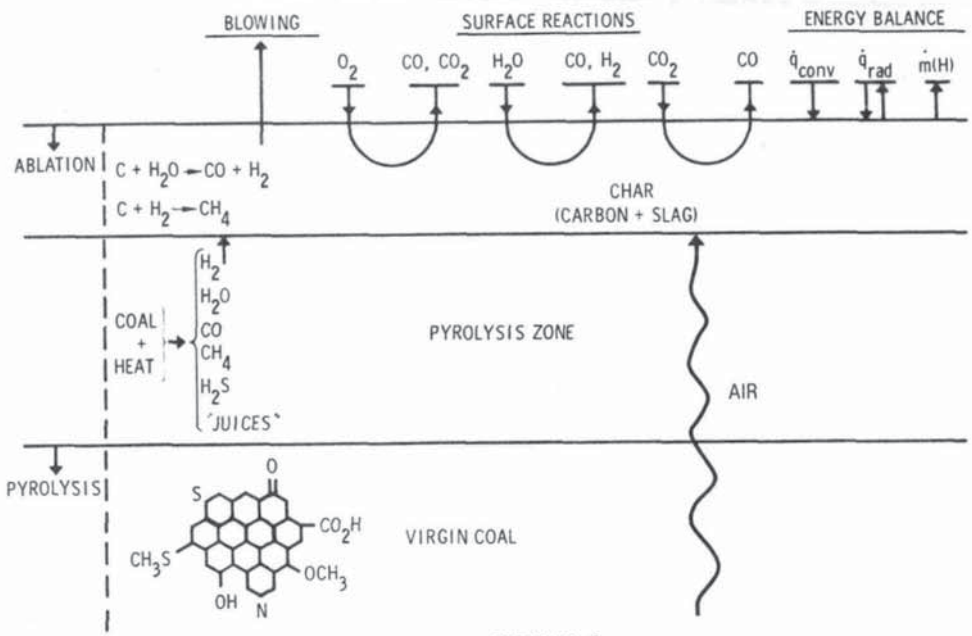


FIGURE 6

and temperature profiles in the coal sample. Provision is also made for introducing a small airflow at the back of the sample to allow simulating ignition in the reverse burning mode.

The experiment is based on a go/no-go approach in which the igniter flow is switched off after a predetermined time. Sustained ignition in a flaming or glowing mode would be detected by visual observation and photography. Temperature profiles measured under critical conditions for ignition would be used to establish an ignition criterion, e.g., based on total energy or on critical surface temperature.

Mathematical modeling studies should be conducted to develop a technique for predicting the growth of the thermal wave at the coal surface during ignition. The analysis, together with the ignition data, would allow predicting the time to ignition at a point on the coal surface for a prescribed set of boundary conditions (local heat flux, gas composition, pressure and flow rates). A promising approach for mathematical modeling is based on existing computer codes developed for predicting the thermal response of charring insulators (figure 6). These materials are chemically and physically similar to model coal compounds and exhibit similar dynamic response when heated.

REFERENCES

1. Shuck, L. Z., and J. Pasini III, "A Report on Progress in Underground Coal Gasification," presented at International Energy Engineering Congress, Chicago, Illinois, November 4-5, 1975.

2. Overby, W. K., C. A. Komar and J. Pasini III, "Underground Gasification of Coal: Proposed Concept for Directional Control of the Combustion Zone," presented at Geol. Soc. of America meeting, Dallas, Texas, November 12-14, 1973.

3. Schrider, L. A., and J. W. Jennings, "An Underground Coal Gasification Experiment, Hanna, Wyoming," AIME Preprint SPE 4993, October 1974.

4. Higgins, G. H., "A New Concept for In-situ Coal Gasification," Lawrence Livermore Laboratory Report UCRL-51217, Rev. 1, September 1972.

5. Gregg, D. W., R. W. Hill, and D. U. Olness, "An Overview of the Soviet Effort in Underground Gasification of Coal," Lawrence Livermore Laboratory Report UCRL-52004, January 1976.

6. Arthur D. Little, Inc., "A Current Appraisal of Underground Coal Gasification," Report No. C73671, December 1971.

7. Martin, Stanley, "Diffusion-Controlled Ignition of Cellulosic Materials by Intense Radiant Energy," Tenth Symposium (International) on Combustion, The Combustion Institute, Pittsburgh, 1965. pp. 877-896.

REVIEW OF CURRENT UCG MODEL CAPABILITIES

by

W. K. SAWYER, RESEARCH MATHEMATICIAN, U.S. ERDA

ABSTRACT

During the past year, several ERDA sponsored papers have appeared in the literature on UCG modeling efforts. As the Russians have done very little modeling work related to their field operations, it is believed that these papers represent the most rigorous, detailed mathematical models ever developed for in situ coal gasification. However, many different simplifying assumptions have been made in these models as the work on the three projects has been essentially three independent efforts.

In this paper, these models are compared as to their merits and weaknesses and recommendations are made as to the nature of future modeling efforts. A second generation model is outlined which includes effects of liquid plugging, gravity segregation, and thermal losses to surrounding strata.

EXISTING UCG MODELS

Dr. S. M. Farouq-Ali of the Pennsylvania State University has been doing contract work related to reaction kinetics of in situ coal gasification for the past three years. The work has been directed by the Morgantown Energy Research Center (U.S. ERDA) and the second year's effort is contained in reference [2].

Dr. R. D. Gunn has recently published two papers [4, 5] working under a cooperative agreement between ERDA's Laramie Energy Research Center and the University of Wyoming. These papers treat the coalbed as a uniform porous medium.

Dr. Alan Winslow of the Lawrence Livermore Laboratory just recently completed a paper [8] on a model of coal gasification in a packed bed. Also, Sawyer and Shuck of the Morgantown Energy Research Center recently presented a paper [6] in which the coal is treated as a fissured medium.

BASIS OF COMPARISON

Since the beginning of ERDA's involvement in underground coal gasification, this is the first opportunity to compare the modeling efforts of the three projects at LERC, LLL, and MERC. Accordingly, the objectives of this paper are: (1) to determine the state-of-the-art in modeling underground coal gasification processes and, (2) to make recommendations as to what should be added (or deleted) to a new generation model.

The five aspects selected for comparison of the models were as follows: (1) geometry, (2) simplifying assumptions, (3) mass and energy transport mechanisms, (4) boundary conditions, and (5) chemical reactions.

References at end of paper

GEOMETRIES

Figure 1 shows the geometry assumed by each of the models. Note that all three assume one-dimensional flow through the coalbed. Only the stream model (Farouq-Ali, Penn State) is two-dimensional. The assumption of linear flow in a first generation model of a sophisticated process such as coal gasification is of course quite reasonable.

Figure 1 also shows that three distinct concepts of flow through the coalbed are being advanced. The LERC models assume the coal to be a uniform porous medium while the Livermore model is based on the idea of a packed bed chemical reactor. The Morgantown model, on the other hand, is pursuing the concept that the coal's natural cleat structure provides the required permeability.

SIMPLIFYING ASSUMPTIONS

It was found that all three models use the assumptions of:

(a) one-dimensional flow of an ideal gas
(b) no mass transport by diffusion
(c) no energy transport by radiation
(d) no heat loss to surroundings
(e) constant inlet gas composition
and (f) zero heat flux at outlet.

A complete list of assumptions covering all three models is given in Table 1. We see that the expanding borehole model is the only one which considers mass transport by diffusion. This is quite natural since within the coalbed forced convection will always dominate except in cases of very low flow rates.

However, the assumptions of no radiation transport and no heat loss to surrounding strata could cause serious errors in model predictions. For example, in thin seams with a relatively low combustion front velocity, radiative transport to the roof and base rock and conductive transport therein could lower peak temperatures to the extent that the process is uneconomical.

The assumption of ideal gas behavior is valid only for pressure ranges up to about 100 psi and hence should not be used to model experiments with large pressure gradients. Of greater concern is LERC's assumption of constant porosity. Laboratory experiments (unpublished) conducted at MERC indicate that the western subbituminous coal ashes at 800°F(427°C). Hence, behind the combustion front the porosity approaches unity.

The present MERC models assume no volatile matter due to the lack of appropriate quantitative laboratory data. However, it is planned to include devolatilization products in the next stage of model development.

The assumption of single phase flow must eventually be dispensed with in order to accurately model the effects of ground water encroachment and liquid tar formation near the combustion zone.

TRANSPORT MECHANISMS AND BOUNDARY CONDITIONS

Mass transport in all three models is by forced convection with radial diffusion included in the borehole model. Energy transport is by conduction in the solid phase and convection in the gas phase. Transfer between solid and gas is via a convective transfer coefficient in all but LERC's models in which thermodynamic equilibrium between solid and gas is assumed.

Table 2 gives the boundary conditions used in each model. Note that LERC has both a forward combustion model and a reverse combustion model, both of which make use of a transformation into a moving coordinate system. A basic assumption for such a transformation is that the velocity of the combustion front is constant. Although of questionable validity, this greatly simplifies the equations to be solved. An iteration scheme based on oxygen depletion and thermal flux is used to determine the frontal velocity.

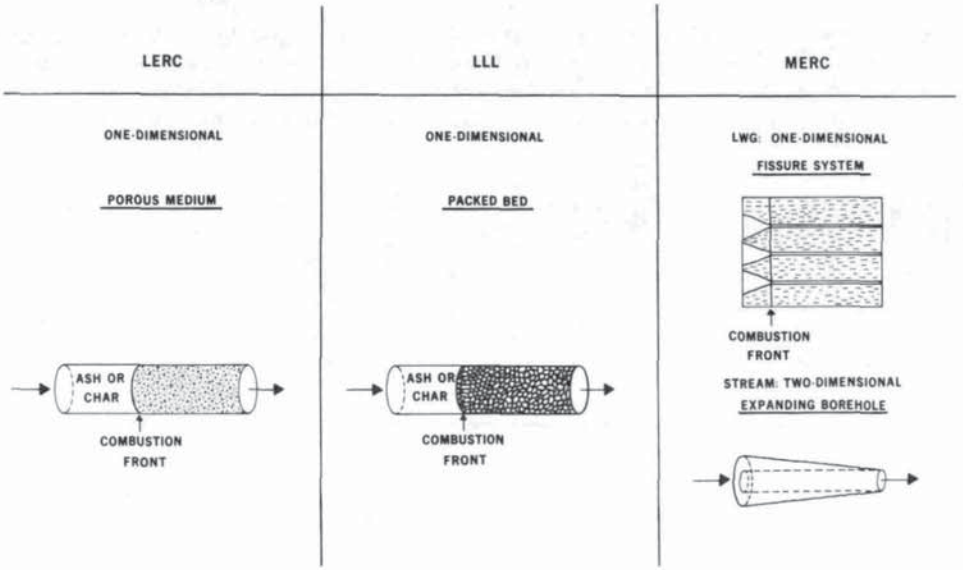


FIGURE 1. COMPARISON OF GEOMETRIES OF EXISTING UGC MODELS

TABLE 1. COMPARISON OF ASSUMPTIONS USED IN EXISTING UGC MODELS

ASSUMPTIONS	LERC	LLL	MERC	
			LWG	BOREHOLE
1. ONE-DIMENSIONAL	●	●	●	
2. TWO-DIMENSIONAL				●
3. SINGLE PHASE FLOW	●		●	●
4. NO MASS TRANSPORT BY DIFFUSION	●	●	●	
5. NO ENERGY TRANSPORT BY RADIATION	●	●	●	●
6. SOLID & GAS AT SAME TEMPERATURE	●			
7. PRESSURE DROP NEGLIGIBLE	●			●
8. CONSTANT POROSITY	●			
9. CONSTANT COMBUSTION FRONT VELOCITY	●			
10. NO HEAT LOSS TO SURROUNDINGS	●	●	●	
11. CONSTANT TEMPERATURE OUTER BOUNDARY				●
12. NO VOLATILES			●	●
13. IDEAL GAS	●	●	●	●

TABLE 2. COMPARISON OF BOUNDRY CONDITIONS USED IN EXISTING UGC MODELS

FORWARD MODE ($\eta = x - vt$) COMBUSTION FRONT: GAS FLUX - - - - - - - - - - - - - CONSTANT SOLID DENSITY - - - - - - - - - - - CONSTANT WT. FRACTION VOLATILES - - - - - - CONSTANT HEAT FLUX = $[(\dot{m}C)_{O_2} + (\dot{m}C)_{N_2}](T - T_{inj}) + (\dot{m}C)_{H_2O}(T - T_{env}) + (\dot{m}\Delta H^V)_{H_2O}$ OUTLET: SOLID DENSITY - - - - - - - - - - - CONSTANT HEAT FLUX - - - - - - - - - - - - - 0 REVERSE MODE ($\eta = x - vt$) AHEAD OF COMBUSTION FRONT: MASS FLUX AIR - - - - - - - - - - -CONSTANT WT. FRACTION O_2 - - - - - - - - - CONSTANT WT. FRACTION FUEL - - - - - - - - 0 TEMPERATURE APPROACHES INITIAL VALUE AT COMBUSTION FRONT: MASS FLUX = $\dot{m}_{air} + V\rho_s^{(o)} S_{wr} W_w$ TEMPERATURE = T_{vap} HEAT FLUX = $[(\dot{m}C)_{air} + V(\rho^{(o)}C)_s + V(\rho\phi C)_g](T_{vap} - T_i) + V(\rho_w \phi S_{wr})\Delta H^V$	GAS FLUX AT INLET - - - - - - CONSTANT GAS COMPOSITION AT INLET - - - CHANGED LINEARLY OVER 5 MINUTES TO CONSTANT HEAT FLUX AT INLET - - - - - - INCREASED LINEARLY FOR 10 MINUTES, CONSTANT FOR 4 MINUTES, THEN TURNED OFF HEAT FLUX AT OUTLET (SOLID) = 0	LWG INLET AND OUTLET PRESSURES - - - - CONSTANT GAS COMPOSITION AT INLET - - - - - CONSTANT GAS TEMPERATURE AT INLET - - - - - CONSTANT SOLID TEMPERATURE AT INLET - - - - CONSTANT HEAT FLUX AT OUTLET (SOLID) = 0 BOREHOLE GAS COMPOSITION AT INLET - - - - - CONSTANT GAS TEMPERATURE AT INLET - - - - - CONSTANT SOLID TEMPERATURE AT INLET - - - - CONSTANT HEAT FLUX AT OUTLET (SOLID) = 0 BOREHOLE SURFACE: (DIFFUSION RATE) = (NET CONSUMPTION RATE) (HEAT GENERATED) = (HEAT CONDUCTED IN SOLID) + (HEAT CONVECTED IN GAS)

The boundary conditions of the Livermore and Morgantown models are straight forward and require no explanation. However, some discussion is in order concerning the inlet heat flux conditions of the Laramie models. In the forward mode, the heat flux equation may be written

$$\begin{pmatrix}\text{inlet}\\ \text{heat flux}\end{pmatrix} = \begin{pmatrix}\text{flux due to}\\ \text{inlet gases}\end{pmatrix} + \begin{pmatrix}\text{flux due to}\\ \text{water encroachment}\end{pmatrix} + \begin{pmatrix}\text{flux due to water}\\ \text{vaporization}\end{pmatrix} \qquad (1)$$

where

$$\begin{pmatrix}\text{flux due to}\\ \text{inlet gases}\end{pmatrix} \sim \begin{pmatrix}\text{local}\\ \text{temperature}\end{pmatrix} - \begin{pmatrix}\text{temperature of}\\ \text{injected air}\end{pmatrix} \qquad (2)$$

and

$$\begin{pmatrix}\text{flux due to}\\ \text{water encroachment}\end{pmatrix} \sim \begin{pmatrix}\text{local}\\ \text{temperature}\end{pmatrix} - \begin{pmatrix}\text{overburden}\\ \text{temperature}\end{pmatrix}. \qquad (3)$$

With the same inlet mass flux, this permits the heat flux into the reaction zone to be proportional to the combustion front temperature. That is, the hotter the combustion front, the more the inlet gas stream is heated and therefore the heat flux into the reaction zone is greater. Thus, conditions (1) is believed to be quite reasonable. Moreover, if the temperature of the inlet air and the overburden were allowed to increase due to backward radiation and conductive heat losses, this type of boundary condition would be even more attractive.

The heat flux for LERC's reverse combustion model is similar to (1) except that T_{vap} and T_i, vaporization and initial temperatures, respectively, are constant.

All three models assume a condition of zero heat flux at the outlet. This is because of the mathematical nature of the energy balance equation. The conduction term renders the equation second order which means that some type of boundary condition must be applied at the outlet to assure a unique solution. However, since the mass flux and temperature are known, a condition of the type used by Gunn at the combustion front would be much more appropriate.

CHEMICAL REACTIONS

A summary of the chemical reactions used in each of the three models is given in Table 3. We see that MERC's borehole model has all the principal coal gasification reactions. As previously mentioned, the devolatilization reaction will be added to the next phase of model development. Also, the Livermore model contains an adequate suite of chemical reactions although it does not include oxidation of hydrogen or carbon monoxide.

The degree of success of any coal gasification project will depend largely on the volumes of carbon monoxide, hydrogen, and methane produced. Hence, the loss of H_2 to form steam, the oxidation of CO to CO_2 and, to some extent, the water-gas-shift reaction are detrimental to the production of a good quality gas. Thus, the reaction kinetics is an extremely important aspect of any UCG modeling effort. However, reaction rate expressions applicable to the in situ gasification of coal are almost non-existent in the literature. Since the rate expressions used in Livermore's model are not available at this writing, a comparison of the reaction kinetics will not be given.

Table 4 summarizes the characteristics common to all three models. Again, the major deficiencies seem to be no radiative transport and no conductive transport to the surrounding strata. Also, the conditions of zero heat flux at the outlet is of questionable validity, particularly for studying the reverse burn mode.

FUTURE UCG MODELING EFFORTS

Each of the models developed has its merits and has produced some interesting results. However, it is impossible to quantify their differences since, due to their different underlying assumptions, reaction kinetics, and areas of applicability, they may not all be used to predict the outcome of a single experiment. Nevertheless, it appears that a "new generation model" should consider (1) natural water encroachment, (2) formation and transport of liquid tars, (3) dip of the coalbed, (4) energy transport by radiation, (5) heat losses to surrounding stratas and (6) mode of operation (method of ignition, inlet gas cycling, etc.). The inclusion of these aspects in a two- or three-dimensional

TABLE 3. COMPARISON OF CHEMICAL REACTIONS USED IN EXISTING UGC MODELS

LERC	LLL	MERC
FORWARD MODE COAL + HEAT → CHAR(C) + CH_4 + CO_2 + H_2 + CO $C + 2O_2 \rightarrow 2CO_2$ $C + H_2O \rightarrow CO + H_2$ REVERSE MODE COAL + HEAT → CHAR(C) + VOLATILES $C + O_2 \rightarrow 2CO$ VOLATILES + O_2 → COMBUSTION PRODUCTS	UNBALANCED FORM DRY COAL + HEAT → π_2 CHAR(C) + π_3 TAR + H_2O + CH_4 + CO_2 + H_2 + CO $C + O_2 \rightarrow CO_2 + H_2O$ $C + H_2O \rightarrow CO + H_2$ $C + CO_2 \rightarrow H_2O + CO$ $C + H_2 \rightarrow CH_4 + CO$ $CO + H_2O \rightarrow CO_2 + H_2$	LWG $C + O_2 \rightarrow CO_2$ $C + CO_2 \rightarrow 2CO$ BOREHOLE $C + O_2 \rightarrow CO_2$ $C + \frac{1}{2}O_2 \rightarrow CO$ $H_2 + \frac{1}{2}O_2 \rightarrow H_2O$ $C + CO_2 \rightarrow 2CO$ $C + H_2O \rightarrow CO + H_2$ $CO + H_2O \rightarrow CO_2 + H_2$ $C + 2H_2 \rightarrow CH_4$ $CO + \frac{1}{2}O_2 \rightarrow CO_2$

TABLE 4. CHARACTERISTICS COMMON TO EXISTING UGC MODELS

SIMPLIFYING ASSUMPTIONS	MASS AND ENERGY TRANSPORT	BOUNDRY CONDITIONS	CHEMICAL REACTIONS
ONE-DIMENSIONAL	MASS TRANSPORT — DARCY FLOW	GAS COMPOSITION AT INLET — CONSTANT	$C + O_2 \rightarrow CO_2$
NO MASS TRANSPORT BY DIFFUSION	ENERGY TRANSPORT — CONDUCTION CONVECTION	HEAT FLUX AT OUTLET — 0	$C + CO_2 \rightarrow 2CO$
NO ENERGY TRANSPORT BY RADIATION			$C + H_2O \rightarrow CO + H_2$
NO HEAT LOSS TO SURROUNDING STRATA			

model, together with the knowledge and experience gained in developing existing models would provide a very powerful tool for advancing the technology of in situ coal gasification. Such a model is outlined in the following section.

AN ADVANCED MODEL FOR UCG

Our objective is to outline the basic conservation equation and functional relationships required to develop a three-dimensional, three-phase (gas, water, tar) immiscible flow model for in situ coal gasification. The oil and gas industry has developed sophisticated models for thermal oil recovery processes (e.g. [1, 3, 7]) and much of this technology can be applied directly to UCG. The primary differences are that in in situ gasification (1) porosity and permeability must be time-dependent, and (2) a mass balance for each gas species must be included according to the particular chemical reactions desired. However, some simplifications may also be made in modifying a thermal oil recovery simulator for UCG modeling. For example, we may assume that (1) capillary pressure effects are negligible, (2) there is no gas dissolved in the coal tar, and (3) fluid viscosities and liquid densities are only functions of temperature.

With the above assumptions, we may write down the following overall mass balance relationships.

(gas) $$\nabla\cdot(A_g\nabla\Phi_g) + M_{ov} + M_{sv} + M_{wv} + q_g = \frac{\partial}{\partial t}(b_g S_g) \tag{4}$$

(water) $$\nabla\cdot(A_w\nabla\Phi_w) - M_{wv} + q_w = \frac{\partial}{\partial t}(\phi b_w S_w) \tag{5}$$

(tar) $$\nabla\cdot(A_o\nabla\Phi_o) - M_{ov} - M_{os} + q_o = \frac{\partial}{\partial t}(\phi b_o S_o) \tag{6}$$

where

$$\Phi_g = P + \frac{1}{144}\frac{g}{g_c}\rho_g D \tag{7}$$

$$\Phi_w = P + \frac{1}{144}\frac{g}{g_c}\rho_w D \tag{8}$$

$$\Phi_o = P + \frac{1}{144}\frac{g}{g_c}\rho_o D \tag{9}$$

$$\rho_g = \frac{P\,\bar{M}}{z\,RT_R},\quad \rho_w = b_w\rho_{wsc},\quad \rho_o = b_o\rho_{osc} \tag{10}$$

$$b_g = \frac{P_{sc}\,T_R z}{P\,T_{sc}} \tag{11}$$

$$b_w = b_{wi}[1 - \beta_w(T - T_i)] \tag{12}$$

$$b_o = b_{oi}[1 - \beta_o(T - T_i)] \tag{13}$$

$$A_{gl} = \frac{b_g k_l k_{rg}}{\mu_g},\ l = x,\ y,\ \text{or } z \tag{14}$$

$$A_{wl} = \frac{b_w k_l k_{rw}}{\mu_w},\ l = x,\ y,\ \text{or } z \tag{15}$$

$$A_{ol} = \frac{b_o k_l k_{ro}}{\mu_o},\ l = x,\ y,\ \text{or } z \tag{16}$$

$$M_{ov} = f_1(T) \tag{17}$$

$$M_{sv} = f_2(T) \tag{18}$$

$$M_{wv} = f_3(T) \tag{19}$$

and

$$M_{os} = f_4(T). \tag{20}$$

We have assumed thermodynamic equilibrium in the fluid phase and that the mass transfer terms are single-valued functions of either the solid or fluid temperature. To complete the mass balance we must include an equation for each gas species. These will be of the form

$$-\nabla\cdot(c_i v_g) + \phi \sum_j a_{ij} R_j + M_{svi} = \frac{\partial}{\partial t}(\phi c_i) \tag{21}$$

where

$$v_g = -\frac{b_g k_g k_{rg}}{\mu_g} \frac{\partial \Phi_g}{\partial l}, \quad l = x, y, \text{ or } z \tag{22}$$

and

$$M_{svi} = f_5(T). \tag{23}$$

Typically, (21) would represent seven components as a minimum: oxygen, hydrogen, nitrogen, water vapor, carbon dioxide, carbon monoxide, and methane. Hence, equations (4-6) and (21) would be 10 equations in 13 unknowns when we include the fluid phase saturations. One additional equation is provided by the simple relationship

$$S_g + S_w + S_o = 1.0 \tag{24}$$

To complete the system, the unknown Φ_w and Φ_o may be eliminated by substituting for P from (7) into (8) and (9) giving 11 equations in 11 unknowns. Finally, to complete the mass conservation segment of the model, we need a solid phase relationship to account for porosity increases due to devolatilization, char combustion, and tar solidification. This may be expressed as

$$-(\dot{m}_c + M_{sv} - M_{os})\phi = \frac{\partial}{\partial t}[(1-\phi)\rho_s] \tag{25}$$

where

$$\dot{m}_c = \sum_{j=1}^{s} R_{cj} \tag{26}$$

assuming solid carbon is consumed in s different reactions.

Next, we must formulate the appropriate energy balance relations for the system. Since we want to include effects of radiation and heat loss to surrounding strata, we shall, for simplicity, assume thermodynamic equilibrium between solid and fluid. Thus, with conduction and convection the primary transport mechanisms, we have

$$\nabla\cdot(K\nabla T) - \nabla\cdot[(\rho_g C_g v_g + \rho_w C_w v_w + \rho_o C_o v_o)T] + E_{hdc} + E_{hlc} + E_{hvw} + E_{hvo} + E_{rad} + E_{hso} + Q_c + Q_L =$$

$$\frac{\partial}{\partial t}[\phi(\rho_g S_g C_g + \rho_w S_w C_w + \rho_o S_o C_o)T]. \tag{27}$$

Here, Q_c is the total heat of all reactions given by

$$Q_c + \sum_{j=1}^{s} \Delta H_{cj} R_{cj} + \sum_{j=1}^{r} \Delta H_{gj} R_{gj} \tag{28}$$

assuming s heterogeneous reactions and r gas phase reactions. The term Q_L is the heat loss to the overburden (or underburden) and is of the form

$$Q_L = -g(T-T_a) \tag{29}$$

where T_a is the adjacent formation temperature and g is a combination convective-radiative transfer coefficient. T_a may be obtained by solving the diffusivity equation in the overburden.

$$\nabla\cdot\nabla T_a + Q_L = \frac{\rho_a C_a}{K_a}\frac{\partial T_a}{\partial t} \tag{30}$$

DISCUSSION

To summarize, we have developed a three-dimensional, three-phase, thermal simulator for any number of chemical reactions occuring in the gas phase or between the gas and the solid. We have allowed for effects of heat loss to surrounding strata, liquid tar formation, migration and solidification, water encroachment (including vaporization and condensation), and the dip of the coalbed. We have also included energy terms for radiation transport as well as all possible phase changes.

Although there are many details remaining to be worked out, the only major one that has not been mentioned is the calculation of permeability. However, this could be handled any number of ways depending upon how one visualizes the internal coal structure. For example, if a fissure system is assumed, the method of Sawyer and Shuck [6] can easily be extended to three dimensions. In fact, for the three-dimensional element of Figure 2 the porosity and permeability are given by

$$\phi = [d_1(1-d_2t) + d_2(1-d_3t) + d_3(1-d_1t)]t + d_1d_2d_3t^3 \tag{31}$$

and

$$k_x = Cd_1t^3 \tag{32a}$$

$$k_y = Cd_2t^3 \tag{32b}$$

$$k_z = Cd_3t^3 \tag{32c}$$

where C is a constant.

On the other hand, if the coal structure is viewed as a porous medium or a packed bed, an empirical relationship based on the Kozeny-Carman formula

$$k \sim \frac{\phi^3}{a}, \tag{33}$$

where a is the solid surface area per unit volume, may be used. This approach was used by Winslow [8].

Finally, it should be pointed out that mass transfer terms of the type given in equations (4)-(6) have been successfully dealt with in previous models. For example, Gunn has developed an expression for devolatilization of Wyoming coal as a function of temperature based on laboratory analysis. Gottfried [3] assumes that the vaporization of water is proportional to the rate at which water vapor diffuses into the gas stream from the gas-water interface. A similar expression should apply to the vaporization of tar. Hence, if appropriate reaction rate and energy generation expressions can be obtained, the proposed model can indeed become a reality.

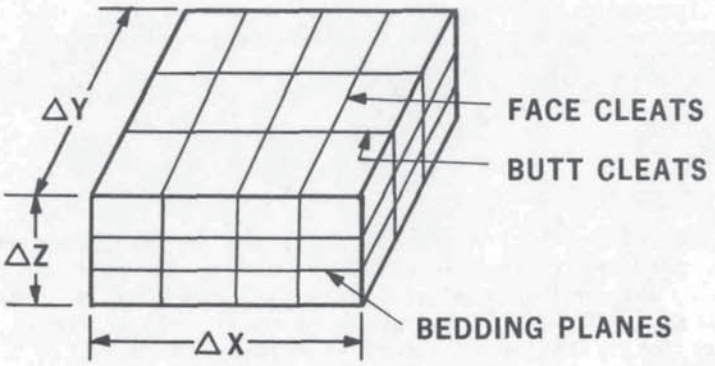


FIGURE 2. THREE DIMENSIONAL FISSURED COAL ELEMENT.

NOMENCLATURE

- a_{ij} = stoichoimetric matrix
- b = volume factor
- c_i = gas species concentration
- C = specific heat
- d = fissure density
- D = elevation above datum
- g = acceleration of gravity
- ΔH = heat of reaction
- k = permeability
- k_r = relative permeability
- K = thermal conductivity
- $\overline{M}$ = mean molecular weight
- M = mass transfer rate
- P = pressure
- q = mass source rate
- Q = energy generation rate
- R_c = char reaction rate
- R_g = gas phase reaction rate
- R_j = jth reaction rate
- S = saturation

t = time

t = fissure thickness

v = apparent velocity

z = gas deviation factor

β = coefficient of thermal expansion

μ = viscosity

ρ = density

ϕ = porosity

Φ = flow potential

Subscripts

o = tar

w = water

g = gas

ov = tar vaporization

os = tar solidification

wv = water vaporization

sv = solid vaporization

svi = solid vaporization of component i

hdc = heat of devolatilization of coal

hlc = heat of liquefaction of coal

hso = heat of solidification of tar

hvw = heat of vaporization of water

hvo = heat of vaporization of tar

rad = radiation

R = Rankine

sc = standard conditions

i = initial condition

a = overburden

REFERENCES

1. Coats, K. H., George, W. D., Chu, Chieh, and Marcum, B. E.: "Three-Dimensional Simulation of Steam-flooding," Paper SPE 4500 presented at 48th Annual Fall Meeting of the Society of Petroleum Engineers of AIME, Sept. 30-Oct. 3, 1973.
2. Farouq-Ali, S. M.: "Modeling and Computer Simulation of Reaction Kinetics Associated with the Underground Gasification of Coal," Annual report, USDI, Bureau of Mines, Grant No. G0133094.
3. Gottfried, B. S.: "A Mathematical Model of Thermal Oil Recovery in Linear Systems," Society of Petroleum Engineers Journal, Sept. 1965, pp. 196-210.
4. Gunn, R. D. and Whitman, D. L.: "An In Situ Gasification Model (Forward Mode) for Feasibility Studies and Design," U.S. ERDA Report of Investigations, LERC/RI-76/2, February 1976.
5. Gunn, R. D. and Kotowski, M. D.: "Theoretical Aspects of Reverse Combustion in the Underground Gasification of Coal," U.S. ERDA Report of Investigations, LERC/RI-76/4, March 1976.
6. Sawyer, W. K. and Shuck, L. Z.: "Numerical Simulation of Mass and Energy Transfer in the Long-wall Process of Underground Gasification of Coal," Paper SPE 5743 presented at the Fourth Symposium on Numerical Simulation of Reservoir Performance of the Society of Petroleum Engineers, Los Angeles, California, February 18-20, 1976.
7. Smith, J. T.: "Numerical Simulation of In Situ Combustion in a Two-Dimensional System," Ph.D. Thesis, Pennsylvania State University, 1971.

8. Winslow, A. M.: "Numerical Model of Coal Gasification in a Packed Bed," Paper prepared for submission to the 16th International Symposium on Combustion, Cambridge, Massachusetts, M.I.T., August 15-21, 1976.

A GENERALIZED THEORY FOR DIFFUSIVE FLUID FLOW THROUGH SOLID, PERMEABLE MEDIA

by

John F. Seeberger, West Virginia University, Morgantown, WV

ABSTRACT

In the last 15 years there has been much work done on the mechanical theory of mixtures of superposed continua to represent the mechanical aspects of diffusion. In this paper the fundamental concepts are reviewed and the applicability of the theory to the flow of fluids and gases through porous solids is examined. A general three-dimensional constitutive theory is established for the partial stresses and the diffusive forces in the following cases: (a) The diffusion of a non-newtonian fluid through a non-linear elastic solid, (b) The diffusion of a newtonian fluid through a linear elastic solid, (c) The diffusion of a newtonian fluid through a rigid solid, (d) The diffusion of an ideal fluid through a linear elastic solid, and finally (e) The diffusion of an ideal fluid through a rigid body. The general 3-D equations of motion are evolved in each of the above cases as being the appropriate generalization of the commonly employed Darcy's law for flow through porous media. Cases where the more general framework reduces to Fick's Law or Darcy's Law are investigated. The object of the study is to supply a generalization, in less restricted circumstances, to the commonly employed Darcy's law as well as to exhibit the appropriate equations of motion in these circumstances.

Introduction

In the last 15 years there has been much work done in the theory of mixtures of superposed continuous media to represent diffusion phenomena (see eg. ref. (1), (2), (3), (4), (6), (10), (11). In this paper we review the fundamental concepts and indicate their applicability to the flow of fluids through porous elastic and rigid bodies. Constitutive equations are layed down for the partial stresses in the individual media as well as for the diffusive forces that one media exerts on the other. The classical approaches based on Fick's law and Darcy's Law are examined in light of the more general theory. Both linear and non-linear theories are examined.

The theory is restricted to a binary mixture, that is, to the superposition of two continuous media C_1, and C_2. It is assumed that each position in space is occupied by one particle from C_1 and one particle from C_2. C_1 will be identified with a solid-like body and will be assumed either elastic or rigid. C_2 will be identified with a fluid-like body and will be assumed to be either a newtonian fluid or an ideal fluid.

In modern continum mechanics the general principles i.e. the balance equations of mass, momentum and energy are clearly distinguished from the constitutive equations which give the stresses in terms of the kinematics. There has been much recent progress in the theory of constitutive equations within the theory of mixtures. A simple mechanical theory based on recognizing that the diffusion process gives rise to forces that produce motions, gives the diffusive forces by constitutive equations depending on the relative motion of C_2 with respect to C_1. The general equations of balance plus the constitutive equations for the partial stresses in C_1 and C_2 as well as the diffusive force results in a complete theory.

Kinematics

It is assumed that the motions of C_1 and C_2 are smooth and can be described by equations relating the present position of a given particle as a given function of a reference position and time.

The motion of C_1 is denoted by $\underset{\sim}{x}_{(1)} = \underset{\sim}{\chi}_{(1)}(\underset{\sim}{X}, t)$

and C_2 by $\underset{\sim}{x}_{(2)} = \underset{\sim}{\chi}_{(2)}(\underset{\sim}{X}, t)$

In all that follows quantities associated with C_1 will be denoted by a (1) underneath the quantity and those associated with C_2 by a (2).

The velocities and accelerations of particles in C_1 and C_2 are given by $\underset{\sim}{v}_{(1)} = \frac{D\,\underset{\sim}{x}_{(1)}}{Dt}$; $\underset{\sim}{v}_{(2)} = \frac{D\,\underset{\sim}{x}_{(2)}}{Dt}$

and $\underset{\sim}{a}_{(1)} = \frac{D\,\underset{\sim}{v}_{(1)}}{Dt}$; $\underset{\sim}{a}_{(2)} = \frac{D\,\underset{\sim}{v}_{(2)}}{Dt}$

It is assumed that the two particles under consideration occupy the same position at the present time, i.e.

$$\underset{\sim}{x}_{(1)} = \underset{\sim}{x}_{(2)} \quad \text{at time } t.$$

The relative positions, velocities, and accelerations of the particle in C_2 with respect to the particle in C_1 are given by

$$\underset{\sim}{x}_{(21)} = \underset{\sim}{x}_{(2)} - \underset{\sim}{x}_{(1)}$$

$$\underset{\sim}{v}_{(21)} = \underset{\sim}{v}_{(2)} - \underset{\sim}{v}_{(1)}$$

$$\underset{\sim}{a}_{(21)} = \underset{\sim}{a}_{(2)} - \underset{\sim}{a}_{(1)}$$

The kinematical quantity associated with straining of the material is the deformation gradient from the reference position to the present position i.e.

$$\underset{\sim}{F}_{(1)} = \nabla \underset{(1)}{\chi}(\underset{\sim}{X}_{(1)}, t)$$

and

$$\underset{\sim}{F}_{(2)} = \nabla \underset{(2)}{\chi}(\underset{\sim}{X}, t)$$

The deformation gradients are second order tensors and serve to define the local deformation in the neighborhood of a given particle. It is assumed that the deformation gradients are nonsingular and can be decomposed into local rotations and local stretches as given by the polar decomposition theorem of linear algebra.

e.g. $\underset{\sim}{F}_{(1)} = \underset{\sim}{R}_{(1)}\underset{\sim}{U}_{(1)} = \underset{\sim}{V}_{(1)}\underset{\sim}{R}_{(1)}$

where $\underset{\sim}{R}_{(1)}$ is an orthogonal second order tensor representing a rotation, and $\underset{\sim}{U}_{(1)}$ and $\underset{\sim}{V}_{(1)}$ are positive definite symmetric tensors representing the stretch in the local neighborhoods. $\underset{\sim}{R}$ is referred to as the rotation tensor, while $\underset{\sim}{U}$ and $\underset{\sim}{V}$ are referred to as the right and left stretch tensors. The stretch tensors are fundamental to the construction of strain tensors used in the theory of

Elasticity. Similar decompositions and identifications hold for $\underset{(2)}{\underset{\sim}{F}}$.

The fundamental kinematical quantity associated with the rate of deformation of a continuous media is the velocity gradient.

It is customary to express the velocity as a function of the present position instead of the reference position.

i.e. $$\underset{(1)}{\underset{\sim}{v}} = \underset{(1)}{\underset{\sim}{\hat{v}}} \left(\underset{(1)}{\underset{\sim}{x}}, t \right)$$

We distinguish between functions and their values by putting a (Λ) over the function. The velocity gradients are given by

$$\underset{(1)}{\underset{\sim}{L}} = \text{grad} \underset{(1)}{\underset{\sim}{v}} \left(\underset{(1)}{\underset{\sim}{x}}, t \right)$$

and

$$\underset{(2)}{\underset{\sim}{L}} = \text{grad} \underset{(2)}{\underset{\sim}{v}} \left(\underset{(2)}{\underset{\sim}{x}}, t \right)$$

Notice that gradients with respect to reference configurations (Δ) are distinguished from gradients with respect to the present configuration (grad).

The velocity gradients are second order tensors and serve to define the rate of deformation in the local neighborhood. The velocity gradients can be decomposed into symmetric and skew-symmetric parts as follows:

$$\underset{(1)}{\underset{\sim}{L}} = 1/2 \left(\underset{(1)}{\underset{\sim}{L}} + \underset{(1)}{\underset{\sim}{L}}^T \right) + 1/2 \left(\underset{(1)}{\underset{\sim}{L}} - \underset{(1)}{\underset{\sim}{L}}^T \right)$$

where $\underset{\sim}{L}^T$ denotes transpose of $\underset{\sim}{L}$.

The symmetric part of the velocity gradient is associated with the stretching of elements in the local neighborhood while the skew part is associated with a rate of rotation or spin.

$$\underset{(1)}{\underset{\sim}{D}} = 1/2 \left(\underset{(1)}{\underset{\sim}{L}} + \underset{(1)}{\underset{\sim}{L}}^T \right)$$

$$\underset{(1)}{\underset{\sim}{W}} = 1/2 \left(\underset{(1)}{\underset{\sim}{L}} - \underset{(1)}{\underset{\sim}{L}}^T \right)$$

The tensors $\underset{(1)}{\underset{\sim}{F}}$, $\underset{(2)}{\underset{\sim}{F}}$ and $\underset{(1)}{\underset{\sim}{L}}$, $\underset{(2)}{\underset{\sim}{L}}$ are the fundamental kinematical quantities which describe the local deformation and rate of deformation in local neighborhoods and are instrumental in the formulation of the constitutive equations for the partial stresses in C_1 and C_2. The $\underset{\sim}{F}$'s are associated with elastic behavior (strain) while the $\underset{\sim}{L}$'s are associated with fluid behavior (rate of strain)

The fundamental quantity describing the motion of C_2 with respect to C_1 is the relative velocity vector $\underset{(21)}{\underset{\sim}{v}}$. It will be instrumental in forming constitutive equations for the diffusive forces exerted by C_2 on C_1 and vice-versa.

The following quantities will also be useful.

The mean velocity is defined by $$\rho \underset{\sim}{v} = \rho_{(1)} \underset{(1)}{\underset{\sim}{v}} + \rho_{(2)} \underset{(2)}{\underset{\sim}{v}}$$

where $\rho = \rho_{(1)} + \rho_{(2)}$ is the total density of the mixture, and similarly, the mean acceleration is given

by

$$\rho \underset{\sim}{a} = \rho \underset{\sim}{a} + \rho \underset{\sim}{a}$$
$$(1)(1) \quad (2)(2)$$

The diffusion velocities with respect to the mean motion are defined by

$$\underset{\sim}{u}_{(1)} = \underset{\sim}{v}_{(1)} - \underset{\sim}{v}$$

$$\underset{\sim}{u}_{(2)} = \underset{\sim}{v}_{(2)} - \underset{\sim}{v}$$

Partial Stresses and Diffusion Forces

The internal forces in a single species are represented by the contact force. The total force on a particle is given by the sum of the contact force and the body force.

$$\underset{\sim}{F} = \underset{\sim}{F}_c + \underset{\sim}{F}_b$$

where

$$\underset{\sim}{F}_c = \int_S \underset{\sim}{T} \cdot d\underset{\sim}{a}$$

$$\underset{\sim}{F}_b = \int_v \rho \underset{\sim}{b} dv$$

$\underset{\sim}{T}$ is the stress tensor given as a force per unit area and $\underset{\sim}{b}$ is the body force density.

The equation expressing the balance of momentum is then given by

$$\frac{d}{dt}\int_v \rho \underset{\sim}{v} dv = \int_s \underset{\sim}{T} \underset{\sim}{da} + \int_v \rho \underset{\sim}{b} dr$$

where under suitable smoothness conditions and the use of the divergence theorem we can derive the equivalent differential form

$$\rho \underset{\sim}{a} = \text{div } \underset{\sim}{T} + \rho \underset{\sim}{b}$$

where div is the divergence operator.

For the case of a binary mixture the above view must be altered slightly. Examining the forces on C_1 we break the body force into two parts; the extraneous body force (e.g. gravitation), and a diffusive body force which is exerted by C_2 on C_1.

Truesdell (11), following an idea of Maxwell, let the interaction force between C_1 and C_2 be represented by a body force proportional to the relative motion of the two media.

We represent this body force by $\underset{(21)}{\tilde{d}}$ i.e. the diffusive body force exerted by C_2 on C_1.

Therefore in the case of a binary mixture we have two stresses $\underset{(1)}{\tilde{T}}$ and $\underset{(2)}{\tilde{T}}$, and a body force $\underset{(21)}{\tilde{d}}$ that describe the nature of the internal forces. The forms of $\underset{(1)}{\tilde{T}}$, and $\underset{(2)}{\tilde{T}}$ and $\underset{(21)}{\tilde{d}}$ are given by constitutive equations that relate these forces to the kinematical quantities. Essentially the constitutive equations for $\underset{(1)}{\tilde{T}}$ and $\underset{(2)}{\tilde{T}}$ define the nature of the constituents C_1 and C_2, while the constitutive equation for $\underset{(21)}{\tilde{d}}$ defines the nature of the diffusion process.

Equations of Balance

In continum mechanics there are four types of balance equations: the balance of mass, momentum, angular momentum, and energy. For what is done here only the balance of mass and momentum are considered.

The balance of mass (or equations of continuity) for the constituents C_1 and C_2 are given by

$$\frac{\partial \rho_{(1)}}{\partial t} + \text{div}(\rho_{(1)} \underset{\sim}{v}_{(1)}) = 0$$

$$\frac{\partial \rho_{(2)}}{\partial t} + \operatorname{div}(\rho_{(2)} \underset{\sim}{v}_{(2)}) = 0$$

when no chemical reactions take place.

In order to derive an equation of balance for the mixture we can add these two equations and get

$$\frac{\partial}{\partial t}(\rho_{(1)} + \rho_{(2)}) + \operatorname{div}(\rho_{(1)} \underset{\sim}{v}_{(1)} + \rho_{(2)} \underset{\sim}{v}_{(2)}) = 0$$

or

$$\frac{\partial \rho}{\partial t} + \operatorname{div} \rho \underset{\sim}{v} = 0$$

where $\rho = \rho_{(1)} + \rho_{(2)}$ is the total density of the mixture, and $\underset{\sim}{v}$ is the mean velocity.

The equations expressing the balance of momentum for C_1 and C_2 are $\operatorname{div} \underset{\sim}{T}_{(1)} + \rho_{(1)} \underset{\sim}{b}_{(1)} + \underset{\sim}{d}_{(21)} = \rho_{(1)} \underset{\sim}{a}_{(1)}$

and $\underset{\sim}{T}_{(2)} + \rho_{(2)} \underset{\sim}{b}_{(2)} + \underset{\sim}{d}_{(12)} = \rho_{(2)} \underset{\sim}{a}_{(2)}$

It is also assumed that the diffusive force exerted by C_1 on C_2 is equal and opposite to that exerted by C_2 on C_1, i.e.

$$\underset{\sim}{d}_{(12)} = -\underset{\sim}{d}_{(21)}$$

The effect of diffusion in the equations of motion is accounted for by the diffusive body force. Recall that $\underset{\sim}{d}_{(21)}$ e.g. is the force that constituent (2) exerts on constituent (1).

If we desire an equation of balance of momentum for the mixture as a whole we can add the above equations and obtain

$$\operatorname{div}(\underset{\sim}{T}_{(1)} + \underset{\sim}{T}_{(2)}) + \rho_{(1)} \underset{\sim}{b}_{(1)} + \rho_{(2)} \underset{\sim}{b}_{(2)} = \rho_{(1)} \underset{\sim}{a}_{(1)} + \rho_{(2)} \underset{\sim}{a}_{(2)}$$

where the diffusive forces have cancelled out because of $\underset{\sim}{d}_{(21)} = -\underset{\sim}{d}_{(12)}$. If the external body forces are the same for both constituents (as is customary), we can write an equation of balance of momentum for the mixture as $\operatorname{div} \underset{\sim}{T} + \rho \underset{\sim}{b} = \rho \underset{\sim}{a}$

where $\rho = \rho_{(1)} + \rho_{(2)}$

and $\underset{\sim}{a}$ is the mean acceleration

and $\underset{\sim}{T} = \underset{\sim}{T}_{(1)} + \underset{\sim}{T}_{(2)}$ the total stress in the mixture.

In what follows the individual equations of motion for the constituents are of more interest than the equation for the mixture.

The continuity equations and the equations of motion for the constituents C_1 and C_2 are incomplete. For a complete theory they must be supplemented by constitutive equations describing the material properties of C_1 and C_2 as well as the diffusion process.

Constitutive Equations for the Partial Stresses

In a general theory of material behavior for a single constituent it is assumed that the stress is determined from a knowledge of the motion in a local neighborhood around the point in question. For what follows it is sufficient to discuss the two cases of elastic and fluid behavior.

The constituent C_1 will be identified with an elastic material in which the stress is determined from a knowledge of the deformation (or strain) of the local neighborhood around the point

in question. For what follows it is sufficient to discuss the two cases of elastic and fluid behavior.

The constituent C_1 will be identified with an elastic material in which the stress is determined from a knowledge of the deformation (or strain) of the local neighborhood around the point in question. In terms of equations, the constitutive function of an elastic material will have the form

$$\underset{\sim}{T}_{(1)} = \hat{\underset{\sim}{T}}_{(1)} \left(\underset{\sim}{F}_{(1)} \right)$$

In the case of a fluid the stress is determined by a knowledge of the rate of strain of the local neighborhood i.e.

$$\underset{\sim}{T}_{(2)} = \hat{\underset{\sim}{T}}_{(2)} \left(\underset{\sim}{L}_{(2)} \right)$$

In what is done here, we assume that the partial stresses in a given constituent are not affected by the kinematics of the other constituent, and the nature of the interaction of the two constituents is represented solely through the nature of the diffusive body force. At the end of the paper we shall give generalizations of the constitutive equations which include interactive phenomena in the partial stresses and the diffusive force.

Constitutive Equation for the Diffusive Force

The constitutive equation that governs the diffusive phenomena gives $\underset{\sim}{d}_{(21)}$ as a function of the constituents C_1 and C_2 and the relative motion between them.

We assume, at first, that the diffusive constitutive equation is given by

$$\underset{\sim}{d}_{(21)} = \hat{\underset{\sim}{d}}_{(21)} \left(\rho_{(1)}, \rho_{(2)}, \underset{\sim}{v}_{(21)} \right)$$

i.e. it depends on the densities of each constituent and the relative velocity of C_2 with respect to C_1. Later we will give reasons for including the viscosity of the fluid (μ_v) in the above relation.

Truesdell (11) discussed the linear while Adkins (1), (3) discussed the non-linear theory.

Principle of Material Frame Indifference

As a general guideline in forming constitutive equations we use the principle of material frame indifference, that is, the constitutive equations governing material behavior should be independent of the frame of reference in which they are viewed. In the language of invariant theory the equations should contain only frame-indifferent or objective quantities.

Changes of frame are transformations of space-time which leave distances, angles, and time intervals unchanged. The most general such transformation in 3-D Euclidean space is

$$\underset{\sim}{x}^* = \underset{\sim}{Q}\,\underset{\sim}{x} + \underset{\sim}{c}$$

$$t^* = t - a$$

where $\underset{\sim}{Q}$ is an orthogonal second order tensor function of t, $\underset{\sim}{c}$ is a point function of t, and a is a scalar.

The above change of frame induces corresponding changes in the kimematical quantities formed from the motions. In general, the quantities are said to be frame-indifferent or objective if they transform in a certain way. Scalars, vectors, and second order tensors are frame-indifferent if they transform as follows

References at end of paper

$$s^* = s \quad \text{for scalars}$$

$$\underset{\sim}{v}^* = \underset{\sim}{Q}\,\underset{\sim}{\bar{v}} \quad \text{for vectors}$$

$$\underset{\sim}{T}^* = \underset{\sim}{Q}\,\underset{\sim}{T}\,\underset{\sim}{Q}^T \quad \text{for second order tensors.}$$

If the angular velocity of the starred frame with respect to the unstarred frame is

$$\underset{\sim}{w} = \underset{\sim}{Q}\,\underset{\sim}{Q}^T$$

where $\underset{\sim}{w}$ is a skew-symmetric second order tensor, then the vectors and tensors we have defined previously transform as follows

$$\underset{\sim}{F}^* = \underset{\sim}{Q}\,\underset{\sim}{F}\ ,\ \underset{\sim}{R}^* = \underset{\sim}{Q}\,\underset{\sim}{R}\ ,\ \underset{\sim}{U}^* = \underset{\sim}{U}$$

$$\underset{\sim}{v}^* = \underset{\sim}{Q}\,\underset{\sim}{V}\,\underset{\sim}{Q}^T\ ,\ \underset{\sim}{L}^* = \underset{\sim}{Q}\,\underset{\sim}{L}\,\underset{\sim}{Q}^T + \underset{\sim}{w}$$

$$\underset{\sim}{D}^* = \underset{\sim}{Q}\,\underset{\sim}{D}\,\underset{\sim}{Q}^T\ ,\ \underset{\sim}{W}^* = \underset{\sim}{Q}\,\underset{\sim}{W}\,\underset{\sim}{Q}^T + \underset{\sim}{W}\ ,\ \underset{(21)}{\tilde{v}}^* = \underset{\sim}{Q}\ \underset{(21)}{\tilde{v}}$$

It is also assumed that the partial stresses and the diffusive forces are indifferent, i.e.

$$\underset{(1)}{\tilde{T}}^* = \underset{\sim}{Q}\,\underset{(1)}{\tilde{T}}\,\underset{\sim}{Q}^T\ ,\ \underset{(2)}{\tilde{T}}^* = \underset{\sim}{Q}\,\underset{(2)}{\tilde{T}}\,\underset{\sim}{Q}^T$$

and

$$\underset{(21)}{\tilde{d}}^* = \underset{\sim}{Q}\ \underset{(21)}{\tilde{d}}$$

Therefore, if the constitutive equations are to contain only indifferent quantities $\underset{(1)}{\tilde{T}} = \underset{(1)}{\tilde{\hat{T}}}\,(\underset{(1)}{\tilde{V}})$

or as is generally used in non-linear isotropic elasticity $\underset{(1)}{\tilde{T}} = \underset{(1)}{\tilde{\hat{T}}}\,(\underset{(1)}{\tilde{B}})$

where $\underset{\sim}{B} = \underset{\sim}{V}^2 = \underset{\sim}{F}\,\underset{\sim}{F}^T$ is the left Gauchy-Green tensor.

On the other hand, the constitutive equation for the fluid-like media C_2 must reduce to a function of $\underset{(2)}{\tilde{D}}$ instead of $\underset{(2)}{\tilde{L}}$.

$$\underset{(2)}{\tilde{T}} = \underset{(2)}{\tilde{\hat{T}}}\,(\underset{(2)}{\tilde{D}})$$

i.e.

Whereas, since $\underset{(21)}{\tilde{v}}$ is already indifferent, the constitutive equation for the diffusive force is as before.

$$\underset{(21)}{\tilde{d}} = \underset{(21)}{\tilde{\hat{d}}}\,(\rho, \rho, \underset{(1)}{\tilde{v}}, \underset{(2)}{\tilde{v}}, \underset{(21)}{\tilde{v}})$$

Representation Theorems for Isotropic Materials

Much work has been accumulated in the last twenty years on the representations of isotropic functions, i.e. a relation involving only indifferent quantities whether scalars, vectors, or tensors. It is well established that such functions must have a certain prescribed form as given by what are called representation theorems.

The earlier work of Rivlin and Ericksen, Spencer, Smith, etc. on isotropic representation theorems has culminated in a recent work by C. C. Wang (15) and (16) where he gives the general representation theorems for isotropic functions which can be scalar, vector, or tensor valued and be a function of any number of scalars, vectors, symmetric tensors, and skew tensors. For the most

References at end of paper

part the theorems are rather long, and the reader is referred to Wang's work.

Since only isotropic materials are treated here the representation theorems are used to reduce the forms of the constitutive equations. The symmetric tensor-valued representation theorems are used to reduce $\underset{\sim}{T}_{(1)}$ and $\underset{\sim}{T}_{(2)}$ and the vector-valued to reduce $\hat{d}_{(21)}$.

Constitutive Equations for the Partial Stresses as Given by the Representation Theorems

The following cases are considered for C_1 and C_2.

C_1 is considered to be one of the following:

(1) a rigid body (porous)
(2) a linear elastic solid (porous)
(3) a non-linear elastic solid (porous),

while C_2 is considered to be either

(1) an ideal fluid
(2) a newtonian fluid
(3) a non-newtonian fluid

Each of the above cases is now considered separately so as to evolve the constitutive equations for the partial stresses.

For

(1) a rigid body.

In this case both $\underset{\sim}{F}$ and $\underset{\sim}{L}$ reduce to the identity tensor i.e. $\underset{\sim}{F}=\underset{\sim}{L}=\underset{\sim}{1}$ and the stress in C_1 is indeterminate.

(2) a linear elastic solid.

Many strain measures are available for elastic materials, none of which are unique.

For the isotropic case $\underset{\sim}{B}$ is frequently used. Other possibilities are the Green non-linear strain measure $2\underset{\sim}{E}=\underset{\sim}{C}-\underset{\sim}{1}$ where $\underset{\sim}{C}=\underset{\sim}{F}^T\underset{\sim}{F}$ is the right Gauch-Freen tensor, or in the case of infinitesimal strain $\underset{\sim}{\tilde{E}}$ i.e. the symmetric part of the infinitesimal displacement gradient.

Since the usual case for the linear elastic material is to use $\underset{\sim}{\tilde{E}}$ as strain measure, we use this. We consider

$$\underset{(1)}{T} = \hat{T}_{(1)}(\underset{\sim}{\tilde{E}})$$

and we assume that this function is linear. In this case the representation theorem gives $\underset{(1)}{T}$ in the form

$$\underset{(1)}{T} = \lambda_e (\mathrm{tr}\,\underset{\sim}{\tilde{E}})\underset{\sim}{1} + 2\mu_e \underset{\sim}{\tilde{E}}$$

which is the clasical form for infinitesimal elasticity. λ_E and μ_e are the Lame constants of linear elasticity. The above $\underset{(1)}{T}$ will give the partial stress in C_1 when C_1 is regarded as a linear elastic material.

(3) Non-Linear elastic solid.

For non-linear isotropic elastic solids the most commonly used strain measure is $\underset{\sim}{B}$.

i.e. $\underset{(1)}{T} = \underset{(1)}{T}(\underset{\sim}{B})$

The representation theorem in this case gives the form for the most general non-linear isotropic elastic material as

$$\underset{(1)}{T} = \hat{T}_{(1)}(\underset{\sim}{B}) = \psi_o \underset{\sim}{1} + \psi_1 \underset{(1)}{\underset{\sim}{B}} + \psi_2 \underset{(1)}{\underset{\sim}{B}^2}$$

where the ψ's are scalar functions of the invariants of $\underset{\sim}{B}$ i.e. trB, trB^2, trB^3 where tr denotes trace. If linearity were enforced on this we would end up with the linear elastic version with $\underset{\sim}{E}$ replaced by $\underset{\sim}{B}$.

In the case of C_2, the fluid-like constituent, we assume

(1) an ideal fluid

In the case of an ideal fluid the stress is hydrostatic (i.e. the material can support no shear stress). In this case the partial stress $\underset{(2)}{T}$ is given by $\underset{\sim}{T} = - p\,(\rho)\,\underset{\sim}{1}$

If this is put into the equation of motion for a single constituent, Euler's dynamical equation for perfect fluids results.

(2) a newtonian fluid

For a newtonian fluid the stress is regarded as a function of the density and the rate of deformation tensor i.e. $\underset{(2)}{\underset{\sim}{T}} = \hat{\underset{(2)}{\underset{\sim}{T}}}\,(\rho, \underset{(2)}{\underset{\sim}{D}})$

Since all the quantities are indifferent the general representation theorem may be applied to give the most general linear isotropic function $\hat{\underset{(2)}{\underset{\sim}{T}}}$ as, $\underset{(2)}{\underset{\sim}{T}} = - p\,\underset{\sim}{1} + \lambda_v\,(tr\,\underset{(2)}{\underset{\sim}{D}})\,\underset{\sim}{1} + 2\mu_v\,\underset{(2)}{\underset{\sim}{D}}$

Putting this into the equation of motion for a single constituent results in the Navier-Stokes equation for classical fluid flow. The constants λ_v and μ_v are the viscosities of the linear theory.

(3) non-newtonian fluids of the Reiner-Rivlin type.

Stokes generalized Newton's concept of a fluid to apply to a non-linear dependence on $\underset{\sim}{D}$ i.e. $\underset{(2)}{\underset{\sim}{T}} = \hat{\underset{(2)}{\underset{\sim}{T}}}\,(\rho, \underset{(2)}{\underset{\sim}{D}})$ where $\underset{(2)}{\underset{\sim}{T}}$ is no longer a linear function of $\underset{\sim}{D}$. The representation theorem gives the following form for the non-linear case,

$$\hat{\underset{(2)}{\underset{\sim}{T}}} = \phi_o\,\underset{\sim}{1} + \phi_1\,\underset{(2)}{\underset{\sim}{D}} + \phi_2\,\underset{(2)}{\underset{\sim}{D}}^2$$

where the ϕ's are scalar functions of ρ and the invariants of $\underset{(2)}{\underset{\sim}{D}}$ i.e. $tr\,\underset{\sim}{D}$, $tr\,\underset{\sim}{D}^2$, $tr\,\underset{\sim}{D}^3$

The scalar coefficients generalize the classical viscosities occuring in the linear case. If the above relation is assumed to be linear, the classical case is recovered.

Constitutive Equations for the Diffusive Force

Two cases will be considered for the diffusive force, the linear representation and the non-linear representation

(1) the linear case

Recall that in general the diffusive force $\underset{(21)}{\underset{\sim}{d}}$ was given as a function of $\rho_{(1)}$, $\rho_{(2)}$ and $\underset{(21)}{\underset{\sim}{v}}$. i.e. $\underset{(21)}{\underset{\sim}{d}} = \hat{\underset{(21)}{\underset{\sim}{d}}}\,(\rho_{(1)}, \rho_{(2)}, \underset{(21)}{\underset{\sim}{v}})$

The vector-valved representation theorem can be applied to this function and in the linear case it gives the following form, $\underset{(21)}{\underset{\sim}{d}} = K\,\rho_{(1)}\,\rho_{(2)}\,\underset{(21)}{\underset{\sim}{v}}$ where K is a constant.

(2) the non-linear case

The representation theorem for the non-linear case impresses the following form on the function $\underset{(21)}{d}$

$$\underset{(21)}{d} = \phi\,(\rho_{(1)}, \rho_{(2)}, |\underset{(21)}{v}|)\,\underset{(21)}{v}$$

where ϕ is in general a non-linear function of $\rho_{(1)}$ and $\rho_{(2)}$ and $|\underset{(21)}{v}|$.

In a later part of the paper we will have occasion to use a slightly different diffusive force. There, it is supposed that the diffusive force is allowed to depend on μ_v as well as on the previous variables $\rho_{(1)}$, $\rho_{(2)}$ and $\underset{(21)}{v}$ i.e. $\underset{(21)}{d} = \hat{\underset{(21)}{d}}\,(\rho_{(1)}, \rho_{(2)}, \mu_v, \underset{(21)}{v})$

In the linear case this results in

$$\underset{(21)}{d} = K\,\rho_{(1)}\,\rho_{(2)}\,\mu_v\,\underset{(21)}{v}$$

while in the non-linear case the representation theorem gives $\underset{(21)}{d} = \phi\,(\rho_{(1)}, \rho_{(2)}, \mu_v, |\underset{(21)}{v}|)\underset{(21)}{v}$

where in general ϕ is non-linear (perhaps a polynomial) in the variables $\rho_{(1)}$, $\rho_{(2)}$, μ_v, and $|\underset{(21)}{v}|$.

Of course, it doesn't follow that if one of the partial stresses is linear the other is, or that the diffusive force is, although we shall in general assume that this is the case.

The following cases are considered and compared. In particular it shall be pointed out that the equations of motion in conjuction with the constitutive equations for the partial stresses and the diffusive force give generalizations of the commonly used Darcy's law for flow through porous media. The cases looked at are:

(a) Diffusion of a non-newtonian fluid through a non-linear elastic solid.

(b) Diffusion of a newtonian fluid through a linear elastic solid.

(c) Diffusion of a newtonian fluid through a rigid body.

(d) Diffusion of an ideal fluid through an elastic solid, and

(e) Diffusion of an ideal fluid through a rigid body

Case (a) Diffusion of a non-newtonian fluid through a non-linear elastic solid.

If the constituent C_1 is represented by a non-linear isotropic elastic solid the partial stress $\underset{(1)}{T}$ is given by $\underset{(1)}{T} = \psi_o\,\underset{}{1} + \psi_1\,\underset{(1)}{B} + \psi_2\,\underset{(1)}{B^2}$

and if the constituent C_2 is represented by a non-linear fluid the partial stress $\underset{(2)}{T}$ in C_2 is given by $\underset{(2)}{T} = \phi_o\,\underset{}{1} + \phi_1\,\underset{(2)}{D} + \phi_2\,\underset{(2)}{D^2}$

where the ψ's and ϕ's are functions of their respective invariants.

It is supposed that the constitutive equation for the diffusive force is given by its most general non-linear form compatible with the isotropic representation theorem

i.e. either $\underset{(21)}{d} = \phi\,(\rho_{(1)}, \rho_{(2)}, |\underset{(21)}{v}|)\,\underset{(21)}{v}$

or $\underset{(21)}{d} = \phi\,(\rho_{(1)}, \rho_{(2)}, \mu_v, |\underset{(21)}{v}|)\,\underset{(21)}{v}$

These three constitutive equations together with the equations of motion and continuity are sufficient to completely describe the dynamical situation.

If we substitute the constitutive equations into the equations of motion we get for C_1

$$\operatorname{div}(\psi_0 \underset{\sim}{1} + \psi_1 \underset{(1)}{\underset{\sim}{B}} + \psi_2 \underset{(1)}{\underset{\sim}{B}}^2) + \rho_{(1)} \underset{(1)}{\underset{\sim}{b}} + \phi(\rho_{(1)}, \rho_{(2)}, |\underset{(21)}{\underset{\sim}{v}}|) \underset{(21)}{\underset{\sim}{v}} = \rho_{(1)} \underset{(1)}{\underset{\sim}{a}}$$

for C_2 $$\operatorname{div}(\phi_0 \underset{\sim}{1} + \phi_1 \underset{(2)}{\underset{\sim}{D}} + \phi_2 \underset{(2)}{\underset{\sim}{D}}^2) + \rho_{(2)} \underset{(2)}{\underset{\sim}{b}} - \phi(\rho_{(1)}, \rho_{(2)}, |\underset{(21)}{\underset{\sim}{v}}|) \underset{(21)}{\underset{\sim}{v}} = \rho_{(2)} \underset{(2)}{\underset{\sim}{a}}$$

recalling that $\underset{(21)}{\underset{\sim}{d}} = -\underset{(12)}{\underset{\sim}{d}}$

Case (b) Diffusion of a newtonian fluid through a linear elastic solid.

If C_1 is taken as a classical linear elastic solid the partial stress $\underset{(1)}{\underset{\sim}{T}}$ is given by

$$\underset{(1)}{\underset{\sim}{T}} = \lambda_e(\operatorname{tr} \underset{(1)}{\underset{\sim}{\hat{E}}}) \underset{\sim}{1} + 2\mu_e \underset{(1)}{\underset{\sim}{\hat{E}}}$$

and if C_2 is regarded as a classical linear fluid, the partial stress $\underset{(2)}{\underset{\sim}{T}}$ is given by

$$\underset{(2)}{\underset{\sim}{T}} = -p \underset{\sim}{1} + \lambda_v (\operatorname{tr} \underset{(2)}{\underset{\sim}{D}}) \underset{\sim}{1} + 2\mu_v \underset{(2)}{\underset{\sim}{D}}$$

and the diffusive force is given by either $\underset{(21)}{\underset{\sim}{d}} = k\rho_{(1)}\rho_{(2)} \underset{(21)}{\underset{\sim}{v}}$ or $\underset{(21)}{\underset{\sim}{d}} = k\rho_{(1)}\rho_{(2)}\mu_v \underset{(21)}{\underset{\sim}{v}}$

Substituting these into the equations of motion the equations become

for C_1 $$\operatorname{div}(\lambda_e(\operatorname{tr}\underset{(1)}{\underset{\sim}{E}}) \underset{\sim}{1} + 2\mu_e \underset{(1)}{\underset{\sim}{E}}) - \rho_{(1)} \underset{(1)}{\underset{\sim}{b}} + K\rho_{(1)}\rho_{(2)}\mu_v \underset{(21)}{\underset{\sim}{v}} = \rho_{(1)} \underset{(1)}{\underset{\sim}{a}}$$

and for C_2 $$\operatorname{div}(-p \underset{\sim}{1} + \lambda_v(\operatorname{tr}\underset{(2)}{\underset{\sim}{D}}) \underset{\sim}{1} + 2\mu_v \underset{(2)}{\underset{\sim}{D}}) + \rho_{(2)} \underset{(2)}{\underset{\sim}{b}} - K\rho_{(1)}\rho_{(2)}\mu_v \underset{(21)}{\underset{\sim}{v}} = \rho_{(2)} \underset{(2)}{\underset{\sim}{a}}$$

As can be seen from the above equations, it is necessary to distinguish clearly between the stress and the hydrostatic pressure; a point that is not clear in many works on flow through porous media.

Case (c) Diffusion of a newtonian fluid through a rigid body

If C_1 is a rigid body the partial stress $\underset{(1)}{\underset{\sim}{T}}$ is indeterminate and this makes the equation of motion for C_1 vacuous.

For C_2 a newtonian fluid, $\underset{(2)}{\underset{\sim}{T}}$ is given by $\underset{(2)}{\underset{\sim}{T}} = -p \underset{\sim}{1} + \lambda_v(\operatorname{tr} \underset{(2)}{\underset{\sim}{D}}) \underset{\sim}{1} + 2\mu_v \underset{(2)}{\underset{\sim}{D}}$

and using $\underset{(21)}{\underset{\sim}{d}} = K\rho_{(1)}\rho_{(2)}\mu_v \underset{(21)}{\underset{\sim}{v}}$

the equation of motion for C_2 becomes

$$\operatorname{div}(-p \underset{\sim}{1} + \lambda_v(\operatorname{tr} \underset{(2)}{\underset{\sim}{D}}) \underset{\sim}{1} + 2\mu_v \underset{(2)}{\underset{\sim}{D}}) + \rho_{(2)} \underset{(2)}{\underset{\sim}{b}} - K\rho_{(1)}\rho_{(2)}\mu_v \underset{(21)}{\underset{\sim}{v}} = \rho_{(2)} \underset{(2)}{\underset{\sim}{a}}$$

Again it is well to keep in mind the difference between the pressure gradient and the divergence of the stress in the above equation.

Case (d) Diffusion of an ideal fluid through an elastic solid

If C_1 is an elastic solid (linear) $\underset{(1)}{\underset{\sim}{T}}$ is $\underset{(1)}{\underset{\sim}{T}} = \lambda_e(\operatorname{tr} \underset{(1)}{\underset{\sim}{E}}) \underset{\sim}{1} + 2\mu_e \underset{(1)}{\underset{\sim}{\hat{E}}}$

while if C_2 is an ideal fluid we have for the partial stress $\underset{(2)}{\underset{\sim}{T}}$, $\underset{(2)}{\underset{\sim}{T}} = -p_{(2)}(\rho_{(2)}) \underset{\sim}{1}$

and using the diffusive force as $\underset{(21)}{\underset{\sim}{d}} = K\rho_{(1)}\rho_{(2)}\mu_v \underset{(21)}{\underset{\sim}{v}}$

the equation of motion for C_1 becomes

$$\operatorname{div}(\lambda_e(\operatorname{tr} \underset{(1)}{\underset{\sim}{E}}) \underset{\sim}{1} + 2\mu_e \underset{(1)}{\underset{\sim}{E}}) + \rho_{(1)} \underset{(1)}{\underset{\sim}{b}} + K\rho_{(1)}\rho_{(2)}\mu_v \underset{(21)}{\underset{\sim}{v}} = \rho_{(1)} \underset{(1)}{\underset{\sim}{a}}$$

while that for C_2 becomes $\operatorname{div}(-p\,\underset{\sim}{1})_{(2)} + \rho_{(2)}\,\underset{\sim}{b}_{(2)} - K\,\rho_{(1)}\,\rho_{(2)}\,\mu_{v_{(21)}}\,\underset{\sim}{v} = \rho_{(2)}\,\underset{\sim}{a}_{(2)}$

Case (e) Diffusion of an ideal fluid through a rigid body

If C_1 is a rigid body $\underset{(\tilde{1})}{T}$ is indeterminate and the equation of motion is of no use.

If C_2 is an ideal fluid, its partial stress is given by $\underset{(2)}{T} = -\,p_{(2)}\,(\rho_{(2)})\,\underset{\sim}{1}$

and a diffusive force of the form $\underset{(21)}{d} = K\,\rho_{(1)}\,\rho_{(2)}\,\mu_{v_{(21)}}\,\underset{\sim}{v}$ is used

The equation of motion becomes

$$\operatorname{div}(-p\,(\rho)\,\underset{\sim}{1})_{(2)(2)} + \rho_{(2)(2)}\,b + K\,\rho_{(1)(2)}\,\rho_{(2)}\,\mu_{v_{(21)}}\,\underset{\sim}{v} = \rho_{(2)(2)}\,\underset{\sim}{a}$$

In this case the divergence reduces to the gradient

i.e. $\operatorname{div}(-p\,(\rho)\,\underset{\sim}{1}) = -\operatorname{grad}(p\,(\rho))$

Only in the case of ideal fluids is the pressure gradient the driving force; in more general cases it is the divergence of the stress.

Cases Where Fick's Law is Applicable

Within the more general framework presented here, it is shown under what assumptions on the general laws and constitutive equations the equations known as Fick's law are precipitated, and the standard diffusion equation results.

According to Truesdell (11), Fick, on no basis beyond an asserted analogy to the flow of heat, proposed that in a binary mixture at uniform total density

$$\rho_{(1)}\,\underset{\sim}{u}_{(1)(\tilde{1})} = -D\,\operatorname{grad}\rho_{(1)}$$

where $\rho_{(1)}$ is the density of C_1, $\underset{\sim}{u}_{(1)}$, its diffusion velocity, and D, a phenomenological coefficient which may depend on the densities

This equation, generally referred to as Fick's law, in conjunction with the equation of continuity for C_1 results in $\frac{d}{dt}(\rho_{(1)}) = \operatorname{div}(D\,\operatorname{grad}\rho_{(1)})$ which is the standard diffusion equation.

Truesdell also points out that the presumptions leading to Fick's law are unsupported by any principle or method of mechanics or physics and cannot be expected to explain or predict motions except in specially simple circumstances.

Adkins (1) has been able, within the framework of the theory presented here, and under special assumptions to derive the classical diffusion equations based on Fick's Law. His analysis holds equally as well for a two component mixture of fluids or a single fluid diffusing into a rigid solid. In the case of a binary mixture of fluids he makes the following assumptions.

(I) The diffusing substances are perfect fluids with similar linear pressure-density relations

(II) The velocity and acceleration components are sufficiently small for the inertia terms in the equations of motion and for products of velocities in the expressions for the diffusion forces to be neglected.

(III) The total density of the mixture is constant.

(IV) The extraneous body forces can be neglected.

References at end of paper

From assumptions (II) and (IV) the equations of motion become $\operatorname{div} \underset{\sim}{T}_{(1)} + \underset{\sim}{d}_{(21)} = 0$ (I) implies $\underset{\sim}{T}_{(1)} = -p_{(1)} \underset{\sim}{1}$ with $p_{(1)} = k \rho_{(1)}$ and $\underset{\sim}{d}_{(21)} = \phi \underset{\sim}{v}_{(21)}$ where ϕ is a scalar fuction of $\rho_{(1)}$ and $\rho_{(2)}$. The equation of motion then become

$$- \operatorname{grad} p_{(1)} + \phi \underset{\sim}{v}_{(21)} = 0$$

$$- \operatorname{grad} \frac{\partial p}{\partial \rho} \operatorname{grad} \rho + \phi \underset{\sim}{v}_{(21)} = 0$$

Recalling that $\rho \underset{\sim}{v} = \rho_{(1)} \underset{\sim}{v}_{(1)} + \rho_{(2)} \underset{\sim}{v}_{(2)}$ where $\underset{\sim}{v}$ is the mean velocity, and $\underset{\sim}{u}_{(1)} = \underset{\sim}{v}_{(1)} - \underset{\sim}{v}$ where $\underset{\sim}{u}_{(1)}$ is the diffusion velocity, the relative velocity $\underset{\sim}{v}_{(21)}$ can be expressed in terms of the diffustion velocity.

i.e. $$\underset{\sim}{u}_{(1)} = \underset{\sim}{v}_{(1)} - \underset{\sim}{v} = \underset{\sim}{v}_{(1)} - \rho_{(1)} \frac{\underset{\sim}{v}_{(1)} - \rho_{(2)} \underset{\sim}{v}_{(2)}}{\rho} = \frac{\rho_{(2)}}{\rho} \underset{\sim}{v}_{(2)} - \underset{\sim}{v}_{(2)}$$

Therefore, in terms of the diffusion velocity, the equation of motion becomes. $-k \operatorname{grad} \rho_{(1)} = \phi \rho_{(1)} \underset{\sim}{u}_{(1)} / \rho_{(2)}$

If it is assumed that $\phi = k \rho_{(1)} \rho_{(2)} / \rho D$ the equation of motion becomes $-k \operatorname{grad} \rho_{(1)} = k \rho_{(1)} \underset{\sim}{u}_{(1)} / D$ so $-D \operatorname{grad} \rho_{(1)} = \rho_{(1)} \underset{\sim}{u}_{(1)}$ i.e. Fick's Law. One can see that it holds only under the most restrictive of circumstances.

This law together with the equation of continuity for C_1, i.e. $\frac{\partial \rho_{(1)}}{\partial t} + \operatorname{div} \rho_{(1)} \underset{\sim}{v}_{(1)} = 0$ the equation of continuity for the mixture $\frac{\partial \rho}{\partial t} + \operatorname{div} \rho \underset{\sim}{v} = 0$ or $\operatorname{div} \underset{\sim}{v} = 0$ since ρ =const), and the definition of the mean derivative of $\rho_{(1)}$, yields

Therefore, $$\frac{D \rho_{(1)}}{Dt} = \frac{\partial \rho_{(1)}}{\partial t} + \underset{\sim}{v} \circ \nabla \rho_{(1)} = \frac{\partial \rho_{(1)}}{\partial t} + \operatorname{div} \rho_{(1)} \underset{\sim}{v}$$

putting this into the continuity equation for C_1 results in $\frac{\partial \rho_{(1)}}{\partial t} = \frac{D \rho_{(1)}}{Dt} - \operatorname{div} \rho_{(1)} \underset{\sim}{v}$

or $$\frac{D \rho_{(1)}}{Dt} - \operatorname{div} \rho_{(1)} \underset{\sim}{v} + \operatorname{div} \rho_{(1)} \underset{\sim}{v} = 0$$

which together with Fick's Law result in the standard diffusion equation $\frac{D \rho_{(1)}}{Dt} = \operatorname{div}(D \operatorname{grad} \rho_{(1)})$

Cases where Darcy's law results

Using roughly the same assumptions as for Fick's Law the equations of motion can be given as

$$-\nabla p + \phi \underset{\sim}{v}_{(21)} = 0$$

or

$$\underset{\sim}{v}_{(21)} = \frac{1}{\phi} \nabla p$$

where ϕ is regarded as a scalar function of the densities and possibly contains a constant that can be identified with the viscosity, e.g. suppose

Then the equation of motion results in $\phi = \mu_v / k$ $\underset{\sim}{v}_{(21)} = \frac{k}{\mu_v} \nabla p$

Again one must be aware of the rather stringent restrictions placed on the more general framework in order for these equations to result. In general, Darcy's Law is usually defined for the uniform flow of an ideal fluid through a rigid solid. The idea of a viscosity being associated with an ideal fluid is somewhat tenuous in itself. We prefer to view Darcy's Law as resulting from special and somewhat unclear assumptions applied to the general equations of motion defined in the section describing the flow of a newtonian fluid througha rigid porous media. It is felt

that within the more rational framework of the continum mixture theories where balance equations and constitutive equations for partial stresses and diffusive forces are clearly delineated and defined, many well founded generalizations of Darcy's law can be found and applied.

Some Other Recent Attempts at a Rational Theory of Diffusion

Recall that in the theory looked at here the following assumptions were made about the constitutive equations for the partial stresses and the diffusive force.

$$\underset{(1)}{\mathbf{T}} = \hat{\underset{(1)}{\mathbf{T}}}\,(\underset{(1)}{\mathbf{F}}) \quad \text{, basically elastic}$$

$$\underset{(2)}{\mathbf{T}} = \hat{\underset{(2)}{\mathbf{T}}}\,(\rho_{(2)}, \underset{(2)}{\mathbf{L}}) \quad \text{, basically fluid}$$

and $$\underset{(21)}{\mathbf{d}} = \hat{\underset{(21)}{\mathbf{d}}}\,(\rho_{(1)}, \rho_{(2)}, \underset{(21)}{\mathbf{v}})$$

or $$\underset{(21)}{\mathbf{d}} = \hat{\underset{(21)}{\mathbf{d}}}\,(\rho_{(1)}, \rho_{(2)}, \mu_{\nabla}, \underset{(21)}{\mathbf{v}})$$

More recently some authors, see e.g. (2), (3), (6) have attempted to generalize the above framework claiming that it doesn't allow for a more general interaction through the partial stresses and diffusion forces.

As a rough first attempt at an interaction theory Adkins (2) suggests that the densities of both constituents be included in the partial stresses

i.e.

$$\underset{(1)}{\mathbf{T}} = \hat{\underset{(1)}{\mathbf{T}}}\,(\rho_{(1)}, \rho_{(2)}, \underset{(1)}{\mathbf{F}}), \quad \underset{(2)}{\mathbf{T}} = \hat{\underset{(2)}{\mathbf{T}}}\,(\rho_{(1)}, \rho_{(2)}, \underset{(2)}{\mathbf{L}}), \text{ and } \underset{(21)}{\mathbf{d}} = \hat{\underset{(21)}{\mathbf{d}}}\,(\rho_{(1)}, \rho_{(2)}, \underset{(21)}{\mathbf{v}})$$

In another attempt at a more general interaction, the diffusive force is allowed to have both elastic and fluid properties by having it depend upon $\underset{(1)}{\mathbf{F}}$, and $\underset{(2)}{\mathbf{L}}$ i.e. $\underset{(21)}{\mathbf{d}} = \hat{\underset{(21)}{\mathbf{d}}}\,(\rho_{(1)}, \rho_{(2)}, \underset{(21)}{\mathbf{v}}, \underset{(1)}{\mathbf{F}}, \underset{(2)}{\mathbf{L}})$

Finally, the interactions are generalized to the extent where each of the partial stresses and the diffusive force is allowed to share in the elastic, fluid, and diffusive properties of the mixture. In such a case it is assumed that

$$\underset{(1)}{\mathbf{T}} = \hat{\underset{(1)}{\mathbf{T}}}\,(\rho_{(1)}, \rho_{(2)}, \underset{(1)}{\mathbf{F}}, \underset{(2)}{\mathbf{L}}\ \underset{(21)}{\mathbf{v}})$$

$$\underset{(2)}{\mathbf{T}} = \hat{\underset{(2)}{\mathbf{T}}}\,(\rho_{(1)}, \rho_{(2)}, \underset{(1)}{\mathbf{F}}, \underset{(2)}{\mathbf{L}}, \underset{(21)}{\mathbf{v}})$$

and

$$\underset{(21)}{\mathbf{d}} = \hat{\underset{(21)}{\mathbf{d}}}\,(\rho_{(1)}, \rho_{(2)}, \underset{(1)}{\mathbf{F}}, \underset{(2)}{\mathbf{L}}, \underset{(21)}{\mathbf{v}})$$

It is felt that this last view is too general inasmuch as it is hard to distinguish what is fluid and what is solid. The two previous views, however, hold promising generalizations within the framework presented here.

Results and Recommendations

It is felt that the commonly used equations for flow of fluids through porous media lacks a well established framework. It was the purpose of this note to try to put the theory within a stronger framework as suggested by that commonly used in modern continuum mechanics. We feel that once established, the theory can be applied to many problems of interest in the study of gaseous or

References at end of paper

fluid media moving through coal. Work is presently being done to examine special solutions to some of the above cases. The two geometries that are felt to yield useful situations are the rectangular cartesian geometry as applicable to flow through coal beds, and the cylindrical geometry as applicable to well problems.

It is also pointed out that recently the mechanical theory has been extended to include thermodynamic fields as well as the possibility of the mixtures chemically reacting. Both of these extensions will be useful in the analysis now being carried out at U.S. ERDA in the underground coal gasification project.

Nomenclature

$\underset{\sim}{1}$ = identity tensor

$\underset{\sim}{a}_{(1)}$, $\underset{\sim}{a}_{(2)}$ = acceleration vectors of C_1 and C_2

$\underset{\sim}{a}$ = mean acceleration vector

$\underset{\sim}{a}_{(21)}$ = relative acceleration vector

$\underset{\sim}{B}$ = left Cauchy-Green tensor

$\underset{\sim}{b}$ = body force density

$\underset{\sim}{C}$ = right Cauchy-Green tensor

C_1, C_2 = constituents of the binary mixture

$\underset{\sim}{D}$ = stretching tensor

$\underset{\sim}{d}_{(21)}$ = diffusive force vector

D = diffusivity in Fick's Law

div = divergence operator

∇ = gradient with respect to the reference configuration

$\underset{\sim}{E}$ = Green's non-linear strain tensor

$\underset{\sim}{\varepsilon}$ = infinitesimal strain tensor

$\underset{\sim}{F}_{(1)}$, $\underset{\sim}{F}_{(2)}$ = deformation gradients of C_1 & C_2

$\underset{\sim}{F}_c$ = contact force

$\underset{\sim}{F}_b$ = body force

$\underset{\sim}{F}_e$ = external body force

$\underset{\sim}{F}_d$ = diffusive body force

grad = gradient with respect to the present configuration

K, k = permeabilities

$\underset{\sim}{L}$ = velocity gradient

λ_e, μ_e = Lame´ constants of elasticity

λ_v, μ_v = Lame´ constants of viscosity

p = pressure

ρ = total density

$\rho_{(1)}$, $\rho_{(2)}$ = densities of C_1 and C_2

ϕ = diffusive coefficient

ψ_0, ψ_1, ψ_2 = non-linear elasticities

ϕ_0, ϕ_1, ϕ_2 = non-linear viscosities

$\underset{\sim}{Q}$ = orthogonal rotation tensor

$\underset{\sim}{R}$ = rotation tensor

$\underset{\sim}{T}_{(1)}$, $\underset{\sim}{T}_{(2)}$ = partial stresses in C_1 and C_2

Tr = trace operator

( ) = transpose of the second order tensor

$\underset{\sim}{U}$ = right stretch tensor

$\underset{\sim}{u}$, $\underset{\sim}{u}$ = diffusion velocities

$\underset{\sim}{V}$ = left stretch tensor

$\underset{\sim}{v}$ = mean velocity

$\underset{\sim}{v}_{(1)}$, $\underset{\sim}{v}_{(2)}$ = velocities of C_1 and C_2

$\underset{\sim}{v}_{(21)}$ = relative velocity

$\underset{\sim}{W}$ = spin tensor

$\underset{\sim}{w}$ = angular velocity of two reference frames

$\underset{\sim}{X}_{(1)}$, $\underset{\sim}{X}_{(2)}$ = reference positions

$\underset{\sim}{x}_{(1)}$, $\underset{\sim}{x}_{(2)}$ = present positions

Acknowledgement

The author wishes to express his thanks to L. Zane Shuck for the opportunity to research and gather together, as well as extend, some of the more recent work in the mechanical theory of mixtures, so as to make it available to a larger audience of researchers working in the flow of fluids and gases through porous media. It is felt that such an approach can be used with much success in many of the ongoing researches at U.S. ERDA.

(1) Adkins, J. E.: "Non-Linear Diffusion I. Diffusion and Flow of Mixtures of Fluids," Phil. Trans. Roy. Soc. Lond. (1963) A 255, 607-633.

(2) Adkins, J. E.: "Non-Linear Diffusion II. Constitutive Equations for Mixtures of Fluids," Phil. Trans. Roy. Soc. Lond. (1963) A 255, 635-648.

(3) Adkins, J. E.: "Non-Linear Diffusion III. Diffusion Through Isotropic Highly Elastic Solids," Phil. Trans. Roy. Soc. Lond. (1964) A 256, 301-316.

(4) Collins, R. E.: "Flow of Fluids Through Porous Materials," Reinhold, New York.

(5) Crochet, M. J., P. M. Naghdi: "Constitutive Equations for Flow of a Fluid Through an Elastic Solid," Intern. J. Engng. Sci. (1966) 4, 383-401.

(6) Green, A. E., and J. E. Adkins: "A Contribution to the Theory of Non-linear Diffusion," Arch. Rational Mech. Anal. (1965) 15, 235-246.

(7) Muskat, M. "The Flow of Homogeneous Fluids through Porous Media," Edwards, Ann Arbor, Michigan.

(8) Streeter, V. L.: "Handbook of Fluid Dynamics," sec. 16, McGraw-Hill Book Co., Inc.

(10) Truesdell, C. L "Sulle basi della termomeccanica," Rend, Accad. Lincei (1958) English translation in Rational Mechanics of Materials. Intl. Sci. Rev. Ser. (1965) Gordon and Breach, New York.

(11) Truesdell, C. : "Mechanical Basis of Diffusion," J. Chem. Phys. (1962) 37, 2336-2344.

(12) Truesdell, C. : "The Elements of Continuum Mechanics," Springer-Verlag, New York Inc. 1966.

(13) Truesdell, C., and W. Noll L Handbuch der Physik, 111/3. Berlin-Heidellberg: Springer 1965.

(14) Truesdell, C., and R. A. Toupin: "Handbuch der Physik, 111/1. Berlin-Gottingen-Heidelberg: Springer 1960.

(15) Wang, C. C. "A New Representation Theorem for Isotropic Functions: Pt I," Arch. Rat. Mech. Anal. (1970) 36, 166-191.

(16) Wang, C. C. "A New Representation Theorem for Isotropic Functions: pt II," Arch. Rat. Mech. Anal. (1970) 36, 198-223.

SURFACE DIRECTIONAL PERMEABILITY ANALYZER

by

J. C. Huston
L. Z. Shuck
B. E. Slonneger
ERDA, Morgantown Energy Research Center
Morgantown, West Virginia

ABSTRACT

An in-situ method is presented which predicts the directional permeability constants of porous reservoir rocks. To accomplish this, a fluid is injected through the center of the permeability analyzer which is placed on a smooth surface of the porous permeable medium. The resulting surface pressure distribution is then measured. A finite difference technique is used which numerically solves the governing differential equations obtaining the three-dimensional pressure distribution. The directional permeability is then determined by applying a modified three-dimensional form of Darcy's law.

Tests were performed on Berea, Bradford, and Ohio sandstones and Pittsburgh coal to obtain the surface pressure distribution and the corresponding directional permeability constants. Oriented core samples were taken from the specimens tested to determine the validation/correlation of the directional permeabilities. The directional properties obtained by both methods were in agreement.

There are advantages of the surface directional permeability analyzer. The apparatus is portable, economical, and convenient which enables the researcher to perform on-site field studies. The device also allows for non-destructive testing. This is particularly useful in underground coal gasification where knowledge of the velocity and flow direction is essential in controlling the gas burn.

INTRODUCTION

In-situ energy extraction/conversion technology can be improved through better methods of characterizing reservoirs and their properties. Improved in-situ characterization techniques are needed for petroleum, natural gas and coal reservoirs. To better understand and control these processes a thorough knowledge of the numerous properties including a directional permeability is required. This paper discusses a new in-situ method for determining the directional permeabilities.

The objectives of this study were to develop a permeability analyzer, (permeameter), which has the following characteristics:

1. Three-dimensional directional permeability measurement
2. In-situ field application
3. Non-destructive testing for both the rock and apparatus
4. Portable
5. Applicable for any porous permeable medium

6. Simple and economical to use

Present permeameters do not contain these characteristics. The most widely used procedure for obtaining the permeability of a porous medium is to cut the rock into cylindrical cores which are placed inside a rubber washer so that air or some other gas will be forced through the rock parallel to the principle axis of that core. By measuring the pressure drop and the volumetric flow rate, the permeability along the axis of the core is obtained from Darcy's law.

Other laboratory methods similar to that described above have been developed by Batra [1] and Zoback [2]. Both of these methods are one-dimensional and still require drilling core samples. Smith and Phillips [3] have developed a simple, destructive in-situ procedure of measuring near surface permeabilitiy by cutting two rectangular chambers in the ground and allowing water to flow from one chamber to the other. Another instrument, developed by Eijpe and Weber [4], forces air through a one centimeter circular hole into the surface of the porous material. The pressure drop along with the flow rate determines the permeability. Two other permeameters, not directly related to this problem, were developed by Brock and Orr [5] using very low pressures, and the Klinkenberg permeability developed by Jones [6].

The study of coal permeability has been limited and confined primarily to the laboratory. The most recent research has been at the University of Pittsburgh [7,8] where a wide variation in the permeability of each coal sample was found. Permeabilities of coal obtained from core specimens are, in general, greatly different from the in-situ determined values. That is, due to the fragility of the cleat planes and the fact that tectonic stresses keep the small fissures closed under reservoir conditions, coring itself is a destructive procedure. This indicates that an in-situ method of measuring coal permeability is almost a necessity.

A number of studies have been concerned with determining the permeability of anisotropic materials, [9, 10, 11, 12, 13]. The majority of this research has been with laboratory techniques evaluating the permeability ratios of various sandstones. These ratios, which are defined as the maximum permeability divided by the minimum permeability of a material, usually range from 1 to 2 with sandstone compared to 1 to 10 with coal. Again, this would indicate a need for an in-situ technique of determining coal permeability.

Research evaluating the effects stress and temperature have on the permeability of materials were conducted by Klock [14], Hamsy [15], and Vairogs [16]. These studies are of interest because the effects are pertinent to the process of underground coal gasification.

The most recent and noteworthy theoretical studies of the flow of fluids through porous materials have been by Greenkorn [17], Al-Hussainy [18], and Whitaker [19]. Each of these papers gives a good state-of-the-art review.

THEORETICAL CONSIDERATIONS

Derivation of the equations is made under the following assumptions:

1. The fluid is assumed to be a perfect gas,
2. The gas is the same throughout the medium,
3. The gas is at a constant temperature everywhere in the field,
4. The porous medium is isotropic and homogeneous with uniform porosity and permeability, (for sandstone), and anisotropic, (for coal).

First, a pressure distribution based upon known flow laws is obtained. The appropriate continuity equation is:

$$-\underline{\nabla} \cdot (\rho \underline{v}) + G = \frac{\partial(\rho\phi)}{\partial\tau}$$

where; ρv - mass flux density, G - sources or sinks, ϕ - porosity.

References at end of paper.

From Collins [20], Darcy's law for an isotropic, porous media represents simple proportionalities between the components of the volumetric flux and the corresponding components of the gradient of the flow potential, thus:

$$\underline{v} = -\frac{\kappa\rho}{\mu}\,\underline{\nabla}\,\Phi$$

where: κ - permeability of the material, μ - viscosity of the fluid, ρ - density of the fluid, Φ - flow potential, and where the flow potential Φ is defined as

$$\Phi = \int_{P_o}^{P} \frac{dP}{\rho(P)}$$

This equation can be solved with the use of the perfect gas law:

$$\rho = \frac{P}{RT}$$

Substituting equation 4 into 3 and integrating yields:

$$\Phi = RT\ \ell n\ (\frac{P}{P_o})$$

Applying the del operator to equation 5 and noting that R, T, P_o are all constants, we obtain:

$$\nabla\Phi = RT\,\frac{P_o}{P}\,\nabla\,(\frac{P}{P_o}).$$

Becuase P_o is a constant, it can be taken out of the del operation sign and cancelled with the other P_o. By then applying the perfect gas law again equation 6 becomes:

$$\nabla\Phi = \frac{1}{\rho}\,\nabla P$$

This value for $\nabla\Phi$ can be substitued into equation 2 of Darcy's law thus:

$$v = -\frac{\kappa}{\mu}\,\nabla P$$

Substituting this equation into the continuity equation and noting that the porosity ϕ, the permeability κ, and the viscosity μ, are all assumed constant and that the system contains no sources or sinks equation 1 becomes:

$$\frac{\kappa}{\mu}\,\nabla(\rho\nabla P) = \phi\,\frac{\partial\rho}{\partial t}$$

By substituting the perfect gas law for ρ, the above equation becomes:

$$v \cdot (P\nabla P) = \frac{\mu\phi}{\kappa}\ \frac{\partial\rho}{\partial t}$$

which can be transformed into:

$$(\nabla P)^2 + P\nabla^2 P = \frac{\mu\phi}{\kappa}\ \frac{\partial\rho}{\partial t}$$

by carrying out the gradient operation. If the following identities are used:

$$\nabla^2 P^2 = 2\,(\nabla P)^2 + 2\,P\nabla^2 P$$

and

$$\frac{\partial P}{\partial t} = \frac{1}{2P}\ \frac{\partial P^2}{\partial t}$$

equation 11 becomes:

$$\nabla^2 P^2 = \frac{\mu\phi}{\kappa P}\ \frac{\partial P^2}{\partial t}$$

Consider now the problem of a flow stream of radium R_1 entering a porous material with a volumetric flow rate q, and pressure P_1. The material is considered to be an infinite half-space but it can also be assumed that the physical boundaries of the medium R_3 and Z_3 are sufficiently large that at least 95% of the total flow pattern has been expelled. The surface boundary condition is such that an impermeable washer barrier of inside and outside radius R_1 and R_2 respectively is placed on the porous material, (z=0), so that all of the gas is subsequently flowing out beyond R_2.

For this problem, it is most convenient to select cylindrical coordinates where the del square operator is defined as:

$$\nabla^2 = \frac{\partial^2}{\partial r^2} + \frac{1}{r}\frac{\partial}{\partial r} + \frac{1}{r^2}\frac{\partial^2}{\partial \theta^2} + \frac{\partial_2}{\partial z^2}$$

On expanding the equation 15 in 14 the following is obtained.

$$\frac{\partial^2 P^2}{\partial r^2} + \frac{1}{r}\frac{\partial P^2}{\partial r} + \frac{1}{r^2}\frac{\partial^2 P^2}{\partial \theta^2} + \frac{\partial^2 P^2}{\partial z^2} = \frac{\phi\mu}{\kappa P}\frac{\partial P^2}{\partial t}$$

If ϕ and κ are assumed constant, and the pressure P is not a function of θ, then

$$\frac{\partial^2 P^2}{\partial \theta^2} = 0$$

and for steady state,

$$\frac{\partial P^2}{\partial t} = 0$$

such that equation [16] becomes

$$\frac{\partial^2 P^2}{\partial r^2} + \frac{1}{r}\frac{\partial P^2}{\partial r} + \frac{\partial^2 P^2}{\partial z^2} = 0$$

There are a number of approaches which can be used to solve equiation [19]. Using the separation of variables method, assume a linear solution in terms of the pressure squared of the form:

$$P^2 = R\,(r)\,Z\,(z)$$

By substituting this equation into [19] and dividing by RZ gives:

$$\frac{R''}{R} + \frac{R'}{rR} + \frac{Z''}{Z} = 0$$

Then by taking the Z terms to the right hand side of the equation and equating both sides to a constant $-\lambda^2$, the following is obtained:

$$\frac{R''}{R} + \frac{R'}{rR} = -\frac{Z''}{Z} = -\lambda^2$$

Equation [22] now contains two ordinary differential equations of the form:

$$Z'' - \lambda^2 Z = 0$$

and

$$R'' + \frac{R'}{r} + \lambda^2 R = 0$$

Equation [23] can be solved as an exponential function with a solution of the form:

$$Z\,(z) = Ae^{-\lambda z} + Be^{\lambda z}$$

Equation [24] is a Bessell function with solution of the form:

$$R(r) = C J_o(\lambda r) + D Y_o(\lambda r)$$

Upon substitution of equations [25] and [26] into equation [20], the expression for the pressure distribution becomes:

$$P^2 = [Ae^{-\lambda z} + Be^{\lambda z}] [CJ_o(\lambda r) + DY_o(\lambda r)]$$

Since this is a physically real problem, the solution must be of the form such that P^2 is a finite number everywhere within the field. It can be concluded then that the constants B and D must be equal to zero such that $Y_o(0) = -\infty$ and $e^{\infty} = \infty$ yield infinite solutions: Thus, P^2 becomes:

$$P^2 = \sum_{n=1}^{\infty} [F_n J_o(\lambda n r) e^{-\lambda n z}]$$

For the particular problem of the washer barrier resting on top of the porous medium the boundary conditions are:

$$\begin{aligned} P(r,0) &= f_0^{P_1}(r) && 0 \le r \le R_1 \\ P(r,Z_3) &= 0 && R_1 \le r \le R_2 \\ P(R_3,z) &= 0 && R_2 \le r \le R_3 \end{aligned}$$

where f(r) is measured from the analyzer. By applying the boundary conditions [30] and [31] to equation [28] and recalling that both R_3 and Z_3 are sufficiently large so that at least 95% of the total flow has been expelled, the λ_n's can be obtained from the zeros of the Bessel functions, $J_o(\lambda_n R_3) = 0$. These boundary conditions are naturally satisfied when R_3 and Z_3 approach infinity. The other boundary condition when z = 0 yields:

$$P^2(r,0) = \sum_{n=1}^{\infty} F_n J_o(\lambda_n r) = \begin{cases} P_1^2 & 0 \le r \le R_1 \\ f(r) & R_1 \le r \le R_2 \\ 0 & R_2 \le r \le R_3 \end{cases}$$

Then from the Fourier-Bessel series, the function F_n is obtained:

$$F_n = \{[\int_0^{R_1} rP_1^2 J_o(\lambda_n r)\, dr + \int_{R_1}^{R_2} rf^2(r) J_o(\lambda_n r)\, dr] \Big/ \int_0^{R_3} rJ_o^2(\lambda_n r)\, dr\}$$

To determine the directional permeability of the porous medium, a three-dimensional modified form of Darcy's law is applied. The cross-sectional area term in the one-dimensional Darcy's law is changed to a hemispherical surface area where:

$$K_z = \frac{q\mu}{2\pi R_1^2 \frac{\partial p}{\partial z}}$$

and

$$K_r = \frac{q\mu}{C_1 \frac{\partial p}{\partial r}}$$

and where $\frac{\partial p}{\partial r}$ and $\frac{\partial p}{\partial z}$ are obtained by differentiating equation [32]. C_1 is an empirically adjusted constant related to the flow area.

The above equations were derived under the assumption that the porous material is isotropic and homogeneous, as is reasonable for many sandstones. However, coal is anisotropic and non-homoge-

Therefore, the derivation is valid only up to equation [16] if K is considered constant or equation [8] if K is allowed to vary. Closed form solutions for the pressure distribution through anistropic material become intractable. Thus, a finite difference technique was employed to solve equation [16]. Here the surface pressure measured from the analyzer along with the requirement of a zero pressure condition elsewhere on the rock's surface is sufficient to solve for the total pressure distribution. The permeability is again obtained through equations [34] and [35]. If K varies significantly, an iterative technique is applied using the predicted permeability values and equation

[8]. The finite difference routine is then repeated until no further change in the permeability values are detected.

Experimental Apparatus and Test Procedure

Two prototype permeability analyzers were constructed for this investigation. The first was made from a 5" (12.7 cm) diameter - 1/2" (1.27 cm) thick stainless steel plate. In this plate, 40 1/8" (0.3175 cm) diameter manometer holes were drilled in a radial pattern. These holes were spaced at 1/2" (1.27 cm) intervals in rows located every 45 degrees. An additional hole, 1/4" (0.635 cm) in diameter, was drilled at the plate's center for an inlet air source. Each manometer was assembled by connecting two 1/100 ml Corning Glass disposable pipets together with 1/4" (0.635 cm) flexible tygon tubing. A third pipet was used to support the manometer and then cemented into one of the plate's 1/8" (0.3175 cm) diameter holes with RTV. Colored water was inserted as the manometer fluid.

The second analyzer, constructed in a similar manner to the first, was made from the 8" (20.32 cm) diameter - 1" (2.54 cm) thick stainless steel plate, (Figure 1). There were 56 - 1/4" (0.635 cm) diameter manometer holes drilled and spaced in a radial pattern, (Figure 2). The inlet air hole was a 1/2" (1.27 cm) diameter hole drilled at the plate's center. Each manometer was assembled from four 1/100 ml glass pipets and filled with mercury. Rubber and plastic gaskets were made to enable a good seal between the analyzer and the porous medium.

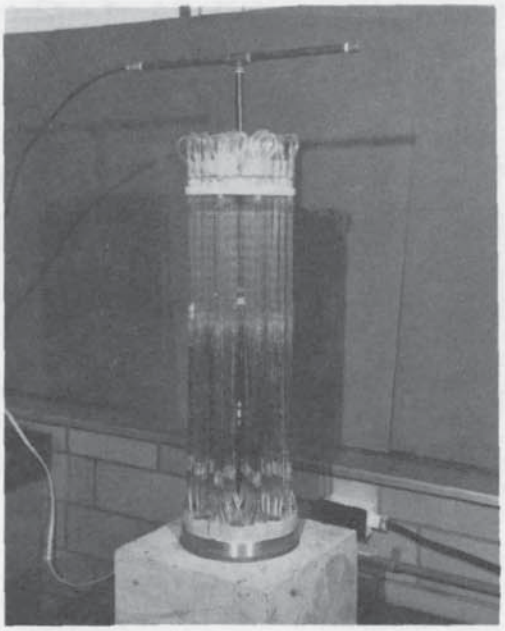


Figure 1
8" Permeability Analyzer

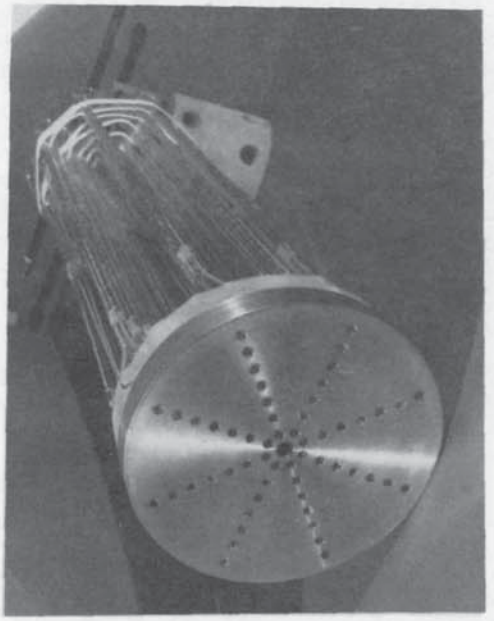


Figure 2
Bottom view of analyzer plate showing pressure response locations.

Figure 3 shows a schematic diagram of the equipment used in the overall setup. Air was obtained from a 100 psi line source and passed through a pressure regulator, volumetric flow meter, and a pressure gage before reaching the analyzer's center inlet air hole. The resulting pressure distribution was obtained from the manometers.

A determination of the amount of overall pressure needed to seal the analyzer to the porous medium was also made. Using both a rubber and a plastic gasket, a 5" (12.7 cm) diameter - 1" (2.54 cm) thick plexiglass plate with one inlet air hole and one manometer hole was placed on a 6" cube of sandstone. This plate was then loaded in a Tinius-Olsen testing machine until no further

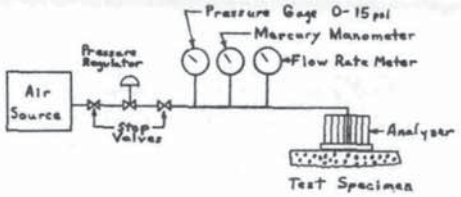


Figure 3 - Schematic Diagram of Experimental Apparatus.

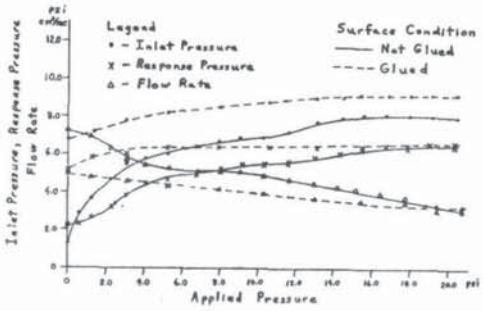


Figure 4 - Analyzer Response Characteristics Under Compressive Loading Using Rubber Gasket.

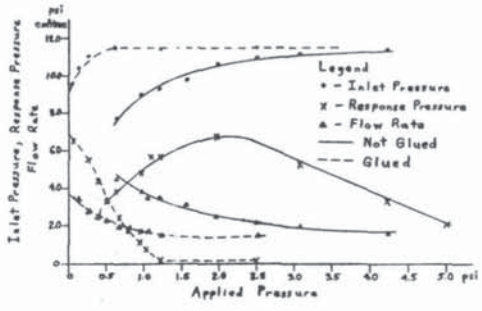


Figure 5 - Analyzer Response Characteristics Under Compressive Loading Using Plastic Gasket.

change in the inlet pressure, manometer deflection, or volumetric flow rate occurred. These results plotted in Figures 4 and 5 show that approximately 2 psi (13790 N/m^2) is needed to make an effective seal for these materials. The inlet pressure applied through the center of the plate tends to lift the analyzer from the rock's surface, and also a counter pressure is needed to close the outer layer of pores or surface features with the gasket.

The experimental procedure for obtaining the surface pressure distribution is as follows:

1. Prepare a smooth flat surface on the porous medium such that the RMS roughness is that of the grain structure. Spray the surface with high pressure air to remove dust particles.

2. Cement the gaskets to the analyzers, assuring that each gasket is aligned properly and that each manometer hole is open.

3. Place the 5" (12.7 cm) diameter analyzer on the test specimen to determine the rock's directional properties. Rotate and translate the analyzer to determine local phenomena and to obtain a statistical average.

4. Use the 8" diameter (20.32 cm) diameter analyzer on the same specimen but in addition, cement the gasket to the rock. Add weight to the plate until the appropriate sealing pressure is reached.

5. Analyze the results of the surface pressure distribution to determine directional permeability by using the finite difference technique and a three-dimensional form of Darcy's law.

6. Validate and correlate the results with standard permeametor core samples taken from the test specimen.

Conclusions

Tests were performed on Berea, Bradford, and Ohio sandstones and Pittsburgh coal to obtain the surface pressure distribution and corresponding directional permeability constants. These results are listed in tabular form in the Appendix. Conventional 3/4" x 1" core samples were drilled and evaluated on the Bradford and Ohio sandstones, (Figure 6), to determine the validation/correlation of their directional permeabilities (see tests 1 through 4). In general, when comparing the results of both methods, the analyzer showed similar directional properties and permeability values as those obtained from the core samples. However, any discrepancy can be accounted for because of the air leakage between the analyzer and the porous medium in addition to using an extended form of Darcy's law in three dimensions.

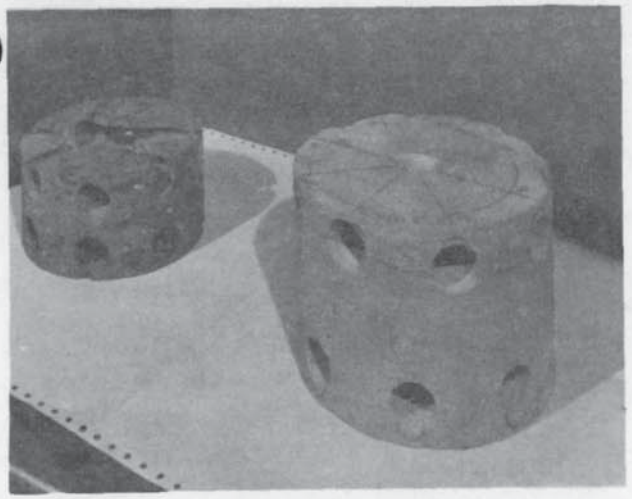


Figure 6 - Cored Samples Bradford and Ohio Sandstone

Tests 5 through 10 included evaluations of Berea sandstone and Pittsburgh coal. Air leakage experienced in the earlier tests was kept to a minimum by using the 8" diameter mercury analyzer with a soft deformable plastic gasket together with applying 7 psi confining pressure.

In summary, the developed surface directional permeability analyzer exhibits the following advantages. It is a non-destructive in-situ field apparatus which can predict the steady-state directional permeability of any porous medium. The analyzer also gives an immediate visualization of the surface pressure distribution. Preliminary results indicate a definite directional permeability pattern coinciding with those obtained from conventional core samples.

Future work for this project includes an on-site field study to determine the directional properties of coal. Also planned is a further development of the experimental apparatus together with refining the theoretical derivation. In addition, development of the bore hole directional permeability analyzer will be performed. This apparatus will have particular applications to underground gasification of eastern coal.

TABLE 1. TEST NO. 1

Flow Rate - 4.4 $cm^3/sec.$
Inlet Pressure - 1.46 psi
Type of Material - Ohio sandstone (6" core)
Analyzer used - 5" water manometers

Pressure Response Mean Values (psi)

Location/Angle	0	45	90	135	189	225	270	315
0.5"	0.239	0.228	0.227	0.225	0.230	0.217	0.214	0.233
1.0"	0.098	0.089	0.087	0.092	0.095	0.095	0.095	0.094
1.5"	0.049	0.020	0.018	0.049	0.046	0.053	0.050	0.046
2.0"	0.022	0.007	0.007	0.022	0.020	0.024	0.016	0.021
2.5"	0.002	0.001	0.001	0.022	0.002	0.003	0.002	0.001
Predicted $K^{(md)}$	1978	2006	1992	2096	2065	2285	2343	2006
Cored K	3508	3723	4009	4781	4348	3646	3198	4239

TABLE 2. TEST NO. 2

Flow Rate - 2.2 $cm^3/sec.$
Inlet Pressure - 0.734 psi
Type of Material - Ohio sandstone (6" core)
Analyzer used - 5" water manometers

Pressure Response Mean Values (psi)

Location/Angle	0	45	90	135	180	225	270	315
0.5"	0.195	0.249	0.252	0.249	0.279	0.256	0.259	0.197
1.0"	0.064	0.068	0.130	0.123	0.140	0.167	0.092	0.067
1.5"	0.036	0.034	0.057	0.082	0.084	0.093	0.043	0.040
2.0"	0.009	0.014	0.022	0.064	0.058	0.049	0.019	0.009
2.5"	0.001	0.002	0.004	0.013	0.019	0.007	0.003	0.001
Predicted $K^{(md)}$	1064	770	1143	1106	1003	1567	835	1072
Cored K	1354	970	590	416	1330	1948	2235	2796

Table 3. Test No. 3

Flow Rate - 0.24 cm^3/sec.
Unlet Pressure - 0.491 psi
Type of Material - Bradford Sandstone (6" Core)
Analyzer used - 5" water monometers

Pressure Response Mean Values (psi)

Location/Angle	0	45	90	135	180	225	270	315
0.5"	0.246	0.236	0.241	0.236	0.254	0.250	0.242	0.229
1.0"	0.140	0.171	0.193	0.163	0.173	0.186	0.150	0.133
1.5"	0.088	0.119	0.185	0.118	0.107	0.122	0.121	0.078
2.0"	0.033	0.082	0.159	0.072	0.058	0.071	0.111	0.038
2.5"	0.003	0.018	0.000	0.014	0.010	0.018	0.039	0.007
Predicted $K^{(md)}$	143	234	317	208	188	238	165	158

Table 4. Test No. 4

Flow Rate - 0.18 cm^3/sec
Inlet Pressure - 0.378 psi
Type of Material - Bradford Sandstone (6" core)
Analyzer used - 5" water monometers

Pressure Response Mean Values (psi)

Location/Angle	0	45	90	135	180	225	270	315
0.5"	0.253	0.255	0.260	0.267	0.266	0.214	0.229	0.269
1.0"	0.185	0.192	0.185	0.186	0.078	0.007	0.010	0.192
1.5"	0.141	0.103	0.057	0.128	0.009	0.003	0.005	0.148
2.0"	0.091	0.082	0.028	0.052	0.003	0.000	0.001	0.061
2.5"	0.016	0.024	0.003	0.008	0.000	0.000	0.000	0.004
Predicted $K^{(md)}$	168	181	152	141	61	55	52	148

Table 5 Test No. 5

Flow Rate - 5.0 cm^3/sec.
Inlet Pressure - 7.4 psi
Type of Material - Berea Sandstone (1' cube)
Analuzer used - 8" Mercury Manometers

Pressure Response Mean Values (psi)

Location/Angle	0	45	90	135	180	225	270	315
0.5	6.664	5.882	2.958	2.652	2.890	3.128	4.964	6.358
1.0	4.250	NR	1.462	1.360	1.224	1.598	1.836	4.896
1.5	3.026	NR	0.612	0.272	0.136	0.442	0.850	0.714
2.0	0.102	0.340	0.102	0.374	0.306	0.272	0.578	0.612
2.5	0.034	0.102	0.034	0.170	0.306	0.272	0.340	0.374
3.0	NR	NR	NR	0.102	0.204	0.238	0.204	0.170
3.5	NR	NR	NR	0.017	0.170	0.170	0.102	0.034
Predicted $K^{(md)}$	131	176	212	245	190	207	101	217
Cored K	56	111	60	101	103	118	70	87

Table 6 Test No. 6

Flow Rate - 5.0 cm^3/sec.
Inlet Pressure - 7.5 psi
Type of Material - Berea Sandstone (1" cube)
Analyzer used - 8" Mercury Monometers

	Pressure Response Mean Value (psi)							
Location/Angle	0	45	90	135	180	225	270	315
0.5	0.868	6.800	6.766	6.834	6.732	6.630	6.578	6.596
1.0	2.074	NR	1.870	2.244	3.094	2.278	1.734	3.672
1.5	1.020	0.782	0.646	0.510	0.986	0.884	0.578	0.782
2.0	0.442	0.340	NR	0.544	0.816	0.204	0.340	NR
2.5	0.272	0.238	0.034	0.374	0.306	0.238	0.170	0.272
3.0	0.034	0.034	0.068	0.170	0.136	0.170	0.068	0.034
3.5	NR	0.034	0.034	0.068	0.034	NR	0.034	0.034
Predicted $K^{(md)}$	66	79	65	69	87	73	66	108
	109	92	115	46	122	91	89	112

Table 7 Test No. 7

Flow Rate - 5.0 cm^3/sec.
Inlet Pressure - 7.8 psi
Type of Material - Berea Sandstone (1' cube)
Analyzer used - 8" Mercury Monometers

	Pressure Response Mean Value (psi)							
Location/Angle	0	45	90	135	180	225	270	315
0.5	7.140	7.106	7.072	6.970	7.072	7.004	6.902	6.868
1.0	2.278	NR	1.564	2.244	1.700	1.802	1.224	3.638
1.5	1.020	0.034	0.612	0.884	1.632	0.680	0.408	0.476
2.0	0.408	0.306	0.306	0.204	0.238	0.270	0.272	0.272
3.0	0.102	0.204	0.068	0.034	0.136	0.170	0.068	0.034
3.5	0.068	0.034	0.034	0.068	0.034	0.034	0.034	0.034
Predicted $K^{(md)}$	65	58	58	67	59	61	56	98
	230	260	256	248	222	268	278	270

Table 8 Test No. 8

Flow Rate - 5.0 cm^3/sec.
Inlet Pressure - 7.6 psi
Type of Material - Berea Sandstone (1' x 2' x 2')
Analyzer Used - 8' Mercury Manometers

	Pressure Response Mean Value (psi)							
Location/Angle								
0.5	6.868	6.766	6.766	7.140	7.038	6.092	6.664	6.800
1.0	3.026	1.734	2.822	3.536	3.672	3.774	2.822	3.944
1.5	1.428	9.340	1.122	0.748	2.006	0.782	0.714	1.224
2.0	0.612	0.374	0.374	0.782	0.952	0.816	0.612	0.442
2.5	0.170	0.340	0.374	0.034	0.476	0.408	0.408	0.340
3.0	0.136	0.204	0.102	NR	0.136	0.306	0.170	0.238
3.5	0.034	0.034	NR	0.068	0.034	0.068	0.170	0.102
Predicted $K^{(md)}$	82	63	80	88	94	101	82	111

Table 9 Test No. 9

Flow Rate - 0.25 cm^3/sec.
Inlet Pressure - 0.5 psi
Type of Material - Pittsburgh Coal
Analyzer used - 5" Water Manometers

Pressure Response Mean Value (psi)

Location/Angle								
0.5	0.244	0.268	0.259	0.216	0.223	0.224	0.254	0.244
1.0	0.223	0.175	0.228	0.149	0.106	0.148	0.200	0.199
1.5	0.149	0.115	0.048	0.053	0.084	0.100	0.104	0.073
2.0	0.028	0.094	0.015	0.021	0.024	0.035	0.069	0.014
2.5	NR	NR	0.001	0.001	NR	NR	0.010	NR
Predicted $K^{(md)}$	748	170	511	236	135	208	293	352

Table 10 Test No. 10

Flow Rate - 0.5 cm^3/sec.
Inlet Pressure - 7.0 psi
Type of Material - Coal (1' cube)
Analyzer used - 8" mercury monometers

Pressure Response Mean Valves (psi)

Location/Angle								
0.5"	4.556	4.794	6.460	NR	3.434	5.984	6.596	6.528
1.0"	NR	NR	NR	NR	NR	NR	NR	NR
$K^{(md)}$	12.9	14.3	58.7	4.5	8.9	31.2	78.4	67.1

NOMENCLATURE:

A - cross sectional area
G - sources and sinks
K - permeability
L - length of core sample
$\dot{m}$ - mass of flow rate
p - pressure
q - volumetric flow rate
R - gas constant
r - radial component
T - temperature
t - time
V - volume
v - velocity
z - vertical component
Θ - transverse component
μ - viscosity
ρ - density
Φ - flow potential
ϕ - porosity

ACKNOWLEDGEMENT

The authors wish to thank Jerry Chidester, Mike Pellegrin, Harold Shoemaker and Frank Slagle of MERC for their helpful suggestions and assistance in conducting the tests.

REFERENCES

1. Batra, V. K. and Dullien, F. A. L., "Measuring Permeability of Porous Media, "Chemical Engineering, Vol. 81, p. 92, Sept. 2, 1974.

2. Zoback, M. D. and Byerlee, J. D., "Permeability and Effective Stress," The American Association of Petroleum Geologists, Vol. 59, No. 1, pp. 154-158, Jan. 1975.

3. Smith, T. N. and Phillips, C. R., "Determination of Permeability Profile of Surface Terrain," Environmental Science and Technology, Vol. 8, pp. 1020-1023, 1974.

4. Eijpe, R. and Weber, K. J., "Mini-Permeameters for Consolidated Rock and Unconsolidated Sand," The American Association of Petroleum Geologists Bulletin, Vol. 55, pp. 307-309, Feb. 1971.

5. Brock, J. F. and Orr, C., "Permeametry in the Knudsen-Flow Regime," Analytical Chemistry, Vol. 44, pp. 1534-1537, 1972.

6. Jones, S. C., "A Rapid Accurate Unsteady-State Klinkenberg-Permeameter," Society of Petroleum Engineers Journal, pp. 383-397, Oct. 1972.

7. Reznik, A. A., Dabbous, M. K., Fulton, P. F., and Taber, T. J., "Air-Water Relative permeability Studies of Pittsburgh and Pocahontas Coals," Society of Petroleum Engineers Journal, Vol. 257, pp. 556-562, 1974.

8. Dabbous, M. K., Reznik, A. A., Taber, J. J., and Fulton, P. F., "The Permeability of Coal to Gas and Water," Society of Petroleum Engineers Journal, Vol. 257, pp. 563-572, 1974.

9. Rinard, R. E., "Analog Simulation of Anisotropic Permeability," Master's Thesis, Department of Petroleum Engineering, Louisianna State University, Baton Rouge, La., May 1974.

10. Gray, D. H., Fatt, I., and Bergamini, G., "The Effect of Stress on Permeability of Sandstone Cores," Society of Petroleum Engineers Journal, pp. 95-100, June 1963.

11. Raghavan, R. and Clark, K. K., "Vertical Permeability from Limited Entry Flow Tests in Thick Formations," Society of Petroleum Engineers Journal, pp. 65-73, Feb. 1975.

12. Ramey, H. J., Jr., "Interference Analysis for Anisotropic Formations - A Case History," Journal of Petroleum Technology, pp. 1290-1298, Oct. 1975.

13. Hollabaugh, G. R., and Slotboom, R. A., "A Vertical Permeability Study," Society of Petroleum Engineers Journal, pp. 199-210, June 1972.

14. Klock, G. O., Boessma, L., and DeBacker, L. W., "Pore Size Distributions as Measured by the Mercury Intrusion Method and Their Use in Predicting Permeability," Soil Science Society of America, Proceedings, Vol. 33, 1969.

15. Homsy, G. M. and Sherwood, A. E., "Convective Instabilities in Porous Media with Through Flow," AIChE Journal, Vol. 22, pp. 168-174, Jan. 1976.

16. Vairogs, J., Hearn, C. L., Dareing, D. W., and Rhoades, V. W., "Effect of Rock Stress on Gas Production from Low-Permeability Reservoirs," Journal of Petroleum Technology, pp. 1161-1167, Sept. 1971.

17. Greenkorn, R. A., and Kessler, D. P., "Dispersion in Heterogeneous Nonuniform Anisotropic Porous Media, " Industrial and Engineering Chemistry, Vol. 61, pp.14-32, Sept. 1969.

18. Al-Hussainy, R., "The Flow of Real Gases Through Porous Media," Journal of Petroleum Technology, pp. 624-642, May, 1966.

19. Whitaker, S., "Advances in Theory of Fluid Motion in Porous Media," Industrial and Engineering Chemistry, Vol. 61, pp. 14-28, Dec. 1969.

20. Collins, R. E., Flow of Fluids through Porous Materials, Reinhold Publishing Corporation, New York, 1961.

ALGORITHM FOR COST EFFECTIVENESS OF DIRECTIONAL VERSUS VERTICAL WELL DRILLING

by

B. E. Slonneger, MERC, ERDA

ABSTRACT

The advantages and disadvantages of directional and vertical well drilling for underground coal gasification are well worth comparing. Basically, directional well drilling involves drilling a hole at a changing angle of inclination to a desired depth, then boring a horizontal hole the length of the coalbed. These are drilled in sets of not less than two wells. In vertical well drilling, vertical holes are spaced in two rows along the coalbed length and connected by burning through the coalbed. The cost ratio between the two methods involves the amount of pipe needed, the length of time for drilling and installation of the pipe, as well as the consideration of other factors influencing cost. Once the ratio of cost is established and compared for various depths of beds, number of vertical wells, and dimensions of gasification cells, the more economical method of drilling can be evaluated.

FACTORS CONSIDERED

Directional and vertical well drilling, Fig. 1, can be compared only after equations are determined for length drilled, time for drilling, and total cost. The simplified and generalized equations are shown in Table I. The time equations reflect the drilling and installation time of the pipe, distance drilled and difficulty of the drilling, as well as the horizontal linkage burn time between vertical wells. The cost equations are based on the cost of the material, pipe, linkage of vertical wells, and the hourly cost of drilling. For consistency, the coalbeds are assumed to be in the Eastern region, approximately 6 ft (1.8 m) in thickness rather than the thicker Western beds. The ratio of costs does not include several factors that influence the final cost because, for simplicity, it is assumed the costs for these are basically the same for both methods. The algorithm could be further refined in future studies to include costs for machinery, preparation, and site surveying. In general, numerous smaller costs such as for drilling mud, etc., are ignored; the rationale being that the costs are proportional to the total length of drilling and cancel out in the final ratio.

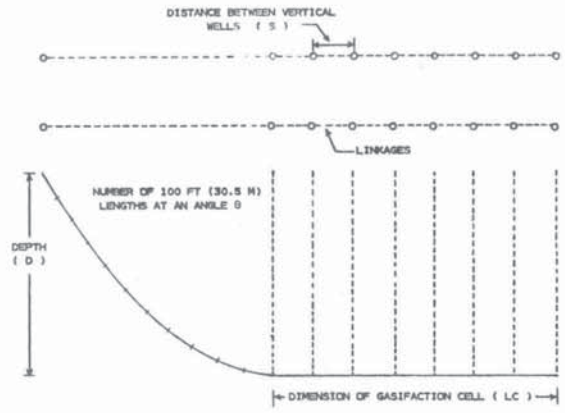


FIG. 1 SUPERIMPOSED SCHEMATIC OF DIRECTIONAL AND VERTICAL DRILLING

FORMULATION

After the equations are set, the next step is substituting values for the variables. As seen in Table II, the total cost of pipe per foot includes the cost of pipe, cement, and cost of installing and cementing the pipe in place. In order that the flow in the pipe of the two methods is equal,

TABLE I. EQUATIONS

$$D = \sum_{x=1}^{Z} 100 \cos (x \Theta) \qquad HN = 2 \cdot (LC / S + 1)$$

Length Drilled*

$$TL1 = 2 \cdot (100 \cdot Z + LC)$$

$$TL2 = (HN \cdot D) + (HN - 1) \cdot S$$

$$RTL = TL2 / TL1$$

Drilling Time*

$$TIME1 = 2 \cdot (100 \cdot Z \cdot TA + LC \cdot TH)$$

$$TIME2 = (HN \cdot D \cdot TV) + ((HN - 1) \cdot S \cdot TL)$$

$$RTIME = TIME2 / TIME1$$

Cost

$$C1 = TL1 \cdot XA + TIME1 \cdot XC$$

$$C2 = (HN \cdot D \cdot XB) + ((HN - 1) \cdot S \cdot XD) + (TIME2 \cdot XC)$$

$$RC = C2 / C1$$

*includes linkage (burned through not drilled) between vertical wells

the diameters are different; thus, the pipe cost also reflects this difference. The drilling times are set realistically, but somewhat arbitrarily. Since the state-of-the-art for both drilling methods is not the same, it is reasonable to make estimates for the various variables in the equations which do not necessarily hold at the present, but which could be true when the technologies are more equal. Even though the ratio of directional/vertical drilling time is approximately sixty at the present, it is expected to decrease to twenty in the future. However, for a matter of comparison, the ratio of directional/vertical drilling time ranges from four to twenty to determine the range in which directional well drilling becomes economical.

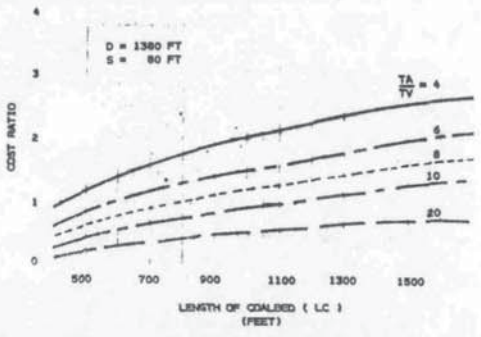


FIG 2. COST RATIO OF VERTICAL TO DIRECTIONAL WELL DRILLING VS. LENGTH OF COALBED

Different cost ratios are obtained by varying the depth to coal bed, horizontal length of bed, well spacing (vertical holes only) and angles of directional drilling by the increments shown in Table II. As expected, the cost ratio (vertical well drilling/ directional well drilling) increases as the horizontal distance in the coal seam becomes longer and the bed deeper, Figs. 2 & 3, and as the vertical wells are drilled closer together, Fig. 4. The cost depends almost entirely on the time for drilling, since time is overwhelmingly the most expensive commodity, Table III.

TABLE II. VALUES FOR VARIABLES

Variance of D, LC, and S

Depth to coalbed (D):
900 ft to 1860 ft (274.3 m to 566.9 m)
(Caused by varying angle drilled Θ from 3° to 6° / 100 ft)

Distance between vertical wells (S):
60 ft to 200 ft (18.3 m to 61.0 m)

Length of horizontal coalbed (LC):
500 ft to 1500 ft (152.4 m to 457.2 m)

Drilling and Linkage Times

TA = 2.60 to 13.00 hr / ft

TH = 2.00 hr / ft

TL = 2.00 hr / ft

TV = 0.65 hr / ft

Costs

XA = $ 11.45 / ft
(Pipe = $ 5.50 / ft
Cement = 2.52 / ft
Cost of cementing in place = 3.43 / ft
TOTAL = $11.45 / ft

XB = $ 8.60 / ft

XD = $ 8.00 / ft

XC = $ 125.00 / ft

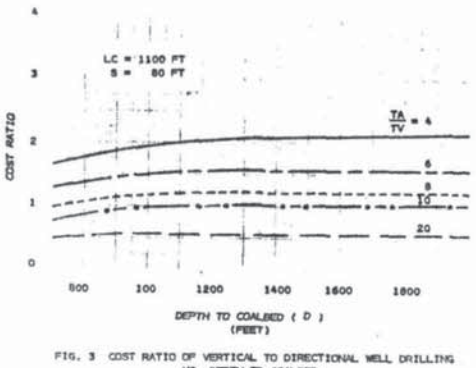


FIG. 3 COST RATIO OF VERTICAL TO DIRECTIONAL WELL DRILLING VS. DEPTH TO COALBED

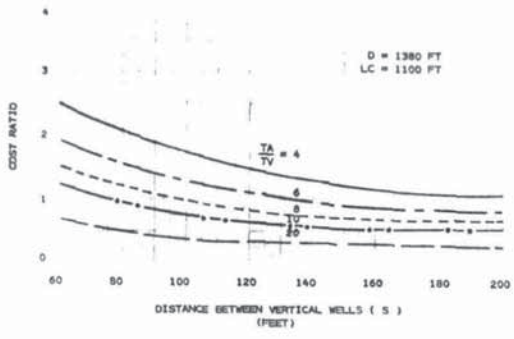


FIG. 4 COST RATIO OF VERTICAL TO DIRECTIONAL WELL DRILLING VS. DISTANCE BETWEEN VERTICAL WELLS

TABLE III. SAMPLE RESULTS

D and S constant (D = 1860 ft
S = 60 ft)

TA/TV = 4

LENGTH OF COALBED (feet)	RATIOS OF VERTICAL TO DIRECTIONAL WELL DRILLING		
	LENGTH DRILLED	DRILLING TIME	TOTAL COST
500	5.1099	1.4023	1.4877
700	6.5629	1.8227	1.9328
900	7.8668	2.2081	2.3404
1100	9.0436	2.5627	2.7153
1300	10.1109	2.8899	3.0610
1500	11.0833	3.1930	3.3810

RESULTS AND CONCLUSIONS

When calculations are made using the data shown in Table II, and setting the directional drilling time equal to four times the vertical drilling time, a cost ratio greater than one is obtained for almost all of the combinations of horizontal distance in the bed and depth of the bed. This shows that directional well drilling is more economical using the above estimates. Slight changes in any of the drilling times or substantial costs adjustments also effect which method is the more economical. For example, increasing the ratio of directional/vertical drilling time to ten and considering drilling horizontally in coalbeds 1000 ft (304.8 m) and over in length, directional well drilling is more economical all the time when the distance between vertical wells is 60 ft (24.4 m), 75% of the time when the distance is 80 ft (18.3 m) and never economical when the holes are spaced 200 ft (61.0 m) apart. Therefore, directional well drilling becomes more economical than vertical well drilling only when the ratio of directional/vertical drilling time is between four and ten, depending on the depth to the coalbed, horizontal distance in the coalbed, and vertical well spacing.

The approach used in this study is purposely simplified, ignoring several factors, and assuming others; but, it leads to the following valid conclusions: The deeper and longer the horizontal hole in the coalbed, the more economical directional well drilling becomes and the amount of time involved in drilling also determines economy. Vertical well drilling is considered by most to be more economical at the present due to the extra time directional drilling involves. However, in the future, if directional well drilling is further advanced so that the ratio of directional/vertical drilling time ranges between four and ten, it could well be economical. It may be too early to tell which will be the method of the future, but it seems logical that the final decision will be based not only on economy, but on other advantages and disadvantages as well.

NOMENCLATURE

C1 = cost of directional drilling, dollars

C2 = cost of vertical drilling, dollars

D = depth to coalbed, ft

HN = number of vertical wells drilled

LC = length of horizontal hole in coalbed, ft

RC = ratio of cost of vertical to directional drilling

RTIME = ratio of drilling time of vertical to directional drilling

RTL = ratio of length drilled of vertical to directional drilling

S = distance between vertical wells (well spacing), ft

TA = directional drilling time (on an angle), hr/ft

TH = horizontal drilling time (directional), hr/ft

TIME1 = total drilling time for directional drilling, hr

TIME2 = total drilling and linking time for vertical drilling, hr

TL = horizontal linkage (burning) time between vertical holes, hr/ft

TL1 = total length drilled (directional), ft

TL2 = total length drilled and linked (vertical), ft

TV = vertical drilling time, hr/ft

XA = cost of pipe and cement (directional), dollars/ft

XB = cost of pipe and cement (vertical), dollars/ft

XC = cost of time (labor), dollars/hr

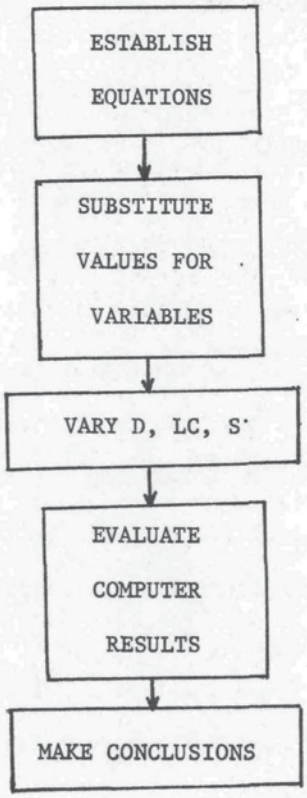
XD = cost of compressors and gas for burning linkages between the vertical holes, dollars/ft

Z = number of 100 ft (30.5 m) lengths drilled at angle Θ

Θ = angle of directional drilling (maximum = 6°)

APPENDIX A

ALGORITHM



APPENDIX B

COMPUTER PROGRAM FOR
DETERMINING A COST RATIO

```
      SIMPLE SYSTEMS STUDY
      OPEN 5,"TMP"
      OPEN 6,"SYSOUT",ATT="AP"
      MC=5
      MP=6
      DRILLING AND LINKAGE TIMES:TA (ANGLE), TH (HORIZONTAL),
           TV (VERTICAL),TL (LINKAGE)
      REAL I,J,K,L,M,N,IL,JM,KN
      READ(MC,10)TA,TH,TV,TL
      COST OF PIPES: XA, XB
      COST OF TIME: XC
      COST OF LINKAGE: XD
      READ(MC,11)XA,XB,XC,XD
      RANGE OF S
      READ(MC,20)I,J,K
      RANGE OF Z
      READ(MC,20)L,M,N
      RANGE OF LC
      READ(MC,20)IL,JM,KN
      RANGE OF ANGLE
      READ(MC,20)A1,A2,A3

      WRITE(MP,40)
      DO 100 S=I,J,K
      DO 100 Z=L,M,N
      DO 100 ANGLE=A1,A2,A3
      D=0.0
 90   X=1.0,Z,1.
 90   D=D+100.*COS((X*ANGLE*3.141593)/180.)
      DO 100 LC=IL,JM,KN
      HN=2.*(LC/S+1.)
      TL1=2.*(100.*Z+LC)
      TL2=(HN*D)+((HN-1.)*S)
      RTL=TL2/TL1
      TIME1=2.*(100.*Z*TA+LC*TH)
      TIME2=(HN*D*TV)+((HN-1.)*S*TL)
      RTIME=TIME2/TIME1
      C1=TL1*XA+TIME1*XC
      C2=(HN*D*XB)+((HN-1.)*S*XD)+TIME2*XC
      RC=C2/C1

      WRITE(MP,50)D,LC,S,HN,RTL,RTIME,RC,Z,ANGLE
100   CONTINUE
      STOP
 10   FORMAT(4F8.2)
 11   FORMAT(4F6.2)
 20   FORMAT(3F6.2)
 30   FORMAT(1F6.5)
 40   FORMAT('   DEPTH',7X,'LENGTH OF COAL',6X,'HOLE SPACING',6X,'NO. OF HOLES'
   1  6X,'LENGTH RATIO',6X,'TIME RATIO',8X,'COST RATIO',4X,'Z',2X,'ANGLE')
 50   FORMAT(6(F10.4,8X),F10.4,3X,F4.1,2X,F3.1)
      END
```

REAL MASS AND ENERGY TRANSPORT COEFFICIENTS DETERMINED FROM UCG PROCESS SIMULATION EXPERIMENTS

M. T. PELLEGRIN, MORGANTOWN ENERGY RESEARCH CENTER

ABSTRACT

The probe method was used to determine the thermal conductivity and thermal diffusivity of eastern bituminous coal for temperatures up to 450°F (250°C). Forward and reverse flows were imposed on the sample during heating in order to simulate in situ gasification conditions. The results were interpreted in terms of moisture content, sample size and orientation, and sample temperature. Spatial temperature distributions for forward and reverse flow were compared with those predicted by a steady-state model.

INTRODUCTION

In the study of in situ gasification processes, it is of interest to know the relevant thermal transport properties of the coal. The thermal conductivity and thermal diffusivity would be expected to depend upon the type of coal, the moisture content, and size of the sample being gasified, the heat flow direction, and the coal temperature. In addition, mass transport mechanisms in the form of forward and reverse flows through the coal (relative to the burn direction) and diffusion properties of water already in the coal could affect the thermal transport properties.

Several early investigations, the results of which are summarized in Clendenin, et al [1], have considered thermal conductivity and thermal diffusivity of both powdered and monolithic coal samples. Most of the work was concerned with bituminous coals, although some results for lower rank coals were presented. Quantitative and qualitative dependence of thermal conductivity and thermal diffusivity on temperature, heat flow direction, and coal type was considered. More recently, Badzioch, et al [2] investigated thermal property changes in English coals at elevated temperatures. The results followed the same trend as those in earlier investigations. Thermal property changes due to mass transport have been included as part of a more general analysis of flow through porous media by Burch, et al [3], and in the particular analysis of in situ gasification by Sawyer [5].

The purpose of this investigation was to determine thermal transport properties of eastern bituminous coal under simulated in situ gasification conditions. A lignite sample was also tested for comparison. Transport property variations were examined with respect to coal type, moisture content, sample temperature, sample size, sample orientation, and air flow direction. Quantitative evaluation of thermal conductivity and thermal diffusivity was made where the data permitted; otherwise, effects were qualitatively assessed.

THEORETICAL CONSIDERATIONS

DETERMINATION OF THERMAL CONDUCTIVITY AND THERMAL DIFFUSIVITY

Thermal properties were determined using the probe method, described in Carslaw and Jaeger [6]. This method was used by Badzioch, et al [2] to determine thermal properties of coal. The method is

based on heating of a specimen of infinite extent by a constant heat flux applied via a borehole of known radius. After a long time has elapsed from the initiationof heating, the temperature at any point in the coal sample is given by

$$T - To = \frac{(q/l)}{4\pi K} \ln \frac{4\kappa t}{Cr^2} + \ldots \text{ smaller terms} \qquad (1)$$

After a long time (when the quantity $\frac{r^2}{4\kappa t}$ becomes small, say less than 0.1) has elapsed, the temperature difference T - To versus the logarithm of time asymptotically approaches a straight line. The slope of this line, i.e.

$$\Delta = \frac{(T - To)_2 - (T - To)_1}{\ell nt_2 - \ell nt_1} \qquad (2)$$

is equal to the quantity $\frac{(q/l)}{4\pi K}$. Thus the thermal conductivity K may readily be determined.

Thermal diffusivity may be determined in a manner similar to that used to determine thermal conductivity. Manipulation of equation (1) and use of equation (2) for long times yields

$$\kappa = \frac{r^2}{4t} \exp\left(\frac{T - To}{\Delta} + 0.5772\right) \qquad (3)$$

for given values of t and T - To. The accuracy of the method may be assessed since the quantity $\frac{r^2}{4\kappa t}$ is easilty evaluated. It should be noted that, although K and κ are determined from the same plot of temperature versus time, the two quantities are determined independently.

The advantage of the probe method lies in the fact that any contact resistance existing where heat is applied to the specimen (borehole surface) may be neglected when considering the long time behaviour of the temperature field. A disadvantage of the method is that long times (on the order of hours) are necessary for the temperature versus logarithm of time plot to approach a linear asymptote. The sample must be large enough so that temperatures in the outer regions do not rise appreciably during the heating time, i.e., the sample must be considered infinite in extent.

EFFECT OF MOISTURE CONTENT

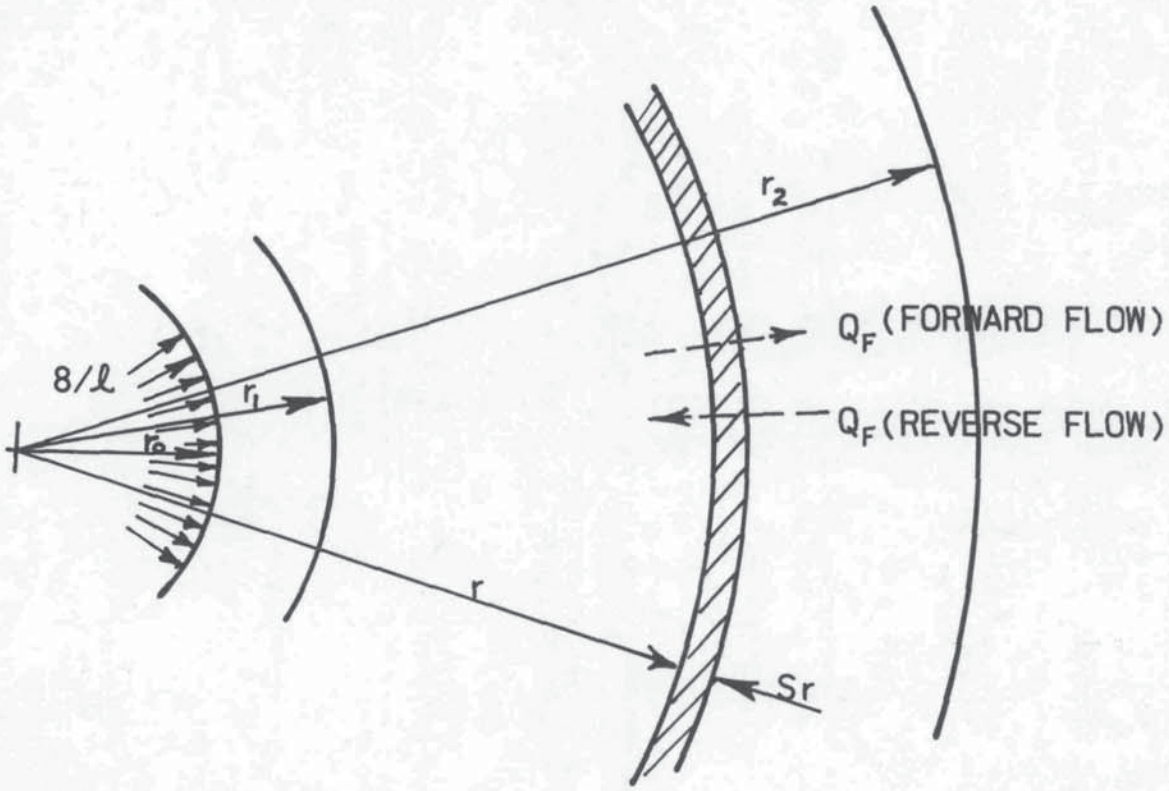
Coal beds, especially lignite beds, are likely to be water saturated. The summary by Clendenin, et al [1] concludes that thermal conductivity of coal rises with increasing moisture content. A definite specification for this increase was not given. One investigation indicated that the thermal conductivity of brown coal approached that of water as moisture content increased.

Several models have been proposed to account for the increase of thermal conductivity with moisture content. Kunii and Smith [7] approached the problem by considering a bed of consolidated particles. Bear [8] summarizes several models, including series and parallel conduction models. A disadvantage of using models to predict the moisture dependence of thermal conductivity is that the fine structure of the coal bed must be known. It may not be possible to determine the fine structure in-situ.

EFFECT OF SAMPLE SIZE AND ORIENTATION

Sample size and orientation are considered together since it could be difficult to separate effects due to anisotropy and inhomogeneity in coal. Directional dependence of thermal conductivity has been pointed out by Clendenin et al [1]. The data show that thermal conductivity is about 10% greater when the heat flux is applied parallel to the bedding planes. However, contradictory results have been obtained. The data scatter in such experiments may preclude an accurate determination of directional thermal properties.

Sample size may also be responsible for data scatter in thermal conductivity determinations. Previous investigations have utilized coal blocks up to roughly 10 cm in diameter. In order to minimize variations due to the amorphous nature of coal, the thermal properties should be



FIGUREI; SECTION OF POROUS CYLINDER
WITH DIFFERENTIAL ELEMENT

determined over a length scale that is comparable to the scale of the actual gasification process. The spatial averaging implied by this procedure may obscure directional dependence of the thermal properties.

EFFECTS OF FLOW THROUGH THE COAL

Burch et al have investigated the dependent transportation heating of porous slabs and cylinders [3], [4]. If the fluid and solid temperatures are not assumed equal, [4], then numerical methods must be employed in order to solve the governing equations [4]. If the fluid and solid temperatures are assumed to be equal, then analytic solutions may be obtained [3], [4]. Since inclusion of a temperature difference between fluid and solid requires the detailed specification of a fluid-solid heat transfer coefficient for the microstructure of coal, the assumption of equal blind and solid temperatures has been retained in this analysis. Furthermore, a steady state temperature distribution is assumed in the investigation of flow effects. The cylindrical geometry characteristic of the probe method leads to transient temperature solutions in terms of Bessel Functions [3] from which it is difficult to evaluate a heat transfer coefficient.

The analysis presented here is similar to that given by Eckert and Drake [9] for flow through porous slabs. Applying the assumptions of a steady state temperature distribution and equal fluid solid temperatures to the cylinder shown in Figure 1 leads to the following expressions for the radial temperature distribution: (see Appendix A).

$$\frac{T(r) - T_2}{T_1 - T_2} = \frac{r^m - r_1^m}{r_1^m - r_2^m} \qquad \text{(Forward Flow)} \qquad (3)$$

$$\frac{T(r) - T_2}{T_1(r) - T_2} = \frac{r^{-m} - r_2^{-m}}{r_1^{-m} - r_2^{-m}} \qquad \text{(Reverse Flow)} \qquad (4)$$

$$\text{where} \quad m = \frac{\rho c Q f}{2\pi K l\,(1-\phi)} \qquad (5)$$

The parameter m may be interpreted as a ratio of heat transported by fluid movement and the heat conducted through the solid. In the limiting case of no fluid movement (m=0), expressions (3) and (4) reduce (with the aid of L'Hospitals Rule) to the standard logarithmic temperature distribution.

An overall heat transfer coefficient for forward or reverse flow may be obtained by forming the ratio of the heat flux to the temperature difference (Appendix A):

$$\text{(Forward Flow)} \qquad U = -\frac{\rho c Q f}{A_{ref}} \left[\frac{r_2^m}{r_1^m - r_2^m} - \frac{T_2}{T_1 - T_2} \right] \qquad (6)$$

$$\text{(Reverse Flow)} \qquad U = \frac{\rho c Q f}{A_{ref}} \left[\frac{r_2^{-m}}{r_1^{-m} - r_2^{-m}} - \frac{T_2}{T_1 - T_2} \right] \qquad (7)$$

It may be seen that the heat transfer coefficient increases for forward flow and decreases for reverse flow. If expression (7) is set equal to zero, a "critical flow rate" can be defined by:

$$m_{cr} = \frac{\ln \left| r_{1/r_2} \right|}{\ln \left| T_{1/T_2} \right|} \qquad (8)$$

Equation (8) represents the case where air flowing toward a burn carries back any heat generated by the burn. For in-situ simulation conditions, this corresponds to a flow rate of 10-15 scfm. Since m must be positive, a critical flow rate does not exist for the forward flow case.

The temperature dependence of thermal conductivity may be considered by defining several "zones" of finite width, each having constant thermal properties.

EFFECT OF ELEVATED TEMPERATURE

Previous investigations [1], [2] have established that thermal conductivity increases with increasing temperatures as the coal is re-formed. In this investigation, the additional effect of moisture diffusion due to a high temperature in the borehole may be significant. The thermal conductivity can be increased as much as 0.1 W/m o k by vapor diffusion effects for temperatures below 100°C. [10].

EXPERIMENTAL METHODS

SAMPLE PREPARATION

Cylindrical coal samples 15.24 cm (6.0") in diameter and 36.83 cm (14.5") long were fixed in the MERC C-size reactor vessel (12" dia., 19" long) with the aid of a castable refractory cement. Care was taken to keep the samples in a water saturated condition. A 30.48 cm (12") platinum coil igniter was installed in a borehole drilled along the reactor axis. For 2 of the samples a 2.54 cm (1") diameter borehole was drilled, while a 1.27 cm (0.5") borehole was drilled in the remaining sample. A schematic drawing of the prepared sample is shown in Figure 2. Test conditions are summarized in Table 1 below.

Sheathed chromel-alumel thermocouples 1.59 mm (1/16") in diameter were installed at various radial and axial locations in the coal and in the castable cement (Figure 2). Due to the construction of the reactor vessel, the thermocouples were installed along radial lines emanating from the reactor axis. Consequently, some error in temperature measurement was to be expected [11]. Thermocouples were installed parallel to and perpendicular to the bedding planes.

DATA ACQUISITION

The MERC in-situ gasification data acquisition system, utilizing an on-line computer, was used to record each of the experimental variables. This system is described by Shuck and Fasching [12].

EXPERIMENTAL PROCEDURE

The experimental procedure consisted of applying a constant known power input to the igniter. The vessel was sealed during heating in order to retain moisture content. Coal temperatures and other system variables (pressures, flow rates where applicable) were recorded on magnetic tape for later processing. Selected variables were also monitored during the tests. A thermocouple placed at the interface between the coal and the castable cement was used to determine the time span for which the coal sample could be considered an infinite solid. Elevated temperatures were obtained by heating the samples with higher power inputs (Table 1).

SIMULATION OF FORWARD AND REVERSE FLOW

Forward flow was simulated by pressurizing the reactor vessel at constant flow rates (0.05 - 0.08 scfm). These flow rates could be maintained for approximately 30 minutes. At this time, the reactor vessel pressure was 60 psig. Pressurizing was initiated after the initial heating period of the sample was completed. Reverse flow was simulated by depressurizing the reactor vessel. Heating was continued during the simulation of forward and reverse flow.

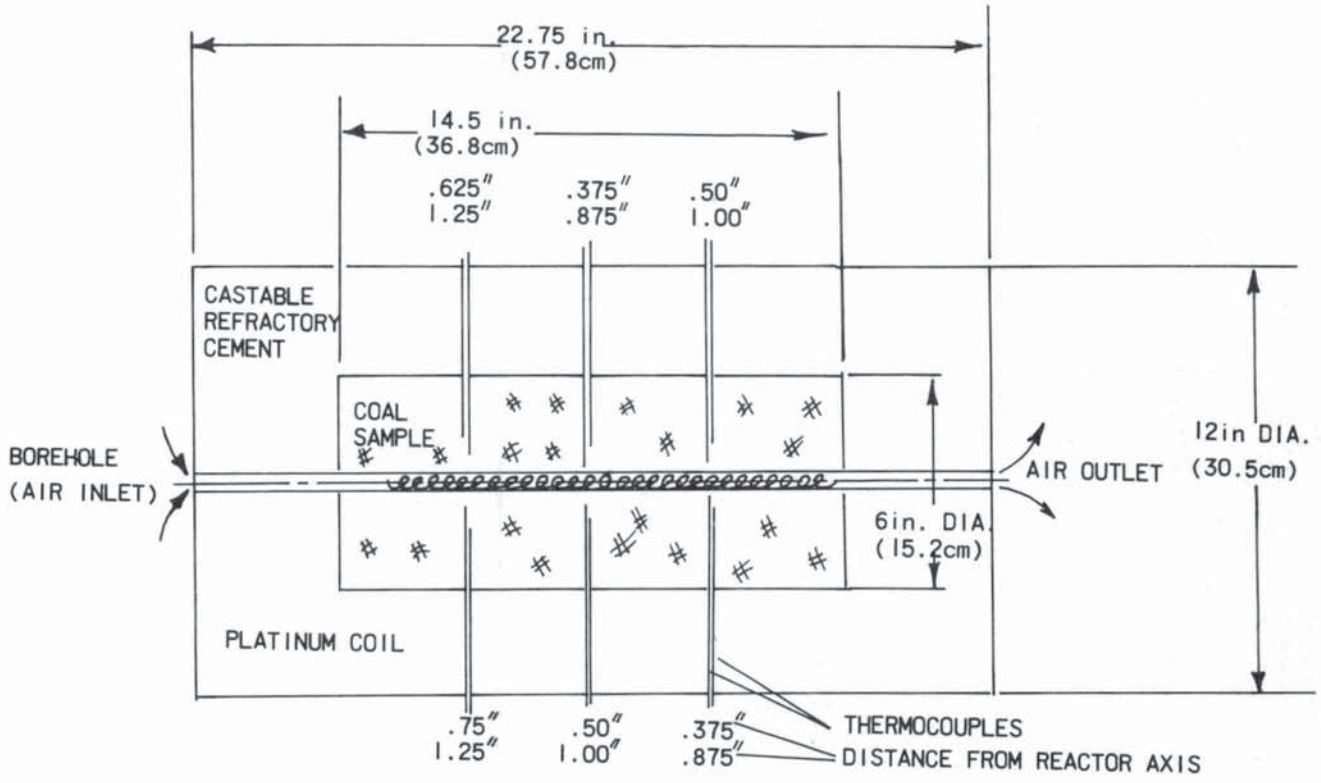


FIGURE 2: REACTOR VESSEL SHOWING TYPICAL THERMOCOUPLE LOCATIONS

TABLE 1: Summary of Test Conditions

Test Number	Coal Type	Borehole Diameter	Power Applied	Heating Time	Forward Flow	Reverse Flow
1	East Bitum.	1.0 in. (2.54 cm)	75 W/ft (246.1 $W/_M$)	4.35 hr	----	----
2	Lignite	1.0 in. (2.54 cm)	70 W/ft (229.7 $W/_M$)	5.16 hr	----	----
3*	East Bitum.	0.5 in. (1.27 cm)	20 W/ft (65.6 $W/_M$)	1.25 hr	0.053 scfm	0.055 scfm
4*	East Bitum.	0.5 in. (1.27 cm)	50 W/ft (164.0 $W/_M$)	1.17 hr	0.06 scfm	0.07 scfm
5*	East Bitum.	0.5 in. (1.27 in)	85 W/ft (278.9 $W/_M$)	1.0 hr	0.08 scfm	0.08 scfm
6*	East Bitum.	0.5 in. (1.27 cm)	130 W/ft (426.5 $W/_M$)	1.0 hr	0.08 scfm	0.08 scfm

*Tests 3-6 performed on the same sample

RESULTS AND DISCUSSION

THERMAL CONDUCTIVITY AND THERMAL DIFFUSIVITY

Figures 3a and 3b show typical temperature time plots from which thermal conductivity and thermal diffusivity were determined. Figures 4 and 5 show K and respectively. The scatter in the data is significant for both K and For temperatures below 100°C., the thermal conductivity is higher than that of water.

TEMPERATURE-DEPENDENT BEHAVIOR

The thermal conductivity decreases as temperature is increased above 100°C. This decrease is evidently due to drying. The large apparent thermal conductivity for temperatures below 100°C. can be explained by a combination of mechanisms: the high water content of the coal at the beginning of each test, (parallel conduction), and the movement of water (diffusion) away from the heat source [10].

DIRECTIONAL PROPERTIES AND INHOMOGENEITY

The scatter in Figures 4a and 5 is indicative of the amorphous nature of coal, since a large amount of scatter exists for thermal properties determined at different points in the same coal sample.

While a definite directional trend is not noticeable for K and , below 100°C, it should be noted that temperatures were much higher for thermocouples placed parallel to the bedding. This

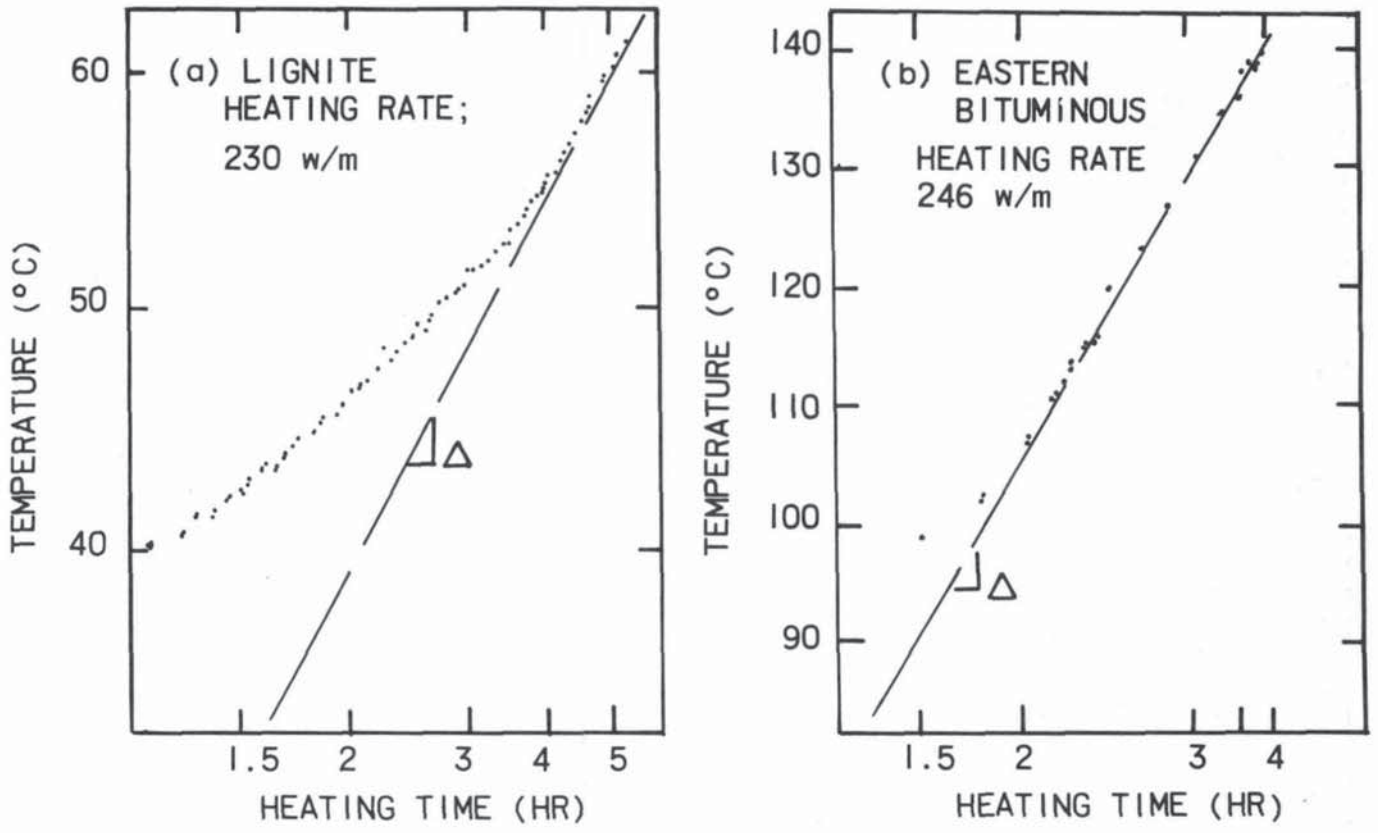


FIGURE 3; TYPICAL TEMPERATURE VS TIME
PLOTS FOR EASTERN BITUMINOUS
COAL AND LIGNITE

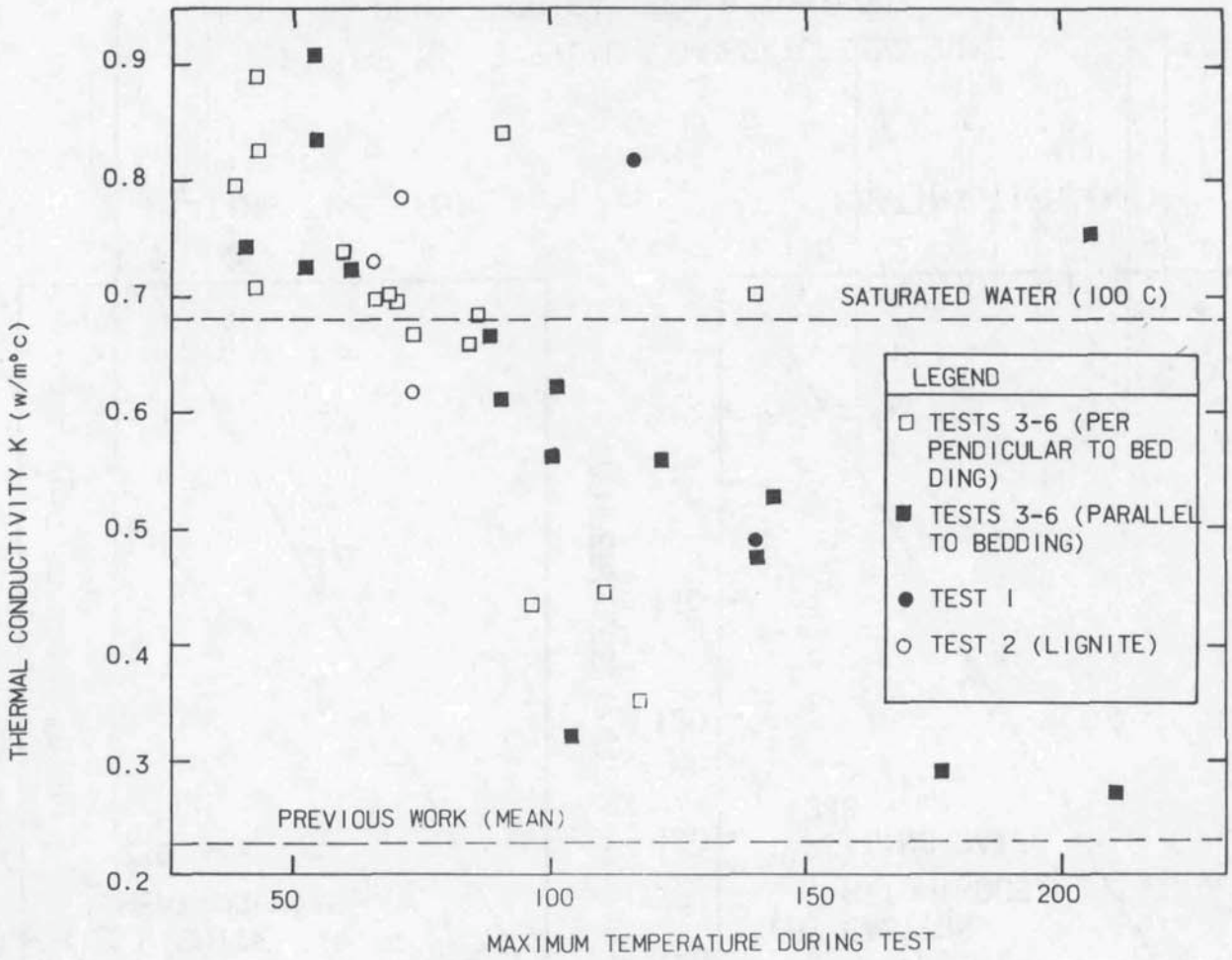


FIGURE 4: APPARENT THERMAL CONDUCTIVITY VERSUS TEMPERATURE

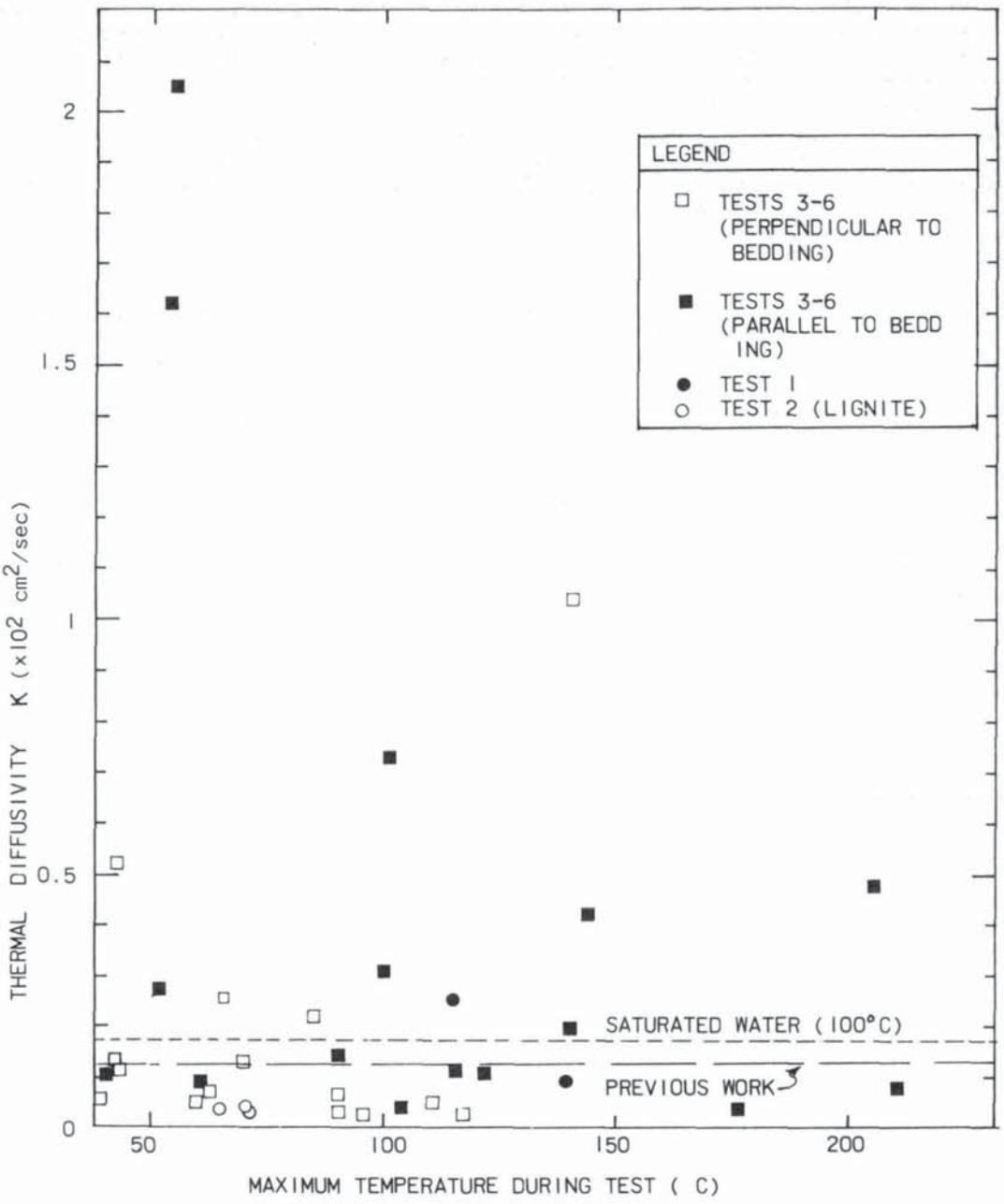


FIGURE 5: APPARENT THERMAL DIFFUSIVITY VS. TEMPERATURE

phenomenon is probably due to vapor diffusion through the face cleats and cracks parallel through the face cleats. Apparently, thermal diffusion is greatest parallel to the bedding plane.

FORWARD AND REVERSE FLOW

There is some question as to whether pressurizing and depressurizing the reactor is a valid simulation of forward and reverse flow. Some of the temperatures decreased during the forward flow simulation while others decreased. The same behavior was characteristic of the reverse flow simulation. Due to data scatter, no clear comparisons can be made for this part of the test.

Predicted temperature distributions are shown in Figure 6. For the quantity calculated for these tests (approximately 0.03), the heat transferred to the coal is increased by 10% for forward flow and is decreased by 10% for reverse flow. For flow rates which are likely to be characteristic of an in-situ conversion process, the heat transfer coefficient will be determined mainly by the flow rate (i.e., by convection).

CONCLUSIONS

1. The thermal conductivity and thermal diffusivity of water saturated bituminous coal is higher than for air dried coal at temperatures below 100°C. Apparent thermal conductivity is increased both by parallel conduction through the water and by thermal diffusion.

2. The thermal conductivities of water-saturated lignite and bituminous coal are approximately the same.

3. Thermal conductivity decreases with increasing temperature for the parameter ranges studied; apparently due to drying of the coal.

4. Scatter in the data indicate the amorphous nature of coal. Heat transfer properties tests should be performed on samples approximately the same size as the sample being gasified. (simulation only).

5. Forward flow increases heat transfer to the outlying coal, while reverse flow decreases the heat transfer.

APPENDIX

STEADY STATE THEORY

Referring to Figure 1, the following heat balances may be made on a differential element. For the solid, the net heat in is given by

$$\delta Q = \text{Heat in} - \text{Heat Out}$$

$$= -KA_s \frac{\partial T_s}{\partial r} - \left[- KA_s \frac{\partial T_s}{\partial r} - K \frac{\partial}{\partial r} \left(A_s \frac{\partial T_s}{\partial r} \right) \delta r \right]$$

$$= (1 - \phi) K \left[r \frac{\partial^2 T_s}{\partial r^2} + K \frac{\partial T_s}{\partial r} \right] 2\pi\ell \qquad \text{(A-1)}$$

where K ∿ thermal conductivity, assumed constant, ϕ ∿ areal porosity, As ∿ area of solid, $A_s = A(1-\phi) = 2\pi r\, 1\, (1-\phi)$

For the fluid, it is noted that the fluid gains heat in the reverse flow mode, and loses heat in the forward flow mode. Thus

$$\delta Q = \pm \rho c\, (U_f A_f) T_f - \left[\pm \rho c\, U_f A_f T_f \pm \rho c \frac{\partial}{\partial r} (U_f A_f T_f)\, \delta r \right]$$

$$= \mp \rho c\, U_f A_f \frac{\partial T_f}{\partial r} \delta r \qquad \text{(A-2)}$$

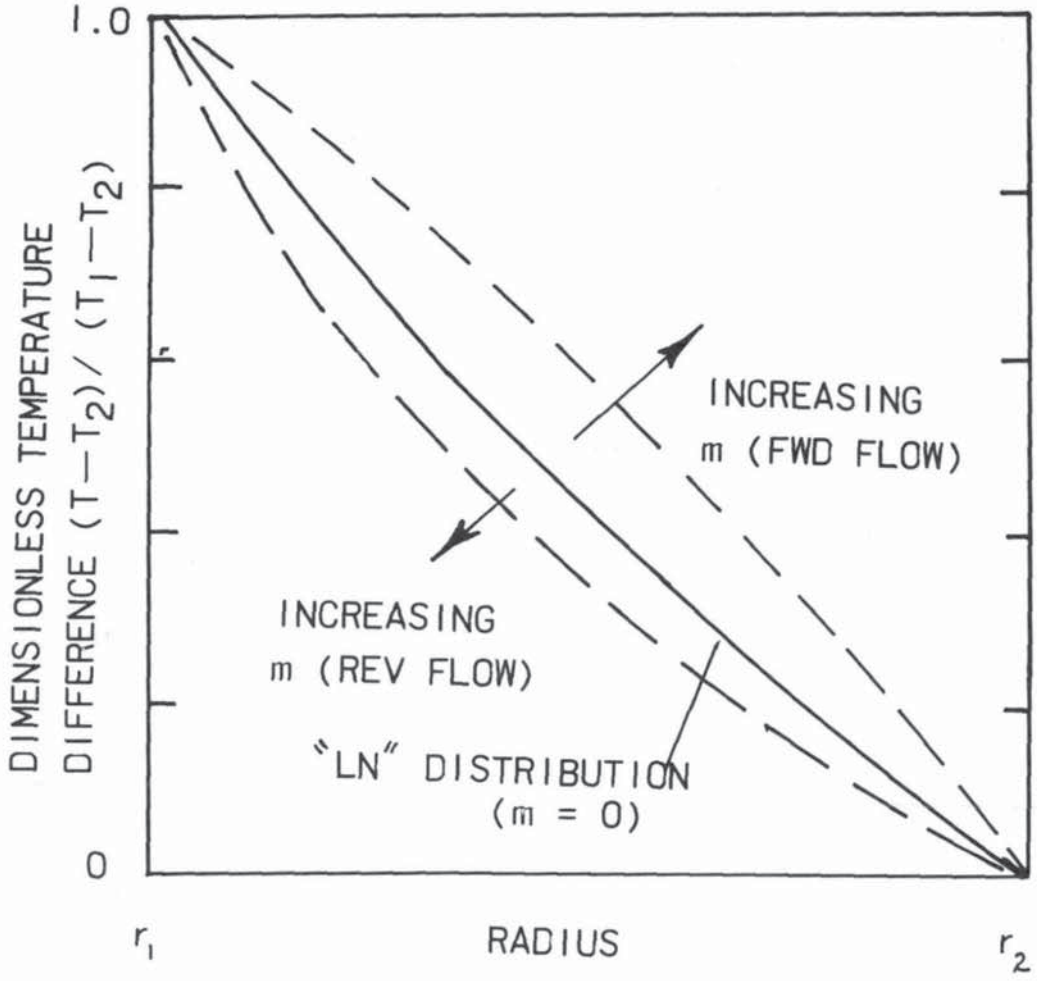


FIGURE 6; PREDICTED RADIAL TEMPERATURE DISTRIBUTIONS WITH FORWARD AND REVERSE FLOW

Assume that Tf = Ts = T and note that the heat added to (lost by) the solid equals the heat lost by (added to) the fluid. Equating δQ in expressions (A-1) and (A-2) results in

$$r \frac{d^2T}{dr^2} + (1 \pm m) \frac{dT}{dr} = 0 \qquad (A-3)$$

where

$$m = \frac{\rho c}{K} \frac{Qf}{2\pi \ell (1 - \phi)} \qquad (A-4)$$

and where the "+" denotes reverse flow, and the "-" denotes forward flow.

The solution of equation (A-3) subject to specified temperatures at r_1 and r_2 is

$$\frac{T(r) - T_2}{T_1 - T_2} = \frac{r^{\mp m} - r_2^{\mp m}}{r_1^{\mp m} - r_2^{\mp m}} \qquad (A-5)$$

where the "-" denotes reverse flow and the "+" denotes forward flow.

An overall heat transfer coefficient U is defined by

$$Q = UA_{ref} (T_1 - T_2) \qquad (A-6)$$

Now Q = Heat added by conduction to solid - Heat lost by convection (reverse flow) + Heat added by convection (forward flow)

$$= - K A_s \frac{dT}{dr} \rho c Q_f T \qquad (A-7)$$

Using (A-4) and (A-5) in (A-7) gives

$$Q = \pm \rho c Q_f \left[(T_1 - T_2) \frac{r_2^{\mp m}}{r_1^{\mp m} - r_2^{\mp m}} - T_2 \right] \qquad (A-8)$$

Employing (A-6) yields

$$U = \pm \frac{\rho c Q_f}{A_{ref}} \left[\frac{r_2^{\mp m}}{r_1^{\mp m} - r_2^{\mp m}} - \frac{T_2}{T_1 - T_2} \right] \qquad (A-9)$$

NOMENCLATURE

A	area
C	Eulers constant
c	Specific Heat (of fluid)
K	Thermal Conductivity
l	Length of Reactor Vessel
m	Flow Rate Parameter
Q, q	Heat Flux
Q_f	Fluid Volume Flow Rate
r	Radius

T	Temperature
t	Time
U	Overall Heat Transfer Coefficient
Uf	Fluid Velocity
Δ	Slope of Temperature vs. ln Time Curve
κ	Thermal Diffusivity $\left(\frac{K}{\rho c}\right)$
ϕ	Area Porosity (A_f/A_s)
ρ	Density (of fluids)

Subscripts

$( )_o$	Initial value, or value at borehole surface
$( )_1$	Value at inner position, or at a specified time
$( )_2$	Value at outer position, or at a specified time later than $( )_1$
$( )_{cr}$	Critical Value
$( )_f$	Value for fluid
$( )_{ref}$	Chosen reference value
$( )_s$	Value for solid

REFERENCES

1. Clendenin, J. D., Barclay, K. M., Donald, H. J., Gillmore, D. W. and Wright, C. C., "Thermal and Electrical Properties of Anthracite and Bituminous Coals", Pennsylvania State College Mineral Industries Experiment Station, Technical Paper 160, 1949.

2. Badzioch, S., Gregory, D. R., and Field, M. A., "Investigation of the Temperature Variation of the Thermal Conductivity and Thermal Diffusivity of Coal", British Coal Utilization Research Association, 1964.

3. Burch, D. M., Peavy, B. A., and Allen, R. W., "Time-Dependent Transpiration Heat Transfer in Porous Cylinders", Trans. ASME, Journal of Heat Transfer, May 1974, pp. 218-224.

4. Burch, D. M., ALlen, R. W., and Peavy, B.A., "Transient Temperature Distributions within Porous Slabs Subjected to Sudden Transpiration Heating", Trans. ASME, Journal of Heat Transfer, May 1976, pp. 221-225.

5. Sawyer, W. K. and Shuck, L. Z., "Numerical Simulation of Mass and Energy Transfer in the Longwall Process of Underground Gasification of Coal", Fourth Symposium of Numerical Simulation of Reservoir Performance, SPE-AIME, Los Angeles, California, Feb. 19-20, 1976.

6. Carslaw, H. S. and Jaeger, J. C., Conduction of Heat in Solids, 2nd Ed., Oxford University Press, 1959.

7. Kunii, D. and Smith, J. M., "Heat Transfer Characteristics of Porous Rocks: I. Effective Thermal Conductivities of Porous Media Containint Stationary Fluid", Symposium on Fundamental Concepts of Thermal Methods of Recovery of Petroleum - In Situ Combustion, 52nd Annual Meeting, San Francisco, California, December 6-9, 1959.

8. Bear, J., Dynamics of Fluids in Porous Media, American Elsevier, 1972.

9. Eckert, E. R. G., and Drake, R. M., Analysis of Heat and Mass Transfer, McGraw Hill, 1972.

10. Hermsen, R. W., Chemical Systems Division, United Technologies, Sunnyvale, California, Personal Communication, 1976.

11. Jakob, M., Heat Transfer, Volume II, John Wiley & Sons, 1957.

12. Shuck, L. Z. and Fasching, G. E., "Instrumentation for In Situ Coal Gasification", MERC SP-75/1. Morgantown Energy Research Center, Morgantown, West Virginia, August 1975.

ACKNOWLEDGEMENTS

The author is indebted to the following employees of the Morgantown Energy Research Center: J. Ernest, L. Kisner, F. Slagle, and T. Yost for vessel preparation; L. Bissett and E. Fisher for testing procedures; E. D'Aurora and J. Downey for computer programming; L. Z. Shuck for technical guidance.

FUNDAMENTAL ASPECTS OF IN SITU ELECTROCARBONIZATION AND ELECTROGASIFICATION OF COAL

By

DR. ERICH SARAPUU

ABSTRACT

The "vertical Borehole Mining Method" of coal by in situ electrocarbonization and electrogasification process can be used for various purposes, such as:

generating permeability between vertical wells drilled several hundred feet apart

producing coke gas of 500 to 600 Btu/cu. ft. of heating value from bituminous coal or hydrogen rich synthesis gas from brown-coal

producing gas by cracking heavy oil in a hot coke channel in situ

The development of the first phase of this process was completed in Hume, Missouri, as part of the fulfillment of a Ph.D. program by Erich Sarapuu at the University of Missouri, School of Mines in Rolla, Missouri.

Subsequent field applications of this process were carried out by the author in Gorgas, Alabama.

INTRODUCTION

Electrofrac's in situ processes for the recovery of fossil fuels, in essence, consist of a portfolio of experimental findings dealing with the electro-energetic gasification of coal, oil shale, crude oil and tar sands.

This paper deals with the development of in situ electrocarbonization and electrogasification of horizontal bituminous coal beds.

The conversion of coal into liquid and gaseous products is one of the technologies which can increase the production of gaseous energy from domestic hydrocarbon resources, such as coal. Gas made from coal can be used for substituting natural gas, although the existing processes of coal gasification need to be improved. However, the gas made from coal with heating values of 100 to 600 Btu/cu. ft. could serve well in various industrial applications.

The in situ gasification, as opposed to mining, has several advantages. The underground processing of coal requires less capital investment than the industrial complex of mining and retorting of coal. In addition, the hazards of underground mining are eliminated, the working conditions for people improved and the productivity per man-hour increased. In situ gasification of coal will eliminate the environmental disturbances which are associated with surface mining, will permit the use of high sulphur coal reserves and eliminate the disposal of residual matter from coal cleaning and gasifacation plants.

The conversion of coal in place can duplicate several gas-making techniques, such as:

- producing hot flue gas
- producing carbonization gas - 500 to 600 Btu/cu. ft.
- conversion of coal into producer and water gas - 100 to 250 Btu/cu. ft.
- use of underground hot coke zone for making carburetted gas by cracking heavy oil in hot coke zone - 500 to 1000 Btu/cu. ft.
- producing hydrogen rich synthesis gas from brown-coal.

The application of in situ electrocarbonization process requires that the electrodes be placed in boreholes and electrical energy be used to carbonize coal between wells which have been drilled several hundred feet apart. The products generated by electrical energy are recovered in gaseous form through the electrode wells. The residual hot coke forms a highly permeable zone which will be used for initiating in situ gasification processes by injecting gasification reactants into the coal stratum.

The process of underground electrocarbonization can be described by several phases of operation, such as:

Electrolinking. It is necessary that "linkages" or permeable channels be induced within the coal seam in order to institute and maintain the complete conversion of coal by subsequent gasification. This has been accomplished by forming a coke zone between wells containing electrodes.

Electrocarbonization. This term is used to designate a relatively long duration, electrical coking of coal before injecting gasification reactants.

Electrogasification. This phase of operation entails simultaneous electrical heating and injection of air, steam or heavy oil into the fuel medium. The electrogasification procedure will yield a gaseous mixture from subsurface fuel deposits that is similar to the enriched producer gas, water gas or oil gas.

THEORETICAL CONSIDERATION

Coal is an aggregate consisting of hydrocarbons and minerals of various compositions and electrical conductivity. When electrodes are placed into the coal seam and electric field is applied, a relatively large electric current may flow through the coal stratum if the electric field intensity exceeds a certain threshold value. The electrically induced ionization (coking) will start acting as a partial conductor to transfer the field concentration at the electrodes to the area between vertical wells until a continuous coke layer is formed between electrodes.

The electrical conductivity of earth material has been the subject of geophysical measurements and investigation for many years. In accord with the physical concepts of the electrical conductivity in the earth, each of the following should be considered: (a) Electrolytic conductivity; (b) Electronic conductivity and (c) Dielectric conductivity.

The pertinent factors effecting the ground conductivity are (a) Type of soil - petrographic composition; (b) Definite anisotrophism of flow of electric current; (c) Chemical impurities in electrolyte; (d) Temperature; (e) Chemical composition of rock-forming minerals.

In order to describe the different types of earth heating problems by ground electrodes, an attempt is made to analyze the flow of electric current in the earth. For instance, in a conductor with fixed cross-sectional area and resistivity, the current flow is normal to the imaginary cross-sectional area between two potentials. However, in the earth the current flow is distributed through a cross section of practically infinite dimensions and continual change of resistance in ground circuit.

Therefore, the current density is highest at the electrode and diminishes as the square of radial distance from the electrode. When current flows from an electrode to the ground, heat is generated in the immediate surrounding of the ground electrode. The temperature limitation of the heating of a ground electrode is given as the boiling point of the electrolyte {1}. When the temperature exceeds the boiling point of water, the electric ground is disrupted. In underground electrocarbonization, however, temperatures far above the boiling point of water are required. The coking and decomposing of hydrocarbons have been accomplished in the the temperature range of 1000^{o} F. When dealing with hydrocarbons, the temperature limit (100^{o} C) of heating geological strata by electric energy has been expanded by replacing electrolytic conductivity of moisture in coal with the conductivity of hot coke which has been formed between electrode wells.

EXPERIMENTAL PROCEDURES

The laboratory and field experimentation of coal {2} was made by using bituminous coal of a Melbourn seam in Hume, Missouri. The primary purpose of this study was to ascertain basic data and secure fundamental knowledge that would later guide the development of large scale underground gasification plants. It was deemed particularly to determine the following controlling factors:

- The magnitude of electric resistivity of coal. The laboratory measurements showed that the electrical resistivity of coal was about 6 orders of magnitude higher than under its original conditions in situ. The increase of the resistivity was due to the loss of moisture of coal samples.

- It was demonstrated that the coal could be electrolinked in the laboratory and the current density to initiate electrolinking was about 0.10 to 0.15 amps/cm^2 of electrode surface ore. Figure 1 illustrates the residual coke after electrocarbonizing a block of raw-coal.

The first field study of underground electrocarbonization was carried out at the Tiger Mine property of the Sinclair Coal Company where a coal seam is about 20 feet below the surface. Successful electrolinking and electrocarbonization of the coal seam was obtained with the electrode spacing of 60 feet. For instance, in an experimental program, the resistance decreased from an initial 11 ohms to approximately 7 ohms in a period of 12 hours; at the end of which time, electrolinking was accomplished and the resistance dropped very rapidly to less than 0.4 ohms. Figure 2 illustrates part of the test facilities of underground electrocarbonization of coal in Hume, Missouri.

References at end of paper



FIGURE 1

Cross-section of electrocarbonized raw-coal.

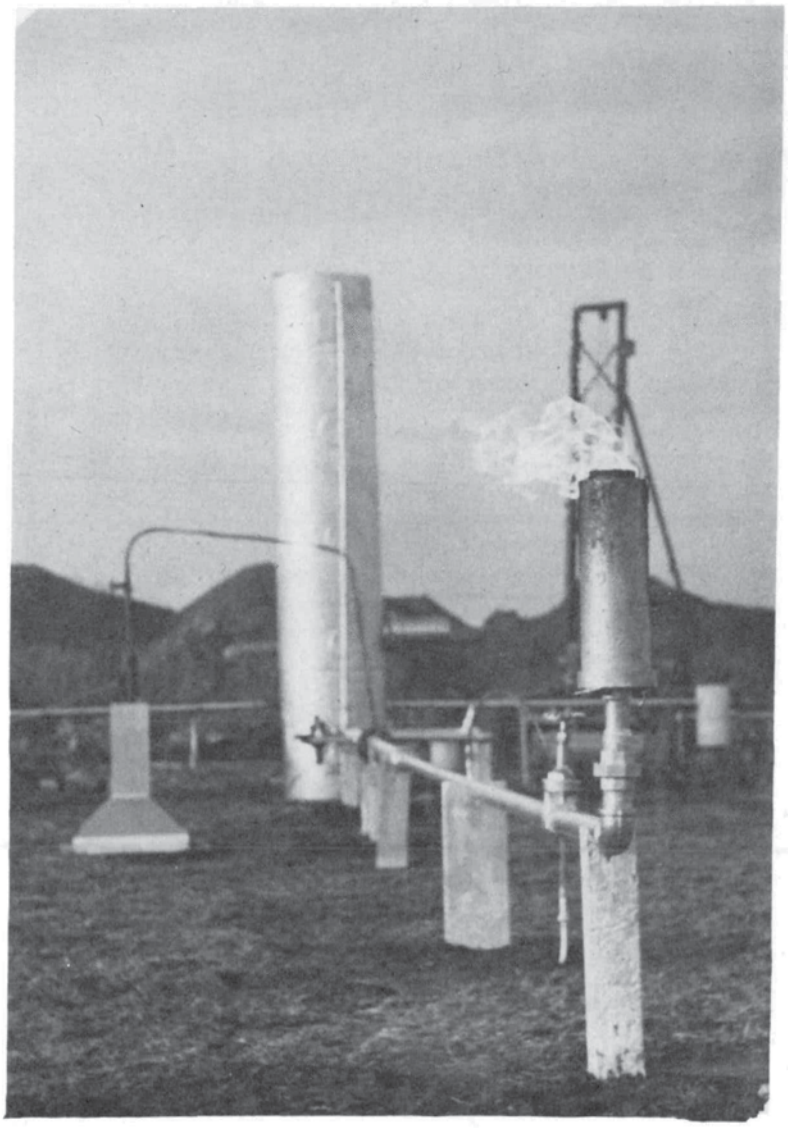


FIGURE 2

In situ electrocarbonization of coal
in Hume, Missouri.

The following is the composition of a random gas sample of coke gas produced during the electrocarbonization of bituminous coal in Hume, Missouri:

CO_2	3.8%
Illuminants	4.0%
O_2	0.3%
CO	12.0%
H_2	54.5%
CH_4	24.1%
N_2	1.3%

Heating value of this sample was 525 Btu/cu. ft.

A laboratory electrocarbonization experiment using Texas lignite resulted in production of 69 percent of hydrogen in pyrolysis gas.

The electrolinking data secured form Hume, Missouri and Gorgas, Alabama {3} experimentation have been plotted comparatively in Figure 3. Graphs No. 1 and No. 2 are of data taken at Hume and they represent results of tests where the electrodes were spaced respectively at 20 feet and 60 feet. Graphs No.'s 3, 4 and 5 are from data obtained at Gorgas where in each case the electrodes were about 150 feet apart. It is felt that No. 3, which shows that electrolinking was accomplished in about 21 hours or at a rate of approximately 7 feet per hour, is the more typical expression of what might be expected from a large-scale operation. Figure 4 illustrates the production of coke gas in Gorgas after the electrolinking was completed.

References at end of paper

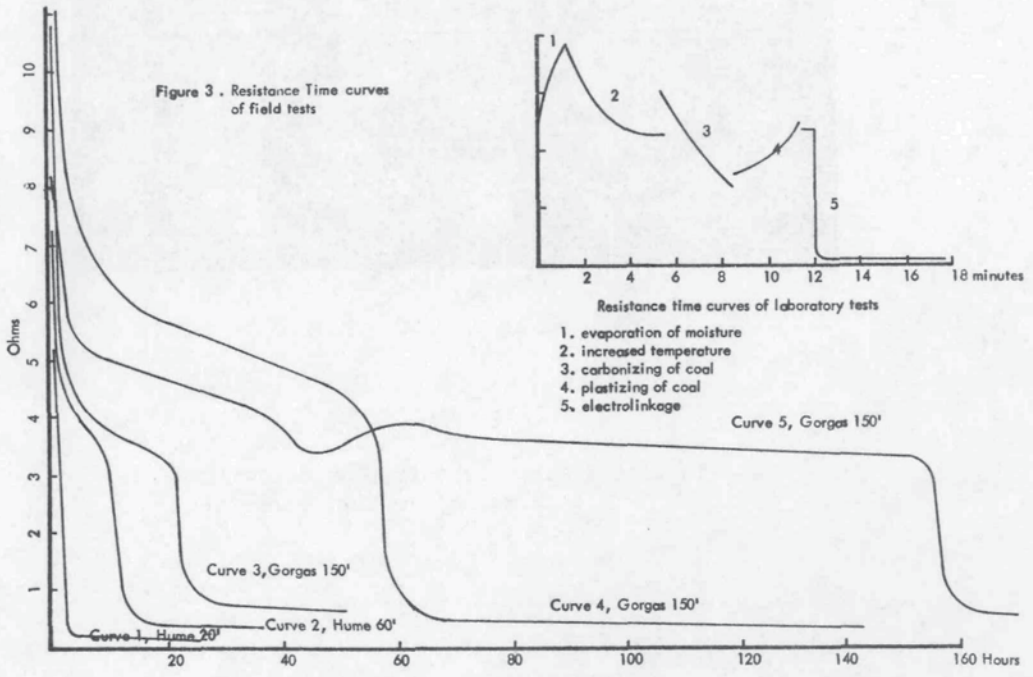


Figure 3. Resistance Time curves of field tests



FIGURE 4

Electrocarbonization of coal in Gorgas, Alabama

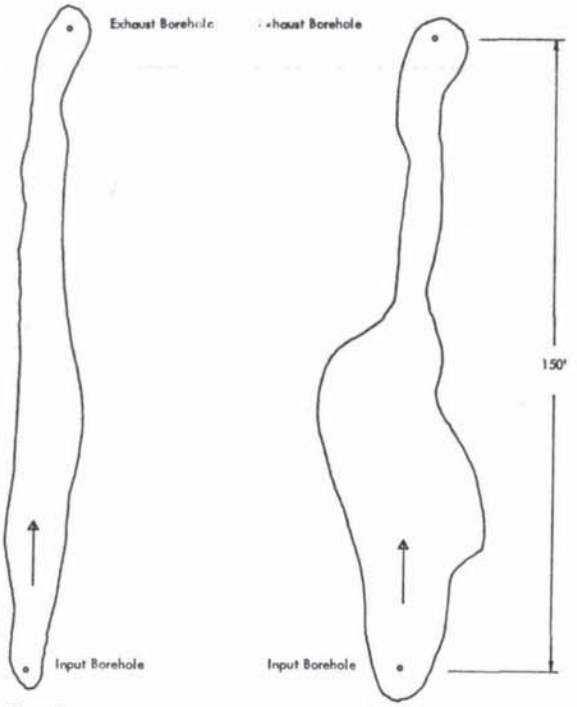


Figure 5

Gasification pattern using oxygen and steam in uniflow operation

Figure 6

Gasification pattern using air in uniflow operation



FIGURE 7

Excavated gasification channel in Hume, Missouri.



FIGURE 8

Fused clinker filled the gasification channel.

Efforts were made at Gorgas to determine the size and shape of the underground gasified area which resulted from the electrocarbonization field research. Figures 5 and 6 illustrate the extent of the gasified area as defined by electrical measurements tracing the distortion of equipotential lines along the high electrical conductivity zone of the gasification channel.

Inasmuch as the field tests at Hume had been made in shallow coal, it was possible to expose the gasified area by stripping the cover with a dragline and thus ascertain the pattern of the affected zone in situ. The gasification by air was carried out for the sole purpose of studying the behavior of residual matter after the gasification of coke zone. Figures 7 and 8 show the excavation of the gasified area. It was found that the gasification channel was completely filled with fused clinker and an idealized schematic of this type of gasification is illustrated in Figure 9.

The need for process control in underground gasification can be appreciated when analyzing the operating differences between gasification in a retort and in situ. This control is obtained by the electrogasification process.

The gasification of coal in surface retort proceeds under controlled physical, thermal and chemical conditions. All factors which affect the results of gasification can be readily designed and selected for the operational requirements. In general, the conditions which regulate the outcome of gasification are:

- physical conditions of the fuel bed
- composition of coal
- height of the fuel bed
- heat losses through the wall of the retort
- tortuosity of gasification channels
- volume of gasification reagent and its composition
- pressure drop in the retort
- reaction temperature

A radical change of any of these factors would greatly degrade the performance of a commercial gasification retort. However, several of these conditions change continually in processing of coal in situ, and reduce the gasification efficiency unless corrective measures and techniques are developed.

A comparison often has been made between the conventional type of gasification retort and the underground gasification unit. With respect to the chemical reactions occurring, there is no difference between the two. However, the technique of underground gasification itself is very different from gasification of coal in a retort.

The following differences exist:

- difference in fuel bed
- difference in fuel used
- difference in environment
- difference in distribution of reaction zones
- difference in controllability of the process

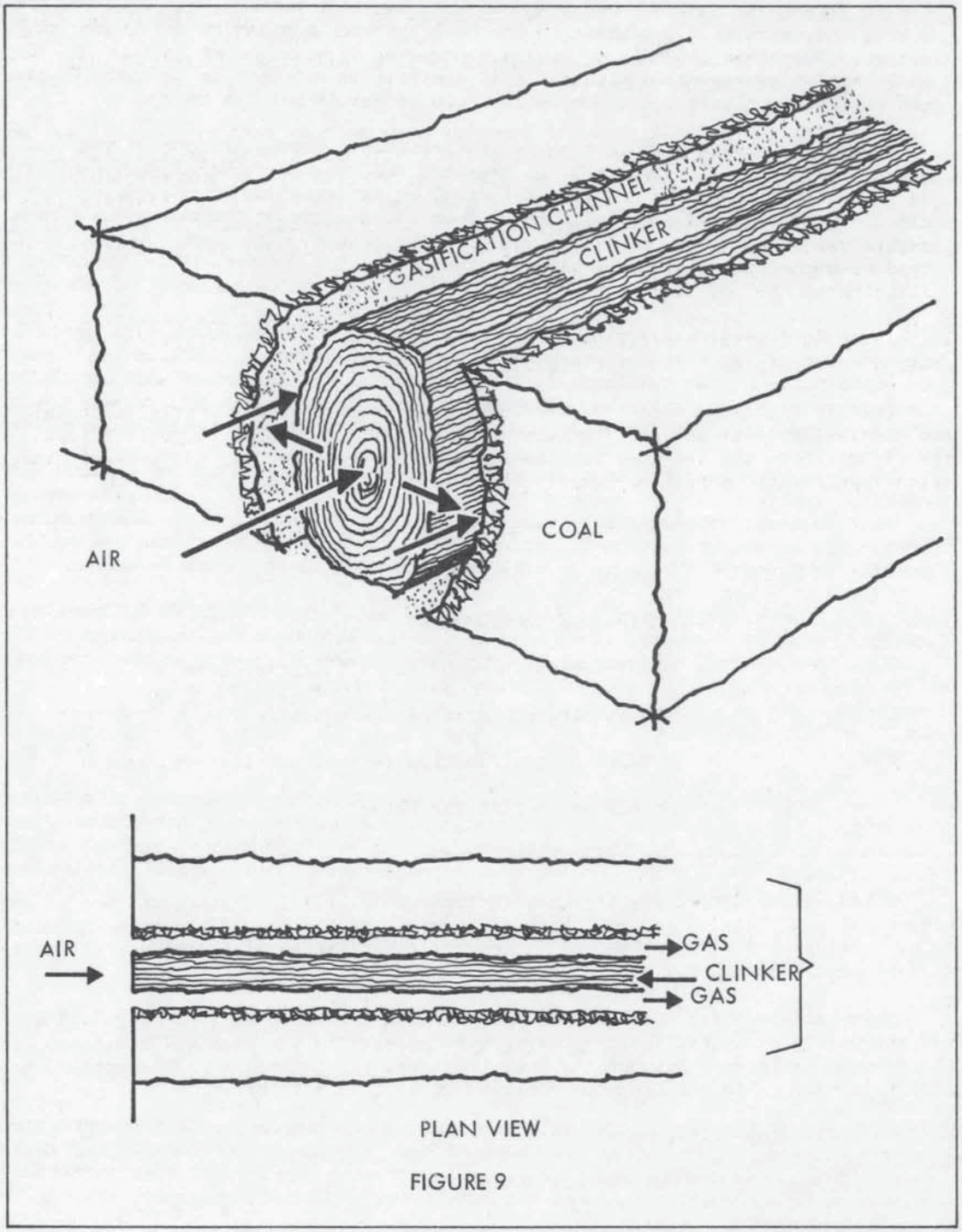


FIGURE 9

Idealized view of thin coal seam during the gasification

In an underground coal gasification unit, a permeable fuel bed must be prepared first. There are numerous methods developed for this purpose, but very few are able to create and maintain a condition in the fuel bed even similar to one in the gasification retort. Permeable channels or openings prepared in situ change in size and shape as gasification progresses. Also the fuel composition adjacent to the gasification channel can change in character and composition due to the impurities in coal.

The underground gasification is started from a permeable zone in the coal seam, which gradually changes in diameter. The consumed fuel is not replaced, but usually the opening is filled by clinker and melting roof-rock, or may stand as an opening for considerable time. An underground coal bed with an open channel can be compared with a gasification retort which has a "vertical hole" through the middle of the fuel charge. In effect, this type of a gasification unit would become a combustion chamber. This situation roughly illustrates the conditions under which an in situ gasification unit has to operate.

The fuel used in a gasification retort is carefully selected. The particle size and ash content are kept at the desired limits. In underground gasification, these advantages do not exist, and the available fuel can contain a high amount of ash and shale partings associated with the coal seam. The non-combustible materials will affect the material change between the gas phase and coal surface and reduce the gasification efficiency.

The surrounding rock in an undergound gasification unit can be compared with the shell of the retort. The ratio of the area of the retort shell to the reactive coal surface is considerably smaller than the ratio of the wall rock to the reactive coal surface in an underground gasification unit. The high ratio between the active coal surface and roof-rock results in a considerable heat loss to the formation.

The actual performance of an underground gasification unit is followed by remote control methods. The gasification in situ cannot be regulated as closely as in a surface retort. The control of chemical reactions by electrical energy is one possibility of improving the outcome of the underground gasification of coal.

SUMMARY

The research of the process of underground electrocarbonization of coal that was conducted in the laboratory and pilot-plant tests demonstrated that the process is feasible as a method of underground gasification and it offers a means of solution of many of the problems that have attended other methods. For example, the fundamental desirable characteristics of electrocarbonization are:

- relatively low construction and installation cost
- comparatively low cost of operation and maintenance
- simple regulation and control of gasification reactions
- high efficiency and resultant good economical yield

Though the economics of the process as a whole depends on many factors such as cost of power, depth of fuel bed, thickness of seam, proximity and character of industrial activities, the research has demonstrated that underground electrocarbonization and electrogasification could assist the development of underground gasification for industrial scale application.

REFERENCES

1. Taylor, H. G., "The Current-Loading Capacity of Earth Electrodes," report (Ref. F/T81) of the British Electrical and Allied Industries.

2. Sarapuu, Erich, "The Process of Underground Electrocarbonization of Mineral Fuels," Dissertation - University of Missouri, School of Mines, Rolla, Missouri, 1951.

3. Elder, J., et al., "Field Scale Experiments in Underground Gasification of Coal at Gorgas, Alabama. Use of Electrolinking-Carbonization as Means of In Situ Preparation," U. S. Bureau of Mines, Report of Investigation 5357, 1957, 101 pp.

APPENDIX A1

SYMPOSIUM STAFF

CHAIRMAN	L.Z. Shuck
VICE-CHAIRMAN & TREASURER	J.D. Spencer
COORDINATOR	H.D. Barlow
ARRANGEMENTS	C.E. Whieldon, Jr. J.A. Bennett
PHOTOGRAPHY & AUDIO-VISUAL	B.B. Samples R.M. Davis
MERC UCG FACILITIES TOUR	L.A. Bissett
GUEST TOUR	D.L. Cooley
ILLUSTRATOR	R.L. Smith, Jr.
ASSISTANTS	M.L. Carson A.J. Casey D.M. Evans R.B. Lowe R.J. McGee R.H. Perkins B.E. Slonnegar

SESSION CHAIRMEN

SESSION I - Major Project Status Report
P.R. Wieber, Act. Branch Chief,
In Situ Coal Gasification Branch,
ERDA HQ, Washington, D.C.

SESSION II - Environmental Studies
L.A. Schrider, Assistant Director,
Extraction and In Situ Conversion Division,
Morgantown Energy Research Center, ERDA

SESSION III - Process Economics
D.R. Stephens, Project Director,
In Situ Coal
Lawrence Livermore Laboratory

SESSION IV - Monitoring & Instrumentation
C.F. Brandenburg, Project Manager
Underground Coal Gasification
Laramie Energy Research Center, ERDA

SESSION V - Theoretical Process Modeling
E.F. Byars, Professor and Chairman,
Mechanical Engineering & Mechanics Dept.
West Virginia University

SESSION VI - Structural & Rock Mechanics
W.K. Sawyer, Research Mathematician
Morgantown Energy Research Center, ERDA

SESSION VII - Field & Systems Studies
S.H. Advani, Professor
Mechanical Engineering & Mechanics Dept.
West Virginia University

SESSION VIII - UCG Technology & Programs in Other Countries
T.F. Edgar, Assistant Professor,
Chemistry Department
University of Texas

SESSION IX - Laboratory Experimentation
A.P. Sikri, Chemical Engineer,
In Situ Coal Gasification Branch,
ERDA HQ, Washington, D.C.

SESSION X - Potpourri Briefs
D.A. Northrop, Division Supervisor
Sandia Laboratories

APPENDIX A2

LIST OF ATTENDEES
2nd Annual Underground Coal Gasification Symposium
August 10 - 12, 1976

Advani, Sunder H.
Professor of Mechanical Engineering
and Mechanics
523 Engineering Sciences Building
West Virginia University
Morgantown, WV 26506
Phone: 304-293-4031

Akers, Dee Ashley
Director, Commonwealth and
Community Services
University of Louisville
Louisville, KY 40208
Phone: 502-588-6508

Arscott, R. L.
Director, Energy Resources Section
Gulf Research & Development
P.O. Box 2038
Pittsburgh, PA 15230
Phone: 412-362-1600

Azoory, Sam
Manager, Process Research
Gulf Oil of Canada
715 - 5th Avenue S.W.
Calgary 1 Alberta, Canada

Balanis, C. A.
Professor, Dept. of Electrical
Engineering
Engineering Sciences Building
West Virginia University
Morgantown, WV 26506
Phone: 304-293-5180

Ball, Keith
Engineer
Alcoa
1501 Alcoa Building
Pittsburgh, PA 15219
Phone: 412-353-4510

Beane, Fred O.
Associate Project Director
Lawrence Livermore Laboratory
P.O. Box 808
Livermore, CA 94550
Phone: 415-447-110 (Ext. 7991)

Beard, S. G.
Member of Technical Staff
Sandia Laboratories
Albuquerque, NM 87115
Phone: 505-264-3377

Beckervordersandforth, Chr. P.
Dr.-Ing. Projektleiter
RWTH in Aachen
Institut für Eisenhüttenkunde
Intzestrabe 1, 5100 Aachen (Germany)

Beckham, L. W.
MTS
Sandia Laboratories
Albuquerque, NM 87115
Phone: 505-264-3377

Bidlack, Duane L.
Sr. Project Engineer
Gulf Research & Development Company
P.O. Drawer 2038
Pittsburgh, PA 15230
Phone: 412-362-1600 (Ext. 305)

Bissett, L. A.
Morgantown Energy Research Center
P.O. Box 880
Morgantown, WV 26505
Phone: 304-599-7266

Booker, J. D.
Associate Planning Advisor
The Carter Oil Company
P.O. Box 2180
Houston, TX 77001

Borer, Ted C.
Process Engineer
Cameron Engineers, Inc.
1315 S. Clarkson Street
Denver, CO 80210
Phone: 303-777-2525

Boyd, R. M.
Geologist
Laramie Energy Research Center
P.O. Box 3395, University Station
Laramie, WY 82071
Phone: 307-742-2115

Brandenburg, C. F.
Research Chemist
Laramie Energy Research Center
P.O. Box 3395, University Station
Laramie, WY 82071
Phone: 307-742-2115

Bray, Bruce G.
Director of Special Projects
Continental Oil Company
Mining Research Division
Drawer 1267 - Rm. 4 WOB
Ponca City, OK 74601
Phone: 405-762-3456 (Ext. 8291)

APPENDIX A2

LIST OF ATTENDEES (con't)

Brown, R. A. S.
Alberta Research Council
11315-87 Avenue
Edmonton, Alberta, Canada T6G2C2
Phone: 403-432-8181

Bryer, C. W.
Morgantown Energy Research Center
P.O. Box 880
Morgantown, WV 26505
Phone: 304-599-7547

Benner, Robert I.
Suntech, Incorporated
503 North Central Expressway
Richardson, TX 75080

Buder, Manfred K.
Engineer
Bechtel Corporation
P.O. Box 3965
San Francisco, CA 94119
Phone: 415-764-3562

Butkovich, Theodore R.
Lawrence Livermore Laboratory
P.O. Box 808
Livermore, CA 94550
Phone: 415-447-1100 (Ext. 3376)

Butler, H. W.
Professor of Mining Engineering
West Virginia University
Morgantown, WV 265056
Phone: 304-293-5360

Calden, Diane L.
Resource Engineer
Pacific Gas & Electric Company
245 Market Street
San Francisco, CA 94106
Phone: 415-781-4211 (Ext. 4176)

Campbell, John H.
Research Chemist
Lawrence Livermore Laboratory
P.O. Box 808
Livermore, CA 94550
Phone: 415-447-1100 (Ext. 4444)

Campbell, G. G.
Petroleum Engineer
Laramie Energy Research Center
P.O. Box 3395, University Station
Laramie, WY 82071
Phone: 307-328-4342

Chaiken, Robert F.
Research Chemist
U. S. Bureau of Mines
4800 Forbes Avenue
Pittsburgh, PA 15213
Phone: 412-892-2400 (Ext. 651)

Chandelle, V.
Senior Research Worker
Institut National des Industries Extractives
rue du Chera, 200
B - 4000 LIEGE (Belgium)

Clarke, Forbes R. Jr.
Asst. to Vice President - Operation
Freeman United Coal Mining Co.
Box 570
Canton, IL 61520
Phone: 309-647-4287

Clements, B. R.
Manager In Situ Gasification Project
Texas Utilities Generating Company
2001 Bryan Tower
Dallas, TX 75201
Phone: 214-653-4017

Coursen, D. L.
Research Fellow
Dupont
Potomac River Laboratory
Martinsburg, WV 25401
Phone: 304-267-2941 (Ext. 336)

Dalverny, L. E.
Physicist
U. S. Bureau of Mines
4800 Forbes Avenue
Pittsburgh, PA 15213
Phone: 412-892-2400

Datta, Rabinder Singh
Senior Minerals Research Engineer
Syracuse Research Corporation
Merrill Lane
Syracuse, NY 13210
Phone: 315-425-5129

Dean, C. S.
Geologist
Morgantown Energy Research Center
P.O. Box 880
Morgantown, WV 26505
Phone: 304-599-7211

Denbina, Eric S.
Senior Research Engineer
Exxon Production Research Company
3120 Buffalo Speedway
P.O. Box 2189
Houston, TX 77001
Phone: 713-965-4145

Douglas, George W.
Associate Professor
The University of Alabama
P.O. Box 2908
University, AL 35486
Phone: 205-348-6311

ATTENDEES (con't)

Eastwood, D. E.
Physicist
Laramie Energy Research Center
P.O. Box 3395, University Station
Laramie, WY 82071
Phone: 307-742-2115 (Ext. 309)

Edgar, T. F.
Asst. Professor
Department of Chemical Engineering
University of Texas
Austin, TX 78712
Phone: 512-471-3080

Ehlenberger, A. E.
Talley-Frac Corporation
P.O. Box 849
Mesa, AR 85201
Phone: 602-832-3830

Enterline, Jack J.
President
Precision Metal Services, Inc.
P.O. Box 2109
Ft. Pierce, FL 33450
Phone: 305-465-8880

Farouq Ali, S. M.
Professor
Pennsylvania State University
20 M. I. Building
University Park, PA 16802
Phone: 814-865-0101

Fischer, D. D.
Research Chemist
Laramie Energy Research Center
P.O. Box 3395, University Station
Laramie, WY 82071
Phone: 307-742-2115

Fischer, Jack
Argonne National Laboratory
9700 S. Cass Avenue
Argonne, IL 60439
Phone: 312-739-7711 (Ext. 2540)

Fisher, E. P.
Chemical Engineer
Morgantown Energy Research Center
P.O. Box 880
Morgantown, WV 26505
Phone: 304-599-7247

Fontenot, Ronald C.
Senior Engineer
Ethyl Corporation R&D Staff
P.O. Box 341
Baton Rouge, LA 70821
Phone: 504-359-2312

Forrester, Richard C. III
Research Staff Member
Oak Ridge National Laboratory
P.O. Box X
Oak Ridge, TN 37830
Phone: 615-483-8611 (Ext. 6282)

Fritz, Jim
Field Engineer
Paramount Exploration, Inc.
Box 551
Waynesburg, PA 15370
Phone: 412-627-6144

Fulton, Paul F.
Professor
University of Pittsburgh
1249 Benedum Hall
Pittsburgh, PA 15261
Phone: 412-621-5274

Gardner, John
General Manager
Paramount Exploration, Inc.
Box 551
Waynesburg, PA 15370
Phone: 412-627-6144

Garon, Allan M.
Sr. Research Engineer
Gulf Research & Development Co.
P.O. Box 2038
Pittsburgh, PA 15230
Phone: 412-362-1600 (Ext. 576)

Gottlieb, Myron
Division of Environmental Control Tech.
U.S. ERDA
Mail Station E201
Washington, D. C. 20545

Gregg, David
Lawrence Livermore Laboratory
P. O. Box 808
Livermore, CA 94550
Phone: 415-447-1100 (Ext. 8639)

Grisafi, Ted W.
Engineer of Coal Property
Chessie System
Box 9447
Huntington, WV 25701

Gunn, R. D.
Chemical Engineer
Laramie Energy Research Center No. 234
P.O. Box 3395, University Station
Laramie, WY 82071
Phone: 307-742-2115 (Ext. 319)

ATTENDEES (con't)

Guthrie, H. D.
Director, Division of Oil, Gas
and Shale Technology
U.S. ERDA
20 Massachusetts Avenue, NW
Washington, D. C. 20545
Phone: 202-376-4693

Hagen, Nancy S.
Program Coordinator
U. S. ERDA, San Francisco
1333 Broadway
Oakland, CA 94612

Hahn, Ottfried J.
Associate Director
Ins-itute for Mining & Mineral Research
Bradley Hall
University of Kentucky
Lexington, KY 40506
Phone: 606-258-5862

Hermsen, Robert W.
Chief, Kinetics & Combustion
Chemical Systems Division, United Technologies
P.O. Box 358
Sunnyvale, CA 94088
Phone; 408-739-4880 (Ext. 2851)

Hill, Richard W.
Physicist
Lawrence Livermore Laboratory
P.O. Box 808
Livermore, CA 94550
Phone: 415-447-1100 (Ext. 7460)

Holighaus, Dr.
KFA - Julich
GMBH
577 Jülich Germany

Holmes, J. J.
Research Assistant
Engineering Building
West Virginia University
Morgantown, WV 26506
Phone: 304-293-5180

Humphrey, A.
Mechanical Engineer
Laramie Energy Research Center
P.O. Box 3395, University Station
Laramie, WY 82071
Phone: 307-742-2115

Humphrey, John P.
Research Manager
Dow Chemical Company
Hydrocarbons and Energy
677 Building
Midland, MI 48640
Phone: 517-636-2296

Hutchinson, H.
Chemist
Laramie Energy Research Center
P.O. Box 3395, University Station
Laramie, WY 82071
Phone: 307-742-2115

Huston, J. C.
Morgantown Energy Research Center
P.O. Box 880
Morgantown, WV 26505
Phone: 304-599-7448

Jensen, Erik J.
Head, Engineering Division
Alberta Research Council
11315-87 Avenue
Edmonton, Alberta, Canada T6G 2C2
Phone: 403-432-8181

Kern, Lloyd R.
Research Scientist
Atlantic Richfield Company
P.O. Box 2819
Dallas, TX 75221
Phone: 214-424-3511

King, S. B.
Chemist
Laramie Energy Research Center
P.O. Box 3395, University Station
Laramie, WY 82071
Phone: 307-742-2115

Komar, C. A.
Research Physicist
Morgantown Energy Research Center
P.O. Box 880
Morgantown, WV 26505
Phone: 304-599-7107

Krauss, Ulrich
Dr. Rer. nat.
BERGBAU-FORSCHUNG GMBH
4300 Essen 13/Bundesrepublik Deutschland
Frillendorfer Str. 351 Germany

Kresse, Thomas J.
Senior Engineer
The Peoples Gas Light and Coke Co.
122 South Michigan Avenue
Chicago, IL 60603
Phone: 312-431-4558

Lane, David M.
Chief Geologist - Non Metallics
Scurry-Rainbow Oil Limited
709-8th Avenue SW
Calgary, Alberta, Canada T2P 1H5
Phone: 403-269-7991

ATTENDEES (con't)

Lanum, W. J.
Research Chemist
Laramie Energy Research Center
P.O. Box 3395, University Station
Laramie, WY 82071
Phone: 307-742-2115

Law, Richard K.
Research Associate
Alberta Research Council
11315-87th Avenue
Edmonton, Alberta, Canada T6G 2C2
Phone: 403-432-8181

Locke, C. D.
Petroleum Engineer
Morgantown Energy Research Center
P.O. Box 880
Morgantown, WV 26505
Phone: 304-599-7216

Lowe, R. L.
Morgantown Energy Research Center
P.O. Box 808
Morgantown, WV 26505
Phone: 304-599-7267

Magee, Robert A.
Scientist
Radian Corporation
8500 Shoal Creek Blvd.
Austin, TX 78758
Phone: 512-454-4797

Mahoney, James V.
Research Engineer
U.S. Steel Research Lab.
125 Jamison Lane
Monroeville, PA 15146
Phone: 412-372-1212 (Ext. 2861)

Martin, J. W.
Physicist
Morgantown Energy Research Center
P.O. Box 880
Morgantown, WV 26505
Phone: 3Q4-599-7447

Mason, Richard Z.
Manager, Process Engineering
Williams Brothers Process Services, Inc.
6600 South Yale Avenue
Tulsa, OK 74136
Phone: 918-496-5000

McFarlane, Samuel B.
Special Assistant for Fossil Energy Programs
Office of the Manager
ERDA - San Francisco
1333 Broadway
Oakland, CA 94612
Phone: 415-273-7881

McKinley, Marvin D.
Associate Professor
The University of Alabama
P.O. Box G
University, AL 35486
Phone: 205-348-6450

Moll, A. J.
Director, Energy Technology Department
Stanford Research Institute
333 Ravenswood Avenue
Menlo Park, CA 94025
Phone: 415-326-6200

Moore, E. T., Jr.
Vice-President/Division Director
Physics International Co.
2700 Merced Street
San Leandro, CA 94577
Phone: 415-357-4610

Neumann, R.
KFA - Juelich GMBH
Postfach 1913
517 Juelich, Germany

Northrop, David A.
Division Supervisor
Division 5732, Sandia Laboratories
Albuquerque, NM 87115
Phone: 505-264-2302

Oliver, Robert W.
Geologist - In Situ Gasification
Texas Utilities Company
2001 Bryan Tower
Dallas, TX 75201
Phone: 214-653-4974

Ottinger, Robert S.
Assistant Project Manager
TRW Energy Systems
7600 Colshire Drive
McLean, VA 22101
Phone: 203-893-2000 (Ext. 2201)

Pasini, J. III
Assistant Director, Advanced Projects
Morgantown Energy Research Center
P.O. Box 880
Morgantown, WV 26505
Phone: 304-599-7103

Pellegrin, Michael T.
Morgantown Energy Research Center
P.O. Box 880
Morgantown, WV 26505
Phone: 304-599-7751

Peters, George T.
Research Engineer
United Technologies Research Center
East Hartford, CT 06108
Phone: 203-565-8428

ATTENDEES (con't)

Peterson, J. L.
Vice President
Resource Sciences Corporation
6600 South Yale
Tulsa, OK 74136

Phillips, Terry
Columbia Gas System
Box 2318
Columbus, OH 43216
Phone: 614-486-3681

Pitrolo, A. A.
Director
Morgantown Energy Research Center
P.O. Box 880
Morgantown, WV 26505
Phone: 304-599-7511

Prats, Michael
Consultant
Shell Development
Box 481
Houston, TX 72001
Phone: 713-667-5661

Robertson, R. L.
Manager, Process Systems Operations
TRW Energy Systems
7600 Colshire Blvd.
McLean, VA 22101
Phone: 203-893-2000 (Ext. 2208)

Roehl, A. A.
Alberta Research Council
11315-87 Avenue
Edmonton, Alberta, Canada T6G 2C2
Phone: 403-432-8181
403-432-8089

Rosenberg, Harold
President
Paramount Exploration Inc.
300 E. 56th St.
New York, NY 10022
Phone: 212-838-3413

Rozsa, Rudolf
Group Leader
Lawrence Livermore Laboratory
P.O. Box 808
Livermore, CA 94550
Phone: 415-447-1100 (Ext. 8629)

Rupert, R. C.
Energy Systems Management Div.
TRW
1 Space Park - E2/10042
Redondo Beach, CA 90274
Phone: 213-535-1687

Sarapuu, Erich
President
Electrofrac Corporation
308 W - 99 Terrace
Kansas City, MO 64114
Phone: 913-649-5611

Sawyer, Walter K.
Mathematician
Morgantown Energy Research Center
Morgantown, WV 26505
Phone: 304-599-7221

Schrider, Leo A.
Assistant Director
Extraction and In Situ Conversion Division
Morgantown Energy Research Center
Morgantown, WV 26505
Phone: 304-599-7492

Schwartz, S. H.
Associate Professor, MEM Department
West Virginia University
Morgantown, WV 26506
Phone: 304-293-5360

Sears, H. V.
SADECO
Box 123
Flat River, MO 63601
Phone: 314-431-3836

Seeberger, J. F.
Morgantown Energy Research Center
Box 880
Morgantown, WV 26505
Phone: 304-599-7450

Shepard, John C.
Senior Research Chemist
Suntech, Incorporated (Sun Oil Co.)
503 North Central Expressway
Richardson, TX 75080
Phone: 214-744-4411

Shoemaker, Harold D.
Mechanical Engineer
Morgantown Energy Research Center
Morgantown, WV 26505
Phone: 304-599-7751

Shuck, L. Z.
Supervisory Mechanical Engineer
Morgantown Energy Research Center
Morgantown, WV 26505
Phone: 304-599-7447

Sikri, Atam P.
Chemical Engineer
Division of Oil, Gas & Shale Technology
U. S. ERDA
20 Masachusetts Avenue, NW
Washington, D. C. 20545
Phone: 202-376-4868

ATTENDEES (con't)

Singer, Joseph M.
Research Chemist
U. S. Bureau of Mines
4800 Forbes Avenue
Pittsburgh, PA 15217
Phone: 412-892-2400

Skidmore, Duane R.
Professor
West Virginia University
108 WH
Morgantown, WV 26506
Phone: 304-293-5695

Spencer, J. D.
Technical Editor
Morgantown Energy Research Center
P.O. Box 880
Morgantown, WV 26505
Phone: 304-599-7341

Stephens, Douglas R.
Project Director - In Situ Coal Program
Lawrence Livermore Laboratory
P.O. Box 808
Livermore, CA 94550
Phone: 415-447-1100 (Ext. 7991)

Sterner, T. E.
Petroleum Engineer Technician
Laramie Energy Research Center
P.O. Box 3395, University Station
Laramie, WY 82071
Phone: 307-742-2115

Stewart, Ian McC
Professor
Department of Chemical Engineering
The University of Newcastle
New South Wales 2308, Australia

Strain, Dennis W.
Assistant Attorney General
Pennsylvania Dept. of Environmental Resources
1200 Kossman Bldg., Forbes at Stanwix St.
Pittsburgh, PA 15222
Phone: 412-565-5363

Taylor, Clifford J.
Graduate Engineer
TransCanada Pipelines
P.O. Box 54, Commerce Court West
Toronto, Ontario, Canada M5L 1C2

Terry R. C.
President
In Situ Technology, Inc.
830 Midland Savings Bldg.
Denver, CO 80202
Phone: 303-825-7957

Thompson, T. W.
Assistant Professor
University of Texas at Austin
Austin, TX 78712
Phone: 512-471-3161

Trentacoste, Nicholas
Manager, Transportation and Environmental
Sciences Division
Science Applications, Inc.
8400 Westpark Drive
McLean, VA 22101
Phone: 703-821-4587

Thakur, P. C.
CONOCO
P.O. Box 4294
Morgantown, WV 26505
Phone: 304-983-2251

Varga, I. E.
Assistant Manager - Operations
Texaco Canada Limited
3rd Floor, 600 - 6th Avenue SW
Calgary, Alberta, Canada T2P 2S4
Phone: 403-269-7381

Vincinelly, Walter J.
Commissioner, Office of Deep Mine Safety
Department of Environmental Resources
6th Floor, Fulton National Bank Bldg.
Harrisburg, PA 17120
Phone: 717-787-1376

Vogt, T. C.
Associate Chemist
Mobil Research and Development Corporation
P.O. Box 900
Dallas, TX 75221
Phone: 214-331-6531

Von Gonton, W. D.
Professor and Department Head
Petroleum Engineering Department
Texas A&M University
College Station, TX 77840

Wertman, W. T.
Deputy Director
Morgantown Energy Research Center
P.O. Box 880
Morgantown, WV 26505
Phone: 304-599-7711

Whieldon, C. E., Jr.
Petroleum Engineer Technician
Morgantown Energy Research Center
P.O.Box 880
Morgantown, WV 26505
Phone: 304-599-7255

ATTENDEES (con't)

White, Les
Alberta Research Council
11315-87 Avenue
Edmonton, Alberta, Canada T6G 7C2
Phone: 403-432-8181

Whitman, David L.
Engineering Technician
Laramie Energy Research Center
P.O. Box 3395. University Station
Laramie, WY 82071
Phone: 307-742-2115 (Ext. 319)

Wieber, Paul R.
Acting Chief, Underground Coal Gasification Branch
U. S. ERDA
20 Massachusetts Avenue, N.W.
Washington, D. C. 20545
Phone: 202-376-4868

Williams, Fred
Operational Research Executive
National Coal Board
Coleorton Hall
Coleorton, Leicester, England

Wilson, Lyndon
U. S. Stamping Company
Moundsville, WV 26041
Phone: 304-845-3110

Wrubleski, R. M.
Senior Process Engineer
Shell Canada Limited
Box 100
Calgary, Alberta, Canada T3B 2H5
Phone: 403-266-7561

Young, J. E.
Chemist
Argonne National Laboratory
9700 S. Cass Avenue
Argonne, IL 60439
Phone: 312-739-7711 (Ext. 5202)

APPENDIX A3

Registration Statistics of 2nd Annual UCG Symposium--1976

Government	55
Industry	61
University	17
Other	5
TOTAL	138

United States

Alabama	2	Missouri	2
Arizona	1	New Mexico	3
California	16	New York	2
Colorado	2	Ohio	1
Connecticut	1	Oklahoma	3
District of Col.	4	Pennsylvania	15
Florida	1	Tennessee	1
Illinois	4	Texas	13
Kentucky	2	Virginia	3
Louisiana	1	West Virginia	31
Michigan	1	Wyoming	12
		TOTAL	121

Other Countries

Australia	1	England	1
Belgium	1	Germany	4
Canada	10	TOTAL	17

Female	4
Male	134

Participants returning from 1st Annual UCG Symposium	37
First time attendees for a UCG Symposium	101



Figure A4-1. - "Arrivals"

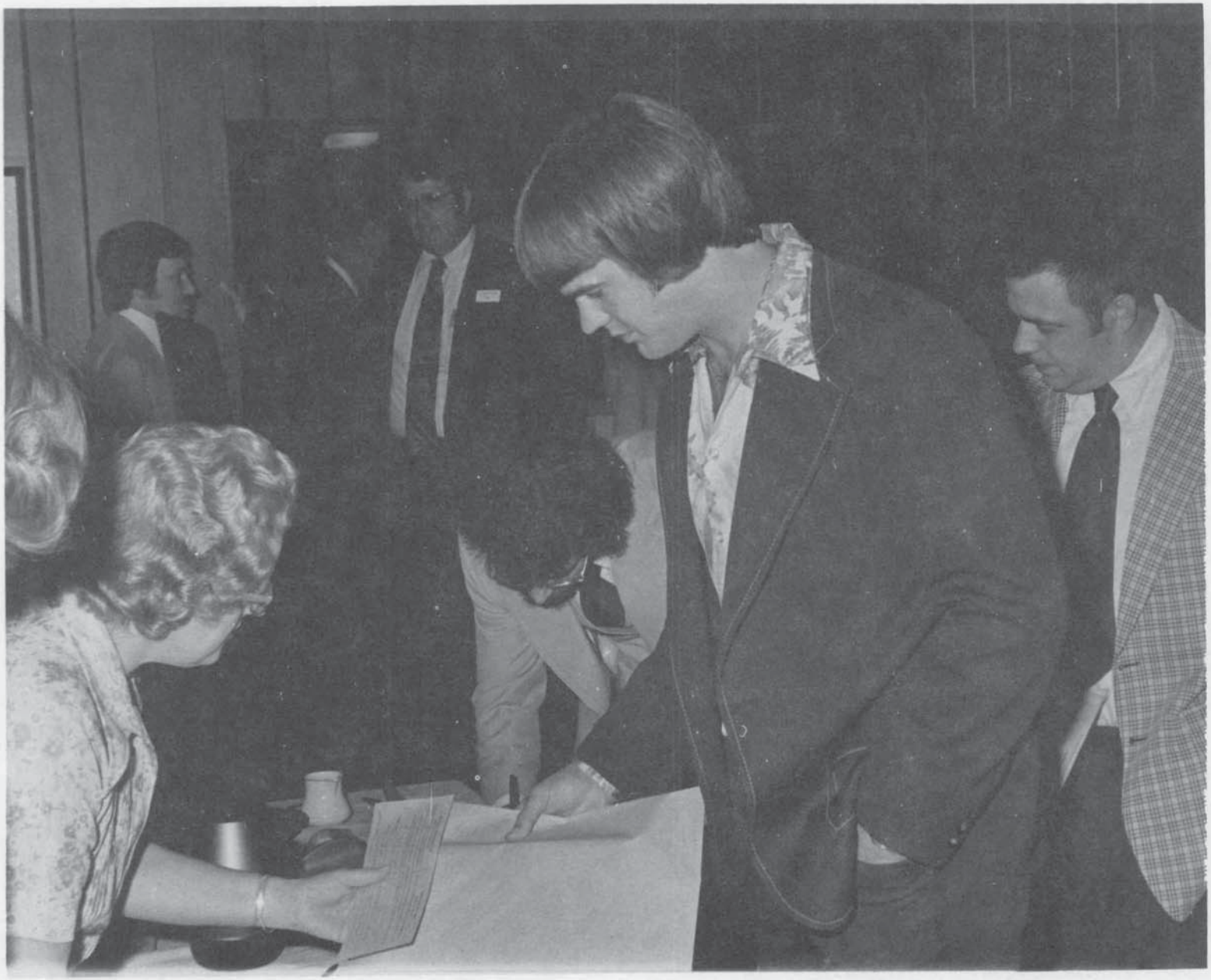


Figure A4-2. - Symposium Registration

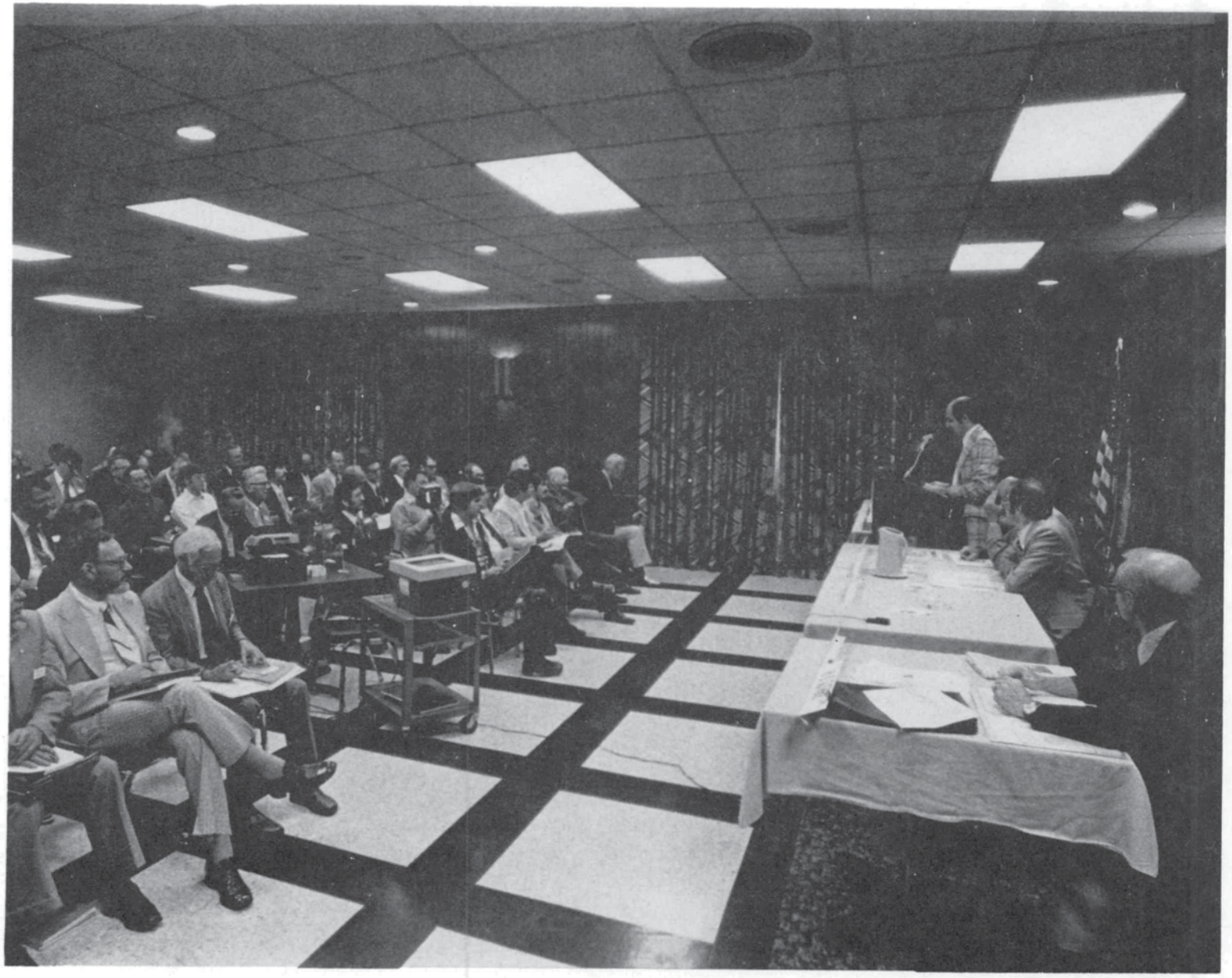


Figure A4-3. - Welcome Address
A. A. Pitrolo
Director, MERC



Figure A4-4. - Opening Remarks
Symposium Chairman
L. Z. Shuck



Figure A4-5. - Keynote Address
H. D. Guthrie
Director, Division of Oil,
Gas, and Shale Technology
ERDA HQ, WASH. D.C.



Figure A4-6. - "A Cooperative, Attentive Lot" for the Message from Washington

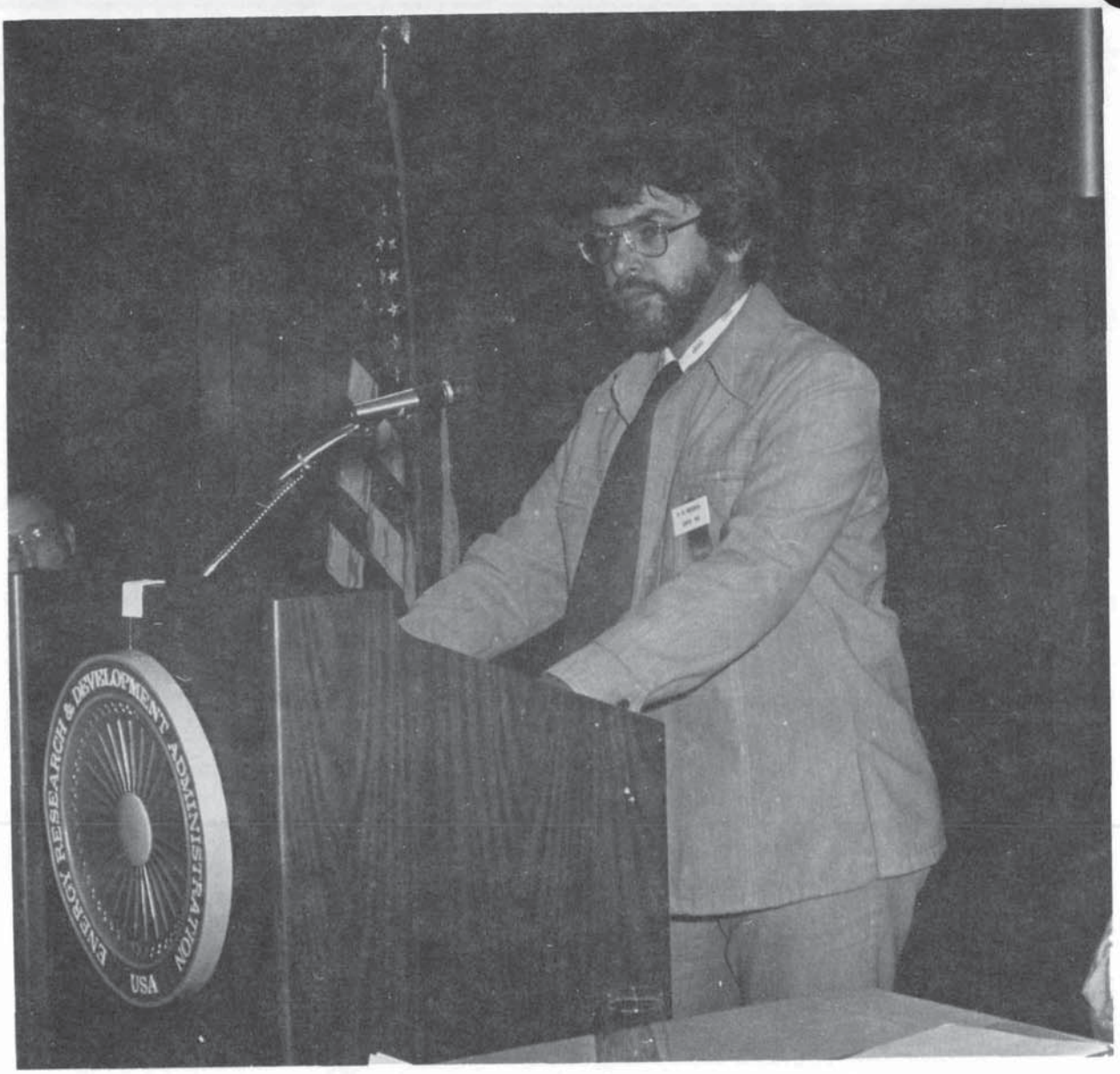


Figure A4-7. - Plenary Paper 1
The ERDA UCG PROGRAM
P. R. Wieber
Acting Branch Chief, ERDA
F.E. In Situ Tech. Branch
ERDA HQ, WASH. D.C.

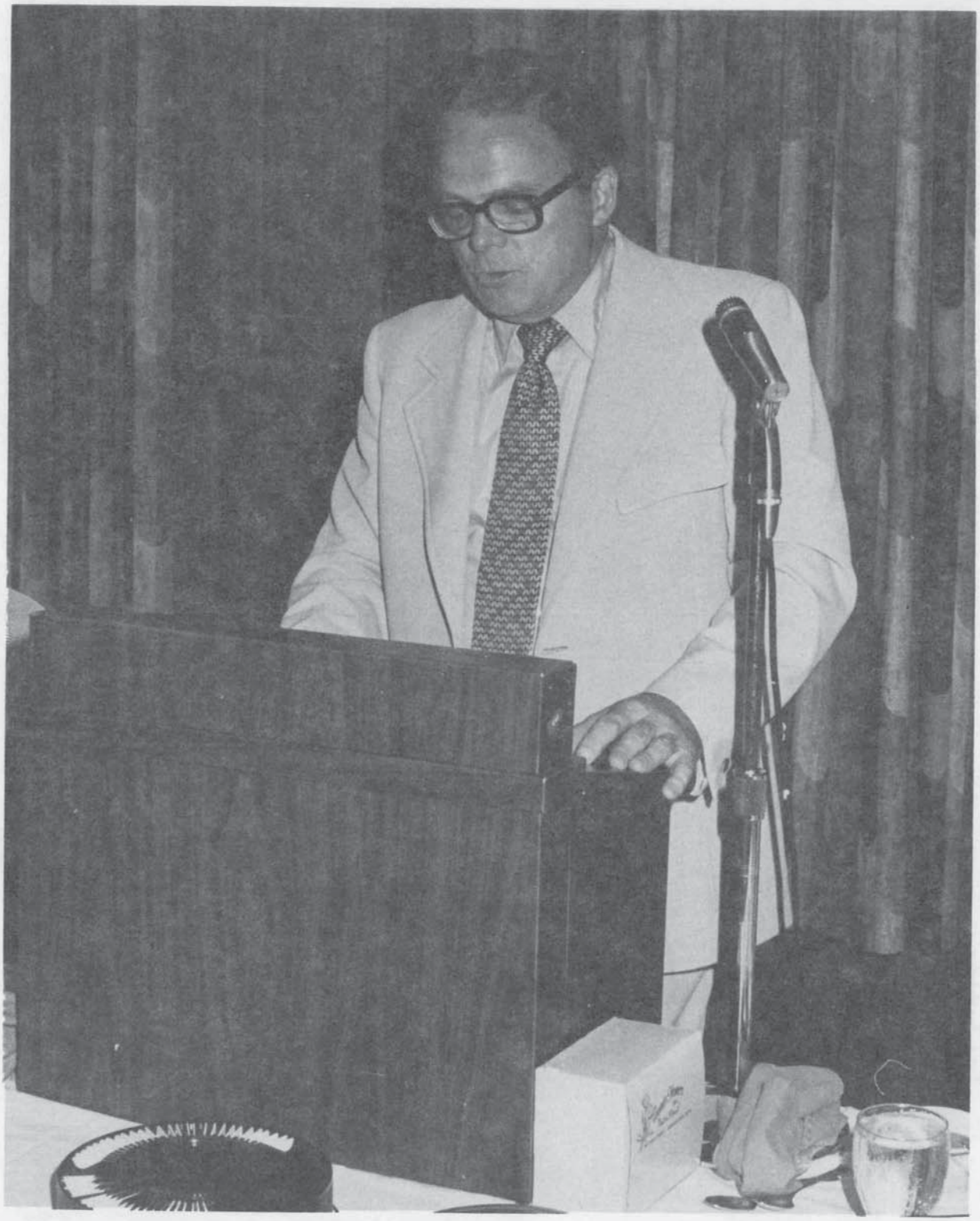


Figure A4-8. - Master of Ceremonies, Banquet
Robert Hart, Manager
Oak Ridge Operations Office

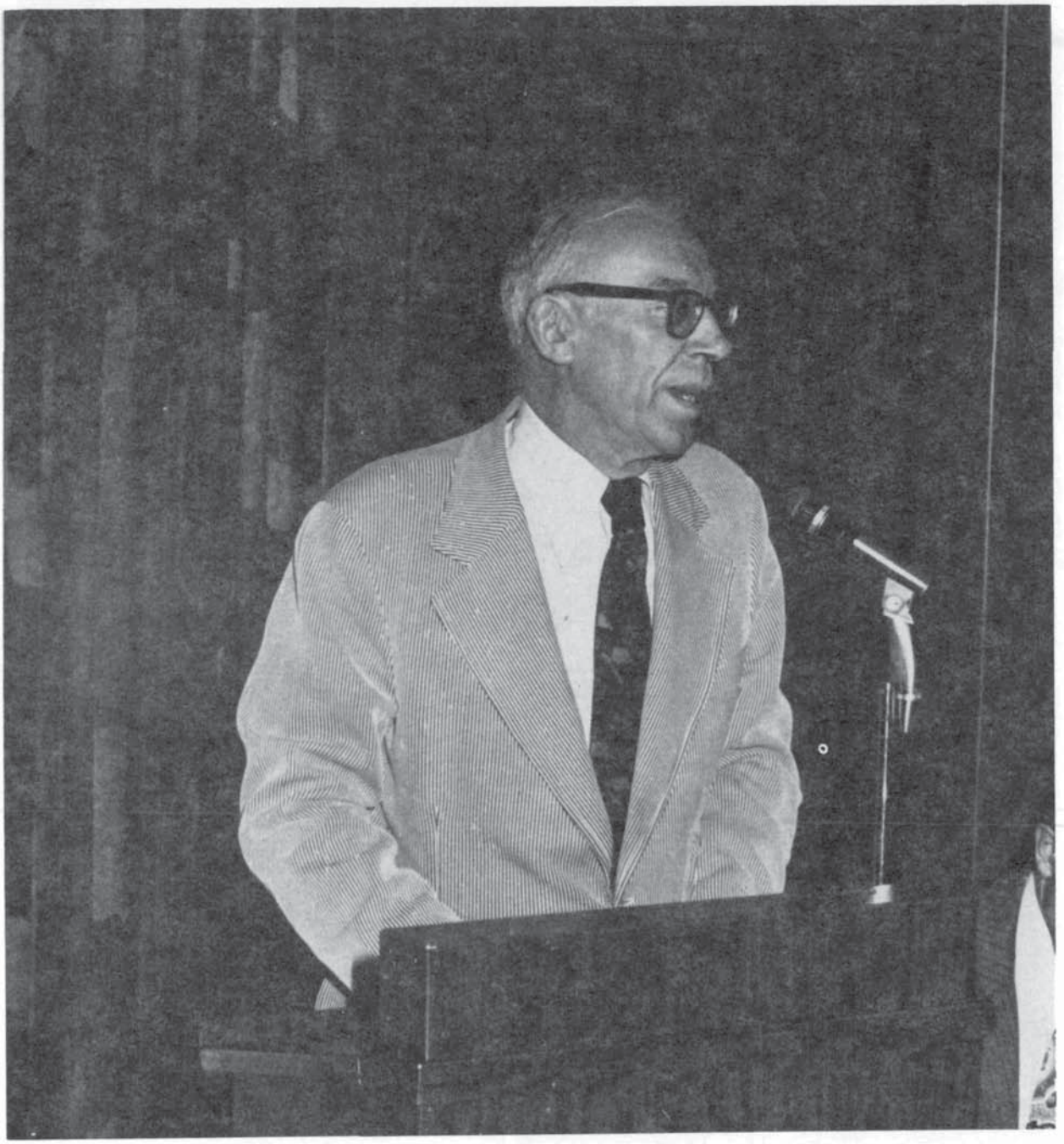


Figure A4-9. - Banquet Speaker
The Honorable Ken Hechler
West Virginia Congressman
Fourth District



Figure A4-10. - "Those who prevailed over the temptations of golf, boating, etc. to be in the group mug shot."

APPENDIX A5

SUBMITTED BIOGRAPHICAL SKETCHES

S. H. ADVANI, West Virginia University, Morgantown, West Virginia

R. L. ARSCOTT, Gulf Research and Development Company, Pittsburgh, Pennsylvania

CONSTANTINE A. BALANIS

Dr. Balanis received his B.S.E.E. degree from Virginia Polytechnic Institute, Blacksburg, in 1964, the M.E.E. degree from the University of Virginia, Charlottesville, in 1966, and the Ph.D. degree in electrical engineering from Ohio State University, Columbus, in 1969.

From 1964 to 1970 he was with NASA, Langley Research Center, Hampton, Virginia. Since 1970 he has been with the Department of Electrical Engineering, West Virginia University where he is presently a Professor. His research interests are in the application of the Geometrical Theory of Diffraction, Fourier transform methods for the inversion of radiometric measurements, and electromagnetic wave propagation and instrumentation for coal applications.

Dr. Balanis is a member of Sigma Xi, Tau Beta Pi, Eta Kappa Nu, Phi Kappa Phi, American Society for Engineering Education, and Radio Technical Commission for Aeronautics. He is listed in American Men of Science, Who's Who in the East and is an Associate Editor of the IEEE Transactions on Antennas and Propagation.

L. C. BARTEL, Sandia Laboratories, Albuquerque, New Mexico

F. O. BEANE, Lawrence Livermore Laboratories, ERDA, Livermore, California

S. G. BEARD

Mr. Beard earned the B.S. and M.S. degrees in Physics at North Carolina State University at Raleigh, N.C. He is a member of the American Institute of Aeronautics and Astronautics. He is presently a Member of the Technical Staff of Sandia Laboratories, Albuquerque, New Mexico. His work at Sandia has included plasma jet diagnostics and reentry vehicle thermal analyses in the RV Aerothermodynamics Division. Presently he is engaged in thermal instrumentation development, data reduction and analysis, and modeling related to underground coal gasification.

L. W. BECKHAM

L. W. Beckham was born in Ogden, Utah on September 9, 1946. He received the B.S.E.E. and M.S.E.E. degrees from the University of Texas - El Paso, in 1973 and 1974, respectively. Since joining Sandia Laboratories he has been associated with the Hanna Instrumentation Program. His special interests include statistical signal processing, signal detection theory and adaptive filtering as applied to array processing. He is a member of Tau Beta Pi, Eta Kappa Nu and the I.E.E.E.

APPENDIX A5

SUBMITTED BIOGRAPHICAL SKETCHES

W. BERTSCH, University of Alabama, University, Alabama

D. L. BIDLACK

Dr. Bidlack is a senior project engineer with the Process Economics Section at Gulf Research & Development Company where he has spent the past several years working on the economics of coal conversion processes and utilization of coal resources. He holds a B.S. Ch.E. degree from Tri-State College and a Ph.D. degree in Chemical Engineering from Michigan State University. He is a member of Sigma Xi, American Chemical Society, and American Institute of Chemical Engineers.

L. A. BISSETT, MERC, ERDA, Morgantown, West Virginia

R. MICHAEL BOYD

Mr. Boyd received his B.S. degree in geology from Bowling Green University in 1966 and his M.A. degree from the same University in 1970.

For the past four years he has been the Project Geologist for the Underground Coal Gasification Project at Hanna, Wyoming. Prior to that time he worked in mineral exploration in the U.S. and Canada.

CHARLES F. BRANDENBURG

Dr. Brandenburg received his B.S. and Ph.D. degrees in chemistry from the University of Wyoming in 1962 and 1969 respectively. Dr. Brandenburg has worked at the Laramie Energy Research Center in research on fossil fuel technology since 1959. Dr. Brandenburg spent several years studying the retorting mechanisms of oil shale.

Dr. Brandenburg has been the Project Leader of the Underground Coal Gasification Program at the Laramie Energy Research Center for the past three years. During this period the Laramie Energy Research Center's underground coal gasification project at Hanna has made significant breakthroughs toward developing underground coal gasification into a commercially viable process.

APPENDIX A5

SUBMITTED BIOGRAPHICAL SKETCHES

MANFRED K. BUDER

Manfred K. Buder is presently with Coal Technology Department at Bechtel Corporation, San Francisco, California, where his major job functions include technical and economic process evaluations and feasibility studies, coal conversion process development, and formulation and testing of novel approaches in coal processing for energy and chemicals. He was previously employed by Standard Oil Company of California in refinery engineering. He received a B.S. degree in chemical engineering from the University of British Columbia, Vancouver, B.C.

T. R. BUTKOVICH, Lawrence Livermore Laboratory, Livermore, California

CHARLES W. BYRER

Mr. Byrer, Geologist, Morgantown Energy Research Center, graduated with a Bachelor's Degree in Geology from Fairmont State College and a Master's Degree from West Virginia University, Morgantown, West Virginia.

G. G. CAMPBELL, LERC, ERDA, Laramie, Wyoming

J. H. CAMPBELL, Lawrence Livermore Laboratories, Livermore, California

R. F. CHAIKEN, Pittsburgh Mining and Safety Research Center, Bureau of Mines, Pittsburgh, Pennsylvania

H. Y. CHANG, West Virginia University, Morgantown, West Virginia

B. R. CLEMENTS, Texas Utilities Service, Inc., Dallas, Texas

R. DATTA, Syracuse Research Corporation, Syracuse, New York

G. W. DOUGLAS, University of Alabama, University, Alabama

D. E. EASTWOOD, LERC, ERDA, Laramie, Wyoming

J. K. EASTLACK, LERC, ERDA, Laramie, Wyoming

APPENDIX A5

SUBMITTED BIOGRAPHICAL SKETCHES

T. F. EDGAR

Dr. Edgar is Director of the In Situ Lignite Gasification Project at the University of Texas at Austin. He received a B.S. in Chemical Engineering from the University of Kansas and his Ph.D. from Princeton University. His principal research interests are in underground coal gasification, process control and optimization, and he has over forty publications in these areas. He is co-authoring, along with Dr. David Gregg if Livermore Laboratory, the chapter on underground coal gasification for the new edition of Chemistry of Coal Utilization to be published in 1977.

G. E. FASCHING, MERC, ERDA, Morgantown, West Virginia

S. M. FAROUQ ALI

Dr. Farouq Ali is professor of petroleum and natural gas engineering at the Pennsylvania State University, where he has been a faculty member since 1962. Prior to this he has worked as petroleum and mechanical engineer. He holds a B.S. in electrical engineering, a B.Sc. in petroleum engineering, and M.S. and Ph.D. degrees in petroleum and natural gas engineering.

Dr. Farouq Ali has conducted research in underground coal gasification simulation, thermal recovery, and simulation of oil production processes. He has authored over 110 papers and two books in these areas. He has taught numerous short courses on thermal recovery and simulation, including many abroad, and has served as consultant to a number of oil companies in the U.S. and abroad.

DENNIS D. FISCHER

Mr. Fischer received his B.S. degree in chemistry from South Dakota State University in 1965. He received the Fulbright Scholarship to Albert-Ludwigs University in Freiburg, West Germany, for the year 1965 to 1966 and did graduate work at Florida State University from 1966 to 1967 and at Scripps Institute of Oceanography, University of California at San Diego from 1967 to 1968.

He was previously employed at the Bureau of Mines' Reno Metallurgy Research Center in Reno, Nevada from 1968 to 1972 and was working on recovery of precious metals from low grade sources and development of hydrometallurgical methods of separating molybdenum and rhenium and of recovering silver and gold using activated carbon from process solutions.

In November 1972 he was transferred to Laramie Energy Research Center to work on the underground coal gasification project with the primary interest being study of environmental impacts of underground coal gasification.

APPENDIX A5

SUBMITTED BIOGRAPHICAL SKETCHES

J. FISCHER, Argonne National Laboratory, Argonne, Illinois

R. C. FORRESTER III, Oak Ridge National Laboratory, Oak Ridge, Tennessee

R. A. FOSCHER, Bechtel Corporation, San Francisco, California

G. V. GANGARAO, West Virginia University, Morgantown, West Virginia

ALLAN M. GARON

Allan M. Garron is a Senior Research Engineer with Gulf Research and Development Company. He received a PhD degree from the University of Minnesota in mechanical engineering with a heat transfer specialty. Since joining Gulf in 1970, Dr. Garon has worked on thermal enhanced oil recovery, specifically involving fireflooding and fire-water flooding, and on tar sand recovery. He has been involved in underground coal gasification for the past three years.

DAVID W. GREGG

Dr. Gregg received an B.A. in Chemistry from Dartmouth in 1957 and a Ph.D. in Chemical Engineering from the University of Illinois in 1961. Upon leaving the University of Illinois he went to work for Lawrence Livermore Laboratory where he has been to the present. Dr. Gregg spent most of that time (1962-74) working for the laser fusion program. In 1974 he joined the LLL Underground Coal Gasification Program and has been working on the alternative system options for UCG, with special emphasis on the Soviet approach.

ROBERT D. GUNN

Dr. Gunn received a B.S. degree in Industrial Chemistry from Kansas State University in 1950, and an M.S. (1958) and Ph.D. (1967) in Chemical Engineering from the University of California at Berkeley.

He spent seven years in the petroleum industry primarily in Saudia Arabia and Venezuela.

He has spent the last 8½ years teaching at the University of Texas and at the University of Wyoming. He is currently an associate professor in the Mineral Engineering Department and an intermittent employee of the Laramie Energy Research Center.

APPENDIX A5

SUBMITTED BIOGRAPHICAL SKETCHES

S. V. GUNN, Rocketdyne Corporation, Canoga Part, California

O. J. HAHN

Dr. Hahn is presently an Associate Professor of Mechanical Engineering Deparment of the University of Kentucky, he is also Associate Director for the Institute of Mining and Minerals Research.

He received his B.S. in Engineering Physics (1958) at the University of Alberta, an M.S. degree (1960) in Nuclear Engineering at the West Virginia University, and an M.A. and Ph.D. degree (1964 in Mechanical Engineering at Princeton University.

Dr. Hahn is presently involved in all phases of coal utilization and conversion.

A. HAYATDAVOUDI, University of Alabama, University, Alabama

R. R. HAYNES, MERC, ERDA, Morgantown, West Virginia

J. F. HENRY, University of Alabama, University, Alabama

ALAN E. HUMPHREY

Mr. Humphrey received his B.S. degree in mechanical engineering from the University of Wyoming in 1973.

He was employed by Ford Motor Company as a design and test engineer from 1973 to 1974. Prior to this transfer to the Laramie Energy Research Center, September 1975, he was employed by the Environmental Protection Agency as a test engineer.

He has worked as a design engineer and field test site supervisor since joining the underground coal gasification project.

R. W. HERMSEN

Dr. Hermsen is Chief, Kinetics and Combuston, Chemical Systems Division, where he is responsible for research on gas dynamics and combustion systems. He holds B.S. and Ph.D. degrees in chemical engineering from Oregon State University and the University of California at Berkeley. His research experience includes studies in thermodynamics, two-phase flow, metal combustion, and radiation from gas particle clouds.

APPENDIX A5

SUBMITTED BIOGRAPHICAL SKETCHES

JOHN J. HOLMES

Mr. Holmes was born in Wheeling, W.Va., on July 27, 1951. He received the B.S. and M.S. degrees in electrical engineering from West Virginia University, Morgantown, WV., in 1973 and 1974, respectively.

From 1973 to 1974 he was a Research Assistant in the Department of Electrical Engineering, West Virginia University. He is currently working towards the Ph.D. degree in electrical engineering under a West Virginia University Foundation Fellowship. His interests are in the area of Radiometric Inversions and electromagnetic wave propagation through lossy media.

Mr. Holmes is a member of Eta Kappa Nu, Tau Beta Pi, Pi Mu Epsilon, Phi Kappa Phi, and is an Associated Member of Sigma Xi.

JEFFREY C. HUSTON

Dr. Huston received his B.S. degree in Engineering Science from Illinois Institute of Technology in May 1972. In June 1972 he enrolled in graduate studies at West Virginia University where he was later granted both a M.S. (May 1973) and Ph.D. (December 1975) degree in Mechanical Engineering Mechanics. Dr. Huston has recently been employed by West Virginia University as a Lecturer and an Assistant Professor in the Department of Mechanical Engineering Mechanics and by Morgantown Energy Research Center as a Mechanical Engineer (Faculty Member). This fall (1976), Dr. Huston has accepted employment at Iowa State University as an Assistant Professor in the Engineering Science and Mechanics department.

J. W. JENNINGS, LERC, ERDA, Laramie, Wyoming

J. E. JONES, JR., University of Kentucky, Lexington, Kentucky

W. R. KAISER, University of Texas at Austin, Texas

S. B. KING, LERC, ERDA, Laramie, Wyoming

W. V. LANUM, LERC, ERDA, Laramie, Wyoming

R. LO, Argonne National Laboratory, Argonne, Illinois

JO MANN

Ms. Mann is a mathematics and economics graduate of the University of Sussex and a member of the OR team at Harrow. Besides UCG, her main fields of interest are in marketing, distribution and manpower.

APPENDIX A5

SUBMITTED BIOGRAPHICAL SKETCHES

JOSEPH W. MARTIN

Mr. Martin is the assistant project manager for the Underground Coal Gasification program at the Morgantown Energy Research Center. He received his B.S. degree in Physics from West Virginia University in 1962 and has pursued extensive graduate work in the related fields of physics, mathematics, and computer science. In 1963, he was employed by the U.S. Bureau of Mines, Morgantown Energy Research Center. From 1963 until 1972, he participated in the application of nuclear radiation to coal by developing a gamma ray-based coal mine dust combustibles meter and completing a neutron-based meter to monitor the sulfur content of flowing tonnage quantities of coal. In 1972, he transferred to the Underground Coal Gasification group to develop automatic data acquisition and process control capabilities for the project and to assist in the construction and operation of the In Situ Hydrocarbon Simulation Laboratory.

A. I. McCONE, Bechtel Corporation, San Francisco, California

M. D. McKINLEY, University of Alabama, University, Alabama

I. McC. STEWART, University of Newcastle, New South Wales, Australia

ALBERT JAMES MOLL

Dr. Moll is Director of the Energy Technology Department, Stanford Research Institute, Menlo Park, California. He was previously employed by Union Carbide Corporation and Chem Systems, Inc. He holds a B.S. degree in chemical engineering from the University of Illinois, and M.S. and Ph.D in chemical engineering from the University of Washington. He is a member of AIChe, ACS and Sigma Xi and is listed in American Men and Women of Science.

D. F. MOORE, LERC, ERDA, Laramie, Wyoming

D. A. NORTHROP, Sandia Laboratories, Albuquerque, New Mexico

M. L. PASHA

Dr. Pasha earned his B.Sc. (1961) and M.Sc. (1964) in Mathematics from Agra and Lucknow Universities in India respectively and his Ph.D. in (1974) in Mathematics at The Penntylvania State University. Since December 1973, he is working in the department of Petroleum and Natural Gas Engineering as a research associate, with Prof. S. M. Farouq Ali on the mathematical modeling of the process of underground coal gasification.

APPENDIX A5

SUBMITTED BIOGRAPHICAL SKETCHES

J. PASINI III, MERC, ERDA, Morgantown, West Virginia

M. T. PELLEGRIN, MERC, ERDA, Morgantown, West Virginia

R. P. REED

Dr. Reed (B.S. in ,.E., M.S. IN E.M., Ph.D.) is a Registered Professional Engineer, a member of the American Society of Mechanical Engineers, and of Sigma Xi. He is a member of the Technical Staff of Sandia Laboratories, Albuquerque, New Mexico where he is an experimenter and consultant for stress wave and thermal measurements on research relating to underground gasification of coal, in situ rubblization and retorting of oil shale, explosive and projectile induced waves in geologic media, safety studies of nuclear reactors, nuclear waste disposal, and nuclear weapons effects.

RUDOLF ROZSA

Mr. Rozsa received a B.S. degree in Chemical Engineering from Tulane University in 1961 and M.S. and Engineering degrees in Chemical Engineering from Stanford in 1963 and 1964, respectively. He has been at the Lawrence Livermore Laboratory since 1966 and has worked on various projects including the Space Power Reactor Program, and several different Weapons Programs. He is currently a Chemical Engineering Group Leader in the Chemistry and Materials Science Department at Lawrence Livermore Laboratory.

ERICH SARAPUU

Dr. Sarapuu, President of Electrofrac Corporation, studied mining engineering and fuel technology in Estonia, Germany and U.S.A. He earned his Diploma-Engineering degree (M.S.) in Mining Academy Freiberg, Germany. His theses was connected with the development of underground electrolinking of oil shale, Later, he spent four years in the University of Missouri, School of Mines where he carried out the development of in situ electrocarbonization of coal. He received his Ph.D. degree in 1951 for this research work.

Since 1953 he has been connected with Electrofrac Corporation. In past twenty-five years, he has been developing in situ electro-energetic processes for recovering coal, oil shale, tar sand and crude oil by underground electropyrolysis and electrogasification techniques. He has been also engaged in the development of electrical rock fragmentation methods and electrical disintegration drilling of blask-holes by means of electrical energy.

He has served as consultant to the U.S. Government, oil and mining companies and for two years was connected with the University of Arizona in Tucson as an associate professor. He has been issued several patents in this country and abroad and has published papers dealing with the electroenergetic in situ processing of fossil fuels and electrical rock fragmentation.

APPENDIX A5

SUBMITTED BIOGRAPHICAL SKETCHES

W. K. SAWYER, MERC, ERDA, Morgantown, West Virginia

LEO A. SCHRIDER

Leo A. Schrider is the Assistant Director, Extraction and In Situ Conversion Division at the Morgantown Energy Research Center. He received his B.S. degree in petroleum engineering from the University of Pittsburgh in 1962. Subsequent post graduate work has been completed in operations research at West Virginia University. After graduating in 1962, he was employed by Shell Oil Company in southern Louisiana as an exploitation engineer. In 1964 he joined the staff of the Bureau of Mines, Morgantown Energy Research Center, as petroleum research engineer. He worked in this capacity for several years and became project leader for the project titled, "Susceptibility of Eastern U.S. Oil Reservoirs to Newer Recovery Techniques." In 1973 he transferred to the Laramie Energy Research Center as the program manager for the Underground Coal Gasification program being conducted by the U.S. Bureau of Mines. He managed the research and technology development for the in situ coal gasification experiments being conducted near Hanna, Wyoming. In July 1976 he transferred back to Morgantown to assume his present duties.

J. F. SEEBERGER, West Virginia University, Morgantown, West Virginia

HAROLD D. SHOEMAKER

Dr. Shoemaker received his B.S. (Dec. 1969) and M.S. (May 1971) degrees in Agricultural Engineering from West Virginia University. In May 1976, he received his PhD degree in Mechanical Engineering and Mechanics from West Virginia University. His doctoral research was performed at the Morgantown Energy Research Center and involved determining the thermo-mechanical properties of coal. Dr. Shoemaker is currently a member of the In Situ Conversion research group at MERC. He is a member of Sigma Xi, Tau Beta Pi, and Alpha Epsilon.

L. Z. SHUCK

Dr. Shuck is the Project Leader for the In Situ Conversion Project, MERC. He earned his B.S. degree (1958) in Mechanical Engineering at the West Virginia Institute of Technology, his M.S. degree (1965) in Mechanical Engineering at West Virginia University, and his Ph.D. in Theoretical and Applied Mechanics (1970) at West Virginia University. Dr. Shuck has spent 15 years either teaching or consulting in the energy area, or conducting and managing energy extraction and conversion programs. During that time, he has served as consultant to several companies in the energy field including: Southern Public Service Co., United Fuel Gas Co., Stonestreet Oil and Gas Co., West Virginia Air Pollution Control Commission, and Gravely Tractor Division, Studebaker Corp., Dunbar, West Virginia. Since 1970, Dr. Shuck has been conducting and managing research at the Morgantown Energy Research Center, ERDA, in the areas of petroleum, natural gas, oil shale and coal in situ extraction and conversion technology.

APPENDIX A5

SUBMITTED BIOGRAPHICAL SKETCHES

A. P. SIKRI, Chemical Engineer, In Situ Coal Gasification Branch, ERDA HQ, Washington, D.C.

J. M. SINGER, Pittsburgh Mining and Safety Research Center, Bureau of Mines, Pittsburgh, Pennsylvania

BARBARA E. SLONNEGER

Ms. Slonneger is a junior majoring in mechanical engineering at Virginia Polytechnic Institute and State University. She spent summer 1976 working at the Morgantown Energy Research Center, ERDA. During the previous summer she helped with the preparation of a report on the Personal Rapid Transit System at West Virginia University.

D. R. STEPHENS, Lawrence Livermore Laboratories, Livermore, California

T. STERNER, LERC, ERDA, Laramie, Wyoming

R. E. D. Stewart

Dr. Stewart received a B.S. in mechanical engineering from the University of Illinois in 1962. Upon graduation, he joined Sandia Laboratories, working in a variety of areas, including timer development, parachute deployment dynamics, and reentry vehicle aero heating and ablation analysis, while simultaneously pursuing graduate studies at the University of New Mexico. He received an M.S. in mechanical engineering from the University of New Mexico in 1964, and was granted a leave of absence in the fall of 1965 to pursue full time doctoral studies at Illinois Institute of Technology. He received a Ph.D. in mechanical and aerospace engineering in 1969 with specialization in the areas of heat transfer and fluid mechanics. Dr. Stewart rejoined Sandia in 1969, working from 1969 to 1972 in thermal stress analysis, and from 1972 to 1975 in surveillance systems and data link security. In early 1975, Dr. Stewart joined Sandia's "Energy Projects and Systems Analysis" division where he is currently conducting systems analysis studies in the areas of coal gasification and solar energy.

O. N. TERICHOW, Bechtel Corporation, San Francisco, California

T. H. TSANG, University of Texas, Austin, Texas

PETER N. THOMPSON

Mr. Thompson is a mining engineer and a graduate of Birmingham University. As Midlands Manager of the NCB Operational Research Executive he is responsible for providing an OR service to wide areas of the coalfields and also to be research establishments of the NCB.

APPENDIX A5

SUBMITTED BIOGRAPHICAL SKETCHES

T. W. THOMPSON

Dr. Thompson received his B.Sc. in Geology from the University of Newcastle upon Tyne, England in 1967. Following one year in the Geology Department of the University of Edinburgh, Scotland he joined the Mining Engineering Department at the University of Newcastle upon Tyne working initially as a graduate studient and later as an Experimental officer and then Senior Research Associate in the Rock Mechanics Laboratory of that Department. During this period he was involved mainly with analytical and experimental studies into the feasibility of gas storage in underground brine cavities. He was awarded a Ph.D. in Applied Science for work in this area in 1973.

In 1975 Dr. Thompson joined the staff of the Center for Earth Sciences and Engineering at the University of Texas at Austin as a Research Engineer, and since then has been conducting research mainly into the rock mechanics aspect of in-situ gasification and geothermal geopressured reservoir exploitation, and in the areas of hydraulic fracturing and laboratory testing techniques. In September, 1976, Dr. Thompson is joining the faculty in the Department of Petroleum Engineering at the University of Texas as an Assistant Professor.

CHARLES THORSNESS

Dr. Thorsness received his B.S. degree in Chemical Engineering from Oregon State University in 1968 and his Ph.D. in Chemical Engineering from the University of Illinois in 1974. He worked as a research engineer for Esso Production Research Company from 1968 to 1971. He joined Lawrence Livermore Laboratory in 1974 and has worked since then on LLL's In-Situ Coal Gasification project.

THOMAS WARREN

Mr. Warren received a B.S. degree in Mineral Engineering at the University of Alabama in 1973 and an M.S. in Mineral Engineering in 1976. He has two years experience as a Petroleum Engineer with Amoco Production Company.

D. L. WHITMAN, University of Wyoming, Laramie, Wyoming

APPENDIX A5

SUBMITTED BIOGRAPHICAL SKETCHES

FRED WILLIAMS

Mr. Williams is a mining engineer and a graduate of Nottingham University. He is a member of the Midlands OR Unit and has experience in line management, smokeless fuel production, coal preparation, pipeline transportation and fluidized bed applications.

JOHN E. YOUNG

Dr. Young received his B.S. (1962) in Chemical Curriculum at Iowa State University, Ames, Iowa, and his Ph.D. (1970) in Organic Chemistry at Cornell University, Ithaca, New York.

Dr. Young was previously employed as a Research Chemist at Gulf Research and Development Co., Pittsburgh, Pa., from 1970 until he joined the Chemical Engineering Division in April, 1975. At that time he became a member of the Coal Technology Group where he has studied coal ash catalysis and simulated in situ gasification reactions. He has approximately 11 publications concerning non-stoichiometric metal oxides, structural properties of ceramics, and various aspects of hydrocarbon and synthetic fuels processing. He also has three patents in the area of hydrocarbon processing. He is a member of the American Chemical Society and the American Association for the Advancement of Science.

All Meetings Held in Lakeview Inn
& Country Club Conference Room A-B

Program Outline

Monday, August 9

REGISTRATION	5:00 - 7:00 p.m.
RECEPTION	7:00 - 8:30 p.m.

Tuesday, August 10

OPENING REMARKS	8:00 a.m.
KEYNOTE ADDRESS	8:15 a.m.
ERDA UCG PROGRAM REVIEW	8:45 a.m.
PROJECT STATUS REPORTS	9:15 a.m.
Coffee Break (15 min.)	*10:25 a.m.*
PROJECT STATUS REPORTS	10:40 a.m.
Lunch (1 hour)	*12:40 p.m.*
PROJECT STATUS REPORTS	1:40 p.m.
Coffee Break (15 min.)	*3:40 p.m.*
ENVIRONMENTAL STUDIES	3:55 p.m.
Break (35 min.)	*5:25 p.m.*
Dinner (1 hour)	*6:00 p.m.*
ECONOMICS	7:00 - 9:00 p.m.

Wednesday, August 11

INSTRUMENTATION	8:00 a.m.
Coffee Break (15 min.)	*10:00 a.m.*
THEORETICAL MODELING	10:15 a.m.
Lunch (1 hour)	*12:15 p.m.*
STRUCTURAL & ROCK MECH.	1:15 p.m.
Break (2 3/4 hours)	*3:45 p.m.*
Optional MERC Tour 4:00	*6:00 p.m.*
Cocktail Hour	*6:30 p.m.*
Banquet:	*7:30 p.m*

Congressman Ken Hechler
Soviet UCG Film & Slide Show

Thursday, August 12

FIELD & INTEGRATED SYS.	8:00 a.m.
Coffee Break (15 min.)	*10:30 a.m.*
UCG IN OTHER COUNTRIES	10:45 a.m.
Luncheon (1½ hour)	*12:15 p.m.*
LABORATORY EXPERIMENTS	1:45 p.m.
Coffee Break (15 min.)	*3:15 p.m.*
LABORATORY EXPERIMENTS	3:30 p.m.
Dinner Break (2 hours)	*5:00 p.m.*
POTPOURRI BRIEFS	7:00 p.m.
CLOSING REMARKS	9:00 p.m.

*U.S.GOVERNMENT PRINTING OFFICE: 1977- 740062/44